Patai Series:
The Chemistry of Functional Groups
Series Editor: Zvi Rappoport

Volume Editors: Zvi Rappoport & Joel F. Liebman

The Chemistry of Hydroxylamines, Oximes and Hydroxamic Acids

Part 1

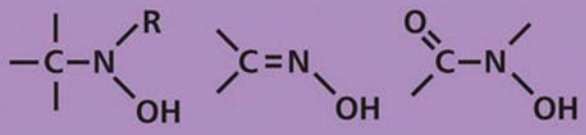

Patai Series online:
http://www.interscience.wiley.com

WILEY

An Interscience® Publication

The chemistry of
Hydroxylamines, Oximes and Hydroxamic Acids

Part 1

Edited by

ZVI RAPPOPORT

The Hebrew University, Jerusalem

and

JOEL F. LIEBMAN

Department of Chemistry and Biochemistry,
University of Maryland, Baltimore County

2009

A John Wiley and Sons, Ltd., Publication

An Interscience® Publication

The chemistry of

Hydroxylamines, Oximes and Hydroxamic Acids

Patai Series: The Chemistry of Functional Groups

A series of advanced treatises founded by Professor Saul Patai and under the general editorship of Professor Zvi Rappoport

The **Patai Series** publishes comprehensive reviews on all aspects of specific functional groups. Each volume contains outstanding surveys on theoretical and computational aspects, NMR, MS, other spectroscopic methods and analytical chemistry, structural aspects, thermochemistry, photochemistry, synthetic approaches and strategies, synthetic uses and applications in chemical and pharmaceutical industries, biological, biochemical and environmental aspects.
To date, 120 volumes have been published in the series.

Recently Published Titles

The chemistry of the Cyclopropyl Group (Volume 2)
The chemistry of the Hydrazo, Azo and Azoxy Groups (Volume 2, 2 parts)
The chemistry of Double-Bonded Functional Groups (Volume 3, 2 parts)
The chemistry of Organophosphorus Compounds (Volume 4)
The chemistry of Halides, Pseudo-Halides and Azides (Volume 2, 2 parts)
The chemistry of the Amino, Nitro and Nitroso Groups (2 volumes, 2 parts)
The chemistry of Dienes and Polyenes (2 volumes)
The chemistry of Organic Derivatives of Gold and Silver
The chemistry of Organic Silicon Compounds (2 volumes, 4 parts)
The chemistry of Organic Germanium, Tin and Lead Compounds (Volume 2, 2 parts)
The chemistry of Phenols (2 parts)
The chemistry of Organolithium Compounds (2 volumes, 3 parts)
The chemistry of Cyclobutanes (2 parts)
The chemistry of Peroxides (Volume 2, 2 parts)
The chemistry of Organozinc Compounds (2 parts)
The chemistry of Anilines (2 parts)
The chemistry of Organomagnesium Compounds (2 parts)

Forthcoming Titles

The chemistry of Metal Enolates
The chemistry of Organocopper Compounds

The Patai Series Online

Starting in 2003 the **Patai Series** is available in electronic format on Wiley InterScience. All new titles will be published as online books and a growing list of older titles will be added every year. It is the ultimate goal that all titles published in the **Patai Series** will be available in electronic format.
For more information see under **Online Books** on:

www.interscience.wiley.com

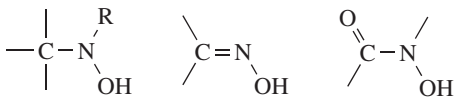

The chemistry of
Hydroxylamines, Oximes and Hydroxamic Acids

Part 1

Edited by

ZVI RAPPOPORT

The Hebrew University, Jerusalem

and

JOEL F. LIEBMAN

Department of Chemistry and Biochemistry,
University of Maryland, Baltimore County

2009

A John Wiley and Sons, Ltd., Publication

An Interscience® Publication

John Wiley & Sons Ltd, The Atrium, Southern Gate, Chichester,
West Sussex PO19 8SQ, England

Telephone (+44) 1243 779777

Email (for orders and customer service enquiries): cs-books@wiley.co.uk
Visit our Home Page on www.wileyeurope.com or www.wiley.com

Other Wiley Editorial Offices

John Wiley & Sons Inc., 111 River Street, Hoboken, NJ 07030, USA

Jossey-Bass, 989 Market Street, San Francisco, CA 94103-1741, USA

Wiley-VCH Verlag GmbH, Boschstr. 12, D-69469 Weinheim, Germany

John Wiley & Sons Australia Ltd, 42 McDougall Street, Milton, Queensland 4064, Australia

John Wiley & Sons (Asia) Pte Ltd, 2 Clementi Loop #02-01, Jin Xing Distripark, Singapore 129809

John Wiley & Sons Canada Ltd, 6045 Freemont Blvd, Mississauga, Ontario, L5R 4J3, Canada

Wiley also publishes its books in a variety of electronic formats. Some content that appears in print may not be available in electronic books.

Library of Congress Cataloging-in-Publication Data:

The chemistry of hydroxylamines, oximes and hydroxamic acids / edited by Zvi Rappoport and Joel Liebman.
p. cm.—(The Chemistry of Functional Groups)
Includes bibliographical references and index.
ISBN 978-0-470-51261-6
1. Hydroxamic acids. 2. Oximes. 3. Hydroxylamine. I. Rappoport, Zvi. II. Liebman, Joel F.
QD305.A7C44 2008
547—dc22

2008046989

British Library Cataloguing in Publication Data

A catalogue record for this book is available from the British Library

ISBN 978-0-470-51261-6

Typeset in 9/10pt Times by Laserwords Private Limited, Chennai, India
Printed and bound in Great Britain by Biddles Limited, Kings Lynn, Norfolk
This book is printed on acid-free paper responsibly manufactured from sustainable forestry in which at least two trees are planted for each one used for paper production.

Dedicated to the memory of

Professor Tuvia Sheradsky

and

to

Kifele bat TC + C, and Moische ben A * C

Contributing authors

Edgars Abele	Latvian Institute of Organic Synthesis, Riga, LV1006, Latvia. Fax: +371-7550338; e-mail: abele@osi.lv
Yacov Ashani	Department of Neurobiology, The Weizmann Institute of Science, Rehovot 76100, Israel. Fax: +972-8-9346017; e-mail: yaacov.ashani@weizmann.ac.il
Yaniv Barda	Department of Organic Chemistry, Weizmann Institute of Science, P.O. Box 26, Rehovot 76100,Israel. Fax: +972-8-9342917; e-mail: yaniv.barda@weizmann.ac.il
Harald Brand	LMU Munich, Butenandt-Str. 5–13, 81377 München, Germany. e-mail: harald.brand@cup.uni-muenchen.de
Erwin Buncel	Department of Chemistry, Queen's University, Kingston, Ontario K7L 3N6, Canada. Fax: +1-613-533-6669; e-mail: buncele@chem.queensu.ca
Marvin Charton	Chemistry Department, School of Liberal Arts and Sciences, Pratt Institute, Brooklyn, NY 11205, USA. Fax: +1-718-722-7706; email: mcharton@pratt.edu
Jacques Fernandes Dias	Departamento de Química e Ambiental, Faculdade de Tecnologia, Universidade do Estado do Rio de Janeiro, Rodovia Presidente Dutra km 298—Pólo Industrial, Resende, RJ, 27537-000, Brazil. Fax: +55-24-3354-7875; e-mail: jacques@fat.uerj.br
Ender Erdik	Ankara University Science Faculty, Department of Chemistry, Beşevler, Ankara 06100, Turkey. Fax: +90-312-223-23-95; e-mail: erdik@science.ankara.edu.tr
Clifford E. Felder	Department of Organic Chemistry, Weizmann Institute of Science, P.O. Box 26, Rehovot 76100, Israel. Fax: +972-8-9342917; e-mail: clifford.felder@weizmann.ac.il
Carlo Galli	IMC-CNR Sezione Meccanismi di Reazione, c/o Dipartimento di Chimica, Università 'La Sapienza', 00185 Roma, Italy. Fax: +39-06-490421; e-mail: carlo.galli@uniroma1.it
Giampaolo Giacomelli	Università degli Studi di Sassari, Dipartimento di Chimica, via Vienna 2, 07100-Sassari, Italy. Fax: +39-079-212069; e-mail: ggp@uniss.it

Stephen A. Glover	Division of Chemistry, School of Science and Technology, University of New England, Armidale, NSW 2351, Australia. Fax: +61-2-67733268; e-mail: stephen.glover@une.edu.au
Joel F. Liebman	Department of Chemistry and Biochemistry, University of Maryland, Baltimore County, 1000 Hilltop Circle, Baltimore, Maryland 21250, USA. Fax: +1-410-455-2608; e-mail: jliebman@umbc.edu
Edmunds Lukevics	Latvian Institute of Organic Synthesis, Riga, LV1006, Latvia. Fax: +371-7550338; e-mail: ign@osi.lv
Artem Melman	Department of Chemistry and Biomolecular Science, Clarkson University, Potsdam, NY 13699, USA. Fax: +1-315-268-6610; e-mail: amelman@clarkson.edu
Jane S. Murray	Department of Chemistry, University of New Orleans, New Orleans, LA 70148, USA *and* Department of Chemistry, Cleveland State University, Cleveland, OH 44115, USA. Fax: +1-440-331-1785; e-mail: jsmurray@uno.edu
Osamu Onomura	Department of Molecular Medicinal Sciences, Graduate School of Biomedical Sciences, Nagasaki University, 1–14, Bunkyo-machi, Nagasaki 852–8521, Japan. Fax: +81-95-819-2476; e-mail: onomura@nagasaki-u.ac.jp
M. Manuela A. Pereira	REQUIMTE/CQFB, Departamento de Química, Faculdade de Ciências e Tecnologia, Universidade Nova de Lisboa, Campus da Caparica, 2829-516 Caparica, Portugal. Fax: +351-212948550; e-mail: mmm@dq.fct.unl.pt
Peter Politzer	Department of Chemistry, University of New Orleans, New Orleans, LA 70148, USA *and* Department of Chemistry, Cleveland State University, Cleveland, OH 44115, USA. Fax: +1-440-331-1785; e-mail: ppolitze@uno.edu
Maja Ponikvar	Department of Inorganic Chemistry and Technology, Jožef Stefan Institute, Jamova 39, SI-1000 Ljubljana, Slovenia. Fax: +386-1-477-31-55; e-mail: maja.ponikvar@ijs.si
Andrea Porcheddu	Università degli Studi di Sassari, Dipartimento di Chimica, via Vienna 2, 07100-Sassari, Italy. Fax: +39-079-212069; e-mail: anpo@uniss.it
Pedro Paulo Santos	Centro de Química Estrutural, Instituto Superior Técnico, Universidade Técnica de Lisboa, Av. Rovisco Pais, 1049-001 Lisboa, Portugal. Fax: +351-218417122; e-mail: pepesantos@ist.utl.pt
Axel Schulz	Universität Rostock, Institut für Chemie, Abteilung Anorganische Chemie, Albert-Einstein-Straße 3a, 18059 Rostock, Germany *and* Leibniz-Institut für Katalyse e.V. an der Universität Rostock, Albert-Einstein-Str. 29a, 18059 Rostock, Germany. Fax: +49-381-498-6382; e-mail: axel.schulz@uni-rostock.de

Peter Rudolf Seidl	Departamento de Processos Orgânicos, Escola de Química, Universidade Federal do Rio de Janeiro, Centro de Tecnologia, Bloco E, Ilha do Fundão, Rio de Janeiro, RJ 21949-900, Brazil. Fax: +55-21-2562-7567; e-mail: pseidl@eq.ufrj.br
Abraham Shanzer	Department of Organic Chemistry, Weizmann Institute of Science, P.O. Box 26, Rehovot 76100, Israel. Fax: +972-8-9342917; e-mail: abraham.shanzer@weizmann.ac.il
Israel Silman	Department of Neurobiology, The Weizmann Institute of Science, Rehovot 76100, Israel. Fax: +972-8-9346017; email: israel.silman@weizmann.ac.il
Suzanne W. Slayden	Department of Chemistry, George Mason University, 4400 University Drive, Fairfax, Virginia 22030, USA. Fax: +1-703-993-1055; e-mail: sslayden@gmu.edu
François Terrier	Laboratoire SIRCOB, UMR 8086, Institut Lavoisier-Franklin, Université de Versailles, 45 Avenue des Etats-Unis 78035, Versailles Cedex, France. Fax: +33-01-3925-4452; e-mail: terrier@chimie.uvsq.fr
Ik Hwan Um	Division of Nano Sciences and Department of Chemistry, Ewha Womans University, Seoul 120–750, Korea. Fax: +82-2-3277-2844; e-mail: ihum@ewha.ac.kr
Alexander Villinger	Universität Rostock, Institut für Chemie, Abteilung Anorganische Chemie, Albert-Einstein-Straße 3a, 18059 Rostock, Germany. e-mail: alexander.villinger@uni-rostock.de

Foreword

The present book, *The Chemistry of Hydroxylamines, Oximes and Hydroxamic Acids*, deals with the chemistry of three related functional groups that were not hitherto treated in 'The Chemistry of Functional Groups' series. Professor Artem Melman, then at the Hebrew University, who felt that such a book would be valuable, suggested the title and we followed his advice; he also contributed a chapter. We will be grateful to other readers who suggest other topics which, in their opinion, deserve to be included in new volumes in the series.

The two parts of the present volume contain 18 chapters written by experts from 14 countries. They include theoretical aspects, structural analysis, thermochemistry and NMR spectra of the three groups, chapters on the synthesis of the groups and on synthetic aspects, such as their use for synthesis of a variety of heterocyclic systems, the use of hydroxylamines and oximes for electrophilic amination, their use as analytical reagents, their electrochemistry and rearrangements both in the laboratory and in large-scale industry. Biological properties and use as therapeutic agents as well as the iron transfer ability of natural hydroxamic acids are covered in several chapters. Mechanistic aspects of these systems, including their effect as substituents, with emphasis on their α-effects, which are important both theoretically and as anti-toxic agents, are covered in two chapters. One sub-group, the *N*-heteroatom-substituted hydroxamic acids, is covered extensively from the synthetic, theoretical and biological aspects. Special chapters are devoted to related topics such as nitroxyl radicals, nitrosomethanides and their acids.

A few of the originally planned topics not covered in the present book are organometallic derivatives, analysis of, mass spectrometry, photochemistry and acidities and basicities of the title groups. We hope that these topics will soon be covered in an additional volume.

The literature coverage is up to the end of 2007, and extends in several chapters into 2008.

One of the editors (J. F. L.) is especially pleased to participate in this volume because the classes of compounds encompassed in the volume figured prominently in his chemical upbringing.

We would be grateful to readers who draw our attention to mistakes in the present volume and to omissions of important chapters related to the three groups.

Jerusalem and Baltimore
October 2008

ZVI RAPPOPORT
JOEL F. LIEBMAN

The Chemistry of Functional Groups Preface to the series

The series 'The Chemistry of Functional Groups' was originally planned to cover in each volume all aspects of the chemistry of one of the important functional groups in organic chemistry. The emphasis is laid on the preparation, properties and reactions of the functional group treated and on the effects which it exerts both in the immediate vicinity of the group in question and in the whole molecule.

A voluntary restriction on the treatment of the various functional groups in these volumes is that material included in easily and generally available secondary or tertiary sources, such as Chemical Reviews, Quarterly Reviews, Organic Reactions, various 'Advances' and 'Progress' series and in textbooks (i.e. in books which are usually found in the chemical libraries of most universities and research institutes), should not, as a rule, be repeated in detail, unless it is necessary for the balanced treatment of the topic. Therefore each of the authors is asked not to give an encyclopaedic coverage of his subject, but to concentrate on the most important recent developments and mainly on material that has not been adequately covered by reviews or other secondary sources by the time of writing of the chapter, and to address himself to a reader who is assumed to be at a fairly advanced postgraduate level.

It is realized that no plan can be devised for a volume that would give a complete coverage of the field with no overlap between chapters, while at the same time preserving the readability of the text. The Editors set themselves the goal of attaining reasonable coverage with moderate overlap, with a minimum of cross-references between the chapters. In this manner, sufficient freedom is given to the authors to produce readable quasi-monographic chapters.

The general plan of each volume includes the following main sections:

(a) An introductory chapter deals with the general and theoretical aspects of the group.

(b) Chapters discuss the characterization and characteristics of the functional groups, i.e. qualitative and quantitative methods of determination including chemical and physical methods, MS, UV, IR, NMR, ESR and PES — as well as activating and directive effects exerted by the group, and its basicity, acidity and complex-forming ability.

(c) One or more chapters deal with the formation of the functional group in question, either from other groups already present in the molecule or by introducing the new group directly or indirectly. This is usually followed by a description of the synthetic uses of the group, including its reactions, transformations and rearrangements.

(d) Additional chapters deal with special topics such as electrochemistry, photochemistry, radiation chemistry, thermochemistry, syntheses and uses of isotopically labeled compounds, as well as with biochemistry, pharmacology and toxicology. Whenever applicable, unique chapters relevant only to single functional groups are also included (e.g. 'Polyethers', 'Tetraaminoethylenes' or 'Siloxanes').

This plan entails that the breadth, depth and thought-provoking nature of each chapter will differ with the views and inclinations of the authors and the presentation will necessarily be somewhat uneven. Moreover, a serious problem is caused by authors who deliver their manuscript late or not at all. In order to overcome this problem at least to some extent, some volumes may be published without giving consideration to the originally planned logical order of the chapters.

Since the beginning of the Series in 1964, two main developments have occurred. The first of these is the publication of supplementary volumes which contain material relating to several kindred functional groups (Supplements A, B, C, D, E, F and S). The second ramification is the publication of a series of 'Updates', which contain in each volume selected and related chapters, reprinted in the original form in which they were published, together with an extensive updating of the subjects, if possible, by the authors of the original chapters. Unfortunately, the publication of the 'Updates' has been discontinued for economic reasons.

Advice or criticism regarding the plan and execution of this series will be welcomed by the Editors.

The publication of this series would never have been started, let alone continued, without the support of many persons in Israel and overseas, including colleagues, friends and family. The efficient and patient co-operation of staff-members of the Publisher also rendered us invaluable aid. Our sincere thanks are due to all of them.

The Hebrew University
Jerusalem, Israel

SAUL PATAI
ZVI RAPPOPORT

Sadly, Saul Patai who founded 'The Chemistry of Functional Groups' series died in 1998, just after we started to work on the 100th volume of the series. As a long-term collaborator and co-editor of many volumes of the series, I undertook the editorship and I plan to continue editing the series along the same lines that served for the preceeding volumes. I hope that the continuing series will be a living memorial to its founder.

The Hebrew University
Jerusalem, Israel
May 2000

ZVI RAPPOPORT

Contents

List of abbreviations used

Ac	acetyl (MeCO)
acac	acetylacetone
Ad	adamantyl
AIBN	azoisobutyronitrile
Alk	alkyl
All	allyl
An	anisyl
Ar	aryl
Bn	benzyl
Bu	butyl (C_4H_9)
Bz	benzoyl (C_6H_5CO)
c-	cyclo
CD	circular dichroism
CI	chemical ionization
CIDNP	chemically induced dynamic nuclear polarization
CNDO	complete neglect of differential overlap
Cp	η^5-cyclopentadienyl
Cp*	η^5-pentamethylcyclopentadienyl
DABCO	1,4-diazabicyclo[2.2.2]octane
DBN	1,5-diazabicyclo[4.3.0]non-5-ene
DBU	1,8-diazabicyclo[5.4.0]undec-7-ene
DIBAH	diisobutylaluminium hydride
DME	1,2-dimethoxyethane
DMF	*N*,*N*-dimethylformamide
DMSO	dimethyl sulphoxide
E-	entgegen
ee	enantiomeric excess
EI	electron impact
ESCA	electron spectroscopy for chemical analysis
ESR	electron spin resonance
Et	ethyl
eV	electron volt

Fc	ferrocenyl
FD	field desorption
FI	field ionization
FT	Fourier transform
Fu	furyl(OC_4H_3)
GLC	gas liquid chromatography
Hex	hexyl(C_6H_{13})
c-Hex	cyclohexyl(*c*-C_6H_{11})
HMPA	hexamethylphosphortriamide
HOMO	highest occupied molecular orbital
HPLC	high performance liquid chromatography
i-	iso
ICR	ion cyclotron resonance
Ip	ionization potential
IR	infrared
LAH	lithium aluminium hydride
LCAO	linear combination of atomic orbitals
LDA	lithium diisopropylamide
LUMO	lowest unoccupied molecular orbital
M	metal
M	parent molecule
MCPBA	*m*-chloroperbenzoic acid
Me	methyl
MNDO	modified neglect of diatomic overlap
MS	mass spectrum
n-	normal
Naph	naphthyl
NBS	*N*-bromosuccinimide
NCS	*N*-chlorosuccinimide
NMR	nuclear magnetic resonance
Pen	pentyl(C_5H_{11})
Ph	phenyl
Pip	piperidyl($C_5H_{10}N$)
ppm	parts per million
Pr	propyl (C_3H_7)
PTC	phase transfer catalysis or phase transfer conditions
Py	pyridine (C_5H_5N)
Pyr	pyridyl (C_5H_4N)
R	any radical
RT	room temperature

s-	secondary
SET	single electron transfer
SOMO	singly occupied molecular orbital
t-	tertiary
TCNE	tetracyanoethylene
TFA	trifluoroacetic acid
TFE	2,2,2-trifluoroethanol
THF	tetrahydrofuran
Thi	thienyl(SC_4H_3)
TLC	thin layer chromatography
TMEDA	tetramethylethylene diamine
TMS	trimethylsilyl or tetramethylsilane
Tol	tolyl(MeC_6H_4)
Tos or Ts	tosyl(*p*-toluenesulphonyl)
Trityl	triphenylmethyl(Ph_3C)
Vi	vinyl
XRD	X-ray diffraction
Xyl	xylyl($Me_2C_6H_3$)
Z-	zusammen

In addition, entries in the 'List of Radical Names' in *IUPAC Nomenclature of Organic Chemistry*, 1979 Edition, Pergamon Press, Oxford, 1979, p. 305–322, will also be used in their unabbreviated forms, both in the text and in formulae instead of explicitly drawn structures.

CHAPTER 1

Some intrinsic features of hydroxylamines, oximes and hydroxamic acids: Integration of theory and experiment

PETER POLITZER and JANE S. MURRAY

Department of Chemistry, University of New Orleans, New Orleans, LA 70148, USA and Department of Chemistry, Cleveland State University, Cleveland, OH 44115, USA
Fax: +440-331-1785; e-mail: ppolitze@uno.edu, jsmurray@uno.edu

The chemistry of hydroxylamines, oximes and hydroxamic acids
Edited by Z. Rappoport and J. F. Liebman

I. INTRODUCTION

A. The Compounds

The structural link between hydroxylamines (**1**), oximes (**2**) and hydroxamic acids (**3**) is the N−OH group:

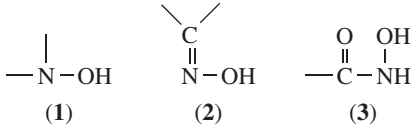

(**1**) (**2**) (**3**)

Formally, they can all be viewed as derivatives of hydroxylamine, H_2N-OH; indeed, oximes can be prepared by the addition of hydroxylamine to aldehydes and ketones (equations 1 and 2), and hydroxamic acids by its reactions with acetyl halides and esters (equations 3 and 4)[1].

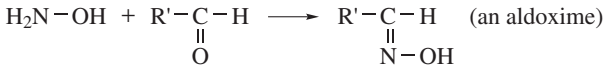

(1)

(2)

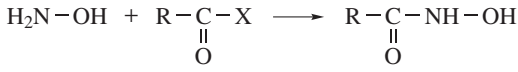

(3)

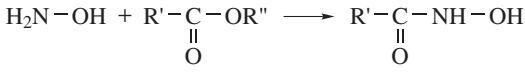

(4)

However, there are also important features that very significantly differentiate between hydroxylamines, oximes and hydroxamic acids: the C=N double bond in **2** and the acetyl group in **3**.

In this chapter, our objective will be to integrate theory and experiment in relating chemical and physical properties of these three classes of compounds to electronic and structural factors. We will begin with an overview and comparison of some computational approaches.

B. Survey of Computational Procedures

The purpose of this section is to present a short overview, with relevant examples, of some aspects of molecular computations. In-depth treatments can be found in textbooks such as that by Levine[2], and in the overview by Irikura and Frurip[3].

Tables 1 and 2 compare the experimental values of several properties of hydroxylamine and acetaldoxime, $H_3C-C(H)=NOH$, with the results obtained by nine different computational procedures. These are of three general types:

(a) Hartree–Fock (HF): Until a few years ago, this was the most widely used *ab initio* method. It does not account for electronic correlation (i.e. the repulsions between electrons are treated in an average rather than instantaneous manner) and therefore is not reliable for predicting interaction energies. However, properties that depend upon the average electronic density distribution $\rho(\mathbf{r})$, such as the dipole moment and the electrostatic potential, are generally reasonably satisfactory. We have used the Hartree–Fock approach in analyzing the electrostatic potentials of carbon and boron/nitrogen model nanotubes with as many as 120 atoms[4].

(b) MP2-FC: Moeller–Plesset second-order perturbation theory is an extension of Hartree–Fock that takes some account of electronic correlation, although not for inner-shell electrons (FC = frozen core). MP2-FC requires more computer time and space, and thus is limited to smaller molecules (25–50 first-row atoms[4]).

(c) B3LYP: This is one of the Kohn–Sham density functional theory (DFT) procedures that have had such a dramatic impact upon computational chemistry since about 1990. Kohn–Sham DFT methods have evolved from the local density approximation, based upon the concept of a uniform electron gas, to gradient-corrected DFT, which recognizes that $\rho(\mathbf{r})$ is not constant, to hybrid gradient-corrected DFT, such as B3LYP, which introduces the Hartree–Fock exchange term into the density functional[2]. Density functional theory does include electronic correlation, to varying degrees, and in the Kohn–Sham formalism it is only somewhat more demanding of computer resources than is Hartree–Fock and therefore can treat equally large systems. Hybrid density functional techniques (e.g. B3LYP, B3PW91) are now very extensively used for molecular calculations.

After choosing a computational procedure, the next decision generally concerns the basis set, by which is meant the mathematical functions (usually corresponding to atomic orbitals) in terms of which the system is to be described. The computed results in Tables 1 and 2 are for three different basis sets; in order of increasing size, they are 6-31G* < 6-311G^{**} $\ll$ cc-pVTZ. While a bigger basis set should permit a better description of the system, the processor time and space requirements increase very rapidly with size; furthermore, as will be seen, the variations in the values of computed properties, other than the energy, do not necessarily improve as the basis set becomes larger. For a given *ab initio* or DFT method, the molecular energy can be expected to decrease monotonically as the basis set increases in size (see Tables 1 and 2).

It seems fair to say that one of the consequences of the evolution and success of Kohn–Sham density functional methodology has been a diminished role for semi-empirical procedures (AM1, PM3, INDO etc.). While these can still be very useful, the capability of DFT to treat relatively large systems, and at an overall higher level of accuracy, has led to its being the method of choice in cases that earlier would have been treated semi-empirically.

Proceeding now to Tables 1 and 2, it is seen that bond lengths and bond angles are predicted well by both B3LYP and MP2-FC, Hartree–Fock being less effective. These results depend relatively little upon the basis set for the three that were used, which can be viewed as medium to large in size.

The atomization enthalpies show sharper distinctions between the nine approaches. The Hartree–Fock are very poor, as expected given the non-inclusion of electronic correlation. The MP2-FC are much better, but do not match the B3LYP, which actually achieve essentially 0% error in the two best cases. (Such perfection should not be expected regularly!) The atomization enthalpies do show a steady improvement as the basis set is increased.

TABLE 1. Comparison of experimental properties of hydroxylamine, H_2NOH, with results of various computational procedures [a]

Property	Experimental	Hartree–Fock			MP2-FC			B3LYP		
		6-31G*	6-311G**	cc-pVTZ	6-31G*	6-311G**	cc-pVTZ	6-31G*	6-311G**	cc-pVTZ
Energy (hartrees) [b]	—	−130.979	−131.028	−131.044	−131.325	−131.418	−131.508	−131.705	−131.757	−131.773
N–O distance (Å)	1.453 [c]	1.404	1.397	1.398	1.452	1.436	1.441	1.447	—	1.447
H–N–O angle (deg)	103.2 [c]	104.7	105.4	105.5	102.9	103.9	103.4	103.2	—	103.7
Atomization enthalpy (kcal mol^{-1}) [d]	340.8 [a]	177	184	188	290	310	330	331	336	340
Dipole moment (D)	0.59 [e]	0.68	0.70	0.64	0.63	—	0.60	0.58	0.64	0.59
Atomic charges: Mulliken										
N	—	−0.525	—	−0.193	−0.528	—	—	−0.496	—	−0.203
O	—	−0.632	—	−0.366	−0.634	—	—	−0.547	—	−0.337
ESP										
N	—	−0.789	—	−0.755	−0.770	—	—	−0.737	—	−0.706
O	—	−0.486	—	−0.461	−0.464	—	—	−0.439	—	−0.434

[a] All computed and some experimental values are from NIST Computational Chemistry Comparison and Benchmark Database, NIST Standard Reference Database No. 101, Release 12 (Ed. R. D. Johnson III), 2005. http://srdata.nist.gov/cccbdb

[b] Energy minimum at 0 K; 1 hartree = 627.5 kcal mol^{-1}.

[c] M. D. Harmony, V. W. Laurie, R. L. Kuczkowski, R. H. Schwendeman, D. A. Ramsey, F. J. Lovas, W. J. Lafferty and A. G. Maki, *J. Phys. Chem. Ref. Data*, **8**, 619 (1979).

[d] Enthalpy required to separate molecule into atoms at 298 K.

[e] D. R. Lide (Ed.), *Handbook of Chemistry & Physics*, 87th edn., CRC Press, Boca Raton, 2006.

TABLE 2. Comparison of experimental properties of acetaldoxime, $CH_3C(H)=NOH$, with results of various computational procedures [a]

Property	Experimental [a]	Hartree–Fock			MP2-FC			B3LYP		
		6-31G*	6-311G**	cc-pVTZ	6-31G*	6-311G**	cc-pVTZ	6-31G*	6-311G**	cc-pVTZ
Energy (hartrees) [b]	—	−207.884	−207.945	−207.970	−208.484	−208.612	−208.750	−209.131	−209.198	−209.221
N−O distance (Å)	1.408	1.375	1.369	1.370	1.417	1.400	1.406	1.409	—	1.407
C−N distance (Å)	1.276	1.251	1.248	1.246	1.286	1.282	1.278	1.276	—	1.268
C−N−O angle (deg)	110	111.8	112.1	112.4	110.0	110.7	110.4	110.9	—	111.5
N−O−H angle (deg)	103	104.3	104.5	104.6	101.7	101.5	101.6	102.2	—	102.6
Atomization enthalpy (kcal mol^{-1}) [c]	781.0	506	508	514	712	738	771	777	776	781
Dipole moment (D)	0.938	0.825	0.857	—	0.629	—	0.683	0.612	0.651	0.722
Atomic charges: Mulliken										
C [d]	—	0.090	0.073	−0.045	0.103	—	—	0.108	0.026	−0.028
N	—	−0.160	−0.149	−0.046	−0.176	—	—	−0.166	−0.132	−0.052
O	—	−0.609	−0.376	−0.310	−0.618	—	—	−0.510	−0.316	−0.254
ESP										
C [d]	—	0.436	—	0.445	−0.462	—	—	0.381	—	0.405
N	—	−0.374	—	−0.388	−0.351	—	—	−0.357	—	−0.375
O	—	−0.508	—	−0.485	−0.454	—	—	−0.430	—	−0.424

[a] All computed and experimental values are from NIST Computational Chemistry Comparison and Benchmark Database, NIST Standard Reference Database No. 101, Release 12 (Ed. R. D. Johnson III), 2005. http://srdata.nist.gov/cccbdb

[b] Energy minimum at 0 K; 1 hartree = 627.5 kcal mol^{-1}.

[c] Enthalpy required to separate molecule into atoms at 298 K.

[d] Carbon bonded to nitrogen.

The situation is quite different for the dipole moment. The Hartree–Fock values are comparable to the MP2-FC and B3LYP for hydroxylamine, and significantly better than the others for acetaldoxime. This reflects the fact that Hartree–Fock electronic density distributions $\rho(\mathbf{r})$ are, overall, reasonably good[5]. The errors in the MP2-FC and B3LYP results may seem rather large, especially on a percentage basis, but it should be noted that dipole moments are obtained as a small difference between two much larger numbers (the electronic and nuclear moments), so that any errors in these are greatly magnified in the former. (The same problem is encountered in computing ΔE or ΔH for chemical reactions. One way of addressing it in this context is by means of isodesmic and related types of equations[2].)

Calculated atomic charges are included in Tables 1 and 2, even though these are not physical observables and cannot be determined experimentally, because they are conceptually convenient and are widely used in analyzing molecular electronic structures and reactive properties. Numerous definitions of atomic charge have been proposed over the years, but all of them are arbitrary and purport to quantify something that has no experimental basis. In Tables 1 and 2 are listed two sets of atomic charges. The Mulliken, which are very popular due to ease of computation, result from partitioning the molecular orbital expression for the electronic density[6]; the ESP are designed to reproduce the electrostatic potential produced by the molecule's electrons and nuclei[7]. Mulliken charges can vary considerably with the basis set[2,8], as is seen in Tables 1 and 2; note, for example, the B3LYP values. This is less of a problem for the ESP since they come from $\rho(\mathbf{r})$, which is much less dependent upon the basis set. What is particularly serious, however, is that the Mulliken and the ESP results actually differ even *qualitatively* in predicting whether the nitrogen or the oxygen in hydroxylamine is the more negative. This example illustrates the inherent uncertainty associated with trying to assign a charge to an atom in a molecule.

We conclude this section with a comment concerning notation. To identify a computational approach, it is customary to write 'procedure/basis set', e.g. MP2-FC/6-311G**. If the geometry is obtained by procedure 1 and basis set 1, and that geometry is then used in calculating a particular property with procedure 2 and basis set 2, this is designated by 'procedure 2/basis set 2//procedure 1/basis set 1'.

II. ANALYSIS OF COVALENT AND NONCOVALENT INTERACTIONS

Three fundamental properties that play key roles in determining covalent and/or noncovalent interactions are the electrostatic potential $V(\mathbf{r})$, the ionization energy I (sometimes written IE) and the polarizability α. All three can be obtained experimentally. It is primarily in terms of these properties that we will examine the inter- and intramolecular interactions of hydroxylamines, oximes and hydroxamic acids. Accordingly we shall first briefly discuss $V(\mathbf{r})$, I and α.

A. Electrostatic Potential

$V(\mathbf{r})$ is the electrostatic potential that is created throughout the space of a system by its nuclei and electrons. It is given by equation 5, which is simply a form of Coulomb's Law:

$$V(\mathbf{r}) = \sum_{\mathrm{A}} \frac{Z_{\mathrm{A}}}{|\mathbf{R}_{\mathrm{A}} - \mathbf{r}|} - \int \frac{\rho(\mathbf{r}')\mathrm{d}\mathbf{r}'}{|\mathbf{r}' - \mathbf{r}|} \tag{5}$$

Z_{A} is the charge on nucleus A, located at $\mathbf{R}_{\mathrm{A}}$, and $\rho(\mathbf{r})$ is the electronic density of the system. Thus $V(\mathbf{r})$ is the net result at any point $\mathbf{r}$ of the positive contributions of the

nuclei and the negative ones of the electrons. Although $V(\mathbf{r})$ is a potential, it is usually given in energy units, e.g. kcal mol^{-1}, which means that the value quoted is actually the interaction energy of the system with a $+1$ point charge placed at $\mathbf{r}$. The general interpretation of $V(\mathbf{r})$ is that regions in which it is positive will interact favorably with negative portions of the surroundings, such as lone pairs, π electrons, anions etc., and unfavorably with positive portions, e.g. hydrogens, cations etc.; negative regions of $V(\mathbf{r})$ will do the reverse.

The electrostatic potential $V(\mathbf{r})$ is a physical observable, which can be determined experimentally by diffraction methods[9,10] as well as computationally. It directly reflects the distribution in space of the positive (nuclear) and the negative (electronic) charge in a system. $V(\mathbf{r})$ can also be related rigorously to its energy and its chemical potential, and further provides a means for defining covalent and ionic radii[11,12].

Noncovalent interactions are primarily electrostatic in nature[13,14], and thus can be interpreted and predicted via $V(\mathbf{r})$. For this purpose, it is commonly evaluated on the surfaces of the molecules, since it is through these surface potentials, labeled $V_S(\mathbf{r})$, that the molecules 'see' and 'feel' each other. We have shown that a number of condensed-phase physical properties that are governed by noncovalent interactions—heats of phase transitions, solubilities, boiling points and critical constants, viscosities, surface tensions, diffusion constants etc.—can be expressed analytically in terms of certain statistical quantities that characterize the patterns of positive and negative regions of $V_S(\mathbf{r})$[15,16].

All of this is of course predicated upon finding some reasonable way to define the surface of a molecule, for which there is no rigorous physical basis. We follow the suggestion of Bader and coworkers[17] in taking this to be the 0.001 au (electrons bohr^{-3}) contour of the molecule's electronic density $\rho(\mathbf{r})$; this contour encompasses about 96% of the electronic charge. (1 bohr $= 0.5292$ Å.) In contrast to another approach to defining a molecular surface, involving fused 'atomic' spheres, the method of Bader and coworkers has the advantage of reflecting features specific to that molecule, such as lone pairs, π electrons and strained bonds. We have confirmed that other outer contours of $\rho(\mathbf{r})$, e.g. the 0.002 au, would be equally effective[18].

Our focus in this chapter shall be primarily upon the surface electrostatic potential, specifically its most positive and most negative values, denoted by $V_{S,max}$ and $V_{S,min}$, respectively. There may be several local and absolute maxima and minima on a given surface. They indicate the most positive and negative sites. The former are often associated with hydrogens, especially acidic ones, and the latter with lone pairs, π electrons of unsaturated molecules and strained bonds[5]. We have demonstrated that $V_{S,max}$ and $V_{S,min}$ correlate well with measures of hydrogen bond donating and accepting tendencies[19].

We will also refer in some instances to the overall most negative potentials, V_{min}, associated with nitrogen and oxygen lone pairs. These can be viewed as indicating the effective 'center' of the lone pair. Such V_{min} are always more negative than the corresponding $V_{S,min}$, and are located within the molecular surface.

B. Ionization Energy

The ionization energy I is the amount of energy required to remove an electron from an atom or molecule. This normally involves the least tightly held electron, which is in the highest occupied orbital. I is clearly a governing factor in any process involving charge transfer from the system.

Whereas $V(\mathbf{r})$ and $V_S(\mathbf{r})$ are local properties, i.e. have a different value at each point $\mathbf{r}$, I is global, in the sense that there is just a single value for the whole system (assuming that only the highest-energy electron is considered). Chemical reactions, however, are site-specific, and so there is a need for a *local* ionization energy, that gives the energy needed to remove an electron at each point $\mathbf{r}$ in the space of a system.

We introduced such a quantity, the average local ionization energy $\overline{I}(\mathbf{r})$[20], in equation 6:

$$\overline{I}(\mathbf{r}) = \sum_i \frac{\rho_i(\mathbf{r})|\varepsilon_i|}{\rho(\mathbf{r})} \tag{6}$$

In equation 6, $\rho_i(\mathbf{r})$ is the electronic density of orbital i, having energy ε_i. The formalism of Hartree–Fock theory (within the framework of which equation 6 was proposed) and Koopmans' theorem[21,22] provide support for interpreting $\overline{I}(\mathbf{r})$ as the local ionization energy, which focuses upon the point in space rather than an orbital.

In analyzing chemical reactivity, we compute $\overline{I}(\mathbf{r})$ on the 0.001 au surface of the molecule, just as we do $V(\mathbf{r})$. The lowest values of the resulting $\overline{I}_S(\mathbf{r})$, its local minima $\overline{I}_{S,min}$, indicate the locations of the least tightly held, most reactive electrons, and are an effective means for identifying and ranking sites favorable for electrophilic attack. $\overline{I}_S(\mathbf{r})$ computed via Kohn–Sham density functional procedures are equally successful for this purpose[23]. It should be pointed out that the $\overline{I}_{S,min}$ are invariably somewhat larger than the magnitude of the highest occupied orbital energy, because $\overline{I}(\mathbf{r})$ averages over *all* of the system's electrons, and there is always some probability of inner, more tightly held ones being at the point in question, even on an outer contour of $\rho(\mathbf{r})$.

The local maxima of $\overline{I}_S(\mathbf{r})$, the $\overline{I}_{S,max}$, reveal the locations of the most strongly bound electrons. While we have found some evidence that these may be sites reactive toward nucleophiles, this is not well-established. Since $\overline{I}_{S,min}$ and $\overline{I}_{S,max}$ are local features, referring to specific points in space, it is quite possible to have one or more of each in the neighborhood of a given atom in a molecule; this simply means that there are both tightly and loosely held electrons in different regions around the atom. Some examples will be seen later in this chapter.

In addition to its role with regard to chemical reactivity, $\overline{I}(\mathbf{r})$ is also linked to atomic shell structure and electronegativity, local temperature (or kinetic energy), radical characterization, bond strain and local polarizability. For a recent overall review, see Politzer and Murray[24].

C. Polarizability

The extent to which an atom or molecule's charge distribution is affected by an external electric field $\mathbf{E}$ (which could be due to an approaching reactant) is governed, to first order, by its polarizability $\boldsymbol{\alpha}$. It was really $\boldsymbol{\alpha}$ to which Pearson was referring in his hard and soft acid–base theory[25], which rationalizes a large number of chemical reactions. The terms 'hard' and 'soft' refer, respectively, to low and high polarizability.

Specifically, the change in the system's dipole moment $\boldsymbol{\mu}$ is given by equation 7:

$$\boldsymbol{\mu}(\boldsymbol{\varepsilon}) - \boldsymbol{\mu}(0) = \boldsymbol{\alpha} \cdot \mathbf{E} \tag{7}$$

Whereas $\boldsymbol{\mu}$ is a vector, with three components, $\boldsymbol{\alpha}$ is a nine-component tensor, which can be represented by a symmetric 3×3 matrix[26] (equation 8):

$$\boldsymbol{\alpha} = \begin{pmatrix} \alpha_{xx} & \alpha_{xy} & \alpha_{xz} \\ \alpha_{xy} & \alpha_{yy} & \alpha_{yz} \\ \alpha_{xz} & \alpha_{yz} & \alpha_{zz} \end{pmatrix} \tag{8}$$

What this means is that a field along one axis, e.g. the x, can influence not only that component of $\boldsymbol{\mu}$, i.e. μ_x, but also the other two, μ_y and μ_z. This is done through α_{xy}

and α_{xz}. Quite often, however, matters are simplified by dealing only with the average, or scalar, polarizability α (equation 9):

$$\alpha = \frac{1}{3}(\alpha_{xx} + \alpha_{yy} + \alpha_{zz}) \tag{9}$$

It has long been recognized that α correlates well with volume[13, 27, 28] (equation 10):

$$\alpha \sim V \tag{10}$$

In fact, α is customarily given in volume units, e.g. Å^3. It seems reasonable, however, that polarizability should also depend inversely upon ionization enery, since I is a measure of how strongly an outer electron is held. It has indeed been confirmed that equation 10 is improved by including an inverse dependence upon I, but even more so by using the average of the local ionization energy $\overline{I}_S(\mathbf{r})$ over the atomic or molecular surface[29]. Thus, for a group of 29 molecules, the relationship (equation 11)

$$\alpha \sim V/\overline{I}_{S,ave} \tag{11}$$

has $R^2 = 0.984$ and root-mean-square error $= 0.48$ Å^3 compared to $R^2 = 0.960$ and root-mean-square error $= 0.76$ Å^3 for equation 10.

Since α does correlate with V (equation 10) and molecular volumes can be treated as summations over atomic and/or group contributions[30, 31], it might be inferred that an analogous approximation (equation 12) could be applied for α:

$$\alpha \approx \sum_i \alpha_i \tag{12}$$

In equation 12, the α_i are the average polarizabilities of the molecule's components. The use of equation 12 for estimating molecular polarizabilities has been quite successful, utilizing atomic, group and/or bond α_i developed by various means[30, 32–35]. The key requirement is of course that the α_i be sufficiently transferable from one molecule to another. We have demonstrated that equation 11 also provides an effective basis for obtaining component polarizabilities, purely computationally[36] (equation 13):

$$\alpha_i = V_i/\overline{I}_{S,ave,i} \tag{13}$$

Thus, with α_i for NH_2 and OH from equation 13, we have predicted[36] that the polarizability of hydroxylamine is 2.55 Å^3; while we are not aware of an experimental value, ours is in good agreement with the 2.76 Å^3 resulting from α_i produced by Miller[35] by a completely different procedure.

Just as it is useful to have a *local* ionization energy, so would it be desirable, in the context of reactive behavior, to have a *local* polarizability, $\alpha(\mathbf{r})$. Reflecting the discussion earlier in this section, we have suggested that $\overline{I}_S(\mathbf{r})$ be viewed as an inverse measure of $\alpha_S(\mathbf{r})$[24, 29, 37, 38]; we focus upon the *surface* local ionization energy and *surface* local polarizability because the outermost electrons are expected to make the greatest contributions to α. The volume dependence that is so important on a macroscopic scale should not be a factor on the local level, which considers only infinitesimal volume elements d$\mathbf{r}$. We have presented evidence[29, 37, 38] in support of the concept expressed by equation 14:

$$\alpha_S(\mathbf{r}) \sim 1/\overline{I}_S(\mathbf{r}) \tag{14}$$

III. COMPUTATIONAL APPROACH

In this chapter, energy minima have been located and geometries obtained with the B3LYP/6-31G** method, since taking account of electronic correlation can be important, especially for bond lengths. (Note the improvement in going from Hartree–Fock to MP2-FC and B3LYP in Tables 1 and 2.) Energy differences ΔE between conformers and between isomers were calculated with these geometries but utilizing a larger basis set, B3LYP/6-311G(3df,2p), for greater accuracy. Zero-point and thermal corrections have been added so that all ΔE will correspond to 298 K.

The same geometries were also used to compute electrostatic potentials and local ionization energies, at the HF/6-31G* level. Hartree–Fock $V(\mathbf{r})$ and $\overline{I}(\mathbf{r})$ are known to be quite satisfactory[5, 21, 22].

Formally, divalent oxygen has two lone pairs, both of which will normally produce regions of negative electrostatic potential, overlapping to some extent. In many instances, each of these regions will have a most negative point, a $V_{S,min}$. On occasion, however, due to extensive overlapping or some other factor, only one $V_{S,min}$ can be identified. This will be seen in the next section, for hydroxylamine.

IV. LONE PAIR–LONE PAIR REPULSION

Hydroxylamines, oximes and hydroxamic acids all have adjacent nitrogen and oxygen atoms, as part of their characteristic N–OH group. Since both of these atoms commonly have significant lone pairs, a major determinant of these molecules' conformations is the need to minimize the repulsion between these lone pairs. This will be illustrated by the example of hydroxylamine, $H_2N–OH$.

We have found two energy minima for $H_2N–OH$, corresponding to two stable conformers **4** and **5**[39]. In the less stable **4**, the nitrogen and oxygen lone pairs are in close proximity; the distance between their effective centers, the respective V_{min}, is only 2.40 Å. (The two oxygen lone pairs give rise to only one V_{min} and one $V_{S,min}$.) When the hydroxyl group is rotated to give **5**, this distance increases to 3.21 Å. The energy simultaneously decreases by 3.9 kcal mol^{-1} [B3LYP/6-311G(3df,2p)].

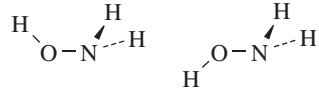

(**4**) (**5**)

It might be thought that **5** may also be stabilized by attractive interactions between the hydroxyl hydrogen and the nitrogen lone pair and/or between the amine hydrogens and the oxygen lone pair(s). To investigate these possibilities, we look at the distances between these hydrogens and the $V_{S,min}$ of the lone pairs. Here it is appropriate to use $V_{S,min}$, because the hydrogens are external to the nitrogen and oxygen surfaces. The respective H---$V_{S,min}$ separations are rather large: H(hydroxyl)---$V_{S,min}$(N) = 2.75 Å, H(amine)---$V_{S,min}$(O) = 3.05 Å. They are indeed greater than the sums of the H---N and H---O van der Waals radii[40], 2.72 Å and 2.69 Å. (The sum of the N---O van der Waals radii is 3.07 Å.) Thus the effect of any such hydrogen bonding interactions in stabilizing **5** should be quite minor (or none) compared to that of separating the lone pairs. In all of the hydroxylamines, oximes and hydroxamic acids treated in this chapter, we have found the hydroxyl group to be rotated so as to achieve this separation.

This section was intended only to demonstrate the importance of minimizing lone pair repulsions. A more representative hydroxylamine will now be discussed in greater detail.

V. COMPARISON OF PROTOTYPICAL EXAMPLES

We shall now compare some properties of prototypical examples of hydroxylamines, oximes and hydroxamic acids. These will be structures **1**, **2** and **3** with methyl groups at the remaining positions, i.e. dimethylhydroxylamine (**6**), acetoxime (**7**) and acetohydroxamic acid (**8**).

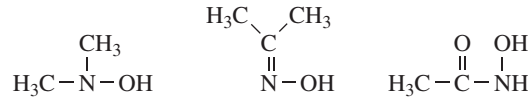

(**6**) (**7**) (**8**)

In Table 3 are reported (a) bond lengths and bond angles, (b) most positive and most negative values of the surface electrostatic potentials, $V_{S,max}$ and $V_{S,min}$, and (c) the highest and lowest local ionization energies, $\overline{I}_{S,min}$ and $\overline{I}_{S,max}$, for **6**, **7** and **8**. (Some of the data in Table 3 are taken from Politzer and coworkers[39].) The electrostatic potentials and local ionization energies on the molecular surfaces are shown graphically in Figures 1–6.

A. Dimethylhydroxylamine (6)

The nitrogen in **6** is pyramidal, with bond angles similar to those in dimethylamine (107, 107, 111.8 deg[41]). Accordingly it has a significant lone pair, as shown in Figure 1(a), which is manifested in a $V_{S,min}$ of -28.1 kcal mol^{-1} (Table 3). The oxygen's lone pairs, Figure 1(b), give it a single but even more negative $V_{S,min}$, -35.0 kcal mol^{-1}. In order that these negative regions associated with the nitrogen and oxygen avoid each other, the hydroxyl group rotates to give the structure shown below, in which the hydrogen is in the plane bisecting the C−N−C angle. The two C−N−O−H dihedral angles were found to be -120.7 and 120.8 deg.

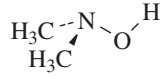

The positive nature of the hydroxyl hydrogen is clearly evident in Figure 1; its $V_{S,max}$ is 44.1 kcal mol^{-1}. To put this into perspective, the methyl hydrogens have $V_{S,max}$ between 7 and 13 kcal mol^{-1}. The bond lengths in **6** are as would be expected. For example, representative C=N and N=O distances in such configurations (in crystals) are 1.469 Å and 1.463 Å, respectively[42].

The dominant feature of the local ionization energy on the surface of **6** is the low $\overline{I}_S(\mathbf{r})$ of the nitrogen lone pair, Figure 2(a). The oxygen lone pairs, so much in evidence in terms of $V_S(\mathbf{r})$, do not stand out at all now, Figure 2(b).

The $V_{S,min}$ and $\overline{I}_{S,min}$ of **6** (Table 3, Figures 1 and 2) illustrate an important point. The more negative $V_{S,min}$ of the oxygen means that (a) it could be the site for a noncovalent electrostatic interaction with a positive portion of another molecule, and (b) an electrophile might initially be attracted to the neighborhood of this oxygen. However, any significant charge transfer and covalent bond formation with an electrophile should occur preferentially at the nitrogen, which has the lower $\overline{I}_{S,min}$ and hence the more reactive, less tightly held electronic charge. Thus $V_S(\mathbf{r})$ is more relevant for noncovalent interactions,

TABLE 3. Some computed properties of dimethylhydroxylamine (**6**), acetoxime (**7**) and acetohydroxamic acid (**8**)[a,b]

Property	$(H_3C)_2N-OH$ (**6**)	$(H_3C)_2C=N-OH$ (**7**)	$H_3C-C(O)-N(H)-OH$ (**8**)
Bond lengths (Å)			
C−N	1.460	1.283	1.368
N−O	1.453	1.414	1.403
O−H	0.967	0.966	0.984
C−C	—	1.505	1.510
C−O	—	—	1.231
N−H	—	—	1.012
Bond angles (deg)			
C−N−O	105.6, 105.7	112.6	115.3
C−N−C	111.7	—	—
N−O−H	102.1	101.5	100.2
C−C−N	—	115.8, 125.9[c]	116.0
C−C−C	—	118.3	—
C−C−O	—	—	124.3
O−C−N	—	—	119.6
C−N−H	—	—	121.0
O−N−H	—	—	110.6
Electrostatic potentials (kcal mol^{-1})			
$V_{S,min}$ (N)	−28.1	−31.5	—
$V_{S,min}$ (hydroxyl O)	−35.0	−28.8, −28.9	−33.0
$V_{S,min}$ (acetyl O)	—	—	−39.7
$V_{S,max}$ (hydroxyl H)	44.1	45.9	30.7
$V_{S,max}$ (amine H)	—	—	54.9
Local ionization energies (eV)			
$\overline{I}_{S,min}$ (N)	12.3	—	13.5
$\overline{I}_{S,min}$ (C=N)	—	12.9, 12.9[d]	—
$\overline{I}_{S,min}$ (hydroxyl O)	15.1, 15.1	15.2, 15.2	15.4, 15.5
$\overline{I}_{S,min}$ (acetyl O)	—	—	14.9, 15.0
$\overline{I}_{S,max}$ (hydroxyl H)	19.1	19.4	20.8
$\overline{I}_{S,max}$ (amine H)	—	—	19.9

[a] Computational levels: bond lengths and bond angles, B3LYP/6-31G**; electrostatic potentials and local ionization energies, HF/6-31G*//B3LYP/6-31G**.
[b] Some of the data for **8** are taken from Reference 39.
[c] The larger C−C−N angle is the one on the same side of the double bond as the hydroxyl group.
[d] These $\overline{I}_{S,min}$ are above and below the central portion of the C=N double bond.

$\overline{I}_S$ (**r**) for covalent ones, although V_S(**r**) may play an important role in guiding an electrophile to the $\overline{I}_{S,min}$. For a more extensive discussion of this distinction between V_S(**r**) and $\overline{I}_S$(**r**), see work by Politzer and coworkers[24,43].

B. Acetoxime (7)

In **7**, the hydroxyl group, the nitrogen and all three carbons are coplanar. The nitrogen can now be viewed as having sp^2 hybridization, but it still has a lone pair, in the nonbonded sp^2 orbital. This produces a $V_{S,min}$ of −31.5 kcal mol^{-1} (Table 3 and Figure 3) and a V_{min} of −57.7 kcal mol^{-1}, both located in the plane of the molecular framework. The angles that these $V_{S,min}$ and V_{min} make with the nitrogen and the oxime carbon are

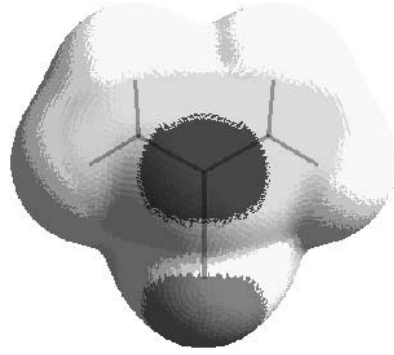

(a)

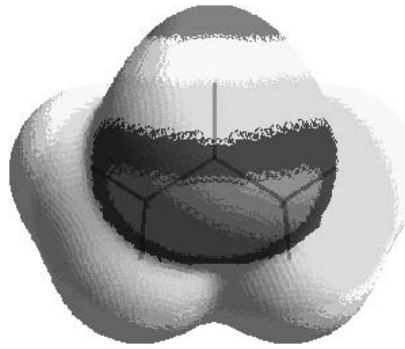

(b)

FIGURE 1. Computed electrostatic potential $V_S(\mathbf{r})$ on the molecular surface of dimethylhydroxylamine, (**6**), $(H_3C)_2N{-}OH$. Color scale, in kcal mol^{-1}: Purple, more negative than −30; blue, between −30 and −20; green, between −20 and 0; yellow, between 0 and 25; red, more positive than 25. Part (a) shows the nitrogen lone pair (blue) and the hydroxyl hydrogen (red). The methyl groups are at the top. Part (b) is the other side of the molecule, with the oxygen lone pairs (purple). The methyls are now at the bottom, the hydroxyl hydrogen at the top (See color plate 1)

126.5 and 128.7 deg, respectively; these are larger than expected for sp^2 hybridization. This may help to account for the deviation of the C−N−O angle from the standard 120 deg (Table 3). The two C−C−N angles differ considerably, the larger being on the same side of the double bond as the hydroxyl group. This may reflect steric features (see Chapter 2). We have found an analogous situation in dimethylimine, $(H_3C)_2C{=}NH$.

In each of the hydroxylamines that have been discussed (**4**, **5** and **6**), the two oxygen lone pairs together have just a single $V_{S,min}$. In the oxime **7**, however, each of the oxygen lone pairs is represented by a $V_{S,min}$; these are located above and below the framework plane. Figure 3 shows very clearly the negative potentials due to the oxygen and nitrogen lone pairs (the latter being stronger) and that they are on opposite sides of the molecule, to minimize lone pair−lone pair repulsion.

The C−N and N−O bond lengths in **7** are quite typical of oximes, the relevant overall values being 1.281 Å and 1.416 Å[42], respectively. Table 3 shows that the N−O distance

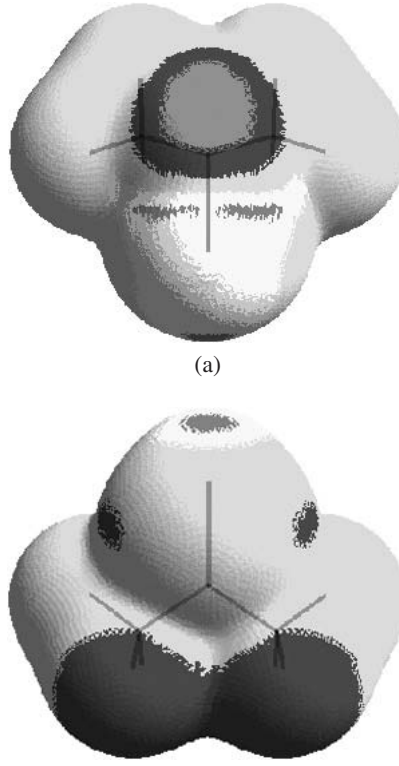

(a)

(b)

FIGURE 2. Computed local ionization energy $\overline{I}_S(\mathbf{r})$ on the molecular surface of dimethylhydroxylamine, (**6**) $(H_3C)_2N-OH$. Color scale, in eV: Purple, less than 13; blue, between 13 and 15.2; green, between 15.2 and 18; yellow, between 18 and 19; red, greater than 19. Part (a) shows the nitrogen lone pair (purple) and the hydroxyl hydrogen (yellow). The methyl groups are at the top. Part (b) is the other side of the molecule, with the oxygen lone pairs and with the methyls at the bottom. The hydroxyl hydrogen is at the top (See color plate 2)

is somewhat shorter in **7** than in **6**. This is consistent with the argument that there is some charge delocalization in oximes[44] (equation 15).

(15)

This would explain the shortening of the N−O bond in **7** relative to **6**, and also the less negative $V_{S,min}$ of the oxygen in **7**, -28.9 kcal mol^{-1} vs -35.0 kcal mol^{-1} in **6**. Equation 15 has been invoked to rationalize the greater stability toward nucleophilic attack of oximes, compared to imines ($R'R''C{=}NH$)[44].

An interesting feature of **7** is that the lowest $\overline{I}_{S,min}$ are not by a specific atom but rather are above and below the central portion of the C=N double bond (Figure 4). This

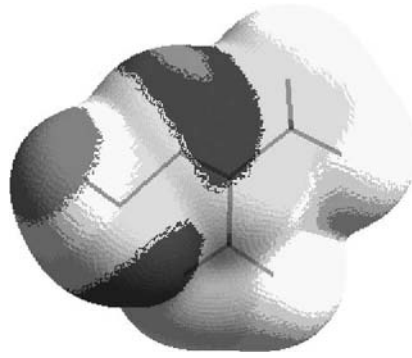

FIGURE 3. Computed electrostatic potential $V_S(\mathbf{r})$ on the molecular surface of acetoxime (**7**), $(H_3C)_2C{=}N{-}OH$. Color scale, in kcal mol^{-1}: Purple, more negative than −30; blue, between −30 and −20; green, between −20 and 0; yellow, between 0 and 25; red, more positive than 25. The hydroxyl hydrogen is at the left (red), the methyl groups are at the right and bottom. In the central portion are the lone pairs of nitrogen at the top (purple) and oxygen at the bottom (blue) (See color plate 3)

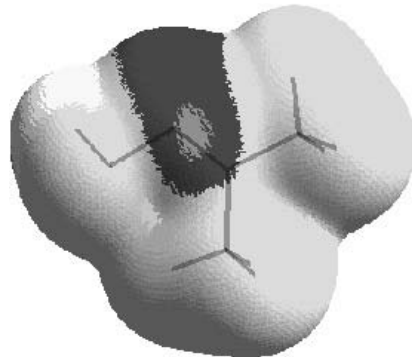

FIGURE 4. Computed local ionization energy $\overline{I}_S(\mathbf{r})$ on the molecular surface of acetoxime (**7**), $(H_3C)_2C{=}N{-}OH$. Color scale, in eV: Purple, less than 13; blue, between 13 and 15; green, between 15 and 18; yellow, between 18 and 19.4; red, greater than 19.4. The hydroxyl hydrogen is at the left (yellow), the methyl groups are at the right and bottom. In the center are seen the low $\overline{I}_S(\mathbf{r})$ of the C=N double bond (purple) and the nitrogen lone pair (blue) (See color plate 4)

is consistent with our earlier finding of $\overline{I}_{S,min}$ associated with C=C double bonds[45,46]. We will return later to this aspect of the $\overline{I}_S(\mathbf{r})$ of **7**.

C. Acetohydroxamic Acid (8)

The hydroxamic acid **8** can be viewed as a derivative of hydroxylamine, $H_2N{-}OH$[39], in which one of the amine hydrogens has been replaced by an acetyl group, $H_3C{-}C(O){-}$. However, the nitrogen in **8** is less pyramidal than might be expected, as can be seen by comparing its bond angles to those in **6** (Table 3). Indeed the C−N bond length in **8**, 1.368 Å, is much closer to the typical C(sp^2)—N(sp^2), 1.355 Å, than the C(sp^2)—N(sp^3),

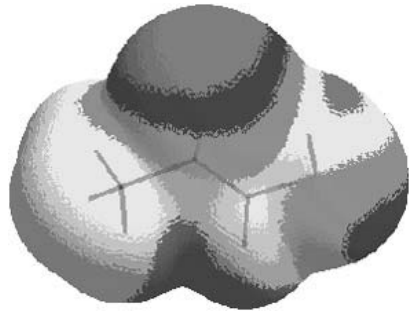

FIGURE 5. Computed electrostatic potential $V_S(\mathbf{r})$ on the molecular surface of acetohydroxamic acid (**8**), $H_3C-C(O)-N(H)-OH$. Color scale, in kcal mol^{-1}: Purple, more negative than −30; blue, between −30 and −20; green, between −20 and 0; yellow, between 0 and 25; red, more positive than 25. The acetyl oxygen is at the top (purple), close to the hydroxyl hydrogen (red) at its right. The amine hydrogen is at the bottom (red), the methyl group at the left and the hydroxyl oxygen lone pairs at the right (blue) (See color plate 5)

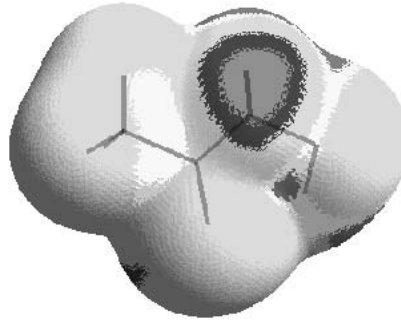

FIGURE 6. Computed local ionization energy $\overline{I}_S(\mathbf{r})$ on the molecular surface of acetohydroxamic acid (**8**), $H_3C-C(O)-N(H)-OH$. Color scale, in eV: Purple, less than 14; blue, between 14 and 15; green, between 15 and 18; yellow, between 18 and 19; red, greater than 19. The acetyl oxygen is at the bottom, the methyl group at the left and the hydroxyl group at the right. The nitrogen lone pair is in the upper center (purple) (See color plate 6)

1.416 Å[42]. The N−O distance, 1.403 Å, is similar to what would be expected for N(sp^2)−O(2), 1.397 Å, rather than for N(sp^3)−O(2), 1.463 Å. In fact, the whole molecular framework of **8**, excluding the methyl and amine hydrogens, is nearly planar. This is indicated by the relevant dihedral angles: C−C−N−O = −171.3, O−C−N−O = 11.9 and C−N−O−H = −7.0 deg.

The near-planarity of **8** can be attributed at least partially to intramolecular hydrogen bonding between the hydroxyl hydrogen and the acetyl oxygen[39]; their separation is 1.95 Å, considerably less than the sum of their van der Waals radii, 2.69 Å[40]. The proximity of these two atoms in **8** is quite evident in Figure 5. When this hydrogen bond is prevented from forming, by forcing the hydroxyl group to rotate through 125 deg, the near-planarity disappears; the aforementioned dihedral angles become, respectively, −26.4, 156.7 and 118.1 deg. In addition, the nitrogen is more pyramidal, the C−N

distance increases by 0.026 Å and the N−O distance by 0.011 Å. The rotation increases the energy [B3LYP/6-311G(3df,2p)] by 1.9 kcal mol^{-1}.

The O−H- - -O hydrogen bonding in **8** accounts for the sizeable decrease in the $V_{S,max}$ of the hydroxyl hydrogen to 30.7 kcal mol^{-1}, in contrast to its values in **6** and **7**. Decreases in the magnitudes of the donor $V_{S,max}$ and the acceptor $V_{S,min}$ have been found in the past to be associated with the presence of hydrogen bonding[47,48]. On the other hand, the $V_{S,max}$ of the amine hydrogen is the highest in Table 3. Both the hydroxyl and the amine hydrogens can readily be identified in Figure 5, as can the lone pairs of the oxygens; however, the nitrogen lone pair is not reflected in this $V_S(\mathbf{r})$ plot. In marked contrast, the nitrogen lone pair is the dominant feature of the $\overline{I}_S(\mathbf{r})$ of **8** (Figure 6), showing that these are indeed the most reactive electrons in the molecule.

VI. OXIME ISOMERISM

The restricted rotation around the C=N double bond in oximes (**2**) gives rise to two possible isomers, **9A** and **9B** for aldoximes and **10A** and **10B** for ketoximes. For aldoximes, these are labeled *syn* (**9A**) and *anti* (**9B**).

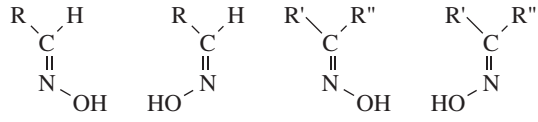

syn (**9A**) *anti* (**9B**) (**10A**) (**10B**)

We will look at three pairs of *syn* and *anti* aldoxime isomers, **9A** and **9B**, corresponding to R = CH_3 (acetaldoxime), R = CH_2Cl (chloroacetaldoxime) and R = C_6H_5 (benzaldoxime). We will also consider the two isomeric forms **10A** and **10B** of acetophenone oxime, a ketoxime in which R′ = CH_3 and R″ = C_6H_5.

Since our interest is in fact in the equilibria between isomers, we have computed both energy and free-energy changes, ΔE and ΔG, for going from one isomer to the other. From ΔG can be determined the equilibrium constant, K_{eq}, by means of equation 16[27],

$$K_{eq} = \exp(-\Delta G^{\circ}/RT) \tag{16}$$

in which R is the universal gas constant and T is the absolute temperature. Our calculations correspond to pressures of one atmosphere, so that our ΔG is the standard value ΔG°, as required by equation 16.

In Table 4 are the computed ΔE, ΔG and K_{eq} for the aldoxime isomerization equilibria *syn* $\rightleftharpoons$ *anti*, and also for the ketoxime equilibrium **10A** $\rightleftharpoons$ **10B**. It should be kept in mind that all of these results come from single-molecule calculations, and do not include any intermolecular interactions.

A. Acetaldoxime, 9 (R = CH_3)

As is the case for acetoxime, **7**, the two isomers of this oxime are both planar (except for two methyl hydrogens in each case). Their energy difference, $E(anti)$—$E(syn)$, is only 0.7 kcal mol^{-1} (Table 4), while ΔG actually has the opposite sign, but is also very small. At the B3LYP/6-311G(3df,2p) computational level, we can only conclude that these two isomers are intrinsically very similar in stability. If one or the other is found to be

TABLE 4. Computed energy and free energy changes, ΔE and ΔG, and equilibrium constants K_{eq}, for isomerization equilibria at 298 K, at the B3LYP/6-311G(3df,2p) level

Oxime	Process	ΔE (kcal mol^{-1})	ΔG (kcal mol^{-1})	K_{eq}
Acetaldoxime, **9** (R = CH_3)	*syn* $\rightleftharpoons$ *anti*	0.7	−0.5	2.2
Chloroacetaldoxime, **9** (R = CH_2Cl)	*syn* $\rightleftharpoons$ *anti*	−1.6	−1.3	9.0
Benzaldoxime, **9** (R = C_6H_5)	*syn* $\rightleftharpoons$ *anti*	2.3	2.4	1.7×10^{-2}
Acetophenone oxime, **10** (R′ = CH_3, R″ = C_6H_5)	**10A** $\rightleftharpoons$ **10B**	−2.7	−3.2	2.2×10^{2}

more stable in a condensed phase (pure liquid or solid, or solution), it is presumably due to intermolecular interactions, such as hydrogen bonding.

B. Chloroacetaldoxime, 9 (R = CH_2Cl)

In each isomer of chloroacetaldoxime, the chlorine is coplanar with the remainder of the molecule (other than the methyl hydrogens) but it points away from the other atoms. When we tried to rotate the chloromethyl and hydroxyl groups in the *anti* structure so as to permit $-CH_2Cl\cdots HO-$intramolecular hydrogen bonding, the molecule preferentially returned to its original conformation, perhaps because these rotations also lead to increased repulsion between the nitrogen and oxygen lone pairs.

Table 4 indicates that the *anti* isomer of chloroacetaldoxime is energetically slightly the more stable one. The equilibrium constant is predicted to be 9.0.

C. Benzaldoxime, 9 (R = C_6H_5)

In both the *syn* and the *anti* isomers of benzaldoxime, the entire molecule was found to be planar. Rotating the aromatic ring out of the plane of the other atoms is energetically unfavorable. The computed energy difference between the isomers is again quite small, but the *syn* is favored, the *syn* $\rightleftharpoons$ *anti* equilibrium constant being 1.7×10^{-2}.

D. Acetophenone Oxime, 10 (R′ = CH_3, R″ = C_6H_5)

In acetophenone oxime, the aromatic ring is rotated out of the plane of the molecular framework, by about 30 deg when it is *syn* to the hydroxyl group but only by about 6 deg when they are *anti*. As was observed for acetoxime, **7** (Table 3), the two C−C−N angles differ notably, the one on the same side of the double bond as the hydroxyl group being the larger: 128.3 vs 113.0 deg for **10A**, 124.1 vs 116.0 deg for **10B**. As in **7**, the C−N−O−angles are smaller than would be expected for sp^2 hydridization: 114.4 deg in **10A**, 113.1 deg in **10B**.

The isomer in which the methyl and hydroxyl groups are *syn* to each other, **10B**, was found to be favored energetically (Table 4); the calculated **10A** $\rightleftharpoons$ **10B** equilibrium constant is 2.2×10^2. The difference in the stabilities of **10A** and **10B** is greater than for any of the other isomer pairs in Table 4.

E. Comments

The magnitudes of the computed ΔE and ΔG are relatively small for all four of the oxime isomerizations that have been considered. Thus the effects of intermolecular interactions with the surroundings—whether the pure liquid or solid phases or a solvent—may often determine which isomer is more stable in a condensed phase. (This point will be addressed again in Section VII.) For example, benzaldoxime is known to be in the *anti* form in an acidic environment but *syn* in a basic one[49]. Temperature also plays a role in affecting K_{eq}. It should further be noted, as can be seen in Table 4, that even ΔE and ΔG in the neighborhood of just $\pm$ 3 kcal mol^{-1} can produce K_{eq} of two orders of magnitude.

VII. HYDROGEN BONDING

The presence of nitrogen and oxygen lone pairs, and hydroxyl and amine hydrogens, means that each hydroxylamine, oxime and hydroxamic acid has several possibilities for accepting and donating hydrogen bonds. These can be characterized in terms of the electrostatic potentials associated with the respective atoms, in particular the $V_{S,min}$ of the nitrogens and oxygens and the $V_{S,max}$ of the hydrogens. It was shown some time ago that the magnitudes of $V_{S,min}$ and $V_{S,max}$ correlate directly, and quantitatively, with empirical measures of hydrogen-bond accepting ($V_{S,min}$) and donating ($V_{S,max}$) tendencies[19].

As points of reference, we will take two well-established hydrogen-bond donor/acceptors, H_2O and NH_3. Their computed gas-phase $V_{S,max}$ and $V_{S,min}$ are in Table 5, along with the same data for all of the molecules that have been discussed: hydroxylamine (**5**), dimethylhydroxylamine (**6**), acetoxime (**7**), acetohydroxamic acid (**8**), and the isomeric pairs of oximes examined in the last section. Finally, we included an additional hydroxamic acid, **11**, to see the effects of the strongly electron-withdrawing cyano group.

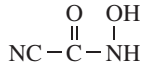

(**11**)

A few generalizations can be made before analyzing individual molecules. The $V_{S,min}$ of the oxygen in H_2O and the nitrogen in NH_3 are more negative than any others in Table 5. This is not surprising; in all of the other molecules, the oxygen and nitrogen are bonded to each other, which diminishes the amount of electronic charge that each of these electronegative atoms can attract. Thus the oxygen and nitrogen in H_2O and NH_3 should be the best hydrogen-bond acceptors in Table 5, although many of the others certainly have that capability as well, and the $V_{S,min}$ of some of the oxygens approach that of H_2O. In fact the two hydroxamic acids have intramolecular hydrogen bonding between the acetyl oxygens and the hydroxyl hydrogens, as was already mentioned for **8** and can readily be seen in Figure 5; the O---H distances in **8** and **11** are 1.95 and 2.05 Å, respectively, much less than the sum of the van der Waals radii, 2.69 Å[40].

The $V_{S,max}$ of the hydroxyl hydrogens are almost all in the neighborhood of 50 kcal mol^{-1}, indicating that these molecules should be as good hydrogen-bond donors as H_2O and better than NH_3. The only low hydroxyl hydrogen $V_{S,max}$ is in the case of acetohydroxamic acid (**8**), in which the hydrogen is already interacting with the acetyl oxygen (Figure 5). In **11**, the effect of the intramolecular hydrogen bonding upon the hydrogen's $V_{S,max}$ is countered by electron withdrawal due to the cyano group (to be discussed later in this section).

There are three amine hydrogens in Table 5, in hydroxylamine (**5**), and in the two hydroxamic acids, **8** and **11**. The magnitudes of their $V_{S,max}$ range from 32.3 to 67.6 kcal

TABLE 5. Most positive and most negative values, $V_{S,max}$ and $V_{S,min}$, of computed surface electrostatic potentials, HF/6-31G*//B3LYP/6-31G** [a]

Molecule	$V_{S,min}$ (kcal mol^{-1})	$V_{S,max}$ (kcal mol^{-1})
H_2O	oxygen: −42.1	hydrogens: 49.0, 49.0
NH_3	nitrogen: −48.1	hydrogens: 27.6, 27.6, 27.6
Hydroxylamines		
H_2N-OH (**5**)	oxygen: −33.6 nitrogen: −31.7	hydroxyl H: 44.5 amine H: 32.3, 32.3
$(H_3C)_2N-OH$ (**6**)	oxygen: −35.0 nitrogen: −28.1	hydroxyl H: 44.1 methyl H: 6.7–12.8
Oximes		
$H_3C-C(H)=NOH$, *syn*	oxygen: −30.5, −30.5 nitrogen: −29.6	hydroxyl H: 47.6 oxime H: 18.4 methyl H: 10.6–14.9
$H_3C-C(H)=NOH$, *anti*	oxygen: −27.3, −27.3 nitrogen: −31.6	hydroxyl H: 47.9 oxime H: 19.3 methyl H: 7.3–14.8
$H_2C(Cl)-C(H)=NOH$, *syn*	oxygen: −25.2, −25.2 nitrogen: −20.6 chlorine: −13.2, −13.4, −13.4	hydroxyl H: 54.7 oxime H: 18.8 methyl H: 23.3, 23.3
$H_2C(Cl)-C(H)=NOH$, *anti*	oxygen: −16.6, −16.6 nitrogen: −25.0 chlorine: −14.0	hydroxyl H: 56.6 oxime H: 22.0 methyl H: 20.6, 20.6
$C_6H_5-C(H)=NOH$, *syn*	oxygen: −29.1, −29.1 nitrogen: −23.4 ring: −15.9, −15.9	hydroxyl H: 49.4 oxime H: 21.5 phenyl H: 11.4–18.2
$C_6H_5-C(H)=NOH$, *anti*	oxygen: −25.0, −25.0 nitrogen: −30.9 ring: −16.3, −16.3	hydroxyl H: 49.9 oxime H: 21.8 phenyl H: 16.1–18.3
$C_6H_5-C(CH_3)=NOH$ (C_6H_5, OH *syn*)	oxygen: −18.0, −34.6 nitrogen: −29.7 ring: −16.3	hydroxyl H: 47.6 phenyl H: 8.4–20.5 methyl H: 8.0, 10.8
$C_6H_5-C(CH_3)=NOH$ (C_6H_5, OH *anti*)	oxygen: −26.2, −27.4 nitrogen: −21.4, −25.0 ring: −17.6, −18.2	hydroxyl H: 48.6 phenyl H: 9.2–19.6 methyl H: 6.2
$(H_3C)_2C=NOH$ (**7**)	oxygen: −28.8, −28.9 nitrogen: −31.5	hydroxyl H: 45.9 methyl H: 5.7–14.5
Hydroxamic Acids		
$H_3C-C(O)-N(H)-OH$ (**8**)	hydroxyl oxygen: −33.0 acetyl oxygen: −39.7 nitrogen: -	hydroxyl H: 30.7 amine H: 54.9 methyl H: 21.0, 22.9 acetyl C: 16.3
$NC-C(O)-N(H)-OH$ (**11**)	hydroxyl oxygen: −18.4 acetyl oxygen: −28.9 amine nitrogen: - cyano nitrogen: −25.6	hydroxyl H: 50.7 amine H: 67.6 acetyl C: 31.1

[a] The data for **5**, **8** and **11** are taken from Reference 39.

mol^{-1}, reflecting their different molecular environments, but all are more positive than the $V_{S,max}$ of the hydrogens in NH_3. Finally, hydrogens attached to carbons have $V_{S,max}$ between 6 and 23 kcal mol^{-1}.

It is particularly interesting to compare the electrostatic potentials of each pair of oxime isomers in Table 5. In the case of acetaldoxime, $H_3C-C(H)=NOH$, the $V_{S,min}$ and $V_{S,max}$ of the *syn* and *anti* forms are quite similar. However, in chloroacetaldoxime, $H_2C(Cl)-C(H)=NOH$, the oxygen $V_{S,min}$ are significantly more negative in the *syn* isomer than in the *anti*, which suggests that the former could be more stabilized by intermolecular hydrogen bonding in a condensed phase. In benzaldoxime, $C_6H_5-C(H)=NOH$, the more negative $V_{S,min}$ of the nitrogen in the *anti* form may have analogous consequences.

A new feature to mention concerns the aromatic rings that are in two of the oximes in Table 5: benzaldoxime, $C_6H_5-C(H)=NOH$, and acetophenone oxime, $C_6H_5-C(CH_3)=NOH$. Most of them have $V_{S,min}$ of about -16 kcal mol^{-1} above and below the central portions of the rings. These can be attributed to the aromatic π electrons; benzene itself has two such $V_{S,min}$ of -20.1 kcal mol^{-1} (HF/6-31G*)[43]. The only exception is the isomer **10A** of acetophenone oxime, in which the C_6H_5 and the OH are *syn*; this is the one in which the ring is most out of the plane of the molecular framework. Only one $V_{S,min}$ was found for this ring, because the negative π potential on the other side merges with one of the oxygen lone-pair regions. This makes the latter more negative, and helps to account for the large difference between the two oxygen $V_{S,min}$, -18.0 and -34.6 kcal mol^{-1}.

Another notable point, pertaining now to **10B**, in which the C_6H_5 and OH are *anti*, is that there are two $V_{S,min}$ associated with the nitrogen. This is not observed for any other nitrogen in Table 5. Thus **10B** has six significant $V_{S,min}$, compared to four for **10A**. If the result is an enhanced capacity for intermolecular hydrogen bonding, then this—together with the intrinsically greater stability of **10B** (Table 4)—may explain why **10B** is much more stable than **10A** in the crystalline phase[49].

Two of the molecules in Table 5 contain strongly electron-withdrawing substituents: chloroacetaldoxime, $H_2C(Cl)-C(H)=NOH$, and the cyanohydroxamic acid **11**, $NC-C(O)-N(H)-OH$. The effects of these substituents are readily apparent. In chloroacetaldoxime, the oxygen and nitrogen $V_{S,min}$ are less negative and the hydrogen $V_{S,max}$ are more positive than in acetaldoxime itself. The contrast between cyanohydroxamic acid, **11**, and its unsubstituted parent **8** is even greater, particularly with regard to the $V_{S,max}$ of the hydrogens. The cyano group also induces a reasonably strong $V_{S,max}$ on the acetyl carbon.

VIII. ACIDITY/BASICITY

The previous section focused upon the numerous hydrogen-bond donating and accepting possibilities of hydroxylamines, oximes and hydroxamic acids: the hydroxyl and amine hydrogens and the oxygen and nitrogen lone pairs. These also translate into possible acidic and basic sites, capable of donating and accepting protons. However, whereas hydrogen bonding is a noncovalent interaction and can be analyzed in terms of molecular surface electrostatic potentials ($V_{S,min}$ and $V_{S,max}$), proton transfer requires local ionization energies, specifically the surface minima $\overline{I}_{S,min}$.

The strength of an acid HA is quantified by means of the pK_a, which is the negative logarithm of the equilibrium constant for the process described in equation 17[27]:

$$HA + H_2O \rightleftharpoons H_3O^+ + A^- \tag{17}$$

(In practice, the concentration of the water is included in K_a.) The smaller the pK_a, the stronger the acid.

One can analogously measure base strength via pK_b, which refers to equation 18:

$$B + H_2O \rightleftharpoons BH^+ + OH^- \tag{18}$$

in which B is the base. Again, the smaller the pK_b, the stronger the base.

The values of $\overline{I}_{S,min}$ on a surface indicate the locations of the most reactive electrons, most readily transferred to a proton. Accordingly, the lower the $\overline{I}_{S,min}$, the more basic should be the site; thus it could be anticipated that $pK_b \sim \overline{I}_{S,min}$.

The same reasoning applies of course to the reverse reaction in equation 17, in which A^- acts as a base. The lower the $\overline{I}_{S,min}$ of A^-, the stronger it is as a base, and hence the weaker is HA as an acid. The pK_a of HA should therefore increase (and its acidity decrease) as the $\overline{I}_{S,min}$ of A^- decreases.

These expectations have been borne out. We have confirmed the anticipated correlations of experimental aqueous acid and base strengths with $\overline{I}_{S,min}$[50,51]. A base becomes stronger, and its pK_b lower, as the $\overline{I}_{S,min}$ of the basic site decreases. An acid becomes stronger, and its pK_a lower, as the $\overline{I}_{S,min}$ of the conjugate base's basic site increases. To assess basicity and predict pK_b, therefore, $\overline{I}_{S,min}$ should be computed for the basic site itself; to assess acidity and predict pK_a, $\overline{I}_{S,min}$ must be obtained for the conjugate base, i.e. A^- for an acid HA.

It should be noted that some literature tabulations list only pK_a values, for bases as well as for acids. For example, the *Handbook of Chemistry and Physics*[41] gives a pK_a of 9.25 for NH_3. This corresponds to the process in equation 19:

$$NH_4^+ + H_2O \rightleftharpoons NH_3 + H_3O^+ \tag{19}$$

whereas our interest is more often in the pK_b for the basic action of NH_3 (equation 20):

$$NH_3 + H_2O \rightleftharpoons NH_4^+ + OH^- \tag{20}$$

If the expressions for K_a and K_b are written out, it is seen that K_aK_b equals K_w, the ion product of water, which is 1.01×10^{-14} at 25 °C[41]. It then follows that $pK_a + pK_b = 14.00$, so that $pK_b = 4.75$ for NH_3. Thus the pK_b for a base can easily be ascertained from its quoted pK_a.

When a molecule contains several potential acidic and/or basic sites, as do those treated in this chapter, the relative $\overline{I}_{S,min}$ can help to rank them and also to clarify possible ambiguities. For example, hydroxylamine, $H_2N{-}OH$, has a reported pK_a of 5.94[41]. Does this correspond to the loss of the hydroxyl proton, or an amine proton? Or is it telling us that the nitrogen, or the oxygen, has $pK_b = 14.00 - 5.94 = 8.06$?

Table 6 presents the computed $\overline{I}_{S,min}$ at the potentially basic sites in hydroxylamine (**5**), dimethylhydroxylamine (**6**), acetoxime (**7**) and acetohydroxamic acid (**8**). In the case of hydroxylamine, for example, this means the $\overline{I}_{S,min}$ at the oxygen and nitrogen. Table 6 also lists the $\overline{I}_{S,min}$ at the conjugate base sites corresponding to the loss of the potentially acidic amine and hydroxyl protons; in the case of hydroxylamine, for instance, these are the $\overline{I}_{S,min}$ for the oxygen in $H_2N{-}O^-$ and for the nitrogen in $HN^-{-}OH$. Finally, for reference purposes, the table provides the nitrogen $\overline{I}_{S,min}$ for the two bases, NH_3 and pyridine, and the conjugate base $\overline{I}_{S,min}$ for acetic acid, $H_3C{-}C(O){-}OH$, i.e. the $\overline{I}_{S,min}$ at either oxygen in $[H_3C{-}C(O){-}O]^-$. Experimental aqueous solution pK_a values are included when available, although, as mentioned above, for **5**–**8** there is some uncertainty as to the process to which these pK_a values refer.

Looking first at the basic sites in Table 6, it is clear that the oxygens $\overline{I}_{S,min}$ are weaker in this respect than the nitrogens; the oxygen $\overline{I}_{S,min}$ are in the neighborhood of 15 eV,

TABLE 6. Values of $\overline{I}_{S,min}$ relevant to the acidities or basicities of hydroxylamine (**5**), dimethylhydroxylamine (**6**), acetoxime (**7**) and acetohydroxamic acid (**8**). The $\overline{I}_{S,min}$ were computed at the HF/6-31G*//B3LYP/6-31G** level and are in eV [a]

Molecule [b]	Acidic site	$\overline{I}_{S,min}$ (conj. base) [c,d]	Basic site	$\overline{I}_{S,min}$ [d]
H_2N-OH (**5**).	hydroxyl H	3.9	O	15.2
$pK_a = 5.94$	amine H	2.3	N	12.8
$(H_3C)_2N-OH$ (**6**)	hydroxyl H	4.4	O	15.1
			N	12.3
$(H_3C)_2C{=}N-OH$ (**7**),	hydroxyl H	6.4	O	15.2
$pK_a = 12.42$	C=N	5.1	C=N	12.9
$H_3C-C(O)-N(H)-OH$ (**8**),	hydroxyl H	6.3	hydroxyl O	15.4
$pK_a = 8.70$	amine H	5.9	acetyl O	14.9
			N	13.5
Reference Values				
$H_3C-C(O)-OH$,	hydroxyl H	7.0		
$pK_a = 4.756$				
NH_3,			N	11.9
$pK_a = 9.25$				
pyridine,			N	12.7
$pK_a = 5.23$				

[a] The data for **5**, **8**, $H_3C-C(O)-OH$, NH_3 and pyridine are taken from Reference 39.
[b] Experimental pK_a values in aqueous solution are from Reference 40.
[c] For the acid sites, the $\overline{I}_{S,min}$ are those of the conjugate bases, i.e. after the removal of the proton.
[d] Only the lowest $\overline{I}_{S,min}$ is given for each site, even if there are two $\overline{I}_{S,min}$ associated with it.

which is at least 2 eV (46 kcal mol^{-1}) higher than most of the nitrogen $\overline{I}_{S,min}$. The oxygen values in Table 6 are also higher than those of H_2O, 14.8 eV.

The nitrogens are accordingly the stronger basic sites in these molecules—but they are not very strong in absolute terms. This can be seen by noting that the lowest nitrogen $\overline{I}_{S,min}$ among the molecules **5**–**8** is for **6**, dimethylhydroxylamine, which is therefore predicted to be the strongest base, but its $\overline{I}_{S,min}$ is approximately midway between those of NH_3 and pyridine, which indicates that the K_b of **6** may be about two orders of magnitude smaller than that of NH_3. Hydroxylamine (**5**) and acetoxime (**7**) are expected to be close to pyridine in basicity, having very similar nitrogen $\overline{I}_{S,min}$. However, that of acetohydroxamic acid (**8**) is significantly higher, which suggests very weak basicity.

It can be concluded therefore that the experimental pK_a of 8.70 of acetohydroxamic acid pertains to its action as an acid. Its K_a is then four orders of magnitude less than that of acetic acid. The rate of change of pK_a with respect to conjugate base $\overline{I}_{S,min}$ is thus roughly the same in magnitude as was observed above for the pK_b and basic site $\overline{I}_{S,min}$ of NH_3 and pyridine, and as was found in our earlier work[50,51]. The $\overline{I}_{S,min}$ for the conjugate bases of **8** in Table 6 indicate that the hydroxyl hydrogen is somewhat more acidic than the amine. There has been considerable disagreement in the literature concerning the relative acidities of the hydroxyl and amine protons in various hydroxamic acids; for a summary of this, see García and coworkers[52].

Hydroxylamine and dimethylhydroxylamine, **5** and **6**, are extremely weak acids, judging from how much less are their conjugate base $\overline{I}_{S,min}$ than that of acetohydroxamic acid, **8**. Accordingly the experimental pK_a of hydroxylamine, 5.94, must refer to its behavior as a base, with $pK_b = 8.06$. Indeed its pK_a and its nitrogen $\overline{I}_{S,min}$ are both quite similar to those of pyridine.

Acetoxime (**7**) is a particularly interesting case. The lowest $\overline{I}_{S,min}$ in both the neutral molecule (Figure 4) and the conjugate base are above and below the central portion of the C=N bond. Acetoxime is also the only molecule in Table 6 for which the lowest $\overline{I}_{S,min}$ of the conjugate base is not at the site from which the proton was lost. The acidity of acetoxime is determined, therefore, by the degree to which the proton resists interacting not with the oxygen from which it came but with the C=N double bond, forming a protonated complex. Taking the C=N $\overline{I}_{S,min}$ of 5.1 eV as the criterion, and comparing it to those of hydroxamic and acetic acids, indicates that acetoxime is a very weak acid, consistent with the experimental pK_a of 12.42.

The $\overline{I}_{S,min}$ of 12.9 eV of neutral acetoxime implies that it should also act as a base, somewhat weaker than pyridine. Indeed an important application, especially of the double oxime dimethylglyoxime (**12**), is in chelating metal ions[53].

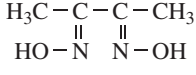

(**12**)

The aldoxime and ketoxime isomers **9** and **10**, which were discussed in Section VI, all follow acetoxime (**7**) in having $\overline{I}_{S,min}$ above and below the C=N double bonds. For the most part, these $\overline{I}_{S,min}$ are the same or slightly larger than those of **7**, ranging from 12.9 to 13.1 eV, the *syn* aldoximes having the higher values. However, the C=N $\overline{I}_{S,min}$ of chloroacetaldoxime (**9**, R = CH_2Cl) are significantly greater than the others, 13.5 eV, reflecting—as do its $V_{S,min}$ and $V_{S,max}$ (Table 5)—electron withdrawal by the chlorine. It should be noted, however, that for the oximes having aromatic rings, the lowest $\overline{I}_{S,min}$ are not those of the C=N but rather are near (above and below) specific carbons of the rings (unlike the $V_{S,min}$ of the rings, which are associated with their central portions; see Section VII). These $\overline{I}_{S,min}$ are between 11.9 and 12.1 eV, and are usually in the vicinities of *ortho* and *para* carbons, but sometimes *meta* as well.

IX. GLOBAL AND LOCAL POLARIZABILITY

The average polarizability α, defined by equation 9, is a global property, which pertains to a molecule as a whole. It is a measure, to the first order, of the overall effect of an external electric field upon the charge distribution of the molecule. We are unaware of any experimentally determined α for the molecules that are included in this chapter. However, they can be estimated using equation 12 and the atomic hybrid polarizabilities, and corresponding group values, that were derived empirically by Miller[35]. These were found to reproduce experimental molecular α with an average error of 2.8%. The relevant data, taken from his work, are in Table 7.

The resulting estimated average polarizabilities for the hydroxylamines, oximes and hydroxamic acids that we have discussed are given in Table 8. (It should be noted that Miller's approach does not distinguish between oxime isomers.) As anticipated from the correlation between average polarizability and volume (equation 10), the α in Table 8 increase with molecular size.

Some idea of the relative polarizabilities of various portions of the molecules in Table 8 can be obtained by looking at the group values in Table 7. However, a more detailed picture is provided by the variation of the local ionization energy $\overline{I}_S(\mathbf{r})$ over the molecular surface, if it is accepted that this is an inverse measure of local polarizability (equation 14).

Proceeding on this basis, Figure 2 shows that the most polarizable portion of dimethylhydroxylamine, $(H_3C)_2N-OH$, is the lone pair of the nitrogen. Although the oxygen lone

TABLE 7. Empirical hybrid atom and group polarizabilities[a]

Atom or group	Atom hybridization[b]	Polarizability α (Å^3)
H		0.387
C	trtrtrπ	1.352
N	te^{2}tetete	0.964
N	tr^{2}trtrπ	1.030
Cl		2.315
CH_2		1.835
CH_3		2.222
C≡N		2.239
C=O		1.921
NH		1.351
NH_2		1.738
OH		1.024
C_6H_5		10.047

[a] Reference 35.
[b] te = tetrahedral, tr = trigonal.

TABLE 8. Estimated average molecular polarizabilities, based on empirical hybrid atom and group values[a] (Table 7)

Molecule	Average polarizability α (Å^3)
H_2N-OH	2.76
$(H_3C)_2N-OH$	6.43
$H_3C-C(H)=N-OH$	6.02
$H_2C(Cl)-C(H)=N-OH$	7.94
$(H_3C)_2C=N-OH$	7.85
$C_6H_5-C(H)=N-OH$	13.84
$C_6H_5-C(CH_3)=N-OH$	15.68
$H_3C-C(O)-N(H)-OH$	6.52
$NC-C(O)-N(H)-OH$	6.54

[a] Reference 35.

pairs are more negative (Table 3 and Figure 1), they are less polarizable than even the methyl groups. Least polarizable is the hydroxyl hydrogen, which is typical for hydroxyl and amine hydrogens (Figures 2, 4 and 6).

Figure 4 provides an interesting contrast to Figure 3. The latter shows very clearly the nitrogen and oxygen lone pairs in acetoxime, $(H_3C)_2C=N-OH$. However, Figure 4 indicates that the most polarizable region is not one of these lone pairs, but rather above and below the C=N double bond. This is followed in polarizability by the nitrogen lone pair, its sp^2 form being very apparent.

Again in the case of acetohydroxamic acid, $H_3C-C(O)-N(H)-OH$, the acetyl and hydroxyl oxygen lone pairs that dominate its $V_S(\mathbf{r})$ (Figure 5) are only intermediate in terms of $\bar{I}_S(\mathbf{r})$ and hence polarizability (Figure 6). The most polarizable region is associated with the nitrogen—which does not manifest itself at all in $V_S(\mathbf{r})$.

X. CONCLUSION

We began this chapter by pointing out that the feature common to all of the molecules to be considered is the NOH group. This has, bonded to each other, two atoms with high electronegativities and significant lone pairs, i.e. basic sites, with an attached potentially

acidic hydrogen. These three atoms in such close proximity give rise to a variety of possible inter- and intramolecular interactions; even more are introduced by other portions of some of the molecules that were studied, e.g. amine hydrogens, acetyl oxygens, aromatic rings and the C=N double bond.

We have approached these multi-faceted systems by looking in particular at two local molecular properties: the electrostatic potential, $V(\mathbf{r})$ and $V_S(\mathbf{r})$, and the local ionization energy, $\overline{I}_S(\mathbf{r})$. In terms of these, we have addressed hydrogen bonding, lone pair–lone pair repulsion, conformer and isomer stability, acidity/basicity and local polarizability. We have sought to show how theoretical and computational analyses can complement experimental studies in characterizing and predicting molecular behavior.

The discussion at the end of Section IX illustrates very well how $V_S(\mathbf{r})$ and $\overline{I}_S(\mathbf{r})$ complement each other in bringing out different aspects of a molecule's reactive tendencies. For example, the $V_S(\mathbf{r})$ of acetohydroxamic acid in Figure 5 shows the availability of its oxygen lone pairs for hydrogen bonding and other noncovalent interactions, while its $\overline{I}_S(\mathbf{r})$ in Figure 6 reveals its most basic and most polarizable site to be the nitrogen. The complementarity of $V_S(\mathbf{r})$ and $\overline{I}_S(\mathbf{r})$ was already mentioned at the end of Section V.A, and it certainly emerges as well from Section IX.

In this chapter, we have looked at some of the intrinsic features of hydroxylamine, oxime and hydroxamic acid molecules. The insights obtained, particularly concerning the electrostatic potentials on their molecular surfaces, should provide a useful basis for proceeding to their gas phase and crystal structures and properties.

XI. ACKNOWLEDGMENT

We thank Dr. Branko Jursič for helpful discussions in the course of preparing this chapter.

XII. REFERENCES

1. J. March, *Advanced Organic Chemistry*, 3rd edn., John Wiley & Sons, Inc., New York, 1985.
2. I. N. Levine, *Quantum Chemistry*, 5th edn., Prentice Hall, Upper Saddle River, NJ, 2000.
3. K. K. Irikura and D. J. Frurip, Chap. 1 in *Computational Thermochemistry* (Eds. K. K. Irikura and D. J. Frurip), ACS Symposium Series 677, American Chemical Society, Washington, 1998.
4. P. Politzer, P. Lane, J. S. Murray and M. C. Concha, *J. Mol. Model.*, **11**, 1 (2005).
5. P. Politzer and J. S. Murray, Chap. 7 in *Reviews in Computational Chemistry*, Vol. 2 (Eds. K. B. Lipkowitz and D. B. Boyd), VCH, New York, 1991 and references cited therein.
6. R. S. Mulliken, *J. Chem. Phys.*, **23**, 1833 (1955).
7. D. E. Williams, Chap. 6 in *Reviews in Computational Chemistry*, Vol. 2 (Eds. K. B. Lipkowitz and D. B. Boyd), VCH, New York, 1991.
8. P. Politzer and R. S. Mulliken, *J. Chem. Phys.*, **55**, 5135 (1971).
9. R. F. Stewart, *Chem. Phys. Lett.*, **65**, 335 (1979).
10. P. Politzer and D. G. Truhlar (Eds.), *Chemical Applications of Atomic and Molecular Electrostatic Potentials*, Plenum Press, New York, 1981.
11. P. Politzer and J. S. Murray, *Theor. Chem. Acc.*, **108**, 134 (2002).
12. P. Politzer, *Theor. Chem. Acc.*, **111**, 395 (2004).
13. J. D. Hirschfelder, C. F. Curtiss and R. B. Bird, *Molecular Theory of Gases and Liquids*, Wiley, New York, 1954.
14. G. Naray-Szabo and G. G. Ferenczy, *Chem. Rev.*, **95**, 829 (1995).
15. J. S. Murray and P. Politzer, *J. Mol. Struct. (Theochem)*, **425**, 107 (1998).
16. P. Politzer and J. S. Murray, *Trends Chem. Phys.*, **7**, 157 (1999).
17. R. F. W. Bader, M. T. Carroll, J. R. Cheeseman and C. Chang, *J. Am. Chem. Soc.*, **109**, 7968 (1987).
18. T. Brinck, J. S. Murray and P. Politzer, *Mol. Phys.*, **76**, 609 (1992).
19. H. Hagelin, J. S. Murray, T. Brinck, M. Berthelot and P. Politzer, *Can. J. Chem.*, **73**, 483 (1995).

20. P. Sjoberg, J. S. Murray, T. Brinck and P. Politzer, *Can. J. Chem.*, **68**, 1440 (1990).
21. T. Koopmans, *Physica*, **1**, 104 (1934).
22. R. K. Nesbet, *Adv. Chem. Phys.*, **9**, 321 (1965).
23. P. Politzer, F. Abu-Awwad and J. S. Murray, *Int. J. Quantum Chem.*, **69**, 607 (1998).
24. P. Politzer and J. S. Murray, Chap. 8 in *Chemical Reactivity* (Ed. A. Toro-Labbé), Elsevier, Amsterdam, 2007.
25. R. G. Pearson, *J. Am. Chem. Soc.*, **85**, 3533 (1963).
26. K. D. Bonin and V. V. Kresin, *Electric-Dipole Polarizabilities of Atoms, Molecules and Clusters*, World Scientific, Singapore, 1997.
27. S. Glasstone, *Text-Book of Physical Chemistry*, Van Nostrand, New York, 1940.
28. J. J. C. Teixeira-Dias and J. N. Murrell, *Mol. Phys.*, **19**, 329 (1970).
29. P. Jin, J. S. Murray and P. Politzer, *Int. J. Quantum Chem.*, **96**, 394 (2004).
30. K. M. Gough, *J. Chem. Phys.*, **91**, 2424 (1989).
31. H. L. Ammon, *Struct. Chem.*, **12**, 205 (2001).
32. A. Vogel, *J. Chem. Soc.*, 1833 (1948).
33. R. J. W. Le Fevre, *Adv. Phys. Org. Chem.*, **3**, 1 (1965).
34. A. J. Stone, *Mol. Phys.*, **56**, 1065 (1985).
35. K. J. Miller, *J. Am. Chem. Soc.*, **112**, 8533, 8543 (1990).
36. P. Jin, J. S. Murray and P. Politzer, *Int. J. Quantum Chem.*, **106**, 2347 (2006).
37. J. S. Murray, Z. Peralta-Inga, P. Politzer, K. Ekanayake and P. LeBreton, *Int. J. Quantum Chem., Biophys. Q.*, **83**, 245 (2001).
38. P. Jin, J. S. Murray and P. Politzer, *Comp. Lett.*, **3**, 373 (2007).
39. P. Politzer, J. S. Murray and M. C. Concha, *J. Phys. Org. Chem.*, **21**, 155 (2008).
40. A. Bondi, *J. Phys. Chem.*, **68**, 441 (1964).
41. D. R. Lide (Ed.), *Handbook of Chemistry and Physics*, 87th Ed., CRC Press, Boca Raton, 2006.
42. F. H. Allen, O. Kennard, D. G. Watson, L. Brammer, A. G. Orpen and R. Taylor, *J. Chem. Soc., Perkin Trans. 2*, S1 (1987).
43. P. Politzer, J. S. Murray and M. C. Concha, *Int. J. Quantum Chem.*, **88**, 19 (2002).
44. F. A. Carey and R. J. Sundberg, *Advanced Organic Chemistry*, 4th edn., Kluwer/Plenum, New York, 2000.
45. J. S. Murray, J. M. Seminario, P. Politzer and P. Sjoberg, *Int. J. Quantum Chem., Quantum Chem. Symp.*, **24**, 645 (1990).
46. J. S. Murray, F. Abu-Awwad and P. Politzer, *J. Mol. Struct. (Theochem)* **501–502**, 241 (2000).
47. J. S. Murray, Z. Peralta-Inga and P. Politzer, *Int. J. Quantum Chem.*, **75**, 267 (1999).
48. W. Hussein, C. G. Walker, Z. Peralta-Inga and J. S. Murray, *Int. J. Quantum Chem.*, **82**, 160 (2001).
49. L. F. Fieser and M. Fieser, *Organic Chemistry*, Heath, Boston, 1944.
50. T. Brinck, J. S. Murray, P. Politzer and R. E. Carter, *J. Org. Chem.*, **56**, 2934 (1991).
51. T. Brinck, J. S. Murray and P. Politzer, *J. Org. Chem.*, **56**, 5012 (1991).
52. B. García, S. Ibeas, J. M. Leal, F. Secco, M. Venturini, M. L. Senent, A. Niño and C. Muñoz, *Inorg. Chem.*, **44**, 2908 (2005).
53. F. A. Cotton and G. Wilkinson, *Advanced Inorganic Chemistry*, 4th edn., Wiley-Interscience, New York, 1980.

CHAPTER 2

Structural analysis of hydroxylamines, oximes and hydroxamic acids: Trends and patterns

PETER POLITZER and JANE S. MURRAY

Department of Chemistry, University of New Orleans, New Orleans, LA 70148, USA and Department of Chemistry, Cleveland State University, Cleveland, OH 44115, USA Fax: 440-331-1785; e-mail: ppolitze@uno.edu, jsmurray@uno.edu

The chemistry of hydroxylamines, oximes and hydroxamic acids
Edited by Z. Rappoport and J. F. Liebman

I. INTRODUCTION

One of the main points emphasized in the first chapter of this volume is the variety of inter- and intramolecular interactions that are available to hydroxylamines, oximes and hydroxamic acids. The structural element common to all of them is the NOH group, which consists of two strongly electronegative atoms with significant lone pairs plus a presumably positive hydrogen. In addition, hydroxylamines and hydroxamic acids often have amine hydrogens, which should have positive character, and hydroxamic acids also have acetyl oxygens, which can be more negative than the hydroxyl ones (see Table 5 of Chapter 1).

All of these features can be expected to affect both the gas phase and the crystal structures of these compounds, our focus in the present chapter. Some evidence of this was given already in the first chapter, e.g. the effects of lone pair repulsion in the NOH groups and intramolecular hydrogen bonding in hydroxamic acids. The scope of our discussion will now be greatly expanded. Our emphasis will be upon (a) identifying and interpreting, insofar as possible, general trends and patterns that may exist, and (b) comparing structures in the gas phase, which reflect intrinsic features of the molecules, to those in the crystalline, which may be influenced by the surroundings.

II. GAS PHASE STRUCTURES

A. Procedure

With the methodology, software and processors that are now available, an appropriate computational approach can be a very reasonable and practical means for obtaining accurate gas phase molecular structures. For example, Table 1 compares calculated and experimentally-determined gas phase geometries for hydroxylamine and for formaldoxime. The agreement is very good; the largest discrepancy is for the H−N−H angle of hydroxylamine, for which the uncertainty in the experimental value is given as $\pm 1^{\circ}$ to $\pm 2^{\circ}$.

We shall accordingly base our discussion of gas phase molecular structures upon computationally-obtained data, resulting from geometry optimizations using the density functional B3LYP/6-31G(d,p) procedure. (For a brief overview of different computational methods, see Section I.B of Chapter 1.) The Gaussian 03 code was utilized[1]. In order to ensure that true energy minima had been achieved, the vibration frequencies were calculated for each molecule and it was confirmed that there were no imaginary values[2].

In Table 2 are listed the hydroxylamines, oximes and hydroxamic acids for which we have determined the gas phase structures. We tried to select a representative group in each category. There are two types of oximes, as indicated, aldoximes and ketoximes. Due to restricted rotation around the C=N double bond, these can exist in two isomeric forms (except when R = H for an aldoxime and $R' = R''$ for a ketoxime). We have investigated both isomers in nearly every instance. For aldoximes, they are generally labeled *syn* when the H and OH are on the same side of the double bond and *anti* when on opposite sides. Note that the ketoximes in Table 2 contain one pair of isomers in which the >C=NOH group is not bonded to two carbons; instead one bond is to a chlorine. One of these isomers will be of interest in Section II.D in the context of hydrogen bonding *vs* lone pair—lone pair repulsion.

As was seen in Chapter 1, in which four pairs of oxime isomers were examined in some detail, the energy difference ΔE within each pair tends to be relatively small (Table 4, Chapter 1). That is true as well for the larger group being considered now; ΔE(0 K), B3LYP/6-31G(d,p), averages about 2 kcal mol^{-1}, just as was found in Chapter 1 for ΔE(298 K) at a higher level, B3LYP/6-311G(3df,2p). Any pronounced preference for one isomer over the other that is observed in condensed phases may be due to interactions

TABLE 1. Comparison of computed [B3LYP/6-31G(d,p)] and experimental structures; the latter are in parentheses[a]

Property	Hydroxylamine, H_2N-OH	Formaldoxime, $H_2C=N-OH$
Bond length (Å)		
N−O	1.448 (1.453)	1.402 (1.408)
C=N	—	1.274 (1.276)
N−H	1.022 (1.016)	—
O−H	0.966 (0.962)[b]	0.967 (0.956)
C−H	—	1.085,1.090 (1.085,1.086)[c]
Bond angle (deg)		
N−O−H	101.7 (101.4)	102.4 (102.7)
C−N−O	—	111.2 (110.2)
H−N−O	103.4 (103.2)	—
H−C−N	—	116.7,123.1 (115.6,121.8)[c]
H−C−H	—	120.2
H−N−H	104.8 (107.1)	—

[a] Experimental data for H_2N-OH and $H_2C=N-OH$ are from M. D. Harmony, V. W. Laurie, R. L. Kuczkowski, R. H. Schwendeman, D. A. Ramsey, F. J. Lovas, W. J. Lafferty and A. G. Maki, *J. Phys. Chem. Ref. Data*, **8**, 619 (1979).
[b] O−H bond is in plane bisecting H−N−H angle.
[c] The longer C−H bond and the larger H−C−N angle are on the OH side of the C=N double bond.

with the surroundings, or may perhaps result from the synthesis process. In our discussion of gas phase structures, we will accordingly include all of the isomers, not just the lower energy member of each pair.

One set of aldoxime isomers merits further comment. These are the ones having R = 2-pyridyl (Table 2). The *syn* and *anti* isomers both have two conformers, arising from rotation of the 2-pyridyl ring. The four optimized geometries are shown in Figure 2; each corresponds to an energy minimum, although the energies of the two *syn* conformers are the same. The *anti-2* conformer is 4.6 kcal mol^{-1} higher in energy than the *anti-1* [ΔE(0 K), B3LYP/6-31G(d,p)], with *syn-1* and *syn-2* between them. [ΔE(0 K) is the difference in the energy minima at 0 K. Note that for transitions between isomers, $\Delta E = \Delta H$ at any temperature, within the ideal gas approximation.]

B. The NOH Group

The NOH group is the structural element that links hydroxylamines, oximes and hydroxamic acids. We will accordingly begin by examining its key features, namely the N−O and O−H bond lengths and the N−O−H angle, for all three families of molecules taken together.

1. O−H bond lengths

Figure 3 is a histogram showing the spread of the O−H bond lengths for the 55 molecules for which we computed optimized geometries (Table 2). The values fall very neatly into two distinct groups. Nearly all of the hydroxylamine and oxime O−H bonds are between 0.965 and 0.969 Å in length; in the two remaining hydroxylamines, they are 0.970 (R′ = H, R″ = CN) and 0.971 Å (R′ = H, R″ = Cl). There is no differentiation between aldoximes and ketoximes, nor between their isomers.

The hydroxamic acids also all have very similar O−H bond distances, but they are slightly longer, 0.981 to 0.984 Å. This can be attributed to the intramolecular hydrogen

TABLE 2. Molecules for which B3LYP/6-31G(d,p) optimized geometries have been computed

	Oximes		
Hydroxylamines 	Aldoximes 	Ketoximes 	Hydroxamic acids 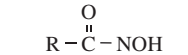
$R' = H$, $R'' = H$	R = H	$R' = CH_3$, $R'' = CH_3$	R = H
$R' = H$, $R'' = CH_3$	R = CH_3 *syn*	$R' = CH_3$, $R'' = C_4H_9$	R = CH_3
$R' = H$, $R'' = C_6H_5$	R = CH_3 *anti*	$R' = C_4H_9$, $R'' = CH_3$	R = C_6H_5
$R' = H$, $R'' = NH_2$	R = C_6H_5 *syn*	$R' = CH_3$, $R'' = C_6H_5$	R = CN
$R' = H$, $R'' = Cl$	R = C_6H_5 *anti*	$R' = C_6H_5$, $R'' = CH_3$	R = NH_2
$R' = H$, $R'' = CN$	R = CH_2Cl *syn*	$R' = CH_3$, $R'' = Cl$	R = CH_2Cl
$R' = H$, $R'' = NO_2$	R = CH_2Cl *anti*	$R' = Cl$, $R'' = CH_3$	R = $C(=O)CH_3$
$R' = H$, $R'' = p\text{-}C_6H_4NO_2$	R = CCl_3 *syn*	$R' = CH_3$, $R'' = CH{=}C(CH_3)_2$	R = $p\text{-}C_6H_4OH$
$R' = CH_3$, $R'' = CH_3$	R = CCl_3 *anti*	$R' = C_6H_5$, $R'' = C_6H_5$	R = $p\text{-}C_6H_4NO_2$
$R' = C_6H_5$, $R'' = C_6H_5$	R = $C(O)CH_3$ *syn*		R = $p\text{-}C_6H_4Cl$
	R = $C(O)CH_3$ *anti*	HON=(C_6H_5)C–$C(C_6H_5)$ = NOH, 1 [a]	
	R = 2-pyridyl *syn-1*	HON=(C_6H_5)C–$C(C_6H_5)$=NOH, 2 [a]	
	R = 2-pyridyl *syn-2*		
	R = 2-pyridyl *anti-1*		
	R = 2-pyridyl *anti-2*		
	HON=C(H)–C(H)=NOH, 1 [a]		
	HON=C(H)–C(H)=NOH, 2 [a]		
	HON=C(H)–$(CH_2)_2$–C(H)=NOH [a]		

[a] Structure is shown in Figure 1.

bonding between the hydroxyl hydrogens and the acetyl oxygens that is known to occur in hydroxamic acids[3–6], as shown in **1**. For example, when we disrupted this hydrogen bonding in the case of acetohydroxamic acid (R = CH_3) by rotating the hydroxyl group away from the acetyl oxygen and reoptimizing the geometry, another energy minimum was obtained, 1.9 kcal mol^{-1} higher [ΔE(298 K), B3LYP/6-311G(3df,2p)][6], and the O–H bond was shortened from 0.984 to 0.969 Å, the latter being exactly in the range observed for the hydroxylamines and oximes. (The intramolecular hydrogen bonding in acetohydroxamic acid was also discussed in Chapter 1, Section V.C.)

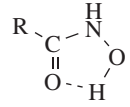

(**1**)

HON=C(H)−C(H)=NOH, *1*

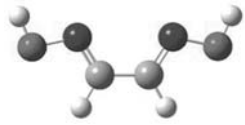

HON=C(H)−C(H)=NOH, *2*

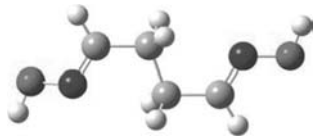

HON=C(H)−$(CH_2)_2$−C(H)=NOH

HON=(C_6H_5)C−C(C_6H_5)=NOH, *1*

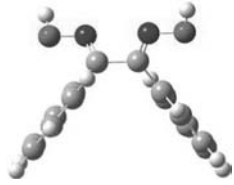

HON=(C_6H_5)C−C(C_6H_5)=NOH, *2*

FIGURE 1. Structures of the five indicated compounds in Table 2

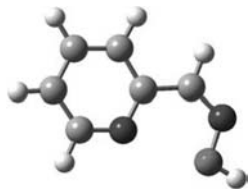

***anti*-2**

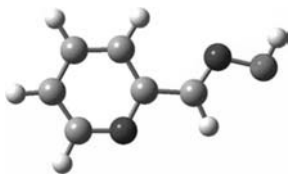

***syn*-1**

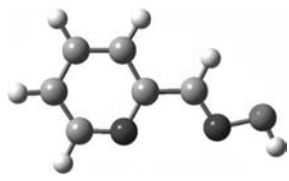

***syn*-2**

FIGURE 2. Structures of the four 2-pyridyl aldoxime isomers in Table 2, shown from top to bottom in order of increasing stability. The black atom in each ring is the nitrogen; the small white atoms are hydrogens. (Figure 2 is continued on the next page.)

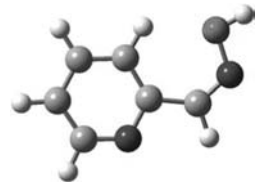

***anti*-1**

FIGURE 2. (*continued*)

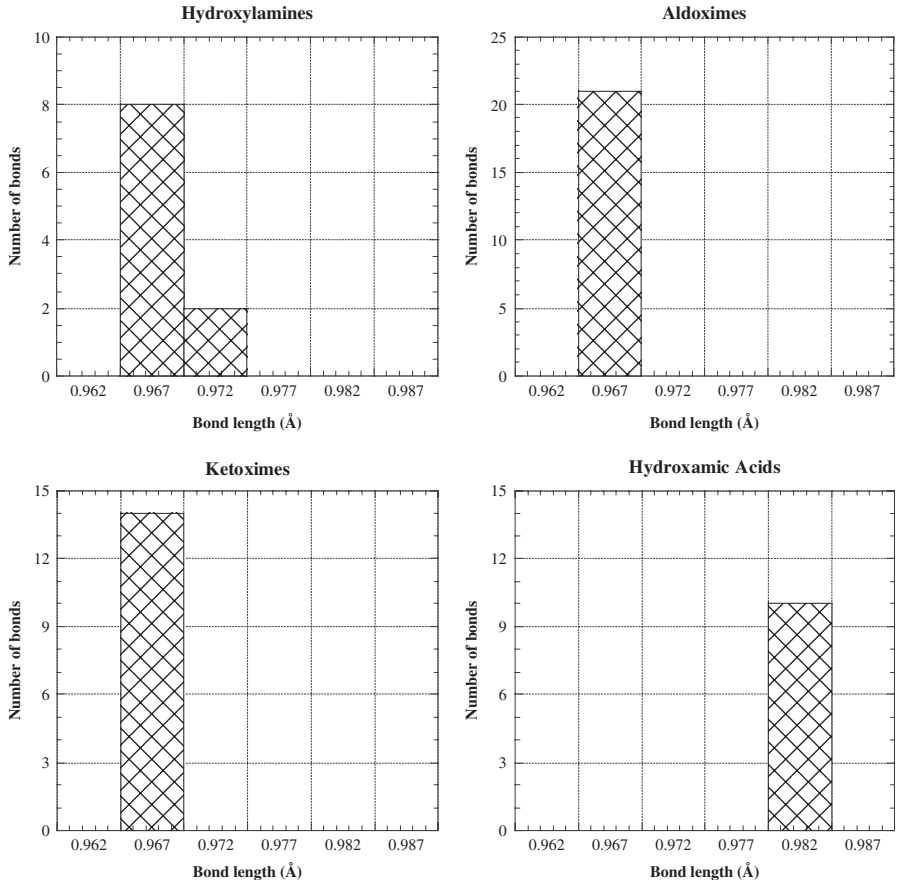

FIGURE 3. Histograms showing distributions of calculated gas phase O−H bond lengths in the hydroxylamines, aldoximes, ketoximes and hydroxamic acids in Table 2. The horizontal axis is the same in each case

The O−H lengthening in the hydroxamic acids that is seen in Figure 3 is typical of what is observed in many hydrogen bond interactions, X−H---Y, and has, in the past, sometimes been viewed as a 'fingerprint' of hydrogen bonding. However, it is now recognized that X−H bond shortening can also occur, depending upon the properties of X−H and Y. Since X−H lengthening is often accompanied by a decrease in the X−H stretching frequency and shortening by an increase, they are frequently labeled 'red-shifting' and 'blue-shifting' hydrogen bonding. For a recent review, see Kryachko[7]. The factors that are involved in red-shifting *vs* blue-shifting have been analyzed in terms of the dipole moment of X−H and the electric field due to Y by Hermansson[8] and by Qian and Krimm[9] and the results of their analyses have been applied to another type of noncovalent interaction, σ-hole bonding (discussed in Section IV), by Murray and coworkers[10].

The hydrogen bonding in hydroxamic acids produces, in effect, five-membered rings (as in **1**) and thus it should not be expected to be linear. For the hydroxamic acids in Table 2, the O−H---O angles are between 118° and 122°.

2. N−O−H bond angles

The N−O−H angles for the 55 molecules in Table 2 do not require a histogram, because they range only between 100° and 103°, except for the hydroxylamine having $R' = H$ and $R'' = NO_2$, for which the angle is 104°. This remarkable uniformity is all the more noteworthy because the molecules encompass a variety of structural features, such as the C=N double bonds in the oximes and the intramolecular hydrogen bonding in the hydroxamic acids.

3. N−O bond lengths

The distribution of N−O distances is in Figure 4. For the aldoximes, ketoximes and hydroxamic acids, they are from 1.38 to 1.42 Å, congregating especially around 1.40 Å. The hydroxylamines are separate, forming two groups, one around 1.43 Å and the other around 1.45 Å, except for two short ones, when $R' = H$ and $R'' = Cl$ or NO_2.

The 'characteristic' gas phase N−O single bond length is given as 1.43 Å[11]. Thus it is the shorter values in Figure 4 that are anomalous. There may be several factors involved. The nitrogens are essentially planar in the oximes and nearly so in most of the hydroxamic acids, in contrast to the usually pyramidal nitrogens in hydroxylamines; this shall be demonstrated in later sections. N(sp^2)−O(2) bonds are typically shorter than N(sp^3)−O(2)[12]. Our longest hydroxamic acid N−O bond, for $R = NH_2$, is indeed for the most pyramidal nitrogen, the sum of its bond angles being 334° compared to 342°−357° for the other hydroxamic acids. For oximes, there may in addition be some charge delocalization[13], as in **2**, which would decrease the N−O bond lengths. (See also Section V.B of Chapter 1.) Some charge delocalization may also be occurring in the two hydroxylamines with short N−O distances, under the influence of the electron-withdrawing Cl and NO_2 substituents, e.g. **3**. This has been invoked to explain the unusually long Cl−N distance, 1.864 Å, in chlorohydroxylamine[6].

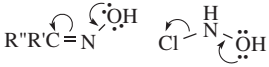

(**2**) (**3**)

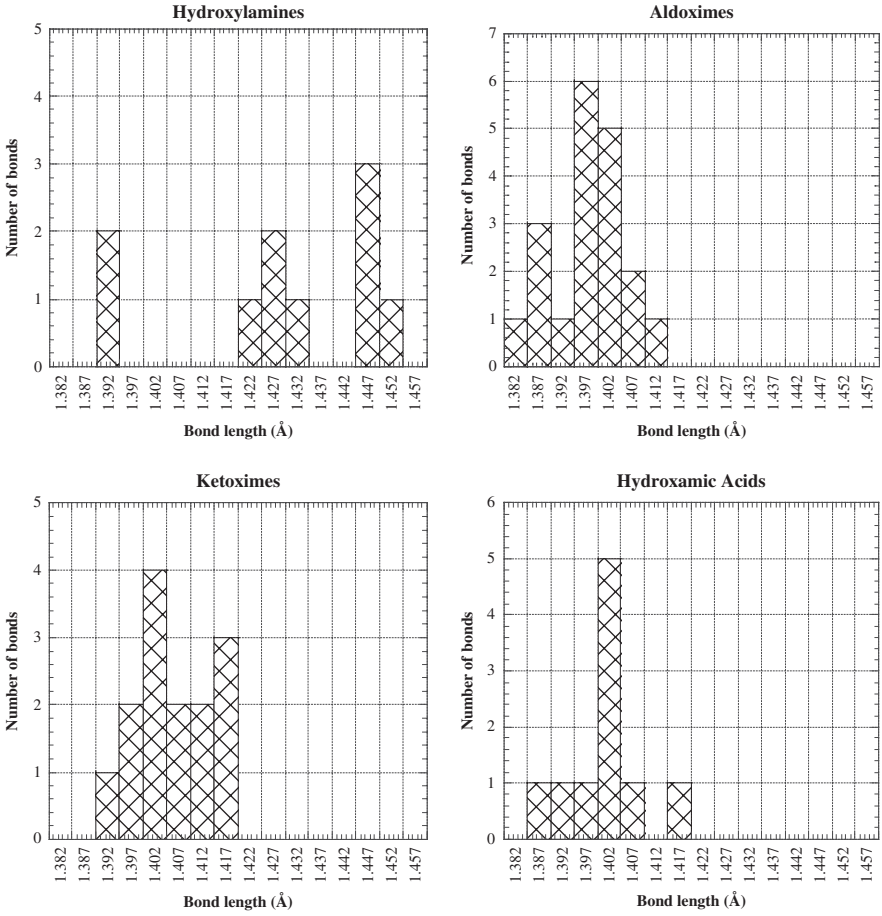

FIGURE 4. Histograms showing distributions of calculated gas phase N−O bond lengths in the hydroxylamines, aldoximes, ketoximes and hydroxamic acids in Table 2. The horizontal axis is the same in each case

C. Hydroxylamine Configuration and Conformations

The nitrogens in the hydroxylamines in Table 2 are pyramidal. The sums of the nitrogen bond angles in nine of the ten hydroxylamines in Table 2 are between 309° and 334°; for comparison, it is 320.1° for NH_3[11]. The molecules in which the NOH is attached to a phenyl group have among the largest values: 329° for $R'' = C_6H_5$, 334° for $R'' = p\text{-}C_6H_4NO_2$ and the outlier, 346° when $R' = R'' = C_6H_5$. These may reflect charge delocalization from the NOH to the ring.

The hydroxylamines illustrate well the importance of intramolecular lone pair—lone pair repulsion. This has been examined in detail for hydroxylamine itself, $H_2N{-}OH$, by Politzer and coworkers[6]; see also Chapter 1, Section IV of this volume. It was demonstrated that the preferred conformation of $H_2N{-}OH$ is **4A**, which maximizes the separation between the nitrogen and oxygen lone pairs and hence minimizes their repulsion. Rotating

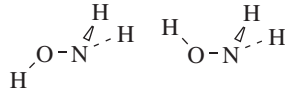

(**4A**) (**4B**)

the OH by 180° to give **4B** does produce another energy minimum, but it is 3.9 kcal mol^{-1} higher in energy [ΔE(298 K), B3LYP/6-311G(3df,2p)].

In **4A**, the OH is in the plane bisecting the H−N−H angle; the H−N−O−H dihedral angles are ±125°. The same qualitative picture as in **4A** holds for most of the other hydroxylamines in Table 2; the OH is oriented so as to minimize lone pair repulsion and is approximately in the R′−N−R″ bisector plane. The two dihedral angles usually have similar magnitudes for each molecule, although differing from one molecule to another. In three instances, however, the dihedral angles differ significantly: R′ = H and R″ = Cl, NH_2 and NO_2. In these molecules, the R′−N−O−H and R″−N−O−H angles are roughly 155° and 90°, respectively. These deviations probably reflect the fact that these R″ introduce additional lone pairs which may interact repulsively with those already present or attractively with the hydroxyl hydrogens.

D. Oximes

The >C=NOH portions of all of the aldoximes and ketoximes in Table 2 are planar. Any nonplanarities in these molecules are within the attached substituents. The lengths of the C=N double bonds fall within a rather narrow range (Figure 5), 1.27–1.29 Å. The longer of these are primarily ketoximes in which both R′ and R″ involve phenyl groups. These distances are significantly longer than what is considered to be characteristic of gas phase C=N double bonds, 1.21 Å[11]. The C−N−O angles are mostly between 110° and 114° (Figure 6), those of the ketoximes tending to be the slightly larger ones. Finally, the C−H bond lengths in the aldoximes are all 1.09 Å, exactly what would be expected[11].

The bond angles around the central carbons in the oximes present some interesting patterns. First, Figure 7 shows that the H−C−R angles in the aldoximes and the R′−C−R″ angles in the ketoximes tend to be 116°–120°. Since these carbons have planar configurations, the sums of the other two angles must be, in nearly all cases, 240°–244°. The distributions of these angles can be seen in Figure 8. In the aldoximes, they are often between 120° and 123°. These are all *syn* isomers; in these, the H−C−N and R−C−N angles are approximately equal. In the *anti* isomers, however, these angles are quite different, the R−C−N being much larger than the H−C−N. This certainly suggests a steric factor. When the OH is on the same side of the double bond as the hydrogen, in the *syn* aldoximes, there is little or no interaction between them and the H−C−N and R−C−N angles can be approximately equal, but when the OH and R are on the same side, in the *anti* isomers, the R−C−N angle expands, to increase their separation; this in turn decreases the H−C−N angle.

The same considerations apply, for the most part, to the ketoximes. The R′−C−N and R″−C−N angles are mainly in one of two groups, 113°–116° and 124°–129°. Now there are substituents and hence steric factors on both sides of the double bond, so the larger angle is always on the side having the OH.

The ketoxime in which R′ = CH_3 and R″ = Cl is worthy of special attention in that it is an example of a molecule needing to choose between two opposing factors. We found two energy minima, corresponding to **5A** and **5B**. **5A** minimizes the repulsion between the nitrogen and oxygen lone pairs. (As shown in Chapter 1, Sections V and VII, the lone pairs of oxime nitrogens are in their nonbonded sp^2 orbitals.) On the other hand, **5B** allows Cl---H hydrogen bonding; their separation is only 2.29 Å, much less

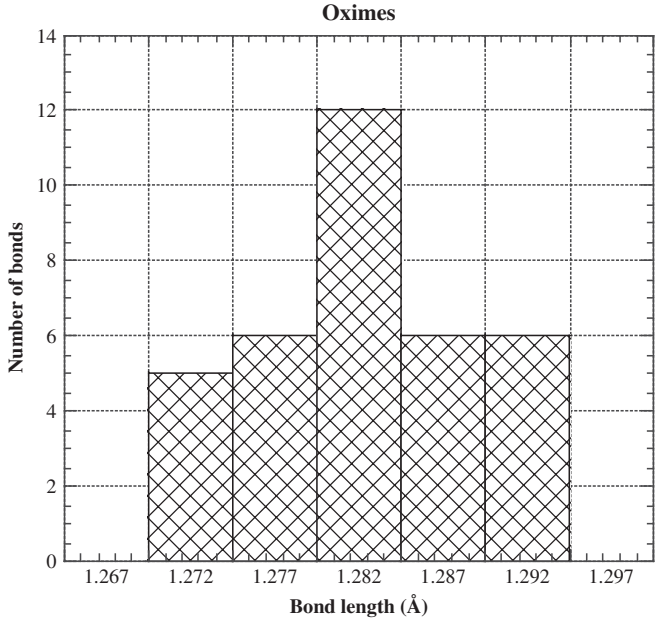

FIGURE 5. Histogram showing distribution of calculated gas phase C=N bond lengths in the aldoximes and ketoximes in Table 2

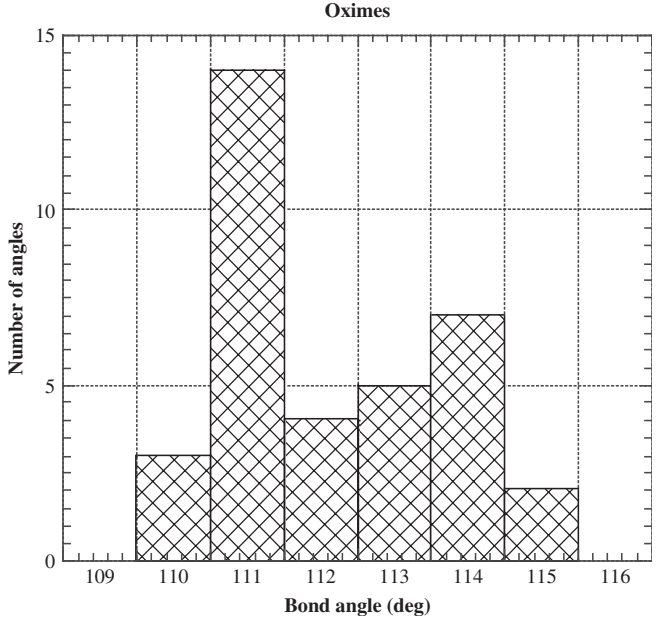

FIGURE 6. Histogram showing distribution of calculated gas phase C−N−O angles in the aldoximes and ketoximes in Table 2

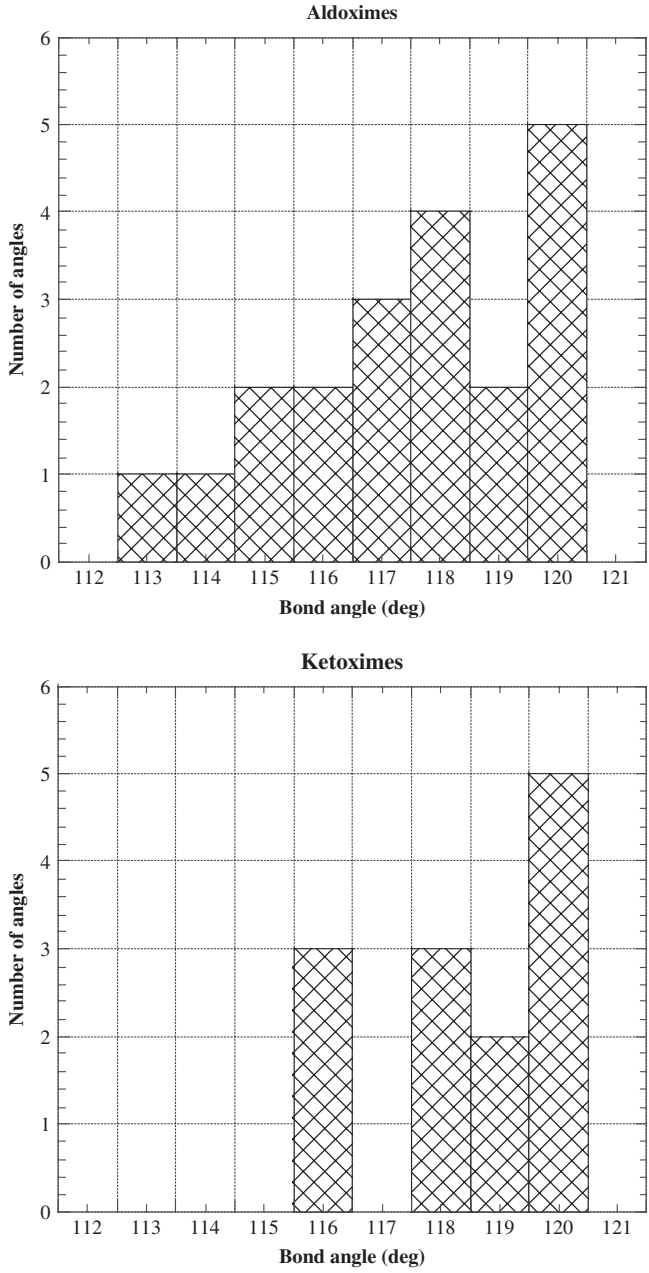

FIGURE 7. Histograms showing distributions of calculated gas phase H−C−R and R′−C−R″ bond angles in the aldoximes and ketoximes in Table 2. Horizontal axes are the same in both cases

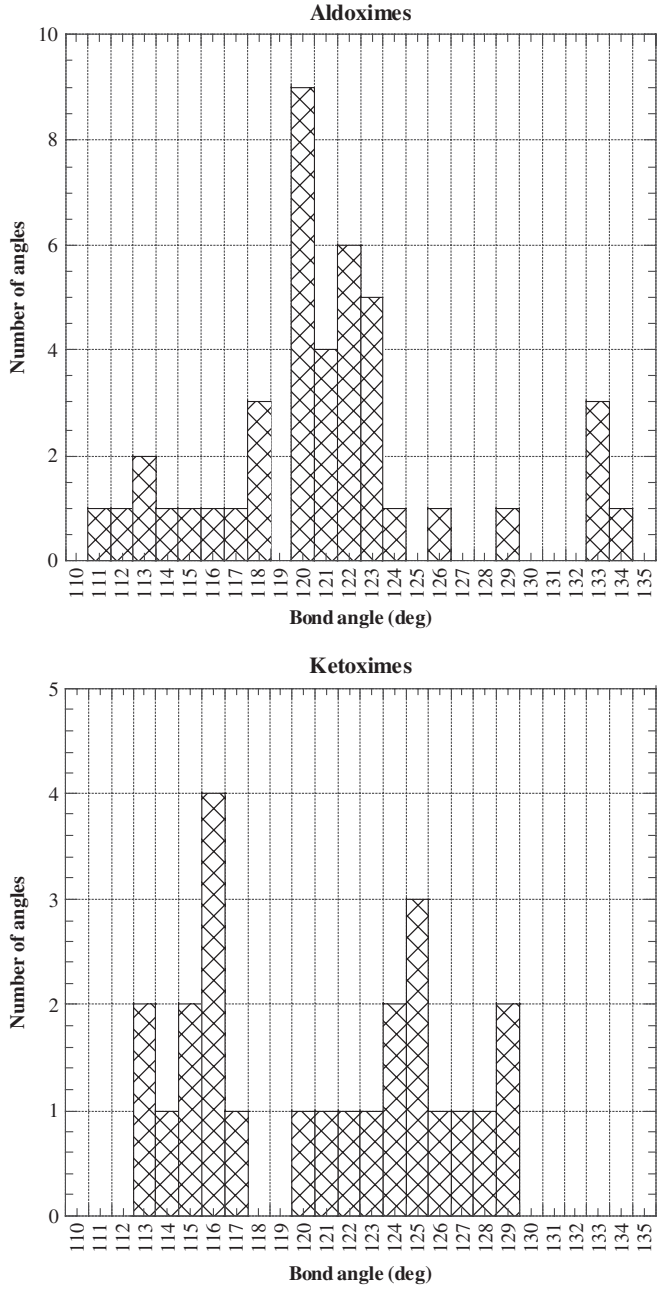

FIGURE 8. Histograms showing distributions of calculated gas phase H−C−N and R−C−N bond angles of the aldoximes and R′−C−N and R″−C−N bond angles of the ketoximes in Table 2. Horizontal axes are the same in both cases

than the sum of their van der Waals radii, 2.95 Å[14]. Which factor will win? In this instance, lone pair repulsion dominates over hydrogen bonding; **5A** is more stable by 1.3 kcal mol^{-1} [ΔE(298 K), B3LYP/6-311G(3df,2p)]. Gas phase oximes typically do have the C−N−O−H conformation of **5A**. In the **5B**-type conformation, the hydroxyl hydrogen would usually interact unfavorably with whatever occupies the position of the Cl, and thus complement the desire to minimize nitrogen/oxygen lone pair repulsion.

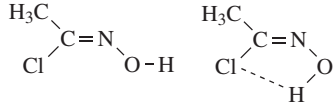

(**5A**) (**5B**)

E. Hydroxamic Acids

The −C(=O)−NOH portions of the hydroxamic acids in Table 2 are near-planar; the C−N−O−H dihedral angle is in no instance greater than 7°. The amine hydrogens are somewhat out of the plane, by an average of about 30°. The near-planarity of the hydroxamic acid frameworks was shown by Politzer and coworkers[6] to be promoted by the intramolecular hydrogen bonding between the hydroxyl hydrogen and the acetyl oxygen (see also Section V.C in Chapter 1).

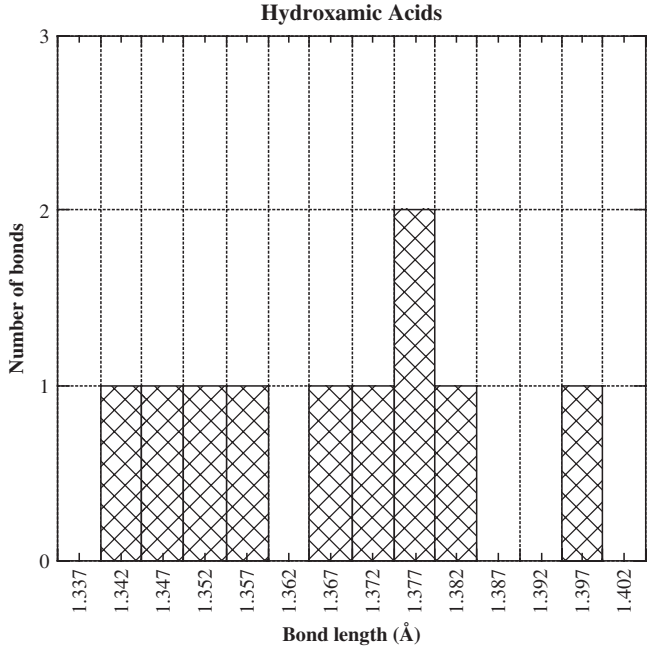

FIGURE 9. Histogram showing distribution of calculated gas phase C−N bond lengths in the hydroxamic acids in Table 2

The C=O distances in the hydroxamic acids congregate around 1.23 Å, slightly longer than the characteristic 1.21 Å[11], and the N−H around 1.01 Å. (In the hydroxylamines, the N−H bonds are all about 1.02 Å, exactly the characteristic value.) In contrast, the C−N bond lengths in the hydroxamic acids are quite dispersed, between 1.34 and 1.40 Å (Figure 9). The C−N−O angles are between 112° and 118°, but 7 of the 10 values are between 114° and 116°.

III. CRYSTAL PHASE STRUCTURES

Due to the unreliability associated with crystallographically-determined positions of hydrogen atoms, our discussion of the molecular structures in crystals will focus on the interatomic distances and angles that do not involve hydrogens. Our data are from the Cambridge Structural Database[15,16] unless stated otherwise.

A. N−O Bond Lengths

The variations in N−O bond lengths can be seen in Figure 10 for hydroxylamines and hydroxamic acids and in Figure 11 for aldoximes and ketoximes. To give an overall picture for just the oximes, the Cambridge Structural Database gives the following summary of the N−O bond lengths in a group of 915 compounds: mean = 1.400 Å, median = 1.404 Å, standard deviation = 0.028 Å.

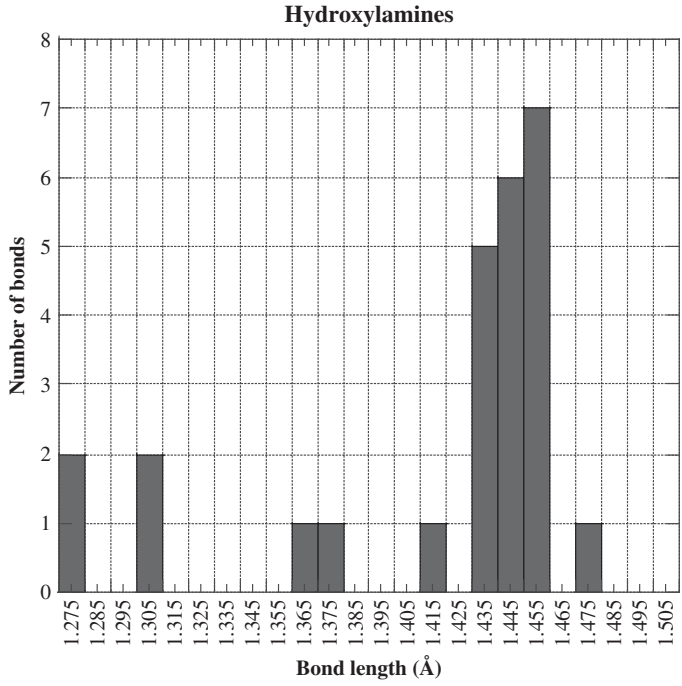

FIGURE 10. Histograms showing the distributions of N−O bond lengths in crystal phase hydroxylamines and hydroxamic acids. The horizontal axes are the same in both cases

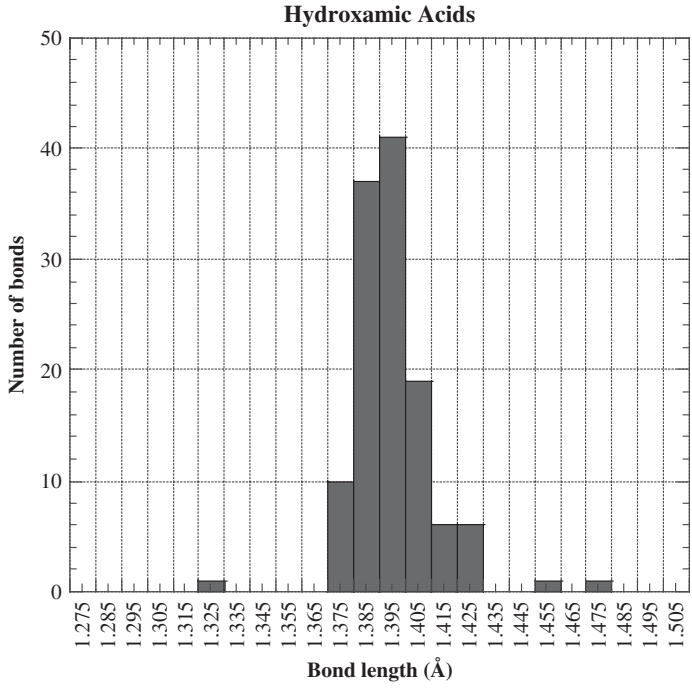

FIGURE 10. (*continued*)

The patterns in Figures 10 and 11 are much like those found in the gas phase; the majority of the aldoximes, ketoximes and hydroxamic acids are between 1.38 and 1.42 Å, with the hydroxylamines mostly slightly higher, 1.43–1.46 Å. The spreads of values are greater than in the gas phase, which is not surprising in view of the intermolecular interactions that must be expected in the crystal.

B. Hydroxylamine Configurations

As was pointed out in Section II.C, the nitrogens in the hydroxylamines in Table 2 are pyramidal to varying degrees. We find the same tendency in the crystalline phase, although we did note an instance in which the effect of the remainder of the molecule is to constrain the nitrogen to planarity. In this case, the nitrogen is part of an unsaturated ring, **6**[17].

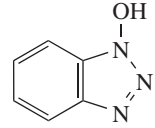

(**6**)

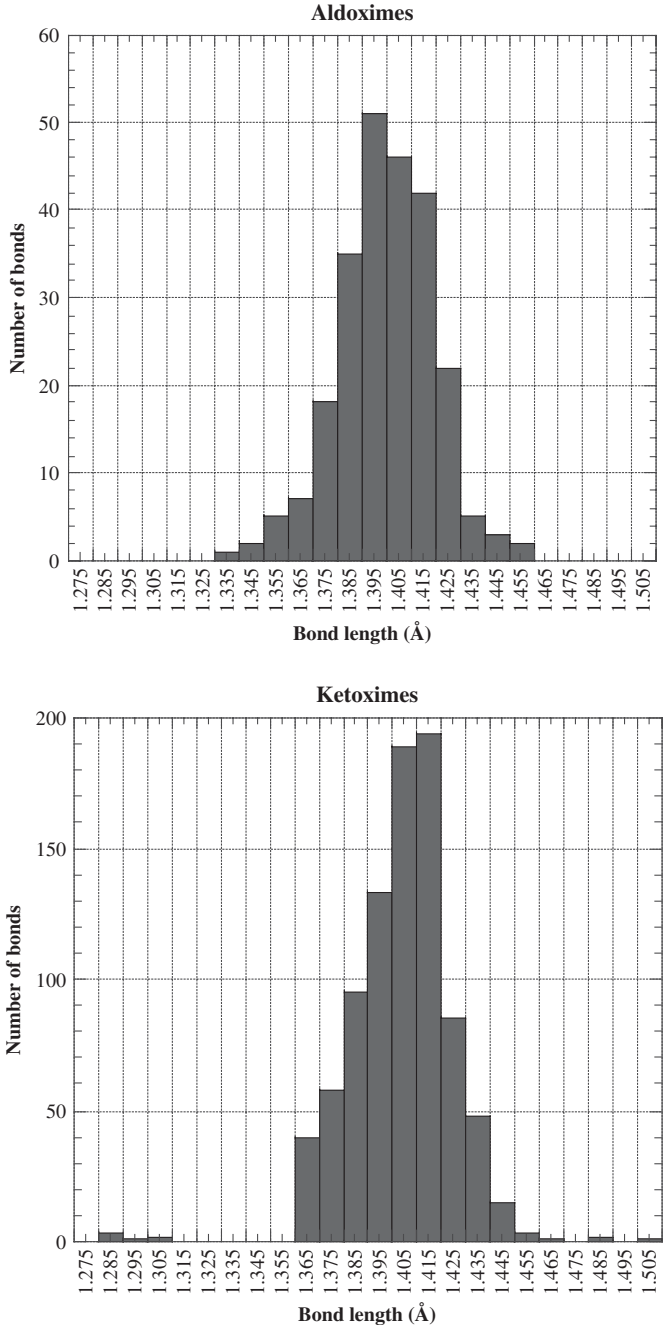

FIGURE 11. Histograms showing the distributions of N−O bond lengths in crystal phase aldoximes and ketoximes. The horizontal axes are the same in both cases

In the crystal phase, hydroxylamines may form intermolecular hydrogen bonds. Two obvious possibilities are the hydroxyl hydrogen of one molecule interacting with the oxygen or nitrogen of the NOH group on a neighbor; an example of the latter is crystalline **7**[18]. In **6**, however, the intermolecular O−H---N interaction involves not the NOH nitrogen but rather the one across from it in the triazole ring[17].

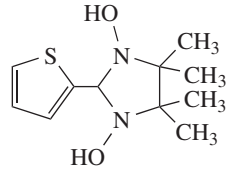

(**7**)

C. Oximes

The molecular geometries of oximes in crystals are quite similar to those in the gas phase. The central carbons are planar. The C=N double bonds are primarily between 1.27 and 1.29 Å in length (Figure 12) and the C−N−O angles are mostly 110°–114° (Figure 13). These histograms, which combine aldoximes and ketoximes, are based on data taken from Bertolasi and coworkers[19]. For comparison, Allen and coworkers give the mean C=N distance in a collection of 67 crystalline oximes as 1.281 Å, with a median of 1.280 Å and standard deviation 0.013 Å[12].

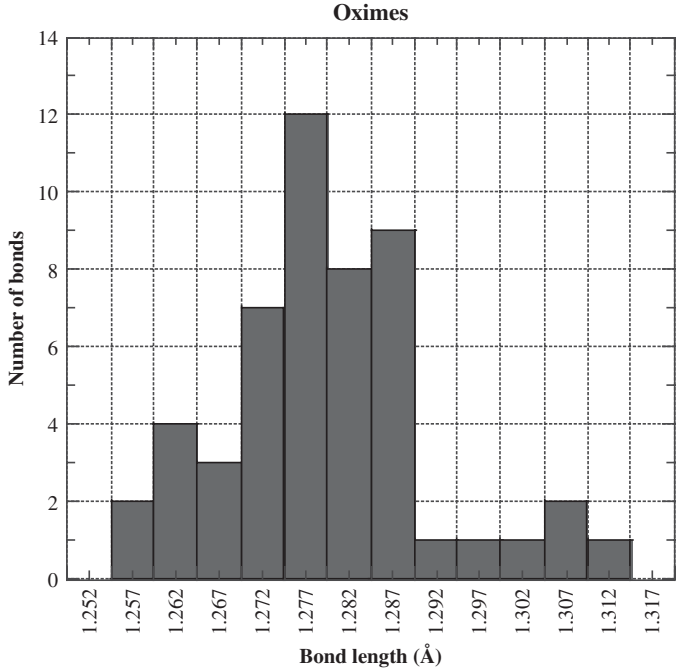

FIGURE 12. Histogram showing distribution of C=N bond lengths in crystal phase oximes

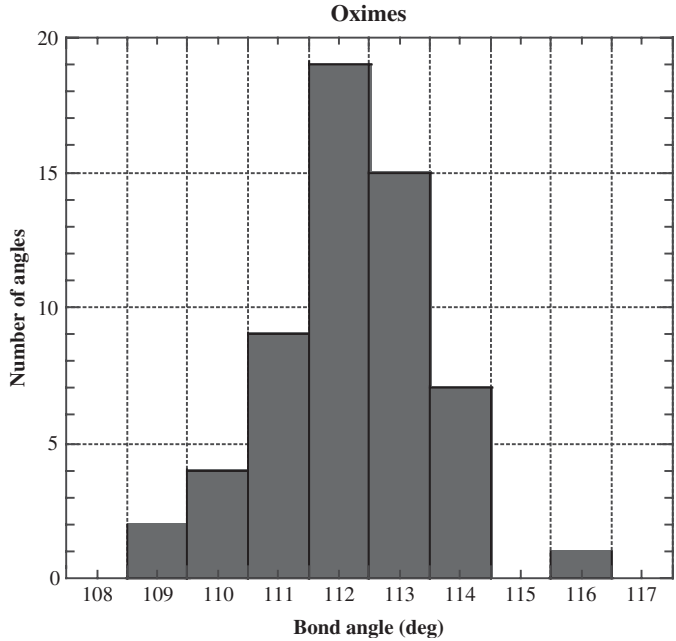

FIGURE 13. Histogram showing distribution of C−N−O bond angles in crystal phase oximes

The R′−C−N and R″−C−N angles again tend to be in two groups, the larger ones being on the same side of the C=N double bond as the OH group. In this context, we noted two interesting exceptions, one in the gas phase (Table 2) and one in the crystalline[20]. Both involve R″ = Cl. Their geometries and the relevant angles, in degrees, are shown below:

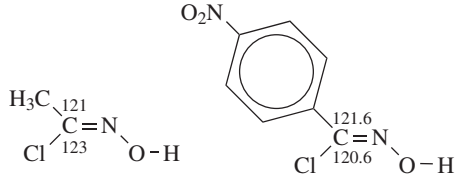

5A, gas phase **8,** crystal phase

In these two examples, the R′−C−N and R″−C−N angles are nearly equal. It might be thought that this is due to O−H---Cl intramolecular hydrogen bonding causing the R″−C−N angles to become smaller than what would normally be the case, but it was pointed out in Section II.D that such hydrogen bonding is energetically not favored, at least for **5** in the gas phase; **5A** is lower in energy than **5B**. It may be that the C−Cl bonds, with lengths of 1.766 Å in **5A** and 1.726 Å in **8**, are sufficiently longer than the C−C more typical of oximes as to greatly diminish the role of the steric factor that seems to be responsible for the differences in the R′−C−N and R″−C−N bond angles that are usually seen.

Intermolecular hydrogen bonding is an important factor in crystalline oximes; Bertolasi and coworkers found it to be present in each of the 57 compounds that they investigated[19]. They identified three different types, i.e. the NOH group acting as a donor or as an acceptor through either the nitrogen or the oxygen. A given NOH group can actually be involved in all three types of interactions, with three other molecules. Much more common, however, occurring in 35 of the 57 oximes, is for each NOH to take part in two hydrogen bonds, forming dimers such as **9** within the crystal. The N---O distances are typically 2.7–2.9 Å. Bertolasi and coworkers observed a rough relationship, the N–O bond tending to lengthen as the number of hydrogen bonds in which the NOH group is participating increases.

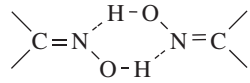

(**9**)

On occasion, a hydrogen bond may be to an acceptor other than an NOH nitrogen or oxygen. This was observed by Bertolasi and coworkers in **10**[19], in which the donor OH interacts with the nitrogen that is linked to the phenyl ring (which has a C–N–C angle of 120°). This results in the crystal containing chains of hydrogen-bonded molecules.

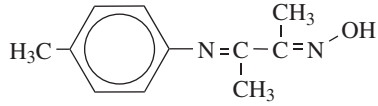

(**10**)

D. Hydroxamic Acids

As in the gas phase, the –C(=O)–NO portions of hydroxamic acids in the crystal phase tend to be near-planar. We have observed this in a series of eight compounds found in the Cambridge Structural Database, and Dietrich and coworkers have reported the same for five out of six others[21], and in the sixth the deviation is rather minor.

There are various opportunities for hydrogen bonding in crystalline hydroxamic acids. The intramolecular O–H---O=C that is seen in the gas phase (Section II.B.1) may be disrupted in favor of intermolecular interactions. Three such have been noted in **11**[22]: O–H---O=C, N–H---O=C and O–H---O(H)N. On the other hand, the thiohydroxamic acid **12** maintains its intramolecular hydrogen bond while also interacting intermolecularly via some C–H---S and C–H---O bonds[23]. When the hydrogen bonding is primarily O–H---O=C, it may simply lead to dimers within the crystal[21,24], but when several different interactions are occurring, as in **11** and **13**, then hydrogen-bonded networks can result. In crystalline **13** are found O–H---O, N–H---O, C=O---C=O and C–H---O links, which produce two-dimensional sheets that then form three-dimensional structures via C–H---π (arene) interactions[25].

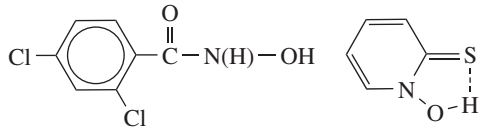

(**11**) (**12**)

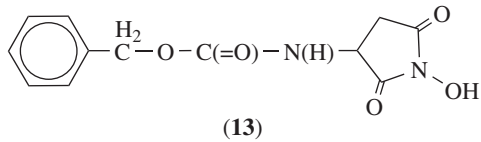

(**13**)

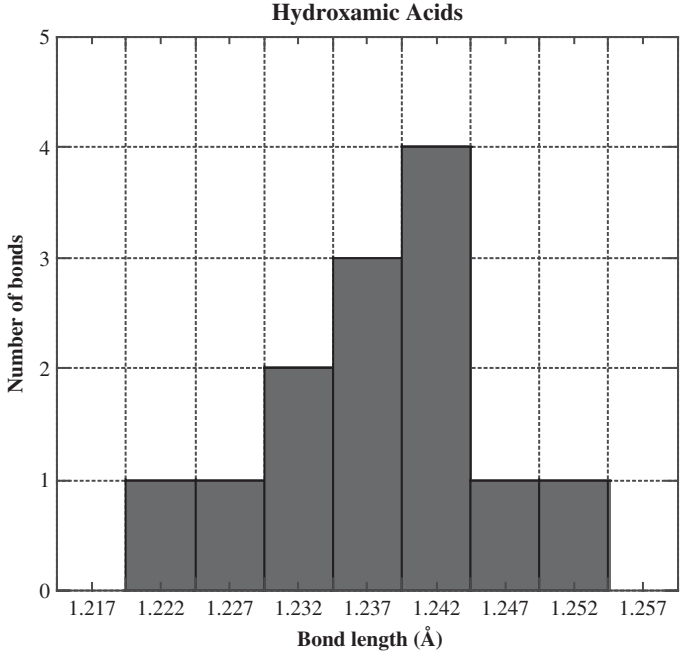

FIGURE 14. Histogram showing distribution of C=O bond lengths in crystal phase hydroxamic acids

The distributions of C=O and C−N bond lengths in a group of 13 crystalline hydroxamic acids are given in Figures 14 and 15. The C=O show slightly greater variation than in the gas phase (Section II.E), 1.22–1.25 Å *vs* 1.23 Å. The C−N bonds tend to be somewhat shorter than in the gas phase, but again have a significant range, now 0.05 Å. The fact that the small overall changes in the C=O and C−N distances in going from the gas phase to the crystal phase are in opposite directions is consistent with the suggestion by Dietrich and coworkers that there is a rough inverse relationship between these bond lengths[21]. Finally, the C−N−O angles have a spread of values, as in the gas phase, but they are a little larger in magnitudes, 115°–123°.

IV. SUMMARY

The basic molecular frameworks of the three classes of compounds examined in this chapter are >N−OH for hydroxylamines, >C=NOH for oximes and $-\overset{|}{C(=O)N}-OH$ for hydroxamic acids. Within the scope of the data that have been presented, the bond lengths

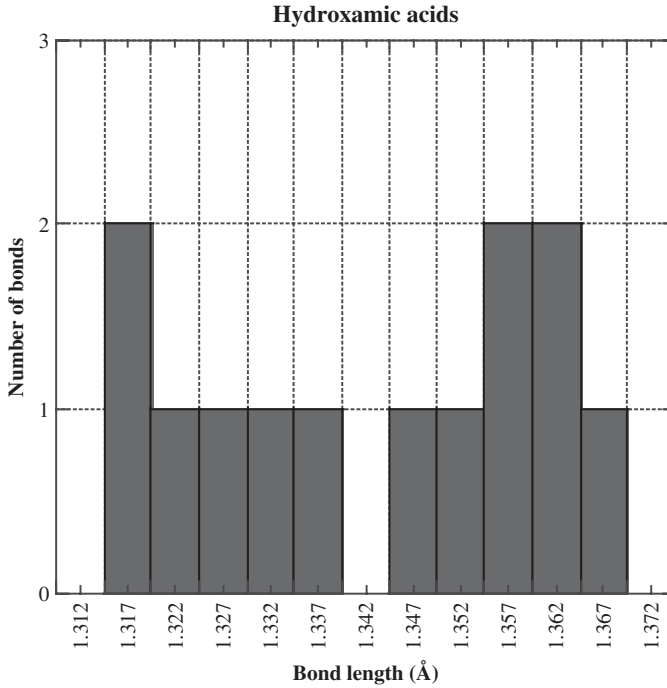

FIGURE 15. Histogram showing distribution of C−N bond lengths in crystal phase hydroxamic acids

and bond angles associated with these frameworks have been found, overall, to be much the same in the crystal as in the gas phase. This can be seen from the histograms in Figures 3–15, and has been pointed out in the discussion for the individual properties, but for convenience, a summary is given in Table 3. The parallels between the gas and the crystal phases are quite evident. Crystal factors appear to be greatest for the hydroxamic acids. The histograms also show the values of some bond lengths and bond angles to be somewhat more dispersed in the crystal phase.

A focus of both Chapters 1 and 2 has been the number of significantly positive and negative sites in hydroxylamines, oximes and hydroxamic acids. The NOH group itself provides three to each molecule—the nitrogen and oxygen lone pairs and the positive hydroxyl hydrogen. The hydroxylamines and hydroxamic acids often have another positive hydrogen, on the amine nitrogen, and the hydroxamic acids also feature lone pairs on the acetyl oxygens. The remainder of each molecule may contain additional positive and/or negative sites.

The structures of these molecules show the effects of intramolecular electrostatic interactions. Two examples are the lone pair—lone pair repulsion that is an important determinant of hydroxylamine and oxime conformations, and the intramolecular hydrogen bonding in hydroxamic acids that promotes the near-planarities of their −C(=O)−NO frameworks.

In the crystals, the prevalent electrostatic intermolecular interaction that has been reported is hydrogen bonding. This has taken several forms, due to the frequent availability of multiple donor and acceptor sites. Thus, O−H---N, O−H---O(H)−N, N−H---N,

TABLE 3. Comparison of gas and crystal phase bond lengths and bond angles encountered most frequently in the present work

Property	Gas phase	Crystal phase
Bond lengths (Å)		
Hydroxylamine N−O	1.42–1.45	1.43–1.46
Aldoxime N−O	1.38–1.42, esp 1.40	1.38–1.42
Ketoxime N−O	1.38–1.42, esp 1.40	1.38–1.42
Hydroxamic acid N−O	1.38–1.42, esp 1.40	1.38–1.41
Oxime C=N	1.27–1.29	1.27–1.29
Hydroxamic acid C−N	1.34–1.40	1.32–1.37
Hydroxamic acid C=O	1.23	1.22–1.25
Bond angles (deg)		
Oxime C−N−O	110–114	110–114
Hydroxamic acid C−N−O	112–118, esp $\sim$ 115	115–123

N−H---O(H)−N, O−H---O=C and N−H---O=C are among the possibilities. Such interactions can have a variety of consequences for crystal packing, which can involve dimers, two-dimensional sheets, three-dimensional networks etc. Examples have been cited.

Before ending this chapter, we would like to draw attention to another type of electrostatic intermolecular interaction that could be quite relevant to hydroxylamines, oximes and hydroxamic acids. We refer to σ-hole bonding. This is a highly-directional, noncovalent interaction between a region of positive electrostatic potential (or σ-hole) on an outer portion of a Group V, VI or VII covalently-bonded atom and a negative site on a neighboring molecule, e.g. the lone pair of a Lewis base[10,26–31]. (When a Group VII atom is involved, this is often called 'halogen bonding.') σ-Hole bonding has now been observed in numerous crystalline compounds[28,32,33] and there is a growing recognition of the importance of halogen bonding, in particular, in molecular biology[27,28]. The possibility of σ-hole bonding is now being increasingly exploited in crystal engineering[28,30,34]. It is certainly to be anticipated that attractive interactions can take place between positive σ-holes on appropriate Group V, VI and VII atoms and the nitrogen and oxygen lone pairs in hydroxylamines, oximes and hydroxamic acids. It is important to be aware of such interactions that may already be present, as well as to make use of them in designing new systems.

V. ACKNOWLEDGMENT

We greatly appreciate the assistance of Dr. Cheryl Klein Stevens in obtaining data from the Cambridge Structural Database.

VI. REFERENCES

1. Gaussian 03, Revision C.02, M. Frisch, G. W. Trucks, H. B. Schlegel, G. E. Scusceria, M. A. Robb, J. R. Cheeseman, J. A. Montgomery, Jr., T. Vreven, K. N. Kuden, J. C. Burant, J. M. Millam, S. S. Iyengar, J. Tomasi, V. Barone, B. Mennucci, M. Cossi, G. Scalmani, N. Rega, G. A. Petersson, H. Nakatsuji, M. Hada, M. Ehara, K. Toyota, R. Fukuda, J. Hasegawa, M. Ishida, T. Nakajima, Y. Honda, O. Kitao, H. Nakai, M. Klene, X. Li, J. E. Knox, H. P. Hratchian, J. B. Cross, V. Bakken, C. Adamo, J. Jaramilo, R. Gomperts, R. E. Stratmann, O. Yazyev, A. J. Austin, R. Cammi, C. Pomelli, J. W. Ochterski, P. Y. Ayala, K. Morokuma, G. A. Voth, P. Salvador, J. J. Dannenberg, V. G. Zakrzewski, S. Dapprich, A. D. Daniels, M. C. Strain, O. Farkas, D. K. Malick, A. D. Rabuck, K. Raghavachari, J. B. Foresman, J. V.

Ortiz, Q. Cui, A. G. Baboul, S. Clifford, J. Ciolowski, B. B. Stefanov, G. Liu, A. Liashenko, P. Piskorz, I. Komaromi, R. L. Martin, D. J. Fox, T. Keith, M. A. Al-Laham, C. Y. Peng, A. Nanayakkara, M. Challacombe, P. M. Gill, B. Johnson, W. Chen, M. W. Wong, C. Gonzalez and J. A. Pople, Gaussian, Inc., Wallingford, CT, 2004.
2. W. J. Hehre, L. Radom, P. v. R. Schleyer and J. A. Pople, *Ab Initio Molecular Orbital Theory*, Wiley–Interscience, New York, 1986.
3. M. Remko and J. Šefčiková, *J. Mol. Struct. (Theochem)*, **528**, 287 (2000).
4. M. Remko, *J. Phys. Chem. A*, **106**, 5005 (2002).
5. B. García, S. Ibeas, J. M. Leal, F. Secco, M. Venturini, M. L. Senent, A. Niño and C. Muñoz, *Inorg. Chem.*, **44**, 2908 (2005).
6. P. Politzer, J. S. Murray and M. C. Concha, *J. Phys. Org. Chem.*, **21**, 155 (2008).
7. E. S. Kryachko, chap. 8 in *Hydrogen Bonding—New Insights* (Ed. S. J. Grabowski), Springer, Dordrecht, 2006.
8. K. Hermansson, *J. Phys. Chem. A*, **106**, 4695 (2002).
9. W. Qian and S. Krimm, *J. Phys. Chem. A*, **106**, 6628 (2002).
10. J. S. Murray, M. C. Concha, P. Lane, P. Hobza and P. Politzer, *J. Mol. Model.*, in press.
11. D. R. Lide (Ed.), *Handbook of Chemistry and Physics*, 87th edn., CRC Press, Boca Raton, 2006.
12. F. H. Allen, O. Kennard, D. G. Watson, L. Brammer, A. G. Orpen and R. Taylor, *J. Chem. Soc., Perkin Trans. 2*, S1 (1987).
13. F. A. Carey and R. J. Sundberg, *Advanced Organic Chemistry*, 4th edn., Kluwer/Plenum, New York, 2000.
14. A. Bondi, *J. Phys. Chem.*, **68**, 441 (1964).
15. F. H. Allen, *Acta Crystallogr., Sect. B*, **58**, 380 (2002).
16. I. J. Bruno, J. C. Cole, M. Kessler, J. Luo, W. D. S. Motherwell, L. H. Purkis, B. R. Smith, R. Taylor, R. I. Cooper, S. E. Harris and A. G. Orpen, *J. Chem. Inf. Comput. Sci.*, **44**, 2133 (2004).
17. R. Bosch, G. Jung and W. Winter, *Acta Crystallogr., Sect. C*, **39**, 1089 (1983).
18. K. Jiang, X.-Q. Wang, L.-Y. Wang and Y.-F. Wang, *Acta Crystallogr., Sect. E*, **62**, o4814 (2006).
19. V. Bertolasi, G. Gilli and A. C. Veronese, *Acta Crystallogr., Sect. B*, **38**, 502 (1982).
20. G. D. Andretti, L. Gavalca, A. Manfredotti and A. Musatti, *Acta Crystallogr., Sect. B*, **25**, 288 (1969).
21. A. Dietrich, D. R. Powell, D. L. Eng-Wilmot, M. B. Hossain and D. van der Helm, *Acta Crystallogr., Sect. C*, **46**, 816 (1990).
22. X.-M. Shang, X.-G. Meng, J.-Z. Wu and Q.-S. Li, *Acta Crystallogr., Sect. E*, **61**, o1961 (2005).
23. A. Bond and W. Jones, *Acta Crystallogr., Sect. C*, **55**, 1536 (1999).
24. W. E. Hunt, C. H. Schwalbe and K. Vaughan, *Acta Crystallogr., Sect. C*, **39**, 738 (1983).
25. P. Stefanowicz, M. Jaremko, L. Jaremko and A. Kochel, *Acta Crystallogr., Sect. C*, **63**, o204 (2007).
26. T. Brinck, J. S. Murray and P. Politzer, *Int. J. Quantum Chem., Quantum Biol. Symp.*, **19**, 57 (1992).
27. P. Auffinger, F. A. Hays, E. Westhof and P. Shing Ho, *Proc. Natl. Acad. Sci. U.S.A.*, **101**, 16789 (2004).
28. P. Metrangolo, H. Neukirsch, T. Pilati and G. Resnati, *Acc. Chem. Res.*, **38**, 386 (2005).
29. P. Politzer, P. Lane, M. C. Concha, Y. Ma and J. S. Murray, *J. Mol. Model.*, **13**, 305 (2007).
30. J. S. Murray, P. Lane, T. Clark and P. Politzer, *J. Mol. Model.*, **13**, 1033 (2007).
31. J. S. Murray, P. Lane and P. Politzer, *Int. J. Quantum Chem.*, **107**, 2286 (2007).
32. T. N. Guru Row and R. Parthasarathy, *J. Am. Chem. Soc.*, **103**, 477 (1981).
33. P. Murray-Rust, W. C. Stallings, C. T. Monti, R. K. Preston and J. P. Glusker, *J. Am. Chem. Soc.*, **105**, 3206 (1983).
34. P. Politzer, J. S. Murray and M. C. Concha, *J. Mol. Model.*, **13**, 643 (2007).

CHAPTER 3

The organic thermochemistry of hydroxylamines, oximes, hydroxamic acids and their derivatives

SUZANNE W. SLAYDEN

Department of Chemistry, George Mason University, 4400 University Drive, Fairfax, Virginia 22030, USA
Fax: (+1)703-993-1055; e-mail: sslayden@gmu.edu

and

JOEL F. LIEBMAN

Department of Chemistry and Biochemistry, University of Maryland, Baltimore County, 1000 Hilltop Circle, Baltimore, Maryland 21250, USA
Fax: (+1)410-455-2608; e-mail: jliebman@umbc.edu

The chemistry of hydroxylamines, oximes and hydroxamic acids
Edited by Z. Rappoport and J. F. Liebman

I. INTRODUCTION: SCOPE OF THE CHAPTER, DEFINITIONS OF KEY TERMS AND SOURCES OF DATA

A. Thermochemical Properties of Interest

As has been the approach for the authors' other reviews on organic thermochemistry (many of which are referenced throughout the current text) this chapter is dominated by discussions of the 'molar standard enthalpy of formation' (also called 'heat of formation') and written symbolically as $\Delta_f H_m^\circ$ (also as ΔH_f or ΔH_f°). This chapter largely foregoes discussion of Gibbs energy and entropy and ignores concerns of heat capacity and excess enthalpy. We have also chosen to ignore questions of acid or base strength and of any complex or chelate forming energy.

The temperature and pressure are assumed to be 25 °C ('298K') and 1 atmosphere or 1 bar (101,325 or 100,000 Pa), respectively. Enthalpies are always given in the thermochemist's preferred units of $kJ\,mol^{-1}$ where 4.184 kJ equals 1 kcal by definition. The descriptors s, lq, g and aq refer to solid, liquid, gas and aqueous, respectively.

Unreferenced enthalpies of formation of organic compounds are taken from the now 'classic' thermochemical archive by Pedley[1]. Other, generally early, data are taken from the archive by Stull, Westrum and Sinke[2]. It is noteworthy, but left unexplained, how few of the species discussed in Stull, Westrum and Sinke appear in Pedley's book written some decades later. Much of the recent data are taken from the NIST WebBook[3] wherein some data evaluation and 'correction' were occasionally performed; the primary reference is given for more complete attribution. Other enthalpy of formation data for a variety of one- through four-carbon species are taken from the recent study[4] by Shaikhlislamov, Talipov and Khursan, where we use their accompanying (but otherwise unreferenced) experimental data with which they compared their highly accurate quantum-chemically derived findings: citations to this source will make clear whether it is their cited (but still sparse) calorimetric or calculational results. We also include in our discussion 'old' numbers ignored by all of these authors where they are the only data for a given species, as well as some new numbers appearing in none of the above archival compendia. Where there are conflicting data, the most recent value is generally preferred,

where we assume that the later authors were cognizant of earlier studies as well as of their presumed greater capability of achieving better sample purity and instrumental precision.

B. The Data

Compared to many other functional groups for which we have reviewed their thermochemistry, we find that our archival sources give us the enthalpy of relatively few species and there are few new values to complement and supplement these sources. Table 1 gives the enthalpy of formation data for hydroxylamines. Tables 2–4 present the admittedly sparse data on monooximes, dioximes and ketooximes, respectively, while Table 5 gives the data for other oxime derivatives. Table 6 is for hydroxamic acids and their derivatives. Furthermore, within each table, the compounds are arranged according to the Chemical Abstracts 'Hill' sort scheme. There will be additional vignettes for each class of compounds that follow the individual tables. These admittedly brief discussions will refer to special species, very often involving estimates and for which the resulting numbers will not appear in the tables because they lack the provenance of literature citations.

In thermochemical discussions, the gas phase is preferred—we wish to avoid what we consider the diverting considerations of intermolecular interactions whenever possible. Indeed, when the phase is left unsaid, the reader should assume we are talking about this ideal and idyllic state. Most often, however, only the condensed phase data are available for the hydroxylamine, oxime or hydroxamic acid that is discussed in this chapter. The unavoidably selected phase will be denoted explicitly. Not uncommonly, we need enthalpy of formation data for the solid phase of some ancillary species and have but liquid (or the other way). Accordingly, we have accepted the enthalpy of fusion data from the compendium cited as Reference 5 without making any temperature corrections as the necessary approximations to do so are generally small and too ill-defined to be of much use. To further simplify the reading and writing of text, we do not give attribution to this source or the primary source found therein. The implicit reference for all inorganic (and aqueous) species in the chapter is Reference 6.

II. HYDROXYLAMINES AND *N*-SUBSTITUTED DERIVATIVES

A. Hydroxylamine

There are few enthalpy of formation data for substituted hydroxylamines of any type—Table 1 presents the available values for these species where we start with the parent compound hydroxylamine itself. Even though hydroxylamine is not organic we start with this species, since it is the parent compound for all of the classes of compounds that fill this chapter and indeed, the current volume. With its recommended[4] gas phase enthalpy of formation of $-41.8\ \mathrm{kJ\,mol^{-1}}$, hydroxylamine is seen to be more stable than the average of its 'homonuclear' counterparts, hydrogen peroxide[6] ($\Delta H_f(g) = -136.3\ \mathrm{kJ\,mol^{-1}}$) and hydrazine[6] ($\Delta H_f(g) = 95.4\ \mathrm{kJ\,mol^{-1}}$). Said differently, the N–O bond energy is larger than the arithmetic average of the N–N and O–O bonds. As such, the relative values are an immediate corollary of the use of Pauling's electronegativity equation and its contemporary analysis and extension[7] to polyatomic species of more general interest to the organic chemistry community.

B. *N*- (and *O*-)Methylated Hydroxylamines and Other Alkyl Derivatives

Thermochemical data on aliphatic hydroxylamines is sparse. Indeed, it is almost totally limited to methylated species and so we include both *N*- and *O*-methyl substituted species

TABLE 1. Enthalpies of formation for hydroxylamines (kJ mol^{-1})

Compound	Formula	ΔH_f(s)	Reference	ΔH_f(lq)	Reference	ΔH_f(g)	Reference
Hydroxylamine	NH_3O	−114.2	6			−41.8	4
N-Methylhydroxylamine	CH_5NO					−50.2	4
O-Methylhydroxylamine	CH_5NO					−25.1	4
N,*O*-Dimethylhydroxylamine	C_2H_7NO					−37.7	4
N,*N*-Diethylhydroxylamine	$C_4H_{11}NO$			−174.8 ± 7	11	−121.8 ± 7	11
N-(2-Nitrophenyl)hydroxylamine	$C_6H_6N_2O_3$			−13.3	2		
N-Phenylhydroxylamine	C_6H_7NO			7.1	2		
1-Hydroxy-2,2,6,6-tetramethyl-4-piperidone	$C_9H_{17}NO_2$	−378.1 ± 0.5	1			−298.0 ± 4.6	1
1-Hydroxy-2,2,6,6-tetramethyl-4-piperidinol	$C_9H_{19}NO_2$	−445.1 ± 1.4	1			−345.0 ± 1.5	1

in this section. It is not surprising that gaseous *O*-methylhydroxylamine is less stable than its *N*-isomer by *ca* 25 kJ mol^{-1}. '*O*-Methylmethanol' is some 51 kJ mol^{-1} less stable than its isomer '*C*-methylmethanol', where we now recognize these latter species as the more commonly named dimethyl ether and ethanol, respectively. The element nitrogen interpolates carbon and oxygen in terms of size and electronegativity and so the value of 25 kJ mol^{-1} falls right between this difference and the necessarily 0 kJ mol^{-1} difference for *O*- and *O'*-methylated hydrogen peroxide (as these last two compounds are the same species, methyl hydroperoxide).

The formal gas phase transmethylation reaction, the sole transalkylation reaction available to us (equation 1), is thermoneutral to within 5 kJ mol^{-1}.

$$\mathrm{MeNHOH + MeONH_2 \longrightarrow NH_2OH + MeNHOMe} \qquad (1)$$

While there are numerous alcohols and ethers for which enthalpies of formation are known[8], the bleak thermochemical situation for hydroperoxides[8,9] (and hydrazines[10]) parallels that of the hydroxylamines. An obvious comparison is between the heteroatom bonds in peroxide, hydrazine and hydroxylamine as shown in equation 2.

$$\mathrm{R^1NHNHR^1 + R^2OOR^2 \longrightarrow 2R^1NHOR^2} \qquad (2)$$

For both $\mathrm{R^1 = R^2 = H}$ and $\mathrm{R^1 = R^2 = Me}$, the enthalpy of reaction is the identical −42.7 and −41.9 kJ mol^{-1}. When $\mathrm{R^1 = Me}$, $\mathrm{R^2 = H}$, the reaction enthalpy is more exothermic, −56.3 kJ mol^{-1}, and for the reverse substitution, $\mathrm{R^1 = H}$, $\mathrm{R^2 = Me}$, the enthalpy is less exothermic, −19.9 kJ mol^{-1}.

There are thermochemical data for only one nonmethyl aliphatic hydroxylamine, *N*,*N*-diethylhydroxylamine[11]. The enthalpy of formation difference between it and *N*-methylhydroxylamine is 71.6 kJ mol^{-1}. This is very nearly the same as the difference of 79.7 kJ mol^{-1} between the corresponding primary and secondary alcohols[8], ethanol and 3-pentanol, where the N of the hydroxylamine is replaced by a CH. Thus, the formal reaction enthalpy of equation 3 is only 8.1 kJ mol^{-1}.

$$\mathrm{Et_2CHOH + MeNHOH \longrightarrow Et_2NOH + MeCH_2OH} \qquad (3)$$

As it may be a useful comparison, it is asked what is the enthalpy change for the formal, simple insertion of an oxygen atom in the NH bond of an amine (*N*-hydroxylation)? For ammonia, the change to hydroxylamine is only +4 kJ mol^{-1}. The exothermicity of the comparable change for the primary methyl amine is −27.2 kJ mol^{-1} (g) and for the secondary diethyl amine it is −49.3 kJ mol^{-1}.

C. Aryl Hydroxylamines

We now turn to the two aryl hydroxylamines, *N*-phenylhydroxylamine and its *o*-nitro derivative. As liquids, the former compound has an enthalpy of formation that is *ca* 20 kJ mol^{-1} more positive than that of the latter. For comparison, we find the enthalpies of the corresponding liquid species without the NHOH group, *i.e.* benzene and nitrobenzene, differ by 36.5 kJ mol^{-1}. Alternatively said, equation 4 is endothermic by 16.1 kJ mol^{-1}.

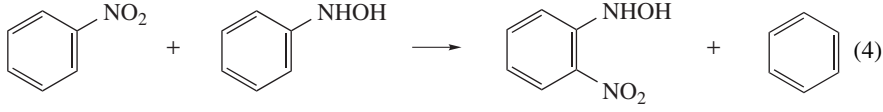

(4)

Similarly, removing only the NH and thus comparing the resulting phenols with hydroxylamines, as in equation 5, the formal reaction enthalpy is 13.3 kJ mol^{-1} using the enthalpies of fusion in Reference 5.

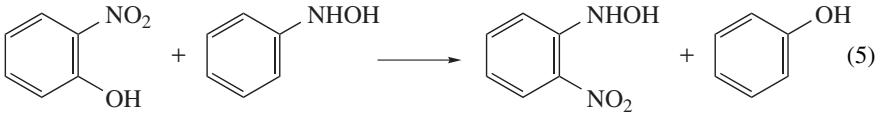

(5)

We might have thought that the *o*-nitro group would provide stabilization for the hydroxylamine and the phenol by two mechanisms: (a) enhanced (*i.e.* zwitterionic, dipolar, quinonoid-like) resonance as is often discussed for *o*- and *p*-nitroaniline, *cf.* Reference 12, and (b) intermolecular $O^{\delta-} \cdots H-O$ hydrogen bonding between the nitro and hydroxyl groups.

However, as seen from the data in Reference 1, reaction 6

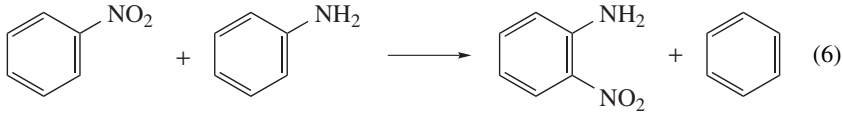

(6)

is exothermic by only *ca* 4 kJ mol^{-1}. There are acknowledged difficulties with the enthalpies of formation of the nitroanilines[12b]. As evidenced by the relative basicities of hydroxylamines[13,14] and related amines[13], the *N*-hydroxyl group inductively destabilizes positively charged nitrogen[15]. This suggests that nitrophenylhydroxylamine 'enjoys' less resonance-derived stabilization than expected. The chronicled enthalpy of formation difference between phenylhydroxylamine and its *o*-nitro derivative is thus plausible. The difference is also apparent in the formal *N*-hydroxylation reaction. For these two primary aromatic amines as liquids, the difference is *ca* 4 kJ mol^{-1} for the nitroaniline and -24 kJ mol^{-1} for aniline itself. Nonetheless, additional measurements on the enthalpies of formation of other hydroxylamines are still welcomed because we cannot appraise the systematics of reactions of the type in equation 7.

$$Ar^1NHOH + Ar^2NH_2 \longrightarrow Ar^1NH_2 + Ar^2NHOH \tag{7}$$

D. Hydroxylated Piperidines

We now turn to the remaining two hydroxylamines that are *N*-hydroxylated derivatives of 2,2,6,6-tetramethyl-4-piperidone and -4-piperidinol. The enthalpies of formation of some simple 4-piperidones and their corresponding 4-piperidinols have recently been determined. The values of gaseous *N*-methyl-4-piperidone[16] and *N*-methyl-4-piperidinol[17] are -160.7 ± 1.7 and -226.8 ± 1.8 kJ mol^{-1} (also see Reference 18). The difference between these contemporary values is -66.1 ± 2.5 kJ mol^{-1} while for the hydroxylated and methylated counterpart species the difference is -47.0 ± 4.8 kJ mol^{-1}. For comparison, the formal enthalpy of reduction of 3-hexanone to 3-hexanol is *ca* -54 kJ mol^{-1}. As has been discussed earlier, reduction enthalpies are not necessarily constant[19]. Relatedly, reaction 8 that exchanges *N*-methyl and *N*-hydroxy and parent and tetramethylpiperidines is endothermic by 19.1 ± 5.4 kJ mol^{-1}. The deviation from thermoneutrality is more

disparate than we would have anticipated even though we don't know the steric effect of four abutting methyl groups on the conformation of the two *N*-hydroxypiperidines.

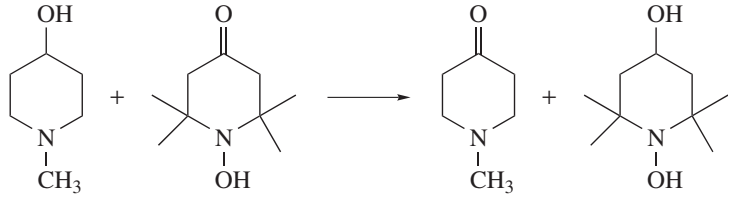

(8)

We close this section with a statement of surprise and disappointment. For no apparent reason there are no published[20] enthalpy of formation measurements for 1-hydroxy-2,2,6,6-tetramethylpiperidine, the 'parent' species for the above 1-hydroxylated piperidines and the hydroxylamine counterpart to probably the most famous nitroxide radical, 'TEMPO'.

III. *O*-SUBSTITUTED HYDROXYLAMINE DERIVATIVES (ALKOXYLAMINES)

A. Aliphatic Examples

The alkoxylamines have a >N−O−C substructure and may be considered O-substituted hydroxylamine ethers. The simplest example of these species is $MeONH_2$ with a gas phase enthalpy of formation[4] of $-25.1\ kJ\,mol^{-1}$ which was discussed in a previous section. Consider now the perfluorinated species $(CF_3)_2NOCF_2CF_2ON(CF_3)_2$ and its synthesis shown in equation 9.

$$2(CF_3)_2NO^{\bullet} + C_2F_4 \longrightarrow (CF_3)_2NOCF_2CF_2ON(CF_3)_2 \qquad (9)$$

With an adequately stable nitroxide radical, this reaction is facile enough that it can be investigated in a calorimetric context, from which a reaction enthalpy of $246 \pm 6\ kJ\,mol^{-1}$ has been determined[21]. Accepting the suggested lower limit for the enthalpy of formation of $-1190 \pm 40\ kJ\,mol^{-1}$ for the fluorinated nitroxide (as derived from ion energetics threshold measurements[22]) and the enthalpy of formation of tetrafluoroethylene ($-656.9 \pm 4.9\ kJ\,mol^{-1}$)[1], we hereby deduce the gas phase enthalpy of formation of the bis hydroxylamine ether to be $-3283 \pm 80\ kJ\,mol^{-1}$. This value—actually these values, the enthalpy of formation and the error bar—seems frightfully large. With regard to the first quantity, there are sixteen C−F bonds and this confers considerable stabilization and a large negative enthalpy of formation. For comparison, the enthalpy of formation of perfluoroheptane, likewise with sixteen C−F bonds, is $-3383.6 \pm 3.6\ kJ\,mol^{-1}$. How do we calibrate our thinking for such values? Dare we suggest that the following reaction in equation 10 is thermoneutral?

$$n\text{-}C_7H_{16} + (CF_3)_2NOCF_2CF_2ON(CF_3)_2 \longrightarrow n\text{-}C_7F_{16} + Me_2NOCH_2CH_2ONMe_2 \qquad (10)$$

Additionally, we posit thermoneutrality for equation 11 in order to to derive[4] the enthalpy of formation of the bis 'hydrocarbon' hydroxylamine ether of $-73\ kJ\,mol^{-1}$.

$$2Me_2NOMe + EtOCH_2CH_2OEt \longrightarrow 2EtOMe + Me_2NOCH_2CH_2ONMe_2 \qquad (11)$$

The calculated value for the perfluoro species in equation 10 is $-3269\ \text{kJ mol}^{-1}$. The literature value is $-3283 \pm 80\ \text{kJ mol}^{-1}$. The agreement is almost too good to be true!

B. Isoxazolidines and Other Cyclic Hydroxylamines

While numerous nitrones react with olefins to form isoxazolidines (1-oxa-2-azacyclopentanes) by a formally simple [3 + 2] cycloaddition reaction, there have been few calorimetric investigations of this process. Among these is the reaction of some *p*-substituted *C*,*N*-diphenyl nitrones (*p*-$XC_6H_4CHN(O)Ph$, X = NO_2, Cl, H, Me and MeO) with *N*-phenylmaleimide to form 2,3,6-triaryl derivatives of 1-oxa-2,6-diazabicyclo[3.3.0]octane-5,7-dione[23]. No enthalpy of formation data are available for *N*-phenylmaleimide or for maleimide itself. However, it is available for the corresponding *N*-methylmaleimide[24] along with some other imides[25]. The gas phase enthalpy of hydrogenation of this species (derived as the difference between its enthalpy of formation and that of *N*-methylsuccinimide[24]) is $133.7 \pm 2.2\ \text{kJ mol}^{-1}$. This value is essentially the same as for ethylene (derived as the difference between its enthalpy of formation and that of ethane) of $136.3 \pm 0.4\ \text{kJ mol}^{-1}$. Therefore, let us assume the reaction of the above parent nitrone with ethylene to form the diphenylated isoxazolidine, shown in equation 12, has very much the same exothermicity as with *N*-phenylmaleimide[23], namely *ca* 82 kJ mol^{-1}. If so, the enthalpy of formation of 2,3-diphenylisoxazolidine would be 233 kJ mol^{-1}. Now, is this value plausible?

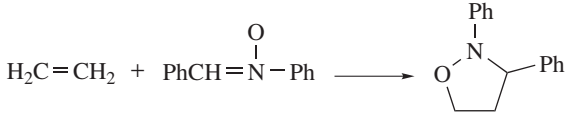

(12)

Let us assume that the 2- and 3-dephenylation reactions to form the parent heterocycle isoxazolidine have the same enthalpies as those of isopropylbenzene and dimethylaniline, 108.7 and 118.6 kJ mol^{-1}, respectively. Therefore, the enthalpy of formation of isoxazolidine is predicted to be *ca* 6 kJ mol^{-1}. Consider the reaction in equation 13.

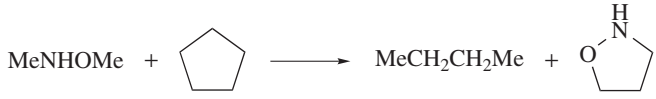

(13)

If this reaction is assumed to be thermoneutral (neglecting the effects of heteroatoms on conformation and on ring strain), the predicted enthalpy of formation of isoxazolidine is 11.6 kJ mol^{-1}. Admitting that it may be simplistic, as well as simple, to have assumed thermoneutrality, we take these two predicted values of 6 and 11.6 kJ mol^{-1} to be in satisfactory agreement and choose an average value of 9 kJ mol^{-1} for the enthalpy of formation of isoxazolidine.

Very different enthalpies of addition are found for the acylnitrone PhC(O)CHN(O)Ph. Instead of the above exothermicity of *ca* 82 kJ mol^{-1} for the addition of PhCHN(O)Ph and its substituted derivatives to a maleimide, the acylated nitrone adds to a variety of norbornenes with an average exothermicity[26] of *ca* 120 kJ mol^{-1}, some 38 kJ mol^{-1} more favorable. This suggests about 40 kJ mol^{-1} destabilization arises from the presence of the adjacent acyl and nitrone groups. No enthalpy of formation data are available for any acylnitrone. To simulate the mutual destabilizing effect of the acyl and nitrone

groups, consider the pair of reactions shown in equations 14 and 15 involving nitriles and acylnitriles.

$$PhCN + C_3H_8 \longrightarrow PhEt + MeCN \tag{14}$$

$$PhCOCN + C_3H_8 \longrightarrow PhCOEt + MeCN \tag{15}$$

The two reactions are exothermic by 7.0 and 47.5 kJ mol^{-1}, respectively, suggesting that acyl and nitrile groups are mutually destabilizing by 40 kJ mol^{-1}. Likewise, consider the same two reactions where the CN group is replaced by COOH[27]. The two enthalpies of reaction differ by 44 kJ mol^{-1} and so the acyl and carboxyl groups are also mutually destabilizing. The suggested 40 kJ mol^{-1} destabilization of acyl and nitrone groups is thus plausible.

C. *N,N*-Dialkoxylamines

Another class of compounds deals with *N*,*N*-dialkoxylamines, species of the general type $R^1N(OR^2)_2$. The reaction of 2-nitroisoxazoline-*N*-oxide in equation 16 has been observed[28] and found to be exothermic by 126 ± 4 kJ mol^{-1}. From archival values for the gas phase enthalpy of formation of both reagents, we deduce the enthalpy of formation of the product, 5-nitro-1-aza-2,8-dioxabicyclo[3.3.0]octane, to be -53 ± 10 kJ mol^{-1}.

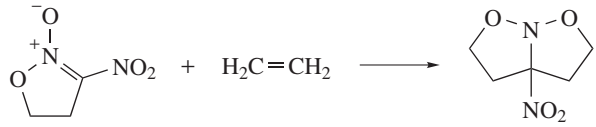

(16)

We ask once again whether this value is plausible. Let us assume that the nitro group is normal, *i.e.* equation 17 is thermoneutral.

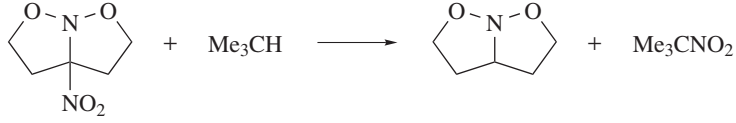

(17)

And so the enthalpy of formation of gaseous 1-aza-2,8-dioxabicyclo[3.3.0]octane is predicted to be -10 kJ mol^{-1}. Consider the 1-ring to 2-ring reaction in equation 18 and its associated exothermicity of 24 kJ mol^{-1}.

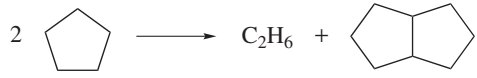

(18)

Assuming strain energies are independent of heteroatoms, then reaction 19 should have roughly the same exothemicity.

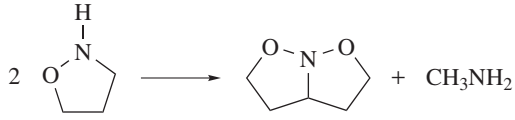

(19)

This results in a predicted enthalpy of formation of 16 kJ mol^{-1} for 1-aza-2,8-dioxabicyclo [3.3.0]octane. This value is plausibly an overestimate. We have neglected any anomeric stabilization arising from the −O−N−O− substructure. However, this effect may be shown to be small. While no species with this functionality has seemingly a measured enthalpy of formation, consider the related F−N−F substructure as found in HNF_2 and the enthalpy of the following equation 20 which is close to thermoneutral.

$$2\ NH_2F \longrightarrow HNF_2 + NH_3 \tag{20}$$

The enthalpy of formation of HNF_2 is known from a reaction calorimetric experiment[29] to be -65 ± 6 kJ mol^{-1}. The enthalpy of formation of NH_2F remains unknown from experiment but the value has been suggested[30] to be *ca* -58 kJ mol^{-1}. We must thus content ourselves with the two values of formation of 1-aza-2,8-dioxabicyclo[3.3.0]octane, -10 and $+16$ kJ mol^{-1}, which, given all of our assumptions, are not that disparate.

D. Dimers of Nitroxide Radicals

Consider species of the general structural type $R_2N-O-O-NR_2$. These compounds may be understood as the dimer of nitroxide radicals and nitrogen analogs of peroxides. Regardless, they qualify as hydroxylamine derivatives as well and so discussion of their thermochemistry is relevant. From Galli's chapter in the current volume we find the recommended O−H bond energy in Et_2NOH of 305 kJ mol^{-1}. As part of our earlier discussion on alkyl hydroxylamine thermochemistry, we find the enthalpy of formation of this dialkylhydroxylamine in its gaseous phase[11] to be -121.8 kJ mol^{-1}. Accordingly, from the gas phase reaction 21 employing the enthalpy of formation of atomic hydrogen of 212.0 kJ mol^{-1} we derive the enthalpy of formation of gas phase nitroxide radical Et_2NO to be *ca* -29 kJ mol^{-1}.

$$Et_2NO^{\bullet} + H^{\bullet} \longrightarrow Et_2NOH \tag{21}$$

Accepting the enthalpy of dimerization for reaction 22 of *ca* 21 ± 10 kJ mol^{-1} (an averaged value from results in two nonpolar solvents[31]) to apply to the gas phase,

$$2Et_2NO^{\bullet} \longrightarrow Et_2N-O-O-NEt_2 \tag{22}$$

the enthalpy of formation of $Et_2NOONEt_2$ is hereby deduced to be -263 ± 20 kJ mol^{-1}.

IV. MONOOXIMES

A casual perusal of the literature shows there are numerous measurements for the enthalpy of formation of monooximes. Table 2 presents available data. There is also a computational study of oximes[4]. However, as is so often the case, there are more data than one thinks and less than one needs.

A. Simple Aliphatic Aldoximes

If there were ever a simple comparison of enthalpies of formation to be investigated as part of this chapter it would be the oximes of the aliphatic aldoximes, RCH=NOH, as R proceeds through Me, Et, *n*-Pr, ... Ideally, we would have the values for at least R = Me and Et and then employ the 'universal methylene increment'[36] to derive the remaining values by addition of -20.6 kJ mol^{-1} for gaseous species and a related *ca* -26.0 kJ mol^{-1} for

TABLE 2. Enthalpies of formation for monooximes (kJ mol^{-1})

Compound	Formula	ΔH_f(s)	Reference	ΔH_f(lq)	Reference	ΔH_f(g)	Reference
Formaldoxime	CH_3NO					29.3[a]	4
Acetaldoxime	C_2H_5NO	−76.1	2	−71.6 ± 0.3	11	−22.6 ± 0.3	11
('High melting isomer')		−77.8	9				
('Low melting isomer')				−81.6	9		
Acetone oxime	C_3H_7NO	−128.9	2			−62.8	4
Butanone oxime	C_4H_9NO			−155.4	2		
Pyrrole-2-carboxaldoxime	$C_5H_6N_2O$	12.1 ± 2.9	1				
Acetylcyclopropane oxime	C_5H_9NO	−27.6 ± 1.1	32				
Pyridine-2-carboxaldoxime	$C_6H_6N_2O$	78.6 ± 2.4	33				
Cyclohexanone oxime	$C_6H_{11}NO$	−152.4 ± 0.8	34	−141.5 ± 1.3	34	−72.8 ± 2.0	34
Benzaldoxime	C_7H_7NO	41.0	2				
Salicylaldoxime	$C_7H_7NO_2$	−183.7 ± 0.7	1				
4-Hydroxybenzaldoxime	$C_7H_7NO_2$	−212.9	2				
Acetophenone oxime	C_8H_9NO	−22.2	2				
2-Hydroxyacetophenone oxime	$C_8H_9NO_2$	−221.3	2				
4-Hydroxyacetophenone oxime	$C_8H_9NO_2$	−199.2	2				
Octanal oxime	$C_8H_{17}NO$	−238.5 ± 2.1	35			−149.4 ± 3.9	35
2-Octanone oxime	$C_8H_{17}NO$			−248.3 ± 2.2	35	−180.1 ± 4.1	35
3-Octanone oxime	$C_8H_{17}NO$			−240.0 ± 1.7	35	−172.8 ± 3.6	35
4-Octanone oxime	$C_8H_{17}NO$			−249.9 ± 1.8	35	−181.1 ± 3.7	35
2-Methylacetophenone oxime	$C_9H_{11}NO$	−239.7	2				
3-Methylacetophenone oxime	$C_9H_{11}NO$	−254.0	2				
4-Methylacetophenone oxime	$C_9H_{11}NO$	−247.7	2				
2-Hydroxy-3-methylacetophenone oxime	$C_9H_{11}NO_2$	−482.8	2				
2-Methoxyacetophenone oxime	$C_9H_{11}NO_2$	−364.8	2				
2-Hydroxy-4-methoxyacetophenone oxime	$C_9H_{11}NO_3$	−593.7	2				
2-Hydroxy-5-methoxyacetophenone oxime	$C_9H_{11}NO_3$	−583.7	2				
Acetylcycloheptane oxime	$C_9H_{17}NO$	−265.7	2				
4-Methoxy-2-methylacetophenone oxime	$C_{10}H_{13}NO_2$	−398.3	2				
4-Methoxy-3-methylacetophenone oxime	$C_{10}H_{13}NO_2$	−418.4	2				
Camphor oxime (1,7,7-trimethyl-2-norbornanone oxime)	$C_{10}H_{17}NO$	−164.0	2				
Benzophenone oxime	$C_{13}H_{11}NO$	−120.1	2				

[a] The quantum chemically calculated value of Reference 8 is 16.8 kJ mol^{-1}.

the liquids. We lack the desired data from experiment for R = Et, there being data only for R = Me[11] and Hep[35], a difference of six carbons. The difference between the enthalpies of formation of gaseous MeCH=CH_2 and EtCH=CH_2 is 19.9 ± 1.2 kJ mol^{-1} and between gaseous MeCH=O and EtCH=O it is 20.8 ± 1.6 kJ mol^{-1}. Both values are statistically indistinguishable from the 'universal' value and so we are confident that the difference between gaseous MeCH=NOH and EtCH=NOH should be very much the same value[37]. As such, the difference between the enthalpies of formation of gaseous MeCH=NOH and HepCH=NOH is expected to be 6•20.6 or 123.6 kJ mol^{-1}. Accordingly, accepting the contemporary value for acetaldoxime of -22.6 ± 0.3 kJ mol^{-1}, the value for the enthalpy of formation of octanal oxime would be expected to be -146.2 kJ mol^{-1}. The literature value is -149.4 ± 3.9 kJ mol^{-1}, experimentally indistinguishable from that predicted within error bars.

B. Simple Aliphatic Ketoximes

The enthalpy of formation of the oximes of acetone and the isomeric 2-, 3- and 4-octanone are seemingly the sole examples of aliphatic ketoximes for which gas phase enthalpies of formation are available. The enthalpies of formation of the octanone oximes[35], as well as the octanone isomers[38] themselves, were all determined by the same research group. The authors suggest an alternation effect for these as one proceeds to substitute the functional groups down the octane chain (an effect which is particularly exaggerated for 3-octanone oxime which is seemingly *ca* 10 kJ mol^{-1} less stable than its isomers). This explanation is dubious based on the accepted enthalpies of formation for other ketones[1]. For the homologous series of 2-*n*-alkanones, Me(C=O)R, where R = Me, Et, Pr, Bu, Hep, Dec, a weighted least-squares analysis of the gaseous enthalpies of formation yields a profoundly linear relationship with a methylene increment of -20.7 kJ mol^{-1}. The enthalpy of formation value for 2-octanone is 24 kJ mol^{-1} more negative than that predicted on the basis of the regression analysis (-321.0 kJ mol^{-1}). The liquid phase value is too negative by *ca* 11 kJ mol^{-1}. The difference between the isomeric 2- and 3-pentanone, 2- and 3-hexanone and 2- and 5-nonanone, in all cases and either phase, is less than 2 kJ mol^{-1} except for the nonanes for which the liquid phase enthalpy difference is *ca* 4 kJ mol^{-1}. Since the three isomeric octanones have nearly the same enthalpy of formation within the uncertainties of their experimental measurements in the liquid phase (-384.5 ± 2.5 kJ mol^{-1}) and gas phase (-344.3 ± 2.5 kJ mol^{-1}), it is thus likely they also are too negative. What about the oximes?

Consider equation 23 that relates the oximes to the corresponding ketones.

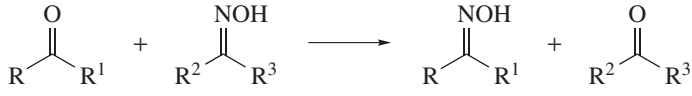

(23)

For the two aldehydes discussed in the previous section (R^1, R^3 = H; R = Me, R^2 = Hep), the reaction is thermoneutral in the gas phase. Thermoneutrality would also be expected for ketones, but which ketone/oxime should be the standard for comparison? In the gas phase there are two possibilities: acetone/acetone oxime and cyclohexanone/cyclohexanone oxime. The latter pair may be assumed to be essentially strainless, or at least that their strain energies are very much the same. The assumption is borne out by substituting these two pairs into equation 23 (R, R^1 = Me; $R^2R^3 = -(CH_2)_5-$) and finding that the enthalpy of reaction is only 1.2 kJ mol^{-1}, essentially thermoneutral. Comparing the C_8 species with the cyclohexyl species ($RR^1 = -(CH_2)_5-$; R^2/R^3 = Me/Hex, Et/Pen, Pr/Bu), the enthalpies

of reaction are −11.7, −12.5 and −14.9 kJ mol^{-1}, respectively. However, because the octanone enthalpies of formation are in error by *ca* −24 kJ mol^{-1}, the enthalpies of reaction 23 for the octanone oximes are likely to be *ca* 12 kJ mol^{-1} when using the octanone correction. Accordingly, the enthalpies of formation of the octanone oximes are probably *ca* 12 kJ mol^{-1} too negative. Additionally, the oximes, like the ketone isomers, are probably of comparable stability. In the liquid phase, the exothermicities of equation 23 are *ca* 7, 13 and 7 kJ mol^{-1}, respectively. Because we offered a correction to the liquid phase enthalpies of formation of the octanones of *ca* 11 kJ mol^{-1}, the resulting correction to the liquid enthalpies of formation of their oximes is *ca* 4 kJ mol^{-1}, except for 3-octanone oxime which, by the foregoing analysis, is fairly accurate.

There remains to be discussed butanone oxime, for which there is an enthalpy of formation value only in the liquid phase. The enthalpy of reaction 23 ($RR^1 = -(CH_2)_5-$; R^2 = Me, R^3 = Et) is +11.8 kJ mol^{-1}. The enthalpy of formation of butanone oxime would seem to be *ca* 12 kJ mol^{-1} too negative.

Finally, assuming a linear relationship between the enthalpies of formation and carbon number for the 2-alkanone oximes, and a gas phase methylene increment of −20.7 kJ mol^{-1}, the same as for the 2-alkanones, the enthalpies of formation of 2-butanone and 2-octanone oximes would be −82.5 and −166.3 kJ mol^{-1}, respectively. The latter value is within 1 kJ mol^{-1} of that derived from equation 23.

C. Formaldoxime

As acknowledged in Table 2, the authors of Reference 4 present a *ca* 13 kJ mol^{-1} discrepancy between the calculated and experimentally determined enthalpy of formation of the simplest oxime, CH_2=NOH. What would our analysis suggest? As has long been known, the universal increment logic very often shows that for any X, the difference between MeX and EtX is generally different from EtX and PrX and higher members of most RX series. The discrepancy is even larger for the enthalpies of formation of HX and MeX. Nonetheless, we will let X = CH=NOH and compare HX and MeX for X = CH=CH_2 and CH=O. We would have ideally considered X = CH=NH, CH=NMe and CH=NNH_2, but the necessary thermochemical data for these species are either absent or problematic. For X = CH=CH_2 the difference is 32.5 ± 0.7 kJ mol^{-1} while for CH=O the difference is 57.6 ± 0.7 kJ mol^{-1}. By simple interpolation, this suggests that the difference should be at least *ca* 44 kJ mol^{-1}. We acknowledge, however, that the combination of electronegative N and O atoms in the oxime plausibly could make the enthalpy difference resemble that of the aldehydes more than the alkenes. Accordingly, the enthalpy of formation of CH_2=NOH is expected to be 22 kJ mol^{-1}, *i.e.* we derive a value that almost Solomonically cuts the difference between the two sets of values. Legitimizing this division are related data for some saturated species. For HCH_2OH and $MeCH_2OH$ we find a difference of 33.7 ± 0.4 kJ mol^{-1} while for HCH_2Me and $MeCH_2Me$ the difference is 20.9 ± 0.6 kJ mol^{-1}. This suggests that the difference between the enthalpies of formation of HCH_2NH_2 and $MeCH_2NH_2$ is 27.1 ± 0.7 kJ mol^{-1}. The actual difference for these species, more commonly written as $MeNH_2$ and $EtNH_2$, is 24.1 ± 1.3 kJ mol^{-1}, in fine agreement.

To what is this discrepancy due? As noted in the chapter in the current volume by Schulz, Brand and Villinger on derivatives of formaldoxime, the parent species and its ionic salts are prone to polymerization and to decomposition. This most assuredly complicates calorimetric measurements. That the calculated[4] enthalpy of formation is more negative than the experimental is surprising in that the polymer is expected to be more stable (with lower ΔH_f as well as necessarily ΔG_f) than the monomer.

D. Acetylcycloalkane Oximes

The enthalpy of formation of two such species has been measured, namely the cyclopropane[32] and cycloheptane[2] derivatives. The difference between the values for these two species, both as solids, is 238.1 kJ mol^{-1}. Is this difference plausible? Consider the difference between the enthalpies of formation of the parent cycloalkanes as solids, 194 kJ mol^{-1}. The *ca* 44 kJ mol^{-1} discrepancy between these two differences seems rather large. However, there are idiosyncracies associated with the enthalpies of formation of compounds with three-membered rings[39] and almost nothing is known at all about the thermochemistry of compounds with seven-membered rings. Rather, we merely note that a seemingly well-defined synthesis of cycloheptyl methyl ketone[40] was shown later to result in a mixture of methyl methylcyclohexyl ketones[41], and superelectrophilic carbonylation of cycloheptane resulted in the same products as methylcyclohexane, namely esters of 1-methylcyclohexanecarboxylic acid[42]. The difference between the enthalpies of formation of the unsubstituted alicyclic hydrocarbons cycloheptane and methylcyclohexane as solids is 33 kJ mol^{-1}. This alternative structural assignment hereby corrects for most of the above 44 kJ mol^{-1} discrepancy in the enthalpies of formation of the two oximes. More thermochemical measurements are needed, of oximes and cycloheptanes alike.

E. Aromatic Oximes

Despite the numerous entries in Table 2, there are few entries that correspond to trustworthy species. More precisely, there are but two derived from contemporary, well-characterized measurements, where contemporary means the primary data were reported since the mid-20th century. These are for pyridine-2-carboxaldoxime and salicylaldoxime. The formal solid phase reaction 24 is but 5 kJ mol^{-1} endothermic.

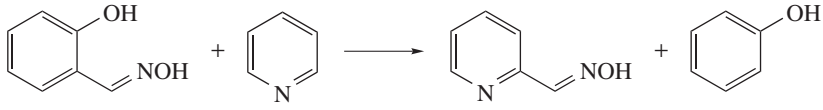

(24)

This near-thermoneutrality gives confidence in both values of the oxime enthalpies of formation, the salicylaldoxime some 50 years old[43] and the pyridine-2-carboxaldoxime within a year from when the chapter was submitted. Consider now the formal solid phase reaction 25 involving the some decades older pyrrole-2-carbaldoxime[44].

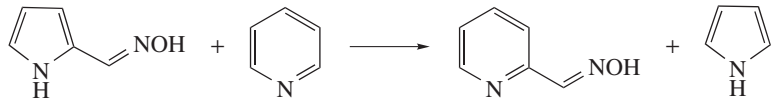

(25)

As written, the reaction is endothermic by *ca* 30 kJ mol^{-1}. Pyrrole and pyridine are both 6-π nitrogen-containing heterocycles. However, the former is electron-rich while the latter is electron-deficient and so conjugative stabilization mechanisms are different for the two species. Furthermore, the former can form one more hydrogen bond per molecule than the latter, a feature that may account for pyrrole-2-carboxaldehyde being a solid while pyridine-2-carboxaldehyde is a liquid. We wonder if either difference accounts for the profound lack of thermoneutrality for the above reaction.

The remaining aromatic oximes are primarily a collection of hydroxyl- and methyl-substituted acetophenones and benzaldehydes. Thwarting a comprehensive analysis is a lack of data for the corresponding carbonyl compounds or even 'deoximated' compounds. A comparison of the benzaldoximes with benzaldehydes would be interesting, except there

are no enthalpy of formation data for either salicylaldehyde or 4-hydroxybenzaldehyde. Data for the corresponding benzoic acids are available however, and we assume that the enthalpy of the reduction reaction to the aldehyde product is constant for all species. 4-Hydroxybenzoic acid is about 10 kJ mol^{-1} more stable than its 2-hydroxy isomer (using the average of the values found for the solid species in Reference 3). This is similar to the *ca* 7 kJ mol^{-1} greater stability of 4-hydroxyacetophenone over 2-hydroxyacetophenone. However, the 4-hydroxybenzaldoxime is 30 kJ mol^{-1} more stable than its 2-isomer while the 4-hydroxyacetophenone oxime is 22 kJ mol^{-1} less stable than the 2-isomer. In that the thermochemistry of phenols has been recognized to be often problematic[45], we recommend the remeasurement of the enthalpies of formation of benzaldoxime and its isomeric 2- and 4-hydroxy derivatives.

F. The Relative Stability of *syn*- and *anti*-Aliphatic Oximes

Although the existence of *syn* and *anti*-isomers of monooximes with the structure $R^1C(=NOH)R^2$ has long been known, there are surprisingly few studies that address the question of the difference in their enthalpies of formation. Reference 6 reports values for two isomeric acetaldoximes, a high melting solid and a low melting liquid; as always, no primary reference is available. The respective condensed phase enthalpies of formation of the two isomers are -77.9 and -81.6 kJ mol^{-1}, respectively.

By comparison of the neutralization energy of a variety of samples of acetaldoxime, it was deduced[46] that there are two isomers with an enthalpy of formation difference of *ca* 8 kJ mol^{-1}. From an NMR study of aqueous acetaldoxime[47], a *syn:anti* isomer ratio of 63:37 was found (where *syn* means the OH is on the same side as the H and opposite from the methyl and *anti* means the opposite locations). If it is assumed that

(a) the ratio of species in aqueous solution reflects the thermodynamic stabilities of the solute isomers as pure species,
(b) the entropy may be ignored and so enthalpy differences may be equated to those of free energies,

we conclude that the difference between the enthalpies of formation of *syn*- and *anti*-acetaldoxime is $RT\ln(63/37) = 1.3$ kJ mol^{-1} favoring the *syn* isomer. From the same source we find for 2-butanone oxime a *syn:anti* ratio (where *syn* means the OH is on the same side as the methyl) of 71:29 favoring the *syn* isomer. (Very much the same ratio, 75:25, was determined by analysis of peaks in the NMR spectrum[47] of a mixture of the two isomers and by chromatographic analysis[48] of the trimethylsilyl derivatives, additionally assuming that silylation did not change the isomer composition.) Making the same assumptions, the difference between the enthalpies of formation of *syn*- and *anti*-2-butanone oxime of *ca* $RT\ln(71/29 \text{ or } 75/25) = 2.5 \pm 3$ kJ mol^{-1} favoring the *syn* isomer. These results and those of a few other aliphatic oximes were shown to track the size of the groups on the oxime-bearing carbon.

Disappointingly absent from experiment are the corresponding gas phase species. Quantum chemical calculations[8] suggest the *syn*-isomer of acetaldehyde is more stable by nearly the same value of 1.6 kJ mol^{-1}; other calculational studies (with different computational protocols, *e.g.* by Politzer and Murray in this volume) have also given small values. Does it follow that there is a negligible difference in intermolecular hydrogen bonding for the two isomers, even though they differ as to phase? This is surprising. Then again, there are few monooximes for which enthalpies of formation in any phase may be trusted, regardless of any other stereochemical assignment. Summarizing, the energetics of *syn*- vs *anti*-oximes remains a largely non-understood aspect of the energetics of oximes.

G. A Brief Discussion of Aliphatic Oximes in Aqueous Solution

Despite a literature that begins early in the 20th century[49], we only briefly discuss the energetics of the aqueous phase synthesis of oximes and bypass the intermediacy of α,*N*-dihydroxylamines (hydroxycarbinolamines) and any zwitterionic or charged species. With great simplification we would thus write equation 26:

$$R^1R^2C{=}O(aq) + NH_2OH(aq) \longrightarrow R^1R^2C{=}NOH(aq) + H_2O(lq) \qquad (26)$$

Acknowledging the multiple sites for hydrogen bonding with the starting materials, we generally lack the necessary data to 'desolvate' the various species to derive the energetics for the pure compounds which we recognize as the desirable subjects of understanding for the current chapter. We thus limit our attention to the two simple oximation reactions for which we have the requisite data: we wish to consider condensed, gaseous and aqueous phases. The first is that of acetaldehyde, equation 27:

$$MeCHO + NH_2OH \longrightarrow MeCH{=}NOH + H_2O \qquad (27)$$

There are three environments that we may consider for this reaction: *syn*-acetaldehyde oxime data in the condensed phase[11], the gas phase[11] and in aqueous solution[6,49]. The reaction exothermicities are 51.0, 56.5 and *ca* 53 kJ mol^{-1}, respectively. The only other case where the values are known for all three phases is that of acetone, equation 28:

$$Me_2C{=}O + NH_2OH \longrightarrow Me_2C{=}NOH + H_2O \qquad (28)$$

In this case, the enthalpies of reaction are 52.1, 45.7 and 44.6 kJ mol^{-1} where the enthalpies of formation of solid and gaseous acetone oxime are from References 1 and 4, respectively, and the enthalpies of oximation in aqueous media are from References 49a and 49c. In both cases, the values are comfortably similar for the three phases. Perhaps we should not be too surprised that the values are close—after all, the number of hydrogen bonds are the same on the two sides of the reaction. However, nothing prepares us for the observation that the aqueous phase oximation enthalpy of propionaldehyde[49d] is 73.2 kJ mol^{-1}, even though we recall 'problems'[25] with the enthalpy of formation of EtCH=NOH.

V. GLYOXIME AND OTHER DIOXIMES

Glyoxime, or ethanedial dioxime, is the simplest dioxime and is the structural paradigm for a large variety of important complexing and chelating agents. For these dioximes, HON=CRCR=NOH, there are three possible stereoisomers that may be considered: the OH and R groups are on the same side of both C=N bonds, the OH and R groups are on opposite sides of both C=N bonds; the OH and R groups are one apiece on the same and opposite sides of the C=N bonds. There has been seemingly little concern from the thermochemist as to which stereoisomer has been employed. As such, we generally lack certainty as to which isomer is meant by historical descriptors such as α- and β- and the stereochemical purity (as opposed to bulk composition) of a given species. Most enthalpy of formation determinations for these dioximes come from rather early in the last century. Additionally, these data are for solids. As such, we are not altogether bothered by this ignorance. See Table 3. Nonetheless, let us be more precise in our comments. We now ask: are these enthalpy of formation values plausible?

TABLE 3. Enthalpies of formation for dioximes (kJ mol^{-1})

Compound	Formula	ΔH_f(s)	Reference	ΔH_f(g)	Reference
Ethanedial dioxime (glyoxime)	$C_2H_4N_2O_2$	-90.5 ± 1.2	1		
1,2-Propanedione dioxime	$C_3H_6N_2O_2$	-126.7 ± 1.9	1		
2,3-Butanedione dioxime (dimethylglyoxime)	$C_4H_8N_2O_2$	-162.8	50	-65.7	1 [a]
1,2-Cyclohexanedione dioxime	$C_6H_{10}N_2O_2$	-130.4	51	-7 ± 17	51
α-Phenylglyoxime	$C_8H_8N_2O_2$	42.1 ± 4.1	1		
β-Phenylglyoxime	$C_8H_8N_2O_2$	-20.4 ± 4.1	1		
α-(*p*-Tolyl)glyoxime	$C_9H_{10}N_2O_2$	158.4 ± 5.0	1		
β-(*p*-Tolyl)glyoxime	$C_9H_{10}N_2O_2$	229.2 ± 5.0	1		
(*Z*,*Z*)-Benzil dioxime	$C_{14}H_{12}N_2O_2$	41.8 ± 7.1	1		
(*E*,*E*)-Benzil dioxime	$C_{14}H_{12}N_2O_2$	18.0 ± 7.1	1		
(*E*,*Z*)-Benzil dioxime	$C_{14}H_{12}N_2O_2$	53.1 ± 7.1	1		

[a] The enthalpy of formation in the gas phase was calculated by summing the enthalpy of formation of the solid species from Reference 50 with the sublimation enthalpy in Reference 1.

A. Dimethylglyoxime

We start with butane-2,3-dione dioxime, more commonly known as dimethylglyoxime (dmg). It is a classic reagent for the analysis of Ni^{II}, the green aqueous solution of metal ions transforming into a vibrantly red precipitate of $Ni(dmg)_2$ complex: it is one of 'the stars of the show' in Ponikvar and Liebman's analytical chemistry chapter in the current volume. Here the stereochemistry is well-established and well-known—both OH groups are found on the same side as their adjacent CH_3 group on the butanedione backbone. There have been several measurements of the enthalpy of formation of this species for which we take the one associated with this inorganic analytical chemistry application, *i.e.* with diverse metal complexes and chelates[50].

First of all, we may compare the values for this species and its lesser-methylated derivatives, the parent ethanedial and 1,2-propanedione dioximes, respectively. The former are only for the solid state. The differences for sequential methylation are the all but indistinguishable 36.2 and 36.1 kJ mol^{-1} and so we feel confident in this set of numbers. We also find that, at least for unstrained species, the gas phase olefin[52] and aldehyde reactions[53] in equations 29 and 30 are roughly endothermic by *ca* 4 kJ mol^{-1}.

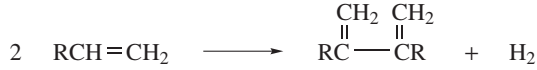

(29)

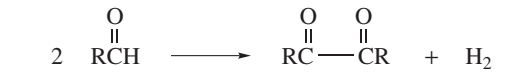

(30)

From the enthalpies of formation of gaseous acetaldoxime and butanedione dioxime we find the corresponding reaction 31 (R = Me) is exothermic by 20 kJ mol^{-1}.

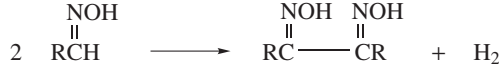

(31)

We have no prior experience with diimines to make any disparaging or supportive comparison but the result is implausible. Since we earlier accepted the enthalpy of formation of acetaldoxime, it is the dioxime that is seemingly suspect. From an expected enthalpy of reaction 32 of *ca* 4 kJ mol^{-1}, the enthalpy of formation of dmg is calculated as -41 kJ mol^{-1}. Not only is this derived value very different from the one presented in Table 3, it is wildly divergent from the one that appears in Reference 1 and which is not in Table 3: -80.8 kJ mol^{-1}.

B. 1,2-Cyclohexanedioxime

From available enthalpies of formation we find the gas phase reaction 32 is endothermic by 15 kJ mol^{-1}.

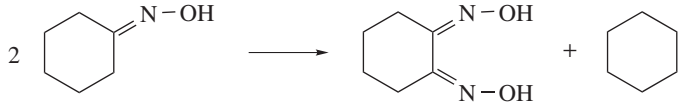

(32)

This is encouragingly small, especially considering the experimental uncertainty for the dioxime enthalpy of formation, although we have no real idea how much repulsion or stabilization we might expect from vicinal dioxime groups. (We likewise lack such information for vicinally substituted alicyclic diones—there are literature[54] enthalpy of formation data for 1,3- and 1,4- but not 1,2-cyclohexanedione; there are also data for 2,3-pentanedione[55] but not 1,2-cyclopentanedione.) Consider now the reaction 33.

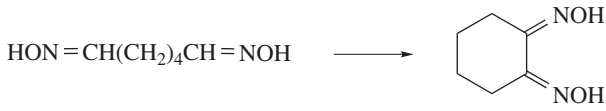

(33)

Although there are no experimental data on the acyclic dioxime, hexanedial dioxime, we have no reason to believe that the gas phase reaction 34 is not essentially thermoneutral.

(34)

Accordingly, we derive an enthalpy of formation of -49 kJ mol^{-1} for the acyclic dioxime and so an endothermicity of 40 kJ mol^{-1} for the cyclohexane dioxime forming reaction 33—only 25 kJ mol^{-1} would have been expected from the above cyclohexanedione reaction if we assume that the cyclohexane dioxime is destabilized by 15 kJ mol^{-1}.

C. Aryl Glyoximes

A quick perusal of Table 3 shows inverted stability for α and β isomers of phenylglyoxime and *p*-tolylglyoxime. Given uncertainties as to stereochemistry it is plausible that the structural assignments of *Z* and *E*, *syn* and *anti*, even α and β were reversed. This is understandable. However, it is inexplicable that the tolyl species have enthalpies of formation at least 150 kJ mol^{-1} more positive than the phenyl compounds. This is an altogether implausible result. The solid phase reaction 35 is calculated to be *ca* 75 kJ mol^{-1} exothermic if we use the averaged value for the various stereoisomers of phenylglyoxime and benzil dioxime. This, too, is implausible.

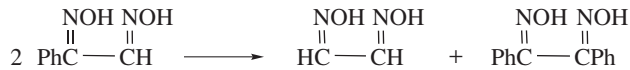

(35)

The related solid phase reaction 36 is exothermic by but 5.0 kJ mol^{-1} [56].

(36)

We can only conclude that these aryl glyoxime data are suspect. As such, although we finally have data for sets of enthalpies of formation of *syn*- and *anti*-isomers, we do not trust these data enough to return to the earlier question of the relative stabilities of these isomers as enunciated in the discussion of monooximes.

VI. QUINONE OXIMES AND NITROSOARENOLS

Quinone oximes and nitrosoarenols are related as tautomers, *i.e.* by the transfer of a proton from an oxygen at one end of the molecule to that at the other (equation 37). While both members of a given pair of so-related isomers can be discussed separately (see, *e.g.*, our earlier reviews on nitroso compounds[12a] and phenols[45]) there are no calorimetric measurements on the two forms separately and so discussions have admittedly been inclusive—or very often sometimes, evasive—as to the proper description of these compounds. Indeed, while quantitative discussions of tautomer stabilities have been conducted for condensed phase and gaseous acetylacetone[57] and ethyl acetoacetate[58], there are no definitive studies for any pair of quinone oximes and nitrosoarenols. In any case, Table 4 summarizes the enthalpy of formation data for these pairs of species.

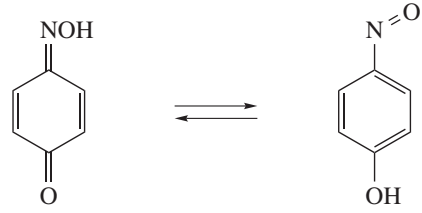

(37)

TABLE 4. Enthalpies of formation for ketooximes (kJ mol^{-1})

Compound	Formula	ΔH_f(s)	Reference	ΔH_f(g)	Reference
5-Cyclohexene-1,2,3,4-tetraone-1,3-dioxime (2,4-dinitrosoresorcinol)	$C_6H_4N_2O_4$	235	59		
p-Benzoquinone oxime (4-nitrosophenol)	$C_6H_5NO_2$	-70.2 ± 2.1	60		
1,2-Naphthoquinone 1-oxime (1-nitroso-2-naphthol)	$C_{10}H_7NO_2$	-50.5 ± 2.2	1	36.1 ± 4.7	1
1,2-Naphthoquinone 2-oxime (2-nitroso-1-naphthol)	$C_{10}H_7NO_2$	-61.8 ± 4.5	1	-5.4 ± 6.1	1
1,4-Naphthoquinone 1-oxime (4-nitroso-1-naphthol)	$C_{10}H_7NO_2$	-107.8 ± 2.4	1	-20.3 ± 4.8	1
5-Isopropyl-2-methyl-benzoquinone oxime (5-methyl-4-nitroso-2-isopropyl phenol)	$C_{10}H_{13}NO_2$	-216.3	2		

A. *p*-Benzoquinone Oxime and 4-Nitrosophenol

Conceptually, the simplest pair to discuss is that of *p*-benzoquinone oxime and 4-nitrosophenol and their substituted derivatives, here all denoted by '*p*-OC_6H_4=NOH/4-HOC_6H_4NO'. In practice, this comparison is complicated by the fact[60] that this species cannot be sublimed without decomposition and so we are prevented from analyzing the energetics of gas phase isodesmic reactions such as equations 38 and 39.

$$\text{4-O=C}_6\text{H}_4\text{=NOH/4-HOC}_6\text{H}_4\text{N=O} + \text{R}^1\text{R}^2\text{C=O} \longrightarrow \text{4-O=C}_6\text{H}_4\text{=O} + \text{R}^1\text{R}^2\text{C=NOH} \quad (38)$$

$$\text{4-O=C}_6\text{H}_4\text{=NOH/4-HOC}_6\text{H}_4\text{N=O} + \text{C}_6\text{H}_6 \longrightarrow \text{PhOH} + \text{PhN=O} \quad (39)$$

The enthalpy of reaction 38 is *ca* 13 kJ mol^{-1} for the case of cyclohexanone wherein $R^1R^2 = -(CH_2)_5-$. This difference is compatible with intermolecular hydrogen bonding as would be found for the benzoquinone oxime tautomer. In order to understand the energetics of reaction 39, we derived the solid phase enthalpy of formation of nitrosobenzene (monomeric PhNO) by

(a) accepting the gas phase enthalpy of formation of this species from thermochemical kinetics studies [61];

(b) combining the enthalpy of formation of the solid nitrosobenzene dimer from Reference 62 and assuming that the solution phase dimerization enthalpy from Reference 63 may be applied to the gaseous state;

(c) combining the enthalpy of formation of the gaseous nitrosobenzene dimer from Reference 62 and assuming that the solution phase dimerization enthalpy from Reference 63 may be applied to the gaseous state; and

(d) equating the sublimation enthalpy of monomeric nitrosobenzene with that of benzaldehyde (the sum of vaporization and fusion enthalpies).

This resulted in an enthalpy of reaction 39 of *ca* 70 kJ mol^{-1}. While this is much larger than what would be predicted for the correction due to nitroso-phenol conjugation and the energies of most hydrogen bonds, the value for the related reaction for *p*-nitrophenol (equation 40) is the rather comparable 80 kJ mol^{-1}.

$$\text{4-HOC}_6\text{H}_4\text{NO}_2 + \text{C}_6\text{H}_6 \longrightarrow \text{PhOH} + \text{PhNO}_2 \quad (40)$$

As such, thermochemical analogies don't help us decide which tautomer is more stable. From the literature we conclude that the quinone oxime tautomer is somewhat the more stable, the precise enthalpy and free energy difference depending on the solvent, substituents and reaction conditions (see the recent paper, Reference 60, and references cited therein).

The situation is simultaneously exacerbated for the corresponding *o*-species, here denoted 2-O=C_6H_4=NOH/2-HOC_6H_4N=O, because there is no experimental determination of the enthalpy of formation of this *o*-benzoquinone oxime/*o*-nitrosophenol pair and there is also intramolecular hydrogen bonding in suitably chosen rotamers of these two species. As such, we cannot investigate, using experimentally determined numbers, the enthalpy of reaction 41 even though there is a recent determination of the gas phase enthalpy of formation of *o*-benzoquinone, as well as two di-*t*-butyl derivatives[56].

$$\text{4-O=C}_6\text{H}_4\text{=NOH/4-HOC}_6\text{H}_4\text{N=O} + \text{2-O=C}_6\text{H}_4\text{=O} \longrightarrow \text{2-O=C}_6\text{H}_4\text{=NOH/2-HOC}_6\text{H}_4\text{N=O} + \text{4-O=C}_6\text{H}_4\text{=O} \quad (41)$$

We note that the difference between the enthalpy of formation of the unsubstituted benzoquinone/nitrosophenol and that of its isopropyl methyl 'cymene-like' disubstituted derivative is 146 kJ mol^{-1}, comparable to that of the corresponding hydrocarbons, benzene and its substituted counterpart as liquids, 127.0 ± 1.2 kJ mol^{-1}, and as the corresponding phenols as solids, 144.4 ± 9.6 kJ mol^{-1}.

B. 5-Cyclohexene-1,2,3,4-tetraone-1,3-dioxime (2,4-Dinitrosoresorcinol)

This species enjoys much tautomeric ambiguity. Besides the two names given above we also recognize this species as tautomerically equivalent to 3-nitroso-4-hydroxy-*o*-benzoquinone 1-oxime and 2-nitroso-3-hydroxy-*p*-benzoquinone 1-oxime. It is this ambiguity that encouraged us to include in this chapter the nearly 100-year-old calorimetry measurements[59] for this species. Without attempting to write and interpret a balanced thermochemical reaction (as we said, there are no data for *o*-benzoquinone oxime/2-nitrosophenol in the experimental literature), nonetheless, this is an intriguing polyfunctionalized species that we feel is worthy of further investigation.

C. Naphthol/Naphthoquinone Derivatives

Much the same confusing situation applies to the energetics of 1,2- and 1,4-disubstituted naphthalene derivatives. That the 1,4-species is meaningfully more stable than either of its 1,2-isomers suggests these species are 1,4- and 1,2-naphthoquinone derivatives—based on other pairs of isomeric naphthalenes such as the naphthols, we do not expect that much difference between the enthalpies of formation of 1- and 2-nitrosonaphthalenes while 1,4-naphthoquinone, as solid, is reported[2] to be *ca* 25 kJ mol^{-1} more stable than its 1,2-isomer. However, that the enthalpy of formation of the 1-oxime of 1,2-naphthoquinone is reported to be *ca* 40 kJ mol^{-1} less stable than the 2-oxime is not explicable in terms of quinone stability, hydrogen bonding or even invocation of the nitrosonaphthol being the more stable tautomer. That the enthalpies of sublimation differ by this *ca* 40 kJ mol^{-1} provides an explanation—the solid phase enthalpies of formation are sensibly nearly the same—but this is a pyrrhic victory. We are forced to ask: Do we now trust the gas phase enthalpy of formation values of any of these quinone oximes/nitrosoarenols at all?

D. Related Nitrogenous Cases

If nitrosophenols are in equilibrium with quinone oximes, are nitrosoanilines in equilibrium with quinonimine oximes? While in solution, 2-nitrosoanilines appear to show such behavior[64] and crystallographic determination shows the benzenoid form is preferred[65]. The enthalpy of formation of 4-nitrosodiphenylamine—or is it *N′*-phenyl-*p*-benzoquinone oxime—has been measured[1] (213.1 ± 3.2 kJ mol^{-1}), but as this value is for the solid we hesitate to make any thermochemical comparisons. Perhaps relatedly, the enthalpy of formation of 3,5-dimethyl-4-nitrosopyrazole has been determined[66] but there are no data for any pyrazolones (1,2-diazacyclopentadienones as opposed to pyrazolinones) with which to make comparison with a putative oxime.

VII. OXIME ETHERS

Oxime ethers have a >C=N−O−C− substructure. Table 5 presents the enthalpy of formation data for such species where there is little structural commonality save the functional group of interest.

TABLE 5. Enthalpies of formation for oxime ethers and esters (kJ mol^{-1})

Compound	Formula	ΔH_f(s)	Reference	ΔH_f(lq)	Reference	ΔH_f(g)	Reference
3-Nitro-2-isoxazoline	$C_3H_4N_2O_3$			-20.0 ± 1.3	1	39.0 ± 1.5	1
1-Nitroacetaldehyde *O*-(1,1-dinitroethyl)oxime (O_{NO}-1,1-dinitroethyl acetonitronate) [a]	$C_4H_6N_4O_7$	-165.5 ± 2.01	1				
7,8-Dimethoxy-1*H*-2,3-benzoxazin-1-one (opianic acid oxime anhydride)	$C_{10}H_9NO_4$	-400.4	2				
cis-3-Phenyl-2-isoxazolinedicarboxylic acid dimethyl ester	$C_{13}H_{13}NO_5$	-864.8	67				
trans-3-Phenyl-2-isoxazolinedicarboxylic acid dimethyl ester	$C_{13}H_{13}NO_5$	-739.3	67				

[a] The structure shown in Reference 3 for this species is for 2-nitroacetaldehyde *O*-(1,1-dinitroethyl)oxime.

This appears to be a rather mixed collection of compounds. We recognize three isoxazolines in the collection. However, the data for the last two species, the *cis* and *trans* isomers of 3-phenyl-2-isoxazolinedicarboxylic acid dimethyl ester from Reference 67, are suspect because the difference of 125 kJ mol^{-1} is implausible—the corresponding difference for the *cis* and *trans* butenedioic acid dimethyl esters from Reference 68 is but *ca* 30 kJ mol^{-1}.

The 3-nitroisoxazoline has gas and liquid phase values available. Given the absence of knowledge about isoxazolines, we accept these data and use them in what follows. We are told[69] that the dehydration reaction of 3-phenyl-Δ^2-isoxazoline-5-ol (an oxime ether) to form 3-phenylisoxazole (equation 42) is exothermic by 16 kJ mol^{-1}. The gas phase enthalpy of formation of the latter species[1] is 139.5 ± 6.2 kJ mol^{-1}. (As the isoxazoles are nominally aromatic, they are not included here as unsaturated oxime ethers.)

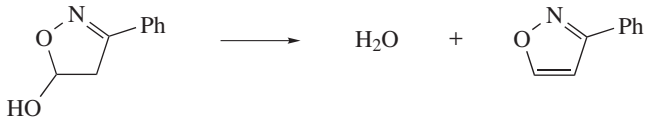

(42)

Assuming that the exothermicity is independent of phase and using the gas phase enthalpy of formation of water (-241.818 kJ mol^{-1}) gives us the desired enthalpy of formation of the isoxazoline of -86 kJ mol^{-1}. If we assume that the liquid phase is appropriate, then with the enthalpies of formation of the liquid phenyl isoxazole and water we find -194 kJ mol^{-1}. Are these values plausible? We will continue with our gas phase preference. Let us make the following assumptions. The introduction of a nitro group into isoxazoline is the same as in benzene, *i.e.* reaction 43 is thermoneutral.

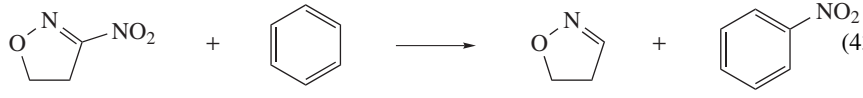

(43)

The strain energies of isoxazolidine and isoxazoline are the same, and so using the derived enthalpy of formation of the former from an earlier section (9 kJ mol^{-1}) and that of the two methyl ethers from the calculations of Reference 8 (MeCH=NOMe is -7.1 kJ mol^{-1} and $MeCH_2NHOMe$ is -60.5 kJ mol^{-1}), equation 44 is thermoneutral.

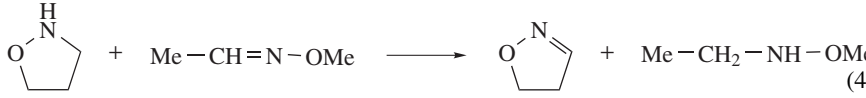

(44)

Equations 43 and 44 are equally valid and so we should average their results of 54 and 62 kJ mol^{-1}, respectively, to derive the enthalpy of formation of isoxazoline to be 59 kJ mol^{-1}.

The introduction of a phenyl group in isoxazole and isoxazoline has the same enthalpic change and equation 45 is thermoneutral, and so the enthalpy of formation of phenylisoxazoline is 116 kJ mol^{-1}.

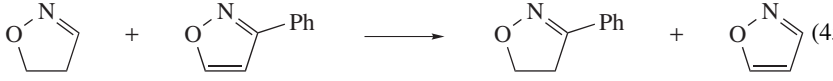

(45)

Hydroxylating 3-phenylisoxazoline is enthalpicly the same as for cyclopentane, with an added 39 kJ mol^{-1} for anomeric stabilization (equation 46)[70].

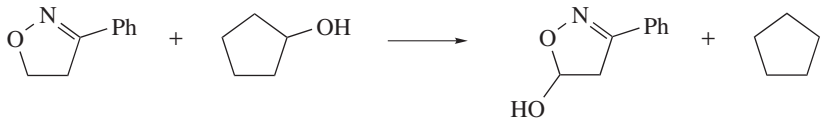
(46)

The resulting value for the enthalpy of formation of 3-phenyl-Δ^2-isoxazoline-5-ol is -86 kJ mol^{-1}, which is in fine agreement with that obtained from the reaction calorimetry.

Interestingly, two of the other species in Table 3 are nitrolates, *i.e.* ethers of α-nitrooximes, an otherwise thermochemically unprecedented class of compounds. We already have briefly discussed one, 3-nitroisoxazoline, and the second is 1-nitroacetaldehyde *O*-(1,1-dinitroethyl)oxime (O_{NO}-1,1-dinitroethyl acetonitronate), MeC$(NO_2)_2-O-N=C(NO_2)$Me. The latter acyclic species is a derivative of 1,1-dinitroethanol—we know of the enthalpy of formation of no other α-nitroalcohol or derivative. Nonetheless, we may ask if the two calorimetric data are internally consistent. Consider the condensed phase reaction 47, which involves formal cleavage of the C^4-C^5 bond in the nitroisoxazoline by the C−H bond of the dinitromethane. It is assumed that the isoxazoline has the same strain energy as the archetypal 5-atom ring species cyclopentane and cyclopentene, *ca* 30 kJ mol^{-1}.


(47)

Equivalently, the enthalpy of reaction 47 is equated to that of the analogous (unsubstituted, saturated, carbocyclic) reaction 48. The difference is 29 kJ mol^{-1}, taken as the strain energy of cyclopentane.


(48)

Using enthalpies of formation of the liquid species from Reference 1, the enthalpy of formation of the liquid 2,2-dinitronitronate ester is *ca* -155 kJ mol^{-1}.

Reaction 49 involves the isomerization of the 2,2-dinitro compound to its 1,1-isomer, which is of direct interest here. The latter is plausibly more strained and so its enthalpy of formation would be more positive. The phase change—from a liquid to a solid—would result in a more negative enthalpy of formation. If these two changes are assumed to cancel, we would predict an enthalpy of formation of 1-nitroacetaldehyde *O*-(1,1-dinitroethyl)oxime of -151 kJ mol^{-1} while the literature value is -165.5 kJ mol^{-1}. That these two values are close suggests that the two nitrolate enthalpy of formation values are at least self-consistent.


(49)

By use of direct combustion calorimetry and that of the isomerization of reaction 50, we are told[71] that 7,8-dimethoxy-1*H*-2,3-benzoxazin-1-one (opianic anhydride oxime) is

220 kJ mol^{-1} less stable than the corresponding dimethoxylated phthalimide (hemipinimide). Again we ask: 'is this value plausible?'

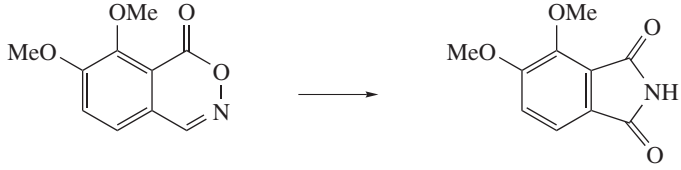

(50)

Let us assume that the effect of the dimethoxy groups is the same for both species and that the enthalpy difference is independent of which phase is chosen for the two species. From combustion and sublimation measurements, the enthalpy of formation[72] of gaseous phthalimide is found to be -211 kJ mol^{-1}. Accordingly, the enthalpy of formation of gaseous 1*H*-2,3-benzoxazin-1-one is predicted to be *ca* 10 kJ mol^{-1}. Now consider isatoic anhydride and its gas phase enthalpy of formation[73] of -406.2 ± 3.5 kJ mol^{-1}. Let us convert the CONH group therein to a C=N group to form 4*H*-5,6-benzoxazin-4-one (reaction 51), and assume that this reaction has the same endothermicity as for other gaseous amides[74] of *ca* 252 ± 20 kJ mol^{-1}. Accordingly 4*H*-5,6-benzoxazin-4-one is predicted to have a gas phase enthalpy of formation of -154.2 kJ mol^{-1}.

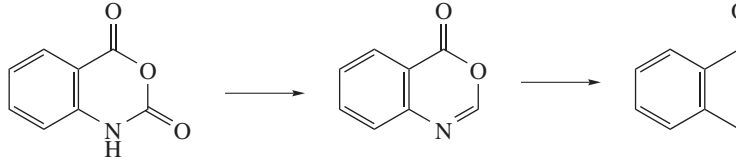

(51)

Reversing the CH=N group position in 4*H*-5,6-benzoxazin-4-one should result in the same isomerization enthalpy as from HC(NMe)OMe to MeCHNOMe. The enthalpy of formation of the latter species was calculated to be -7.1 kJ mol^{-1} from the high-level quantum chemical calculations of Reference 4. The enthalpy of formation of the former species is unknown. However, if we accept the gas phase isomerization enthalpy of dimethylamides to methyl imidates (69.6 ± 13.4 kJ mol^{-1}) in equation 52 from Reference 75,

(52)

and the enthalpy of formation of dimethylformamide from Reference 1, -192.4 ± 1.8, we derive the enthalpy of formation of the desired formimidate ester to be -123 ± 13 kJ mol^{-1}. The isomerization enthalpy in equation 51 is thus calculated to be 116 kJ mol^{-1}, resulting in the predicted enthalpy of formation of 1*H*-2,3-benzoxazin-1-one of *ca* -38 kJ mol^{-1}. The two values, $+10$ and -38 kJ mol^{-1}, are disparate by 48 kJ mol^{-1}.

Now where does the discrepancy lie? An acyclic paradigm was used for the oximate/imidate interconversion. Had we used the plausibly aromatic paradigm of isoxazole/oxazole, the isomerization enthalpy would have been 95 kJ mol^{-1} where the requisite enthalpies of formation are from References 76 and 1, respectively. This difference is meaningfully distinct from that of the acyclic paradigm but still does not particularly ameliorate the difference. Is it possible that the N–O bond in aryl and alkyl oxime ethers are profoundly different? Could it be that we have neglected any antiaromaticity in the 8 π

phthalimide and aromaticity in the 10 π 1*H*-2,3-benzoxazin-1-one? The former contribution is quite negligible[77]; the latter remains undetermined[78]. The only other conclusion is that the initial isomerization enthalpy of hemipinimide into opianic oxime anhydride is in error[79].

The last species is $Ph_2C{=}N{-}OPh$, where its enthalpy of formation does not appear in our table of enthalpies of formation of oxime ethers. The N−O bond dissociation energy, *i.e.* roughly the enthalpy of reaction 53, has been measured[80] and the enthalpy of formation of $PhO^{\bullet}$ is quite reliably known, *e.g.* see Reference 81.

$$Ph_2C{=}N{-}OPh \longrightarrow Ph_2C{=}N^{\bullet} + PhO^{\bullet} \tag{53}$$

What is known about the enthalpy of formation of the other fragment radical, $Ph_2C{=}N^{\bullet}$? The enthalpy of formation of $H^{\bullet}$ is well-established and that of $Ph_2C{=}NH$ has been calorimetrically determined[82]. The N−H bond energy in this imine, *i.e.* roughly the enthalpy of reaction 54, has been reported, twice[80,83].

$$Ph_2C{=}NH \longrightarrow Ph_2C{=}N^{\bullet} + H^{\bullet} \tag{54}$$

These data should allow us to derive the desired enthalpy of formation of the iminyl radical. The problem is that the two results differ by *ca* 100 kJ mol^{-1}! The effect of substituents on the thermochemistry of oximes, their ethers and related imines are not so well-established for us to attempt deciding between these two bond energies.

VIII. HYDROXAMIC ACIDS AND THEIR DERIVATIVES

Hydroxamic acids are a highly important class of compounds as discussed in other chapters in this volume. Nonetheless, their thermochemistry appears limited to surprisingly few species. See Table 6.

Hydroxamic acids are related to amides as hydroxylamines are related to amines. *N*-Hydroxylation of a gaseous primary amine is *ca* −27 kJ mol^{-1} and greater exothermicity is expected for the condensed phase because of intermolecular hydrogen-bonding. Is this true for amides as well? The enthalpy of formation of solid oxalamide, $(H_2NC{=}O)_2$, is -504.5 ± 5 kJ mol^{-1} corresponding to a *ca* −19 kJ mol^{-1} difference between the diamide and the corresponding dihydroxamic acid, oxalohydroxamic acid, per structural unit. The change is thus smaller than for amines. *N*-Hydroxylation of 2-pyridone, from its archival enthalpy of formation of -166.3 ± 1.8 kJ mol^{-1}, to *N*-hydroxy-2-pyridone in Table 6, is -32.4 ± 0.4 kJ mol^{-1}. The structurally dissimilar diamide and aromatic pyridine would not be expected to have closely similar differences.

What about the isomers of the hydroxamic acids, the *O*-acyl derivatives of hydroxylamine? Having mentioned early in this study that *N*-methylhydroxylamine is more stable than its *O*-isomer, we are thus intrigued by the finding[87] that *N*-benzoylhydroxylamine (benzohydroxamic acid), or at least its *N*-*t*-butyl derivative, is less stable than its corresponding *O*-benzoyl isomer as shown by the thermal isomerization of the former to the latter, equation 55.

$$PhC(O)N(Bu\text{-}t)OH \longrightarrow (t\text{-}Bu)NHOC(O)Ph \tag{55}$$

Although perhaps explicable, or at least precedented, in terms of the greater resonance energy of esters than corresponding amides[88], nonetheless, a further study is welcomed as this is the only thermochemical information we have on this class of compounds.

We close this section with a mention of the enthalpy of formation[86] of 1,2-benzisothiazol-3(2*H*)-one (dideoxysaccharin). This compound is thermochemically unique as it is

TABLE 6. Enthalpies of formation for hydroxamic acids ($kJ\,mol^{-1}$)

Compound	Formula	ΔH_f(s)	Reference	ΔH_f(lq)	Reference	ΔH_f(g)	Reference
Oxalohydroxamic acid (dihydroxyglyoxime)	$C_2H_4N_2O_4$	−542.7	84				
N-Hydroxy-2-pyridone	$C_5H_5NO_2$	−198.7 ± 1.7	85			−109.3 ± 1.3	85
1,2-Benzisothiazol-3(2*H*)-one (dideoxysaccharin)	C_7H_5NOS	−98.6 ± 2.6	86			13.6 ± 3.6	86

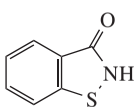

the sole example for a thiohydroxamic acid ester. Indeed, there are no other examples of thiohydroxamic derivatives for which there is a measured enthalpy of formation and so this species remains in sweet, solitary splendor[89]. What about sulfur analogs of our classes of compounds, such as species with S−N bonds reminiscent of hydroxylamines? Species with the N−S−N functionality that have been thermochemically studied are $Et_2NSO_2NEt_2$, $Et_2NS(O)NEt_2$ and Et_2NSNEt_2, although the last is admittedly unmeasured, but plausibly understood[90] in terms of the related measured disulfide, $Et_2NSSNEt_2$. The enthalpy of formation has also been measured[91] for the heterocyclic S_7NH, also with the S−N−S functionality. Only quantum chemical calculations[92] are available for the archetypal N−S species NH_2SH. The sparse organic thermochemistry of such species, recognized as sulfenamides, has been reviewed[93]. It appears that we cannot compare the energetics of isoelectronically related N−S and N−O containing species. Perhaps this will be realizable in a future review of the thermochemistry of hydroxylamines, oximes and hydroxamic acids.

IX. REFERENCES AND NOTES

1. J. B. Pedley, *Thermochemical Data and Structures of Organic Compounds*, Vol. 1, TRC Data Series: College Station, TX, 1994.
2. D. R. Stull, E. F. Westrum, Jr and G. C. Sinke, *The Chemical Thermodynamics of Organic Compounds*, Wiley, New York, 1969. (We used the slighly amended, reprinted edition from R.E. Krieger Publishing Co., Malabar, FL, 1987.)
3. H. Y. Afeefy, J. F. Liebman and S. E. Stein, '*Neutral Thermochemical Data*', in *NIST Chemistry WebBook, NIST Standard Reference Database Number 69* (Eds. W. G. Mallard and P. J. Linstrom), June 2005, National Institute of Standards and Technology, Gaithersburg, MD 20899 (http://webbook.nist.gov).
4. D. S. Shaikhlislamov, M. R. Talipov and S. L. Khursan, *Russ. J. Phys. Chem. A*, **81**, 235 (2007).
5. J. S. Chickos, W. E. Acree, Jr. and J. F. Liebman, *J. Phys. Chem. Ref. Data*, **28**, 1535 (1999).
6. D. D. Wagman, W. H. Evans, V. B. Parker, R. H. Schumm, I. Halow, S. M. Bailey, K. L. Churney and R. L. Nuttall, *J. Phys. Chem. Ref. Data*, **11** (Supplement No. 2) (1982).
7. N. Matsunaga, D. W. Rogers and A. A. Zavitsas, *J. Org. Chem.*, **68**, 3158 (2003).
8. S. W. Slayden and J. F. Liebman, in *The Chemistry of Functional Groups Supplement E2: The Chemistry of Hydroxyl, Ether and Peroxide Groups* (Ed. S. Patai), Wiley, Chichester, 1993, p. 103.
9. S. W. Slayden and J. F. Liebman, in *The Chemistry of Peroxides*, Vol. 2 (Ed. Z. Rappoport), Wiley, Chichester, 2006, p. 145.
10. J. F. Liebman, H. Y. Afeefy and S. W. Slayden, in *The Chemistry of Hydrazo, Azo and Azoxy Groups*, Vol. 2 (Ed. S. Patai), Wiley, Chichester, 1997, p. 79.
11. W. V. Steele, R. D. Chirico, A. Nguyen, I. A. Hossenlopp and N. K. Smith, *Am. Inst. Chem. Eng. Symp. Ser. (AIChE Symp. Ser.)*, 138 (1990).
12. (a) J. F. Liebman, M. S. Campbell and S. W. Slayden, in *The Chemistry of Functional Groups Supplement F2: The Chemistry of Amino, Nitroso, Nitro and Related Groups* (Ed. S. Patai), Wiley, Chichester, 1996, p. 337.
    (b) S. W. Slayden and J. F. Liebman, in *The Chemistry of Anilines* (Ed. Z. Rappoport), Wiley, Chichester, 2007, p. 259.
13. E. P. Hunter and S. G. Lias, *J. Phys. Chem. Ref. Data*, **27**, 413 (1998).
14. F. Angelelli, M. Aschi, F. Cacace, F. Pepi and G. de Petris, *J. Phys. Chem.*, **99**, 6551 (1995).
15. A. Johansson, P. A. Kollman, J. F. Liebman and S. Rothenberg, *J. Am. Chem. Soc.*, **96**, 3750 (1974).
16. M. A. V. Ribeiro da Silva and J. I. T. A. Cabral, *J. Chem. Eng. Data*, **51**, 1556 (2006).
17. M. A. V. Ribeiro da Silva and J. I. T. A. Cabral, *J. Chem. Eng. Data*, **51**, 767 (2006).
18. Y. B. Tewari, D. J. Vanderah, M. M. Schantz, R. N. Goldberg, J. D. Rozzell, J. F. Liebman, R. W.-M. Hui, Y. Nissenbaum and A. R. Parniani, *J. Chem. Thermodyn.* **40**, 661 (2008).

19. S. W. Slayden and J. F. Liebman, in *The Chemistry of Functional Groups Supplement A3: The Chemistry of the Double-bonded Functional Groups* (Ed. S. Patai), Wiley, Chichester, 1997, p. 537.
20. We note now the conference proceedings paper, M. V. Roux, J. Z. Dávalos and P. Jiménez, 12th International Congress on Thermal Analysis and Calorimetry, August 14–18, 2000, Copenhagen, Denmark, pp. 305–306.
21. P. E. Coles, R. N. Haszeldine, A. J. Owen, P. J. Robinson and B. J. Tyler, *J. Chem. Soc., Chem. Commun.*, 340 (1975).
22. P. W. Harland, *Int. J. Mass Spectrom.*, **25**, 61 (1977).
23. Y. D. Samuilov, R. L. Nurullina, S. E. Solov'eva and A. I. Konovalov, *Zh. Obshch. Khim.*, **48**, 2586 (1978); *Chem. Abstr.*, **90**, 71412 (1979).
24. M. V. Roux, P. Jiménez, M. A. Martin-Luengo, J. Z. Dávalos, Z. Sun, R. S. Hosmane and J. F. Liebman, *J. Org. Chem.*, **62**, 2732 (1997).
25. The enthalpy of formation of *N*-phenylphthalimide was recently reported, M. A. V. Ribeiro da Silva and C. P. F. Santos, *J. Therm. Anal. Calor.*, **87**, 21 (2007).
26. Y. D. Samuilov, A. I. Movchan, S. E. Solov'eva and A. I. Konovalov, *Zh. Org. Khim.*, **21**, 1772 (1985); *Chem. Abstr.*, **104**, 206450 (1986).
27. W. V. Steele, R. D. Chirico, A. Nguyen, I. A. Hossenlopp and N. K. Smith, *J. Chem. Thermodyn.*, **23**, 101 (1991).
28. E. A. Miroshnichenko, V. A. Tartakovskii and Y. A. Lebedev, *Khim. Geterotsikl. Soedin.*, 351 (1968); *Chem. Abstr.*, **69**, 70842 (1968).
29. A. V. Pankratov, A. N. Zercheninov, V. I. Chesnokov and N. N. Zhdanova, *Zh. Fiz. Khim.*, **43**, 394 (1969); *Chem. Abstr.*, **70**, 118752 (1969).
30. K. Sudlow and A. A. Woolf, *J. Fluorine Chem.*, **73**, 47 (1995).
31. D. F. Bowman, T. Gillan and K. U. Ingold, *J. Am. Chem. Soc.*, **93**, 6555 (1971).
32. N. D. Lebedeva, N. M. Gutner and L. F. Nazarova, *Termodin. Org. Soedin.*, 26 (1977); *Chem. Abstr.*, **89**, 128950 (1978).
33. Q. Shi, Z.-C. Tan, B. Tong, Y.-Y. Di, Z.-H. Zhang, J.-L. Zeng, L.-X. Sun and Y.-S. Li, *J. Chem. Thermodyn.*, **39**, 817 (2007).
34. (a) W. V. Steele, R. D. Chirico, A. B. Cowell, S. E. Knipmeyer and A. Nguyen, *J. Chem. Eng. Data*, **47**, 725 (2002).
    (b) Note, there is another, also contemporaneous, study with nearly indistinguishable results: A. A. Kozyro, G. J. Kabo, V. S. Krouk, M. S. Sheiman, I. A. Yursha, V. V. Simirsky, A. P. Krasulin, V. M. Sevruk and V. I. Gogolinsky, *J. Chem. Thermodyn.*, **24**, 883 (1992).
35. G. Geiseler, M. Rätzsch, K. Ebster and E. Ziegel, *Ber. Bunsenges. Phys. Chem.*, **70**, 221 (1966).
36. J. D. Cox and G. Pilcher, *Thermochemistry of Organic and Organometallic Compounds*, Academic Press, London, 1970. In addition, the 'universal methylene increment' has been a major tool in our analyses of literature thermochemical data in many of our earlier Patai/Rappoport chapters, *e.g.* References 8 and 9.
37. The difference between the calculated enthalpies of formation of MeCH=NOH and EtCH=NOH (Reference 4) is but 14 kJ mol^{-1}, an anomalously small value, while that between EtCH=NOH and PrCH=NOH is 26 kJ mol^{-1}, correspondingly large. The difference between the experimentally measured enthalpies of formation of MeCHO and EtCHO is 19.5 ± 0.9 kJ mol^{-1} and that between EtCHO and PrCHO is 19.2 ± 1.6 kJ mol^{-1}—neither value is anomalous. We thus wonder if there is an error in the calculation for propanal oxime, especially since the average of the enthalpies of formation for MeCH=NOH and PrCH=NOH is essentially the same as the value we derived.
38. G. Geiseler and M. Rätzsch, *Ber. Bunsenges. Phys. Chem.*, **69**, 485 (1965).
39. (a) J. F. Liebman and A. Greenberg, *Chem. Rev.*, **89**, 1225 (1989).
    (b) J. F. Liebman and A. Greenberg, in *The Chemistry of the Cyclopropyl Functional Group* (Ed. Z. Rappoport), Wiley, Chichester, 1987, p. 1083.
    (c) J. F. Liebman, in *The Chemistry of the Cyclopropyl Group*, Vol. 2 (Ed. Z. Rappoport), Wiley, Chichester, 1995, p. 223.
40. C. D. Nenitzescu and E. Cioranescu, *Ber. Dtsch. Chem. Ges.*, **69B**, 1820 (1936).
41. S. L. Friess and R. Pinson, Jr., *J. Am. Chem. Soc.*, **73**, 3512 (1951).
42. I. S. Akhrem, L. V. Afanas'eva, P. V. Petrovskii, S. V. Vitt and A. V. Orlinkov, *Russ. Chem. Bull.*, **50**, 2394 (2001).

43. J. A. Young, J. E. Keith, P. Stehle, W. C. Dzombak and H. Hunt, *Ind. Eng. Chem.*, **48**, 1375 (1956).
44. A. Stern and G. Klebs, *Ann. Chim.*, **505**, 295 (1933).
45. S. W. Slayden and J. F. Liebman, in *The Chemistry of Phenols* (Ed. Z. Rappoport), Wiley, Chichester, 2003, p. 223.
46. A. Dorabialska, *Rocz. Chem.*, **5**, 386 (1925).
47. (a) E. Lustig, *J. Phys. Chem.*, **65**, 491 (1961).
    (b) M. D. Mosher and S. Meisenbach, *Chem. Educ.*, **7**, 356 (2002).
48. R. Yanagi, C. Matui, M. Chinda and Y. Yamamoto, *Bull. Chem. Soc. Jpn.*, **67**, 1740 (1994).
49. References include:
    (a) P. Landrieu, *Compt. Rendu*, **140**, 867 (1905).
    (b) J. E. Dubois, W. Wolf and H. Herzog, *Compt. Rendu, Ser. C*, **263**, 349 (1966).
    (c) J. Vulterin, P. Straka, M. Stastny and R. Volf, *Chem. Prumysl.*, **24**, 618 (1974).
    (d) J. Vulterin, P. Straka, M. Stastny and R. Volf, *Cesko-Slovenska Farmacie*, **24**, 10 (1975).
    We limit our attention to only those cases where we have trustworthy values of the enthalpy of formation of the parent carbonyl compounds, and even here we are hesitant.
50. J. L. Wood and M. M. Jones, *J. Phys. Chem.*, **67**, 1049 (1963).
51. C. R. Brent, 'A thermochemical study of the C=N and N−O bonds energies in tetramethylene furoxan and cyclohexanedione dioxime', Ph.D. Thesis, Tulane University, 1963; *Chem. Abstr.*, **60**, 79426 (1964).
52. W. R. Roth, H. W. Lennartz, W. v. E. Doering, W. R. Dolbier, Jr. and J. C. Schmidhauser, *J. Am. Chem. Soc.*, **110**, 1883 (1988).
53. J. F. Liebman, *Struct. Chem.*, **3**, 449 (1992).
54. G. Pilcher, O. G. Parchment, I. H. Hillier, F. Heatley, D. Fletcher, M. A. V. Ribeiro da Silva, M. L. C. C. H. Ferrão, J. S. Monte and F. Jiye, *J. Phys. Chem.*, **97**, 243 (1993).
55. J. P. Kercher, E. A. Fogleman, H. Koizumi, B. Sztaray and T. Baer, *J. Phys. Chem. A*, **109**, 929 (2005).
56. A. Fattahi, S. R. Kass, J. F. Liebman, M. A. R. Matos, M. S. Miranda and V. M. F. Morais, *J. Am. Chem. Soc.*, **127**, 6116 (2005).
57. M. Temprado, M. V. Roux, P. Umnahanant, H. Zhao and J. S. Chickos, *J. Phys. Chem. B*, **109**, 12590 (2005).
58. P. Umnahanant and J. S. Chickos, *J. Chem. Eng. Data*, **50**, 1720 (2005).
59. W. Swientoslawski, *Z. Phys. Chem.*, **72**, 49 (1910).
60. M. D. M. C. Ribeiro da Silva, M. A. R. Matos, M. L. C. C. H. Ferrão, L. M. P. F. Amaral, M. S. Miranda, W. E. Acree, Jr. and G. Pilcher, *J. Chem. Thermodyn.*, **31**, 1551 (1999).
61. K. Y. Choo, D. M. Golden and S. W. Benson, *Int. J. Chem. Kinet.*, **7**, 713 (1975).
62. V. I. Pepekin, V. P. Lebedev, A. A. Balepin and Yu. A. Lebedev, *Dokl. Phys. Chem. (Engl. Transl.)*, **221**, 370 (1975).
63. K. G. Orrell, V. Sik and D. Stephenson, *Magn. Reson. Chem.*, **25**, 1007 (1987).
64. I. M. El-Nahhal and G. S. Heaton, *J. Chem. Res. (S)*, 299 (1989).
65. R. G. Pritchard, G. S. Heaton and I. M. El-Nahhal, *Acta Crystallogr.*, **C45**, 829 (1989).
66. M. D. M. C. Ribeiro da Silva, S. C. C. Ferreira, I. A. P. Rodrigues, L. C. M. da Silva, W. E. Acree, Jr., S. Pandey and L. E. Roy, *J. Chem. Thermodyn.*, **33**, 1227 (2001).
67. G. S. D'Alcontres, *Acta Cient. Venez.*, **4**, 63 (1953).
68. M. A. R. Matos, M. S. Miranda, V. M. F. Morais and J. F. Liebman, *Org. Biomol. Chem.*, **1**, 2930 (2003).
69. A. V. Chapman, M. J. Cook, A. R. Katritzky, M. H. Abraham, M. A. F. Danil de Namor, L. Dumont and J. Reisse, *Tetrahedron*, **34**, 1571 (1978).
70. S. P. Verevkin, W.-H. Peng, H.-D. Beckhaus and C. Rüchardt, *Eur. J. Org. Chem.*, 2323 (1998).
71. C. Liebermann, *Ber. Dtsch. Chem. Ges.*, **25**, 89 (1892); *Chem. Abstr.*, **0**, 78838 (1906).
72. M. A. V. Ribeiro da Silva, C. P. F. Santos, M. J. S. Monte and C. A. D. Sousa, *J. Therm. Anal. Calorimetry*, **83**, 533 (2006).
73. V. M. F. Morais, M. A. R. Matos, M. S. Miranda and J. F. Liebman, *Org. Biomol. Chem.*, **2**, 1647 (2004).
74. V. M. F. Morais, M. S. Miranda, M. A. R. Matos and J. F. Liebman, *Mol. Phys.*, **104**, 325 (2006).
75. P. Beak, J.-K. Lee and J. M. Zeigler, *J. Org. Chem.*, **43**, 1536 (1978).

76. W. V. Steele, R. D. Chirico, S. E. Knipmeyer, A. Nguyen, N. K. Smith and I. R. Tasker, *J. Chem. Eng. Data*, **41**, 1269 (1996).
77. Benzo-annelation of benzene results in the less aromatic naphthalene. Benzo-annelation of the antiaromatic cyclobutadiene results in the less antiaromatic benzocyclobutadieene; cf. A. Fattahi, L. Lis, Z. Tian and S. R. Kass, *Angew. Chem. Int. Ed.*, **45**, 4984 (2006) and K. M. Broadus and S. R. Kass, *J. Am. Chem. Soc.*, **122**, 10697 (2000). This suggests that phthalimide will be less antiaromatic than maleimide, which is only marginally so (cf. Reference 24). See also M. A. R. Matos and J. F. Liebman, in *Topics in Heterocyclic Chemistry: Aromaticity in Heterocyclic Chemistry* (Eds. T. M. Krygowski and M. K. Cyranski), Springer, Heidelberg (in press).
78. While there are enthalpy of formation data for coumarin [L. E. Watik and R. Sabbah, *Bull. Soc. Chim. Fr.*, **128**, 344 (1991)], there are none for its isomer with the CO and O exchanged, nor for α-pyrone missing the benzene ring, and so extrapolation of the benzoxazinone is problematic.
79. In the original abstract there is the following text: '... a difference of 52.6 Cal. [i]s the heat evolved by the molecular change. This amount of heat is 10 times that developed in the change of allocinnamic into cinnamic acid and more than six times the amount due to the change of maleic into fumaric acid'. Translating to our preferred set of units, as noted above the difference between the species of interest is 220 kJ mol^{-1}, while the contemporary values for maleic and fumaric acid give a difference of 22.3 kJ mol^{-1}. Translating allocinnamic acid as the (*Z*)-isomer, the contemporary difference for these isomers is 24.8 kJ mol^{-1}. Neither contemporary 'conversion rate' corresponds to the arithmetic values offered, suggestive of experimental complications.
80. J. A. Blake, D. A. Pratt, S. Lin, J. C. Walton, P. Mulder and K. U. Ingold, *J. Org. Chem.*, **69**, 3112 (2004).
81. R. M. Borges dos Santos and J. A. Martinho Simões, *J. Phys. Chem. Ref. Data*, **27**, 707 (1998).
82. S. P. Verevkin, J. Morgenthaler and C. Rüchardt, *J. Chem. Thermodyn.*, **29**, 1175 (1997).
83. F. G. Bordwell and G. Z. Ji, *J. Am. Chem. Soc.*, **113**, 8398 (1991).
84. E. E. Baroody and G. A. Carpenter, *Heats of Formation of Propellant Compounds*, Rep. Naval Ordnance Systems Command Task No. 331-003/067-1/UR2402-001 for Naval Ordnance Station, Indian Head, MD, 1972, pp. 1–9.
85. M. D. M. C. Ribeiro da Silva, M. A. R. Matos, M. S. Miranda, V. M. F. Morais and W. E. Acree, *J. Chem. Thermodyn.*, **36**, 107 (2004).
86. M. A. R. Matos, M. S. Miranda, V. M. F. Morais and J. F. Liebman, unpublished results.
87. S. A. Hussain and M. J. Perkins, *J. Chem. Soc. Pakistan*, **8**, 217 (1986); *Chem. Abstr.*, **106**, 101832 (1987).
88. J. F. Liebman and A. Greenberg, *Biophys. Chem.*, **1**, 222 (1974).
89. The enthalpy of formation of the corresponding sulfonamide (more commonly known as the artificial sweetener, saccharin) has also been measured, M. A. R. Matos, M. S. Miranda, V. M. F. Morais and J. F. Liebman, *Mol. Phys.*, **103**, 221 (2005).
90. Y. Kudo and S. Hamada, *Bull. Chem. Soc. Jpn.*, **60**, 239 (1987).
91. J. F. Liebman, *Struct. Chem.*, **8**, 85 (1997).
92. O. Mo, M. Yáñez, M. Eckert-Maksić, Z. B. Maksić, I. Alkorta and J. Elguero, *J. Phys. Chem. A*, **109**, 4359 (2005).
93. J. F. Liebman, K. S. K. Crawford and S. W. Slayden, in *The Chemistry of Functional Groups Supplement S: The Chemistry of Sulphur-containing Functional Groups* (Eds. S. Patai and Z. Rappoport), Wiley, Chichester, 1993, p. 197.

CHAPTER 4

NMR spectra of hydroxylamines, oximes and hydroxamic acids

PETER RUDOLF SEIDL

Departamento de Processos Orgânicos, Escola de Química, Universidade Federal do Rio de Janeiro, Centro de Tecnologia, Bloco E, Ilha do Fundão, Rio de Janeiro, Brazil, RJ, 21949-900
Fax: +55 21 2562 7567; e-mail: pseidl@eq.ufrj.br

and

JACQUES FERNANDES DIAS

Departamento de Química e Ambiental, Faculdade de Tecnologia, Universidade do Estado do Rio de Janeiro, Rodovia Presidente Dutra km 298—Pólo Industrial, Resende, Brazil, RJ, 27537-000
Fax: +55 24 3354 7875; e-mail: jacques@fat.uerj.br

The chemistry of hydroxylamines, oximes and hydroxamic acids
Edited by Z. Rappoport and J. F. Liebman

I. INTRODUCTION

A. NMR Applied to Hydroxylamines, Oximes and Hydroxamic Acids

Nuclear magnetic resonance spectroscopy was adopted enthusiastically by chemists as a structural and analytical tool after the discovery in 1950 of the phenomenon of the chemical shift. As commented by Prof. J. D. Roberts in the Foreword of Reference 1, those who were fortunate to be present at the beginning of the application of NMR to chemistry in the mid-1950s were able to more or less 'grow' with the field and enter the modern arena of multipulse and multidimensional NMR with substantial experience with NMR fundamentals. Others, who may now consider using NMR in their research, surely must feel at least somewhat overwhelmed by the enormity and sophistication of the currently available knowledge of NMR. The problem is that to properly use modern NMR requires a lot of rather specialized knowledge. The effects of couplings, of exchange, of relaxation times, of low sensitivity, of solvents and so on make selection of conditions for taking spectra and interpreting results far from routine. Serious errors may result from the misuse or improper consideration of these factors[1].

There are a large number of structural parameters for NMR of different nuclei and many examples of how they can be applied to the analysis of hydroxylamines, oximes and hydroxamic acids. Fortunately though, there are many very clear, meticulously written descriptions of INEPT, DEPT, INADEQUATE, COSY, NOESY and the like, in one- and two-dimensional NMR spectroscopy, that are cited in the references. Since their content is beyond the scope of the present chapter, a brief mention of some of the fundamental concepts that are essential for its understanding by the nonspecialist is in order.

B. Basic Concepts of NMR

Most atomic nuclei have an angular momentum ($\mathbf{L}$) resulting from their nuclear spin. Hydroxylamines, oximes and hydroxamic acids are made up of hydrogen, carbon, nitrogen and oxygen nuclei. Some of their derivatives of interest may also contain fluorine, phosphorus and silicon. Owing to their complexing ability they may also coordinate with metals or with elements in different types of materials. Thus, spectra from hydrogen, deuterium, tritium as well as carbon-13, nitrogen-14 and nitrogen-15, oxygen-17 and other nuclei may be observed. Whether their use is practical for different types

TABLE 1. Properties of selected nuclides of importance in NMR spectroscopy

Nuclide	Spin I	Electric quadrupole moment eQ $(10^{-28}\mathrm{m}^2)$ [a]	Natural abundance (%)	Relative sensitivity [b]	Gyromagnetic ratio γ $(10^7\ \mathrm{rad\,T^{-1}\,s^{-1}})$ [a]	NMR frequency (MHz) $(B_o = 2.3488\ \mathrm{T})$ [b]
^{1}H	1/2	—	99.985	1.00	26.7519	100.0
^{2}H	1	2.87×10^{-3}	0.015	9.65×10^{3}	4.1066	15.351
^{3}H[c]	1/2	—	—	1.21	28.5350	106.664
^{10}B	3	8.5×10^{-2}	19.58	1.99×10^{-2}	2.8747	10.746
^{11}B	3/2	4.1×10^{-2}	80.42	0.17	8.5847	32.084
^{12}C	0	—	98.9	—	—	—
^{13}C	1/2	—	1.108	1.59×10^{-2}	6.7283	25.144
^{14}N	1	1.67×10^{-2}	99.63	1.01×10^{-3}	1.9338	7.224
^{15}N	1/2	—	0.37	1.04×10^{-3}	−2.7126	10.133
^{16}O	0	—	99.96	—	—	—
^{17}O	5/2	-2.6×10^{-2}	0.037	2.91×10^{-2}	−3.6280	13.557
^{19}F	1/2	—	100	0.83	25.1815	94.077
^{23}Na	3/2	0.1	100	9.25×10^{-2}	7.0704	26.451
^{29}Si	1/2	—	4.70	7.84×10^{-3}	−5.3190	19.865
^{31}P	1/2	—	100	6.63×10^{-2}	10.8394	40.481
^{39}K	3/2	5.5×10^{-2}	93.1	5.08×10^{-4}	1.2499	4.667
^{57}Fe	1/2	—	2.19	3.37×10^{-5}	0.8687	3.231
^{59}Co	7/2	0.42	100	0.28	6.3015	23.614
^{133}Cs	7/2	3.0×10^{-3}	100	4.74×10^{-2}	3.5339	13.117
^{195}Pt	1/2	—	33.8	9.94×10^{-3}	5.8383	21.499

[a] Values from References 2 and 3.
[b] Values from the Bruker Almanac, 1992; sensitivity is expressed relative to ^{1}H for constant field and equal numbers of nuclei.
[c] ^{3}H is radioactive.

of work depends on the natural abundance of these isotopes (or techniques available for enrichment) as well as on properties related to their behavior in the presence of a magnetic field.

Quantum mechanical considerations show that, like many other atomic quantities, this angular momentum is quantized and depends on I, which is the angular momentum quantum number, commonly referred to as nuclear spin. The nuclear spins of $I = 0$, 1/2, 1, 3/2, 2 ... up to 6 have been observed (see also Table 1). Neither the values of I nor those of **L** (see below) can yet be predicted from theory.

The angular momentum **L** has associated with it a magnetic moment μ. Both are vector quantities and they are proportional to each other. The proportionality factor γ is a constant for each nuclide (i.e. each isotope of each element) and is called the gyromagnetic ratio, or sometimes the magnetogyric ratio. The detection sensitivity of a nuclide in the NMR experiment depends on γ; nuclides with a large value of γ are said to be sensitive (i.e. easy to observe), while those with a small γ are said to be insensitive.

Nuclides with spin $I = 0$ therefore have no nuclear magnetic moment. Two very important nuclei, the ^{12}C isotope of carbon and the ^{16}O isotope of oxygen, belong to this class of nuclides—this means that the main building blocks of organic compounds cannot be observed by NMR spectroscopy.

For most nuclides the nuclear angular momentum vector **L** and the magnetic moment vector $\boldsymbol{\mu}$ point in the same direction, i.e. they are parallel. However, in a few cases, for example, ^{15}N, they are antiparallel.

C. 'Other' Nuclides

It is possible to obtain NMR spectra of nearly all elements, although not always from observing the isotope with the highest natural abundance, as can be seen from the examples of carbon and oxygen. For reasons connected with the historical development of NMR spectroscopy, nuclei of all species other than ^{1}H are referred to as *heteronuclei*.

The procedures for recording spectra of heteronuclei often differ considerably from those for ^{1}H and ^{13}C (which would today be considered 'routine') since it is necessary, even for routine measurements, to adjust the experimental conditions to suit the special properties of the nuclei to be observed. For example, the spin–lattice relaxation times for some nuclides, such as ^{15}N, are very long, whereas for others (especially those with an electric quadrupole moment, such as ^{14}N) they are very short. Also, the spectra observed for some nuclides contain interfering signals caused by other materials present, for example the glass of the sample tube (^{11}B, ^{29}Si), the spectrometer probe unit (^{27}Al) or the transmitter/receiver coil. For many nuclides the sample temperature and its constancy are important factors; for example, quadrupolar nuclides such as ^{17}O give narrower signals when the temperature is increased.

The behavior in a magnetic field of any nucleus with spin $I = 1/2$ is similar to that of ^{1}H and ^{13}C. This group includes ^{3}H, ^{15}N and many others. Some of these nuclides, such as ^{3}H, are easy to observe (*sensitive* nuclides), as they have a large gyromagnetic ratio γ and a large magnetic moment π, whereas others, such as ^{15}N, are not so favorable. These insensitive nuclides suffer from the additional disadvantage of low natural abundances (e.g. 0.37% for ^{15}N; see Table 1). For nuclides such as these the pulsed method of observation is essential, as in the case of ^{13}C. However, this often presents technical problems owing to the fact that the range of chemical shifts for nuclei that differ in their substituents or coordination is usually very large, requiring a correspondingly large spectral width.

By far the majority of heteronuclides belong to the group with $I > 1/2$. A small selection of these is listed in Table 1. All such nuclides have an electric quadrupole moment eQ, and they usually give broad NMR signals due to shortening of the relaxation times through the interaction of the quadrupole moment with local electric field gradients. Often this means that one is unable to observe any multiplet splitting due to coupling with other nuclei, or even to resolve chemical shift differences. Exceptions to this are those nuclides that have a relatively small quadrupole moment, such as deuterium, ^{2}H. Other exceptions occur when the quadrupolar nucleus is in a symmetrical environment; a typical example is the ^{14}N resonance of the symmetrical ammonium ion NH_4^+.

1. Nitrogen (^{14}N and ^{15}N)

The isotope ^{14}N, with a natural abundance of 99.9%, has nuclear spin $I = 1$ and gives broad signals which are of little use for structural determinations. The ^{15}N nucleus, with $I = 1/2$, is therefore preferred. However, the low natural abundance of about 0.4% and the extremely low relative sensitivity (Table 1) make measurements so difficult that ^{15}N NMR spectroscopy was slow to become an accepted analytical tool. A further peculiarity is the negative magnetogyric ratio since, in proton decoupled spectra, the nuclear Overhauser effect can strongly reduce the signal intensity. DEPT and INEPT pulse techniques are therefore particularly important for ^{15}N NMR spectroscopy.

The two isotopes ^{14}N ($I = 1$) and ^{15}N ($I = 1/2$) both have only small values of δ and thus belong to the class of insensitive nuclides. Although the electric quadrupole moment of ^{14}N is relatively small and the signals are therefore not very greatly broadened, the overwhelming majority of nitrogen NMR studies are now performed on ^{15}N using natural abundance samples, despite the difficulties involved. The spread of chemical shifts for

the widest possible variety of compounds is about 900–1000 ppm. Nitrogen nuclei in amines are the most strongly shielded, while those in nitroso compounds are the least shielded.

2. Oxygen (^{17}O)

^{17}O is the only oxygen isotope that gives NMR signals. With a nuclear spin of 5/2, a natural abundance of only 0.037% and an electric quadrupole moment (even though this is not very large), ^{17}O is not a favorable nuclide for NMR measurements. Nevertheless, owing to the great importance of oxygen, numerous studies have been carried out, mostly confined to the measurement of chemical shifts. The most strongly shielded ^{17}O nuclei are those in compounds with singly-bonded oxygen, such as alcohols and ethers ($\delta = -50$ to $+100$, referred to $\delta[H_2O] = 0$). The least shielded are those in nitrites (δ *ca* 800) and nitro compounds (δ *ca* 600), where the oxygen atom is doubly bonded. A carboxy group OC=O gives only one signal, showing that the two oxygen nuclei are isochronous.

D. Spectral Parameters: A Brief Survey

1. The chemical shift

Nuclear resonance is influenced in characteristic ways by the environments of the observed nuclei. However, nuclei are always surrounded by electrons and other atoms. Thus, in diamagnetic molecules the effective magnetic field B_{eff} at the nucleus is always smaller than the applied field B_o, i.e. the nuclei are shielded. The effect, although small, is measurable. This observation is expressed by equation 1:

$$B_{eff} = B_o - \sigma B_o = (1 - \sigma) B_o \tag{1}$$

Here σ is the *shielding constant*, a dimensionless quantity which is of the order of 10^{-5} for protons, since the shielding increases with the number of electrons. It should be noted that σ-values are molecular constants which do not depend on the magnetic field. They are determined solely by the electronic and magnetic environment of the nuclei being observed.

2. Spin–spin coupling

a. The indirect spin–spin coupling. Neighboring magnetic dipoles in a molecule interact with each other. This *spin–spin coupling* affects the magnetic field at the positions of the nuclei being observed. The effective field is stronger or weaker than it would be in the absence of the coupling and alters the resonance frequencies. The cause of this fine structure is usually explained by taking examples from ^1H NMR spectroscopy, but the same considerations can be extended to ^{13}C and other nuclides with $I = 1/2$.

The fine structure is caused by the so-called *indirect spin–spin coupling*, indirect because it occurs through the chemical bonds. Nuclear dipoles can also be coupled to each other directly through space.

b. Coupling between protons and other nuclei; ^{13}C satellite spectra. In the ^1H NMR spectra of organic molecules one normally only sees H,H couplings. However, for molecules containing carbon, nitrogen or other nuclei which have a magnetic moment, the couplings to these nuclei are also seen. The same rules apply as for H,H couplings. For these heteronuclear couplings there is the additional simplification that $\Delta\nu \gg |J|$, and

thus the condition for first-order spectra is nearly always fulfilled. Special mention must be made of the couplings between protons and ^{13}C nuclei. These C,H couplings make themselves apparent in the ^{1}H NMR spectrum by the ^{13}C satellite signals.

3. The intensities of the resonance signals

The area under the signal curve is referred to as the *intensity* or the *integral* of the signal. Comparing these intensities in a spectrum directly gives the ratios of the protons in the molecule. In the case of multiplets one must, of course, integrate over the whole group of peaks.

Signal intensities are next in importance to chemical shifts and direct spin–spin coupling constants as aids to structure determination: they also make possisle the quantitative analysis of mixtures. However, this only applies to more abundant isotopes, i.e. protons and ^{19}F. For nuclei of relatively low natural abundance and sensitivity, detection methods are used which have the undesirable side effect of distorting the integrals that are used to determine the signal intensity. Details of these causes are given in NMR texts[1]. It must be pointed out here that spectra for more insensitive nuclei are usually recorded under conditions in which signals are amplified by the nuclear Overhauser effect (NOE). For the present purposes, an NOE can be defined as an increase in signal intensity of insensitive nuclei (^{13}C, ^{15}N, for example) when more abundant nuclei (^{1}H, ^{19}F, for example) are irradiated.

E. Data on NMR of Hydroxylamines, Oximes and Hydroxamic Acids

As the first commercial NMR instruments became available, a significant part of the empirical knowledge related to the structure and reactivity of organic compounds was under close scrutiny. Model compounds that could be used to test certain concepts or effects were subject to spectroscopic techniques and a framework for interpreting spectra based on structural properties began to develop.

Although some of this early work was based on ^{14}N nuclei which are of special interest for studies of hydroxylamines, oximes and hydroxamic acids, a variety of reasons led to a concentration of work on ^{19}F and, particularly, ^{1}H nuclei. These include the sensitivity of these nuclei to the method, the advent of commercially available instrumentation to allow exploitation of this sensitivity, the abundance of ^{1}H compounds and the unfavorable spectral characteristics of ^{14}N[4].

Moreover, NMR studies of protons attached to ^{14}N were complicated by the same agency and in many cases broadening was accentuated by the ability of the N–H bond, which permitted rapid proton exchange. Hydrogen bonding (which renders proton shifts very sensitive to conditions of temperature, concentration and solvent) initially also limited the usefulness of proton magnetic resonance for structural analytical studies of compounds containing nitrogen. On the other hand, there are periodic revivals of interest on the part of NMR spectroscopists in nitrogen systems, which are probably inevitable owing to the importance of nitrogen compounds to preparative inorganic and organic chemistry, and particularly to biochemists.

NMR parameters, such as chemical shifts and coupling constants, have been extensively investigated through the use of organic compounds that exhibit restricted rotation, such as oximes. NMR data are routinely used in determination of the stereochemistry of organic compounds and rigid structures, such as oxime conformers, can help in the interpretation of many of the physical and chemical properties that are associated with effects of lone pairs on different types of systems that contain nitrogen.

NMR data on hydroxylamines, oximes and hydroxamic acids appeared at roughly the same periods as those of other types of compounds with a small delay for ^{14}N relative

to ^{1}H and for ^{15}N relative to ^{13}C. The development of NMR techniques applied to more abundant nuclei (in this case ^{14}N) quickly highlighted some of the difficulties which would face chemists trying to use ^{14}N NMR spectroscopy as an analytical tool. For example, it became apparent that problems would arise from varying linewidths due to the effects of electric quadrupole induced relaxation of ^{14}N. Similarly there was a dearth of studies employing the low abundance ^{15}N isotope, no doubt due to pessimistic individual judgments that extensive studies on enriched compounds would be not only expensive but would prove as unspectacular as the ^{14}N studies. Nevertheless, the factors which complicate nitrogen spectra did not discourage several laboratories that invested considerable effort in the nitrogen area.

More recently, single and double resonance techniques on both ^{14}N and ^{15}N compounds are being employed for accurate shift and coupling constant measurements including relative signs. Use of enrichment with ^{15}N has grown because of its favorable spectral characteristics in proton magnetic resonance studies.

The last few years have seen the usual 'dramatic' increase in the number of publications in this area, coming from an impressive array of groups using the full range of NMR techniques, and NMR data have been used to determine the stereochemistry of rather complex systems containing hydroxylamines, oximes and hydroxamic acids, but systematic studies have been concentrated mainly on oximes.

F. Scope and Limitation

In spite of the relatively large amount of work on the NMR of hydroxylamines, oximes and hydroxamic acids, a comprehensive treatment of their NMR parameters is still not at hand. They are usually studied in conjunction with other functional groups containing double bonds and serve to illustrate differences in parameters between *E*/*Z* isomers or tautomeric forms of functional groups containing carbon, nitrogen and oxygen. The dependence of certain carbon, nitrogen and hydrogen chemical shifts (and, sometimes, coupling constants) on isomer populations is a complicating factor. However, substituents or hydrogen bonding in certain systems may stabilize one of the conformations, simplifying studies of dynamic equilibrium of rather well-defined geometries, which may be used for stereochemical analysis.

Owing to their tendency to form complexes, there is a considerable amount of data on the NMR spectra of these types of molecules. However, unless they provide relevant data for the interpretation of NMR properties of the uncomplexed moiety, studies of complexes with metals or elements on surfaces or in cavities of materials have not been included.

G. Organization and Classification

The intimate relationship between NMR parameters such as chemical shifts and spin–spin coupling constants and molecular geometry is particularly evident for derivatives with rigid frameworks. Therefore, structural and conformational effects are treated first as a separate topic and then in conjunction with specific compounds. As data on hydroxylamines, oximes and hydroxamic acids are not as extensive as those for other types of systems containing nitrogen or oxygen, comparisons with their respective parameters or effects have also been included wherever they are considered relevant.

Discussion of NMR data have been organized according to the nucleus and type of parameter. They are used to exemplify general aspects of NMR data and are followed by more specific examples. This material is arranged by parameter (chemical shifts, coupling constants) and then by nucleus, in their order in the periodic table. Wherever general aspects of discussions of substituent or conformational effects are at hand, they are treated

separately. In other cases they are included along with the respective data on a certain structure.

II. STRUCTURAL AND CONFORMATIONAL EFFECTS

NMR plays an important role in the determination of chemical structures. Steric effects are reflected by chemical shifts and coupling constants may be used to probe spatial proximity or dihedral angles involving magnetic nuclei. Nuclear Overhauser effects are widely used to determine distances between magnetic nuclei. In fact, protocols used to determine structures of complex molecular systems are based on combinations of these parameters. Stereochemical investigations of hydroxylamines, oximes and hydroxamic acids are based on comparisons of these parameters for similar compounds or their combinations that are incorporated into techniques such as COSY, NOESY, HMBC, HSQC and the like which are used to determine the connectivity among magnetic nuclei and establish the corresponding structural features. Historically, hydrogen NMR played an important role in establishing the relationship between geminal coupling constants and molecular geometry for oximes. The influence of substituents on restricted rotation and the relative population of the respective conformers were also investigated in oximes[5].

There is a strong influence of certain substituents on conformational equilibria. Data on substituted cyclohexanone oximes and oxime ethers reflect hyperconjugative effects that can be investigated by vicinal interproton coupling constants and anisotropic deshielding by the oxime oxygen[6]. More recent work[7] is also based on fluorine coupling to protons, carbon and nitrogen and includes theoretical calculations.

III. SPECTRAL PARAMETERS

There are a few compilations of NMR parameters that include hydroxylamines, oximes and hydroxamic acids. Representative examples are given here and compared with data on similar systems in order to establish specific relationships between molecular structure and spectral parameters.

Chemical shifts are measured in ppm from the appropriate standard. The early literature on ^{13}C shifts is given relative to certain compounds, but nowadays the same standard as hydrogen is used (tetramethylsilane; TMS). With other nuclei the situation is more complex and there has been some discussion on the use of a certain standard. To avoid this problem, all data are given relative to the standard used in the original literature whereas its conversion to other scales for chemical shifts is given for each nucleus of interest. No such problem exists, of course, with coupling constants.

A. Chemical Shifts

1. Proton spectra

The electric quadrupole effects of ^{14}N which limit the lifetimes of the spin states for nitrogen are made manifest in the NMR spectra of nuclei coupled to ^{14}N. The commonest example is the N−H group. In the absence of exchange and if the relaxation for ^{14}N is slow, three equally intense proton lines are expected, arising from the three magnetic spin states, +1, 0 and −1, for the nitrogen (^{15}N in the same circumstance gives two lines arising from the two magnetic spin states +1/2 and −1/2). For more rapid relaxation, however, the lines broaden and, in the limit when the relaxation rate is large compared with $J(^{14}N-H)$, the lines collapse to a single broad line which narrows if the relaxation rate increases further.

The broadening effects of ^{14}N may be removed not only by ^{15}N substitution but also by proton$-^{14}N$ decoupling produced by double resonance techniques. The information concerning $J(N-H)$ is, however, lost in a decoupling experiment.

There are excellent texts on proton chemical shifts listed in the references and this topic will not be discussed here. Specific aspects of substituent electronegativity, hyperconjugation and solvent effects are treated separately whenever a sufficient amount of data is available for the purpose of interpretation.

2. Carbon-13

Carbon chemical shifts were employed in studies of conformational effects on aldoximes and ketoximes. They appear in the region 145 to 163 ppm[8] and several values are illustrated in Table 2. Such resonances are some 50 ppm to higher field relative to the corresponding carbonyl resonance. Where substitution is asymmetrical, differences in oxime carbon chemical shifts are observed, depending upon the conformation of the oxime N$-$OH. Such conformational isomerism also has a profound effect upon the chemical shift of the α-carbon.

The carbon-13 NMR spectrum of acetone oxime has three resonances, the derivatized carbonyl carbon at 154.5 ppm and the two nonequivalent CH_3 groups at 21.5 and 14.7 ppm. The difference between the chemical shifts of the two methyl groups, 6.8 ppm, is primarily a steric compression shift. This is clearly indicated in the carbon NMR spectrum of methyl ethyl ketoximes (Scheme 1), where the two oxime substituents are not sterically identical and thus the two isomers are not present in equal amounts. In methyl

TABLE 2. Carbon-13 chemical shifts of oxime carbons[8]

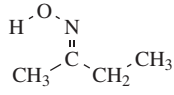	159.2	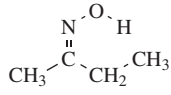	158.7
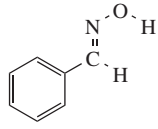	149.6	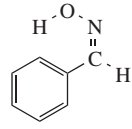	146.4
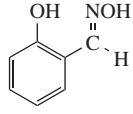	152.4	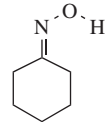	159.4
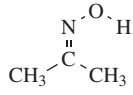	154.3	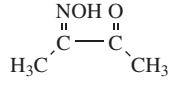	156.6

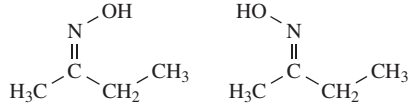

SCHEME 1. Isomers of methyl ethyl ketoxime

ethyl ketoxime the observed isomer ratio is 77:23 in favor of the isomer with the N−OH group facing the methyl group[8].

3. Nitrogen-14 and -15[9]

Nitrogen chemical shifts of organic compounds are reviewed in Chapter 5 of Reference 4. The range of ^{15}N chemical shifts is about 600 ppm wide. If extreme values for metal complexes are included, it extends to over 1400 ppm. Nitromethane is the recommended reference (it can be added in a sealed-off capillary). Values are also frequently quoted with respect to a saturated aqueous solution of ammonium chloride or ammonium nitrate. The following ^{15}N shift values can be used to convert the δ-values:

$$\begin{aligned} &CH_3NO_2 && \delta = 0.0 \\ &NH_4Cl && \delta = -352.9 \\ &NH_4NO_3 && \delta(NH_4^+) = -359.5 \\ & && \delta(NO_3^-) = -3.9 \end{aligned}$$

In principle, ^{15}N NMR spectroscopy is very important for structural analysis, since N-containing functional groups and N atoms in molecular skeletons are frequently encountered. Table 3 gives a summary of the shift ranges of the more important classes of compounds. When quoting specific δ-values it should be remembered that the ^{15}N NMR signals often depend strongly on the concentration and temperature, and particularly on the solvent. Intermolecular hydrogen bonds often play an important role.

^{15}N shifts can often show remarkable differences. Thus $\Delta\delta$ in the azene resonance forms below **1** ↔ **2** is almost 600 ppm. The charge distribution would, as in a diazo compound, suggest the reversed signal assignment; however, the large paramagnetic term, attributed to low-energy electronic transitions ($n \rightarrow \pi^*$ transitions), is decisive for the chemical shift. The nitrene nitrogen of the aminonitrene therefore appears at very low field.

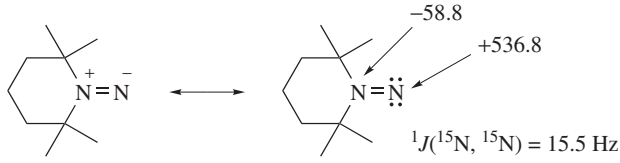

(**1**) (**2**)

On formation of the hydrochloride **4** of diethylamine **3**, a low field shift $\Delta\delta$ of less than 4 ppm is observed.

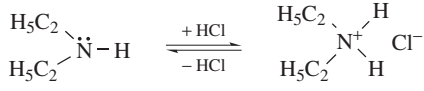

–333.7 –330.1

(**3**) (**4**)

A comparison with the ^1H and ^{13}C NMR of ammonium salts **5/7** and zwitterion **6** shows that the positive charge is essentially located not on the central nitrogen atom, but on the substituents.

TABLE 3. ^{15}N chemical shifts of examples of the more important classes of compounds (δ-values referred to CH_3NO_2); for chemically nonequivalent ^{15}N nuclei the δ-values are given in the order of the number indicating the atoms[9]

Class of compound	Example		Solvent	δ
Amides 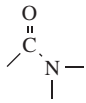	Formamide	$HCO-NH_2$	Neat liquid	−267.6
	N-Methylformamide	$HCO-NH-CH_3$	Neat liquid	−270.1
	N,*N*-Dimethylformamide	$HCO-N(CH_3)_2$	Neat liquid	−275.2
	Benzamide	$C_6H_5-CONH_2$	DMF	−279.3
	Methyl dimethylcarbamate	$CH_3O-CO-N(CH_3)_2$	Chloroform	−314.2
	Urea	$H_2N-CO-NH_2$	Water	−305.0
	Thiourea	$H_2N-CS-NH_2$	Water	−273.3
Imines, Oximes, Hydrazones 	*N*-Methylbenzaldimine	$C_6H_5-CH=N-CH_3$	Chloroform	−62.1
	N-Phenylbenzaldimine	$C_6H_5-CH=N-C_6H_5$	Chloroform	−54.1
	Acetone oxime	$(CH_3)_2C$	Chloroform	−45.9
	Benzaldehyde oxime	$C_6H_5-CH=NOH$	Chloroform	−26.3
	Benzaldehyde *N*-phenylhydrazone	C_6H_5-CH=N(2)-NH(1)C_6H_5	DMSO	−237.0 −54.0
Azo-compounds Azoxy-compounds 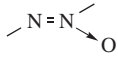	(*Z*)-Azobenzene	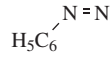	Chloroform	+146.5
	(*Z*)-Azoxybenzene	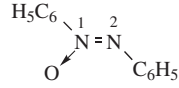	Chloroform	−57.1 −46.7
	(*E*)-Azoxybenzene	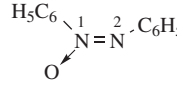	Chloroform	−36.0 −19.8

Amino acids show the expected dependency of the δ(N)-values on pH:

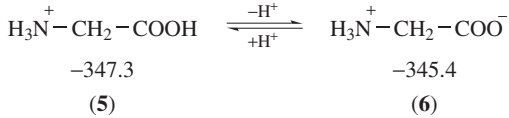

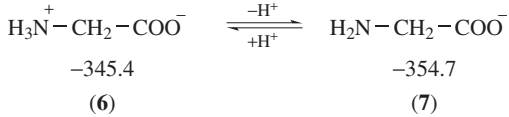

The rapid tautomerism due to the intermolecular exchange of protons between two N atoms in azoles can be slowed down by using DMSO as solvent to such an extent that even at room temperature different ^{15}N signals appear.

Apart from tautomerism between identical structures, ^{15}N NMR can also be used to investigate tautomeric equilibria between states of different energy. Thus it can be shown that barbituric acid exists as a urea derivative and is only formally a pyrimidine derivative.

In this group of molecules there is a double bond at the nitrogen atom in a structure which may be conventionally written as

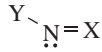

where X = C, Y = OH or OR for oximes and their ethers, respectively. The corresponding *N*-oxide structure

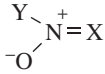

is characteristic of nitrones (X, Y = alkyl) and azoxy compounds (X = N, Y = alkyl, aryl). These structures resemble those in azines and their *N*-oxides, respectively, and the corresponding nitrogen chemical shifts are also alike, as can be seen from Tables 3 and 4. There is also a downfield shift for compounds with the N=N structure as compared with the C=N structure. The nitrogen resonance signals of the *N*-oxide structures such as azoxybenzene, nitrone or furoxan are shifted upfield relative to the parent structures of azobenzene, imines and furazan, respectively, similarly to azine *N*-oxides relative to azines.

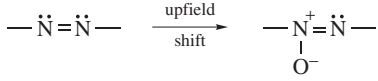

azo azoxy

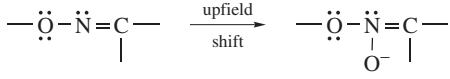

oxime (furazan) furoxan

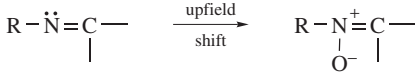

imine nitrone

Nitrogen chemical shifts are clearly different for the isomeric structures of nitrones, oximes and nitroso compounds.

	Screening-constant scale (ppm)	Frequency scale (ppm)
Oxime, $R_2C{=}N{-}OR$	*ca* +30	*ca* +300
	ca +100	*ca* +230
Nitrone, $R{-}\overset{+}{N}(O^-){=}CR_2$		
Nitroso compound, $R_3C{-}N{=}O$	−400 to −500	+700 to +800

For azo compounds R−N=N−R, it has been suggested that the nitrogen resonance signal moves to higher fields (lower frequencies) with increasing electronegativity of the

TABLE 4. Nitrogen chemical shifts (ppm) of some oximes and related structures[4]

Compound	Solvent	Screening-constant scale referred to internal $MeNO_2$ or NO_3^- [a]	Frequency scale J referred to $Me_4N^+X^-$	^{14}N Resonance half-height width (Hz)
		δ (N)		
MeCH=NOH	CCl_4	$+27 \pm 4$	+306	900
Me_2C=NOH	CCl_4	$+44 \pm 5$	+288	1100
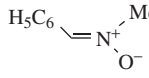	acetone (satd)	$+103 \pm 4$	+230	70
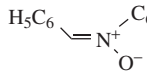	acetone (satd)	$+94 \pm 1$	+238	100

[a] Direct ^{14}N measurements, referred to internal $MeNO_2$.

groups R, but the low accuracy of the ^{14}N measurements in this case and the rather arbitrary classification of substituents R according to electronegativity makes the conclusion rather premature.

Molecules which contain the nitroso group  give nitrogen NMR signals at very low fields (high frequencies). Their chemical shifts are clearly outside the spectral range of all other organic compounds. Their ^{14}N resonance linewidths are usually large. It is possible to make a spectroscopic distinction in this group of molecules between the following subgroups:

	Screening-constant scale (ppm)	Frequency scale (ppm)
Nitrosamines, R_2NNO and nitrites, R−O−NO	*ca* −150 to −200	+480 to +530
Thionitrites, R−S−NO and nitrosoalkanes, R−NO	*ca* −350 to −450	+680 to +780
Aromatic nitroso compounds	*ca* −500	+830

The shifts for nitrites RONO distinguish them from the isomeric nitro compounds, RNO_2. There is also a remarkable difference in nitrogen chemical shifts between the isomeric structures of nitroso compounds and oximes:

	Screening-constant scale (ppm)	Frequency scale (ppm)
Nitroso compounds, R_2CH−NO	−400 to −500	+730 to +830
Oximes, R_2C=N−OH	*ca* +30	*ca* +300

The nitrogen chemical shifts of the nitroso group show a roughly linear correlation with the energies of the lowest transitions observed in the electronic absorption spectra. The

decreasing energy is accompanied by a downfield nitrogen chemical shift. The nitroso structure is a very peculiar case: theoretical calculations indicate a dominant contribution (deshielding) to the nitrogen screening constant by the lowest-energy excitation connected with the presence of the lone electron pair at the nitrogen atom in the NO group. This is an exception which constitutes an explanation of the observed relationship between the shifts and the transition. For other organic compounds, attempts to explain nitrogen chemical shifts in terms of experimental electronic transitions have not been very successful.

The ^{15}N chemical shifts for *Z* and *E* forms of 21 aliphatic ketoximes (**8**–**29** in Table 5) were thoroughly investigated[10]. They are found in the range 31.4–63.9 ppm. Shieldings for ten aliphatic aldoximes appear between −4.0 and 30.1 ppm (Table 6).

The shifts listed in Table 5 show that the ^{15}N resonances of the *Z* isomers of acyclic ketoximes appear *upfield* of the resonances of the corresponding *E* isomers. The differences range from 2.2–5.1 ppm and increase with the increased branching at the β carbon, where β is defined in the following notation:

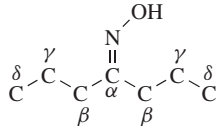

The ^{15}N resonances of the *Z* aldoximes **31a–43a** (Table 6) differ in being downfield of those for the corresponding *E* isomers **31b–43b** and of formaldoxime **30**. The differences between the aldoxime isomer pairs decrease from 4.3 to about 0 ppm as branching increases at the β carbon. In general, ^{15}N shifts of *E* isomers are relatively insensitive to the bulk of R and remain approximately the same throughout a series, whereas the shifts of the *Z* isomers move upfield as the steric interaction between R and the OH group increases as a result of introduction of bulkier R groups.

Solvent effects indicate that the chemical shifts of the nitrogen of oximes, like other azine nitrogens, are significantly influenced by the second-order paramagnetic effect associated with the unshared pairs of nitrogen. If this is true, then the shift difference between acetaldoxime isomers may be ascribed to a lowering of the $n \rightarrow \mu^*$ transition energy when the CH_3 is *trans* to the lone pair, despite the steric interactions which should produce an upfield shift. The ^{13}C resonance of the methyl carbon of *Z*-acetaldoxime is 3.8 ppm upfield of the methyl carbon of *E*-acetaldoxime. Apparently with increasing size of R, the influence of steric interactions on the nitrogen shifts of *Z*-aldoximes tends to overcome the direct effect of the methyl group on the $n \rightarrow \mu^*$ transition energy and the *Z*–*E* shift differences become *smaller*. In the ketoxime series, the *Z*-oxime ^{15}N resonances appear to be always upfield of the *E*-oxime resonances.

Substitution of methyl for hydrogen at the α carbon of an oxime causes an upfield shift of the nitrogen resonance. Although these shifts are similar in direction, they are about twice the magnitude of those observed for the corresponding carbons of alkenes. Examples are

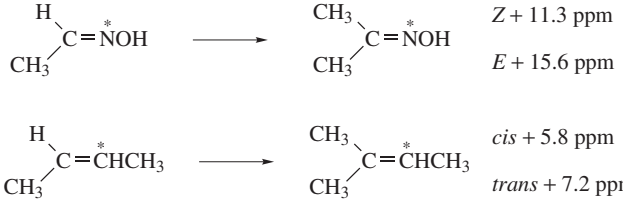

TABLE 5. ^{15}N chemical shifts[a] of ketoximes[10]

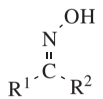	No.		$\delta^{15}N$		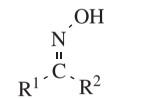	No.		$\delta^{15}N$	
	Z	*E*	*Z*	*E*		*Z*	*E*	*Z*	*E*
	**8**		39.7(293.1)		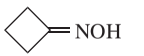	**19**		46.2(286.6)	
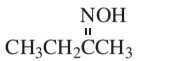	**9a**	**9b**	41.4(291.4)	38.3(294.5)	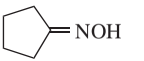	**20**		46.8(286.0)	
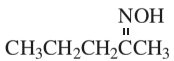	**10a**	**10b**	38.9(293.9)	36.0(296.8)	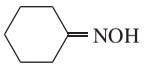	**21**		46.4(286.4)	
	**11a**	**11b**	43.4(289.4)	38.3(294.5)	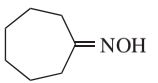	**22**		40.6(292.2)	
	**12a**	**12b**	—	37.0(295.8)	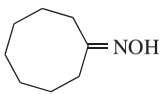	**23**		39.5(293.3)	
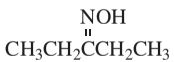	**13**		40.1(292.7)		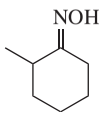	**24a**	**24b**	49.0(283.8)	44.4(288.4)

(*continued overleaf*)

TABLE 5. (*continued*)

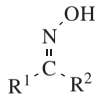	No.		$\delta^{15}N$		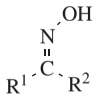	No.		$\delta^{15}N$	
	Z	*E*	*Z*	*E*		*Z*	*E*	*Z*	*E*
	**14a**	**14b**	40.3(292.5)	38.1(294.7)	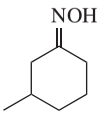	**25a**	**25b**	46.1(286.7)	46.1(286.7)
	**15a**	**15b**	—	37.5(295.3)	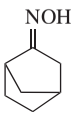	**26a**	**26b**	53.4(279.4)	51.4(281.4)
	**16**		37.3(295.5)		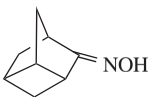	**27a**	**27b**	63.9(268.9)	59.0(273.8)
	**17a**	**17b**	39.1(293.7)	36.1(296.7)		**28a**	**28b**	41.6[b](291.2)	—
	**18a**	**18b**	—	31.4(301.4)	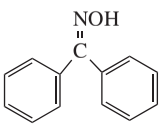	**29**		28.0(304.8)	

[a] In ppm upfield from external 1 M $D^{15}NO_3$ capillary. In parentheses are given calculated ^{15}N shift values (downfield shifts taken as positive relative to external 2 M $(CH_3)_4N^+Cl^-$, which we have found to be 332.8 ppm upfield from an external 1 M $D^{15}NO_3$ capillary).
[b] Only one signal is observed. However, two methyl resonances were found in the ^1H NMR spectrum.

TABLE 6. ^{15}N chemical shifts[a] of aldoximes[10]

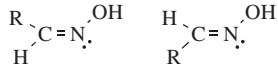

No.			$\delta^{15}N$	
R	*Z*	*E*	*Z*	*E*
H	**30**		−4.0(336.8)[b]	
CH_3	**31a**	**31b**	24.1(308.7)	28.4(304.4)
CH_3CH_2	**32a**	**32b**	26.6(306.7)	28.2(304.6)
$CH_3CH_2CH_2$	**33a**	**33b**	25.4(307.4)	27.2(305.5)
$(CH_3)_2CH$	**34a**	**34b**	30.0(302.8)	30.1(302.7)
$(CH_3)_2CHCH_2$	**35a**	**35b**	26.0(306.8)	26.5(306.3)
$CH_3CH_2(CH_3)CH$	**36a**	**36b**	28.9(303.9)	28.8(304.0)
$CH_3CH_2(CH_3)CHCH_2$	**37a**	**37b**	26.0(306.8)	26.0(306.8)
$(CH_3CH_2)_2CH$	**38a**	**38b**	25.8(307.0)	28.0(304.8)
	**39a**	**39b**	28.3(304.5)	28.5(304.3)
	**40a**	**40b**	—	20.1(312.7)
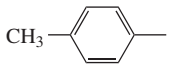	**41a**	**41b**	—	23.1(309.7)
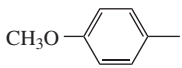	**42a**	**42b**	—	24.7(308.1)
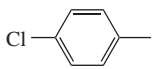	**43a**	**43b**	—	17.3(315.5)

[a] See footnote *a* in Table 5.
[b] Measured as a 20 mol% solution in water.

(where * marks the atom undergoing the NMR transition). These shift changes contrast with the downfield ^{15}N and ^{13}C shifts generally observed for attachment of methyl to a carbon connected to the nucleus being observed by a single bond, as in the following structures:

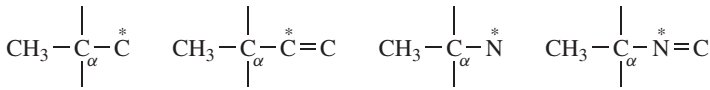

These effects are well established for alkanes and alkenes, and also for alkylamines and *N*-benzylidenealkylamines[10].

The effect of different substituents on ^{1}H, ^{13}C and ^{15}N spectra of salicylaldoximes (**44**–**51**) was investigated.[11]

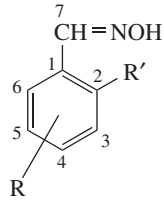

No	R′	R
44	OH	5-NO_2
45	OH	5-Cl
46	OH	5-Br
47	OH	5-OMe
48	OH	H
49	OH	4-OMe
50	OH	4-NMe_2
51	H	4-NMe_2

It has been found that the chemical shift of the benzylidene carbon, δ_{C7}, in ring-substituted benzaldoximes (Scheme 2) correlates well with Hammett σ constants. On the other hand, it is known that the chemical shift of that atom in the NMR spectra of benzaldoximes depends mainly on the substituents' inductive effect and its resonance effect is of reduced importance. Multiparameter correlations of δ_{C7} with the inductive and resonance substituents' constants are of better quality. It is known that the ^{15}N chemical shifts of *para*-substituted benzaldoximes are linearly dependent on Hammett σ constants. Correlations between the ^{17}O NMR chemical shifts of the oximino oxygen and σ, σ^* and σ_I substituent constants for substituted benzaldoximes are poor. These results show that coplanarity of Ar−CH=NOH creates difficulties in transmission of the substituents' effect, especially the resonance effect, to the CH=NOH group[11].

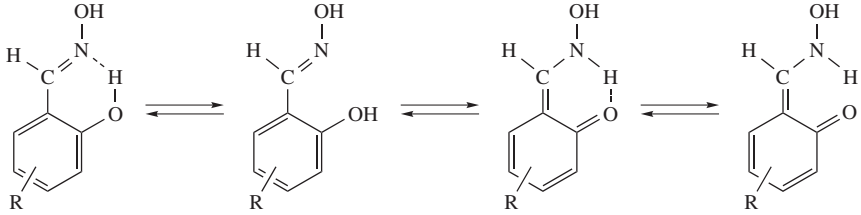

SCHEME 2

The chemical shifts of the protons in the ^1H NMR spectra of salicylaldoximes are given in Table 7. The hydroxyl proton varies between 11.61 and 10.82 ppm. The chemical shifts of carbon atoms in the ^{13}C NMR spectra of the salicylaldoximes are given in Table 8. The signal of C7 shifts downfield when the substituent becomes a stronger electron donor ($\Delta\delta = 149.58 - 144.64$ ppm $= 4.94$ ppm). Comparison of the spectra of **50** and **51** shows that the 2-OH group shifts the signal of C7 upfield. Since the most important interactions between the solvent and the aldoxime probably involve the 2-OH group, the solvent chemical shifts in the spectra of **50** and **51** are not parallel.

TABLE 7. ^{1}H NMR chemical shifts (ppm from internal TMS) of oximes **44**–**51** measured for 0.1 M solutions in DMSO-d_6[11]

Compound	H2	H3	H4	H5	H6	H7	NOH	Other H
44	11.46	7.02	8.06	—	8.37	8.32	11.61	—
45	10.29	6.92	7.17	—	7.45	8.31	11.46	—
46	10.30	6.83	7.30	—	7.60	8.29	11.45	—
47	9.66	6.82	6.82	—	7.04	8.33	11.33	—
48	— [a]	6.89	7.21	6.85	7.46	8.37	— [a]	—
49	10.33	6.47	—	6.44	7.31	8.27	11.11	3.39
50	10.08	6.16	—	6.25	7.18	8.18	10.82	2.89
	9.99 [b]	6.18 [b]	—	6.31 [b]	7.09 [b]	8.16 [b]	10.01 [b]	2.97 [b]
51	7.40	6.71	—	6.71	7.40	7.97	10.64	2.92
	7.44 [b]	6.71 [b]	—	6.71 [b]	7.44 [b]	7.99 [b]	9.71 [b]	2.96 [b]

[a] Overlapping signals at 10.9 ppm were found for H2 and NOH.
[b] In acetone-d_6.

The values of the one-bond carbon–hydrogen spin–spin coupling constants in the NMR spectra of the salicylaldoximes are also given in Table 8. J^{1}(C*n*, H*n*) values are 8.6, 9.8 and 6.5 Hz for $n = 3$, 6 and 7, respectively.

The chemical shifts of the nitrogen atoms in the ^{1}H, ^{15}N HMBC correlation maps of salicylaldoximes are given in Table 9. The range of ^{15}NOH chemical shifts, i.e. 24.7 ppm, is comparable to that of *para*-substituted benzaldoximes. Electron-donor substituents shift the signal of oximino nitrogen upfield. Comparison of the spectra of **50** and **51** shows that the 2-OH group shifts the signal of ^{15}NHO upfield. This is inferred to be a result of superposition of the inductive/resonance effect of 2-OH and the intramolecular hydrogen bonding, N•••H-OC2.

4. Oxygen-17[12]

a. Hydroxamic acids and oximes. The ^{17}O NMR characteristics of hydroxamic acids are essentially unexplored. In a detailed study of the structure of benzohydroxamic acids, ^{17}O NMR data on the carbonyl oxygen of four enriched benzohydroxamic acids (**52** to **55**) were recorded. No data were reported for the oxygen bound to nitrogen for these compounds. Table 10 gives the data from the earlier report for **52** to **55** and the data for both types of oxygen for **52**.

The downfield trends of the carbonyl signal for **52**–**55** correspond to the tendencies noted on the introduction of methyl groups in simple amides. The carbonyl signal for these hydroxamic acids (**52**–**55**) was shown to be sensitive to both intramolecular and intermolecular hydrogen bonding effects arising from interactions with solvent. The data for the oxygen bound to nitrogen for **52** and **55** show relatively small differences. These signals doubtlessly are also sensitive to hydrogen bonding. Clearly, additional work is needed to characterize the ^{17}O chemical shift properties of this functional group.

The chemical shifts for the *O*-methyl derivative of acetaldoxime ($CH_3CH{=}N{-}OCH_3$), **56**, has been reported to be 157 ppm. Table 11 contains the chemical shift value[12] for some representative oximes (**57**–**62**). The chemical shift range for these compounds is not large. It remains to be determined if ^{17}O NMR data can be used to distinguish between *syn* and *anti* forms of the oximes. Since the oxime group can function both as a hydrogen bond donor and acceptor, it will be necessary to carefully work out the influence of hydrogen bonding on the chemical shift of the oxygen in this functional group.

TABLE 8. ^{13}C NMR chemical shifts and one-bond carbon–hydrogen spin–spin coupling constants of oximes **44**–**51** measured for saturated solutions in DMSO-d_6[11]

	δ (ppm from internal TMS)								^1J(C, H) (Hz)					
Compound	C1	C2	C3	C4	C5	C6	C7	Other C	C3	C4	C5	C6	C7	Other C
44	119.36	161.44	116.63	125.89	139.91	122.72	144.64	—	165.2	174.3	—	167.2	170.1	—
45	120.11	154.95	117.90	129.98	123.24	126.96	146.60	—	162.3	165.8	—	164.7	168.1	—
46	120.64	155.35	118.36	132.80	110.65	129.87	146.49	—	162.0	166.2	—	166.2	168.1	—
47	118.52	150.37	117.11	117.11	152.40	112.06	148.11	55.46	161.1	161.1	—	159.4	166.5	143.7
48	118.24	156.29	116.18	130.57	119.48	128.46	148.42	—	159.4	159.5	162.0	159.4	166.2	—
49	111.26	158.11	101.33	161.50	106.22	130.10	149.10	55.21	159.4	—	162.7	159.6	165.4	144.5
50	106.41	157.73	98.46	152.08	104.19	129.89	149.58	39.84	156.6	—	160.3	157.4	163.6	135.9
	107.18[a]	159.85[a]	99.59[a]	153.56[a]	105.01[a]	132.18[a]	152.67[a]	40.17[a]	—	—	—	—	—	—
	(−0.77)[b]	(−2.12)[b]	(−1.13)[b]	(−1.48)[b]	(−0.82)[b]	(−2.29)[b]	(−3.09)[b]	(−0.33)[b]	—	—	—	—	—	—
51	120.54	127.43	111.86	150.89	111.86	127.43	148.07	39.77	—	—	—	—	—	—
	122.05[a]	128.73[a]	112.51[a]	152.06[a]	112.51[a]	128.73[a]	149.62[a]	40.27[a]	—	—	—	—	—	—
	(−1.51)[b]	(−1.30)[b]	(−0.65)[b]	(−1.17)[b]	(−1.65)[b]	(−1.30)[b]	(−1.55)[b]	(−0.50)[b]	—	—	—	—	—	—

[a] In acetone d_6.
[b] Solvent chemical shift, $\Delta\delta$ (ppm).

TABLE 9. ^{15}N NMR chemical shifts (ppm from external CH_3NO_2 ($\delta = 0.0$ ppm)) of oximes **44**–**51** measured for solutions in DMSO-d_6 based on *z*-gradient selected ^{1}H, ^{15}N HMBC experiments[11]

Compound	NOH	Other N
44	−17.5	−10.0
45	−19.6	—
46	−25.3	—
47	−22.6	—
48	−21.8	—
49	−34.9	—
50	−42.2	−327.0
51	—	−329.1

TABLE 10. ^{17}O chemical shift data (ppm) for hydroxamic acids and esters[a]

Compound no.	Structure	Chemical shift (ppm) C=O	Chemical shift (ppm) (NHOH)
52	$C_6H_5CONHOH$	333 (302)[b]	79[b]
53	$C_6H_5CON(CH_3)OH$	330	
54	$C_6H_5CONHOCH_3$	341	
55	$C_6H_5CON(CH_3)OCH_3$	348	

[a] Data from Reference 12 in dioxane solvent unless otherwise noted.
[b] Data for 0.5 M acetonitrile solutions cited in Reference 12.

TABLE 11. ^{17}O chemical shift data (ppm) of oximes[a]

Compound no.	Structure	Chemical shift (ppm)
57	Cyclopentanone oxime	179
58	Cyclohexanone oxime	170
59	Dicyclopropyl ketone oxime	167
60	2,6-Dimethylbenzaldehyde oxime	188
61	2,6-Dichlorobenzaldehyde oxime	196.5
62	Fluorenone oxime	195

[a] Data from 0.5 *M* acetonitrile solutions cited in Reference 12.

Selected ^{1}H, ^{13}C and ^{15}N chemical shifts of oximes **65**–**67** are compared to those of similar compounds **63**, **64** and **68**–**72** in Table 12.

B. Coupling Constants

1. Hydrogen–hydrogen

Nowadays, the NMR specialist finds an arsenal of assignment techniques at his disposal for structural determination. Long before they became available this responsibility lay mostly in the hands of chemists who could treat the information gleaned from coupling constants. Older NMR texts dedicated a large part of their content to the descriptions of spin–spin coupling patterns (order of spectra, two and higher order systems) as exemplified by Reference 5, which contains relevant *J* values. This content has been updated and placed on a very sound theoretical basis that is described in recent reviews[13, 14].

TABLE 12. Selected ^{13}C and ^{1}H chemical shifts of imines, oximes, hydrazones, carbodiimides and azo compounds[9]

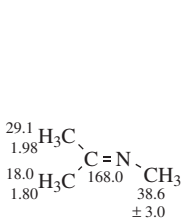

N-Isopropylidene methylamine

(**63**)

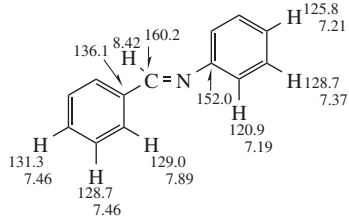

N-Benzylidene aniline

(**64**)

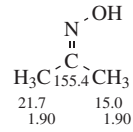

Acetone oxime

(**65**)

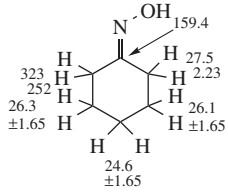

Cyclohexanone oxime

(**66**)

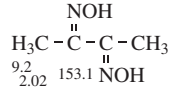

2,3-Butanedione dioxime

(**67**)

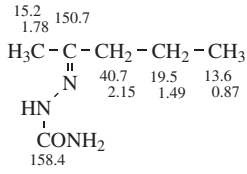

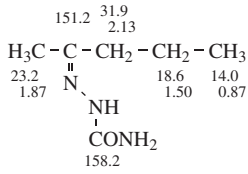

2-Pentanone semicarbazone

(**68a**) (**68b**)

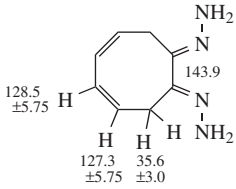

Cycloocta-4,5-diene-1,2-dione-(*E*,*E*)-dihydrazone

(**69**)

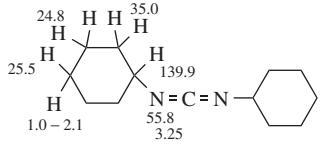

Dicyclohexylcarbodiimide

(**70**)

TABLE 12. (*continued*)

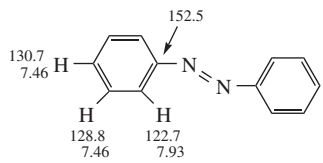

Azobenzene

(**71**)

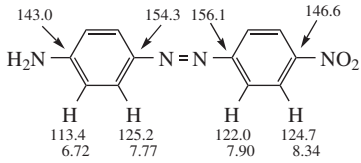

4-Amino-4'-nitroazobenzene

(**72**)

The role of lone pairs, the effect of their geometry and of electronegative substituents on coupling constants (mostly proton–proton) have been studied for oximes. Specific examples are given in the corresponding tables.

2. Carbon–hydrogen

Carbon–hydrogen spin–spin coupling constants are included in a review by Hansen[15] and discussed in terms of ring strain, steric effects, electronegativity, lone pair effects and electric field effects. Additivity of these effects in a few systems is commented on.

3. Nitrogen–hydrogen

Nitrogen–hydrogen coupling constants are thoroughly discussed in Chapter 5 of Reference 4. Their medium and temperature effects are also analyzed.

$^1J(^{15}N,^1H)$ coupling constants lie in the range of (-80 ± 15) Hz. Some examples, including exceptions, are tabulated in Table 13. $^2J(^{15}N,^1H)$ coupling constants are generally less than 2 Hz in magnitude:

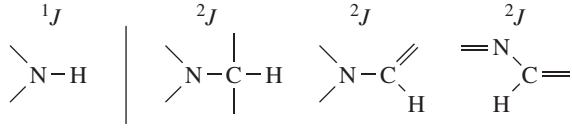

Only where there are sp^2-hybridized C and/or N atoms do the magnitudes reach 3–12 Hz. In compounds with C=N double bonds the coupling constants can be as large as −16 Hz (Table 12). The sign of the $^2J(^{15}N,^1H)$ coupling can be positive or negative. The same applies to $^1J(^{15}N,^1H)$ couplings and long-range couplings $^nJ(^{15}N,^1H)$. The latter only have significant values when there are multiple coupling pathways.

In the case of nitrogen the gyromagnetic ratio is positive for ^{14}N and negative for ^{15}N. It is convenient to compare the reduced coupling constants, $^nK(A–X)$, which are obtained by dividing the observed coupling constant by the product of the gyromagnetic ratios of the coupled nuclei (equation 2)[4]. The reduced coupling constant is a measure of the electronic interactions in the molecule and is independent of the specific properties of the nuclei.

$$^nK(A-X) = \frac{2\pi}{h\gamma_A\gamma_X}\ ^nJ(A-X) \qquad (2)$$

TABLE 13. $^{n}J(^{15}N,^{1}H)$ coupling constants ($n = 1, 2, 3, 4$) of selected compounds[9]

Compound	Solvent	^{1}J	^{2}J	^{3}J	^{4}J
	Neat liquid	−64.5	1.0		
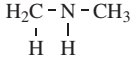	Neat liquid	−67.0	0.9		
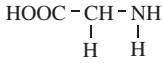	Water	−74.7 −88.3	0.5		
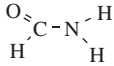	Neat liquid	 −90.7 −88.4	14.6		
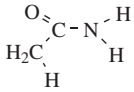	Water	−90.9		1.3	
	Diethyl ether	−70.2	2.3	2.2	
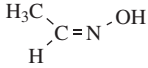	Water		−15.9		
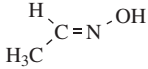	Water		+2.90		
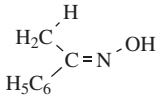	Chloroform			−2.0	
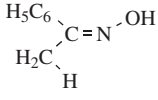	Chloroform			−4.2	
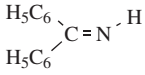	Pentane	−51.2			
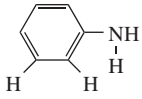	Chloroform Benzene	−78.0		 −1.9	 −0.5
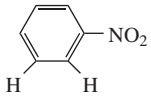	Acetone			−1.90	−0.8

TABLE 13. (*continued*)

Compound	Solvent	^1J	^2J	^3J	^4J
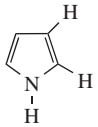	Benzene Neat liquid	−96.5	−4.5	−5.4	
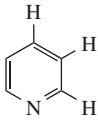	Neat liquid		−10.8	−1.5	0.2
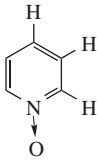	Chloroform		0.5	−5.3	1.1

Directly bonded nuclei are predicted to have positive reduced couplings unless one of the nuclei, such as fluorine, has tightly bound *s*-valence electrons. Single resonance experiments have been used to determine the relative signs of spin couplings, but these are limited to spin systems exhibiting second-order features which are not usually encountered in heteronuclear couplings. Double resonance techniques, which include selective decoupling, spin tickling, nuclear Overhauser and localized saturation effects, are generally used to obtain relative signs of coupling constants. Absolute signs of couplings whose relative values are known can be related to the $^{13}C-H$ coupling which is predicted to be positive. Liquid crystal solvent studies on methyl fluoride have confirmed that $J(^{13}C-H)$ is positive and $J(^{13}C-F)$ is negative, in agreement with theory.

Table 14 summarizes the magnitudes and absolute signs of a variety of couplings involving nitrogen in oximes. The entries include examples of spin coupling between other nuclei and ^{14}N and ^{15}N. Spin coupling between ^{14}N and ^1H nuclei is not usually observable because of the rapid quadrupolar relaxation of the ^{14}N nucleus.

TABLE 14. Values and signs of some experimentally determined nitrogen coupling constants of oximes[4]

Compound	J, (Hz)	$K \times 10^{-20}(cm^{-3})$
N−C−H Coupling		
$CH_3CH=^{15}N-OH$	−15.9[a]	+13.1[a]
$CH_2=^{15}N-OH$	−13.9[a], +2.7[b]	+11.4[a], −2.2[b]
N−C−C−H Coupling		
$CH_3CH=^{15}N-OH$	−4.2[a], −2.6[b]	+3.4[a], +2.1[b]
$(CH_3)_2C-^{15}N-OH$	−4.0[a], −2.2[b]	+3.2[a], 1.8[b]

[a] Coupling to proton *trans* to oxygen atom.
[b] Coupling to proton *cis* to oxygen atom.

In oximes, of which formaldoxime (**73**) is representative, the two geminal $^{15}N-C-H$ couplings are found to be of different magnitudes and also of opposite signs:

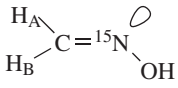

$^2K(NH_A) = +11.4 \times 10^{20}\ cm^{-3}$
$^2K(NH_B) = -2.2 \times 10^{20}\ cm^{-3}$

(**73**)

A similar reversal of the signs of the N−C−H coupling with stereochemistry is not, however, found for the geometric isomer, *E*-formanilide (**74**) and *Z*-formanilide (**75**). In both cases, the one- and two-bond reduced coupling constants have been shown to be positive.

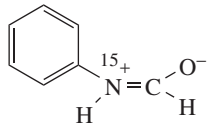

(**74**)

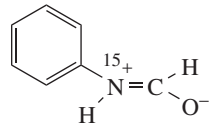

(**75**)

Signs and magnitudes of two- and three-bond N−H couplings in oximes along with quinoline derivatives have been thoroughly investigated in terms of solvent effects and stereochemistry. It is observed that protonation in aldoximes produces an algebraic decrease in two-bond reduced coupling to each of the geometrically different protons without any accompanying change in sign, whereas in quinoline, $^2K(N{=}C-H)$, which is also positive, undergoes a similar algebraic decrease on protonation or quaternization. For all three-bond couplings that have been investigated so far, the reduced coupling constants are found to be positive and protonation results in an algebraic increase in $^3K(N-H)$. Directly bonded N–H couplings are also found to have positive reduced coupling constants, and evidence shows that protonation similarly leads to an algebraic enhancement in $^1K(N-H)$. This alternating effect of protonation on the reduced coupling constants for one-, two- and three-bond couplings has been suggested as a means of determining the signs of spin coupling.

The coupling interaction between directly bonded $^{15}N-H$ is generally dominated by the Fermi contact term, as evidenced by the dependence of $^1J(^{15}N-H)$ on the amount of *s* character in the bond. Table 15 lists some illustrative $^{15}N-H$ coupling constants, determined under comparable solvent conditions, as a function of the *s* character in the bonding orbitals.

Kintzinger and Lehn[16] have uncovered a very striking effect of the orientation of the nitrogen lone-pair on $^{15}N-H$ coupling constants in the $^{15}N{=}C-H$ group. In oximes the measured $^{15}N{=}C-H$ coupling constants are *ca* 3 Hz and *ca* 16 Hz for the *syn* and *anti* isomers, respectively.

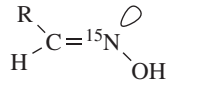

syn

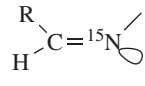

anti

TABLE 15. Representative $^{15}N-H$ coupling constants as a function of nitrogen hybridization[4]

Compound	Solvent	Hybridization	$^1J(^{15}N-H)$, (Hz)
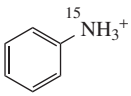	$HFSO_3$	sp^3	76.9
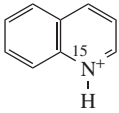	$HFSO_3$	sp^2	96.0
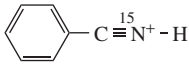	$HFSO_3-SbF_5-SO_2$	sp	136.0

Coupling comparable with that found in *anti*-oximes is also observed in cyclic systems such as pyridine, quinoline, 5-phenylisothiazole and isoxazole in which the nitrogen lone-pair lies *E(cis)* to the adjacent hydrogen. Confirmation of the importance of the lone-pair orientation is further derived from the fact that removal of the nitrogen lone-pair by protonation or quatenization results in the reduction of $^2J(^{15}N-H)$ to the value found in *syn*-oximes and pyrrole.

An extensive analysis of the effect of lone pairs on the nitrogen atom on spin–spin coupling constants is reviewed in the context of a description of molecular electronic structure[17]. Several oximes are analyzed in studies of these effects and their relevance for structural determination has been pointed out.

4. Carbon–carbon

Factors affecting carbon–carbon coupling constants have been studied using ^{13}C-labeled compounds[18,19]. Small substituent effects on directly-bonded carbons are observed. Aliphatic vicinal $^{13}C-^{13}C$ couplings are shown to parallel vicinal $^1H-^1H$ couplings in similar geometric surroundings and a similar dependence on bond and dihedral angles.

One-bond carbon–carbon spin–spin coupling constants are included in a review by Krivdin and Kalabin[20]. They are analyzed in terms of hybridization, substitution effects, lone pair effects and steric effects as well as respective applications to structural determination. The carbon–carbon spin–spin coupling constants between carbons that are separated by more than one bond were reviewed by Krivdin and Della[21] and are discussed in terms of experimental techniques, the effects of hybridization, substituent effects, steric effects and respective additivity patterns.

5. Carbon–nitrogen

Couplings between ^{15}N and ^{13}C are difficult to measure without isotopic enrichment. Values of $^1J(^{15}N,^{13}C)$ are generally less than 20 Hz. The sign can be positive or negative. If the value of ^1J is close to zero, it can be exceeded by ^2J or ^3J couplings. Some examples of known $^nJ(^{15}N,^{13}C)$ couplings are given in Table 16.

6. Coupling to other nuclei

^{15}N, ^{15}N couplings will not be treated here. They can only be measured for singly or doubly labeled compounds and are almost totally worthless for structural purposes. On the

TABLE 16. $^{n}J(^{15}N, ^{13}C)$ coupling constants ($n = 1$, 2, 3) of selected compounds in Hz (if the sign is not known, the magnitude is given)[9]

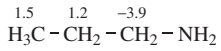	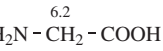
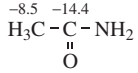	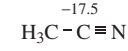
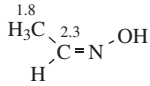	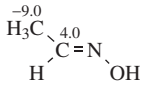
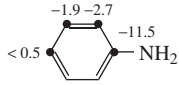	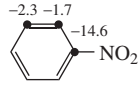
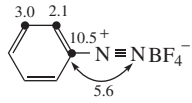	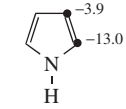
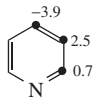	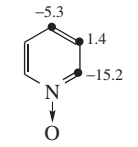
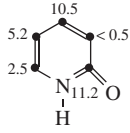	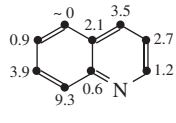

other hand, fluorine coupling constants are very large and, if this element is present, its coupling can be very useful in interpreting spectra and determining structural relationships including those via nonbonded interactions[22].

C. Relaxation Times

In order to discuss the width of an NMR line it is necessary to consider the relaxation mechanism involved (i.e. spin–lattice and spin–spin mechanism). Longitudinal relaxation times (T_1) for ^{13}C nuclei cover a large range of values. Those for cyclic ring systems are intermediate between the very short ones observed for macromolecules and the longer ones that are characteristic of quaternary carbons or those in highly symmetric molecules. Carbon-13 chemical shifts and spin–lattice relaxation times were determined for hydroxamic acid analogues[23]. The quadrupole moment of the ^{14}N nucleus leads to very fast relaxation and line broadening. Its particular effects are treated in Chapter 3 of Reference 4.

IV. SOLVENT EFFECTS

In some very early work the conformation of α-methyl groups in cyclohexanone oximes (**76**) was assigned from solvent shifts[24]. Results are summarized in Table 17. In solutes bearing a lone pair of electrons on nitrogen, the benzene–solute collision complex is likely to occur at a site as far as possible from the nitrogen[24]. Shifts have been summarized for aziridines, oximes and imines, and for the latter a complex of type **77** was proposed.

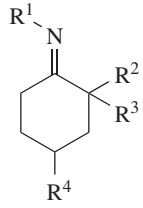

(**76**)

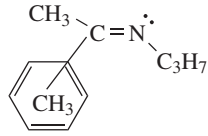

(**77**)

Oximes show strong intermolecular hydrogen bonding, in nonpolar solvents, which affects the ^{1}H NMR chemical shifts and coupling constants. The influence of this interaction on the conformational equilibrium and on some selected coupling constants ($^4J_{HF}$, $^1J_{CF}$ and $^2J_{CF}$) was evaluated[7]. Thus the ^{1}H and ^{13}C NMR spectra in different solvents were obtained. Both $^4J_{HF}$ and $^1J_{CF}$ are sensitive to the F–C–C=N orientation (Tables 18 and 19).

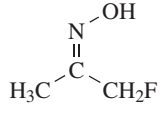

(**78a**)

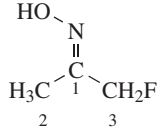

(**78b**)

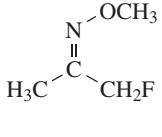

(**79a**)

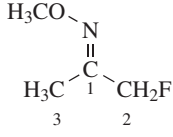

(**79b**)

The NMR data, combined with theoretical calculation and solvation theory, provide a consistent analysis of the conformational isomerism in **78b** and **79b** in solvents of

TABLE 17. Solvent shifts in cyclohexanone oximes[24]

Group	$\Delta\nu$	$\Delta\nu^*$
2-CH_3 (eq)	−6.3 to −11.4	4.8 to 12.2
2-CH_3 (ax)	−7.0 to −11.0	−1.6 to 1.8
	$\Delta\nu = \nu(CCl_4) - \nu(C_6H_6)$	
	$\Delta\nu^* = \nu(CCl_4) - \nu(C_5H_5N)$	
	(Both in Hz at 60 MHz)	

TABLE 18. Chemical shifts (ppm) and couplings constants (Hz) for **78b**[7]

Solvent	δ(OH)	δH_2	δH_3	δC_1	δC_2	δC_3	δN	$^2J_{HF}$	$^4J_{HF}$	$^1J_{CF}$	$^2J_{CF}$	$^3J_{CF}$	$^3J_{NF}$
CCl_4	9.44	4.78	1.97	153.8	82.6	10.8	−27.3	47.16	0.86	169.5	20.4	1.1	7.8
$CDCl_3$	9.00	4.84	1.99	154.6	83.8	11.1		46.90	0.90	168.2	19.4	1.3	
CD_2Cl_2	9.00	4.84	1.97	154.8	83.8	11.0		46.90	0.95	167.2	18.8	1.4	
Pure liquid	10.95	5.20	2.32	155.2	83.3	10.6	−23.5	47.91	0.76	166.2	18.7	1.4	7.9
Acetone-d_6	10.24	4.83	1.91	153.4	85.1	10.9	−23.5	47.34	1.58	163.2	19.0	0.9	8.0
CD_3CN	8.96	4.82	1.89	154.4	85.2	11.2		47.16	1.46	163.0	18.7	1.1	
DMSO-d_6	10.76	4.84	1.83	151.7	84.2	11.0	−16.6	47.25	1.70	161.9	18.5	0.7	8.1

TABLE 19. Chemical shifts (ppm) and coupling constants (Hz) for **79b**[7]

Solvent	δH_2	δH_3	δH_4	δC_1	δC_2	δC_3	δC_4	δN	$^2J_{HF}$	$^4J_{HF}$	$^6J_{HF}$	$^1J_{CF}$	$^2J_{CF}$	$^3J_{CF}$	$^3J_{NF}$
CCl_4	4.72	1.88	3.83	151.6	82.7	61.9	11.1	0.9	47.34	1.10	0.73	168.2	20.6	1.1	7.7
$CDCl_3$	4.81	1.93	3.89	152.7	83.5	61.8	11.5	−1.6	47.07	1.15	0.60	166.8	19.6		7.8
CD_2Cl_2	4.79	1.90	3.86	152.9	84.0	61.9	11.5		47.17	1.25		165.7	19.2	0.9	
Pure liquid	4.89	2.02	3.91	152.9	83.9	61.5	10.9		47.11	1.23	0.60	165.4	19.8	0.9	
Acetone-d_6	4.83	1.88	3.83	153.3	84.4	61.9	11.5	1.2	47.17	1.40	0.66	164.0	19.0	1.1	7.8
CD_3CN	4.81	1.88	3.84	153.5	84.4	61.9	11.4	0.2	47.05	1.38	0.70	163.6	18.7		8.0
DMSO-d_6	4.86	1.85	3.82	152.6	83.3	61.4	11.5	−0.2	46.92	1.31	0.68	163.2	18.4		8.0

different polarity. In **78b** the isomerism is between the *cis* and *gauche* forms. The energy difference is 3.30 kcal mol^{-1} in the vapor phase, which compares very well with that calculated (3.4 kcal mol^{-1}) by DFT at the B3LYP/6-311++g(2df, 2p) level. In **79b** the isomerism is similar to that of **78b**, and the observed energy difference of 2.2 kcal mol^{-1} is also in fair agreement with that calculated (3.2 kcal mol^{-1}).

Hydrogen bonding usually affects proton chemical shifts, and this is observed in the spectra of pure liquid **78b**, in comparison with the data in solution (Table 18). However, it is noteworthy that similar changes do not occur for the coupling constants (Table 18), since no change was detected when the concentration was changed in nonpolar and polar solvents, and when the OH was replaced by OCH_3 to prevent the formation of hydrogen bonds (Tables 18 and 19).

The $^1J_{CF}$ and $^4J_{HF}$ couplings for **78b** are 159.7 and 1.94 Hz (*cis*) and 170.0 and 0.70 Hz (*gauche*), and for **79b** 161.6 and 1.50 Hz (*cis*) and 168.9 and 1.02 (*gauche*). In fluoroacetone, its precursor, $^1J_{CF}$ and $^4J_{HF}$ are 179.6 and 3.4 Hz (*cis*) and 188.0 and 5.0 Hz (*trans*). For the compounds studied here, the C=N group leads to smaller coupling than C=O (fluoroacetone), probably owing to a reduced interaction between the coupled nuclei in **78b** and **79b**.

It was noted that for **78b** and **79b**, $^4J_{HF}$ and $^1J_{CF}$ are dependent on the molecular conformation, but this is not the case with $^3J_{NF}$, which is independent of the conformation. It is well known that the internuclear couplings are electron coupled interactions[25] for which there are three possible mechanisms: (1) the nuclear moments interact with the electronic currents produced by the orbiting electrons; (2) there is a dipolar interaction between the nuclear and electronic magnetic moments; (3) there is an interaction between the nuclear moments and the electronic spins in *s*-orbitals, the so-called Fermi contact term[25].

For all couplings involving hydrogen the Fermi contact term is dominant, and the other terms may be neglected. Hence this term is dependent on the molecular conformation. Recent studies[25–29] using *ab initio* and DFT techniques to calculate the various

contributions, such as Fermi contact (FC), paramagnetic spin–orbit (PSO), diagmagnetic spin–orbit (DSO) and spin–dipolar (SD) for J_{CH}, J_{CF} and J_{HF}, confirmed the predominance of the Fermi contact contributions and agreed with experiment[30–36] that these couplings are dependent on the molecular conformation.

DFT calculations were also used to study the NMR spectra of salicylhydroxamic acid in DMSO-d_6 solution[37]. Best fit with experimental results was observed for association with two solvent molecules. Assignments could be made for the specific structure formed in solution. Similar studies were made on other types of hydroxamic acids[38, 39].

V. REFERENCES

1. H. Friebolin, *Basic One- and Two-Dimensional Spectroscopy*, 3rd Edn., Wiley-VCH, Weinheim, 1998.
2. R. K. Harris, *Nuclear Magnetic Resonance Spectroscopy, A Physicochemical View*, Pitman, London, 1983.
3. J. Masen (Ed.), *Multinuclear NMR*, Plenum Press, New York, 1987.
4. M. Witanowski and G. A. Webb (Eds.), *Nitrogen NMR*, Plenum Press, London, 1973.
5. F. Bovey, *Nuclear Magnetic Resonance Spectroscopy*, Academic Press, New York, 1969.
6. S. E. Dermark, M. S. Dappen, N. L. Sear and R. T. Jacobs, *J. Am. Chem. Soc.*, **112**, 3466 (1990).
7. C. F. Tormena, R. Rittner, R. J. Abraham, E. A. Basso and B. C. Fiorin, *J. Phys. Org. Chem.*, **17**, 42 (2004).
8. G. C. Levy and G. L. Nelson, *Carbon-13 Nuclear Magnetic Resonance for Organic Chemists*, Wiley, New York, 1972.
9. M. Hesse, H. Maier and B. Zeeh, *Spectroscopic Methods in Organic Chemistry*, Georg Thieme Verlag, Stuttgart, 1997.
10. R. E. Botto, P. W. Westerman and J. D. Roberts, *Org. Magn. Res.*, **11**, 510 (1978).
11. E. Kolehmainen, R. Gawinecki, B. Osmialowski and K. Tzebiatowska, *Magn. Res. Chem.*, **35**, 778 (1997).
12. D. W. Boykin, *^{17}O NMR Spectroscopy in Organic Chemistry*, CRC Press, Boca Raton, 1991.
13. J. Kowalewski, *Annu. Rep. NMR Spectrosc.*, **12**, 81 (1982).
14. R. Contreras and J. C. Facelli, *Annu. Rep. NMR Spectrosc.*, **27**, 255 (1993).
15. P. E. Hansen, *Progress in NMR Spectroscopy*, Vol. 14, Pergamon, Oxford, 1981, pp. 175–296.
16. J. P. Kintzinger and J. M. Lehn, *Chem. Commun.*, 660 (1967).
17. V. M. S. Gil and W. Phillipsborn, *Magn. Res. Chem.*, **27**, 409 (1989).
18. M. Stockler and M. Klessinger, *Org. Magn. Res.*, **12**, 107 (1979).
19. J. Jokisaari, *Org. Magn. Res.*, **11**, 157 (1978).
20. L. B. Krivdin and G. A. Kalabin, *Progress in NMR Spectroscopy*, Vol. 21, Pergamon, Oxford, 1989, pp. 243–448.
21. L. B. Krivdin and E. W. Della, *Progress in NMR Spectroscopy*, Vol. 23, Pergamon, Oxford, 1991, pp. 301–610.
22. F. M. Mallory and C. W. Mallory, *J. Am. Chem. Soc.*, **107**, 4816 (1985).
23. L. Cavali, *J. Chem. Soc. B*, 1453 (1968).
24. N. C. Lim, M. D. Morton, H. A. Jenckins and C. Bruckner, *J. Org. Chem.*, **68**, 9233 (2003).
25. T. Enevoldsen, J. Oddershede and S. P. A. Sauer, *Theor. Chem. Acc.*, **100**, 275 (1998).
26. J. E. Peralta, V. Barone and R. H. Contreras, *J. Am. Chem. Soc.*, **123**, 9162 (2001).
27. J. E. Peralta, V. Barone, M. C. R. Azua and R. H. Contreras, *Mol. Phys.*, **99**, 655 (2001).
28. R. Barone, J. E. Peralta and R. H. Contreras, *J. Comput. Chem.*, **22**, 1615 (2001).
29. L. B. Krivdin, S. P. A. Sauer, J. E. Peralta and R. H. Contreras, *Magn. Reson. Chem.*, **40**, 187 (2002).
30. R. J. Abraham, A. D. Jones, M. A. Warne, R. Rittner and C. F. Tormena, *J. Chem. Soc., Perkin Trans. 2*, 533 (1996).
31. R. J. Abraham, C. F. Tormena and R. Rittner, *J. Chem. Soc., Perkin Trans. 2*, 1663 (1999).
32. C. F. Tormena, R. Rittner, R. J. Abraham, E. A. Basso and R. M. Pontes, *J. Chem. Soc., Perkin Trans. 2,* 2054 (2000).

33. R. J. Abraham, C. F. Tormena and R. Rittner, *J. Chem. Soc., Perkin Trans. 2,* 815 (2001).
34. C. F. Tormena, R. Rittner and R. J. Abraham, *J. Phys. Org. Chem.*, **15**, 211 (2002).
35. C. F. Tormena, N. S. Amadeus, R. Rittner and R. J. Abraham, *J. Chem. Soc., Perkin Trans. 2*, 773 (2002).
36. M. P. Freitas, R. Rittner, C. F. Tormena and R. J. Abraham, *J. Phys. Org. Chem.*, **14**, 317 (2001).
37. A. Kaczor and L. M. Proniewicz, *J. Mol. Struct. (THEOCHEM)*, **640**, 133 (2003).
38. A. Kaczor and L. M. Proniewicz, *J. Mol. Struct.*, **704**, 189 (2004).
39. A. Kaczor and L. M. Proniewicz, *Spectrosc. Acta, Part A*, **62**, 1023 (2005).

CHAPTER 5

Synthesis of hydroxylamines

ARTEM MELMAN

Department of Chemistry and Biomolecular Science, Clarkson University, Potsdam, NY 13699, USA
Fax: +1-315-268-6610; e-mail: amelman@clarkson.edu

The chemistry of hydroxylamines, oximes and hydroxamic acids
Edited by Z. Rappoport and J. F. Liebman

I. INTRODUCTION

Hydroxylamines and related hydroxamic acids are polyfunctional organic molecules possessing a number of distinctive chemical properties. In addition to traditional applications of hydroxylamine and hydroxamate derivatives as analytical and organic reagents, these compounds recently attracted considerable interest as drug candidates with a wide range of biological effects. Particularly important biological activities of hydroxamate and hydroxylamines are matrix metalloprotease inhibition[1], antidoting for nerve amine poisoning[2,3], chelation therapy for iron overload[4,5], antimalarial activity[6], cancer treatment through histone deacetylase inhibition[7] and iron deprivation[8], and many others.

This chapter is devoted to synthetic methods most commonly used for preparation of hydroxylamines. The synthesis of hydroxylamines has been previously reviewed, most recently in 1990[9]. The present review covers chemical literature up to 2007 with particular attention to the progress achieved in stereoselective synthesis of hydroxylamines.

The main first part of the review (Section III) summarizes preparation of hydroxylamine derivatives through alkylation, arylation, and addition reaction of hydroxylamine, or its derivatives such as hydroxamic acids and *N*-oxysulfonamides. The second main part (Sections IV–VIII) describes methods of creation of hydroxyamino groups *de novo* from other functionalities. Due to easy interconversion outlined in Section II, syntheses of hydroxylamines and hydroxamic acids are considered together. For the same reason, the chapter also relates to synthesis of *N*-oxysulfonamides and *N*-oxyphosphonamides as far as these methods are of interest for the preparation of hydroxylamines.

II. HYDROXYLAMINES THROUGH HYDROLYSIS OF HYDROXAMIC ACIDS, OXIMES AND NITRONES

Hydrolysis of nitrones, oximes and hydroxamic acids is frequently used as a final step in the preparation of substituted hydroxylamines. Although hydrolysis is the most commonly utilized method for oximes, oxime ethers and nitrones, formation of sensitive hydroxylamines can also be achieved under milder reaction conditions by treatment of

their precursors with excess of hydroxylamine or hydrazine. Hydrolysis of oximes and oxime ethers has been reviewed[10].

Conversion of hydroxamic acids into hydroxylamines is usually performed by hydrolysis or alcoholysis under acidic[11–14] or basic catalysis[15,16], although other methods like reaction with trimethylsilyl iodide[17] have also been sparingly used.

Preparation of hydroxamic acids through acylation of hydroxylamines is a common and straightforward reaction. However, acylation of *N*-alkylhydroxylamines is known to proceed on both the oxygen and nitrogen atoms and can result in mixtures of *N*- and *O*-acylation products[18,19]. In *N*-alkylhydroxylamines possessing a bulky[20] or an electron-poor[21] substituent on nitrogen atom, *O*-acylation is predominant.

III. SYNTHESIS OF HYDROXYLAMINES THROUGH ALKYLATION AND ARYLATION OF OTHER HYDROXYLAMINES

A. *N*-Alkylation of Hydroxylamines through Displacement of C–X Bonds

1. N-Alkylation of hydroxylamines through nucleophilic substitution

Hydroxylamines and alkylhydroxylamines possess high nucleophilicity and can react with a variety of primary and secondary alkylating agents. The reactivity of hydroxylamines in the majority of these reactions resembles that of primary and secondary amines. While hydroxylamine and *N*-alkylhydroxylamines **1** are ambident nucleophiles, under neutral or weakly basic reaction conditions alkylation proceeds exclusively on nitrogen atom to give products of type **2** (equation 1). Deprotonation of the OH group of hydroxylamines results in *O*-alkylation products.

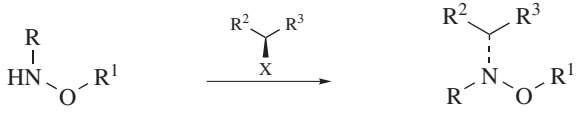

(**1**) (**2**) (1)

R, R^1, R^2, R^3 = H, Alk, Ar X = Hal, OSO_2Alk, OSO_2Ar, OH

The main advantages of preparation of hydroxylamines through *N*-alkylation of other hydroxylamines are versatility and predictable stereochemical outcome that allow the introduction of the hydroxyamino group at advanced stages of multistep syntheses. The use of nucleophilic displacement is however problematic for sterically hindered alkyl halides and sulfonates. Apart from several examples mentioned below, alkylation of hydroxylamines with tertiary alkyl halides does not take place.

Alkylation of hydroxylamine with primary halides and sulfonates is rarely used nowadays for preparation of *N*-alkylhydroxylamines due to the competing formation of *N*,*N*-dialkylhydroxylamines. A number of older procedures have been reported with low to moderate yields of *N*-alkylhydroxylamines. Yet, in many cases the reported low yields can be attributed to workup losses during distillation and crystallization steps rather than to the polyalkylation. Use of excess of hydroxylamine in reactions with primary alkyl halides (e.g. **3**) improves the yields of monoalkylation (equation 2). Most of the examples of alkylation of hydroxylamine in good yield involve a substitution of an activated halogen atom at benzylic positions[22] as well as in haloacetamides **4**[23] leading to alkylhydroxylamines such as **5** where dialkylation rates are lower (equation 3).

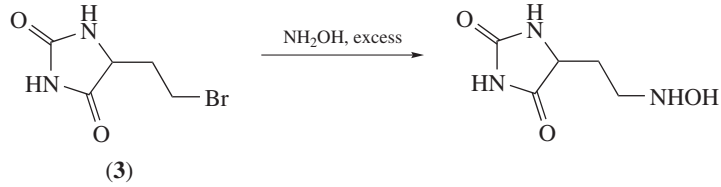

(**3**) (2)

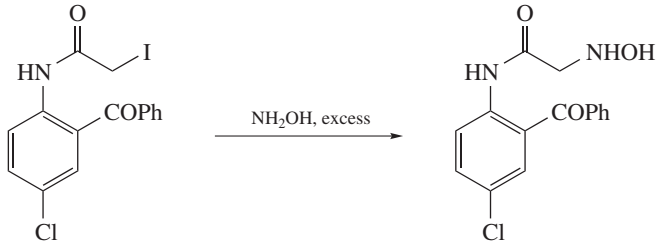

(**4**) (**5**) (3)

N,*N*-Dialkylation of hydroxylamine (equation 4) with an excess of alkylating reagent such as **6** usually proceeds in a good to excellent yield[24]. *N*,*N*-Dialkylation has also been successfully employed for cyclization reactions (equation 5) with formation of *N*-hydroxyazaheterocycles[25] of type **7**.

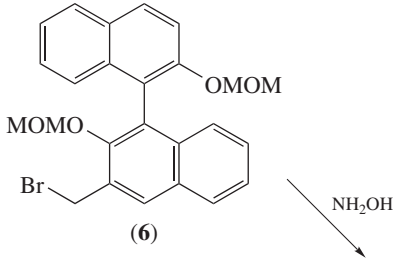

(**6**)

MOM = CH_2OCH_3

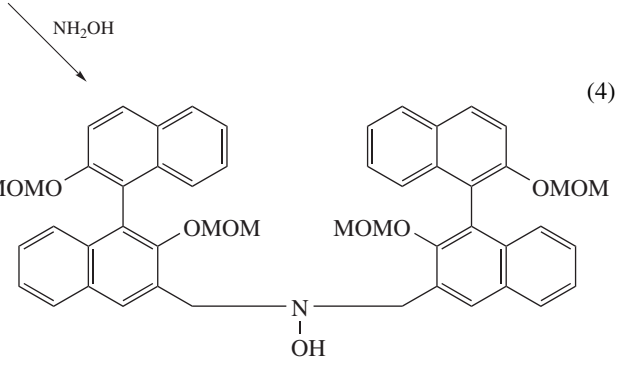

(4)

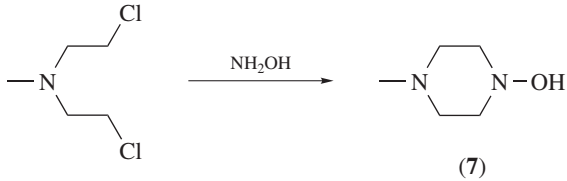

(**7**) (5)

Because of their lower hydrophilicity and higher stability to oxidation, *O*-protected hydroxylamines are more convenient substrates for alkylation than hydroxylamine itself. Commercially available *O*-benzylhydroxylamine was successfully alkylated with alkyl halides[26–28] and alkyl sulfonates[29–31].

Due to a much lower danger of dialkylation, alkylation of *N*-alkyl- and *N*-alkyl-*O*-protected hydroxylamines (e.g. **8**, equation 6) with primary alkyl halides proceeds substantially more selectively giving high yields of *N*,*N*-disubstituted products[32–34] of type **9**.

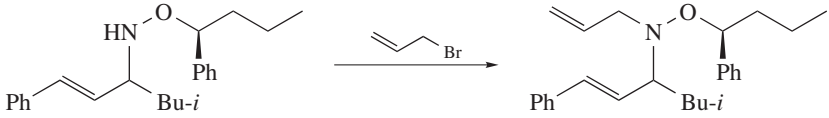

(**8**) (**9**) (6)

Alkylation of hydroxylamines with secondary alkyl halides and alkyl sulfonates like **10** (equation 7) is one of the most frequently used synthetic approaches, especially to enantiomerically pure hydroxylamines such as **11** (equation 7). The reaction proceeds with inversion of configuration and does not produce appreciable amounts of dialkylation products. Both hydroxylamine as well as *N*- and *O*-alkylhydroxylamines have been successfully used. Alkyl triflates[35–37] are probably the most useful substrates for these transformations since they can be prepared from a large pool of commercially available enantiomerically pure chiral secondary alcohols.

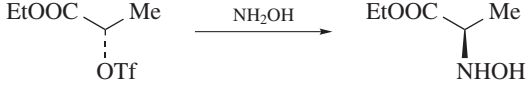

(**10**) (**11**) (7)

Intermolecular reactions of hydroxylamines with secondary alkyl halides and mesylates proceed slower than with alkyl triflates and may not provide sufficiently good yield and/or stereoselectivity[38]. A useful alternative for these reactions is application of more reactive anions of *O*-alkylhydroxamic acids[39] or *O*-alkoxysulfonamides[40] like **12** (equation 8) as nucleophiles. The resulting *N*,*O*-disubstituted hydroxamic acids or their sulfamide analogs of type **13** can be readily hydrolyzed to the corresponding hydroxylamines. The same strategy is also helpful for synthesis of hydroxylamines from sterically hindered triflates[41,42] and from chiral alcohols (e.g. **14**) through a Mitsunobu reaction[43–45] (equation 9).

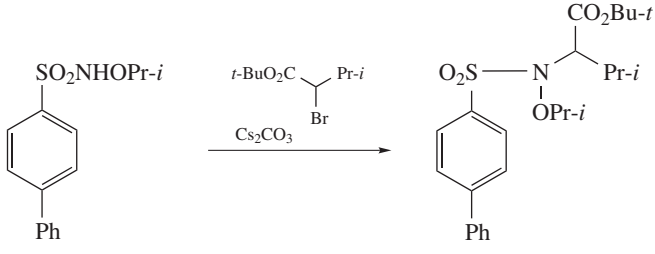

(**12**) (**13**) (8)

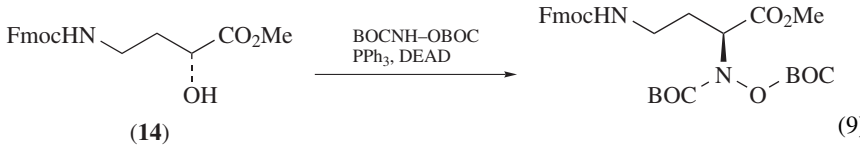

(**14**) (9)

Fmoc = 9-Fluorenylmethoxycarbonyl
BOC = *t*-Butoxycarbonyl
DEAD = Diethyl azodicarboxylate

Tertiary electrophiles alkylate hydroxylamines through the S_N1 mechanism. These reactions (e.g. equation 10) are practically feasible only for compounds forming highly stabilized carbocations such as trityl[46, 47], or 2-(*p*-alkoxyphenyl)propyl[48]. All these reactions proceed exclusively on the nitrogen atom and have been used for *N*-protection of the amino groups in hydroxylamines.

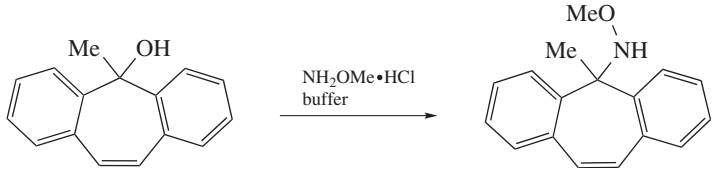

(10)

S_N1 substitutions also proceed easily in compounds forming highly stabilized secondary carbocations such as benzyhydrol[49], ferrocene[50] and analogous systems[51]. A variety of leaving groups can be utilized in these reactions including halides, alkoxy and alkylthio in the presence of mercury salts and ethers.

2. Palladium-catalyzed N-allylation of hydroxylamines

N-Alkylhydroxylamines react with substituted allyl acetates (e.g. **15**, equation 11) in palladium catalyzed addition–elimination reactions giving the corresponding *N*-alkyl, *N*-allylhydroxylamines **16**[52]. The reaction proceeds with high regioselectivity but complete racemization. A similar reaction with *O*-acyl hydroxamic acids has been carried out using allylic α-alkoxycarbonyloxyphosphonates[53].

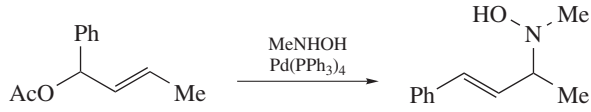

(**15**) (**16**) (11)

3. N-Alkylation of hydroxylamines through ring opening of epoxides

Ring opening of terminal epoxides with *O*-protected hydroxylamines proceeds regiospecifically under mild reaction conditions. As in the case of alkyl halides and sulfonates, formation of dialkylation products has been observed in epoxides opening with *O*-alkylhydroxylamines[54] but not *N*-alkylhydroxylamines[55]. Highly chemoselective ring opening in terminal epoxides of type **17** into β-hydroxyaminohydroxylamine **18** without

any appreciable amount of dialkylation product has been achieved using *O*-trimethylsilylhydroxylamine in the presence of lithium perchlorate[56] (equation 12).

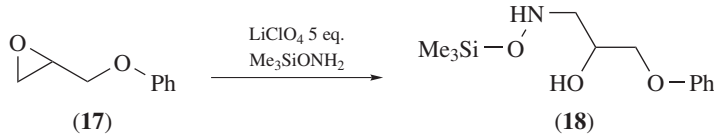

(**17**) (**18**) (12)

The reactions of 2,3-disubstituted epoxides with hydroxylamines[57] and hydroxamates[58] tend to proceed more slowly, giving variable yields of ring-opening products. Catalysis with chiral Lewis acids **20** was reported to allow asymmetric opening of *meso*-epoxide **19** in a good yield and *ee*[59] (equation 13).

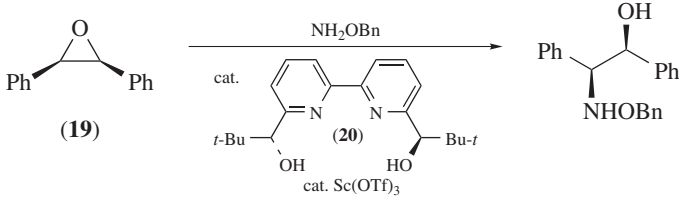

(**19**) (**20**) (13)

B. *O*-Alkylation of Hydroxylamines

Selective *O*-alkylation of hydroxylamines and their derivatives can be done through deprotonation of the OH group. *O*-Alkylation (equation 14) of *N*-substituted hydroxamic acid[60–62] (e.g. **21**) followed by hydrolysis of the resultant *O*-alkylation product **22** is the most commonly used approach. Since alkylation of *N*-unsubstituted hydroxamic acid results in a mixture of *O*- and *N*-alkylation products, the corresponding *O*-alkylhydroxylamines are better prepared through alkylation of *N*-hydroxysuccinimide[63,64] or *N*-hydroxyphthalimide[65,66] followed by hydrolysis.

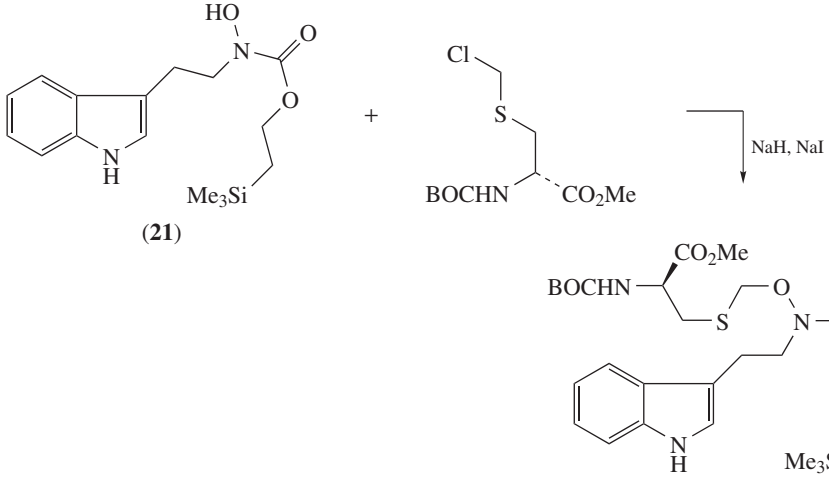

(**21**) (**22**) (14)

O-Alkylation of oxime anions[67,68] followed by hydrolysis is another efficient approach toward *O*-alkylhydroxylamines. *O*-Alkylation of oximes of type **24** (equation 15) can also be done through Michael addition with Baylis–Hillman adducts of type **23** catalyzed by triphenylphosphine[69].

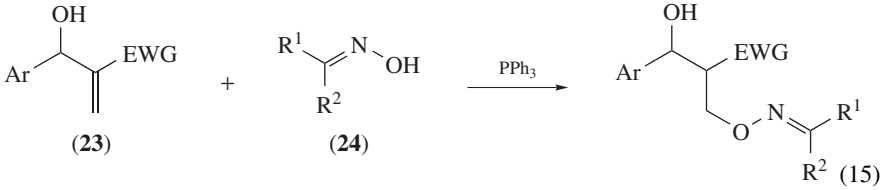

(**23**) (**24**) (15)

EWG (Electron Withdrawing Group) = CO_2Me, COMe, CN

R^1 = Ar, R^2 = H, Me

Other *O*-alkylation methods are exploited less frequently. *O*-Allylation of *N*-substituted hydroxamic acids of type **25** with allyl carbonates such as **26** and related compounds has been achieved through palladium catalyzed addition–elimination[70] (equation 16).

(**25**) (**26**) (16)

EWG = BOC, Bz, Ac, Cbz

R = Alk, Ar

N,*N*-Dialkyl *O*-allylhydroxylamines can be obtained through rearrangement of *N*-allyl substituted *N*-oxides[71].

C. *N*-Arylation and *N*-heteroarylation of hydroxylamines

Nucleophilic substitution of halogen atom in aromatic and heteroaromatic halides with a hydroxyamino group proceeds only in substrates that are activated by a strong electron-withdrawing substituent in the benzene ring (e.g. **27**, equation 17). Despite this limitation this reaction is useful for synthesis of arylhydroxylamines and usually provides good yields of products[72]. Along with activated aryl halides and sulfonates, activated methyl aryl ethers such as **28** can be used[73] (equation 18).

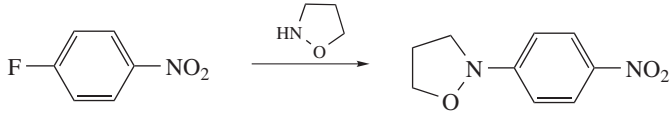

(**27**) (17)

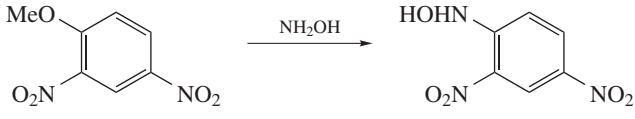

(**28**) (18)

Perfluoroarenes also undergo facile and selective monosubstitution with hydroxylamine[74]. This reaction is general and proceeds with different *N*-alkylhydroxylamines and a number of perfluorinated arenes (e.g. **29**, equation 19) and pentafluoropyridine.

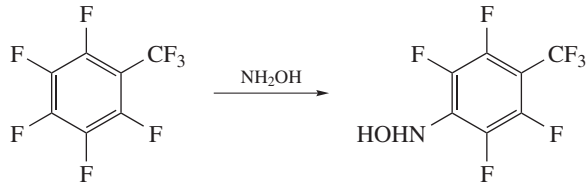

(19)

(**29**)

Electron-poor fused heterocyclic systems can activate a neighboring benzene ring for nucleophilic substitution. Fluoroquinolines of type **30** were shown to react efficiently with hydroxylamine (equation 20)[75,76].

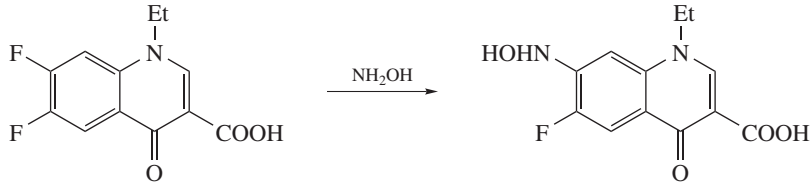

(20)

(**30**)

In contrast to *N*-alkylation of hydroxylamines, *N*-arylation is not complicated by polysubstitution. In the presence of two or more activated halogen substituents clean monosubstitution is possible (equation 21)[77].

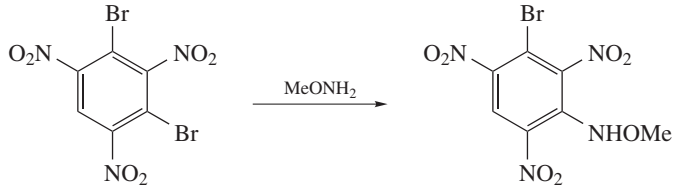

(21)

Hydroxamic acids undergo facile nucleophilic *N*-arylation with activated aryl halides such as **31** (equation 22). While hydroxamates are known to be ambident nucleophiles in alkylation reactions, arylation of hydroxylamines results exclusively in *N*-substituted hydroxamates of type **32** (equation 22)[78].

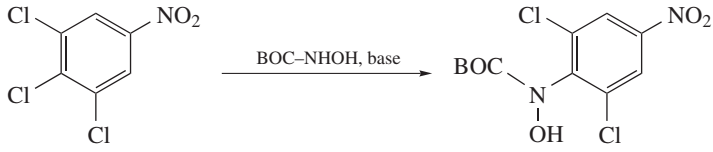

(22)

(**31**) (**32**)

Substitution of halogen atom in non-activated rings such as **33** (equation 23) is substantially more difficult. Palladium couplings are the most promising approach, although

only few examples of *N*-arylation with hydroxamates (e.g. **34**, equation 23) have been reported[79]. Nevertheless, it can be assumed that in analogy to numerous successful studies on other aryl–nitrogen couplings[80] this reaction is of general utility.

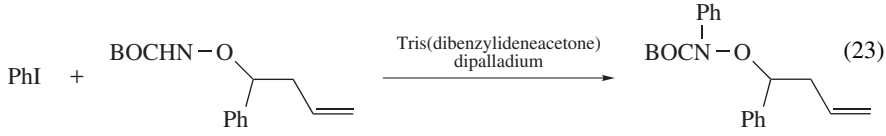

(23)

(**33**) (**34**)

A different approach to *N*-arylation of hydroxamic acid involves reaction with aromatic iodonium salt[81,82], but this reaction has been used for *N*-phenylation only.

Nucleophilic substitution with heteroaryl halides is a particularly useful and important reaction. Due to higher reactivity of heteroaryl halides (e.g. **35**, equation 24) in nucleophilic substitution these reactions are widely employed for synthesis of *N*-heteroaryl hydroxylamines such as **36**. Nucleophilic substitution of halogen or sulfonate functions has been performed at positions 2 and 4 of pyridine[83,84], quinoline[83], pyrimidine[85,86], pyridazine[87], pyrazine[88], purine[89,90] and 1,3,5-triazine[91] systems. In highly activated positions nucleophilic substitutions of other than halogen functional groups such as amino[92,93] or methoxy[94] are also common.

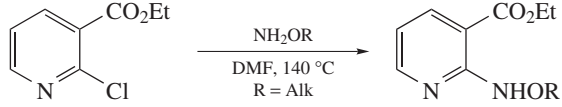

(24)

(**35**) (**36**)

No nucleophilic substitution in five membered heterocycles with hydroxylamines has been reported so far, although any nucleophilic substitution reaction known for amines should be suitable for hydroxylamines as well.

As in the case of aryl halides, no polysubstitution reaction has been reported in heteroarylion of hydroxylamines. If two or more identical chlorine atoms are present in the molecule, substitution of the first chlorine atom can be done selectively in most cases.

D. *O*-Arylation of Hydroxylamines

The general approach to *O*-arylation of hydroxylamines involves *N*-protection followed by *O*-arylation. Activated aryl halides and heteroaryl halides easily alkylate oxime salts[95] (equation 25), *N*-alkyl hydroxamic acids[96] and *N*-hydroxysuccinimide[97]. *N*-Hydroxyphthalimide can be also *O*-phenylated through a reaction with diphenyliodonium salt, although in lower yield[98].

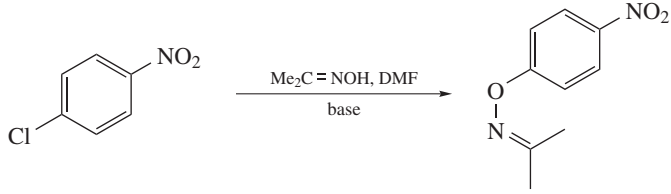

(25)

An alternative approach to *O*-arylation involves converting the OH function of hydroxylamine to a leaving group, followed by nucleophilic substitution with phenolate ions. Reaction of hydroxylaminesulfonic acid[99] as well as *O*-sulfonylhydroxylamines[100] (e.g. **37**, equation 26) with phenolates produces *O*-arylhydroxylamines of type **38**.

$$\underset{(\mathbf{37})}{H_2N-OR} \xrightarrow{ArOH/Base} \underset{(\mathbf{38})}{H_2N-OAr} \qquad (26)$$

R = SO_3H, SO_2Ar, 2,4-Dinitrophenyl

E. Nucleophilic Addition of Hydroxylamines to Activated C=C Bonds

Intermolecular or intramolecular 1,4-addition of hydroxylamines as well as *N*- and *O*-alkylhydroxylamines **39** to activated carbon–carbon double bonds (e.g. **40**, equation 27) is widely used for preparation of both *N*-substituted, and *N*,*N*-disubstituted hydroxylamines. The addition proceeds regiospecifically. The most commonly utilized activating groups are ester[101], carboxyl[102], sulfone[103], ketone[104] and 2-pyridyl[105]. Depending on reaction conditions, addition of hydroxylamines to α,β-unsaturated ketones can be accompanied by formation of oximes[106, 107].

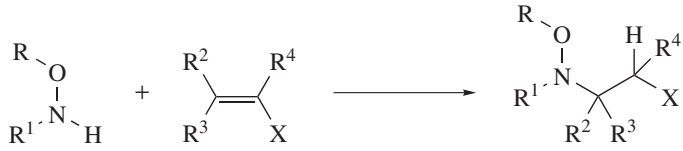

(**39**) (**40**) (27)

R, R^1, R^2, R^3, R^4 = H, Alk, Ar

X = COR, COOH, COOAlk, NO_2, SO_2Alk, $P(O)(OAlk)_2$, 2-pyridyl, 3-oxazolidone, 1-imidazolidone

In most cases monoaddition products can be obtained in good yields[108], even in reactions with Michael acceptors possessing a terminal double bond[109]. Further reaction with an excess of a Michael acceptor produces diaddition products in excellent yields[69]. Sequential additions of hydroxylamine to endocyclic double bonds such as in **41** have also been applied for preparation of bridged heterocyclic systems of type **42** (equation 28)[110].

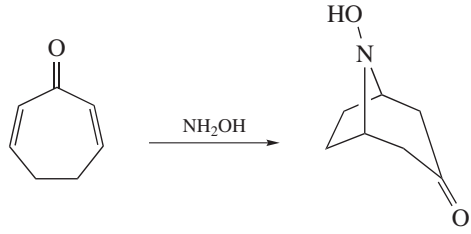

(**41**) (**42**) (28)

Addition of hydroxylamines to an endocyclic bond is possible if the double bond is a part of an aromatic heterocyclic system (e.g. **43**, equation 29)[111, 112].

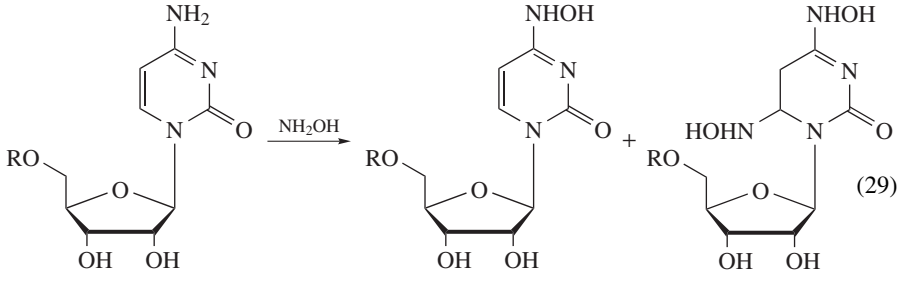

(29)

(**43**)

Addition of hydroxylamines to Michael acceptors **44** possessing an allylic leaving group results in formation of tandem addition–elimination products of type **45** (equation 30)[113].

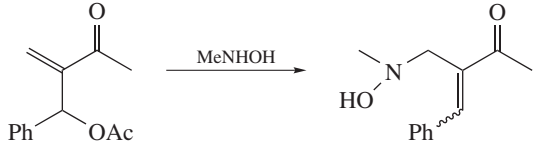

(30)

(**44**) (**45**)

Hydroxamic acids, possessing a free NH group[114] (e.g. **46**), as well as *N*-hydroxy sulfonamides[115, 116] also undergo addition to an activated double bond of type **47** (equation 31) under basic catalysis.

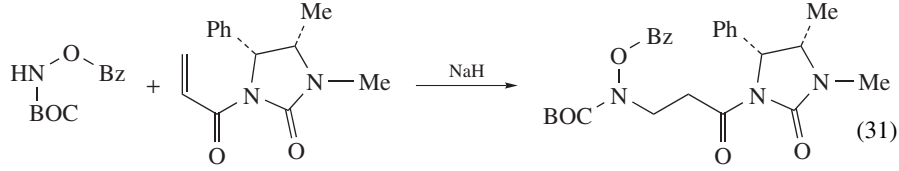

(31)

(**46**) (**47**)

Addition of hydroxylamines as well as hydroxamates **48** to activated di- and trisubstituted alkenes **49** (equation 32) results in the formation of one or two stereogenic centers at the α- and β-positions of the product **50**.

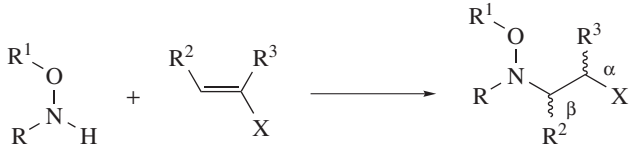

(32)

(**48**) (**49**) (**50**)

R = H, Alk, Ar, COAlk, COOAlk; R^1, R^2, R^3 = H, Alk, Ar

X = COR, COOH, COOAlk, NO_2, SO_2Alk, P(O)$(OAlk)_2$, 2-pyridyl

The stereochemistry of the addition can be controlled through the attachment of a chiral auxiliary or using asymmetric catalysis. Addition of *O*-benzylhydroxylamine to unsaturated imide **51** (equation 33) bearing a chiral auxiliary was found to proceed with high diastereoselectivity at the α-position[117].

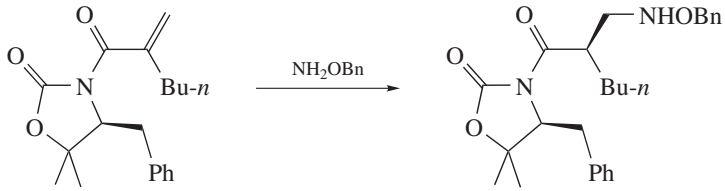

(33)

(**51**)

Steric induction at the β-position (equation 34) using analogous chiral auxiliaries of type **52**[118, 119] was found to be considerably weaker.

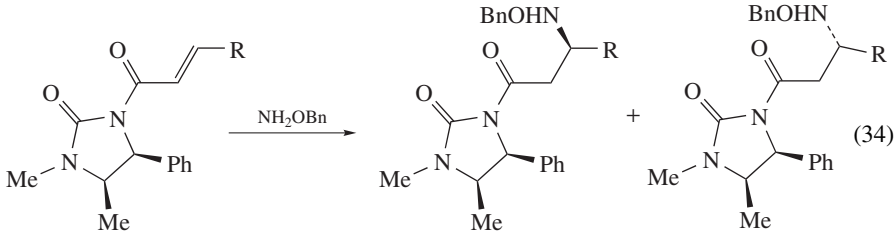

(34)

(**52**) R = CH_3, *n*-C_3H_7 4:1

Control of enantioselectivity in addition of hydroxylamines to prochiral activated double bonds has also been achieved through chiral catalysis. Substoichiometric amounts of magnesium bromide–chiral oxazolidine complex **54** (equation 35) catalyze asymmetric addition of *O*-benzylhydroxylamine to pyrazolides of α,β-unsaturated acids **53** with moderate to good enantioselectivity[120].

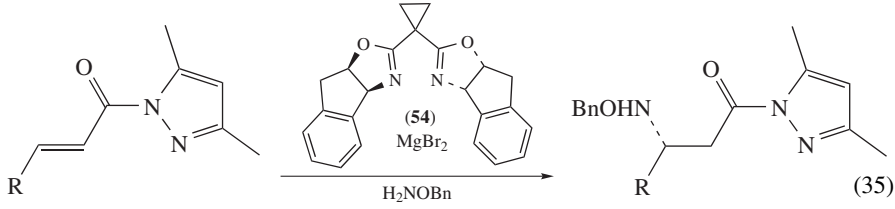

(35)

(**53**)

R = Alk, Ar

Analogous addition with scandium–(*S*,*S*-2,6-bis(oxazolinyl)pyridine) complex resulted in lower enantioselectivity[121]. A chiral heterobimetallic complex of $Y(OTf)_3$ and Li-BINOL provided high *ee* in addition of *O*-methylhydroxylamine to enones of type **55** (equation 36)[122–124].

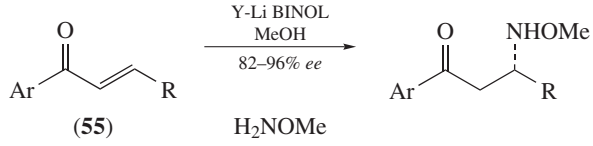

(55)

R = Ar, Alk (36)

F. Nucleophilic Addition of Hydroxylamines to Unactivated C=C Bonds

Thermal addition of hydroxylamines to non-activated C=C bonds has been observed only during cyclization processes[125, 126]. The reaction proceeds through a thermal retro-Cope mechanism as evidenced by its suprafacial stereospecificity (equation 37)[127].

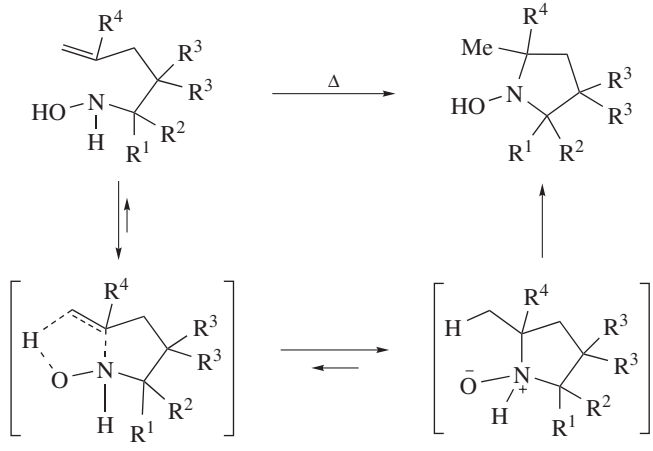

(37)

Intramolecular addition of hydroxylamines and hydroxamic acids to the non-activated double bonds is possible through oxidative cyclization. Reaction of *O*-Acyl β,γ-unsaturated hydroxamates (e.g. **56**, equation 38) with bromine provides 3,4-substituted *N*-hydroxy β-lactams such as **57** with high diastereoselectivity. Analogous reaction of *O*-benzyl hydroxylamine **58** (equation 39) with iodine results in five-membered cyclization with 2:1 ratio of diastereomers[128].

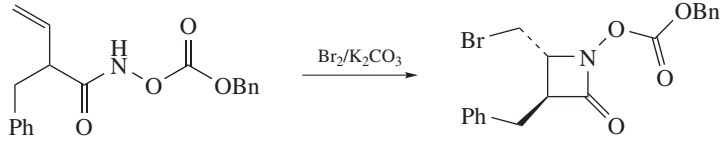

(56) (57) (38)

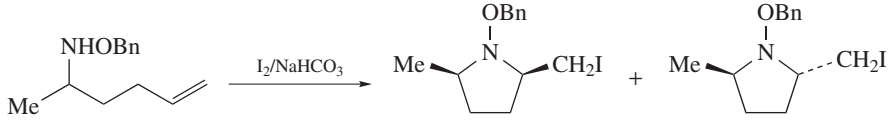

(58) 1:2 (39)

G. Nucleophilic Addition of Hydroxylamines to C=N Bond

Addition of hydroxylamines to C=N double bonds produces stable compounds only for endocyclic C=N bonds. Addition of hydroxylamine to azirines of type **59** results in stable adducts **60** as seen in equation 40. Similar reactions have been observed in benzoxazoles[129] and 1,2,3-triazolo[4.5-*d*]pyrimidones[130,131].

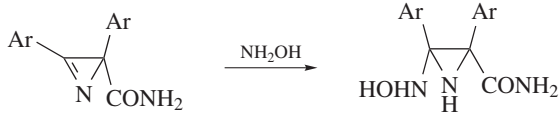

(40)

(**59**) (**60**)

Ar = Ph, *p*-MeC_6H_4, *p*-ClC_6H_4

Iminium cations obtained *in situ* from heterocyclic compounds possessing a hydroxy or alkoxy group in the α position to nitrogen atom (e.g. **61**, equation 41) react smoothly with hydroxylamines through iminium cations providing stable products such as **62**[132].

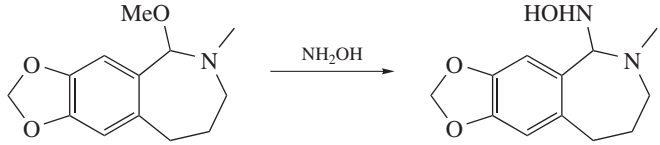

(41)

(**61**) (**62**)

H. Hydroxylamines through Reactions of Oxyiminium Cations

Reaction of hydroxylamine as well as *O*- and *N*-substituted hydroxylamines with aldehydes **63** results in formation of oximes and/or oxyiminium salts of type **64** (equation 42). Subsequent reaction with carbon, nitrogen, oxygen or phosphorous nucleophiles provides *N*-substituted hydroxylamines of type **65**.

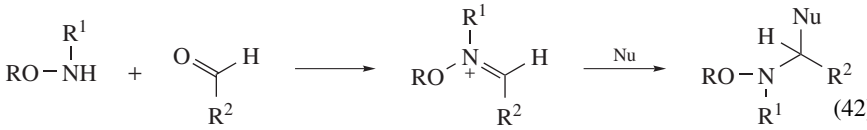

(42)

(**63**) (**64**) (**65**)

R = H, Alk, Me_3Si R^1, R^2 = H, Alk, Ar

Intermolecular reactions with *O*- and *N*-nucleophiles produce labile adducts of type **65** (equation 42). These adducts can be used for reversible generation of oxyiminium cations *in situ*[133]. In contrast, reaction of hydroxylamines with δ- or ε-lactols results in intramolecular additions of an oxygen nucleophilic group to intermediate oxyiminium cation, thus providing stable cyclic products. Reactions of this type have been extensively used for glycosidation of hydroxylamine derivatives such as **66** (equation 42), resulting in neoglycosides of type **67**[134–136].

Reactions of oxyiminium cation with carbon and phosphorous nucleophiles are irreversible. Strecker reaction of *N*-phenyl-*O*-trimethylsilylhydroxylamine **68** (equation 44)

with aliphatic aldehydes of type **69** and trimethylsilyl cyanide in the presence of Lewis acid catalyst produces α-hydroxyaminonitriles such as **70** in high yield[137].

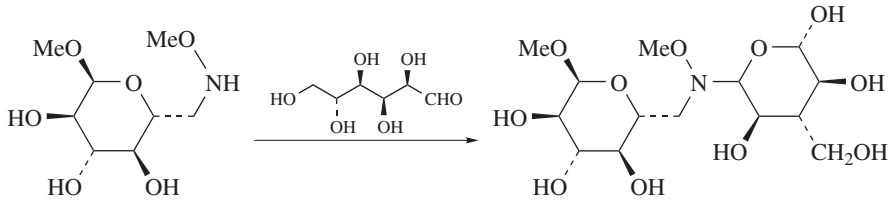

(**66**) (**67**) (43)

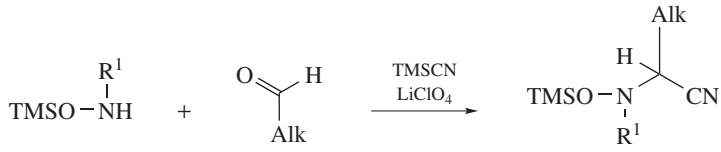

(**68**) (**69**) (**70**) (44)

R^1 = H, Ph

Reaction of oxyiminium cations with trimethylphosphite under catalysis with $LiClO_4$/TMSCl results in the corresponding α-oxyaminophosphonates of type **71** (equation 45) in good yield[138–140].

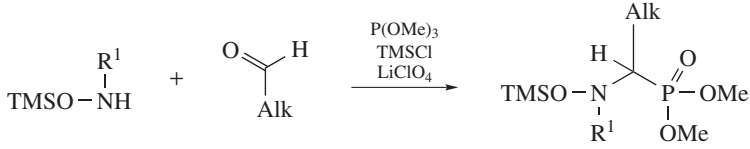

R^1 = H, Ph (**71**) (45)

The use of hydroxyamino instead of amino components in a Ugi reaction (equations 46 and 47) gives access to the corresponding hydroxamic acid of type **72** (equation 46)[141], hydroxylamines such as **73** (equation 47)[142] or *N*-hydroxyamidines[143].

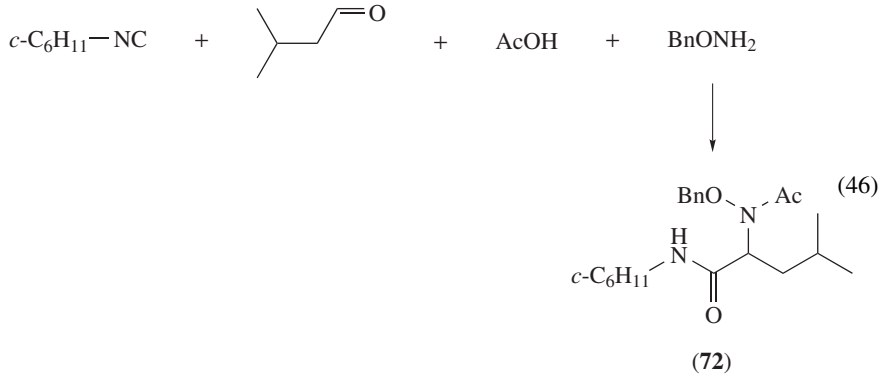

(**72**) (46)

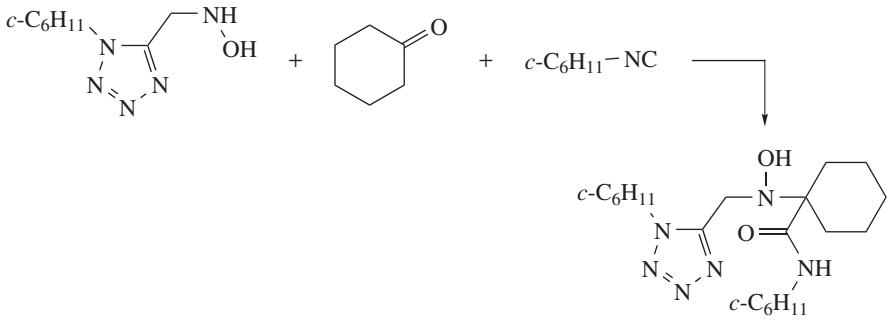

(**73**) (47)

Oxyiminium cations formed from *N*,*O*-dialkyhydroxylamines and formaldehyde are sufficiently reactive for Mannich reactions with activated arenes. Mannich reactions of oxyiminium cations with indoles (e.g. **74**, equation 48)[144] as well as pyrroles and furans but not phenol and thiophene[133] have been reported.

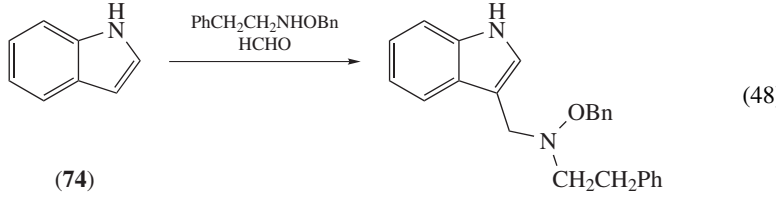

(**74**) (48)

IV. HYDROXYLAMINES THROUGH REDUCTION REACTIONS

A. Hydroxylamines through Reduction of Nitro Compounds

Hydroxylamines can be synthesized from various aliphatic and aromatic nitro compounds by reduction with metals and other one-electron donors, with complex hydrides and other two-electron donors, and by hydrogenation. In all cases the reduction proceeds stepwise and, depending on reaction conditions, can provide both amines and hydroxylamines.

1. Reduction of nitro compounds with one-electron donors

In general, ionic reductions of nitro compounds in neutral or weakly acidic media produce hydroxylamines while strongly acidic conditions provide amines. An exception is made by tin(II) chloride that can convert nitro compounds into hydroxylamines also under acidic conditions.

Zinc in the presence of ammonium chloride reduces primary, secondary and tertiary aliphatic nitro compounds but yields of hydroxylamines are moderate[145,146] and formation of coupling products is common[147]. Zinc with[148,149] or without[150,151] ammonium chloride reduces aromatic nitro compounds (e.g. **75**, equation 49) into hydroxylamines in moderate to good yield. However, it has been mentioned that the reaction is sensitive to the grade and quality of zinc dust (equation 50) and aromatic amines have been obtained as major products in zinc reduction reactions[151].

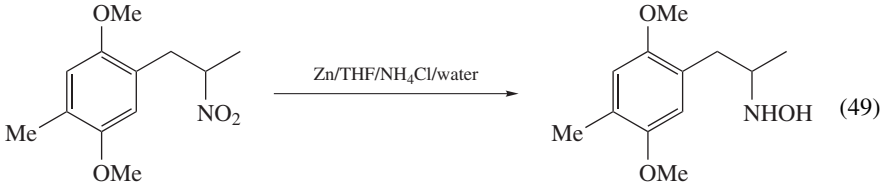

(**75**) (49)

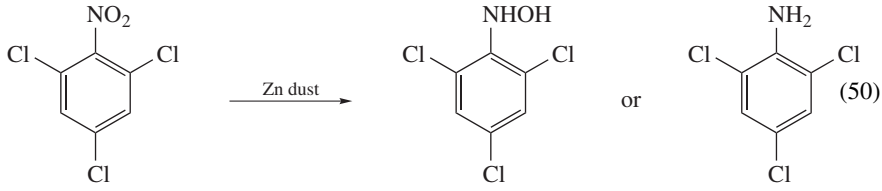

(50)

Aluminum amalgam reduces aliphatic[152, 153] and aromatic[154] nitro compounds to hydroxylamines in consistently good yields[155, 156] (equation 51) and this can be the method of choice for large-scale reductions.

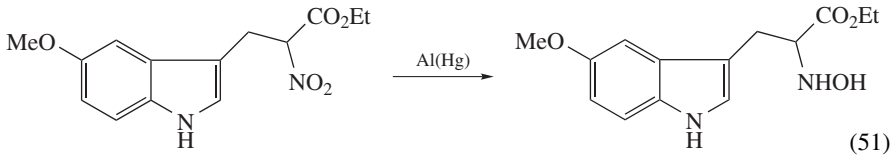

(51)

Samarium(II) iodide smoothly reduces primary, secondary[157] and tertiary[158, 159] aliphatic as well as aromatic[160] nitro compounds to hydroxylamines (equation 52). This reaction was found to be highly versatile although with limited scalability, since at least four equivalents of SmI_2 are necessary. Most functional groups, except aldehydes and sulfones, are compatible with SmI_2 reduction (equation 53).

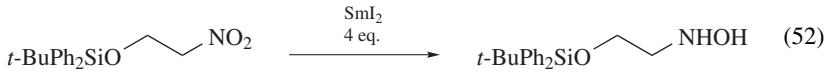

(52)

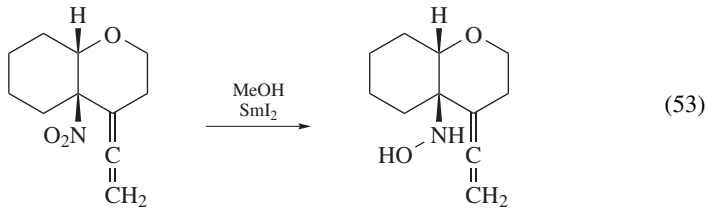

(53)

Tin(II) chloride in the presence of hydrochloric acid reduces aliphatic nitro compounds (e.g. **76**, equation 54)[161]. Aromatic nitro compounds are also reduced into hydroxylamines in moderate to excellent yields[162].

Furthermore, aromatic nitro compounds may be reduced to hydroxylamines by titanium(III) chloride[163] or ammonium sulfide[164], as well as by electrochemical reduction[165].

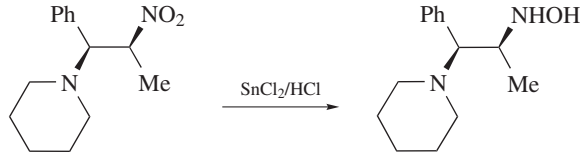

(**76**) (54)

2. Reduction of nitro compounds with complex hydrides

Metal hydrides such as $LiAlH_4$[166, 167], DIBAL[160, 168] and $NaBH_4$ in the presence of Te[169], Se[170], $NiCl_2$[171] or $BiCl_3$[172] reduce nitro compounds into hydroxylamines, although they are not usually considered as reagents of choice for this reduction.

Readily available α,β-unsaturated nitro compounds such as **77** undergo facile reduction into alkylhydroxylamines of type **78** (equation 55) with borane/THF complex in the presence of catalytic amounts of sodium borohydride[173, 174].

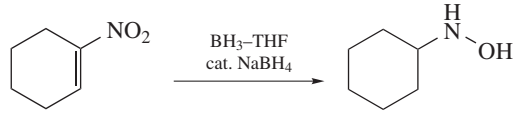

(**77**) (**78**) (55)

3. Hydrogenation of nitro compounds

In hydrogenation of nitro compounds, careful control of reaction conditions is needed to avoid formation of amines instead of hydroxylamines. In general, transfer hydrogenation is the most commonly used method to obtain hydroxylamines. Transfer hydrogenation of aryl nitro compounds with hydrazine on rhodium catalyst provides hydroxylamines in good yield. A number of functionalities can be tolerated including chloroaryl, and conjugated double bond[175, 176]. Palladium-catalyzed transfer hydrogenation of aliphatic and aromatic nitro compounds with triethylsilane[177] and hydrazine[178] also produces hydroxylamines in good yield. Raney nickel catalyzed transfer hydrogenation of aromatic nitro compounds with hydrazine has been reported to produce hydroxylamines in good yield[179]. Chemoselective reduction of nitro compounds into hydroxylamines with molecular hydrogen is more difficult, but can be achieved through specially prepared iridium catalyst[180].

4. Microbiological reduction of nitro compounds

Enzymatic reduction of aromatic nitro compounds such as **79** into hydroxylamines (equation 56) by plant cells has been recently reported[181].

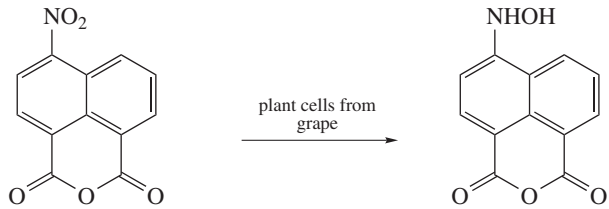

(**79**) (56)

B. Hydroxylamines through Reduction of Nitroso Compounds

Hydroxylamines are usually more accessible than the corresponding nitroso compounds, so only few examples of this reaction have been described in the literature. Aromatic nitroso compounds have been reduced into hydroxylamines with ascorbic acid[182], glyoxylic acid[183] and by NADH[184]. It can be safely assumed that any reagent capable of reducing nitro compounds should reduce nitroso compounds as well.

C. Hydroxylamines through Reduction of Oximes, Oxime Ethers and Nitrones

Complex hydrides are reagents of choice for reduction of oximes, oxime ethers and nitrones. Hydrogenation is rarely used for reduction of these compounds although several examples are known. Other methods, especially reduction with silanes in the presence of acid, can also be useful for providing alternative stereochemical outcomes.

1. Reduction of oximes and nitrones with complex hydrides

Sodium cyanoborohydride is the most commonly used reagent for reduction of oximes and oxime ethers. Although this reaction is highly versatile, and does not interfere with a majority of functional groups, careful control of reaction conditions is necessary. A considerable problem in the reduction, especially for aldoximes **80** (equation 57), is the reaction of initially formed *N*-alkylhydroxylamine **81** with the starting oxime **80**. The obtained nitrone **82** is subsequently reduced to *N*,*N*-dialkylhydroxylamine **83**, which was found to be a major reaction product at pH = 4 and above[185]. This side reaction can be avoided by adjusting the pH of the reaction mixture to 3 or below.

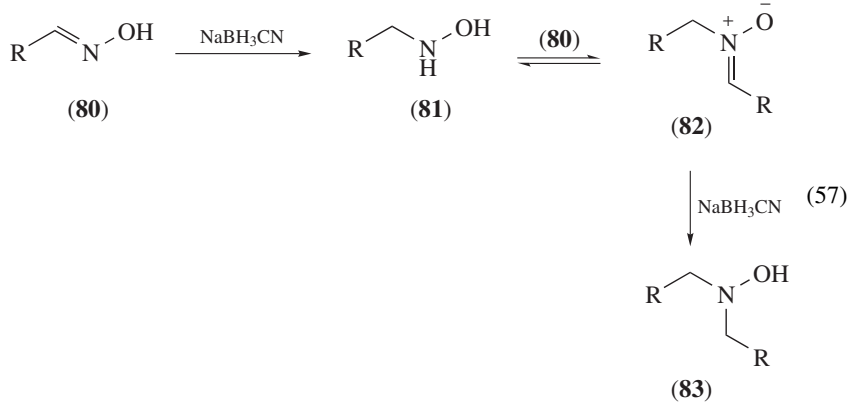

Lithium cyanoborohydride reduces oximes to hydroxylamines in good yield. Careful pH control is not necessary in this case and reduction can be done efficiently in the presence of acetic acid at pH 5[186]. Lithium borohydride reduces oximes as well[187]. Sodium borohydride in acetic acid[188] or on silica gel[189] has been used for reduction of oximes, but reported yields were low to moderate only. Lithium aluminum hydride[190] and DIBAL[191, 192] are capable of reducing oximes, but are sufficiently chemoselective for reduction of polyfunctional oximes.

Diborane in THF has been successfully used for reduction of aliphatic and aromatic oximes to hydroxylamines. Reported yields are highly variable[193, 194] although the low

yields should be attributed to non-optimal workup procedures rather than to low chemoselectivity. Other borane complexes also reduce oximes in good yield. Reduction of aldo- and ketoximes with borane–pyridine[195–197] and borane–trimethylamine[198] complexes proceeds smoothly giving good to excellent yields of hydroxylamines.

Silanes in the presence of trifluoroacetic acid reduce *O*-acyloximes **84** into *O*-acylhydroxylamines **85** (equation 58)[199,200].

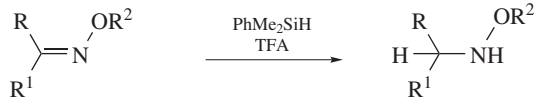

(**84**) (**85**) (58)

R, R^1 = H, Alk, Ar; R^2 = Bn, Ac, Bz

Oximes also have been reduced to hydroxylamines with bis(trifluoroacetoxy) borane[201] and photochemically with PhSeH[202].

Reduction of chiral ketoximes results in formation of a new stereogenic center. Although mixtures of stereoisomers are generally obtained, kinetically controlled reduction of cyclic oximes (e.g. **86**, equation 59 and **87**, equation 60) with sodium cyanoborohydride can proceed with high diastereoselectivity[203,204]. Stereoselectivity in these reactions closely resembles that of reduction of ketones with complex hydrides featuring attack from the least hindered side.

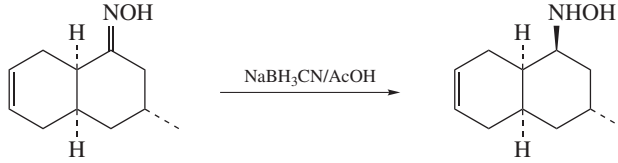

(**86**) (59)

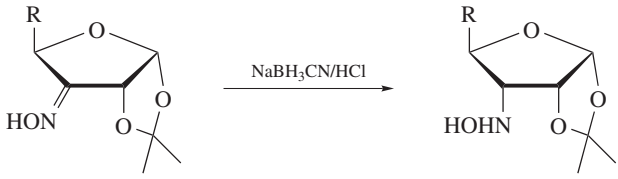

(**87**) (60)

Opposite stereoselectivity in reduction of cyclic oximes (e.g. **88**, equation 61) can be achieved with silane-trifluoroacetic acid[205].

Stereoselectivity in reductions of acyclic oximes depends on the configuration of C=N bond. (*E*)-Isomer of oxime **89** produced syn-hydroxylamine **90** in excellent stereoselectivity in reaction with phenyldimethylsilane-trifluroacetic acid while giving anti-product in the reaction with lithium aluminium hydride. Stereoselectivity in reductions of (*Z*)-isomers of **89** was substantially lower in both cases (equation 62)[199]. It can be assumed that the rules of stereoselectivity established in diastereoselective reduction of ketones[206] can be applied to reduction of oximes as well.

Syn stereoselectivity in reduction of acylic chiral ketoxime ethers of type **91** (equation 63) can be obtained using bulky tetramethylammonium triacetoxyborohydride that produces Felkin-type products with high selectivity[207]. Reaction of α-tolylsulfinylketoximes **92** (equation 64)[208] with L-Selectride also results in *syn* products **93**.

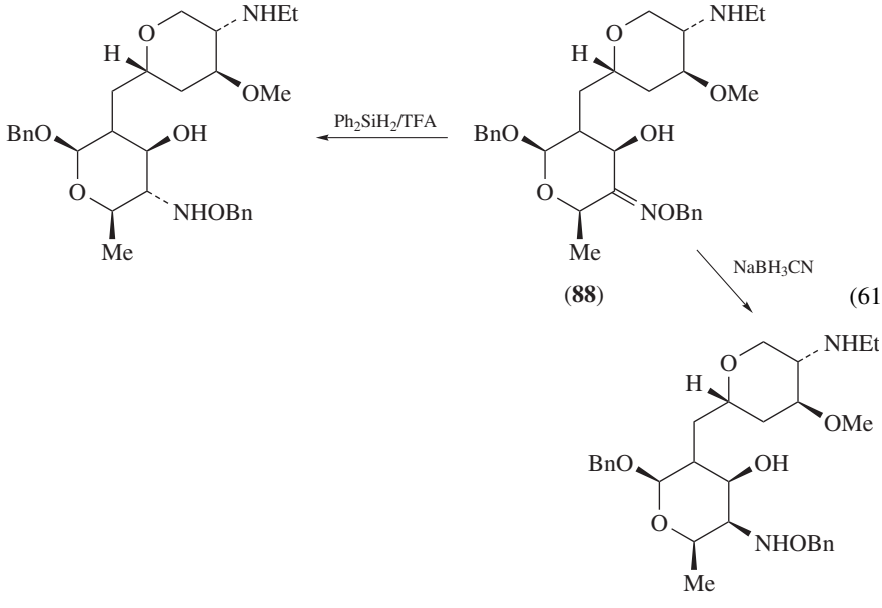

(**88**) (61)

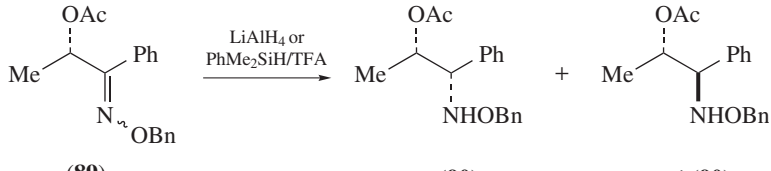

(**89**) *syn*-(**90**) *anti*-(**90**) (62)

	reducing agent	*anti*/*syn* (**90**)
(*E*)-(**89**)	$PhMe_2SiH$	99:1
(*E*)-(**89**)	$LiAlH_4$	82:18
(*Z*)-(**89**)	$PhMe_2SiH$	24:76
(*Z*)-(**89**)	$LiAlH_4$	58:42

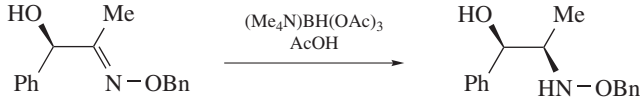

(**91**) (63)

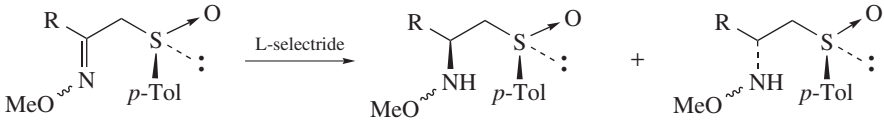

(**92**) (**93**) 96:4 (64)

Enantioselective reduction of ketoxime ethers with chiral boron hydrides produces chiral *O*-alkylhydroxylamines with variable *ee*. Reduction of oxime ethers of type **94** (equation 65) with norephedrine-derived oxazoborolidine **95** proceeds with very high *ee*[209]. However, an analogous reduction of acyclic aromatic oximes with chiral oxaborazolidines produced a mixture of amine and hydroxylamine[210].

Reduction of nitrones closely resembles that of oximes, although this reaction is rarely used for synthesis of hydroxylamines. All reagents capable of reducing oximes should reduce nitrones to *N*,*N*-dialkylhydroxylamines. Sodium cyanoborohydride reduces nitrones to hydroxylamines in moderate to excellent yields[211]. The zwitterionic structure of nitrones allows reduction without acid catalysis. Both sodium borohydride[212] and lithium aluminum hydride[213] convert nitrones to hydroxylamines in good yields. Two other reagents reducing nitrones in good yield are trichlorosilane[214] and germanium hydrides[215].

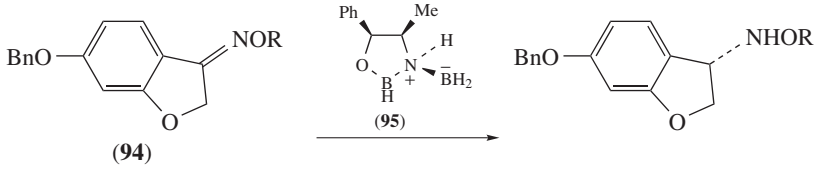

(65)

R = $XC_6H_4CH_2$; X = H, *p*-MeO, *o*-NO_2

2. Hydrogenation of oximes and nitrones

Oximes undergo hydrogenation to hydroxylamines and/or amines depending on reaction conditions. Platinum oxide is the most frequently used catalyst[216, 217] for selective hydrogenation of oximes to hydroxylamines. Reduction of chiral oxime **96**[218] over palladium catalyst (equation 66) proceeds in high yield and stereoselectivity. High stereoselectivity was observed in catalytic hydrogenation of α-alkoxyoximes[219].

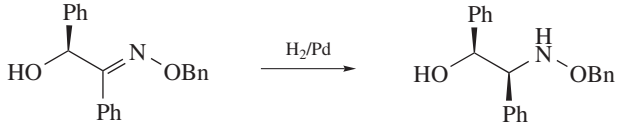

(66)

Other hydrogenation methods are less chemoselective. Use of Raney nickel provides hydroxylamines in low yield[220]. Hydrogenation of 1-acetonaphthone oxime over rhodium–chiral phosphine catalysts was found to proceed under harsh conditions and provided low *ee*[221].

V. HYDROXYLAMINES THROUGH ADDITION TO THE C=N DOUBLE BOND OF OXIMES, OXIME ETHERS AND NITRONES

A. Addition of Organometallic Reagents to Oximes, Oxime Ethers and Nitrones

Organolithium and Grignard reagents are capable of addition to the C=N bond of oximes and oxime ethers. Oxime ethers can react directly[222, 223] while addition to oximes requires two equivalents of an organometallic reagent[224]. The majority of experimental

data involve reactions of organometallic reagents with aldoxime ethers. Additions to ketoximes and ketoxime ethers (e.g. **97**) usually proceed in lower yields[224] (equation 67), yet are useful for preparation of *N*-*tert*-alkylhydroxylamines of type **98** that are difficult to synthesize by other methods. Addition of organometallic reagents to nitrones proceeds similarly, resulting in *N*,*N*-dialkylhydroxylamines of type **99** (equation 68)[225–226].

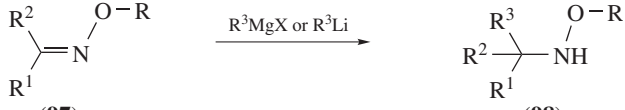

(**97**) (**98**) (67)

R, R^1, R^2 = H, Alk; R^3 = Alk, Ar

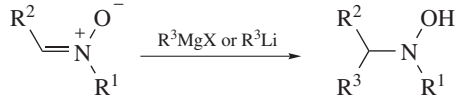

(**99**) (68)

R, R^1, R^2 = H, Alk; R^3 = Alk, Ar

Coordination of organometallic species has been used in studies of stereocontrol of the addition. These stereocontrolled addition reactions possess considerable preparative potential as outlined in the following examples. Addition of Grignard reagents to chiral aldoxime ethers such as **100** (equation 69) was found to proceed with a substantial stereoselectivity[227].

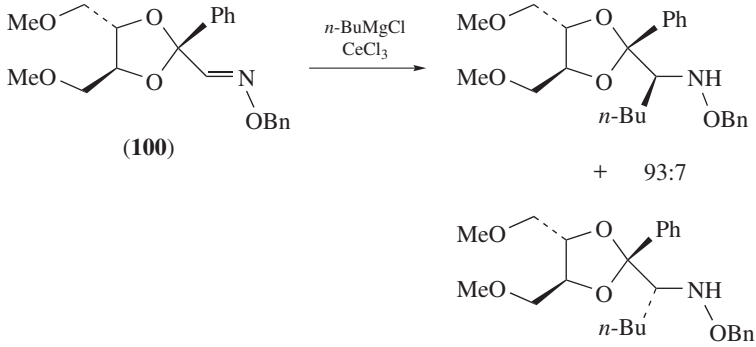

(**100**) (69)

High diastereoselectivity of addition was observed in acyclic oxime ethers bearing bulky chiral auxiliaries on the oxygen atom of the oxime function[228–231] (equations 70 and 71).

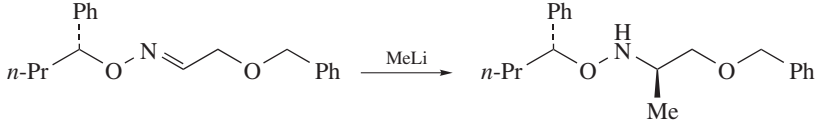

(70)

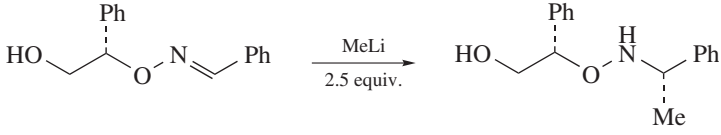

(71)

Additions of alkynylzinc compounds to nitrones possessing an easily recoverable mannose-derived chiral auxiliary of type **101** (equation 72) proceed with good steroeselectivity (93–98% dr)[232].

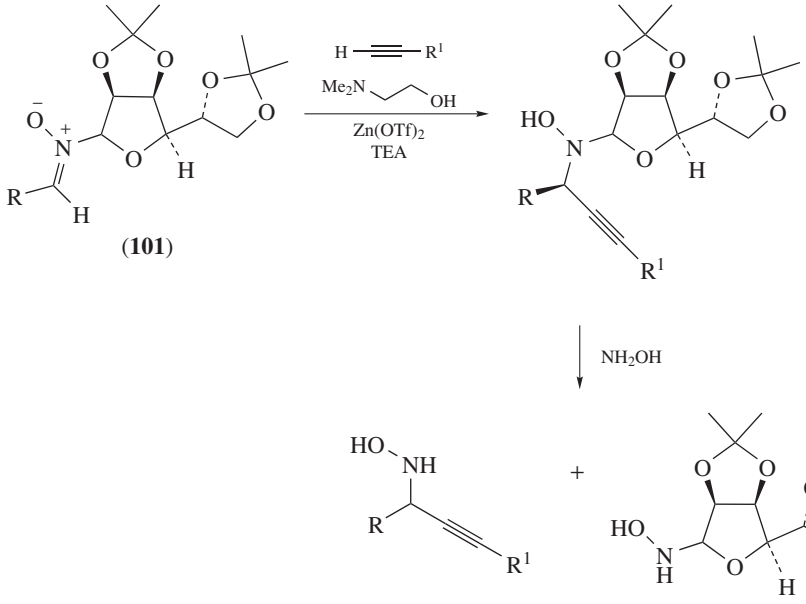

(**101**)

(72)

Allylboronates of type **103** react with equivalent amounts of aldoximes **102** (equation 73) giving allylhydroxylamines **104** in good yields. Similar reactions of aldoximes[233] and glyoxylate oxime ethers[234] with allyl bromide and indium also provide hydroxylamines. Additions of substituted allyl boronates to oximes produce mixtures of stereoisomers with ratio highly dependent on the steric size of substituents in both molecules[235]. Addition of allyltri-*n*-butyltin to aldoxime ether **105** (equation 74) was found to proceed with a considerable diastereoselectivity[236].

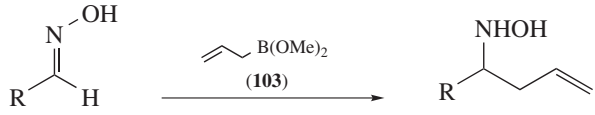

(**102**) (**104**)

(73)

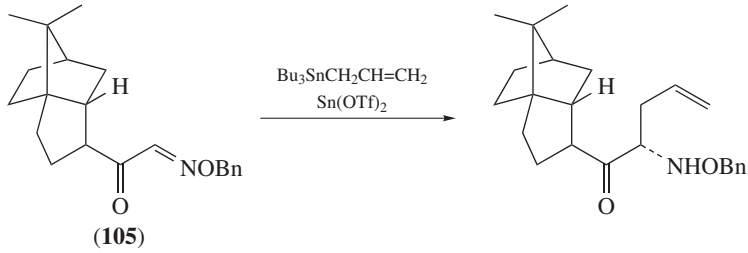

(**105**) (74)

B. Free Radical Additions to Oximes, Oxime Ethers and Nitrones

Free radical addition to oximes and oxime ethers emerged as a useful alternative to addition of organometallic reagents, particularly for intramolecular reactions. The most important advantage of free radical *vs*. organometallic addition is its tolerance for almost any functional group (with the exception of thiocarbonyl and iodoalkyl functions).

Free radicals generated by zinc and alkyl iodides[237] easily add to oxime ethers (e.g. **106**, equation 75), providing good yield of corresponding hydroxylamines **107**. This reaction has also been performed in solid-phase bound oxime ethers[238].

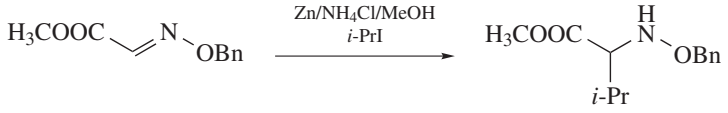

(**106**) (**107**) (75)

Similar results were achieved in a free-radical chain addition reaction with free radicals generated from an Et_3B–air[239,240] or Et_3B–air/alkyl iodide system (equation 76)[241].

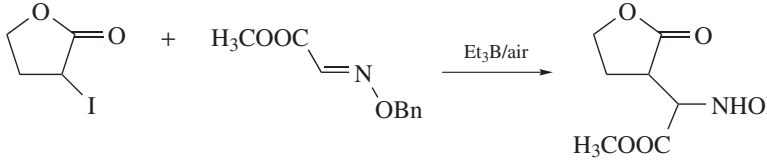

(76)

Free-radical cyclizations using ethyl radicals generated by Et_3B/air system[242] or stannyl radicals[243–248] systems provide a range of carbocyclic and heterocyclic hydroxylamines (equation 77). Stereoselectivity in these reactions is variable but can be semiqualitatively predicted by Beckwith–Houk models[249]. Depending on the substitution pattern of the emerging cyclic system, stereoselectivity can be very high, especially in fused polycyclic systems (equation 78)[250].

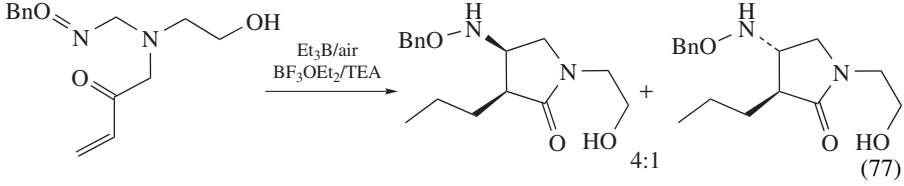

(77)

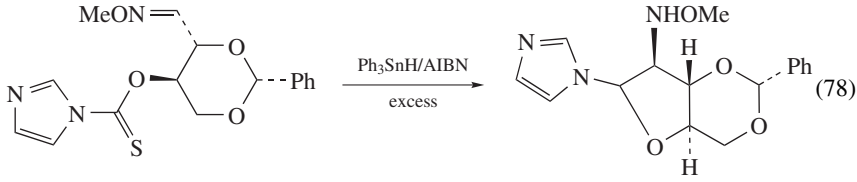

(78)

A high degree of stereoselectivity was achieved in reductive radical cyclizations with SmI_2[251, 252]. Coordination of the oxime function (e.g. **108**) with samarium cation seems to play an important role, since the identical reaction with a tributyltin hydride/radical initiator system produces poor stereoselectivity (equation 79)[248].

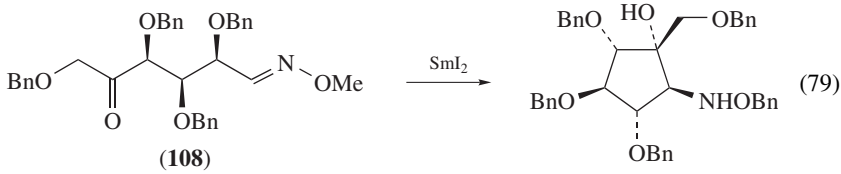

(**108**) (79)

VI. HYDROXYLAMINES THROUGH ADDITION TO THE N=O DOUBLE BOND OF NITROSO AND NITRO COMPOUNDS

A. Addition of Organometallic Reagents to Nitro and Nitroso Compounds

Tertiary and aromatic nitroso compounds react with aryl Grignard[253, 254] or aryllithium[255] reagents giving the corresponding hydroxylamines[256]. This reaction is useful for preparation of alkyl- and arylhydroxylamines (e.g. **109**, equation 80 and **110**, equation 81) and can be considered as complementary to arylation of hydroxylamines with activated aryl halides. It has been used for functionalization of cyclophanes with the hydroxyamino group[257]. The main limitation of the reaction is the relatively restricted choice of available aliphatic nitroso components, so most of reactions were done with 2-nitroso-2-methylpropane. There is no literature data about the possibility of removal of the *tert*-butyl group from these compounds.

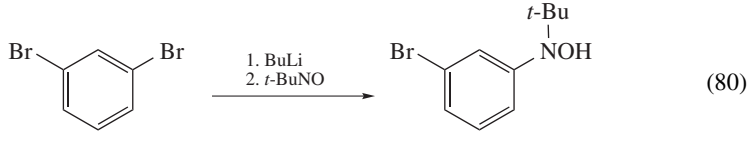

(80)

(**109**)

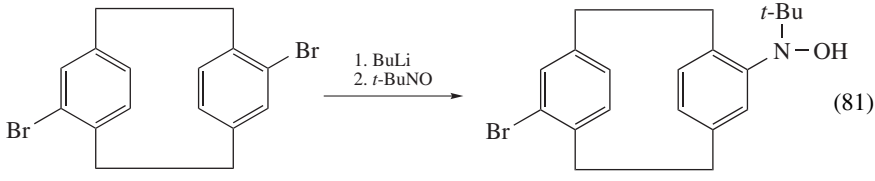

(81)

(**110**)

Enolates obtained from aliphatic catboxylic acids such as **111** undergo similar transformation, giving α-*N*-*tert*-butyl(hydroxy)amino acids of type **112** (equation 82)[258].

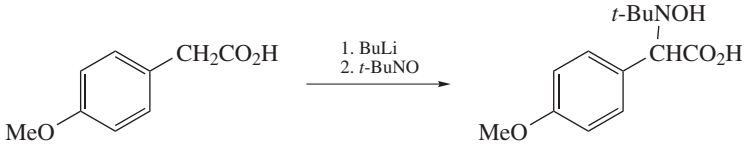

(**111**) (**112**) (82)

Addition of organometallic reagents to nitro compounds is possible but is sparingly used. Reaction of aromatic nitro compounds with large excess of phenyl magnesium bromide produces hydroxylamines in moderate yield[259]. Similar addition of Grignard compounds to nitromethane proceeds in low yield[260] while addition of excess methyllithium to tertiary nitro compound **113** results in formation of hydroxylamine **114** (equation 83)[261].

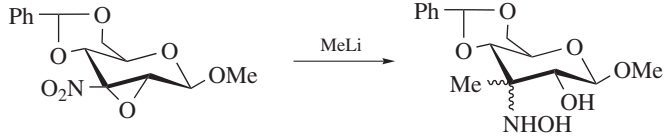

(**113**) (**114**) (83)

Chiral non-racemic *O*-(2-ketoalkyl) *N*-phenylhydroxylamines such as **115** (equation 84) can be prepared through catalytic enantioselective α-aminoxylation of carbonyl compounds catalyzed by proline. This reaction proceeds with a variety of ketones and aldehydes although it has been tried only with a nitrosobenzene component[262, 263].

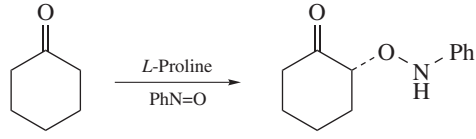

(**115**) (84)

B. Ene Reactions of Nitroso Compounds

Nitroso compounds (e.g. **116**, equation 85) that are unable to tautomerize to oximes undergo an ene reaction with alkenes **117** giving *N*-allylhydroxylamines **118** (equation 85). Both trifluoromethyl and aryl nitroso compounds react with alkenes[264, 265], although in many cases the resulting *N*-allylhydroxylamines are prone to subsequent chemical transformations. If allylzinc compounds are used as the alkene components, the chemoselectivity of the reaction is reversed and *O*-allylation products are preferably formed[266].

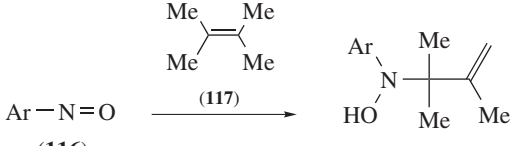

(**116**) (**118**) (85)

Reactions of alkenes such as **120** with α-chloronitrosoalkanes of type **119** proceed under very mild conditions and result in the formation of nitrones **121** that can be easily hydrolyzed into hydroxylamines **122** (equation 86)[267]. Chiral carbohydrate-derived α-chloronitrosoalkenes **123** possess enhanced reactivity and produce good stereoselectivity in reaction with prochiral alkenes such as **124** (equation 87)[268].

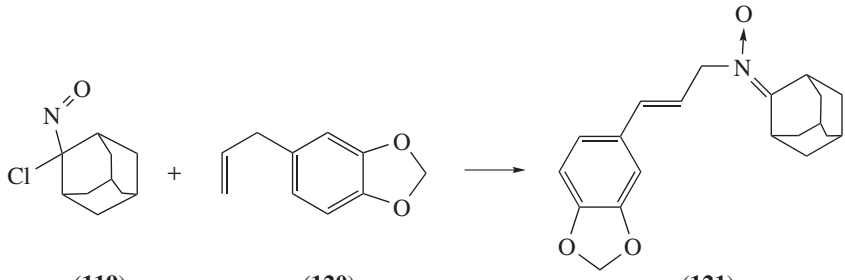

(**119**) (**120**) (**121**)

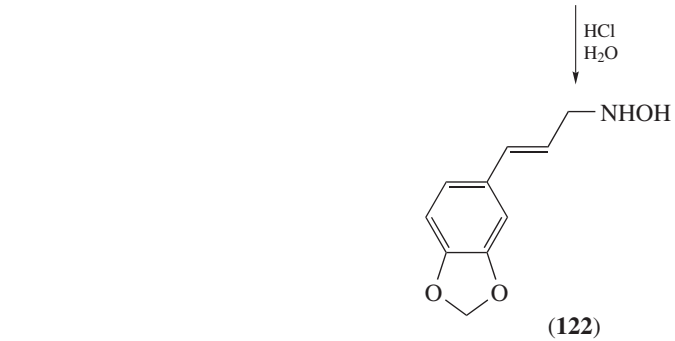

(**122**)

(86)

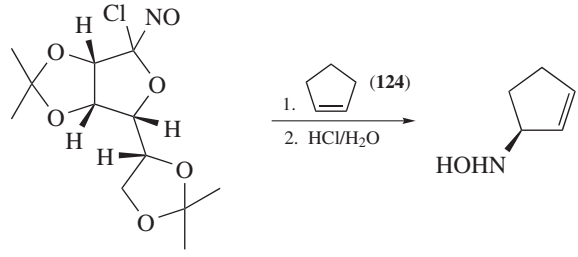

(**123**)

(87)

VII. HYDROXYLAMINES THROUGH OXIDATION OF AMINES

Preparation of hydroxylamines through oxidation of an amino group is an attractive approach since a variety of primary and secondary amines are commercially available, including compounds with high enantiomeric purity. A number of reagents have been suggested for the oxidation. However, yields are variable and sometimes are difficult to predict, since primary hydroxylamines can undergo further oxidation into nitroso and nitro compounds. The overoxidation is less a problem for *N*,*N*-disubstituted hydroxylamines

which can be usually obtained in a good yield, although formation of nitroxyl radicals with excess of oxidizing reagent is still possible.

Direct oxidation of primary amines with peroxide oxidants does not provide appreciable yield of hydroxylamines. As was mentioned above, oxidation of secondary amines usually proceeds smoothly giving moderate to good yields of *N*,*N*-disubstituted hydroxylamines. Oxidation of sterically hindered secondary amines such as **125** (equation 88) can also be done with peracids[269]. Further oxidation of the resulting *N*,*N*-disubstituted hydroxylamines **126** with an excess of *m*-chloroperbenzoic acid is known to end up with the corresponding nitroxyl radicals of type **127** (equation 88)[270] although the reaction can be stopped at the hydroxylamine stage.

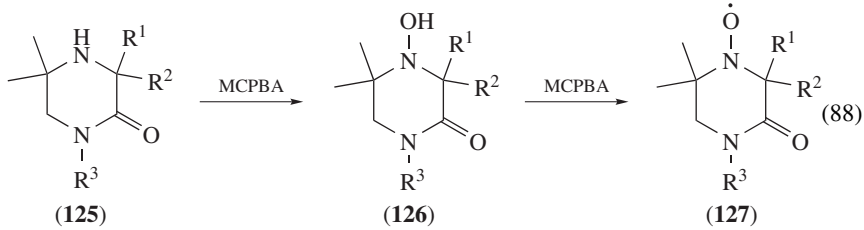

(88)

(**125**) (**126**) (**127**)

To avoid overoxidation, primary amines (e.g. **128**, equation 89) can be converted into Schiff bases with an aromatic aldehyde. Subsequent oxidation of the resultant imines **129** with an excess of peracids produces oxaziridines **130** and/or nitrones **131**. Both of them produce hydroxylamines **132** (equation 89) upon hydrolysis in moderate to good overall yields. Yields of hydroxylamines are considerably better if anisaldehyde instead of benzaldehyde is used for the protection[271–273].

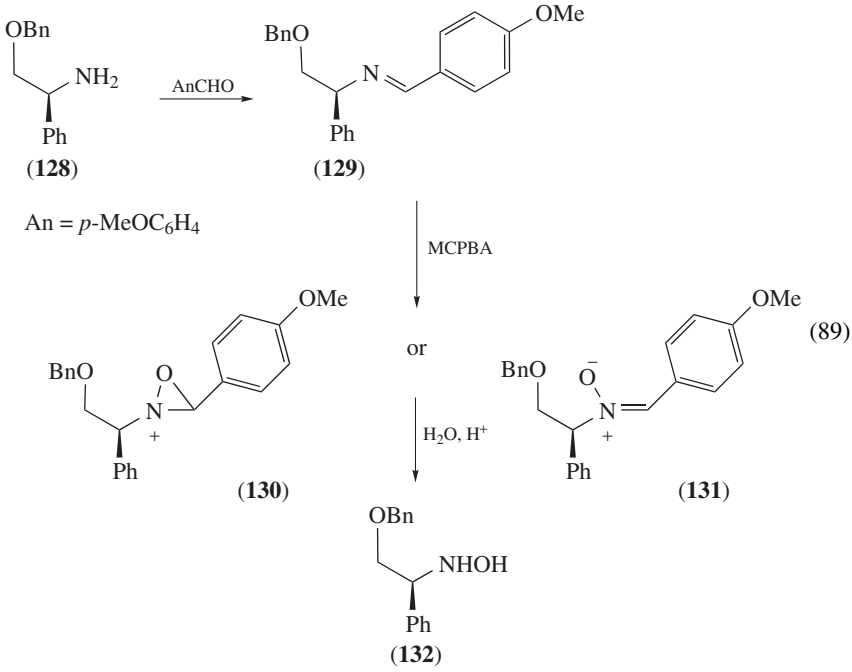

(89)

(**128**) (**129**) (**130**) (**131**) (**132**)

Another approach toward protection against overoxidation of primary amines is based on a three-step sequence involving selective mono-cyanomethylation of a primary amine such as **133** (equation 90) to cyanomethyl secondary amine **134**, regioselective nitrone **135** formation using MCPBA and hydroxylaminolysis[274, 275] of the resultant nitrones releasing hydroxylamine **136** (equation 90).

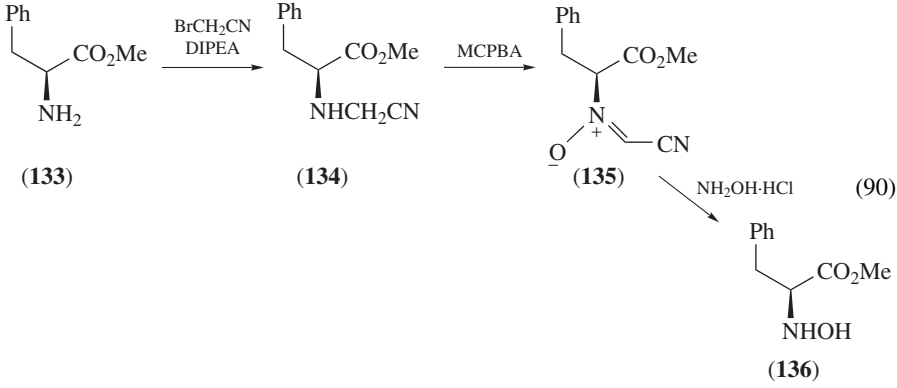

(**133**) (**134**) (**135**) (**136**) (90)

In an analogous way, secondary amines can be protected through attachment of β-cyanoethyl or a similar function. The cyanoethyl group undergoes facile Cope elimination from initially formed *N*-oxide (e.g. **137**, equation 91) thus giving the corresponding hydroxylamine **138** in a good yield[276, 277].

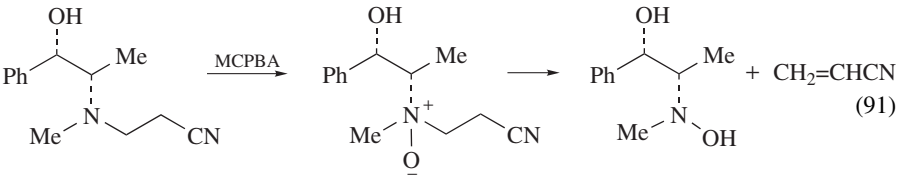

(**137**) (**138**) (91)

An alternative strategy preventing further oxidation of hydroxylamines is based on concomitant *O*-protection of the hydroxyamino group. Reaction of primary amines with benzoyl peroxide affords *O*-benzoyl hydroxylamines of type **139** (equation 92) that can be deprotected under mildly basic conditions. The oxidation is compatible with a number of functionalities and does not interfere with other functionalities such as an isolated double bond in the molecule of amine[278]. This reaction is versatile and a number of hydroxylamines has been prepared in this way, although yields are only moderate in most cases[279–281]. Oxidation of secondary amines with benzoyl peroxide[282] is also possible and usually proceeds in better yields.

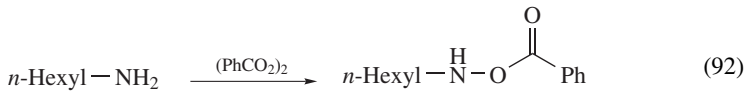

(**139**) (92)

Oxidation with diphenylphosphinyl peroxide occurs similarly and has been tried on both primary[283] and secondary[284] amines (equation 93).

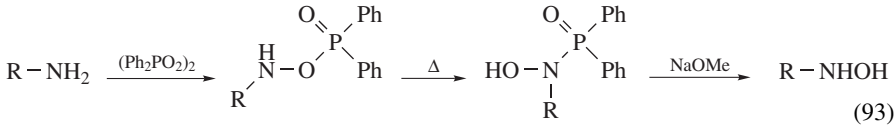

(93)

Silicon-supported OXONE reagent oxidizes *n*-hexylamine into the corresponding hydroxylamine in good yield[285].

2,2-Dimethyldioxirane was reported to provide superior yields of hydroxylamines in comparison to other peroxide oxidizing agents. This reaction worked well on polyfunctional amines such as *O*-protected aminosaccarides **140** (equation 94), yet it was found to be substrate-sensitive and failed to provide hydroxylamines in several cases[286].

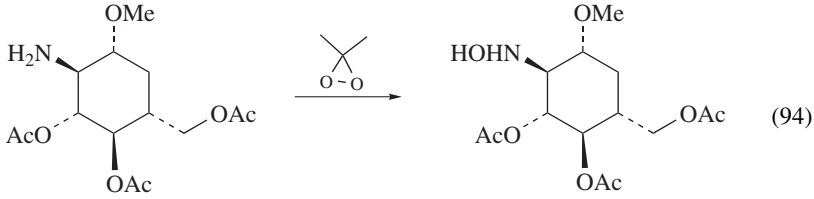

(**140**) (94)

Lithium salts of *N-tert*-alkylamines **141** (equation 95) undergo direct oxidation with *tert*-butyl peroxybenzoate **142** through a free-radical mechanism and afford *O-tert*-butylhydroxylamines **143** (equation 95)[287], although in low yields.

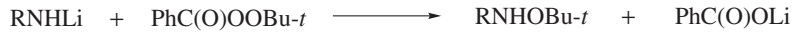

(**141**) (**142**) (**143**) (95)

Oxidation of secondary amines with oxaziridine **144** provides moderate yields of hydroxylamines **145**, although overoxidation invariably results in formation of nitrones **146** (equation 96)[288].

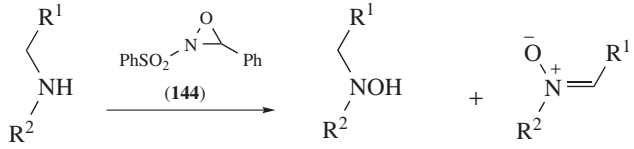

(**145**) (**146**) (96)

VIII. HYDROXYLAMINES THROUGH CYCLOADDITION REACTIONS

Both [4 + 2] and [3 + 2] cycloadditions are a direct and versatile method for preparation of cyclic hydroxylamines. These reactions have been extensively studied, used and reviewed[289, 290] so reactivity and chemoselectivity in these reactions can be reliably

predicted. Recent publications also demonstrate considerable progress in steric control of these cycloaddition reactions.

Hydroxylamines of type **149** (equation 97) can be prepared directly through cycloaddition of nitroso compounds of type **147** to dienes of type **148**. Hydroxylamines of type **153** can be easily obtained through cycloaddition of nitrone **151** to alkene **152** (equation 98).

Furthermore, cyclic hydroxylamines **149** and **153** possessing heteroatomic substituents R^1 can be further converted to acyclic hydroxylamines **150** (equation 97) and **154** (equation 98) through selective cleavage of the NO−C bond.

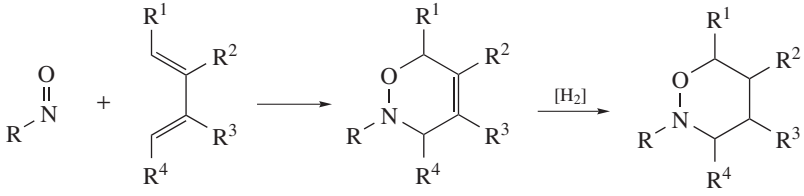

(**147**) (**148**) (**149**)

R = Alk, Ar, COAlk, COAr, CO_2Alk R^1 = H, Alk, Hal, OAlk
R^2, R^3, R^4 = H, Alk, Ar,

R^1= Hal, OAlk (97)

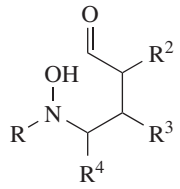

(**150**)

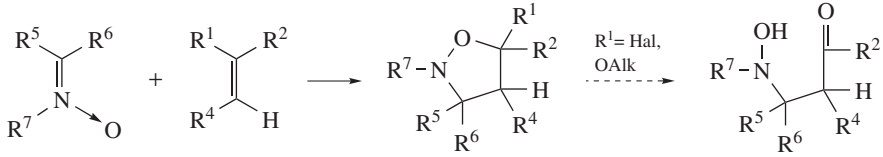

(**151**) (**152**) (**153**) (**154**)

R = Alk, Ar, COAlk, COAr, CO_2Alk R^1 = H, Alk, Hal, OAlk
R^2, R^4, R^5, R^6, R^7 = H, Alk, Ar, (98)

A. Hydroxylamines through [4 + 2] Cycloaddition of Nitroso Compounds to Dienes

Aliphatic and aromatic nitroso compounds are powerful dienophiles and react with a variety of acyclic, cyclic and heterocyclic 1,3-dienes producing cyclic hydroxylamines. The reaction proceeds with a high regioselectivity at room temperature (equation 99)[291–293]. Asymmetric variation of the reaction with chiral copper–BINAP catalyst has been reported[294]. The cycloaddition is reversible and some amounts of diene and nitroso components may be observed in reaction products.

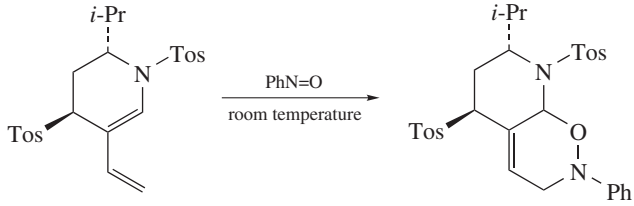

(99)

Due to the restricted availability of nitroso components, it more convenient to prepare acylnitroso compounds *in situ* from *N*-acyl or *N*-carbamoyl hydroxylamines with $NaIO_4$ (equation 100)[295]. Subsequent deprotection results in an *N*-unsubstituted dihydro-1,2-oxazine cycle. The reaction is also commonly employed for intramolecular cycloadditions[296,297].

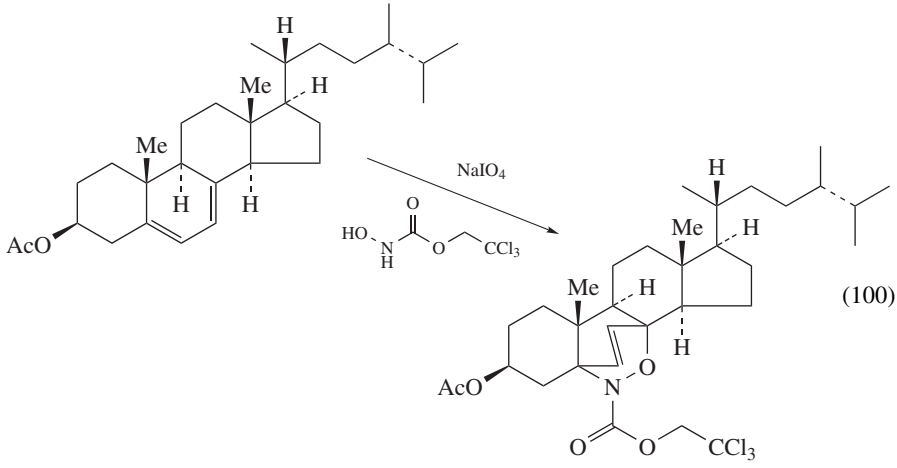

(100)

Another approach toward *N*-unsubstituted dihydro-1,2-oxazines involves cycloaddition of easily available α-chloro nitrosoalkanes **155** to 1,3-dienes (e.g. **156**, equation 101). Subsequent alcoholysis results in the removal of the alkyl function and provides *N*-unsubstituted cyclic hydroxylamines of type **157** (equation 101)[298–300].

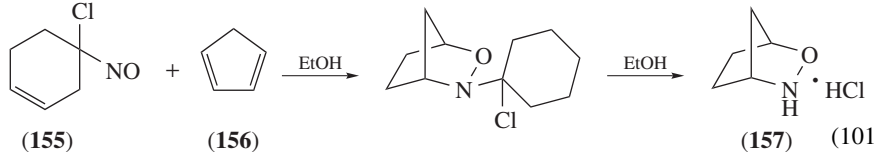

(**155**) (**156**) (**157**) (101)

Cycloaddition of enantiomerically pure α-chloro nitroso compounds derived from steroids[301] and carbohydrates[301,302] (e.g. **158**, equation 102) proceeds with considerable stereoselectivity. Final removal of the chiral auxiliary results in *N*-unsubstituted cyclic hydroxylamines of high *ee*.

Reactions with 1-halogeno[303,304], 1-oxy[305], 1-silyl[306] and 1-amino[307,308] susbstituted 1,3-dienes proceed similarly and provide complete regioselectivity (equation 103). Due

to the presence of the hetero substituent, the resultant cyclic hydroxylamines (e.g. **159**) can be easily converted to acylic *N*-mono- and *N*-disubstituted hydroxylamines[309].

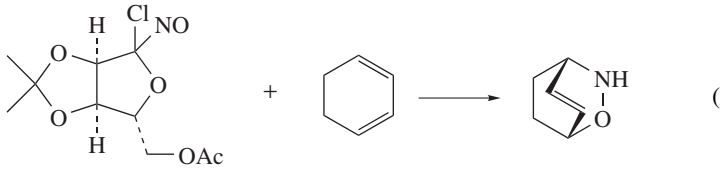

(**158**) (102)

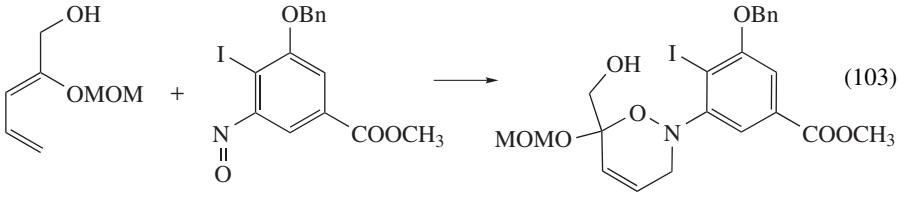

(**159**) (103)

Finally, nitrosoarenes **160** (equation 104) prepared *in situ* by reacting nitroarenes with CO over a palladium catalyst add to dienes **161**, forming cyclic hydroxylamines **162** in good yields[310].

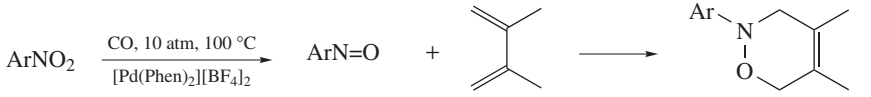

(**160**) (**161**) (**162**) (104)

B. Hydroxylamines through [3 + 2] Cycloaddition Reactions of Nitrones and Oximes to Alkenes

[3 + 2] Dipolar cycloaddition of nitrones to alkenes produces isooxazolidines. This reaction has been widely studied and exploited in a number of total syntheses.

The reaction is versatile and proceeds with a variety of cyclic and acylic alkenes substituted with alkyl, aryl, vinyl and heteroatom substituents. Allene derivatives also undergo cycloaddition with nitrones[311]. A variety of cyclic and acyclic aliphatic nitrones bearing aliphatic and aromatic substituents has been tested. The reaction is, however, relatively sensitive to steric constraints and proceeds easily only for mono- and disubstituted alkenes. Steric requirements for a nitrone molecule are similar and, although several reactions with R^1, $R^2 \neq H$ are known[312], good yield has been achieved only with $R^1 = H$ (equation 105).

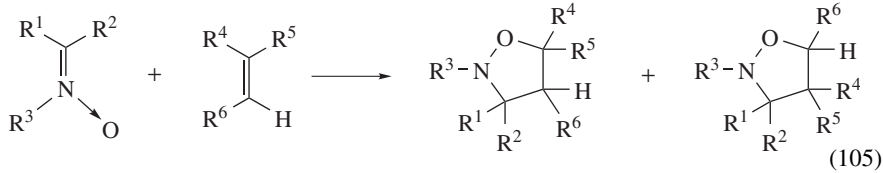

(**163**) (**164**) (105)

While monosubstituted alkenes usually react with high regioselectivity, it is not true for disubstituted alkenes. Formation of mixtures of type **163** and **164** (equation 105) has been observed in most cases when unsymmetrical alkenes bearing two different substituents possess similar stereoelectronic properties. In general, regioselectivity is controlled by a combination of HOMO–LUMO interactions, steric effects and hydrogen bonding between suitable substituents in both alkene and nitrone molecules[313, 314].

It has been shown that the cycloaddition of highly unreactive sterically hindered nitrones of type **165** can be catalyzed by magnesium salts that provide temporary tethering of allyl alcohol in the nitrone moiety (equation 106)[315]. This results in complete regio- and stereoselectivty of the cycloaddition.

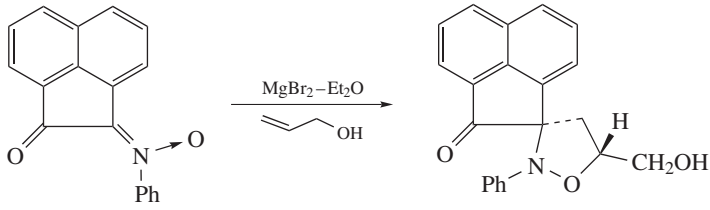

(106)

(**165**)

Cycloaddition of nitrones (e.g. **166**, equation 107) to alkoxyalkenes proceeds in high yield with complete diastereoselectivity, giving 1,2-isoxazolidines of type **167**. Similar reactions have been reported for vinyl ethers[316], vinyl acetate[317, 318], enamines[319], vinyl imidazoles[320], enamides[321], vinyl sulfones[322, 323] and vinyl sulfides[324, 325]. Since the resultant 1,2-oxazolidines of type **167** and its analogs can be hydrolyzed under acidic conditions, this reaction may also be considered as an approach to *O*-unsubstituted *N*-alkylhydroxylamines[326].

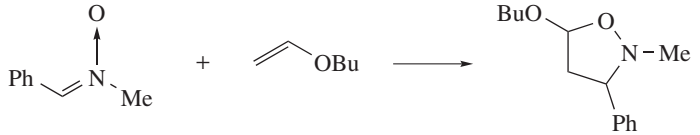

(107)

(**166**) (**167**)

Depending on the size of the forming cycle, alkenylnitrones (e.g. **168**, equation 108) undergo intramolecular cycloaddition with high regio- and stereoselectivity[327, 328].

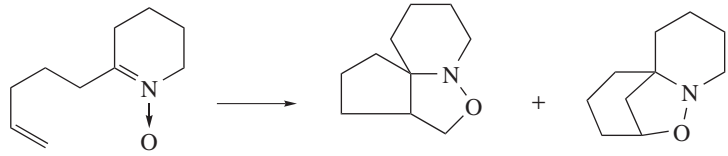

(108)

(**168**) 64% 1%

Most commonly, alkenylnitrones are produced *in situ* from alkenylketones (e.g. **169**, equation 109)[329, 330], alkynes (e.g. **170**, equation 110)[331] or oximes[332].

Oximes undergo similar cycloaddition with alkenes. This reaction provides more flexibility because oximes are easily available and are stable compounds. The reaction is, however, slower than cycloaddition of nitrones and generally requires high temperatures

(equation 111), although it can be considerably accelerated by Lewis acid catalysis[333]. Cycloaddition of oximes is most frequently used for intramolecular cylcoadditions[334,335], although intermolecular examples are also known[336,337].

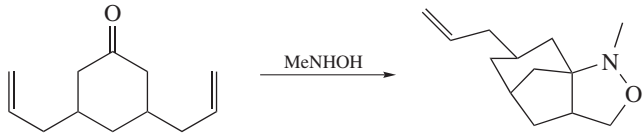

(109)

(**169**)

(110)

(**170**)

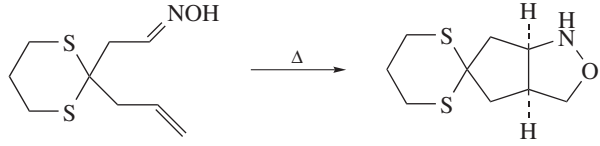

(111)

Intramolecular oxime–alkene cycloaddition has been proved to proceed with complete stereoselectivity in carbohydrate derived hydroxylamine[338] **171** (equation 112).

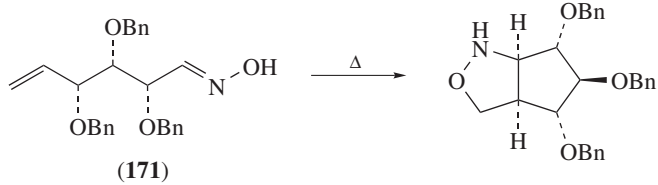

(112)

(**171**)

Lewis acid catalyzed reaction of oximes **172** (equation 113) with divinyl ketone (**173**) provided 1-aza-7-oxabicyclo[3.2.1]octan-4-ones **174** through a sequential Michael addition and [3 + 2] cycloaddition. The reaction occurred with complete stereoselectivity giving the same product with both *cis*- and *trans*-oximes[339].

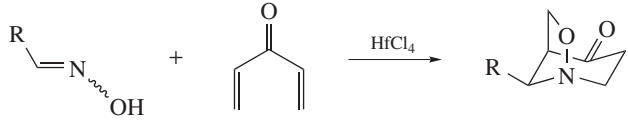

(113)

(**172**) (**173**) (**174**)

Reaction of lithium alkoxyallenes (e.g. **176**, equation 114) with nitrones such as **175** proceeded through two sequential additions and provided good yield of six-membered

cyclic hydroxylamine **177**, thus giving a formal [3 + 3] addition. Nitrones possessing a carbohydrate derived chiral auxiliary have been shown to react with good stereoselectivity[340].

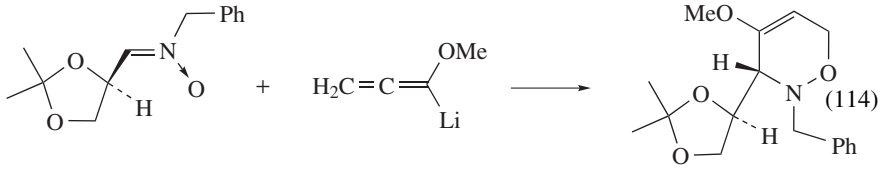

(**175**) (**176**) (**177**)

IX. REFERENCES

1. E. Nuti, T. Tuccinardi and A. Rossello, *Curr. Pharm. Design*, **13**, 2087 (2007).
2. J. V. Peter, J. L. Moran and P. L. Graham, *Expert Opin. Pharmacother.*, **8**, 1451 (2007).
3. K. Kuca, D. Jun and K. Musilek, *Mini Rev. Med. Chem.*, **6**, 269 (2006).
4. J. C. Barton, *Curr. Gastroenterol. Rep.*, **9**, 74 (2007).
5. E. D. Weinberg, *Pharm. Pharmacol.*, **58**, 575 (2006).
6. J. B. Hynes and L. G. Hack, *J. Med. Chem.*, **15**, 1194 (1972).
7. M. Fouladi, *Cancer Invest.*, **24**, 521 (2006).
8. D. R. Richardson, *Crit. Rev. Oncol. Hematol.*, **42**, 267 (2002).
9. D. Klamann (Ed.), *Houben-Weyl, Methoden der Organischen Chemie*, Ed 4, Vol. 16a, Georg Thieme Verlag, Stuttgart, 1990, pp, 1–394.
10. A. Corsaro, U. Chiacchio and V. Pistarà, *Synthesis*, 1903 (2001).
11. N. Amlaiky and G. Leclerc, *Synthesis*, 426 (1982).
12. Y. S. Cheng, A. T. Lupo and F. W. Fowler, *J. Am. Chem. Soc.*, **105**, 7696 (1983).
13. V. K. Khlestkin, D. G. Mazhukin, A. Ya. Tikhonov, T. V. Rybalova, I. Yu. Bagryanskaya and Y. V. Gatilov, *Synthesis*, 681 (2000).
14. B. P. Martin, M. E. Cooper, D. K. Donald and S. D. Guile, *Tetrahedron Lett.*, **47**, 7635 (2006).
15. Y. Jin and D. H. Kim, *Synlett*, 1189 (1998).
16. G. W. Kirby and M. Nazeer, *Tetrahedron Lett.*, **29**, 6173 (1988).
17. G. I. Nikishin, E. I. Troyansky, I. V. Svitanko and O. S. Chizhov, *Tetrahedron Lett.*, **25**, 97 (1984).
18. D. Noeteberg, J. Branalt, I. Kvarnström, M. Linschoten, D. Musil, J-E. Nyström, G. Zuccarello and B. J. Samuelsson, *J. Med. Chem.*, **43**, 1705 (2000).
19. A. R. Katrizky, N. Kirichenko and B. V. Rogovoy, *Synthesis*, 2777 (2003).
20. R. Plate, M. A. J. Akkerman, H. C. J. Ottenheijm and J. M. M. Smits, *J. Chem. Soc., Perkin Trans. 1*, 2481 (1987).
21. T. I. Orlova, S. P. Epshtein, A. F. Rukasov, N. S. Magomedova, V. K. Bel'skii, V. P. Tashchi and Y. G. Putsykin, *Khim. Geterotsikl. Soedin.*, 1280 (1987); *Chem. Abstr.*, **108**, 167366 (1988).
22. G. C. Lancini, E. Lazzari and A. Diena, *Farmaco*, **24**, 169 (1969).
23. Z. I. Zhilina, A. V. Bogatskii, S. A. Andronati and N. I. Danilina, *Khim. Geterotsikl. Soedin.*, 545 (1979); *Chem. Abstr.* **91**, 157698 (1979).
24. K. Majima, R. Takita, A. Okada, T. Ohshima and M. Shibasaki, *J. Am. Chem. Soc.*, **125**, 15837 (2003).
25. S. M. Rida, A. S. Issa and Y. A. Beltagy, *Pharmazie*, **33**, 711 (1978).
26. A. Alanine, A. Bourson, B. Büttelmann, R. Gill, M-P. Heitz, V. Mutel, E. Pinard, G. Trube and R. Wyler, *Bioorg. Med. Chem. Lett.*, **13**, 3155 (2003).
27. N. Nishino, D. Yoshikawa, L. A. Watanabe, T. Kato, B. Jose, Y. Komatsu, Y. Sumida and M. Yoshida, *Bioorg. Med. Chem. Lett.*, **14**, 2427 (2004).
28. X. Hu, J. Zhu, S. Srivathsan and D. Pei, *Bioorg. Med. Chem. Lett.*, **14**, 77 (2004).
29. N. Koshti, V. R. Gantla, H. K. Jacobs and A. S. Gopalan, *Synth. Commun.*, **32**, 3779 (2002).
30. T. Y. H. Wu, C. Hassig, Y. Wu, S. Ding and P. G. Schultz, *Bioorg. Med. Chem. Lett.*, **14**, 449 (2004).

31. Y.-H. Woo, R. P. M. Fernandes and P. J. Proteau, *Bioorg. Med. Chem.*, **14**, 2375 (2006).
32. J. C. A. Hunt, P. Laurent and C. J. Moody, *Chem. Commun.*, 1771 (2000).
33. M. Strasser, P. Cooper, B. Dewald and T. Payne, *Helv. Chim. Acta*, **71**, 1156 (1988).
34. A. O. Miller and G. G. Furin, *J. Fluorine Chem.*, **36**, 247 (1987).
35. R. W. Feenstra, E. H. M. Stokkingreef, R. J. F. Nivard and H. C. J. Ottenheijm, *Tetrahedron*, **44**, 5583 (1988).
36. G. V. Shustov, M. K. Chandler and S. Wolfe, *Can. J. Chem.*, **83**, 93 (2005).
37. H. Schedel, W. Dmowski and K. Burger, *Synthesis*, 1681 (2000).
38. S. Wolfe, M.-C. Wilson, M.-H. Cheng, G. V. Shustov, C. I. Akuche, *Can. J. Chem.*, **81**, 937 (2003).
39. R. Sulsky and J. P. Demers, *Tetrahedron Lett.*, **30**, 31, (1989).
40. A. Rossello, E. Nuti, P. Carelli, E. Orlandini, M. Macchia, S. Nencetti, M. Zandomeneghi, F. Balzano, B. G. Uccello, A. Albini, R. Benelli, G. Cercignani, G. Murphy and A. Balsamo, *Bioorg. Med. Chem. Lett.*, **15**, 1321 (2005).
41. R. L. Halcomb, M. D. Wittman, S. H. Olson, S. J. Danishefsky, J. Golik, H. Wong and D. Vyas, *J. Am. Chem. Soc.*, **113**, 5080 (1991).
42. S. H. Kim, D. Augeri, D. Yang and D. Kahne, *J. Am. Chem. Soc.*, **116**, 1766 (1994).
43. T. Tuccinardi, A. Martinelli, E. Nuti, P. Carelli, F. Balzano, G. Uccello-Barretta, G. Murphy and A. Rossello, *Bioorg. Med. Chem.*, **14**, 4260 (2006).
44. J. Seo and R. B. Silverman, *Tetrahedron Lett.*, **47**, 4069 (2006).
45. J. J.-W. Duan, Z. Lu, C.-B. Xue, X. He, J. L. Seng, J. J. Roderick, Z. R. Wasserman, R.-Q. Liu, M. B. Covington, R. L. Magolda, R. C. Newton, J. M. Trzaskos and C. P. Decicco, *Bioorg. Med. Chem. Lett.*, **13**, 2035 (2003).
46. B. Cebon, J. N. Lambert, D. Leung, H. Mackie, K. L. McCluskey, X. Nguyen and C. Tassone, *Aust. J. Chem.*, **53**, 333 (2000).
47. M. Canle, W. Clegg, I. Demirtas, M. R. J. Elsegood, J. Haider, H. Maskill and P. C. Miatt, *J. Chem. Soc., Perkin Trans. 2*, 1742 (2001).
48. A. O. Stewart and J. G. Martin, *J. Org. Chem.*, **54**, 1221 (1989).
49. S. S. Adams, B. J. Armitage, N. W. Bristow and B. V. Heathcote, US Patent 3855406 (1974); *Chem. Abstr.*, **72**, 121369 (1970).
50. H. Martin, R. Herrmann and I. Ugi, *J. Organomet. Chem.*, **269**, 87 (1984).
51. R. D. Larsen, P. Davis, E. G. Corley, P. J. Reider, T. R. Lamanec and E. J. J. Grabowski, *J. Org. Chem.*, **55**, 299 (1990).
52. S.-I. Murahashi, Y. Imada, Y. Taniguchi and Y. Kodera, *Tetrahedron Lett.*, **29**, 2973 (1988).
53. E. Öhler and S. Kanzler, *Synthesis*, 539 (1995).
54. A. E. Wroblewski and A. Halajewska-Wosik, *Tetrahedron: Asymmetry*, **15**, 3201 (2004).
55. S. Jordan, R. E. Markwell and B. S. Woolcott, *J. Chem. Soc., Perkin Trans. 1*, 928 (1978).
56. A. Heydari, M. Mehrdad, A. Maleki and N. Ahmadi, *Synthesis*, 1563 (2004).
57. I. A. O'Neil and J. M. Southern, *Tetrahedron Lett.*, **39**, 9089 (1998).
58. W. R. Roush and B. C. Follows, *Tetrahedron Lett.*, **35**, 4935 (1994).
59. C. Schneider, A. R. Sreekanth and E. Mai, *Angew. Chem., Int. Ed.*, **43**, 5691 (2004).
60. M. Inglesi, M. Nicola and S. Magnetti, *Farmaco*, **45**, 1327 (1990).
61. J. H. Van Maarseveen, P. H. H. Hermkens, E. De Clercq, J. Balzarini, H. W. Scheeren and C. Kruse, *J. Med. Chem.*, **35**, 3223 (1992).
62. P. H. H. Hermkens, J. H. Van Maarseveen, H. C. J. Ottenheijm, C. G. Kruse and H. W. Scheeren, *J. Org. Chem.*, **55**, 3998 (1990).
63. S. Cao, F. D. Tropper and R. Roy, *Tetrahedron*, **51**, 6679 (1995).
64. L. A. Marcaurelle, Y. Shin, S. Goon and C. R. Bertozzi, *Org. Lett.*, **3**, 3691 (2001).
65. H. Iwagami, M. Nakazawa, M. Yatagai, T. Hijiya, Y. Honda, H. Naora, T. Ohnuki and T. Yukawa, *Bull. Chem. Soc. Jpn.*, **63**, 3073 (1990).
66. T. Ishikawa, K. Kamiyama, N. Matsunaga, H. Tawada, Y. Iizawa, K. Okonogi and A. Miyake, *J. Antibiot.*, **53**, 1071 (2000).
67. S. Itsuno, K. Tanaka and K. Ito, *Chem. Lett.*, 1133 (1986).
68. R. J. Brown, G. Annis, A. Casalnuovo, D. Chan, R. Shapiro and W. J. Marshall, *Tetrahedron*, **60**, 4361 (2004).
69. D. Bhuniya, S. Gujjary and S. Sengupta, *Synth. Commun.*, **36**, 151 (2006).
70. H. Miyabe, K. Yoshida, M. Yamauchi and Y. Takemoto, *J. Org. Chem.*, **70**, 2148 (2005).
71. A. C. Cope and P. H. Towle, *J. Am. Chem. Soc.*, **71**, 3423 (1949).

72. S. D'Andrea, Z. B. Zheng, K. DenBleyker, J. C. Fung-Tomc, H. Yang, J. Clark, D. Taylor and J. Bronson, *Bioorg. Med. Chem. Lett.*, **15**, 2834 (2005).
73. I. R. Bryant and L. K. Dyall, *Aust. J. Chem.*, **42**, 2275 (1989).
74. A. O. Millerand and G. G. Furin, *J. Fluorine Chem.*, **36**, 247 (1987).
75. C. B. Ziegler, P. Bitha and Y. I. Lin, *J. Heterocycl. Chem.*, **25**, 719 (1988).
76. K. S. Kim, *Heterocycles*, **31**, 87 (1990).
77. R. L. Atkins, A. T. Nielsen, C. Bergens and W. S. Wilson, *J. Org. Chem.*, **49**, 503 (1984).
78. D. C. Boyles, T. T. Curran, D. Greene, D. Macikenas and R. V. Parlett, *Tetrahedron Lett.*, **43**, 6735 (2002).
79. K. G. Dongol and B. Y. Tay, *Tetrahedron Lett.*, **47**, 927 (2006).
80. C. C. Mauger and G. A. Mignani, *Aldrichimica Acta*, **39**, 17 (2006).
81. T. Sheradsky and E. Nov, *J. Chem. Soc., Perkin Trans. 1*, 2781 (1980).
82. Y. Kikugawa and M. Kawase, *Chem. Lett.*, 581 (1990).
83. J. K. Pratt, P. Donner, K. F. McDaniel, C. J. Maring, W. M. Kati, H. Mo, T. Middleton, Y. Liu, T. Ng, Q. Xie, R. Zhang, D. Montgomery, A. Molla, D. J. Kempf and W. Kohlbrenner, *Bioorg. Med. Chem. Lett.*, **15**, 1577 (2005).
84. G. M. Shutske and F. P. Huger, *J. Heterocycl. Chem.*, **25**, 703 (1988).
85. A. Tomazic, M. Tišler and B. Stanovnik, *Tetrahedron*, **37**, 1787 (1981).
86. D. T. Hurst, *Heterocycles*, **22**, 79 (1984).
87. A. Tomazic, M. Tišler and B. Stanovnik, *Heterocycles*, **12**, 1157 (1979).
88. I. M. El-Deen and F. F. Mahmoud, *Phosph. & Sulfur*, **165**, 205 (2000).
89. R. Volpini, D. Dal Ben, C. Lambertucci, S. Taffi, S. Vittori, K.-N. Klotz and G. Cristalli, *J. Med. Chem.*, **50**, 1222 (2007).
90. M. R. Harnden and R. L. Jarvest, *J. Chem. Soc., Perkin Trans. 1*, 2207 (1989).
91. I. Ekeltchik, J. Gun, O. Lev, R. Shelkov and A. Melman, *Chem. Commun.*, 5319 (2005).
92. A. Nohara, T. Ishiguro, K. Ukawa, H. Sugihara, Y. Maki and Y. Sanno, *J. Med. Chem.*, **28**, 559 (1985).
93. L. M. Werbel and M. J. Degnan, *J. Med. Chem.*, **30**, 2151 (1987).
94. H. Reimlinger, F. Billiau, W. R. F. Lingier and M. A. Peiren, *Chem. Ber.*, **108**, 3799 (1975).
95. D. Kaminsky, J. Shavel and R. I. Meltzer, *Tetrahedron Lett.*, 859 (1967).
96. R. G. Baughman, K. R. Fountain, D. P. Fountain and A. M. Tappmeyer, *J. Org. Chem.*, **54**, 5819 (1989).
97. C. Leguault and A. B. Charette, *J. Org. Chem.*, **68**, 7119 (2003).
98. J. I. G. Cadogan and A. G. Rowley, *Synth. Commun.*, 365 (1977).
99. C. L. Bumgardner and R. L. Lilly, *Chem. Ind.*, 559 (1962).
100. H. Kagechika, T. Himi, K. Namikawa, E. Kawachi, Y. Hashimoto and K. Shudo, *J. Med. Chem.*, **32**, 1098 (1989).
101. F. Berree, Y. Malvaut, E. Marchand and G. More, *J. Org. Chem.*, **58**, 6072 (1993).
102. M. C. Fournie-Zaluski, A. Coulaud, R. Bouboutou, P. Chaillet, J. Devin, G. Waksman, J. Costentin and B. P. Roques, *J. Med. Chem.*, **28**, 1158 (1985).
103. H. G. Aurich, T. M. Schmidt and T. Schwerzel, *Chem. Ber.*, **118**, 1086 (1985).
104. V. Y. Sosnovskikh, M. A. Barabanov and B. I. Usachev, *J. Org. Chem.*, **69**, 8297 (2004).
105. I. A. Cliffe, A. D. Ifill, H. L. Mansell, R. S. Todd and A. C. White, *Tetrahedron Lett.*, **32**, 6789 (1991).
106. G. Drefahl, K. Ponsold, B. Schoenecker and U. Rott, *Chem. Ber.*, **99**, 386 (1966).
107. A. S. Amarasekara, *Tetrahedron Lett.*, **46**, 2635 (2005).
108. S. Seko and N. Tani, *Tetrahedron Lett.*, **39**, 8117 (1998).
109. X. Hu, J. Zhu, S. Srivathsan and D. Pei, *Bioorg. Med. Chem. Lett.*, **14**, 77 (2004).
110. Y. Kashman and S. Cherkez, *Synthesis*, 885 (1974).
111. P. J. Atkins and C. D. Hall, *J. Chem. Soc., Perkin Trans. 2*, 155 (1983).
112. Y. Ishido, N. Sakairi, K. Okazaki and N. Nakazaki, *J. Chem. Soc., Perkin Trans. 1*, 563 (1980).
113. K. Y. Lee, C. G. Lee, T. H. Kim and J. N. Kim, *Bull. Korean Chem. Soc.*, **25**, 33 (2004).
114. G. Cardillo, L. Gentilucci, I. R. Bastardas and A. Tolomelli, *Tetrahedron*, **54**, 8217 (1998).
115. V. Krchnak and G. A. Slough, *Tetrahedron Lett.*, **45**, 4649 (2004).
116. D. Colantoni, S. Fioravanti, L. Pellacani and P. A. Tardella, *Org. Lett.*, **6**, 197 (2004).
117. L. M. Pratt, R. P. Beckett, S. J. Davies, S. B. Launchbury, A. Miller, Z. M. Spavold, R. S. Todd and M. Whittaker, *Bioorg. Med. Chem. Lett.*, **11**, 2585 (2001).

118. R. Amoroso, G. Cardillo, P. Sabatino, C. Tomasini and A. Trere, *J. Org. Chem.*, **58**, 5615 (1993).
119. I. Braschi, G. Cardillo and C. Tomasini, *Tetrahedron*, **50**, 2955 (1994).
120. M. P. Sibi, J. J. Shay, M. Liu and C. P. Jasperse, *J. Am. Chem. Soc.*, **120**, 6615 (1998).
121. S. Kikuchi, H. Sato and S. Fukuzawa, *Synlett*, 1023 (2006).
122. N. Yamagiwa, S. Matsunaga and M. Shibasaki, *Angew. Chem., Int. Ed.*, **43**, 4493 (2004).
123. N. Yamagiwa, S. Matsunaga and M. Shibasaki, *J. Am. Chem. Soc.*, **125**, 16178 (2003).
124. N. Yamagiwa, H. Qin, S. Matsunaga and M. Shibasaki, *J. Am. Chem. Soc.*, **127**, 13419 (2005).
125. D. S. C. Black and J. E. Doyle, *Aust. J. Chem.*, **31**, 2317 (1978).
126. H. O. House and J. F. Lee, *J. Org. Chem.*, **41**, 863 (1976).
127. W. Oppolzer, A. C. Spivey and C. G. Bochet, *J. Am. Chem. Soc.*, **116**, 3139 (1994).
128. D. R. Williams, M. H. Osterhout and J. M. McGill, *Tetrahedron Lett.*, **30**, 1327 (1989).
129. A. M. Osman, M. Z. A. Badr, A. M. Mahmoud and Z. A. Hezien, *J. Indian Chem. Soc.*, **59**, 763 (1982).
130. A. Albert and W. Pendergast, *J. Chem. Soc., Perkin Trans. 1*, 1625 (1973).
131. T. Nishiwaki and S. Onomura, *J. Chem. Soc. C*, 3026 (1971).
132. F. Dallacker, D. Bernabei, R. Katzke and P.-H. Benders, *Chem. Ber.*, **104**, 2526 (1971).
133. R. Grigg, Z. Rankovic and M. Thoroughgood, *Tetrahedron*, **56**, 8025 (2000).
134. S. Cicchi, M. Corsi, M. Marradi and A. Goti, *Tetrahedron Lett.*, **43**, 2741 (2002).
135. F. Peri, J. Jimenez-Barbero, V. Garcia-Aparicio, I. Tvaroska and F. Nicotra, *Chem. Eur. J.*, **10**, 1433 (2004).
136. A. Dondoni, P. P. Giovannini and D. Perrone, *J. Org. Chem.*, **67**, 7203 (2002).
137. A. Heydari, H. Larijani, J. Emami and B. Karami, *Tetrahedron Lett.*, **41**, 2471 (2000).
138. A. Heydari, M. Zarei, R. Alijanianzadeh and H. Tavakol, *Tetrahedron Lett.*, **42**, 3629 (2001).
139. A. Heydari, M. Mehrdad, M. Schaffie, M. S. Abdolrezaie and R. Hajinassirei, *Chem. Lett.*, 1146 (2002).
140. A. Heydari, M. Mehrdad and H. Tavakol, *Synthesis*, 1962 (2003).
141. A. Basso, L. Banfi, G. Guanti, R. Riva and A. Riu, *Tetrahedron Lett.*, **45**, 6109 (2004).
142. G. Zinner and O. Hantelmann, *Arch. Pharm.*, **308**, 321 (1975).
143. D. Moderhack, G. Zinner and W. Heuer, *Z. Chem.*, **15**, 55 (1975).
144. J. Thesing, H. Uhrig and A. Muller, *Angew. Chem.*, **67**, 31 (1955).
145. J. Gal, L. D. Gruenke and N. Castagnoli, *J. Med. Chem.*, **18**, 683 (1975).
146. K. A. Petrov, L. V. Treshchalina and V. M. Chizhov, *Zh. Obshch. Khim.*, **46**, 590 (1979); *Chem. Abstr.*, **91**, 5305 (1979).
147. T. Hino, A. Hasegawa, J. J. Liu and M. Nakagawa, *Chem. Pharm. Bull.*, **38**, 59 (1990).
148. T. B. Patrick, J. A. Schield and D. G. Kirchner, *J. Org. Chem.*, **39**, 1758 (1974).
149. R. J. Cummings, M. F. Grundon, A. C. Knipe and A. S. Wast, *J. Chem. Soc., Perkin Trans. 2*, 105 (1983).
150. S. D. Nelson, W. L. Nelson and W. F. Trager, *J. Med. Chem.*, **21**, 721 (1978).
151. H. W. Heine and B. J. Barchiesi, *J. Org. Chem.*, **49**, 2560 (1984).
152. S. E. Denmark and J. I. Montgomery, *J. Org. Chem.*, **71**, 6211 (2006).
153. P. H. H. Hermkens, J. H. Van Maarseveen, H. C. J. Ottenheijm, C. G. Kruse and H. W. Scheeren, *J. Org. Chem.*, **55**, 3998 (1990).
154. W. R. Dolbier, G. E. Wicks and C. R. Burkholder, *J. Org. Chem.*, **52**, 2196 (1987).
155. J. C. Anderson and H. A. Chapman, *Synthesis*, 3309 (2006).
156. P. H. H. Hermkens, J. H. Van Maarseveen, P. L. H. M. Cobben, H. C. J. Ottenheijm, C. G. Kruse and H. W. Scheeren, *Tetrahedron*, **46**, 833 (1990).
157. A. S. Kende and J. S. Mendoza, *Tetrahedron Lett.*, **32**, 1699 (1991).
158. E. Dumez, R. Faure and J.-P. Dulcere, *Eur. J. Org. Chem.*, 2577 (2001).
159. G. Durand, A. Polidori, J.-P. Salles and B. Pucci, *Bioorg. Med. Chem. Lett.*, **13**, 859 (2003).
160. B. M. Trost and M. K. Ameriks, *Org. Lett.*, **6**, 1745 (2004).
161. P. C. Southwick and J. R. Stemniski, *Synthesis*, 599 (1982).
162. D. J. Anderson and A. J. Taylor, *J. Heterocycl. Chem.*, **23**, 1091 (1986).
163. R. T. Coutts and J. L. Malicky, *Can. J. Chem.*, **51**, 1402 (1973).
164. T. B. Patrick, J. A. Schield and D. G. Kirchner, *J. Org. Chem.*, **39**, 1758 (1974).
165. M. Masui, H. Sayo and K. Kishi, *Chem. Pharm. Bull.*, **12**, 1397 (1964).
166. A. E. Feiring, *J. Org. Chem.*, **48**, 347 (1983).
167. G. Yamamoto, F. Nakajo, N. Endo and Y. Mazaki, *Bull. Chem. Soc. Jpn.*, **74**, 1467 (2001).

168. N. M. Yoon and Y. S. Gyoung, *J. Org. Chem.*, **50**, 2443 (1985).
169. S. Uchida, K. Yanada, H. Yamaguchi and H. Meguri, *Chem. Lett.*, 1069 (1986).
170. K. Yanada, H. Yamaguchi, H. Meguri and S. Uchida, *J. Chem. Soc., Chem. Commun.*, 1655 (1986).
171. E. Rozners, D. Katkevica, E. Bizdena and R. Stroemberg, *J. Am. Chem. Soc.*, **125**, 12125 (2003).
172. P.-D. Ren, X.-W. Pan, Q.-H. Jin and Z.-P. Yao, *Synth. Commun.*, **27**, 3497 (1997).
173. M. S. Mourad, R. S. Varma and G. W. Kabalka, *J. Org. Chem.*, **50**, 133 (1985).
174. R. S. Varma, Y. Z. Gai and G. W. Kabalka, *J. Heterocycl. Chem.*, **24**, 767 (1987).
175. I. D. Entwistle and T. Gilkerson, *Tetrahedron*, **34**, 213 (1979).
176. C. S. Rondestved and T. A. Johnson, *Synthesis*, 850 (1977).
177. R. J. Rahaim and R. E. Maleczka, *Synthesis*, 3316 (2006).
178. F. Peri, C. Airoldi, S. Colombo, S. Mari, J. Jimenez-Barbero, E. Martegani and F. Nicotra, *Eur. J. Org. Chem.*, 3707 (2006).
179. N. R. Ayyangar, K. C. Brahme, U. R. Kalkote and K. V. Srinivasan, *Synthesis*, 938 (1984).
180. K. Taya, *Chem. Commun.*, 464 (1966).
181. F. Li, J. Cui, X. Qian, R. Zhang and Y. Xiao, *Chem. Commun.*, 1901 (2005).
182. E. Borel and H. Deuel, *Helv. Chim. Acta*, **36**, 801 (1953).
183. M. D. Corbett and B. R. Corbett, *Experientia*, **38**, 1310 (1982).
184. S. Fukuzumi, M. Chiba and T. Tanaka, *J. Chem. Soc., Chem. Commun.*, 941 (1989).
185. R. F. Borch, M. D. Bernstein and H. D. Durst, *J. Am. Chem. Soc.*, **93**, 2897 (1971).
186. A. Ahmad, *Bull. Chem. Soc. Jpn.*, **47**, 1819 (1974).
187. B. T. Chao and S. Y. Seong, *Bull. Korean Chem. Soc.*, **9**, 322 (1988).
188. G. W. Gribble, R. W. Leiby and M. M. Sheehan, *Synthesis*, 856 (1977).
189. F. Hodosan and V. Ciurdaru, *Tetrahedron Lett.*, **12**, 1997 (1971).
190. A. H. Bekket, G. R. Jones and S. J. Al-Sarray, *Pharm. Pharmacol.*, **26**, 945 (1974).
191. N. M. Yoon and Y. S. Gyoung, *J. Org. Chem.*, **50**, 2443 (1985).
192. H. L. Lee, E. G. Raggiolini and M. R. Uskokovic, *Tetrahedron*, **43**, 4887 (1987).
193. H. K. Kim, H. K. Yaktin and R. E. Bambury, *J. Med. Chem.*, **13**, 238 (1970).
194. H. Feuer, B. F. Vincent and R. S. Bartlett, *J. Org. Chem.*, **30**, 2877 (1965).
195. M. Kawase and Y. Kikugawa, *J. Chem. Soc., Perkin Trans. 1*, 643 (1979).
196. M. Kawase and Y. Kikugawa, *Chem. Pharm. Bull.*, **29**, 1615 (1981).
197. C. Yuan, S. Chen, H. Zhou and L. Maier, *Synthesis*, 955 (1993).
198. H. C. J. Ottenhejm, R. Plate, J. H. Noordik and J. D. M. Herscheid, *J. Org. Chem.*, **47**, 2147 (1982).
199. M. Fujita, H. Oishi and T. Hiyama, *Chem. Lett.*, 837 (1986).
200. M. Fujita and T. Hiyama, *J. Org. Chem.*, **53**, 5415 (1988).
201. B. E. Maryanof, D. F. McComsey and S. O. Nortey, *J. Org. Chem.*, **46**, 355 (1981).
202. M. J. Perkins, B. V. Smith and E. S. Turner, *J. Chem. Soc., Chem. Commun.*, 977 (1980).
203. W. Oppolzer and M. Petrzilka, *Helv. Chim. Acta*, **61**, 2755 (1978).
204. J. M. Tronchet, F. Habashi, J. P. Fasel, G. Zosimolandolfo, F. Barbalat-Rey and G. Moret, *Helv. Chim. Acta*, **69**, 1132 (1986).
205. K. C. Nicolaou, E. P. Schreiner and W. Stahl, *Angew. Chem., Int. Ed. Engl.*, **30**, 585 (1991).
206. T. Oishi and T. Nakata, *Acc. Chem. Res.*, **17**, 338 (1984).
207. D. R. Williams, M. H. Osterhout and J. P. Reddy, *Tetrahedron Lett.*, **34**, 3271 (1993).
208. K. Miyashita, T. Toyoda, H. Miyabe and T. Imanishi, *Synlett*, 1229 (1995).
209. J. T. Dougherty, J. R. Flisak, J. Hayes, I. Lantos, L. Liu and L. Tucker, *Tetrahedron: Asymmetry*, **8**, 497 (1997).
210. E. Fontaine, C. Namane, J. Meneyrol, M. Geslin, L. Serva, E. Roussey, S. Tissandié, M. Maftouh and P. Roger, *Tetrahedron: Asymmetry*, **12**, 2185 (2001).
211. K. Shishido, K. Hiroya, H. Komatsu, K. Fukumoto and T. Kametani, *J. Chem. Soc., Chem. Commun.*, 904 (1986).
212. H. Mohrle and M. Lappenberger, *Chem. Ber.*, **109**, 1106 (1976).
213. A. H. Beckett, R. T. Coutts and F. A. Ogunbona, *Tetrahedron*, **29**, 4189 (1973).
214. A. G. Hortmann, J. Koo and C. C. Yu, *J. Org. Chem.*, **43**, 2289 (1978).
215. P. Riviere, S. Richelme, M. Riviere-Baudet and J. Satge, *J. Chem. Res. (M)*, 2817 (1978).
216. F. Benington, R. D. Morin and L. C. Clark, *J. Med. Chem.*, **8**, 1004 (1965).

217. G. H. Rasmusson, G. F. Reynolds, N. G. Steinberg, E. Walton, G. F. Patel, T. Liang, M. A. Cascieri, A. H. Cheung, J. R. Brooks and C. Berman, *J. Med. Chem.*, **29**, 2298 (1986).
218. M. Shimizu, K. Tsukamoto and T. Fujisawa, *Tetrahedron Lett.*, **38**, 5193 (1997).
219. K. Harada and S. Shiono, *Bull. Chem. Soc. Jpn.*, **57**, 1040 (1984).
220. W. Ried and K. Lotterhos, *Chem. Ber.*, **88**, 38 (1955).
221. A. S. C. Chan, C.-C. Chen, C.-W. Lin, Y.-C. Lin, M.-C. Cheng and S.-M. Peng, *J. Chem. Soc., Chem. Commun.*, 1767 (1995).
222. T. Kolasa, S. Sharma and M. J. Miller, *Tetrahedron Lett.*, **28**, 4973 (1987).
223. K. E. Rodriques, A. Basha, J. B. Summers and D. W. Brooks, *Tetrahedron Lett.*, **29**, 3455 (1988).
224. H. G. Richey, R. C. McLane and C. J. Phillips, *Tetrahedron Lett.*, **17**, 233 (1976).
225. C. Schenk, M. L. Beekes and Th. J. de Boer, *Recl. Trav. Chim. Pays-Bas*, **99**, 246 (1980).
226. E. Gossinger and B. Witkop, *Monatsh. Chem.*, **111**, 803 (1980).
227. H. Fujioka, M. Fuji, Y. Okaichi, T. Yoshida, H. Annoura, Y. Kita and Y. Tamura, *Chem. Pharm. Bull.*, **37**, 602 (1989).
228. T. S. Cooper, A. S. Larigo, P. Laurent, C. J. Moody and A. K. Takle, *Org. Biomol. Chem.*, **3**, 1252 (2005).
229. T. S. Cooper, P. Laurent, C. J. Moody and A. K. Takle, *Org. Biomol. Chem.*, **2**, 265 (2004).
230. T. S. Cooper, A. S. Larigo, P. Laurent, C. J. Moody and A. K. Takle, *Synlett*, 1730 (2002).
231. M. Atobe, N. Yamazaki and C. Kibayashi, *J. Org. Chem.*, **69**, 5595 (2004).
232. R. Fassler, D. E. Frantz, J. Oetiker and E. M. Carreira, *Angew. Chem., Int. Ed.*, **41**, 3054 (2002).
233. L. Bernardi, V. Cere, C. Femoni, S. Pollicino and A. Ricci, *J. Org. Chem.*, **68**, 3348 (2003).
234. D. J. Ritson, R. J. Cox and J. Berge, *Org. Biomol. Chem.*, **2**, 1921 (2004).
235. R. W. Hofmann and A. Endesdelder, *Justus Liebigs Ann. Chem.*, 215 (1987).
236. N. A. Kulkarni and K. Chen, *Tetrahedron Lett.*, **47**, 611 (2006).
237. M. Ueda, H. Miyabe, H. Sugino and T. Naito, *Org. Biomol. Chem.*, **3**, 1124 (2005).
238. H. Miyabe, A. Nishimura, Y. Fujishima and T. Naito *Tetrahedron*, **59**, 1901 (2003).
239. H. Miyabe, K. Fujiim and T. Naito, *Org. Biomol. Chem.*, **1**, 381 (2003).
240. H. Miyabe, C. Konishi and T. Naito, *Chem. Pharm. Bull.*, **51**, 540 (2003).
241. S. B. McNabb, M. Ueda and T. Naito, *Org. Lett.*, **6**, 1911 (2004).
242. H. Miyabe, M. Ueda, K. Fujii, A. Nishimura and T. Naito, *J. Org. Chem.*, **68**, 5618 (2003).
243. E. J. Enholm, J. A. Bumoff and L. M. Jaramillo, *Tetrahedron Lett.*, **31**, 3727 (1990).
244. J. Marco-Contelles, P. Gallego, M. Rodríguez-Fernández, N. Khiar, C. Destabel, M. Bernabé, A. Martínez-Grau and J. L. Chiara, *J. Org. Chem.*, **62**, 7397 (1997).
245. J. Marco-Contelles, C. Destabel, P. Gallego, J. L. Chiara and M. Bernabé, *J. Org. Chem.*, **61**, 1354 (1996).
246. O. Miyata, S. Kajisa, M. Ueda, M. Yamauchi and T. Naito, *Chem. Pharm. Bull.*, **53**, 995 (2005).
247. H. Miyabe, H. Tanaka and T. Naito, *Chem. Pharm. Bull.*, **52**, 74 (2004).
248. T. Kiguchi, K. Tajiri, I. Ninomiya and T. Naito, *Tetrahedron*, **56**, 5819 (2000).
249. A. L. J. Beckwith and C. H. Schiesser, *Tetrahedron*, **41**, 3925 (1985).
250. J. U. Rhee, B. I. Blissm and T. V. RajanBabu, *J. Am. Chem. Soc.*, **125**, 1492 (2003).
251. A. Boiron, P. Zillig, D. Faber and B. Giese, *J. Org. Chem.*, **63**, 5877 (1998).
252. S. Bobo, I. Storch de Gracia and J. L. Chiara, *Synlett*, 1551 (1999).
253. K. Torssell, J. Goldman and T. E. Petersen, *Justus Liebigs Ann. Chem.*, 231 (1973).
254. J. F. W. Keana, V. S. Prabhu, S. Ohmiya and C. E. Klopfstein, *J. Org. Chem.*, **51**, 3456 (1986).
255. K. Torsell, *Tetrahedron*, **33**, 2287 (1977).
256. Y. Xie, C. Liao, P. M. Lahti, R. T. Weber, J. Jiang and D. P. Barr, *J. Org. Chem.*, **64**, 5176 (1999).
257. A. R. Forrester and R. Ramasseual, *J. Chem. Soc., C*, 1638 (1971).
258. J. F. Keana, *J. Org. Chem.*, **54**, 2418 (1989).
259. Y. Yost, H. R. Gutmann and C. C. Muscoplat, *J. Chem. Soc., C*, 2119 (1971).
260. S. Wawzonek and J. V. Kempf, *J. Org. Chem.*, **38**, 2763 (1973).
261. H. H. Baer and C. B. Madumelu, *Carbohydr., Res.*, **67**, 329 (1978).
262. S. Brown, M. P. Brochu, C. J. Sinz and D. W. C. MacMillan, *J. Am. Chem. Soc.*, **125**, 10808 (2003).

263. Y. Hayashi, J. Yamaguchi, K. Hibino and M. Shoji, *Tetrahedron Lett.*, **44**, 8293 (2003).
264. R. A. Abramovitch, S. R. Challand and Y. Yamada, *J. Org. Chem.*, **40**, 1541 (1975).
265. M. G. Barlow, R. N. Haszeldine and K. W. Murray, *J. Chem. Soc., Perkin Trans. 1*, 1960 (1980).
266. S. V. Filip and N. Sewald, *Synthesis*, 3565 (2005).
267. C. Schenk and T. J. De Boer, *Tetrahedron*, **35**, 147 (1979).
268. H. Braun, H. Felber, G. Kresse, A. Ritter, F. P. Schmidtchen and A. Schneider, *Tetrahedron*, **47**, 3313 (1991).
269. A. H. Beckett and M. A. Salami, *J. Pharm. Pharmacol.*, **24**, 900 (1972).
270. J. T. Lai, *Synthesis*, 124 (1984).
271. R. W. Feenstra, E. H. M. Stokkingreef, A. M. Reichwein, W. B. H. Lousberg, H. C. J. Ottenheijm, J. Kamphuis, W. H. J. Boesten, H. E. Schoemaker and E. M. Meijer, *Tetrahedron*, **46**, 1745 (1990).
272. D. Thomas and D. H. Aue, *J. Org. Chem.*, **39**, 3855 (1974).
273. G. Grundke, W. Keese and M. Rimpler, *Synthesis*, 1115 (1987).
274. H. Tokuyama, T. Kuboyama, A. Amano, T. Yamashita and T. Fukuyama, *Synthesis*, 1299 (2000).
275. H. Tokuyama, T. Kuboyama and T. Fukuyama, *Org. Synth.*, **80**, 207 (2003).
276. I. A. O'Neil, E. Cleator and D. J. Tapolczay, *Tetrahedron Lett.*, **42**, 8247 (2001).
277. A. Albini, *Synthesis*, 263 (1993).
278. A. Heesing and W. Herdering, *Tetrahedron Lett.*, **22**, 4675 (1981).
279. O. Phanstiel, Q. X. Wang, D. H. Powell, M. P. Ospina and B. A. Leeson, *J Org. Chem.*, **64**, 803 (1999).
280. L. Grierson and M. J. Perkins, *Tetrahedron Lett.*, **34**, 7463 (1993).
281. A. Nemchik, V. Badescu and O. Phanstiel, *Tetrahedron*, **59**, 4315 (2003).
282. A. J. Biloski and B. Ganem, *Synthesis*, 537 (1983).
283. G. Boche and R. H. Sommerlade, *Tetrahedron*, **42**, 2703 (1986).
284. J. Yaouanc, G. Masse and G. Sturz, *Synthesis*, 807 (1985).
285. J. D. Fields and P. J. Kropp, *J. Org. Chem.*, **65**, 5937 (2000).
286. M. D. Wittman, R. L. Halcomb and S. J. Danishefsky, *J. Org. Chem.*, **55**, 198 (1990).
287. A. C. M. Meesters and M. H. Benn, *Synthesis*, 679 (1978).
288. W. W. Zajac, T. R. Walters and M. G. Darcy, *J. Org. Chem.*, **53**, 5856 (1988).
289. H. Pellissier, *Tetrahedron*, **63**, 3235 (2007).
290. P. F. Vogt and M. J. Miller, *Tetrahedron*, **54**, 1317 (1998).
291. J.-C. Adelbrecht, D. Craig, A. J. Fleming and F. M. Martin, *Synlett*, 2643 (2005).
292. G. Calvet, R. Guillot, N. Blanchard and C. Kouklovsky, *Org. Biomol. Chem.*, **3**, 4395 (2005).
293. H. Ren, S. Grady, D. Gamenara, H. Heinzen, P. Moyna, S. L. Croft, H. Kendrick, V. Yardley and G. Moyna, *Bioorg. Med. Chem. Lett.*, **11**, 1851 (2001).
294. Y. Yamamoto and H. Yamamoto, *J. Am. Chem. Soc.*, **126**, 4128 (2004).
295. G. W. Kirby, H. McGuigan, J. W. M. Mackinnon, D. McLean and R. P. Sharma, *J. Chem. Soc., Perkin Trans. 1*, 1437 (1985).
296. H. Abe, S. Aoyagi and C. Kibayashi, *J. Am. Chem. Soc.*, **122**, 4583 (2000).
297. T. P. Burkholder and P. L. Fuchs, *J. Am. Chem. Soc.*, **110**, 2341 (1988).
298. E. Muller, H. Metzger and D. Fries, *Chem. Ber.*, **87**, 1449 (1954).
299. G. Kresze and E. Kysela, *Justus Liebigs Ann. Chem.*, 202 (1981).
300. E. Kesler, *J. Heterocycl. Chem.*, **17**, 1113 (1980).
301. H. Felber, G. Kresze, R. Prewo and A. Vasella, *Helv. Chim. Acta*, **69**, 1137 (1986).
302. A. Defoin, M. Joubert, J.-M. Heuchel, C. Strehler and J. Streith, *Synthesis*, 1719 (2000).
303. T. Hudlicky and H. F. Olivo, *Tetrahedron Lett.*, **32**, 6077 (1991).
304. T. Hudlicky, U. Rinner, D. Gonzalez, H. Akgun, S. Schilling, P. Siengalewicz, T. A. Martinot and G. R. Pettit, *J. Org. Chem.*, **67**, 8726 (2002).
305. A. Defoin, J. Pires and J. Streith, *Synlett*, 111 (1990).
306. P. Kefalas and D. S. Grierson, *Tetrahedron Lett.*, **34**, 3555 (1993).
307. E. E. Knaus, K. Avasthi and C. S. Giam, *Can. J. Chem.*, **58**, 2447 (1980).
308. S. K. Dubey and E. E. Knaus, *J. Org. Chem.*, **50**, 2080 (1985).
309. J. M. Schkeryantz and S. J. Danishefsky, *J. Am. Chem. Soc.*, **117**, 4722 (1995).
310. F. Ragaini, S. Cenini, D. Brignoli, M. Gasperini and E. Gallo, *J. Org. Chem.*, **68**, 460 (2003).

311. W. R. Dolbier, C. R. Burkholder, G. E. Wicks, G. J. Palenik and M. Gawron, *J. Am. Chem. Soc.*, **107**, 7183 (1985).
312. G. Bianchi, A. Gamba and R. Gandolfi, *Tetrahedron*, **28**, 1601 (1972).
313. S. Niwayama, S. Dan, Y. Inouye and H. Kakisawa, *Chem. Lett.*, 957 (1985).
314. C. De Micheli, A. G. Invernizzi, R. Gandolfi and L. Scevola, *J. Chem. Soc., Chem. Commun.*, 246 (1976).
315. S. Kanemasa and T. Tsuruoka, *Chem. Lett.*, 49 (1995).
316. G. Tacconi, P. P. Righetti and G. Desimoni, *J. Prakt. Chem.*, **322**, 679 (1980).
317. U. Chiacchio, D. Iannazzo, A. Piperno, R. Romeo, G. Romeo, A. Rescifina and M. Saglimbeni, *Bioorg. Med. Chem.*, **14**, 955 (2006).
318. C. M. Dicken and P. De Shong, *J. Org. Chem.*, **47**, 2047 (1982).
319. A. Bened, R. Durand, D. Pioch., P. Geneste, C. Guimon, G. G. Pfister, J. P. Declercq, G. Germain and P. Briard, *J. Chem. Soc., Perkin Trans. 2*, 1 (1984).
320. C. Kashima, A. Tsuzuki and T. Tajima, *J. Heterocycl. Chem.*, **21**, 201 (1984).
321. T. B. Nguyen, C. Gaulon, T. Chapin, S. Tardy, A. Tatibouet, P. Rollin, R. Dhal, A. Martel and G. Dujardin, *Synlett*, 3255 (2006).
322. A. Padwa, D. N. Kline, K. F. Koehler, M. Matzinger and M. K. Venkatramanan, *J. Org. Chem.*, **52**, 3909 (1987).
323. A. Padwa, D. N. Kline and B. H. Norman, *Tetrahedron Lett.*, **29**, 265 (1988).
324. M. Yamamoto, T. Suenaga, K. Suzuki, K. Naruchi and K. Yamada, *Heterocycles*, **26**, 755 (1987).
325. L. Di Nunno and A. Scilimati, *Tetrahedron*, **49**, 10965 (1993).
326. W. R. Doblier, C. R. Burkholder, G. E. Wicks, G. J. Palenik and M. Gawron, *J. Am. Chem. Soc.*, **107**, 7183 (1985).
327. E. Gossinger, R. Imh and H. Wehrli, *Helv. Chim. Acta*, **58**, 96 (1975).
328. O. Tamura, T. Mitsuya, X. Huang, Y. Tsutsumi, S. Hattori and H. Ishibashi, *J. Org. Chem.*, **70**, 10720 (2005).
329. R. L. Funk, G. L. Bolton, J. U. Dagett, M. M. Hansen and L. H. M. Horcher, *Tetrahedron*, **41**, 3479 (1985).
330. T. Kusimi, S. Takahashi, Y. Sato and H. Kakisawa, *Heterocycles*, **10**, 257 (1978).
331. A. Padwa and G. S. Wong, *J. Org. Chem*, **51**, 3125 (1986).
332. R. Grigg, J. Markandu, T. Perrior, S. Surendrakumar and W. J. Warnock, *Tetrahedron Lett.*, **31**, 559 (1990).
333. O. Tamura, T. Mitsuya and H. Ishibashi, *Chem. Commun.*, 1128 (2002).
334. A. Hassner, R. Maurya, A. Padwa and W. H. Bullock, *J. Org. Chem.*, **56**, 2775 (1991).
335. E. Mernyak, G. Benedek, G. Schneider and J. Woelfling, *Synlett*, 637 (2005).
336. N. K. A. Dalgaard, K. E. Larsen and K. B. G. Torssell, *Acta Chem. Scand., Ser. B*, **B38**, 423 (1984).
337. P. Armstrong, R. Grigg and W. J. Warnock, *J. Chem. Soc., Chem. Commun.*, 1325 (1987).
338. P. J. Dransfield, S. Moutel, M. Shipman and V. Sik, *J. Chem. Soc., Perkin Trans. 1*, 3349 (1999).
339. P. J. Dunn, A. B. Graham, R. Grigg, P. Higginson and M. Thornton-Pett, *Tetrahedron*, **58**, 7727 (2002).
340. M. Helms, W. Schade, R. Pulz, T. Watanabe, A. Al-Harrasi, L. Fisera, I. Hlobilova, G. Zahn and H.-U. Reissig, *Eur. J. Org. Chem.*, **6**, 1003 (2005).

CHAPTER 6

Synthesis of oximes and hydroxamic acids

ANDREA PORCHEDDU and GIAMPAOLO GIACOMELLI

Università degli Studi di Sassari, Dipartimento di Chimica, via Vienna 2, 07100-Sassari, Italy
Fax: +39 079 212069; e-mail: anpo@uniss.it

The chemistry of hydroxylamines, oximes and hydroxamic acids
Edited by Z. Rappoport and J. F. Liebman

I. SYNTHESIS OF OXIMES

A. Introduction

Oximes are a class of chemical compounds with general formula $R^1R^2C{=}NOH$, where R^1 is an organic side chain and R^2 may be either hydrogen, forming an aldoxime, or another organic residue, forming a ketoxime (Chart 1).

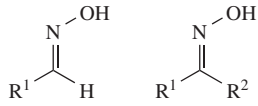

Aldoxime Ketoxime

CHART 1

The term oxime dates to the 19th century, a combination of the words oxygen and imide. Oximes exist as two stereoisomers: *syn* (*Z*) and *anti* (*E*). Aldoximes, except for aromatic aldoximes, exist for the most part as the *syn* isomer[1], while ketoximes are obtained as both *syn* and *anti* isomers, which can be separated almost completely. Recently, Kolandaivel and Senthilkumar[2] have studied the molecular structure and conformational stability of *anti* and *syn* conformers of some aliphatic aldoximes by employing the *ab initio* and density functional theory (DFT) methods.

Most oximes are weakly amphoteric[3,4] in character due to the mildly acidic hydroxy group and the slightly basic nitrogen atom, and may dissolve in aqueous sodium hydroxide to form the sodium salt, from which they can be liberated by the addition of a weak acid, e.g. acetic acid.

B. Carbonyl Groups as Synthetic Starting Compounds

The condensation of a primary amine with $R^1R^2C{=}O$ compound was first reported by Schiff in 1864[5] and since then a great number of these reactions were actively investigated[6].

When hydroxylamine is used, the condensation gives oximes, along with water as a by-product (Scheme 1). It is known that the oxime is formed via an intermediate because its C=N double bond, which is responsible for the IR absorption at 1400 cm^{-1} absorption, hardly appears until after the carbonyl 1710 cm^{-1} absorption has almost completely disappeared[7].

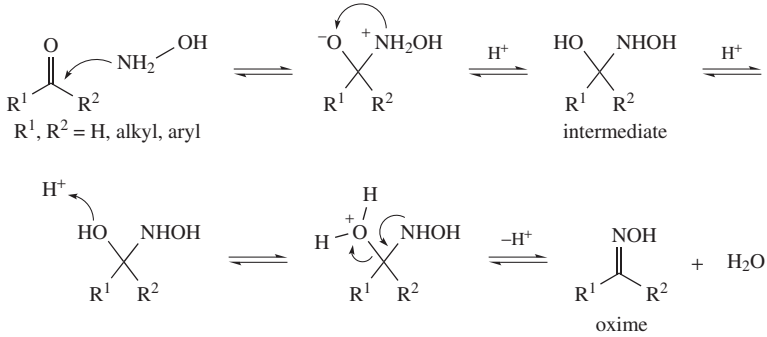

SCHEME 1

Since hydroxylamine is usually available only in the form of its salts, e.g. the hydrochloride or sulfate, the aqueous solution of these salts has to be treated with sodium acetate or hydroxide to liberate the base before treatment with the aldehyde or ketone.

Oximes are highly crystalline and the oximation is a very efficient method for characterization and purification of carbonyl compounds. Impure aldehydes and ketones are sometimes purified by conversion into the corresponding oximes and, after recrystallization, they are hydrolyzed by boiling with dilute sulfuric acid.

The acid, protonating the hydroxylamine, prevents the reverse reaction and thus causes rapid and complete hydrolysis: distillation of the final solution then drives off the aldehyde or ketone, and the hydroxylamine sulfate remains behind. This method must be used with care, however, as the acid may cause a Beckmann rearrangement to occur.

The experimental conditions used to prepare oximes depend mostly on the nature of the parent materials and the basicity of the reaction medium; usually, reactions proceed smoothly at pH close to neutral. In organic chemistry, it is generally believed that reactions of RR′C=O and hydroxylamine at a pH close to neutral proceed through nucleophilic attack of the nitrogen electron pair on the electrophilically activated C=O carbon[8]. Usually, the preparation of oximes via condensation of the carbonyl compounds and hydroxylamine hydrochloride needs long reaction times[9].

Oxime ligations can be significantly accelerated by using aniline as a nucleophilic catalyst[10]. Rate enhancements are achieved by changing the electrophile from a weakly populated protonated carbonyl (Scheme 2a) to a more highly populated protonated aniline Schiff base (Scheme 2b). The transimination of the protonated aniline Schiff base to the oxime proceeds rapidly under aqueous acidic conditions.

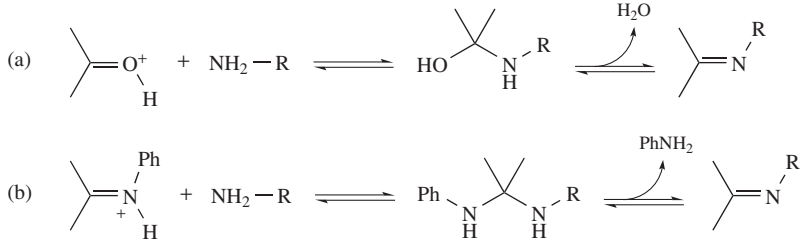

SCHEME 2

The resulting ligation rates (k_{obs}) are increased up to 400-fold in aqueous solution at pH 4.5 and up to 40-fold at pH 7. Such rate enhancements enable the use of equimolar concentrations of reactants, meeting the rigorous requirements of challenging macromolecular ligation. With the exception of symmetrical ketones, both isomeric oximes (*Z* and *E*), which have different physical properties and biological activities, are usually produced[11,12]. They could be separated by chromatography or recrystallization techniques.

A small number of examples is available for the synthesis of *E* and *Z* isomers of oximes[13]. In many cases, *E* isomers were obtained either from the *Z* forms (by the hydrochloride method) or isolated by column chromatography. Often, the reagents that have been used for oximation of aldehydes and ketones also catalyze the interconversion of *Z* and *E* isomers. The rate of equilibration of a mixture of *Z* and *E* isomers and the position of the equilibrium is temperature-dependent[14]. In 2001, Sharghi and Sarvani[15] reported a convenient method for controlling the stereochemistry of the reaction of hydroxylamine hydrochloride with aldehydes or ketones in the solid state. The highly stereoselective conversion of aldehydes and ketones to their corresponding oximes

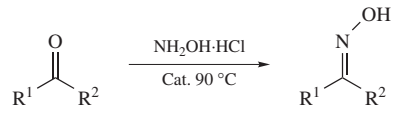

Cat. = $CuSO_4$, K_2CO_3

R^1, R^2 = H, Me, Ph, *p*-ClC_6H_4, *p*-HOC_6H_4, *p*-MeC_6H_4, 2- and 3-thienyl, 2- and 4-pyridyl

SCHEME 3

with hydroxylamine hydrochloride is catalyzed by $CuSO_4$ and K_2CO_3 (Scheme 3). This method occurs under mild reaction conditions with high yields.

Various types of aromatic aldehydes with electron donating and withdrawing groups were cleanly and rapidly condensed with hydroxylamine hydrochloride at 90 °C, giving the corresponding *E*-isomer of oximes (with OH *anti* to aryl) in excellent yields in the presence of $CuSO_4$. However, aromatic ketones such as benzophenone did not afford the corresponding oximes under these conditions.

Nowadays, synthetic chemists continue to explore new methods to carry out chemical transformations. One of these new methods is to run reactions on the surface of solids. As the surfaces have properties which differ from those in solution or the gas phase, entirely new chemistry may occur.

Several classes of solids have commonly been used for surface organic chemistry including aluminas, silica gels and clays. Zinc oxide (ZnO) is certainly one of the most interesting of these solids because it has surface properties that suggest that a very rich organic chemistry may occur there.

Sarvari[16] has prepared a number of aldoximes using ZnO/CH_3COCl (Scheme 4). It was carried out by simple condensation between hydroxylamine hydrochloride and the desired aldehyde in the presence of zinc oxide (ZnO) as catalyst at 60 °C for a few minutes.

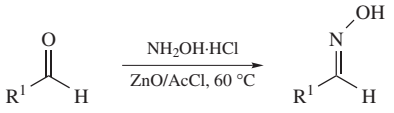

R^1 = *n*-Bu, *n*-pentyl, Ph, *o*-ClC_6H_4, *p*-HOC_6H_4, *p*-MeC_6H_4, 2-thienyl, 3-pyridyl

SCHEME 4

N,*N*′-Disalicylideneethylenediamine (Salen) and its analogues are most versatile chelate ligands in inorganic and organometallic chemistry (Chart 2)[17]. The synthesis of unsymmetrical salen derivatives which consist of two different salicylideneimine moieties

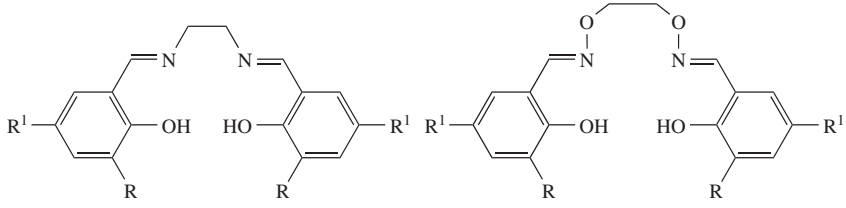

CHART 2

is difficult, because a statistical mixture of three possible condensation products is usually obtained[18].

To develop stable analogues of Salen-type ligands (Chart 2), Dong and colleagues have synthesized a series of new 1,2-bis(salicylideneaminooxy)ethane (Salamo) ligands on the basis of *O*-alkyl oxime instead of the imine moiety (Scheme 5)[19]. Eight salamo ligands **3a**–**h** were prepared as colorless crystals from the corresponding salicylaldehydes **1a**–**h** and *O*,*O*′-(ethane-1,2-diyl)bis(hydroxylamine) **2**. The crystal structure of **3a**–**c** suggests that the oxime-OH form is more predominant than the keto-NH form. In fact, the corresponding salen analogues show a band around 400 nm assigned to their keto-NH form and the $\pi-\pi^*$ bands (at *ca* 315 nm)[20]; **3a**–**c** showed no absorption around 400 nm. This fact confirms that the population of the keto-NH form of salamo is negligibly small.

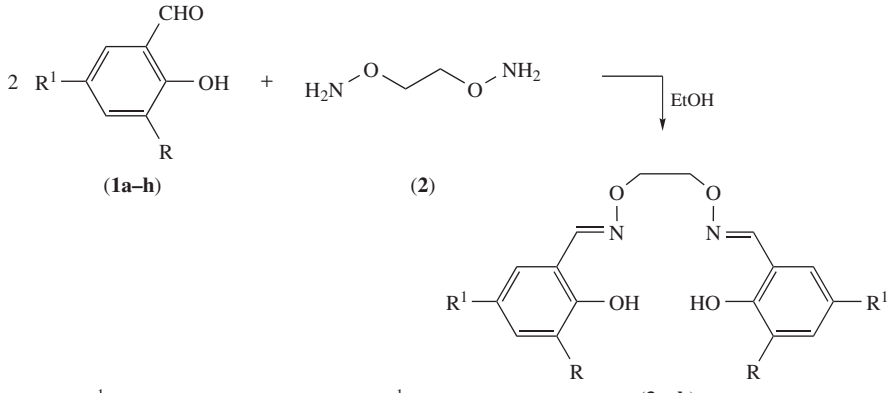

(**1a–h**) (**2**) (**3a–h**)

Salamo (R, R^1 = H)

(**3a**) R = R^1 = H	83%	(**3e**) R = H, R^1 = Br	64%
(**3b**) R = OMe, R^1 = H	79%	(**3f**) R = H, R^1 = OH	77%
(**3c**) R = R^1 = *t*-Bu	74%	(**3g**) R = OH, R^1 = H	88%
(**3d**) R = SMe, R^1 = H	74%	(**3h**) R = H, R^1 = NO_2	79%

SCHEME 5

O-Substituted oxime derivatives are synthetically useful in a wide variety of transformations. Hoffman and Butani[21] have observed that reaction of a series of aldehydes and ketones with the potassium salt of *N*,*O*-bis(trimethylsilyl)hydroxylamine **4a** or **4b** (a rapid equilibrium between **4a** and its *N*,*N*-bis(silylated) isomer **4b** probably exists in solution) gave high yields of the corresponding oximate anion **5**, formed via the Peterson-type reaction, together with the silyl ether **6**. Anion **5** could be protonated to the oxime **7** or trapped *in situ* with a variety of electrophiles to give *O*-substituted oxime derivatives (Scheme 6).

During the last years, the microwave oven has become a very popular device in the laboratories of synthetic organic chemists. Since the early articles of the groups of Gedye and Giguere[22,23], application of the microwave heating technique has been under intensive investigation and has been recently reviewed[24,25]. The effects usually observed are: (a) decreased reaction time and (b) cleaner reaction with easier work-up. After several controversies, it was demonstrated that the acceleration of the reaction rate is caused by combination of the heat and non-specific interaction between the microwaves and reacting molecules[26].

In 1992, Puciova and Toma[27] published the synthesis of a broad range of oximes by microwave irradiation. They observed that the application of microwave heating enhanced

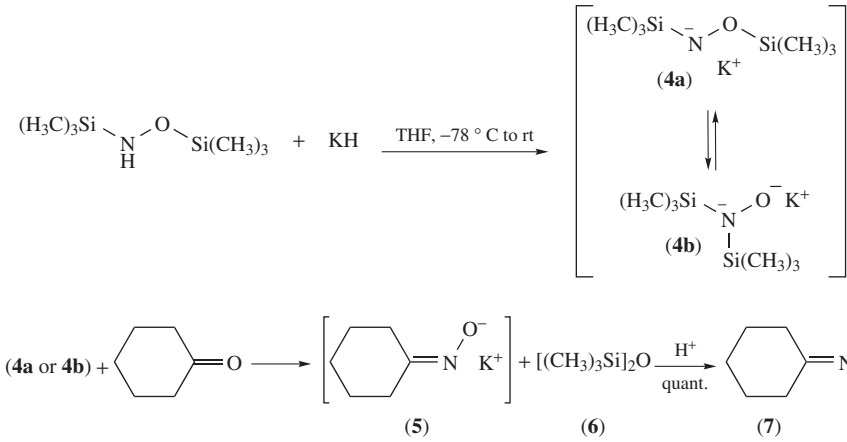

SCHEME 6

dramatically the reaction rate, and practically quantitative yields of oximes were isolated after less than 1 min heating in most cases. The effect of solvents on the course of the reaction was studied.

The ketoximes **9** were synthesized by refluxing the ketones **8** and hydroxylamine hydrochloride in a mixture of pyridine and ethanol as solvent (Scheme 7). The microwave heating reduced markedly the reaction time (1–3 min versus 45 min in an oil bath).

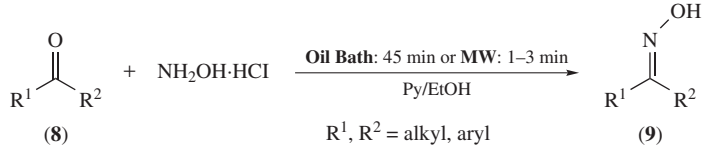

SCHEME 7

In 1999, Hajipour[28] reported that silica gel, without any base, could be a useful catalyst for the preparation of oximes in dry media coupled with microwave irradiation. Hydroxylamine hydrochlorides were reacted with several aliphatic and aromatic aldehydes and ketones affording the desired oximes.

The chemical applications of ultrasound (Sonochemistry) have become an exciting new field of research during the past decade. Recently, Li and coworkers[9] have found an efficient and convenient procedure for the preparation of oximes via the condensation of aldehydes and ketones in ethanol with hydroxylamine hydrochloride under ultrasound irradiation (Scheme 8). Compared with conventional methods, the main advantages of the sonochemical procedure are milder conditions, higher yields and shorter reaction periods. The reason may be the phenomenon of cavitations produced by ultrasound.

Na_2SO_4 has a noteworthy effect on the reaction time, while its amount has little effect on the reaction yield. In fact, in the absence of Na_2SO_4, a prolonged period of ultrasonication (u.s.) is needed to get similar yields.

The synthesis of chemical libraries loaded with structural diversity is an emerging field with direct applications in biomedical research. Strategies for library synthesis have mainly focused on combinatorial synthesis of molecules that vary substituents with a core

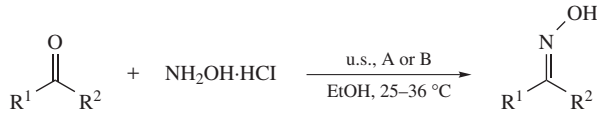

A: Na_2SO_4 (1.0 mmol). **B**: without Na_2SO_4
R^1, R^2 = H, alkyl, aryl
u.s.: ultrasounds

SCHEME 8

structural type. Diversity-oriented synthesis is a new strategy for constructing libraries with both skeletal and functional group diversity.

In an effort to formulate novel approaches to complex library synthesis, Porco and coworkers[29] have prepared a hybrid oxime library (**10**) via 'chemical domain shuffling'. In this approach, discrete fragments or 'chemical domains' may be shuffled to prepare complex hybrid structures (Scheme 9).

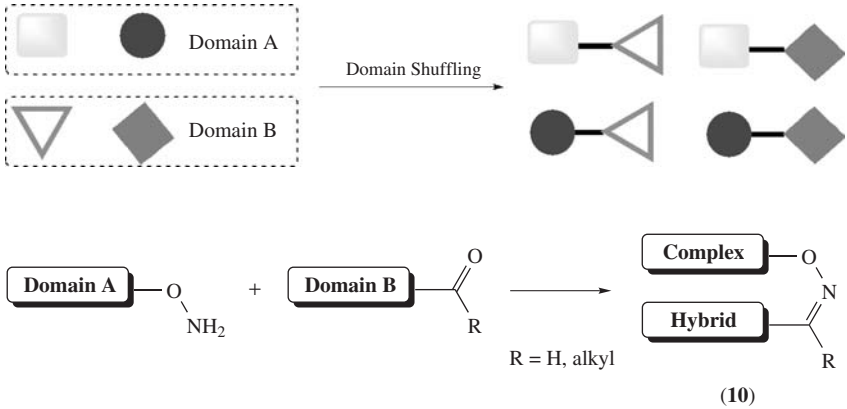

SCHEME 9

Aldehydes or ketones were found to smoothly condense with *O*-alkylhydroxylamine at room temperature using 20 mol% of AcOH in EtOAc. Polymer-supported methylisatoic anhydride (PL-MIA) was employed to scavenge the excess of alkoxyamines (Scheme 10).

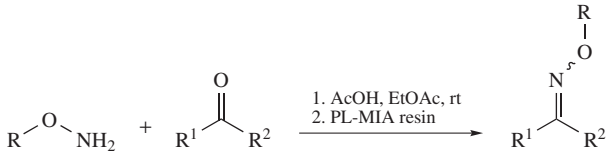

Complex Oxime Library

R = alkyl or cycloalkyl; R^1 = H, Me; R^2 = alkyl, cyclohexyl, aryl

SCHEME 10

In 2002, Kanno and Taylor[30] successfully developed a simple one-pot procedure using $MnO_2/NH_2OMe{\bullet}HCl$ for the conversion of activated primary alcohols into *O*-methyl oximes (Scheme 11). They also developed a modification using Amberlyst 15-supported alkoxylamines, which can be employed to prepare other types of *O*-alkyl oximes as well as the parent hydroxylamines. This latter procedure has been used as the cornerstone of an efficient synthesis of the antifungal natural product citaldoxime **11** (Scheme 11). Citaldoxime is an antifungal natural product first obtained as a radiation-induced stress metabolite of *Citrus sinensis*[31,32], and later isolated from the roots of several different *citrus* plants[33].

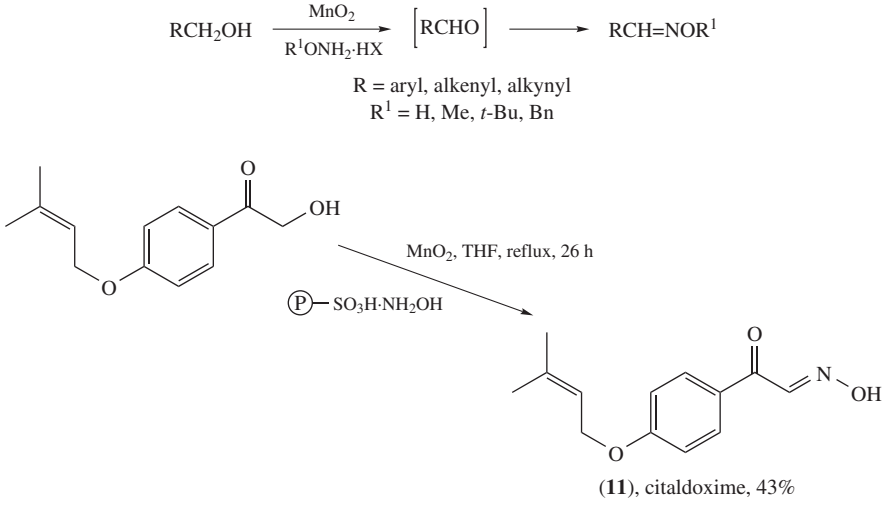

SCHEME 11

Oximes are usually prepared by reaction of ketones with hydroxylamine while, especially in industrial processes, ketoximes are synthesized by the reaction shown in Scheme 12[34].

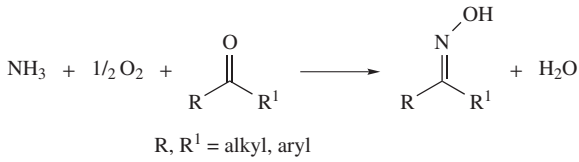

SCHEME 12

This process of synthesis of ketoximes as described by Scheme 12 is termed ammoximation. The source of NH_2OH is the oxidation of NH_3 to NO (or NO_2) followed by reduction with H_2 or SO_2. The reactants were passed over a Pt catalyst at low pressures and high temperatures (>800 °C).

C. Nitro Compounds as Starting Material

The action of carbon monoxide (CO) upon solutions of copper salts leads to the formation of cuprous CO complexes that have pronounced activity as reducing agents[35]. In

1972, Knifton[36] reported that solutions of cuprous salts in amine solvents are excellent catalysts for the selective reduction of nitroalkanes to the corresponding oximes.

In an interesting paper published by Barton and coworkers[37] in 1987, aliphatic nitro compounds were reduced to oximes using carbon disulfide in the presence of an excess of triethylamine under homogeneous conditions. The process is particularly suitable for the reduction of allylic nitro derivatives. The choice of the base is a crucial factor for a good outcome of the reaction; the use of a stronger base such as *N″-tert*-butyl-*N*,*N*,*N′*,*N′*-tetramethylguanidine afforded a mixture of oxime and nitrile. As was recently demonstrated by Penso and colleagues[38], wet potassium carbonate is a more versatile and effective reagent for promoting base-catalyzed reactions, especially under solid–liquid phase transfer catalysis (SL-PTC) conditions (Scheme 13).

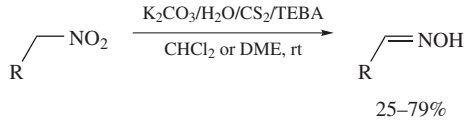

R = 4-methylcyclohexyl, *i*-propyl, 2-phenylcyclohexyl

SCHEME 13

The chemistry of nitro compounds forms the basis of a number of well-known processes, such as the Henry or the Nef reactions[39]. Transformations such as the latter permit the interconversion between nitro and other functional groups and are therefore of prime importance. The most commonly employed methods for the reduction of primary nitroalkanes to oximes involve the use of Bu_3SnH, $Se/NaBH_4$, CS_2 or $SnCl_2$ (often in combination with thiophenol)[40].

In this context, Czekelius and Carreira[41] have recently documented a convenient heavy-metal-free transformation of optically active nitroalkanes **12** to chiral aldoximes **13** at room temperature by employing inexpensive reagents: benzyl bromide, KOH and 5 mol% *n*-Bu_4NI (Scheme 14). This provides an environmentally friendly reaction that excludes the potential contamination of the products by metal impurities.

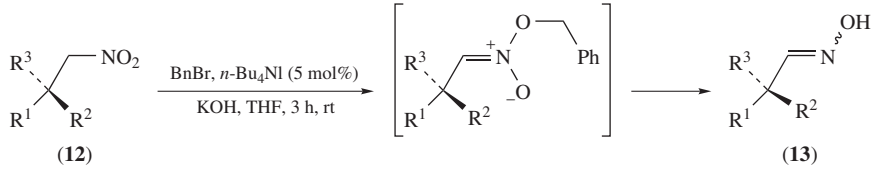

R^1, R^2, R^3 = H, Me, Ph, 2-thienyl, 2-furfuryl ratio major/minor isomer: around 70/30

SCHEME 14

The use of soluble amine bases failed to give products, whereas the heterogeneous conditions KOH/THF proved optimal in promoting aldoxime formation for a broad range of substrates. Optically active nitroalkanes including aromatic (both electron-rich and electron-deficient), heteroaromatic, branched and unbranched aliphatic substrates, as well as substrates that incorporate unprotected alcohol functionalities were successfully reduced.

The reduction of an aliphatic nitro compound containing an α-hydrogen ($R^1R^2CHNO_2$) may be stopped at the stage of the oxime ($R^1R^2C{=}NOH$). Despite the great synthetic importance of these nitro compounds, their photochemical conversion to oximes has not

been deeply studied, except for the direct reduction of α-nitroketone to the corresponding oxime in 2-propanol[42]. In this paper, Takechi and Machida have described a preparatively useful photochemical conversion of nitro compounds **14** to oximes **15** (Scheme 15). The nitro compounds are irradiated in acetone in the presence of NEt_3 using a 500-W high-pressure mercury lamp through a Pyrex filter.

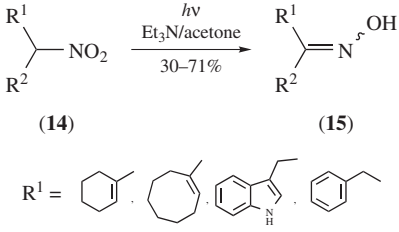

(**14**) (**15**)

R^1 =

$R^2 = EtO_2CCH_2CH_2$, $NCCH_2CH_2$

SCHEME 15

More recently, Kim and coworkers[43] have developed a novel radical alkylation reaction of organic nitro derivatives **16a–d** via bis(silyloxy)enamines **17a–d** (Scheme 16). This method enables not only β-alkylation to the nitro group, but also the conversion of the nitro group (**16a–d**) into an oxime ether functionality (**18a–d**). The irradiation of a solution of **16a–d** with iodomethyl phenyl sulfone (or ethyl iodoacetate) and hexamethylditin in benzene at 300 nm give the oxime ethers **18a–d** in good yields.

Tin-based reagents are not always suitable owing to the toxicity of organotin derivatives and the difficulties often encountered in removing tin residues from the final product. Therefore, the same authors have carried out additional experiments with **17d** and several different alkyl halides under tin-free conditions. The treatment of **16d** with *tert*-butyldiphenylsilyl chloride (TBDPSCl) and triethylamine in the presence of silver triflate in CH_2Cl_2 affords the bis(silyloxy)enamine **17d** in 92% yield (Scheme 17). When the radical reaction was carried out with ethyl iodoacetate in the presence of 2,2′-azobis(4-methoxy-2,4-dimethylvaleronitrile) (V-70) as the initiator in CH_2Cl_2, the oxime ether **19** was obtained in 83% yield (Scheme 17).

Most of the current preparative methods of oximes from nitroalkenes are not versatile. Reduction of nitroalkenes by $CrCl_2$ or NaH_2PO_2 in the presence of palladium was reported to afford the corresponding oximes, but the yields are not satisfactory. Zn-acetic acid and Na_2SnO_2 reductions are limited to the preparation of ketoximes only. Electroreduction of alkenes was reported to yield mixtures of ketones and ketoximes, or oximes and acetals (or ketones) depending on the structure of nitroalkanes.

Sera and coworkers[44], during their investigation on electroreduction of nitroalkenes, found that plates of powder or metallic lead can reduce nitroalkene **20** to give oxime **21** in acetic acid–DMF solution 'without electricity' (Scheme 18). The reduction of 1-nitro-1-alkenes afforded the corresponding aldoximes or ketoximes in excellent yield.

The reduction of conjugated nitroalkenes such as β-nitrostyrenes to oximes provides easy access to a large number of versatile organic intermediates[45]. However, despite their potential utility, many of these methods suffer from the use of strongly acidic[46] or basic conditions[47], requirement of anhydrous conditions, and incompatibility with halogenated arenes. Further, some of the methods are inefficient for the preparation of aldoximes due

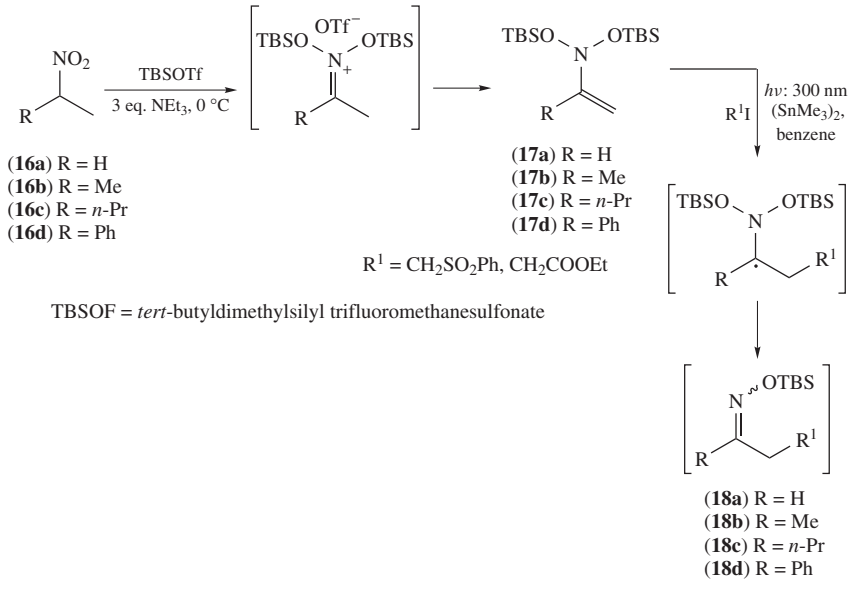

(**16a**) R = H
(**16b**) R = Me
(**16c**) R = *n*-Pr
(**16d**) R = Ph

(**17a**) R = H
(**17b**) R = Me
(**17c**) R = *n*-Pr
(**17d**) R = Ph

$R^1 = CH_2SO_2Ph$, CH_2COOEt

TBSOF = *tert*-butyldimethylsilyl trifluoromethanesulfonate

(**18a**) R = H
(**18b**) R = Me
(**18c**) R = *n*-Pr
(**18d**) R = Ph

SCHEME 16

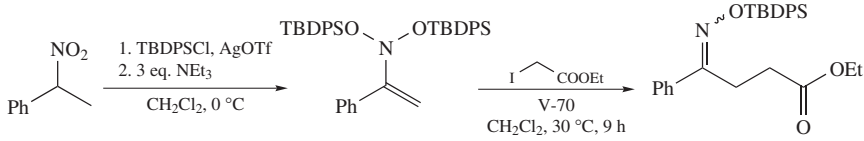

(**16d**) (**17d**) 92% (**19**) 83%

TBDPSCl = *tert*-butyldiphenylsilyl chloride
V-70 = 2.2′-azobis(4-methoxy-2, 4-dimethylvaleronitrile)

SCHEME 17

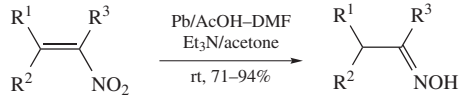

(**20**) (**21**)

R^1 = phenyl, 1-naphthyl, C_6H_{13}; R^2 = H, Ph; R^3 = H, Me, Ph

SCHEME 18

to competing side reactions such as the Nef reaction[48] under acidic conditions[49], and polymerization of nitrostyrenes.

Due to the close similarity of indium to magnesium[50,51] in several aspects, indium could be a potential reducing agent[52]. Since indium has special properties in water, the application of indium for the reduction of β-nitrostyrenes to oximes is of great interest.

In this context, Yadav and coworkers[53] have recently developed a mild and efficient procedure for the selective reduction of β-nitrostyrenes **22** to oximes **23** using indium metal in aqueous methanol under neutral reaction conditions (Scheme 19). Similarly, α-alkoxy oximes **24** are formed in good yields by the treatment of nitroolefins with metallic indium and trimethylsilyl chloride in anhydrous methanol (Scheme 19).

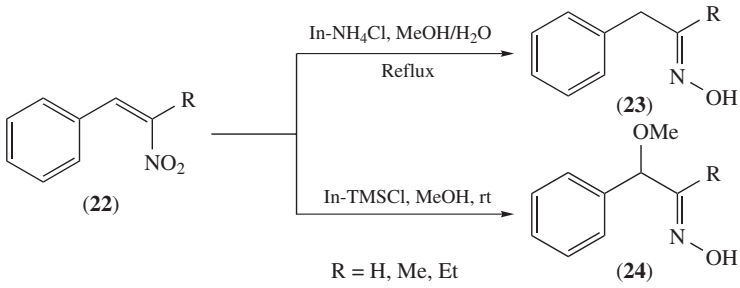

SCHEME 19

The reduction of β-nitrostyrenes with indium metal in aqueous ammonium chloride gave a mixture of *E* and *Z* isomers while the reduction of β-methyl-β-nitrostyrenes with indium powder in the presence of trimethylsilyl chloride gave exclusively the *E* isomer.

N,*N*-Bis(siloxy)enamines **26**, the products of double silylation of aliphatic nitro compounds **25**, react with nucleophiles to give various functionalized α-oximes **27**, α-hydroxy oximes **28** (or their bis(siloxy) derivatives **29**) as side products (Scheme 20)[54].

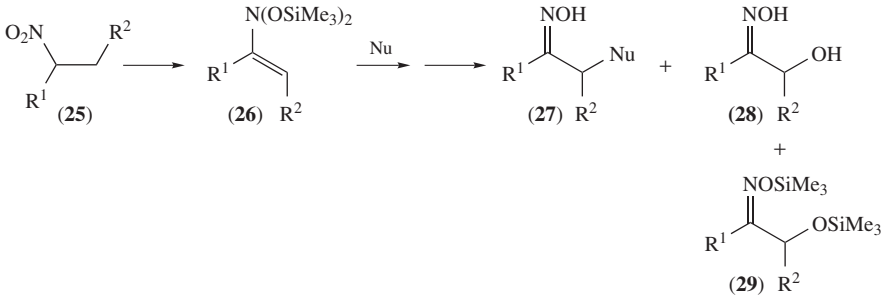

SCHEME 20

Oximes **28** are interesting precursors to β-amino acids, as well as different heterocyclic systems, so it is advantageous to develop the synthesis of the oximes **28** maximizing the side process shown in Scheme 20. This problem was solved in the earlier paper, which dealt with the double silylation of **26** with Me_3SiOTf/Et_3N, but the yields of target derivatives were modest as a rule[55].

Very recently, Ioffe and coworkers[56] have developed a new convenient two-step procedure for the conversion of **26** to **28** via intermediate *N*,*N*-bis(siloxy)enamines **29** (Scheme 21). It was observed that $Zn(OTf)_2$ is the most effective catalyst, whereas the use of chlorine-containing Lewis acids leads to the formation of the corresponding chloro derivative, as the product.

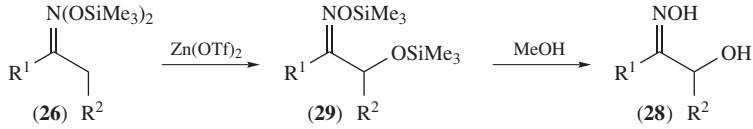

R^1 = H, Me, Ph, Bn, COOMe; R^2 = H, Me; R^1R^2 = -$(CH_2)_4$-

SCHEME 21

D. Nitrite Oxidation as a Means for Obtaining Oximes

In a paper published in the early 1950s Touster[57] found that sodio derivatives of many alkyl-substituted heteroaromatic compounds or of allyl-substituted benzenes **30** can be oximated with alkyl nitrites in refluxing anhydrous liquid ammonia at atmospheric pressure according to Scheme 22.

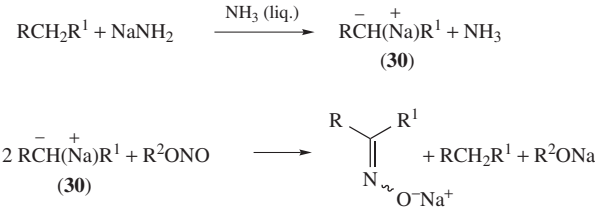

R = heteroaromatic, Ph; R^1 = H, Me, allyl; R^2 = lower alkyl

SCHEME 22

Subsequently, Kato and Goto[58] have reported the synthesis of 2- and 4-pyridinecarboxaldoximes from 2- and 4-picoline with potassium amide and amyl nitrite in liquid ammonia at −33 °C, although they failed to obtain either of these oximes when the reaction was carried out with sodium amide in liquid ammonia at room temperature in a sealed tube. Finally, in 1964, alkyl-substituted heteroaromatic compounds and allyl-substituted benzenes were oximated in liquid ammonia at −33 °C with sodamide and an alkyl nitrite[59].

The preparation of oximes from olefins is a valuable approach for the synthesis of nitrogen-containing compounds such as amino acids and heterocycles. Okamoto and colleagues[60] have reported that a catalytic reduction–nitrosation of styrenes **31** with ethyl nitrite and tetrahydroborate anion by the use of bis(dimethylglyoximato)cobalt(II) complex afford the corresponding acetophenone oximes **32** (Scheme 23).

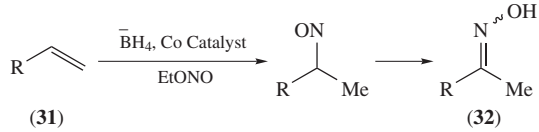

R = Ph, XC_6H_4 (X = *p*-Cl, *p*-OMe, *p*-NO_2, *o*-Cl, *o*-Me)

SCHEME 23

Sugamoto and colleagues[61] have attempted the reduction–nitrosation of the conjugated olefins **33** by the use of *t*-butyl nitrite instead of oxygen (Scheme 24). Various olefins such as styrenes, α,β-unsaturated carbonyl compounds and $\alpha,\beta,\gamma,\delta$-unsaturated carbonyl compounds were directly converted to the corresponding acetophenone oximes, α-hydroxyimino carbonyl compounds and γ-hydroxyimino-α,β-unsaturated carbonyl compounds in good or moderate yields by reduction–nitrosation with *t*-butyl nitrite and triethylsilane in the presence of cobalt(II) porphyrin as a catalyst (Scheme 24).

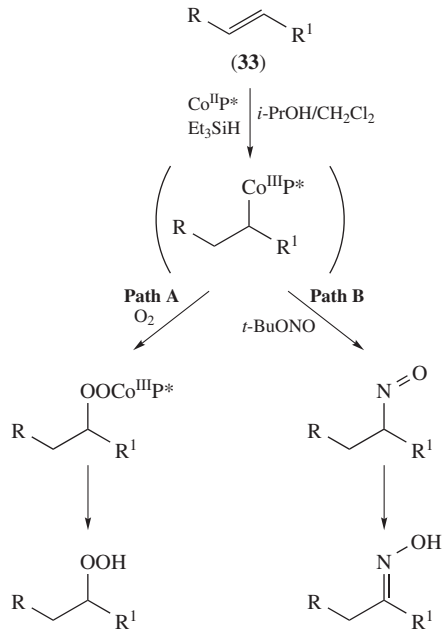

R = alkyl; R^1 = aryl, COR^2, CH=CHCOR^2; R^2 = H, Me, Et, Bu
P* = Porphyrin

SCHEME 24

The combined use of 3.0 equivalents of *t*-butyl nitrite and 3.0 equivalents of triethylsilane with **34** was found to be required for the complete consumption of **34**. Under these conditions, oxime **35** was obtained in 91% yield along with 2% yield of ketone **36** (Scheme 25).

More than a century ago, Fileti and Ponzio reported that 1,2-diketones can be prepared by treating α-methylene ketones with sodium nitrite in aqueous HCl[62]. However, this procedure has been limited to a few applications of water-soluble substrates.

In a very interesting paper, Rüedi and colleagues[63] have presented a convenient α-oximation method that allows for the selective preparation of 1,2-dione monoximes **38a**, **40a**, **41a** and/or their hydrolyzed 1,2-diketone derivatives **38b**, **40b**, **41b** simply by using the appropriate amount of the *in situ* generated nitrosyl chloride and ketones **37** or **39** (Scheme 26; route a or b).

The versatility and high efficiency coupled with the synthetic significance of 1,2-dicarbonyl compounds make this procedure a powerful tool in organic synthesis. In

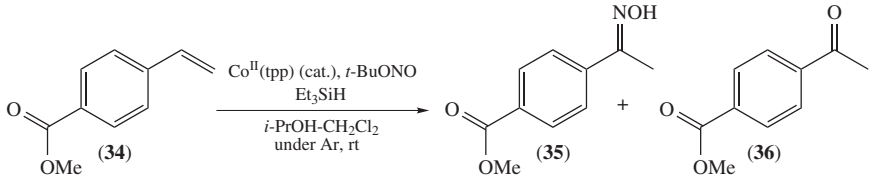

tpp: 5,10,15,20-tetraphenylporphyrine

SCHEME 25

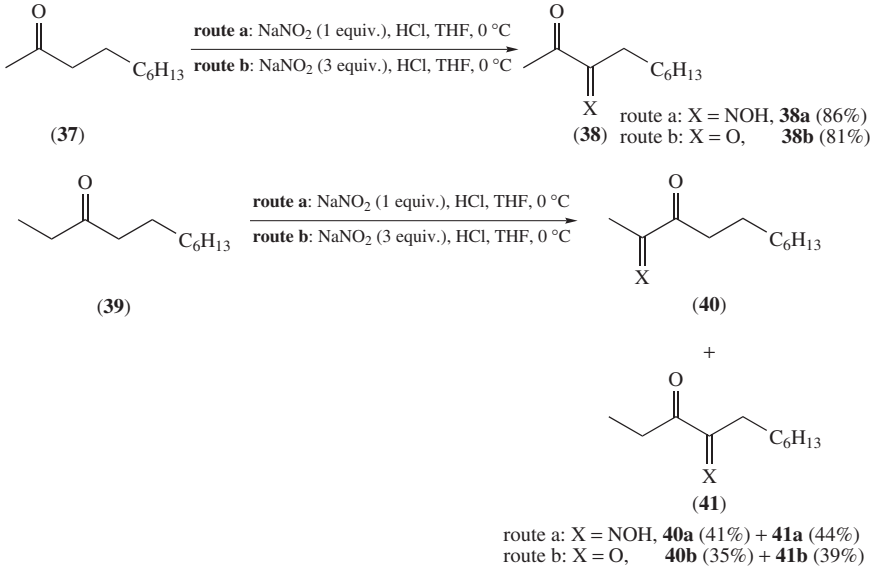

SCHEME 26

addition, the reaction can be carried out on a preparative scale with no significant change in yield, rendering this procedure also promising for industrial applications.

Diketo oxime **43** (Scheme 27) find extensive use in organic synthesis. These compounds are useful building blocks in five-membered heterocyclic chemistry. These oximes can be used for the synthesis of pyrroles[64], thiazoles[65], oxazoles[66] and pyrazoles[67]. The diketo oxime **43** was synthesized in high yield by addition of an aqueous solution of sodium nitrite to a 0 °C solution of 1-benzoylacetone **42** in AcOH[68].

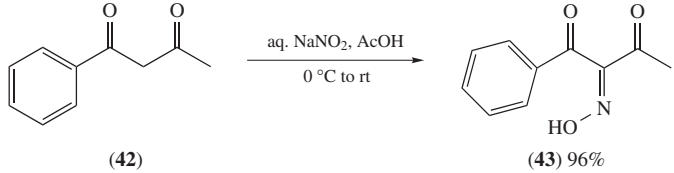

SCHEME 27

Acylation is one of the most fundamental and useful reactions in organic synthesis and is normally achieved by the reaction either with carboxylic acid derivatives and organometallic compounds or with masked acyl anions and alkyl halides.

Recently, Kim and colleagues[69] have described a new efficient method for the preparation of α-keto esters **48** via a free-radical acylation approach using (phenylsulfonyl) methoxycarbonyl oxime ether **46** as carbonyl equivalent radical acceptor (Scheme 28). The oxime **46** was conveniently prepared from readily available methylphenylsulfonyl acetate **44** by a two-step sequence (via oxime **45**) as shown in Scheme 28. Nitrosation of **44** with isoamyl nitrite in the presence of sodium methoxide gave oxime **47** in 78% yield.

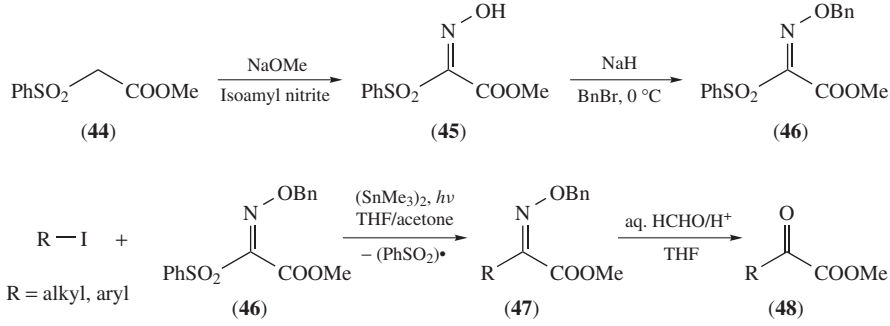

SCHEME 28

This approach involves additions of alkyl radicals to C=N bonds and subsequent β-expulsion of the phenylsulfonyl group (as a radical) which react with bis(trialkyl)tin to propagate a chain. The phenylsulfonyl group lowers the energy of the LUMO of the radical acceptor, increasing the rate of addition of alkyl radicals[70].

In a communication by Tanimoto and coworkers[71], ketene *O*-alkyl *O′*-trimethylsilyl acetals **49** provide either α-nitroso esters **50** or their oximes **51** on reaction with nitric oxide or isoamyl nitrite in the presence of titanium(IV) chloride (Scheme 29). These reactions seem to provide a relatively direct way to introduce a nitrogen substituent at the α-carbon atom of carboxylic esters.

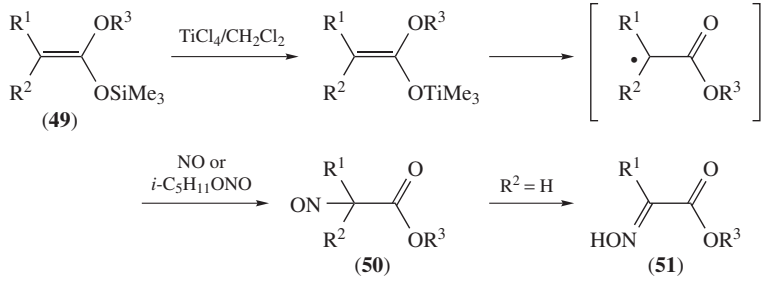

R^1 = Me, Et, Ph; R^2 = Me, Ph; R^3 = Me, Et

SCHEME 29

ε-Caprolactam is one of the monomers most widely used for the production of nylon-6. Nowadays, ε-caprolactam[72] is produced by a Beckmann rearrangement of cyclohexanone oxime or by nitrosation of cyclohexanecarboxylic acid with $NOHSO_4$ (Route C, Scheme 30).

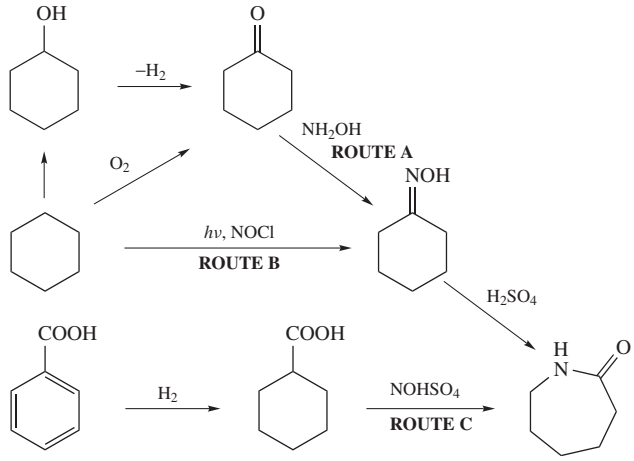

SCHEME 30

Currently, cyclohexanone oxime is synthesized starting from cyclohexanone and hydroxylamine (Route A, Scheme 30) or by photonitrosation of cyclohexane with NOCl (PNC process, Route B, Scheme 30). Of these approaches, Route A is most often employed and accounts for about 70% of the total production of ε-caprolactam worldwide. However, this method has several drawbacks[73].

Ishii and coworkers[74], in the course of their studies on the *N*-hydroxyphthalimide (NHPI)-catalyzed functionalization of cyclohexane, have observed that the nitrosation of cyclohexane **52** by *tert*-butyl nitrite **53** can be successfully achieved without photoirradiation and under halogen-free conditions by using NHPI as a catalyst (Scheme 31).

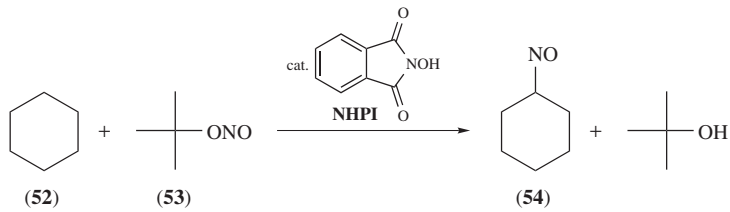

SCHEME 31

This procedure is the first example of a catalytic transformation of **52** into **54** under relatively mild conditions (at 80 °C for 2 h). In this process the majority of **53** is converted into *tert*-butyl alcohol (see below). Since *tert*-butyl alcohol is known to react with NO_2 or with sodium nitrite to produce **53**, reagent **53** may be regenerated from the *tert*-butyl alcohol formed (Scheme 32).

A plausible reaction pathway for the reaction of **52** with **53**, catalyzed by NHPI, is showed in Scheme 33.

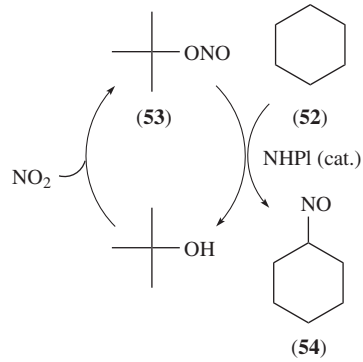

SCHEME 32

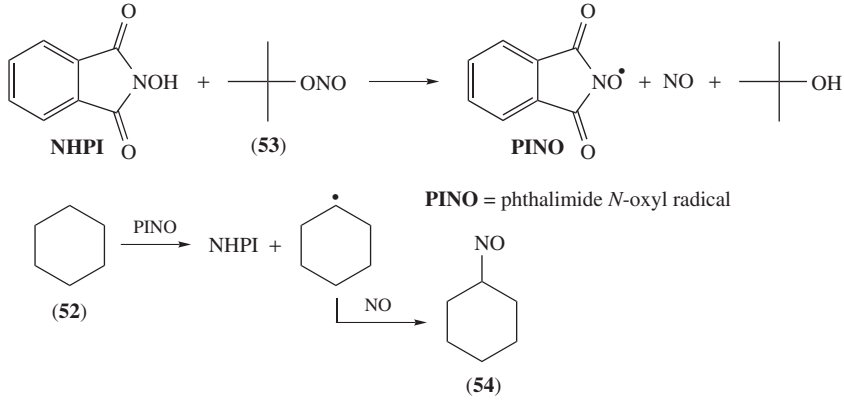

SCHEME 33

In a recent paper, Kim and Ryu[75] have demonstrated that the reaction of some stable nitrile oxides with uracil nucleosides cleanly gave products of l,3 addition (Scheme 34). The 5-aroylpyrimidine nucleoside oximes **57**–**64** were prepared in moderate to good yield by the reaction of hydroximoyl chlorides **55a**–**e** with the corresponding pyrimidine nucleosides **56a**–**d**.

The nitrile oxides were generated *in situ* from the corresponding hydroximoyl chlorides **55a**–**e**. From these reactions, only the l,3 addition products **57**–**64** were obtained. No products of cycloaddition could be isolated.

Nitrile oxides are widely used as dipoles in cycloaddition reactions for the synthesis of various heterocyclic rings. In order to promote reactions between nitrile oxides and less reactive carbon nucleophiles, Auricchio and coworkers[76] studied the reactivity of nitrile oxides towards Lewis acids. They observed that, in the presence of gaseous BF_3, nitrile oxides gave complexes in which the electrophilicity of the carbon atom was so enhanced that it could react with aromatic systems, stereoselectively yielding aryl oximes **65** and **66** (Scheme 35)[77].

Pyridine *N*-oxides are potential starting materials for the synthesis of a multitude of target molecules. Rapid addition of Grignard reagents to pyridine *N*-oxides **67** under mild conditions gave stereodefined dienal oximes **68** in good to excellent yields (Scheme 36)[78].

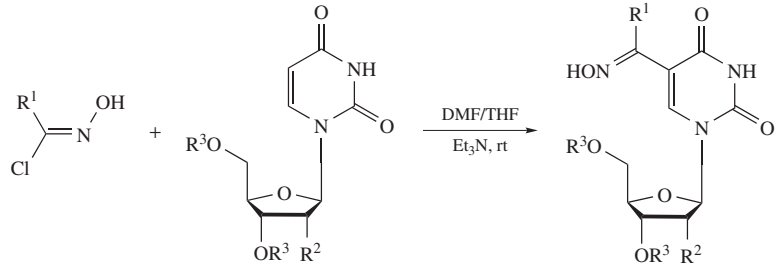

(**55a**) $R^1 = 2,6\text{-}Cl_2C_6H_3$
(**55b**) $R^1 = 2\text{-}Cl\text{-}6\text{-}FC_6H_3$
(**55c**) $R^1 = 2,6\text{-}F_2C_6H_3$
(**55d**) $R^1 = 2,3,5,6\text{-}F_4C_6H$
(**55e**) $R^1 = 2,3,6\text{-}Cl_3C_6H_2$

(**56a**) $R^2 = OH$, $R^3 = H$
(**56b**) $R^2 = OBz$, $R^3 = Bz$
(**56c**) $R^2 = H$, $R^3 = Ac$
(**56d**) $R^2 = H$, $R^3 = H$

(**57**) $R^1 = 2,6\text{-}Cl_2C_6H_3$, $R^2 = OH$, $R^3 = H$
(**58**) $R^1 = 2,6\text{-}Cl_2C_6H_3$, $R^2 = OBz$, $R^3 = Bz$
(**59**) $R^1 = 2,6\text{-}Cl_2C_6H_3$, $R^2 = H$, $R^3 = Ac$
(**60**) $R^1 = 2,6\text{-}Cl_2C_6H_3$, $R^2 = H$, $R^3 = H$
(**61**) $R^1 = 2\text{-}Cl\text{-}6\text{-}FC_6H_3$, $R^2 = H$, $R^3 = H$
(**62**) $R^1 = 2,3,5,6\text{-}F_4C_6H$, $R^2 = H$, $R^3 = H$
(**63**) $R^1 = 2,6\text{-}F_2C_6H_3$, $R^2 = H$, $R^3 = H$
(**64**) $R^1 = 2,3,6\text{-}Cl_3C_6H_2$, $R^2 = H$, $R^3 = H$

SCHEME 34

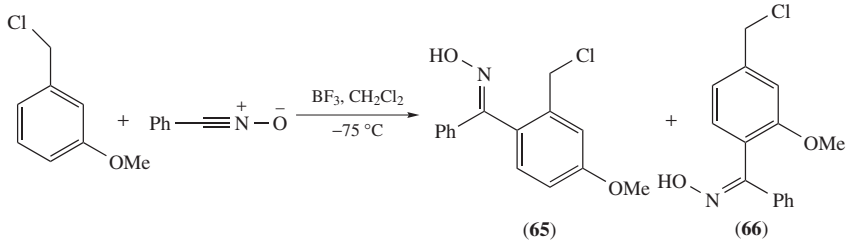

(**65**) (**66**)

SCHEME 35

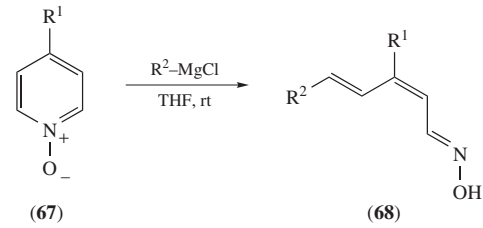

(**67**) (**68**)

R^1 = Cl, OBn; R^2 = Ph, 2-naphthyl, 2-thienyl

SCHEME 36

E. Oximes via Radical Reactions

Recent advances in radical reactions have greatly benefited from the efficiency of organotin reagents as mediators. Radical reaction of alkyl iodides with trifluoromethyl phenylsulfonyl oxime ether **69** and hexamethylditin at 300 nm in benzene afforded the corresponding trifluoromethyl oxime ethers **70** in high yields (Scheme 37)[79].

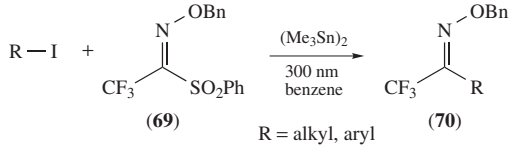

SCHEME 37

F. Polymer-bound Oximes in Solid-phase Synthesis

In recent years, combinatorial synthesis has rapidly emerged as a powerful methodology for the preparation of a wide variety of diverse molecular structures. The generation of non-oligomeric, small-molecule libraries has especially attracted great attention for new drug lead discovery and optimization due to their preferable physiochemical and pharmacokinetic properties[80].

In general, solid-phase synthesis, rather than solution-phase synthesis, can be the preferred method for the generation of combinatorial libraries because of the greater ability to automate a solid-phase protocol, primarily due to the use of excess reagents in solution to effect cleaner reactions and to the ease of workup by simple filtration. The solid-phase method of peptide synthesis has had many notable successes. However, the preparation of peptides containing more than 20 amino acids in length using the solid-phase technique often causes major problems in that very extensive purification of the final product is needed.

A series of polystyrene-bound substituted benzophenone oximes **71a–d** have been synthesized and tested by DeGrado and Kaiser as potential supports for the solid-phase preparation of protected peptide fragments (Scheme 38)[81].

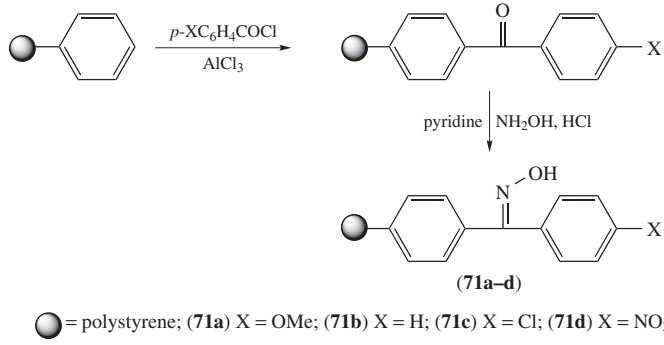

SCHEME 38

The polymer-bound *p*-nitrobenzophenone oxime (**71d**) has been found to be a suitable support for stepwise peptide synthesis. Protected peptides can be assembled on **70d** by coupling and deprotection steps similar to those employed in the usual Merrifield solid-phase procedures (Scheme 39). Cleavage of peptides from **71d** can be accomplished with hydrazine and amino acid esters under mild conditions, which do not affect benzyl ester side-chain protecting groups.

The oxime **71d** has several advantages over other resins, since the protected peptide segment can be cleaved by aminolysis under conditions which do not affect benzyl ester protecting groups. Moreover, the whole procedure is compatible with the Boc group employed for α-amino protection. The synthesis of several peptides using **71d** has been

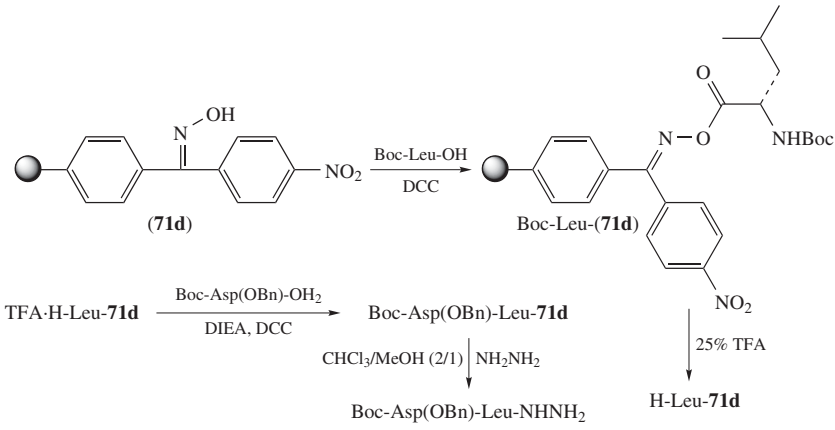

SCHEME 39

shown to be essentially free from racemization. A further advantage is that acetic acid has been reported to be a potent catalyst for the aminolysis of oxime esters[82].

Nakagawa and Kaiser[83] have further increased the versatility of this polymer in peptide synthesis by use of 1-hydroxypiperidine to cleave the *C*-terminal amino acid anchored on the solid support (Scheme 40).

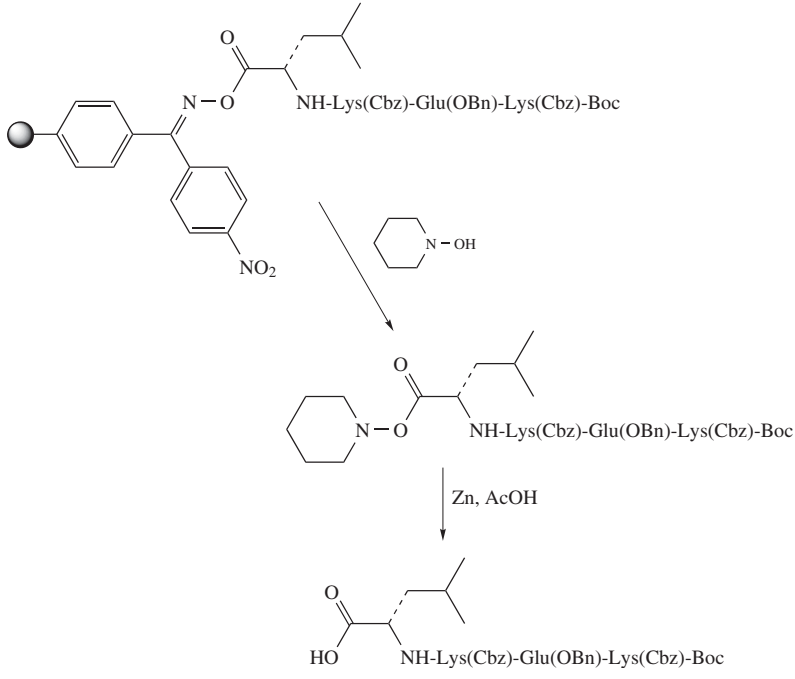

SCHEME 40

Although resin-to-resin transfer reactions were demonstrated as early as 1975, they have had very limited applications for preparative purposes. In Scialdone's group[84] it was demonstrated that, under optimized conditions, acyl- and aminoacyl-transfer reactions proceed in good yield and high chemical and stereochemical purity. The authors have described a convergent approach to solid-phase synthesis in which two fragments of a molecule are synthesized on independent supports (**72** and **73**) and then condensed in a key resin-to-resin transfer reaction (Scheme 41). This approach has been utilized for the synthesis of ureas **75** (via **74** after cleavage from the solid support) by transferring acyl groups and aminoacyl groups from *p*-nitrophenyl(polystyrene)ketoxime resin to amino-acid-functionalized Wang resins.

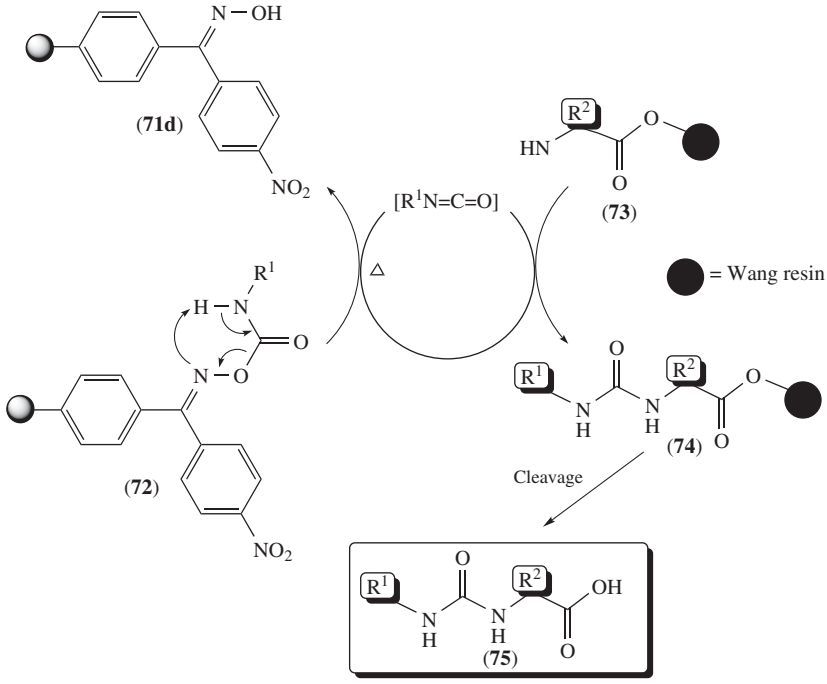

SCHEME 41

Recently, Scialdone and colleagues[85] have employed phosgenated *p*-nitrophenyl(polystyrene) ketoxime (Phoxime, **76**) resin in the synthesis (via **77** and **78**) of acyclic and heterocyclic amino-acid-derived ureas **79** too (Scheme 42). Resin **75** was first reacted with an amino acid and TMSCl in pyridine, and the resulting carbamate acid resin **77** was then coupled with an amine under standard carbodiimide protocol (HOBt/DIC in DMF) to obtain the carbamate amide resin **79**.

Integrin receptors are a family of heterodimeric transmembrane glycoproteins, which are involved in cell–cell and cell–matrix interactions. The search for inhibitors of integrin receptors led to the discovery of several cyclic and linear arginine–glycine–aspartate (RGD) sequences containing peptidic constructs showing potent antagonistic activity[86].

Five novel RGD peptides **81** containing either one or twice furanoid SAAs **80** were recently synthesized via an efficient solid-phase strategy based on Kaiser's oxime resin **71d** (Scheme 43).

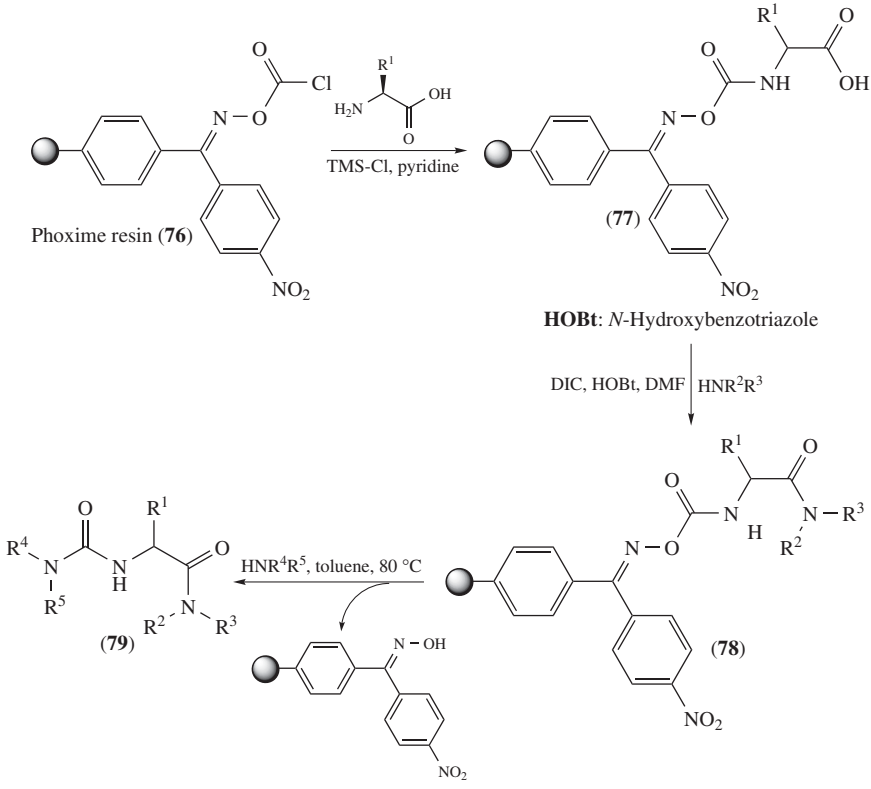

SCHEME 42

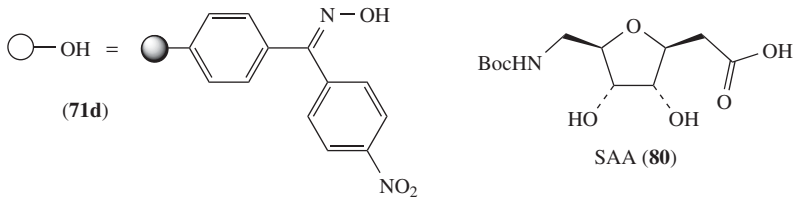

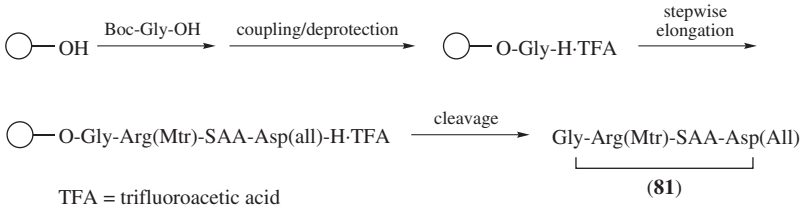

SCHEME 43

Design and development of synthetic protocols for oligonucleotide conjugation have recently attracted considerable research interest[87,88]. The most common approach used to prepare oligonucleotide (ODN) conjugates involves separate preparation and purification of the oligonucleotide followed by their solution-phase coupling. Oxime linkages formed by the reaction of an aldehyde with an aminooxy group remain the most widely used chemical linkage for ODN conjugation. This is due to the fact that reactions leading to the formation of oxime bonds are chemoselective and give high coupling efficiency.

Thus, a new and convenient procedure has been developed by Defrancq and coworkers[89] for the synthesis of 3′-oligonucleotide conjugates **83** through the formation of glyoxylic oxime bonds (Scheme 44). This has been achieved by using a novel solid support **82** for ODN synthesis. Support **82** was conveniently prepared from a commercially available serine derivative in a few steps. The glyoxylic oxime bonds showed higher stability than aldoxime bonds at acidic to neutral pH but lower stability at alkaline pH.

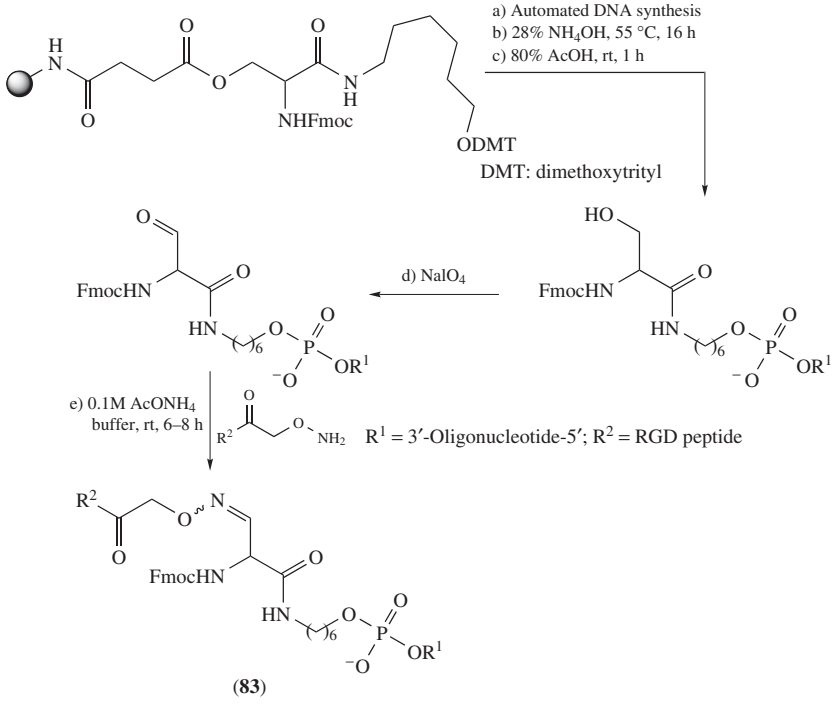

SCHEME 44

Solid-phase organic synthesis of heterocycles plays an increasing role in modern drug discovery[90]. In 1999 Lepore and Wiley[91], during an attempt to identify new ligands for biological targets, developed an efficient method for the solid-phase synthesis of 3-aminobenzisoxazoles **86** (Scheme 45). Their approach involves the first application of the Kaiser oxime **71d** resin to S_NAr reactions and can be used successfully with 2-fluorobenzonitriles **84** containing a variety of electron-withdrawing/-donating groups. The intermediate aryl oxime linkage in **85** is stable to anhydrous acid and can support Boc-deprotection and amidation reactions, holding promise for compatibility with a broader variety of organic transformations.

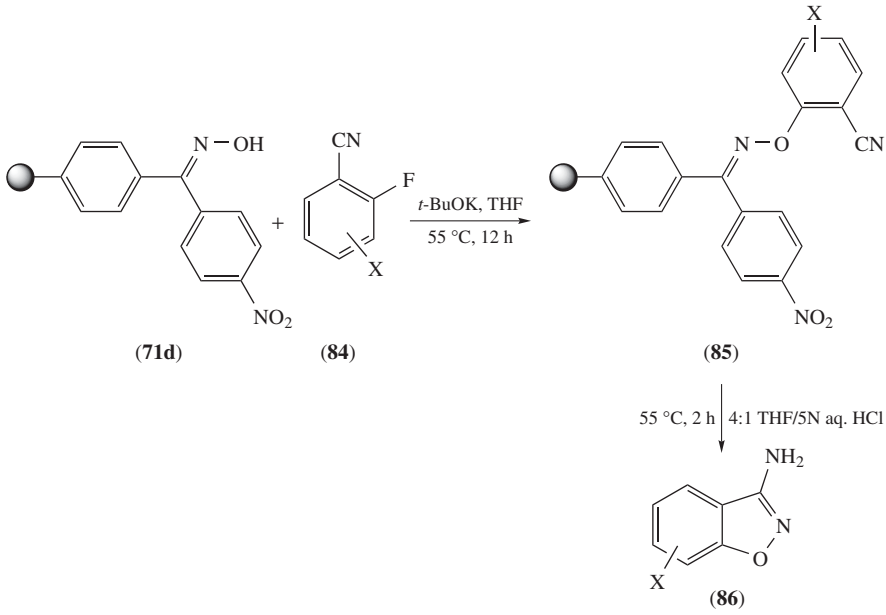

SCHEME 45

Sulfahydantoins **87** and **88** are analogues of hydantoins and provide heterocyclic scaffolds with a great potential for the construction of bioactive compounds. A total of 28 derivatives, with crude purity generally higher than 85%, were prepared by parallel synthesis using an oxime resin as a solid support (Scheme 46)[92]. The results constitute the first report of successful Mitsunobu reactions and reductive alkylations on the oxime resin.

II. SYNTHESIS OF HYDROXAMIC ACIDS

A. Introduction

Hydroxamic acids of general structure R−CO−NH−OH, having R as an organic residue, have been known since 1869 with the discovery of oxalohydroxamic acid by Lossen[93]. Despite this, researches on these compounds were lacking until the 1980s, after which an enormous amount of information has accumulated with respect to their biomedical applications, synthesis, and the determination of the structures of their metal complexes[94].

Complexation of metal ions by hydroxamic acids is the starting point of a number of analytical determinations[95]. All hydroxamic acids, in acid solutions, react with ferric chloride to give rust brown complex salts **89** (Scheme 47). These colored complexes form the basis for the sensitive qualitative and quantitative determination of carboxylic acids and their derivatives too.

The authors do not intend to review all the reactions that have been reported for the synthesis of hydroxamic acids, but rather to limit the section to the most relevant studies which have appeared in the literature in recent years.

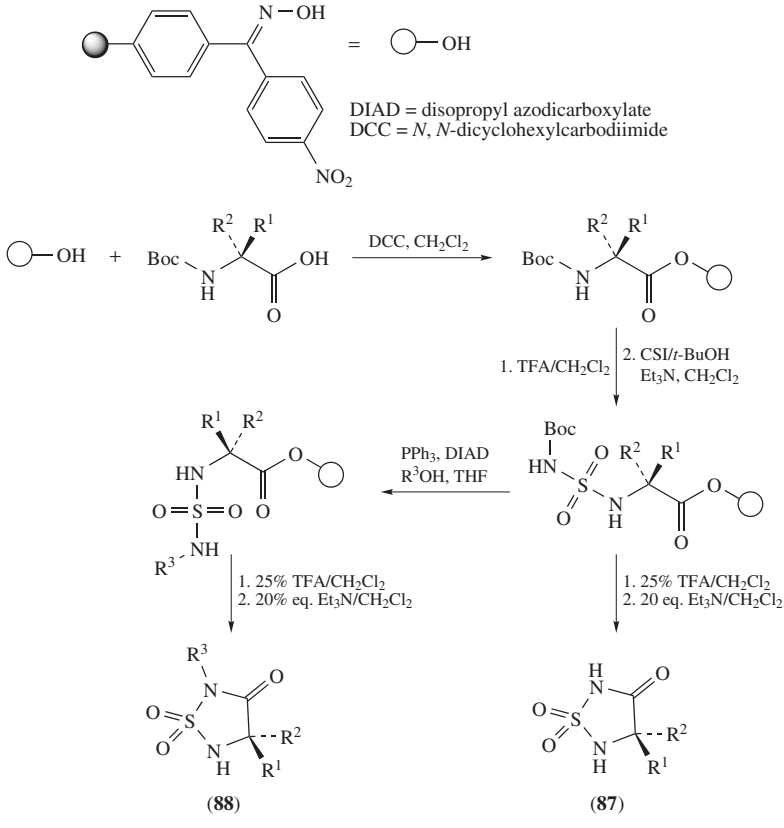

SCHEME 46

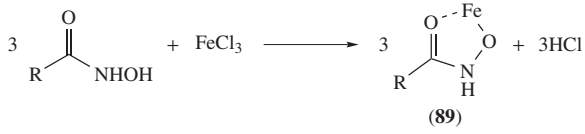

SCHEME 47

B. Synthesis of Hydroxamic Acids from Carboxylic Acids

The *N*-hydroxycarboxamide group is a key fragment of many siderophores so that a convenient synthesis of this group is crucial for further progress. A variety of methods have been attempted for the preparation of hydroxamic acids starting from carboxylic acids. Although some of these methods are quite efficient for the preparation of substituted hydroxamic acids, the preparation of the parent compound is still a problem and yields are often moderately unacceptable, in part due to the low solubility of the parent hydroxylamine hydrochloride in organic solvents.

In 1985, Nakonieczna and coworkers[96] observed that *N*,*N*-dimethylchloromethaniminium chloride **91** formed from *N*,*N*-dimethylformamide and oxalyl dichloride is an

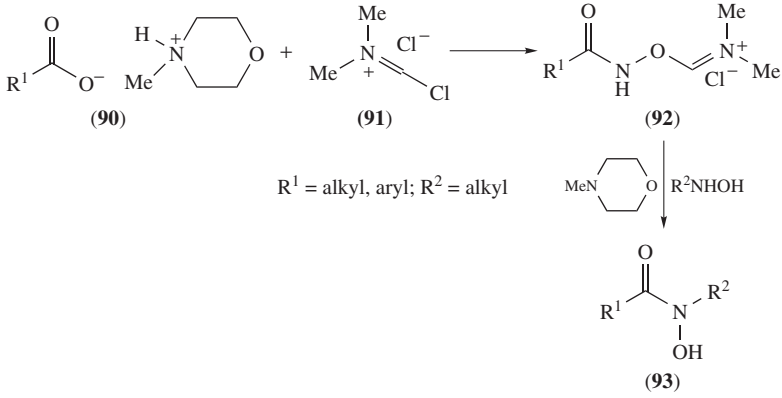

SCHEME 48

efficient reagent for the synthesis of *N*-substituted hydroxamic acids **93** from carboxylic acids **90** and *N*-substituted hydroxylamines **92** in the presence of a base (Scheme 48).

Nowadays, the most economical way of preparing hydroxamic acid derivatives is the reaction of hydroxylamine with acid chlorides or esters[97]. Unfortunately, the preparation of acid chlorides is often tedious. In addition, it is very difficult to avoid further acylation during the reaction with hydroxylamine.

It is not possible to carry out the reaction between hydroxylamine and an ester under neutral conditions (Scheme 49) since it always requires a pH >10. Hence, this method is not suitable for ester derivatives that contain halides, and other base-sensitive groups.

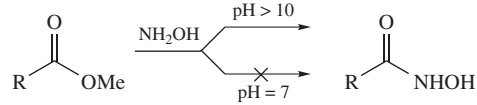

SCHEME 49

In 2000, Reddy and colleagues[98] developed a one-step conversion of carboxylic acid to hydroxamic acid under neutral pH conditions using ethyl chloroformate as an activating reagent (Scheme 50).

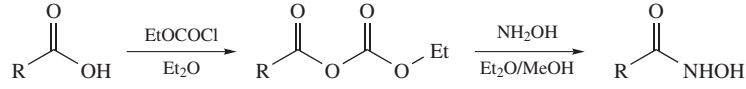

SCHEME 50

This simple, selective and efficient method was applied to a wide range of aliphatic/aromatic carboxylic acid derivatives that contain hydroxyl-, halo-, ester and other base-sensitive groups as substituents.

Benzotriazoles are neutral acylating agents, successfully used for the preparation of amides, oxamides and hydrazides[99, 100]. The acylbenzotriazoles **95a–d** are prepared from carboxylic acids **94a–d** by reaction with 1-methanesulfonyl-1*H*-benzotriazole (Scheme 51). Reaction of 1-benzoyl-1*H*-benzotriazole with hydroxylamine hydrochloride in the

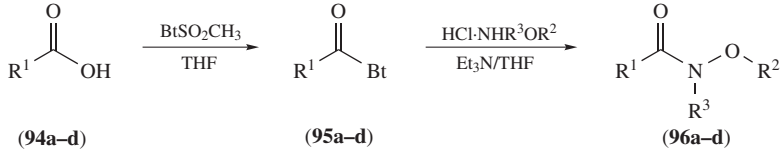

(**94a–d**) (**95a–d**) (**96a–d**)

(**a**) R^1 = Ph
(**b**) R^1 = 2-furyl
(**c**) R^1 = 2-pyridyl
(**d**) R^1 = *n*-butyl

R^2 = H, Me, Et, Bn; R^3 = H, Me
Bt = Benzotriazole

SCHEME 51

presence of potassium *tert*-butoxide gives the desired hydroxamic acid **96a** in only 17% yield[101].

Changing the base to triethylamine improves the yield of benzoylhydroxamic acid (**96a**) up to 91%; the purification required column chromatography. Independently of the substituent in both *N*-acylbenzotriazole and hydroxylamine, the desired *O*-alkyl, *N*-alkyl and *O*,*N*-dialkyl hydroxamic acids were obtained as sole products as a result of nucleophilic displacement of the benzotriazolyl moiety by the hydroxylamine nitrogen.

Although the simplest route to prepare hydroxamic acid derivatives remains the reaction of hydroxylamine with acid chlorides, this last method cannot be applied to all *N*-protected-α-amino acids. The synthesis of Fmoc-protected amino acid hydroxamates represents the only exception to this rule[102]. In fact, Fmoc-amino acid hydroxamates **98** can be synthesized by the acylation of hydroxylamine using Fmoc-amino acid chlorides **97** in the presence of MgO (Scheme 52). The route is simple, efficient, and affords good yields of products.

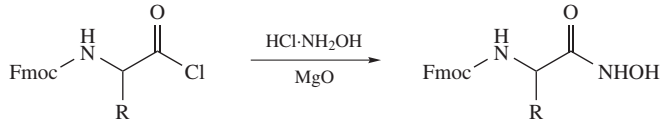

(**97**) (**98**)

SCHEME 52

In this context, Giacomelli and coworkers[103] have reported a new simple, mild, and high-yielding one-flask synthesis of hydroxamic acids (**101**) from carboxylic acids and *N*-protected amino acids (**99**) that uses the very cheap 2,4,6-trichloro-1,3,5-triazine **100** (cyanuric chloride) as a coupling agent (Scheme 53). The method allows the preparation of hydroxamic acids in a single-step ('one flask') reaction. Moreover, the procedure is compatible with the common *N*-protecting groups (Boc, Cbz and Fmoc) and no deprotection was noted even with the less stable Boc-*N*-protected amino acids.

The triazine by-products are easily removed by this simple aqueous workup. The reaction is not fast and requires from 6 to 12 h for completion in most cases. In addition, this method can be also successfully applied on a large scale. The yields are high in all cases examined, and no *O*-acylated or di- and triacylated products were found in the reaction mixture. The method is compatible with the common *N*-protecting groups and no significant racemization of the chiral center on the R-substituted carbon atom occurred during the synthesis.

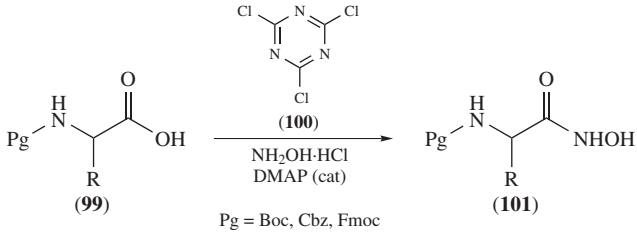

SCHEME 53

Despite continuous progress in amide bond formation, the acylation of hydroxylamine under carbodiimide promotion is often contaminated by *N*,*O*-diacylation even with substoichiometric amounts of acids. Appendino and colleagues[104] have developed a practical solution to the problem by combining the *in situ* activation of carboxylic acids **102** with the cyclic phosphonic anhydride PPAA (**103**), and the generation of hydroxylamine from its corresponding hydrochloride to form **104** (Scheme 54).

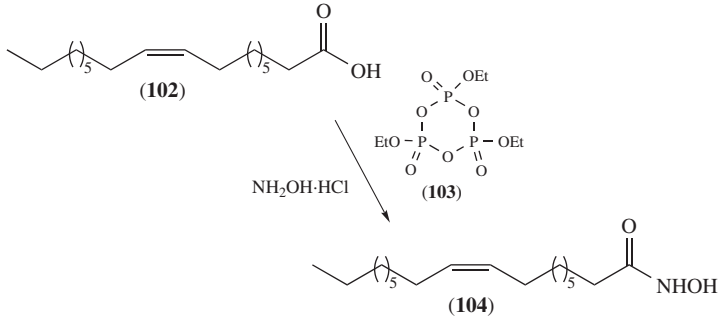

SCHEME 54

This experimentally simple one-pot operation addresses the issue of polyacylation without resorting to a large excess of hydroxylamine or to protection.

The authors have also observed that reverse addition of a carboxylic acid to a mixture of PPAA, hydroxylamine and TEA gave a lower hydroxamate yield (16% with oleic acid) compared to the direct addition, suggesting a certain competition between carboxylate and hydroxylamine for phosphonylation.

Although the procedures for the synthesis of hydroxamic acids are well documented, the methods for the synthesis of α-chloro hydroxamic acids are limited to a few examples[105, 106]. However, these compounds have synthetic value, as they are interesting starting materials for the synthesis of intermediate aziridinones used *in situ*, as precursors to α-hydroxy acids and α-amino acids[107].

The reaction of dicyano epoxides **105** with hydroxylamines hydrochlorides **106** in acetonitrile represents a direct route via **107** to a number of new and higher α-chloro hydroxamic acids and their derivatives **108** (Scheme 55)[108].

Multicomponent reactions[109] have recently become one of the favored methods to prepare pharmacologically important compounds. Ugi condensations with *O*-protected hydroxylamines have been successfully performed in THF using $ZnCl_2$ as activating agent (Scheme 56). This synthetic strategy opens up the route to a very convergent assembly of 'internal' hydroxamic acid derivatives (*N*-acyl-*N*-hydroxypeptides **109**)[110].

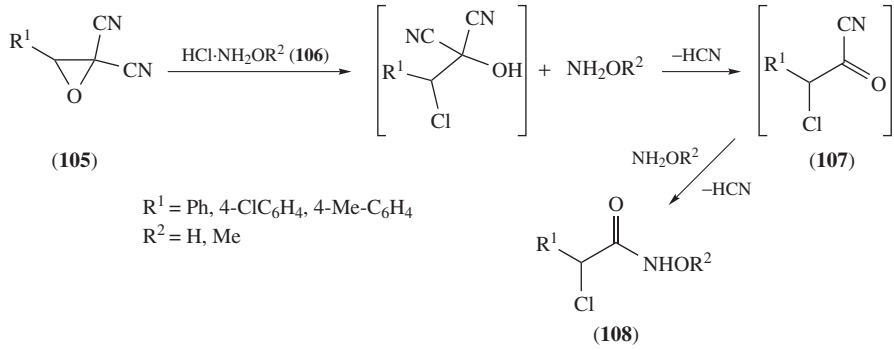

SCHEME 55

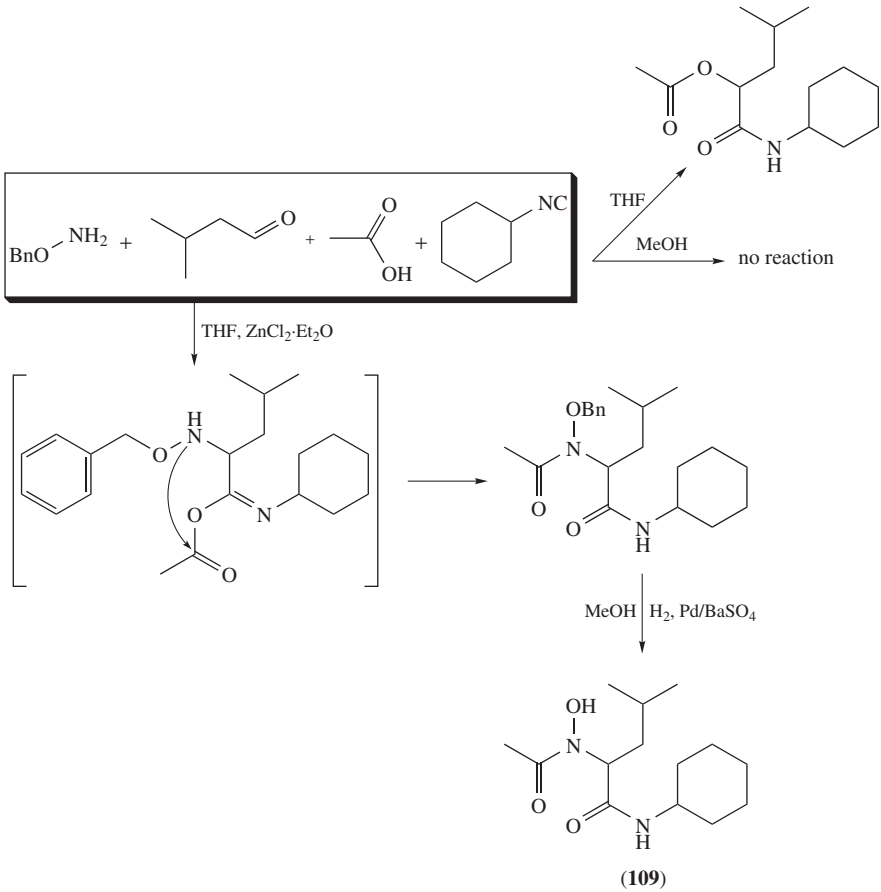

SCHEME 56

Very recently, Shinde and colleagues have prepared the interesting amide coupling reagent diethyl 2-phenylbenzimidazol-1-yl phosphonate **110** and demonstrated that it is an efficient reagent for the preparation of *O*-alkyl hydroxamic acids too (Scheme 57)[111]. The *O*-alkyl hydroxamic acids of *N*-protected amino acids were also synthesized.

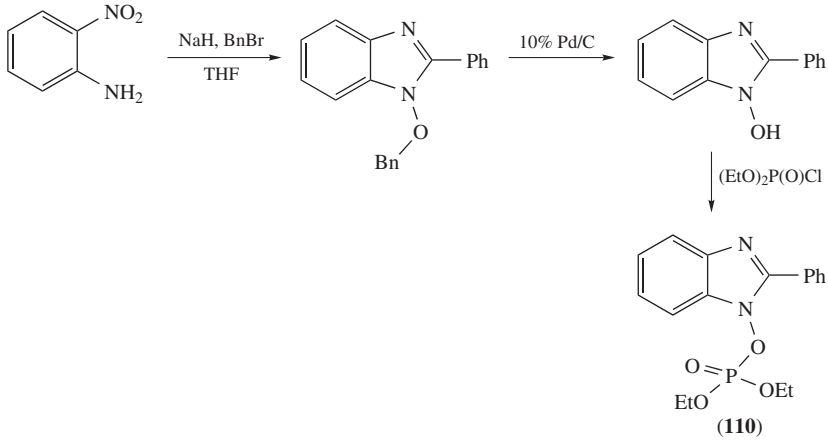

(**110**)

SCHEME 57

C. Synthesis of Hydroxamic Acids from Esters

The direct solution-phase hydroxyamination of esters is commonly accomplished by a two-step preparation of the potassium salt of hydroxylamine followed by the addition of the ester in alcohol[112]. Alternatively, the stepwise saponification of the ester to the acid is followed by activation of the acid as acyl chloride or mixed anhydride and then by quenching with an *O*-protected hydroxylamine analogue[113]. In special cases, the hydroxyamination of ester substrates has been achieved via enzymatic methods[114] or, for more reactive esters, by treatment with excess hydroxylamine in alcohol[115].

Ho and coworkers[116] have observed that the addition of small amounts of solid KCN (0.2 equivalents) can effectively accelerate the formation of hydroxamic acids **112** from methyl esters **111** (Scheme 58). The authors suggested that this reaction proceeds through an acylcyanide intermediate followed by nucleophilic substitution by 50% aqueous hydroxylamine at room temperature. The use and advantage of this methodology have been demonstrated for both solution-phase and solid-phase applications.

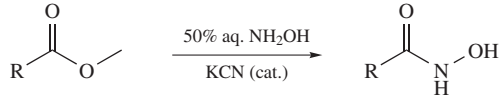

(**111**) R = aryl, alkyl (**112**)

SCHEME 58

Zanda and colleagues[117] have developed an alternative one-step method for the synthesis of hydroxamate derivatives **114** directly from a broad range of inactivated esters **113** and the anion of *O*-benzylhydroxylamine generated *in situ* (Scheme 59).

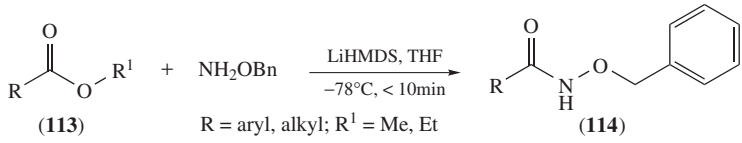

(**113**) R = aryl, alkyl; R^1 = Me, Et (**114**)

SCHEME 59

The method was successfully employed with enolizable esters, including chiral α-amino acid esters and peptides, and no trace of racemization/epimerization at the α carbon was detected.

Very recently, Mordini and coworkers[118] have overcome the problems associated with the long reaction times that are normally required for the synthesis of hydroxamic acids from esters by performing these transformations under MW irradiation. The protective groups are also well tolerated under these reaction conditions, though a partial deprotection of the *tert*-butoxycarbonyl (Boc) group was observed in the reaction with Boc-proline ester. Amidic bonds and ketals also survive without any detectable decomposition. All the reactions go to completion in about six minutes, except in the case of the conversion of Boc-protected phenylalanine methyl ester, which required longer reaction times (12 min).

Nowadays, malaria remains the world's most devastating parasitic disease. According to the World Health Organization, at least one million deaths and over 300 million acute illnesses can be attributed to malaria[119]. Leishmaniasis, which is estimated to cause 59,000 deaths each year[120], is sparked by another unrelated protozoan parasite. In the search for orally active drug candidates inhibiting the growth of *Plasmodium falciparum*[121] and *Leishmania donovani* parasites[122], the causative agents of severe malaria and visceral leishmaniasis, Hua and coworkers[123] investigated the inhibition potencies of three symmetrical bishydroxamic acids **119**–**121** (Scheme 60). Presumably, the ability of bishydroxamic acids to complex with metallic iron in hemoglobin may be responsible for antimalarial activity of these compounds.

The syntheses of the methyl esters **116**–**118** from **115** and hydroxamic acids **119**–**121** were carried out via a typical alkylation of the hydroxy function of methyl 4-hydroxybenzoate **116** followed by either reaction with hydroxylamine to provide bishydroxamic acids **119**–**121** containing an alkyl spacer between two aromatic rings.

D. Synthesis of Hydroxamic Acids from Amides

Oxazolidinone is a versatile functional group and chiral oxazolidinones, readily prepared from amino acids, are premiere auxiliaries with broad utility in synthetic chemistry[124].

Treatment of *N*-acyloxazolidinone **122** with hydroxylamines using samarium triflate as a Lewis acid gives the corresponding hydroxamic acids **123** in 50–98% yields at room temperature (Scheme 61). The conversion proceeds with a high degree of chemoselectivity and without racemization of chiral centers at the α-position to the acyl group.

The catalyst choice was based on several unique properties of the rare-earth Lewis acids: (1) ready availability, (2) a large number of triflates with varied Lewis acidity, (3) compatibility with amine nucleophiles and (4) potential for reactions in aqueous medium.

E. Synthesis of Hydroxamic Acids from Aldehydes

Formation of hydroxamic acids via the reaction of the carbonyl group of aldehydes and α-oxo acids with the aromatic or aliphatic *C*-nitroso group belongs to the small number of nucleophilic reactions of the *C*-nitroso group[125].

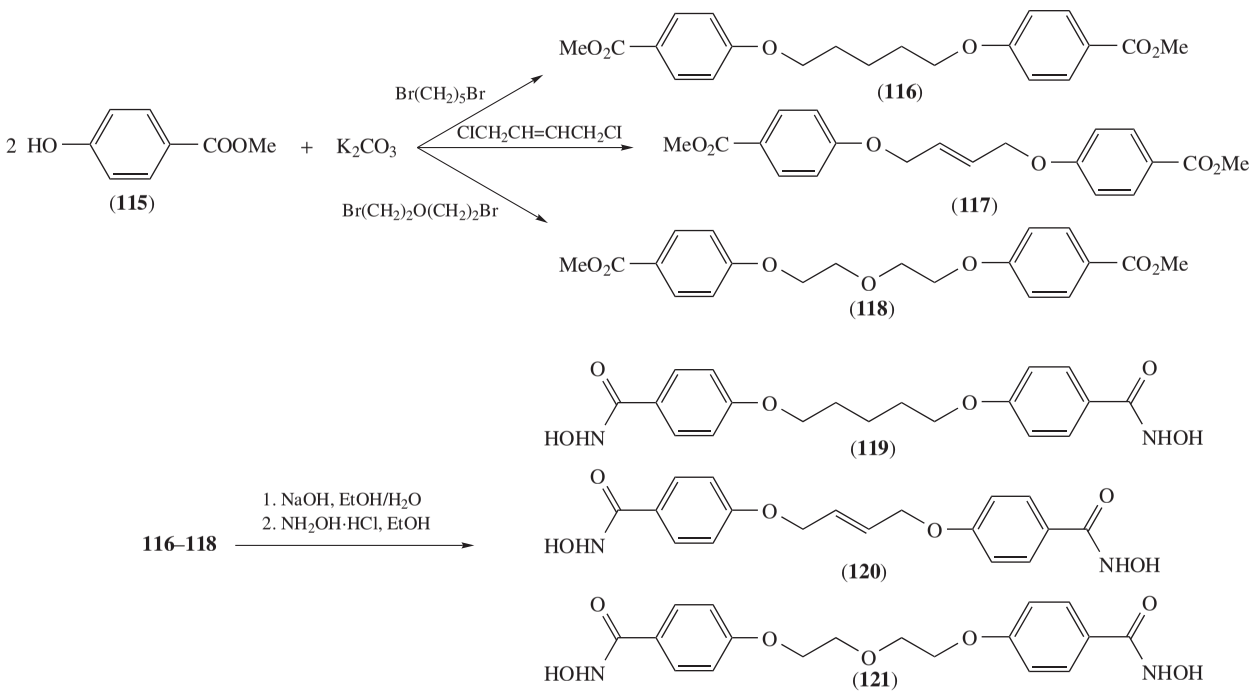
2 HO
COOMe
(115)
+ K2CO3
Br(CH2)5Br
ClCH2CH=CHCH2Cl
Br(CH2)2O(CH2)2Br
MeO2C
CO2Me
(116)
(117)
(118)
HOHN
NHOH
(119)
(120)
(121)
116–118
1. NaOH, EtOH/H2O
2. NH2OH·HCl, EtOH

SCHEME 60

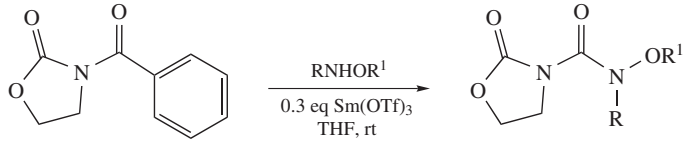

(**122**) (**123**)

R = H, Me; R^1 = H, Me, 4-MeOBn

SCHEME 61

The reactions are complex, and ordinarily the first step involves carbon–nitrogen bond formation while the final products are the corresponding hydroxamic acids.

The preparation of *N*-phenyl-substituted hydroxamic acids **125** in the reaction of formaldehyde with nitrosobenzene to give **124** is strongly catalyzed by Fe^{3+} ions, which stabilize the transition states **126** and **127** for the rate-controlling proton transfer from the carbon atom of nitrosocarbinolic cation intermediate **125** leading to the product **128** (Scheme 62)[126].

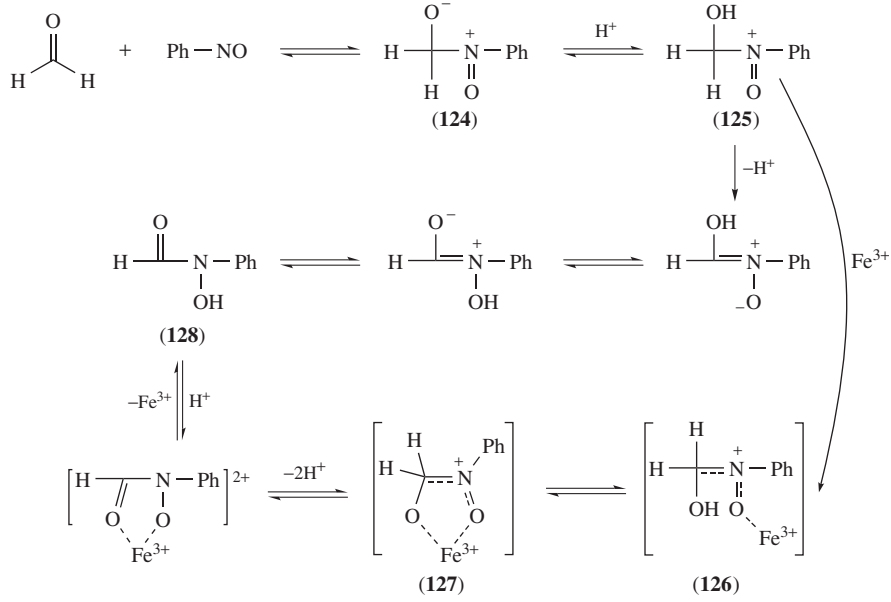

(**124**) (**125**) (**128**) (**127**) (**126**)

SCHEME 62

In aqueous solution, substituted aromatic nitroso compounds **129** react rapidly with glyoxylic acid to produce *N*-hydroxyformanilides **131**–**132** (via **130**) and CO_2 (Scheme 63)[127]. The reaction is nearly quantitative for all nitroso aromatics and serves as a convenient synthetic route to *N*-hydroxyformanilides. The reaction is strongly inhibited by organic cosolvents but is not affected by hydroquinone, H_2O_2, catalase, superoxide dismutase, or O_2. The rate of reaction was found to increase with increasing electron donation by ring substituents.

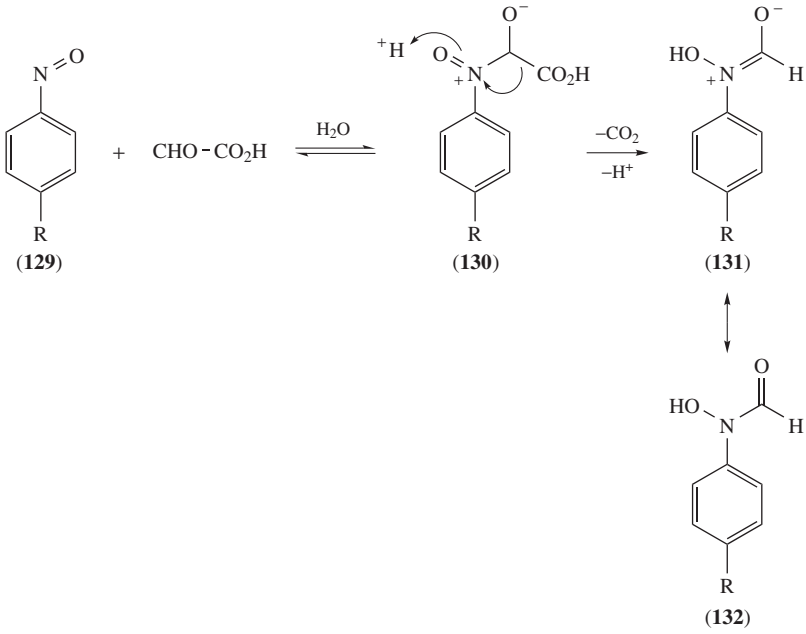

SCHEME 63

Recently, Ursic and colleagues have observed an unexpected reaction sequence in the interaction of the acyl halides with nitrosobenzenes **133**, which involves carbon–nitrogen bond formation followed by heterolytic nitrogen–chlorine bond cleavage, giving the corresponding unsubstituted *N*-phenylalkylhydroxamic acids **137** (or *N*-phenylarylhydroxamic acids) and chlorine as the products (Scheme 64)[128].

The kinetic and other evidence obtained suggest that the carbon–nitrogen bond formation is the consequence of a nucleophilic interaction of an *N*-phenylchlorohydroxylamine intermediate **135**, formed in the second reaction step from **134**, and the acyl halide, which leads to an *N*-acyl-*N*-chlorophenylhydroxylamine cation intermediate **136**. The latter loses chlorine with the formation of **137**.

F. Hydroxamic Acids from Carbonylation

In 2000, Szarka and coworkers[129] reported some preliminary results on the facile synthesis of steroidal hydroxamic acid derivatives via the palladium-catalyzed functionalization of skeletons (**138–141**) possessing iodoalkene moieties (Scheme 65).

Successively, they prepared steroidal hydroxamic acid derivatives (**138a**, **138b**, **138b–140b**, **138c–141c)** in moderate to high yields by palladium-catalyzed carbonylation reactions of the corresponding iodoalkenyl compounds **138–141** or enol triflates **142** and **143** in the presence of *O*-substituted hydroxylamines under mild reaction conditions (Scheme 66)[130].

The substrates with the alkenyl iodide (**138–141**) moiety could be totally converted into the desired products **(138a**, **139a**, **138b–140b**, **138c–141c)** in 4–8 h, while the enol triflate (**142**) reacted slowly. The bromo derivative (**144**) is unreactive and no carbonylation product was observed even after prolonged reaction times.

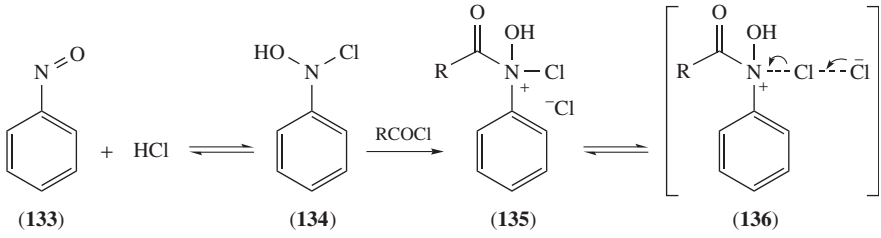

(**133**) (**134**) (**135**) (**136**) (**137**)

SCHEME 64

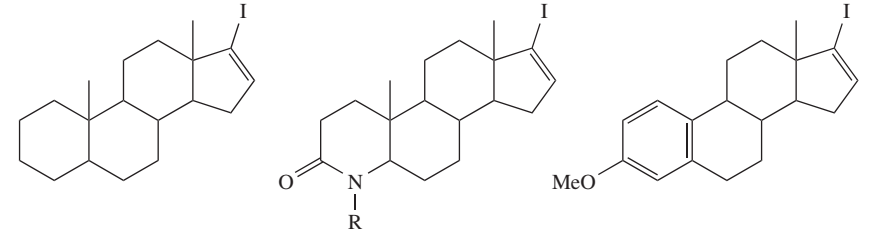

(**138**) (**139**) R = Me (**140**) R = H (**141**)

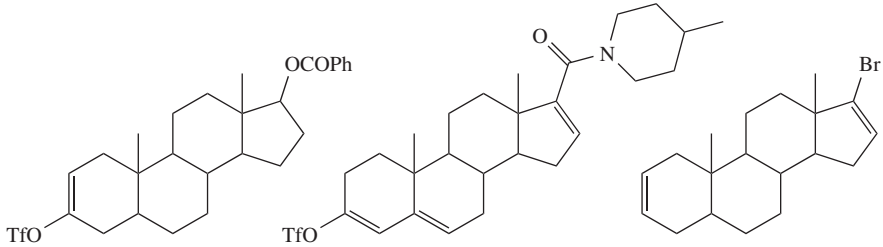

(**142**) (**143**) (**144**)

SCHEME 65

The carbonylation of the same substrates (**138**–**144**) with several *N*-substituted hydroxylamines proceeds with the same order of substrate reactivity (Scheme 67). In particular, with steroidal alkenyl iodides **138**–**141** and enol triflates **142** and **143** complete conversion of the substrates could be achieved, in the latter cases (**142** and **143**) with long reaction times. The analogue bromo derivative **144** is completely unreactive.

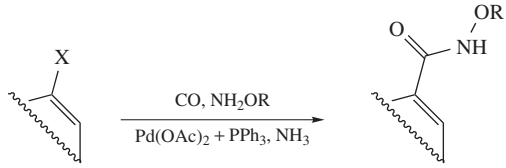

(**138–141**) X = I
(**142–143**) X = OTf
(**144**) X = Br

(**138a–139a**) R = $SiMe_3$
(**138b–140b**) R = CH_2Ph
(**138c–142c**) R = Me

SCHEME 66

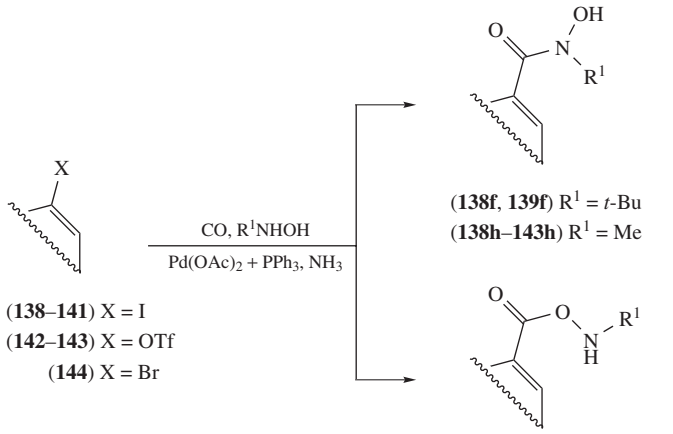

(**138–141**) X = I
(**142–143**) X = OTf
(**144**) X = Br

(**138f**, **139f**) R^1 = *t*-Bu
(**138h–143h**) R^1 = Me

(**138e**, **139e**) R^1 = C(O)Me
(**138g**,**139g**) R^1 = *t*-Bu
(**138i–142i**) R^1 = Me

SCHEME 67

The most interesting point in this reaction is its regioselectivity. Theoretically, the acylating agent (the palladium–acyl intermediate) could react either with the NH or the OH group of the hydroxylamine derivative. The regioselectivity of the reaction appears to be strongly influenced by the nature of both the substrate and solvent.

G. Hydroxamic Acids Protective Group

The ability of hydroxamic acids to act as bidentate ligands has made this functional group a key component in the design of most matrix metalloproteinase inhibitors. Due to its labile and diprotic nature, the hydroxamate is typically installed in its protected form at the end of the synthetic sequence[131].

In 2002, Couturier and coworkers investigated the possibility of using a dioxazole as an aprotic hydroxamic acid protective group[132]. In this context, the masked hydroxamic acid could be introduced earlier in the synthesis and could perhaps be released in a single operation at the end of the sequence.

Dioxazoles **146** are readily prepared by transketalization of 2,2-diethoxypropane, where both the NH and OH moieties are protected in a non-protic form (Scheme 68). The dioxazoles **146** are stable to a wide variety of reaction conditions and readily revert back to the hydroxamic acids **145** and isopropyl ester **147** (**145/147**: 50/1) by treatment with Nafion-H in 2-propanol. The method is applicable to primary, secondary, tertiary and aromatic hydroxamic acids, and the acidity of the protons adjacent to the dioxazole allows R-functionalization.

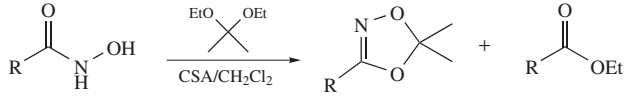

(**145**) (**146**)

R = Ph, 4-PhC$_6$H$_4$, 4-O$_2$NC$_6$H$_4$, PhCH$_2$CH(Me), PhCH=CH

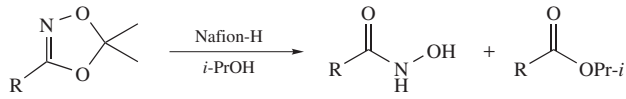

(**146**) (**145**) (**147**)

145 / **147** ratio: 50/1

SCHEME 68

H. Hydroxamic Acids Inserted into a Cycle

Since the discovery and clinical introduction of penicillin, considerable industrial and academic effort has been addressed to the design and synthesis of β-lactam antibiotics[133]. However, among the numerous methods developed for β-lactam synthesis, no single method is compatible with all possible functional groups and/or the chirality needed on the β-lactamic ring.

In this context Miller[134] has demonstrated that all these issues could be overcome by hydroxamic-acids-based heteroatom activation.Therefore, β-halo or β-hydroxy carboxylic acids **148a** and **148b** are converted to the corresponding hydroxamates **149a** and **149b** by active ester condensation with *O*-substituted hydroxylamines (Scheme 69). Since chiral

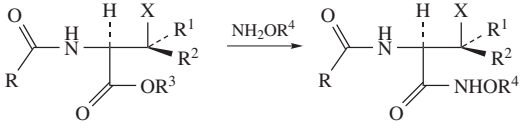

(**148a**) X = Cl
(**148b**) X = OH
(**148c**) X = OMs

(**149a–c**)

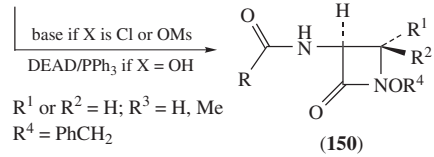

R^1 or R^2 = H; R^3 = H, Me
R^4 = PhCH$_2$

(**150**)

SCHEME 69

β-hydroxy acids **148b** are much more readily available than β-halo acids **148a**, the corresponding β-hydroxy hydroxamates **149b** (X = OH) represent the key reagent to prepare β-lactams **150**. Reaction of several β-hydroxy hydroxamates **148b** under Mitsunobu conditions provided the desired β-lactams in high yields.

The major problems with industrial-scale applications of this procedure are the use of expensive reagents, the required chromatographic separation of the side products and the competitive formation of oxazolines. The use of carbamate protecting groups avoided the oxazoline problem and is usually preferred, since the resulting protected 3-amino-substituted β-lactams **150** can later be deprotected and reacylated.

Later, Krook and Miller[135] found that β-mesylates of benzyl hydroxamate of α-acylserine (**149c**: X = OMs; $R^1 = R^2 = H$; $R^4 = CH_2Ph$) can be directly cyclized under careful conditions (t-BuOK/DMF/$-23\,^{\circ}C$) without β-elimination or formation of oxazolines or aziridines.

Often, the use of expensive O-substituted hydroxylamines and the azodicarboxylates could be avoided by direct hydroxaminolysis of protected amino acid esters **151** with hydroxylamine itself, followed by *in situ* acylation and finally substitution of Ph_3P/CCl_4/Et_3N for Ph_3P/DEAD during the cyclization step from **152** to **153** (Scheme 70)[136].

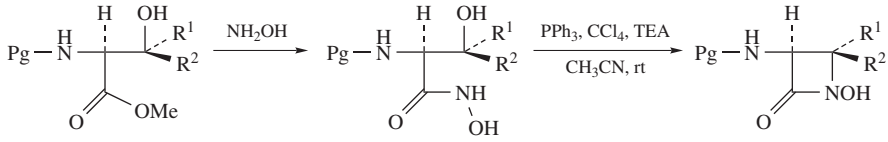

(**151**) (**152**) (**153**)

Pg = Boc, Cbz, Fmoc
R^1 or R^2 = H, alkyl

SCHEME 70

Deprotection of the hydroxyl group in **150** followed by reduction of the free-N-hydroxy β-lactam **154** with buffered $TiCl_3$[137, 138] (the pH maintained at 7 with 3 N NaOH) provide access to a variety of chiral N-unsubstituted β-lactams **155** (Scheme 71)[139, 140].

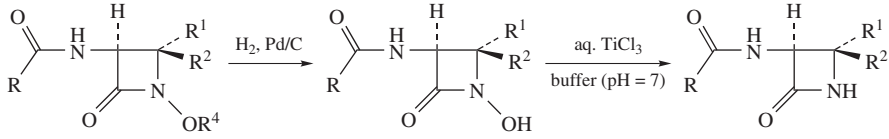

(**150**) (**154**) (**155**)

R^4 = OBn

SCHEME 71

Romo and colleagues[141] subsequently reported a samarium diiodide-mediated reduction of the N–O bond of a functionalized 1-(benzyloxy)-2-azetidinone (Scheme 72). Use of the samarium protocol allows elaboration of the 4-(methyl)-1-(benzyloxy)-2-azetidinones **156a** and **156b** to their Boc-protected coupling precursors **158a** and **158b**, via the hydroxy compounds **157a** and **157b**, as shown in Scheme 72[142].

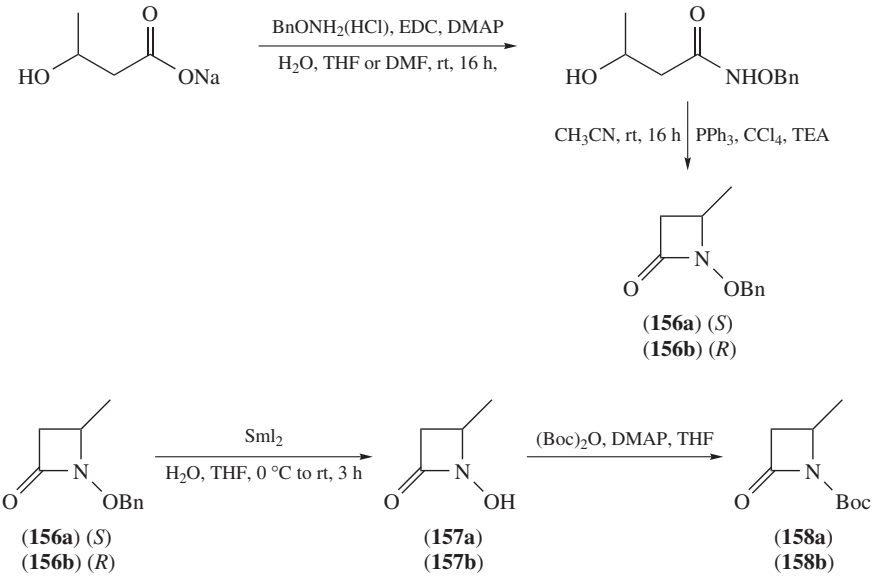

SCHEME 72

Making use of a *O*-trityl-hydroxylamine linker, Meloni and Taddei[143] reported the first example of Miller hydroxamate on solid phase (**161**, Scheme 73). β-Lactams **162** and **163** were prepared on solid support starting from serine, threonine or other β-hydroxyacids derived from naturally occurring amino acids and a resin bound hydroxylamine **159**. The ring closure of **160** was carried out under Mitsunobu conditions.

Thomas and Rajappa have described a novel method for the synthesis of five-membered α-substituted cyclic hydroxamic acids from aliphatic nitro compounds including nitroacetic acid derivatives (Scheme 74)[144]. Michael addition of allyl acrylate to these compounds (**164a–c**) gave **165a–c**, which then gave **166a–c** by Pd(0)-catalyzed intramolecular allyl transfer. Subsequent reduction of the tertiary nitro group results in a new class of compounds related to *N*-hydroxy pyroglutamic acid (**167a–c**) and their ester derivatives (**168a–c**).

1,2-Dihydro-1-hydroxy-2-oxoquinolines containing a cyclic hydroxamic acid group exhibit antibacterial activity, which is influenced by the type of substituents at positions 3 and 4. Noble and Wibberley[145] have synthesized a series of 3-alkyl-1,2,3,4-tetrahydro-1-hydroxy-2-oxoquinolines **169** by the route showed in Scheme 75.

Due to its labile and diprotic nature, the hydroxamate is typically installed in its protected form at the end of the synthetic sequence[131]. In general, only the alcohol proton is derivatized, and examples include *O*-Bn[146], *O*-*t*-Bu[147], *O*-Bz[148], *O*-TMS[149], *O*-TBS[150], and *O*-SEM (2-(trimethylsilyl)ethoxymethyl)[151]. On rare occasions, both differentially protecting groups can be cleaved in a single operation: *N*,*O*-bis-(Boc), *N*-Boc-*O*-THP, and *N*-Boc-*O*-TBS[152].

In a very interesting paper Hu and Miller have described the synthesis of a *L*-lysine-derived cyclic hydroxamic acid **174** starting by the oxidation of protected *Z*-*L*-lysine **171** (formed from **170)** with dimethyldioxirane (DMD) in acetone, followed by nitrone

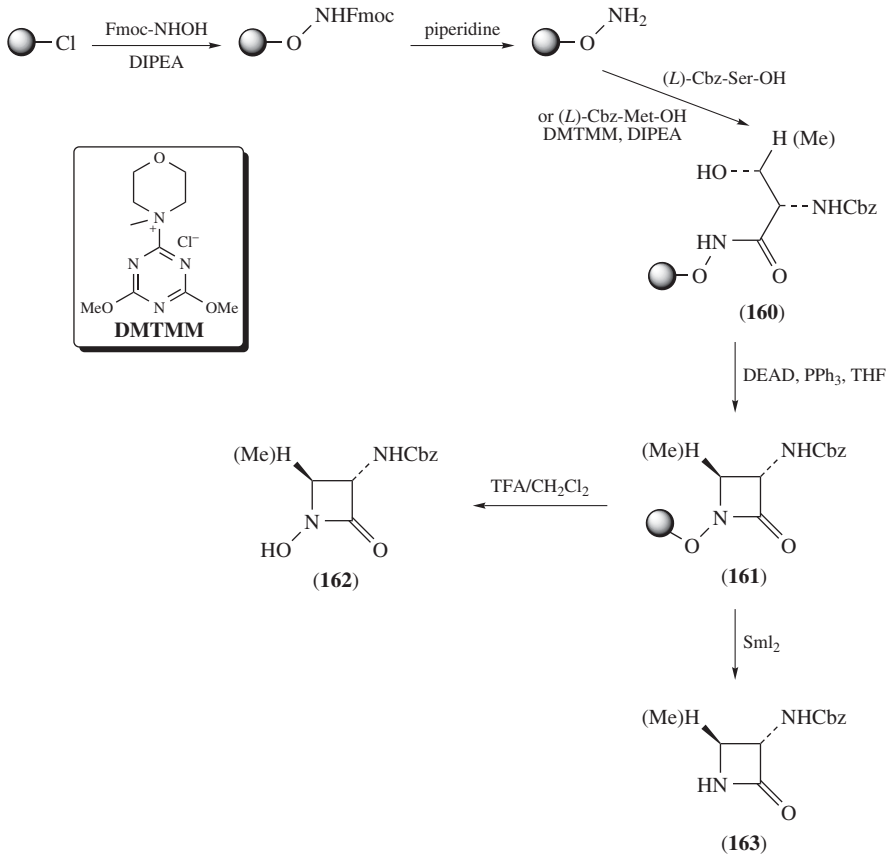

SCHEME 73

formation **172** (Scheme 76). Cyclization of the intermediate hydroxylamine **173** to **174** was accomplished with a 5-fold excess of DCC, DMAP and DMAP(HCl)[153].

An alternative procedure that generates stable, storable nitrone intermediates **175** from **170**, mediated by dry *m*-CPBA as oxidating reagent, is shown in Scheme 77[154]. Conversion of the nitrone **175** to the hydroxylamine by an exchange reaction with hydroxylamine hydrochloride was followed by EDC/HOAt-mediated cyclization to hydroxamic acid **174** (HOAt: 1-hydroxy-7-azabenzotriazole).

I. Synthesis of Sulfonyl Hydroxamic Acids

In 2004, Rossello and colleagues[155] synthesized some matrix *N*-arylsulfonyl-substituted alkoxyaminoacetohydroxamic acid derivatives designed as oxa-analogues of known sulfonamide-based metalloproteinases.

The synthetic route to the *N*-arylsulfonylhydroxamic acids **177** is shown in Scheme 78; *para*-substituted arylsulfonyl chlorides **176** are coupled with the appropriate *O*-alkylhy-

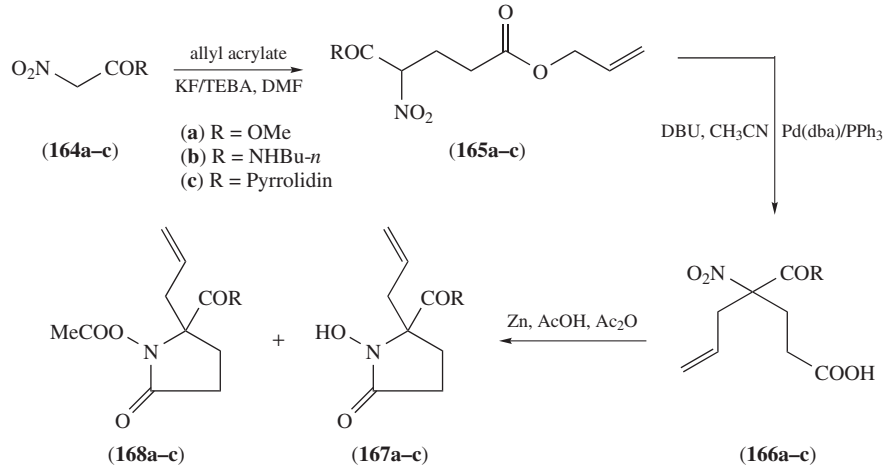

SCHEME 74

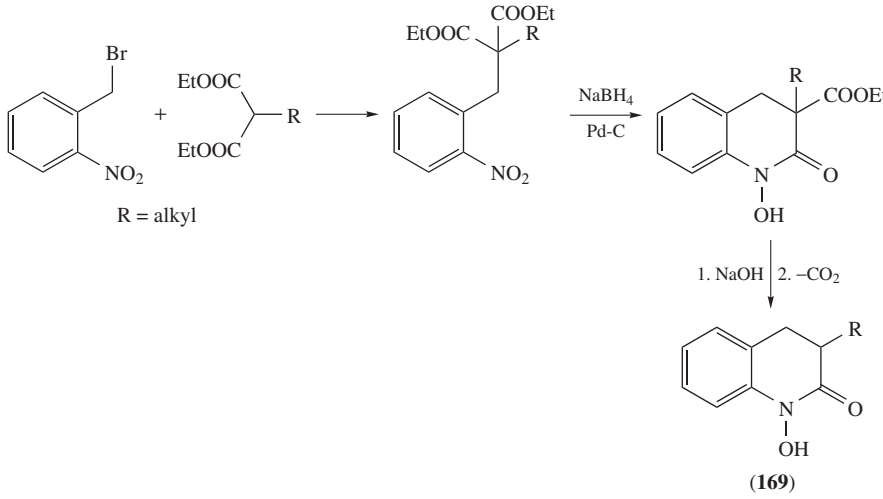

SCHEME 75

droxylamines in the presence of *N*-methylmorpholine (NMM) to give the corresponding *O*-alkylsulfonamides **177**.

J. Solid-phase Synthesis of Hydroxamic Acids

The recent development of parallel and combinatorial chemical library synthesis has created a renewed interest in polymeric solid-phase reagents. They offer the advantage of

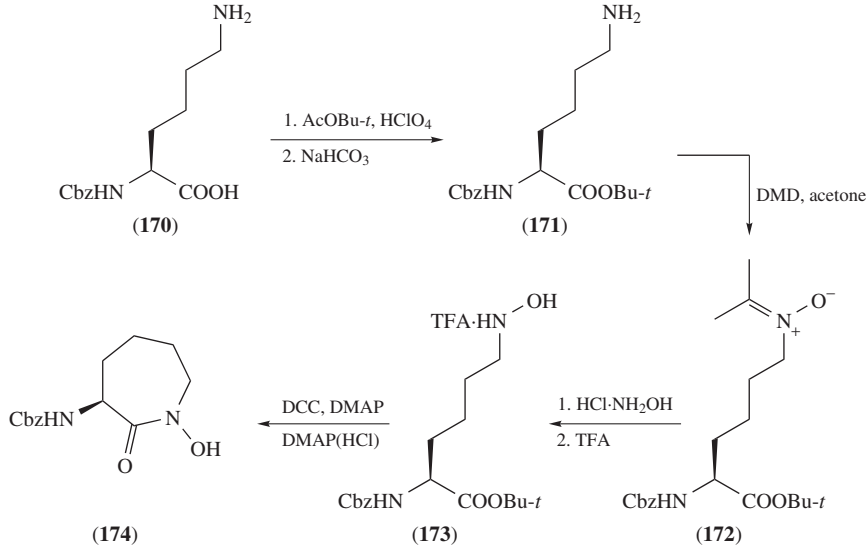

SCHEME 76

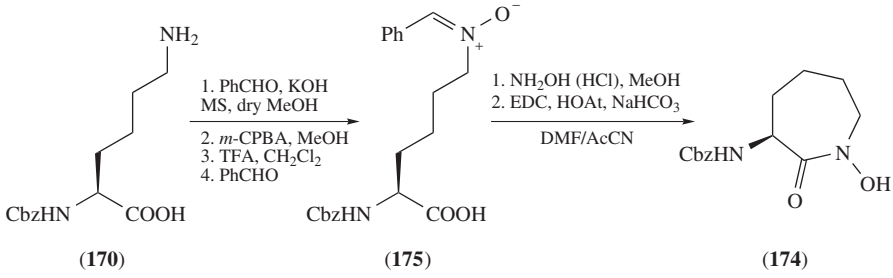

HOAt = 1-hydroxy-7-azabenzotriazole

SCHEME 77

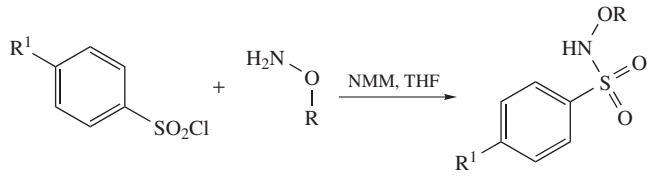

R = *i*-Pr, Et, Allyl, *p*-BnOBn

R^1 = Ph, OMe

SCHEME 78

easy separation from low molecular weight reactants or products by filtration or selective precipitation and are very suitable for automation of chemical library synthesis.

The solid-phase synthesis of hydroxamic acids has been of interest in the recent chemical literature[156]. Typically, hydroxylamine derivatives are tethered to solid supports via the oxygen (Scheme 79), although immobilization through the nitrogen has also been observed.

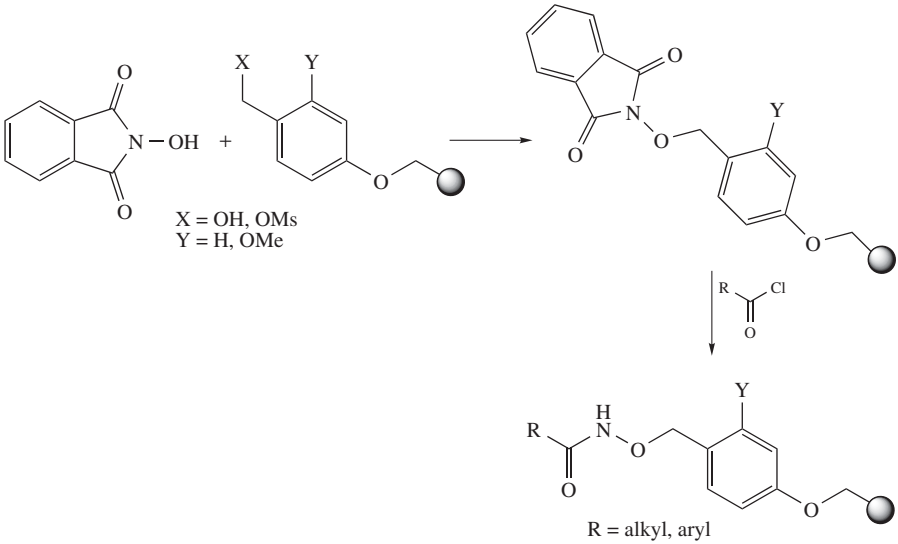

SCHEME 79

The reaction of *N*-hydroxyphthalimide **178** with Wang or Sasrin **179** resins under Mitsunobu conditions to give **180** is one of the common preparative routes to *O*-immobilized hydroxylamine **181** (Scheme 80)[157].

In 1997, Bauer and colleagues[158] described the preparation of a hydroxylamine resin **183** using trityl chloride resin **182** as the base matrix as well as its application to the synthesis of various hydroxamic acids (Scheme 81).

N-Hydroxyphthalimide **178** was used as a source of the hydroxylamine reacting with trityl chloride resin **182** in the presence of triethylamine to obtain the *N*-hydroxyphthalimide derivative **183**. This intermediate is transformed to the desired hydroxylamine resin **184** by treatment with hydrazine. The peptidic and peptidomimetic hydroxamic acids **185** and **186** were synthesized using the described solid-supported reagent (Scheme 82).

Richter and Desai[159] have claimed the synthesis of a TFA-cleavable hydroxamate linkage, which takes advantage of the linkage as a 'protecting group' for the requested functionality, and overcome solution-phase synthesis of protected building blocks. Thus mesylate displacement from the formed **187** with *N*-hydroxyphthalimide **179** resulted in formation of the resin-linked hydroximide **180** (Scheme 83). Complete deprotection of the phthalimido group was accomplished under mild conditions, and the solid-supported hydroxylamine **181** can be manipulated using classical procedures for Fmoc-peptide synthesis. Quantitative cleavage from the solid support is carried out with 50% TFA/5% $(i\text{-Pr})_3SiH$/45%CH_2C1_2 or 90% TFA/anisole.

Using the *N*-Fmoc-hydroxylamine **189**, which was formed from **188**, Chan and colleagues generated a facile route to a high-loading, acid-labile, solid-phase resin **190**

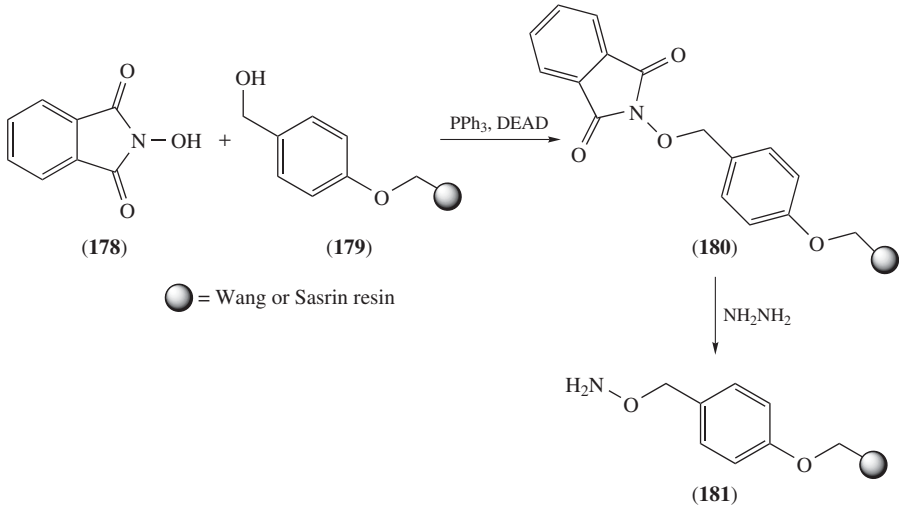

(**178**) (**179**) (**180**) (**181**)

SCHEME 80

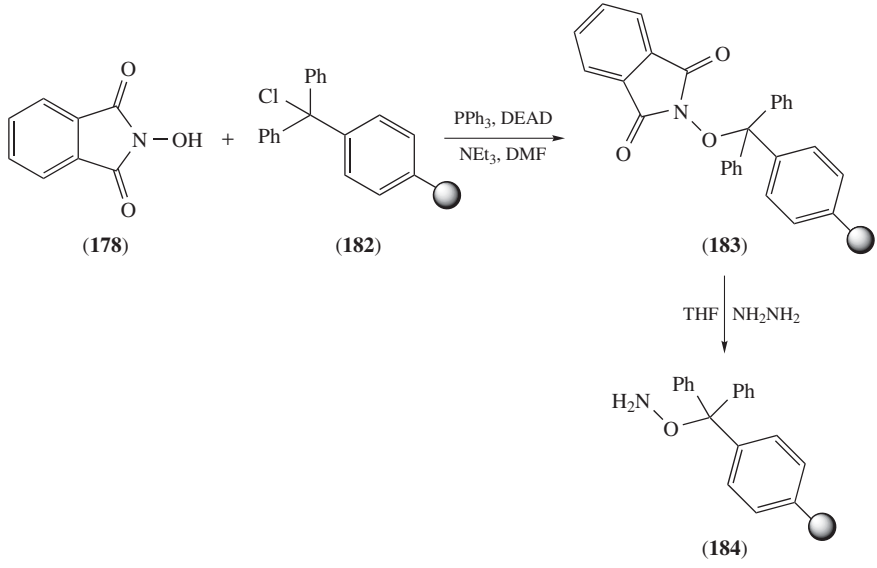

(**178**) (**182**) (**183**) (**184**)

SCHEME 81

bearing a hydroxylamine linker (Scheme 84)[160]. The *N*-Fmoc-aminooxy-2-chlorotrityl polystyrene **190** showed generic utility for the construction of hydroxamic acids, including peptidyl hydroxamic acids.

A very interesting approach to the solid-supported synthesis of hydroxamic acids was developed by Golebiowski and Klopfenstein[161]. It employs an oxime resin (Kaiser resin) **171d** and, unlike all previouxsly reported methods, allows the use of acid-labile protecting

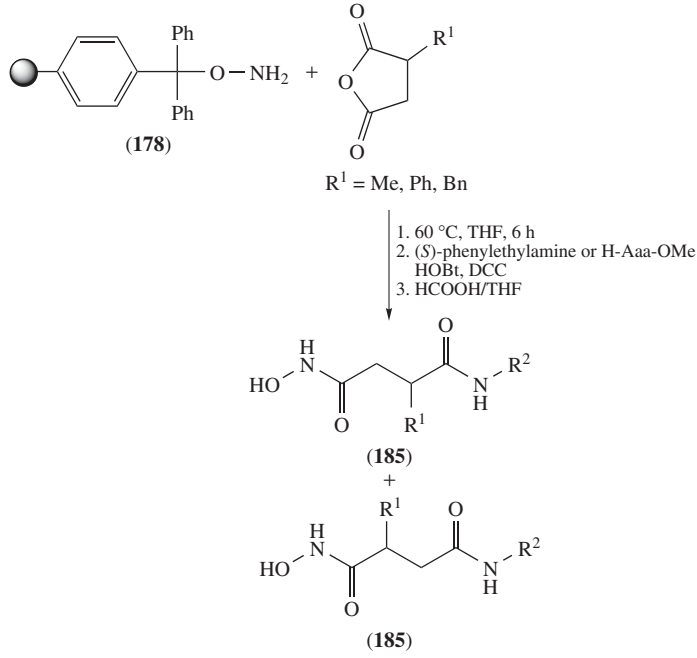

a. R^2 residue from H-Aaa-OMe: H-Phe-OMe or H-Val-OH
b. R^2 moiety from (*S*)-phenylethylamine

SCHEME 82

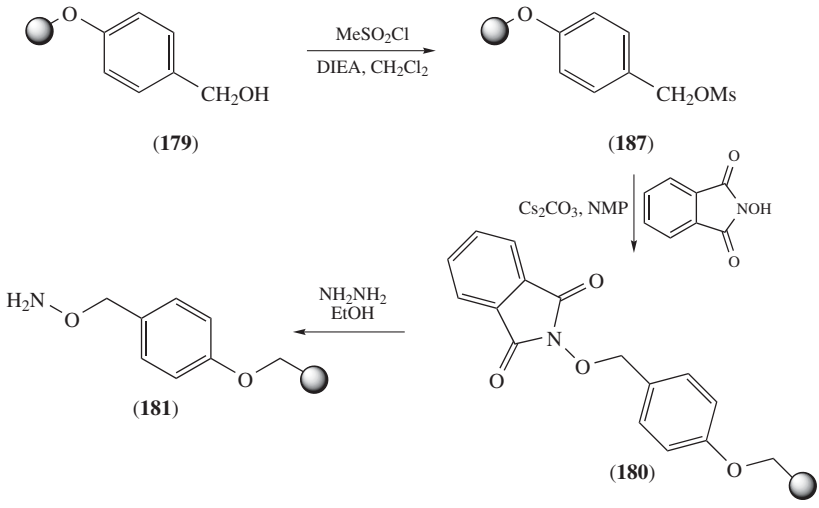

SCHEME 83

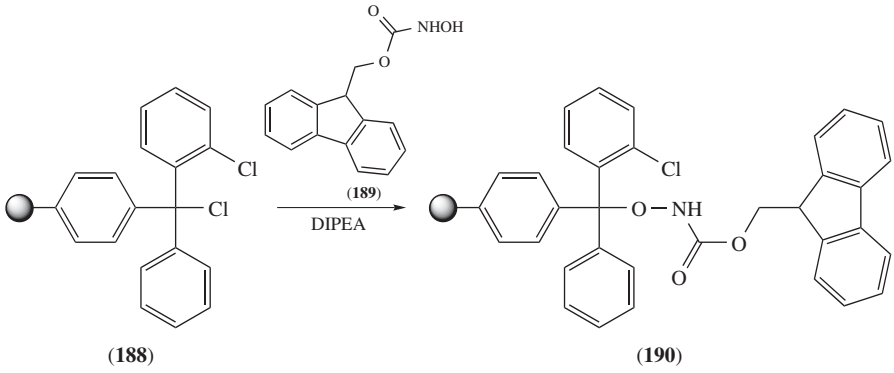

(**188**) (**190**)

SCHEME 84

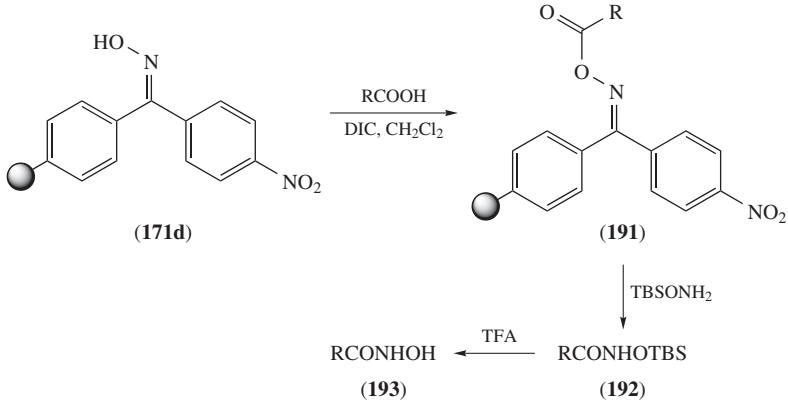

(**171d**) (**191**)

(**193**) (**192**)

SCHEME 85

groups (Scheme 85). Cleavage of **191** is induced by treatment with *tert*-butyldimethylsilyl-*O*-hydroxylamine to give **192**, followed by silyl group deprotection with trifluoroacetic acid to give the hydroxamic acids **193**.

Although several routes have been published for the preparation of hydroxamic acids on solid phase, these generally involve the preparation of a special linker to which hydroxylamine is attached. Dankwardt's approach[162] obviates the need for special linkers or protecting groups, by displacing the desired hydroxamic acid from the resin directly using hydroxylamine, as illustrated in Scheme 86. Carboxylic-acid-ester-linked, polymer-supported, Cbz-protected amino acids **195** (formed from **194**) were displaced from the resin with aqueous hydroxylamine to provide the corresponding hydroxamic acids **196**.

Nevertheless, the direct nucleophilic displacement of support-bound carboxylates to prepare hydroxamates presents some limitations. For example, *O*-*tert*-butyldimethylsilyl-protected hydroxylamine displaces common acids from oxime resin; however, further treatment with trifluoroacetic acid (TFA) is necessary to remove completely the silyl

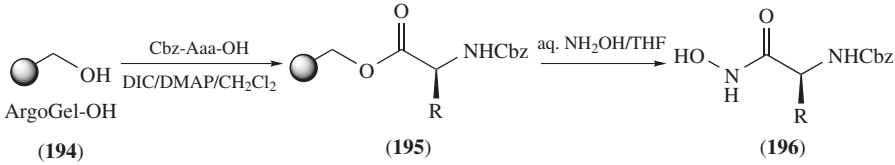

SCHEME 86

group. Moreover, 25 equivalents of hydroxylamine and a reaction time of 2 days are required to cleave *N*-(Cbz)amino esters from ArgoGel-OH^{TM} resin.

Thouin and Lubell[163] have overcome some of these issues by exposing oxime resin-bound(acyl)amino acids **197**–**200** to a solution of anhydrous hydroxylamine in 1:6 MeOH: $CHCl_3$ (Scheme 87). Enantiopure hydroxamates, possessing a variety of functional groups, are isolated by simple evaporation of volatile solvents.

Since the thioester linkage is susceptible to nucleophilic attack but stable to TFA treatment during solid-phase peptide synthesis (using standard Boc protection), Weigel and colleagues[164] have envisioned that hydroxylamine derivatives could directly cleave resin-bound peptide thioesters **201** or **202** to form the corresponding peptide hydroxamates **203** (Scheme 88).

In 2003, Devocelle and colleagues[165] reported a convenient two-step procedure for the parallel synthesis of hydroxamic acids (or *O*-protected hydroxamic acids **207**) from carboxylic acids and hydroxylamine. It involves the formation of a polymer-bound HOBt active ester **206** from **204** and the acid **205** and subsequent reaction with *O*-protected or free hydroxylamine (Scheme 89). The use of free hydroxylamine leads to increased yields while maintaining high purities. Recycling of the exhausted resin **204** to produce the same or a different hydroxamic acid has been achieved by a three-step protocol, which is easily amenable to automation and cost-economical.

The polymer-supported *N*-benzyloxy-2-nitrobenzenesulfonamide linkers **208a** and **208b** are versatile substrates for *N*-alkylation using different types of carbon-based building blocks such as alcohols, alkyl bromides and α,β-unsaturated carbonyl compounds (Scheme 90). *N*-Alkylation reactions to give **209a** and **209b** proceed under mild conditions, are amenable to manual parallel synthesis and gave *N*-alkylhydroxamic acids **210a** and **210b** in high yield and excellent purity after convenient cleavage conditions.

Angeli[166] and Rimini[167] discovered that *N*-hydroxybenzenesulfonamide **211** formed hydroxamic acids in fair to good yields if treated with aldehydes in the presence of sodium methoxide in MeOH (Scheme 91)[168, 169]. Unfortunately, the acidic workup afforded the desired hydroxamic acid together with the benzenesulfinic acid **212** as a byproduct.

Because this impurity is not easily removed from the desired product, the Angeli–Rimini reaction has been seldom used in organic synthesis.

Recently, Porcheddu and Giacomelli[170] have reported a convenient one-step procedure for the synthesis of hydroxamic acids **215** starting from aldehydes **213** and solid-supported *N*-hydroxybenzenesulfonamide **214** (Scheme 92). The hydroxamates are isolated in good to high yields and purities by simple evaporation of the volatile solvents, after treatment of the crude reaction mixture with sequestering agents (**216** and **217**).

Aromatic or conjugated aldehydes react in excellent yields, whereas the reaction with aliphatic aldehydes requires longer times and leads to *N*-hydroxyamides in lower, although satisfactory, yield. When both aldehyde and ketone groups are present on the same

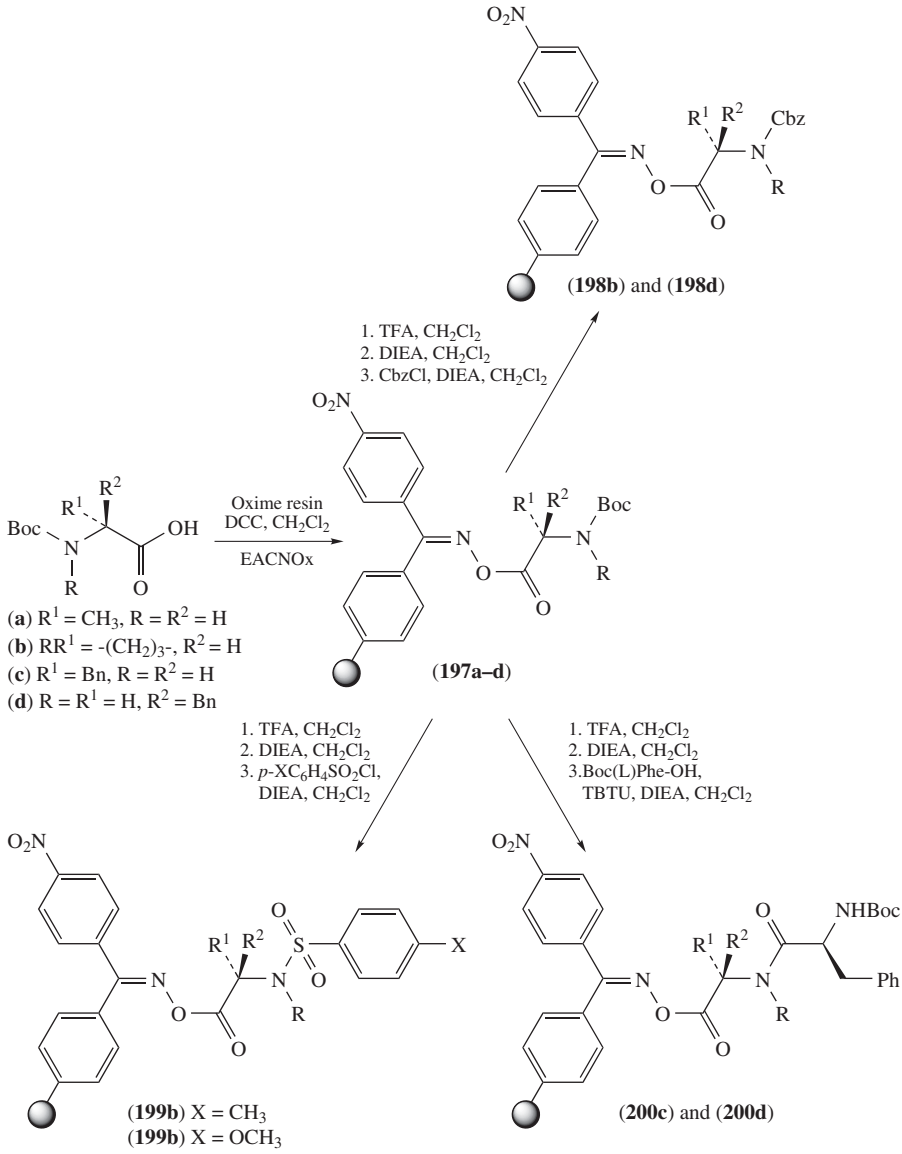

EACNOx = ethyl 2-(hydroxyimino)-2-cyanoacetate
TBTU = *O*-(Benzotriazol-1-yl)-*N*, *N*, *N*′, *N*′-tetramethyluronium tetrafluoroborate

SCHEME 87

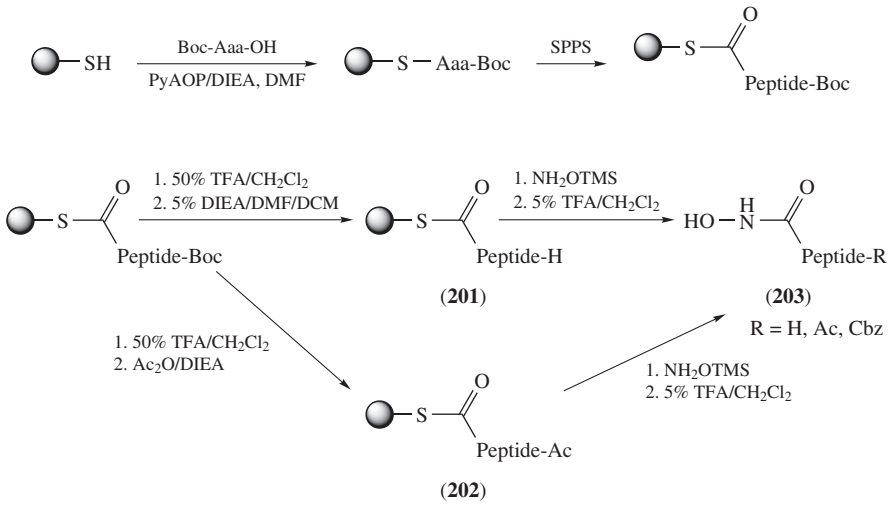

PyAOP = azabenzotriazol-1-yloxytris(pyrrolidino)phosphonium hexafluorophosphate

SCHEME 88

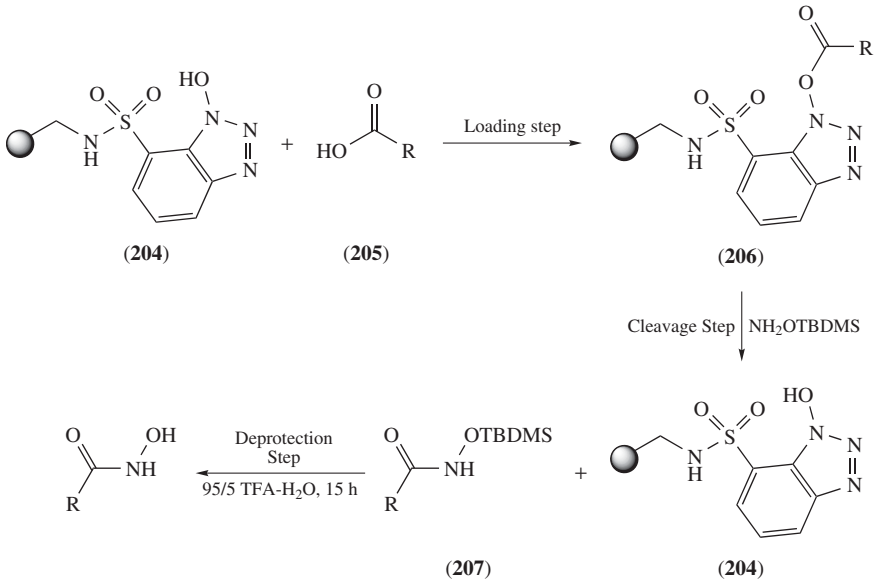

$NH_2OTBDMS$: O-*tert*-butyldimethylsilylhydroxylamine

SCHEME 89

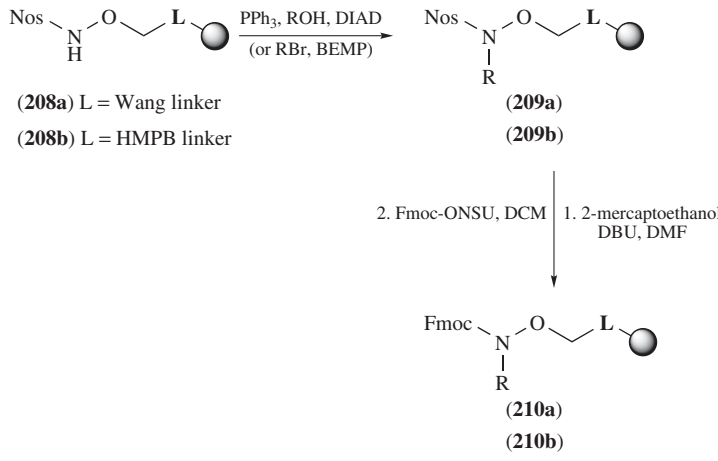

(**208a**) L = Wang linker

(**208b**) L = HMPB linker

(**209a**)

(**209b**)

(**210a**)

(**210b**)

Fmoc-ONSu = *N*-(9-Fluorenylmethoxycarbonyl) succinimide

SCHEME 90

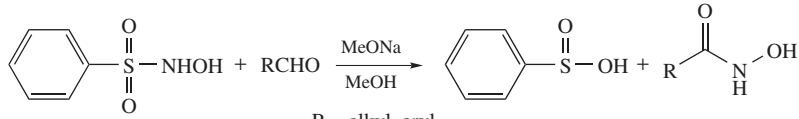

(**211**)

R = alkyl, aryl

(**212**)

SCHEME 91

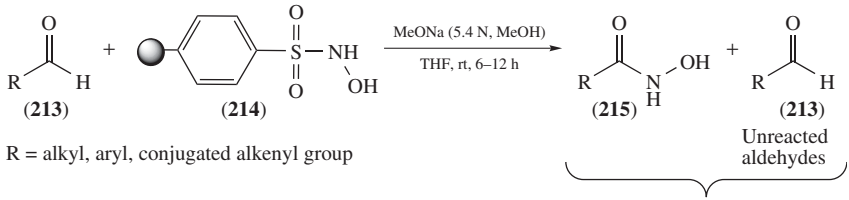

(**213**)

(**214**)

R = alkyl, aryl, conjugated alkenyl group

(**215**)

(**213**)

Unreacted aldehydes

crude reaction mixture

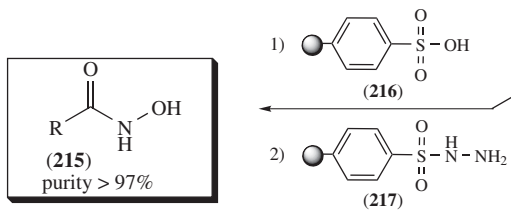

THF/MeOH (3/1), pH~5,
4 h, rt

SCHEME 92

substrate, only the aldehyde moiety is selectively transformed into the corresponding *N*-hydroxyamide function.

This synthetic approach indicates even an interesting solution for the preparation of monohydroxamic acids (**219a** and **219b**), in a single step, from substrates containing carboxylic acid functions (**218a** and **218b**), too, without implementing protection/deprotection strategies (Scheme 93).

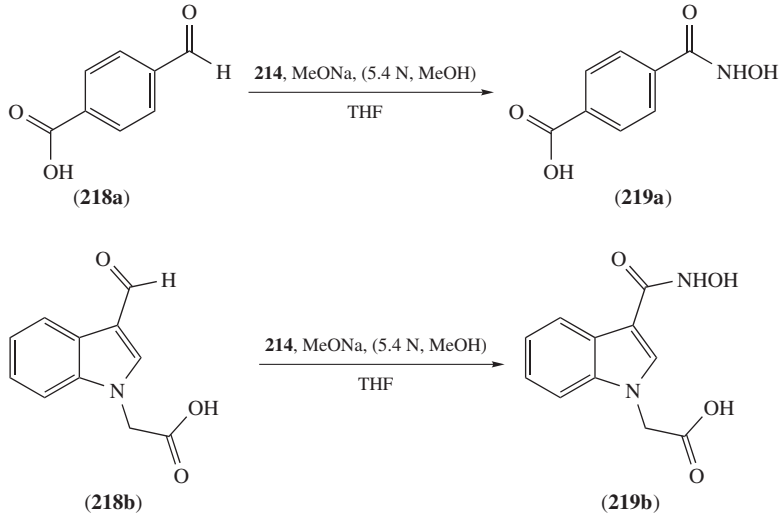

SCHEME 93

K. *O*-Linked Polymer-bound *N*-Substituted Hydroxamic Acids

O-linked polymer-bound *N*-substituted hydroxylamines are prepared by reduction of resin-bound oximes with borane–pyridine complex in the presence of dichloroacetic acid (Scheme 94). Other reducing systems commonly used for imine or oxime reduction are ineffective, including borane–pyridine in the presence of acetic acid. Subsequently, the *N*-substituted products are acylated and cleaved from the resin to afford *N*-substituted hydroxamic acids **220**[171].

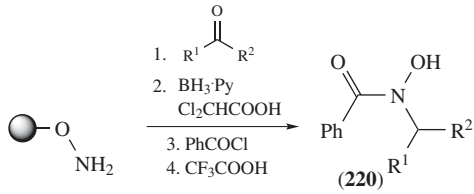

SCHEME 94

The problem of antibiotic-resistant bacteria[172] has created a pressing demand for new antibacterial agents with novel mechanisms of action. *N*-Formylhydroxylamines, also known as reverse- or retro-hydroxamates, are one of the few novel targets that are currently being pursued against a variety of metalloenzyme targets, including carboxy

peptidase A (CPA)[173], tumor necrosis factor-R converting enzyme (TACE)[174], matrix metalloproteinases (MMPs)[175], thermolysin (TLN)[176], histone deacetylase (HDAC)[177] and peptide deformylase (PDF)[178], an essential enzyme involved in bacterial protein biosynthesis and maturation.

Although solution-phase[177] synthetic routes to such compounds have been reported, these are often lengthy and involve purification at each stage. Current methodologies on homogeneous phase are extremely time-consuming, rendering this approach unsuitable for the preparation of libraries of *N*-formylhydroxylamines.

Recently, Price and and Osborne[179] have developed a synthetically convergent route to produce libraries of *N*-formylhydroxylamines that utilizes commercially available starting materials. In particularly, they have investigated the reaction of several electrophiles with the nitrogen atom of a solid-supported *O*-protected *N*-formylhydroxylamine **221**.

N-Formyl-Wang-*O*-hydroxylamine **222** resin was prepared by treating Wang-*O*-hydroxylamine resin **221** with *p*-nitrophenyl formate and 10% pyridine in DMF at room temperature for 16 h (Scheme 95).

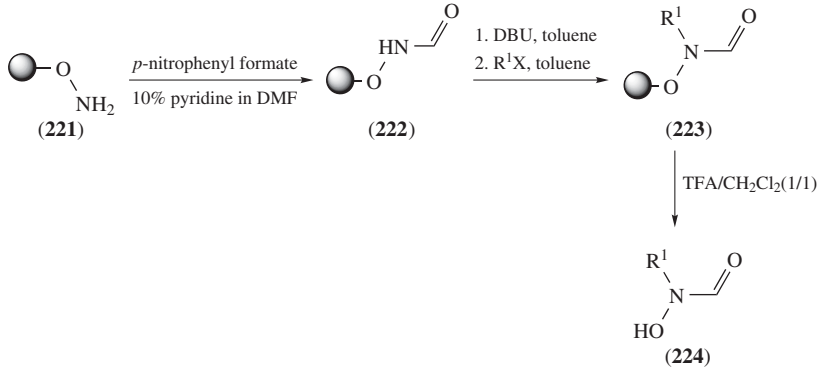

SCHEME 95

N-Alkylation was achieved by treating the *N*-formyl Wang-*O*-hydroxylamine resin **222** with DBU in toluene for 1 h, followed by addition of an alkyl halide in toluene and stirring for an additional 16 h. The final treatment of the *N*-alkyl, *N*-formyl Wang-*O*-hydroxylamine resin **223** with a solution of TFA/CH_2Cl_2 (1/1) affords the *N*-formylhydroxylamines **224**. These original approaches allow the introduction of diversity at the penultimate stage of any synthetic route (i.e. prior to liberation of the free *N*-formylhydroxylamine **224** itself).

In addition, they have also shown that further synthetic routes may be accessible utilizing Mitsunobu chemistry and commercially available alcohols (Scheme 96).

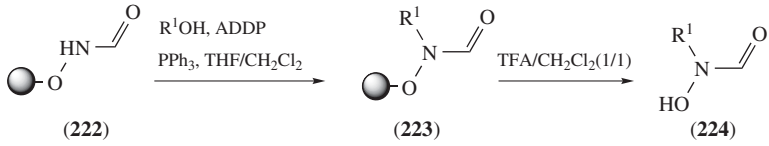

R^1 = H, Et, Ph; R^2 = H, Et; R^3 = H, Ph

SCHEME 96

In 2006, Stanger and Krchnak[180] described a solid-phase synthesis of several hydroxamates employing the Nos-derivatized polymer-supported benzyloxyamine **225** (Schemes 97 and 98). The synthesis of NH hydroxamates includes protection of the nitrogen with a 2,4-dimethoxybenzyl group at the stage of polymer-supported benzyloxyamine (**226**). The protecting group eliminates side reactions caused by the presence of a free hydroxamate NH group and is simultaneously removed during cleavage of the target compounds from the solid support. The method allows the concurrent synthesis of both *N*-alkyl and *N*-*H* hydroxamates and is compatible with a wide range of chemical transformations.

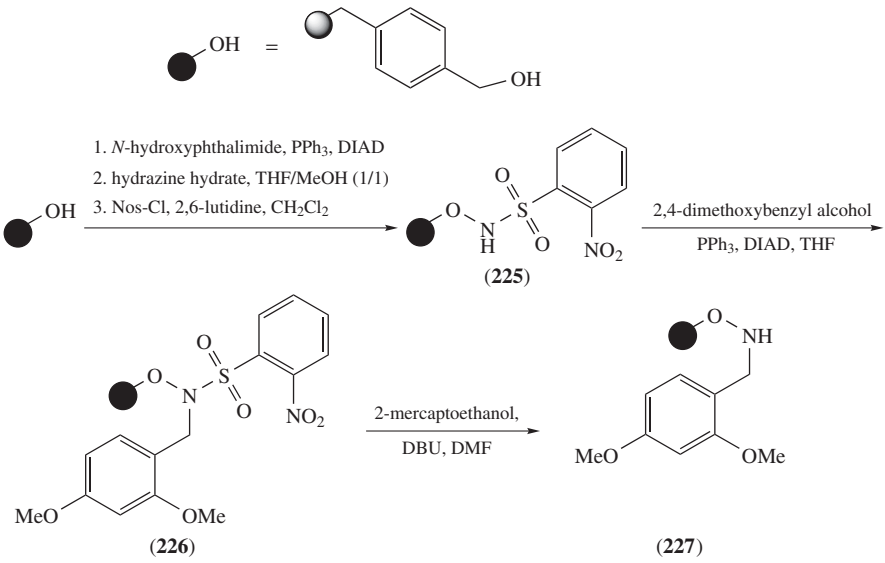

SCHEME 97

Acylation of **227** by *N*-Fmoc-protected amino acids give, after removal of the Fmoc group, the polymer-supported hydroxamates **228** ready for further chemical transformation on the side chain. The free amino group was then reacted with sulfonyl chlorides to afford resin-bound sulfonamides **229**. A final Mitsunobu reaction or electrophilic substitution *N*-alkylated the sulfonamide to yield the solid-supported compounds **230**. Complete recovery of **231** from the Wang linker and removal of the protecting group required treatment with 90% TFA for 1 h. Typical conditions for cleavage of carboxylic acids (50% TFA in DCM for 30 min) caused an incomplete cleavage of hydroxamates from the Wang linker, and the product **231** is contaminated by the side product **232**. This drawback was completely addressed making use of the more acid-labile 2,4,6-trimethoxybenzyl protecting group together with a more acid-labile linker, such as the 4-(4-hydroxymethyl-3-methoxyphenoxy)butyric acid (HMPB) linker.

L. Hydroxamic Acids as Ligands

Hydroxamic acids are important bioligands[181] and are involved in numerous biological processes including metal-ion transport and inhibition of metalloenzymes[182, 183]. 1:1 Metal binding to hydroxamic acids usually occurs in a bidentate fashion (Scheme 99) with

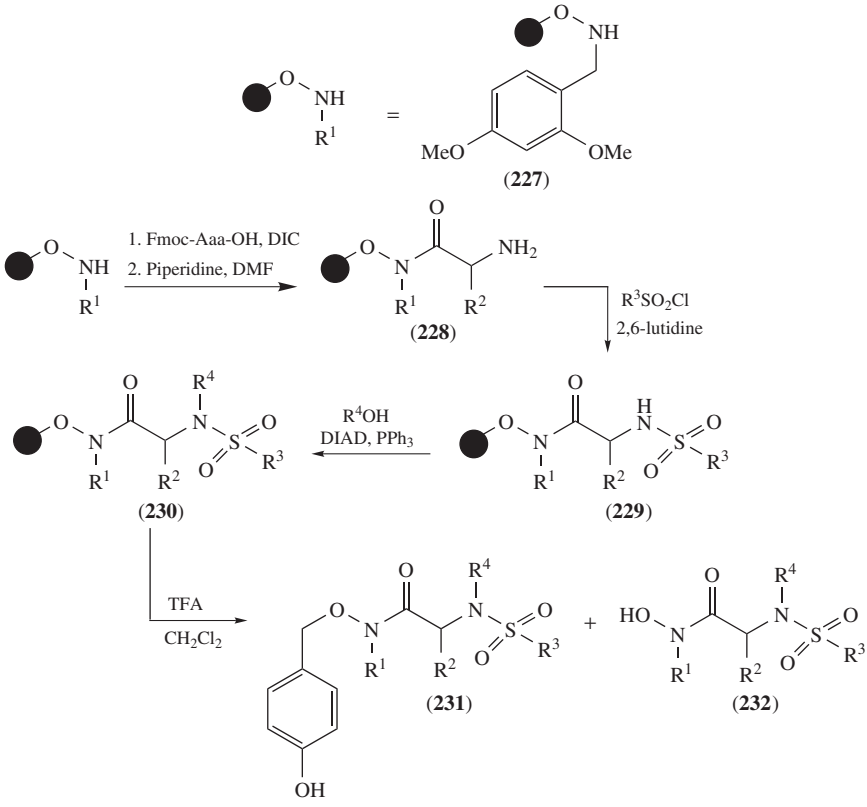

SCHEME 98

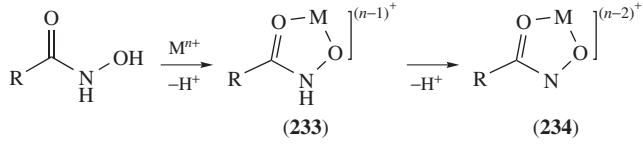

SCHEME 99

the formation of singly **233** or doubly deprotonated **234** (hydroxamato or hydroximato) ligands.

Since the first report of Sharpless's titanium tartrate catalyst[184, 185], a number of useful methods for asymmetric oxidation have been developed[186, 187]. Recently, Yamamoto and coworkers[188] have reported a vanadium-catalyzed epoxidation of allylic alcohols with newly designed bishydroxamic acid (BHA) ligands (**235a** and **235b**), which has the following features: (1) high enantioselectivity for a wide scope of allylic alcohols, (2) less than 1 mol% catalyst loading, (3) mild reaction conditions and (4) use of aqueous *tert*-butyl hydroperoxide (TBHP) as an achiral oxidant instead of anhydrous TBHP7-9 (Scheme 100).

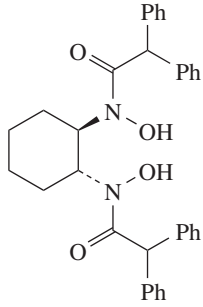

(**235a**)

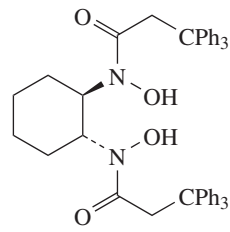

(**235b**)

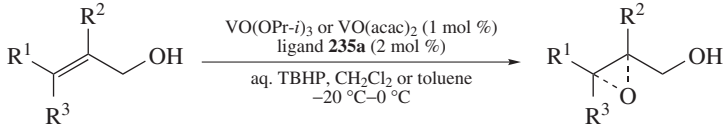

e.e.> 95%

R^1 = H, Me, Ph, C_3H_7, C_5H_{11}; R^2 = H, Me, Ph; R^3 = H.

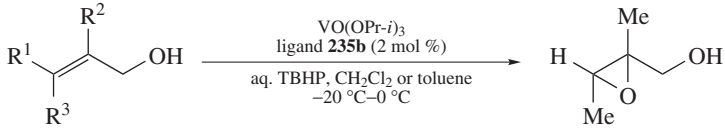

e.e.> 95%

R^1 = H, Me, Ph; R^2 = H; R^3 = C_6H_{13},C_6H_{11}

SCHEME 100

These chiral bishydroxamic acids **235a** and **235b** were synthesized starting from a readily available diamine tartrate salt as shown in Scheme 101.

The catalyst derived from vanadium and **235a** induces excellent enantioselectivities during the epoxidation of *trans*-substituted allylic alcohols. An interesting feature of this method is also the high enantioselectivity of the epoxidation of *cis*-substituted allylic alcohols with catalyst having BHA **235b** as ligand.

In a recent paper, Zhang and Yamamoto[189] have described a modified BHA ligand (**235d**) that is suitable for highly enantioselective vanadium-catalyzed epoxidation of homoallylic alcohols (Scheme 102). Both *trans*- and *cis*-substituted epoxides were achieved with nearly complete enantioselectivities and good yields.

The design of a new C_2-symmetric bis-hydroxamic acid (BHA) ligand has also accomplished the successful asymmetric oxidation of unfunctionalized olefins[190] and sulfides[191] (Scheme 103).

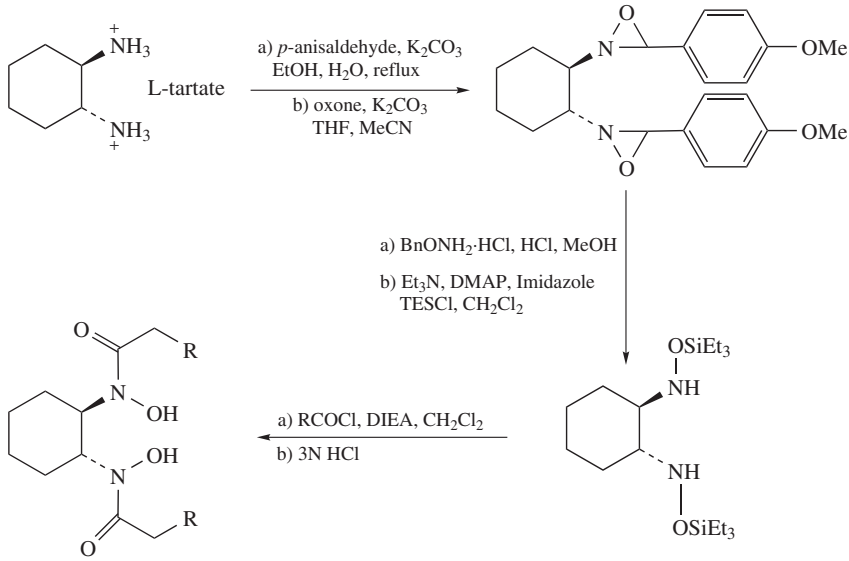

(**235a**) R = $CHPh_2$
(**235b**) R = CH_2CPh_3

DIEA = *N*, *N*-diisopropylethylamine
Bn = benzyl, DMAP = 4-dimethylaminopyridine
TESCl = triethylsilyl chloride

SCHEME 101

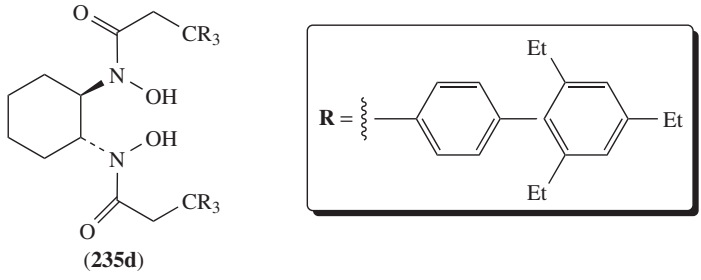

(**235d**)

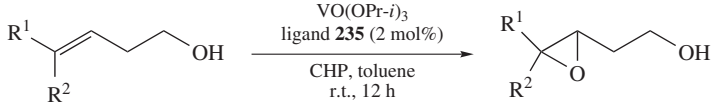

CHP: cumene hydroperoxide

yield > 85
e.e > 96%

R^1, R^2 = H, Et, C_3H_7, C_4H_9, C_5H_{11}, C_6H_{13}, Ph

SCHEME 102

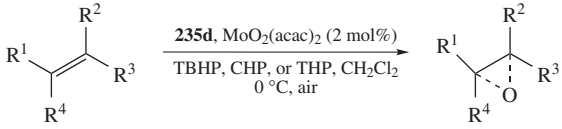

R^1, R^2, R^3 = H, Me, Ph, C_6H_{13} ee: 50–96%

TBHP: *tert*-butyl hydroperoxide, CHP: cumene hydroperoxide, THP: trityl hydroperoxide

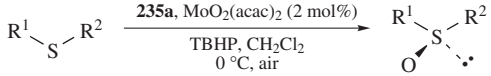

R^1 = Ph, *p*-MeC_6H_4, *o*-MeC_6H_4, 2-$C_{10}H_7$ ee: 54–86%
R^2 = Me, Et, *i*-Pr

SCHEME 103

While coordination chemistry of hydroxamic acids has been studied extensively (particularly with Cu(II), Zn(II), Fe(III), Co(III), and Cr(III) ions)[192, 193], there have been only few reports in the literature on the formation of Cr(V) complexes of these ligands. The current interest in coordination chemistry of Cr(V) arises mainly from the proposed crucial role of reactive Cr(V) intermediates in Cr(VI)-induced genotoxicity and carcinogenicity[194].

M. Some Interesting Hydroxamic Acids

1. Weinreb amides

The so-called Weinreb amides[195] (or *N*-methoxy-*N*-methylamides) are versatile building blocks in organic synthesis[196]. Their preparation can be accomplished by coupling carboxylic acids and *N*,*O*-dimethylhydroxylamine. The majority of the methods reported use peptide coupling reagents such as chloroformates[197], BOP[198], DCC[199] and others[200] or phosphonic derivatives[201]. These reactive reagents are expensive in some cases, and the removal of their excess (and/or the removal of byproducts) from the reaction mixtures may be difficult. Additional purification of the reaction product is often required.

In 2001, De Luca and Giacomelli[202] reported a new simple and high-yielding one-flask synthesis of Weinreb amides from carboxylic acids and *N*-protected amino acids that uses different 1,3,5-triazine derivatives (such as **236**) as the coupling agents (Scheme 104). The method allows the preparation of Weinreb amides **237** and hydroxamates as *O*-benzyl and *O*-silyl hydroxamates that can be easily transformed into hydroxamic acids.

A variety of *N*-methoxy-*N*-methylamides were thus prepared from commercially available carboxylic acids and amino acids. This methodology is applicable to the synthesis of other *O*-alkylhydroxamates and also to the preparation of *O*-silyl hydroxamates.

Deoxo-Fluor reagent is a versatile reagent for acyl fluoride generation and subsequent one-flask amide coupling. Georg and coworkers have explored the utility of this reagent for the one-flask conversion of acids to hydroxamic acids and Weinreb amides (Scheme 105)[203].

The conversion of sterically hindered carboxylic acids to *N*-methoxy-*N*-methyl amides can be efficiently carried out with methanesulfonyl chloride, 3 equivalents of triethylamine and *N*-methoxy-*N*-methylamine. Yields for this process range from 59% to 88%

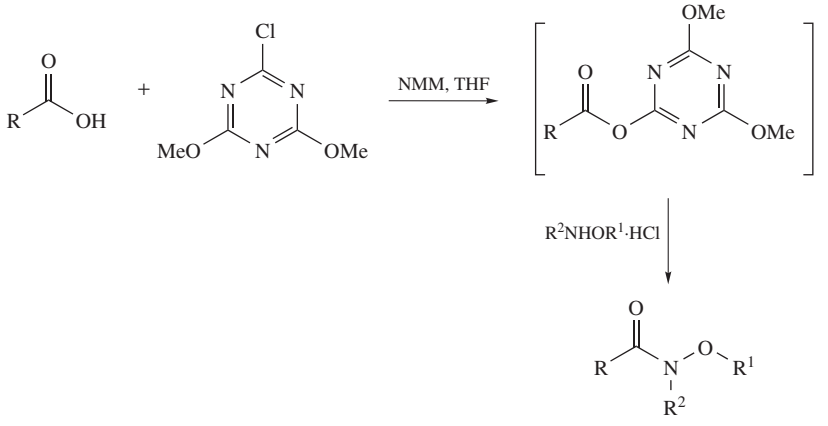

(**237**)

R^1 = Me, Bn, *t*-$BuPh_2Si$; R^2 = H, Me

SCHEME 104

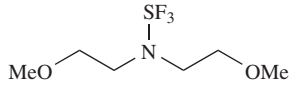

Deoxo-Fluor™

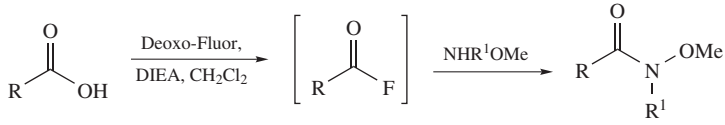

R = alkyl, aryl, hetaryl; R^1 = H, Me

SCHEME 105

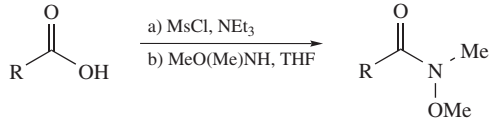

SCHEME 106

(Scheme 106)[204]. The major byproduct in these reactions, *N*-methoxy-*N*-methylmethanesulfonamide, can be removed by placing the product mixture under vacuum for 14–24 h.

The advantage of using the supported reagent as opposed to the solution method becomes apparent during the workup of the reaction. The solid-phase method offers an extremely simple filtration workup in contrast to the aqueous extractive workup necessary for the solution method.

In 1999, Salvino and coworkers[205] developed a novel supported Weinreb amide resin **238** that facilitates parallel synthesis of aldehydes and ketones on a scale useful for chemical library synthesis (Scheme 107).

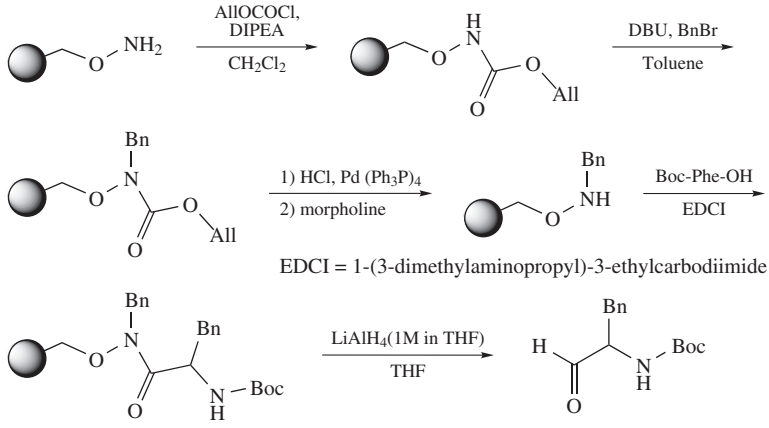

SCHEME 107

This new resin makes it possible to produce custom aldehydes and ketones from a wide range of carboxylic acids, including *N*-Boc-amino acids. No alcohol side product is observed, and the purity of the resulting aldehyde or ketone is so high that it may be used directly as a building block in parallel synthesis of chemical libraries.

2. N-Alkylhydroxamic acids

Recent studies have shown that *N*-arylhydroxamic acids, **239**, have found extensive applications as reagents in spot tests, gravimetric and colorimetric analyses, and in separations involving solvent extraction (Chart 3)[206].

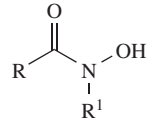

(**239**)

R^1 = aryl, heteroaryl

CHART 3

In 1972, Gupta and coworkers reported the preparation of twelve *N*-arylhydroxamic acids by the condensation of *N*-1-naphthylhydroxylamine and acid chloride in diethyl ether medium[207]. An aqueous suspension of sodium bicarbonate was added to neutralize the liberated hydrochloric acid. The formation of a diacylated derivative was practically prevented by carrying out the reaction at low temperature, preferably below 0 °C.

Most of the reactions proceeded as usual with 40–50% yield. The *ortho*-substituted benzoyl chlorides reacted with difficulty. They readily formed reddish-black products

during reaction. For this reason the hydroxamic acids derived from *o*-nitro-, *o*-chloro- and *o*-iodobenzoic acids could not be prepared. Once prepared, they are generally stable except for those derived from lower fatty acids, which gradually become brown on storage. They are soluble in benzene, alcohol, chloroform, and *o*-dichlorobenzene, and the solutions, are stable for about a week if stored in air-tight brown bottles. This property is of great use from the standpoint of analytical applications. These acids were synthesized with the object of using them as possible organo-analytical reagents for metal ions. All of these acids formed chloroform-extractable reddish-violet/violet complexes with vanadium(V) from concentrated hydrochloric acid media.

General protocols for the preparation of enantiomerically pure *N*-hydroxy α-amino acids have not been accorded enough attention in the literature[208]. These 'oxidized' α-amino acids are important in metabolism[209], in biological processes relevant to human and animal tumors[210], and as naturally occurring metabolites[211]. In 1995, Hanessian and Yang[212] described a very interesting synthesis of *N*-alkoxycarbonyl derivatives **241** of α-hydroxyamino acids **240** by a Mitsunobu displacement reaction of the corresponding readily available α-hydroxy esters. In general, the reactions carry on in excellent yields via an S_N2-type mechanism, affording products of high enantiomeric purity (ee >93%) as shown in Scheme 108.

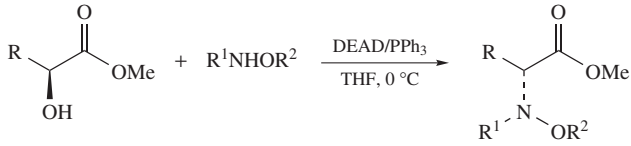

(**240**) (**241**)

R = Me, Bn, Me_2CH, Me_2CHCH_2
R^1 = Cbz, PhOCO-, R^2 = Cbz

Yield: 68–91%
ee: 93–96%

SCHEME 108

3. *O*-Alkylhydroxamic acids

Surprisingly, despite the rising interest in *O*-glycosyl hydroxamates **243**, no direct method for the glycosylation of hydroxamic acids has been reported in the literature. To date, the sole known methodology for preparing such carbohydrate derivatives involves amidation of the corresponding carboxylic acids with *O*-glycosyl hydroxylamines **242** (Scheme 109)[213].

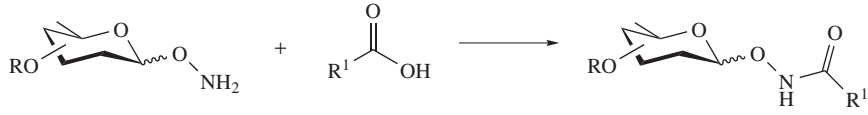

(**242**) (**243**)

SCHEME 109

Papot and colleagues[214] have reported the first efficient *O*-glycosylation of hydroxamic acids **246** (Scheme 110). This process involves the use of glycosyl *N*-phenyl trifluoroacetimidates **244** as glycosyl donors to acids **245** in the presence of TMSOTf and 4 Å molecular sieves in dichloromethane.

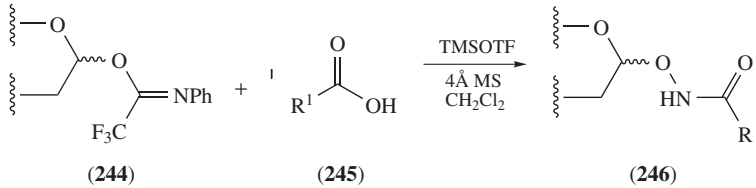

(**244**) (**245**) (**246**)

R = Ph, Bn, Me, $(CH_2)_6CONHPh$

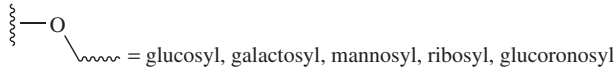

SCHEME 110

Under such conditions, a wide range of new glycosyl donors, including glucosyl, galactosyl, mannosyl, glucuronyl and ribosyl hydroxamates, was prepared in good to high yields. This procedure appears to be an advantageous alternative for the synthesis of glycosyl hydroxamates of biological interest.

4. N-Hydroxyphthalimide: A versatile reagent in organic synthesis

N-Hydroxyphthalimide **178a** (**NHPI**; Chart 4), described for the first time in 1880[215], is a weak acid ($pK_a = 7$), which forms highly colored salts with alkali metals, heavy metals, ammonia or amines. More precisely, the two crystalline forms of NHPI reported in the literature[216,217] display different colors, colorless (white) and yellow, with the colors depending on the solvent in which the NHPI is prepared. The variations in physical properties, including color, have been attributed to synthetic problems[218], such as impurities, and contamination from a fluorescent compound that could not be isolated or characterized.

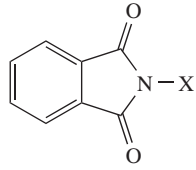

(**178a**) X = H, **NHPI**
(**178b**) X = alkyl
(**178c**) X = Ac
(**178d**) X = Bz

CHART 4

In 2007, in a very exhaustive paper, Paradies and coworkers[219] carried out a comprehensive structural characterization of the colorless and yellow forms of *N*-hydroxyphthalimide (NHPI) by means of single-crystal X-ray diffraction, FTIR and Raman spectroscopies and scanning electron microscopy. In the yellow form, the *N*-hydroxyl group is significantly out of the plane (1.19°), but the *N*-hydroxyl group in the colorless form is only 0.06° out of the plane. The irreversible conversion of the colorless crystalline form to the yellow crystalline form is more like a dynamic isomerism than a polymorphic transformation.

Colorless *N*-hydroxyphthalimide ethers **178b** undergo hydrolysis to *O*-alkylhydroxylamines, H_2NOR[220]. On acylation, *N*-hydroxyphthalimide yields acyl derivatives as **178c** and **178d**[221].

N-Hydroxyphthalimide is a cheap and non-toxic reagent easily prepared by the reaction of hydroxylamine with phthaloyl chloride[215], phthalic anhydride[222] or ethyl phthalate in the presence of sodium ethoxide (Scheme 111)[223]. A hydroxylammonium salt of *o*-carboxybenzohydroxamic acid (**247**) is isolated by use of an excess of hydroxylamine during the synthesis of **178a** from phthalic anhydride (Scheme 111).

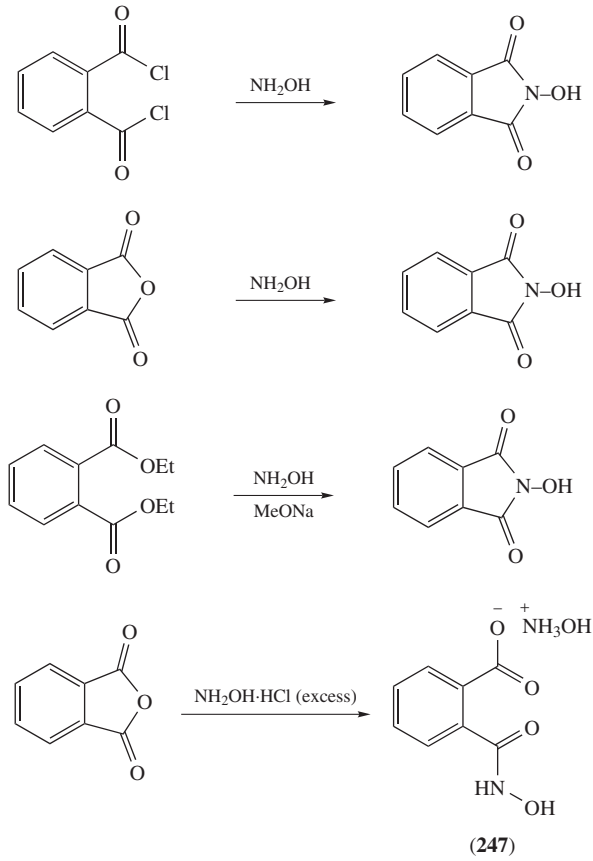

SCHEME 111

N-Hydroxyphthalimide has received significant attention in recent years as a useful catalyst on an industrial scale in the production of cyclohexyl nitrate from cyclohexane and 2-methyl-2-nitropropane from isobutene[224].

Over the past decade, NHPI has emerged as a powerful and popular catalyst for organic oxidation reactions where, together with acetaldehyde, it has been employed as oxidation mediator[225,226]. The use of molecular oxygen for the selective oxidation of organic substrates, especially hydrocarbons under mild conditions, is still a major challenge for organic chemistry[227]. It constitutes an environmentally safe alternative to more

conventional oxidants used in stoichiometric amounts and is therefore of high economic value in industrial chemistry[228]. NHPI has also been used in selective catalytic oxidation, using dioxygen as the primary oxidant. This represents a critical technology in an area of continuing research and development[229, 230].

The molecule has been found to be an efficient electron carrier in electrochemical oxidation, converting secondary alcohols to ketones[231]. Daicel of Tokyo has used NHPI in the development of custom production in proprietary air-oxidation technology[232], and it can also be used to oxidize cyclohexane to adipic acid and *p*-xylene to *p*-toluic acid in the presence of Mn^{2+} or Co^{2+} salts. The new process produces no nitrogen oxides, is more environmentally friendly and does not require the use of denitration equipment.

A further use of the system is to mediate the reaction of adamantane with carbon monoxide and oxygen to form 1-adamantanecarboxylic acid[233]. When long-wavelength light (>300 nm) is used, hydroperoxides efficiently generate hydroxyl radicals without the use of metal ions and would be an extremely useful source of hydroxyl radicals, particularly in the design of DNA-cleaving molecules[234].

III. REFERENCES

1. P. G. Kolandaivel, N. Kuze, T. Sakaizumi, O. Ohashi and K. Iijima, *J. Phys. Chem., A*, **101**, 2873 (1997).
2. P. G. Kolandaivel and K. Senthilkumar, *J. Mol. Struct. (Theochem)*, **535**, 61 (2001).
3. J. Matulic-Adamic and L. Beilgelman, U.S. patent 6316612 (2001); http://www.patentstorm.us/patents/6316612-description.html.
4. F. G. Mann and B. C. Saunders, *Practical Organic Chemistry*, 4th edn., Longmars, Green and Co., New York, 1974, p. 93.
5. T. T. Tidwell, *Angew. Chem. Int. Ed.*, **46**, 2 (2007).
6. S. Dayagi and Y. Degani, in *The Chemistry of Carbon–Nitrogen Double Bond* (Ed. S. Patai), Interscience, London, 1970, p. 61.
7. J. Clayden, N. Greeves, S. Warren and P. Wothers, *Organic Chemistry*, University Press, Oxford, 2001, p. 348.
8. V. Y. Kukushkin and A. J. L. Pombeiro, *Coord. Chem. Rev.*, **181**, 147 (1999).
9. J.-T. Li, X.-L. Li and T.-S. Li, *Ultrasonics Sonochem.*, **13**, 200 (2006).
10. A. Dirksen, T. M. Hackeng and P. E. Dawson, *Angew. Chem. Int. Ed.*, **45**, 7581 (2006).
11. U. Brandt and G. Von Jagow, *FEBS Lett.*, **287**, 215 (1991).
12. H. Tecie, D. J. Lauffer, T. Mirzadegan, W. H. Moos, D. W. Moreland, M. R. Pavia, R. D. Schwarz and R. E. Davis, *Life Sci.*, **52**, 505 (1993).
13. T. Urro, B. Gong and P. G. Schultz, *J. Am. Chem. Soc.*, **116**, 1145 (1994).
14. P. A. S. Smith and E. P. Antoniades, *Tetrahedron*, **9**, 210 (1960).
15. H. Sharghi and M. H. Sarvari, *Synlett*, 99 (2001).
16. M. H. Sarvari, *Synthesis*, 787 (2005).
17. T. Katsuki, *Coord. Chem. Rev.*, **140**, 189 (1995).
18. I. Sasaki, D. Pujol and A. Gaudemer, *Inorg. Chim. Acta*, **134**, 53 (1987).
19. S. Akine, T. Taniguchi, W. Dong, S. Masubuchi and T. Nabeshima, *J. Org. Chem.*, **70**, 1704 (2005).
20. H. E. Smith, *Chem. Rev.*, **83**, 359 (1983).
21. R. V. Hoffman and G. A. Butani, *Synthesis*, 831 (1987).
22. R. J. Gedye, K. Westaway, H. Ali, L. Baldisera, L. Laberge and J. Rousell, *Tetrahedron Lett.*, **27**, 279 (1986).
23. R. J. Giguere, T. L. Bray, S. M. Duncan and G. Majetich, *Tetrahedron Lett.*, **27**, 4945 (1986).
24. D. M. P. Mingos and D. R. Baghurst, *Chem. Soc. Rev.*, **20**, 1 (1991).
25. S. Caddick, *Tetrahedron*, **51**, 10403 (1995).
26. C. O. Kappe and A. Stadler, in *Microwaves in Organic and Medicinal Chemistry Methods and Principles in Medicinal Chemistry* (Eds. R. Mannhold, H. Kubinyi and G. Folkers), Vol. 25, Wiley-VCH, Weinheim, 1995.
27. M. Puciova and S. Toma, *Collect. Czech. Chem. Commun.*, **57**, 2407 (1992).

28. A. R. Hajipour, *J. Chem. Res. (S)*, 228 (1999).
29. S. Su, D. E. Acquilano, J. Arumugasamy, A. B. Beeler, E. L. Eastwood, J. R. Giguere, P. Lan, X. Lei, G. K. Min, A. R. Yeager, Y. Zhou, J. S. Panek, J. K. Snyder, S. E. Schaus and J. A. Porco Jr., *Org. Lett.*, **7**, 2751 (2005).
30. H. Kanno and R. J. K. Taylor, *Synlett*, 1287 (2002).
31. I. A. Dubery, C. W. Holzhapfel, G. J. Kruger, J. C. Schabort and M. Van Dyk, *Phytochemistry*, **27**, 2769 (1988).
32. I. A. Dubery, A. E. Louw and F. R. van Heerden, *Phytochemistry*, **50**, 983 (1999).
33. C. Ito, S. Tanahashi, Y. Tani, M. Ju-ichi, M. Omura and H. Furukawa, *Chem. Pharm. Bull.*, **38**, 2586 (1990).
34. J. N. Armor, *J. Am. Chem. Soc.*, **102**, 1453 (1980).
35. J. J. Byerley and E. Peters, *Can. J. Chem.*, **41**, 314 (1969).
36. J. F. Knifton, British Patent 1, **269**, 483 (1972).
37. D. H. R. Barton, I. Fernandez, C. S. Richard and S. Z. Zard, *Tetrahedron*, **43**, 551 (1987).
38. D. Albanese, D. Landini and M. Penso, *Synthesis*, 333 (1990).
39. N. Ono, *The Nitro Group in Organic Synthesis*, Wiley-VCH, New York, 2001.
40. A. Nielsen, *Nitro Compounds—Recent Advances in Synthesis and Chemistry*, VCH, Weinheim, 1990.
41. C. Czekelius and E. M. Carreira, *Angew. Chem. Int. Ed.*, **44**, 612 (2005).
42. H. Takechi and M. Machida, *Synthesis*, 206 (1989).
43. J. Y. Lee, Y.-T. Hong and S. Kim, *Angew. Chem.*, **118**, 6328 (2006).
44. A. Sera, H. Yamauchi, H. Yamada and K. Itoh, *Synlett*, 477 (1990).
45. G. W. Kabalka, L. H. M. Guindi and R. S. Varma, *Tetrahedron*, **46**, 7443 (1990).
46. B. C. Ranu and R. Chakraborty, *Tetrahedron*, **48**, 5317 (1992).
47. G. W. Kabalka and N. M. Goudgaon, *Synth. Commun.*, **18**, 693 (1988).
48. E. W. Noland, *Chem. Rev.*, **55**, 137 (1955).
49. M. S. Mourad, R. S. Varma and G. W. Kabalka, *Synthesis*, 654 (1955).
50. C. J. Moody and M. R. Pitts, *Synlett*, 1028 (1998).
51. C. J. Moody and M. R. Pitts, *Synlett*, 1575 (1999).
52. B. C. Ranu, *Eur. J. Org. Chem.*, **13**, 2347 (2000).
53. J. S. Yadav, B. V. Subba Reddy, R. Srinivas and T. Ramalingam, *Synlett*, 1447 (2000).
54. A. D. Dilman, A. A. Tishkov, I. M. Lyapkalo, S. L. Ioffe, V. V. Kachala, Y. A. Strelenko and V. A. Tartakovsky, *J. Chem. Soc., Perkin Trans. 1*, 2926 (2000).
55. H. Feger and G. Simchen, *Liebigs Ann. Chem.*, 428 (1986).
56. A. A. Tabolin, A. V. Lesiv, Y. A. Khomutova, P. A. Belyakov, Y. A. Strelenko and S. L. Ioffe, *Synthesis*, 1656 (2005).
57. O. Touster, *Org. React.*, **7**, 327 (1953).
58. T. Kato and Y. Goto, *Chem. Pharm. Bull. (Tokyo)*, **11**, 461 (1963).
59. S. E. Forman, *J. Org. Chem*, **29**, 3323 (1964).
60. T. Okamoto, K. Kobayashi, S. Oka and S. Tanimoto, *J. Org. Chem.*, **53**, 4897 (1988).
61. K. Sugamoto, Y. Hamasuna, Y.-I. Matsushita and T. Matsui, *Synlett*, 1270 (1998).
62. M. Fileti and G. Ponzio, *Gazz. Chim. Ital.*, **25**, 239 (1895).
63. G. Rüedi, M. A. Oberli, M. Nagel, C. Weymuth and H.-J. Hansen, *Synlett*, 2315 (2004).
64. S. E. Boiadjiev and D. A. Lightner, *Tetrahedron*, **58**, 7411 (2002).
65. H. Yamamoto, T. Eikyu, S. Okuda, K. Kawabata, H. Takasugi, H. Tanaka, S. Matsumoto, Y. Matsumoto and S. Tawara, *Bioorg. Med. Chem.*, **10**, 1535 (2002).
66. W. M. Abdou, Y. O. El-Khoshnieh, M. A. I. Salem and R. F. Barghash, *Synlett*, **9**, 1417 (2002).
67. M. Cameron, B. G. Gowenlock and A. S. F. Boyd, *J. Chem. Soc., Perkin. Trans. 2*, 2271 (1996).
68. T. Majid, C. R. Hopkins, B. Pedgrift and N. Collar, *Tetrahedron Lett.*, **45**, 2137 (2004).
69. S. Kim, J. Yong and I. Y. Lee, *Synlett*, 475 (1997).
70. S. Kim, I. Y. Lee, J.-Y. Yoo and D. H. Oh, *J. Am. Chem. Soc.*, **118**, 5138 (1996).
71. S. M. Ali, Y. Matsuda and S. Tanimoto, *Synthesis*, 805 (1988).
72. For the worldwide production of ε-caprolactam, see: http://unit.aist.go.jp/rics/event04/040624ws/Boero.pdf.
73. D. D. Davis and D. R. Kemp, in *Kirk-Othmer Encyclopedia of Industrial Chemistry*, 4th edn., Vol. 1 (Ed. J. I. Kroschwitz), Wiley, New York, 1990, pp. 71–480 and references cited therein.

74. T. Hirabayashi, S. Sakaguchi and Y. Ishii, *Angew. Chem. Int. Ed.*, **43**, 1120 (2004).
75. J. N. Kim and E. K. Ryu, *J. Org. Chem.*, **57**, 1088 (1992).
76. S. Auricchio, A. Bini, E. Pastormerlo, A. Ricca and A. M. Truscello, *Tetrahedron*, **50**, 7589 (1994).
77. S. Auricchio, C. Magnani and A. M. Truscello, *Eur. J. Org. Chem.*, 2411 (2002).
78. H. Andersson, X. Wang, M. Bjorklund, R. Olssonb and F. Almqvista, *Tetrahedron Lett.*, **48**, 6941 (2007).
79. S. Kim and R. Kavali, *Tetrahedron Lett.*, **43**, 7189 (2002).
80. K. S. Lam, M. Lebl and V. Krchnak, *Chem. Rev.*, **97**, 411 (1997).
81. W. F. DeGrado and E. T. Kaiser, *J. Org. Chem.*, **45**, 1295 (1980).
82. W. F. DeGrado and E. T. Kaiser, *J. Org. Chem.*, **47**, 3258 (1982).
83. S. H. Nakagawa and E. T. Kaiser, *J. Org. Chem.*, **48**, 678 (1983).
84. Y. Hamuro, M. A. Scialdone and W. F. DeGrado, *J. Am. Chem. Soc.*, **121**, 1636 (1999).
85. Y. Hamuro, W. J. Marshall and M. A. Scialdone, *J. Comb. Chem.*, **1**, 163 (1999).
86. R. M. van Well, H. S. Overkleeft, G. A. van der Marel, D. Bruss, G. Thibault, P. G. de Groot, J. H. van Booma and M. Overhand, *Bioorg. Med. Chem. Lett.*, **13**, 331 (2003).
87. D. M. Klinman, *Int. Rev. Immunol.*, **25**, 135 (2006).
88. S. L. Beaucage, *Curr. Med. Chem.*, **8**, 1213 (2001).
89. N. Spinelli, O. P. Edupuganti, E. Defrancq and P. Dumy, *Org. Lett.*, **9**, 219 (2007).
90. R. G. Franzen, *J. Comb. Chem.*, **2**, 195 (2001).
91. S. D. Lepore and M. R. Wiley, *J. Org. Chem.*, **64**, 4547 (1999).
92. M. Tremblay, N. Voyer, S. Boujabi and G. F. Dewynter, *J. Comb. Chem.*, **4**, 429 (2002).
93. H. Lossen, *Liebigs Ann. Chem.*, **150**, 314 (1869).
94. C. J. Marmion, D. Griffith and K. B. Nolan, *Eur. J. Inorg. Chem.*, 3003 (2004).
95. M. Ponikvar and J. F. Liebman, Chapter 11 of this book.
96. L. Nakonieczna, M. Milewska, T. Kolasa and A. Chimiak, *Synthesis*, 929 (1985).
97. J. P. Devlin, W. D. Ollis and J. E. J. Thorpe, *J. Chem. Soc., Perkin Trans. 1*, 846 (1975).
98. A. S. Reddy, M. S. Kumar and G. R. Reddy, *Tetrahedron Lett.*, **41**, 6285 (2000).
99. A. R. Katritzky, H.-Y. He and K. Suzuki, *J. Org. Chem.*, **65**, 8210 (2000).
100. A. R. Katritzky, B. V. Rogovoy, N. Kirichenko and V. Vvedensky, *Bioorg. Med. Chem. Lett.*, **12**, 1809 (2002).
101. A. R. Katritzky, N. Kirichenko and B. V. Rogovoy, *Synthesis*, 2777 (2003).
102. G.-R. Vasanthakumar and V. V. S. Babu, *Tetrahedron Lett.*, **44**, 4099 (2003).
103. G. Giacomelli, A. Porcheddu and M. Salaris, *Org. Lett.*, **5**, 2715 (2003).
104. A. Ech-Chahad, A. Minassi, L. Berton and G. Appendino, *Tetrahedron Lett.*, **46**, 5113 (2005).
105. Y. Ogata, T. Harada, K. M. Suyama and T. Lkejiri, *J. Org. Chem.*, **40**, 2960 (1975).
106. J. T. Lai, *Tetrahedron Lett.*, **23**, 595 (1982).
107. P. LeGrel, M. Baudy-Floch and A. Robert, *Tetrahedron*, **44**, 4805 (1988).
108. B. Said, S. Abdelaziz and R. Albert, *Tetrahedron Lett.*, **37**, 179 (1996).
109. I. Ugi, A. Domling and B. J. Werner, *J. Heterocycl. Chem.*, **37**, 647 (2000).
110. A. Basso, L. Banfi, G. Guanti, R. Riva and A. Riu, *Tetrahedron Lett.*, **45**, 6109 (2004).
111. N. D. Kokare, R. R. Nagawade, V. P. Ranea and D. B. Shinde, *Tetrahedron Lett.*, **48**, 4437 (2007).
112. C. R. Hauser and W. B. Renfrow, *Organic Synthesis*, Vol. 2, John Wiley & Sons, Inc, New York, 1943, pp. 67–68.
113. C. J. Burns, R. D. Groneberg, J. M. Salvino, G. McGeehan, S. M. Condon, R. Morris, M. Morrissette, R. Mathew, S. Darnbrough, K. Neuenschwander, A. Scotese, S. Djuric, J. Ullrich and R. Labaudiniere, *Angew. Chem. Int. Ed.*, **37**, 2848 (1998).
114. S.-T. Chen, S.-L. Lin, S.-C. Hsiao and K.-T. Wang, *Bioorg. Med. Chem. Lett.*, **2**, 1685 (1992).
115. J. Spengler and K. Burger, *Synthesis*, 67 (1998).
116. C. Y. Ho, E. Strobel, J. Ralbovsky and R. A. Galemmo Jr., *J. Org. Chem.*, **70**, 4873 (1995).
117. A. Gissot, A. Volonterio and M. Zanda, *J. Org. Chem.*, **70**, 6925 (2005).
118. A. Massaro, A. Mordini, G. Reginato, F. Russo and M. Taddei, *Synthesis*, 3201 (2007).
119. http://www.who.int/mediacentre/factsheets/fs094/en/index.html.
120. http://www.who.int/tdr/diseases/leish/diseaseinfo.htm.
121. P. Zhang, D. E. Nicholson, J. M. Bujnicki, X. Su, J. J. Brendle, M. Fedig, D. E. Kyle, W. K. Milhous and P. K. J. Chiang, *Biomed. Sci.*, **9**, 34 (2002).
122. G. Bhattacharya, M. Salem and K. A. Werbovetz, *Bioorg. Med. Chem. Lett.*, **12**, 2395 (2002).

123. D. H. Hua, M. Tamura, M. Egi, K. Werbovetz, D. Delfin, M. Salem and P. K. J. Chiang, *Bioorg. Med. Chem.*, **11**, 4357 (2003).
124. M. P. Sibi, *Aldrichimica Acta*, **32**, 93 (1999).
125. V. Pilepic and S. Ursic, *Tetrahedron Lett.*, **35**, 7425 (1994).
126. S. Ursic, B. Nigovic, V. Vrcek and V. Pilepic, *Tetrahedron Lett.*, **36**, 9547 (1995).
127. M. D. Corbett and B. R. Corbett, *J. Org. Chem.*, **45**, 2834 (1980).
128. I. V. Vrcek, V. Pilepic and S. Ursic, *Tetrahedron Lett.*, **45**, 699 (2004).
129. Z. Szarka, R. Skoda-Foldes, L. Kollar, J. Horvath and Z. Tuba, *Synth. Commun.*, **30**, 1945 (2000).
130. Z. Szarka, R. Skoda-Foldes, L. Kollar, Z. Berente, J. Horvath and Z. Tuba, *Tetrahedron*, **56**, 5253 (2000).
131. S. R. Sandler and W. Karo, in *Organic Functional Group Preparations*, Vol. III, 2nd edn. (Ed. H. H. Wasserman), Academic Press, New York, 1989, pp. 482–522.
132. M. Couturier, J. L. Tucker, C. Proulx, G. Boucher, P. Dube, B. M. Andresen and A. Ghosh, *J. Org. Chem.*, **67**, 4833 (2002).
133. R. B. Kammer, in *Chemistry and Biology of β-Lactam Antibiotics*, Vol. 3, Chap. 5, (Eds. R. B. Morin and M. Gorman), Academic Press, New York, 1982.
134. M. J. Miller, *Acc. Chem. Res.*, **19**, 49 (1986).
135. M. A. Krook and M. J. Miller, *J. Org. Chem.*, **50**, 1126 (1985).
136. M. J. Miller, A. Biswas and M. A. Krook, *Tetrahedron*, **39**, 2571 (1983).
137. J. E. McMurry. *Acc. Chem Res.*, **7**, 281 (1974).
138. L. A. Paquette (Ed.), *The Encyclopaedia of Reagents for Organic Synthesis*, Vol. 7, Wiley, New York, 1995, 4911 pp.
139. P. G. Mattingly and M. J. Miller, *J. Org. Chem.*, **45**, 410 (1980).
140. M. J. Miller, P. G. Mattingly, M. A. Morrison and F. G. Jr. Kerwin, *J. Am. Chem. Soc.*, **102**, 7026 (1980).
141. D. Romo, R. M. Rzasa, H. A. Shea, K. Park, J. M. Lanhgenhan, L. Sun, A. Akheizer and J. O. Liu, *J. Am. Chem. Soc.*, **120**, 12237 (1998).
142. A. J. Walza and M. J. Miller, *Tetrahedron Lett.*, **48**, 5103 (2007).
143. M. Meloni and M. Taddei, *Org. Lett.*, **2**, 337 (2000).
144. A. Thomas and S. Rajappa, *Tetrahedron*, **51**, 10571 (1995).
145. D. Noble and D. G. Wibberley, *J. Med. Chem.*, **9**, 974 (1966).
146. S. S. Nikam, B. E. Kornberg, D. R. Johnson and A. M. Doherty, *Tetrahedron Lett.*, **36**, 197 (1995).
147. S. Hanessian and S. Johnstone *J. Org. Chem.*, **64**, 5896 (1999).
148. Q. X. Wang and O. Phanstiel, *J. Org. Chem.*, **63**, 1491 (1998).
149. M. H. Jakobsen, O. Buchardt, A. Holm and M. Meldal, *Synthesis*, 1008 (1990).
150. P. J. Hajduk, G. Sheppard, D. G. Nettesheim, E. T. Olejniczak, S. B. Shuker, R. P. Meadows, D. H. Steinman, G. M. Carrera, P. A. Marcotte, J. Severin, K. Walter, H. Smith, E. Gubbins, R. Simmer, T. F. Holzman, D. W. Morgan, S. K. Davidsen, J. B. Summers and S. W. Fesik, *J. Am. Chem. Soc.*, **119**, 5818 (1997).
151. T. Sakamoto and Y. Kikugawa, *J. Org. Chem.*, **59**, 929 (1994).
152. J. M. Altenburger, C. Mioskowski, H. d'Orchymont, D. Schirlin, C. Schalk and C. Tarnus, *Tetrahedron Lett.*, **33**, 5055 (1992).
153. J. Hu and M. J. Miller, *J. Am. Chem. Soc.*, **119**, 3462 (1997).
154. A. J. Walz and M. J. Miller, *Org. Lett.*, **4**, 2047 (2002).
155. A. Rossello, E. Nuti, E. Orlandini, P. Carelli, S. Rapposelli, M. Macchia, F. Minutolo, L. Carbonaro, A. Albini, R. Benelli, G. Cercignani, G. Murphy and A. Balsamo, *Bioorg. Med. Chem.*, **12**, 2441 (2004).
156. K. Yang and B. Lou, *Min-Rev. Med. Chem.*, **3**, 349 (2003).
157. C. D. Floyd, C. N. Lewis, S. R. Patel and M. Whittaker, *Tetrahedron Lett.*, **37**, 8045 (1996).
158. U. Bauer, W.-B. Ho and A. M. P. Koskinen, *Tetrahedron Lett.*, **38**, 7233 (1997).
159. L. S. Richter and M. C. Desai, *Tetrahedron Lett.*, **38**, 321 (1997).
160. S. L. Mellor, C. McGuire and W. C. Chan, *Tetrahedron Lett.*, **38**, 3311 (1997).
161. A. Golebiowski and S. Klopfenstein, *Tetrahedron Lett.*, **39**, 3397 (1998).
162. S. M. Dankwardt, *Synlett*, 761 (1998).
163. E. Thouin and W. D. Lubell, *Tetrahedron Lett.*, **41**, 457 (2000).

164. W. Zhang, L. Zhang, X. Li, J. A. Weigel, S. E. Hall and J. P. Mayer, *J. Comb. Chem.*, **3**, 151 (2001).
165. M. Devocelle, B. M. McLoughlin, C. T. Sharkey, D. J. Fitzgerald and K. B. Nolan, *Org. Biomol. Chem.*, 850 (2003).
166. A. Angeli. *Gazz. Chim. Ital.*, **26**, 17 (1896).
167. E. Rimini, *Gazz. Chim. Ital.*, **31**, 84 (1901).
168. W. Lwowsky, *Angew. Chem., Int. Ed. Engl.*, **6**, 897 (1967).
169. H. L. Yale, *Chem. Rev.*, **33**, 209 (1943).
170. A. Porcheddu and G. Giacomelli, *J. Org. Chem.*, **71**, 7057 (2006).
171. D. E. Robinson and M. W. Holladay, *Org. Lett.*, **2**, 2777 (2000).
172. http://www.fda.gov/Fdac/features/795_antibio.html.
173. D. H. Kim and J. Y. Jin, *Bioorg. Med. Chem. Lett.*, **9**, 691 (1999).
174. N. Kamei, T. Tanaka, K. Kawai, K. Miyawaki, A. Okuyama, Y. Murakami, Y. Arakawa, M. Haino, T. Harada and M. Shimano, *Bioorg. Med. Chem. Lett.*, **14**, 2897 (2004).
175. C. K. Wada, J. H. Holms, M. L. Curtin, Y. Dai, A. S. Florjancic, R. B. Garland, Y. Guo, H. R. Heyman, J. R. Stacey, D. H. Steinman, D. H. Albert, J. J. Bouska, I. N. Elmore, C. L. Goodfellow, P. A. Marcotte, P. Tapang, D. W. Morgan, M. R. Michaelides and S. K. Davidsen, *J. Med. Chem.*, **45**, 219 (2002).
176. J. D. Park and D. H. Kim, *Bioorg. Med. Chem. Lett.*, **13**, 3161 (2003).
177. T. Y. H. Wu, C. Hassig, Y. Wu, S. Ding and P. G. Schultz, *Bioorg. Med. Chem. Lett.*, **14**, 449 (2004).
178. X. Hu, K. T. Nguyen, C. L. M. J. Verlinde, W. G. J. Hol and D. Pei, *J. Med. Chem.*, **46**, 3771 (2003).
179. S. Price and S. E. Osbourne, *Org. Lett.*, **7**, 3761 (2005).
180. K. J. Stanger and V. Krchnak, *J. Comb. Chem.*, **8**, 435 (2006).
181. C. J. Marmion, D. Griffith and K. B. Nolan, *Eur. J. Inorg. Chem.*, 3003 (2004) and references cited therein.
182. K. Rudzka, M. M. Makowska-Grzyska, E. Szajna and A. M. Arif, *Chem. Commun.*, 489 (2005) and references cited therein.
183. K. Rudzka, A. M. Arif and L. M. Berreau, *Inorg. Chem.*, **44**, 7234 (2005).
184. http://nobelprize.org/nobel_prizes/chemistry/laureates/2001/sharpless-lecture.pdf.
185. T. Katsuki, E. N. Jacobsen and M. H. Wu, in *Comprehensive Asymmetric Catalysis I–III* (Eds. E. N. Jacobsen, A. Pfaltz and H. Yamamoto), Springer, Berlin, 1999, pp. 621–678.
186. I. Ojima (Ed.), *Catalytic Asymmetric Synthesis*, Wiley-VCH, New York, 2000, pp. 231–325.
187. H. Adolfsson, in *Modern Oxidation Methods* (Ed. J.-E. Bäckvall), Wiley-VCH, Weinheim, 2004, pp. 21–49.
188. W. Zhang, A. Basak, Y. Kosugi, Y. Hoshino and H. Yamamoto, *Angew. Chem. Int. Ed.*, **44**, 4389 (2005).
189. W. Zhang and H. Yamamoto, *J. Am. Chem. Soc.*, **129**, 286 (2007).
190. A. Barlan, A. Bask and H. Yamamoto, *Angew. Chem. Int. Ed.*, **45**, 45849 (2006).
191. A. Basak, A. Barlan and H. Yamamoto, *Tetrahedron: Asymmetry*, **17**, 508 (2006).
192. B. Kurzak, H. Kozlowski and E. Farkas, *Coord. Chem. Rev.*, **114**, 169 (1992).
193. K. Abu-Dari and K. N. Raymond, *Inorg. Chem.*, **19**, 2034 (1980).
194. S. Gez, R. Luxenhofer, A. Levina, R. Codd and P. A. Lay, *Inorg. Chem.*, **44**, 2934 (2005).
195. S. Nahm and S. M. Weinreb, *Tetrahedron Lett.*, **22**, 3815 (1981).
196. D. Lucet, T. Le Gall, C. Mioskowski, O. Ploux and A. Marquet, *Tetrahedron: Asymmetry*, **7**, 985 (1996).
197. M. Falorni, G. Giacomelli and A. M. Spanedda, *Tetrahedron: Asymmetry*, **9**, 3039 (1998).
198. I. Maugras, J. Poncet and P. Jouin, *Tetrahedron*, **46**, 2807 (1990).
199. M. Braun and D. Waldmuller, *Synthesis*, 856 (1989).
200. M. P. Sibi, C. C. Stessman, J. A. Schultz, J. W. Christensen, J. Lu and M. Marvin, *Synth. Commun.*, **25**, 1255 (1995).
201. M. A. Dechantsreiter, F. Burkhart and H. Kessler, *Tetrahedron Lett.*, **39**, 253 (1998).
202. L. De Luca and G. Giacomelli, *J. Org. Chem.*, **66**, 2534 (2001).
203. J. M. White, A. R. Tunoori, B. J. Turunen and G. I. Georg, *J. Org. Chem.*, **69**, 2573 (2004).
204. J. C. S. Woo, E. Fenster and G. R. Dake, *J. Org. Chem.*, **69**, 8984 (2004).
205. J. M. Salvino, M. Mervic, H. J. Mason, T. Kiesow, D. Teager, J. Airey and R. Labaudiniere, *J. Org. Chem.*, **64**, 1823 (1999).

206. R. J. W. Cremlyn and R. H. Still, *Named and Miscellaneous Reactions in Practical Organic Chemistry*, Heinemann, London, 1967, p. 127.
207. V. K. Gupta and S. G. Tandon, *J. Chem. Eng. Data*, **17**, 248 (1972).
208. R. O. Duthaler, *Tetrahedron*, **50**, 1539 (1994).
209. B. L. Moller, in *Cyanide in Biology* (Eds. B. Venesland, E. E. Conn, C. J. Knowles, J. Westley and F. Wissing), Academic Press, London, 1983, p. 197.
210. J. D. M. Herscheid, G. H. J. N. Knops, S. Boele and A. Hoekstra, *Int. J. Nucl. Med. Biol.*, **13**, 63 (1986).
211. N. Shinmon, M. P. Cava and R. F. C. Brown, *J. Chem. Soc., Chem. Commun.*, 1020 (1980).
212. S. Hanessian and R.-Y. Yang, *Synlett*, 633 (1995).
213. M. Thomas, F. Rivault, I. Tranoy-Opalinski, J. Roche, J.-P. Gesson and S. Papot, *Bioorg. Med. Chem. Lett.*, **17**, 983 (2007).
214. M. Thomas, J.-P. Gesson and S. Papot, *J. Org. Chem*, **72**, 4262 (2007).
215. L. L. Cohn, *Ann. Chem.*, **205**, 295 (1880).
216. L. A. Carpino, *J. Am. Chem. Soc.*, **79**, 98 (1957).
217. D. E. Ames and T. F. Grey, *J. Chem. Soc.*, 3518 (1955).
218. W. R. Roderick and W. G. Brown, *J. Am. Chem. Soc.*, **79**, 5196 (1957).
219. H. Reichelt, C. A. Faunce and H. H. Paradies, *J. Phys. Chem. A*, **111**, 2587 (2007).
220. O. L. Brady, L. C. Baker, R. F. Goldstein and S. Harris, *J. Chem. Soc.*, 529 (1928).
221. C. M. Buess and L. Bauer, *J. Org. Chem.*, **20** 33 (1955).
222. A. Karakurt, S. Dalkara, M. Ozalp, S. Ozbey, E. Kendi and J. P. Stables, *Eur. J. Med. Chem.*, **36**, 421 (2001).
223. L. Bauer and S. V. Miarka, *J. Am. Chem.*, **79**, 1983 (1957).
224. M. Hamamoto, K. Nakayama, Y. Nishiyama and Y. Ishii, *Angew. Chem. Int. Ed.*, **40**, 222 (2001).
225. Y. Ishii, S. Sakaguchi and T. Iwahama, *Adv. Synth. Catal.*, **343**, 393 (2001).
226. C. Einhorn, J. Einhorn, J. Marcadal and J.-L. Pierre, *J. Chem. Soc., Chem. Commun.*, 447 (1997).
227. D. H. R. Barton, A. E. Martell and D. T. Sawyer, *The Activation of Dioxygen and Homogeneous Catalytic Oxidation*, Plenum Press, New York, 1993.
228. U. Schuchardt, W. A. Carvalho and E. V. Spinace, *Synlett*, 713 (1993).
229. F. Minisci, C. Punta, F. Recupero, F. Fontana and G. F. Pedulli, *J. Org. Chem.*, **67**, 2671 (2002).
230. F. Recupero and C. Punta, *Chem. Rev.*, **107**, 3800 (2007).
231. K. Kaneda, S. Ueno, T. Imanaka, E. Shiumotsuma, Y. Nishiyama and Y. Ishii, *J. Org. Chem.*, **59**, 2915 (1994).
232. M.Daicel, *Chem. Eng. News*, **99**, 25 (2001).
233. J. Saito, M. Takayama and T. Matsuura, *J. Am. Chem. Soc.*, **112**, 883 (1990).
234. T. Tezuka and N. Narita, *J. Am. Chem. Soc.*, **101**, 7413 (1979).

CHAPTER 7

Synthesis of heterocycles from oximes

EDGARS ABELE and EDMUNDS LUKEVICS

Latvian Institute of Organic Synthesis, Riga, LV1006, Latvia
Fax: +371-7550338; e-mail: abele@osi.lv and ign@osi.lv

The chemistry of hydroxylamines, oximes and hydroxamic acids
Edited by Z. Rappoport and J. F. Liebman

I. INTRODUCTION

Oximes and their derivatives are widely used in organic synthesis. A number of reviews are devoted to the chemistry and biological activity of oximes and their derivatives[1–10]. The synthesis, reactions and biological activity of oximes containing a heterocyclic substituent, e.g. furan and thiophene[11], indole and isatin[12], pyridine[13], pyrrole[14], quinoline[15] and five-membered heterocycles with two heteroatoms[16] have been reviewed.

Synthesis of heterocycles from amino amide oximes has been described[17]. Recently we have reviewed the synthesis of oximes, oxime *O*-ethers and esters[18], and also the synthesis of heterocycles from oximes covering the literature data published in 1990–1999[19].

Although some of these papers discuss also the synthesis of heterocyclic compounds, no general reviews on the synthesis of heterocyclic compounds from oximes and their derivatives have been published.

The aim of the present review is to describe the methods of synthesis of heterocyclic compounds from oximes and their derivatives.

II. SYNTHESIS OF HETEROCYCLIC COMPOUNDS FROM OXIMES

A. Three-membered Rings

Ketoximes containing α-methylene group can be transformed into aziridines by the action of LAH or Grignard reagent. The reduction of dibenzyl ketoxime (**1**) with LAH in boiling THF led to *cis*-2-phenyl-3-benzylaziridine (**2**) (equation 1). Similarly, *O*-alkylated or acylated dibenzyl oxime derivatives were reduced[20].

(**1**) (**2**) (1)

Highly substituted chalcones and one equivalent of NH_2OH afforded substituted *trans*-2-benzoyl-3-phenyl-1*H*-aziridines[21].

Trifluoromethyl derivatives of aziridine are intensively studied as biologically active substances. (Trifluoromethyl)aziridines **4** were prepared from (trifluoromethyl)ketoximes **3** and Grignard reagents (equation 2). However, this reaction is not general. For example, reaction does not occur with phenyl and allyl Grignard reagents, but when it works the *Z* stereoisomer is formed[22, 23].

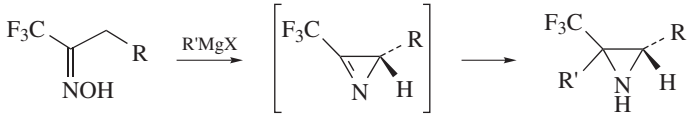

(**3**) (**4**) (2)

An efficient synthesis of 2*H*-azirines **6** substituted with a phosphate group is described. Its key step is an alkaloid catalyzed Neber reaction[24] of β-ketoxime tosylates **5** (equation 3)[25]. Similarly, azirines containing an ester group in position 2 were obtained from tosylated oximes[26]. A novel approach to substituted 2*H*-azirines using benzotriazole (Bt) methodology was recently presented. The reaction of benzotriazole oxime tosylates formed from the oxime **7** and TsCl with aqueous KOH yielded 2-(benzotriazol-1-yl)-2H-azirines.

These intermediates with benzylmagnesium bromides gave 2-benzyl-2*H*-azirines **8** in 50–80% yields, but potassium phthalimide and sodium salt of benzenethiol converted them into the corresponding azirines **9** and **10** in good yields (equation 4)[27]. Similar Neber-type cyclization of α-lithio oxime ethers to highly reactive azirines was recently reported[28].

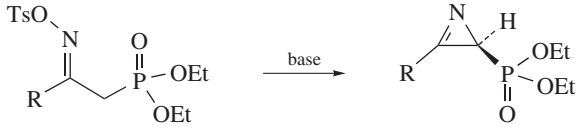

(**5**) (**6**) (3)

85–95%
ee 2–52%

base = quinidine, (–)-sparteine, hydroxyquinidine, quinine

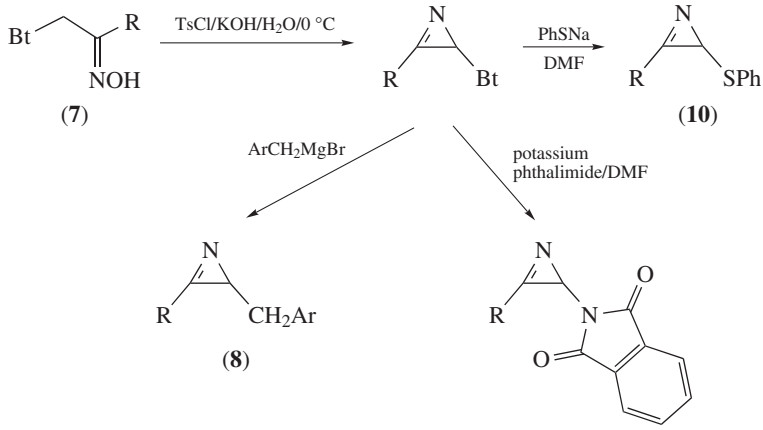

(**7**) (**10**)

(**8**) (**9**) (4)

R = aryl

Synthesis of novel bicyclic heterocyclic systems involving aziridine ring formation has been described. The sodium salts of tosylhydrazones **11** decomposed by heating in benzene and gave aziridinopyrroloindoles **12** in yields up to 73% (equation 5)[29]. Intramolecular cyclization of oxime ether **13** in the presence of base (for example, DBU) in acetonitrile afforded aziridinopyrrolidine **14** in yields up to 51% (equation 6)[30].

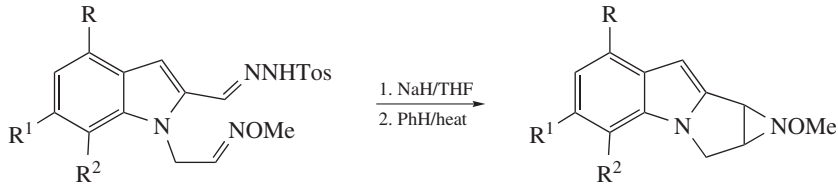

(**11**) R, R^1, R^2 = H, OAlk (**12**) (5)

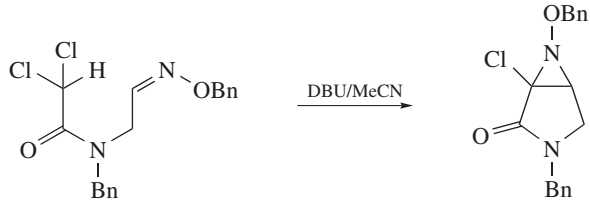

(6)

(**13**) (**14**)

DBU = 1,8-diazabicyclo[5.4.0]undec-7-ene

The oxaziridine ring system has been formed by the oxidation of C=N double bond[31–34]. The two-step synthesis of *N*-phosphinoyloxaziridines **16** from oximes **15** was described (equation 7)[31,32]. Irradiation of hydroperoxynitrones **18**, prepared by dye-sensitized photooxygenation of 2-methoxyfuran in the presence of oximes **17**, led to *trans*-oxaziridines **19** in yields up to 89% (equation 8)[33,34].

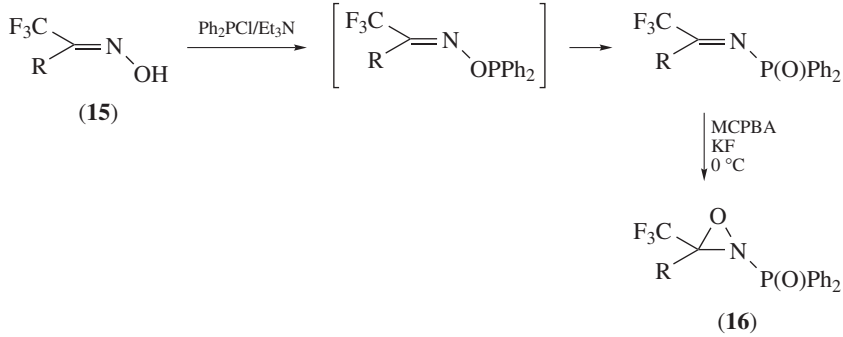

(**15**) (**16**)

(7)

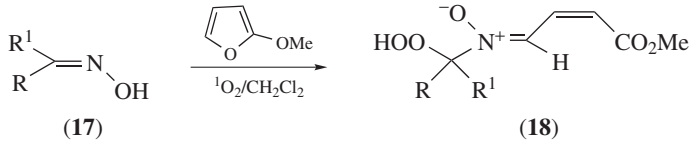

(**17**) (**18**)

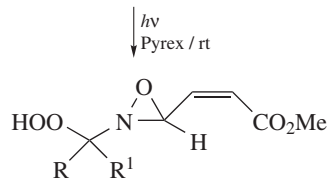

(**19**)

(8)

R, R^1 = H, alkyl, aryl; MCPBA = *meta*-chloroperbenzoic acid

Diazirine ring formation from oxime *O*-tosylates[35–39] or *O*-sulfonates[40] and NH_3 or primary amines has been described. Recently, it was found that this reaction was catalyzed

by ytterbium(III) triflate. Thus, oxime tosylate **20** in the system $NH_3/Yb(OTf)_3/CH_2Cl_2$ afforded 3*H*-diazirine ring system **21** (equation 9)[39].

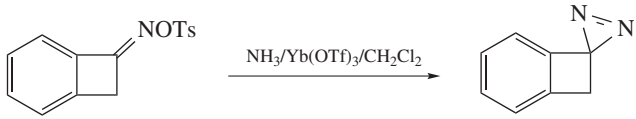

(**20**) (**21**) 10% (9)

B. Four-membered Rings

Photosensitized decomposition of oxime oxalyl amides proceeded via carbamoyl radicals which underwent 4-*exo* cyclizations forming four-membered β-lactams as main products. Irradiation of solution of oxime derivative **22** and 4-methoxyacetophenone (MAP) in toluene at 100 °C with a 400 W UV lamp led to azetidinone **23** in 3:1 ratio of diastereoisomers (equation 10)[41,42].

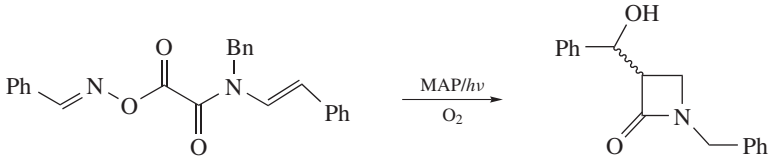

(**22**) (**23**) 69% (10)

C. Five-membered Ring Systems

1. Furan and thiophene

Synthesis of a benzofuran ring was successfully realized from *O*-arylated oximes in the presence of acidic catalyst (Fisher method)[43–46]. For example, oximes **24** in the presence of a mixture of trifluoroacetyl triflate (TFAT) and 4-dimethylaminopyridine (DMAP) in CH_2Cl_2 at room temperature afforded 2-arylbenzofurans (**25**) in yields up to 99% (equation 11)[43].

Synthesis of dihydrofuran derivatives by cyclization of oxime derivatives has been described. Thus, reduction of 2-quinolineacetaldoxime (**26**) with H_2/PtO_2 afforded furanoquinoline **27** as a single product (equation 12)[47]. 4-Formyl-3-hydroxy-5-hydroxymethyl-2-methylpyridine oxime (**28**) in the system $NaNO_2/HCl/H_2O$ cyclized to furopyridine **29** (equation 13)[48].

Dihydro- and tetrahydrofuroisoxazoline rings were constructed by intramolecular cycloaddition of nitrile oxides or nitrones, generated from oximes[49–51]. Thus, oxime **30** and sodium hypochlorite afforded furoisoxazolines **31** (equation 14). Similarly, furanyl or thienyl oximes **32** in the presence of NaOCl afforded tricyclic products **33** in 35–90% yields (equation 15). Nitrostyrenes ($ArCH{=}CHNO_2$) and various nucleophiles (for example, allyl mercaptan) also generated hydroximoyl chlorides which underwent similar cycloaddition leading to bicyclic tetrahydrothiophene and tetrahydrofuran derivatives[52,53].

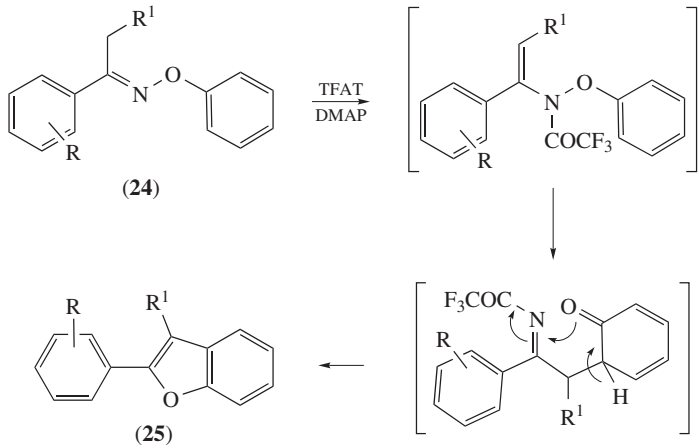

(**24**) (**25**) (11)

R = H, Br, OH, OR, NO_2; R^1 = H, Me

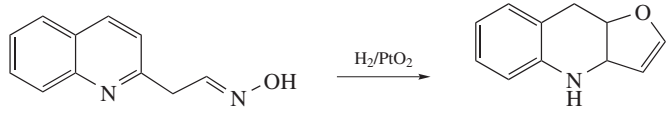

(**26**) (**27**) (12)

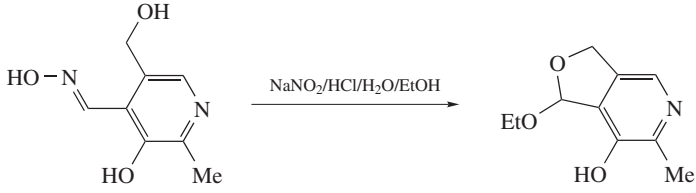

(**28**) (**29**) (13)

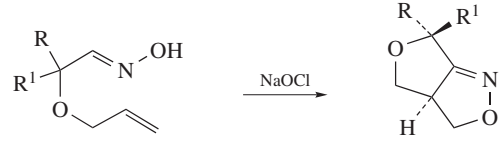

(**30**) R, R^1 = H, Me, Ph (**31**) (14)

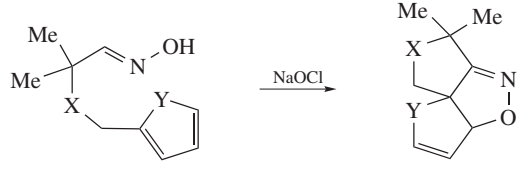

(**32**) (**33**) (15)

X, Y = O; X = O, Y = S; X = S, Y = O

Intramolecular cycloaddition reaction of *O-tert*-butyldimethylsilyloximes having allyloxy moieties **34** was efficiently catalyzed by BF_3•OEt_2. Bicyclic products **35** were isolated in yields up to 87% (equation 16)[54,55].

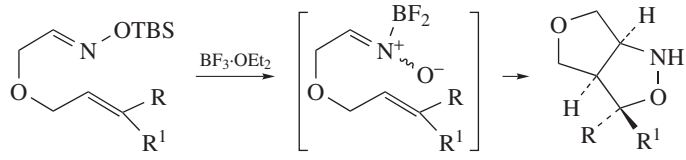

(**34**) (**35**) (16)

TBS = *t*-$BuMe_2Si$; R, R^1= H, Me, Ph

Radical cyclization of oxime ethers having allylic substituents to five-membered rings including furan and pyrrole derivatives was described in reviews[56,57]. A thiophenol-promoted radical cyclization of oxime ethers into tetrahydrofurans was recently described. For example, oxime derivative **36** in the presence of thiophenol and azobisisobutyronitrile (AIBN) afforded substituted tetrahydrofurans **37** and **38** in a ratio 1.2–3:1 (equation 17)[58–61]. Radical cyclization of oxime ethers **39** to tetrahydrofurans **40** was successfully realized in the presence of alkyl iodides and Et_3B in refluxing toluene (equation 18)[62].

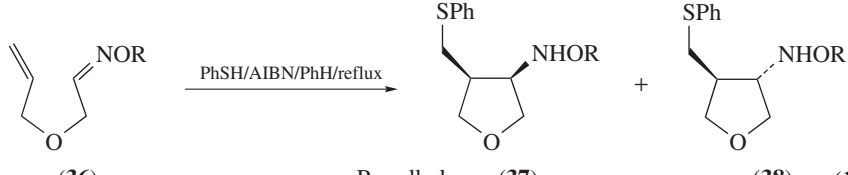

(**36**) R = alkyl (**37**) (**38**) (17)

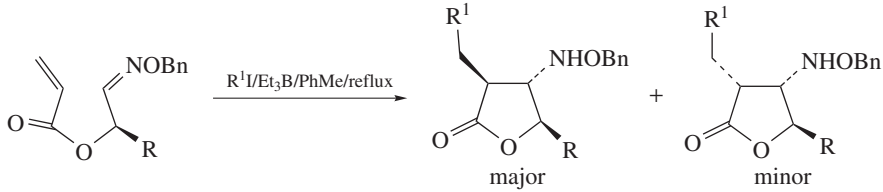

(**39**) R^1 = alkyl (**40**) (18)

Cobaloxime-mediated intramolecular radical cyclization of oxime ethers **41** to furan derivatives **42** occurred during electrolysis in yields up to 76% (equation 19)[63].

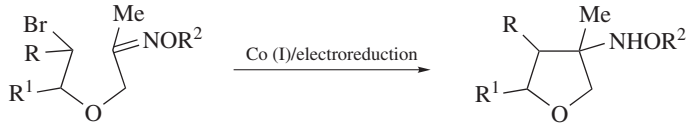

(**41**) (**42**) (19)

R, R^1 = H, Alk, OAlk, RR^1 = -$(CH_2)_n$O-, n = 2,3; R^2 = Me, Bn

2. Trioxolanes

Ozonolysis of acyclic ketoximes **43** in the presence of ketones resulted in the formation of tetrasubstituted cross-ozonolides (1,2,4-trioxolanes) **44** in yields up to 73% (equation 20). Ozonolysis of *O*-methylated monooximes of 1,4-, 1,5- and 1,6-dicarbonyl compounds afforded bicyclic oxonides[64].

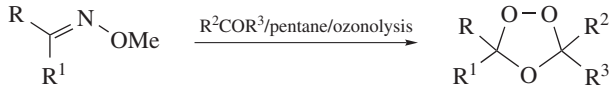

(**43**) (**44**) 11–73% (20)

Ozonolysis of the *O*-methyl oximes of cyclic ketones in the presence of 1,4-cyclohexanedione and ozonolysis of the *O*-methylated dioxime of 1,4-cyclohexanedione in the presence of cyclic ketones afforded the corresponding diozonides[65].

3. Dithioles

The cyclobutanone oxime derivatives **45** reacted with disulfur dichloride, *N*-chlorosuccinimide (NCS) and Hunig's base to give three unexpected 10π pseudoazulenes in low yield: the dark blue cyclopenta-1,2-dithiole (**46**), its red isomer **47** as well as orange cyclopenta-1,2-thiazine **48** (equation 21). The mechanism of formation of compound **46** included cyclobutane ring opening, with subsequent reaction with S_2Cl_2 and formation of the dithiole ring system[66].

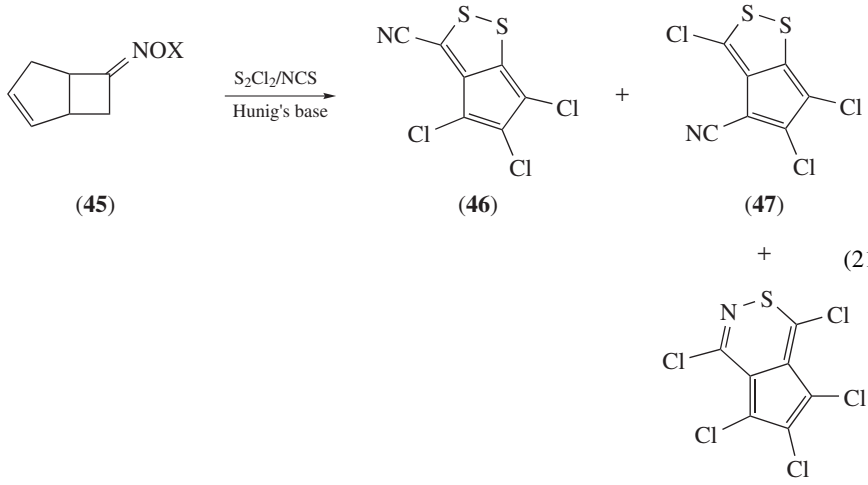

(**45**) (**46**) (**47**) (21)

X = H, $SiMe_3$ (**48**)

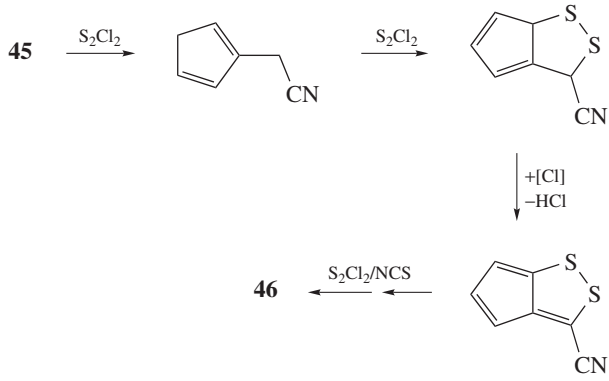

4. Pyrroles

General synthesis of pyrroles and 1-vinylpyrroles by the reaction of ketoximes with acetylenes and their synthetic equivalents (vinyl halides and dihaloethanes) in the presence of the strongly basic KOH/DMSO system (Trofimov reaction) has been reviewed[67–70] in recent years. Therefore, in the present work this reaction will be described very shortly. In principle, pyrrole (**51**) synthesis can be carried out as a one-pot procedure by treating ketones (**49**) with hydroxylamine and then reacting the ketoximes (**50**) formed with acetylenes (equation 22).

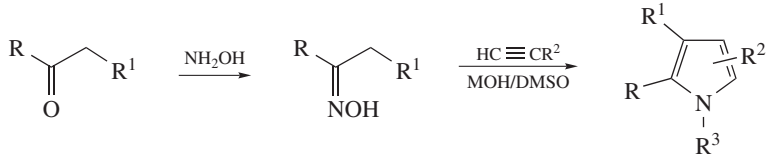

(22)

(**49**) (**50**) (**51**)

R, R^1 = alkyl, aryl, hetaryl; R^2 = H, Me, Ph; R^3 = H, CH_2=CH, PhCH=CH; M = Li, Na, K, Rb

2-(2-Benzofuranyl)pyrroles[71], 2-(2-thienyl)pyrroles[72–74], 2,2′-dipyrroles[75], 3-(2-pyrrolyl)indoles[76,77], 2-(2-benzimidazolyl)pyrroles[78] and 2-(2-, 3- and 4-pyridyl)pyrroles[79–81] were prepared using this method. Reaction of alkynes (for example, propyne) or allene with ketoximes in a superbase system (MOH/DMSO) leads to 2,5-di- or 2,3,5-trisubstituted pyrroles[82,83]. Pyrroles and dipyrroles were synthesized also from corresponding dioximes and acetylene in a KOH/DMSO system[84–86]. It has also been shown that 1,2-dichloroethane can serve as a source of acetylene in pyrrole synthesis[87]. Oxime **52** in the system acetylene/RbOH/DMSO at 70 °C afforded a mixture of three pyrroles **53–55** in low yields (equation 23). The formation of product **53** occurred through recyclization of pyrrolopyridine intermediate[88].

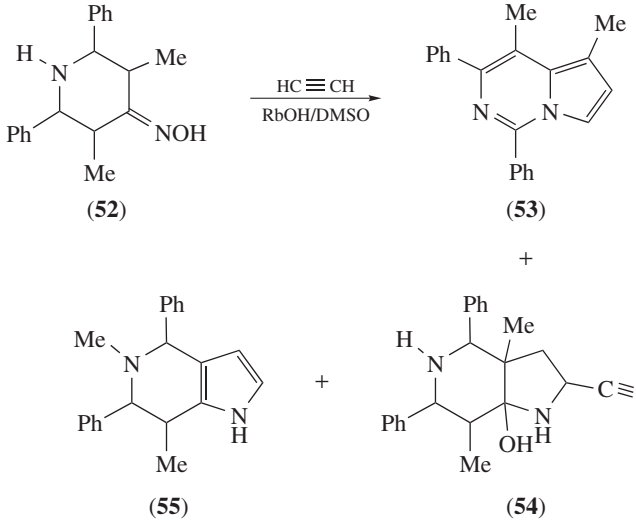

(**52**) (**53**) (23)

(**55**) (**54**)

2-Phenyl- and 2-(2-thienyl)-3,3-dimethyl-3*H*-pyrroles (**58**) were obtained by the reaction of the corresponding ketoximes **56** with acetylene catalyzed by MOH (M = Na, K) in DMSO. The reaction intermediate observed is the corresponding *O*-vinyl oxime **57** which undergoes [3,3] sigmatropic rearrangement and cyclization to products **58** (equation 24). The yield of the products obtained strongly depends on the structure of the ketoxime[89].

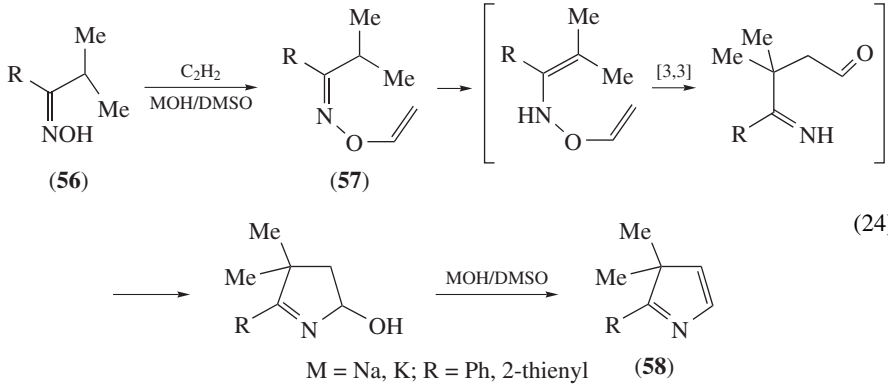

(**56**) (**57**) (24)

M = Na, K; R = Ph, 2-thienyl (**58**)

Reaction of cyclohexanone oxime (**59**) with phenylacetylene in the presence of KOH/DMSO afforded *Z*-[1-(2-phenylvinyl)]-3-phenyl-4,5,6,7-tetrahydroindole (**60**) (equation 25)[90]. Transformation of *O*-vinylacetophenone oxime (**61**) in the system *t*-BuOK/THF has been studied. The reaction at 60–65 °C afforded 2,4-diphenylpyrrole (**62**) and oligomeric products instead of the desired 2-phenylpyrrole (equation 26)[91].

Regioselective synthesis of 2-substituted pyrroles using oximinocyanoacetate esters or related compounds in a Knorr-type reductive condensation with diketones was described[92–96]. Thus, oximinocyanoacetates **63** reacted with pentane-2,4-diones **64** in hot

acetic acid in the presence of zinc dust, giving pyrrole-2-carbonitriles **65** when the acetic acid was wet (equation 27)[92].

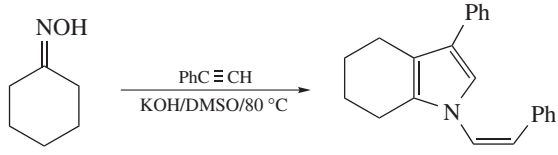

(**59**) (**60**) 42% (25)

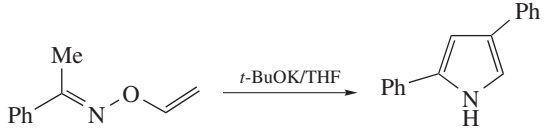

(**61**) (**62**) 21% (26)

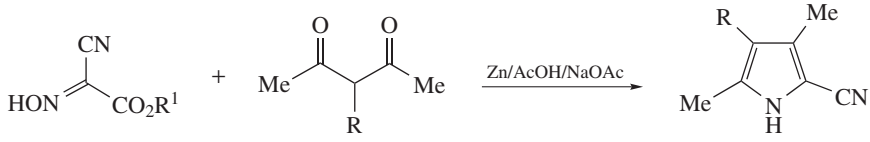

(**63**) (**64**) (**65**)

R = H, $CH_2CH_2CO_2Me$ 23–28% (27)

The pyrrolo[2,3-d]pyrimidine **67** ring system can be obtained from 4-amino-substituted pyrimidine oxime **66** and Dowex-50 in water (equation 28)[97]. Similar cyclization was realized in the presence of benzaldehyde and concentrated HCl[98].

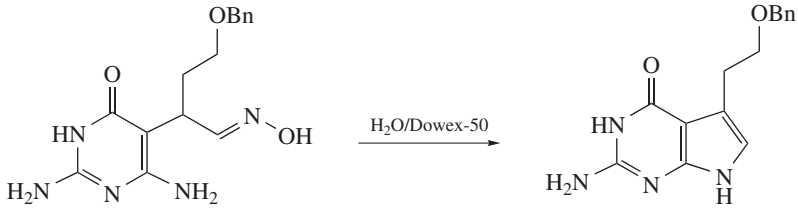

(**66**) (**67**) 71% (28)

Pyrrole and dihydropyrrole derivatives were obtained by palladium-[99–105] or copper-[106] catalyzed intramolecular Heck-type amination of the olefinic moiety in oximes of unsaturated ketones[107]. Substituted pyrroles **69** were synthesized from γ,δ-unsaturated ketone *O*-pentafluorobenzoyl oximes **68** (equation 29). The formation of products **69** proceeds via 3,4-dihydro-2*H*-pyrroles, which undergo aromatization by treatment with Me_3SiCl[99].

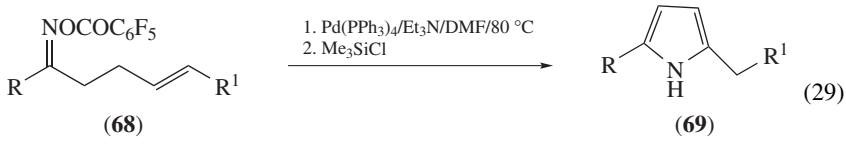

(**68**) (**69**) (29)

R = Alkyl, aryl; R^1 = H, Me, CO_2Et 35–88%

Heck-type cyclization of oxime ethers which contain a halogenated aryl group is a new route to dihydroindole oxime ethers. Thus, oxime ethers **70** in the system $Pd(PPh_3)_4/K_2CO_3$/dioxane afforded dihydroindoles **71** in 59–89% yields (equation 30)[108].

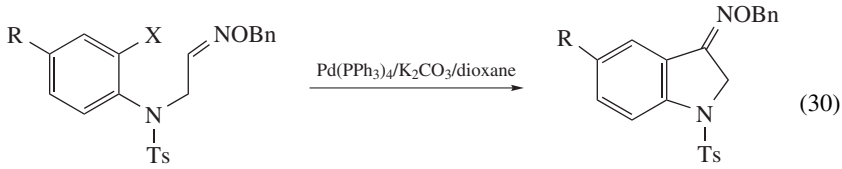

(**70**) X = Br, I; R = H, Me, OMe, CO_2Me (**71**) (30)

Cyclization of *p*-hydroxybenzylacetone derivatives **72** proceeds when treated with tetrabutylammonium perrhenate and trifluoromethanesulfonic acid in refluxing $ClCH_2CH_2Cl$, affording azaspirodienones **73** in moderate to good yields (equation 31). The azaspirodienones are easily transformed into quinolines via dienone–phenol rearrangement[109–111].

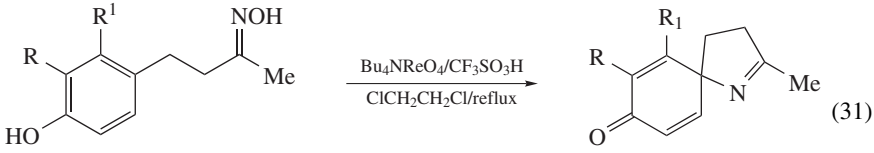

(**72**) (**73**) (31)

R, R^1 = H, alkyl 52–91%

3,4-Dihydro-2*H*-pyrroles were prepared by base-catalyzed cyclization of oxime esters or activated ethers. Thus, 3,4-dihydropyrroles **75** were obtained from (*E*)-*O*-methylsulfonyl oximes **74** having an active methine group at the γ-position by treatment with DBU (equation 32). The stereoselectivity of the cyclization is evidence that S_N2 substitution occurs at the nitrogen atom of oximes **74**[112]. Alkylidene radicals can be easily generated from *O*-2,4-dinitrophenyl oximes **76** of γ,δ-unsaturated ketones by treatment with NaH and phenols, 3,4-methylenedioxyphenol being the best. The resulting radical species intramolecularly add to the olefinic moiety to afford 3,4-dihydro-2*H*-pyrroles **77** (equation 33) in moderate to good yields[113, 114].

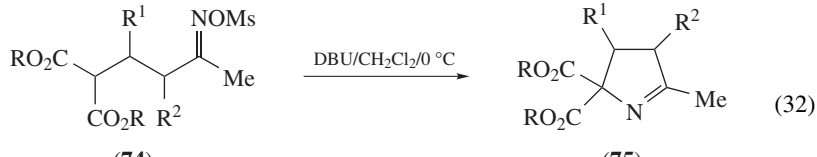

(**74**) (**75**) (32)

R = Me, Bn; R^1 = H, alkyl, Ph; R^2 = H, Me 85–99%

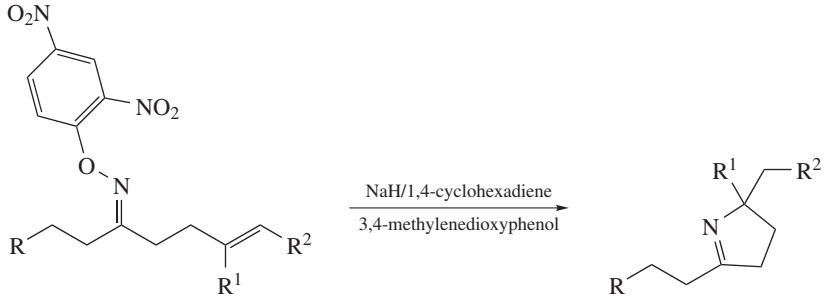

(**76**) (**77**) (33)

R = alkyl, Ph; R^1 = H, Me; R^2 = H, Ph; R^1R^2 = cycloalkyl 54–86%

The oxime esters or benzyl ethers having alkene substituents were readily cyclized to the corresponding dihydropyrroles or related polycyclic pyrrole derivatives in the presence of radical initiators or irradiation[115–124]. Thus, oxime benzoates react with Bu_3SnH in the presence of AIBN to give iminyl radicals, which can be captured by an internal olefin. Thus, slow addition of Bu_3SnH and AIBN to refluxed solution of oxime **78** in cyclohexane afforded pyrrolenine **79** in good yield (equation 34)[115,116]. Irradiation of ketoxime *O*-(*S*-methyl)xanthates **81,** prepared *in situ* from oximes **80** and NaH/CS_2/MeI, leads to dihydropyrroles **82** through cyclization of an intermediate iminyl radical in a radical chain reaction (equation 35). The last reaction step involves transfer of a dithiocarbonate group and various external radical traps can be incorporated into the medium, allowing access to a variety of substituted dihydropyrroles[117].

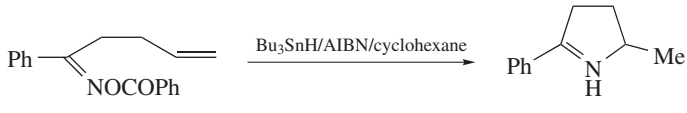

(**78**) (**79**) (34)

88%

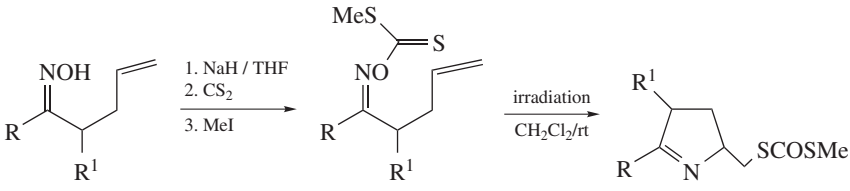

(**80**) (**81**) (**82**)

R = alkyl, aryl; R^1 = H, alkyl; R, R^1 = cycloalkyl (35)

The intramolecular cyclization of oximes with alkene substituents to dihydropyrroles in the presence of radical initiator or by heating was also described[125–130]. Thus, oxime **83** underwent a tandem 1,2-prototropy–cycloaddition sequence and gave an unstable cycloadduct **84,** which on treatment with NaOH afforded indolizine **85** (equation 36)[125].

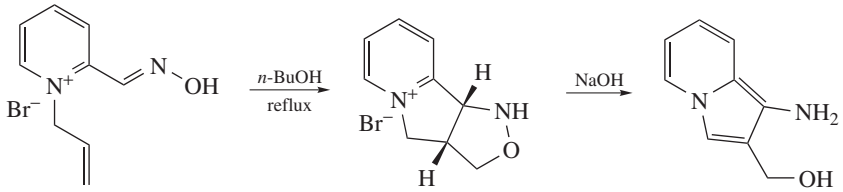

(**83**) (**84**) (**85**)

60% (36)

[2-(1-Hydroxyiminoethyl)phenyl]acetic acid (**86**) was easily transformed to 3-methyl-1*H*-isoindole-1-carboxylic acid (**87**) in the presence of hydrochloric acid (equation 37)[131].

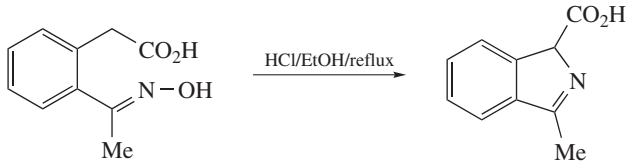

(**86**) (**87**) (37)

Recently, it was described that interaction of 1,2,2,3,3-pentacyanocyclopropane-1-carboxamide **88**, obtained by reaction of tetracyanoethylene and monobromocyanoacetamide, with oximes leads to 4,4-bis(alkylideneaminooxy)-2-amino-*N*,*N*-dimethyl-1,5,6-tricyano-3-azabicyclo[3.1.0]hex-2-en-6-carboxamides **89** as main products (equation 38)[132, 133].

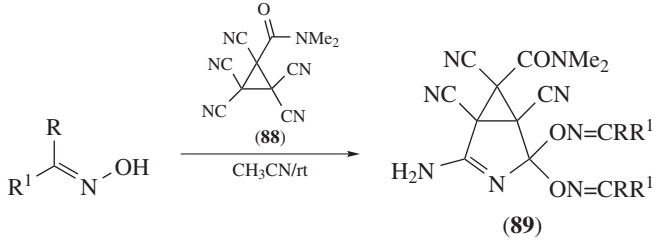

(**89**) (38)

R = Me, R^1 = Me, Et; RR^1 = –$(CH_2)_4$– 25–44%

Reduction of oxime **90** with $NaBH_4$ leads to a mixture of three products **91**–**93**. At low temperatures (−10 °C) pyrroloindole **91** was isolated as the main product (equation 39)[134].

1,3-Diphenyl-2-hydroxyimino-1,3-propanedione (**94**) reacted with phosphonium ylides to give as main products 1-hydroxy-2,3-dihydropyrroles **95** along with novel ylides (equation 40)[135].

Radical cyclization of oximes or oxime ethers having allylic substituents or an aldehyde group to tetrahydropyrrole derivatives was described[136–140]. Thus, SmI_2-induced 5-*exo*-*trig* radical cyclization of oxime ethers containing a formyl group was found to be particularly effective for the preparation of cyclic *trans*-amino alcohols. For example, oxime **96** in the system SmI_2/THF/*t*-BuOH at 25 °C or −78 °C afforded pyrrolidin-3-ols **97** and **98** in a ratio 3:2 or 9:1 (equation 41)[136]. Cyclization of oxime ether **99** in the

system *i*-PrI/Et_3B/hexane at 80 °C leads to product **100** in 63% yield (equation 42)[139]. Similar cycloadditions were realized also by heating of reaction mixtures[141, 142].

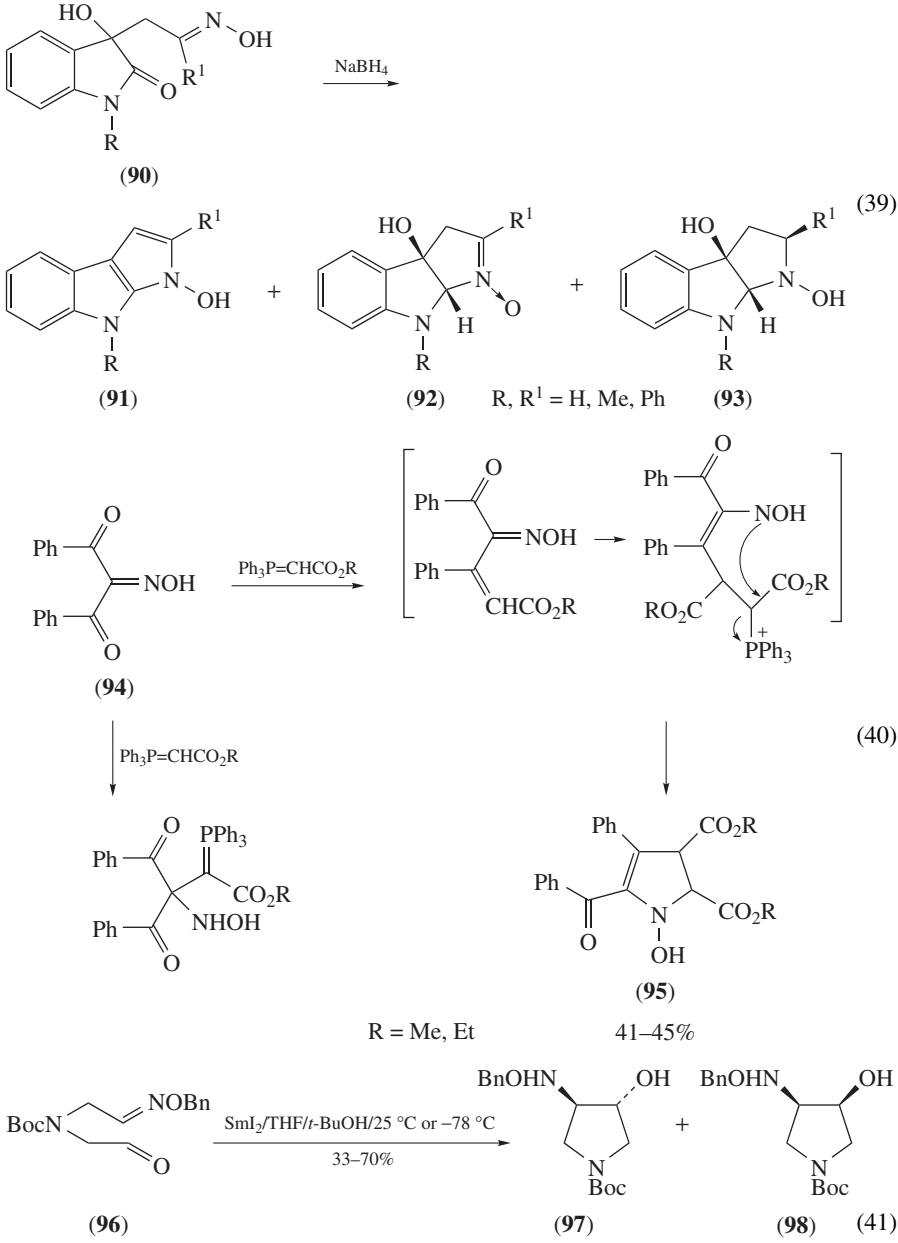

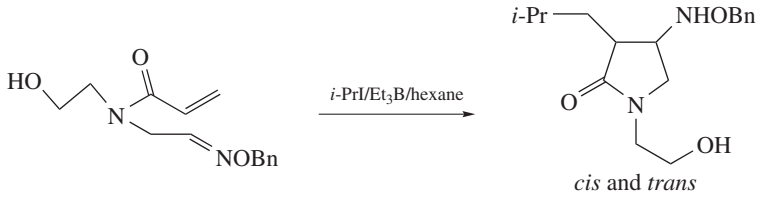

(42)

(**99**) (**100**)

Thermal hetero [3 + 2] cycloaddition reaction of dipolar alkene with *O*-alkyloximes produces substituted pyrrolidines. Thus, heating a mixture of alkylidenecyclopropane **102** with *anti*-*O*-alkyloximes **101** yields substituted pyrrolidines, which upon hydrolysis under mild conditions give 3-alkoxycarbonylpyrrolidines **103** in moderate to good yields (equation 43)[143].

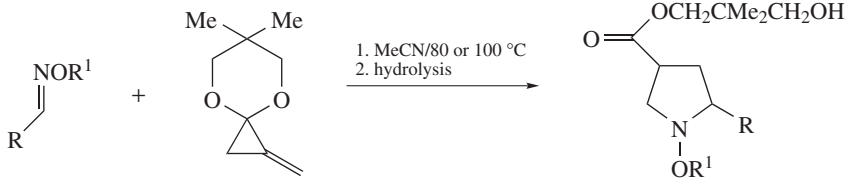

(43)

(**101**) (**102**) R = aryl, hetaryl, CO_2Me; R^1 = Me, Bn (**103**)

The consecutive reduction and cyclization of *O*-benzoyl protected 5-*O*-methylhexose *O*-(*tert*-butyldiphenylsilyl)oxime (**104**) with dimethylphenylsilane in trifluoroacetic acid afforded a *N*-hydroxypyrrolidine (**105**) ring system in good yield (equation 44). The mechanism involves a cascade of neighboring group participation steps involving the *O*-benzoyl protecting groups[144].

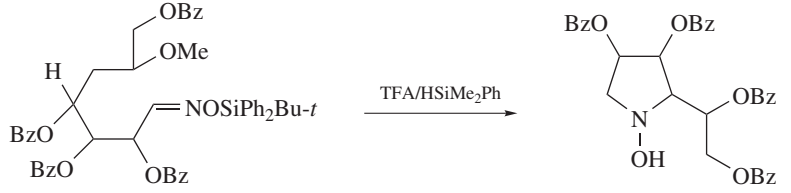

(44)

(**104**) (**105**)

70–73%

Reduction of oxirane oxime **106** with LAH in ether leads to pyrrolidine **107** as a 1:1 mixture of *cis*- and *trans*-isomers (equation 45)[145].

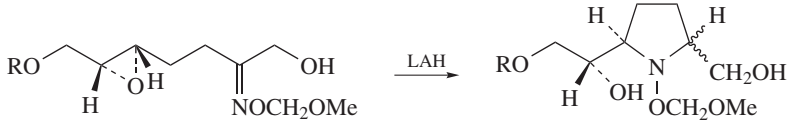

(45)

(**106**) R = $SiMe_2Bu$-*t* (**107**)

Synthesis of isatin **109** derivatives readily proceeds from anilide-derived oximes **108** by interaction with sulfuric acid (equation 46)[146–148].

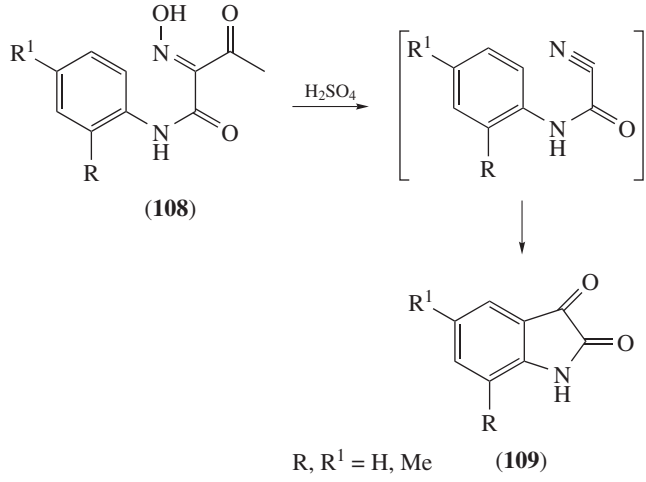

(46)

5. Pyrazole and imidazole

Synthesis of some pyrazole derivatives from amidoximes was reviewed by Karbonits and Horvath[17]. It has been shown that acrylophenone or methacrylophenone oximes (**110**) on treatment with BuONO in the presence of pyridine and copper(II) sulfate, and with subsequent interaction with dilute NaOH and acidification, gives 3(5)-phenyl-1-hydroxypyrazole 2-oxide or 4-methyl-3(5)-phenyl-1-hydroxypyrazole 2-oxide (**111**), respectively (equation 47)[149,150].

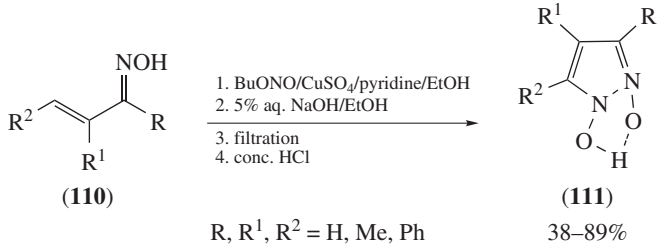

(47)

Similar synthesis of 1-hydroxypyrazole-2-oxides was realized in the presence of Co(II) ions[151] or HNO_2[152] as nitrosating agent. Pyrazole-*N*-oxides were successfully obtained from 1,3-dioximes and $SOCl_2$[153].

Conjugated oximes were converted to pyrazoles in a one-pot reaction by refluxing with hydrazine and iodine in ethanol. The process proceeds via an inverse electron-demand Diels–Alder reaction involving electron-deficient heterodienes and diimide species as dipolarophiles[154].

Pyrazoles were obtained from corresponding 2-hydroxy(or alkoxy-)imino-1,3-diketones or related ketoesters and hydrazine[155–158]. Thus, reaction of oximes **112** with hydrazine in ethanol afforded aminopyrazoles **113** in 48–95% yields (equation 48)[157]. Interaction of

3-hydroxyimino-2,4-dioxopentanone (**114**) and hydrazine hydrate leads to *trans*-bis(3,5-dimethyl-4-nitrosopyrazole) dimer (**115**) in 42% yield (equation 49)[158].

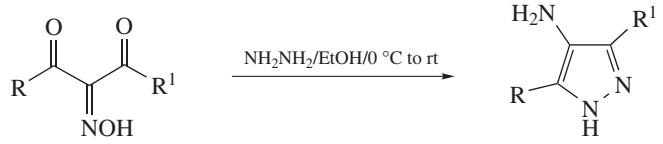

(48)

(**112**) (**113**)

R = alkyl, aryl; R^1 = Me, Et, $CHMe_2$, CO_2Et

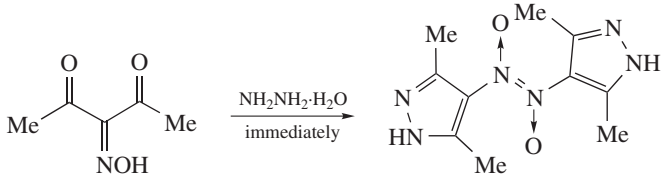

(49)

(**114**) (**115**)

Esters of oximes of $R(C{=}NOR^1)CH_2Het$ type (where Het is a nitrogen-containing heterocycle, R = H, alkyl; R^1 = $COCF_3$, $SO_2C_6H_4R^2$-*p*) readily undergo Beckmann rearrangement forming bicyclic pyrazole-containing heterocycles[159–164]. Benzothiazole oxime **116** in the presence of an excess of trifluoroacetic anhydride (TFAA) at room temperature afforded 2-methyl-3-trifluoroacetylpyrazolo[5,1-*b*]benzothiazole **117** in 92% yield (equation 50)[160]. Pyridine oximes **118** were transformed to pyrazolo[1,5-*a*]pyridines **119** by a two-step process (equation 51)[161].

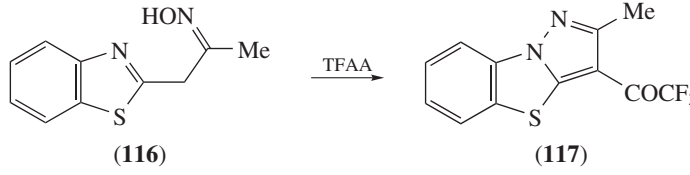

(50)

(**116**) (**117**)

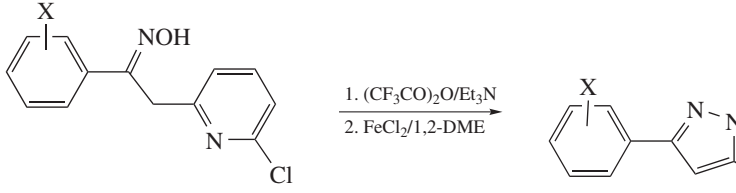

(51)

(**118**) (**119**)

X = H, F, Cl, Br, alkyl, aryl, NH_2, $CONH_2$, NHR

The treatment of substituted ethyl 1-(3,4-dihydro-3,3-dimethylisoquinolyl)-1-oximinoacetates **120** with hydrazine hydrate leads to a 3,4-dihydroisoquinoline ring enlargement

with the annulation of a pyrazole ring to form substituted 5,5-dimethyl-2,3,5,6-tetrahydro-3-oxopyrazolo[3,4-*b*]benzo-3-azepines **121** in 47–74% yields (equation 52)[164].

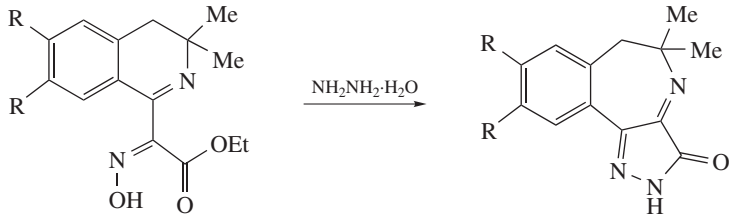

(52)

(**120**) R = H, OMe (**121**)

Oximes can be also used for the imidazole ring synthesis. Thus, reaction of α-amino-oximes **122** and orthoesters leads to imidazole *N*-oxides **123** (equation 53)[165]. Interaction of α-ketooxime **124** with triazinanes also afforded imidazole *N*-oxides **125** in good yields (equation 54)[166]. Similarly, α-ketooximes in the system NH_3/H_2O/aromatic aldehyde afforded trisubstituted 1-hydroxyimidazoles[167].

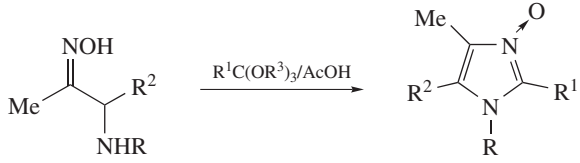

(53)

(**122**) (**123**)

R = alkyl, aryl; R^1 = alkyl; R^2 = H, Me

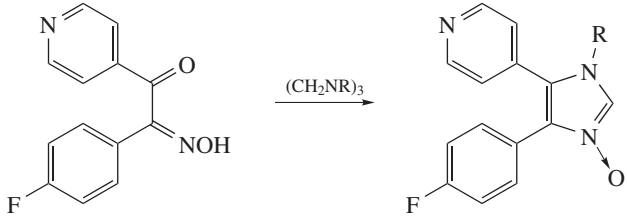

(54)

(**124**) R = alkyl (**125**)

The reaction of α-halogenoximes **126** with amidines in the presence of iron carbonyls gives imidazoles **127** in 31–79% yields. The reaction occurred via deoxygenation of 4*H*-1,2,5-oxadiazines by iron carbonyls (equation 55). Efficiency of carbonyls decreased in the following order: $Fe_3(CO)_{12} > Fe_2(CO)_9 > Fe(Co)_5$[168].

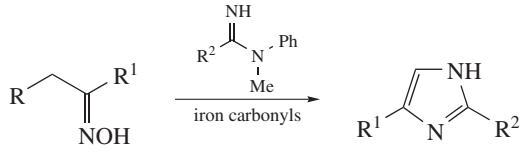

(55)

(**126**) (**127**)

R = Cl, Br; R^1 = alkyl, aryl; R^2 = aryl

1-Benzyl-4-methylimidazoles with substituents at 2-position were prepared from *O*-pentafluorobenzoylamidoximes containing *N*-allyl group in the presence of a palladium catalyst. For example, oxime ester **128** in the system $Pd(PPh_3)_4/Et_3N$ gave imidazole **129** (equation 56)[169].

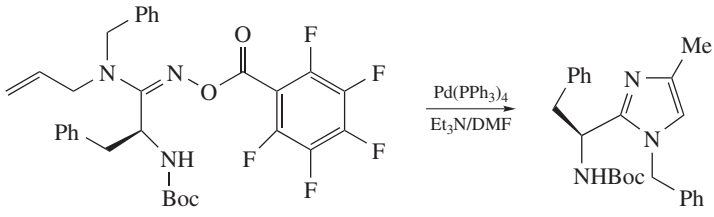

(**128**) (**129**) 70% (56)

1,2-Benzoquinone dioximes and aldehydes in the presence of acidic catalyst (for example, $HClO_4$) in EtOH afforded 1-hydroxybenzimidazole 3-oxides[170].

Imidazo[1,2-*a*]pyridine[171–175], imidazo[5,1-*a*]isoquinoline[176] and imidazo[2,1-*a*]isoquinoline[177,178] rings were successfully obtained from pyridine or isoquinoline oximes or their ethers. Thus, oxime ethers **130** were converted to imidazopyridines **131** in the presence of Et_3N in methanol (equation 57)[174]. Isoquinoline oxime **132** by treatment with ethylenediaminetetraacetic acid (EDTA)/HgO and then Ac_2O gave imidazoisoquinoline **133** (equation 58)[178]. Similar mercury(II)/EDTA mediated cyclization of pyridine oximes afforded fused dihydroimidazoles[179].

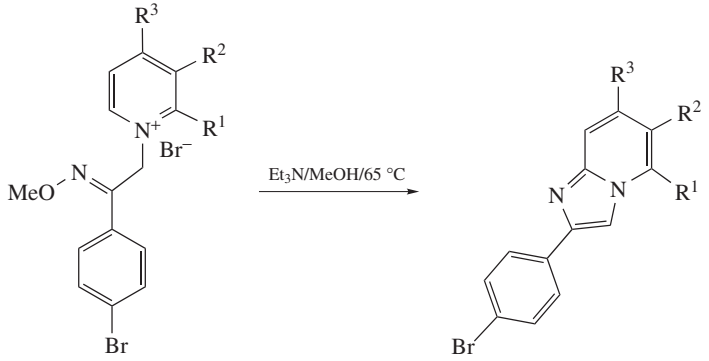

(**130**) (**131**)

R, R^1, R^2, R^3 = H, alkyl 78–96% (57)

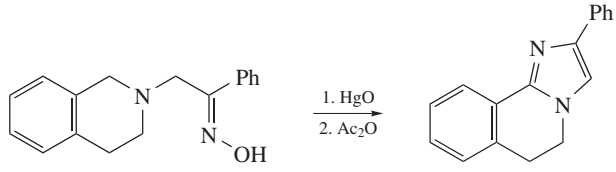

(**132**) (**133**) (58)

Syntheses of xanthines, uracils and related compounds from the corresponding α-iminooxime derivatives were described[180–183]. For example, oxime ester **134** in refluxing ethanol afforded theophyllin **135** in good yield (equation 59)[183].

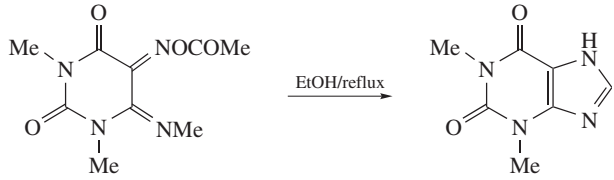

(**134**) (**135**) (59)

Synthesis of 1-hydroxy-3-oxyimidazolines from α-hydroxylaminooximes has been reviewed[184]. Therefore, in the present work it will be described very briefly. In general, the reaction of oximes **136** with aldehydes, ketone or triethyl orthoformate leads to imidazolines **137** or **138**, respectively (equation 60).

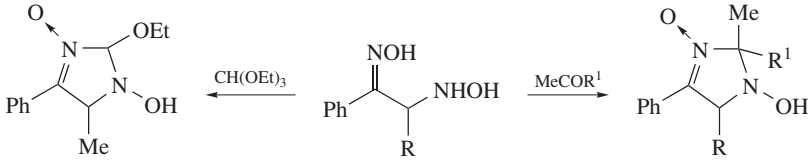

(**137**) (**136**) (**138**) (60)

R, R^1 = H, Me

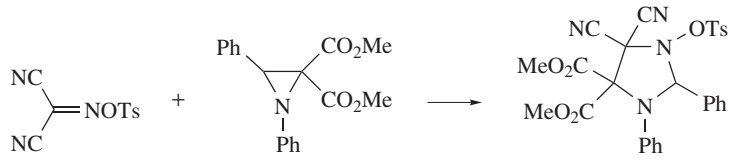

(**139**) (**140**) (**141**) (61)

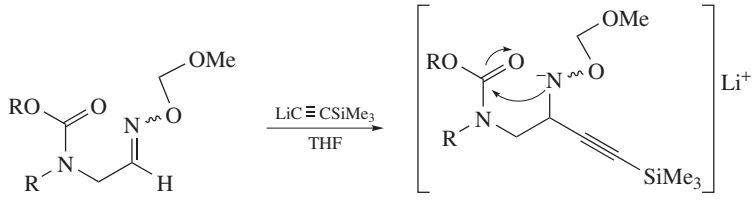

(**142**) (62)

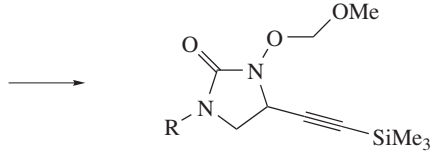

R, R^1 = alkyl, aryl (**143**)

In some cases *O*-substituted oximes reacted with azomethine ylides. Thus, reaction of *O*-substituted oxime $(NC)_2C{=}NOTs$ **139** with azomethine ylide derived from aziridine **140** afforded imidazoline **141** in 44% yield (equation 61)[185]. Addition of lithium derivative of silylated alkyne to oxime ethers **142** leads to 4-ethynyl-*N*-hydroxy-2-imidazolines **143** in 49–72% yields (equation 62)[186].

Reaction of isatin 3-monooxime sulfonate **144** with allylamine proceeds with ring opening and recyclization to 1-arylimidazoline **145** (equation 63)[187]. Isatin 2,3-dioxime (**146**) in the refluxing acetic anhydride afforded a new tetracyclic ring **147** in 31% yield (equation 64)[188].

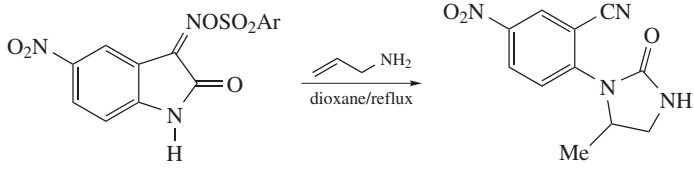

(**144**) (**145**) 77% (63)

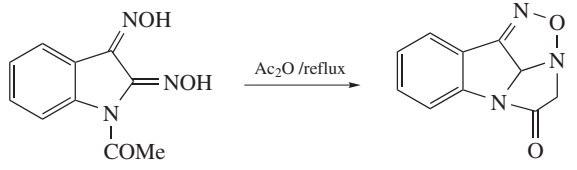

(**146**) (**147**) (64)

6. Triazoles

4,5-Disubstituted 2-phenyl-2*H*-1,2,3-triazole-1-oxides (**150**) can be easily obtained from the corresponding bis(hydroxyimino)butanes **148** in three steps. Thus, treatment of dioximes **148** with diluted HCl in dioxane with subsequent interaction with $PhNHNH_2$/EtOH/AcOH afforded α-hydrazinooximes **149** in excellent yields. Reaction of **149** with *N*-iodosuccinimide (NIS) in CCl_4 or with $CuSO_4$ in aqueous pyridine afforded triazoles **150** (equation 65)[189]. Similar cyclization in the presence of $SOCl_2$ also leads to 1,2,3-triazoles[190].

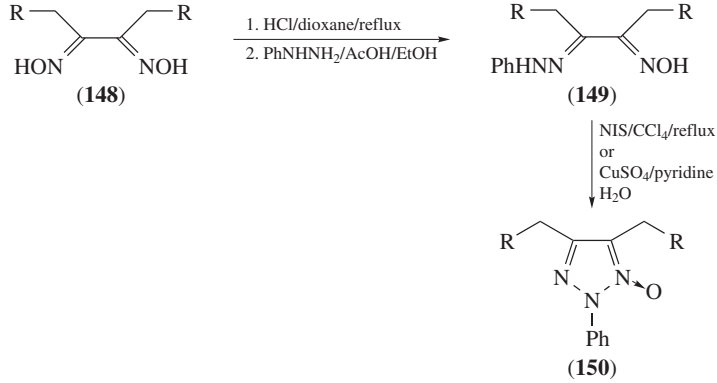

(**148**) (**149**) (**150**) (65)

R = aryl, cyclohexyl 44–68%

Oximino cyanoacetate or malonate esters ($MeO_2CC(CN)$=NOTs or $(MeO_2C)_2C$=NOCOPh) reacted with diazoalkanes ($RCHN_2$) to give unstable 1,2,3-triazolines[191]. Synthesis of *N*-imidoylbenzotriazoles via benzotriazole-mediated Beckmann rearrangement of oximes is also described[192].

Hydrazine derivatives of oximes **151** in the system aromatic aldehyde/catalytic amounts of conc. H_2SO_4/MeCN leads to 1,2,4-triazoles **152** in 50–92% yields (equation 66)[193].

(**151**) (**152**) (66)

Pyrazolo[1,5-*b*]-1,2,4-triazole **154**[194] and 1,2,4-triazolo[1,5-a]pyridine **156**[195] ring systems were successfully obtained from the corresponding formamidoximes or related amidoximes **153** and **155**, respectively, and acylating agent (TsCl or TFAA) (equations 67 and 68). Similarly, 1,2,4-triazolo[1,5-a]pyrimidines were obtained from pyrimidine formamidoximes[196].

(**153**) R, R^1 = alkyl (**154**) (67)

(**155**) (**156**) (68)

R = H, Br, Me, CO_2Me 41–91%

Cycloalkanone oximes **157** reacted with nitrile imines forming spirotriazolines **158** in 48–61% yields (equation 69)[197].

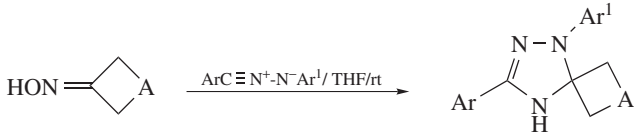

(**157**) (**158**) (69)

A = $CH_2CHMeCH_2$; $CH_2CH(Bu\text{-}t)CH_2$, $(CH_2)_4$, $(CH_2)_5$

Reaction of isatin 3-monooxime sulfonate **159** with hydrazides leads to 1-aryltriazolinones **160** with 41–46% yields (equation 70)[198]. Interaction of oxime PhC(=NHPh)CCl=

NOH with $H_2NC(CH_2OH)_3$ afforded 2,5-diphenyl-2,4-dihydro-1,2,4-triazol-3-one[199].

(**159**) Ar = *p*-$MeCH_4$; R = aryl (**160**) (70)

7. Tetrazoles

Tetrazoles were successfully prepared from corresponding azidooximes in acidic media[200–202]. Thus, oximes **161** in ether in the presence of gaseous HCl afforded tetrazoles **162** in yields up to 85% (equation 71)[200].

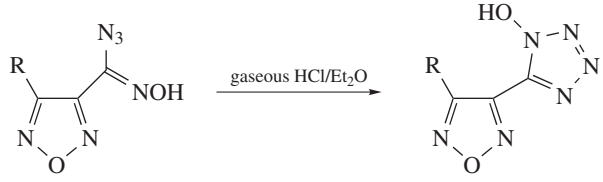

(**161**) $R = NH_2, N_3$ (**162**) (71)

8. Isoxazoles, oxazoles and isothiazoles

The [2 + 3] cycloaddition reaction of nitrile oxides, easily accessible from corresponding aldoximes, with different alkenes is known as an excellent route to isoxazoline derivatives[203, 204]. The reactions of asymmetric addition[205] or addition of unsaturated germanes and stannanes to nitrile oxides[206] were reviewed in recent years. In this subsection only the main directions of the synthesis of isoxazole derivatives are briefly reported.

Cycloadditions with monosubstituted olefins proceed rapidly and regioselectively to yield the 5-substituted dihydroisoxazoles. Thus, addition of styrene to nitrile oxide **164**, formed from oxime **163**, results in the formation of the 5-phenyl- **165** and 4-phenyldihydroisoxazoles **166** in a 99:1 ratio (equation 72)[204, 207].

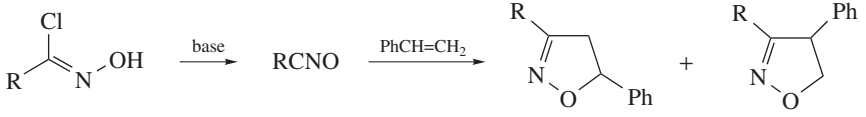

(**163**) (**164**) (**165**) (**166**) (72)

On the other hand, reactions of nitrile oxides with 1,2-disubstituted olefins are slower and regioselectivity usually was not so high. For example, benzonitrile oxides, obtained from the corresponding chlorooximes **167**, undergo 1,3-dipolar cycloaddition reaction with methyl cinnamate to produce the 5-phenyl **168** and 4-phenyl **169** regioisomers in approximately an 80:20 ratio[208]. However, use of *N*,*N*-diethylcinnamamide as the dipolarophile

unexpectedly resulted in the formation of the 5-phenyl and 4-phenyl regioisomers in a 23:77 ratio (equation 73).

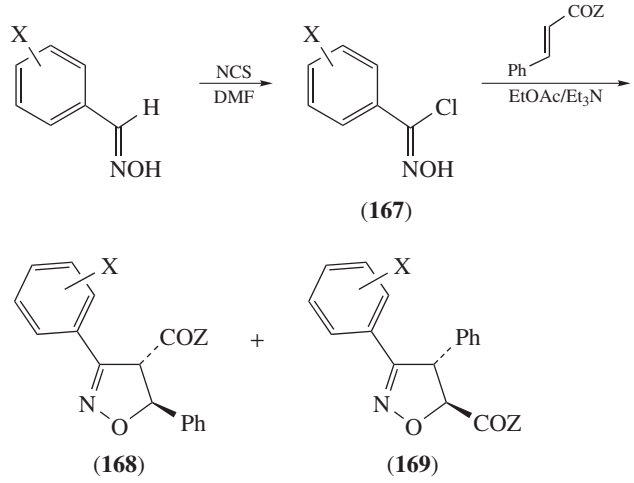

(73)

X = H, Cl, OMe, NO_2; Z = OMe, NH_2, NHPh, NMe_2, NEt_2

Usually nitrile oxides, necessary for the synthesis of isoxazoline derivatives, were generated from hydroximoyl halides by interaction with Et_3N[209], AgOAc in CH_2Cl_2[210] or from the corresponding aldoximes in the presence of *N*-chloro- and *N*-bromosuccinimide/Et_3N[211,212], NaOCl/Et_3N[213], *t*-BuOCl[214], chloramine-T[215], 1-chlorobenzotriazole/base[216], $Pb(OAc)_4$[217], hypervalent iodine compounds[218], ceric ammonium nitrate[219], dimethyldioxirane[220] and MnO_2[221]. Isoxazolines are also prepared from aldoximes and olefins in the presence of $Ca(OCl)_2/CH_2Cl_2$[222] and 1-sodio 3,5-dichloro-*s*-triazine-2,4,6-trione/Al_2O_3/CH_2Cl_2 systems[223] under ultrasonic irradiation or in the presence of Al_2O_3 and Al_2O_3/NCS under microwave irradiation[224,225]. For example, benzothiophene derivative can be easily transformed to corresponding fused isoxazoline **171** by treatment with aldoxime **170**/NCS/Al_2O_3 under microwave irradiation (equation 74).

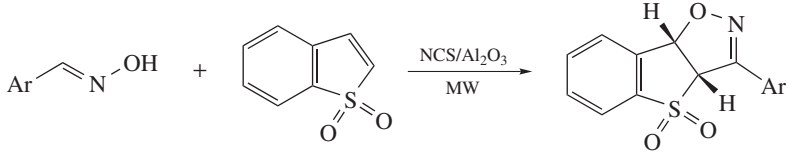

(170) (171)
84–95%

(74)

Nitrile oxides were also readily generated by reaction of aldoximes **172** with *tert*-butyl hydroperoxide and bis(tributyltin) oxide. The reaction proceeded under mild conditions, in which *O*-stannylated aldoximes **173** were the key intermediates. This reaction system was applicable to the one-pot synthesis of isoxazoline **174** or isoxazole **175** derivatives

from the corresponding alkenes or alkynes (equation 75)[226].

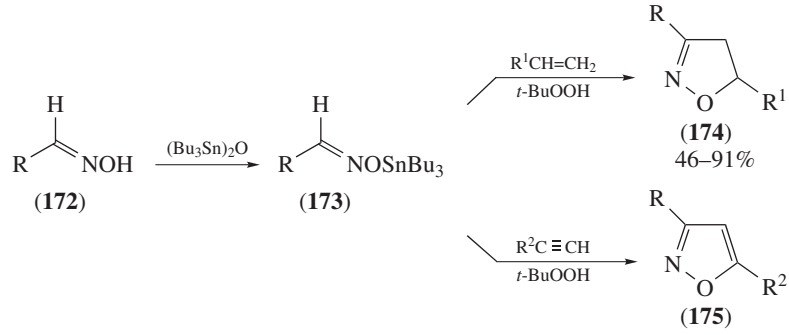

(**172**) (**173**) (**174**) 46–91% (**175**) (75)

R = alkyl, Ph; R^1, R^2 = alkyl, alkoxy, aryl, alkoxycarbonyl 55–70 %

It has been shown that magnesium ions dramatically accelerate nitrile oxide cycloaddition reaction to allylic alcohols, improving both the regio- and stereoselectivity of the reaction. For example, cycloaddition of hydroximoyl chloride **176** to terminal allylic alcohols produces *syn*-stereoisomers of 2-oxazolines **177** selectively (equation 76)[227]. Metal salts other than magnesium, such as lithium, zinc and aluminum, are less effective. An excellent enantioselectivity is obtained in asymmetric 1,3-dipolar cycloaddition of nitrile oxide to (*E*)-and (*Z*)-2-buten-1-ols **178** (equation 77). The reactions were performed using diisopropyl (*R*,*R*)-tartrate ((*R*,*R*)-DIPT) as a chiral auxiliary to afford the corresponding 3,4,5-trisubstituted 2-isoxazolines **179** with high regioselectivity[228].

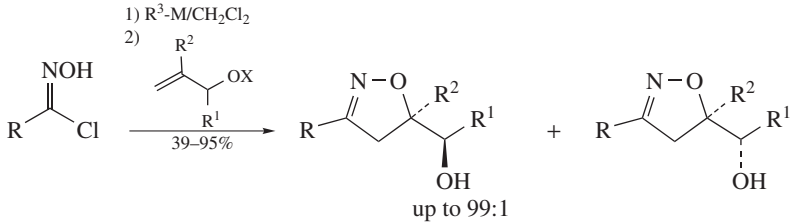

(**176**) *syn*-(**177**) *anti*-(**177**) (76)

R = aryl; R^1 = alkyl; R^2 = H, alkyl; R^3-M = BuLi, EtMgBr, Et_2Zn, Et_3Al; X = H, MgBr

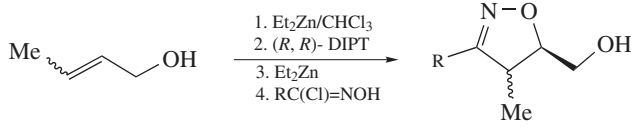

(**178**) (**179**) 20–59% *ee* 88–98% (77)

The synthesis of silyl-substituted tetrahydrofuro[2,3-*d*]isoxazoles **181** by [2 + 3] cycloaddition of benzonitrile oxide, prepared *in situ* from benzhydroxamic chloride **180** and E_3N, to 5-(2,3-dihydrofuryl)silanes was described (equation 78). Compounds with two

condensed bicycles at the silicon atom were also prepared by the addition of acetonitrile oxide to the corresponding bis[5-(2,3-dihydrofuryl)]silanes[229]. Synthesis of silyl and germyl substituted 2-oxazolines from nitrile oxides and unsaturated silanes and germanes has been also reported[230, 231]. Thus, the reaction of *o*-difluoromethoxybenzhydroxamic acid chloride **182** with vinyl- and divinylgermanes in the presence of Et_3N afforded 2-isoxazolines **183** (equation 79).

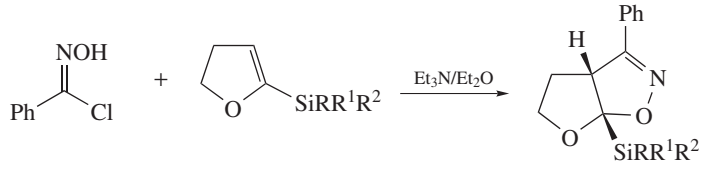

(78)

(**180**) R, R^1, R^2 = Me, Ph, 2-thienyl (**181**)

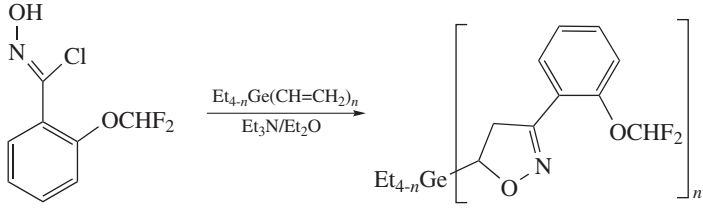

(79)

(**182**) n =1, 2 (**183**)

Fluoride ion catalyzed 1,3-dipolar cycloaddition of bromo nitrile oxide, obtained *in situ* from dibromoformaldehyde oxime **184**, to nonactivated alkynes provides a new approach to the synthesis of neuroactive isoxazoles. However, the regioselectivity of cycloaddition in this case is not high—products **185** and **186** are obtained in a 1:1 to 1:1.4 ratio (equation 80)[232]. Cycloaddition reaction of hydroximoyl chlorides and acetylene was successfully carried out also in the presence of $NaHCO_3$ as a base[233]. For instance, α-keto oximes **187** were reacted with acetylene and $NaHCO_3$ to give isoxazoles **188** in good yields (equation 81).

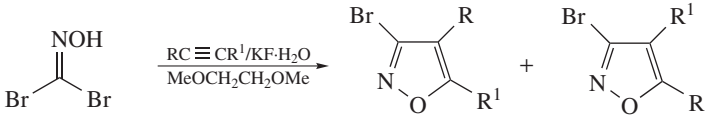

(80)

(**184**) (**185**) (**186**)

R = Me, CH_2OH, CH_2Cl; R^1 = $(CH_2)_4Me$, CH_2OH, CH_2CH_2OH, CH_2Cl

(**187**) R, R^1 = H, alkyl, alkoxy, halo (**188**)

Intramolecular cyclization of α-halooximes or nitrile oxides having allylic or propargylic substituents leading to isoxazolines has been described. 3-Substituted 5-hexenyl

nitrile oxides, which are easily obtained *in situ* from the corresponding unsaturated oximes **189**, undergo intramolecular dipolar cycloaddition to afford bicyclic isoxazoline derivatives **190** with good *cis*-diasteroselectivity (*ca* 9:1) (equation 82)[234].

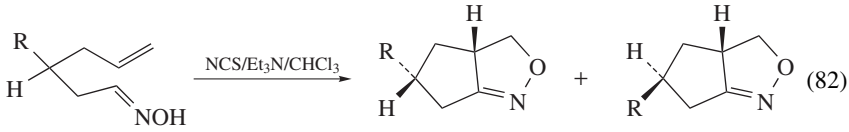

(**189**) *cis*-(**190**) *trans*-(**190**) (82)

Novel polycyclic heterocyclic systems including the isoxazoline ring were described. Thus, oximes **191** and **193** in the presence of sodium hypochlorite afforded heterocycles **192**[235] or **194**, respectively[236] (equations 83 and 84). Intramolecular cycloaddition of nitrile oxide was used in the synthesis of the A-ring fragments of 1α,25-dihydrovitamin D_3 and taxane diterpenoids[237], sulphur-containing isoxazoles[238], fluoro-substituted aminocyclopentanols[239] and aminocyclopentitols[240]. New *gem*- and *vic*-disubstituted effects in such cyclization reactions have been reviewed by Jung[241].

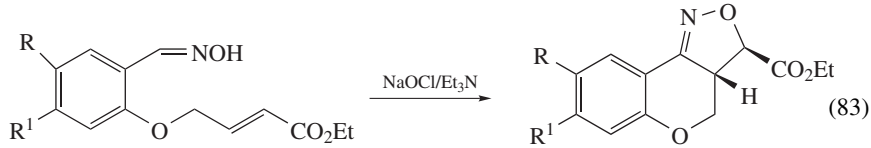

(**191**) (**192**)

R, R^1 = H, OMe 42–85% (83)

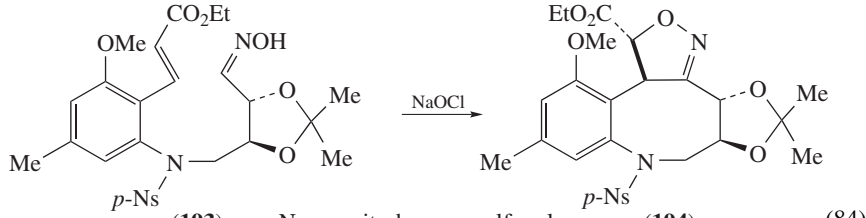

(**193**) *p*-Ns = *p*-nitrobenzenesulfonyl (**194**) (84)

β,γ-Acetylenic oximes undergo in a similar manner conversion to 3,5-disubstituted isoxazoles. Thus, oximes **195** in the system K_2CO_3/MeOH at room temperature afforded isoxazoles **196** in excellent yields (equation 85)[242]. α,β-Unsaturated ketoximes **197** can be also easily transformed to the corresponding 5-arylisoxazoles **198** (yield up to 95%) by treatment with iodine and potassium iodide. The presence of isoxazoline was detected in the reaction mixture (equation 86)[243a]. α,β-Unsaturated ketoximes in the presence of palladium catalyst afforded isoxazolines[243b].

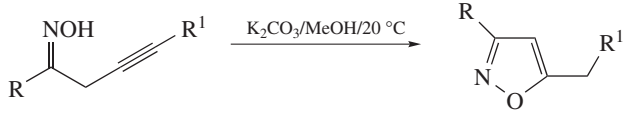

(**195**) (**196**) (85)

R = alkyl, aryl, hetaryl; R^1 = alkyl, aryl, $SiMe_3$ 62–95%

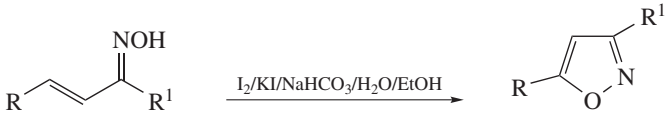

(86)

(**197**) R = aryl, hetaryl; R^1 = alkyl, aryl (**198**)

Synthesis of 3,5-diarylisoxazoles **200** and **201** (overall yield up to 85%) by the reaction of asymmetrically substituted β-diketones (**199**) with hydroxylamine was investigated (equation 87). It has been found that the reaction occurs with a low degree of site selectivity unless steric effects are operating. The isoxazole that has the more electron-deficient aryl group in position 3 is formed preferably when the reaction is performed with hydroxylamine hydrochloride. When the reaction is carried out in a neutral medium, a reversed site stereoselectivity is observed[244]. Similar cyclization occurred using β-dioximes as starting material[245, 246].

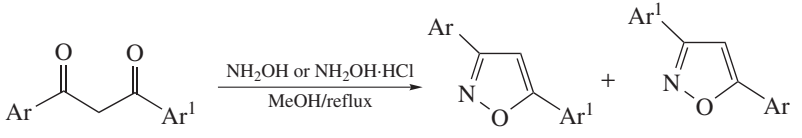

(87)

(**199**) (**200**) (**201**)

3-Substituted 5-alkylisoxazoles **203** are successfully obtained from oxime dianions, prepared from acetone oxime **202** and BuLi, and then by interaction with *N*-methoxyamides of type RCON(OMe)Me (equation 88)[247].

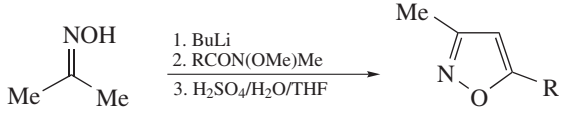

(88)

(**202**) (**203**)
38–94%

The reaction of α-halo ketone oximes **204** with isocyanides leads to formation of 5-aminoisoxazole derivatives **205**. The reaction involves formation of nitrosoalkenes as intermediates (equation 89)[248].

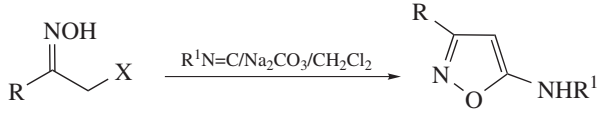

(89)

(**204**) (**205**)

R, R^1 = alkyl, aryl; X = Cl, Br 40–93%

Surprisingly, 3-(2-dialkylaminoethyl)-1,2-benzisoxazoles **207** can be easily obtained by direct cyclization of the corresponding Mannich bases oxime acetates **206** in refluxing benzene in the presence of anhydrous K_2CO_3 (equation 90). The known methods for ring closure to 1,2-benzisoxazole were ineffective for this class of pharmacologically relevant compounds[249].

(90)

(**206**) (**207**)

R = H, Me; R^1 = H, Me; R^2 = alkyl 38–61%

1,2-Benzisoxazoles and isoxazoles are also accessible in excellent yields by intramolecular Mitsunobu reaction or related reactions of *o*-hydroxy- or α-hydroxyoximes[250–256]. Thus, treatment of oxime **208** in the presence of diethyl azodicarboxylate (DEAD) and PPh_3 in THF leads to benzisoxazoles **209** (equation 91)[250].

(91)

(**208**) (**209**)

R = H, Me, Ph; R^1 = H, OMe; R^2 = H, alkyl; R^3 = H, Br

o-Cyanooxime derivatives gave isoxazole derivatives in the presence of a basic[257,258] or acidic[259,260] catalyst. For example, interaction of 2-bromo-3-cyano-4,6-diaminopyridine (**210**) with acetone oxime/*tert*-BuOK and subsequent treatment of intermediate **211** with aqueous NaOH afforded 3,4,6-triaminoisoxazolo[5,4-*b*]pyridine (**212**) (equation 92)[257].

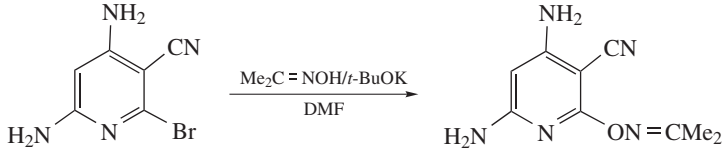

(**210**) (**211**)

(92)

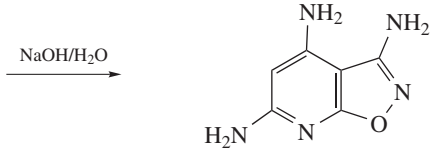

(**212**)

29%

Reaction of *C*,*O*-dilithiooximes **213**, obtained from the corresponding oximes with BuLi, and α-chloroketones afforded 5-hydroxymethylisoxazolines **214** (equation 93). α,β-Unsaturated aldehydes reacted with dilithio salts **213** to give the acyclic 1,2-addition products **215**, which were easily cyclized to the corresponding 5-vinylisoxazolines **216**[261].

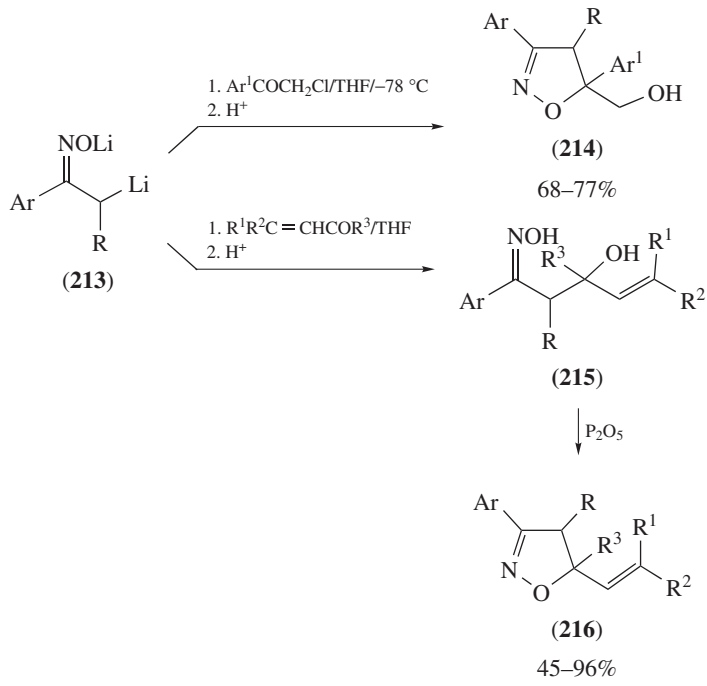

(93)

Ar, Ar^1 = aryl; R = H, alkyl; R^1, R^2, R^3 = H, alkyl, aryl

Effective synthesis of spiroisoxazoline derivatives was elaborated using hypervalent iodine reagents. Thus, treatment of *o*-phenolic oximes **217** with phenyliodonium diacetate (PIDA) in MeCN at 0 °C afforded spiroisoxazolines **218** in moderate yields (equation 94)[262]. Oximes **219,** prepared *in situ* from 2-trifluoromethylchromones, in the acidic media also led to spiroisoxazolines **220** (equation 95)[263].

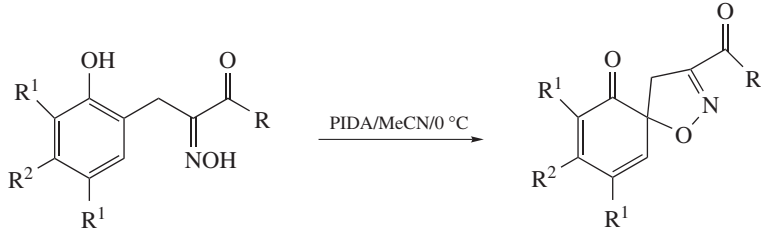

(94)

R = alkoxy, amino; R^1 = H, Br; R^2 = H, OMe 40–72%

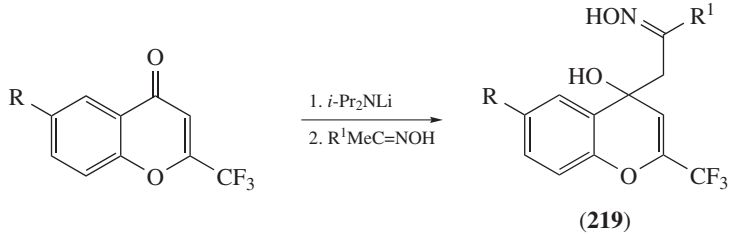

(**219**)

(95)

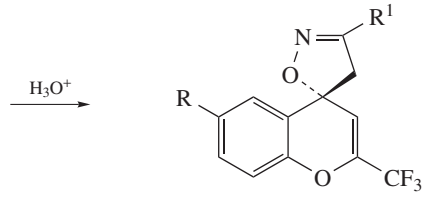

(**220**)

R = H, Me; R^1 = Me, *t*-Bu, Ph 22–64%

It has been shown that phenylselenyl halides easily reacted with *O*-allyl oximes **221** to give cyclic iminium salts **222,** which by reaction with water afforded isoxazolidines **223** in moderate to good yields (equation 96)[264]. Compounds **222** can be reduced *in situ* by sodium borohydride to produce *N*-alkyl-substituted isoxazolidines **224** in 50–95% yields[265].

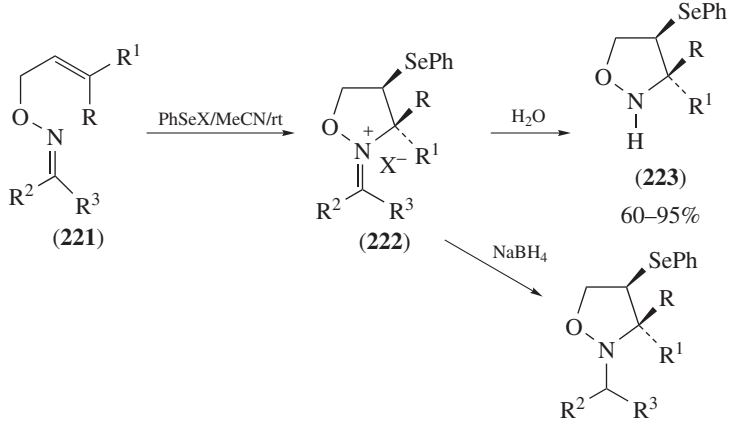

(**221**) (**222**) (**223**) 60–95% (**224**)

(96)

R = H, Me; R^1 = H, Me, Ph; R^2, R^3 = H, alkyl, Ph

Cycloaddition reactions of oxime derivatives having vinyl substituents leading to polycyclic compounds containing isoxazolidine ring were widely described by Grigg and coworkers[266–271]. For example, aldoxime **225** undergoes a cyclization–cycloaddition cascade in boiling THF with *N*-methylmaleimide (NMM) in the presence of $PdCl_2$ to give

the product **226** in 81% yield as a 10:1 mixture of *exo*- and *endo*-isomers (equation 97)[271].

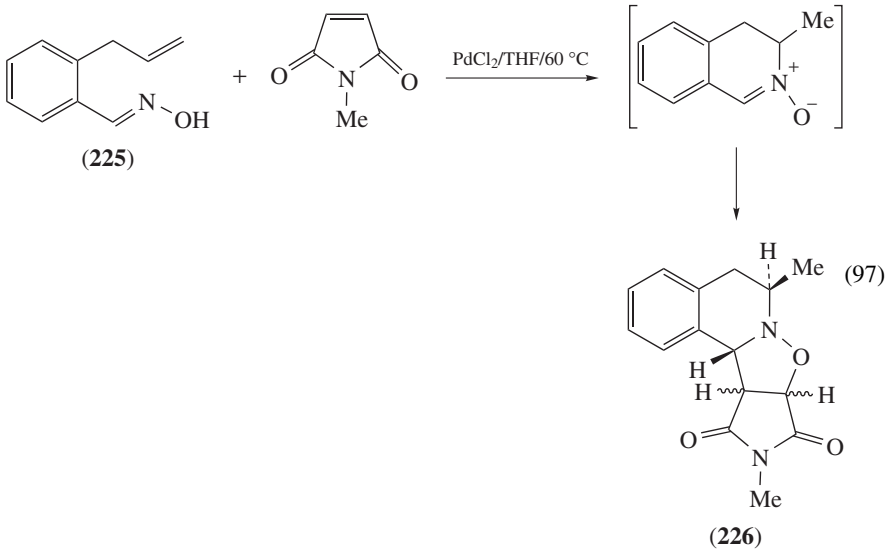

(97)

Hydrogenated isoxazole derivatives were obtained by single electron transfer (SET) cyclization of β,γ-unsaturated oximes[272,273], by thermal [4 + 2] cycloaddition of aldoximes or ketoximes to conventional dienophiles[274] or isomerization/cyclization of an *ortho* halogeno or nitro-substituted amidoximes[275]. Preparation of 1,4-disubstituted 3-hydroximino-2-nitro-1-butenes and their oxidative cyclization to 4-nitroisoxazoles are reported[276]. Synthesis of fluorine-containing substituted isoxazolidines[277,278] as well as isoxazoles by ultrasonic methods[279] has been also described.

Not only isoxazole but also oxazole derivatives are easily accessible from oximes. Benzoxazoles are widely used in organic synthesis due to their importance as intermediates for the preparation of polyether antibiotics or fluorescent whitening agents. For example, 2-methylbenzoxazole (**228**) was obtained from *o*-hydroxyacetophenone oxime (**227**) by Beckmann rearrangement, followed by intramolecular ring closure (equation 98). The best yield of the product **228** (86%) was obtained in solvent-free conditions in the presence of equimolar amounts of $ZnCl_2$ under microwave irradiation[280]. $POCl_3$ is also used as a Lewis acid in the synthesis of benzoxazole derivatives[281]. Benzobisoxazole (**230**) was prepared by rearrangement–cyclization of dioxime (**229**) in the presence of polyphosphoric acid (PPA) (equation 99)[282].

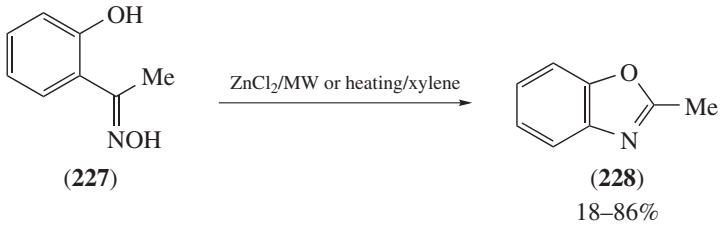

(98)

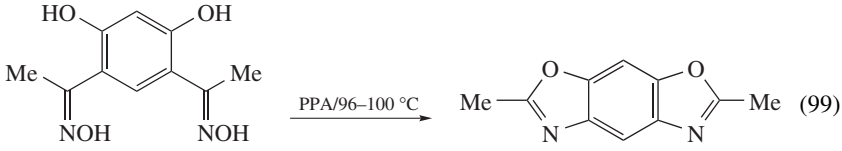

(**229**) (**230**) 58% (99)

The preparation of 1,3-azoles (benzoxazoles, benzimidazoles and benzothiazoles) from oximes using oxidants on mineral supports such as $Ca(OCl)_2/Al_2O_3$ or MnO_2/SiO_2 or by fusion 'in dry media' has been described. For instance, benzoxazoles **232** can be obtained by reaction of *o*-aminophenols (R, R′ = H, NO_2,Cl) with substituted benzaldehyde oximes **231** in the presence of $Ca(OCl)_2/Al_2O_3$ under microwave irradiation (equation 100)[283].

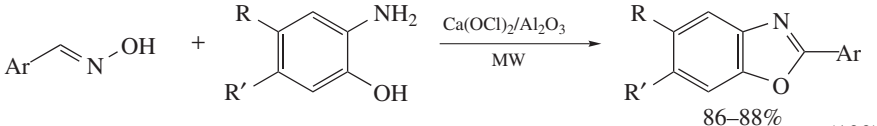

86–88%

(**231**) (**232**) (100)

Activated *O*-vinyloxime **233** undergoes a thermal rearrangement to afford 2-alkenyloxazole **234** in 31% yield (equation 101)[284].

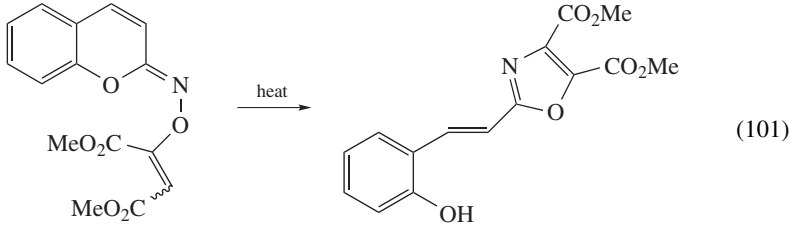

(**233**) (**234**) (101)

Thermal synthesis of 2-substituted phenanthroxazoles and related compounds by cyclization of *O*-methyl *o*-quinone oximes with compounds $ArCH_2Y$ (Ar = aryl, hetaryl; Y = H, OH, Cl, Br, OAc, SH, COR, NH_2) or with amines ($PhCH_2NMe_2$, PhNHMe, $PhNMe_2$) has been described[285]. Cyclization of α-oxooximes in the system alkyl halide or sulfate/DMF/K_2CO_3 also leads to oxazole derivatives[286].

The reaction of ketoximes **235** with dimethyl carbonate in the presence of K_2CO_3, carried out in an autoclave at 180–190 °C, afforded 3-methyl-4,5-disubstituted 4-oxazolin-2-ones **236** (equation 102)[287]. The formation of compounds **236** occurred via [3,3]sigmatropic rearrangement of intermediates of the oxime methylated with dimethyl carbonate.

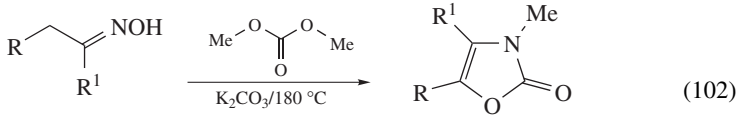

(**235**) (**236**) (102)

R, R^1 = alkyl 22–48%

Cyclization of 2-hydroxy ketoxime ether is used in the synthesis of the alkaloid (−)-cytoxazone containing 4,5-disubstituted 2-oxazolidinone ring[288]. Thus, treatment of 2-hydroxy ketoxime ether **237** with $LiAlH_4/Et_2O$ and Boc_2O/DMAP/MeCN and then with TFA/CH_2Cl_2, O_3/CH_2Cl_2 and $NaBH_4$ afforded racemic cytoxazone **238** (equation 103). Optical resolution of racemic **238** was readily accomplished via the conventional separation of the corresponding diasteroisomers obtained by acylation of racemic cytoxazone with (−)camphanic chloride.

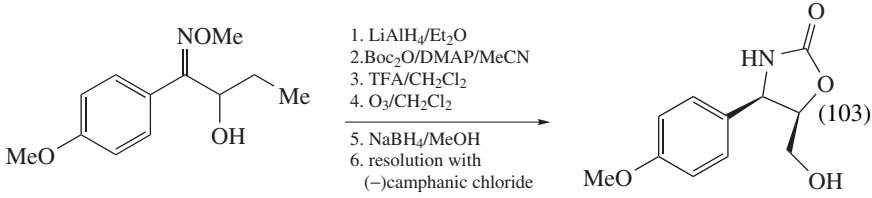

(**237**) (**238**)

o-Mercapto- or *o*-alkylthiooximes were transformed to benzoisothiazoles in the presence of PPA[289,290] or strong acid (H_2SO_4, *p*-TsOH)[291]. Thus, treatment of compound **239** with PPA at 20 °C leads to isothiazolo[5,4-*b*]indole (Brassilexin) **240** in 18% yield (equation 104)[290].

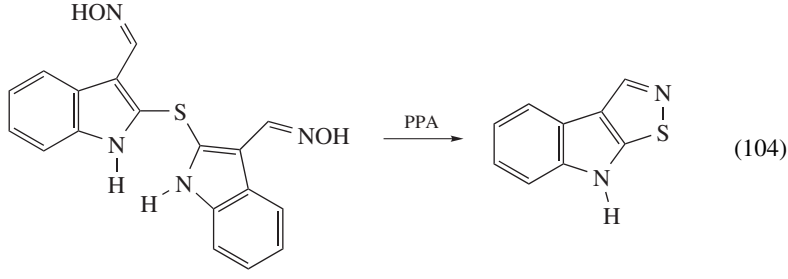

(**239**) (**240**)

9. Dioxazoles, oxadiazoles, oxathiazoles, thiadiazoles and dithiazoles

o-Benzoquinones are unique conjugated 1,2-diones which easily react with various dipoles. Thus, di- **242** and tri-substituted *o*-benzoquinones on interaction with nitrile oxides, generated from the corresponding benzohydroximoyl chlorides **241** and Et_3N, afforded monospirodioxazole derivatives **243** and **244** in overall yields up to 100% (equation 105). The reaction of monosubstituted *o*-benzoquinones with stable nitrile oxides (mesityl nitrile oxide and 2,6-dichlorobenzonitrile oxide) leads to formation of bis adducts[292,293]. Reaction of α-hydroxyiminonitrile oxide **245** and carbonyl compounds also leads to 1,4,2-dioxazole **246** ring formation (equation 106)[294].

The main group of methods for the preparation of a 1,2,4-oxadiazole ring is based on cyclization of amidoxime derivatives in the presence of acylating agents[295–304]. A surprisingly easy cyclization of *O*-benzoyl-β-piperidinopropioamidoxime **247** to oxadiazole **248** in DMSO at room temperature was described (equation 107)[299]. 3-(3-Aryl-1,2,4-oxadiazol-5-yl)propionic acids **250** were obtained by the reaction of amidoximes **249** with succinic anhydride under microwave irradiation or conventional heating (equation 108)[300].

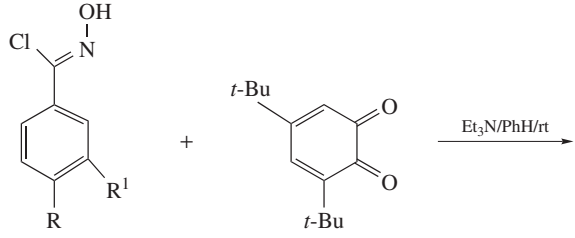

(**241**) (**242**) (105)

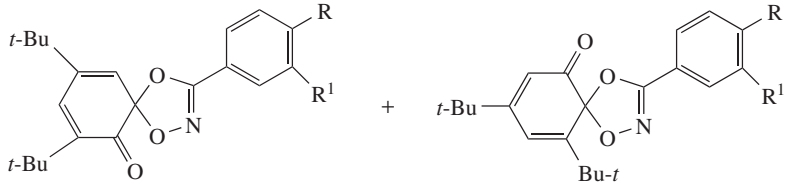

(**243**) (**244**)

R, R^1 = H, Me, OMe, Cl

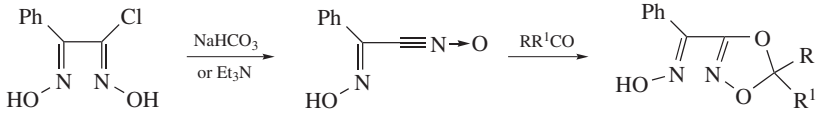

(**245**) R, R^1 = H, alkyl (**246**) (106)

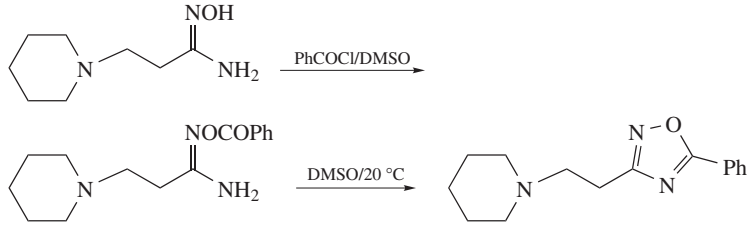

(**247**) (**248**) (107)

73%

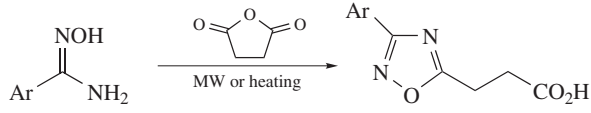

(**249**) (**250**) (108)

70–75%

1,2,4-Oxadiazoles can be sucessfully obtained from amidoximes and diethyl carbonate/*t*-BuOK[305], triethyl orthoformate/BF_3•OEt_2[306, 307] or by reaction of hydroximoyl chlorides with nitriles[308].

Alkyl 2-(substituted cinnamoylamino)-3-dimethylaminopropenoates **251** are transformed to *N*-cinnamoyloxalic acid hydroxyimidic amides **252** by treatment with sodium nitrite in aqueous HCl at 0 °C. The latter can be further transformed into substituted 5-styryl-1,2,4-oxadiazole-3-carboxylates **253** by standing in aqueous HCl at room temperature (equation 109)[309].

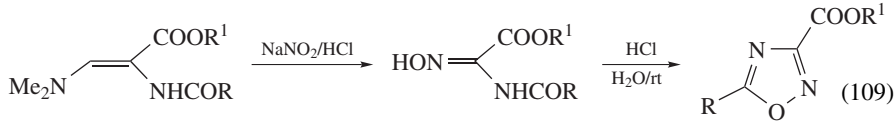

(109)

(**251**) (**252**) (**253**)

R = CH=CHAr; R^1 = Me, Et; Ar = aryl

It has been found that 1,2,4-oxadiazoles **255** can be obtained from amidoximes **254** and aryl iodides by the palladium-mediated reaction in the presence of carbon monooxide. This reaction was applicable to both electron rich and deficient aryl iodides (equation 110)[310]. Amidoximes in the system ArI^+ Ph X^-/CO/$PdCl_2$/K_2CO_3/NMP/toluene also afforded 5-aryl-1,2,4-oxadiazoles[311].

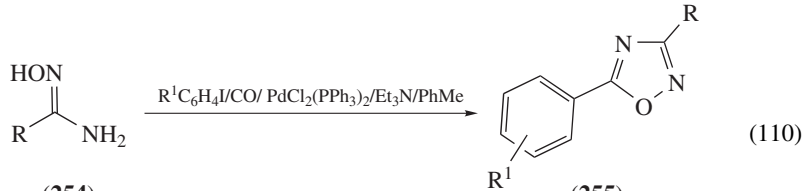

(110)

(**254**) (**255**)

40–68%

R = Me, CO_2Et; R^1 = 4-CO_2Et, 2-, 4-OMe, 4-NO_2, 4-Br

A two-step synthesis of 1,2,4-oxadiazoles from aziridinylbenzaldoximes is described. Thus, aziridinyloximes **256**, obtained by reaction of hydroximoyl chlorides with 2,2-dialkylaziridines in the presence of Et_3N, undergo ring opening in hydrogen chloride–dioxane solution to give (*Z*)-*N*-hydroxy-*N′*-(2-chloro-2-methylpropyl)benzenecarboximidates **257**. Reaction of oximes **257** with NaH in dioxane afforded 4,5-dihydro-1,2,4-oxadiazoles **258** which, on treatment with *N*-chlorosuccinimide, gave heteroaromatic 1,2,4-oxadiazoles **259** (equation 111)[312].

Heating of 4-hydroxyiminoimidazoles **260** in boiling water causes the hydrolytic opening of the imidazole ring and by subsequent cyclization leads to 5-amino-1,2,4-oxadiazoles **261** in 79–86% yields (equation 112)[313].

3-Phenyl-5-bromodifluoromethyl-1,2,4-oxadiazole was obtained in the system PhC(=NOH)NH_2/$BrCF_2COOEt$/Et_3N/toluene[314]. 1,2,4-Oxadiazoles can be also successfully obtained from amidoximes linked to solid resin and $(ClCH_2CO)_2O$ in 2-methoxyethyl ether $(MeOCH_2CH_2)_2O$[315].

Substituted 1,2,4-oxadiazoles were prepared by addition of nitrile oxides to imines[316] or hydrazones. It has been reported that interaction of hydroximoyl chlorides **262** with chiral hydrazones **263** in the presence of Et_3N leads to intermediates **264** with diastereoselectivity up to 97%. A subsequent N–N bond cleavage to remove chiral auxiliary by formic acid leads to 1,2,4-oxadiazolines **265** with *ee* up to 91% (equation 113)[317].

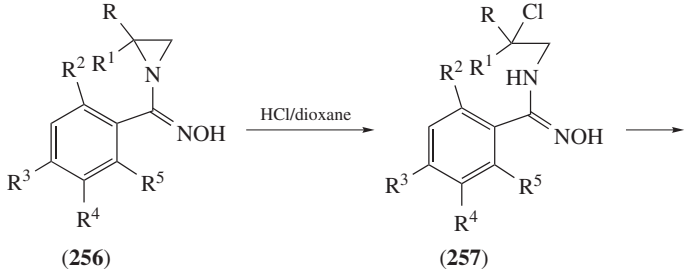

(**256**) (**257**)

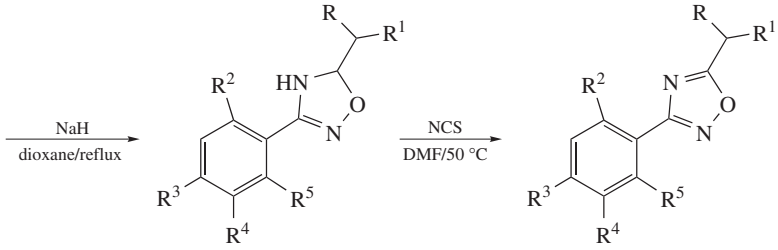

(**258**) (**259**)

66–95% 81–85%

R, R^1 = alkyl, R^2-R^5 = H, Me, Cl, NO_2 (111)

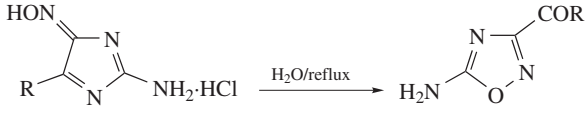

(**260**) (**261**) (112)

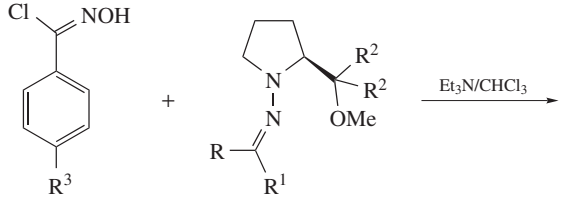

(**262**) (**263**)

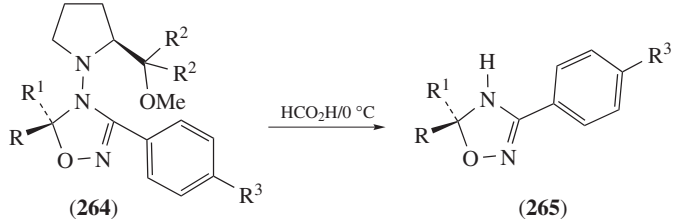

(**264**) (**265**) (113)

50–100% 25–100%

R = alkyl, aryl; R^1, R^2 = H, alkyl, Ph; R^3 = H, F, OMe

2-Hydroxyimino-1,2,3,4-tetrahydroquinoxaline in the presence of an acylating agent afforded 1-oxo-4,5-dihydro-1,2,4-oxadiazolo[4,3-a]quinoxaline[318]. The reaction of 2-aminobenzamide oxime in the presence of aldehydes leads to oxadiazoloquinoxalines[319].

A review dedicated to the reactions of oximes of 1,2,4-oxadiazoles and 1,2,5-oxadiazoles has been published[320]. Beside this, the preparation of monocyclic furazans (1,2,5-oxadiazoles) was also described in a monograph[321]. Therefore, in this chapter only the main directions of the synthesis of oxadiazole derivatives are briefly reported.

Interestingly, on treatment of 1,2,4-oxadiazole-3-carbohydroximoyl chlorides **266** with ethyl hydrazinecarboxylate they rearrange to 4-amino-3-(2-ethoxycarbonylhydrazino)-1,2,5-oxadiazole **267** (equation 114). The formation of product **267** proceeded through an unstable hydrazidoxime[322].

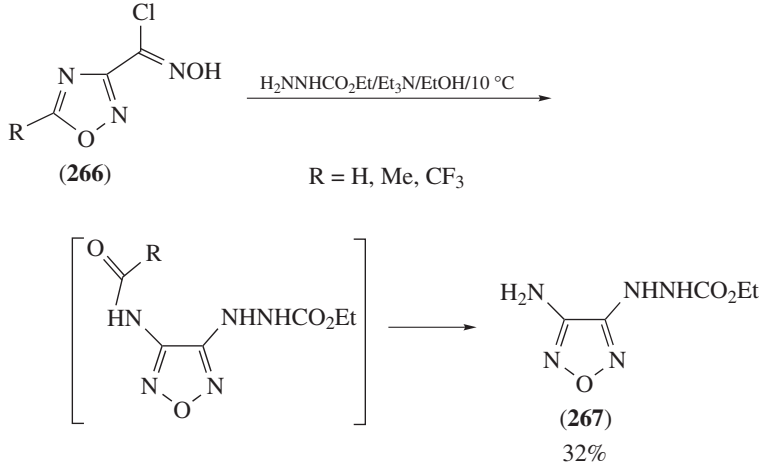

(114)

1,2,5-Oxadiazole-2-oxides (furoxans) **269** can be obtained by treatment of aldoximes **268** with *N*-chlorosuccinimide (NCS)/THF and subsequent interaction with Et_3N in Et_2O (equation 115)[323].

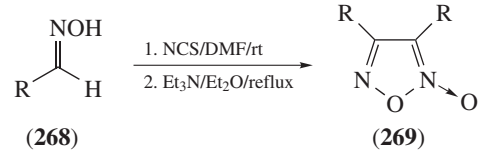

(115)

The synthesis of 1,2,5-oxadiazoles is based on cyclization of 1,2-dioximes[324–326] or α-nitrooxime[327,328] derivatives. The chemistry of dioximes is reviewed by Kotali and Papageorgiou[5]. Thus, reaction of dioximes **270** with 5% aqueous NaOCl in the presence of NaOH in EtOH afforded 1,2,5-oxadiazole-2-oxides **271** in good yields (equation 116)[329]. Bromocyan[330], N_2O_4/CH_2Cl_2[331], bis(trifluoroacetoxy)iodobenzene[332] and SiO_2 at 150 °C[333] were also used as reactants in the cyclization of 1,2-dioximes to 1,2,5-oxadiazoles.

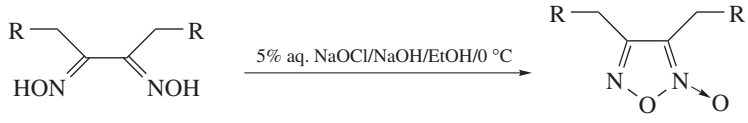

(116)

(**270**) (**271**)

R = aryl, cyclohexyl 81–98%

Bicyclic derivatives of furazan *N*-oxide are prepared by nitrile oxide dimerization reaction. Dioxime **272** (R, R′ = Me) undergoes cyclization to the corresponding 4,4-tetramethylperhydrocycloocta[*c*]furazan *N*-oxide **273** (84% yield) by treatment with $NaOCl/H_2O/CH_2Cl_2$ at 0 °C and then refuxing in toluene (equation 117). However, in the cases of sterically less hindered oximes **272** (R = H, Me; R′ = H) only complex mixtures of oligomerization and cyclization products could be obtained[334]. Interestingly, the reaction of pyridyl oxime *E*-**274** with TsCl afforded 1,2,5-oxadiazole **275** as single product (equation 118). On the other hand, the reaction of *Z*-isomer of oxime **274** leads only to *O*-tosylated oxime[335].

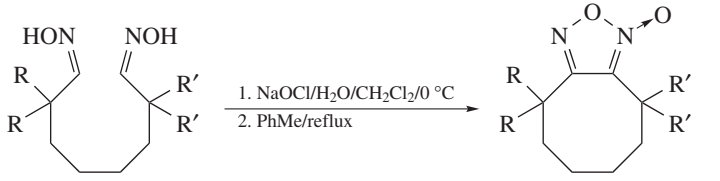

(117)

(**272**) (**273**)

R, R′ = H, Me up to 84%

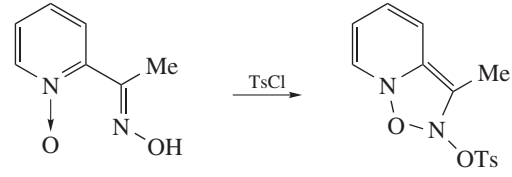

(118)

(**274**) (**275**)

Isothiazole aldoxime tosylate **276** in aqueous solution of K_2CO_3 afforded the oxathiazole ring system **277** in 87% yield (equation 119)[336].

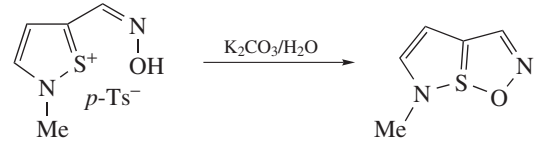

(119)

(**276**) (**277**)

5-Oxo-1,2,4-thiadiazoles were prepared from the corresponding amidoximes and 1,1′-thiocarbonyldiimidazole/BF_3•OEt_2[337] or ClSCOCl/Et_3N[338]. Thus, amidoximes **278** and ClSCOCl in the presence of Et_3N afforded 1,2,4-thiadiazoles **279** in yields up to 20% (equation 120).

(278) (279) (120)

R = aryl

3-Aryl-1,2,5-thiadiazoles or 3-aryl-4-halogeno-1,2,5-thiadiazoles can be readily prepared from 1-aryl-2-haloethanone or 1-aryl-2,2-dihalogenoethanone oximes and tetrasulfur tetranitride[339–341]. For instance, interaction of dichloroacetophenone oxime **280** with S_4N_4/dioxane at reflux afforded 3-phenyl-4-chloro-1,2,5-thiadiazole **281** in 98% yield (equation 121).

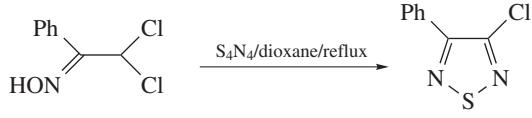

(280) (281) (121)

98%

The 1,2,5-thiadiazole system was also constructed from ketoximes and S_4N_4•$SbCl_5$[342] and by rearrangement of 4-hydroxyimino-2,3,5,6-tetrahydro-3,5-dioxo-1,2,6-thiadiazines in the presence of acid[343].

Synthesis of the dithiazole ring from ketoximes and S_2Cl_2 has been described[344–346]. Cyclopentanone oxime **282** reacts with S_2Cl_2 at 4 °C in tetrahydrofuran containing Hunig's base (*i*-Pr_2NEt), or in dimethylformamide without base, to give trichlorocyclopentadieno-1,2,3-dithiazole **284** without isolable intermediates. Similarly, benzylidene acetophenone oxime **283** afforded monocyclic dithiazole **285** (equation 122)[344].

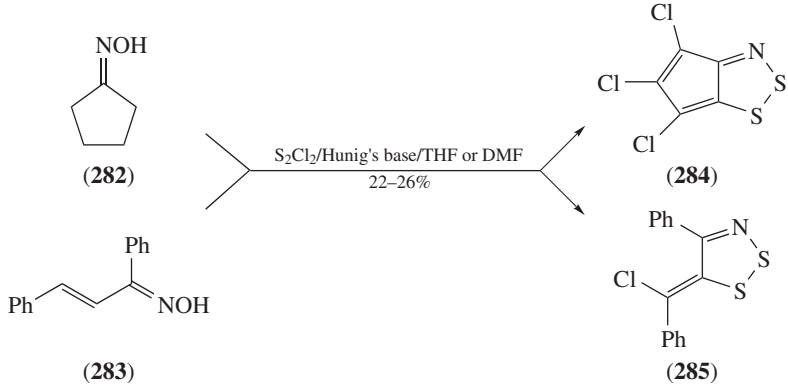

(282) (283) (284) (285) (122)

10. Oxadiazaboroles

Reaction of amidoximes **286** with boronic acids in refluxing toluene leads to 1,3,5,2-oxadiazaboroles **287** in yields up to 95% (equation 123)[347].

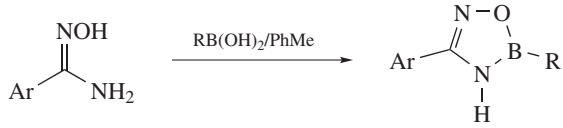

(123)

(**286**) (**287**)

Ar = aryl, hetaryl; R = alkyl, aryl, OH

D. Six-membered Ring Systems

1. Pyrylium salts and chromanes

Beckmann rearrangement of ketoketoximes **288** (R,R^1 = alkyl, aryl) with thionyl chloride unexpectedly afforded 2-aryl(or alkyl)amino-4,6-disubstituted pyrylium salts **289** (equation 124). This reaction is the first example of rearrangement/cyclization involving carbonylic oxygen as terminator[348].

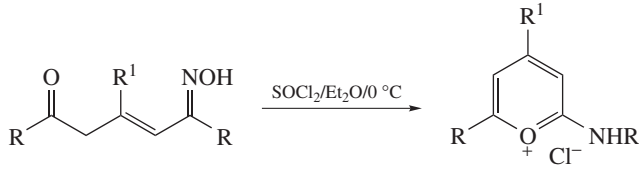

(124)

(**288**) (**289**)

27–55%

2-(2-Bromoallyloxy)phenyl oxime *O*-ethers **290** have been cyclized with Bu_3SnH and azoisobutyronitrile (AIBN) to alkoxyamino-3-methylidenechromanes **291** (equation 125). The cyclization of oxime **290** proceeds through formation of vinyl radicals[349].

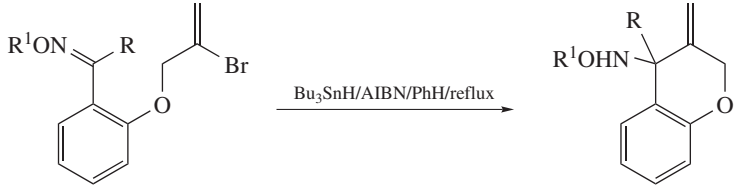

(125)

(**290**) (**291**)

R = H, Me; R^1 = Me, Bn 71–81%

2. Pyridines and quinolines

Oximes of type XON=CW_2 (X = Ts, Tf, Ac; W = CN, CO_2Et) are of interest as cycloaddition partners in [4 + 2] cycloaddition reactions of dienes[350,351]. For example, addition of acetoxyimino Meldrum's acid to dienes at high pressure afforded tetrahydropyridine derivatives[352]. Recently, such reactions were studied in detail by Renslo and Danheiser[353]. Thus, Diels–Alder cycloaddition of oximinotosylate **292** with a variety of 1,3-dienes afforded tetrahydropyridines **293**, which can be easily transformed to

the corresponding pyridines **294** by treatment with NaOMe/NCS in MeOH/THF (1:1) (equation 126).

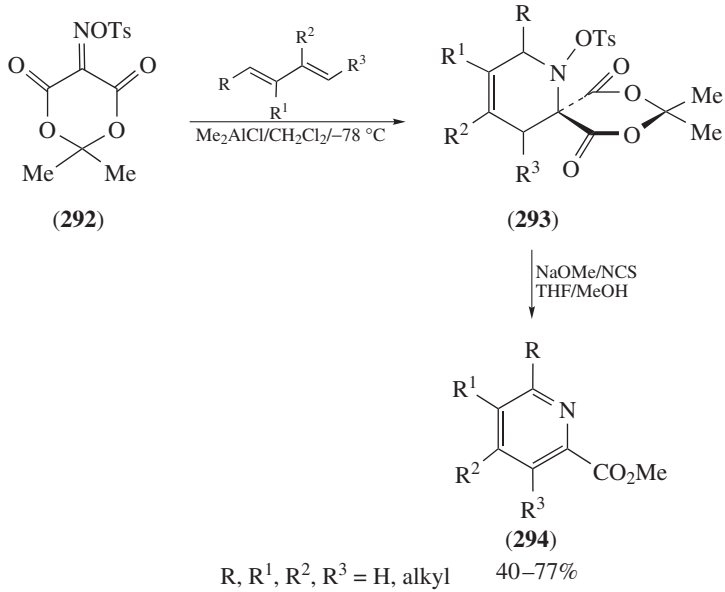

(126)

Reaction of cyclopentadienylzirconium derivatives having C=C bonds with $(NC)_2C$= NOTs also leads to pentasubstituted pyridines[354].

The reaction of α,β-unsaturated oximes with ethyl acetoacetate and related β-dicarbonyl compounds in the presence of $FeCl_3$[355] or $InCl_3$[356] leads to polysubstituted pyridines. Thus, oxime **295** in the system ethyl acetoacetate/$FeCl_3$ (5 mol%) at 150–160 °C formed the pyridines **296** in 41–81% yield (equation 127).

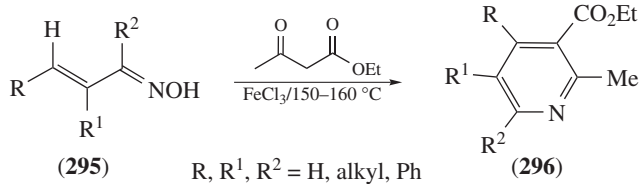

(127)

Synthesis of quinolines by nucleophilic substitution of nitrogen atom in oxime derivatives was described by Narasaka and coworkers[357]. β-Aryl ketone oximes **297** in the presence of trifluoroacetic anhydride and 4-chloranil afforded quinolines **298** in 72–82% yield (equation 128). However, interaction of oxime **299** with 48% HBr at 105 °C proceeded with elimination of hydroxyimino group and gave 2,3-dimethoxynaphtho[1,2-*b*]quinolizinium bromide (**300**) in 45% yield (equation 129)[358].

The diazaphenanthrene system was isolated in the reaction of 1-methyl-3,6,8-trinitro-2-quinolone with PhCH=CHCPh=NOH[359].

Indole oximes are widely used in the synthesis of α-, β- and γ-carbolines. Synthesis of α-carbolines **302** was easily realized from *O*-2,4-dinitrophenyl-substituted oximes **301**

using $NaBH_3CN/NaH$ in 1,4-dioxane (equation 130)[360].

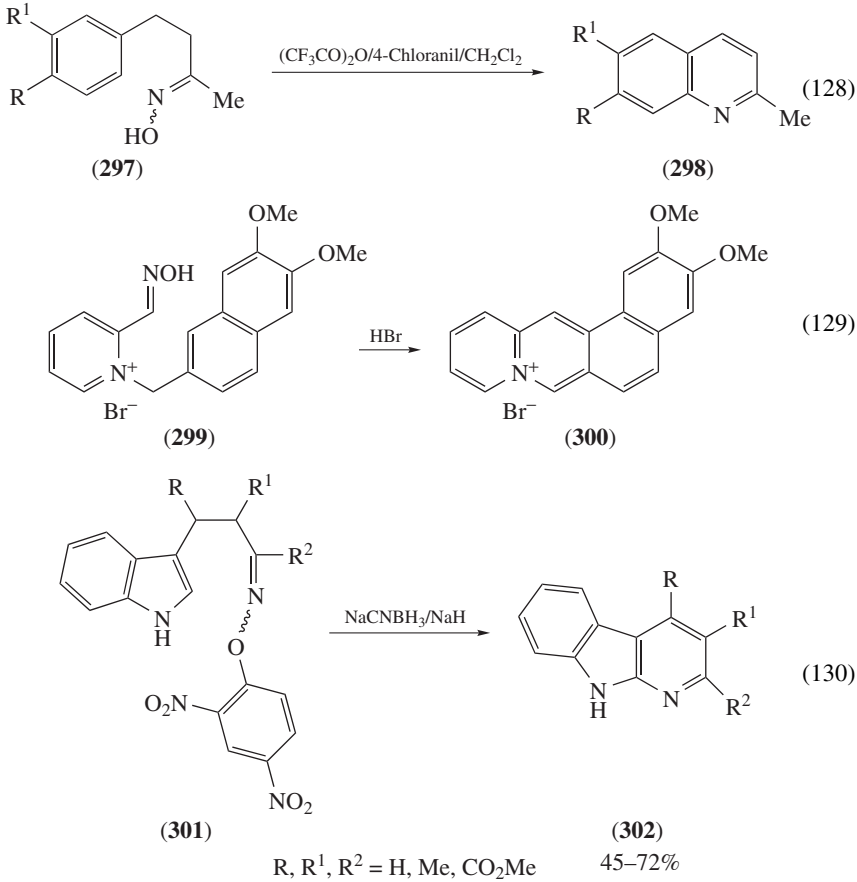

8-Hydroxy-1,2,3,4-tetrahydroquinolines **304** were obtained by cyclization of oxime 2,4-dinitrophenyl ethers **303** in the presence of system $NaBH_3CN/NaH$/1,4-dioxane (equation 131)[361]. If the reductive cyclization was followed by oxidation with DDQ (2,3-dichloro-4,5-dicyano-*p*-benzoquinone) the corresponding 8-hydroxyquinolines **305** were obtained[362].

Oxime derivatives having allyl and vinyl groups can be intramoleculary cyclized to pyridine or quinoline derivatives[363–372].

Syntheses of β-carbolines[373–379] and β-carboline derived alkaloid 17α-epoxyapovincaminate[380] from indole oximes were described. For example, oxime **306** in *o*-dichlorobenzene at 190 °C cyclized to carboline **307** in 81% yield (equation 132).

Derivatives of γ-carbolines were also sucessfully obtained by cyclization of indole oxime derivatives. Refluxing of oximes **308** in xylene gave the γ-carbolines **309** in 51–55% yields (equation 133)[381].

Polysubstituted pyridines **312** can be prepared by a sequence involving an intramolecular thermal or high-pressure Diels–Alder cycloaddition of oximino dienophile **310**,

followed by a mild aromatization of the resulting cycloadduct **311** with Cs_2CO_3 in DMF at room temperature (equation 134)[382]. 3,6-Dihydropyridines **314** can be successfully prepared by 6-*endo* radical cyclization of β-allenyl ketoxime benzoates **313** in the presence of tosyl bromide and AIBN in cyclohexane (equation 135)[383].

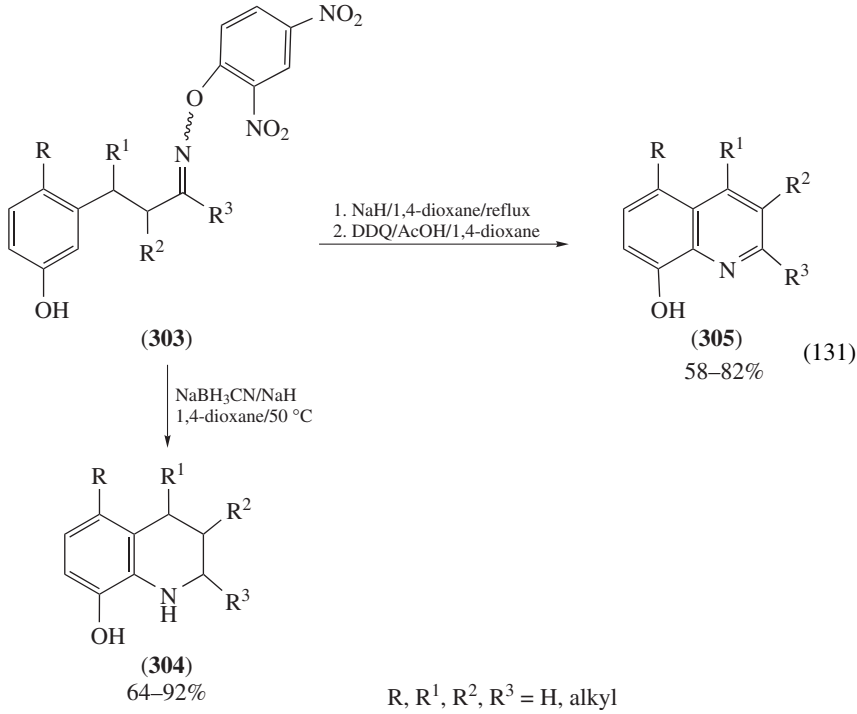

(**303**) (**305**) 58–82% (131)

(**304**) 64–92%

R, R^1, R^2, R^3 = H, alkyl

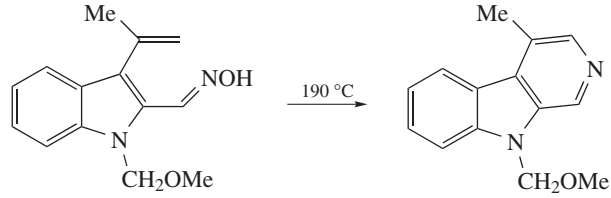

(**306**) (**307**) (132)

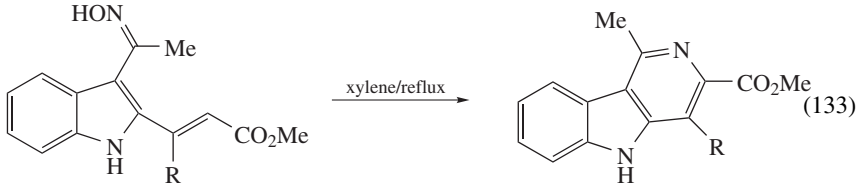

(**308**) (**309**) (133)

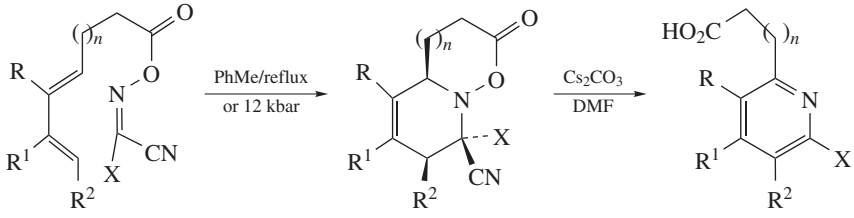

(**310**) (**311**) (**312**)
35–70% 38–79%

R, R^1, R^2 = H, Me, Ph; X = CN, CO_2Et; n = 0, 1 (134)

(**313**) (**314**) (135)

R = alkyl; R^1 = H, alkyl 42–94%

o-Ethynylbenzaldehyde oximes[384] or *o*-ethynylpyridinealdehyde oximes[385] afforded the corresponding isoquinoline *N*-oxides or naphthyridine *N*-oxides. For example, oxime **315** in refluxing methanol afforded 3-hexylisoquinoline 2-oxide **316** in 96% yield (equation 136).

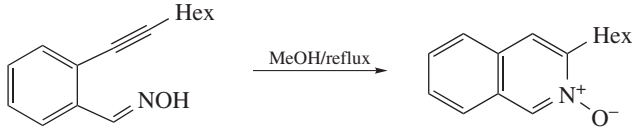

(**315**) (**316**) (136)

A method was developed for preparation of the tetracyclic carboline alkaloids isocanthine, isocanthin-6-one and 1-methylisocanthin-3-one by an intramolecular hetero-Diels–Alder reaction. For example, oxime **317** in sulfolane at 285 °C afforded isocanthine **318** in 8% yield (equation 137)[386].

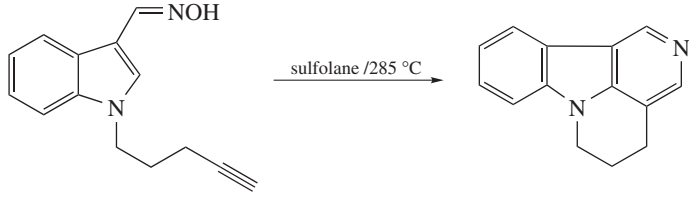

(**317**) (**318**) (137)

Reaction of aldoximes with dimedone derivatives under microwave irradiation leads to partially hydrated acridine derivatives[387]. Fused heterocyclic compounds containing partially hydrogenated pyridine and quinoline rings were prepared by intramolecular cycloaddition reaction of δ-alkynyl oxime derivatives[267, 268]. (*Z*)-1,10*a*-Dihydropyrrolo[1,2-*b*]

isoquinoline-3,10(2*H*,5*H*)-dione oxime undergoes Semmer–Wolf-type aromatization in the presence of polyphosphoric acid and gives 1,4-dihydrobenzo[*c*]-1,5-naphthyridin-2(3*H*)one[388].

Desilylative cyclization of oxime silyl ethers **319** in the presence of TBAT (tetrabutylammonium triphenyldifluorosiliconate)/THF or benzene afforded tetrahydropyridine *N*-oxides **320** in 67–71% yields (equation 138)[389].

(**319**) (**320**) (138)

TBDPS = $SiPh_2Bu$-*t*; R = Bn, TBDPS; R^1 = alkyl

Total synthesis of (+)-lycoricidine, (−)-lycoricidine and (+)-narciclasine via 6-*exo* cyclization of substituted vinyl radicals with oxime ethers has been reported[390]. Thus, interaction of oxime ether **321** with thiophenol and then with SmI_2 and TFA afforded (+)-lycoricidine **322** in good overall yield (equation 139).

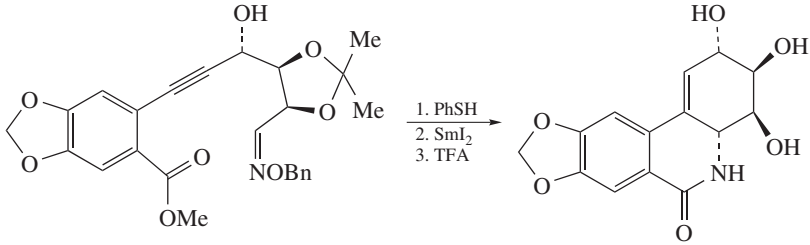

(**321**) (**322**) (139)

Derivatives of cyclopentanone oximes undergo Beckmann rearrangement to corresponding tetra- or hexahydropyridines or quinolines in the presence of Lewis acid ($AlCl_3$[391,392], $BF_3{\bullet}OEt_2$[393] or PPA[394]) or DIBAH (*i*-Bu_2AlH)/CH_2Cl_2[395].

3. Pyridazines, pyrimidines and pyrazines

The reaction of oxime **323** with concentrated aqueous HCl proceeded with a ring contraction and afforded pyridazine **324** as a single product (equation 140)[396]. On the contrary, the rearrangement of pyrrol-3-one oxime in the presence of hydrazine proceeded with ring enlargement and led to 1*H*-pyridazin-4-one oxime[397].

A general method for the synthesis of pyrimidine *N*-oxides from amidoximes is described. The conversion involves treatment of various carboxamide oximes **325** with 1,1,3,3-tetramethoxypropane, 2,4-pentanedione or 3-ethoxy-2-methylpropenal in the presence of CF_3COOH to afford pyrimidine 1-oxides **326** (equation 141)[398,399].

Cyclic amidoxime **327** was reacted with DMAD (dimethyl acetylenedicarboxylate) in CH_3CN and then in refluxing *o*-xylene to give after addition of Bz_2O a bicyclic pyrimidine derivative **328** in 31% yield (equation 142)[400]. The adducts **330**, prepared *in situ*

from amidoxime **329** and DMAD, under microwave irradiation in MeOH transform to pyrimidones **331** in 39–67% yields (equation 143)[401].

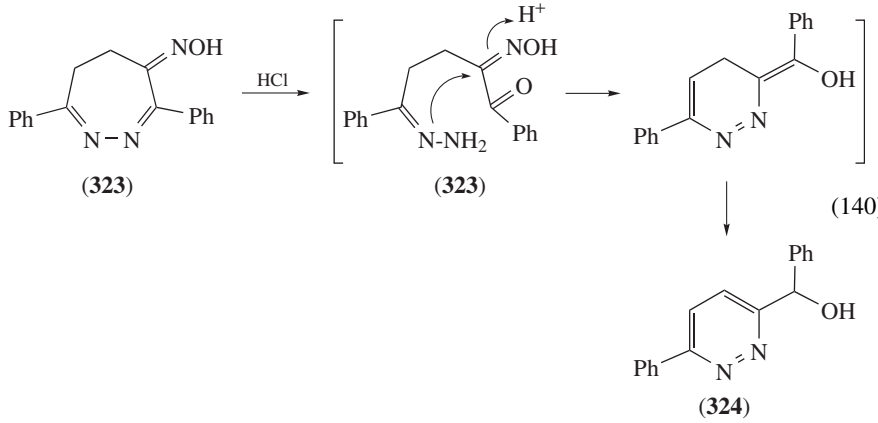

(**323**) (**323**) (140)

(**324**)

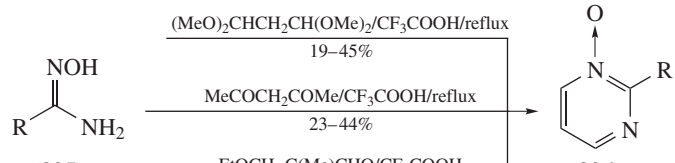

(**325**) (**326**) (141)

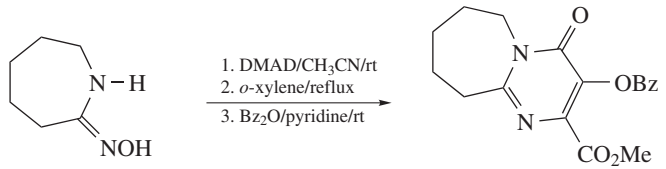

(**327**) (**328**) (142)

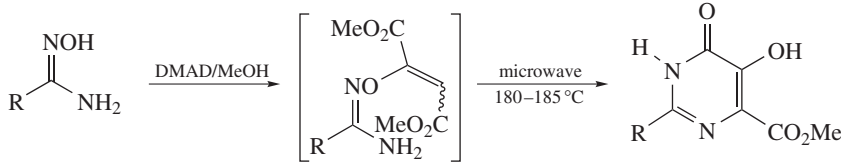

(**329**) (**330**) (**331**) (143)

R = alkyl, aryl, hetaryl

Reaction of amidoximes with dicarbonyl compounds in the presence of $Ru_3(CO)_{12}$ afforded pyrimidine derivatives[402]. Reaction of oximes of type RCH=CMeC(=NOH)Me with R'_2NCN also leads to pyrimidines[403]. α-Halo- and dihaloketoximes and Grignard reagents undergo dimerization to 2,4,6-trisubstituted pyrimidines[404, 405]. For example,

oxime ethers **332** and RMgBr in THF afforded pyrimidines **333** in 55–80% yields (equation 144)[405].

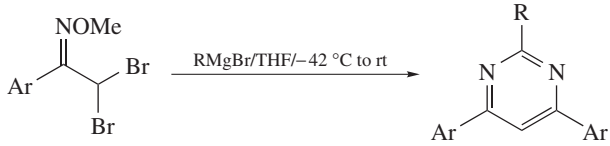

(144)

(**332**) Ar = aryl, 2-furyl; R = alkyl, aryl (**333**)

o-Aminooximes or related compounds reacted with carbonyl compounds or acetals to give pyrimidine mono-*N*-oxides[406–408] or pyrimidines[409]. Thus, interaction of oximes **334** with orthoformates leads to fused pyrimidine *N*-oxides **335** in 22–93% yields (equation 145)[408]. Similarly, *o*-acetamidobenzaldoximes and HCl afforded pyrimidine *N*-oxides[410].

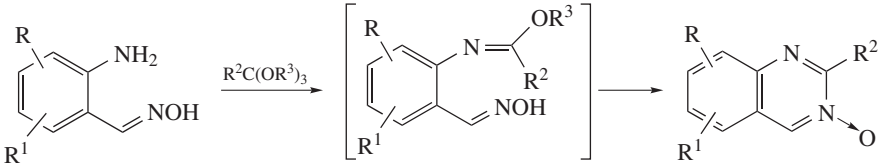

(**334**) R, R^1 = alkyl, aryl, hetaryl; R^2 = H, alkyl; R^3 = alkyl (**335**) (145)

Dihydro-[411], tetrahydro-[411,412] and hexahydropyrimidines[412] were synthesized from aminoamidoximes and carbonyl compounds too.

Reaction of ketoxime **336** with 5-aryl-2,3-dihydrofuran-2,3-diones afforded 4-methyl-1,2-dihydroquinazoline **337** in 70–75% yields (equation 146)[413].

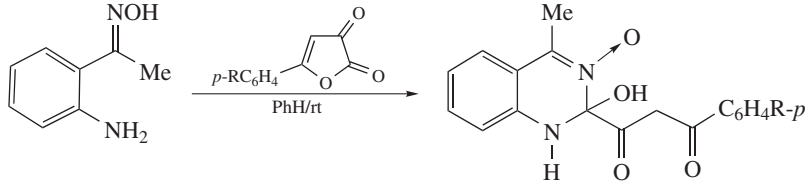

(146)

(**336**) R = H, Me, Cl (**337**)

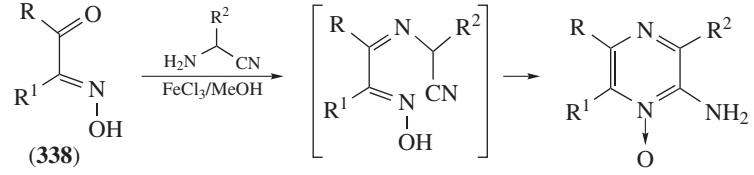

(**338**)

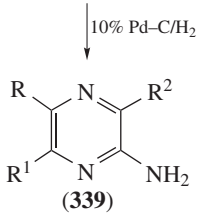

(147)

R = Me, Ph; R^1 = H, Me; R^2 = H, alkyl, Ph (**339**)

The direct reaction of α-hydroxyiminoketones with aminoacetonitriles was found to be a good route to pyrazine derivatives[414,415]. However, in some cases the yields of products were not high. Recently, it was described that the reaction of oximes **338** with aminoacetonitriles was catalyzed by $FeCl_3$. In this case 2-aminopyrazines **339** were obtained in 55–80% yields (equation 147)[415].

5-Methoxypyrazine-2-one *N*-oxides **341** were prepared from oxime derivatives **340** by one-pot cyclization in the presence of DCC/DMF with subsequent interaction with Me_2SO_4/K_2CO_3 and NaOH (equation 148)[416]. Similar intramolecular cyclization of ester and oxime *O*-ethers groups in the presence of lithium arylthiolate also leads to pyrazin-2-one ring formation[417].

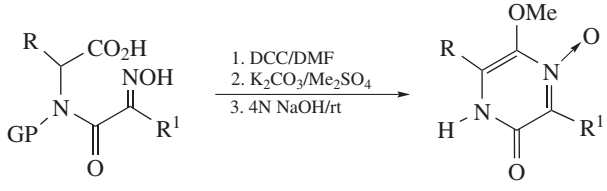

(148)

(**340**) (**341**)

R, R^1 = alkyl, aryl; PG = protecting group 22–56%

4. Triazines and tetrazines

The 1,2,3-triazine ring was constructed from *o*-aminophenyl oximes in the conditions of nitrosation ($NaNO_2$/HCl)[418], while hydrazinooximes were used for the synthesis of the 1,2,4-triazine ring[419–421]. Thus, cyclization of α-hydrazinooxime **342** with Pb_3O_4 in the presence of acetic acid afforded 1,2,4-triazines **343** in 44–54% yields (equation 149)[419]. Interaction of oxime **344** with hydrazine leads to the spiro compound product **345** in 73% yield (equation 150)[420].

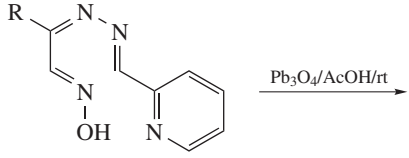

(149)

(**342**) R = alkyl, aryl (**343**)

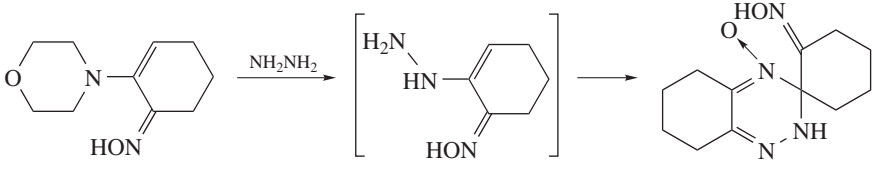

(**344**) (**345**) (150)

1,3,5-Triazines **347** were obtained from amidoximes **346** and ethyl orthoacetate (equation 151). The mechanism of formation of products **347** includes Beckmann rearrangement of amidoximes to carbodiimides, followed by reaction with amidoxime and orthoester[422].

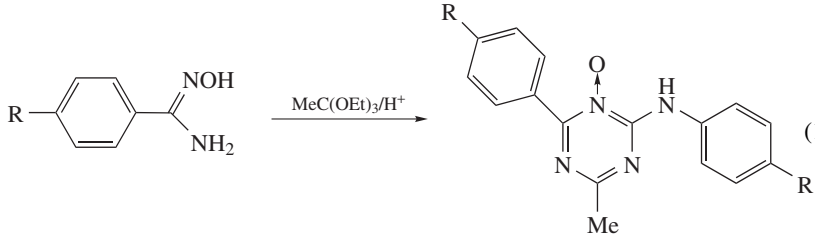

(151)

(**346**) R = H, 1-pyrrolyl (**347**)

Autocondensation of quinoxaline oxime **348** in the presence of $CoCl_2$ in ethanol afforded 1,2,4,5-tetrazino[1,6-a:4,3-*a′*]diquinoxaline (**349**) as main product (equation 152)[423].

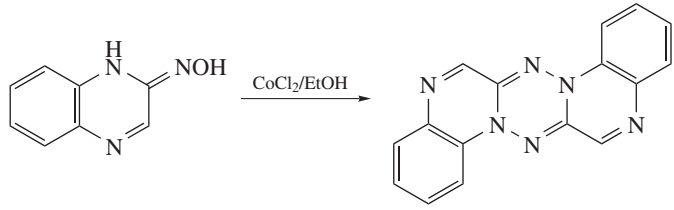

(152)

(**348**) (**349**)

5. Oxazines and dioxazines

Nitroso alkenes, generated from α-halogeno oximes and base, undergo addition with olefinic compounds affording 5,6-dihydro-4*H*-1,2-oxazines as main products[424]. Silyl enol ethers also can be used as dienophiles in this hetero Diels–Alder reaction. Thus, interaction of α-halogeno oximes **350** with silyl enol ethers in the presence of Na_2CO_3 in ether afforded oxazine derivatives **351** in yields up to 96% as a mixture of *cis*- and *trans*-isomers (equation 153)[425]. Similarly, ketene silyl acetals and substituted α-chloroacetophenone oximes **352** in the presence of K_2CO_3 in tetrahydrofuran afforded 6-alkoxy-3-aryl-6-trimethylsiloxy-5,6-dihydro-4*H*-1,2-oxazines **353** in moderate yields (equation 154)[426]. *N*,*N*-Bis(trimethylsilyl)enamines were also used in the synthesis of 1,2-oxazine ring[427].

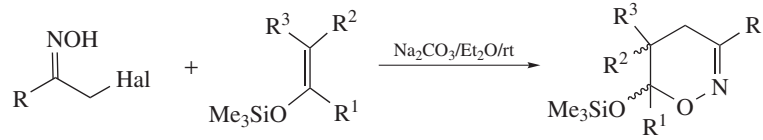

(153)

(**350**) R = Ph, CO_2Et; R^1, R^2, R^3 = H, alkyl, $OSiMe_3$ (**351**)

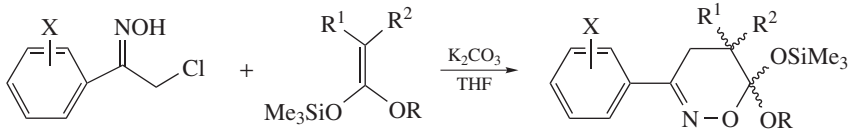

(154)

(**352**) X = H, Cl, alkyl, OMe; R, R^1, R^2 = alkyl, aryl (**353**)

Substituted nitrosoalkenes, prepared *in situ* from corresponding α-bromo oximes, can be added to furan[428], pyrrole[429] or indole[430] to afford fused oxazine derivatives. Recently, there was reported a preparation of novel heterocyclic oxazinotetrahydroquinoline **355** and **356** or oxazinotetrahydroisoquinoline **357** derivatives by reaction of the corresponding dihydroquinolines or dihydroisoquinolines with α-bromo oximes **354** in the presence of Na_2CO_3 in CH_2Cl_2 (equation 155)[428a].

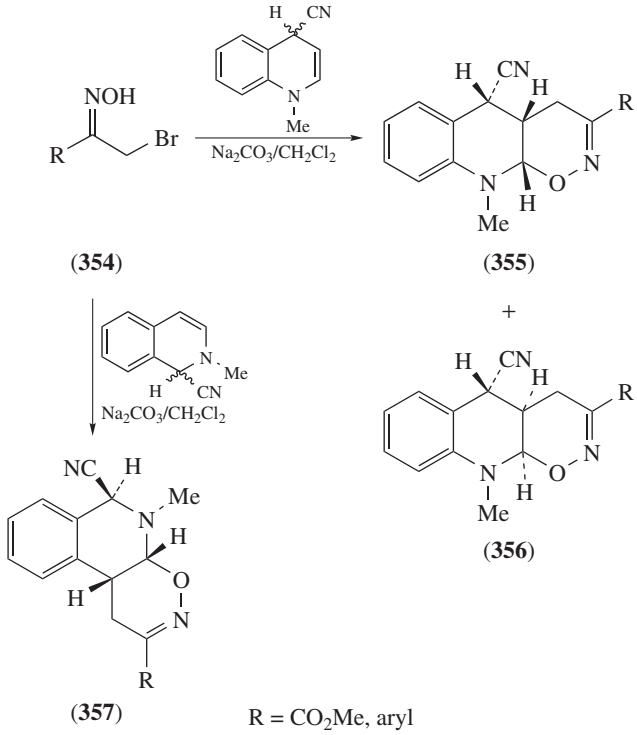

(155)

Enantiomerically pure oxazine derivatives can be obtained from epoxy pyranosides and β-ketoester oximes in the presence of a base. For instance, oxime **358** and epoxy pyranoside **359** in the presence of BuLi/THF gave oxazine **360** in 70% yield (equation 156)[431]. 6-Hydroxymethyl-5,6-dihydro-4*H*-1,2-oxazines were obtained from ketoximes and epibromohydrin in the presence of *n*-BuLi[432].

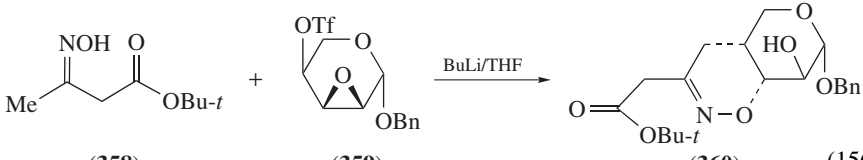

(156)

The photooxygenation of furans in the presence of acetaldoxime, followed by Et_2S reduction and treatment with SiO_2, leads to 1,2-oxazin-6-ones **361** in 37–50% yields (equation 157)[433].

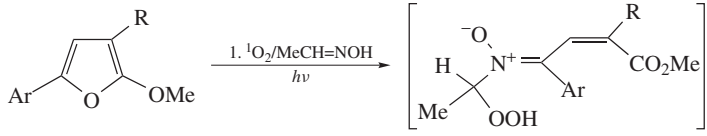

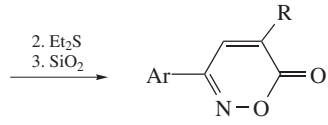

R = COMe, CO_2Me (**361**) (157)

Synthesis of the 1,2-oxazine ring by intramolecular cyclization of γ-hydroxyoximes using Mitsunobu reaction was described[434].

Beckmann rearrangement of 2,2,5,5-tetramethyltetrahydro-3-furanone oxime (**362**) afforded 1,3-oxazine **363** in 64% yield (equation 158)[435]. 1,4-Oxazines **365** were obtained by acidic deprotection–spirocyclization of oxime ethers **364** (equation 159)[436].

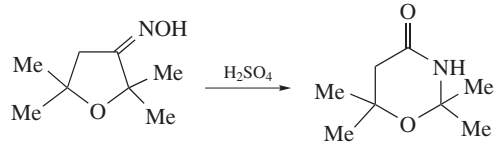

(**362**) (**363**) (158)

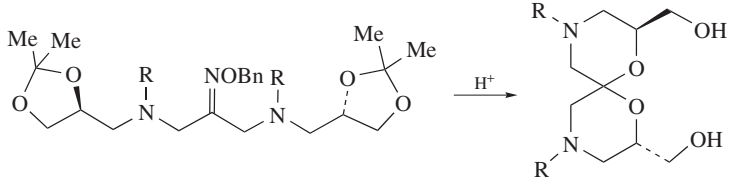

(**364**) (**365**) (159)

Reactions of α-hydroxyoxime **366** with NaH/*i*-PrOH/$ClCO_2Et$ or CS_2 afforded 1,5,2-dioxazines **367** and **368** in 79 or 76% yields, respectively (equation 160)[437].

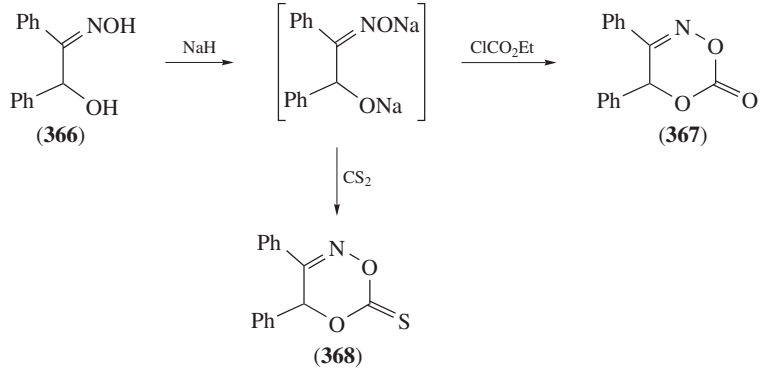

(**366**) (**367**) (**368**) (160)

6. Oxadiazines and dioxadiazines

1,2,4-Oxadiazine **370** was obtained from aziridinooxime **369** and concentrated HCl in 51% yield (equation 161)[438]. Cyclization of acylated amidoxime **371** in the presence of K_2CO_3 in DMF also leads to formation of oxadiazine ring **372** (yield 12%), along with quinoline derivative **373** (equation 162)[439].

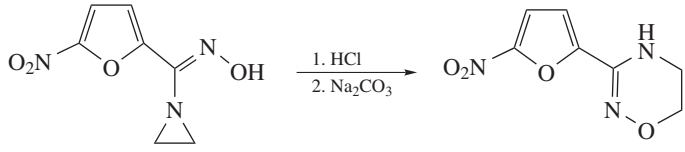

(**369**) (**370**) (161)

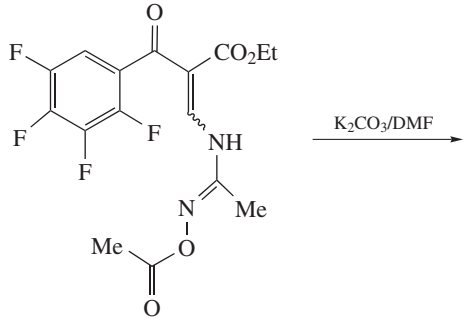

(**371**)

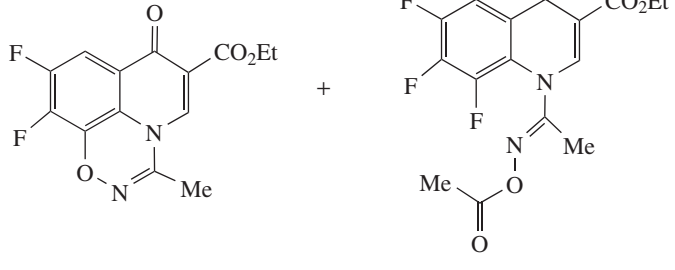

(**372**) (**373**) (162)

Reaction of α-aminoketoximes **374** with 1,1′-carbonyldiimidazole (CDI) in THF afforded 1,2,5-oxadiazin-6-ones **375** in 41–65% yields (equation 163)[440].

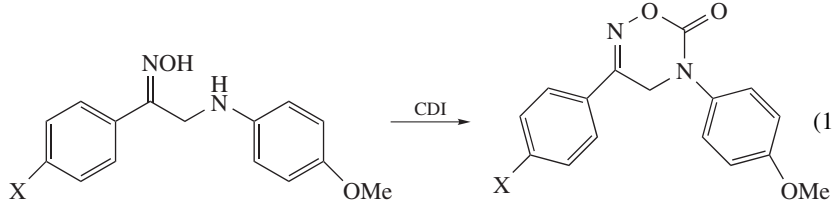

(**374**) X = H, NO_2 (**375**) (163)

1,4,2,5-Dioxadiazine ring **377** was successfully obtained by dimerization of the corresponding hydroximoyl chloride **376** in the presence of Et_3N (equation 164)[441].

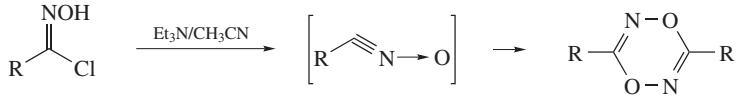

(**376**) R = 4-amino-1,2,5-oxadiazol-3-yl (**377**) (164)

7. Dithiatriazines

The reactions of 1-aryl-2,2,2-trifluoroethanone oximes **378** with tetrasulfur tetranitride (S_4N_4) in toluene at reflux gave 5-aryl-5-trifluoromethyl-4*H*-1,3,2,4,6-dithiatriazines **379**, 1-aryl-2,2,2-trifluoroethylideneaminosulfenamides **380** and sulfur (equation 165)[442].

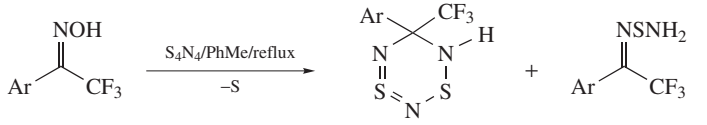

(**378**) (**379**) 17–37% (**380**) 7–53% (165)

8. Oxadiazaphosphinine

A derivative of the new heterocyclic ring system 4-benzyl-3-(2,6-dichlorophenyl)-6-ethoxy-4,5-dihydro-1,2,4,6-oxadiazaphosphinine 6-oxide (**382**) is prepared by the reaction of sterically hindered hydroximoyl chloride **381** with aminomethylphosphonate (equation 166)[443].

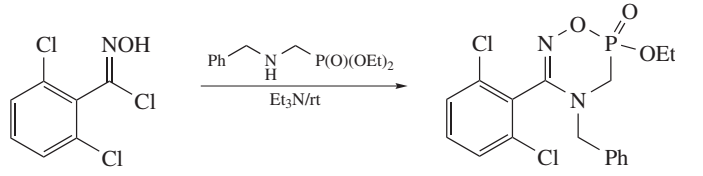

(**381**) (**382**) 44% (166)

E. Seven-membered Ring Systems

2-(2-Bromobenzyloxy)benzaldehyde *O*-alkyloximes **383** are converted to the corresponding dibenzo[*b*, *e*]oxepines **384** by radical addition reaction with Bu_3SnH and AIBN (equation 167)[349].

Beckmann rearrangement is extensively used in organic chemistry for construction of a heterocyclic seven-membered nitrogen-containing ring system. Beckmann rearrangement of cyclohexanone oxime derivatives to the corresponding ε-caprolactams[444] by sulfuric acid[445], tetrabutylammonium perrhenate/trifluoromethanesulfonic acid[446], NBS[447], P_2O_5/ionic liquid[448], PCl_5/ionic liquid[449], borate-pillared layered double peroxides[450], montmorillonite KSF[451], montmorillonite K-10/microwave irradiation[452], in gas phase

over crystalline BPO_4[453], noncatalytic high pressure in supercritical H_2O[454] or other similar methods are reported. Beckmann rearrangement of oximes in the presence of *P*-nucleophiles ($(EtO)_3P$ and $HP(O)(OEt)_2$) afforded the corresponding aminomethylene *gem*-diphosphonates. For example, interaction of tetralone oxime **385** with $(EtO)_3P$ and $POCl_3$ in CH_2Cl_2 afforded 2,2-bis(diethylphosphono)-2,3,4,5-tetrahydro-1*H*-1-benzazepine **386** in 30% yield (equation 168)[455]. 5,6,7,8-Tetrahydro-4*H*-thieno[3,2-*b*]azepine, tetrahydro-4*H*-furo[3,2-*b*]azepine and hexahydropyrrolo[3,2-*b*]azepine derivatives **388** can be easily obtained by ring expansion of heterocyclic fused cyclohexanone oximes **387** with diisobutylaluminium hydride (equation 169)[456].

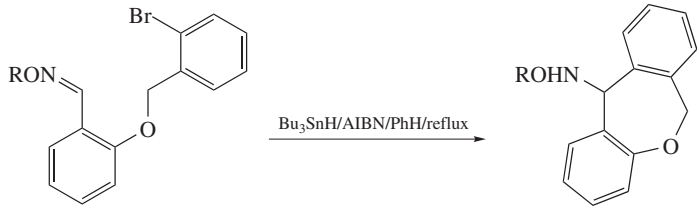

(**383**) (**384**)

R = Me, *t*-Bu 47–49% (167)

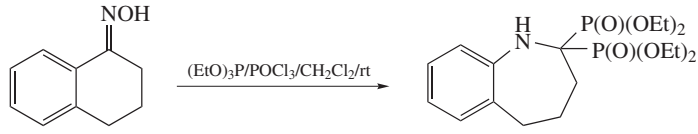

(**385**) (**386**) (168)

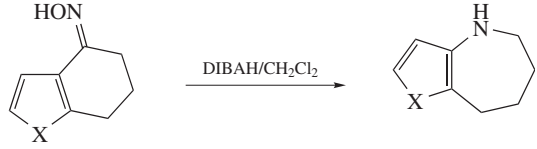

(**387**) X = O, S, NH, NMe (**388**) (169)

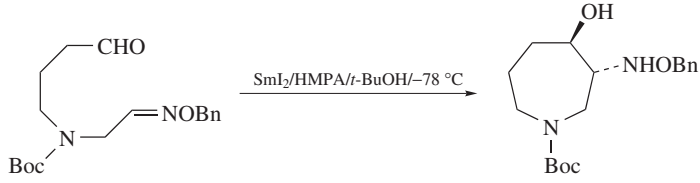

(**389**) (**390**) (170)

A free radical cyclization of oxime ethers tethered to an aldehyde has been used in the synthesis of azepine derivatives[457]. For example, oxime ether **389** is cyclized to azepine **390** by reaction with SmI_2 in HMPA and *t*-BuOH at −78 °C (equation 170)[458]. Similar free radical cyclization of oxime ethers can be carried out also in the presence of Bu_3SnH/AIBN in benzene[459]. Oxime *O*-methyl ether **391** underwent thermal cyclization in refluxing *o*-dichlorobenzene (ODCB) leading to the mixture of two products **392** and **393** in ratio 69:31 in overall yield of 91% (equation 171)[460]. Rearrangement of oxime *O*-tosylates in the presence of piperidine also leads to azepine ring formation[461].

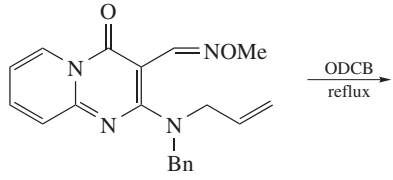

(**391**)

(171)

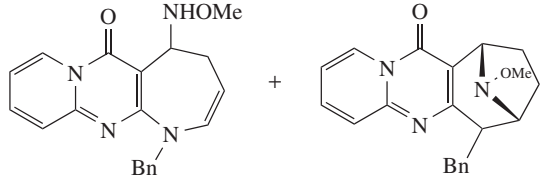

(**392**) (**393**)

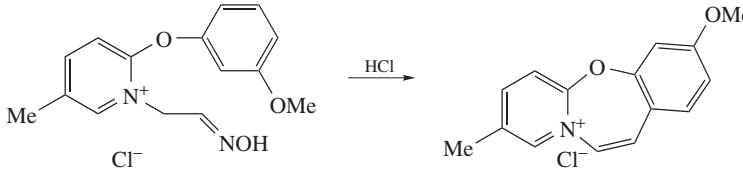

(**394**) (**395**) (172)

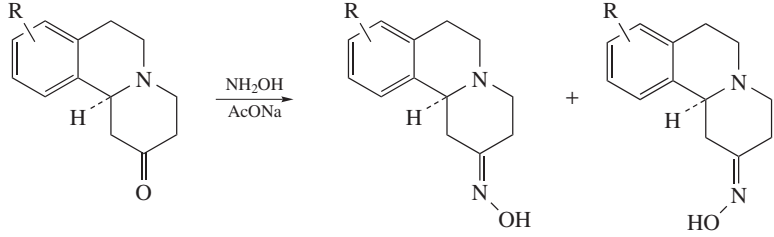

(**396**) (**397**)

TsCl/Na_2CO_3/acetone
45–50%

(173)

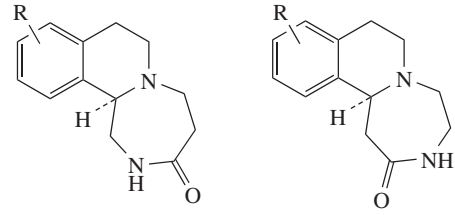

R = H, OMe (**398**) (**399**)

Pyridinium oxime **394** in the presence of concentrated HCl gives oxazepine **395** in 61% yield (equation 172)[462]. Beckmann rearrangement of 4-chromanone oximes in the presence of polyphosphoric acid[463] or diisobutylaluminium hydride[464] also afforded substituted benzoxazepinone ring.

Z- and *E*-oximes of benzo[*a*]quinolizin-2-ones **396** and **397** were converted into isomeric diazepinoisoquinolines **398** and **399**, respectively, by treatment with TsCl and Na_2CO_3 in acetone (equation 173)[465].

Oxime ether **400** with the system $I_2/NaHCO_3/EtOH$ afforded diazepine **401** in 75% yield (equation 174)[466].

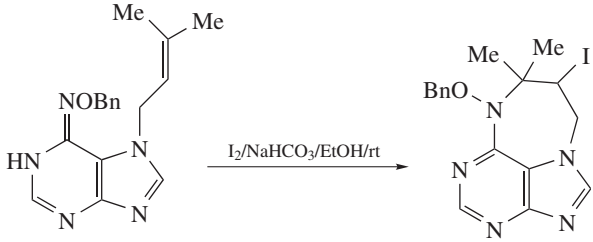

(**400**) (**401**) (174)

Cyclization of amidoxime *O*-ether **402** in the presence of NaH in MeCN leads to 1,2,4-oxadiazepine **403** (equation 175)[467].

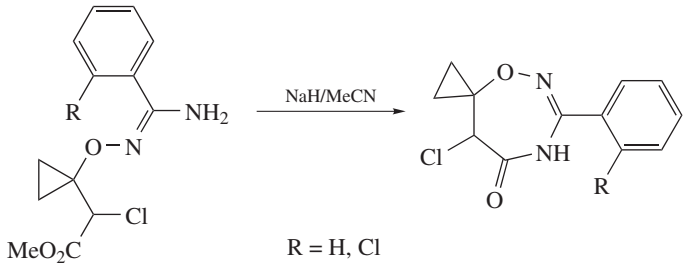

(**402**) (**403**) (175)

III. CONCLUSIONS

Oximes and their derivatives are valuable starting materials for the preparation of many classes of heterocyclic compounds. The main group of reactions includes the cyclization of unsaturated oxime derivatives. Using these starting materials furans, pyrroles, isoxazoles and pyridines were prepared. Imidazoles were synthesized from α-ketooximes and hydrazine. Dioximes were successfully transformed to triazole, dioxazole and oxadiazole ring systems. Amidoximes is an excellent starting material for the synthesis of triazoles, oxadiazoles and pyrimidines. Some heterocyclic systems (for example, pyridines and seven-membered rings) were obtained using classical Beckmann rearrangement. Application of aromatic or heterocyclic oximes in the cyclizations led to different polycyclic heterocyclic compounds.

IV. REFERENCES

1. G. M. Robertson, in *Comprehensive Organic Functional Group Transformation* (Eds. A. R. Katritzky, O. Meth-Cohn and C. W. Rees), Vol. 3, Elsevier, Oxford, 1995, pp. 425–441.

2. J. P. Adams and G. Robertson, *Contemp. Org. Synth.*, **4**, 183 (1997).
3. J. P. Adams, *Contemp. Org. Synth.*, **4**, 517 (1997).
4. J. P. Adams, *J. Chem. Soc., Perkin Trans. 1*, 125 (2000).
5. A. Kotali and V. P. Papageorgiou, *Org. Prep. Proced. Int.*, **23**, 593 (1991).
6. S.-C. Tsay, H. V. Patel and J. R. Hwu, *Synlett*, 939 (1998).
7. Q. X. Zhu, R. O. Hutchins and M. K. Hutchins, *Org. Prep. Proced. Int.*, **26**, 193 (1994).
8. D. Enders and U. Reinhold, *Tetrahedron: Asymmetry*, **8**, 1895 (1997).
9. M. Yurovskaya and A. V. Karchava, *Tetrahedron: Asymmetry*, **9**, 3331 (1998).
10. S. Kobayashi and H. Ishitani, *Chem. Rev.*, **99**, 1069 (1999).
11. E. Abele and E. Lukevics, *Chem. Heterocycl. Compd.*, **37**, 141 (2001).
12. E. Abele, R. Abele, O. Dzenitis and E. Lukevics, *Chem. Heterocycl. Compd.*, **39**, 3 (2003).
13. E. Abele, R. Abele and E. Lukevics, *Chem. Heterocycl. Compd.*, **39**, 825 (2003).
14. E. Abele, R. Abele and E. Lukevics, *Chem. Heterocycl. Compd.*, **40**, 1 (2004).
15. E. Abele, R. Abele, K. Rubina and E. Lukevics, *Chem. Heterocycl. Compd.*, **41**, 825 (2005).
16. (a) E. Abele, R. Abele and E. Lukevics, *Chem. Heterocycl. Compd.*, **43**, 387 (2007).
    (b) E. Abele, R. Abele and E. Lukevics, *Chem. Heterocycl. Compd.*, **43**, 945 (2007).
17. D. Karbonits and K. Horvath, *Heterocycles*, **37**, 2051 (1994).
18. E. Abele and E. Lukevics, *Org. Prep. Proced. Int.*, **32**, 235 (2000).
19. E. Abele and E. Lukevics, *Heterocycles*, **53**, 2285 (2000).
20. K. Kotera, Y. Matsukawa, H. Takahashi, T. Okada and K. Kitahonoki, *Tetrahedron*, **24**, 6177 (1968).
21. T. Kammermeier, A. Kaiser, G. S. Lee, T. Burgemeister and W. Wiegrebe, *Arch. Pharm.*, **327**, 207 (1994).
22. C. P. Felix, N. Khatimi and A. J. Laurent, *Tetrahedron Lett.*, **35**, 3303 (1994).
23. C. Felix, A. Laurent, S. Lesniak and P. Mison, *J. Chem. Res. (S)*, 32 (1991).
24. P. W. Neber and A. Burgard, *Liebigs Ann. Chem.*, **493**, 281 (1932).
25. F. Palacios, A. M. Ochoa de Retana and J. I. Gil, *Tetrahedron Lett.*, **41**, 5363 (2000).
26. T. Sakai, Y. Liu, H. Ohta, T. Korenaga and T. Ema, *J. Org. Chem.*, **70**, 1369 (2005).
27. A. R. Katritzky, M. Wang, C. R. Wilkerson and H. Yang, *J. Org. Chem.*, **68**, 9105 (2003).
28. T. Tsuritani, K. Yagi, H. Shinokubo and K. Oshima, *Angew. Chem. Int. Ed.*, **42**, 5613 (2003).
29. G. B. Jones, C. J. Moody, A. Padwa and J. M. Kassir, *J. Chem. Soc., Perkin Trans. 1*, 1721 (1991).
30. T. Naito, A. Saito, M. Ueda and O. Miyata, *Heterocycles*, **65**, 1857 (2005).
31. W. B. Jennings, J. H. O'Shea and A. Schweppe, *Tetrahedron Lett.*, **42**, 101 (2001).
32. S. D. Cook, T. A. Hamor, W. B. Jennings, A. A. Tebbutt, S. P. Watson and D. R. Boyd, *J. Chem. Soc., Perkin Trans. 2*, 1281 (1991).
33. M. R. Iesce, F. Cermola and A. Guitto, *Synthesis*, 657 (1997).
34. M. R. Iesce, F. Cermola, A. Guitto, F. Giordano and R. Scarpati, *J. Org. Chem.*, **61**, 8677 (1996).
35. Yu. V. Zeifman, E. G. Abduganiev, E. M. Rokhlin and I. L. Knunyants, *Izv. Akad. Nauk SSSR, Ser. Khim.*, 2737 (1972); *Chem. Abstr.*, **78**, 97752t (1973).
36. R. G. Kostyanovskii, G. V. Shustov and G. V. Markov, *Izv. Akad. Nauk SSSR, Ser. Khim.*, 2823 (1974); *Chem. Abstr.*, **82**, 97962u (1975).
37. A. N. Mikhailyuk, N. N. Makhova, A. E. Bova, L. I. Khmel'nitskii and S. S. Novikov, *Izv. Akad. Nauk SSSR, Ser. Khim.*, 1566 (1978); *Chem. Abstr.*, **89**, 215263m (1978).
38. Y. Hatanaka, H. Nakayama and Y. Kanaoka, *Heterocycles*, **35**, 997 (1993).
39. K. M. Broadus and S. R. Kass, *J. Org. Chem.*, **65**, 6566 (2000).
40. A. N. Mikhailyuk, V. Yu. Petukhova and N. N. Makhova, *Mendeleev Commun.*, 60 (1997).
41. E. M. Scanlan and J. C. Walton, *Chem. Commun.*, 2086 (2002).
42. G. A. DiLabio, E. M. Scanlan and J. C. Walton, *Org. Lett.*, **7**, 155 (2005).
43. O. Miyata, N. Takeda and T. Naito, *Org. Lett.*, **6**, 1761 (2004).
44. (a) T. Sheradsky, *J. Heterocycl. Chem.*, **4**, 413 (1967).
    (b) M. Aram, US Patent 3558667; *Chem. Abstr.*, **75**, 20176p (1971).
45. K. Ishibashi, K. Nakajima, Y. Sugioka, M. Sugiyama, T. Hamada, H. Horikoshi and T. Nishi, *Chem. Pharm. Bull.*, **47**, 226 (1999).
46. C. Majdik, A. Kovendi, S. Matei and D. Breazu, *Rev. Roum. Chim.*, **36**, 1321 (1991).
47. K. Eiter and E. Mrazek, *Monatsh. Chem.*, **83**, 926 (1952).
48. D. Heyl, S. A. Harris and K. Folkers, Brit. Patent 613824; *Chem. Abstr.*, **43**, 4702h (1949).

49. A. Hassner, K. S. K. Murthy, A. Padwa, U. Chiacchio, D. C. Dean and A. M. Schoffstall, *J. Org. Chem.*, **54**, 5277 (1989).
50. W. Dehaen and A. Hassner, *J. Org. Chem.*, **56**, 896 (1991).
51. A. Hassner and R. Maurya, *Tetrahedron Lett.*, **30**, 2289 (1989).
52. K.-H. Kao, C.-S. Yang, J.-T. Liu, W.-W. Lin, H.-Y. Fang, C.-F. Yao and K. Chen, *Tetrahedron*, **54**, 13997 (1998).
53. M.-C. Yan, J.-Y. Liu, W.-W. Lin, K.-H. Kao, J.-T. Liu, J.-J. Jang and C.-F. Yao, *Tetrahedron*, **55**, 12493 (1999).
54. O. Tamura, T. Mitsuya and H. Ishibashi, *Chem. Commun.*, 1128 (2002).
55. O. Tamura, T. Mitsuya, X. Huang, Y. Tsutsumi, S. Hattori and H. Ishibashi, *J. Org. Chem.*, **70**, 10720 (2005).
56. G. K. Friestad, *Tetrahedron*, **57**, 5461 (2001).
57. H. Miyabe, O. Miyata and T. Naito, *J. Synth. Org. Chem. Jpn.*, **60**, 1087 (2002).
58. E. El Kaim, A. Gacon and A. Perroux, *Tetrahedron Lett.*, **39**, 371 (1998).
59. O. Miyata, K. Muroya, J. Koide and T. Naito, *Synlett*, 271 (1998).
60. O. Miyata, K. Muroya, T. Kobayashi, R. Yamanaka, S. Kajisa, J. Koide and T. Naito, *Tetrahedron*, **58**, 4459 (2002).
61. O. Miyata, S. Kajisa, M. Ueda, M. Yamauchi and T. Naito, *Chem. Pharm. Bull.*, **53**, 995 (2005).
62. H. Miyabe, K. Fujii, T. Goto and T. Naito, *Org. Lett.*, **2**, 4071 (2000).
63. T. Inokuchi and H. Kawafuchi, *Synlett*, 421 (2001).
64. K. Griesbaum, X. Liu, A. Kassiaris and M. Scherer, *Liebigs Ann. Chem./Recueil*, 1381 (1997).
65. K. Griesbaum, X. Liu and Y. Dong, *Tetrahedron*, **53**, 5463 (1997).
66. O. A. Rakitin, C. W. Rees, D. J. Williams and T. Torroba, *J. Org. Chem.*, **61**, 9178 (1997).
67. B. A. Trofimov, *Adv. Heterocycl. Chem.*, **51**, 177 (1990).
68. B. A. Trofimov and A. I. Mikhaleva, *Heterocycles*, **37**, 1193 (1994).
69. B. A. Trofimov and A. I. Mikhaleva, *Zh. Org. Khim.*, **32**, 1127 (1996); *Chem. Abstr.*, **126**, 251030z (1997).
70. S. E. Korostova, A. I. Mikhaleva and B. A. Trofimov, *Russ. Chem. Rev.*, **68**, 459 (1999); *Chem. Abstr.*, **131**, 228588g (1999).
71. A. B. Zaitsev, E. Yu. Schmidt, A. M. Vasil'tsov, A. I. Mikhaleva, A. V. Afonin, I. A. Ushakov and D.-S. D. Toyashinova, *Chem. Heterocycl. Compd.*, **41**, 444 (2005).
72. S. E. Korostova, A. I. Mikhaleva, R. N. Nesterenko, N. V. Maznaya, V. K. Voronov and N. M. Borodina, *Zh. Org. Khim.*, **21**, 406 (1985); *Chem. Abstr.*, **103**, 53894w (1985).
73. G. A. Pinna, M. A. Pirisi and G. Paglietti, *J. Chem. Res. (S)*, 210 (1993).
74. E. N. Deryagina, N. V. Russavskaya and V. Yu. Vvedenskii, *Russ. J. Org. Chem.*, **35**, 1225 (1999).
75. S. E. Korostova, S. G. Shevchenko, M. V. Sigalov and N. I. Golovanova, *Chem. Heterocycl. Compd.*, **27**, 363 (1991).
76. M. A. Yurovskaya, V. V. Druzhinina, M. A. Tyurekhodzhaeva and Yu. G. Bundel, *Khim. Geterotsikl. Soedin.*, 69 (1984); *Chem. Abstr.*, **100**, 191693u (1984).
77. M. A. Yurovskaya, V. V. Druzhinina, E. V. Snetkova and Yu. G. Bundel, *Khim. Geterotsikl. Soedin.*, 356 (1983); *Chem. Abstr.*, **99**, 5475n (1983).
78. B. A. Trofimov, A. I. Mikhaleva, A. N. Vasil'ev, V. A. Lopyrev, I. A. Titova, V. M. Bzhezovskii and M. V. Sigalov, *Khim. Geterotsikl. Soedin.*, 1422 (1981); *Chem. Abstr.*, **96**, 199581a (1982).
79. O. V. Petrova, A. I. Mikhaleva, L. N. Sobenina, E. Yu. Schmidt and E. I. Kositsyna, *Mendeleev Commun.*, 162 (1997).
80. A. V. Afonin, I. A. Ushakov, O. V. Petrova, L. N. Sobenina, A. I. Mikhaleva, V. K. Voronov and B. A. Trofimov, *Russ. J. Org. Chem.*, **36**, 1043 (2000); *Chem. Abstr.*, **134**, 237174h (2001).
81. B. A. Trofimov, A. M. Vasil'tsov, E. Yu. Schmidt, N. V. Zorina, A. V. Afonin, A. I. Mikhaleva, K. B. Petrushenko, I. A. Ushakov, L. B. Krivdin, V. K. Belsky and L. I. Bryukvina, *Eur. J. Org. Chem.*, 4338 (2005).
82. B. A. Trofimov, O. A. Tarasova, A. I. Mikhaleva, N. A. Kalinina, L. M. Sinegovskaya and J. Henkelmann, *Synthesis*, 1585 (2000).
83. B. J. J. Aiscar, H. Becker, J. Henkelmann and T. Preiss, Ger. Patent 19924041; *Chem. Abstr.*, **134**, 4860p (2001).

84. A. B. Zaitsev, E. Yu. Schmidt, A. M. Vasil'tsov, A. I. Mikhaleva, O. V. Petrova, A. V. Afonin and N. V. Zorina, *Chem. Heterocycl. Compd.*, **42**, 34 (2006).
85. A. B. Zaitsev, E. Yu. Schmidt, A. I. Mikhaleva, A. V. Afonin and I. A. Ushakov, *Chem. Heterocycl. Compd.*, **41**, 722 (2005).
86. B. A. Trofimov, A. B. Zaitseva, E. Yu. Schmidt, A. M. Vasil'tsov, A. I. Mikhaleva, I. A. Ushakov, A. V. Vashchenko and N. V. Zorina, *Tetrahedron Lett.*, **45**, 3789 (2004).
87. S. E. Korostova, R. N. Nesterenko, A. I. Mikhaleva, R. I. Polovnikova and N. I. Golovanova, *Khim. Geterotsikl. Soedin.*, 901 (1989); *Chem. Abstr.*, **112**, 178530s (1990).
88. L. G. Vosskresensky, T. N. Borisova and A. V. Varlamov, *Chem. Heterocycl. Compd.*, **40**, 326 (2004).
89. S. E. Korostova, S. G. Shevchenko and M. V. Sigalov, *Khim. Geterotsikl. Soedin.*, 1371 (1991); *Chem. Abstr.*, **117**, 48251u (1992).
90. S. E. Korostova, A. I. Mikhaleva, B. A. Trofimov, S. G. Shevchenko and M. V. Sigalov, *Khim. Geterosikl. Soedin.*, 485 (1992); *Chem. Abstr.*, **117**, 233764b (1992).
91. B. A. Trofimov, O. A. Tarasova, E. Yu. Schmidt, A. I. Mikhaleva and L. M. Sinegovskaya, *Russ. Chem. Bull.*, **46**, 594 (1997); *Chem. Abstr.*, **127**, 190610k (1997).
92. L. Cheng and D. A. Lightner, *Synthesis*, 46 (1999).
93. V. A. Samsonov and L. B. Volodarsky, *Khim. Geterotsikl. Soedin.*, 1676 (1993); *Chem. Abstr.*, **122**, 9954j (1995).
94. S. Hebbe and L. Dechoux, *Lett. Org. Chem.*, **1**, 257 (2004).
95. D. H. Cho, J. H. Lee and B. H. Kim, *J. Org. Chem.*, **64**, 8048 (1999).
96. D. Shi, C. Shi, X. Wang, Q. Zhuang, S. Tie and H. Hu, *Synlett*, 2239 (2004).
97. D. Edmont and D. M. Williams, *Tetrahedron Lett.*, **41**, 8581 (2000).
98. C. L. Gibson, S. La Rosa, K. Ohta, P. H. Boyle, F. Leurquin, A. Lemacon and C. J. Suckling, *Tetrahedron*, **60**, 943 (2004).
99. H. Tsutsui and K. Narasaka, *Chem. Lett.*, 45 (1999).
100. K. Hiroyuki, K. Uchiyama, Y. Yamashita and K. Narasaka, *Chem. Lett.*, 715 (1995)
101. A. Furstner, K. Radkowski and H. Peters, *Angew. Chem. Int. Ed.*, **44**, 2777 (2005)
102. M. Kitamura, S. Chiba, O. Saku and K. Narasaka, *Chem. Lett.*, 606 (2002)
103. S. Zaman, M. Kitamura and K. Narasaka, *Bull. Chem. Soc. Jpn.*, **76**, 1055 (2003).
104. K. Sakoda, J. Mihara and J. Ichikawa, *Chem. Commun.*, 4684 (2005).
105. M. Kitamura, S. Zaman and K. Narasaka, *Synlett*, 974 (2001).
106. Y. Koganemaru, M. Kitamura and K. Narasaka, *Chem. Lett.*, 784 (2002)
107. K. Narasaka and M. Kitamura, *Eur. J. Org. Chem.*, 4505 (2005).
108. H. Ohno, A. Aso, Y. Kadoh, N. Fujii and T. Tanaka, *Angew. Chem. Int. Ed.*, **46**, 6325 (2007).
109. H. Kusama, K. Uchiyama, Y. Yamashita and K. Narasaka, *Chem. Lett.*, 715 (1995).
110. H. Kusama, Y. Yamashita, K. Uchiyama and K. Narasaka, *Bull. Chem. Soc. Jpn.*, **70**, 965 (1997).
111. S. Mori, K. Uchiyama, Y. Hayashi, K. Narasaka and E. Nakamura, *Chem. Lett.*, 111 (1998).
112. K. Uchiyama, M. Yoshida, Y. Hayashi and K. Narasaka, *Chem. Lett.*, 607 (1998).
113. K. Uchiyama, Y. Hayashi and K. Narasaka, *Chem. Lett.*, 1261 (1998).
114. K. Uchiyama, Y. Hayashi and K. Narasaka, *Tetrahedron*, **55**, 8915 (1999).
115. J. Boivin, A.-M. Shirano and S. Z. Zard, *Tetrahedron Lett.*, **35**, 249 (1994).
116. J. Boivin, A.-C. Callier-Dublanchet, B. Quiclet-Sire, A. M. Schiano and S. Z. Zard, *Tetrahedron*, **51**, 6517 (1995).
117. F. Gagosz and S. Z. Zard, *Synlett*, 1978 (1999).
118. T. Mikami and K. Narasaka, *C. R. Acad. Sci., Chim.*, **4**, 477 (2001)
119. T. Mikami and K. Narasaka, *Chem. Lett.*, 338 (2000).
120. M. Yoshida, M. Kitamura and K. Narasaka, *Chem. Lett.*, 144 (2002).
121. F. Portela-Cubillo, J. S. Scott and J. C. Walton, *Chem. Commun.*, 4041 (2007).
122. (a) M. Kitamura, Y. Mori and K. Narasaka, *Tetrahedron Lett.*, **46**, 2373 (2005).
(b) H. Sakurai, T. Ichikawa and K. Narasaka, *Chem. Lett.*, 508 (2000).
123. M. Departure, J. Diewok, J. Grimaldi and J. Hatem, *Eur. J. Org. Chem.*, 275 (2000).
124. Y. Takeda, T. Nakabayashi, A. Shirai, D. Fukumoto, T. Kiguchi and T. Naito, *Tetrahedron Lett.*, **45**, 3481 (2004).
125. R. Grigg, F. Heaney, J. Markandu, S. Surendrakumar, M. Thornton-Pett and W. J. Warnock, *Tetrahedron*, **47**, 4007 (1991).
126. X. Lin, G. D. Artman, III, D. Stien and S. M. Weinreb, *Tetrahedron*, **57**, 8779 (2001).

127. M. Tiecco, L. Testaferri, L. Bagnoli, V. Purgatorio, A. Temperini, F. Marini and C. Santi, *Tetrahedron: Asymmetry*, **12**, 3297 (2001).
128. H. Ali Dondas, R. Grigg, M. Hadjisoteriou, J. Markandu, W. A. Thomas and P. Kennewell, *Tetrahedron*, **56**, 10087 (2000).
129. B. B. Snider and J. Zhou, *J. Org. Chem.*, **70**, 1087 (2005).
130. R. E. Gawley and E. J. Termine, *J. Org. Chem.*, **49**, 1946 (1984).
131. H. Kotake, H. Kinoshita and S. Miyashita, *Chem. Lett.*, 445 (1972).
132. S. Siaka, P. M. Lukin, O. E. Nasakin, M. Yu. Antipin and V. N. Khrustalev, *Russ. J. Org. Chem.*, **35**, 269 (1999).
133. O. E. Nasakin, P. M. Lukin, E. V. Vershinin, O. V. Yashkanova, A. N. Lyshikov, Ya. G. Urman, S. V. Lindeman, Yu. T. Struchkov and A. Kh. Bulai, *Zh. Org. Khim.*, **31**, 370 (1995); *Chem. Abstr.*, **124**, 145946b (1996).
134. N. Shoji, Y. Kondo and T. Takemoto, *Heterocycles*, **1**, 251 (1973).
135. W. M. Abdou, Y. O. El-Khoshnieh, M. A. I. Salem and R. F. Barghash, *Synlett.*, 1417 (2002).
136. H. Miyabe, S. Kanehira, K. Kume, H. Kandori and T. Naito, *Tetrahedron*, **54**, 5883 (1998).
137. H. Miyabe, H. Tanaka and T. Naito, *Chem. Pharm. Bull.*, **52**, 74 (2004).
138. H. Miyabe, *Yakugaku Zasshi*, **120**, 667 (2000); *Chem. Abstr.*, **133**, 266262v (2000).
139. H. Miyabe, M. Ueda and T. Naito, *J. Org. Chem.*, **65**, 5043 (2000).
140. C. M. McGinley, H. A. Relyea and W. A. van der Donk, *Synlett.*, 211 (2006).
141. H. Ali Dondas, R. Grigg, J. Markandu, T. Perrior, T. Suzuki, S. Thibault, W. A. Thomas and M. Thornton-Pett, *Tetrahedron*, **58**, 161 (2002).
142. A. Hassner, R. Maurya, O. Friedman, H. E. Gottlieb, A. Padwa and D. Austin, *J. Org. Chem.*, **58**, 4539 (1993).
143. S. Yamago, M. Nakamura, X. Q. Wang, M. Yanagawa, S. Tokumitsu and E. Nakamura, *J. Org. Chem.*, **63**, 1694 (1998).
144. C. W. Holzapfel, R. Crous, H. F. Greyling and G. H. Verdoorn, *Heterocycles*, **51**, 2801 (1999).
145. D. R. Williams, J. W. Benbow, T. R. Sattleberg and D. C. Ihle, *Tetrahedron Lett.*, **42**, 8587 (2001).
146. D. I. Iljushkin, E. C. Semichenko and G. A. Suboch, *Russ. J. Org. Chem.*, **40**, 1543 (2004).
147. T. E. Khoshtariya, L. N. Kurkovskaya, L. T. Bochoidze, K. T. Batsikadze, N. T. Mirziashvili, I. G. Abesadze, M. I. Sikharulidze, V. G. Turabelidze, V. O. Ananiashvili, T. O. Dzhashi and M. G. Maisuradze, *Chem. Heterocycl. Compd.*, **41**, 208 (2005).
148. P. Polychronopoulos, P. Magiatis, A.-L. Skaltsounis, V. Myrianthopoulos, E. Mikros, A. Tarricone, A. Musacchio, S. M. Roe, L. Pearl, M. Leost, P. Greengard and L. Meijer, *J. Med. Chem.*, **47**, 935 (2004).
149. J. F. Hansen and M. L. Luther, *J. Heterocycl. Chem.*, **30**, 1163 (1993) and references cited therein.
150. J. F. Hansen and J. A. Easter, *J. Heterocycl. Chem.*, **31**, 1481 (1994).
151. B. Unterhalt, *Tetrahedron Lett.*, 1841 (1968).
152. A. A. Fadda, *Indian J. Chem., Sect. B*, **30B**, 749 (1991).
153. H. Gnichtel and H.-J. Schoenherr, *Chem. Ber.*, **99**, 618 (1966).
154. A. Shahadat, M. Longchar and R. C. Boruah, *Indian J. Chem., Sect. B*, **38B**, 125 (1999).
155. Z. E. Skryabina, Ya. V. Burgart and V. I. Saloutin, *Russ. J. Org. Chem.*, **33**, 392 (1997).
156. E. Aiello, S. Aiello, F. Mingoia, A. Bacchi, G. Pelizzi, C. Musiu, M. G. Setzu, A. Pani, P. La Colla and M. E. Marongiu, *Bioorg. Med. Chem.*, **8**, 2719 (2000).
157. T. Majid, C. R. Hopkins, B. Pedgrift and N. Collar, *Tetrahedron Lett.*, **45**, 2137 (2004).
158. Z. A. N. Al-Shamkhani and A. H. Essa, *Tetrahedron Lett.*, **48**, 5547 (2007).
159. J. Suwinski and K. Walczak, *Pol. J. Chem.*, **58**, 1077 (1984).
160. D. K. Bates, J. T. Kohrt, H. Folk and M. Xia, *Heterocycl. Commun.*, **3**, 201 (1997).
161. K. S. Gudmundsson, B. A. Johns, Z. Wang, E. M. Turner, S. H. Allen, G. A. Freeman, F. L. Boyd, Jr., C. J. Sexton, D. W. Selleseth, K. R. Moniri and K. L. Creech, *Bioorg. Med. Chem.*, **13**, 5346 (2005).
162. H. Gnichtel and B. Moeller, *Liebigs Ann. Chem.*, 1751 (1981).
163. Y. Tamura, J.-H. Kim, Y. Miki, H. Hayashi and M. Ikeda, *J. Heterocycl. Chem.*, **12**, 481 (1975).

164. Y. V. Shklyaev, V. A. Glushkov, V. V. Davidov, V. I. Sokol and V. S. Sergienko, *Mendeleev Commun.*, 36 (2000).
165. H. Cerecetto, A. Gerpe, M. Gonzalez, Y. Fernandez Sainz, O. E. Piro and E. E. Castellano, *Synthesis*, 2678 (2004).
166. S. Laufer, G. Wagner and D. Kotschenreuther, *Angew. Chem. Int. Ed.*, **41**, 2290 (2002).
167. H. Takasugi, K. Ito, S. Nishino, A. Tanaka and T. Takaya, Eur. Patent 257897; *Chem. Abstr.*, **110**, 8207h (1989).
168. S. Nakanishi, J. Nantaku and Y. Otsuji, *Chem. Lett.*, 341 (1983).
169. S. Zaman, K. Mitsuru and A. D. Abell, *Org. Lett.*, **7**, 609 (2005).
170. F. Paetzold, H. J. Niclas and H. J. Foerster, East Ger. Patent 276281; *Chem. Abstr.*, **113**, 231377w (1990).
171. L. N. Azerbaev, I. A. Poplavskaya, R. G. Kurmangalieva and S. F. Khalilova, *Chem. Heterocycl. Chem.*, **14**, 1241 (1978).
172. (a) C. Parkanyi, A. O. Abdelhamid, J. C. S. Cheng and A. S. Shawali, *J. Heterocycl. Chem.*, **21**, 1029 (1984).
(b) A. Krowczynski and L. Kozerski, *Heterocycles*, **24**, 1209 (1986).
173. J. Mayrargue, S. Labidalle, J. Randriatsoa, H. Moskowitz and M. Miocque, *J. Heterocycl. Chem.*, **21**, 1765 (1984).
174. V. A. Artyomov, A. M. Shestopalov and V. P. Litvinov, *Synthesis*, 927 (1996).
175. V. A. Artemov and A. M. Shestopalov, *Zh. Org. Khim.*, **31**, 595 (1995); *Chem. Abstr.*, **124**, 260791j (1996).
176. K. Harssnyi, M. Szentivanyi, J. Szeredi, G. Leszkovszky and C. Vertesi, Ger. Patent 2821226; *Chem. Abstr.*, **90**, 168592b (1979).
177. F. Kroehnke and W. Zecher, *Chem. Ber.*, **95**, 1128 (1962).
178. H. Moehrle and B. Grimm, *Arch. Pharm.*, **319**, 774 (1986).
179. H. Moehrle, D. Ottersbach and A. Steigel, *Pharmazie*, **47**, 403 (1992).
180. H. Goldner, G. Dietz and E. Carstens, French Patent 1367786; *Chem. Abstr.*, **62**, 575e (1965).
181. W. Pfleiderer and F. E. Kempter, *Angew. Chem., Int. Ed. Engl.*, **6**, 259 (1967).
182. H. Goldner, G. Dietz and E. Carstens, *Liebigs Ann. Chem.*, **692**, 134 (1966).
183. W. Pfleiderer and F. E. Kempter, *Chem. Ber.*, **103**, 901 (1970).
184. L. B. Volodarskii, *Khim. Geterotsikl. Soedin.*, 1299 (1973); *Chem. Abstr.*, **80**, 27129n (1974).
185. J. Perrocheau and R. Carrie, *Bull. Soc. Chim. Belg.*, **103**, 9 (1994).
186. T. Ullrich, P. Sulek, D. Binder and M. Pyerin, *Tetrahedron*, **56**, 3697 (2000).
187. A. P. Stankevicius, P. B. Terentiev, L. N. Janusiene and M. V. Vainauskas, *Chem. Heterocycl. Compd.*, **39**, 1645 (2003).
188. M. Takahashi, *Bull. Chem. Soc. Jpn.*, **43**, 2986 (1970).
189. V. Armani, C. Dell'Erba, M. Novi, G. Petrillo and C. Tavani, *Tetrahedron*, **53**, 1751 (1997) and references cited therein.
190. D. M. Patel, V. C. Desai, M. M. Patel and M. R. Patel, *J. Indian Chem. Soc.*, **64**, 342 (1987).
191. J. Perrocheau and R. Carne, *Bull. Soc. Chim. Belg.*, **102**, 749 (1993).
192. A. R. Katritzky, D. A. Monteux and D. O. Tymoshenko, *Org. Lett.*, **1**, 577 (1999).
193. M.-H. Shih, M.-Y. Yeh, M.-J. Lee and Y.-S. Su, *Synthesis*, 2877 (2004).
194. T. Sato, T. Kawagishi and N. Koyakata, Jpn. Patent 60197688 (1985); *Chem. Abstr.*, **104**, 148869b (1986).
195. E. Huntsman and J. Balsells, *Eur. J. Org. Chem.*, 3761 (2005).
196. H. J. Barnes, G. Haran, N. J. Holman and D. T. Vowles, PCT Int. WO Patent 0056733; *Chem. Abstr.*, **133**, 252454x (2000).
197. H. M. Dalloul, *Chem. Heterocycl. Compd.*, **40**, 1402 (2004).
198. A. P. Stankevicius, P. B. Terentiev, L. N. Janushene and A. A. Zhevzhikoviene, *Chem. Heterocycl. Compd.*, **39**, 1525 (2003).
199. L. A. Kayukova, I. A. Poplavskaya, E. I. Khokhlova and R. U. Nysenbaeva, *Izv. Nats. Akad. Nauk Resp. Kaz., Ser. Khim.*, 80 (1983); *Chem. Abstr.*, **123**, 33030w (1995).
200. I. V. Tselinskii, S. F. Mel'nikova and T. V. Romanova, *Russ. J. Org. Chem.*, **37**, 430 (2001) and references cited therein.
201. V. G. Andrianov, V. G. Semenikhina and A. V. Eremeev, *Chem. Heterocycl. Compd.*, **25**, 1419 (1989).

202. M.-H. Shih, M.-J. Lee and M.-Y. Yeh, *J. Chin. Chem. Soc.*, **49**, 361 (2002).
203. D. P. Curran, *Adv. Cycloaddition*, **1**, 129 (1988).
204. (a) K. B. G. Torsell, *Nitrile Oxides, Nitrones and Nitronates in Organic Synthesis*, VCH Publishers, Weinheim, 1988.
(b) C. Grundman and P. Grunanger, *The Nitrile Oxides*, Springer, Berlin, 1971.
205. K. V. Gothelf and K. A. Jorgensen, *Chem. Rev.*, **98**, 863 (1998).
206. E. Lukevics and P. Arsenyan, *Chem. Heterocycl. Compd.*, **34**, 989 (1998).
207. P. Grunanger and P. Vita-Finzi, *Isoxazoles—Part 1;* Vol. 49 of *'Chemistry of Heterocyclic Compounds'*, Wiley, New York, 1991 and references cited therein.
208. M. A. Weidner-Wells, S. A. Fraga-Spano and I. J. Turchi, *J. Org. Chem.*, **63**, 6319 (1998).
209. P. Quadrelli, M. Mella and P. Caramella, *Tetrahedron. Lett.*, **39**, 3233 (1998).
210. Y. Tokunaga, M. Ihara and K. Fukumoto, *Heterocycles*, **43**, 1771 (1996).
211. S. K. Armstrong, E. W. Collington, J. G. Knight, A. Naylor and S. Warren, *J. Chem. Soc., Perkin Trans. 1*, 1433 (1993).
212. A. N. Boa, D. A. Dawkins, A. R. Hergueta and P. R. Jenkins, *J. Chem. Soc., Perkin Trans. 1*, 953 (1994).
213. E. Malamidou-Xenikaki, X. N. Stampelos and E. Coutouli-Argyropoulou, *J. Heterocycl. Chem.*, **33**, 563 (1996).
214. N. Lohse-Fraefel and E. M. Carreira, *Org. Lett.*, **7**, 2011 (2005).
215. G. Ahmad, P. K. Mishra, P. Gupta, P. P. Yadav, P. Tiwari, A. K. Tamrakar, A. K. Srivastava and R. Maurya, *Bioorg. Med. Chem. Lett.*, **16**, 2139 (2006).
216. J. N. Kim and E. K. Ryu, *Synth. Commun.*, **20**, 1373 (1990).
217. S. J. Barrow, C. J. Easton, G. P. Savage and G. W. Simpson, *Tetrahedron Lett.*, **38**, 2175 (1997).
218. A. S. Radhakrishna, K. Sivaprakash and B. B. Singh, *Synth. Commun.*, **21**, 1625 (1991).
219. M. Giurg and M. Mlochowski, *Pol. J. Chem.*, **71**, 1093 (1997).
220. S. Tanaka, S. Kohmoto, M. Yamamoto and K. Yamada, *Nippon Kagaku Kaishi*, 420 (1992); *Chem. Abstr.*, **117**, 7859e (1992).
221. J. Kiegel, M. Poplawska, J. Jozwik, M. Kosior and J. Jurczak, *Tetrahedron Lett.*, **40**, 5605 (1999).
222. K. Bougrin, M. Lamiri and M. Soufiaoui, *Tetrahedron Lett.*, **39**, 4455 (1998).
223. B. Syassi, B. El Bakkali, G. A. Benabdellah, A. Hassikou, M. N. Dinia, M. Riviere, K. Bougrin and M. Soufiaoui, *Tetrahedron Lett.*, **40**, 7205 (1999).
224. B. Syassi, K. Bougrin and M. Soufiaoui, *Tetrahedron Lett.*, **38**, 8855 (1997).
225. B. Touaux, F. Texier-Boullet and J. Hamelin, *Heteroatom Chem.*, **9**, 351 (1998); *Chem. Abstr.*, **129**, 4600a (1998).
226. O. Moriya, H. Takenaka, M. Iyoda, Y. Urata and T. Endo, *J. Chem. Soc., Perkin Trans. 1*, 413 (1994).
227. S. Kanemasa, M. Nishiuchi, A. Kamimura and K. Hori, *J. Am. Chem. Soc.*, **116**, 2324 (1994).
228. Y. Yoshida, Y. Ukaji, S. Fujinami and K. Inomata, *Chem. Lett.*, 1023 (1998).
229. E. Lukevics, V. Dirnens, N. Pokrovska, I. Zicmane, J. Popelis and A. Kemme, *J. Organomet. Chem.*, **586**, 200 (1999).
230. E. Lukevics and P. Arsenyan, *Chem. Heterocycl. Compd.*, **34**, 502 (1998).
231. E. Lukevics, V. Dirnens, A. Kemme and J. Popelis, *J. Organomet. Chem.*, **521**, 235 (1996).
232. P. Pevarello, R. Amici, M. Colombo and M. Varasi, *J. Chem. Soc., Perkin Trans. 1*, 2151 (1993) and references cited therein.
233. H. Kai, A. Takase and M. Tomida, PCT Int. Appl. WO Patent 9816517; *Chem. Abstr.*, **128**, 321634s (1998).
234. M. E. Jung and B. T. Vu, *Tetrahedron Lett.*, **37**, 451 (1996) and references cited therein.
235. J. I. Andres, J. Alcazar, J. M. Alonso, R. M. Alvarez, J. M. Cid, A. I. De Lucas, J. Fernandez, S. Martinez, C. Nieto, J. Pastor, M. H. Bakker, I. Biesmans, L. I. Heylen and A. A. Megens, *Bioorg. Med. Chem. Lett.*, **13**, 2719 (2003).
236. M. Kambe, E. Arai, M. Suzuki, H. Tokuyama and T. Fukuyama, *Org. Lett.*, **3**, 2575 (2001).
237. T. Ishikawa, S. Ikeda, M. Ibe and S. Saito, *Tetrahedron*, **54**, 5869 (1998).
238. S.-S. P. Chou and Yu-Ju Yu, *J. Chin. Chem. Soc.*, **45**, 163 (1998).
239. A. Arnone, M. Cavicchioli, A. Donadelli and G. Resnati, *Tetrahedron: Asymmetry*, **5**, 1019 (1994).

240. P. J. Dransfield, S. Moutel, M. Shipman and V. Sik, *J. Chem. Soc., Perkin Trans. 1*, 3349 (1999).
241. M. E. Jung, *Synlett*, 843 (1999).
242. K. M. Short and C. B. Ziegler, Jr., *Tetrahedron Lett.*, **34**, 75 (1993).
243. (a) A. Alberola, J. M. Banez, L. Calvo, M. T. Rodriguez and M. C. Sanudo, *J. Heterocycl. Chem.*, **30**, 467 (1993).
(b) M. D. Mosher, L. G. Emmerich, K. S. Frost and B. Anderson, *J. Heterocycl. Chem.*, **43**, 535 (2006).
244. T. Bandiera, P. Grunanger and F. Marinone Albini, *J. Heterocycl. Chem.*, **29**, 1423 (1992) and references cited therein.
245. H. Uno, M. Kurokawa and H. Nishimura, *Chem. Pharm. Bull.*, **24**, 644 (1976).
246. N. P. Bainbridge, A. C. Currie, N. J. Cooper, J. C. Muir, D. W. Knight and J. M. Walton, *Tetrahedron Lett.*, **48**, 7782 (2007) and references cited therein.
247. T. J. Nitz, D. L. Volkots, D. J. Aldous and R. C. Oglesby, *J. Org. Chem.*, **59**, 5828 (1994).
248. C. Buron, L. El Kaim and A. Uslu, *Tetrahedron Lett.*, **38**, 8027 (1997).
249. E. Comanita, I. Popovici, G. Roman, G. Robertson and B. Comanita, *Heterocycles*, **51**, 2139 (1999) and references cited therein.
250. G. Poissonnet, *Synth. Commun.*, **27**, 3839 (1997).
251. U. R. Kalkote and D. D. Goswami, *Aust. J. Chem.*, **30**, 1847 (1977).
252. A. Camparini, S. Chimichi, F. Ponticelli and P. Tedeschi, *Heterocycles*, **19**, 1511 (1982).
253. G. Stokker, *J. Org. Chem.*, **48**, 2613 (1983).
254. P. Supsana, P. G. Tsoungas and G. Varvounis, *Tetrahedron Lett.*, **41**, 1845 (2000).
255. T. Ogamino, Y. Ishikawa and S. Nishiyama, *Heterocycles*, **61**, 73 (2003).
256. R. J. Cvetovich, J. Y. L. Chung, M. H. Kress, J. S. Amato, L. Matty, M. D. Weingarten, F.-R. Tsay, Z. Li and G. Zhou, *J. Org. Chem.*, **70**, 8560 (2005).
257. M. Mascal, N. M. Hext, R. Warmuth, J. R. Arnall-Cuiliford, M. H. Moore and J. P. Turkenburg, *J. Org. Chem.*, **64**, 8479 (1999).
258. E. Vogl, R. Bruns, O. Kretschik, H. Uhr, J. Kaulen, M. Kugler, P. Wachtler, W. Kreiss and G. Eberz, *Bioorg. Med. Chem. Lett.*, **15**, 625 (2005).
259. G. M. Shutske and K. J. Kapples, *J. Heterocycl. Chem.*, **26**, 1293 (1989).
260. S. D. Lepore and M. R. Wiley, *J. Org. Chem.*, **64**, 4547 (1999).
261. A. A. Jarrar, A. Q. Hussein and A. S. Madi, *J. Heterocycl. Chem.*, **27**, 275 (1990).
262. M. Murakata, K. Yamada and O. Hoshino, *J. Chem. Soc., Chem. Commun.*, 443 (1994).
263. V. Ya. Sosnovskikh, B. I. Usachev, A. Yu. Sizov and M. I. Kodess, *Tetrahedron Lett.*, **45**, 7351 (2004).
264. M. Tiecco, L. Testaferri, M. Tingoli and L. Bagnoli, *J. Chem. Soc., Chem. Commun.*, 235 (1995).
265. M. Tiecco, L. Testaferri, M. Tignoli, L. Bagnoli and C. Santi, *Tetrahedron*, **51**, 1277 (1995).
266. R. Grigg, M. J. Dorrity, F. Heaney, J. F. Malone, S. Rajviroongit, V. Sridharan and S. S. Surendrakumar, *Tetrahedron*, **38**, 8297 (1991).
267. R. Grigg, J. Markandu, T. Perrior, S. Surendrakumar and W. J. Warnock, *Tetrahedron*, **48**, 6929 (1992).
268. R. Grigg, T. R. Perrior, G. J. Sexton, S. Surendrakumar and T. Suzuki, *J. Chem. Soc., Chem. Commun.*, 372 (1993).
269. H. Ali Dondas, J. E. Cummins, R. Grigg and M. Thornton-Pett, *Tetrahedron*, **57**, 7951 (2001).
270. (a) J. Markandu, H. Ali Dondas, M. Fredrickson and R. Grigg, *Tetrahedron*, **53**, 13165 (1997).
(b) M. Blackwell, P. J. Dunn, A. B. Graham, R. Grigg, P. Higgison and M. Thornton-Pett, *Tetrahedron*, **58**, 7715 (2002).
(c) P. J. Dunn, A. B. Graham, R. Grigg, P. Higgison and M. Thornton-Pett, *Tetrahedron*, **58**, 7727 (2002).
271. M. Fredrickson, R. Grigg, J. Markandu and J. Redpath, *J. Chem. Soc., Chem. Commun.*, 2225 (1994).
272. D. Armesto, A. Ramos, M. J. Ortiz, W. M. Horspool, M. J. Mancheno, O. Caballero and E. P. Mayoral, *J. Chem. Soc., Perkin Trans. 1*, 1535 (1997).
273. W. M. Horspool, G. Hynd and U. Ixkes, *Tetrahedron Lett.*, **40**, 8295 (1999).
274. R. Kusurkar, L. Gadre and M. Kulkarni, *Synth.Commun.*, **24**, 635 (1994).
275. D. M. Fink and B. E. Kurys, *Tetrahedron Lett.*, **37**, 995 (1995).

276. C. Dell'Erba, M. Novi, G. Petrillo and P. Stagnaro, *J. Heterocycl. Chem.*, **31**, 861 (1994) and references cited therein.
277. (a) V. G. Nenaidenko, A. V. Sanin, O. L. Tok and E. S. Balenkova, *Chem. Heterocycl. Compd.*, **35**, 348 (1999).
(b) V. F. Snegirev and I. A. Naumenko, *Izv. Akad. Nauk, Ser. Khim.*, 1449 (1994); *Chem. Abstr.*, **122**, 187463f (1995).
278. B. A. Trofimov, E. Yu. Schmidt, A. I. Mikhaleva, A. M. Vasil'tsov, L. I. Larina and L. V. Klyba, *Mendeleev Commun.*, 238 (1999).
279. C. J. Valduga, D. B. Santis, H. S. Braibante and M. E. F. Braibante, *J. Heterocycl. Chem.*, **36**, 505 (1999).
280. A. Loupy and S. Regnier, *Tetrahedron Lett.*, **40**, 6221 (1999) and references cited therein.
281. M. B. Bagade and B. J. Ghiya, *Asian J. Chem.*, **3**, 158 (1991); *Chem. Abstr.*, **115**, 71443a (1991).
282. J. Kawachi, H. Matsubara, Y. Nakahara and H. Watanabe, Jpn. Patent 1180163 (1999); *Chem. Abstr.*, **130**, 237556b (1999).
283. K. Bougrin, A. Loupy and M. Soufiaoui, *Tetrahedron*, **54**, 8055 (1998).
284. M. Yokoyama, M. Irie, K. Sujino, T. Kagemoto, H. Togo and M. Funabashi, *J. Chem. Soc., Perkin Trans. 1*, 2127 (1992).
285. D. N. Nicolaides, R. Wajih Awad, G. K. Papageorgiou, E. Kojanni and C. A. Tsoleridis, *J. Heterocycl. Chem.*, **34**, 1651 (1997) and references cited therein.
286. A. R. Katritzky, Z. Wang, C. D. Hall, N. G. Akhmedov, A. A. Shestopalov and P. J. Steel, *J. Org. Chem.*, **68**, 9093 (2003).
287. C. A. Marques, M. Selva, P. Tundo and F. Montanari, *J. Org. Chem.*, **58**, 5765 (1993).
288. O. Miyata, H. Asai and T. Naito, *Synlett*, 1915 (1999).
289. T. Vitali, E. Gaetani, F. Ronchini, M. Nardelli and G. Pelizzi, *J. Chem. Soc., Perkin Trans. 2*, 1114 (1977) and references cited therein.
290. M. Devys and M. Barbier, *Synthesis*, 214 (1990).
291. H.-R. Kaenel, A. Wegmann and D. Neff, Eur. Patent 655446; *Chem. Abstr.*, **123**, 83358e (1995).
292. V. Nair, K. V. Radhakrishnan, A. G. Nair and M. Bhadbhade, *Tetrahedron Lett.*, **37**, 5623 (1996).
293. V. Nair, K. V. Radhakrishnan, K. C. Sheela and N. P. Rath, *Tetrahedron*, **55**, 14199 (1999).
294. V. G. Andrianov and A. V. Eremeev, *Chem. Heterocycl. Compd.*, **25**, 1197 (1989).
295. R. F. Vieira, D. J. Brondani, A. R. de Faria, R. M. Srivastava and A. C. Lima Leite, *Heterocycl. Commun.*, **5**, 521 (1999) and references cited therein.
296. C. Chen, C. H. Senanayake, T. J. Bill, R. D. Larsen, T. R. Verhoeven and P. J. Reider, *J. Org. Chem.*, **59**, 3738 (1994).
297. J. Mindl, J. Kavalek, H. Strakova and V. Šterba, *Collect. Czech. Chem. Commun.*, **64**, 1641 (1999) and references cited therein.
298. J. Jesse and H. Kanter, Ger. Patent 3905242; *Chem. Abstr.*, **114**, 81838b (1991).
299. L. A. Kayukova, K. D. Praliev, I. S. Zhumadildaeva and S. G. Klepikova, *Chem. Heterocycl. Compd.*, **35**, 630 (1999).
300. R. Mohan Srivastava, M. da Canceicao Pereira, F. Hallwass and C. R. N. Pacheco, *Heterocycles*, **51**, 2961 (1999).
301. M. D. Evans, J. Ring, A. Schoen, A. Bell, P. Edwards, D. Berthelot, R. Nicewonger and C. M. Baldino, *Tetrahedron Lett.*, **44**, 9337 (2003).
302. A. L. Braga, D. S. Ludtke, E. E. Alberto, L. Dornelles, E. A. Severo Filho, V. A. Corbellini, D. M. Rosa and R. S. Schwab, *Synthesis*, 1589 (2004).
303. Y. Wang, R. L. Miller, D. R. Sauer and S. W. Djuric, *Org. Lett.*, **7**, 925 (2005).
304. D. A. Berry, T.-C. Chien and L. B. Townsend, *Heterocycles*, **63**, 2475 (2004).
305. A. E. Moormann, J. L. Wang, K. E. Palmquist, M. A. Promo, J. S. Snyder, J. A. Scholten, M. A. Massa, J. A. Sikorski and R. K. Webber, *Tetrahedron*, **60**, 10907 (2004).
306. V. G. Andrianov, V. G. Semenikhina and A. V. Eremeev, *Chem. Heterocycl. Compd.*, **27**, 646 (1991).
307. B. Stanovnik, U. Urleb and M. Tišler, *Heterocycles*, **23**, 2819 (1985).
308. G. A. Shvekhgeimer, V. I. Shvedov, L. Dyankova, D. Stefanova and M. Nikolova, *Tr. Nauchnoissled. Khim.-Farm. Inst.*, 70 (1981); *Chem. Abstr.*, **97**, 6230z (1982).
309. M. Kmetič and B. Stanovnik, *J. Heterocycl. Chem.*, **34**, 1705 (1997).

310. J. R. Young and R. J. DeVita, *Tetrahedron Lett.*, **39**, 3931 (1998).
311. H.-C. Ryu, Y.-T. Hong and S.-K. Kang, *Heterocycles*, **54**, 985 (2001).
312. J. E. Johnson, D. Nwoko, M. Hotema, N. Sanchez, R. Alderman and V. Lynch, *J. Heterocycl. Chem.*, **33**, 1583 (1996).
313. B. Cavalleri, P. Bellani and G. Lancini, *J. Heterocycl. Chem.*, **10**, 357 (1973).
314. X. Yang, Z. Wang, X. Fang, X. Yang, F. Wu and Y. Shen, *Synthesis*, 1768 (2007).
315. N. Hebert, A. L. Hannah and S. C. Sutton, *Tetrahedron Lett.*, **40**, 8547 (1999).
316. J.-X. Xu, H.-T. Wu and S. Jin, *Chin. J. Chem.*, **17**, 84 (1999).
317. D. Enders, I. Meyer, J. Runsink and G. Raabe, *Heterocycles*, **50**, 995 (1999).
318. K. Harsanyi, C. Gonczi, G. Horvath and D. Karbonits, *Chem. Ber.*, **105**, 805 (1972).
319. D. Karbonits, E. Tobias-Heja, K. Simon and P. Kolonits, *Chem. Ber.*, **124**, 2065 (1991).
320. V. G. Andrianov and A. V. Eremeev, *Khim. Geterotsikl. Soedin.*, 1443 (1990); *Chem. Abstr.*, **114**, 164046t (1991).
321. A. B. Sheremetev, N. N. Makhova and W. Friedrichsen, *Adv. Heterocycl. Chem.*, **78**, 65 (2001).
322. V. G. Andrianov, V. G. Semenikhina and A. V. Eremeev, *Khim. Geterotsikl. Soedin.*, 969 (1992); *Chem. Abstr.*, **119**, 49310r (1993).
323. K.-J. Hwang, Y. C. Park, H. J. Kim and J. H. Lee, *Biosci. Biotechnol. Biochem.*, **62**, 1693 (1998).
324. A. B. Sheremetev and E. V. Mantseva, *Mendeleev Commun.*, 246 (1996).
325. A. B. Sheremetev, *Mendeleev Commun.*, 135 (1998).
326. I. V. Tselinski, S. F. Melnikova, S. V. Pirogov and S. D. Shaposhnikov, *Russ. J. Org. Chem.*, **36**, 758 (2000).
327. E. Biekert and H. Koessel, *Liebigs Ann. Chem.*, **662**, 93 (1963).
328. M. Curini, F. Epifano, M. C. Marcotullio, O. Rosati, R. Ballini and G. Bosica, *Tetrahedron Lett.*, **41**, 8817 (2000) and references cited therein.
329. V. Armani, C. Dell'Erba, M. Novi, G. Petrillo and C. Tavani, *Tetrahedron*, **53**, 1751 (1997) and references cited therein.
330. V. N. Yarovenko, I. V. Zavarzin and M. M. Krayushkin, *Izv. Akad. Nauk SSSR, Ser. Khim.*, 2159 (1991); *Chem. Abstr.*, **116**, 21000d (1992).
331. G. Sorba, G. Ermondi, R. Fruttero, U. Galli and A. Gasco, *J. Heterocycl. Chem.*, **33**, 327 (1996).
332. J. Brendel, H. Bohn and K. Schoenafinger, Ger. Patent 4218977; *Chem. Abstr.*, **120**, 270408w (1994).
333. Y. Kamitori, *Heterocycles*, **51**, 627 (1999).
334. N. Maugein, A. Wagner and C. Mioskowski, *J. Org. Chem.*, **64**, 8428 (1999).
335. Y. Tagawa, N. Honjo, Y. Goto and T. Kato, *Chem. Pharm. Bull.*, **34**, 4984 (1986) and references cited therein.
336. A. G. Briggs, J. Czyzewski and D. H. Reid, *J. Chem. Soc., Perkin Trans. 1*, 2340 (1979).
337. Y. Kohara, K. Kubo, E. Imamiya and T. Naka, *J. Heterocycl. Chem.*, **37**, 1419 (2000).
338. (a) E. Kawashima, Y. Ando, T. Takada and K. Tabei, *Heterocycles*, **26**, 181 (1987).
(b) A. Castro, T. Castano, A. Encinas, W. Porcal and C. Gil, *Bioorg. Med. Chem.*, **14**, 1644 (2006).
339. K. Kim and J. Cho, *Heterocycles*, **38**, 1859 (1994).
340. S. C. Yoon, J. Cho and K. Kim, *J. Chem. Soc., Perkin Trans. 1*, 109 (1998).
341. J. Cho and K. Kim, *J. Chem. Soc., Perkin Trans. 1*, 2345 (1993).
342. K.-J. Kim and K. Kim, *Tetrahedron*, **63**, 5014 (2007).
343. V. J. Aran, A. G. Bielsa, J. R. Ruiz and M. Stud, *J. Chem. Soc., Perkin Trans. 1*, 643 (1986).
344. M. J. Plater, C. W. Rees, D. G. Roe and T. Torroba, *J. Chem. Soc., Chem. Commun.*, 293 (1993).
345. Shell International Research Maatschappij B.V. Jpn. Patent 5800987 (1983); *Chem. Abstr.*, **98**, 179392c (1983).
346. S. Macho, D. Miguel, T. Gomez, T. Rodriguez and T. Torroba, *J. Org. Chem.*, **70**, 9314 (2005).
347. H. L. Yale, *J. Heterocycl. Chem.*, **8**, 205 (1971).
348. C. Uncuta, A. Tudose, M. T. Caproiu, M. Plaveti and R. Kakou-Yao, *Tetrahedron*, **55**, 15011 (1999).

349. S. E. Booth, P. R. Jenkins, C. J. Swain and J. B. Sweeney, *J. Chem. Soc., Perkin Trans. 1*, 3499 (1994).
350. S. M. Weinreb, in *Comprehensive Organic Synthesis* (Eds. B. M. Trost and I. Fleming), Vol. 5, Pergamon Presss, Oxford, 1991, pp. 401–413.
351. B.-C. Chen, *Heterocycles*, **32**, 529 (1991).
352. N. Katagiri, H. Nochi, A. Kurimoto, H. Sato and C. Kaneko, *Chem. Pharm. Bull.*, **42**, 1251 (1994).
353. A. R. Renslo and R. L. Danheiser, *J. Org. Chem.*, **63**, 7840 (1998).
354. T. Takahashi, Y. Li, T. Ito, F. Xu, K. Nakajima and Y. Liu, *J. Am. Chem. Soc.*, **124**, 1144 (2002).
355. A. M. Chibiryaev, N. De Kimpe and A. V. Tkachev, *Tetrahedron Lett.*, **41**, 8011 (2000).
356. P. Saikia, D. Prajapati and J. S. Sandhu, *Tetrahedron Lett.*, **44**, 8725 (2003).
357. M. Kitamura, M. Yoshida, T. Kikuchi and K. Narasaka, *Synthesis*, 2415 (2003).
358. T. M. Bargar, J. K. Dulworth and M. C. Graham, *J. Heterocycl. Chem.*, **21**, 261 (1984).
359. M. Asahara, C. Shibano, K. Koyama, M. Tamura, Y. Tohda, N. Nishiwaki and M. Ariga, *Tetrahedron Lett.*, **46**, 7519 (2005).
360. A. Ono and K. Narasaka, *Chem. Lett.*, 146 (2001).
361. A. Ono, K. Uchiyama, Y. Hayashi and K. Narasaka, *Chem. Lett.*, 437 (1998).
362. K. Uchiyama, Y. Hayashi and K. Narasaka, *Synlett*, 445 (1997).
363. T. Kusumi, K. Yoneda and H. Kakisawa, *Synthesis*, 221 (1979).
364. C. L. Hickson and H. McNab, *Synthesis*, 464 (1981).
365. J. Koyama, T. Sugita, Y. Suzuta and H. Irie, *Chem. Pharm. Bull.*, **31**, 2601 (1983).
366. (a) S. Hibino, E. Sugino, T. Choshi and K. Sato, *J. Chem. Soc., Perkin Trans. 1*, 2429 (1988). (b) T. Kumemura, T. Choshi, J. Yukawa, A. Hirose, J. Nabuhiro and S. Hibino, *Heterocycles*, **66**, 87 (2005).
367. R. S. Kusurkar and D. K. Bhosale, *Tetrahedron Lett.*, **32**, 3199 (1991).
368. D. L. Boger, S. Ichikawa and H. Jiang, *J. Am. Chem. Soc.*, **122**, 12169 (2000).
369. J. M. Chezal, E. Moreau, O. Chavignon, C. Lartigue, Y. Blache and J. C. Teulade, *Tetrahedron*, **59**, 5869 (2003).
370. T. Kumemura, T. Choshi, A. Hirata, M. Sera, Y. Takahashi, J. Nobuhiro and S. Hibino, *Heterocycles*, **61**, 13 (2003).
371. N. Kawabara, H. Hayashi, N. Hiramatsu, T. Choshi, T. Kamemura, J. Nobuhira and S. Hibino, *Tetrahedron*, **60**, 2943 (2004).
372. M. L. Meketa, S. M. Weinreb, Y. Nakao and N. Fusetani, *J. Org. Chem.*, **72**, 4892 (2007).
373. K. I. Kuchkova and A. A. Semenov, *Chem. Heterocycl. Compd.*, **3**, 878 (1967).
374. K. I. Kuchkova, A. A. Semenov and I. V. Terent'eva, *Chem. Heterocycl. Compd.*, **6**, 182 (1970).
375. K. I. Kuchkova, E. P. Styngach, F. Sh. Rivilis, N. M. Frolova and A. A. Semenov, *Chem. Heterocycl. Compd.*, **12**, 329 (1976).
376. T. Choshi, Y. Matsuya, M. Okita, K. Inada, E. Sugino and S. Hibino, *Tetrahedron Lett.*, **39**, 2341 (1998).
377. N. Kanekiyo, T. Choshi, T. Kuwada, E. Sugino and S. Hibino, *Heterocycles*, **53**, 1877 (2000).
378. U. C. Mashelkar and R. N. Usgaonkar, *Indian J. Chem.*, **16B**, 782 (1978).
379. R. S. Kusurkar and S. K. Goswami, *Tetrahedron*, **60**, 5315 (2004).
380. F. Sori, M. Incze, Z. Kardos-Bologh, M. Kajtar-Peredy and C. Szantay, *Arch. Pharm.*, **326**, 227 (1993).
381. S. A. Snyder, D. A. Vosburg, M. G. Jarvis and J. H. Markgraf, *Tetrahedron*, **56**, 5329 (2000).
382. D. C. Bland, B. C. Raudenbush and S. M. Weinreb, *Org. Lett.*, **2**, 4007 (2000).
383. M. Departure, D. Siri, J. Grimaldi, J. Hatem and R. Faure, *Tetrahedron Lett.*, **40**, 4547 (1999).
384. T. Sakamoto, A. Numata and Y. Kondo, *Chem. Pharm. Bull.*, **48**, 669 (2000).
385. A. Numata, Y. Kondo and T. Sakamoto, *Synthesis*, 306 (1999).
386. S. Hibino, E. Sugino, T. Kuwada, N. Ogura, K. Sato and T. Choshi, *J. Org. Chem.*, **57**, 5917 (1992).
387. S. Tu, C. Miko, Y. Gao, F. Fang, Q. Zhuang, Y. Feng and D. Shi, *Synlett*, 255 (2004).
388. L. L. Martin, S. J. Scott, M. N. Agnew and L. L. Setescak, *J. Org. Chem.*, **51**, 3697 (1986).
389. O. Tamura, A. Toyao and H. Ishibashi, *Synlett*, 1344 (2002).
390. G. E. Keck, T. T. Wager and J. Felix Duarte Rodriquez, *J. Am. Chem. Soc.*, **121**, 5176 (1999).

391. L. L. Martin, L. L. Setescak and S. J. Scott, US Patent 4742061; *Chem. Abstr.*, **110**, 114817s (1989).
392. Y. Torisawa, T. Nishi and J. Minamikawa, *Bioorg. Med. Chem.*, **11**, 2205 (2003).
393. M. Ortiz-Marciales, L. D. Rivera, M. De Jesus, S. Espinosa, J. A. Benjamin, O. E. Casanova, I. G. Figueroa, S. Rodriguez and W. Correa, *J. Org. Chem.*, **70**, 10132 (2005).
394. D. G. Hilmey and L. A. Paquette, *Org. Lett.*, **7**, 2067 (2005).
395. N. S. Mani and M. Wu, *Tetrahedron: Asymmetry*, **11**, 4687 (2000).
396. N. A. Evans, R. B. Johns and K. R. Markham, *Aust. J. Chem.*, **20**, 713 (1967).
397. T. Aiello, V. Spiro and G. Vaccaro, *Gazz. Chim. Ital.*, **59**, 2232 (1959).
398. M. Kočevar, B. Mlakar, M. Perdih, A. Petrič, S. Polank and B. Verček, *Tetrahedron Lett.*, **33**, 2195 (1992).
399. B. Mlakar, B. Štefane, M. Kočevar and S. Polanc, *Tetrahedron*, **54**, 4387 (1998).
400. M. Ferrara, B. Crescenzi, M. Donghi, E. Muraglia, E. Nizi, S. Pesci, V. Summa and C. Gardelli, *Tetrahedron Lett.*, **48**, 8379 (2007).
401. Y.-L. Zhong, H. Zhou, D. R. Gauthier, Jr. and D. Askin, *Tetrahedron Lett.*, **47**, 1315 (2006) and references cited therein.
402. M. Akazome, T. Kondo and Y. Watanabe, *J. Mol. Catal.*, **80**, 383 (1993).
403. M. Mazik and W. Zielinski, *Monatsh. Chem.*, **127**, 1161 (1996).
404. T. Tsuritani, H. Shinokubo and K. Oshima, *Chem. Lett.*, **32**, 122 (2004).
405. H. Kakiya, K. Yagi, H. Shinokubo and K. Oshima, *J. Am. Chem. Soc.*, **124**, 9032 (2002).
406. T. Higashino, Y. Iwai and E. Hayashi, *Chem. Pharm. Bull.*, **24**, 3120 (1976).
407. J. Lessel, *Arch. Pharm. (Weinheim)*, **328**, 397 (1995).
408. S. Ostrowski, *Heterocycles*, **43**, 399 (1996).
409. H. Goncalves, M. Bon, J. Barrans and C. Foulcher, *C. R. Acad. Sci.*, **274**, 1750 (1972).
410. J. Fortea, *J. Prakt. Chem.*, **317**, 705 (1975)
411. H. Goncalves, C. Foulcher and F. Mathis, *Bull. Soc. Chim. Fr.*, 2615 (1970).
412. D. Karbonits, E. Tobias-Heja and P. Kolonits, *Chem. Ber.*, **124**, 1199 (1991) and references cited therein.
413. D. D. Nekrasov, V. G. Chizh and Yu. S. Andreichikov, *Russ. J. Org. Chem.*, **36**, 263 (2000) and references cited therein.
414. J. B. Neilsen, H. S. Broadbent and W. J. Hennen, *J. Heterocycl. Chem.*, **24**, 1621 (1987).
415. T. Itoh, K. Maeda, T. Wada, K. Tomimoto and T. Mase, *Tetrahedron Lett.*, **43**, 9287 (2002) and references cited therein.
416. K. Matoba, H. Tone, K. Shinhama, F. Goto, M. Saka and J. Minamikawa, *J. Synth. Org. Chem. Jpn.*, **57**, 401 (1999) and references cited therein.
417. K. Shinhama, K. Matoba, Y. Torisawa and J. Minamikawa, *Tetrahedron*, **56**, 7427 (2000).
418. (a) J. Meisenheimer, O. Senn and P. Zimmer, *Chem. Ber.*, **60**, 1736 (1927).
(b) A. Monge, J. A. Palop, J. I. Recalde and E. Fernandez-Alvarez, *An. Quim., Ser. C*, **85**, 72 (1989); *Chem. Abstr.*, **112**, 216880r (1990).
419. V. N. Kozhevnikov, D. N. Kozhevnikov, T. V. Nikitina, V. L. Rusinov, O. N. Chupakhin, M. Zabel and B. Konig, *J. Org. Chem.*, **68**, 2882 (2003).
420. BASF A.-G. Belg. Patent 843299; *Chem. Abstr.*, **87**, 135421e (1977).
421. Y. Kurasawa, Y. Okamoto and A. Takada, *J. Heterocycl. Chem.*, **22**, 1715 (1985).
422. G. Kaugars and W. Watt, *J. Heterocycl. Chem.*, **30**, 497 (1993).
423. A. Kocak and O. Bekaroglu, *Helv. Chim. Acta*, **67**, 1503 (1984).
424. H.-U. Reissig, C. Hippeli and T. Arnold, *Chem. Ber.*, **123**, 2403 (1990).
425. C. Hippeli and H.-U. Reissig, *Liebigs Ann. Chem.*, 217 (1990).
426. S. Tanimoto, H. Matsumoto, M. Hojo and A. Toshimitsu, *J. Chem. Soc., Perkin Trans. 1*, 3153 (1991).
427. K. Paulini, H.-U. Reissig and P. Rademacher, *J. Prakt. Chem./Chem.-Ztg.*, **337**, 209 (1995).
428. (a) A. Tahdi, S. Lafquish Titouani and M. Soufiaoui, *Tetrahedron*, **54**, 65 (1998) and references cited therein.
(b) T. L. Gilchrist, W. Stretch and E. J. T. Chrystal, *J. Chem. Soc., Perkin Trans. 1*, 2235 (1987).
429. T. L. Gilchrist and A. Lemos, *J. Chem. Soc., Perkin Trans. 1*, 1391 (1993).
430. T. J. Gilchrist and T. G. Roberts, *J. Chem. Soc., Chem. Commun.*, 847 (1978).
431. R. A. Al-Qawasmeh, T. H. Al-Tel, R. J. Abdel-Jalil and W. Voelter, *Chem. Lett.*, 541 (1999).
432. U. Albrecht, K. Gerwien and P. Langer, *Tetrahedron Lett.*, **46**, 1017 (2005).

433. M. R. Iesce, F. Cermola and A. Guitto, *Synlett*, 417 (1999).
434. H. Kai and T. Nakai, *Tetrahedron Lett.*, **42**, 6895 (2001).
435. C. F. Hennion and J. L. O'Brien, *J. Am. Chem. Soc.*, **71**, 2933 (1949).
436. M. Goubert, L. Toupet, M.-E. Sinibaldi and I. Canet, *Tetrahedron*, **63**, 8255 (2007).
437. M. S. Singh and A. K. Singh, *Synthesis*, 837 (2004).
438. T. Sasaki and T. Yoshioka, *Bull. Chem. Soc. Jpn.*, **42**, 556 (1969).
439. H. Miao, V. Cecchetti, O. Tabarrini and A. Fravolini, *J. Heterocycl. Chem.*, **37**, 297 (2000).
440. G. N. Everson and R. B. Moffett, *J. Heterocycl. Chem.*, **17**, 351 (1980).
441. S. D. Shaposhnikov, T. V. Romanova, N. P. Spiridonova, S. F. Mel'nikova and I. V. Tselinskii, *Russ. J. Org. Chem.*, **40**, 894 (2004) and references cited therein.
442. K.-J. Kim, H.-S. Lee and K. Kim, *J. Heterocycl. Chem.*, **33**, 295 (1996).
443. W. Johnson, A. Faux and G. Fallon, *Heterocycles*, **51**, 2479 (1999).
444. M. J. Mphahlele and T. A. Mondo, *J. Chem. Res. (S)*, 198 (1998) and references cited therein.
445. F. Cavani and F. Trifiro, *Appl. Catal. A. General*, **88**, 15 (1992).
446. K. Narasaka, H. Kusama, Y. Yamashita and H. Sato, *Chem. Lett.*, 489 (1993).
447. O. Kitagawa, M. Fujita, M. Okada and T. Taguchi, *Chem. Pharm. Bull.*, **45**, 32 (1997).
448. R. X. Ren, L. D. Zueva and W. Ou, *Tetrahedron Lett.*, **42**, 8441 (2001).
449. J. Peng and Y. Deng, *Tetrahedron Lett.*, **42**, 403 (2001).
450. T.-S. Lin, S.-J. Tsai and S. Cheng, *J. Chin. Chem. Soc.*, **46**, 779 (1999).
451. H. M. Meshram, *Synth. Commun.*, **20**, 3253 (1990).
452. A. I. Boosch, P. de la Cruz, E. Diez-Barra, A. Loupy and F. Langa, *Synlett*, 1259 (1995).
453. H. Tsuji and T. Setoyama, *Chem. Lett.*, **34**, 1232 (2005).
454. Y. Ikushima, K. Hatakeda, O. Sato, T. Yokoyama and M. Arai, *J. Am. Chem. Soc.*, **122**, 1908 (2000).
455. T. Yokamatsu, Y. Yoshida, N. Nakabayashi and S. Shibuya, *J. Org. Chem.*, **59**, 7562 (1994).
456. H. Cho, K. Murakami, H. Nakanishi, H. Isoshima, K. Hayakawa and I. Uchida, *Heterocycles*, **48**, 919 (1998).
457. L. Yet, *Tetrahedron*, **55**, 9349 (1999).
458. H. Miyabe, M. Torieda, T. Kiguchi and T. Naito, *Synlett*, 580 (1997).
459. T. Naito, K. Tajiri, T. Harimoto, I. Ninomiya and T. Kiguchi, *Tetrahedron Lett.*, **35**, 2205 (1994).
460. M. Noguchi, T. Mizukoshi, T. Uchida and Y. Kuroki, *Tetrahedron*, **52**, 13097 (1996).
461. A. P. Stoll and F. Troxler, *Helv. Chim. Acta*, **51**, 1864 (1968).
462. R. W. L. Kimber and J. C. Parham, *J. Org. Chem.*, **28**, 3205 (1963).
463. A. Levai, G. Toth, J. Halasz, T. Timar, L. Frank and S. Hosztafi, *Heterocycles*, **38**, 305 (1994).
464. N. W. Nand, T. Beghyn, G. Nowogrocki, J.-C. Gesquiere and B. Deprez, *Tetrahedron Lett.*, **45**, 1051 (2004).
465. P. Scheiber and P. Nemes, *Heterocycles*, **41**, 2189 (1995).
466. D. Pappo, S. Shimony and Y. Kashman, *J. Org. Chem.*, **70**, 199 (2005).
467. N. W. Notzel, K. Rauch, T. Labahn and A. De Meijere, *Org. Lett.*, **4**, 839 (2002).

CHAPTER 8

Electrophilic *C*-amination with *O*-substituted hydroxylamines, oximes and *O*-substituted oximes

ENDER ERDIK

Ankara University Science Faculty, Department of Chemistry, Beşevler, Ankara 06100, Turkey
Fax: +90 312 223 23 95; e-mail: erdik@science.ankara.edu.tr

The chemistry of hydroxylamines, oximes and hydroxamic acids
Edited by Z. Rappoport and J. F. Liebman

I. INTRODUCTION

Electrophilic amination is an important reaction in which an electrophilic nitrogen atom (R_2N^+) carried out by an amination reagent (R^1R^2N-L) is transferred to all kinds of nucleophiles (Nu^-) (equation 1). The leaving group L^- is displaced by the nucleophile in the amination reaction.

$$Nu^- + R_2N-L \longrightarrow Nu-NR_2 + L^- \quad (1)$$

This methodology is also an important and potentially valuable method for C−N bond formation using the amination of carbon nucleophiles with electrophilic nitrogen transfer reagents (Scheme 1)[1–8]. Amination of ordinary carbanions and α-carbanion derived from carbonyl compounds and nitriles provides an important method for the synthesis of amines[9,10] and α-amino carbonyl compounds and nitriles[11], respectively. For this purpose, a number of electrophilic amination reagents, which are synthetic equivalents of the R_2N^+ synthon, have been developed and the synthetic potential of electrophilic amination of carbon nucleophiles has been studied in detail[4,7].

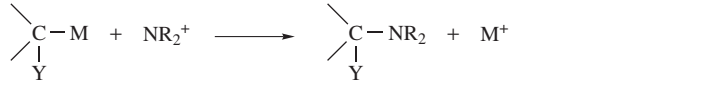

M = Li, Na, K, Mg, Ca
B, Cu, Zn
R = H, organyl

Amine
(Y = R^1)
α-Amino carbonyl compounds and nitriles
(Y = COX (X = H, R^1, OH, OR^1, $NR^1{}_2$), CN)

SCHEME 1

Due to the synthetic and biological importance of amines and α-aminoketones, acids and esters, the introduction of amino functionality into carbon nucleophiles provides a convenient and practical route for their synthesis[8–10]. In addition, a number of electrophilic amination methodologies have been developed for the asymmetric synthesis of amines and α-aminocarbonyl compounds[7–9,11].

Amines are generally prepared by nucleophilic amination, which is a coupling of carbon electrophiles with a nucleophilic amination reagent, NR_2^-, and Ni and Pd catalyzed reaction of aryl halides with arylamines (Hartwig–Buchwald amination)[9]. Thus, the direct C−N bond formation between carbon nucleophiles and electrophilic nitrogen functionality R_2N^+ constitutes an example of the umpolung methodology.

Electrophilic amination reagents (Scheme 2) contain an sp^3 nitrogen, sp^2 nitrogen or sp nitrogen which will be transferred to carbon nucleophiles. sp^3-Nitrogen-containing reagents are *O*-substituted hydroxylamines **1**–**5** such as *O*-organylhydroxylamines **1**, *O*-acylhydroxylamines **2**, *O*-sulfonylhydroxylamines **3**, *O*-phosphinylhydroxylamines **4** and *O*-silylhydroxylamines **5** and oxaziridines **6**. sp^2-Nitrogen-containing reagents are *O*-sulfonyloximes **7**, azides **8** and dialkyl azodicarboxylates **9** and sp-nitrogen containing reagent is arenediazonium salt **10**.

O-Substituted hydroxylamines **1**–**5** ($R^1 = R^2 = H$) and their *N*-mono- or *N*,*N*-disubstituted derivatives **1**–**5** have been used extensively for electrophilic amination of both carbanions and enolates since the first report in 1938[12] on the use of *O*-methylhydroxylamine **1** (R = Me) for conversion of Grignard reagents to primary amines. Oximes **7** (Z = H) have found limited applicability as amination reagents for carbon nucleophiles and their use was first reported in 1907[13]. Ketone *O*-sulfonyloximes **7** ($Z = SO_2R$) have recently been developed.

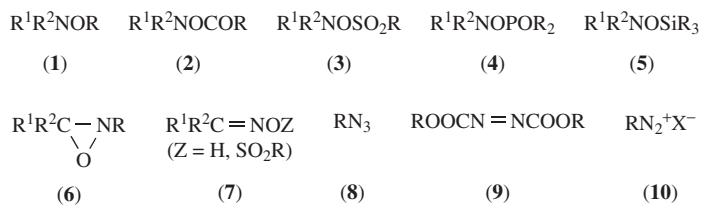

SCHEME 2

This chapter on electrophilic amination using *O*-substituted hydroxylamines **1**–**5** and oximes **7** is focused on the various methods that have been reported for the amination of carbon nucleophiles. Synthetic aspects and applications of the methods for C−N bond formation are accompanied by a brief discussion of the reaction mechanisms. The preparation of *O*-substituted hydroxylamines and oximes has not been considered in detail. This review covers the literature up to August 2007 and is partly based on reviews on the electrophilic amination of carbanions[4] and α-amination of carbonyl compounds[7].

The chapter has been arranged from an amination reagent and method-based division to a carbon nucleophile-based subdivision. As carbon nucleophiles, ordinary carbanions and α-metallated carbonyl compounds have been discussed. For each amination reagent, amination methods for Group 1, 2, 11, 12 and 13 organometallic compounds (ordinary carbanions derived from organolithium, -sodium, -potassium, -magnesium, -copper and -zinc reagents and organoboron compounds) as well as amination methods for α-carbanions derived from carbonyl compounds and nitriles have been reviewed. Asymmetric versions of these methods have been also included in each subdivision. Following the synthetic information for the amination methods using each type of reagent, a short description of the amination mechanisms has been given.

II. ELECTROPHILIC *C*-AMINATION WITH *O*-SUBSTITUTED HYDROXYLAMINES

There are quite a large number of reported methods on the amination of carbon nucleophiles with *O*-substituted hydroxylamines **1**–**5** ($R^1 = R^2 = H$) and their *N*-mono- and *N*,*N*-disubstituted derivatives **1**–**5**. Amination of Group 1, 2, 11 and 12 organometallic compounds and α-metallated carbonyl compounds with these reagents takes place by a direct introduction of the $R_1R_2N^+$ group to carbanions and enolates and for completion the reactions require only hydrolytic work-up (Scheme 3).

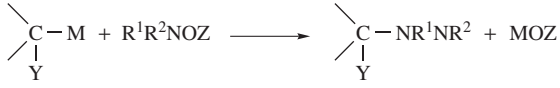

Y = R, COX (X = H, R, OH, OR, NR_2), CN
M = Li, Na, K, Mg, B, Cu, Zn
Z = R (**1**), COR (**2**), SO_2R (**3**), POR_2 (**4**), SiR_3 (**5**)

SCHEME 3

The amination of organoboranes with H_2NOZ-type reagents involves initial nucleophilic attack of NH_2OZ on the organoborane to yield an organoborate complex followed

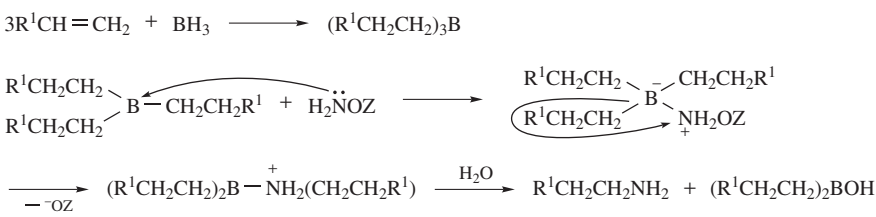

SCHEME 4

by 1,2-migration of an organyl anion from boron to the electrophilic nitrogen with concurrent loss of the OZ group (Scheme 4)[14].

The conversion of alkenes to amines has a considerable synthetic value and hydroboration–amination methodology has been applied using different protocols. However, only two of the three organyl groups can be aminated because of the low reactivity of $RB(NHR)_2$ towards electrophilic nitrogen (equation 2).

$$R_3B \xrightarrow[2.\ H_2O]{1.\ H_2NOZ} R_2B(NHR) \xrightarrow[2.\ H_2O]{1.\ H_2NOZ} RB(NHR)_2 \xrightarrow{H_2NOZ} \not\rightarrow B(NHR)_3 \quad (2)$$

In order to solve this problem, mixed organoboranes $R_T(R_R)_2B$ were used, in which the R_T transferable group reacts but R_R residual groups do not react due to their limited transfer ability[14]. Organodimethylboranes, RMe_2B, are useful reagents for this purpose, since (i) a methyl group is one of the most used R_R groups as it is inexpensive[15–17], and (ii) organodimethylboranes can be easily prepared by addition of dimethylborane to alkenes (equation 3)[10–21].

$$R^1CH{=}CH_2 + Me_2BH \longrightarrow R^1CH_2CH_2BMe_2 \xrightarrow[2.\ H_2O]{1.\ H_2NOZ} R^1CH_2CH_2NH_2 \quad (3)$$

A number of protocols have been reported for the amination of organoboranes and have been reviewed in detail[9].

A. *O*-Organylhydroxylamines

O-Alkyl- and *O*-arylhydroxylamines and their *N*-substituted derivatives have been the most extensively used reagents for amination of C-nucleophiles (Table 1). *O*-Methyl hydroxylamine **1a** is the most extensively used *O*-organylhydroxylamine-type reagent.

Several methods have been reported for the synthesis of *O*-alkylhydroxylamines[22–24]. *O*-Methylhydroxylamine **1a** can be prepared by a one-step procedure[23] or can be obtained from its commercially available hydrochloride salt[25,26]. Methods for the preparation of *O*-(nitrophenyl) hydroxylamines have been reviewed[27]. They are stable and commercially available.

1. Amination of Group 1, 2, 11, 12 and 13 organometallic reagents

The use of an *O*-organylhydroxylamine-type reagent for conversion of organometallic reagents to amines was first reported by Schverdina and Kotscheschkow in 1938[12]. They found that alkyl and aryl Grignard reagents react with *O*-methylhydroxylamine **1a** in a 2:1 molar ratio in diethyl ether at −15 °C and, after hydrolysis, primary amines are obtained in good yields. Brown and Jones[28] also used **1a** for synthesis of primary amines from organylmagnesium bromides (Scheme 5).

TABLE 1. *O*-Organylhydroxylamine-type electrophilic amination reagents

R^1R^2NOR
(**1a–l**)

1	R^1	R^2	R	**1**	R^1	R^2	R
1a	H	H	Me	**1g**	H	H	Ph
1b	H	H	Et	**1h**	H	H	$C_6H_3(NO_2)_2$-2,4
1c	H	H	Pr-*i*	**1i**	H	Me	Me
1d	H	H	Bu-*t*	**1j**	H	CHMePh	Me
1e	H	H	CH_2Ph	**1k**	Me	Me	Me
1f	H	H	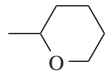	**1l**	H	Cl	$C_6H_3(NO_2)_2$-2,4

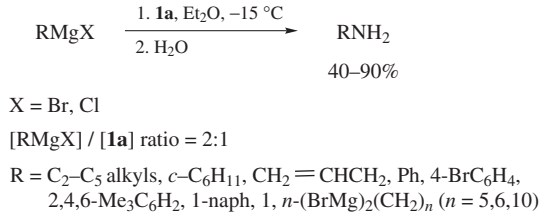

SCHEME 5

Gilman and coworkers prepared amino derivatives of some heterocyclic compounds such as 1- and 4-aminodibenzofurans[29,30], 4-aminodibenzothiophene[31], 1-aminothianthrene[32,33] and 2-aminothianthrene[34] with good yields using 3, 2 or 1 equivalent of corresponding organolithiums and 1 equivalent of the amination reagent **1a**.

Low-yield amination of lithioferrocene with **1a** was also reported[35].

Reaction of a homoallylic Grignard reagent with **1a** resulted in formation of the expected amine as well as the amination product of the rearranged Grignard reagent[36].

The problem in the amination of RM (M = Li, MgBr) with *O*-methylhydroxylamine **1a** is the requirement of 3 equivalents of RM for 1 equivalent of **1a**, i.e. 2 equivalents are consumed for the deprotonation of amino hydrogens and 1 equivalent is used in the amination reaction. Schverdina and Kotscheschkow[12] and Brown and Jones[28] used 2:1 molar ratio of RM: **1a** for the amination of Grignard reagents whereas 3, 2 or 1 equivalent of RLi were used by Gilman in the amination of organolithiums[29–34]. These results are in accordance with the reports on the protodemetallation of RMgBr and RLi reagents, since Grignard reagents are known to abstract one hydrogen atom of the NH_2 group while organolithiums can abstract both hydrogen atoms depending on the reaction conditions[37a]. For solution of this problem, treatment of **1a** with an expandable organolithium reagent at a low temperature in a 2:1 molar ratio before treating with the organolithium reagent to be aminated, was tried as suggested by Wakefield[37b]. Erdik found that maximum amination yield of phenylmagnesium bromide or phenyllithium could be obtained using 3:1 molar ratio of PhM to **1a**[38]. However, using *n*-butyllithium for protodemetallation before amination of either phenyllithium or phenylmagnesium bromide resulted in quite low yields[38].

Beak and coworkers[25] generated *N*-lithio derivative of *O*-methylhydroxylamine **1a** by treating 2 equivalents of methyllithium with 2 equivalents of **1a** in ether at −78 °C for the

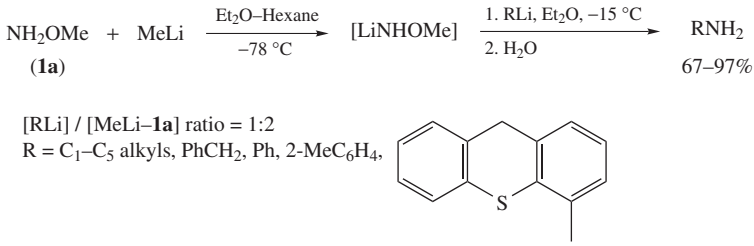

SCHEME 6

amination of 1 equivalent of an organolithium reagent at −15 °C (Scheme 6). Better yields of arylamines compared to alkylamines were obtained by amination of organolithiums, but amination of Grignard reagents gave much lower yields than those of organolithiums.

Successful use of *O*-methylhydroxylamine **1a** for the amination of organozinc reagents has been reported by Erdik and Daşkapan[39,40]. Organozinc reagents provide an important carbanion source due to their high reactivity, easy preparation by Li−or Mg−to Zn transmetallation, and tolerance of electrophilic functional groups. Diorganozincs and bromomagnesium triorganozincates have been shown to react with **1a** in the presence of CuCN catalyst under mild conditions to give primary amines in good yields (Scheme 7). Considering the Li− or Mg− to Zn transmetallation, this method also provides a one-flask method for converting organolithiums and Grignard reagents to primary amines[40].

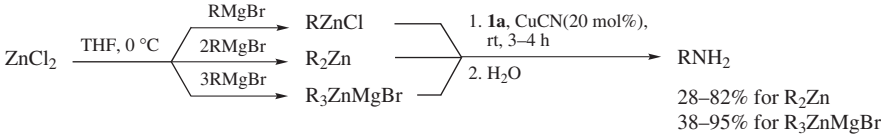

[RM] / [**1a**] ratio = 1.5:1
R = Ph, XC_6H_4 (X = 4-Me, 4-MeO, 4-Br), *n*-C_6H_{13}, *c*-C_6H_{11}, $PhCH_2$

SCHEME 7

The only reported example of the use of *O*-phenylhydroxylamine **1g** for electrophilic amination of carbanions is the conversion of phenylmagnesium bromide into aniline[41].

For the synthesis of secondary amines, Beak, Basha and Kokko used *N*-alkyl-*O*-methylhydroxylamines **1i** and **1j**. The method of treating 1 equivalent of amination reagent with 1 equivalent of methyllithium, followed by reaction with 1 equivalent of organolithium to be aminated, was found more effective than reacting 1 equivalent of amination reagent with 2 equivalents of the organolithium (Scheme 8)[42].

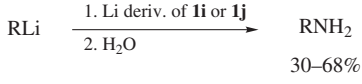

[RLi] / [Li deriv. of **1i** or **1j**] ratio = 1:1
R = C_1–C_4 alkyls, Ph, $PhCH_2$

SCHEME 8

Amination of phenyllithium with *N*,*N*,*O*-trimethylhydroxylamine **1k** did not lead to the formation of the expected tertiary amine; instead *N*-methylbenzylamine was isolated (equation 4).

$$\underset{}{\text{PhLi}} + \underset{(\mathbf{1k})}{\text{Me}_2\text{NOMe}} \xrightarrow[\text{Et}_2\text{O}]{} \underset{52\%}{\text{PhCH}_2\text{NHMe}} \tag{4}$$

In summary, amination of organolithiums, Grignard reagents and diorganozincs with *O*-methylhydroxylamine **1a** using at least a 2:1 molar ratio of RM to **1a** provides a potentially synthetic methodology for the synthesis of primary amines. For the amination of organolithium and Grignard reagents which are expensive or difficult to prepare, treating 2 equivalents of *O*-methylhydroxylamine **1a** with 2 equivalents of methyllithium before the introduction of the *N*-lithiated **1a** to 1 equivalent of carbanion is an advantageous application of the C−N coupling using *O*-methylhydroxylamine **1a**.

Mechanistic investigations on the amination of carbanions using *O*-organylhydroxylamines are limited. Beak and coworkers carried out a series of detailed mechanistic studies of the amination of organolithiums[26,43] with *O*-alkylhydroxylamines and their *N*-substituted derivatives. They found supporting evidence for the initial deprotonation of H_2NOR- and NHR^1OR-type reagents, followed by substitution involving the transition state of an S_N2-type mechanism (Scheme 9). A trigonal bipyramidal transition state for the displacement of oxygen by a carbon nucleophile from neutral and anionic nitrogen was proposed[44,45].

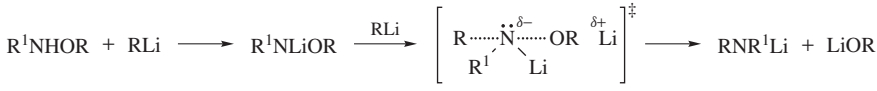

SCHEME 9

Theoretical studies also supported the reaction mechanism of *N*-lithium derivatives of NH_2OR- and NHR^1OR-type reagents with organolithiums[44,46,47]. Erdik also provided experimental evidence for the reaction of *N*-lithium and *N*,*N*-dilithium derivatives of NH_2OMe **1a** by trapping these intermediates with electrophiles[38].

Erdik and coworkers[48] reported competitive kinetic studies and analysis of rate data by the Hammett relationship for the amination of substituted phenylmagnesium bromides, bromomagnesium diphenylcuprates and CuCN-catalyzed diphenylzincs with NH_2OMe **1a**. They also proposed S_N2 mechanisms for these aminations of RMgBr reagents. Amination of $R_2CuMgBr$ or catalytic RCu(CN)ZnCl reagents can take place by a rate-determining addition of the *N*-metallated derivative of **1a** to the cuprate to give the Cu(III) intermediate, followed by reductive elimination of the intermediate to the *N*-metallated amine. The other product is RCu in the amination of $R_2CuMgBr$ whereas the other product is CuCN in the amination of RZnCl in the presence of CuCN as a catalyst (Scheme 10).

2. Amination of α-metallated carbonyl compounds and nitriles

For the synthesis of α-aminocarbonyl compounds, a number of *O*-organylhydroxylamine-type reagents have been used. Several *O*-alkylhydroxylamines **1a**–**e** were screened for amination of α-lithiated carboxylic acids (Scheme 11)[49,50]. However, the yields are

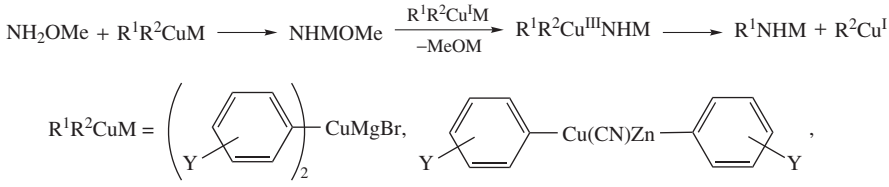

Y = H, 3-Me, 4-Me, 3-MeO, 4-MeO, 3-Br, 4-Br

SCHEME 10

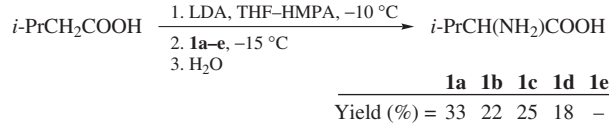

	1a	1b	1c	1d	1e
Yield (%) =	33	22	25	18	–

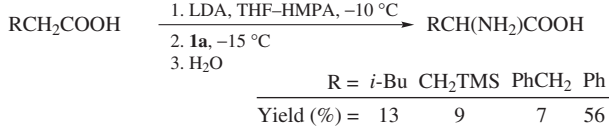

R =	*i*-Bu	CH_2TMS	$PhCH_2$	Ph
Yield (%) =	13	9	7	56

SCHEME 11

low, except in the amination of α-lithiophenylacetic acid with **1a** (Scheme 11). It was observed that the electron-releasing character of the *O*-alkyl groups decreased the amination yield, as expected.

For conversion of α-lithiophenylacetic acid to α-phenylglycine, the use of *O*-2-tetrahydropyranylhydroxylamine **1f** was also tried (equation 5)[49,50].

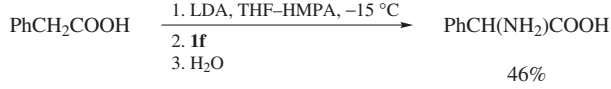

(5)

Amination of α-lithiated derivatives of *t*-butyl acetate and α-phenylacetamide with **1a** were reported to be unsuccessful. However, α-amino derivatives of *N*-mono- and *N*,*N*-disubstituted carboxamides could be prepared by reaction of their α-lithiated derivatives with **1a** (Scheme 12)[34,51].

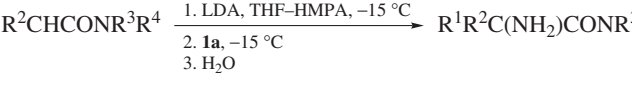

R^1, R^2 = Ph, H; $PhCH_2$, H; Ph, Ph
R^3, R^4 = H, *n*-Bu; H, *c*-C_6C_{11}; H, Ph; Et, Et; *n*-Bu, *n*-Bu

SCHEME 12

The use of 2,4-dinitrophenylhydroxylamine (DPH) **1h** as an amination reagent for α-metallated methyl 9-fluorenecarboxylate and diethyl α-phenylmalonate (equation 6a and b) was reported by Sheradsky and coworkers[52,53].

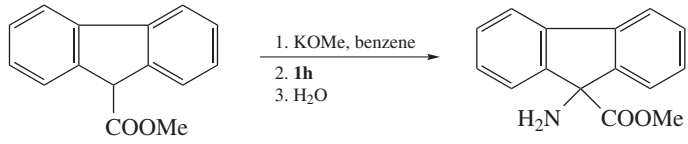

(6a)

$$PhCH(COOEt)_2 \xrightarrow[2.\ \mathbf{1h}\ 3.\ H_2O]{1.\ NaH,\ DMF} PhC(NH_2)(COOEt)_2 \qquad (6b)$$

Radhakrishna and coworkers showed that DPH **1h** reacts with sodium enolates of substituted diethyl malonates to afford α-amino carboxylic acids in good yields (Scheme 13)[54].

$$RCH(COOEt)_2 \xrightarrow[2.\ \mathbf{1h},\ rt,\ 12\ h]{1.\ NaH,\ THF} RC(NH_2)(COOEt)_2 \xrightarrow[Heat]{H_2O} RCH(NH_2)COOH$$

46–84%

R = C_1–C_3 alkyls, $PhCH_2$, Et, CH_2COOEt

SCHEME 13

This strategy also provides a convenient method for amination of various ester enolates with DPH **1h** (Scheme 14). The amination of lithium eniminate of phenyl acetonitrile, the silyl enolate of ethyl phenylacetate and the Reformatsky reagent derived from ethyl α-bromoacetate with DPH were found to be unsuccessful. A failure of DPH for the amination of sodium enolates of β-diketones and the lithium enolate of 3-methylbutanoic acid was also reported[50].

$$R^1R^2CHCOOEt \xrightarrow[2.\ \mathbf{1h}\ 3.\ H_2O]{1.\ Base} R^1R^2C(NH_2)COOH$$

12–65%

Base = NaH, *c*-C_6C_{11}NHPr-*i*

R^1, R^2 = H, Ph; Me, Ph; H, COOEt; Ph, COOEt; Ph, CN

SCHEME 14

Radhakrishna and coworkers also found a direct substitution on the electrophilic nitrogen of enolates in their reaction with DPH[54].

B. *O*-Acylhydroxylamines

N-Mono- and *N*,*N*-disubstituted *O*-benzoylhydroxylamines **2a**–**i** recently developed for amination of organozinc and Grignard reagents and *O*-acylhydroxylamines **2j**–**l** for amination of enolates have been listed in Table 2. *O*-Benzoylhydroxylamines were prepared by Berman and Johnson[55–59] by oxidation of primary and secondary amines with

TABLE 2. *O*-Acylhydroxylamine-type electrophilic amination reagents

$R^1R^2NOCOPh$
(**2a–i**)

2	R^1R^2N	**2**	R^1R^2N
2a	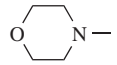	**2e**	$(CH_2{=}CHCH_2)_2N-$
2b	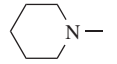	**2f**	$(PhCH_2)_2N-$
2c	Et_2N-	**2g**	*s*-BuNH−
		2h	*i*-BuNH−
2d	*i*-Pr_2N-	**2i**	(*t*-$BuCH_2CMe_2$)NH−

NH_2OCOR
(**2j–l**)

R = 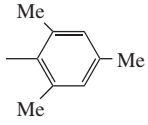 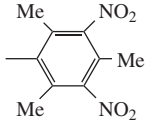 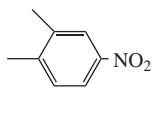

2j **2k** **2l**

benzoyl peroxide and an inorganic base, as originally reported by Biloski and Ganem[60]. Methods for the preparation of *O*-acylhydroxylamines have been reviewed[27]. These compounds are crystalline solids and show good stability.

1. Amination of Group 1, 2, 11 and 12 organometallic reagents

Johnson and Berman used *O*-benzoylhydroxylamine-type reagents for amination of diorganozincs[55,56,58,59], organozinc halides[55,57] and Grignard reagents. They developed general and efficient protocols for high-yield preparation of secondary and tertiary amines under mild reaction conditions. They first reported $Cu(OTf)_2$-catalyzed amination of simple and functionalized diorganozincs[56,58] with *N*,*N*-disubstituted *O*-benzoylhydroxylamines, e.g. *N*-benzoyloxymorpholine **2a**, *N*-benzoyloxypiperidine **2b**, *N*,*N*-dibenzyl *O*-benzoylhydroxylamine **2f** and *N*,*N*-diethyl *O*-benzoylhydroxylamine **2c**, for the preparation of tertiary amines (Schemes 15 and 16). Simple diorganozincs were prepared by transmetallation of the corresponding organolithiums or Grignard reagents[55,56] and functionalized diarylzincs were prepared by transmetallation of functionalized arylmagnesium halides derived by I/Mg exchange using Knochel's procedure[56,58].

$$2RM \xrightarrow[THF,\ rt]{ZnCl_2} R_2Zn \xrightarrow[THF,\ rt,\ 15\text{–}60\ min]{\textbf{2a-c}, \textbf{2f}, Cu(OTf)_2{\cdot}C_6H_6(1.25\ mol\%)} RNR^1R^2$$

M = Li, MgBr
R = C_2–C_4 alkyls, $PhCH_2$, Ph, 2-MeC_6H_4, 4-$MeOC_6H_4$, 2-pyr

SCHEME 15

Other Cu salts, such as CuI and $CuCl_2$, were also tried in the $Cu(OTf)_2$-catalyzed amination of simple and functionalized diorganozincs and identical yields were obtained[55,56,58].

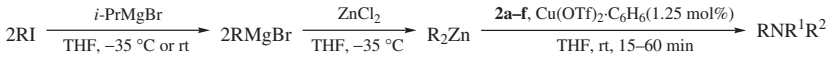

R = XC_6H_4 (X = 2-NO_2, 4-MeO, 4-Cl, 4-F, 4-CF_3, 4-AcO, 4-TfO, 4-EtOOC, 4-CN, 4-CMe  , 2,4-$(NO_2)_2C_6H_3$, 2-pyr, 1-naph

SCHEME 16

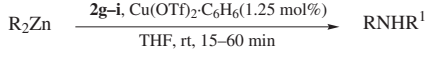

R =	Ph	*n*-Bu
Yield (%) =	71–80	43 (with **2i**)

SCHEME 17

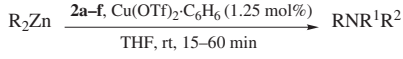

R = C_2–C_4 alkyls, $PhCH_2$, Ph, 2-MeC_6H_4, 4-$MeOC_6H_4$, 2,4,6-$Me_3C_6H_2$, 2-pyr

SCHEME 18

The authors screened a number of *N*-monosubstituted *O*-benzoylhydroxylamines **2g**–**i** and *N*,*N*-disubstituted *O*-benzoylhydroxylamines **2a**–**f** as amination reagents for diorganozincs, and these reagents were found to couple with simple and functionalized diorganozincs in the presence of Cu salts to provide secondary amines (Scheme 17) and tertiary amines (Scheme 18), respectively[58].

For conversion of functionalized diorganozincs into tertiary amines, aromatic compounds which contain a directed metallation group, such as *N*,*N*-dialkylbenzamides, methoxymethyl phenyl ether, phenyl oxazolines and phenyl *N*,*N*-dialkylcarbamates, were ortho-lithiated, transmetallated and then aminated with **2a** in good yields, but with a slower reaction rate (Scheme 19).

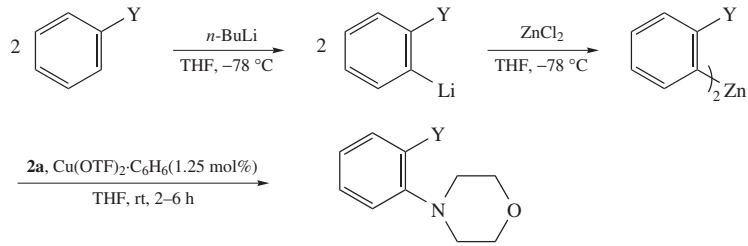

Y = $CONPh_2$, CH_2OMe, 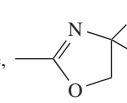 , $OCONEt_2$

SCHEME 19

As outlined, electrophilic amination of diorganozincs with *N*-mono- and *N*,*N*-disubstituted *O*-benzoylhydroxylamines is a general procedure and an easy route for the preparation of secondary and tertiary amines from diorganozincs.

The synthesis of 4-phenylmorpholine by Cu-catalyzed amination of diphenylzinc with *N*-benzoyloxymorpholine **2a** has been also presented as an Organic Synthesis procedure[59].

Berman and Johnson observed that amination of phenylzinc halide and *n*-butylzinc chloride with *N*-benzoyloxymorpholine **2a** and *N*,*N*-dibenzyl *O*-benzoyl hydroxylamine **2f**, respectively, under Cu catalysis was not effective (equation 7)[55].

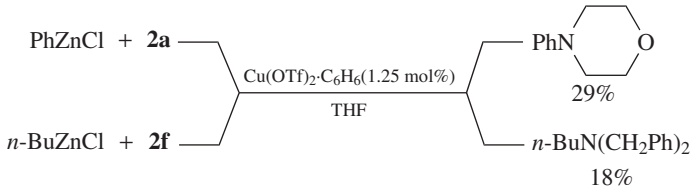

(7)

They tried Ni catalysts with chelating amine and phosphine ligands in the reaction of phenylzinc bromide with *N*-benzoyloxymorpholine **2a** and observed that in the presence of $NiCl_2(PPh_3)_2$, *n*-alkyl, aryl and functionalized arylzinc chlorides can be aminated with *N*,*N*-disubstituted *O*-benzoylhydroxylamines in good yields (Schemes 20 and 21). Attempted amination of secondary and tertiary alkylzinc chlorides failed to yield the expected product.

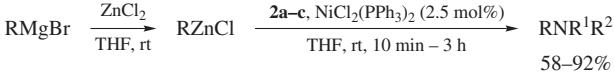

R = *n*-C_8H_{17}, $PhCH_2$, Ph, 2-MeC_6H_4, 4-$MeOC_6H_4$

SCHEME 20

R = XC_6H_4 (X = 3-CF_3, 4-Cl, 4-EtOOC, 4-CN) 56–84%

SCHEME 21

Berman and Johnson also tested Cu-catalyzed amination of a catalytic organozinc reagent[58]. As Mg → Zn → Cu transmetallation and resulting amination occurs faster than C-acylation of Grignard reagents, good yields of the aminated product were obtained when CuOTf and $ZnCl_2$ were used as catalysts in the amination of the Grignard (equation 8).

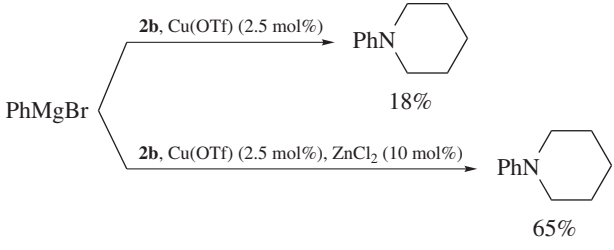

(8)

Recently, Campbell and Johnson also reported that amination of Grignard reagents take place with high yields in the presence of $CuCl_2$ catalyst and Mg → Zn → Cu transmetallation using stoichiometric or catalytic amounts of copper salts can be eliminated (Scheme 22)[61]. The yields of tertiary amines are moderate to excellent depending on the type of the amination reagent, the Grignard reagent and also the catalyst amount. However, amination of phenylmagnesium bromide with *N*-*s*-butyl-*O*-benzoylhydroxylamine **2g** to obtain a secondary amine was not successful. The authors also observed that *N*,*N*- disubstituted *O*-acylhydroxylamines containing large acyl groups such as mesitoyl $COC_6H_2Me_3$-2,4,6 and pivaloyl COBu-*t* can aminate phenylmagnesium bromide with 85% and 54% yields, respectively, without Cu catalysis.

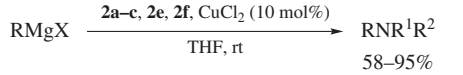

R = C_2–C_4 alkyls, *c*-C_6H_{11}, $PhCH_2$, Ph,
XC_6H_4 (X = 2-Me, 4-F, 4-MeO), 2,4,6-$Me_3C_6H_2$

SCHEME 22

Campbell and Johnson offered an S_N2 mechanism for the Cu(I)-catalyzed amination of diorganozinc reagents with *N*,*N*-disubstituted *O*-benzoylhydroxylamines, showing that the configuration at the nucleophilic carbon is retained in the C−N coupling[61].

2. Amination of α-metallated carbonyl compounds and nitriles

The use of *O*-acylhydroxylamine-type reagents for amination of α-metallated carbonyl compounds is limited. The use of *O*-mesitoylhydroxylamine **2j** or *O*-(3,5-dinitromesitoyl) hydroxylamine **2k** in the amination of the enolate derived from 3-methylbutanoic acid was unsuccessful[50].

Recently, Smulik and Vedejs have reported that amination of ester enolates and eniminates with *O*-(*p*-nitrobenzoyl)hydroxylamine **2l** takes place with good yields[62]. However, reaction of enolates derived from ethyl phenylacetate and phenylacetonitrile gave lower yields compared with stabilized enolates derived from diethyl malonate, diethyl 2-phenylmalonate and 2-phenyl-2-cyanopropionate (Scheme 23).

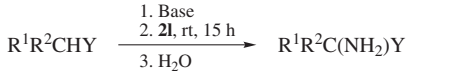

Base = NaH, at rt; KOBu-*t*, at −78 °C
R^1, R^2, Y = H, COOEt, COOEt; Ph, COOEt, COOEt;
Ph, CN, COOEt; Ph, Ph, CN

SCHEME 23

C. *O*-Sulfonylhydroxylamines

A list of *N*-mono- and *N*,*N*-disubstituted *O*-sulfonylhydroxylamines used for amination of ordinary carbanions and enolates are given in Table 3. Except for **3h** and **3p,** they are *O*-(arenesulfonyl)hydroxylamines and their *N*-substituted derivatives. Methods for the syntheses of various *O*-(arenesulfonyl)hydroxylamines have been reported[63–65]

TABLE 3. *O*-Sulfonylhydroxylamine-type electrophilic amination reagents

$R^1R^2NOSO_2R$
(**3a**–**p**)

3	R^1	R^2	SO_2R	**3**	R^1	R^2	SO_2R
3a[a]	H	H	SO_2Mes[b]	**3i**	H	Boc[d]	SO_2Mes[b]
3b	Me	Me	SO_2Mes[b]	**3j**	H	Alloc[e]	SO_2Mes[b]
3c	Et	Et	SO_2Mes[b]	**3k**	H	COOEt	*p*-Tos[c]
3d	Me	Me	SO_2Ph	**3l**[f]	H	Boc	*p*-Tos[c]
3e	Et	Et	SO_2Ph	**3m**	H	Alloc	*p*-Tos[c]
3f	Me	Me	*p*-Tos[c]	**3n**	H	COOEt	SO_2-$C_6H_4NO_2$-4
3g	$PhCH_2$	$PhCH_2$	*p*-Tos[c]	**3o**	H	Boc	SO_2-Py-2
3h	Me	Me	SO_2Me	**3p**[g]	H	H	SO_2OH

[a] Abbreviated name: MSH(*O*-Mesitylenesulfonyl)hydroxylamine.
[b] Mesitylenesulfonyl: $SO_2C_6H_2Me_3$-2,4,6.
[c] *p*-Tosyl: $SO_2C_6H_4Me$-*p*.
[d] *t*-Butoxycarbonyl: COOBu-*t*.
[e] Allyloxycarbonyl: $COOCH_2CH{=}CH_2$.
[f] Abbreviated name for $R^1 = Li$ derivative: LiBTOC (*N*–lithio *t*-butyl *N*-(tosyloxy) carbamate [*N*-lithio *N*-(*t*-butoxycarbonyl) *O*-tosylhydroxylamine].
[g] Abbreviated name: HOSA (Hydroxylamine *O*-sulfonic acid).

and reviewed[27]. *O*-(Mesitylenesulfonyl) hydroxylamine (MSH) **3a** can be stored below 0 °C for a month without change; however, its preparation prior to use is strongly recommended[66]. *N*,*N*-Dialkyl *O*-(arenesulfonyl)hydroxylamines can be stored in a refrigerator for several weeks[67].

N-(Alkoxycarbonyl) *O*-(arenesulfonyl)hydroxylamines [alkyl *N*-(arenesulfonyloxy) carbamates] **3i**–**o**[68,69] can be easily obtained by sulfonylation of commercially available *N*-(alkoxycarbonyl)hydroxylamines (alkyl *N*-hydroxy carbamates). *N*-(Alkoxycarbonyl) hydroxylamines can be also prepared from hydroxylamine and alkyl chloroformate[70,71].

In order to eliminate the requirement of using at least 2 equivalents of RM (M = Li, MgBr) in their amination with the reagents **3i**–**o**, e.g. 1 equivalent for the deprotonation of amino hydrogen and 1 equivalent for the amination reaction, *N*-metallated derivatives of **3i**–**o** have been used. The lithium derivative of **3l**, e.g. *N*-lithio *N*-(*t*-butoxycarbonyl) *O*-*p*-tosylhydroxylamine (*N*-lithio *t*-butyl *N*-tosyloxycarbamate), is also known as LiBTOC.

Boche and coworkers crystallized the lithium derivative of **3i**, e.g. *N*-lithio *N*-(*t*-butoxycarbonyl) *O*-(mesitylenesulfonyl)hydroxylamine[71].

Hydroxylamine *O*-sulfonic acid **3p** has found wide application in the nonsymmetric and asymmetric amination of organoboron compounds and its use as an amination reagent has been well reviewed[9].

1. Amination of Group 1, 2, 11, 12 and 13 organometallic reagents

Boche and coworkers have reported amination of organolithium and Grignard reagents with *N*,*N*-dialkyl-*O*-(arenesulfonyl) hydroxylamines **3b**–**c** (Scheme 24)[67].

In the amination of phenyl-and cycloexylmagnesium bromides, **3f** was also used and yields of 54% and 14%, respectively, were obtained[72].

The method for the introduction of NR^1R^2 groups to organolithium reagents was used in the preparation of 10-(diethylamino)-5,10-dihydroindene [1,2-*b*]indole (equation 9)[73] and

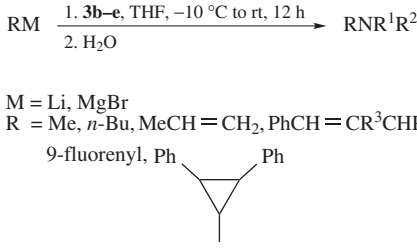

SCHEME 24

N,*N*-dimethyl-1,3-cyclopentadienylamine (equation 10)[74] using **3c** and **3h** as amination reagents, respectively.

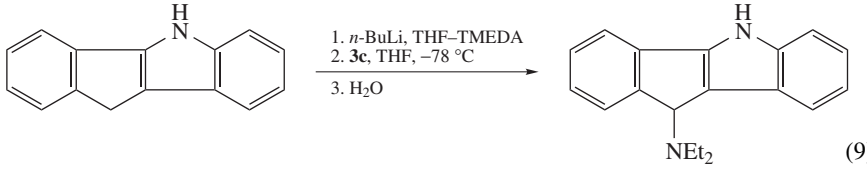

Boche and coworkers also reported that coupling of 1-alkynyl carbanions with *N*,*N*-dialkylamino groups could be achieved in preparing higher-order lithium 1-alkynylcuprates and they used **3h** as the amination reagent (Scheme 25)[75].

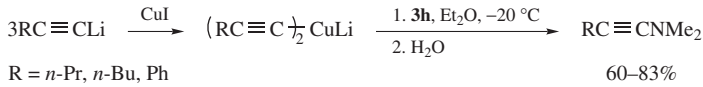

SCHEME 25

The use of *N*,*N*-dibenzyl *O*-*p*-tosylhydroxylamine **3g** for amination of organolithiums by Sheradsky and Itzhak did not give the expected product, but elimination took place leading to formation of the Schiff base (equation 11)[76]. Following hydrolytic work-up, benzaldehyde and benzylamine were obtained.

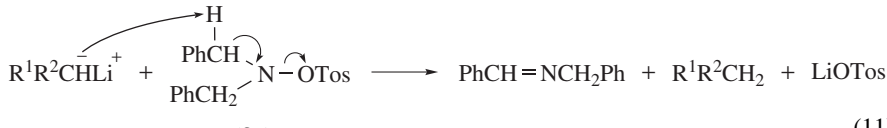

Erdik and Ateş have reported a synthesis of *N*,*N*-dimethylamines via a Barbier–Grignard-type electrophilic amination using *N*,*N*-dimethyl *O*-(mesitylenesulfonyl)hydroxylamine **3b** as amination reagent[77]. The amination of *in situ* prepared Grignard reagents, e.g. reaction of aryl bromides with Mg in the presence of **3b** at room temperature (Scheme 26), gave good yields of *N*,*N*-dimethylanilines, which were not lower than those obtained by using preformed Grignard reagents. However, amination of *in situ* benzylmagnesium bromide gave medium yield; but amination of *n*-hexylmagnesium bromide was found to be unsuccessful.

$$\mathrm{RBr} + \mathrm{Mg} + \underset{(\mathbf{3b})}{\mathrm{Me_2NOMes}} \xrightarrow[\text{rt, 2 h}]{\text{THF}} \underset{54\text{–}83\%}{\mathrm{RNMe_2}}$$

R = *n*-C_6H_{13}, Ph, XC_6H_4, (X = 2-Me, 3-Me, 3-MeO, 4-Me, 4-MeO)

SCHEME 26

N-Metal derivatives of *N*-(alkoxycarbonyl) *O*-(arenesulfonyl)hydroxylamines alkyl *N*-metal *N*-(arenesulfonyloxy)carbamates **3j**, **3l** and **3m** have been used for amination of organolithiums[69,78], organocoppers and diorganocuprates[69]. Amination reagents were first treated with *n*-butyllithium, ethylmagnesium bromide or potassium hexamethyldisilazane, and *N*-metallated reagents were used to prepare *N*-Boc [N(COOBu-*t*)][69,78] or *N*-Alloc [$N(COOCH_2CH{=}CH_2)$] protected primary amines (Scheme 27).

$$\underset{(\mathbf{3f},\ \mathbf{3l}\ \text{or}\ \mathbf{3m})}{\mathrm{NH(COOR^1)OSO_2R^2}} \xrightarrow[\text{THF}]{\text{Base}} \mathrm{M^+N^-(COOR^1)OSO_2R^2}$$

Base = *n*-BuLi, EtMgBr, LiHMDS

$$\mathrm{RM} + \mathrm{Li^+N^-(COOR^1)OSO_2R^2} \xrightarrow[-78\ ^\circ\mathrm{C}]{\text{THF}} \xrightarrow{H_2O} \mathrm{RNH(COOR^1)}$$

3	R	M	Yield (%)	Reference
3l	C_1–C_4 alkyls	Li	42–71	69, 78
	Ph, XC_6H_4 (2-MeO, 4-F)	Cu	50–73	69, 78
	2-pyr, 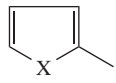 (X = O, S)			
3j, 3m	Ph, XC_6H_4 (X = 2-F, 4-Me, 4-MeO), 1-naph	Cu	38–68	70

SCHEME 27

N-Lithium and *N*-potassium derivatives of *N*-Boc *O*-*p*-tosylhydroxylamines have been also reported to react rapidly with organoboranes to give *N*-Boc protected primary amines in modest to good yields (Scheme 28)[79].

$$\mathrm{R_3B} \xrightarrow[2.\ H_2O]{\text{1. N-Li or N-K deriv. of } \mathbf{3l}} \underset{36\text{–}81\%}{\mathrm{RNHBoc}}$$

R = *n*-Bu, *s*-Bu, *n*-C_8H_{17}, *c*-C_6H_{11}

SCHEME 28

Recently, a direct kinetic study on the amination of substituted phenylmagnesium bromides using *N*,*N*-dimethyl *O*-mesitylenesulfonyl hydroxylamine **3b** as amination reagent has been reported by Erdik and Ateş Ülkü[80]. Rate data, the Hammett relationship and activation entropy support an S_N2 displacement of the carbon nucleophile on the electrophilic nitrogen. These results are consistent with the competition kinetics for electrophilic amination of substituted phenyl Grignard reagents with *O*-methylhydroxylamine **1a**[48].

There are a number of reports on the nonsymmetric and symmetric amination of organoboranes and boronic esters with hydroxylamine *O*-sulfonic acid (HOSA) **3p**[9].

The reaction of organodimethylboranes with HOSA gave quantitative yield of primary amines (Scheme 29)[14].

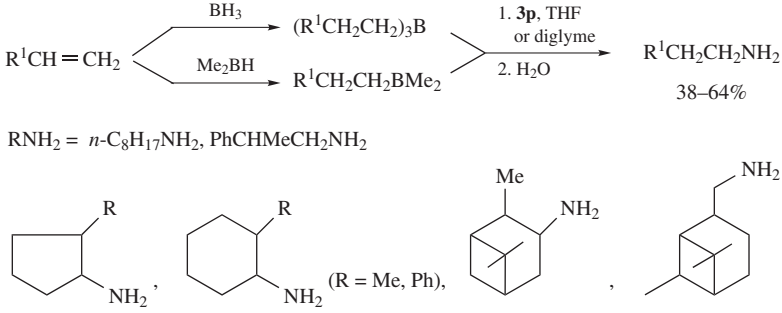

SCHEME 29

Triphenylborane prepared from phenylmagnesium bromide and boron trifluoride etherate also reacted with HOSA, but gave a low yield of aniline (equation 12)[81].

$$3PhMgBr \xrightarrow[Et_2O]{BF_3\cdot Et_2O} Ph_3B \xrightarrow[2.\ H_2O]{1.\ \mathbf{3p},\ Et_2O} PhNH_2 \quad (35\%) \qquad (12)$$

Stereoselective synthesis of primary amines have been successful using chiral boranes and boronic esters. As the 1,2-migration of the organyl group from boron to nitrogen in the organoborate complex (Scheme 4) takes place with complete retention of configuration, chiral primary amines were prepared from chiral boranes R^*BH_2, R^*_2BH or R^*_2BMe or boronate esters $R^*B(OR)_2$ with high enantiomeric excess. The preparation and use of chiral boranes[82] and boronate esters[83] in asymmetric synthesis have been reviewed by Brown and coworkers and by Matteson, respectively.

Hydroboration–amination methodology affords chiral amines from chiral mono- or diorganoboranes and HOSA in high yields and enantiomeric purity (Scheme 30)[14,8].

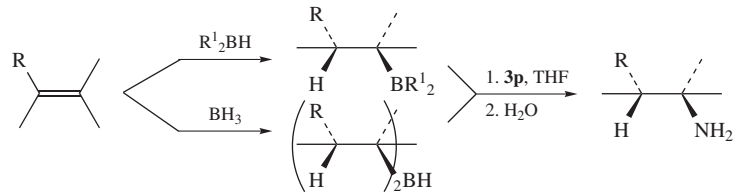

SCHEME 30

Chiral boronate esters can be converted to chiral amines through the intermediate formation of organyl methyl borinate esters (Scheme 31). Reaction of an alkene with a chiral monoorganoborane gives a diorganoborane, which is reduced with acetaldehyde to the chiral boronate ester and regenerates the chiral alkene. Chiral boronate esters are converted to more reactive chiral organylmethyl borinate esters, which are reacted with HOSA to obtain primary amines. The yields and enantiomeric excess of chiral amines are very high[84–86].

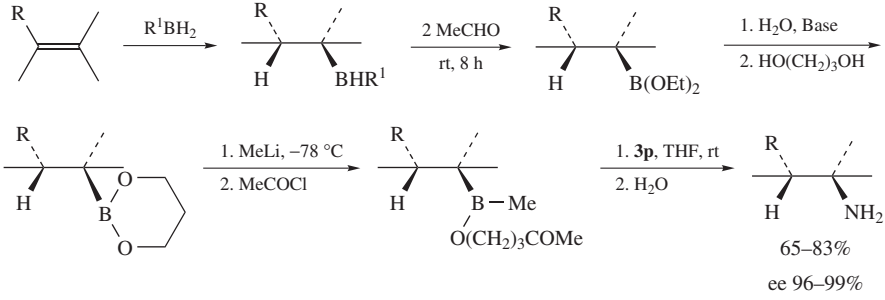

R = $MeCHR^1$ (R^1 = Et, *i*-Pr, *t*-Bu, CH_2Ph, *c*-C_6C_{11}, Ph)

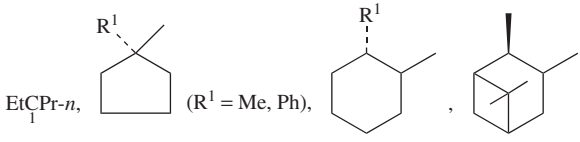

SCHEME 31

Recently, chiral diorganomethylboranes have been prepared and aminated with HOSA in high yields and high enantiomeric excess by Brown and coworkers (Scheme 32)[87,88]. Hydroboration with $BH_2Cl{\bullet}Me_2S$ produces chiral diorganochloroboranes, which are reacted with trimethylaluminum reagents or methyl magnesium bromide to obtain chiral diorganomethylboranes.

As an alternative to the stoichiometric enantioselective hydroboration, catalytic hydroboration using chiral catalysts has been also developed for enantioselective hydroboration[89,90]. The catalytic hydroboration–amination methodology has been successfully applied as a one-pot reaction for the asymmetric synthesis of primary amines[91].

2. Amination of α-metallated carbonyl compounds and nitriles

There are a few reports on the amination of α-metallated carbonyl compounds with *O*-(arenesulfonyl)hydroxylamine-type reagents. However, in recent years there has been substantial progress in *N*-(alkoxycarbonyl) *O*-(arenesulfonyl)hydroxylamine [alkyl *N*-(arenesulfonyloxy)carbamate]-type reagents for the amination of enolates and eniminates.

O-(Mesitylenesulfonyl)hydroxylamine **3a** has been used in the amination of sodium derivative of malononitrile and ammoniomalononitrile tosylate was obtained with a medium yield (equation 13)[66].

$$NaCH(CN)_2 \xrightarrow[\text{2. TosOH}]{\text{1. 3a, THF, 0 °C}} H_3N^+CH(CN)_2{}^-OTos \qquad (13)$$

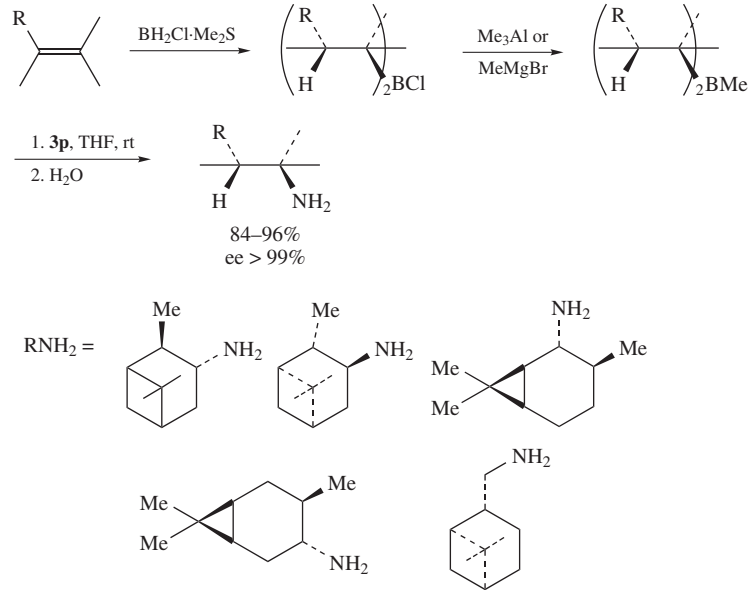

SCHEME 32

Methyl diethylphosphonoacetate was also α-aminated by treating its sodium salt with **3a** (equation 14).

$$(EtO)_2P(=O)CHNaCOOMe \xrightarrow[2.\ H_2O]{1.\ \mathbf{3a},\ THF,\ rt} (EtO)_2(P=O)CH(NH_2)COOMe \quad 39–47\% \qquad (14)$$

A high yield could be achieved in the amination of ethyl phenylcyanoacetate with *N*,*N*-dimethyl *O*-(mesitylenesulfonyl)hydroxylamine **3b** (equation 15)[67].

$$PhCH(CN)COOEt \xrightarrow[3.\ H_2O]{1.\ n\text{-BuLi};\ 2.\ \mathbf{3b},\ THF,\ -10\ ^\circ C} PhC(NMe_2)(CN)COOEt \quad 95\% \qquad (15)$$

N-Metal derivatives of *N*-(alkoxycarbonyl) *O*-(arenesulfonyl)hydroxylamines, [alkyl *N*-metal *N*-(arenesulfonyloxy)carbamates] **3i–o** have been used in the amination of α-metallated carbonyl compounds to give *N*-Boc [N(COOBu-*t*)] or *N*-Alloc [N(COOCH$_2$CH=CH)] protected α-aminocarbonyl compounds.

Among the early attempts of amination of lithium and copper enolates were those which involved formation of α-*N*-(Boc)- or *N*-(Alloc)amino-substituted carboxylic esters, *N*-acyloxazolidinones and diethyl phosphonates (Scheme 33)[70,78]. α-Lithum or α-copper derivatives of these enolates were aminated using *N*-lithium derivatives of *N*-Alloc *O*-(mesitylenesulfonyl)hydroxylamine **3j**, NHBocOTos **3l** and NHAllocOTos **3m**.

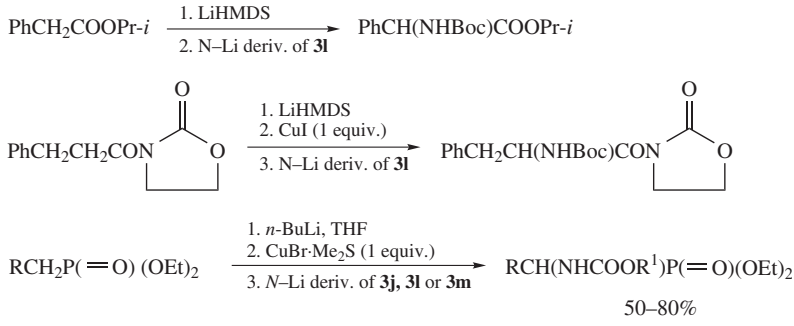

SCHEME 33

Pellacani, Tardella and coworkers recently developed an interesting set of protocols for α-amination of carbonyl compounds using *N*-(alkoxycarbonyl) *O*-(arenesulfonyl) hydroxylamines **3k**, **3l** and **3n** and obtained α-*N*-Boc amino- and α-*N*-(ethoxycarbonyl)amino-carbonyl compounds in medium yields. They reported that synthesis of α-amino β-oxoesters can be achieved by reacting **3n** with β-enaminoesters. Treating ethyl 2-butynoate with pyrrolidine gives β-enaminoester and its reaction with **3n** in the presence of an inorganic or organic base produces α-monoaminated[92, 93] and also α-bisaminated products (Scheme 34)[94]. However, in the absence of a base the amination takes place with a higher yield, implying that the base in this case is either the pyrrolidine present in trace amounts or formed as a product in the reaction medium, or the substrate itself.

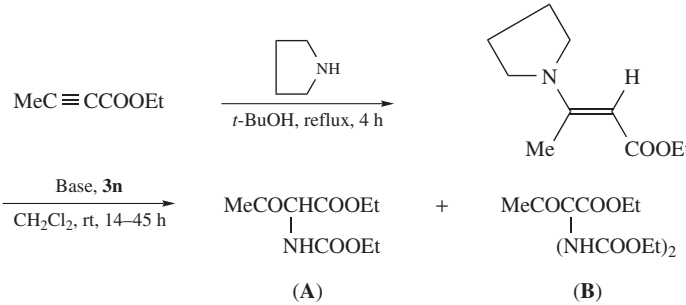

Base	Yields(%) A	B
Et_3N	18	5
CaO	26	8
—	40	–

SCHEME 34

The formation of ethoxycarbonylnitrene from the anion of *N*-(ethoxycarbonyl) *O*-(*p*-nitrobenzenesulfonyl)hydroxylamine **3n** by elimination of *p*-nitrobenzenesulfonate was already reported (equation 16)[95].

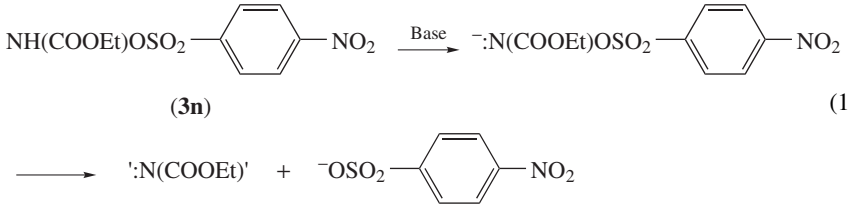

In the amination of β-enaminoesters with **3n**, aziridination was considered as a possible pathway which might transform ethoxycarbonylnitrene 'N(COOEt)' to the olefinic double bond (equation 17)[93,96].

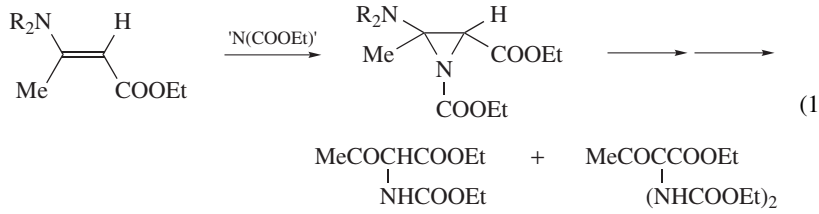

The same group expanded their study to see how well nitrenes derived from *N*-(alkoxycarbonyl) *O*-(arenesulfonyl)hydroxylamines **3i**–**o** perform in α-amination of α,β-unsaturated carbonyl compounds by aziridination. Good results are obtained when α,β-unsaturated carboxylates[97,98] and γ-lactones[99] are reacted with the amination reagents **3k**, **3l** and **3n** in the presence of CaO.

Similar investigations were reported by this group using β-oxoesters as the precursors to be aminated products in the presence of CaO and **3n** as amination reagent[100]. Ethyl acetoacetate gave α-monoaminated and α-bisaminated products (Scheme 35) depending on the substrate:base ratio. An *N*-aminated product was also obtained in the amination of ethyl α-methylacetoacetate.

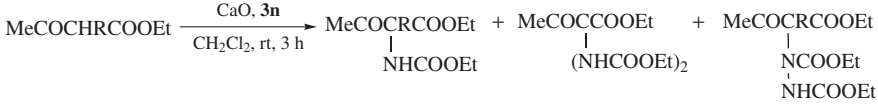

R	Molar ratio of substrate:CaO:**3n**	Yields (%) **A**	**B**	**C**
H	1:3:1	4	41	–
H	1:2:1	58	8	–
Me	1:6:2	42	–	14
Me	1:6:6	22	–	43

(**A**) (**B**) (**C**)

SCHEME 35

Barani, Fioravanti, Pellacani and Tardella also compared the reactivities of **3k** and **3n** in their reaction with trimethylsilyl enol ether of cylohexanone in the presence of an inorganic base (Scheme 36)[101]. The use of triethylamine as a base yielded no aminated product.

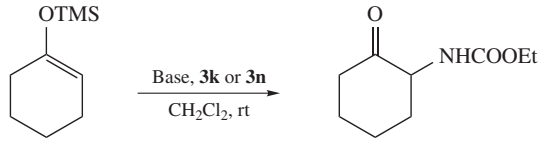

3	Base	Reaction time (h)	Yield (%)
3k	Cs_2CO_3	24	51
3n	CaO	3.5	67

SCHEME 36

N-Boc-*O*-(2-pyridinesulfonyl)hydroxylamine **3o** also reacts with the α-sodium salts of β-dicarbonyl compounds such as malonates, β-ketoesters, α-(alkoxycarbonyl)cycloalkanones, α-(alkoxycarbonyl)lactones and β-ketosulfones, but the reaction gives α-(*t*-butoxyaminocarbonyl)-substituted carbonyl compounds instead of their expected α-*N*-Boc amino derivatives (Scheme 37)[102]. The use of Lewis bases (HMPA, TMEDA) or Lewis acids (LiCl or LiBr) as additives, lithium and potassium enolates as substrates and **3l** as amination reagent decreased the yield. The outcome of the reaction of α-metallated β-dicarbonyl compounds with **3o** and **3l** was rationalized by proposing that the mechanism is a Lossen-type rearrangement.

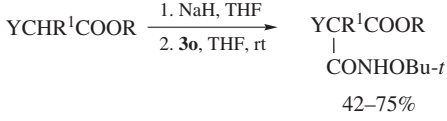

Y = MeCO, R^2OOC, $PhSO_2$
R, R^1, R^2 = C_1–C_4 alkyls, $CH_2{=}CHCH_2$

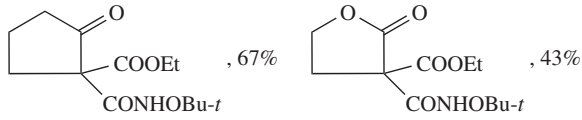

SCHEME 37

For stereoselective synthesis of α-aminocarbonyl compounds, a number of protocols have been reported using chiral enolates and *N*-(alkoxycarbonyl)-*O*-(arenesulfonyl) hydroxylamines.

Chiral carboxyamides derived from acid chlorides and *N*-chiral *cis*-aminoindanol can be protonated and Li $\rightarrow$ Cu transmetallated to generate copper enolates which react with *N*-lithium derivative of *N*-Boc-*O*-tosylhydroxylamine (LiBTOC) **3l** to give α-*N*-Boc amino carboxamides in high yields and enantiomeric excess (Scheme 38)[103]. The chiral auxiliary can be removed by acidic hydrolysis to obtain the α-aminocarboxylic acid.

Tardella's group have developed effective protocols for preparation of chiral α-aminocarbonyl compounds using α-*N*-(ethoxycarbonyl) *O*-(*p*-nitrobenzenesulfonyl)hydroxylamine **3n** in the presence or absence of a base[100]. A chiral β-ketocarboxamide carrying

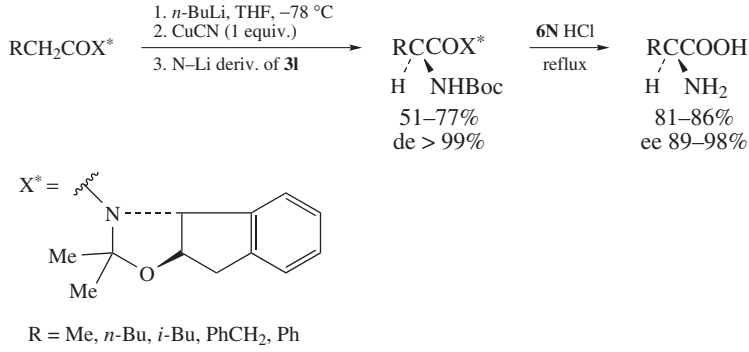

SCHEME 38

bornane [10,2] sultam (Oppolzer sultam) as chiral auxiliary reacts with **3n** in the presence of CaO to produce α-*N*-(ethoxycarbonyl)-β-ketocarboxamide (equation 18)[100].

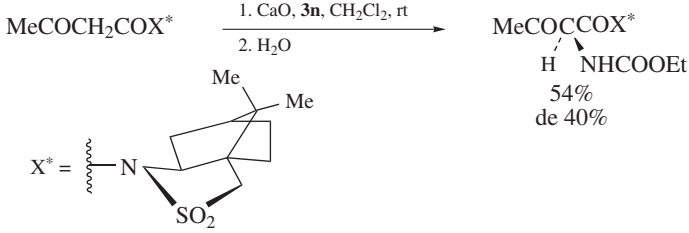

(18)

They also reported amination of chiral β-enaminoesters derived from 2-ethoxycarbonyl-cyclohexanone (equation 19)[92] and ethyl 2-butynoate (equation 20)[93] using (*R*)-1-phenyl ethylamine and chiral pyrrolidine, respectively. Amination was carried out without a base.

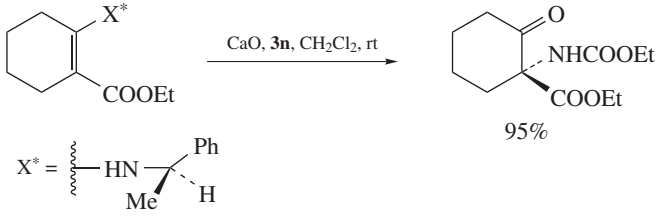

(19)

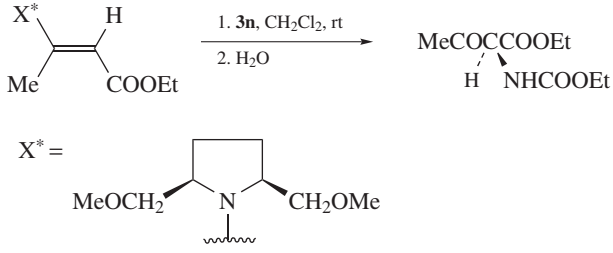

(20)

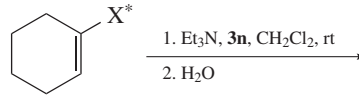

X*	Yield(%)	ee (%)	Reference
N CH_2OY (Y = Me, TMS)	12–18	52–77	104
$OCHR^1CHR^2OTMS$ ((*R*,*R*)- or (*S*,*S*)-)	24–36	60–75	105
R^1,R^2 = Me, Ph, CH_2OMe, CH_2OCH_2Ph			

SCHEME 39

Successful amination of chiral enamines[104] and enol ethers[105] by the same group took place using **3n** in the presence of Et_3N as a base. They obtained α-*N*-(ethoxycarbonyl) aminoketones in low yields and stereoseletivities (Scheme 39).

There are a few published reports on the use of HOSA **3p** for enolate amination. Some β-diketo compounds were reacted with HOSA in 10% aqueous K_2CO_3 solution at room temperature to give substituted pyrroles (equation 21)[106, 107].

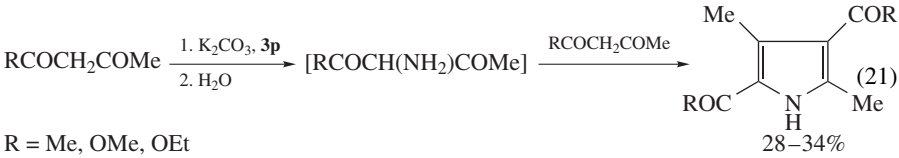

However, amination of β-lithiated carboxylic acids with HOSA was unsuccessful[49].

D. *O*-Phosphinylhydroxylamines

Successful use of *O*-phosphinylhydroxylamines as aminating reagents for amination of carbanions and enolates has been reported. A list of these reagents is given in Table 4.

O-(Diphenylphosphinyl)hydroxylamine **4a** and its *N*,*N*-dialkyl derivatives **4c** and **4d** are stable compounds and can be stored at $-20\,^{\circ}C$. Preparation methods for **4a** have been discussed in detail[107] and a direct method for the preparation of **4c** and **4d** has been reported[108].

1. Amination of Group 1, 2, 11 and 12 organometallic reagents

Colvin and coworkers have reported the amination of phenyl and hexylmagnesium bromides with *O*-(diphenylphosphinyl)hydroxylamine **4a** (equation 22)[109].

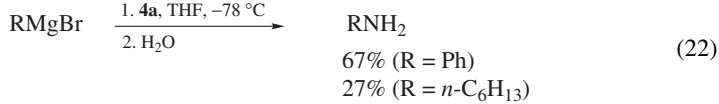

(22)

TABLE 4. *O*-Phosphinylhydroxylamine-type electrophilic amination reagents

$R^1R^2NOP(=O)R_2$
(**4a–e**)

4	R^1	R^2	R	**4**	R^1	R^2	R
4a	H	H	Ph	**4d**	*i*-Pr	*i*-Pr	Ph
4b	H	H	*p*-Tol	**4e**	Me	Me	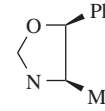
4c	Me	Me	Ph				

An amination procedure for organolithiums and Grignard reagents using **4a** has been also published by Boche and coworkers and moderate yields of alkylamines and arylamines were obtained (Scheme 40)[110]. The use of *N*,*N*-dimethyl-*O*-phosphinylhydroxylamine **4c** for amination gave higher yields.

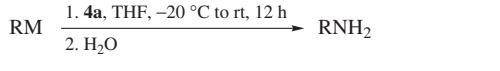

M	R	Yield (%)
Li	Ph_2CH, Ph_3C, PhCH=CHCHPh, Ph, 9-fluorenyl	30–78
MgBr	$PhCH_2$, $PhCMe_2$, Ph, 1-naph	22–51

SCHEME 40

Boche and coworkers described high-yield conversion of lithium alkynylcuprates to alkynylamines using **4c** as amination reagent (Scheme 41)[111].

SCHEME 41

A chiral *O*-phosphinylhydroxylamine-type reagent, such as (2*R*,4*S*,5*R*)-2-[*O*-(*N*,*N*-dimethylhydroxylamino)]-3,4-dimethyl-5-phenyl-1,3,2-oxazaphospholidin-2-one **4e**, was also used for stereoselective amination of carbanions (equation 23)[112].

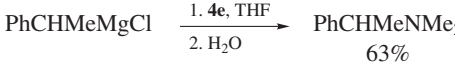

(23)

2. Amination of α-metallated carbonyl compounds and nitriles

Colvin and coworkers[109] and also Boche and coworkers[110] have reported amination procedures with **4a** for the introduction of NH_2 group into sodium enolates[109] (Scheme 42)

$$(EtO)_2P(=O)CH_2CHNaCOOCH_2Ph \xrightarrow[2.\ H_2O]{1.\ \mathbf{4a},\ THF,\ -78\ ^\circ C} (EtO)_2P(=O)CH(NH_2)COOCH_2Ph \quad 57\%$$

$$NaCHY_2 \xrightarrow[2.\ H_2O]{1.\ \mathbf{4a},\ THF,\ -78\ ^\circ C} CH(NH_2)Y_2$$

60% (Y = COOEt)
50% (Y = CN)

SCHEME 42

$$RCHPhY \xrightarrow[3.\ H_2O]{1.\ n\text{-BuLi, THF, } -78\ ^\circ C;\ 2.\ \mathbf{4a},\ rt,\ 12\ h} RCPh(NH_2)Y \quad 31–96\%$$

R,Y = H, COOEt ; COOEt, COOEt ; H, CN; Ph, CN; CN, COOEt;

SCHEME 43

and lithium enolates[110] of phenylacetates, phenylacetonitriles, malonates and β-cyanoesters (Scheme 43).

The efficiency of the amination methodology of enolates with *O*-phoshinylhydroxylamine-type reagents was further demonstrated by Boche and Schrodt in the high-yield amination of *O*-(trimethylsilyl)cyanohydrin anions with **4c** (Scheme 44)[113]. *O*-(Trimethylsilyl)cyanohydrins prepared by treatment of aryl, hetaryl and conjugated aldehydes with trimethylsilyl cyanide were lithiated to the eniminates. This is a practical method that enables the easy conversion of aldehydes to *N*,*N*-dimethylamides under mild conditions.

$$RCHO \xrightarrow{TMSCN} RCH(CN)OTMS \xrightarrow[2.\ \mathbf{4a},\ -78\ ^\circ C,\ rt,\ 5\ h]{1.\ LDA} RC(NMe_2)(CN)OTMS \xrightarrow{H_2O} RCONMe_2 \quad 51–98\%$$

R = Ph, XC_6H_4 (X = 2-Cl, 4-Me, 4-Cl, 4-Br, 4-MeO, 4-NMe_2)

2, 4-$Me_2C_6H_3$, PhCH=CH, 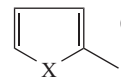 (X = O, S, NMe)

SCHEME 44

Recently, Smulik and Vedejs have reported that sodium and potassium salts of phenylacetates, phenylacetonitriles, malonates and β-cyanoesters can be converted to their α-amino derivatives in good yields using **4a** and **4b** as amination reagents (Scheme 45)[62]. Amination can be accomplished at lower temperature using **4b**.

$$R^1R^2CHY \xrightarrow[2.\ \mathbf{4a}\ or\ \mathbf{4b},\ rt,\ 15\ h]{1.\ Base,\ THF;\ 3.\ H_2O} R^1R^2C(NH_2)Y$$

31–96% with **4a**
41–92% with **4b**

Base = NaH at rt; KOBu-*t* at −78 °C

R^1, R^2, Y = Ph, H, COOEt; Ph, H, CN; Ph, Ph, CN; H, COOEt, COOEt

SCHEME 45

Beak and coworkers offered an S_N2-type mechanism for the amination of α-lithiated nitriles with *N*,*N*-disubstituted *O*-phosphinylhydroxylamines[45].

For stereoselective synthesis of α-aminocarbonyl compounds using *O*-phosphinylhydroxylamines, a few procedures have been developed. Attempted amination of enolates of chiral alkyl 3-hydroxybutanoates with *O*-(diphenylphosphinyl)hydroxylamine **4a** or with its *N*,*N*-diisopropyl derivative **4d** were found to be unsuccessful[112].

Successful amination of chiral α-cyanoesters with **4a** has been reported (Scheme 46)[114]. Appropriate reduction and removal of the chiral auxiliary give α,β-diaminopropionic acids with good yield and enantiomeric excess.

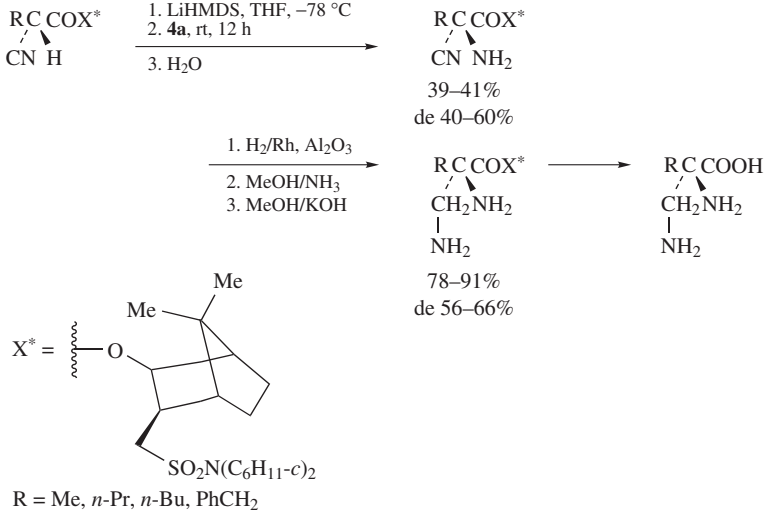

SCHEME 46

As an extension of the use of chiral *O*-phosphinylhydroxylamine **4e** for stereoselective amination, the reaction of lithium enolates with **4e** was also tried. However, low levels of enantiomeric purity were obtained (Scheme 47)[112].

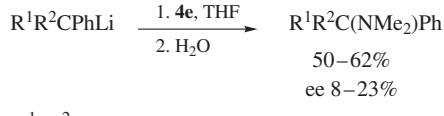

SCHEME 47

E. *O*-Silylhydroxylamines

O-Silylhydroxylamine-type reagents have been listed in Table 5. *O*-Silylhydroxylamine **5a** and **5b**[115], the *N*-alkyl derivatives **5c** and **5g**[115,116] and *N*,*O*-bis(trimethylsilyl) hydroxylamine **5h**[115,117] were prepared by Ricci and coworkers by adapting the method of Wannagat[118,119].

TABLE 5. *O*-Silylhydroxylamine-type electrophilic amination reagents

$R^1NHOSiMe_2R$
(**5a**–**h**)

5	R^1	R	5	R^1	R
5a	H	Me	**5e**	*t*-Bu	Me
5b	H	*t*-Bu	**5f**	$PhCH_2$	Me
5c	Me	Me	**5g**	Me	*t*-Bu
5d	*i*-Pr	Me	**5h**	Me_3Si	Me

Ricci and coworkers reported that the higher order cyanocuprates prepared from aryl- and heteroaryllithiums react with *N*,*O*-bis(trimethylsilyl)hydroxylamine **5h** to yield primary amines in good yields (Scheme 48)[117].

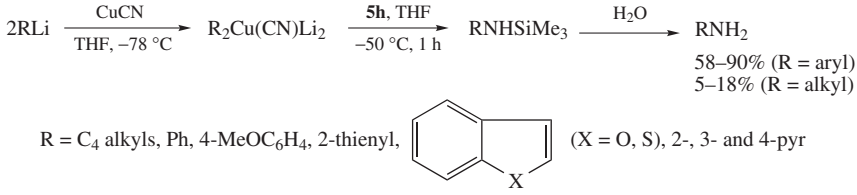

SCHEME 48

A mechanism involving formation of the *N*-lithium derivative of **5h** by proton abstraction with higher-order cyanocuprate, followed by C−N coupling of cyano cuprate, was suggested (Scheme 49)[6,117].

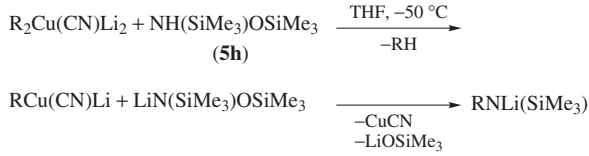

SCHEME 49

A lithiated chiral ferrocene was also converted to the bis(ferrocenyl)cyano cuprate and aminated with **5h** to yield an aminoferrocene (Scheme 50)[120].

Ricci and coworkers also investigated the synthetic utility of *N*-alkyl *O*-silylhydroxylamines **5c–e** in the amination of aryl and heteroaryl higher cyanocuprates and obtained secondary amines in good yields (Scheme 51)[116].

Amination of chiral catechol boronate esters with *O*-silylhydroxylamine-type reagents **5a–c**, **e–h** have been investigated in detail by Brown, Ricci and coworkers (Scheme 52)[115]. However, formation of both alcohol and amine as products in compatible amounts were present on initial nucleophilic attack of oxygen as well as of nitrogen on the organoborane (Scheme 4). Reagents **5a** and **5b** were used, following deprotonation with *n*-butyllithium or methylmagnesium chloride.

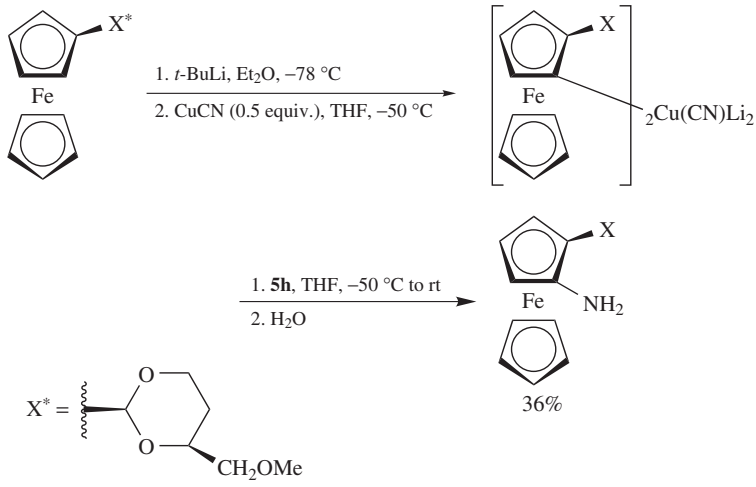

SCHEME 50

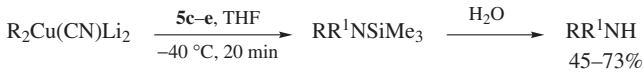

R^1 = Me, *i*-Pr, *t*-Bu

R = Ph, XC_6H_4 (X = 3-MeO, 4-Me, 4-MeO, 4-F), 2-thienyl, 2-pyr

SCHEME 51

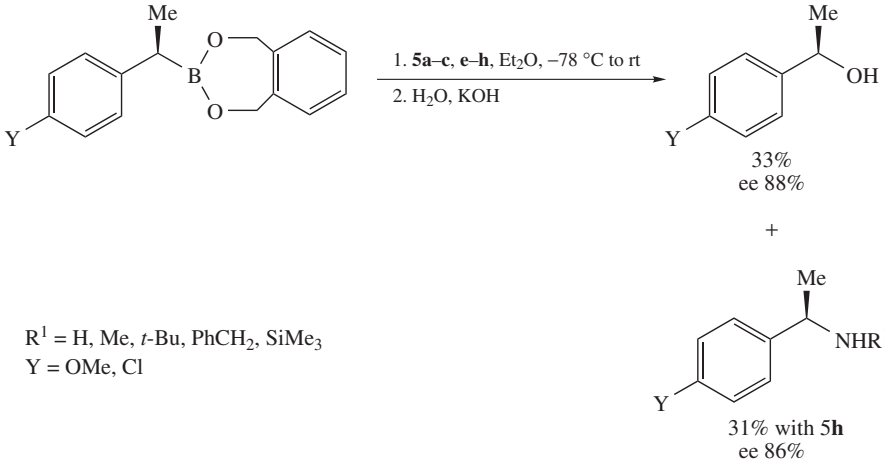

R^1 = H, Me, *t*-Bu, $PhCH_2$, $SiMe_3$
Y = OMe, Cl

SCHEME 52

III. ELECTROPHILIC *C*-AMINATION WITH OXIMES AND *O*-SUBSTITUTED OXIMES

There are a few reports on the use of oximes as electrophilic amination reagents. Since 1984, ketone *O*-sulfonyloximes have found applicability as amino transfer reagents to carbanions. In the reaction of organometallic compounds with oximes, carbanions attack the carbonyl carbon of the oxime, giving *N*-substituted hydroxylamines as addition products (Scheme 53, path a). However, a number of scattered reports have been also published on the formation of aziridines by α-deprotonation, followed by addition (path b) or formation of azirines by α-deprotonation before addition (path c). Addition of carbanions to azirines also yields aziridines, which are hydrolyzed to α-aminoalcohols.

In this chapter, C−N couplings, e.g. substitution reactions of carbanions on nitrogen atom of oximes to yield primary amines, have been reviewed. A list of oximes and *O*-sulfonyloximes used for electrophilic amination is given in Table 6. These reagents aminate carbanions to *N*-organylimines as isolable intermediates which are hydrolyzed to primary amines (Scheme 53, path d; Scheme 54). Depending on the organometallic

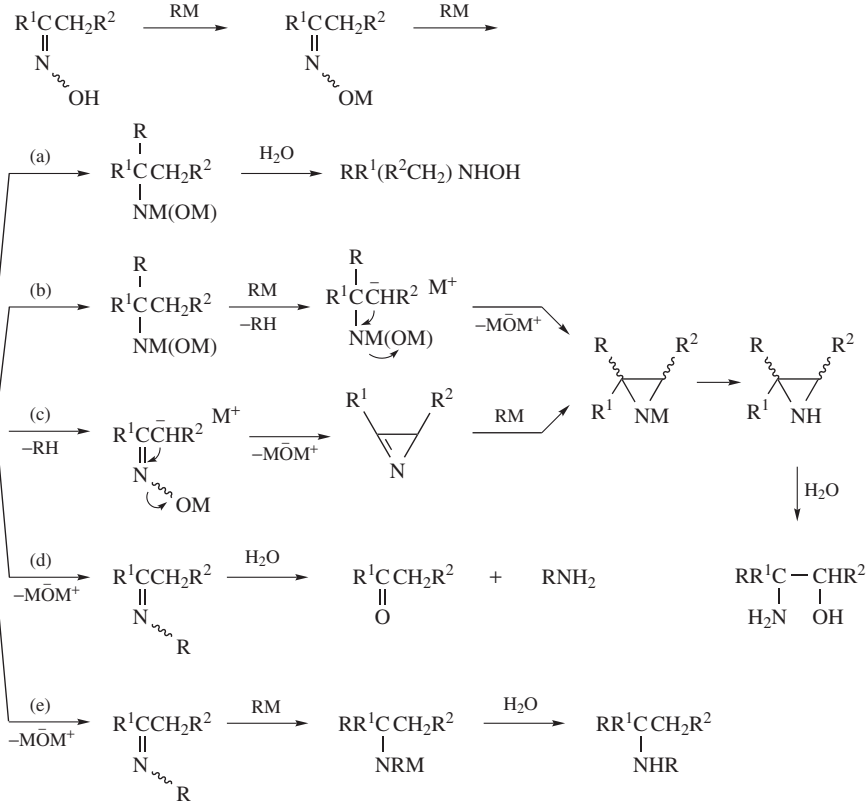

SCHEME 53

TABLE 6. Oxime and *O*-sulfonyloxime-type electrophilic amination reagents

$R^1R^2C=NOZ$
(**6a–l**)

6	$R^1R^2C=$	Z	**6**	$R^1R^2C=$	Z
6a	PhHC=	H	**6h**	$(p\text{-}CF_3C_6H_4)_2C=$	SO_2Me
6b	Ph(*i*-Pr)C=	H			
6c	$Me_2C=$	H	**6i**	$(p\text{-}CF_3C_6H_4)_2C=$	*p*-Tos[b]
6d	MeEtC=	H			
6e	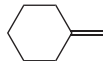	H	**6j**	$(3,5\text{-}(CF_3)_2C_6H_3)_2C=$	*p*-Tos[b]
6f	$Me_2C=$	SO_2Mes[a]	**6k**		*p*-Tos[b]
6g	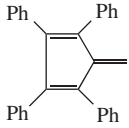	*p*-Tos[b]	**6l**	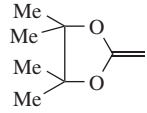	*p*-Tos[b]

[a] Mesitylenesulfonyl: $SO_2C_6H_2Me_3$-2,4-6.
[b] *p*-Tosyl: $SO_2C_6H_4Me$-*p*.

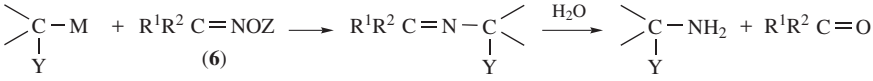

SCHEME 54

reagent and reaction conditions, carbanions also add to *N*-organylimines to produce secondary amines (Scheme 53, path e).

The first example of the amination of Grignard reagents with oximes is the reaction of benzaldoxime **6a** with α-naphthylmagnesium bromide (equation 24, path a)[13] to yield α-naphthylamine (Scheme 53, path d, electrophilic amination product). In contrast, the reaction of benzaldoxime with phenylmagnesium bromide (equation 24, path b) was reported to give *N*-benzhydrylaniline (Scheme 53, path e product).

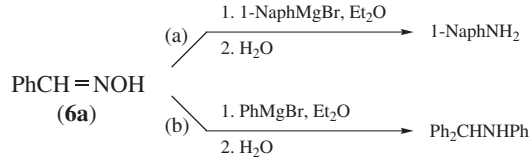

(24)

In the amination of phenylmagnesium bromide with isobutyrophenone oxime **6b**, the amination product and aziridine (Scheme 53, path c product) were obtained (equation 25)[121].

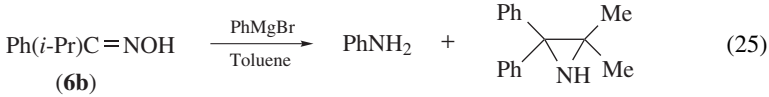

(25)

Alvernhe and Laurent first developed a procedure for conversion of Grignard reagents to primary amines using acetone oxime **6c** and butanone oxime **6d** (Scheme 55)[122, 123]. However, the yields were low. They expanded their study to investigate how well organolithiums perform in their reaction with **6c** or **6d**[123]. Phenyllithium gave a 1:4 mixture of aniline and the addition product of phenyllithium to the imine (Scheme 53, path e product) in the reaction with **6c** while aziridine was obtained in the reaction with **6d** (Scheme 56).

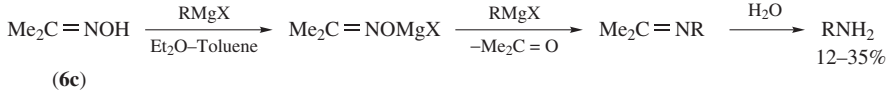

[RMgX] / [**6c**] ratio = 2:1
R = *n*-Bu, $PhCH_2CH_2$, Ph, XC_6H_4 (X = 2-MeO, 4-Me, 4-MeO, 4-Cl)

SCHEME 55

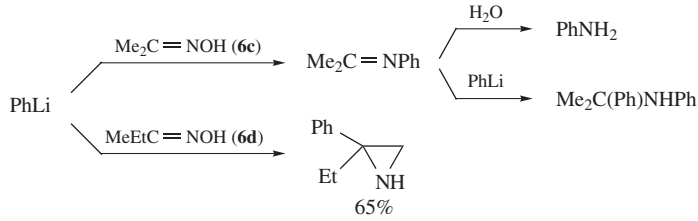

SCHEME 56

When cyclohexanone oxime **6e** was used as amination reagent, primary amines were obtained from phenylmagnesium bromide. Reaction of **6e** with alkyl Grignard reagents gave aziridines, whereas reaction with phenyllithium gave aziridine and the addition product of phenyllithium to the imine (Scheme 57)[124].

Erdik and coworkers developed acetone *O*-(mesitylenesulfonyl) oxime **6f** as amination reagent and investigated its application in the amination of Grignard reagents[125–127] and organozinc reagents[39, 40] in detail. **6f** is easily prepared and conveniently stored[128]. Grignard reagents react with **6f** in the presence of CuI catalysis in ether–toluene[125] or without catalysis in THF[126], both at reflux temperature (Scheme 58, Method a). Amination of Grignard reagents with **6f** can be also successfully carried out under Barbier conditions (Scheme 58, Method b)[127].

Reaction of aryl and benzyl zinc reagents with **6f** in the presence of CuCN catalyst provides an alternative method for the synthesis of primary amines in medium yields (Scheme 59). Amination of diorganozincs, R_2Zn, and bromomagnesium triorganozincates, $R_3ZnMgBr$, seemed to give higher yields of amination than those of organozinc chlorides, RZnCl[40].

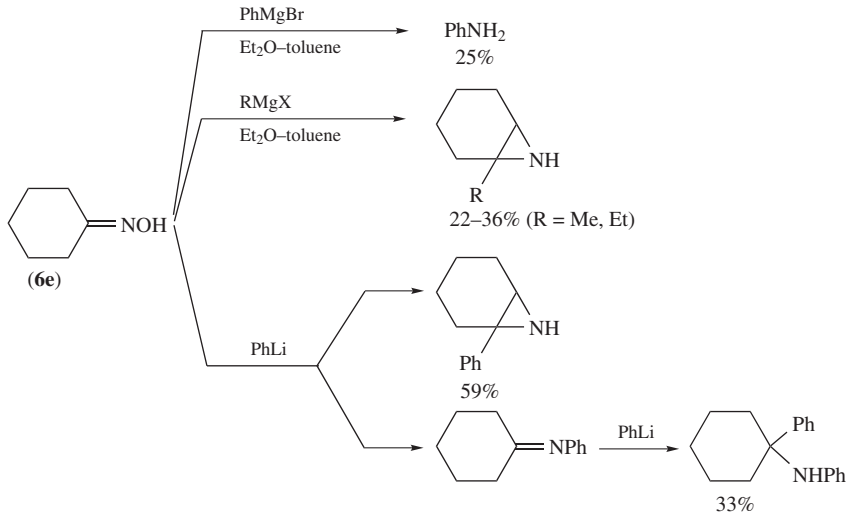

SCHEME 57

Method a

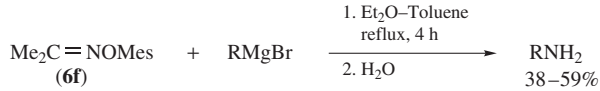

R = Ph, 4-MeC$_6$H$_4$, 4-MeOC$_6$H$_4$

Method b

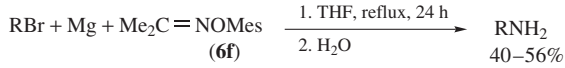

R = Ph, 4-MeC$_6$H$_4$, 4-MeOC$_6$H$_4$, *c*-C$_6$H$_{11}$

SCHEME 58

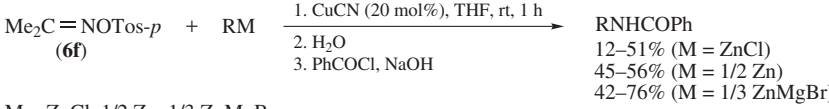

M = ZnCl, 1/2 Zn, 1/3 ZnMgBr
R = Ph, XC$_6$H$_4$ (X = 4-Me, 4-MeO, 4-Br, 4-EtOOC), PhCH$_2$, *c*-C$_6$H$_{11}$

SCHEME 59

The use of DMPU (1,3-dimethyl-3,4,5,6-tetrahydro-2(1*H*)-pyrimidinone) as a cosolvent in THF has been reported to increase the amination yield of arylzinc chlorides with **6f**[129].

Erdik and Ömür[130] also reported competitive kinetic studies for the amination of substituted phenylmagnesium bromides and CuCN-catalyzed phenylzinc chlorides with acetone *O*-(mesitylenesulfonyl)oxime **6f** in THF and analyzed the rate data via the Hammett

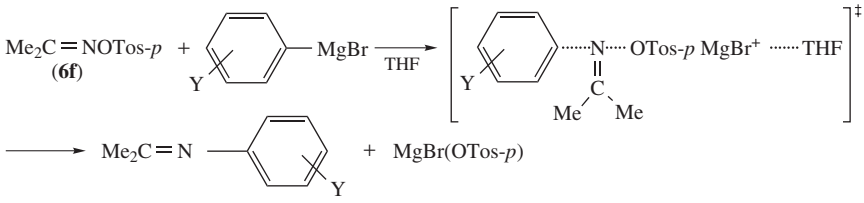

Y = H, 3-Me, 4-Me, 3-MeO, 4-MeO, 3-Br, 4-Br

SCHEME 60

relationship to propose a mechanism. The amination of Grignard reagents seems to be a formal S_N2 displacement by carbanions on the electrophilic nitrogen at the N−OTos bond of **6f** (Scheme 60).

So far, numerous efforts by Erdik and coworkers for amination of lithium and zinc enolates with **6f** were found to be unsuccessful[131].

Murdoch and coworkers carried out amination reactions of aryl Grignard reagents and aryllithiums with oximes using *O*-*p*-toluenesulfonyl tetraphenylcyclopentanone oxime (*O*-tosyltetracyclone oxime) **6g** (Scheme 61)[132]. The imine is extracted with benzene, purified, and then converted to amine and oxime by reacting with excess hydroxylamine in aqueous pyridine at room temperature. Amines are obtained following acidic hydrolysis.

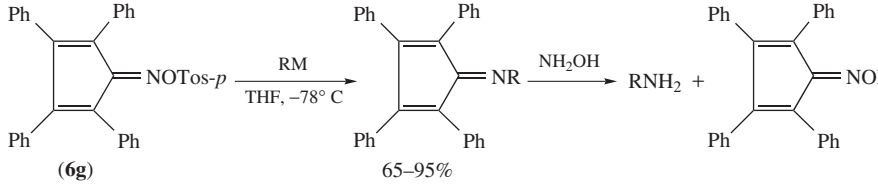

M = Li; R = 2- and 3-furyl
M = MgBr; R = Ph, 2,3,5,6-Me_4C_6H, 1- and 2-naph

SCHEME 61

Narasaka and coworkers prepared a number of benzophenone *O*-sulfonyloxime derivatives[133–137]. They reported that 4,4′-bis(trifluoromethyl) benzophenone *O*-sulfonyl oximes **6h**, **6i** react with Grignard reagents in the presence of CuCN catalyst to give *N*-alkylimines. After hydrolysis and benzoylation, *N*-alkylbenzamides are obtained (Scheme 62)[133, 134]. Cu(I)-catalyzed amination of alkyl Grignard reagents was reported to take place in high yields in polar solvents while amination of aryl Grignard reagents was unsuccessful.

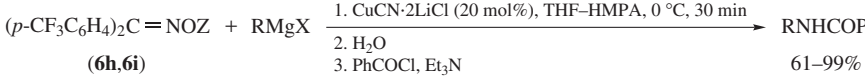

R = C_3, C_4 alkyls, *c*-C_6H_{11}, $PhCH_2CH_2$, 1-adanantyl, 1-norbornyl

SCHEME 62

Amination of alkylcoppers also produced alkyl amines in quantitative yields in polar solvents (Scheme 63, path a). In the amination of dialkylcuprates, imines were obtained

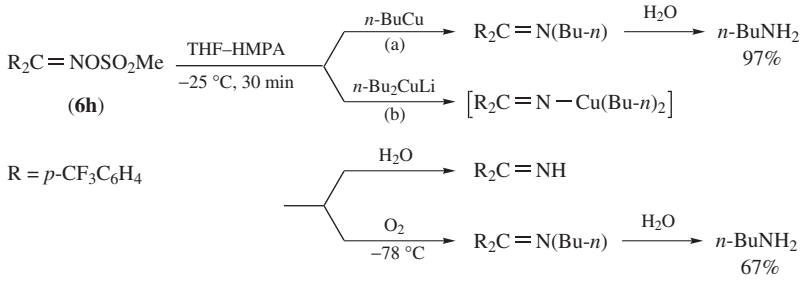

SCHEME 63

and oxidation of the aminocopper intermediate afforded alkylamines (Scheme 63, path b)[134].

Amination of aryl Grignard reagents without a Cu(I) catalyst could succeed using 3,3′,5,5′-tetrakis(trifluoromethyl)benzophenone *O*-tosyloxime **6j** as an amination reagent in toluene (Scheme 64)[134].

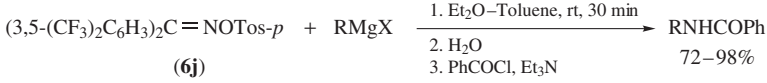

R = Et, *t*-Bu, *c*-C_6H_{11}, Ph, XC_6H_4 (X = 2-MeO, 3-MeO, 4-MeO, 4-F), 2,6 -$Me_2C_6H_3$, 1-naph
X = Br, Cl

SCHEME 64

2-Imidazolidinone *O*-tosyloxime **6k** was also reported to react with alkyl and aryl Grignard reagents in good yields (Scheme 65)[135]. The resulting *N*-organylimines can be hydrolyzed with CsOH to afford primary amines and/or reduced with $LiAlH_4$ to *N*-methyl secondary amines.

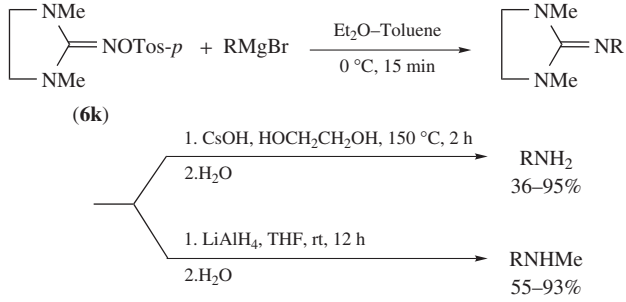

R = $PhCH_2CH_2$, $PhCH_2CH_2CHMe$, 1-adamantyl, Ph, 2,4-$Me_2C_6H_3$, 1-naph, 2-MeC_6H_4, 2-$MeOC_6H_4$

SCHEME 65

High-yield amination of aryl-, benzyl- and alkenyl magnesium bromides has been successful using 1,3-dioxolan-2-one *O*-(benzenesulfonyl)oxime **6l** (Scheme 66)[136].

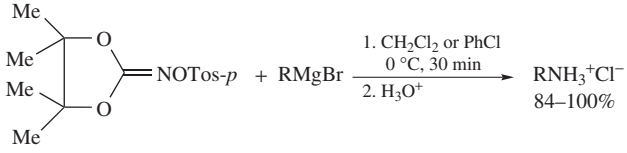

R = $PhCHMeCH_2$, $PhCH_2CHMe$, *c*-C_6H_{11}
1-adamantyl, 1-norbornyl, $R^1CH{=}CR^2$ (R^1, R^2 = Ph, H; H, Me), Ph,
XC_6H_4 (X = 4-Me, 2-MeO, 3-MeO, 4-MeO, 4-F, 4-CF_3), 2,4-$(MeO)_2C_6H_3$

SCHEME 66

Narasaka reviewed the synthesis of arylamines by amination of Grignard reagents with 4,4′-bis(trifluoromethyl)benzophenone *O*-*p*-tosyloxime **6i** and 3,3′,5,5′-tetrakis(trifluoromethyl)benzophenone *O*-tosyloxime **6j**[137].

IV. OVERVIEW AND CONCLUDING REMARKS

The use of *O*-substituted hydroxylamines and oximes as amino transfer reagents to carbanions and α-metallated carbonyl compounds has been outlined. For synthesis of amines and α-amino carbonyl compounds, a number of electrophilic amination reagents and methods are available. However, *O*-substituted hydroxylamines are especially important because they are easy to use as reagents and C–N coupling of *C*-nucleophiles with these reagents can be successful in a one-step procedure under very mild conditions with good yields. *O*-Methylhydroxylamines and *O*-benzoylhydroxylamine exhibit a potential as efficient electrophilic amination reagents for synthesis of amines from organolithium, -magnesium, -copper and -zinc reagents. *O*-Phosphinylhydroxylamines and *O*-sulfonylhydroxylamines give good results in asymmetric amination of α-metallated carbonyl compounds.

O-Sulfonylhydroxylamines and hydroxylamine *O*-sulfonic acid have found wide application in synthesis of amines from achiral or chiral organoboranes and boronate esters and the hydroboration–amination methodology is successfully used for direct amination of alkenes. *O*-Sulfonyloximes were also found to be good reagents for synthesis of amines from organomagnesium, -copper and -zinc reagents.

The discussion in this chapter highlights the performance of *O*-substituted hydroxylamines and oximes as electrophilic amino transfer reagents. In conclusion, the scope of electrophilic amination will be greatly enhanced by developing new *O*-substituted hydroxylamines and oximes and further improvements in electrophilic amination would be of great synthetic interest.

Acknowledgements: I gratefully acknowledge the kind help of Editor Professor Z. Rappoport in preparing the chapter. He gave me valuable suggestions and reviewed the manuscript thoroughly. I also thank Professor J. F. Liebmann for his comment on the hybridization type of electrophilic nitrogen in arenediazonium salts.

V. REFERENCES

1. R. Askani and D. F. Taber, in *Comprehensive Organic Synthesis*, Vol. 7 (Ed. B. M. Trost), Pergamon, Oxford, 1996, p. 1881.
2. G. Boche, in *Houben–Weyl, Methods of Organic Chemistry*, Vol. E21e (Eds. G. Heimchen, R. W. Hoffmann, J. Mulzer and E. Schaumann), Thieme, Stuttgart, 1995, p. 5133.
3. J. Mulzer, H. J. Altenbach, M. Brown, K. Krohn and H. U. Reissing, *Organic Synthesis Highlights*, VCH, Weinheim, 1991, p. 45.

4. E. Erdik and M. Ay, *Chem. Rev.*, **89**, 1947 (1989).
5. J. P. Genet and C. Greck, *Synlett*, 741 (1997).
6. P. Dembech, G. Seconi and A. Ricci, *Chem. Eur. J.*, **6**, 1281 (2002).
7. E. Erdik, *Tetrahedron*, **60**, 8747 (2004).
8. C. Greck, B. Drauillat and C. Thomosigny, *Eur. J. Chem.*, **10**, 1377 (2004).
9. A. Ricci (Ed.), *Modern Amination Methods*, Wiley–VCH, Weinheim, 2000.
10. S. A. Lawrence, *Amines: Synthesis, Properties, and Applications*, Cambridge University Press, Cambridge, 2004.
11. R. M. Williams, *Synthesis of Optically Active α-Aminoacids*, Pergamon, Oxford, 1989, p. 167.
12. N. I. Schverdina and Z. Kotscheschkow, *J. Gen. Chem. USSR (Engl. Transl.)*, **8**, 1825 (1938); *Chem. Zentralbl.*, **I**, 360 (1940).
13. M. Bush and R. Hubein, *Ber. Dtsch. Chem. Ges.*, **40**, 2096 (1907).
14. H. C. Brown, K. B. Kim, M. Srebnik and B. Singaram, *Tetrahedron*, **43**, 4071 (1987).
15. G. Zweifel and H. C. Brown, *J. Am. Chem. Soc.*, **86**, 393 (1964).
16. G. Zweifel and A. Horng, *Synthesis*, 672 (1973).
17. E. J. Corey and W. L. Seibel, *Tetrahedron Lett.*, **27**, 905 (1986).
18. G. W. Kabalka, K. A. R. Sastry, G. W. McCollum and H. Yoshioka, *J. Org. Chem.*, **46**, 4296 (1981).
19. H. C. Brown, T. E. Cole, M. Srebnik and K. W. Kim, *J. Org. Chem.*, **52**, 730 (1987).
20. H. C. Brown, T. E. Cole, M. Srebnik and K. W. Kim, *J. Org. Chem.*, **51**, 4925 (1986).
21. G. W. Kabalka, Z. Wang and N. M. Goudgaon, *Synth. Commun.*, **19**, 2409 (1989).
22. W. Theilacker and K. Ebbe, *Angew. Chem.*, **68**, 303 (1956).
23. A. Chimiak, T. Kolasa, *Bull. Acad. Pol. Sci.*, **22**, 1975 (1974).
24. H. Hjeds, *Acta Chem. Scand.*, **19**, 1764 (1965).
25. P. Beak, A. Basha and B. Kokko, *J. Org. Chem.*, **47**, 2822 (1982).
26. P. Beak, A. Basha, B. Kokko and D. Leo, *J. Am. Chem. Soc.*, **108**, 6016 (1986).
27. Y. Tamura, J. Minamikawa and M. Ykeda, *Synthesis*, 1 (1977).
28. R. Brown and W. G. Jones, *J. Chem. Soc.*, 781 (1946).
29. H. Gilman and S. Avakian, *J. Am. Chem. Soc.*, **68**, 580 (1946).
30. H. Gilman and R. K. Ingham,, *J. Am. Chem. Soc.*, **75**, 4843 (1953).
31. H. Gilman and S. Avakian,, *J. Am. Chem. Soc.*, **68**, 1514 (1946).
32. H. Gilman and D. R. Swayampati, *J. Am. Chem. Soc.*, **65**, 1461 (1943).
33. H. Gilman and D. R. Swayampati, *J. Am. Chem. Soc.*, **79**, 208 (1957).
34. H. Gilman and D. R. Swayampati, *J. Am. Chem. Soc.*, **77**, 5944 (1955).
35. A. N. Nesmeyanov, E. Perevalova, R. V. Golovaya and L. S. Shilovtseva, *Dokl, Akad. Nauk SSSR*, **102**, 535 (1955); *Chem. Abstr.*, **50**, 4925g (1956).
36. M. Silver, P. R. Shafer, J. E. Nordlander, C. Rüchardt and J. D. Roberts, *J. Am. Chem. Soc.*, **82**, 2646 (1960).
37. B. J. Wakefield, *The Chemistry of Organolithium Compounds*, Pergamon, Oxford, 1974, (a) p. 161, (b) p. 215.
38. E. Erdik. *Commun. Fac. Sci. Univ. Ankara, Ser. B*, **26**, 83 (1980); *Chem. Abstr.*, **95**, 115634p (1981).
39. E. Erdik and T. Daşkapan, *Tetrahedron Lett.*, **43**, 6237 (2002).
40. E. Erdik and T. Daşkapan, *J. Chem. Soc., Perkin Trans. 1*, 3139 (1999).
41. C. L. Bumgardner and R. Lilly, *Chem. Ind.*, 559 (1962).
42. P. Beak, A. Basha and B. Kokko, *Tetrahedron Lett.*, **24**, 561 (1983).
43. P. Beak and G. W. Selling, *J. Org. Chem.*, **54**, 5574 (1989).
44. G. Boche and H. U. Wagner, *J. Chem. Soc., Chem. Commun.*, 1591 (1984).
45. P. Beak, K. J. Basu and J. J. Li, *J. Org. Chem.*, **64**, 5218 (1999).
46. D. R. Armstrong, R. Smith and G. T. Walker, *J. Chem. Soc., Chem. Commun.*, 789 (1985).
47. M. L. McKee, *J. Am. Chem. Soc.*, **107**, 859 (1985).
48. E. Erdik, F. Eroğlu and D. Kâhya, *J. Phys. Org. Chem.*, **18**, 950 (2005).
49. S. Yamada, T. Oguri and T. Shiori, *J. Chem. Soc., Chem. Commun.*, 623 (1972).
50. T. Oguri, T. Shiori and S. Yamada, *Chem. Pharm. Bull.*, **23**, 167 (1975).
51. T. Oguri, T. Shiori and S. Yamada, *Chem. Pharm. Bull.*, **23**, 173 (1975).
52. T. Sheradsky, G. Salemnick and Z. Nir, *Tetrahedron*, **28**, 3833 (1972).
53. T. Sheradsky and Z. Nir, *Tetrahedron Lett.*, 77 (1969).
54. A. S. Radhakrishna, G. M. Loudon and M. J. Miller, *J. Org. Chem.*, **44**, 4836 (1979).

55. A. M. Berman and J. S. Johnson, *J. Am. Chem. Soc.*, **126**, 5680 (2004).
56. A. M. Berman and J. S. Johnson, *J. Org. Chem.*, **70**, 364 (2005).
57. A. M. Berman and J. S. Johnson, *Synlett*, 1799 (2005).
58. A. M. Berman and J. S. Johnson, *J. Org. Chem.*, **71**, 219 (2006).
59. A. M. Berman and J. S. Johnson, *Org. Synth.*, **83**, 31 (2005).
60. A. Biloski and B. Ganem, *Synthesis*, 537 (1983).
61. M. J. Campbell and J. S. Johnson, *Org. Lett.*, **9**, 1521 (2007).
62. A. J. Smulik and A. Vedejs, *Org. Lett.*, **5**, 4187 (2003).
63. Y. Tamura, J. Minamikawa, K. Sumoto, S. Feyi and M. Ikeda, *J. Org. Chem.*, **38**, 1239 (1973).
64. L. A. Carpino, *J. Am. Chem. Soc.*, **82**, 3133 (1960).
65. L. A. Carpino, *J. Org. Chem.*, **29**, 2820 (1964).
66. E. C. Taylor and J. H. Sun, *Synthesis*, 801 (1980).
67. G. Boche, N. Mayer, M. Bernheim and K. Wagner, *Angew. Chem., Int. Ed. Engl.*, **17**, 687 (1978).
68. L. A. Carpino, C. A. Giza and B. A. Carpino, *J. Am. Chem. Soc.*, **81**, 955 (1959).
69. C. Greck, L. Bishoff, A. Girard, J. Hajicek and J. P. Genet, *Bull. Soc. Chim. Fr.*, **131**, 429 (1994).
70. C. Greck, L. Bishoff, F. Ferreira and J. P. Genet, *J. Org. Chem.*, **60**, 7010 (1995).
71. G. Boche, C. Boie, F. Bosold, K. Harms and M. Marsch, *Angew. Chem., Int. Ed. Engl.*, **33**, 115 (1997).
72. D. H. R. Barton, L. Bould, D. L. J. Clive, P. D. Magnus and T. Hose, *J. Chem. Soc., Chem. Commun.*, 2204 (1971).
73. T. Abraham and D. Curran, *Tetrahedron*, **38**, 1019 (1982).
74. M. Bernheim and G. Boche, *Angew. Chem., Int. Ed. Engl.*, **19**, 1010 (1980).
75. G. Boche, M. Bernheim and M. Niedner, *Angew. Chem., Int. Ed. Engl.*, **22**, 53 (1983).
76. T. Sheradsky and N. Itzhak, *J. Chem. Soc., Perkin Trans. 1*, 13 (1980).
77. E. Erdik and S. Ateş, *Synth. Comun.*, **36**, 2183 (2006).
78. J. P. Genet, S. Malart, C. Greck and E. Piveteau, *Tetrahedron Lett.*, **32**, 2359 (1991).
79. J. P. Genet, J. Hajicek, L. Bischoff and C. Greck, *Tetrahedron Lett.*, **33**, 2677 (1992).
80. E. Erdik and S. Ateş Ülkü, *J. Phys. Org. Chem.*, **20**, 671 (2007).
81. G. W. Kabalka and J. W. Ferrell, *Synth. Commun.*, **9**, 443 (1979).
82. H. C. Brown and B. Singaram, *Acc. Chem. Res.*, **21**, 287 (1988).
83. D. S. Matteson, *Acc. Chem. Res.*, **21**, 294 (1988).
84. M. V. Rangaishenvi, B. Singaram and H. C. Brown, *J. Org. Chem.*, **56**, 3286 (1991).
85. H. C. Brown, K. W. Kim, T. E. Cole and B. J. Singaram, *J. Am. Chem. Soc.*, **108**, 6761 (1986).
86. L. Verbit and P. J. Heftron, *J. Org. Chem.*, **32**, 3199 (1967).
87. P. V. Ramachandran, M. V. Rangaishenvi, B. Singaram, C. T. Goralski and H. C. Brown, *J. Org. Chem.*, **61**, 341 (1996).
88. H. C. Brown, S. V. Malhotra and P. V. Ramachandran, *Tetrahedron: Asymmetry*, **7**, 3527 (1996).
89. K. Burgess and M. J. Ohlmeyer, *Chem. Rev.*, **91**, 1179 (1991).
90. I. Beletskaya and A. Pelter, *Tetrahedron*, **53**, 4957 (1997).
91. D. I. C. Scopes, A. F. Kluge and J. A. Edwards, *J. Org. Chem.*, **42**, 376 (1977).
92. S. Fioravanti, L. Olivieri, L. Pellacani and P. A. Tardella, *Tetrahedron Lett.*, **39**, 6391 (1998).
93. E. Felice, S. Fiorovanti, L. Pellacani and P. A. Tardella, *Tetrahedron Lett.*, **40**, 4413 (1999).
94. S. Fiorovanti, L. Olivieri, L. Pellacani and P. A. Tardella, *J. Chem. Res. (S)*, 338 (1998).
95. W. Lwowski and J. M. Maricich, *J. Am. Chem. Soc.*, **87**, 3630 (1965).
96. S. Fiorovanti, M. A. Loreto, L. Pellacani and P. A. Tardella, *J. Org. Chem.*, **50**, 5365 (1985).
97. S. Fioravanti, L. Pellacani, S. Stabile, P. A. Tardella and R. Ballini, *Tetrahedron*, **54**, 6169 (1998).
98. M. Carducci, S. Fioravanti, M. A. Loreto, L. Pellacani and P. A. Tardella, *Tetrahedron Lett.*, **37**, 3777 (1996).
99. T. Gasperi, M. A. Loreto, P. A. Tardella and E. Veri, *Tetrahedron Lett.*, **44**, 4953 (2003).
100. S. Fioravanti, A. Morreale, L. Pellaconi and P. A. Tardella, *Tetrahedron Lett.*, **42**, 1171 (2001).
101. M. Barani, S. Fioravanti, L. Pellacani and P. A. Tardella, *Tetrahedron*, **50**, 11235 (1994).

102. S. Hanessian and S. Johnstone, *J. Org. Chem.*, **64**, 5896 (1999).
103. N. Zheng, J. D. Armstrong, J. C. McWilliams and R. P. Volante, *Tetrahedron Lett.*, **38**, 2817 (1997).
104. S. Fiorovanti, M. A. Loreto, L. Pellacani and P. A. Tardella, *J. Chem. Res. (S)*, 310 (1987).
105. S. Fiorovanti, M. A. Loreto, L. Pellacani and P. A. Tardella, *Tetrahedron*, **47**, 5877 (1991).
106. M. J. P. Harger, *J. Chem. Soc., Chem. Commun.*, 768 (1979).
107. Y. Tamura, S. Kato and M. Ikeda, *Chem. Ind.*, 767 (1971).
108. J. J. Yaquanc, G. Mase and G. Sturtz, *Synthesis*, 807 (1985).
109. E. W. Colvin, G. W. Kirby and A. C. Wilson, *Tetrahedron Lett.*, **23**, 3835 (1982).
110. G. Boche, M. Bernheim and W. S. Schrodt, *Tetrahedron Lett.*, **23**, 5399 (1982).
111. G. Boche, M. Bernheim and M. Niedner, *Angew. Chem., Int. Ed. Engl.*, **22**, 53 (1983).
112. G. Boche, F. Bosold and M. Niehner, *Tetrahedron Lett.*, **23**, 3256 (1982).
113. G. Boche and W. Schrodt, *Tetrahedron Lett.*, **23**, 5403 (1982).
114. R. Badorrey, C. Cativiela, M. D. Diaz-de-Villegas and J. A. Galvez, *Tetrahedron: Asymmetry*, **6**, 2787 (1995).
115. F. I. Knight, J. M. Brown, D. Lazzari, A. Ricci and A. J. Blacker, *Tetrahedron*, **53**, 11411 (1997).
116. P. Bernardi, P. Dembech, G. Fabbri, A. Ricci and G. Seconi, *J. Org. Chem.*, **64**, 641 (1999).
117. A. Casarini, P. Dembech, D. Lazari, E. Marini, G. Reginato, A. Ricci and G. Seconi, *J. Org. Chem.*, **58**, 5620 (1993).
118. O. Smrekar and U. Wannagat, *Monatsh. Chem.*, **100**, 760 (1969).
119. U. Wannagat and O. Smrekar, *Monatsh. Chem.*, **100**, 750 (1969).
120. O. Riant, O. Samuel, T. Flessner, S. Taudier and H. B. Kagan, *J. Org. Chem.*, **62**, 6733 (1997).
121. H. M. Kissman, D. S. Tarbel and T. J. Williams, *J. Am. Chem. Soc.*, **75**, 2959 (1953).
122. G. Alvernhe and A. Laurent, *Tetrahedron Lett.*, 1007 (1972).
123. G. Alvernhe and A. Laurent, *J. Chem. Res. (S)*, 28 (1978).
124. R. Chaabouni and A. Laurent, *Bull. Soc. Chim. Fr.*, 2680 (1973).
125. E. Erdik and M. Ay, *Synth. React. Inorg. Met.-Org. Chem.*, **19**, 663 (1989).
126. T. Daşkapan, Ph.D. Thesis, Science Faculty, Ankara University, 1999.
127. E. Erdik and T. Daşkapan, *Tetrahedron Lett.*, **43**, 6237 (2002).
128. L. A. Carpino, *J. Am. Chem. Soc.*, **82**, 3133 (1960).
129. T. Daşkapan, *Tetrahedron Lett.*, **47**, 2879 (2006).
130. E. Erdik and Ö. Ömür, *Appl. Organomet. Chem.*, **19**, 887 (2005).
131. Ö. Ömür, M.Sc. Thesis, Science Faculty, Ankara University, 2004.
132. P. A. Hagopian, M. J. Therien and J. R. Murdoch, *J. Am. Chem. Soc.*, **106**, 5753 (1984).
133. H. Tsutsui, Y. Hayashi and K. Narasaka, *Chem. Lett.*, 317 (1997).
134. H. Tsutsui, T. Ichikawa and K. Narasaka, *Bull. Chem. Soc. Jpn.*, **72**, 1869 (1999).
135. M. Kitamura, S. Chiba and K. Narasaka, *Bull. Chem. Soc. Jpn.*, **76**, 1063 (2003).
136. M. Kitamura, T. Suga, S. Chiba and K. Narasaka, *Org. Lett.*, **6**, 4619 (2004).
137. K. Narasaka, *Pure Appl. Chem.*, **74**, 143 (2002).

CHAPTER 9

Rearrangements of hydroxylamines, oximes and hydroxamic acids

M. MANUELA A. PEREIRA

REQUIMTE/CQFB, Departamento de Química, Faculdade de Ciências e Tecnologia, Universidade Nova de Lisboa, Campus da Caparica, 2829-516 Caparica, Portugal
Fax: +351212948550; e-mail: mmm@dq.fct.unl.pt

and

PEDRO PAULO SANTOS

Centro de Química Estrutural, Instituto Superior Técnico, Universidade Técnica de Lisboa, Av. Rovisco Pais, 1049-001 Lisboa, Portugal
Fax: +351218417122; e-mail: pepesantos@ist.utl.pt

The chemistry of hydroxylamines, oximes and hydroxamic acids
Edited by Z. Rappoport and J. F. Liebman

I. INTRODUCTION

A. Abbreviations

BMIM	1-butyl-3-methylimidazolium ion	MPM	4-methoxybenzyl
BOP-Cl	bis(2-oxo-3-oxazolidinyl) phosphinic chloride	Ms	Mesyl
Bt	benzotriazol-1-yl	MTBE	methyl *tert*-butyl ether
cod	1,5-cyclooctadiene	nbd	Norbornadiene
DIAD	diisopropyl azodicarboxylate	PPA	polyphosphoric acid
DMAP	4-dimethylaminopyridine	PPE	polyphosphoric acid ethyl ester
dr	diastereomeric ratio	TBDMS	*tert*-butyldimethylsilyl
FMO	Frontier Molecular Orbital	TBDPS	*tert*-butyldiphenylsilyl
HFIP	1,1,1,3,3,3-hexafluoro-2-propanol	Tf	Trifluoromethanesulfonyl
HMDS	Hexamethyldisilazane	TFAA	trifluoroacetic anhydride
MNDO	Modified Neglect of Diatomic Overlap	TIPS	Triisopropylsilyl
MOM	Methoxymethyl		

B. General Introduction

Rearrangement reactions of hydroxylamines (**1**), oximes (**2**) and hydroxamic acids (**3**) will be covered in this chapter with emphasis on the developments made during the last 15 years. All referred compounds possess a relatively low energy N−O bond (*ca* 53 kcal mol^{-1}) which facilitates the ability of these compounds to rearrange.

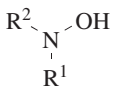

(**1**)

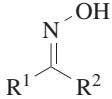

(**2**)

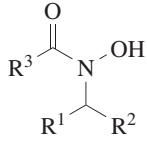

(**3**)

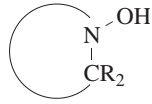

(**4**)

Hydroxylamines may be acyclic (**1**) with one or two substituents or cyclic (**4**). Cyclic compounds **5** where both the nitrogen and the oxygen atoms are ring members like oxaziridines (**6**), 1,2-oxazetidines (**7**), tetrahydro-1,2-oxazoles (**8**) (usually named isoxazolidines) and tetrahydro-1,2-oxazines (**9**) will not be considered in this chapter. Each of these compounds is regarded as a compound class on their own and their chemistry has usually been reviewed individually.

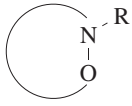

(**5**)

(**6**)

(**7**)

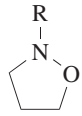

(**8**)

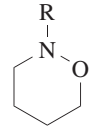

(**9**)

The hydroxylamines are well known by their nucleophilic properties. The presence of the low energy N−O bond gives these compounds the ability to rearrange. The driving force of the rearrangements is usually the simultaneous cleavage of the N−O bond and the formation of new stronger bonds. Oximes and hydroxamic acids which present similar structural features also rearrange under appropriate conditions.

The most frequent rearrangement of substituted hydroxylamines is the thermal [3,3]-sigmatropic rearrangement, the 3-aza-4-oxa-Cope rearrangement[1] also called 3-aza-4-oxy-Cope rearrangement, that proceeds by a cyclic six-membered transition state (equation 1). Albeit the difficulty to prepare hydroxylamine derivatives, this rearrangement proceeds in mild conditions and is useful in the synthesis of several heterocyclic compounds.

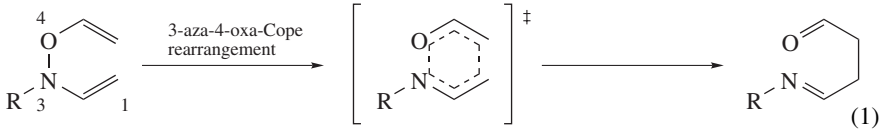

(1)

Despite the relative weakness of the N−O bond which is an important feature for a successful rearrangement reaction of oximes, oximes are fairly stable and do not rearrange spontaneously, due to the inability of the *N*-hydroxyl group to behave as a leaving group. When this hydroxyl group is converted to a better leaving group, rearrangement reactions become more favourable. The Beckmann and Neber rearrangements are classical rearrangement reactions of oximes and their esters, the former being more general than the latter. Scheme 1 illustrates classical Beckmann and Neber rearrangements.

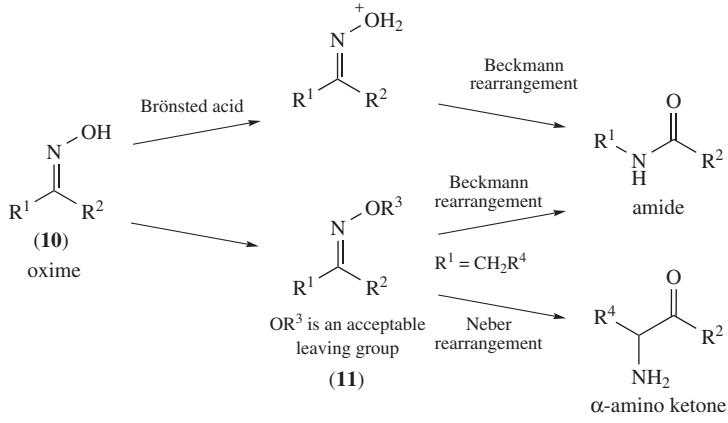

SCHEME 1

Both oximes (**10**) and their ester (**11**) or ether derivatives can be used in the classical Beckmann rearrangement and the reaction usually proceeds under acidic or neutral conditions (although basic conditions may also be used). In sharp contrast, only *O*-oxime esters can be used as starting materials for the Neber rearrangement and basic conditions are always necessary. The Neber rearrangement is not stereospecific, as the stereochemistry of the starting material (*E* or *Z*) does not influence the outcome of the reaction. In

contrast, the Beckmann rearrangement is stereospecific. Both reactions will be covered in this review. Several other related synthetic processes, e.g. rearrangement of nitrones, isoxazolidines or *N*-halogenated imines, are beyond the scope of this chapter and will not be discussed here.

Finally, the Lossen rearrangement provides a practical procedure for replacing the hydroxamic group of a hydroxamic acid (**12**) by an amino group (**14**) (equation 2). The initial rearrangement product is an isocyanate (**13**) which readily reacts with nucleophiles, for example with OH and NH functionalities to give amines (**14**) and ureas (**15**).

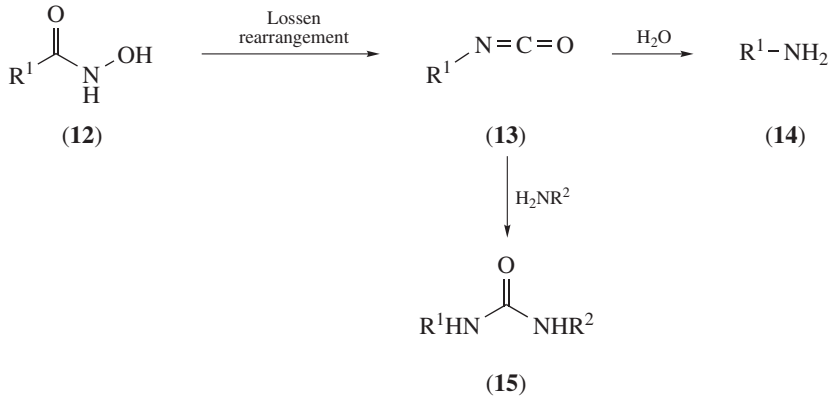

(**12**) (**13**) (**14**) (2)

(**15**)

Essentially, the present chapter reports the concerted and ionic rearrangements of hydroxylamines, oximes and hydroxamic acids. The rearrangement reactions are grouped according to mechanistic pathways and not by the functional group of the precursors. However, the sigmatropic rearrangements are generally characteristic of hydroxylamine derivatives while the ionic Beckmann rearrangement occurs essentially in oximes derivatives and the Lossen rearrangement in hydroxamic acid derivatives. Although it is beyond the scope of this account to provide exhaustive coverage of the subject, close attention has been paid to work published during the last 15 years.

II. THE [3,3]-SIGMATROPIC REARRANGEMENTS

The [3,3]-sigmatropic rearrangements have found many synthetic applications and particular use for the stereocontrolled preparation of carbon–carbon bonds (equation 3). The rearrangement proceeds through a six-membered ring transition state, usually in a chair conformation, unless prohibited by strong steric interactions. The stereochemical outcome of the reaction may be predicted and the diastereomeric ratio is usually very high. The [3,3]-sigmatropic rearrangements of 1,5-dienes and related compounds are reversible processes and the position of the equilibrium depends on the experimental conditions and substitution pattern.

The Cope rearrangement refers to the rearrangement of systems with no heteroatoms. The Claisen and aza-Claisen rearrangements are those of vinyl allyl ethers and amines, respectively. The hetero-Cope rearrangement is related to the rearrangement of 1,5-dienic systems with one heteroatom or more differing from oxygen or nitrogen. The activation energy for the rearrangements could be lowered and thus milder reaction conditions could be applied by the introduction of charge or suitable heteroatoms onto Cope systems.

Furthermore, the use of heteroatoms can lead to new functionalities on the rearrangement product. The hetero-Cope rearrangement has been reviewed[1–3].

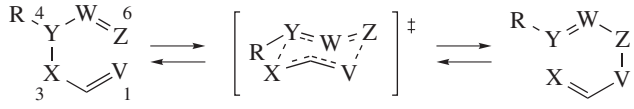

preferentially chair or almost chair conformation

(3)

V = W = X = Y = Z = C	Cope rearrangement
V = W = Y = Z = C, X = O	3-oxa-Cope or Claisen rearrangement
V = W = Y = Z = C, X = N	3-aza-Cope or 3-aza-Claisen rearrangement
V = W = Z = C, X = N, Y = O	3-aza-4-oxa-Cope rearrangement
V or W or Z ≠ C, X = N, Y = O	hetero-Cope rearrangement

Hydroxylamines, hydroxamic acids and related compounds with the adequate structure can rearrange by a [3,3]-sigmatropic shift in favourable reaction conditions. The reactions involving *N*-allyl-*N*-vinyl and *N*-vinyl-*O*-vinyl hydroxylamine derivatives as precursors are known as the 3-aza-Claisen and 3-aza-4-oxa-Cope rearrangements. Polyhetero-Cope rearrangements, which differ in the number, type and position of the heteroatoms, are known and are useful in synthetic processes. The rearrangements take place by concerted mechanisms through cyclic six-membered transition states. Their synthetic value stems from the ability to form a carbon–carbon bond at the expense of a carbon–nitrogen or an oxygen–nitrogen bond. If a concerted cyclic transition state is not formed, homolytic or heterolytic cleavage of the N–O bond can alternatively afford the [3,3] rearrangement product. The electronic nature of the oxygen and nitrogen substituents in the hydroxylamine derivatives is important in determining these alternative pathways[4].

Scheme 2 demonstrates that [3,3] rearrangements of hydroxylamines, oximes or hydroxamic acids are a versatile synthetic tool to prepare different heterocyclic rings such as indoles, imidazoles, benzofurans and oxazolidines which are useful synthetic precursors of natural products.

A. The 3-Aza-Claisen Rearrangements

The 3-aza-Claisen rearrangement concerning the rearrangement of allyl vinyl amines, contrary to its Cope analogue, has not been used extensively to form carbon–carbon bonds, probably due to the high temperatures (>180 °C) required for the uncatalysed variant and to the limited number of catalysts available for promoting the reaction at moderate temperatures[5] (equation 4).

Semiempirical calculations support a spin-paired chair-like transition state for the 3-aza-Claisen rearrangement[6]. The kinetic and thermodynamic parameters of the conversion of *N*-allyl-*N*-vinylamines (**16**, R = H, O^-, OH, F, NH^-) to imines (**18**, R = H, O^-, OH, F, NH^-) through transition state **17** were calculated. The geometry of transition state **17** is predicted to be intermediate between those of the transition states for the Cope and Claisen rearrangements and the predicted activation free energy for the 3-aza-Claisen rearrangement of **16**, R = H, falls between the experimental values for the other two, 31.3 kcal mol^{-1} and 40.8 kcal mol^{-1}, respectively. Substitution on the nitrogen atom changes both the geometry and the energy of the corresponding transition state

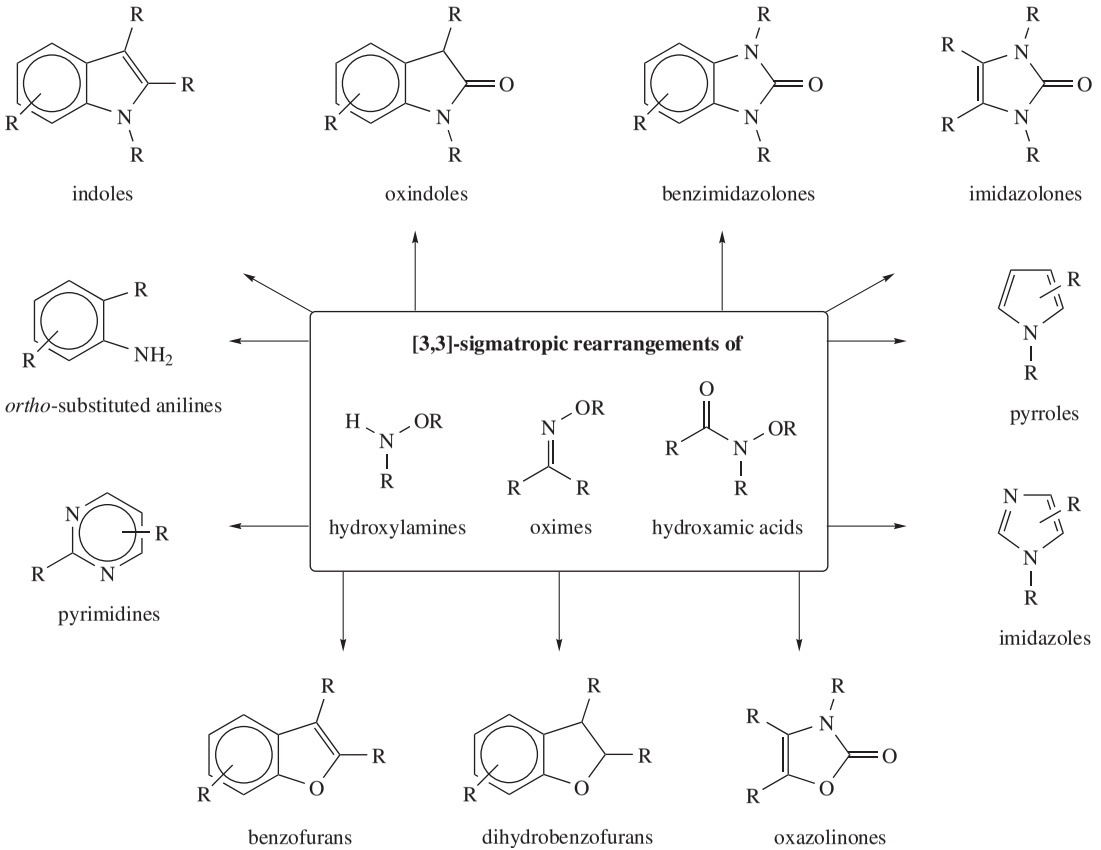
indoles
oxindoles
benzimidazolones
imidazolones
ortho-substituted anilines
[3,3]-sigmatropic rearrangements of
hydroxylamines
oximes
hydroxamic acids
pyrroles
pyrimidines
imidazoles
benzofurans
dihydrobenzofurans
oxazolinones

SCHEME 2

structure, and appropriate substitution might reduce the activation energies required for the rearrangement. The most promising substituents were predicted by MNDO calculations to be an atom or group bearing a negative charge adjacent to the nitrogen atom.

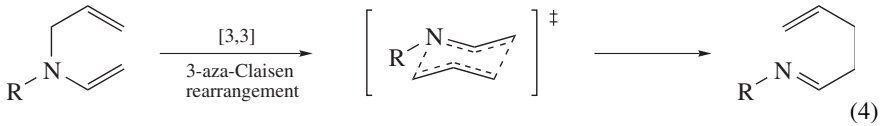

(4)

(**16**) (**17**) (**18**)

$$\Delta G^{\ddagger} \text{ (calc.)} = 35 - 40.1 \text{ kcal mol}^{-1} \text{ for R = H}$$

On thermolysis, appropriately substituted *N*-allyl-*N*-silyloxy enamines **19** undergo smooth [3,3]-sigmatropic rearrangements to the corresponding *N*-silyloxy imino ethers **20**[7] (equation 5). Two stereogenic centers are created but no reference to chiral induction is referred. High diastereoselectivity was observed and short reaction times favoured the *syn* *N*-silyloxy imino ether diastereomers.

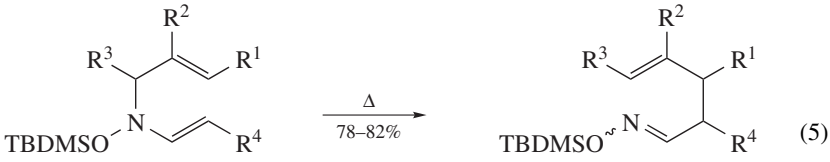

(5)

(**19**) (**20**)

R^1, R^2, R^3 = H, Me, Ph; R^4 = Tos, CO_2Me

B. The 3-Aza-4-oxa-Cope Rearrangements

1. The rearrangements through 3-aza-4-oxa-1,5-dienic systems

The 3-aza-4-oxa-Cope rearrangement in which the weak N−O bond is cleaved and a new carbon−carbon bond is generated (equation 6) is the most frequently used hydroxylamine rearrangement. Low temperature and moderated reaction conditions make this rearrangement an important synthetic tool.

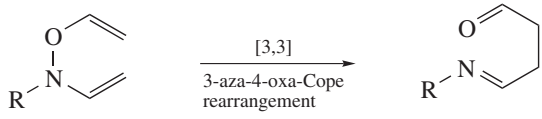

(6)

N-Vinylhydroxylamine derivatives **21** are good candidates for the hetero-Cope rearrangement due to their two adjacent functional groups, the hydroxylamine and the enamine nitrogen (equation 7). Sheradsky and colleagues[8] studied the Cope rearrangement of the *N*-aryl-*O*-vinylhydroxylamines (**22**). They observed that the nitrogen−oxygen bonds were highly unstable and cleaved spontaneously with rearrangement.

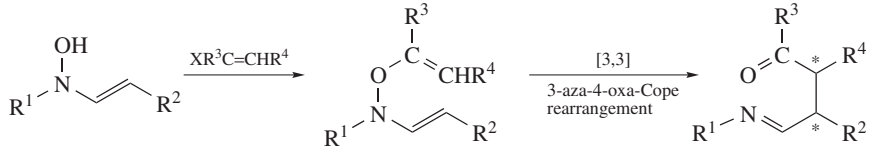

(**21**)

X = leaving group (7)

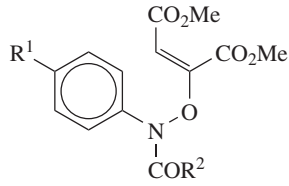

R^1 = Me, Cl, R^2 = Ph, OCH_2Ph

(**22**)

[3,3]-Sigmatropic rearrangement of *O*-vinyl derivatives of enehydroxylamines **23**, R^1 = H, Me, spontaneously provide 2,3-disubstituted cyclohexenones which gave fused pyrrolocyclohexenones after heating[9] (equation 8). A study of the rearrangement using deuterium-labelled compounds showed that no crossover occurs, indicating the intramolecular nature of the transformation. Enehydroxylamines **23** react with methyl propiolate (**24**, R^3 = H) and dimethyl acetylenedicarboxylate (**24**, $R^3 = CO_2Me$) to give the corresponding *O*-vinyl derivatives **25** that rearrange spontaneously, at room temperature, to **26**. Fused pyrrolocyclohexenones **28** are formed when **27**, resulting from cyclization of **26**, are refluxed in toluene.

During the synthesis of the aziridinomitoseno skeleton **29** Vedejs and colleagues[10] used an adaptation of the 3-aza-4-oxa-Cope method developed by Prabhakar and colleagues[9] to prepare bicyclic pyrrole ketones **28**. The introduction of a potentially removable nitrogen substituent, the *N*-benzenesulfanylethyl group, in compound **23**, $R^2 = C_2H_4SPh$ turns this transformation useful in the NH pyrrole synthesis **28**, R^2 = H (equation 8).

Indole derivatives **34** are accessible through 3-aza-4-oxa-Cope rearrangement of *O*-vinyl-*N*-phenylhydroxamic derivatives (**33**) (equation 9). Methyl propiolate (**24**, R^1 = H), dimethyl acetylenedicarboxylate[11] (**24**, $R^1 = CO_2Me$), vinyl acetate[12–14] (**31**) or electron deficient allenes[15] (**32**) were added to *N*-arylhydroxamic acids (**30**) to yield the corresponding *O*-substituted hydroxamic acids (**33**). A [3,3]-sigmatropic rearrangement followed by dehydration afforded the corresponding substituted indoles **34**, usually in high to excellent yields. This method was used to prepare the precursors of the antitumor antibiotic *CC-1065*[11] (**35**) as well as the phosphordiesterase inhibitors *PDE-I* (**36**, $R = NH_2$) and *PDE-II*[11] (**36**, $R = CH_3$).

Saczewski and colleagues[16] reported a similar pathway when the *N*-aryl-*N*-(4,5-dihydro-1*H*-imidazol-2-yl)hydroxylamine hydrochlorides **37** were refluxed in acetone in the presence of acetylenic derivatives **38** carrying electron-withdrawing substituents (equation 10). However, when **37** free bases were used, the adducts rearranged at room temperature, producing only the ketene aminals **39** in poor yields (equation 11).

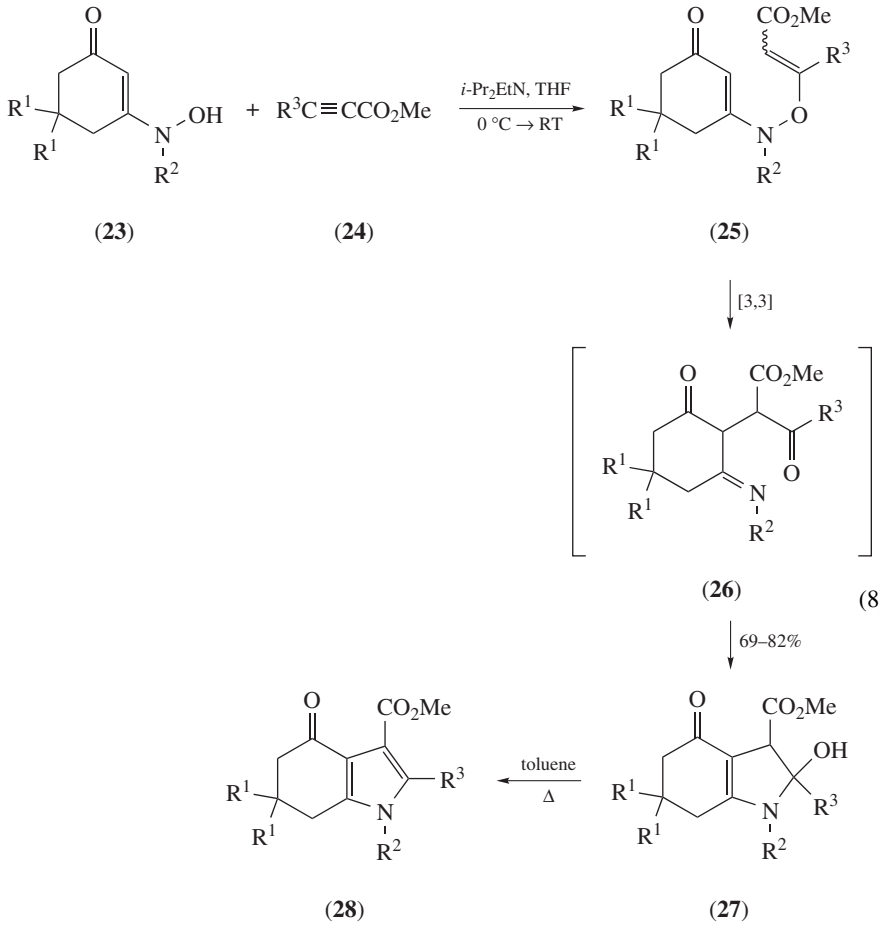

R^1= H, Me, R^2 = Me, C_2H_4SPh, R^3 = H, CO_2Me

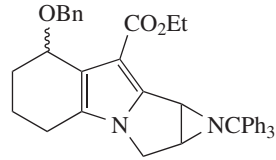

(**29**)

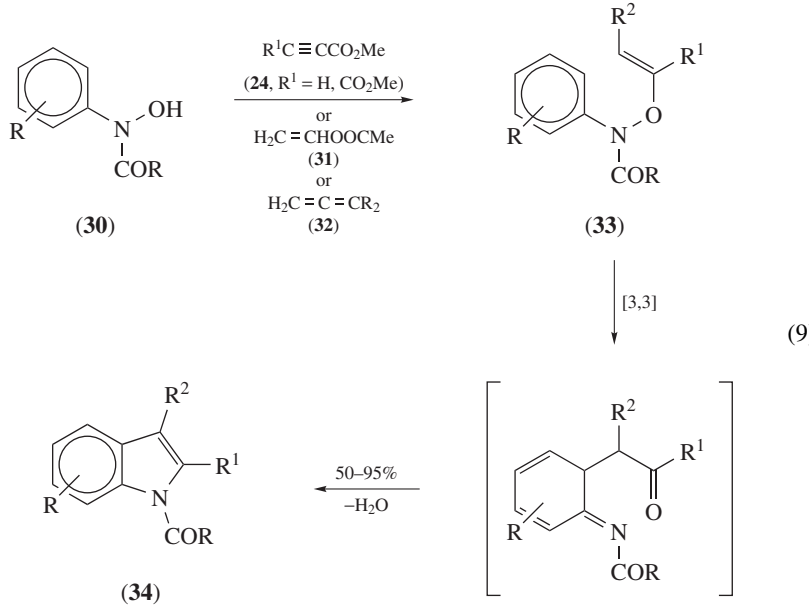

(9)

$R^1 = R^2 = H$; $R^1 = H$, $R^2 = CO_2Me$; $R^1 = R^2 = CO_2Me$; $R^1 = CR_2$, $R^2 = H$

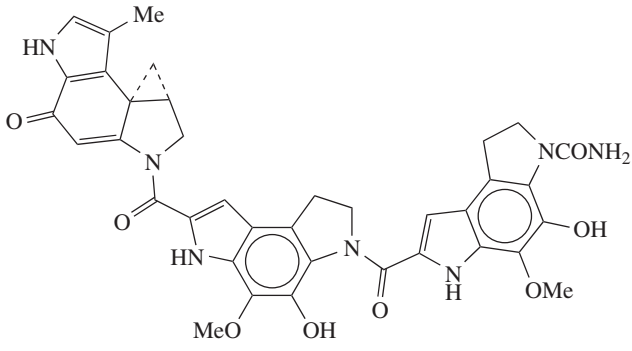

(35)

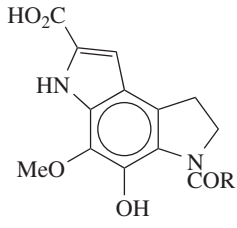

(36)

R = NH_2, CH_3

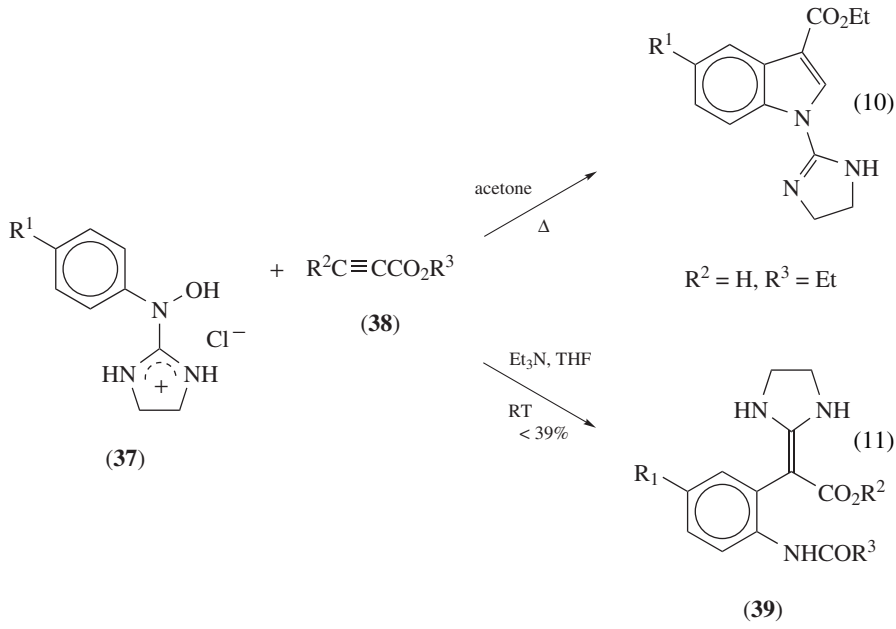

An alternative mechanism leading to compound **39** was proposed[16] (equation 12). The rearrangement product **40** undergoes a retro-ene reaction leading to reopening of the indoline ring with formation of **41**. In the presence of Et_3N, the intermediate **41** can subsequently undergo an intramolecular nucleophilic substitution reaction, giving the ketene aminal (**39**).

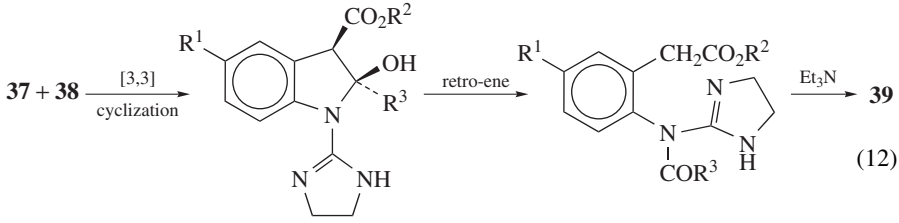

Prabhakar and colleagues[17] used ethyl propiolate (**38**, $R^1 = H$, $R^2 = Et$) to synthesize the *Amaryllidaceae* alkaloid Pratosine (**43**) (equation 13). On heating **42** in DMSO in the presence of water, a cascade of reactions is initiated, namely a [3,3]-sigmatropic rearrangement, ester hydrolysis, decarboxylation and cyclization, to afford Pratosine (**43**) in one step, albeit in modest yield.

In contrast, the *O*-aryl derivative of *N*-methyl-6-(hydroxyamino)-1,3-dimethylpyrimidine-2,4(1*H*,3*H*)-dione **44**, prepared by reaction with 2,4-dinitrofluorobenzene (DNFB), yields the corresponding barbiturate **45** by a spontaneous [3,3]-sigmatropic rearrangement[9] (equation 14).

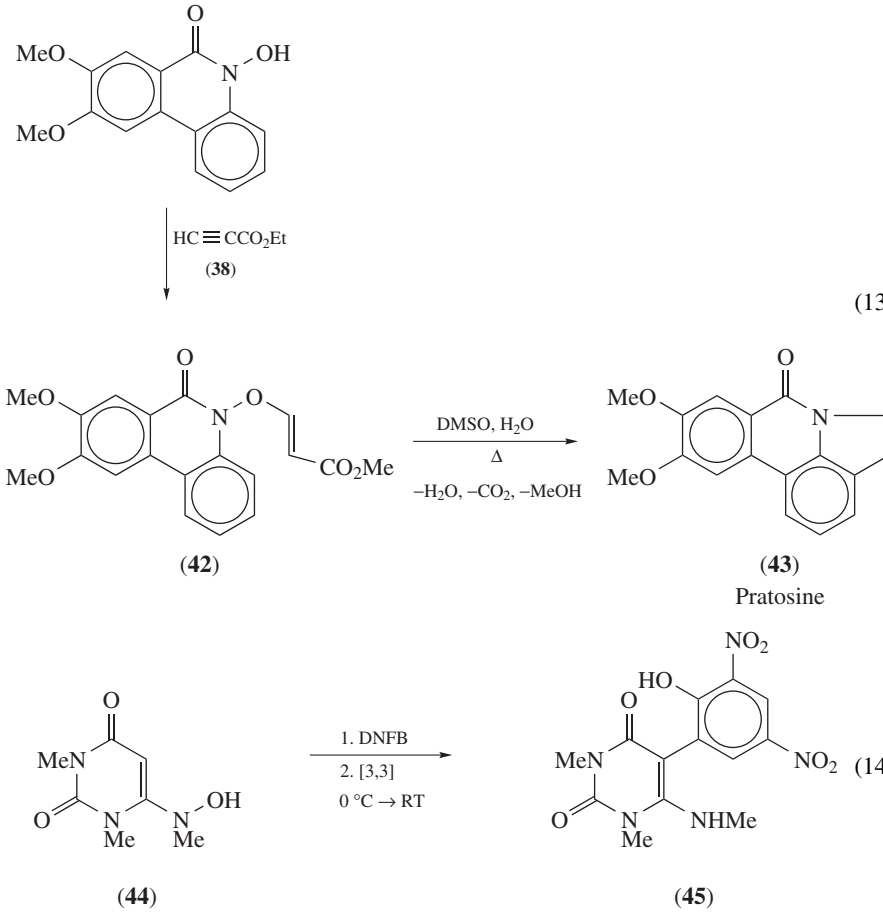

2. The rearrangements through hydroxylamine enol derivatives

3-Aza-4-oxa-Cope rearrangement of *N*-aryl-*O*-vinyl hydroxylamines or hydroxamic acids is an adequate and mild method to produce *ortho* alkylaniline derivatives in complex substrates. Recently, increasing attention has been focussed on the use of easily rearranging non isolable hetero-Cope systems bearing a central N−O bond. The rearrangement appears to be exothermic[18] and the inconvenience of its synthetic application is due to the synthesis and instability of the *O*-vinyl hydroxylamines. Different approaches have been explored to provide stable *O*-vinyl hydroxylamine derivatives and different heteroaromatic nuclei have been synthesized through [3,3]-sigmatropic rearrangements.

Coates and Said[19] reported the successful [3,3]-sigmatropic rearrangement of compound **46** at 110 °C, presumably through the enol tautomer **47** (equation 15).

The intermediate generated in pyrolysis of *N*-acylacetyl-*N*-phenylhydroxylamines **48** can form a 3-aza-4-oxa-1,5-diene system[20] (**50**) (equation 16). A homolytic cleavage of the O−H bond with subsequent rearrangement to the aniline radical, followed by recombination with the hydrogen radical to give the corresponding *O*-acyl hydroxylamine **49**,

was proposed. Heating **48** at reflux in toluene or xylene provided the [3,3]-sigmatropic rearrangement product **51** that, after cyclization, decarboxylation and dehydration, gave **52** in 53–67% yield. The presence of a radical intermediate is supported by yield increase when the rearrangement proceeds in the presence of a radical initiator, whereas no rearrangement product is identified in the presence of a radical trapping agent.

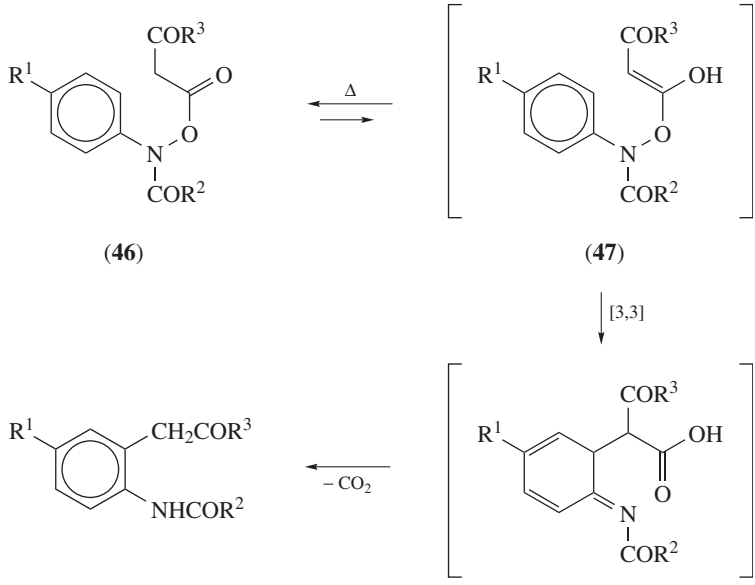

(15)

R^1 = H, Me, Cl, CO_2Me, R^2 = Me, Ph, R^3 = Me, Ph, OEt

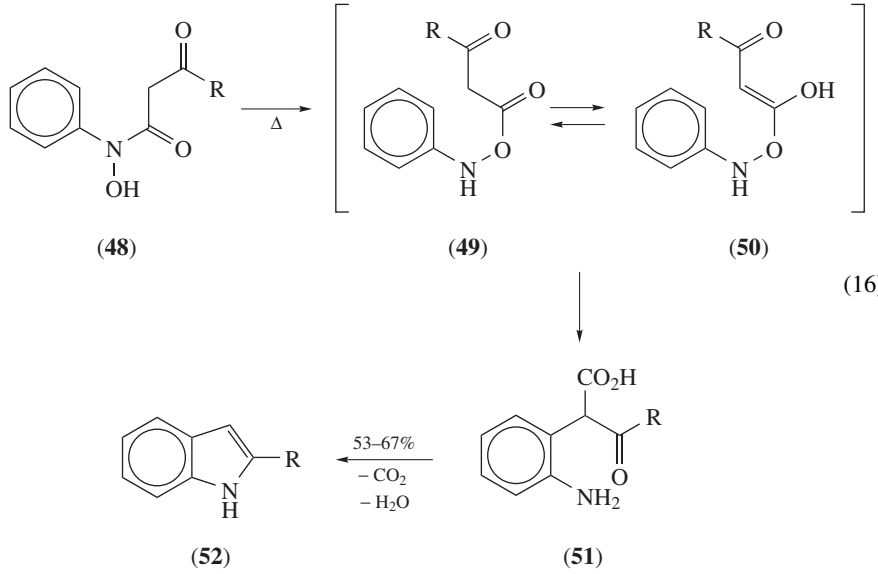

(16)

The 3-aza-4-oxa-[3,3]-sigmatropic rearrangement in which the vinyl ether grouping is generated simply by enolization of an *O*-acyl substituent has been explored (equation 17). The stable *O*-derivatives (**53**) are synthesized by a direct acylation of the hydroxyl group of the corresponding *N*-arylhydroxylamine[21] or hydroxamic acid[22]. To avoid the very high reaction temperatures required to promote the rearrangement, base catalysts have been used to form the enol **54**, sometimes in the presence of silylating agents[22]. Treatment of the *O*-acyl derivatives (**53**) with base forms the corresponding enolates (**54**) and provides the adequate 3-aza-4-oxa-1,5-dienes framework required for the [3,3]-sigmatropic rearrangement. The use of carbanion stabilizing groups α to the carbonyl function in the acyl fragment **53** is necessary to prevent a rapid reversion to the parent hydroxamic acid and to favour the [3,3]-sigmatropic rearrangement at low temperature.

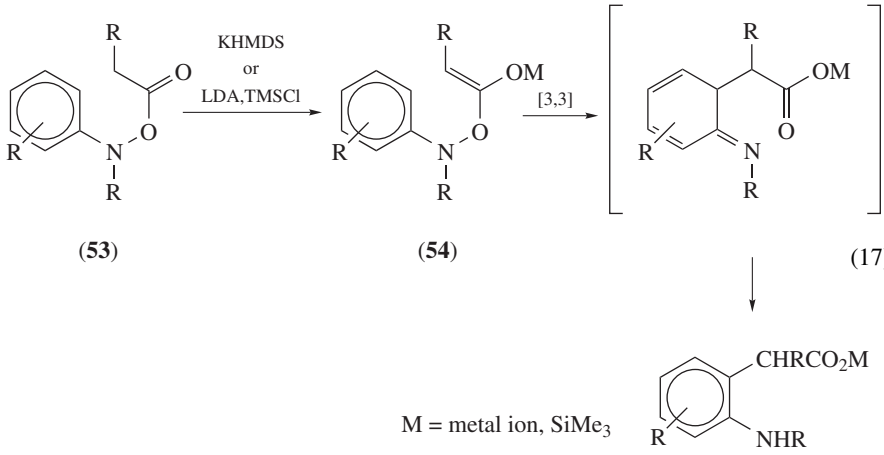

(**53**) (**54**) (17)

Endo and Shudo[21] observed that *O*-acyl-*N*-arylhydroxamic acids (**55**, $R^1 = COMe$) rearranged at a lower rate than the hydroxylamine analogues (**55**, $R^1 = t$-Bu) (equation 18). Succinic acid derivatives **57**, resulting from side-chain rearrangement, were isolated together with the major product **56**. The authors explained these facts by the sp^2 character of the *N*-atom in hydroxamic acid derivatives (**55**, $R^1 = COMe$) and the consequent formation of a disfavoured chair-type six-membered cyclic transition state during the [3,3]-sigmatropic rearrangement.

Spirocyclic oxindole **60** was synthesized by [3,3]-sigmatropic rearrangement of the *N*-phenyl-*O*-acylhydroxamic acid **58** (equation 19). The potassium enolate formed by treatment of **58** with potassium hexamethyldisilazide at low temperature rearranged to **59**, which easily cyclized to the spirocyclic oxindole **60**[23]. Spirooxindoles were previously synthesized by Wolff and Taddei[24]. The spirooxindole **60** was formed in 51% yield from cyclohexanecarboxylic acid after heating the preformed lithium salts of phenyl hydrazide **61** to 205–210 °C.

O-acyloxybenzanilides (**63**) are formed by a thermally induced [3,3]-sigmatropic rearrangement of *O*-acyl-*N*-aryl hydroxamic acid derivatives **62**[22] (equation 20). However, in the presence of LDA and TMSCl the rearrangement proceeds at low temperature and the amide **64** is formed in poor to moderated yields. Substituted oxindoles are obtained by dehydration of **64** with *N*,*N*′-dicyclohexylcarbodiimide (DCC) (equation 21).

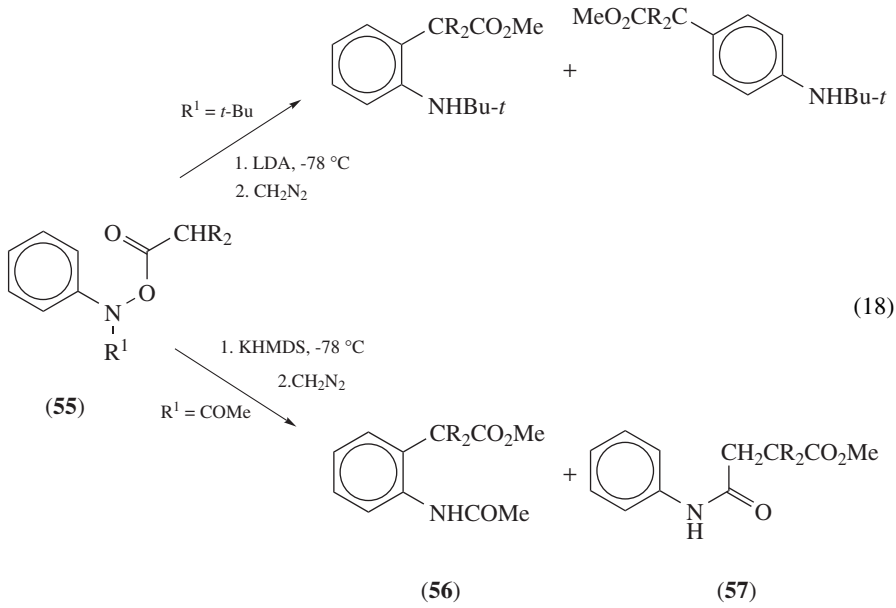

(**55**) (18)

(**56**) (**57**)

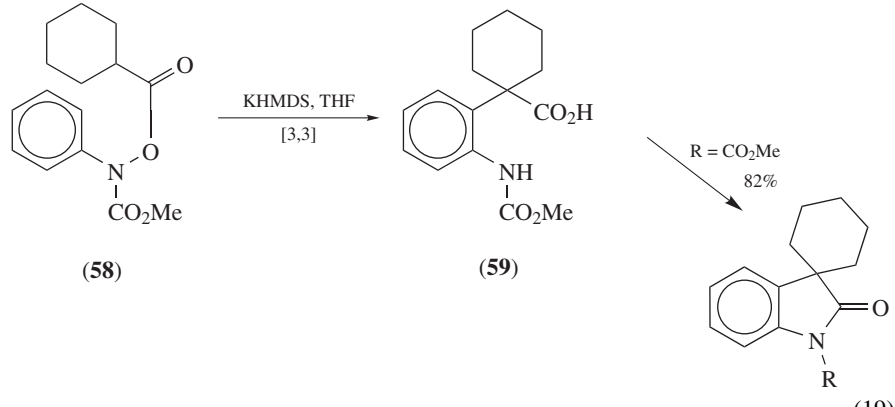

(**58**) (**59**) (**60**) (19)

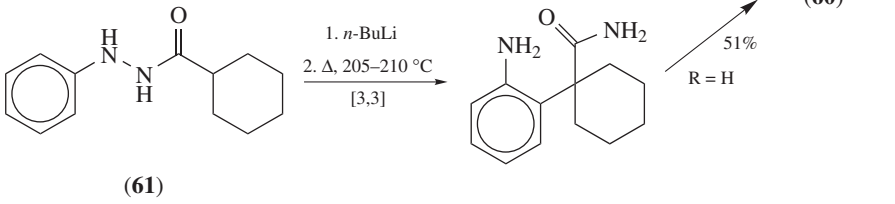

(**61**)

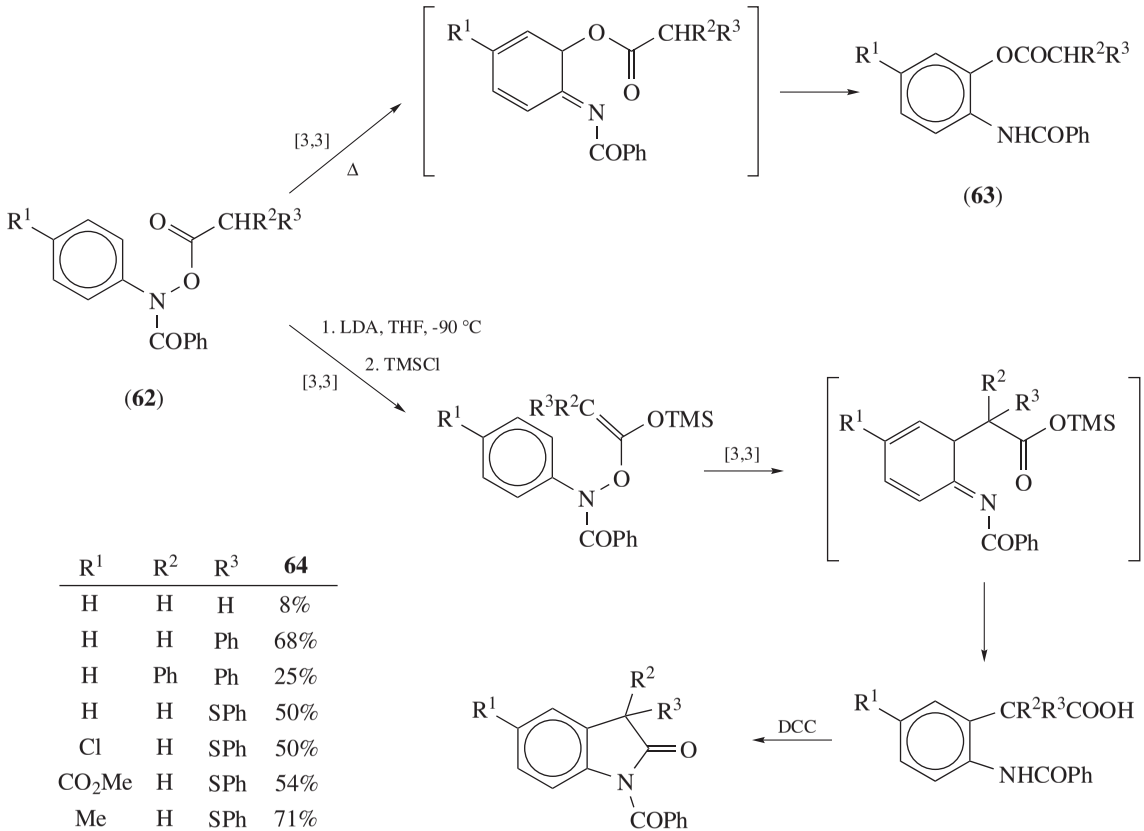

(20)

(21)

R^1	R^2	R^3	**64**
H	H	H	8%
H	H	Ph	68%
H	Ph	Ph	25%
H	H	SPh	50%
Cl	H	SPh	50%
CO_2Me	H	SPh	54%
Me	H	SPh	71%

A formal synthesis of (±)-Eseroline (**69**) via a 3-aza-4-oxa-Cope rearrangement was reported[25]. An *N*-aryl *N*-hydroxycarbamate was reacted with 2-phenylsulfanylpropanoic acid to yield the *O*-acylhydroxamic acid derivative **65**, R = H that rearranged in the presence of potassium bis(trimethylsilyl)amide. The [3,3] and [3,5] rearrangement products, respectively **66** and **67**, were formed (equation 22). If the *para*-substituted hydroxamic acid **65**, R = OCOBu-*t* is used, no [3,5] rearrangement product is observed and the [3,3] rearrangement product **68** is the only product formed (equation 23). The authors proposed two parallel mechanisms, a concerted pathway and an ionic mechanism by an ion-pair recombination.

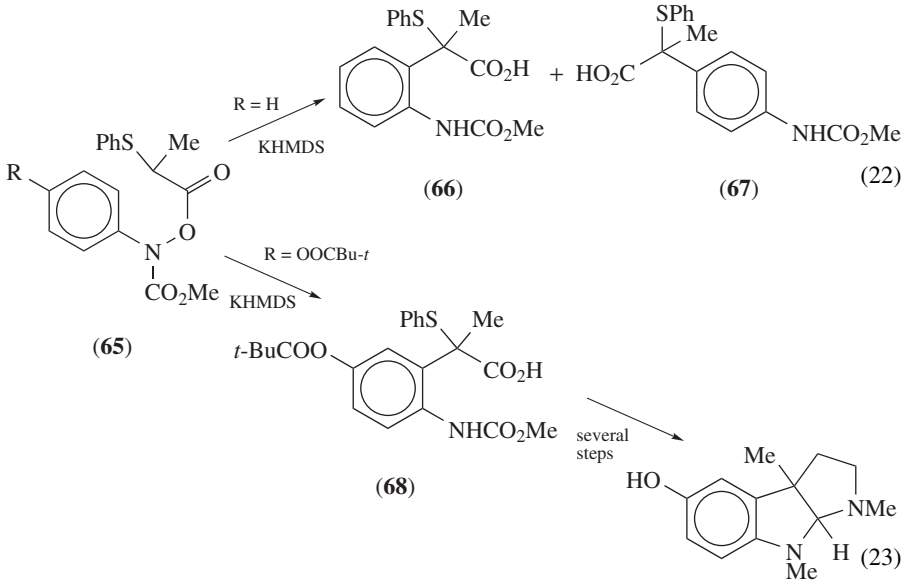

Similarly, a 3-aza-4-oxa-Cope rearrangement of *O*-carbamate derivatives of enehydroxylamines (**70**) in basic medium was reported[9] (equation 24). The base promoted the formation of the imidate ion **71**, providing the adequate 1,5-diene system to [3,3]-sigmatropic rearrangement. Sodium hydride was found necessary to induce the **70**, $R^1 = H$, $R^2 = CH_2$, transformation while experiments in refluxing toluene and in the presence of the weaker base *i*-Pr_2EtN were unsuccessful. However, the pyrimidine derivative **70**, $R^1R^1 = =O$, $R^2 = NMe$, rearranged in refluxing toluene in the presence of *i*-Pr_2EtN to yield **72** in 55% yield.

In adequate basic conditions or on heating, activated *O*-acylhydroxamic acids **73** isomerize to the corresponding enols **74** to generate an adequate 3-aza-4-oxa-1,5-dienic system suitable for a [3,3]-sigmatropic rearrangement (equation 25).

Activated *N*-alkyl-*O*-acylhydroxamic acid derivatives **75** undergo base catalysed rearrangement to give 2-acyloxyamides **76** in good to excellent yields (50–100%)[26] (equation 26). These precursors of 2-hydroxyamides (**77**) are good intermediates to prepare ethanolamines, oxindoles and oxazolidinediones.

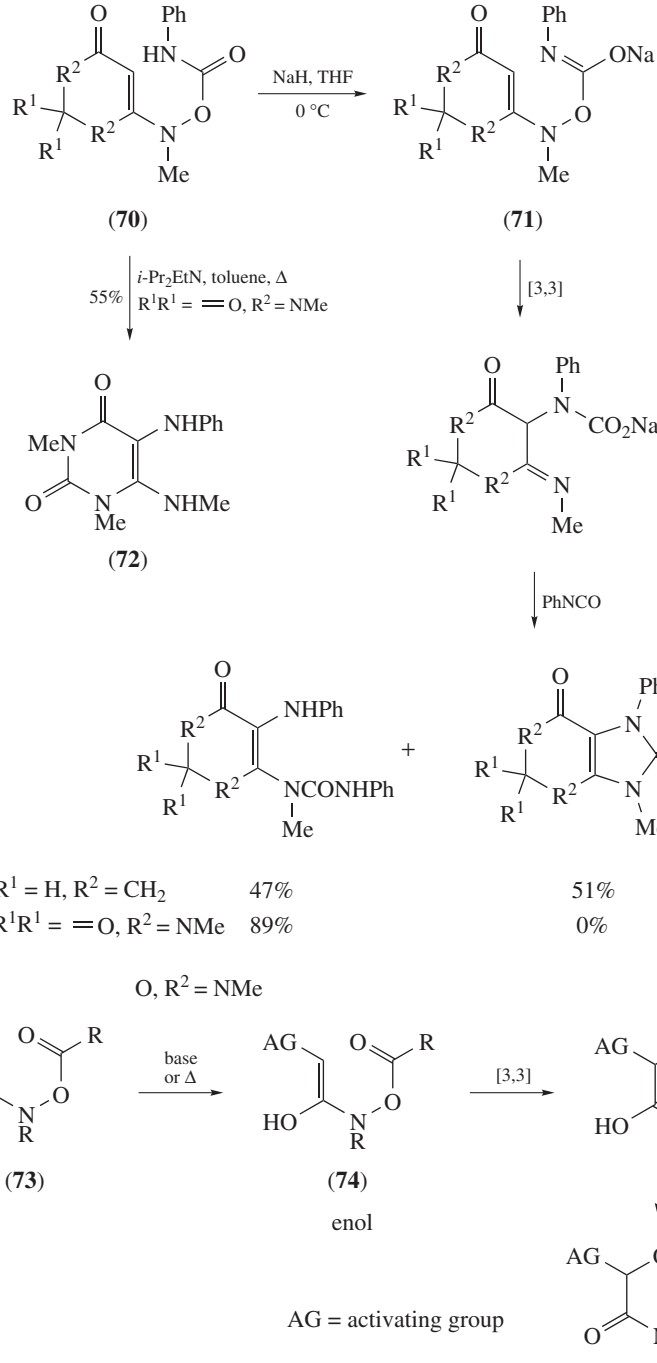
NaH, THF
0 °C
(70)
(71)
55%
i-Pr2EtN, toluene, Δ
R1R1 = =O, R2 = NMe
[3,3]
(72)
PhNCO
+
R1 = H, R2 = CH2 47% 51%
R1R1 = =O, R2 = NMe 89% 0%
O, R2 = NMe
base
or Δ
[3,3]
(73)
(74)
enol
AG = activating group

(24)

(25)

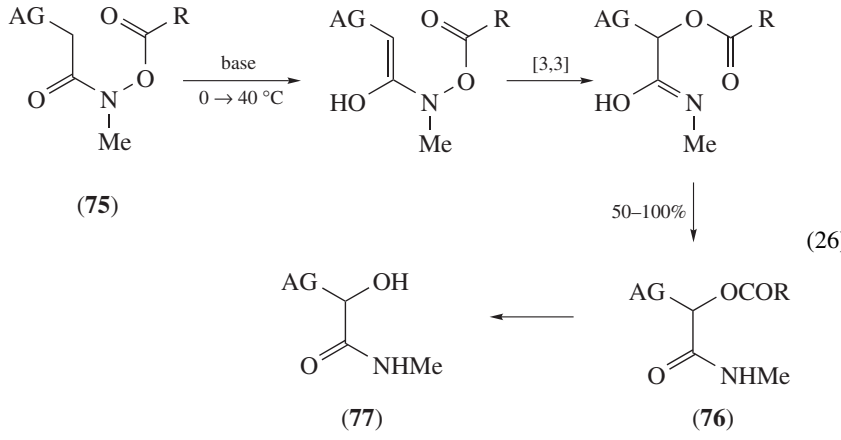

(**75**) (**77**) (**76**) (26)

AG = CH=CH$_2$, Ph, Ar, CH=CHPh, *p*-Tol, R = Me, Et, *t*-Bu, Ph, Ar

A similar thermal rearrangement was reported[27] during the synthesis of the natural benzoxazinone **78**, an allelochemical isolated from plants belonging to the *Poaceae* family.

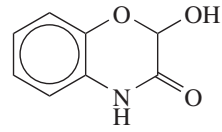

(**78**)

However, malonic acid derivatives **79** failed to rearrange and afforded isozaxole derivatives **84** by direct attack of the anions **83** on the ester group of the *O*-acyl substituents, followed by the elimination of water[28] (equation 27). Rearrangements are slow in the absence of base and **84** is the predominant product. When LiHMDS, NaHMDS or KHMDS are used, the failure to form the rearrangement product **81** was explained by the presence of the counter-ion (M^+) and the assumption that the enolate **83** could not adopt a cyclic chair conformation in the transition state. Triethylamine, the Hunig's base (*i*-Pr$_2$EtN) and phosphazene superbase **80** promoted the formation of the [3,3] rearrangement product **82**. Both aromatic and aliphatic derived *O*-acyl groups were tolerated in the reaction and the presence of electron-withdrawing groups (4-$O_2NC_6H_4$ and 4-ClC_6H_4) increased the observed rate while electron-donating groups (4-MeC_6H_4 and 4-$MeOC_6H_4$) decreased it. The rate and yield of the reaction were heavily dependent upon the steric nature of the *N*-alkyl substituent[29]. Studies on the mechanism demonstrated that either the acidity of the α-carbonyl protons or the nature of the nitrogen leaving group are rate-determining. While the mechanism for the transformation still remains unclear, the observation that crossover of acyloxy substituents occurs during the course of the reaction indicates that a free acyloxy anion is likely to be involved. Homolytic cleavage of the N−O bond in *O*-acylhydroxamic derivatives was previous reported by Clark and colleagues in the rearrangement of activated *O*-benzoylhydroxamic acid derivatives in the presence of Bu_3SnH

and AIBN in refluxing benzene[30,31]. In addition to the rearrangement product, β-lactam derivatives and the corresponding reduced amides were detected.

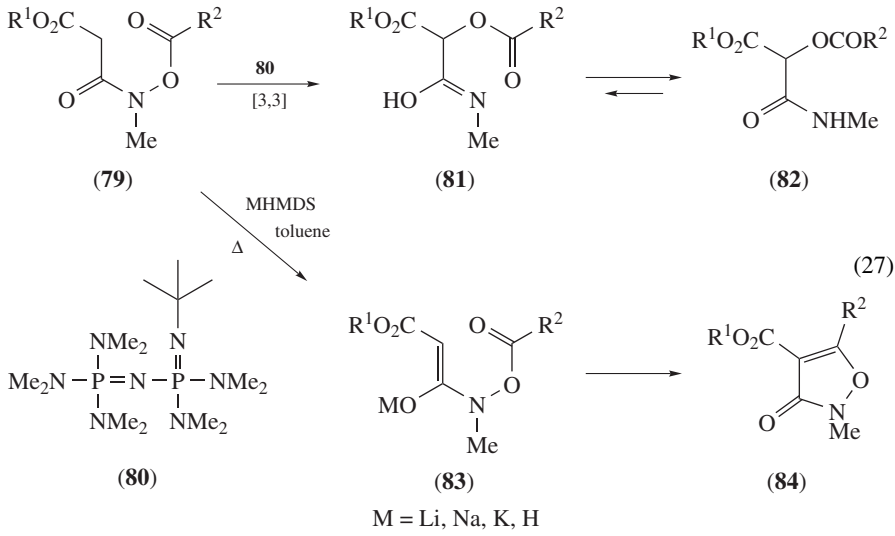

(27)

[3,3]-Sigmatropic rearrangement of *N*,*O*-divinyl hydroxylamine derivatives **86** and **87**, generated *in situ* by treatment of *N*,*O*-diacyl-*N*-alkylhydroxylamines **85** with base, was reported[3,32] (equation 28). The rearrangement product **90** can be rationalized in terms of [3,3]-sigmatropic shifts of ester-amide dienolated *N*,*O*-diacyl hydroxylamines, **87** to **89**. The presence of **88** can be explained in terms of a [3,3]-sigmatropic rearrangement of the ester enolates **86**. Since a cyclic six-membered intermediate is involved in [3,3]-sigmatropic rearrangement, a favourable conformation for [3,3]-shifts can be expected and, consequently, a sterically bulky substituent on the nitrogen atom increased the yield of the rearrangement product **90**, $R^1 = t$-Bu (65– 75%).

In the case of the rearrangement of *O*-phenylacetyl-*N*-methylsulfenylacetyl-*N*-methylhydroxylamine **85**, $R^1 = Me$, $R^2 = CH_2SMe$, $R^3 = Ph$, the unexpected [3,5] rearrangement product **91** was observed and isolated in 10% yield along with the [3,3] rearrangement products **90**, $R^1 = Me$, $R^2 = CH_2SMe$, $R^3 = Ph$[3]. The [3,5] rearrangement requires a sulfur substituent on the amide enolate component. The [3,5] rearrangement product is also obtained when compound **85**, $R^2 = CH_2SMe$, $R^3 = C_2H_2Ph$ is treated with KHMDS at low temperature. The authors proposed that this [3,5] rearrangement proceeds via an intermolecular concerted pathway involving a polarized transition state of the form $N^{\delta+}-O^{\delta-}$, in which the electrostatic factor predominates over the orbital symmetry factor.

An analogous method was used by Endo and colleagues[3] in α-amination of unreactive carboxylic acids. Treatment of *N*-acylhydroxylamine *O*-carbamates **92** by KHMDS or LDA followed by [3,3]-sigmatropic rearrangement and decarboxylation provided α-amino acid analogues **93** (equation 29).

Aliphatic 3-aza-4-oxa-Cope rearrangement of ester-amide dienolates increases the synthetic utility of anionic [3,3]-sigmatropic rearrangement initiated by N−O bond cleavage. Treatment of the enehydroxylamine **94** with KHMDS in the presence of TMSCl at −80 °C provided a mixture of *N*,*O*-disilylated **95** and *O*,*O*-disilylated **96** derivatives[9] (equation 30). Both of these would, on [3,3]-sigmatropic rearrangement, provide the corresponding silyl ethers **97** and **98**, from which **99** and **100** are obtained on workup.

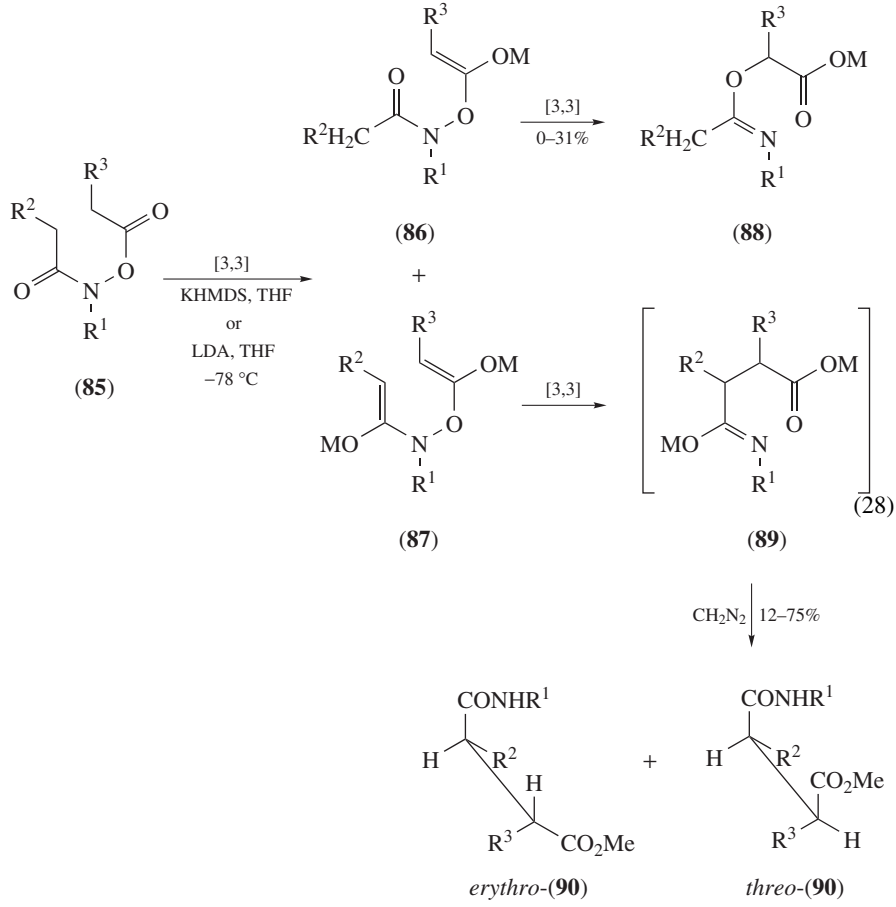

M = K, Li, R^1 = *t*-Bu, Me, R^2 = H, Cl, Ph, OMe, CH_2SMe, R^3 = H, Me, Ph, Ar, C_2H_2Ph

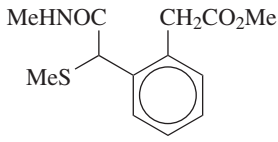

(**91**)

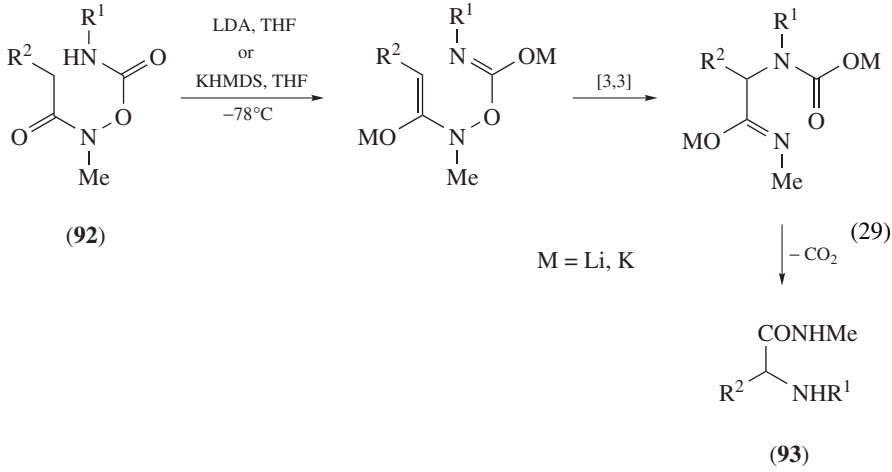

(**92**)

(**93**)

(29)

3. The rearrangements of oxime derivatives

Enehydroxylamines (**102**) are invoked as intermediates in the rearrangement of *O*-vinyl, acyl or aryl oximes (**101**) (equation 31). Varlamov and coworkers[33] demonstrated that the heterocyclization of ketoximes (**103**) with acetylene in super basic medium and in the presence of metal hydroxides proceeds by a [3,3]-sigmatropic rearrangement of the enehydroxylamine **105** of the corresponding oxime vinyl ethers **104** (equation 32). The unreactivity of 3-methyl-2-azabicyclo[3.3.1]nonan-9-one oxime (**106**) in the same reaction conditions was explained by its inability to isomerize to the corresponding enehydroxylamine.

Tundo and colleagues[34, 35] reported the synthesis of 4-oxazolin-2-one **110** by [3,3]-sigmatropic rearrangement of an enehydroxylamine derivative **109** resulting from the reaction of a ketoxime with dimethyl carbonate at high temperatures and in basic medium (equation 33).

The authors proposed that **109** may be formed through a pathway involving deprotonation of the oxime ester **107** to give a resonance-stabilized enamino anion **108** which then undergoes alkylation. The resulting enehydroxylamine **109** after [3,3]-sigmatropic rearrangement and cyclization yields the corresponding 4-oxazolin-2-one **110**. This mechanism is supported by the observation that in *O*- and *N*-methylation, products resulting from normal oxime alkylation competition are detected. The required geometry of the highly ordered transition state required by the sigmatropic rearrangement is perhaps not achieved when a more strained C=C bond is involved as it occurs in the rigid cyclopentanone ring **107**; $R^1R^2 = -(CH_2)_3-$ where no 4-oxazolin-2-one **110** was observed[35].

Recently, [3,3]-sigmatropic rearrangement of the adducts **112**, formed by reaction of aminoximes **111** and dimethyl acetylenedicarboxylate **38**, was used to synthesize pyrimidine carboxylates derivatives **115**, reversible inhibitors of the hepatitis C virus NS5B polymerase (equation 34). The aminoxime isomer **112** undergoes a [3,3]-sigmatropic rearrangement to afford the intermediate **113** which, after tautomerization of the amidine, could cyclize to give the imidazole **114** and compound **115**, formed by nitrogen attack on the ester substituent.

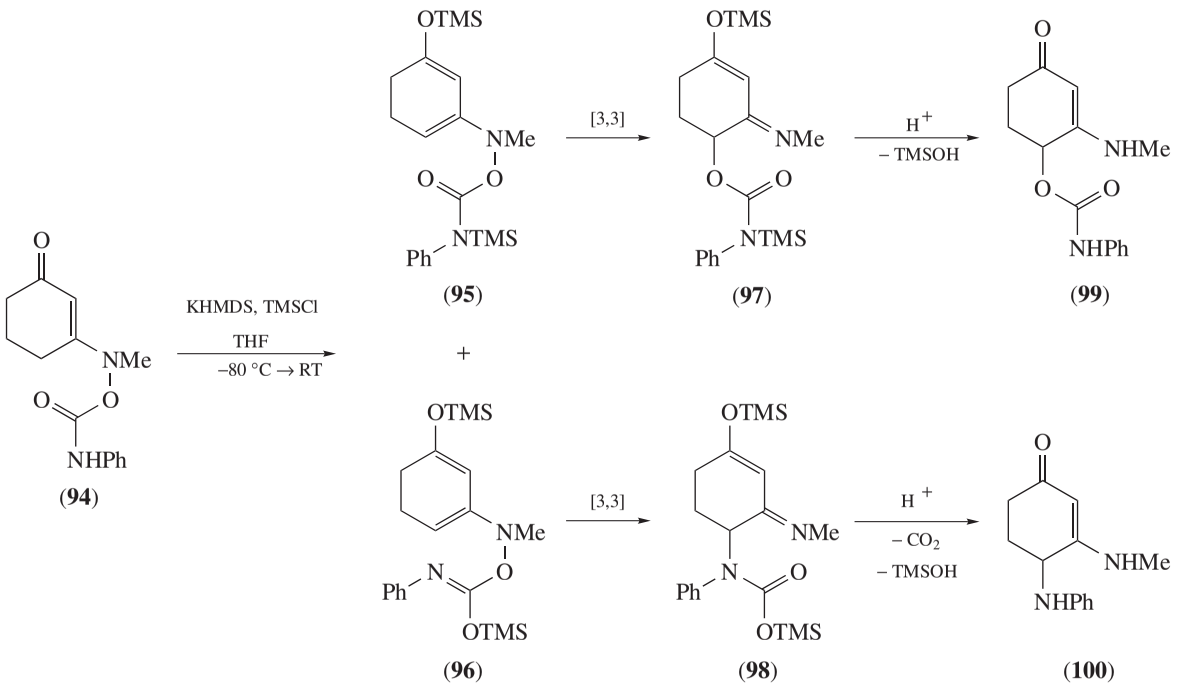
O
NMe
O
O
NHPh
(94)
KHMDS, TMSCl
THF
–80 °C → RT
OTMS
NMe
O
O
NTMS
Ph
(95)
+
OTMS
NMe
Ph
N
O
OTMS
(96)
[3,3]
OTMS
NMe
O
O
NTMS
Ph
(97)
[3,3]
OTMS
NMe
Ph
N
O
OTMS
(98)
H+
– TMSOH
O
NHMe
O
O
NHPh
(99)
H+
– CO2
– TMSOH
O
NHMe
NHPh
(100)

(30)

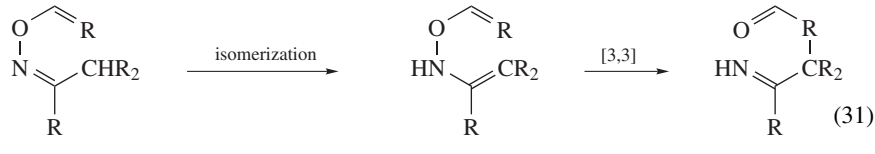

(**101**) (**102**) (31)

R = CH_2, CHR, O

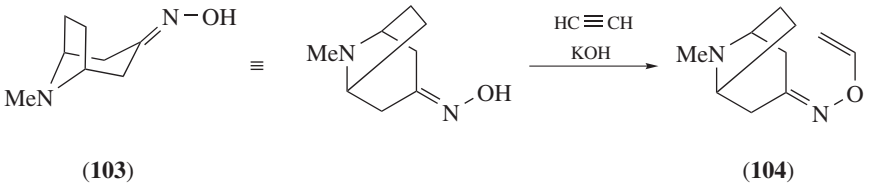

(**103**) (**104**)

(**106**) (**105**) (32)

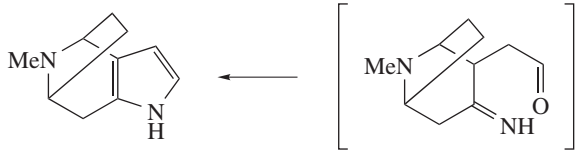

Lantos and colleagues[36] reported a different imidazole synthesis via hetero-Cope rearrangement. Oximes **116** reacted with benzenecarboxidoyl chloride affording adducts **117** that readily underwent a [3,3]-sigmatropic rearrangement at high temperatures (equation 35) to substituted imidazoles **118**.

The [3,3]-sigmatropic rearrangement of *O*-aryl oximes was first described by Sheradsky[37] and it has been used as an adequate route to benzofuran ring, a structural unit largely present in natural products.

One potential approach for the preparation of benzofuran derivatives involves the acid-catalyzed cyclization of *O*-aryl oximes **119**[38,39] (equation 36). The transformation is analogous to well-known Fisher indole synthesis. The reaction proceeds through a [3,3]-sigmatropic rearrangement of enehydroxylamine **120** to compound **121** followed

by condensation to form the benzofuran ring **122**. On the basis of the proposed mechanism, an electron-donating substituent on the aromatic ring would favour the [3,3]-sigmatropic rearrangement. Conversely, electron-withdrawing substitution will inhibit the [3,3]-sigmatropic rearrangement process and when R = F the rearrangement required elevated temperatures and low yields (0–47%) of rearrangement product were observed.

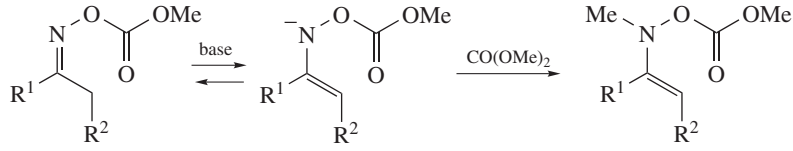

(**107**) (**108**) (**109**)

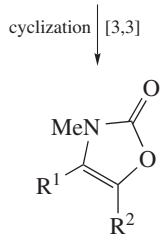

(33)

(**110**)

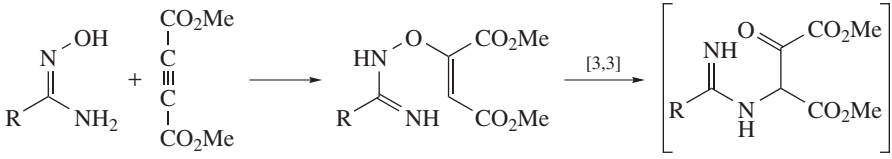

(**111**) (**38**) (**112**) (**113**)

(34)

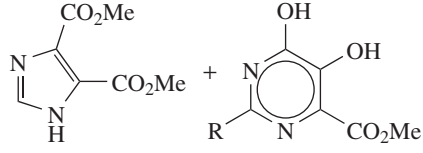

(**114**) (**115**)

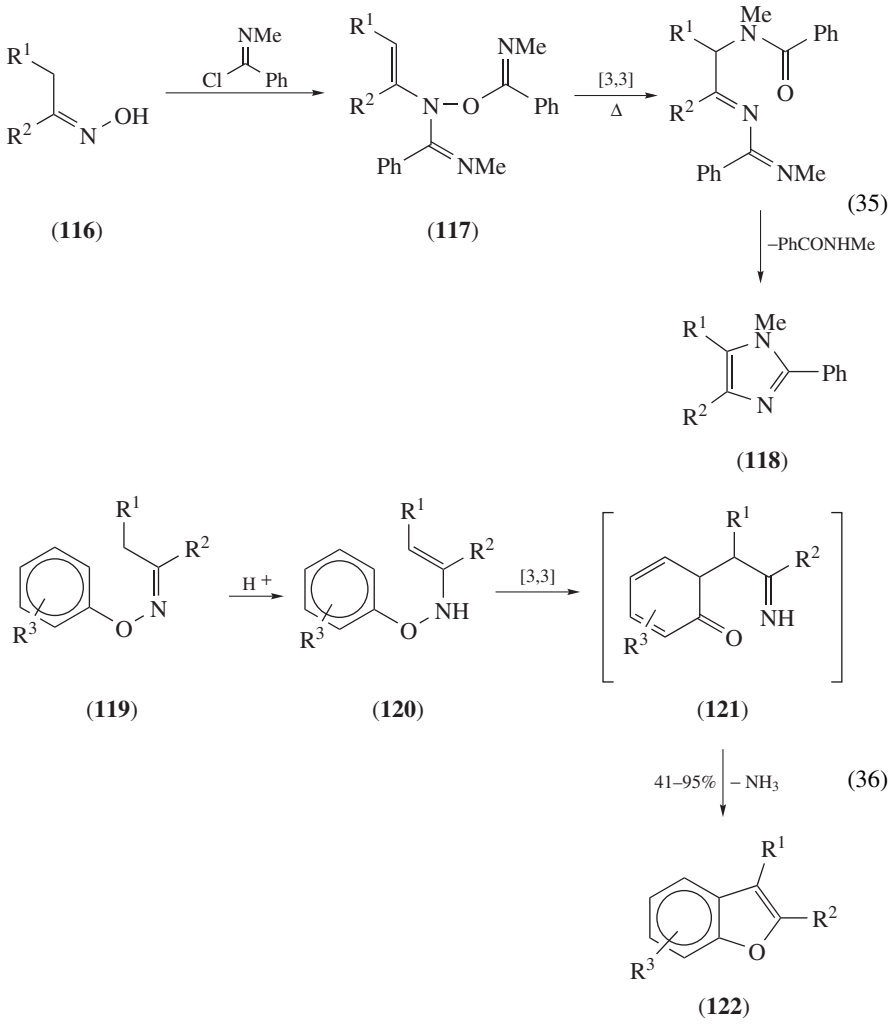

R^1 = H, 2-Me, 3-Me, 4-Me, 3-OMe, 2-Cl, 3-Cl, 4-Cl, R^2 = Me, R^3 = H, Me, R^1R^2 = -$(CH_2)_4$-

Laronze and colleagues[40,41] used a similar procedure to built the dihydrofuran ring of the marine sesquiterpene Aplysin (**123**).

However, when *O*-aryl oximes **124** were treated with a Lewis acid, like $ZrCl_4$, a different rearrangement was observed[42] (equation 37). An intramolecular migration of the imino group from the oxygen to the *ortho* position of the *O*-aryl group occurs via an electron-deficient nitrogen intermediate. The authors proposed an ionic mechanism via a tight ion-pair intermediate **125** analogous to the iminium cation formed in the Beckmann

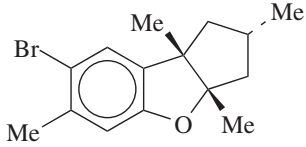

(**123**)

fragmentation (see Section VI). The formation of this intermediate presumably prevents the Beckmann rearrangement and promotes rearrangement of the imino group to the vicinal *ortho* position of the aryl group.

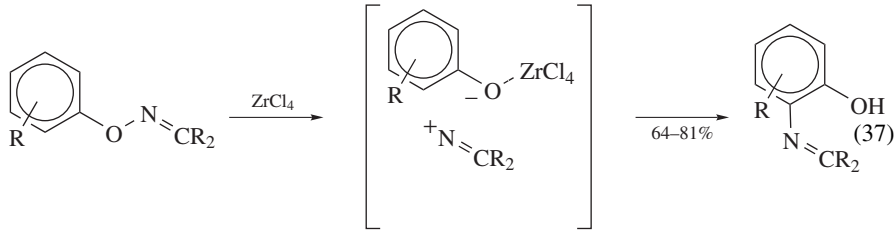

(**124**) (**125**)

Nevertheless, an enehydroxylamine intermediate was recently proposed by Tomkinson and colleagues[43] for the direct α-oxycarbamoylation of carbonyl compounds through a [3,3]-sigmatropic rearrangement (equation 38). Previously, α-oxycarbonates were synthesized by an analogous method[44]. Condensation of *N*-methyl-*O*-carbamoyl hydroxylamines **126** or *N*-methyl-*O*-alkoxyformate hydroxylamines **126** with aldehydes and both acyclic and cyclic ketones **127** yield the iminium ion **128** in equilibrium with both enehydroxylamines **129** and **130** (equation 38). Concerted [3,3]-sigmatropic rearrangement of **129** and **130** yields, respectively, the imines **131** and **132** that, after hydrolysis, provide the two α-oxycarbonyl isomers **133** and **134** in 50–88% yields. The uselessness of this method to functionalize primary carbon center allows complete regiospecificity in the reaction of non-symmetrical methyl ketones **127**, $R^2 = H$, $R^3 = i$-Pr, Bu.

A new synthetic method of benzofuran was reported[45] (equation 39). The [3,3]-sigmatropic rearrangement of *N*-trifluoroacetyl enehydroxylamines **136** obtained *in situ* by acylation of oxime ethers **135** in the presence of trifluoroacetic anhydride lead to the synthesis of cyclic or acyclic dihydrobenzofurans **138**. The effects of base and temperature on the reaction products were studied. A similar pathway to that of Fisher indolization was proposed. The acylimine formed by the [3,3]-sigmatropic rearrangement of the *N*-trifluoroacetyl enehydroxylamine **136** gave the dihydrobenzofuran **137** by an intramolecular cyclization or the benzofuran **138** after elimination.

During the synthesis of the natural and biologically active natural products, Stemofuran A[46] (**139**), Eupomatenoid 6[46] (**140**) and Coumestan[45] (**141**), the [3,3]-sigmatropic rearrangements of a hydroxylamine were used.

The use of a chiral auxiliary to induce stereochemical selectivity in the 3-aza-4-oxa-Cope rearrangement of *O*-aryl oximes **142** was reported by Citivello and Rapoport[47]

during the synthesis of **143**, precursor of (−)- and (+)-Aflatoxins B_1 (**144**), B_2 (**146**), G_1 (**145**) and G_2 (**147**) (equation 40). The diastereomeric ratio of 60/40 indicated little chiral induction.

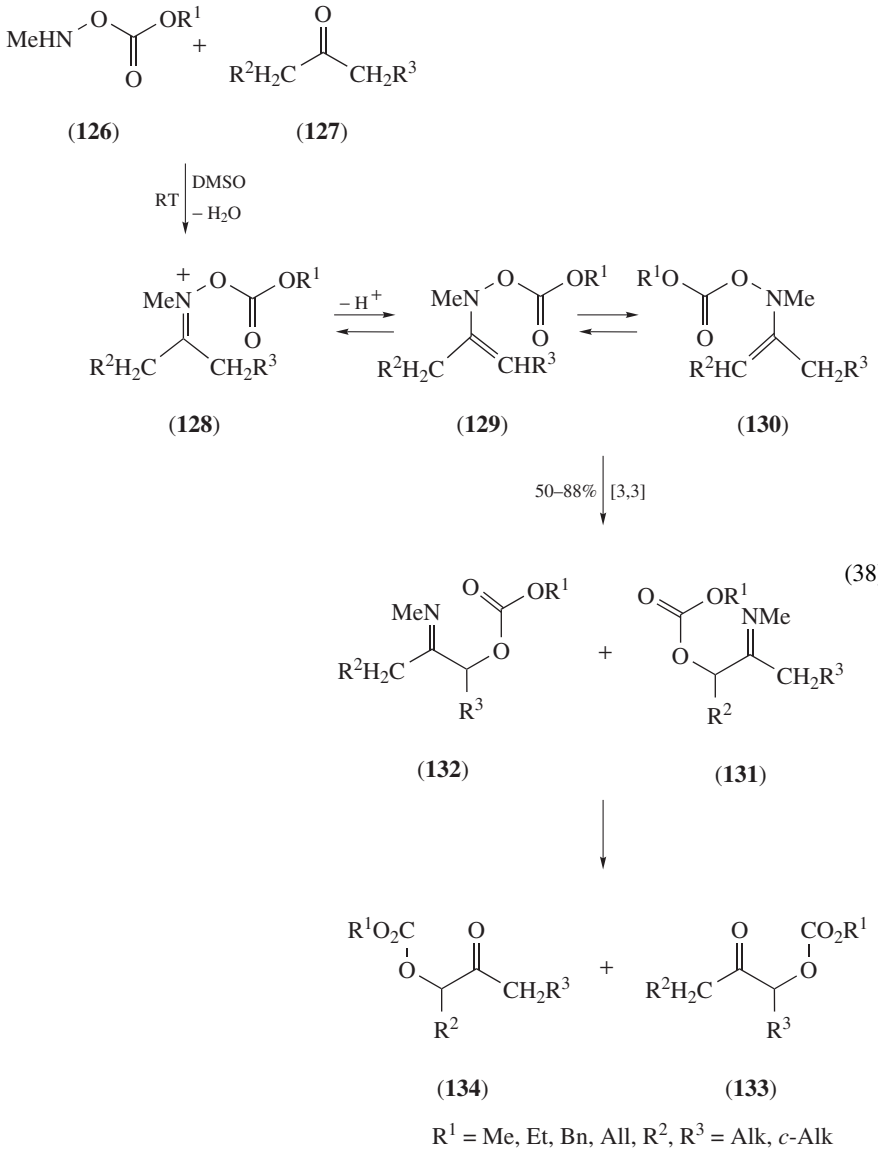

(38)

R^1 = Me, Et, Bn, All, R^2, R^3 = Alk, *c*-Alk

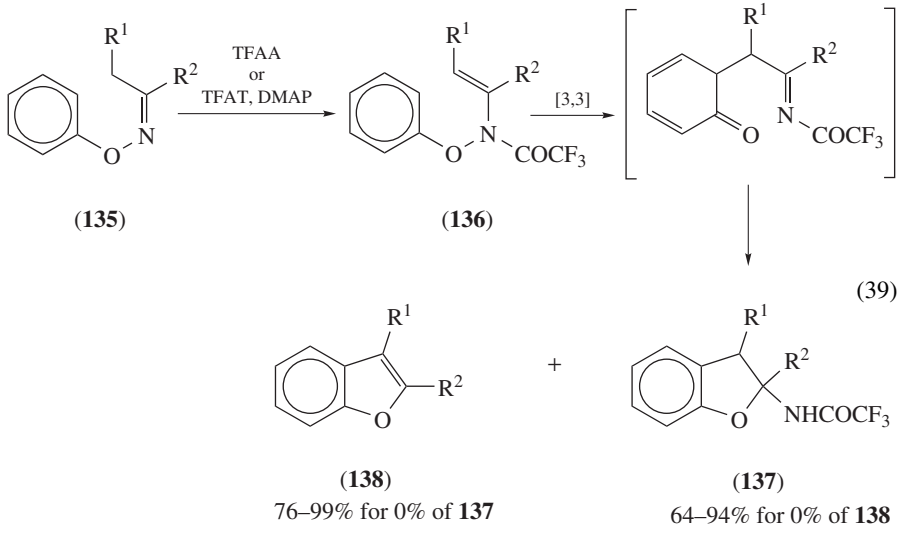

(**135**) (**136**) (39)

(**138**)
76–99% for 0% of **137**

(**137**)
64–94% for 0% of **138**

R^1 = H, Me, R^2 = Me, Et, Ph, Ar; R^1R^2 = -$(CH_2)_3$-, -$(CH_2)_4$-

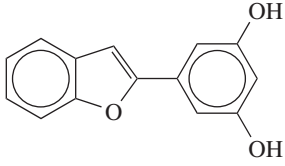

(**139**)
Stemofuran A

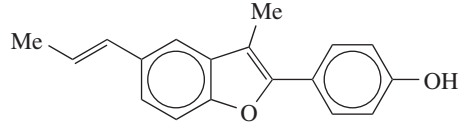

(**140**)
Eupomatenoid 6

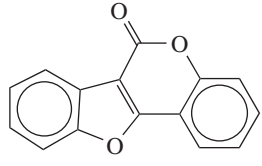

(**141**)
Coumestan

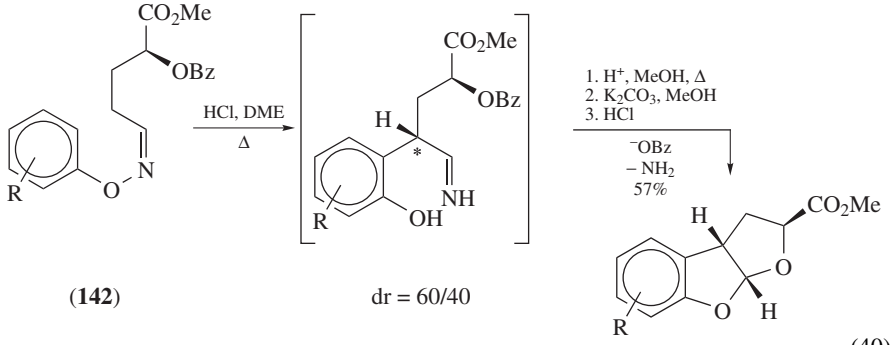

(**142**) dr = 60/40 (**143**) (40)

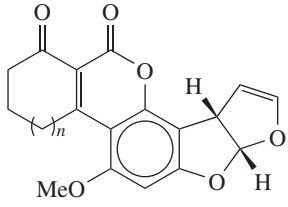

$n = 0$ (+)-(**144**)
$n = 1$ (+)-(**145**)

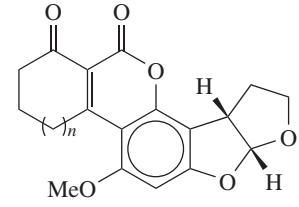

$n = 0$ (+)-(**146**)
$n = 1$ (+)-(**147**)

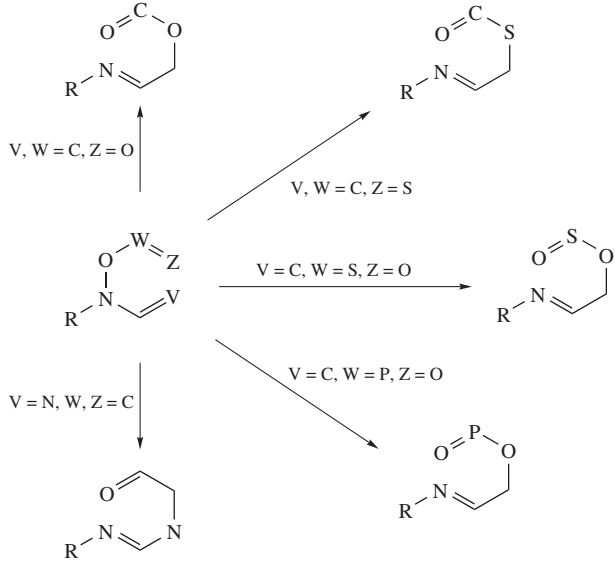

SCHEME 3

C. The Polyhetero-Cope Rearrangements

1. Systems incorporating more heteroatoms

The incorporation of other heteroatoms in the dienic system producing a polyhetero-Cope system have also been used in [3,3]-sigmatropic rearrangements of hydroxylamines, hydroxamic acids and analogues. Sulfur, phosphorus, oxygen and nitrogen are some of the heteroatoms used (Scheme 3). In some cases, the rearrangement proceeds at room temperature but in others, the rearrangement only occurs under heating.

Enehydroxylamine *O*-derivatives **149** and **151**, prepared from the reactions of *N*-alkyl-3-(hydroxyamino)cyclohex-2-enone (**148**, $R^1 = H$) and *N*-alkyl-3-(hydroxyamino)-5,5-dimethylcyclohex-2-enone (**148**, $R^1 = Me$) with MsCl (equation 41) and $Me_2NC(S)Cl$ (equation 42), respectively, in the presence of base rearrange spontaneously providing the corresponding [3,3]-sigmatropic rearranged products **150** and **152** in moderate to excellent yield[9]. However, the diethyl phosphate **153** (equation 43) and the *O*-benzoyl hydroxylamine **154** rearrange under reflux in toluene (equation 44).

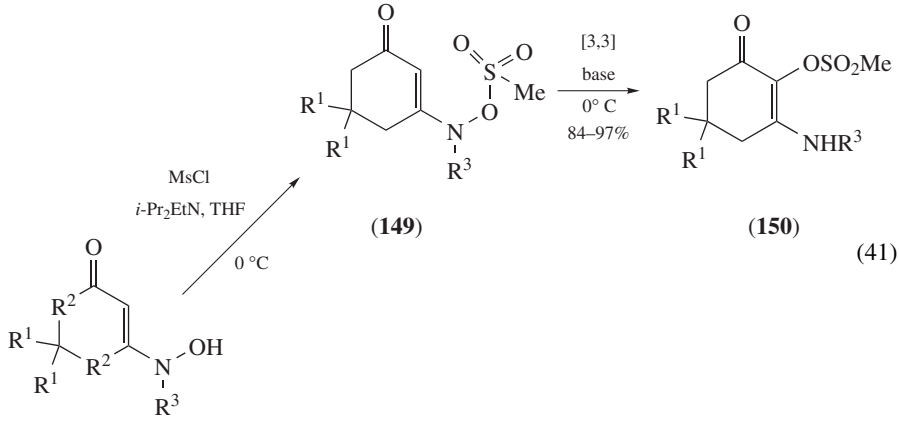

(41)

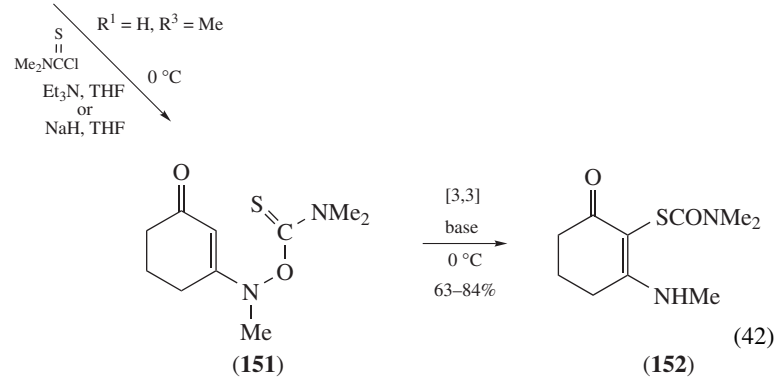

(42)

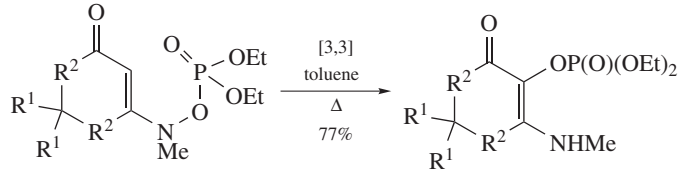

(**153**)

(43)

(**148**, R^3 = Me)

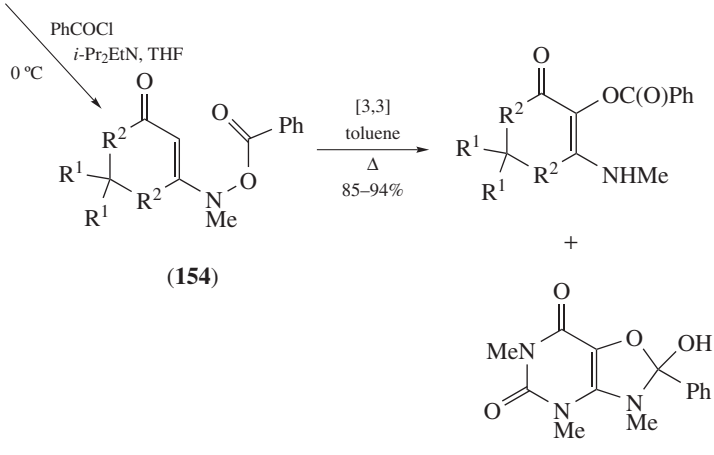

(**154**)

only when (44)

R^1R^1 = =O, R^2 = NMe

R^1 = H, Me, R^2 = CH_2; R^1R^1 = =O, R^2 = NMe

In analogous conditions, compound **148**, R^1R^1 = =O, R^2 = NMe, R^3 = Me, did not react or only provided the rearrangement product **155** in low yield[9] (equation 45). The authors explained this behaviour by the formation of a side product **156** resulting from the attack of the anion liberated from the electrophile at the adjacent carbon atom C(2) prior to rearrangement, or through the decomposition of an earlier intermediate.

Rearrangement of **157**, the reaction product of *N*-4-*tert*-butylphenyl-*N*-*tert*-butylhydroxylamine with $SOBr_2$, provides the corresponding aniline **158** by losing sulfur dioxide[48] (equation 46).

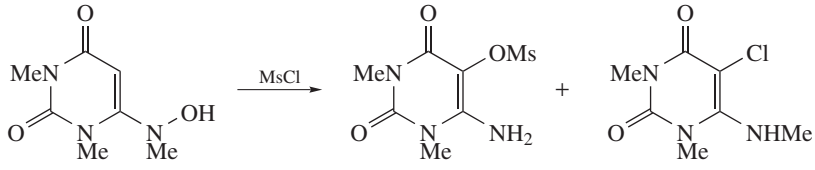

(**148**, R^1R^1 = =O, R^2 = NMe, R^3 = Me) (**155**) (**156**) (45)

41% 47%

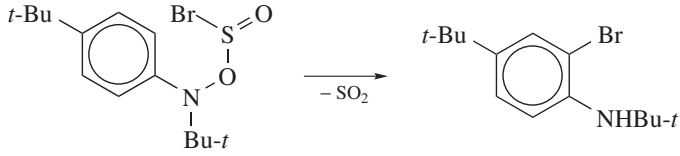

(**157**) (**158**) (46)

Previously, Ayyangar and colleagues[49] reported the synthesis of 2-chloroanilide and aniline derivatives by a [3,3]-sigmatropic rearrangement of the adduct obtained by the treatment of hydroxamic acid and hydroxylamine derivatives with thionyl chloride.

A similar intermediate is invoked when α-amino nitrones **159** are treated with mesyl chloride in the presence of triethylamine[50]. The corresponding mesyloxyamidines **161** are formed formally by [3,3]-sigmatropic rearrangement of **160** (equation 47).

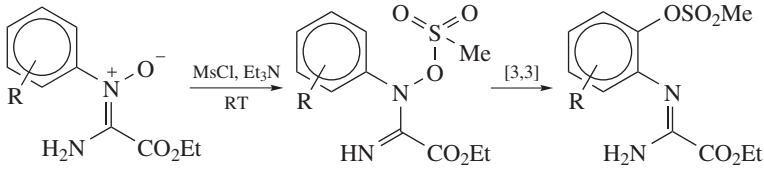

R	**161**
H	60%
4-Me	56%
5-Me	50%
3-Me	15%
4-Br	40%

(**159**) (**160**) (**161**) (47)

Saczewski and Debowski[51] reported a 1-thia-3-oxa-4-aza-Cope rearrangement of the adduct **163** formed when the *N*-aryl-*N*-(4,5-dihydro-1*H*-imidazol-2-yl)-hydroxylamine **162** reacted with carbon disulfide in the presence of triethylamine at room temperature (equation 48). The intermediate **164** formed after the [3,3] rearrangement lost a fragment and after successive or simultaneous rearomatization afforded a thiophenol derivative that provided **165.**

The *N*-acyl-*O*-arylhydroxylamine **166** rearranges in the presence of trifluoroacetic acid to **168** by a [3,3]-sigmatropic shift. An isourea intermediate **167** was proposed to explain the observed transformation[52] (equation 49).

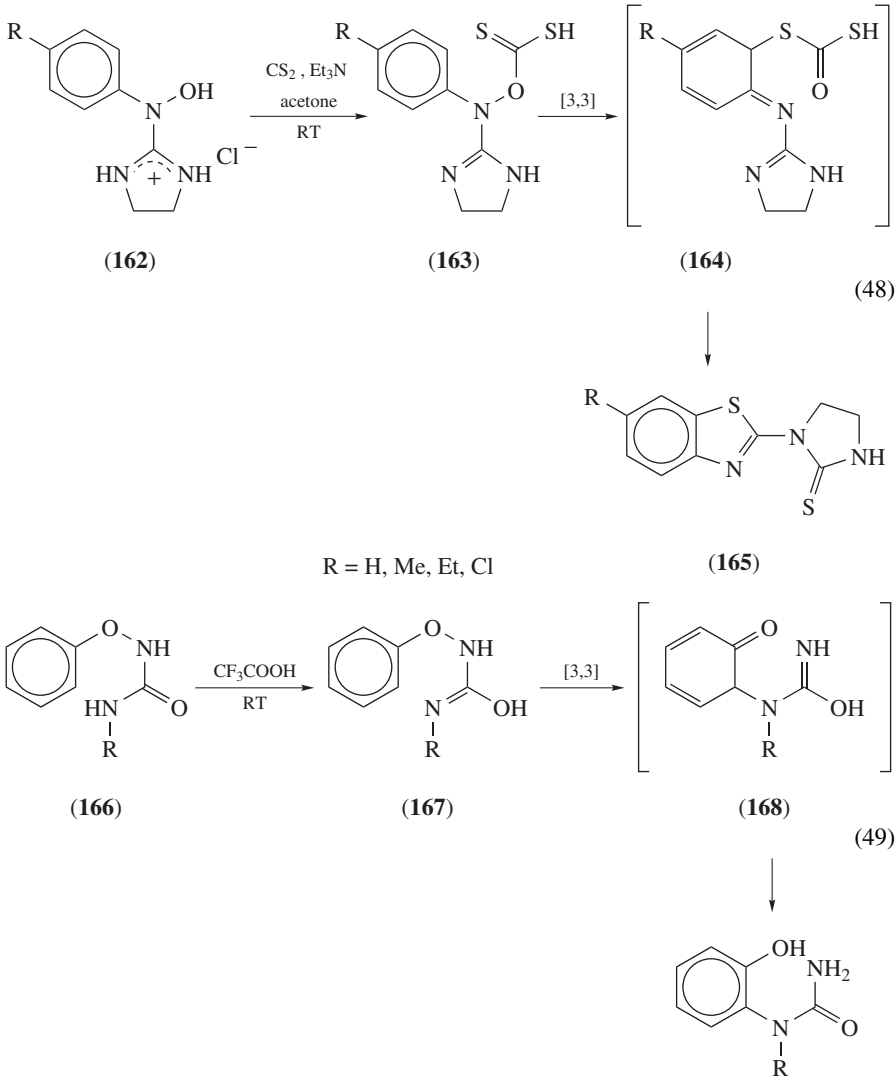

The new metabolite from Red Sea marine invertebrates, Asmarine B (**169**), presents a hydroxylamine functional group (equation 50). When treated with acetic anhydride at room temperature the Asmarine B (**169**) underwent an unexpected [3,3]-sigmatropic rearrangement to give **170**. After 1,6-addition of methanol and concomitant loss of acetic acid **170** produced the pyrimidine **171**[53].

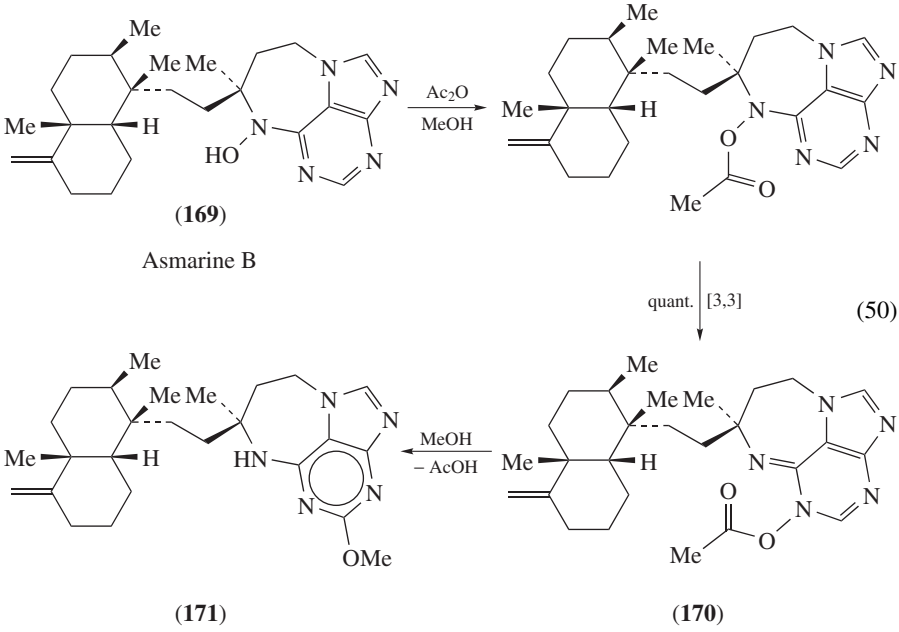

(**169**)

Asmarine B

(50)

(**171**) (**170**)

2. Systems incorporating a triple bond

Despite the typical use of the 1,5-dienic system in the hetero-Cope rearrangement the participation of triple bonds, C≡N and C≡C, in the [3,3]-sigmatropic rearrangement was also reported. Synthesis of *N*-substituted benzimidazolinones **175** by a hetero-Cope rearrangement of the adduct **174** formed by reaction of *N*-arylhydroxamic acids **172** with cyanogen bromide **173** in the presence of triethylamine and at low temperatures was reported by Almeida, Lobo and Prabhakar[54] (equation 51).

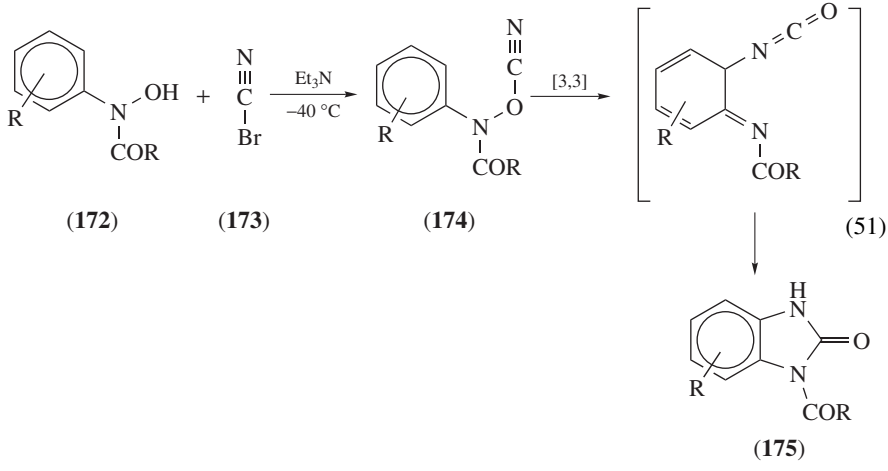

(**172**) (**173**) (**174**) (51)

(**175**)

Saczewski and Debowski[55] reported the 1,4-diaza-3-oxa-Cope rearrangement of *N*-cyanate anilides (equation 52). Prototropic rearomatization of **176** and internal nucleophilic addition afford the corresponding benzimidazolinone **177**, usually in moderate yields (32–78%). A concerted [3,3]-sigmatropic rearrangement is proposed based on the absence of *para* rearrangement product that usually results from homolysis or heterolysis of the N–O bond followed by recombination of the two radicals or ions.

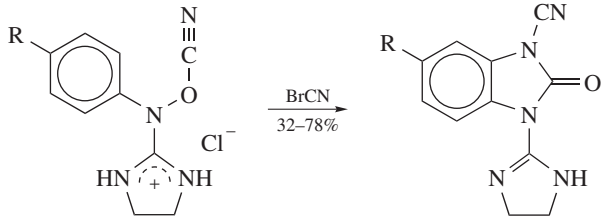

(52)

(**176**) R = H, Me, Cl, OMe (**177**)

A system incorporating a cyano group linked to the *N*-hydroxy group of enehydroxylamines (**178**) was examined in order to accomplish a short synthesis of *N*-monosubstituted imidazolones **180**[9] (equation 53). Indeed, enehydroxylamine on treatment with BrCN in the presence of Et_3N furnished the [3,3]-sigmatropic rearrangement product **179** that cyclized to **180**, albeit in modest yield (36%). When DABCO was used as base a vastly improved yield (81%) of **180** was obtained. Other enehydroxylamines with bulky alkyl substituents at the nitrogen atom, such as isopropyl and cyclohexyl, were found to give poorer yields or no reaction.

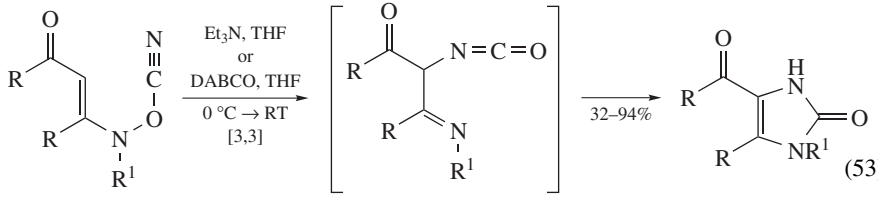

(53)

(**178**) (**179**) (**180**)

R^1 = Alk

The synthesis of 3- and 7-substituted indoles (**184** and **185**) by [3,3]-sigmatropic rearrangement of *N*-hydroxyindole derivatives (**181**) was reported[56] (equation 54). *N*-hydroxyindole **181** in the presence of cyanogen bromide (**182**, R^1 = Br, R^2 = N) and base afforded **183** that rearranged to the NCO substituted at position 3 and position 7, leading to two isomeric isocyanates, **184** and **185**, respectively. Different behaviour was found when an acetylenic sulfone **182**, R^1 = H, R^2 = CTos, was used where the 3-substituted indole **186** was the only rearrangement product identified.

Similar behaviour was reported by Prabhakar and colleagues[50] when the nitrones **187** were treated with cyanogen bromide (**182**, R^1 = Br, R^2 = N) (equation 55). The intermediates **188** underwent a [3,3]-sigmatropic rearrangement and rearomatization producing *N*-substituted benzimidazolones **189**. The authors explained the absence of alternative 3,3-hetero-oxa-Cope rearrangement leading to triazolones **190** by a considerable weakening of the N–O bond with significant positive charge already developed in the aromatic ring of the intermediates **188**.

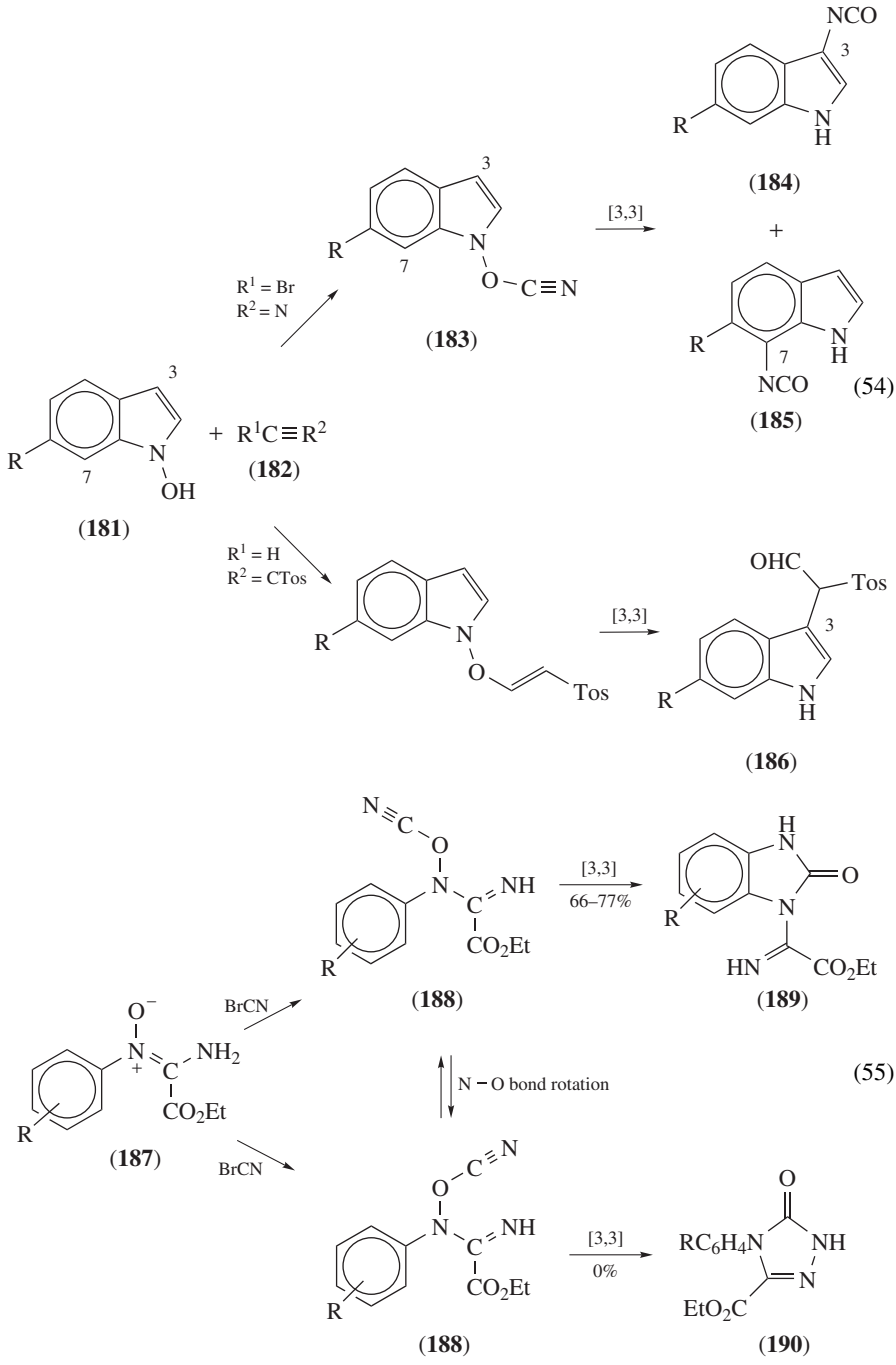
NCO
3
R
N
H
(184)
3
R
7
N
O
C≡N
(183)
[3,3]
+
R1 = Br
R2 = N
R
N
H
7
NCO
(185)
(54)
3
R
7
N
OH
(181)
+ R1C≡R2
(182)
R1 = H
R2 = CTos
R
N
O
Tos
[3,3]
OHC
Tos
3
R
N
H
(186)
N≡C
O
N
C
NH
CO2Et
R
(188)
[3,3]
66–77%
H
N
O
R
N
HN
CO2Et
(189)
O−
N+
C
NH2
CO2Et
R
(187)
BrCN
BrCN
N − O bond rotation
(55)
N≡C
O
N
C
NH
CO2Et
R
(188)
[3,3]
0%
O
RC6H4N
NH
N
EtO2C
(190)

III. THE [2,3]-SIGMATROPIC REARRANGEMENTS

[2,3]-Sigmatropic rearrangements have received considerable attention as a method for carbon–carbon and carbon–heteroatom bond formation[57]. In [2,3]-sigmatropic rearrangement the new σ-bond forms at the end of the allylic system by a concerted process with simultaneous cleavage of the allylic–heteroatom bond. Benzylic, propargylic or allenylic systems are also allowed. The rearrangement leads to formation of a new double bond between C(1) and C(2). When two different substituents are attached to C(1) this double bond may have an *E* or *Z* configuration (Scheme 4).

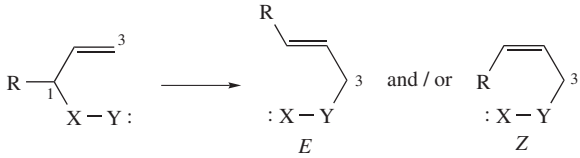

SCHEME 4

The reaction occurs suprafacially across the allyl unit through a five-membered ring envelope-shaped transition state. The five-membered cyclic transition state of [2,3]-sigmatropic rearrangement shows greater conformational 'flexibility' than the six-membered transition state of [3,3]-sigmatropic rearrangements and should therefore be far more susceptible to the effects of stereochemical control by substituents[58].

A new [2,3]-sigmatropic rearrangement of the lithium salt **192** of the *N*-benzyl-*O*-allylhydroxylamines (**191**) affording *N*-benzyl-*N*-allylhydroxylamines (**193**) in moderate yields was reported[59–61] (equation 56). The absence of crossover products confirms the intramolecular character of the transformation and an envelope transition state is proposed. The rearrangement proceeds via a transition state where facial selectivity is determined by stereoelectronic effects.

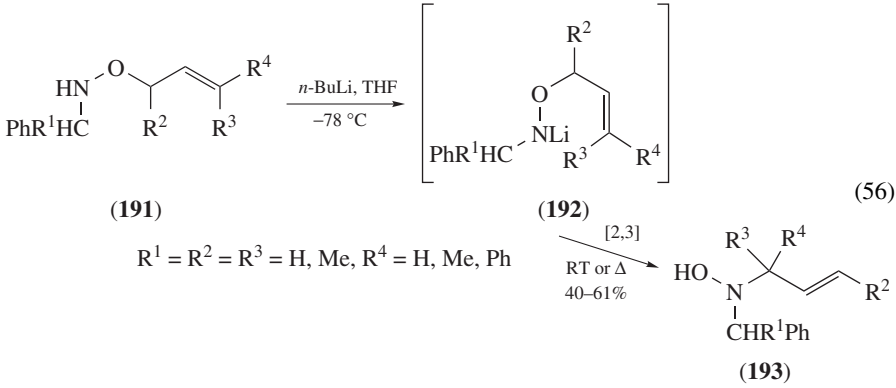

(56)

Diastereoselective [2,3]-sigmatropic rearrangement of lithium *O*-allyl-*N*-benzylhydroxylamides (**195**) bearing a stereogenic center adjacent to the migration terminus was reported[62,63] (equation 57). When the (*E*) and (*Z*)-*N*-benzyl-*O*-(4-methoxy-4-phenylbut-2-enyl)hydroxylamines (**194**) rearrange, a chelation by the lithium ion occurs and the (*Z*)-(1*RS*,2*RS*)-1-phenyl-1-methoxy-3-*N*-benzylaminobut-3-ene (**196**) is the major product

formed (>90% de and 80% yield). Models for the transition states of diastereoselective *N*,*O*-rearrangement are proposed and discussed.

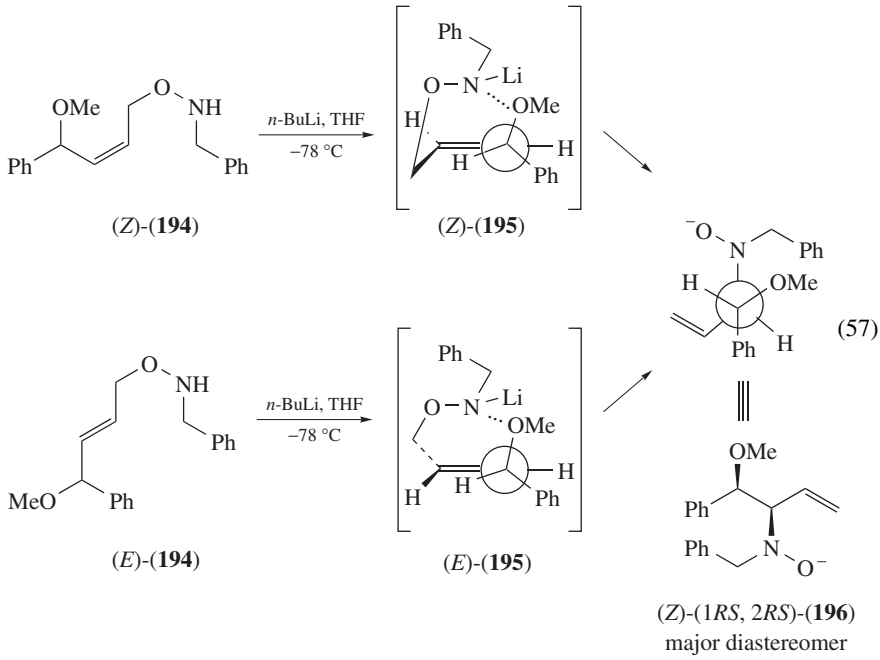

Furthermore, the rearrangement of (*E*)-*N*-allylhydroxylamines into (*E*)-*O*-allylhydroxylamines at room temperature was reported[64]. An aminoxyl radical was detected by EPR and its participation in a Meisenheimer [2,3]-rearrangement was proposed.

Recently, [2,3]-sigmatropic rearrangement of *O*-propargylic hydroxylamines **197** was described[65,66] and claimed as a simple procedure for the synthesis of 2-isoxazolines **200** in moderate to good yields (60–84%) (equation 58). The authors proposed the formation of *N*-allenic hydroxylamines (**198**) by an initial [2,3]-sigmatropic rearrangement. These rearranged to the corresponding α,β-unsaturated oximes that underwent cyclization to give the 3-isoxazolines **199** yielding the related 2-isoxazolines (**200**), after isomerization.

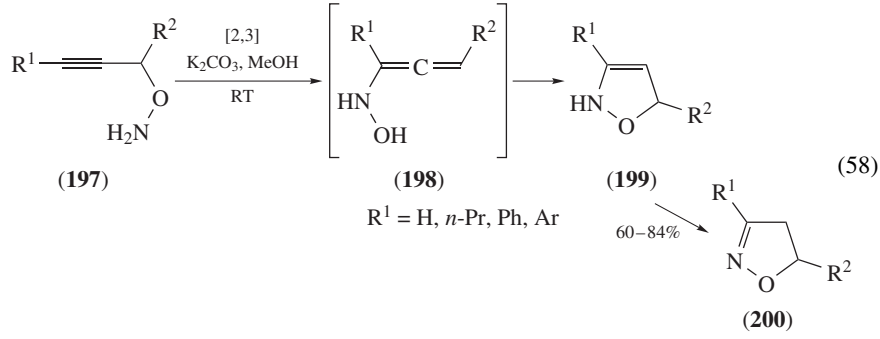

IV. THE DYOTROPIC REARRANGEMENTS

Dyotropic rearrangement is an uncatalysed process in which two σ bonds simultaneously migrate intramolecularly by a dyotropic transition state **202** and has been observed in organosilylhydroxylamine derivatives **201** (equation 59).

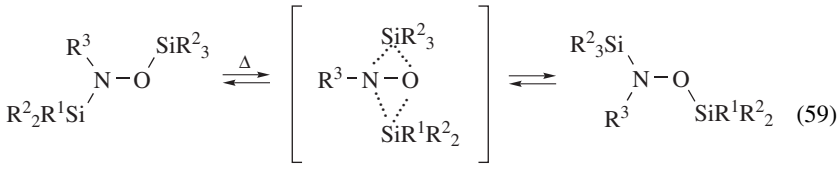

(59)

(**201**) (**202**)

dyotropic transition state

Klingebiel and colleagues[67,68] reported the thermal dyotropic rearrangement of lithium salt of *N*,*O*-bis(silyl)hydroxylamine (**201**, $R^1 = t$-Bu, R^2 = Me, R^3 = Li) during the synthesis of *N*,*N*,*O*-tris(organylsilyl)hydroxylamines from the *N*,*O*-bis(organylsilyl)hydroxylamine (**201**, $R^1 = t$-Bu, R^2 = Me, R^3 = H) (equation 59). The lithium salt **201**, $R^1 = t$-Bu, R^2 = Me, R^3 = Li, was isolated in 50% yield and characterized. This implies an irreversible intramolecular 1,2-anionic silyl group migration from the oxygen to the nitrogen atom[69] to form the oxyanion due to the β-donor bonding in SiON systems[70]. The energy gained in the rearrangement must outweigh the 125 kJ mol^{-1} difference in energy between the Si−O and Si−N bond energies (443 and 318 kJ mol^{-1}, respectively). Earlier, Frainnet and coworkers[71] had reported 1,2-shifts exchange of trialkylsilyl groups in neutral bis(organosilyl)hydroxylamines, and a reversible rearrangement involving positional exchange between the organosilicon groups on oxygen and nitrogen was reported later[72] and a dyotropic transition state was suggested. Meller and colleagues[73] used the ability of the dyotropic rearrangement of *N*,*O*-bis(trimethylsilyl)hydroxylamine (**201**, R^1, R^2, R^4 = Me, R^3 = H) to prepare *N*,*O*-bis(trimethylsilyl)-*N*-β-halogeno-borylhydroxylamines (**203**) (equation 60).

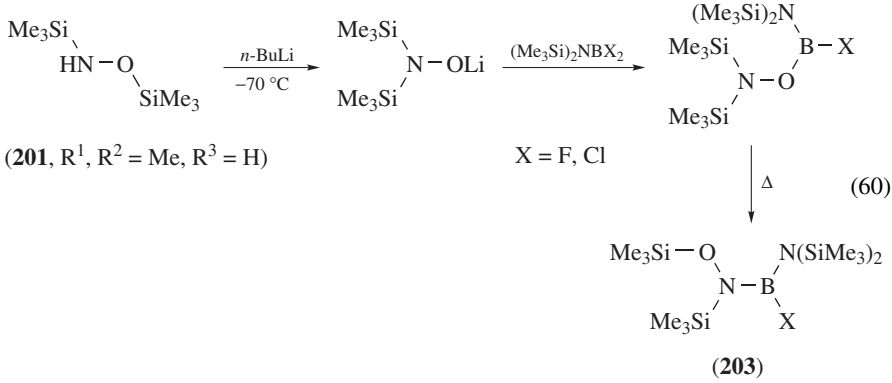

(**201**, R^1, R^2 = Me, R^3 = H) X = F, Cl (60)

(**203**)

However, the *O*-(fluorosilyl)-*N*,*N*-bis(organosilyl)hydroxylamine **204** undergoes an irreversible rearrangement yielding the isomeric *N*-(fluorosilyl)-*N*,*O*-bis(organosilyl) hydroxylamine **205**[74–76]. The rearrangement proceeds via a dyotropic transition state to yield the hydroxylamine **205**. An intermolecular thermal rearrangement with the insertion

of a silyl moiety into the N−O bond and transfer of a methyl group from silicon to nitrogen atom give the unexpected compound **206** (equation 61).

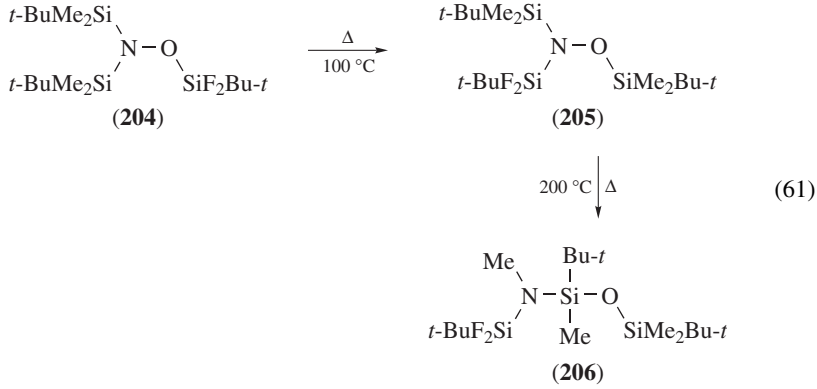

(**204**) (**205**) (**206**) (61)

Recently, density functional calculations (B3LYP) on the thermal rearrangement of tris(silyl)hydroxylamines to silylamino disiloxane for model compounds concluded that the insertion of a silyl group into the N−O bond is energetically favoured if it occurs from the nitrogen atom[77].

To explore the dyotropic rearrangement of silyl hydroxylamines, Schmatz, Klingebiel and colleagues[68] studied the behaviour of *O*-lithium-*N*,*N*-bis(*t*-butyldimethylsilyl) hydroxylamine **207** in the presence of chlorotrimethylstannane (equation 62). They found that the primarily formed *N*,*N*-bis(*t*-butyldimethylsilyl)-*O*-(trimethylstannyl)hydroxylamine **208** underwent a dyotropic rearrangement to form **209**. This reaction mechanism is corroborated by quantum chemical calculations partly employing an effective core potential for tin.

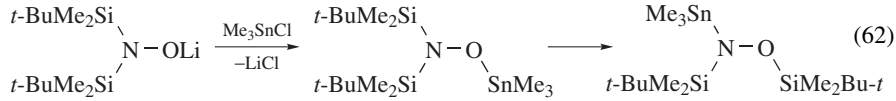

(**207**) (**208**) (**209**) (62)

V. THE BAMBERGER REARRANGEMENTS

The Bamberger rearrangement concerns the treatment of *N*-phenylhydroxylamines (**210**, R^1, R^2, R^3 = H) with aqueous mineral acid to produce 2-aminophenol (**213**, R^1, R^3, R^4 = H) and 4-aminophenol[78] (**214**, R^1, R^3, R^4 = H) (equation 63). The rearrangement is intermolecular and occurs by an S_N1 mechanism. The water-elimination step from the intermediate $ArNHO^+H_2$ (**211**) is rate-determining[79,80]. The mechanism of this reaction is considered to involve the generation of the nitrenium ion **212**, which can be attacked by water or other nucleophiles[81]. The *para* rearrangement product **214** is predominant and occasionally the only one. *N*,*O*-Disubstituted arylhydroxylamines (**210**, $R^1 \neq$ Acyl) can also rearrange.

Recently, a Bamberger rearrangement in gas phase was reported[82]. The rearrangement of *N*-phenylhydroxylamine (**210**, R^1, R^2, R^3 = H) into 4-aminophenol (**214**, R^1, R^3, R^4 = H) occurred on the acid sites of H-ZSM-5 zeolite. However, *N*-phenylhydroxylamine with K-10 montmorillonite clay and its various cation-exchanged forms failed to rearrange into aminophenols[83,84].

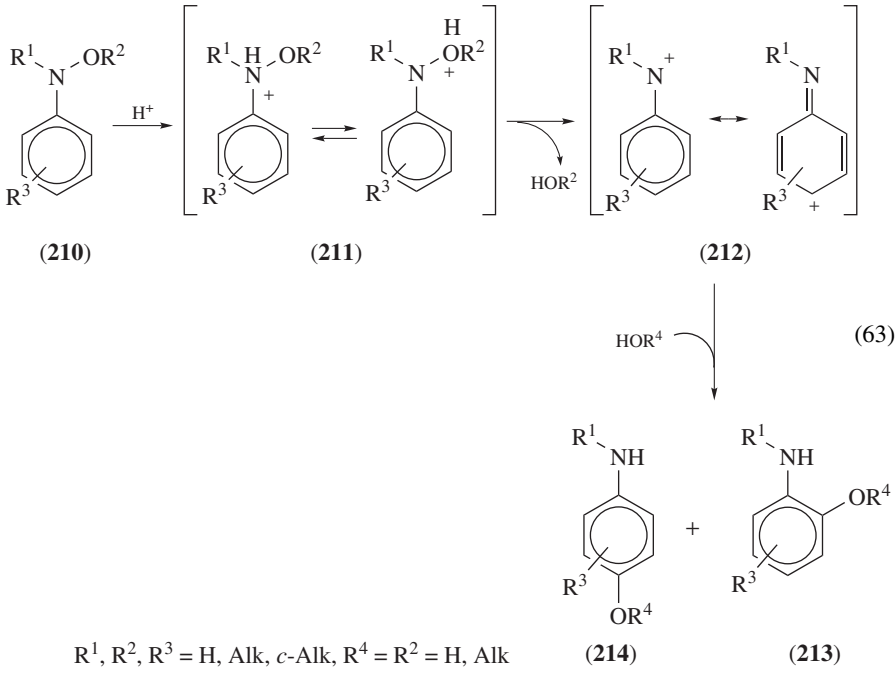

(**210**) (**211**) (**212**) (63)

R^1, R^2, R^3 = H, Alk, *c*-Alk, $R^4 = R^2$ = H, Alk (**214**) (**213**)

N-Arylhydroxylamines rearrange to the corresponding aminophenols during the bacterial degradation of nitroaromatic compounds catalysed by a mutase from *Pseudomonas pseudoalcaligenes* JS45 and other microorganisms[85–88]. The acid-promoted reactions of different *N*-arylhydroxylamines have been studied at constant ionic strength and in the presence of various amounts of NaBr and NaCl[89]. Each system resulted in the corresponding 4-aminophenol, the product of Bamberger rearrangement, as the only detectable product in the absence of halide ion. The addition of halide ion reduced the yield of this product, with the appearance of the corresponding 4-haloaniline, 2-haloaniline (in 2-unsubstituted anilines) and the parent aniline. However, *O*-phenylhydroxylamine in the presence of trifluoroacetic acid rearranges to 2- and 4-aminophenol[90]. The predominance of the *ortho* rearrangement clearly distinguishes this process from the Bamberger rearrangement. The authors proposed an ion–molecule pair involving a phenoxenium ion and an ammonia molecule as intermediate. In this pair, intramolecular combination with the *ortho* position proceeds preferentially over that to the *para* position.

Ester derivatives of *N*-arylhydroxamic acids[91,92] and *N*-arylhydroxylamines[93] have been the focus of attention due to their recognition as ultimate carcinogens in mammals, including humans[94]. During the mechanistic study of the solvolysis of *N*-acetyl-*N*-biphenyl-*O*-pivaloylhydroxylamine (**210**, R^1 = COMe, R^2 = COBu-*t*, R^3 = 4-Ph) in acetate buffer, Novak and colleagues[94] identified the product **216** resulting from the rearrangement of *N*-arylhydroxylamine (equation 64). Similar behaviour was observed with *N*-aryl-*O*-acylhydroxylamine[95,96]. To explain the observation they proposed an intermediate arylnitrenium ion **215**/pivalate ion formed by heterolytic cleavage of the N–O bond and responsible for the formation of DNA adducts[97]. The rearrangement also occurs in aprotic solvent and at low temperatures[98].

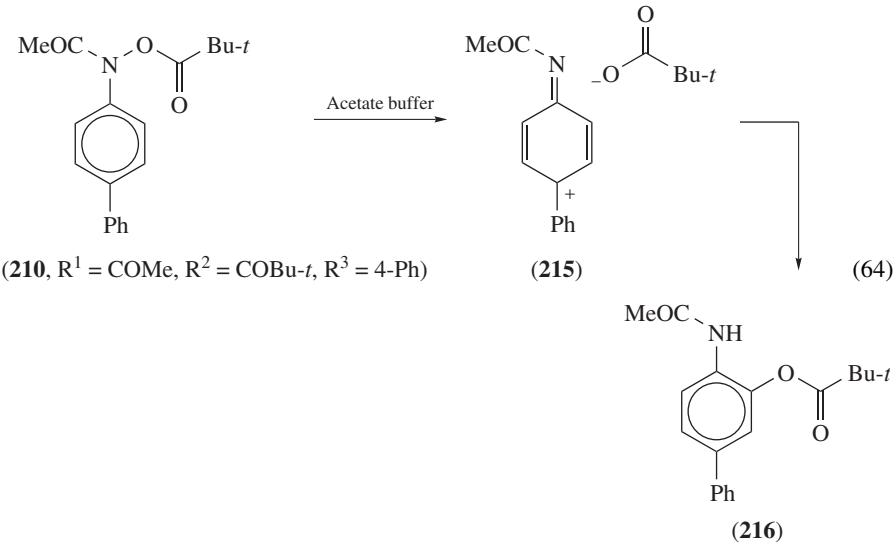

(**210**, R^1 = COMe, R^2 = COBu-*t*, R^3 = 4-Ph) (**215**) (64)

(**216**)

VI. THE BECKMANN REARRANGEMENTS

The rearrangement of ketoximes to amides was discovered more than a century ago, by Beckmann in 1886[99], but remains a topic of current interest and still retains great synthetic utility. During the last century the Beckmann rearrangement has been frequently reviewed[100–102], although the last major review was almost two decades ago.

This reaction remains as one of the most reliable transformations to incorporate efficiently a nitrogen atom in cyclic or acyclic systems, providing a powerful synthetic method (Scheme 5).

Successive investigations cleared its mechanism. The scope of this rearrangement is quite broad, as both α-groups (R^1, R^2) may be alkyl, aryl or heteroaryl groups and one of them to be a hydrogen. In the classical Beckmann rearrangement aldoximes **217** (R^1 or R^2 = H) and ketoximes **217** (R^1, $R^2 \neq$ H) or the corresponding esters **217** (R^3 = OTos, OMs) rearrange in the presence of certain acids, including Lewis acids, to give amides **218** and **220** or lactams **222**. In general, this rearrangement is stereospecific for ketoximes, involving the migration of the residue *anti* to the leaving group on the nitrogen atom of the oxime; the nature of the substituents of the oxime usually do not influence the outcome of the reaction (Scheme 5). Of course, if the starting material consists of a mixture of *E* and *Z* oximes or if oxime isomerization could not be prevented during the rearrangement reaction, a mixture of amides is usually obtained. Primary amides are usually the result of the Beckmann rearrangement of aldoxime, independently of its geometry (*E* or *Z*). A possible side reaction is the Beckmann fragmentation producing nitriles **219**, **221** and **223** which is sometimes predominant over the rearrangement. The factors that govern the selectivity will be analysed later.

Perhaps the most notable application of the Beckmann rearrangement is in the industrial production of ε-caprolactam from cyclohexanone (or its oxime), which is used as monomer for the polymerization to a polyamide for the production of synthetic fibres (for example, nylon 6). Furthermore, Beckmann rearrangement provides a facile route for the

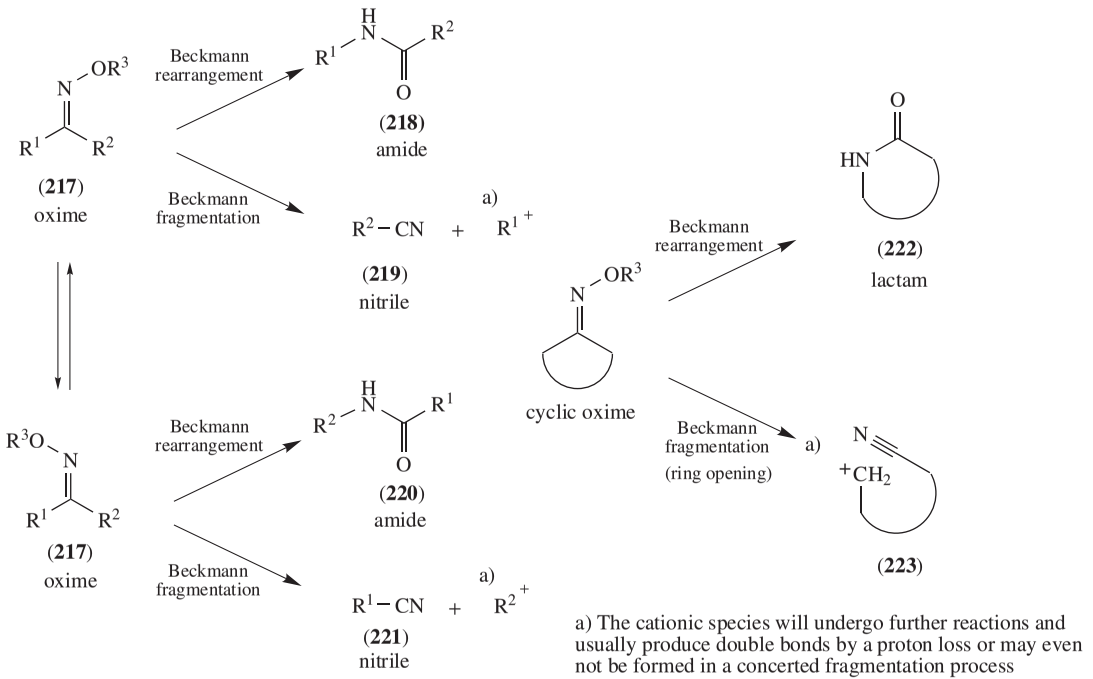

a) The cationic species will undergo further reactions and usually produce double bonds by a proton loss or may even not be formed in a concerted fragmentation process

R^1, R^2 = Alk, Ar, heteroaryl, R^1 or R^2 may be H, OR^3 = OH, OTos, OMs

SCHEME 5

incorporation of nitrogen into polycyclic structures for the synthesis of either important pharmaceuticals or natural products.

A. Mechanism

1. Beckmann rearrangements

The generally accepted mechanism for the Beckmann rearrangement is presented in Scheme 6. The inertness of the oximes to rearrangement in the absence of acid catalyst contrasts with the spontaneous rearrangement of the corresponding oxime tosylate to imidoyl tosylates in the same conditions. These facts demonstrate the necessity to transform the *N*-hydroxy group of the oxime into a better leaving group, either by protonation, etherification or esterification.

Following protonation, etherification or esterification of the oximino hydroxyl group, *a quasi* three-membered transition state (**224**) is formed, in which the group *anti* to the hydroxyl migrates with synchronous lengthening of the N−O bond. The departure of the leaving group (OR^3) is simultaneous with the [1,2]-shift of the *anti* R^1 group. The concept of a three-membered transition state was involved in order to explain the observed retention of configuration of the migrating group and also the stereospecificity of the reaction.

The main intermediate of the rearrangement may be a nitrilium ion (**225**) in some cases or an imidate (**226**) in others. The resulting intermediate reacts with water to produce the amide (**218**) after tautomerization. If other nucleophiles (Nu^-) are present, they can intercept the reactive intermediates (both inter- or intra-molecularly) and several different imino-substituted derivatives (**227**) can be formed. These rearrangement–addition reactions will be analysed later in this chapter as they can effectively broaden the scope of the Beckmann rearrangement reaction (Sections VI.D.2 and VI.E.2).

The study of the Beckmann rearrangement mechanism and the development of new reaction conditions and new catalysts for liquid and vapour-phase reactions are still an intense field of investigation. Kinetic studies showed that the rate-determining step of the Beckmann rearrangement in liquid phase is the migration of the R^1 group that shifts with its bonding electrons by an intramolecular and a stereospecific pathway. The rate of rearrangement increases with the electron donation to the migrating group while electron-withdrawing substituents have the reverse effect[103]. The observed lack of crossover, the retention of configuration at the migration center and the preferential migration of the group *anti* to the OH group proved the intramolecular and the stereospecific character of the rearrangement. Kinetic and spectroscopic studies of the Beckmann rearrangement of ketoximes in trifluoromethanesulfonic acid showed that the nitrilium ion is an intermediate whose stability is determined by the structure of the starting oxime and by solute–solvent interactions[104].

Nguyen and colleagues[105, 106] investigated the mechanism of the Beckmann rearrangement in the gas phase. They suggested that the Beckmann rearrangement constitutes a strong case of active solvent catalysis where the solvent molecules act as a homogenous catalyst in the chemical process and the larger the solvent proton affinity, the faster the hydrogen transfer and the stronger the catalytic effect induced by the solvent. Consequently, they proposed a two-key-step reaction pathway using a proton to model the Brønsted acid of the catalyst interacting with the oxime molecule. The first step, called the [1,2]-*H*-shift, converts the *N*-protonated complex to the *O*-protonated complex. The second step, called the Beckmann rearrangement, is a migration of the *anti*-alkyl group to the nitrogen atom and the elimination of the water molecule, producing the nitrilium ion. The first step was found to be the rate-determining step.

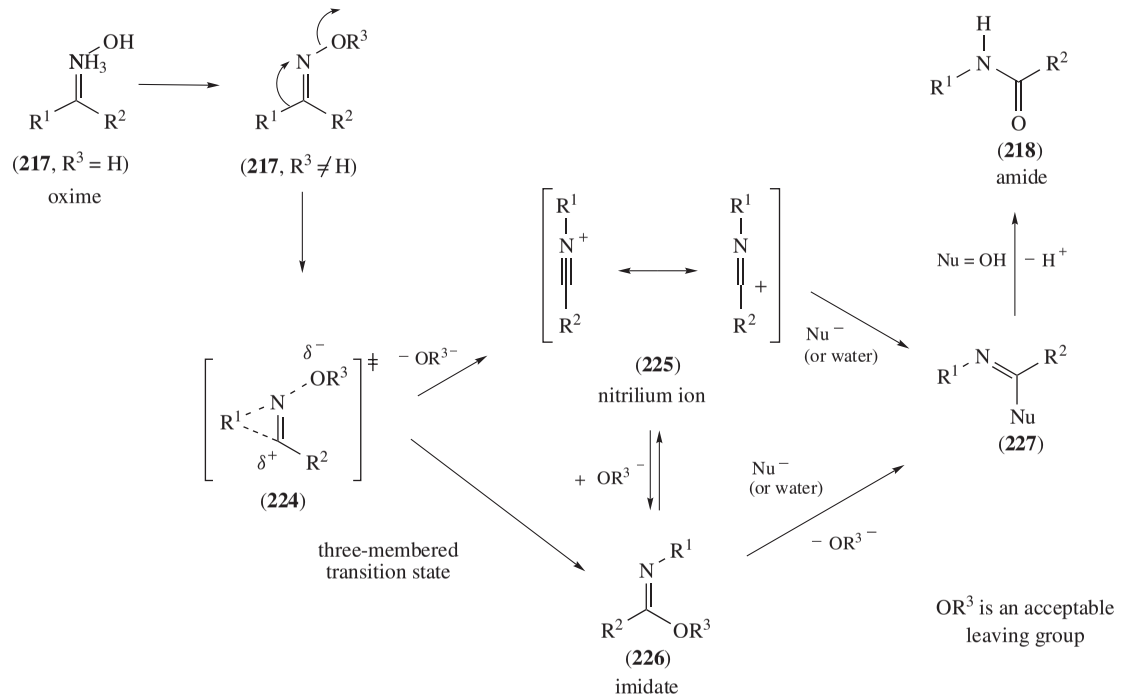
(217, R3 = H)
oxime
(217, R3 ≠ H)
(224)
three-membered transition state
(225)
nitrilium ion
(226)
imidate
(218)
amide
(227)
Nu = OH
− H+
Nu−
(or water)
+ OR3−
− OR3−
OR3 is an acceptable leaving group

SCHEME 6

Recently, computational studies[107] in terms of FMO theory led to the proposal of three different mechanisms of the Beckmann rearrangement (equations 65, 66 and 67). Three different substrates, acetone oxime **228**, acetophenone oxime **230** and cyclohexanone oxime **233**, were used as models for starting materials. Acidic solvents were modelled by $H^+(CH_3COOH)_3$ and $H_3O^+(H_2O)_6$ systems and reaction pathways were determined precisely. In every case the migration and the N−O bond cleavage occurred simultaneously. For acetone oxime **228**, a two-step process involving a σ-type cationic complex **229** was obtained (equation 65). For acetophenone oxime **230**, a three-step process with π- and σ-type complexes (**231**, **232**) was found in $H^+(CH_3COOH)_3$ and a two-step process involving a σ-type cationic complex was obtained in $H_3O^+(H_2O)_6$ (equation 66). However, for cyclohexanone oxime **233**, a concerted process without any π- and σ-complexes was calculated, leading to the ε-caprolactam **234** (equation 67).

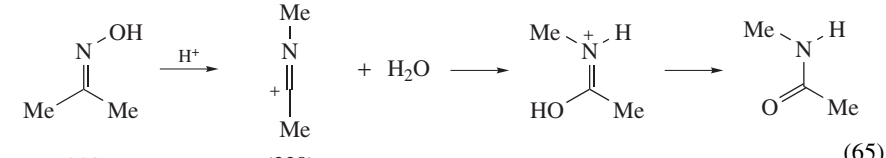

(**228**) acetone oxime — (**229**) σ-complex — amide

(65)

Two-step process with a σ-complex

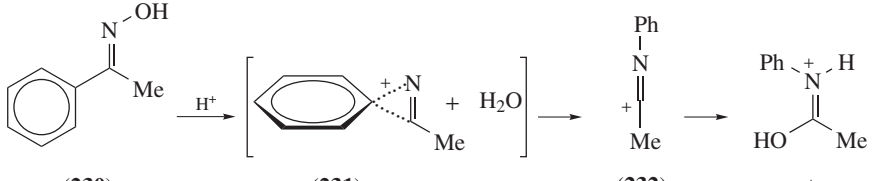

(**230**) acetophenone oxime — (**231**) π-complex — (**232**) σ-complex

(66)

amide

Three-step process with a π and a σ-complex in $H^+(AcOH)_3$ and a two-step process with a σ-complex in $H^+(H_2O)_6$

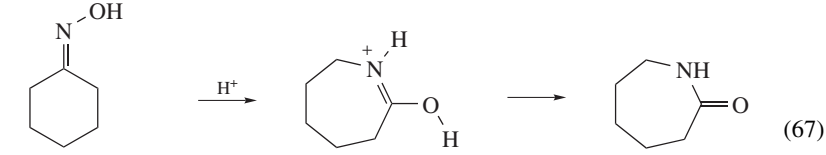

(**233**) cyclohexanone oxime — Concerted process — (**234**) ε-caprolactam

(67)

2. Beckmann fragmentations

A very common side reaction of the Beckmann rearrangement is the Beckmann fragmentation (or sometimes called 'abnormal' or 'second-order' Beckmann rearrangement) (Scheme 5). Fragmentation occurs when the α-carbon–carbon bond breaks, rather than migrates. Some substrates are more prone to fragmentation, but both reaction conditions and reagents used may also have a strong influence on the product distribution.

Ketoximes bearing an R group (R^1 or R^2) that forms a relatively stable positive ion and R being *anti* to the oxygen of the oxime group undergo the Beckmann fragmentation preferentially, instead of the Beckmann rearrangement. In some circumstances the degradation pathway becomes dominant, particularly when there is assistance from a neighbouring center, either by hyperconjugation or by mesomeric donation (note that these effects occur in the migrating group for the Beckmann rearrangement reaction). An increasing ability of the α-carbon atom to support positive charge is normally related to the formation of increasing levels of fragmentation products. It should be noted that many oximes and derivatives that undergo extensive fragmentation under acidic reaction conditions may undergo the Beckmann rearrangement when photolysed[108].

As this side reaction may strongly limit the use of the Beckmann rearrangement, it will be further analysed later (Section VI.E.3).

Several pathways may be possible for the Beckmann fragmentation reaction (equations 68 and 69). Stepwise processes may occur (equation 68), but stereospecific concerted fragmentations are also common (equation 69). Stepwise processes may follow different routes, but in most cases the fragmentation may have the same intermediate as the Beckmann rearrangement: the nitrilium ion.

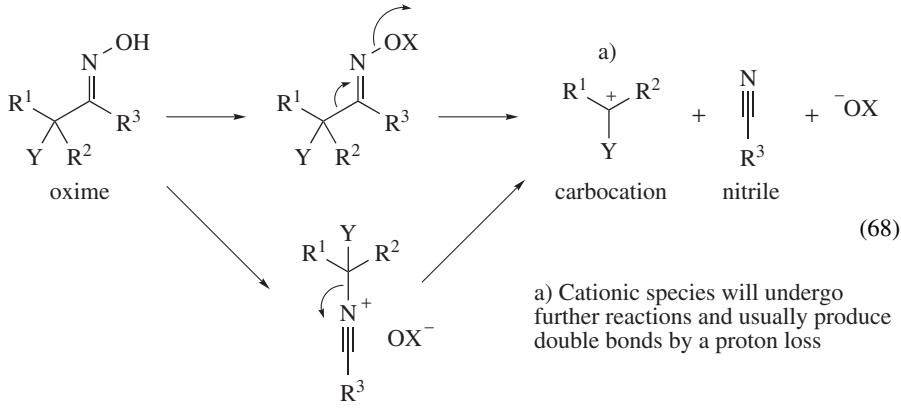

(68)

R^1, R^2, R^3 = alkyl, aryl, H, Y = *N*-, *O*- or *S*-substituent, alkyl, aryl, H

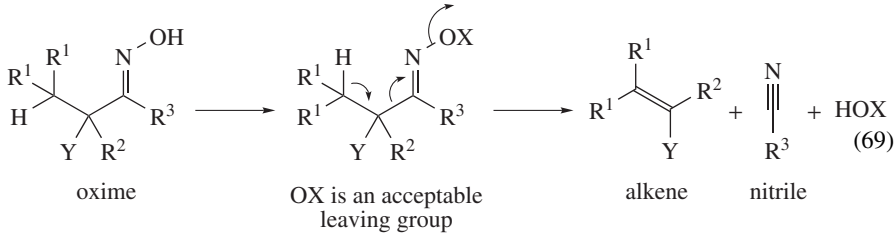

(69)

R^1, R^2, R^3 = Alk, Ar, H, Y = *N*-, *O*– or *S*-substituent, Alk, Ar, H

Examples of Beckmann degradation reactions with assistance by mesomeric donation of electron lone pairs (example: Y = N, O, S) or π electrons (example: R^1 = Ph or aromatic group) are well documented in the literature[101].

3. Beckmann pathways: the nitrilium and iminium routes

In the Beckmann reaction alternative ionic intermediates, two nitrilium ions (**225**, via route a or b and **237**, via route c) or one iminium ion (**235**, via route b or c), may be formed from the activated oximes (Scheme 7).

The iminium ion (**235**) is formed by N−O bond fission before migration of the oxime substituents (via route b or c). Its formation turns this pathway to non-selective, as both R groups can migrate and the two nitrilium ions may be formed. By fragmentation, the nitrilium ions (**225** and **237**) produce the nitrile **219** and carbocation **236** (via route a or b) or nitrile **221** and carbocation **238** (via route c). In the absence of other nucleophiles the carbocations may recombine with the nitriles to re-form the nitrilium ions which, after treatment with water, results in amides (**218** and **220**). Contrary to the Beckmann rearrangement, these processes allow the isomerization of R^+ to its most stable configuration, yielding the corresponding amides (**218** and **220**) without retention of its original configuration.

B. Regioselectivity and Oxime Isomerization

Owing to the relative rigidity of the carbon−nitrogen double bond, oximes can exist in two discrete geometrically isomeric forms: the *E* or *anti* isomer (*anti*-*E*-**217**) and the (*Z*) or *syn* isomer (*syn*-*Z*-**217**) (equation 70). In solid state, both oximes show high configurational stability and discrete existence. In solution, equilibrium between both isomers is rapidly established, favouring the thermodynamically most stable isomer[109, 110].

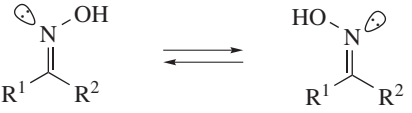

anti-(*E*)-(**217**) ⇌ *syn*-(*Z*)-(**217**)

R^1 has higher priority than R^2 in the Cahn–Ingold–Prelog rules (70)

In contrast, oxime ethers and esters are usually stable in solution but the *E*/*Z* isomerization can be induced by acids[111] or by irradiation[108]. Recently, Narasaka and colleagues[112, 113] studied the equilibration−isomerization of (*E*)-*O*-acyl oximes **239** in the presence of an acid in a nucleophilic solvent (equation 71). Isomerization probably proceeds via protonation of the oxime nitrogen followed by addition−elimination of a nucleophilic solvent until the equilibrium of *E* and *Z* isomers is achieved. The isomerization of the more labile *O*-acyloximes occurs either by an S_N2 substitution at the oxime nitrogen with acids and/or by acyl exchange through the formation of a mixed anhydride and the free oxime.

Lee and coworkers[111], studying the Beckmann rearrangement of 1-indanone oxime derivatives **240**, observed that the pure *E* and *Z* oximes isomerize under mild acidic conditions such as silica gel (equation 72). In the presence of Brønsted or Lewis acids as silica gel or $AlCl_3$ the high rotational barrier of C=N double bond would be lowered by the formation of a complex between the tosylate and $AlCl_3$ **241**. This fact makes the

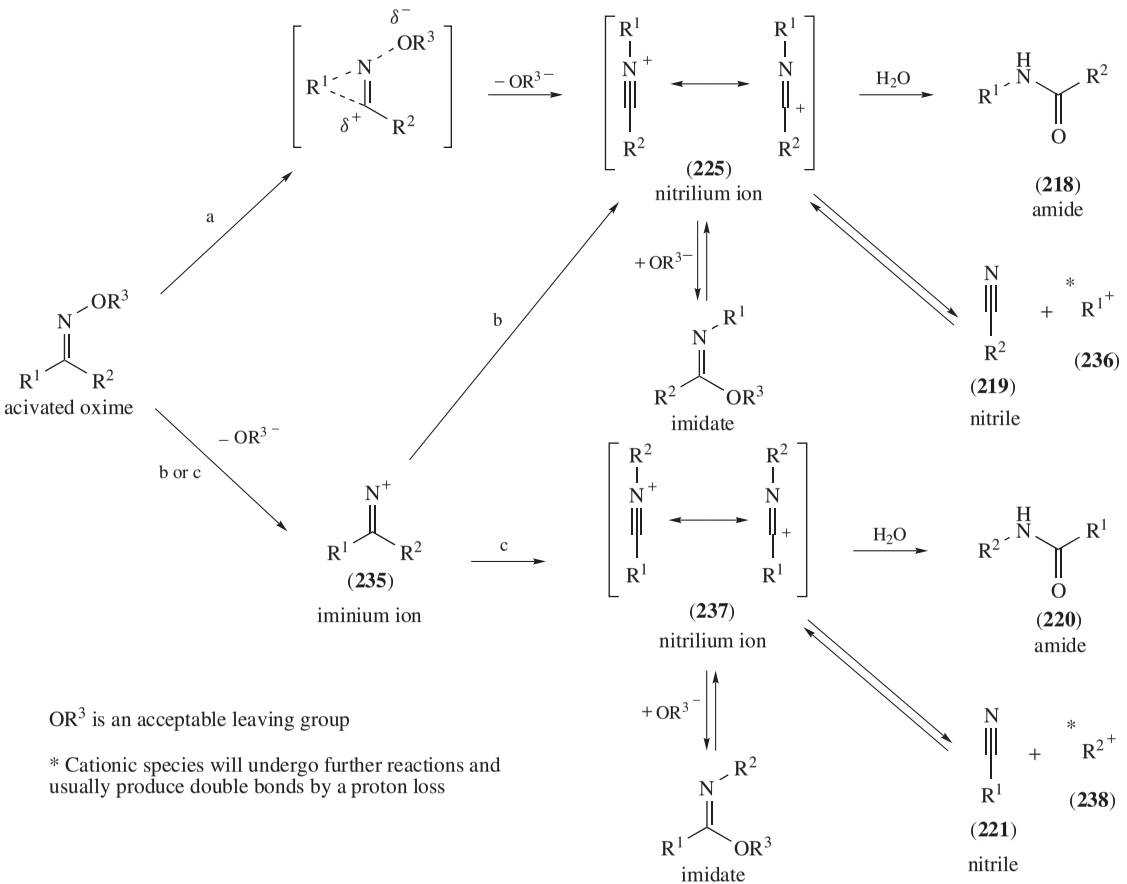
acivated oxime
a
b
b or c
– OR3 –
iminium ion
(235)
c
(225)
nitrilium ion
– OR3 –
+ OR3–
imidate
H2O
(218)
amide
(219)
nitrile
(236)
(237)
nitrilium ion
+ OR3 –
imidate
H2O
(220)
amide
(221)
nitrile
(238)
OR3 is an acceptable leaving group
* Cationic species will undergo further reactions and usually produce double bonds by a proton loss

SCHEME 7

double bond rotation possible and the product distribution of the Beckmann rearrangement would be determined by the relative stability of the $E-Z$ isomers.

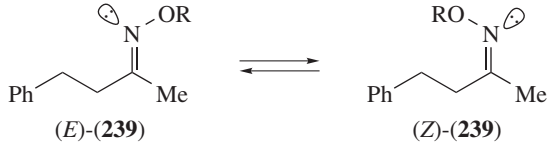

(*E*)-(**239**) (*Z*)-(**239**)

OR	Conditions	(E)/(Z)
OH	CF_3SO_3H (2.0 eq.), CH_2Cl_2	2 / 1
OMe	CF_3SO_3H (2.0 eq.), CH_2Cl_2	>99 / <1
OMe	CF_3SO_3H (2.0 eq.), CD_3OD	2 / 1
OAc	$PhCO_2H$, toluene, 80 °C	3 / 1
$OCOCF_3$	CF_3CO_2H, $CDCl_3$	3 / 1

(71)

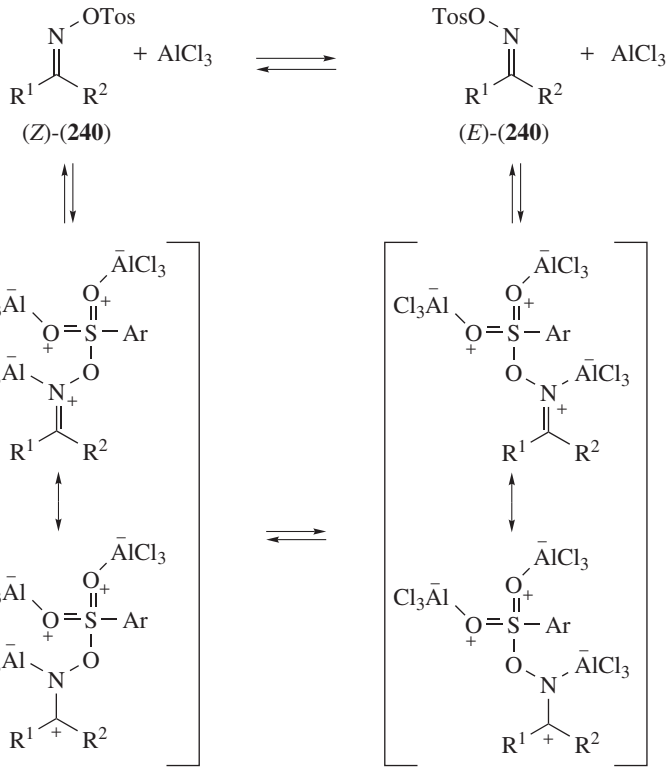

(*E*)-(**241**) (*Z*)-(**241**)

(72)

As stated before, the Beckmann rearrangement is stereospecific: the α-group *anti* to the leaving group on the nitrogen atom of the oxime usually migrates. If the starting material consists of a mixture of *E*/*Z* oximes or if isomerization occurs during the rearrangement reaction, a mixture of amides is usually obtained[111]. The isomerization of the oxime may

have an important role for a successful Beckmann rearrangement. The synthetic utility of the Beckmann rearrangement depends on the substituents (R^1 and R^2) of the oxime. If the geometry of the oxime cannot be easily controlled, this may be a drawback for the synthetic utility of the Beckmann rearrangement. Generally, oximes where one isomer is much more stable than the other and where *E*/*Z* isomerization is difficult are the best substrates for the Beckmann rearrangement. For example, this condition is met in alkyl aryl ketoximes, in which the bulky aryl group takes up the *anti* position and therefore migrates in preference to the alkyl group. This generalization is reversed only when the alkyl group is more bulky, like a branched chain, in which case the alkyl group therefore becomes the *anti* substituent. Dialkyl ketoximes tend to give mixed amides[114]. When both alkyl groups can migrate, the amide formed in the higher proportion is that from migration of the more bulky group.

C. Activation of Oximes Towards Rearrangements

1. Classical methods

Classical media for Beckmann rearrangement of unsubstituted oximes are strongly acidic media. Concentrated sulfuric acid (oleum)[115], anhydrous hydrogen fluoride[116], aluminium trichloride[117,118] and polyphosphoric acid[119,120] are classically used to mediate the rearrangement and usually produce good results. Albeit the good yields, these strongly acidic media prevent their application to sensitive substrates. On the other hand, the toxic by-products generated from these reagents and the inevitable interaction of acidic catalyst with basic substrates (including the starting ketoximes and amides) makes the isolation and purification of the product difficult. Removal of the solid catalyst is problematic and a large amount of neutralization agent (base) is normally required. In strongly acidic conditions, isomerization of the starting oxime is inevitable, which can reduce the selectivity of the amide formation.

Alternatively, oximes may be converted to *O*-substituted oximes (typically *O*-tosyl oximes) making the rearrangement much easier. Sometimes, these oxime derivatives rearrange spontaneously under the condition of their formation and cannot be isolated. Usually, *O*-tosyl ketoximes rearrange smoothly with exclusive *anti* migration. Relative to the acid-promoted Beckmann rearrangement, the rearrangement of *O*-tosyl oximes is much milder and specific.

2. Environmental friendly methods

The previous referred inconveniences have prompted an increasing interest in the development of alternative, essentially neutral and more environmental-friendly catalysts to promote the rearrangement of *O*-unsubstituted oximes. The development of highly efficient and selective transformations and also of processes for catalyst recovery and its reuse are the aim of some of the more recent studies. Much of this work is being done in industry to improve current production processes and is the subject of new patent applications. During the last two decades environment concerns have led to the development of green, simple and cost-effective catalytic systems for the Beckmann rearrangement.

a. Solid catalysts—zeolites and mesoporous materials. The interest in vapour-phase Beckmann rearrangement has increased recently. Several solid catalysts had been studied, such as boria-hydroxyapatite[121], metal ilerite[122,123], supported oxide[124,125] and zeolites, including MCM-41[126–129], MCM-22[130,131], SAPO-11[132] and MgCoAlPO-36[133]. These processes mainly deal with ε-caprolactam synthesis, but low selectivity or rapid decay of catalyst activity is generally observed, partially caused by high reaction

temperatures[123, 127]. As for the liquid-phase process, it usually proceeds under milder conditions and can be applied to the synthesis of different amides.

Zeolites and other mesoporous materials are excellent catalysts for industrial and laboratory applications[134]. Favourable characteristics are their capacity to immobilize homogenous catalysts rendering them heterogeneous, their thermal stability, and the ease of separation from the reaction products and reuse in liquid- and gas-phase conditions. The pore size and Brønsted and Lewis acidic properties are determinant for their use as catalyst in the Beckmann rearrangement. Recently, a review on the use of zeolites and mesoporous materials in the Beckmann rearrangement was published[135].

The nature and location of the active sites for the Beckmann rearrangement in microporous and mesoporous solids was studied by *in situ* infrared spectroscopy, comparing the reactivity of oximes with different molecular sizes[136]. The rearrangements of acetophenone and cyclododecanone oximes into acetanilide and laurolactam, respectively, were studied using siliceous and Al-containing zeolites Beta and MFI and mesoporous MCM-41 as catalysts. The results indicated that Brønsted acid sites, as well as strongly hydrogen-bonded silanol groups and silanol nests, located in the pores of zeolites and MCM-41, were active in the reaction. When the external surface or the outer shell of MFI-type crystals was considered, the bridging hydroxyl groups appeared to be active, whereas no activity in the Beckmann rearrangement of cyclododecanone was observed over silanol groups. However, it was shown that these sites favour the formation of by-products, and both the activity and selectivity of the amide is improved in the presence of high-silica zeolites with medium or weak Brønsted acid sites[137–139]. Discrepancies are also found for the location of the active sites, which have been proposed to be inside the micropores[140, 141], just at the aperture[142] or at the zeolite surface[137, 138].

Theoretical studies on the Beckmann rearrangement mechanism over zeolite catalyst supported by experimental data have increased. The catalytic activity of the zeolite is determined by Brønsted and Lewis acid sites created by protonation or activation by metallic cations. The reactivity of the acid sites is strongly influenced by the geometry and flexibility of the zeolite framework[143].

The initial adsorption of the oxime in zeolites was studied through a combination of solid-state NMR spectroscopy and theoretical calculations[139, 144]. The calculated adsorption complexes formed over silanol groups and complexes over Brønsted acid sites in zeolites are depicted. This study suggests that the *N*-protonated oxime is formed over Brønsted acid centers, but not over weakly acidic silanol groups. It has been also suggested that weakly acidic or neutral silanol groups or silanol nests are active catalysts of the rearrangement reaction[137, 138].

A periodic DFT *ab initio* technique was used by Bucko and coworkers[145] to investigate the reaction mechanisms for the Beckmann rearrangement of cyclohexanone oxime catalysed by mordenite. They found that the most favourable active site is the Brønsted acid site, where the rate-determining step of the reaction is the [1,2]-*H*-shift step with an energy barrier of about 20 kcal mol^{-1}. According to Limtrakul and colleagues[143, 146] who investigated the mechanism of rearrangement of oximes with different molecular sizes over *H*-Faujasite zeolite, the rearrangement step using the bare cluster model is the rate-determining step of the entire reaction of these oxime molecules of which the energy barrier is between 50 and 70 kcal mol^{-1}. The more accurate embedded cluster model, in which the effect of the zeolitic framework is included, yields as the rate-determining step the formaldehyde oxime reaction rearrangement with an energy barrier of 50.4 kcal mol^{-1}. With the inclusion of the methyl substitution at the carbon-end of formaldehyde oxime, the rate-determining step of the reaction becomes the [1,2]-*H*-shift step for *Z*-acetaldehyde oxime (30.5 kcal mol^{-1}) and acetone oxime (31.2 kcal mol^{-1}), while, in the *E*-acetaldehyde oxime, the rate-determining step is either the [1,2]-*H*-shift

(26.2 kcal mol^{-1}) or the rearrangement step (26.6 kcal mol^{-1}). These results signify the important role that the effect of the zeolite framework plays in lowering the activation energy by stabilizing all the ionic species in the process. It should, however, be noted that the sizeable turnover of a reaction catalysed by the Brønsted acid site might be delayed by the quantitatively high desorption energy of the product and readsorption of the reactant at the active center.

According to Limtrakul and colleagues[143] the mechanism of the Beckmann rearrangement of the oxime molecule on the Brønsted acid site of a zeolite proceeds according to the following steps outlined in equation 73.

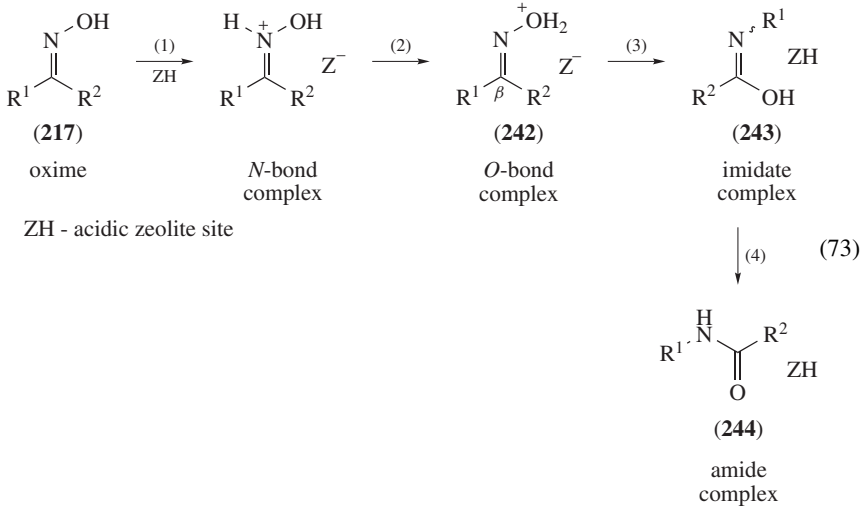

(73)

Step (1) is the adsorption of the oxime molecule, by interaction between the nitrogen atom of the oxime molecule **217** and the Brønsted acid site of zeolite; protonation at the nitrogen atom of the oxime molecule occurs. In the second step (step 2), a [1,2]-*H*-shift, the hydrogen is transferred from the nitrogen-end **218** to the oxygen atom of the oxime molecule. Step (3) is the rearrangement step, which involves the rearrangement of the *O*-bond complex **242** to the enol–amide complex **243**. During this step an R^1 group (R^1 = alkyl, aryl or hydrogen) at the β-position moves to the nitrogen atom and a water molecule is displaced. Subsequently, the displaced water molecule binds to the carbon atom, simultaneously transferring a proton to the acid catalyst. Step (4), the last transforming step, is the tautomerization of the imidate complex **243** to the amide complex **244**, and finally desorption of the amide molecule from the catalyst occurs in the final fifth step (not shown).

Rare-earth exchanged [Ce^{III}, La^{III}, Sm^{IIII} and RE^{III} (RE = La/Ce/Pr/Nd)] Na–Y zeolites, K-10 montmorillonite clay and amorphous silica–alumina have also been employed as solid acid catalysts for the vapour-phase Beckmann rearrangement of salicylaldoxime **245** to benzoxazole **248**[147] (equation 74) and of cinnamaldoxime to isoquinoline[148,149]. Under appropriate reaction conditions on zeolites, salicyl aldoxime **245** undergoes *E*–*Z* isomerization followed by Beckmann rearrangement and leads to the formation of benzoxazole **248** as the major product. Fragmentation product **247** and primary amide **246** are formed as minor compounds. When catalysts with both Brønsted and Lewis acidity were used, a correlation between the amount of Brønsted acid sites and benzoxazole **248** yields was observed.

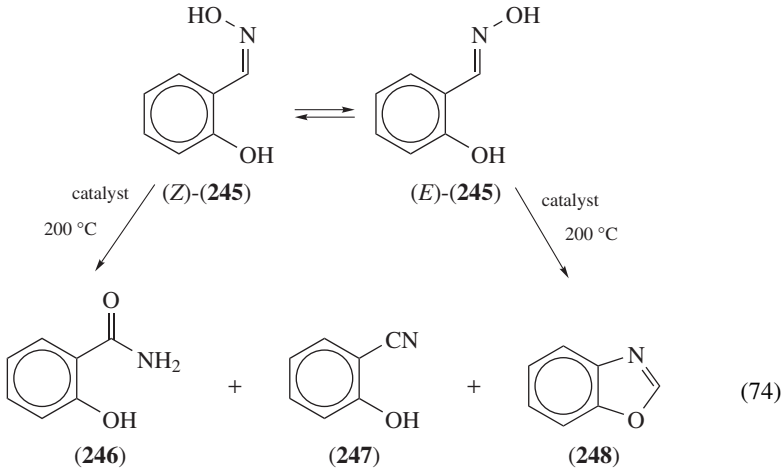

(74)

Catalyst	Yield (%)		
	246	**247**	**248**
Na-Y	32.9	4.3	51.8
CeNa-Y	2.5	8.7	83.7
LaNa-Y	9.2	7.6	79.8
RENa-Y	4.5	10.1	82.3
SmNa-Y	1.3	9.0	84.5
K-10 clay	24.0	5.3	50.4
Al_2O_3 - SiO_2	29.2	4.8	49.5

Acidic zeolites, K-10 clay and silica are highly active and selective catalysts for the dehydration/Beckmann rearrangement reactions of aldoximes (benzaldoxime and 4-methoxybenzaldoxime) for the synthesis of nitriles and amides[150].

b. Mild conditions—Beckmann rearrangements of sensitive compounds. The drastic reaction conditions used in classical Beckmann rearrangement limit its use to acid non-sensitive compounds. The interest in Beckmann rearrangement in milder and essential neutral conditions, adequate for use in sensitive compounds, has increased. To achieve this goal, OH must be converted into a more efficient leaving group. The resulting more unstable specie, an 'activated oxime', may be isolated in some cases or it may be a very reactive intermediate that rearranges spontaneously.

Tamura's reagent ($2,4,6\text{-}Me_3C_6H_2SO_2NH_2$)[151] has been used to convert ketones directly to amides.

Sulfamic acid ($^+H_3NSO_3^-$) has been proved to be an efficient and green catalyst for liquid Beckmann rearrangement of ketoxime in anhydrous acetonitrile[152]. Due to its intrinsic zwitterionic property, the use of a base for the neutralization is avoided and wastes can be reduced.

A variety of ketones **249** can be directly converted into the secondary amides **253** (the expected product of a Beckmann rearrangement of the corresponding oximes **250**) in high yield, by heating them with hydroxylamine hydrochloride and anhydrous oxalic acid[153] (equation 75). Aromatic aldehydes afforded mixtures of nitriles and amides. The

transformation is apparently kinetically driven by the coupled decomposition of the intermediate **251** to CO, CO_2 and imidate **252**, affording the amide **253**.

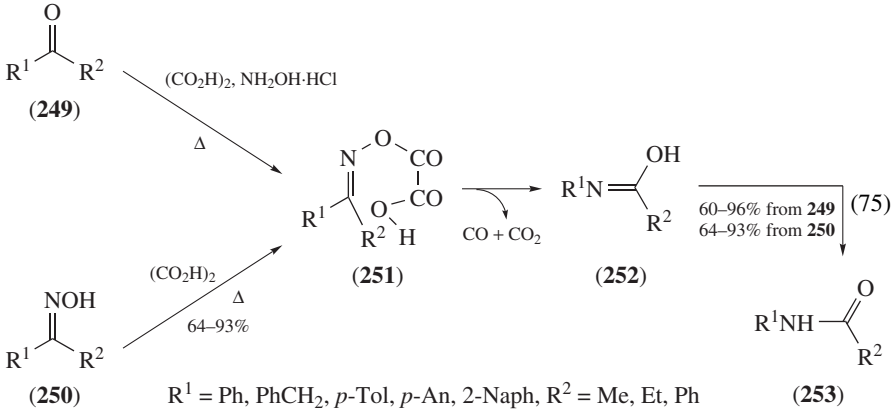

Diazotisation of ketoxime carbamates **254** in concentrated sulfuric acid with either isoamyl nitrite or sodium nitrite leads to the Beckmann rearrangement products in moderate to excellent yields with CO_2 and N_2 as the only by-products[154] (equation 76).

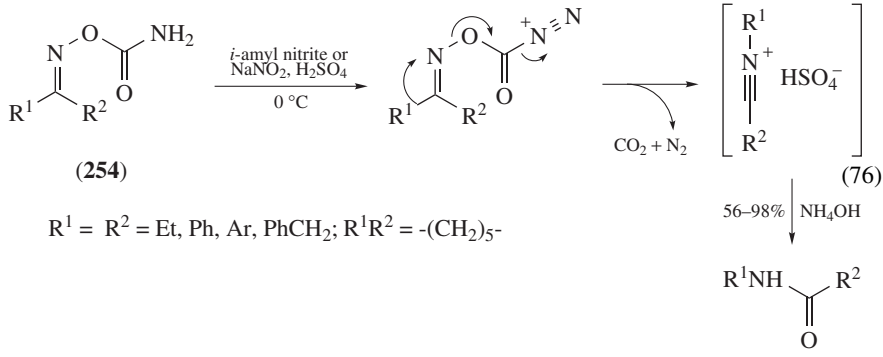

A variety of oximes **255** undergo the Beckmann rearrangement upon treatment with 2,4,6-trichloro-1,3,5-triazine (cyanuric chloride, **256**) in *N*,*N*-dimethylformamide (DMF, **257**) at room temperature in excellent yields[155] (equation 77).

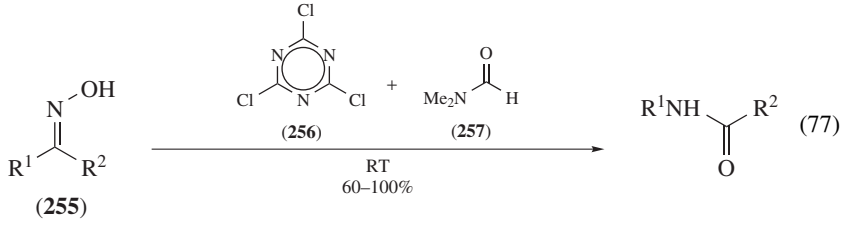

The formation of a very electrophilic intermediate **258** from **256** and **257** is proposed (equation 78). The hydroxyl group of the oxime adds to **259**, giving a reactive cationic species **260** that rearranges and affords the nitrile **261** (in the case of aldoxime, equation 79), or the amide **262** upon hydrolytic workup (equation 80). The conversion of **260** to the nitrilium ion should occur through a concerted [1,2]-intramolecular shift. This procedure can be applied in the conversion of aldoximes to nitriles. It was observed that the stereochemistry of the ketoximes has little effect on the reaction, this fact being explained by the $E-Z$ isomerization of the oxime isomers under the reaction conditions.

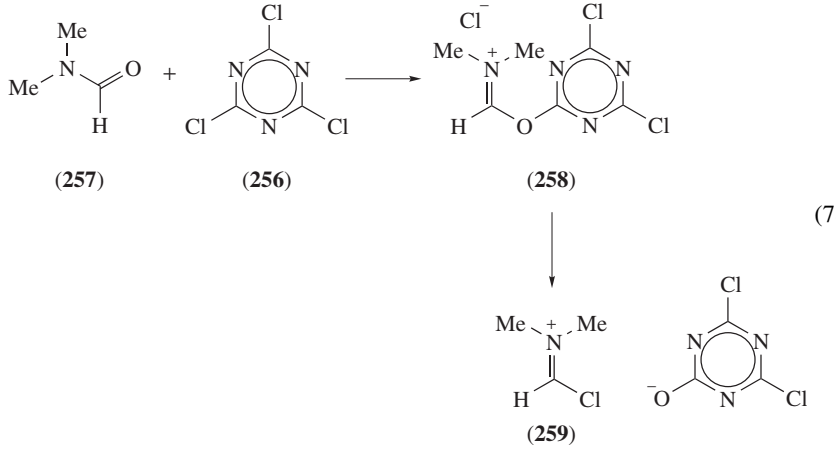

(**257**) (**256**) (**258**) (**259**) (78)

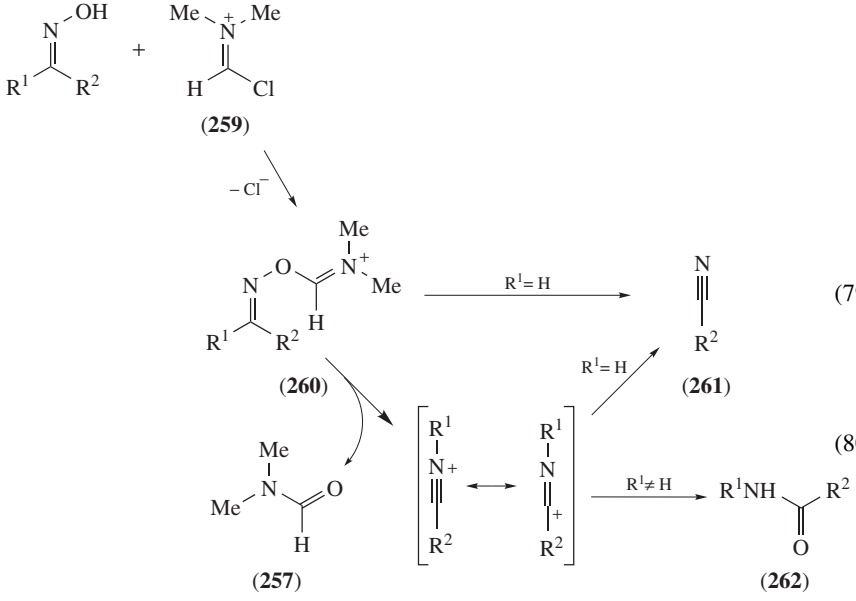

(**259**) (**260**) (**261**) (79)

(**257**) (**262**) (80)

Yamamoto, Ishihara and coworkers[156] proposed a different mechanism for the Beckmann rearrangement of ketoximes catalysed by cyanuric chloride **256** and other chloroarenes (**263**, **267**, **268**) bearing several strong electron-withdrawing groups (equation 81). The authors suggested the formation of the corresponding *O*-aryl ketoximes (**264**), an *O*-aryl imidate (**265**) intermediate and a Meisenheimer complex (**266**) to explain the results. Acids such as HCl and $ZnCl_2$ are effective as co-catalysts.

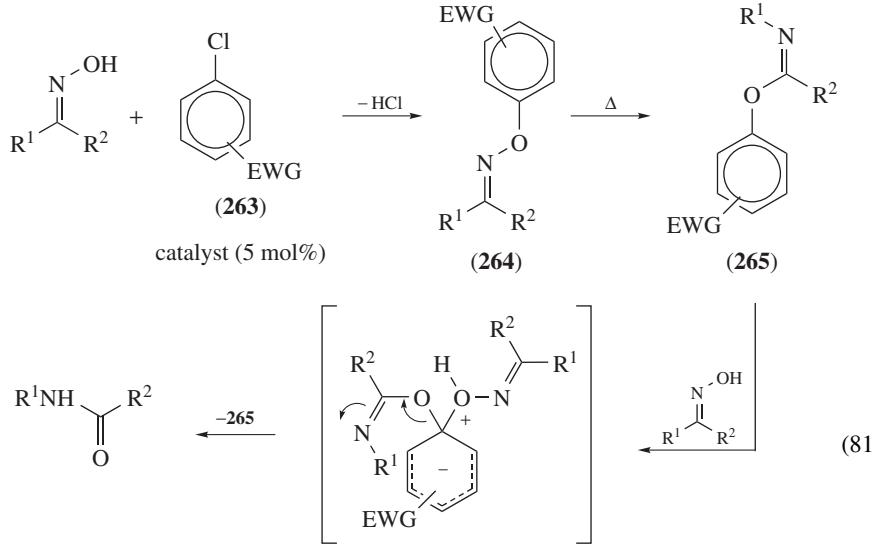

(81)

Catalysts

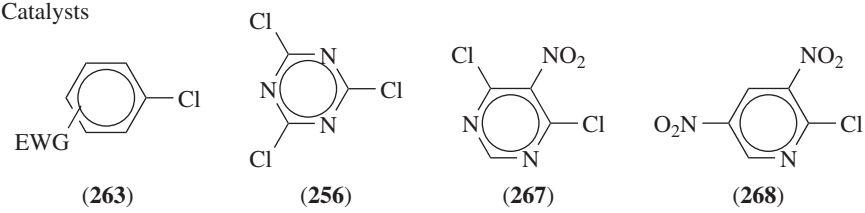

EWG = 2,4,6-$(NO_2)_3$, 2,6-$(NO_2)_2$-4-CN

It was also found that the rearrangement of cyclic oximes into lactams in the presence of cyanuric chloride is markedly facilitated by the use of 1,1,1,3,3,3-hexafluoro-2-propanol (HFIP) as solvent[157].

A similar mechanism to the previous ones was proposed by Deng, Shi and coworkers[158] for the bis(2-oxo-3-oxazolidinyl)phosphinic chloride (BOP-Cl, **269**) catalytic Beckmann rearrangement (equation 82). Addition of the Lewis acid zinc chloride improved the catalyst performance and amides were synthesized in excellent yields (92–99%).

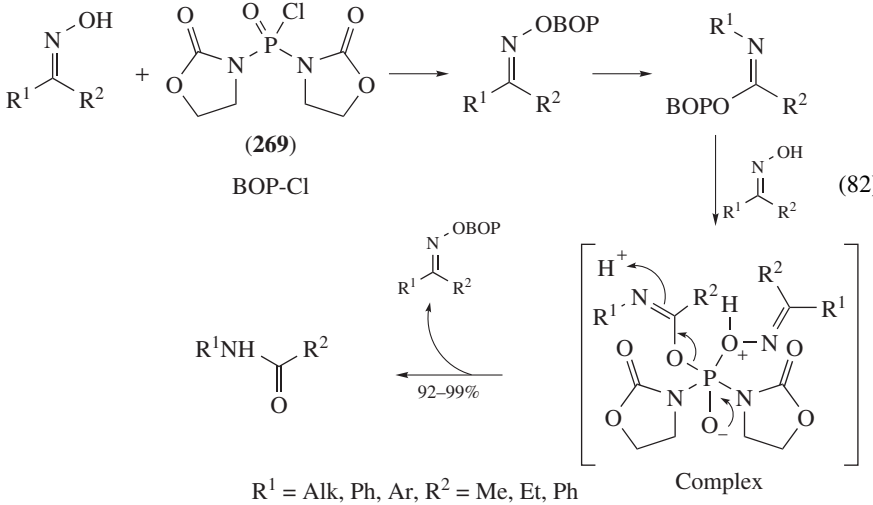
(269)
BOP-Cl
92–99%
Complex
R1 = Alk, Ph, Ar, R2 = Me, Et, Ph

(82)

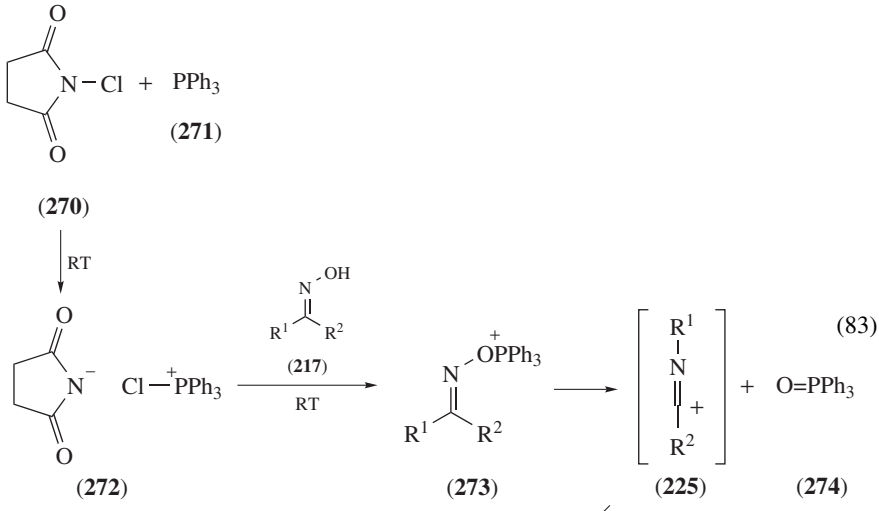
(270)
(271)
RT
(272)
(217)
RT
(273)
(225)
(274)
R1 = H
R1 ≠ H
(219)
77–97%
(218)
75–82%

(83)

The Beckmann rearrangement of ketoximes with triphenylphosphine and *N*-chlorosuccinimide occurs at room temperature almost instantaneously and their corresponding secondary amides are obtained in high yields[159] (equation 83). The triphenylphosphine **271** is activated by the *N*-chlorosuccinimide **270** affording the salt **272**, which is attacked by the *N*-hydroxy group of the oxime **217** forming the intermediate **273**.

Rearrangement of **273** with simultaneous loss of triphenylphosphine oxide **274** produces the intermediate nitrilium ion **225** that affords the corresponding amide **218**. Aldoximes are easily converted to their corresponding nitriles **219** under the same reaction conditions.

Also, chlorosulfonic acid was demonstrated to be an efficient catalyst in the Beckmann rearrangement of a variety of ketoximes in refluxing toluene, and excellent conversion and selectivity was observed[160, 161]. This procedure can also be applied to the dehydration of aldoximes yielding the corresponding nitriles.

In the presence of a catalytic amount of an antimony(V) salt ($SbCl_4^+$ SbF_6^-), generated from antimony(V) chloride and silver hexafluoroantimonate, the Beckmann rearrangement of several ketoxime trimethylsilyl ethers proceeds smoothly to give the corresponding amides or lactams in good yields[162].

Oximes such as cyclohexanone oxime and benzaldehyde oxime were catalytically transformed to the corresponding lactams in *N*,*N*-dimethylformamide solutions of alkylating reagents such as trialkyloxonium salts. *O*-Alkyl-*N*,*N*-dimethylformamidinium salt was suggested as the active catalyst species[163].

c. Transition metal complexes. Transition metal complexes can assist Beckmann rearrangement under essentially neutral conditions. The process is characterized to be atom-economical and environmentally friendly because the transformation occurs generally in the absence of any additives except for the catalyst and it does not generate any by-products[164].

The catalytic activities of a diverse range of ruthenium complexes for the rearrangement of benzaldoxime were investigated. Some ruthenium catalysts showed measurable activities for conversion of aldoximes to the corresponding amides. When benzaldoxime was treated with $[RuCl_2(p\text{-cymene})]_2$ catalyst (5 mol%) in DMF over 4 hours at 150 °C, conversion was incomplete (53%) in the absence of any additives such as molecular sieves, and the ratio of formed benzonitrile to benzamide was determined to be 1:2. Other ruthenium catalysts were investigated but displayed rather lower activities or decreased selectivities under the same conditions: $RuH_2(PPh_3)_4$ (77% conversion, 1:1), $Ru_3(CO)_{12}$ (19% conversion, 3:1) and $RuCl_3$ (67% conversion, 1:1). Compared to the ruthenium complexes, rhodium catalysts exhibit enhanced selectivity for the production of benzamide. Some examples are $[Rh(OAc)_2]_2$ (in DMF, 150 °C, 4 h, 88% conversion, nitrile:amide, 1:4), $[RhCl(cod)]_2$ (67%, 1:4), $[(PPh_3)_3Rh(nbd)]^+$ PF_6^- (77%, 1:6) and $RhCl(PPh_3)_3$ (92%, 1:6). However, Wilkinson's catalyst ($RhCl(PPh_3)_3$) **275** has been found to catalyse the transformation of aldoximes to the corresponding amides with high selectivity and efficiency (equation 84).

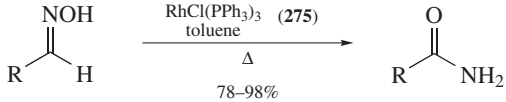

(84)

R = *c*-Hex, Ph, Bn, Ar

The same activity is presented by an iridium complex $[Ir(Cp^*)Cl_2]_2$ that catalyses the Beckmann rearrangement of aromatic, aliphatic and heteroaromatic aldoximes **276** into the corresponding primary amide **277** in good to excellent yields (78–97%)[165] (equation 85).

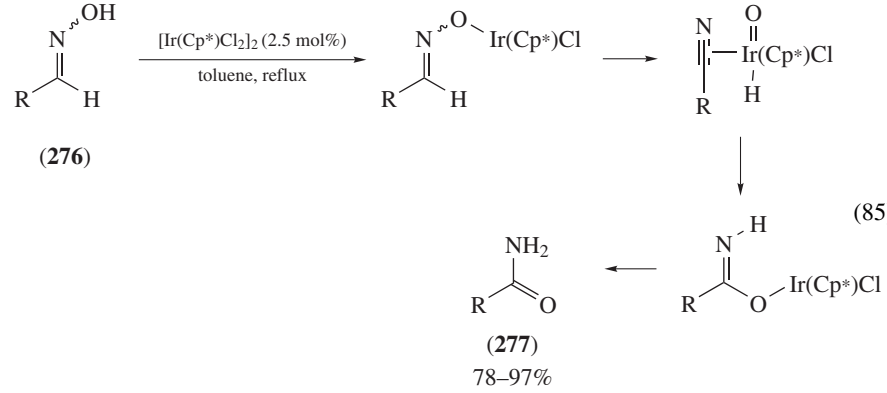

R = Ph, 4-MeOC$_6$H$_4$, *n*-C$_3$H$_7$, (*E*)-PhCH=CH, 2-Fu, 3-Pyr

The isomerization of the (*Z*)-isomer into the (*E*)-isomer promoted by the iridium complex explains the lack of stereospecificity of the transformation. *O*-Alkylated oximes and ketoximes do not react and this fact suggests that the presence of both hydrogen and a hydroxyl group is required for the success of the transformation. The authors proposed that the initial displacement of a chloride ion of the iridium complex by the oxime allows the iridium to remove both the oxygen and the hydride from the initial oxime. Swapping places of both substituents produces the amide.

Arisawa and Yamaguchi[166] compared the catalytic activities of several rhodium complexes in promoting the Beckmann rearrangement of benzophenone oxime in the presence of trifluoromethanesulfonic acid and tris(*p*-tolyl)phosphine. While RhCl(PPh$_3$)$_3$ and [RhCl(cod)]$_2$ plus PPh$_3$ are active, RhH(PPh$_3$)$_4$, RhH(CO)(PPh$_3$)$_3$, RhCl(CO)(PPh$_3$)$_3$, RhH(OAc)(PPh$_3$)$_3$ and RhCl(PPh$_3$)$_3$ are not.

d. Lewis acids and superacids. The Beckmann rearrangement of substituted benzophenone and acetophenone oximes was promoted by using 'silferc' (anhydrous FeCl$_3$ supported on silica-gel by a co-grinding method)[167] under milder conditions. The yields of the rearrangement product were low and fragmentation product was always observed.

However, gallium triflate was found to be an excellent homogeneous catalyst for the rearrangement of a wide variety of ketoximes into the corresponding amides in acetonitrile solution[168]. The best results were attained in acetonitrile in the presence of 5 mol% of catalyst. Diethyl ether, dimethoxyethane and dichloromethane are not suitable solvents due to the poor solubility of the catalyst and polar solvents deactivate the catalyst to some extent. The authors explained the lack of selectivity suggesting that *syn–anti* isomerization of oximes is catalysed by gallium triflate under the reaction conditions. The equilibrium among the oxime isomers is faster than the rearrangement and thus the product composition is determined by the relative rates of migration of the involved groups and is independent of the stereochemistry of the starting oximes. Also in refluxing acetonitrile, a variety of ketoximes undergo the Beckmann rearrangement upon treatment with a catalytic amount of Yb(OTf)$_3$ to afford the corresponding amides and lactams in excellent yields and high selectivity[169]. Good results have also been obtained using AlCl$_3$/6H$_2$O/KI/H$_2$O/CH$_3$CN[170].

In the presence of indium(III) chloride, 3-acyl-1*H*-quinolin-4-ones ketoximes **278** rearrange to the corresponding oxazoloquinolines **279**[171] (equation 86). Isooxazoloquinolines **280** are also formed as minor products.

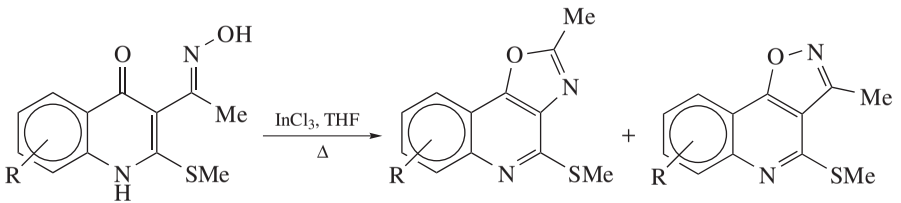

(**278**) (**279**) (**280**)

	Yield (%)	
R[a]	**279**	**280**
H	86	7
8-Ph	65	17
6,8-di-Me	82	16
7-MeO	78	1
7-CF_3	76	12
5,7-di-Cl	62	28
6-NO_2	82	5
8-F	80	7

[a] *E* isomer.

(86)

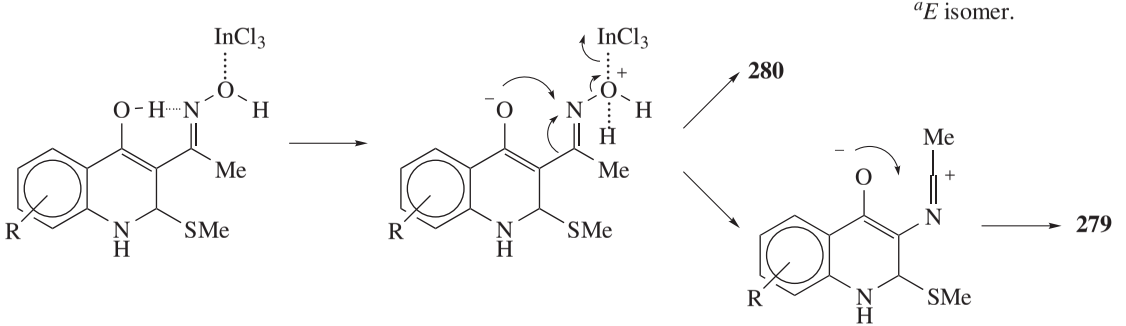

(87)

It is proposed that **279** are formed in the presence of $InCl_3$ by trapping of the nitrilium ion intermediate by the β-hydroxy group of the tautomeric form of the ketoximes (equation 87).

Indium trifluoromethanesulfonate was found to be an effective high-yielding catalyst for the facile dehydration of aldoximes to nitriles and Beckmann rearrangement of ketoximes to anilides[172].

Due to its Lewis acidic properties, the use of chloral (trichloroacetaldehyde) in the Beckmann rearrangement was investigated[161]. When a variety of ketoximes is admixed with chloral hydrate and the mixture is heated at low pressure in nitrogen atmosphere, the Beckmann rearrangement afforded the corresponding amides in excellent yields (73–98%). The transformation occurs under neutral, relatively mild and solvent-free conditions.

The Beckmann rearrangement of oxime esters is catalysed by Brønsted or Lewis acids and these conversions are usually non-stereospecific, as demonstrated by the studies of Beckmann rearrangement of 1-indanone oximes derivatives **240a** with aluminium chloride as a catalyst[111] (equation 88).

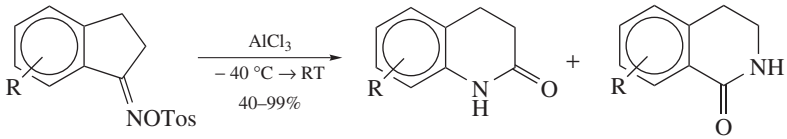

(**240a**) (**281**) (**282**)

(88)

	Precursor	Yield (%)	
R	**(*E*)-240a/(*Z*)-240a**	**281**	**282**
H	97/3	92	8
4-CH_3	100/0	85	15
4-OCH_3	100/0	74	26
4-NO_2	80/20	27	73
6-NO_2	84/16	96	4

To explain these results, Lee and colleagues[111] showed that in the absence of Lewis acids the rotational barrier of the C=N double bond is fairly high, but in the presence of catalysts the rotational barrier is lowered. The complex formation of tosylate and $AlCl_3$ makes the double bond rotation possible and the product distribution is determined by the relative stability of the oxime $E-Z$ isomers (equation 89). A cyclic transition state affords the corresponding quinolinone **281** and the isoquinolinone **282**.

However, *O*-arylketoximes do not afford the rearrangement product under the Beckmann conditions in the presence of Lewis acids such as $AlCl_3$ and $ZrCl_4$[42] (equation 90). A different mechanism involving an initial heterolytic N−O bond cleavage of the oxygen complexed to the Lewis acids was proposed by Kikugawa and coworkers for the intramolecular migration of the imino group from the oxygen to the *ortho* position of the aryl group.

A variety of ketoxime ethyl carbonates undergo the Beckmann rearrangement in excellent yields (74–99%), upon treatment with 1 equivalent of boron trifluoride etherate at room temperature[173] (equation 91).

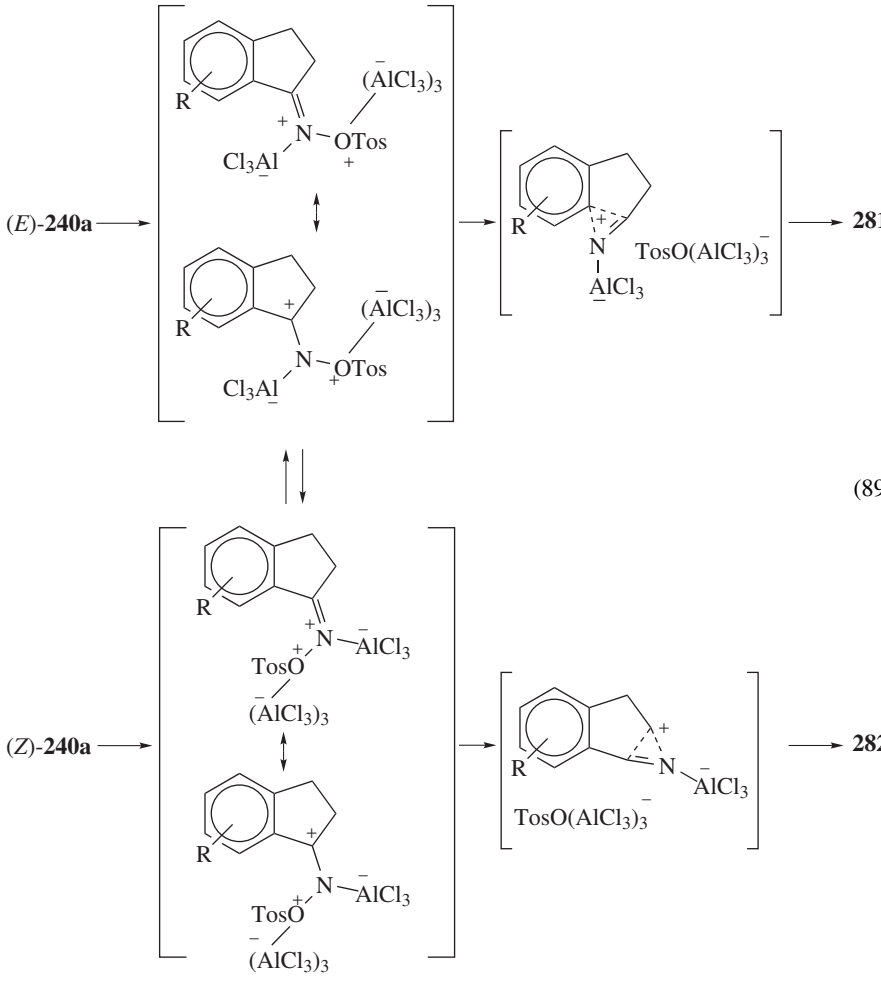

(89)

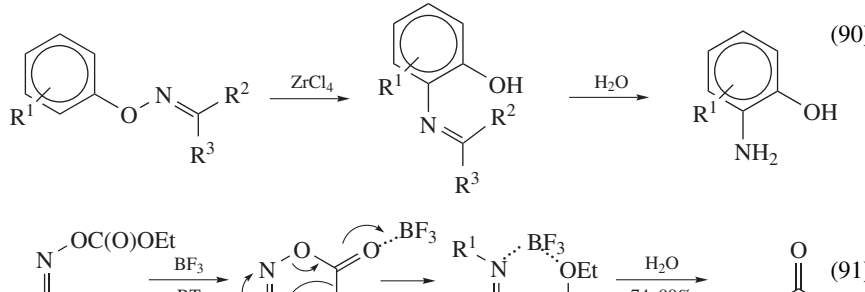

(90)

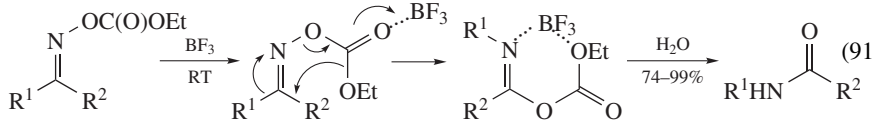

(91)

R^1 = Et, Ph, $PhCH_2$, Ar, R^2 = Me, Et, Ph, $PhCH_2$, Ar

Boron trifluoride etherate was used in conjunction with the reducing agent borane to rearrange aromatic *O*-triisopropylsilyl ketoximes to cyclic and acyclic aniline derivatives[174]. The steric hindrance of the substituents on the silicon atom, the size of the aliphatic ring and the presence of alkoxy substituents on the aryl group played important roles in the aniline formation.

Superacid-catalysed (SbF_5 and $SbCl_5$) Beckmann rearrangement of oximes in the solid state was studied[175] (equation 92). Products resulting from alkyl group shift or hydride migration were identified. These conclusions were supported by *ab initio* calculations and the use of cryogenic matrices enabled one to isolate intermediate cations. The authors found that cyclic oximes with smaller rings (cyclobutanone oxime and cyclopentanone oxime) undergo hydride migration rather than alkyl group shift. It is proposed that the mechanism should involve the formation of a stable cation **283** by a [1,3]-*H*-shift. In contrast, cyclohexanone oxime rearranges by a classical Beckmann mechanism to a cyclic seven-membered nitrilium cation **284**.

It is supposed that hydrogen bonds between halogen atoms of the superacid and the α-hydrogens of the oxime in the Lewis acid–oxime complex can play a role in the hydride transfer either by inter- or by intra-molecular processes.

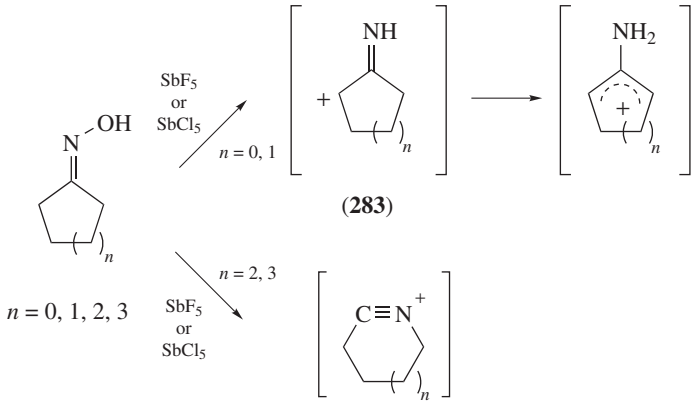

(92)

e. Solvent-free transformations. Considerable attention has been paid to solvent-free reactions[176, 177]. These reactions are not only of interest from an environment point of view, but in many cases also offer considerable synthetic advantages in terms of yield, selectivity and simplicity of execution. Solvent-free Beckmann rearrangement has also been explored.

Beckmann rearrangement of ketoximes is achieved efficiently with anhydrous $FeCl_3$ in the absence of solvent[178]. The rearrangement was selective, producing only one amide isomer in usually good yield.

Under solvent-free conditions, one-step Beckmann rearrangement of a variety of ketones and aldehydes proceeded in the presence of alumina sulfuric acid **285**[179] (equation 93). Good selectivities were also obtained in the rearrangement of aldoximes to primary amides using zinc oxide as catalyst[180] (equation 93).

The Beckmann rearrangement of cyclohexanone oxime catalysed by solid metaboric acid (**286**) has also been investigated[181] (equation 94). When ketoximes, mixed with **286** (formed from boric acid at 100 °C/0.1 Torr), are heated (140 °C/7–42 h) the corresponding amides or lactams are produced in excellent yields (62–92%). Under the

same reaction conditions, aromatic aldoximes undergo both fragmentation to the nitrile and a non-stereospecific rearrangement to primary amide.

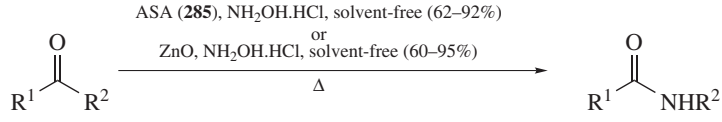

(93)

ASA = alumina sulfuric acid

R^1, R^2 = H, Alk, Ar, *c*-Alk

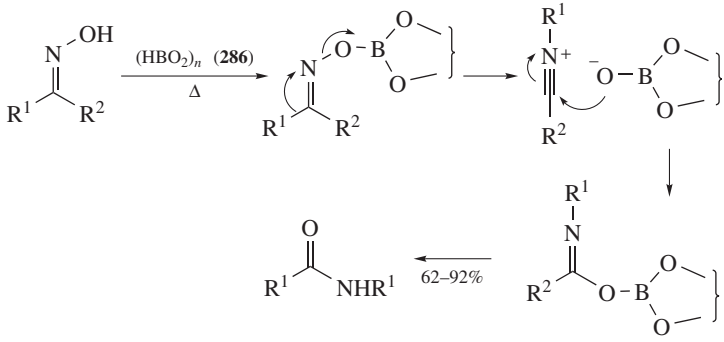

(94)

R^1 = Ph, Ar, 1-Naph, R^2 = H, Me, Ph; R^1R^2 -$(CH_2)_5$–

The use of microwave (MW) activation was common in various attempts to improve the solvent-free Beckmann rearrangement (equation 95). Ketoximes give amides by Beckmann rearrangement in the presence of P_2O_5/SiO_2 in dry media under microwave irradiation[114]. In the same conditions nitriles are obtained by Beckmann fragmentation from the corresponding aldoximes[182]. Also, $AlCl_3–ZnCl_2$ catalyst supported on silica gel[183] is efficient for the Beckmann rearrangement of alkyl aryl ketoximes under microwave irradiation in solvent-free conditions[183]. The corresponding amides are obtained in moderate to excellent yields. As expected, electron-donating groups on the aromatic ring (the migrating group) lead to better yields compared to electron-withdrawing groups. Silica sulfuric acid ($SiO_2–OSO_3H$) as catalyst in Beckmann reaction promoted by microwaves has the advantage of high conversion, high selectivity and short reaction times[184, 185].

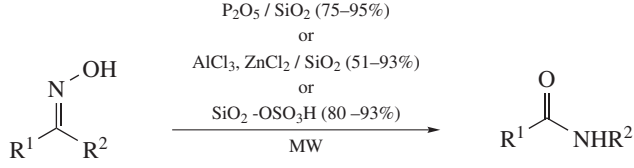

(95)

R^1, R^2 = H, Alk, *c*-Alk, Ar, Heterocyclic

Activated Fly ash[186], an industrial waste pollutant, is found to be a good catalyst in Beckmann rearrangement promoted by microwaves under solvent-free conditions. The amides are obtained from the corresponding ketoximes in high yields (75–94%).

Neutral alumina-supported sodium hydrogen sulfate was also used as a heterogenous catalyst for the 'one' pot conversion of ketones to a great variety of amides in the presence of hydroxylamine under microwave irradiation in solvent-free conditions[103].

f. Ionic liquids. Recently, ionic liquids have gained recognition as environmentally benign alternatives to more volatile organic solvents. Ionic liquids have some interesting properties, such as wide liquid temperature range, negligible vapour pressure, high thermal stability and good solvating ability for a wide range of substrates and catalysts[187].

Beckmann rearrangements using ionic liquids as solvents have been reported. These procedures have the advantages of short reaction time, high yield, no pollution, simple operation and easy work-up[188]. $POCl_3$, P_2O_5/PCl_5[189] metaboric acid[190], $CeCl_3 \cdot 7H_2O-NaI/SiO_2$ system[191] as catalysts and 1-butyl-3-methyl imidazolium trifluoroacetate, [BMIM] TFA, tetrafluoroborate [BMIM] BF_4 and butylpyridinium tetrafluoroborate [N-BuPy] BF_4 ionic liquids as solvent were used[189]. Cyclohexanone oxime was usually selected as the precursor for the rearrangement. The best results were achieved with the [N-BuPy] BF_4 with full conversion to the product and 99% selectivity observed. The use of pure ionic liquid (without any catalyst) did not produce any amide.

The Beckmann rearrangement of cyclohexanone oxime in [BMIM]PF_6 and [BMIM]BF_4 catalysed by P_2O_5 and P_2O_5–methanesulfonic acid (Eaton's reagent) was also reported[192]. Reaction times varied from 16 h to 24 h and generally excellent yields were obtained when using [BMIM]PF_6. No product was formed in the case of [BMIM]BF_4.

Lee and colleagues studied the ionic-liquid-mediated Beckmann rearrangement under microwaves[193] (equation 96). They screened several ionic liquids and investigated the amount of sulfuric acid needed as catalyst. The microwave methodology was found to be superior to analogous conventional heating. All the ionic liquids tested worked well in the microwave and only 5 mol% sulfuric acid was needed. The BMIM ionic liquids ([BMIM]PF_6, [BMIM]BF_4, [BMIM]SbF_6 and [BMIM]OTf) were found to be thermally stable.

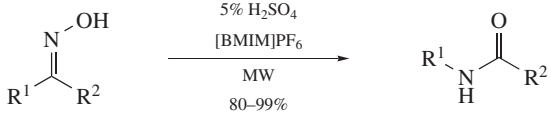

(96)

R^1 = Et, Ph, Ar, R^2 = Et, Ph

Recently, novel sulfonyl chloride functionalized ionic liquids (**287**, **288**, **289** and **290**) were used as solvent and catalyst in Beckmann rearrangements[194, 195]. The use of these

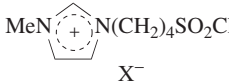

(**287**)

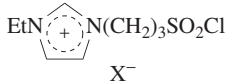

(**288**)

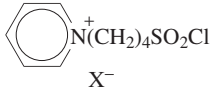

(**289**)

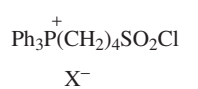

(**290**)

X = PF_6, CF_3SO_3 , CF_3CO_2 , *p*-TolSO_3

task-specific ionic liquids affords the Beckmann rearrangement of different ketoximes. The corresponding amides are easily obtained in high yields after an aqueous extraction. The observed results were better than those previously reported for catalyst/ionic liquid systems.

To explain the difficulties encountered in the reuse of sulfonyl chloride functionalized ionic liquids during Beckmann rearrangement, Deng and colleagues proposed a mechanism for rearrangement of cyclohexanone oxime[194] (equation 97).

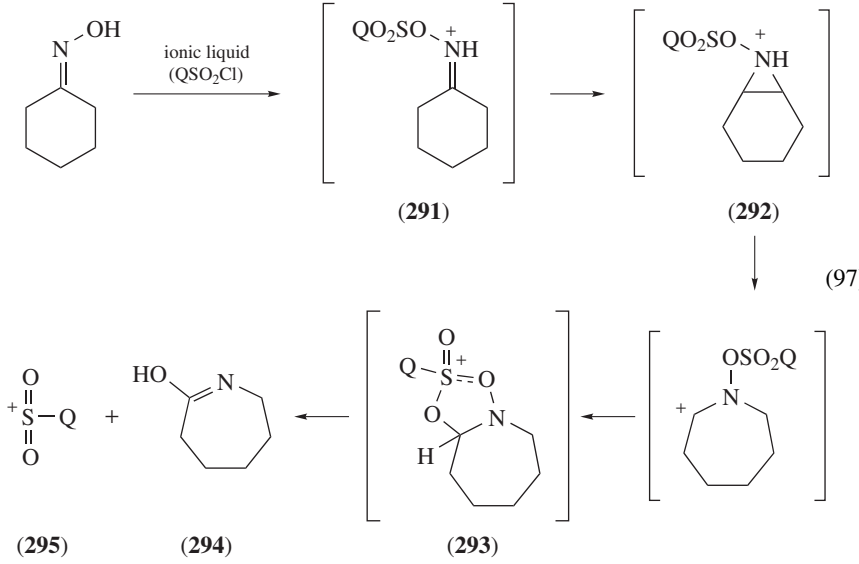

Initially, the oxygen atom of the oxime attacks the SO_2Cl group, which leads to elimination of chloride ion to form the salt **291**; then a three-member-ring aziridinium ion **292** and five-member-ring sulfonium salt **293** might be formed, and finally Q-SO_2^+ **295** is released and the product **294** is produced. Species **292** and **293** should be the key intermediates during the rearrangement. These authors also studied the Beckmann rearrangement of cyclohexanone oxime to afford caprolactam using a novel ε-caprolactam-based Brønsted acidic ionic liquid **296** as catalyst and reaction medium. The ε-caprolactam was recovered with high conversion and selectivity. Difficulties encountered to isolate the product resulted probably from the possible dynamic exchange between caprolactam and the ionic liquid.

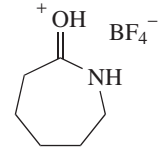

(**296**)

g. Supercritical water. Recent experiments have revealed that the Beckmann rearrangement of cyclohexanone oxime, which requires an acidic catalyst in the ambient water,

proceeds in the absence of any catalyst in supercritical water to produce ε-caprolactam in low to moderate yield[196–200]. Theoretical studies of the mechanism demonstrate that the reaction is catalysed by proton transfers along the hydrogen bonds connecting the solute and the solvent water molecules[201,202]. It has been revealed that the promotion of the chemical reaction is due to the hydration and mainly originates from the interaction between the non-polarized solute and the solvent water molecules at the supercritical state. Although there is no serious corrosion associated and despite the excellent selectivity for ε-caprolactam observed, low conversions and highly demanding reaction conditions make the industrial process unattractive.

D. Synthetic Usefulness

As mentioned previously, the Beckmann reaction remains one of the most reliable transformations to incorporate efficiently a nitrogen atom in acyclic or cyclic systems, providing a powerful synthetic method (Scheme 8).

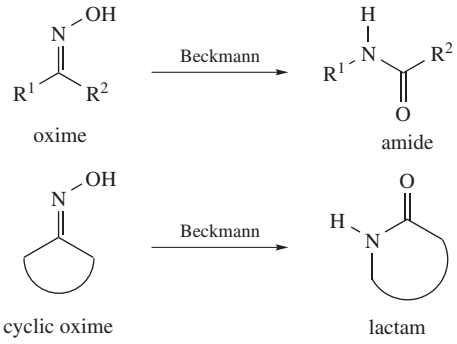

SCHEME 8

Summarizing, the key important features of the reaction are:

a) Starting material requirements
It is usually an oxime, either isolated or prepared *in situ*. The α-groups of the oxime may be alkyl, aryl, heteroaryl (ketoxime) and one may be hydrogen (aldoxime).
b) Reaction conditions
Classical methods use strongly acidic medium. Oximes may be converted to their ester or ether derivatives and these may be used to promote the rearrangement (less vigorous reaction conditions are usually needed). Some other milder reaction conditions and reagents may be used (Section VI.C).
c) Side reactions
The Beckmann fragmentation with nitrile formation is the main side reaction and may be predominant. This side reaction is more important when R^1 and/or R^2 can form a relatively stable carbocation (equations 68 and 69).
d) Selectivity
   a. Aldoximes: both the *E* and *Z* isomer will produce primary amides (non-selective rearrangement). Beckmann fragmentation may be important.
   b. Ketoximes: the rearrangement is usually stereospecific for ketoximes, involving the migration of the residue *anti* to the leaving group on the nitrogen atom of the oxime. Of course, if the starting material consists of a mixture of *E*/*Z* oximes or

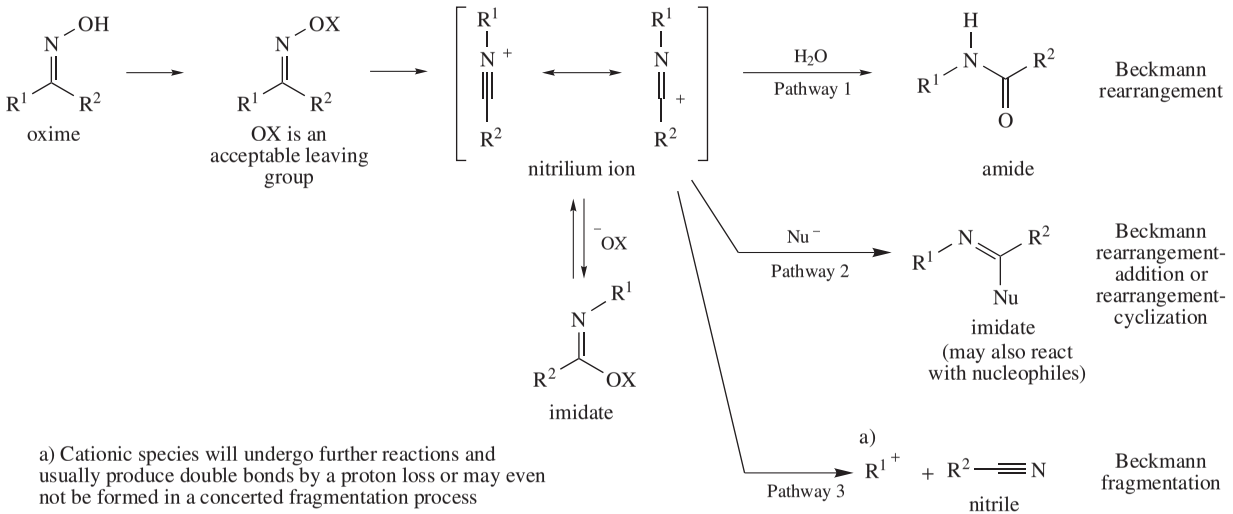
oxime
OX is an acceptable leaving group
nitrilium ion
imidate
amide
imidate (may also react with nucleophiles)
nitrile
Pathway 1
Pathway 2
Pathway 3
Beckmann rearrangement
Beckmann rearrangement-addition or rearrangement-cyclization
Beckmann fragmentation
a) Cationic species will undergo further reactions and usually produce double bonds by a proton loss or may even not be formed in a concerted fragmentation process

SCHEME 9

if oxime isomerization could not be prevented during the rearrangement reaction, a mixture of amides is usually obtained.

e) Mechanism

A simplified mechanism for the Beckmann rearrangements and important related reactions is shown in Scheme 9. Summarizing the 'mechanism' section, the key step of the reaction is the migration of an α-carbon group to the electronically deficient nitrogen atom of the oxime. A nitrilium ion in some cases or an imidate in others are key intermediates in the reaction. Their destiny determines the course of the transformation. Basically, three different pathways may be possible and can be synthetically exploited:

- Water attack on the electrophilic carbon to produce an amide after tautomerization: this reaction is the classical Beckmann rearrangement (Scheme 9, pathway 1).
- The intermediate may be trapped by other nucleophiles (different from water) and diverse products may be obtained. The interception of the intermediate may occur inter- or intra-moleculary, the latter providing a helpful tool to produce a new ring system (Scheme 9, pathway 2). These reactions are sometimes referred to, respectively, as Beckmann rearrangement–addition and Beckmann rearrangement–cyclization reactions.
- Fragmentation of the intermediate or concerted formation of nitriles from the activated oxime (Scheme 9, pathway 3): this is the Beckmann fragmentation. In some circumstances this pathway becomes dominant, particularly when there are quaternary carbons adjacent to the oxime. This transformation has found particular utility in ring-cleavage processes (sometimes called 'abnormal' or 'second-order' Beckmann rearrangements).

1. The Beckmann rearrangements as a synthetic tool

Primary amides may be produced by a Beckmann rearrangement both from *E* or *Z* oximes which are commonly obtained from the corresponding carbonyl compound (aldehyde). Retrosynthetic analysis follows equation 98.

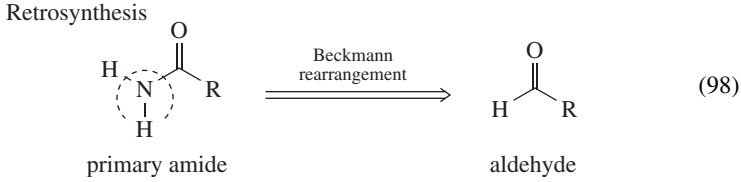

(98)

Synthetically speaking, the Beckmann rearrangement of an aldoxime (*E* or *Z*) will produce a primary amide (equation 99).

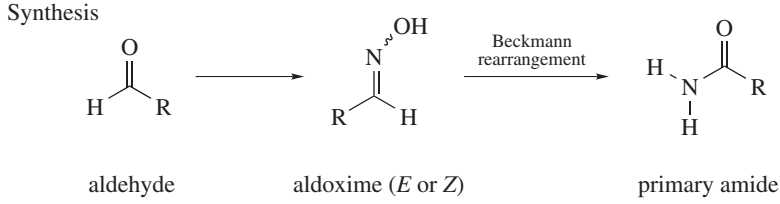

(99)

In the same way, a secondary amide containing identical groups attached to the nitrogen and to the carbonyl group may be produced from an oxime by a rearrangement

(equations 100 and 101) and the selectivity of the Beckmann reaction is unimportant: only one oxime exists.

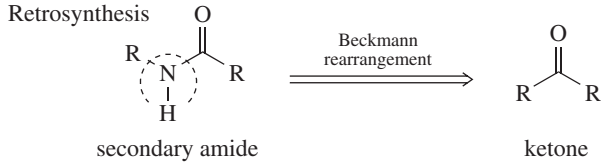

(100)

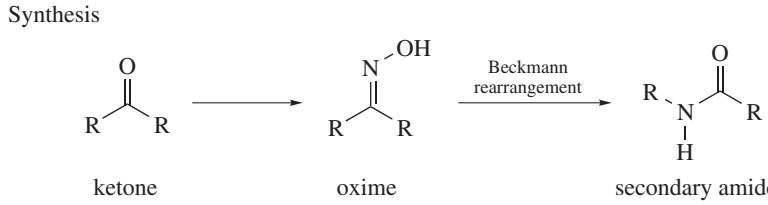

(101)

When the starting ketone is not symmetric, selectivity problems arise, as more than one amide may be obtained, depending on the oxime geometry. If the proper oxime (or derivative) can be exclusively obtained and if the rearrangement reaction conditions can avoid its isomerization, usually only one product resulting from the migration of the group *anti* to the leaving group can be obtained.

However, the stereochemistry of the oxime cannot be easily controlled and this may be a drawback for the synthetic utility of the Beckmann rearrangement. When a mixture of oximes is obtained from the ketone and when the isomerization of the oxime cannot be prevented during the rearrangement reaction, a mixture of amides is obtained. In other less favourable cases, the intended oxime cannot be obtained and the wrong amide will result from the rearrangement reaction.

Because of such lack of general methods available for the controlled production of oxime geometry, Beckmann rearrangements have not been extensively applied in total synthesis. When using the retro-Beckmann in a retrosynthetic analysis, care must be taken of the oxime geometry: the migrating group must be *anti* to the oxime oxygen atom (equation 102).

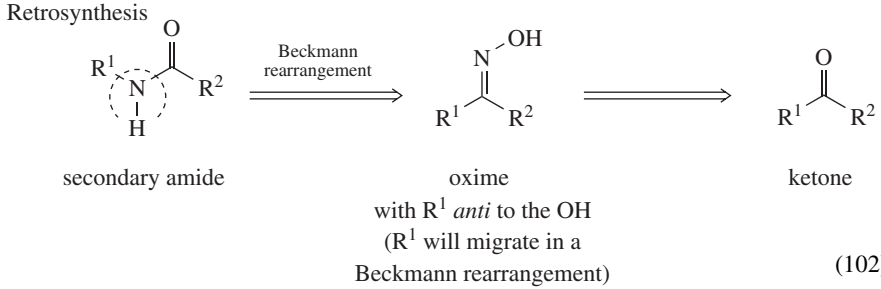

(102)

Amines **297** and/or carboxylic acids **298** may be obtained by amide hydrolysis and the latter compound may be produced from a ketone by a Beckmann rearrangement (equation 103). Therefore, the Beckmann rearrangement of a ketone oxime followed by amide hydrolysis provides a synthetic method to cleave the C−C bond between the carbon

atom of a ketone and an α-carbon atom, producing indirectly amines and/or carboxylic acids from ketones.

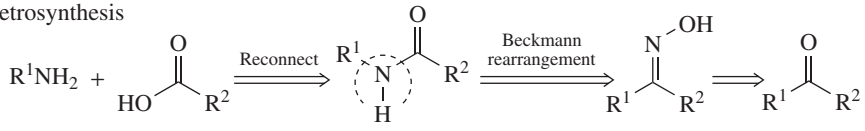

(**297**) (**298**)

(103)

amine carboxylic acid secondary amide oxime ketone

By this strategy, anilines **299** can be obtained from aromatics ketones **300** (equation 104). The Beckmann rearrangement/hydrolysis sequence is able to replace an acyl group by an amine and has been used in aromatic synthesis[203] to attach directly nitrogen atoms to aromatic rings, providing an alternative strategy to the classical nitration/reduction sequence.

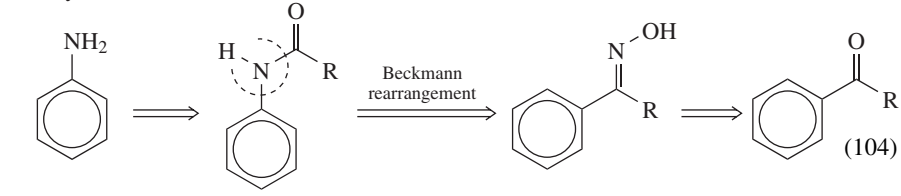

(104)

(**299**) (**300**)

aromatic amine aromatic amide oxime ketone

The same strategy was applied to other substrates and some examples are shown (Scheme 10).

The Beckmann rearrangement is particularly useful to obtain lactams from cyclic ketones (equation 105). Ring enlargement occurs in the synthesis and, as discussed above, selectivity issues may limit the synthetic utility of the reaction. If the proper oxime can be exclusively obtained, good yields can be usually achieved. For various oximes, diverse reagents for OH activations and also diverse reactions conditions may have a strong influence on the selectivity of the Beckmann rearrangement. To increase or change the selectivity, a full investigation of reaction conditions may be necessary.

By a similar strategy, saturated nitrogen heterocycles **301** can be produced from analogous cycloketones **302** (equation 106), containing the same number of carbon atoms (during the synthetic process ring expansion occurs; the ring size is increased by one atom, the nitrogen atom).

A ketone **302** may be produced from the hydrolysis of an enamine **303** (equation 107). Applying the same retrosynthetic analysis as in the previous examples, an α,β-unsaturated compound **304** is obtained as the starting material.

This sequence has great synthetic utility to replace carbonyl chains by a new carbonyl group and found application to degrade steroid side chains[101] (equation 108).

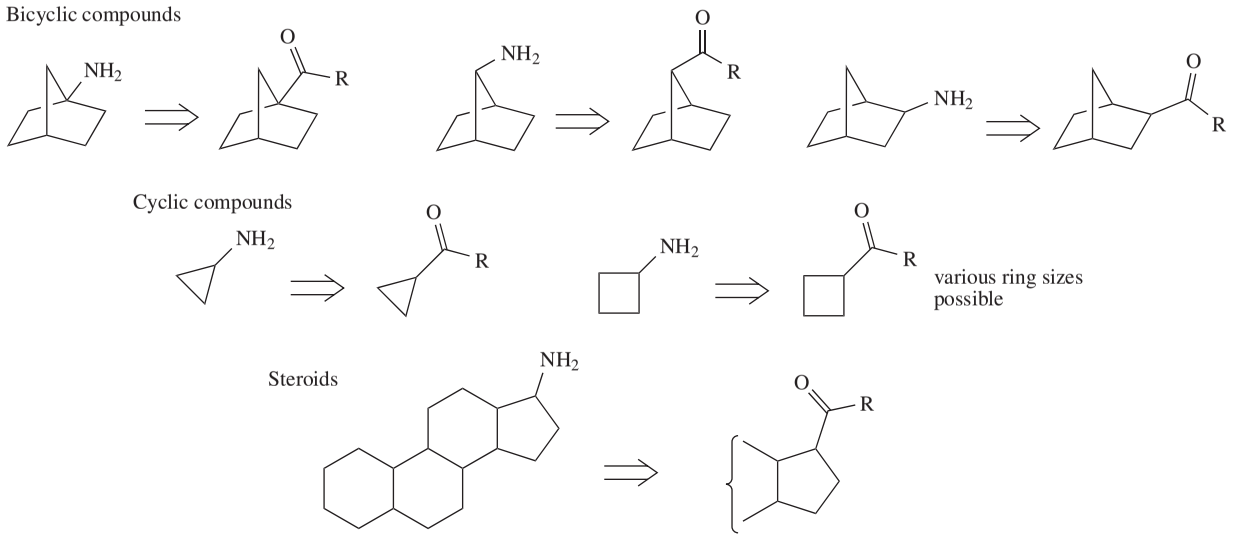
Bicyclic compounds
NH2
O
R
NH2
O
R
NH2
O
R
Cyclic compounds
NH2
O
R
NH2
O
R
various ring sizes
possible
Steroids
NH2
O
R

SCHEME 10

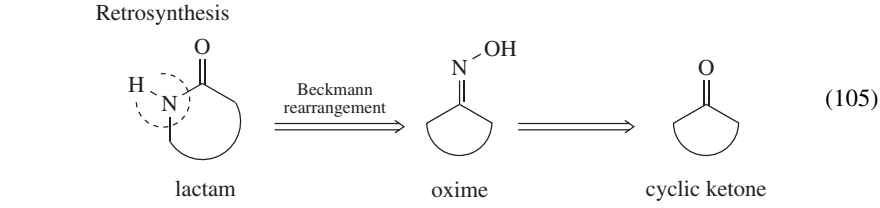

(105)

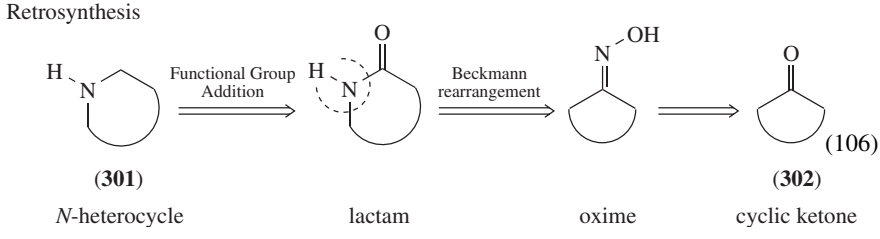

(106)

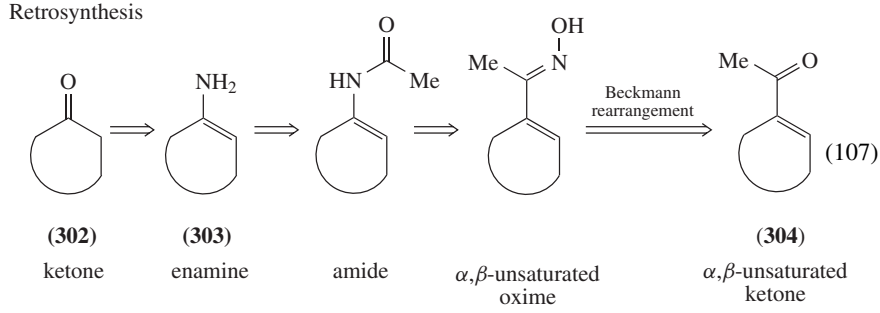

(107)

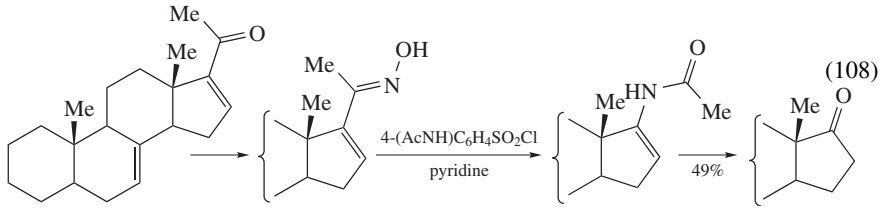

(108)

2. The Beckmann rearrangement–addition as a synthetic tool

Various imidates **227** can be produced by trapping the electrophilic intermediate of the Beckmann rearrangement with a nucleophile (Nu^-) other than water (equation 109).

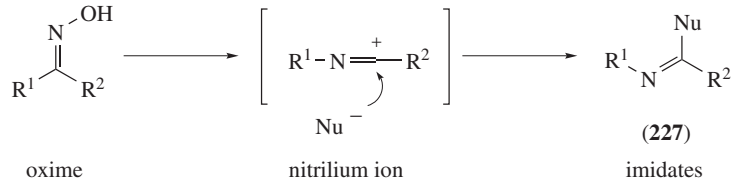

(109)

Pathway 2 of Scheme 9 corresponds to one of the most interesting developments in the Beckmann rearrangement chemistry. By trapping of the electrophilic intermediate with a nucleophile (Nu^-) other than water, an imine derivative **227** is produced that may be used for further transformations. Carbon or heteroatom nucleophiles have been used to trap the nitrilium intermediate. Reducing agents promote the amine formation. More than one nucleophile may be added (for example, two different Grignard reagents can be introduced at the electrophilic carbon atom). Some of the most used transformations are condensed in Scheme 11.

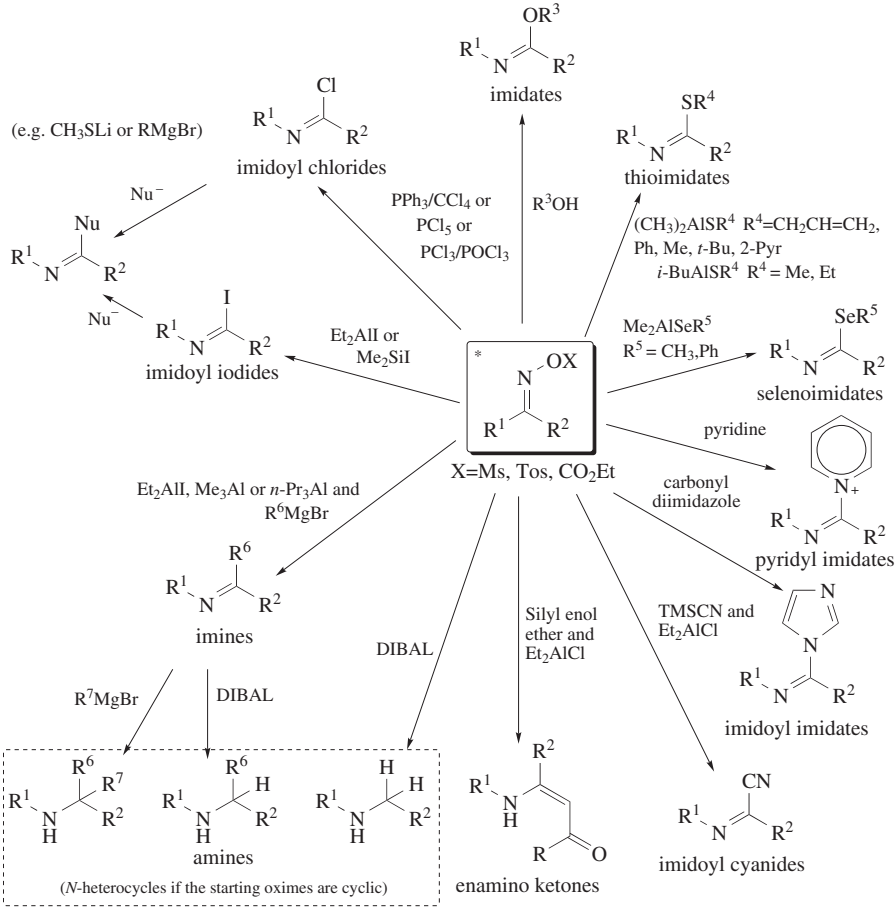

*Cyclic compounds may be used as starting material for these transformations. Regioselectivity of the reaction follows the general Beckmann rearrangement with preferential migration of the *anti* group

SCHEME 11

Imidates, or even nitrogen compounds produced from imidates by the addition of nucleophiles, may be obtained from oximes by a Beckmann rearrangement–addition process.

General retrosynthesis of these compounds follows equation 110.

Retrosynthesis

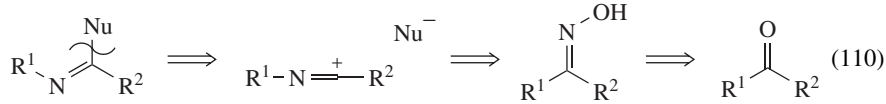

(110)

imidates nitrilium ion oxime ketone

When the nucleophile is already present as a part of the starting oxime (for example, a heteroatom or a C=C double bond), intramolecular trapping of the electrophilic intermediate is possible and a new cycle is formed. This transformation is usually referred to as a Beckmann Rearrangement–Cyclization reaction. Two modes of ring closure may be possible, depending on the oxime structure (equations 111 and 112):

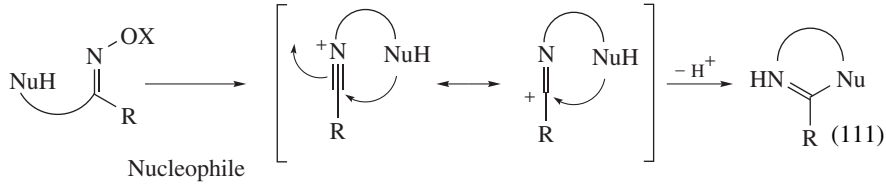

(111)

(**305**) Nucleophile (Nu) *anti* to OX (**306**)

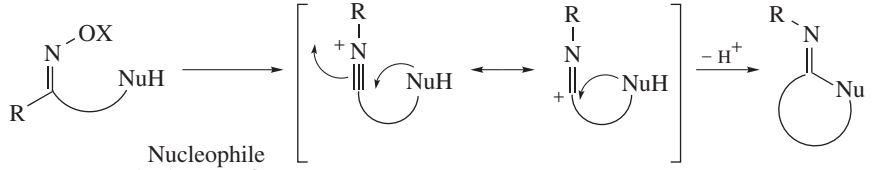

(112)

(**307**) Nucleophile (Nu) *syn* to OX (**308**)

1) In oximes **305** with a nucleophile *anti* to the oxime oxygen atom, the cyclization is *endo* and a nitrogen heterocycle **306** is formed. These cyclizations are extremely useful in natural product syntheses.
2) In oximes **307** with a nucleophile *syn* to the oxime oxygen atom, the cyclization is *exo* and **308** is formed.

In many of these cases, the nucleophile is a C=C double bond (usually an alkenic group and less frequently an aromatic group). Alkenic oxime mesylates enable intramolecular cyclization by an electrophilic addition of the double bond to the electrophilic intermediate. These reactions are terminated by a proton loss.

Four distinct cyclization modes may be possible: *endo–endo, endo–exo, exo–endo* and *exo–exo*. As before, the first two modes of cyclization produce heterocycles (**309**, **310**) directly (equation 113) while the other two cyclizations give imine-carbocycles (**311**, **312**) (equation 114). Five- or six-membered cycles may be easily produced directly by this strategy. A wide variety of structurally different hetero- and carbocyclic systems can be obtained.

Aromatic double bonds may also be used effectively to trap the electrophilic intermediate (electrophilic aromatic substitution). The Beckmann rearrangement–cyclization sequence has found utility in the synthesis of the isoquinoline nucleus[204].

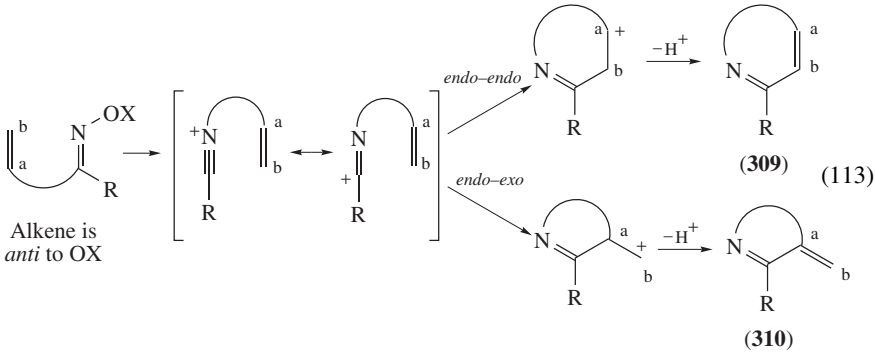

(113)

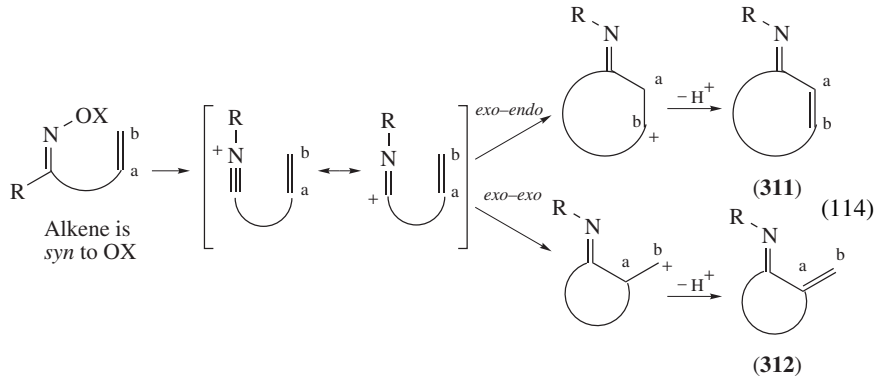

(114)

E. Synthetic Uses

1. The classical Beckmann rearrangements

a. Open-chain amide synthesis. Conversion of acyl aromatics into aromatic amides was successfully performed in various substrates. After hydrolysis of the aromatic amide, a carboxylic acid and an aromatic amine are obtained. This strategy provides a method to cleave the CC bond between the carbonyl carbon atom and one of the α-carbon atoms, and found application both for production of carboxylic acid derivatives or aromatic amines.

A multigram preparation of a useful chiral building block was developed, using the Beckmann rearrangement as a key synthetic step (equation 115)[205]. The enantiomeric addition of thiophenol to a chalcone **313**, catalysed by (+)-cinchonine, provided the chiral enantiomeric carbonyl compound **314**. The Beckmann rearrangement of its oxime **315** gives the anilide of (*R*)-(+)-3-phenyl-3-phenylsulfanylpropanoic acid **316**. Alcoholysis produced the expected enantiomerically pure ethyl ester **317**.

3-Aminophenoxathiin **319** was synthesized from the oxime derivative **318** of 3-acetylphenoxathiin[206] (equation 116).

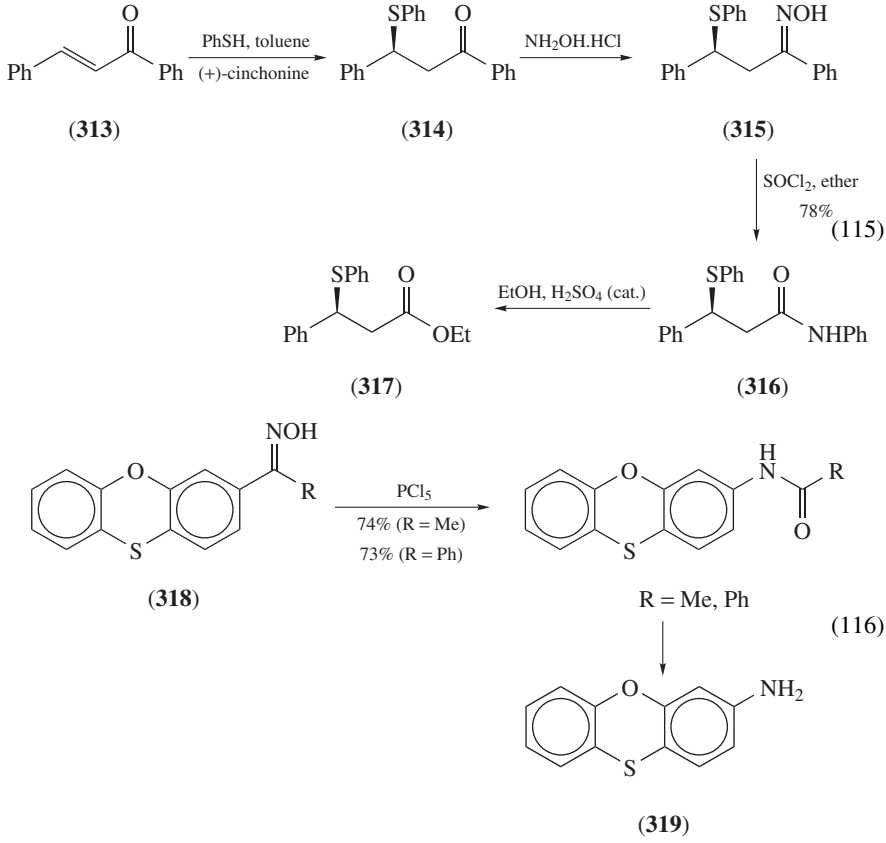

(**313**) (**314**) (**315**) (115)

(**316**) (**317**)

(**318**) (116)

(**319**)

By the same strategy, other amino-substituted heterocycles were obtained from the corresponding acyl derivatives.

The furan oxime **320** was boiled with hydrochloric acid and a mixture of the Beckmann rearranged heterocycle **321** and 2-acetylfuran derivative **322** (resulting from the oxime hydrolysis) was obtained[207] (equation 117).

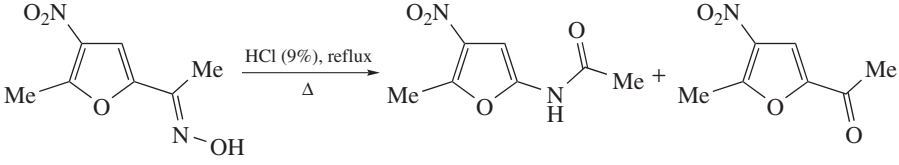

(**320**) (**321**) 18% (**322**) 59% (117)

Several different reaction conditions were tested to perform the Beckmann rearrangement of the substituted thiophene **323** (equation 118). The reaction of the tosyl oxime derivative was found to be the best available method, and **324** was obtained in high yield[208].

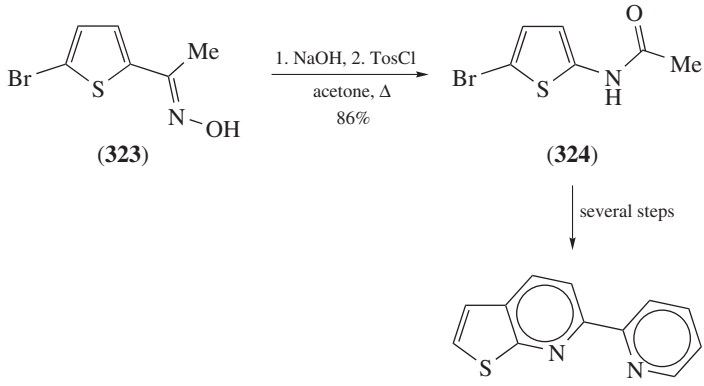

(**323**) (**324**) (118)

The same strategy had application in several other heterocyclic compounds, to obtain either amine or carboxylic acid derivatives. A process for the production of 4-amino-5-methylpyrazole derivative **325** using the Beckmann rearrangement as a key step was the subject of a new patent[209] (equation 119).

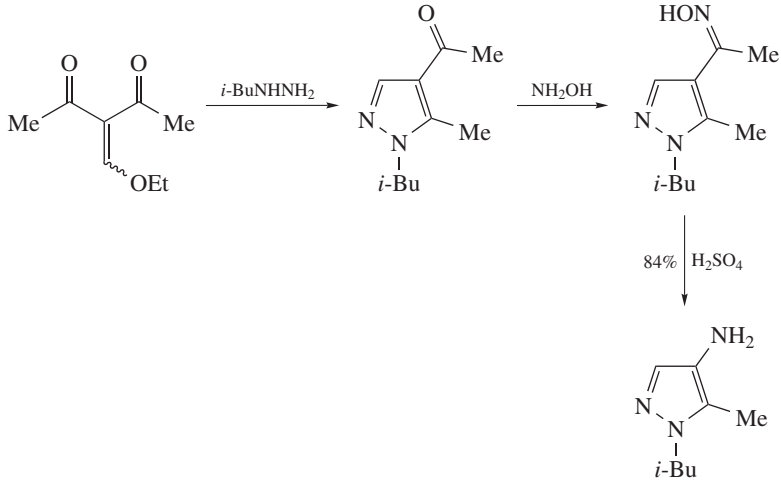

(**325**) (119)

The rearrangement of the oximes obtained from 2-acyl-1,3-selenazoles **326** provides an efficient synthesis of 2-carbamoyl-1,3-selenazoles **327**[210] (equation 120).

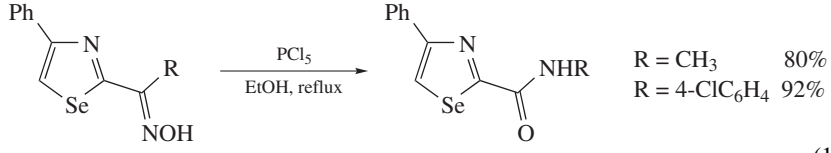

(**326**) (**327**) (120)

Beckmann rearrangements are useful to produce cycloalkylamines from ketoximes. This strategy was applied to produce cyclobutylamine derivatives **328** from the corresponding acyl derivatives during the synthesis of 4(3*H*)-quinazolinones[211] (equation 121).

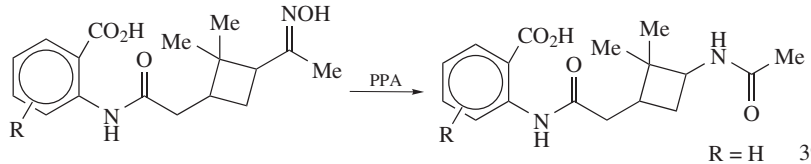

(**328**)

R = H 39%
R = 5-Br 47%
R = 4-Cl 52%

(121)

The Beckmann rearrangement is known to occur with retention of configuration at the migrating carbon[101]. Treatment of **329** with hydroxylamine-*O*-sulfonic acid enabled a Beckmann rearrangement with complete retention of configuration at the migrating carbon and enantiopure cyclobutane amino acid **330** could be obtained[212] (equation 122).

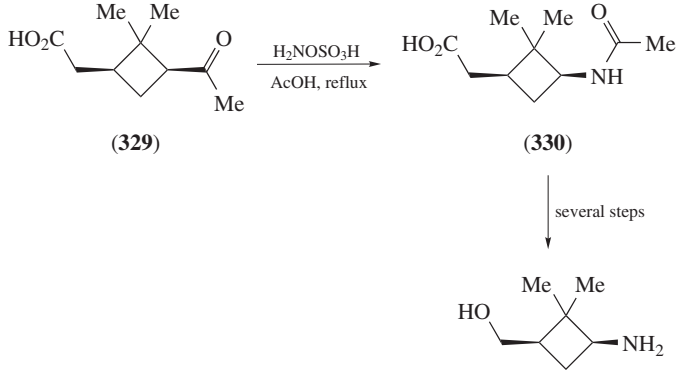

(**329**) (**330**)

(122)

The synthesis of chiral, non-racemic α-amino acids remains an interesting field of investigation and the synthesis of fully protected α,α-disubstituted α-amino acids **331** via the Beckmann rearrangement of tosylated oximes was achieved (equation 123). As expected, the migrating group was able to retain the original stereochemistry and good yields and excellent enantioselectivities were observed[213].

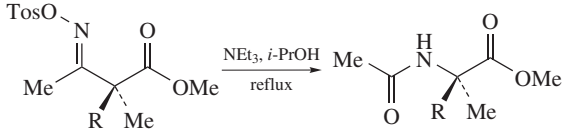

(**331**)

	Yield (%)	ee (%)
R = Ph	70	99.7
R = 4-BrC_6H_4	65	98.5
R = 3-ClC_6H_4	66	99.0
R = CH=CH_2	51	95.0
R = 2-Naph	57	98.0

(123)

Novel α,β-unsaturated amide derivatives at C(4) of chromones **335** were synthesized[214, 215] (equation 124). Oximes **332** and **333** rearranged in the presence of PCl_5 into the same amides **335** in high yields. Spiroisoxazolines **334**, formed from oxime **332** by acid treatment, also produce **335** under Beckmann rearrangement conditions.

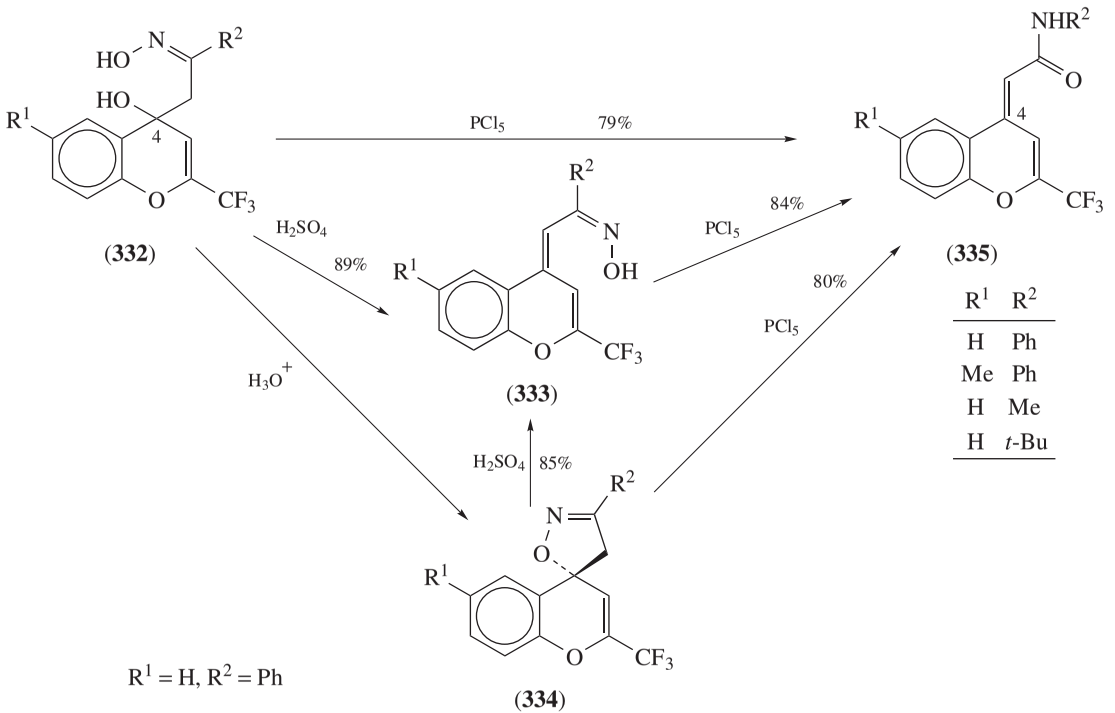

R^1	R^2
H	Ph
Me	Ph
H	Me
H	*t*-Bu

(124)

Attempts have been made to cyclize oxime **336** into isoxazolo[4,3-*c*]pyridones (equation 125). However, only the expected Beckmann rearrangement product **337** was observed in relatively good yields[216].

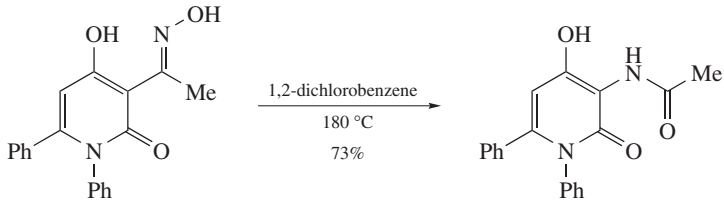

(125)

(**336**) (**337**)

During the synthesis of Camptothecin analogues, Sugimori and colleagues[217] made use of the Beckmann rearrangement to introduce selectively an amino group in an aromatic ring (equation 126). The use of the rearrangement in a cyclic oxime produces a lactam. After hydrolysis and recyclization, a new amine group was successfully introduced in a selective manner.

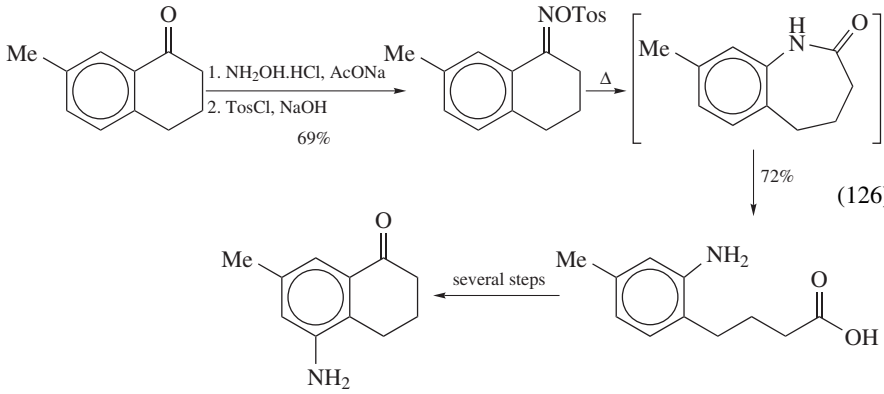

(126)

b. Lactam synthesis. The use of the Beckmann rearrangement to promote ring expansion with lactam formation is still one of the major fields of application of the reaction. In many cases, the rearrangement is very efficient, providing a very powerful synthetic method, and various ring sizes are acceptable as the starting material.

As reported above, the selectivity of the Beckmann rearrangement is mainly dependent on the oxime geometry or, to be more precise, on the 'activated oxime' that undergoes the rearrangement step. In many cases, the geometry of the starting oxime or derivative is controlled by steric hindrance. The oxime group with the hydroxyl group (or its derivatives) on the opposite side of the more bulky substituent has usually less steric repulsion; this geometric isomer is the stable. As a consequence, the more bulky group usually migrates preferentially.

i. γ-Lactams. The application of the Beckmann rearrangement for cyclobutanone oximes is still a challenge, as amide yields are often low, and the Beckmann fragmentation

pathway normally prevails. However, in some cases, γ-lactams can be effectively synthesized from the corresponding cyclobutanone oximes.

Several steroidal cyclobutanone oximes were used to investigate the rearrangement reaction[218]. The oxime **338**, treated with thionyl chloride in benzene solution at room temperature, gave the expected pyrrolidinone **339** in 71% isolated yield (equation 127).

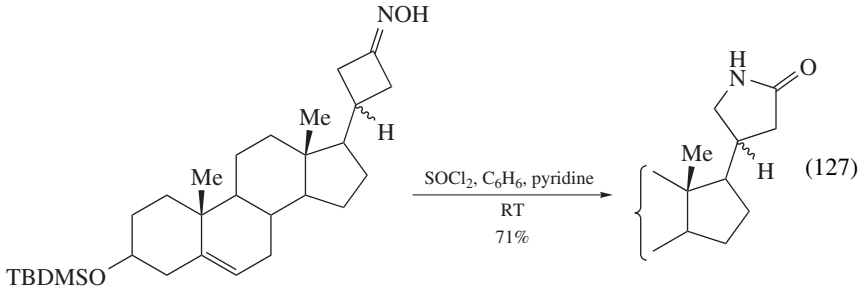

(127)

(**338**) (**339**)

Under the same standard rearrangement conditions, the analogous α-chloroxime **340** gave a low yield of an azacardenolide **341** (14%) as a result of the normal Beckmann rearrangement; the nitrile **342** was isolated as the major reaction product (equation 128).

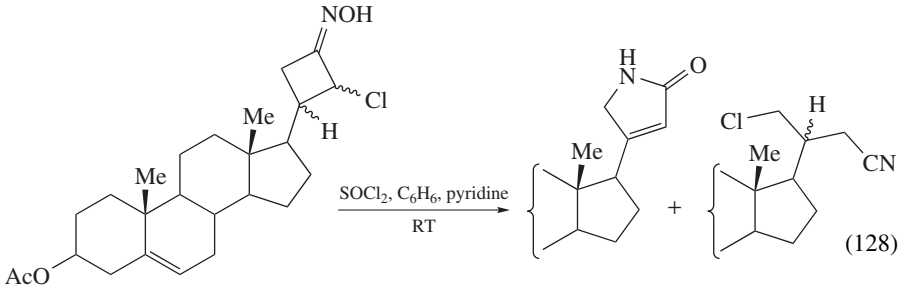

(128)

(**340**) (**341**) (**342**)

14% 45%

α-Chlorocyclobutanone oximes **343** were anticipated to give access to steroids with a spiro chloropyrrolidinone fragment, which are compounds of biological importance. With some exceptions, the rearrangements of α-chlorocyclobutanone oximes were characterized by the prevailing Beckmann fragmentation (equation 129).

Some other syntheses of γ-lactams by the Beckmann rearrangement were also tested without great success, the nitrile being the major product of the transformation[218] (equations 130 and 131).

Delair and colleagues[219] found that an asymmetric pyrrolidone **344** might serve as a common precursor of (+)-Retronecine **345** and (+)-Amphorogynine A and D (equation 132). The ring expansion was a key and efficient step during the synthetic process and was performed with Tamura's Beckmann reagent.

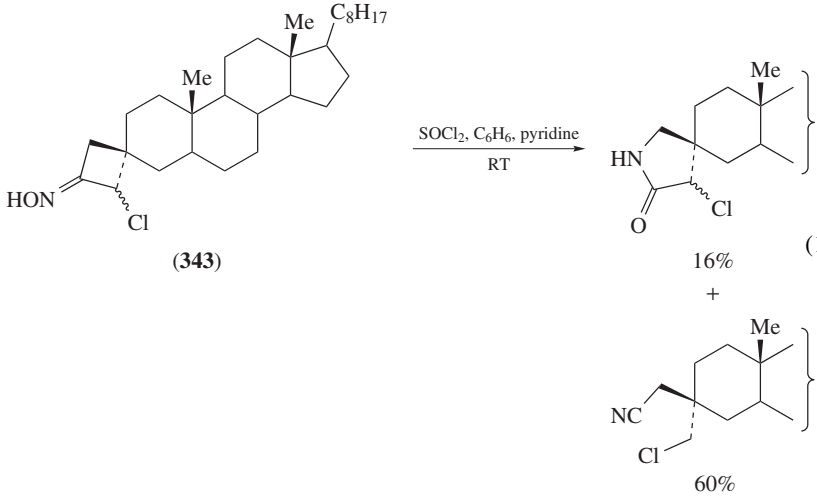
Me
C8H17
Me
HON
Cl
(343)
SOCl2, C6H6, pyridine
RT
Me
HN
O
Cl
16%
+
Me
NC
Cl
60%

(129)

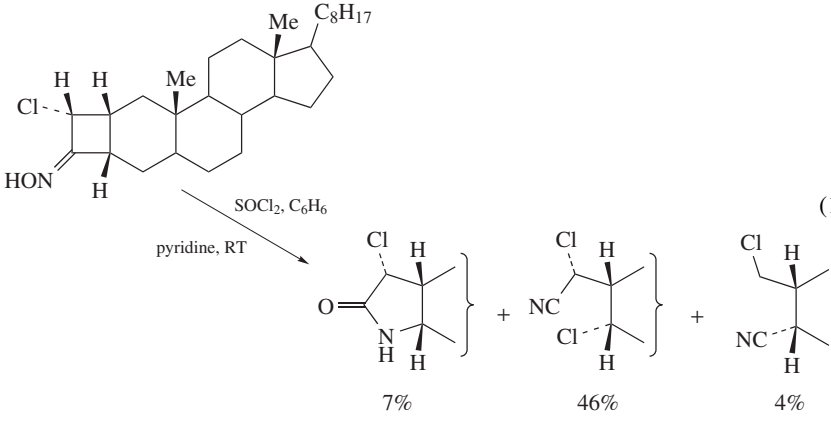
Me
C8H17
H
H
Me
Cl
HON
H
SOCl2, C6H6
pyridine, RT
Cl
H
O
N
H
H
+
Cl
H
NC
Cl
H
+
Cl
H
NC
H
7%
46%
4%

(130)

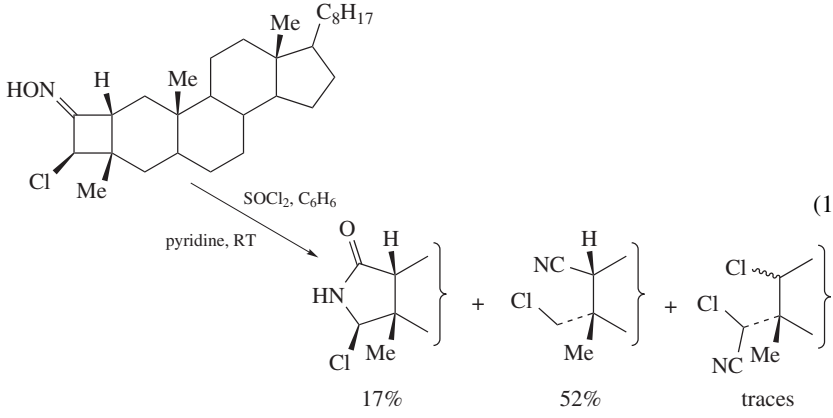
Me
C8H17
HON
H
Me
Cl
Me
SOCl2, C6H6
pyridine, RT
O
H
HN
Cl
Me
+
H
NC
Cl
Me
+
Cl
Cl
NC
Me
17%
52%
traces

(131)

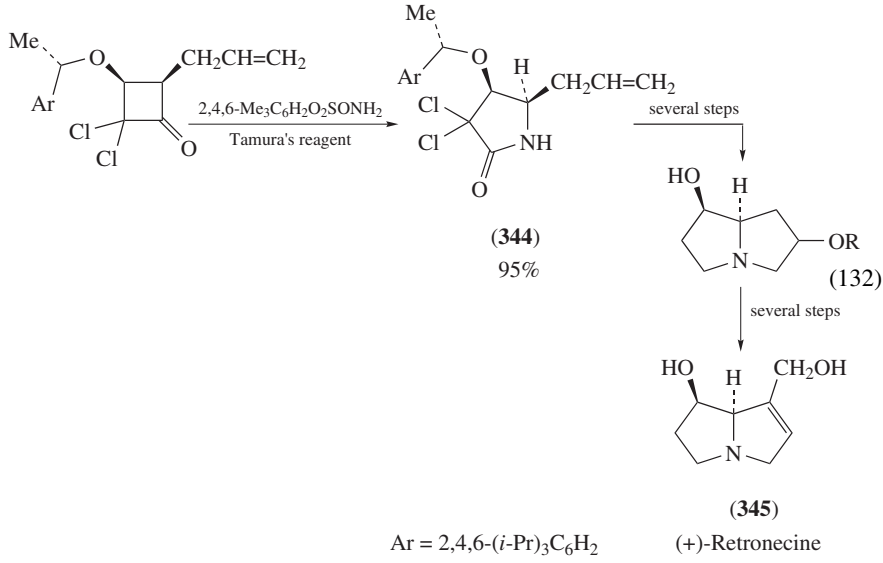

(**344**)
95%

(**345**)
Ar = 2,4,6-(*i*-Pr)$_3$C$_6$H$_2$ (+)-Retronecine

(132)

ii. δ-Lactams. In contrast, six- and seven-membered lactams are usually prepared in good yields from the corresponding oximes. The oxime geometry may limit the application of the reaction.

A series of analogues of 2-iminopiperidine have been prepared and have been shown to be potent inhibitors of the human nitric oxide synthase isoforms[220]. The cyclopentanone oxime **346** was esterified with sodium hydroxide and benzenesulfonyl chloride and the subsequent Beckmann rearrangement afforded the 6-propylvalerolactam **348** as the major product and 3-propylvalerolactam **347** as a minor product (equation 133). The major product was converted into the intended 2-iminopiperidine **349**.

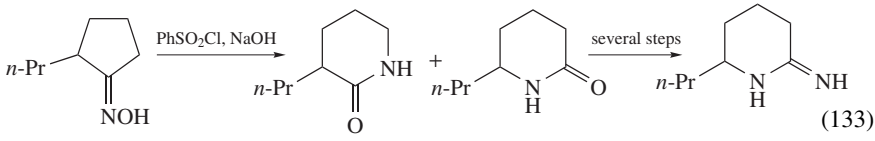

(**346**) (**347**) Minor (**348**) Major (**349**)

(133)

A new piperidine alkaloid Adalinine **352** was prepared in racemic form, using a rearrangement as a key step[221] (equation 134). Enolate chemistry allowed double α-alkylation of cyclopentanone, producing **350** after oxime formation. Rearrangement provided a clear conversion into the lactam **351**, easily converted to racemic Adalinine **352**.

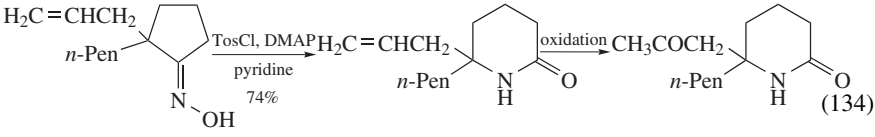

(**350**) (**351**) (**352**)
(±)-Adalinine

(134)

Since the migrating group retains its configuration, the use of enantiomerically enriched oximes provides a direct entry to enantiomerically pure lactams. These lactams may be used as a key building block for the synthesis of diverse compounds. Westermann and Gedrath applied this strategy to the stereoselective synthesis of enantiomerically pure α,α-disubstituted α-amino acids[222] (equation 135), bicyclic lactams[223] and the spirocyclic framework of Histrionicotoxins[224] (equation 136).

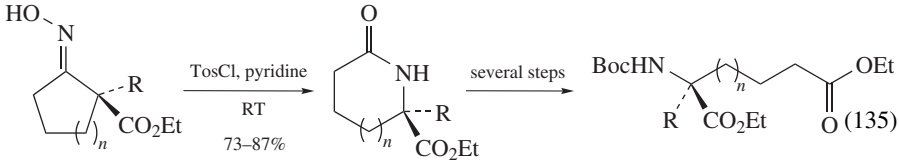

(**353**) $n = 1, 2$ (**354**) (135)

R = Et, $(CH_2)_2CH{=}CH_2$, $CH{=}CH_2$

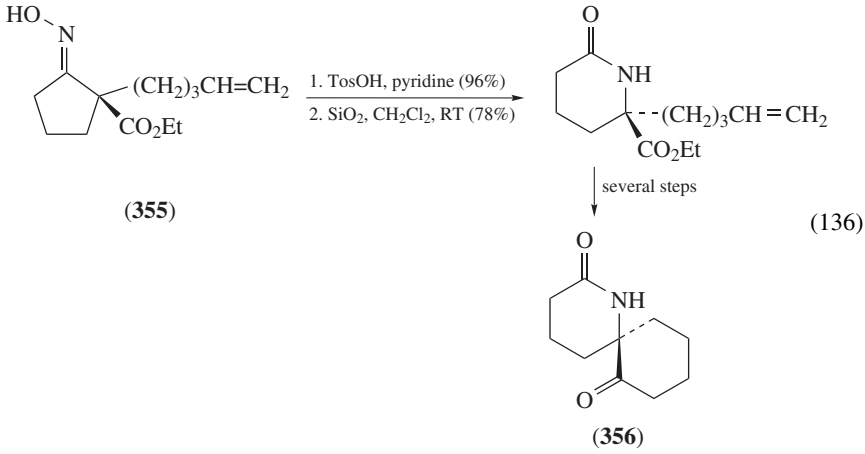

(**355**) (**356**) (136)

Pure α,α-disubstituted α-amino acids were synthesized from the readily available β-ketoesters using a Beckmann rearrangement followed by lactam protection and ring opening[222] (equation 135).

Both enantiomers of the oximes **353**, R = $(CH_2)_2CH{=}CH_2$, $n = 1, 2$ could be obtained in a pure form by lipase-catalysed kinetic resolution of its racemic oxime esters. Applying the previous sequence, both isomers of compounds **354** could be easily obtained[223]. The synthesis of the framework of Histrionicotoxin **356** was obtained from **355** and is shown in equation 136[223].

Another similar application was in the production of bicyclic lactams **357** that might serve as building blocks for the synthesis of conformationally restricted peptides[224] (equation 137).

A double Beckmann rearrangement was used in the synthesis of (±)-Sparteine **358**[225, 226] (equation 138). As usual, complete retention of configuration at the migrating carbons was observed.

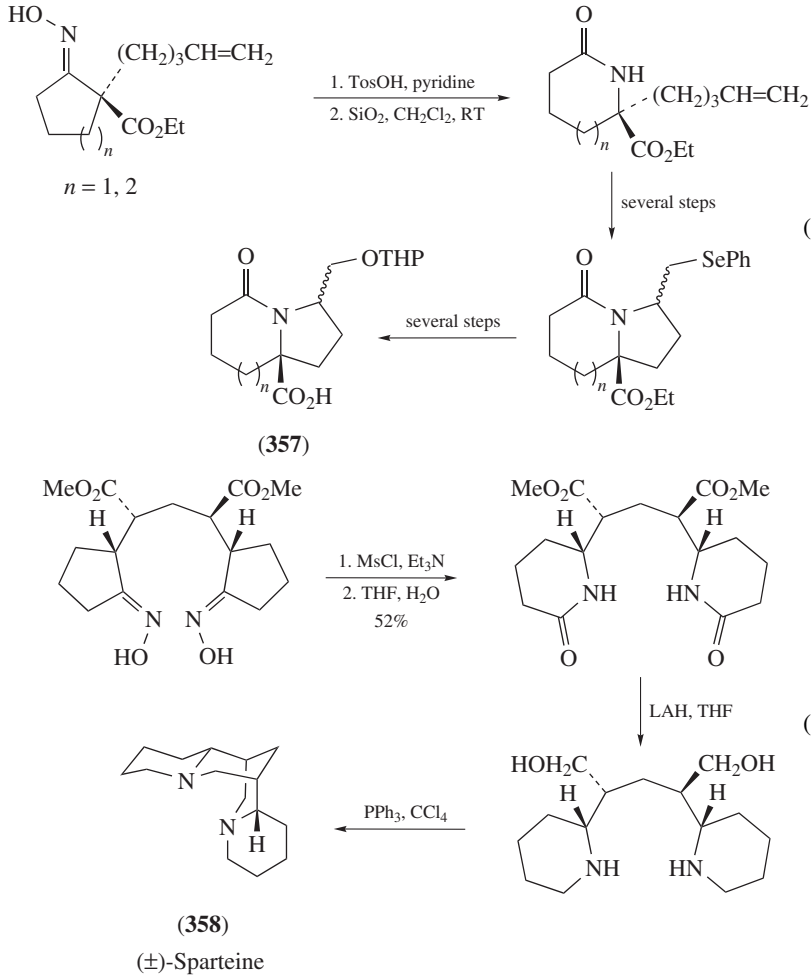

(137)

(138)

In fused ring systems, the Beckmann rearrangement of oximes at the carbon adjacent to a common carbon of the two rings usually proceeds by preferential migration of the ring system (the common carbon atom undergoes migration preferentially). This behaviour can be mainly attributed to the increased stability of the oxime in which the *N*-hydroxyl (or derivative) is directed towards the outside of the molecule.

The Beckmann rearrangement was used as a key step (41% yield, under standard conditions) for the synthesis of the natural alkaloid Pumiliotoxin C **359**, which was originally isolated from the skin extracts of *Dendrobates pumilio* (a strikingly coloured Panamanian poison arrow frog)[227] (equation 139). (±)-Pumiliotoxin C was also synthesized by a similar ring formation process by Mehta and Praveen[228].

During the synthesis of ligands for the vesicular acetylcholine transporter, a octahydroquinoline nucleus **361** was prepared via a ring-expansion rearrangement followed by a hydride reduction[229] (equation 140). The yield was moderate but only one lactam **360** was produced by the Beckmann rearrangement.

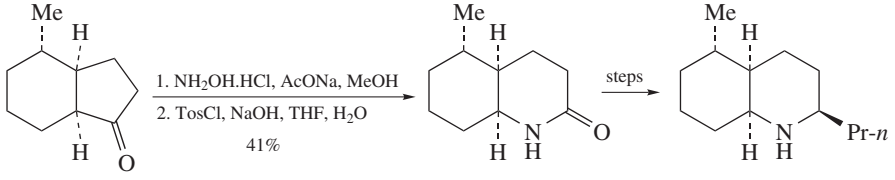

(**359**)

(+)-Pumiliotoxin C

(139)

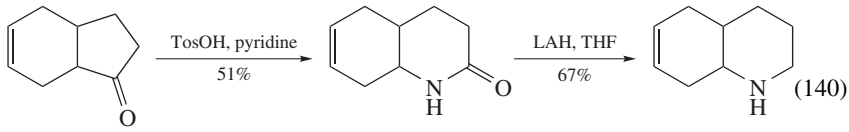

(**360**) (**361**)

(140)

The synthesis of 4-aza triterpenic derivative **362** (ring A modification) made use of the oxime rearrangement to promote the lactam formation[230] (equation 141). Again, only one isomer of the product was observed.

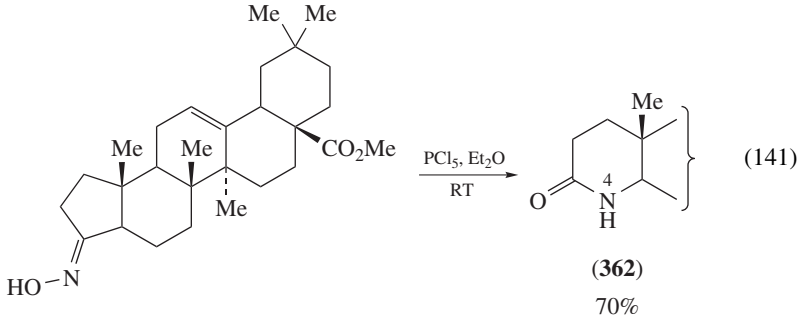

(**362**)

70%

(141)

New azacyclic diterpenoid compounds were also prepared in good yields by ring expansion and only one isomer of the lactam **363** product was obtained[231] (equation 142). However, when the oxime was tosylated, a nitrile compound resulting from ring opening was obtained in good yield (72%) as a result of the Beckmann degradation reaction.

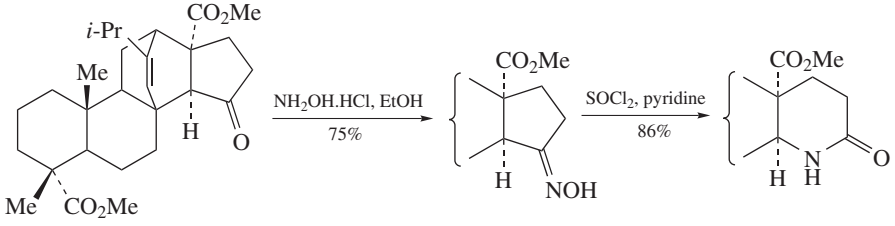

(**363**)

(142)

Stanetty and colleagues[232] applied the Beckmann rearrangement to produce selectively and almost in quantitative yield the lactam **364**, corresponding to the migration of the more bulky alkyl group: the stereochemical control (an α-methyl group) was essential to obtain the desired regioselectivity control of the rearrangement (equation 143).

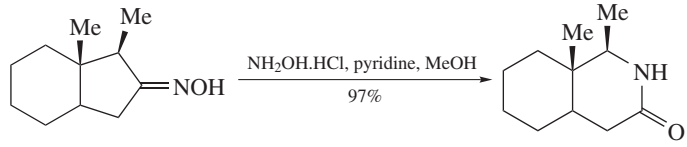

(143)

(**364**)

The Beckmann rearrangement of 1,3-diketones has been investigated and appropriate conditions were developed to be used in the synthesis of indolizidinones[233]. Symmetric and non-symmetric spirocyclic 1,3-diketones (**365** and **366**) were tested as starting materials for the rearrangement. In all cases, the nitrogen was inserted between a carbonyl group and the C(2) spirocyclic carbon atom. In non-symmetric 1,3-diketones only the carbonyl group with less steric hindrance will rearrange (equations 144 and 145).

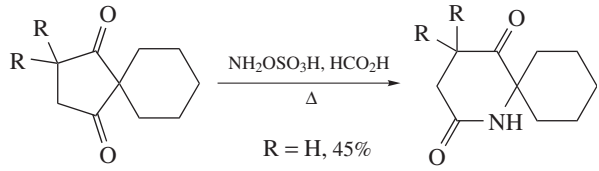

(144)

(**365**)

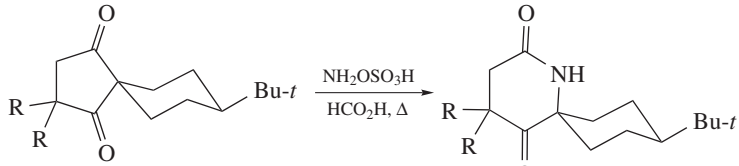

(**366**)

R = H 14%
R = Me 51%

(145)

+

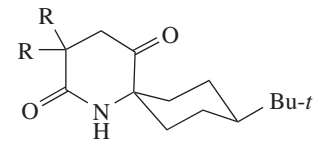

27%
0%

Similarly, the application of Tamura's Beckmann rearrangement reagent to ketones **367** and **370** afforded the appropriate lactams **368** and **371** to be cyclized to the indolizidine nucleus **369** and **372**[234] (equations 146 and 147).

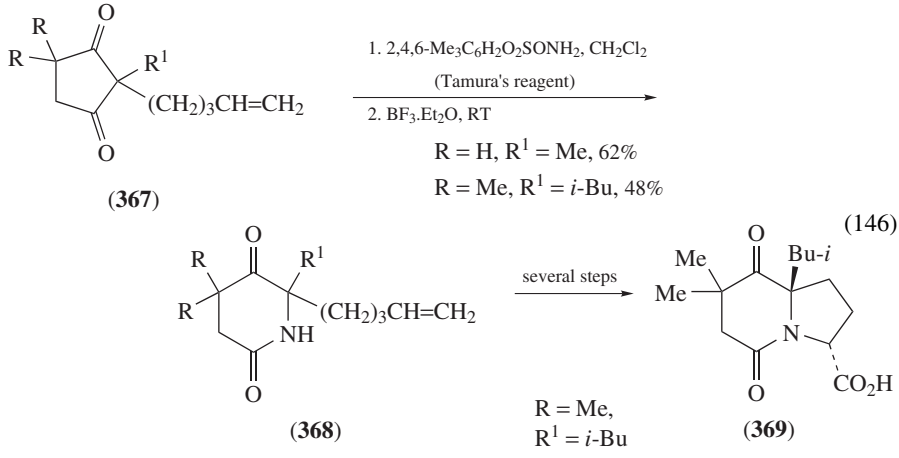

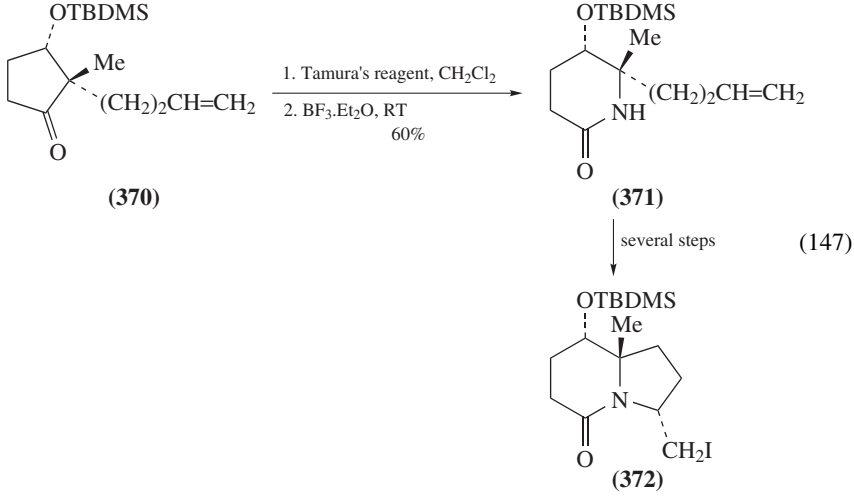

The activation of enantiomeric pure spirocyclic oximes **373** was performed by several acidic reagents to promote the Beckmann rearrangement[235] (equation 148). Best results were obtained with PPE (polyphosphate ester) and the rearrangement was stereospecific (the *E* isomer produces **374**, while the *Z* isomer gives only **375**). Using PPA, the reaction becomes non-stereospecific probably due to isomerization of the starting oxime (in the *Z* isomer an intramolecular hydrogen bonding may be possible and this may be the reason for the isomerization of the *E* into the *Z* isomer).

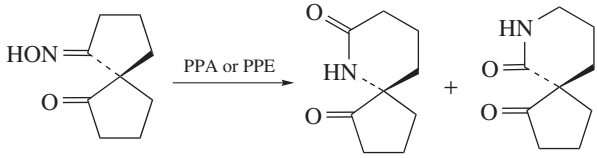

(**373**) (**374**) (**375**) (148)

Precursor	Reagent	Products	Yield (%)
(*E*)-**373**	PPE	**374**	70
(*Z*)-**373**	PPE	**375**	70
(*E*)-**373**	PPA	**374** + **375**	4 + 30
(*Z*)-**373**	PPA	**375**	23

The spirobicyclic lactam **377** possessing the common azaspirodecane unit present in several alkaloids was prepared by rearrangement of the oxime **376**. Beckmann fragmentation products (olefins) are the main side products (15%) (equation 149).

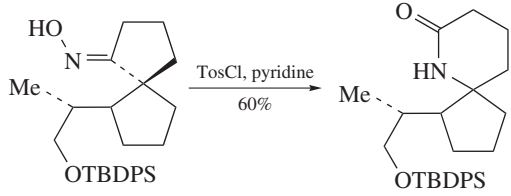

(**376**) (**377**) (149)

Oximes at a carbon atom adjacent to an aromatic ring are more prone to produce mixtures of lactams. In some cases, the product resulting from alkyl migration becomes dominant. Some examples are shown below.

The stereoselectivity of the acidic rearrangement of indanone oximes **378** into the carbostyril core was found to be dependent on the substituents of the aromatic ring[236] (equation 150). Moderate yields were observed.

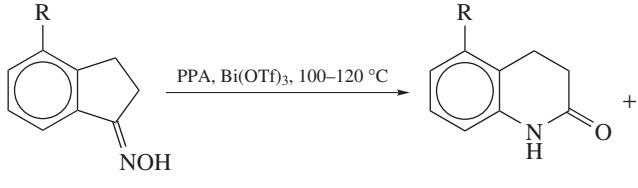

(**378**)

R = H	28%	19%
R = OMe	0%	30%

(150)

Oxime **379** produces exclusively the product of alkyl migration[237] (equation 151).

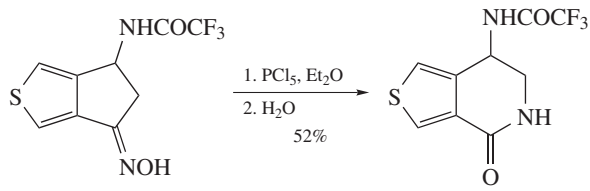

(151)

(**379**)

Expansion of the D-ring of steroids to produce azasteroids is very common. Usually, the nitrogen is inserted between C(17) and the C ring and this kind of transformation was very popular in the search for new active pharmaceutical ingredients. Schönecker and colleagues[238] performed the D ring expansion of **380** in-route to 17-aza-D-homosteroids (equation 152).

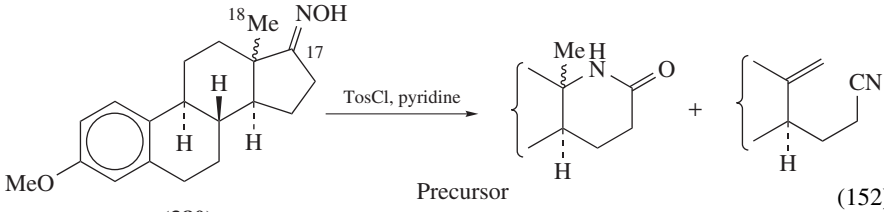

(**380**)

(152)

Precursor		
18α-(**380**)	74%	8%
18β-(**380**)	53%	3%

Azasteroids **381** derived from fusidic acid were prepared in moderate yields[239] (equation 153).

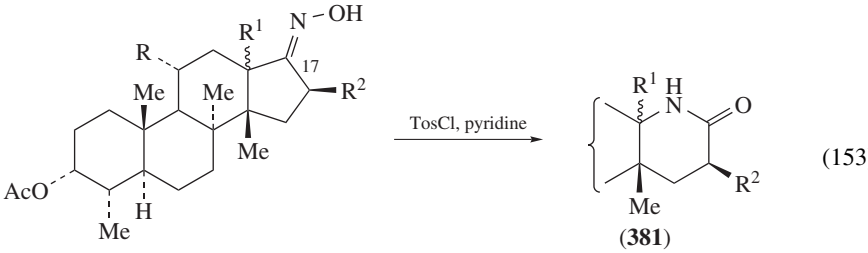

(**381**)

(153)

R = OAc, R^1 = α-H, R^2 = OAc, 45%
R = H, R^1 = β-H, R^2 = H, 67%

Unusual rearrangements of 17-oximino steroids were also observed, with insertion of the nitrogen between C(16) and C(17). As an example, the reaction of pyrrolidine-substituted androstene **382** gave the lactam **383**[240] (equation 154).

Hu and colleagues[241] prepared (5α)-17-azaandrostan-3-ols **385** and (5α)-17-aza-D-homoandrostan-3-ols **386** using the Beckmann rearrangement for the expansion of the D-ring of the steroid **384** (equation 155).

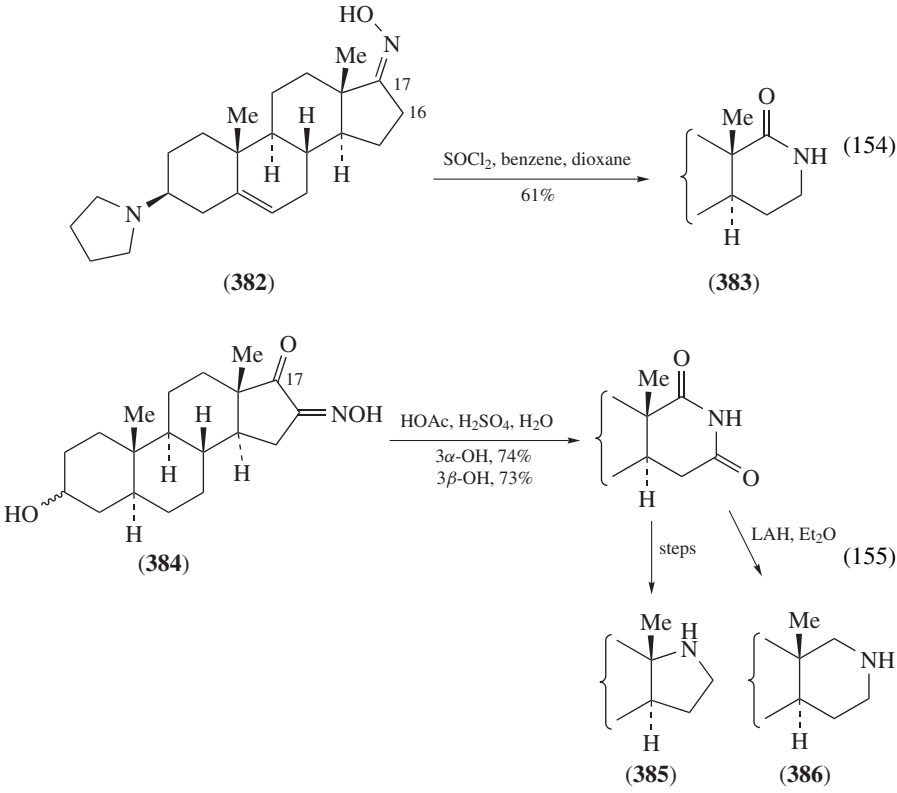

Expansions of oximes of B-ring steroid systems are much less common. Recently, during the synthesis of a 6-aza-pregnane derivative **387**, the introduction of the nitrogen was made using the Beckmann rearrangement reaction[242] (equation 156).

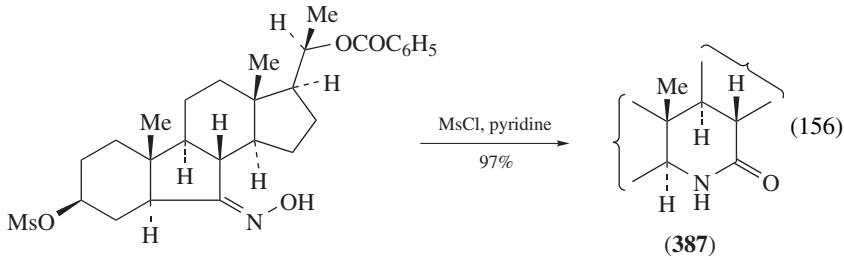

iii. ε-Lactams. Seven-membered lactams (ε-lactams) can be efficiently produced by a Beckmann rearrangement. The most important and well known compound of this kind is ε-caprolactam, which has great industrial importance due to its extensive use in polymer production (for example, in nylon 6). ε-Caprolactam can be conveniently produced from cyclohexanone or its oxime (Section VI.F).

Several substituted caprolactams were produced as intermediates for the synthesis of 2-iminohomopiperidinium salts **390**[220, 243] (equation 157). The privileged migration of the more bulky group was observed once again, as the 2-substituted cyclohexanones **388** gave preferentially the 7-substituted caprolactams **389**.

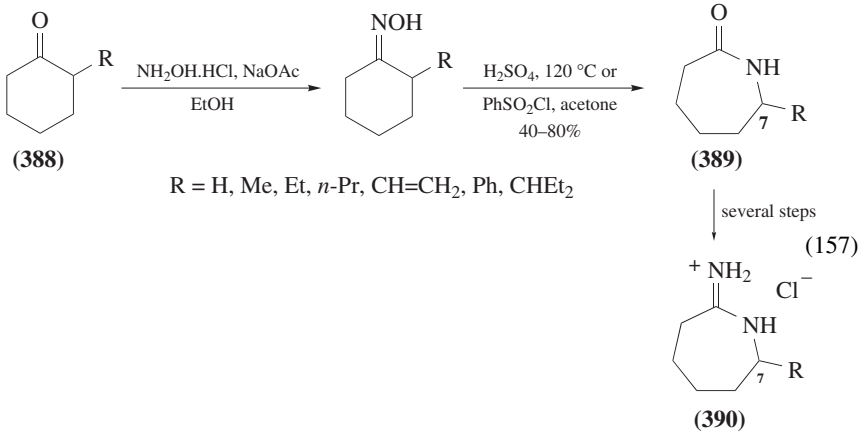

(**388**) (**389**)

R = H, Me, Et, *n*-Pr, $CH{=}CH_2$, Ph, $CHEt_2$

(**390**) (157)

A ring-expansion process was used to produce efficiently diazepinone **392** and homopiperazine **393** from commercially available 4-piperidone **391**[244] (equation 158).

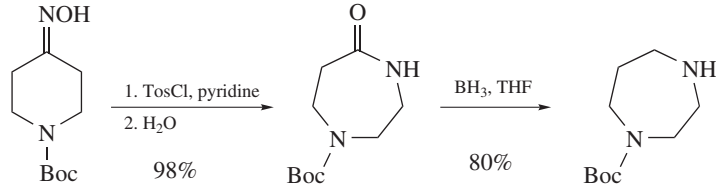

(**391**) (**392**) (**393**) (158)

New seven-membered diazepinone alkoxyamines **394** for nitroxide-mediated radical polymerization were prepared through the Beckmann rearrangement[245, 246] (equation 159).

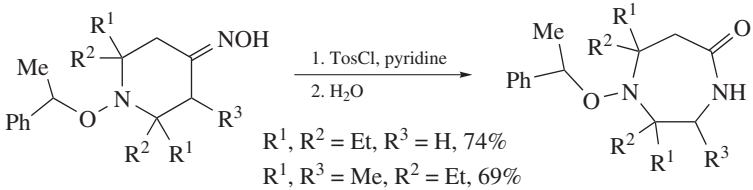

R^1, R^2 = Et, R^3 = H, 74%
R^1, R^3 = Me, R^2 = Et, 69%
R^1, R^2 = Me, R^3 = H, 45%

(**394**) (159)

Various efforts have been made to produce the Balanol nucleus, a chiral azepine ring, and many of the synthetic routes include a Beckmann rearrangement to produce the

seven-membered ring. Hu and colleagues[247] developed a route to the racemic nucleus (equation 160). Only *anti* migration was observed in the rearrangement step.

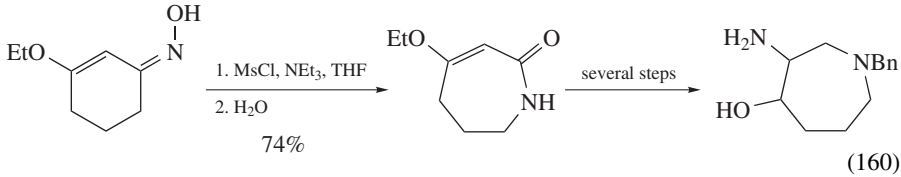

(160)

Pollini and colleagues[248] converted D(−)-quinic acid in five steps into a chiral oxime **395**, R = H in an enantiomeric pure form and subjected this oxime to a Beckmann rearrangement (equation 161). Even though the reaction lacked selectivity, **395** was useful in the synthesis of the chiral epoxide **396**, a key intermediate in the synthesis of (−)-Balanol **397**. The same authors[249] also prepared the isomeric epoxide **398**.

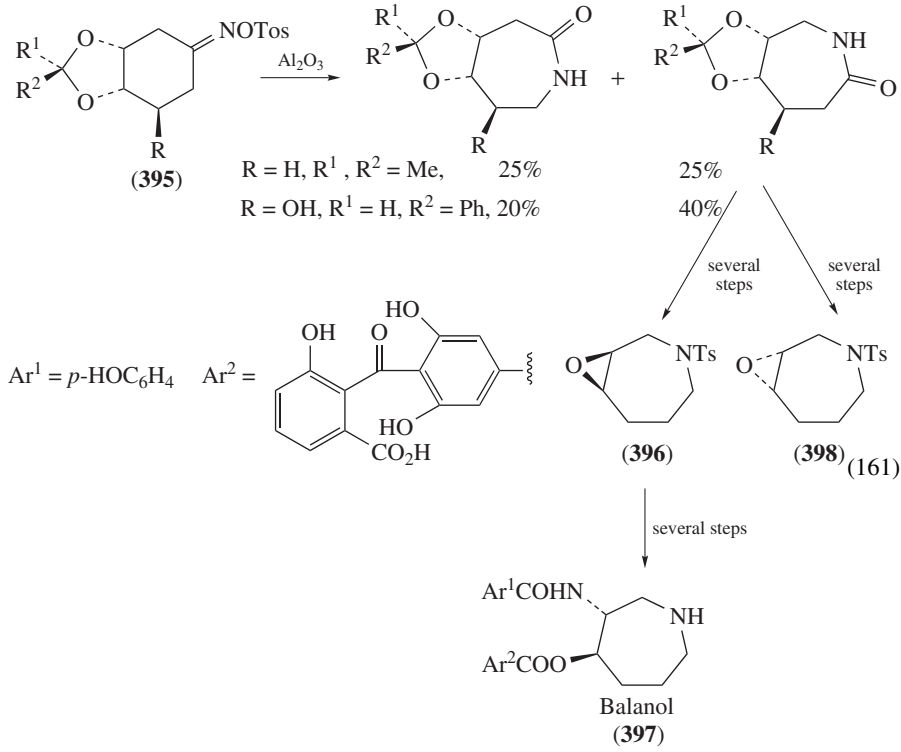

Another chiral synthesis of the azepine nucleus of Balanol (**397**) was developed by Wu and Jacobsen[250], once again converting a cyclohexanone oxime tosylates **399** to a seven-membered lactam (equation 162). The use of a mixture of oxime isomers did not cause

selectivity concerns as endocyclic unsaturated substituents are apparently more reluctant to migrate[101].

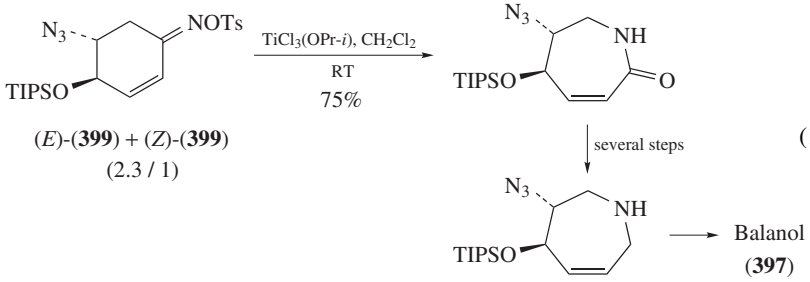

(*E*)-(**399**) + (*Z*)-(**399**)
(2.3 / 1)

(**397**)

(162)

This general trend was also observed during the rearrangement of **400** during the synthesis of pesticides[251] (equation 163). Endocyclic unsaturated double bonds usually migrate less efficiently and lower yields are obtained.

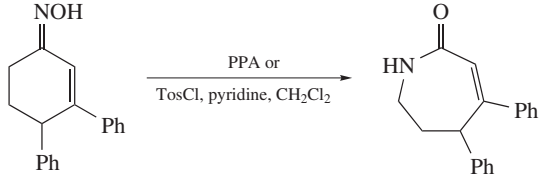

(**400**)

(163)

Precursor	Reagent	Yield (%)
(*E*)-**400**	PPA	50
(*Z*)-**400**	PPA	90
(*E*)-**400**	TosCl, pyridine	71
(*Z*)-**400**	TosCl, pyridine	0

Beckmann rearrangement of the oxime from 3-phosphonoalkylcyclohexenones **401** afforded lactams and regioselective migration of the non-unsaturated substituent was observed[252] (equation 164).

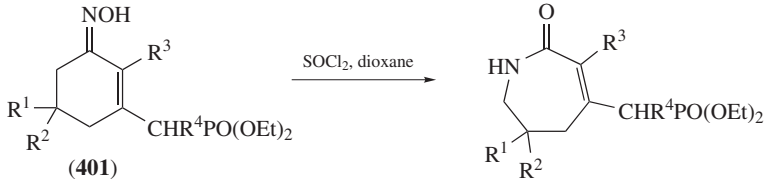

(**401**)

(164)

R^1	R^2	R^3	R^4	Yield (%)
H	H	H	H	40
H	H	Me	H	50
Me	Me	H	H	60
Me	H	H	H	35
Me	H	H	Me	54

Thiazoloazepines **402** may be produced by a ring-expansion reaction[253] (equation 165).

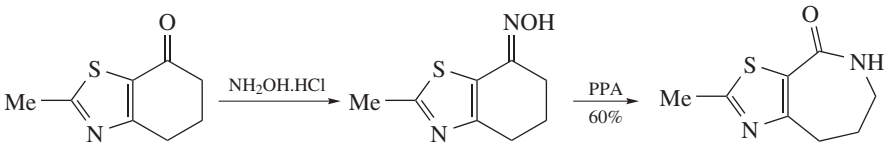

(**402**) (165)

A flexible approach to the synthesis of substituted benzazepines **403** was devised[254] (equation 166). As before, the seven-membered ring was made by the use of a ring-expansion reaction and exclusive migration of the aromatic ring was observed.

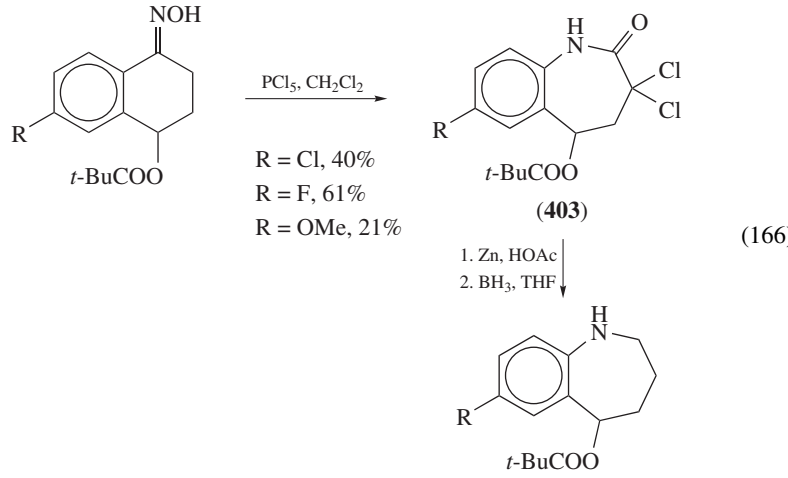

(166)

In fused-ring systems, Beckmann rearrangement of oximes at the carbon adjacent to a common carbon of the two rings usually proceeds by preferential migration of the ring system (the common carbon atom undergoes migration preferentially). This behaviour can be mainly attributed to the increased stability of the oxime in which the *N*-hydroxyl (or derivative) is directed towards the outside of the molecule. The referred selectivity of the Beckmann rearrangement was observed in various substrates, and some recent examples of azepine formation are shown in the following examples. Pyrido[3,2-*b*]azepin-6-ones **404** were obtained in moderate yields[255] (equation 167).

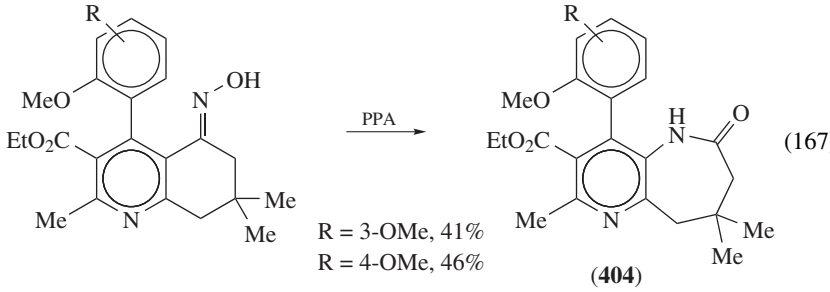

(167)

The *N*-heterocyclic ring of the alkaloid Stenine **406** was made by the use of a ring-expansion reaction and a high-yield lactam **405** formation was observed[256] (equation 168).

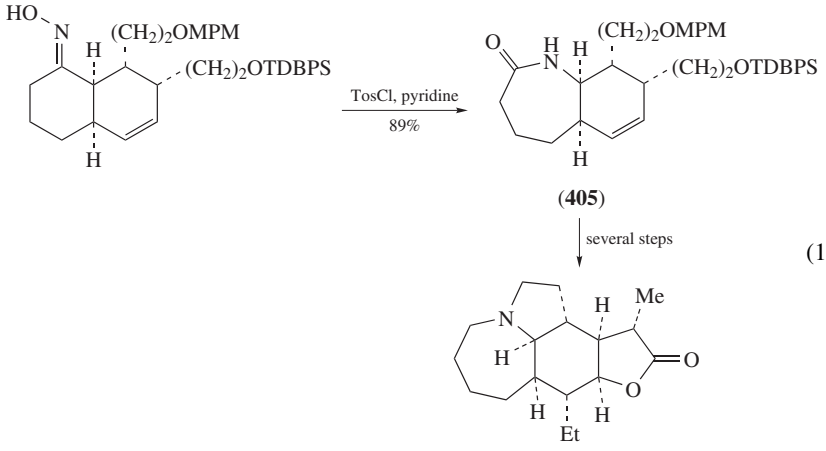

(**405**)

(**406**)
Stenine

(168)

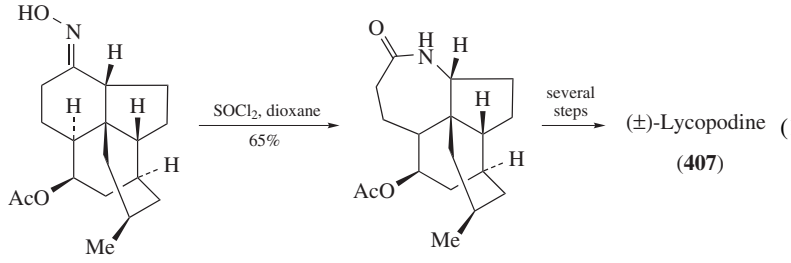

(**407**)

(169)

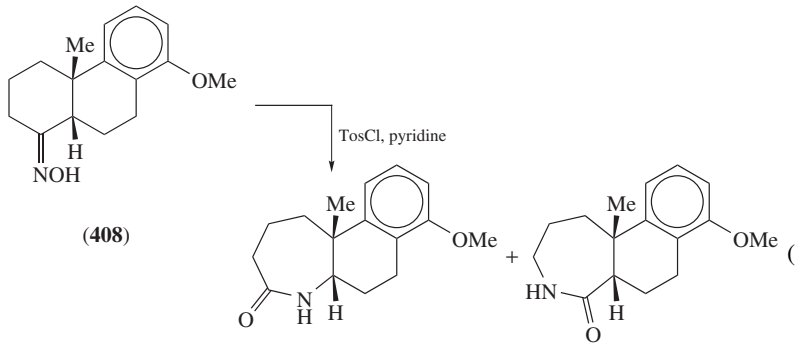

(**408**)

(**409**)

(**410**)

(170)

Precursor	Product	Yield (%)
(*E*)-**408**	**409**	50%
(*Z*)-**408**	**410**	78%

The production of the intricate carbon framework of Lycopodine **407** by Grieco and Dai[257] included an azepine formation by the classical Beckmann rearrangement method (equation 169).

If both oxime individual isomers can be isolated, both isomeric lactams can be usually obtained. Oxime (*E*)-**408** produces **409** exclusively, while the (*Z*)-**408** oxime gives the isomeric amide **410** (equation 170).

iv. Large-ring lactams. The Beckmann rearrangement is usually an extremely efficient synthetic method to introduce a nitrogen atom in a ring cycle, independently of its size. Large-ring lactams can usually be synthesized in moderate to good yields from the appropriate oxime.

Colchicine derivatives with an eight-membered B-ring lactam were prepared via Beckmann reactions. Berg and colleagues[258] synthesized both geometric isomers of **411** and their rearrangements were promoted (equation 171). The reaction of the *Z* isomer proceeded as expected (**412** is formed with a yield of 55%) but the lactam that resulted from the *E* isomer could not be isolated. Instead, compound **413** was obtained, as a result of the lactam ring opening followed by a Friedel–Crafts acylation of the activated aromatic ring.

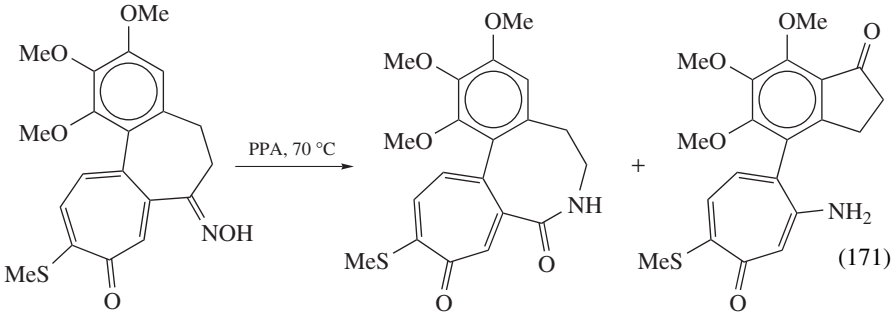

(**411**) (**412**) (**413**)

Precursor	Product	Yield (%)
(*Z*)-**411**	**412**	55%
(*E*)-**411**	**413**	64%

A similar strategy was applied to the synthesis of novel allocolchicinoids **414** and **415** to evaluate their inhibitor effects on tubulin assembly[259,260] (equation 172).

Bhawal and colleagues[261] promoted a ring expansion to produce diazocines **417** from the oximes of dioxomorphanthridines **416** (equation 173). In all examples, migration of the aromatic ring was completely selective.

Another example of azepinone formation was in the synthesis of new tetracyclic compounds **418**[262] (equation 174).

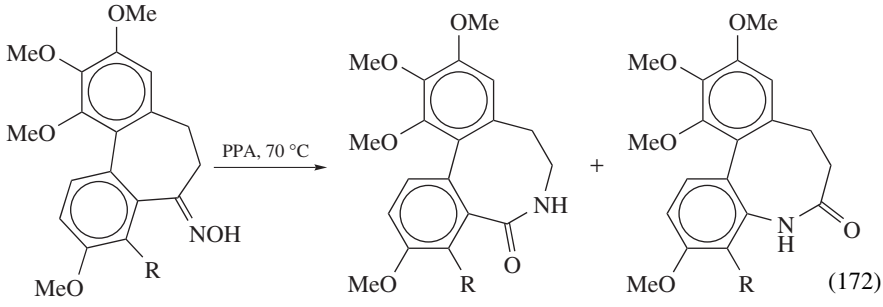

(172)

(**414**) (**415**)

R	**414**	**415**
H	7%	65%
OMe	25%	41%

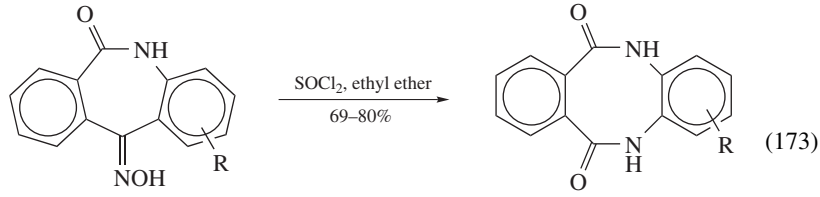

(173)

(**416**) (**417**)

R = H, CH_3, OCH_3, Br, Cl, NO_2

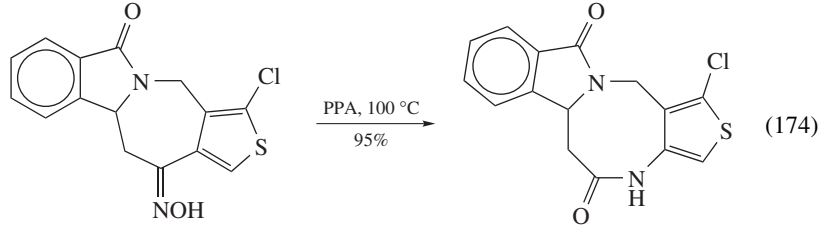

(174)

(*Z*)+(*E*) (80 / 20) (**418**)

Nine-membered lactam rings can also be produced by the Beckmann rearrangement. The azonane ring **420** was selectively formed from an eight-membered cyclic ketone **419** by a rearrangement/reduction sequence[233] (equation 175).

An ingenious synthesis of the functionalized bicyclo[6.2.1]undecane ring **423** system was recently devised[263] (equation 176). After rearrangement of **421**, an eight-ring lactam **422** was formed. Cleavage of the amide provided the basic ring framework of the bicyclic compound **423**.

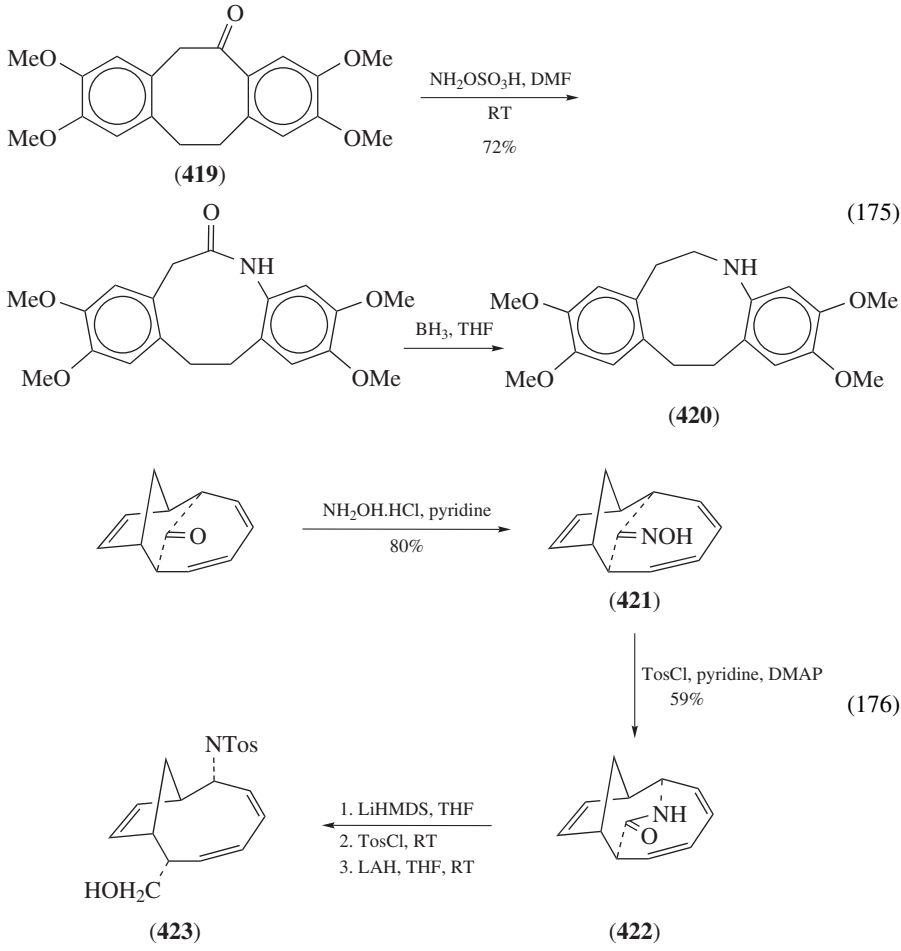

Other large-ring systems may also undergo the Beckmann rearrangement successfully. The Beckmann rearrangement has been applied frequently to the ring expansion of Erythromycin derivatives and intramolecular trapping of the nitrilium ion is frequent, producing imino ethers[264] (equation 177). One example[265] of a successful ring expansion is shown below.

v. Bicyclic compounds. The Beckmann rearrangement is also frequently applied to bicyclic compounds. In the vast majority of cases, the migration of the most substituted group occurs. When the original carbonyl group is at the carbon atom next to the bridgehead atom, this group normally migrates (the lactam formation is normally completely stereoselective, in contrast with other similar transformations, as, for example, the Schmidt rearrangement where two isomeric compounds may be formed).

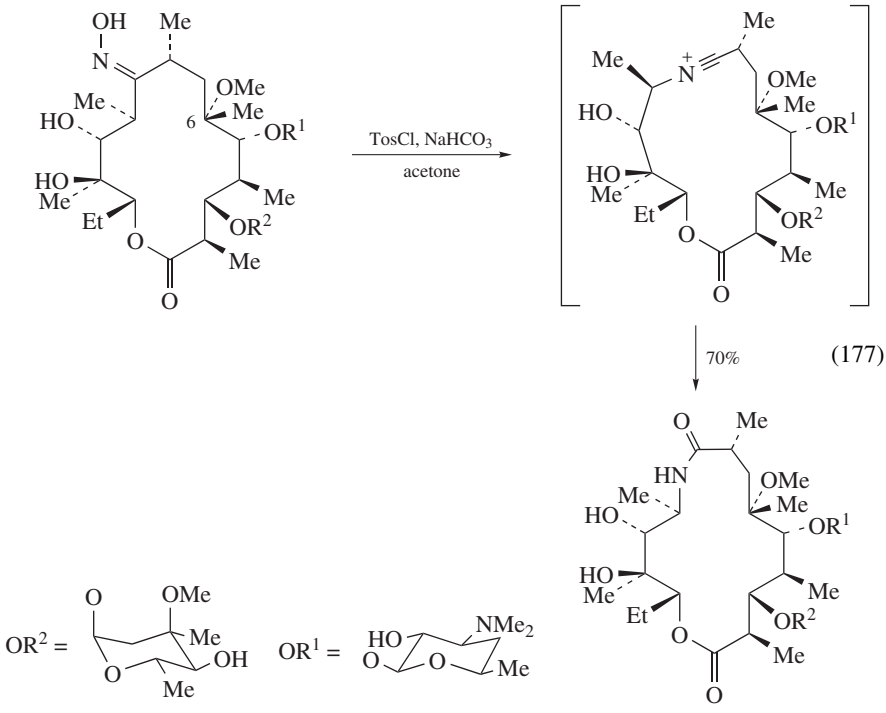

(177)

Krow and colleagues[266] investigated the migratory preferences of the Schmidt and Beckmann rearrangements in norcamphors. Two isomeric lactams are usually formed in the Schmidt reaction but one lactam is obtained almost exclusively in a Beckmann reaction (equation 178).

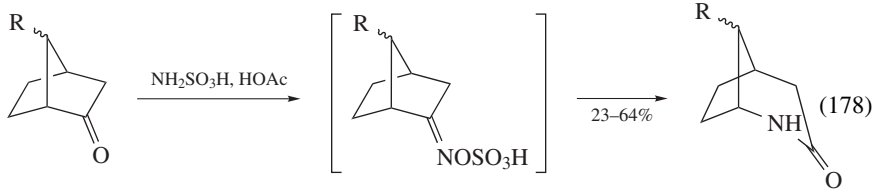

(178)

R = H, OMe, Cl, Br, OTos, CO_2Me

Novel 2,6-diazabicyclo[3.2.*x*]alkan 3-ones (**424**, $n = 1$ to 3) were synthesized by the same authors[267] using the Beckmann rearrangement. The insertion of the nitrogen occurred next to the bridgehead atom (equation 179).

Similarly, azabicyclo[3.2.2]nonanes **426** were produced from bicyclo[2.2.2]octan-2-ones **425**[268] (equation 180).

1,5-Benzodiazocines **429** were prepared to be tested as calcium-sensitizing agents[269] (equation 181). A mixture of isomeric lactams was obtained when the Schmidt rearrangement was applied to **427**, but only one product **428** was produced using the Beckmann reaction.

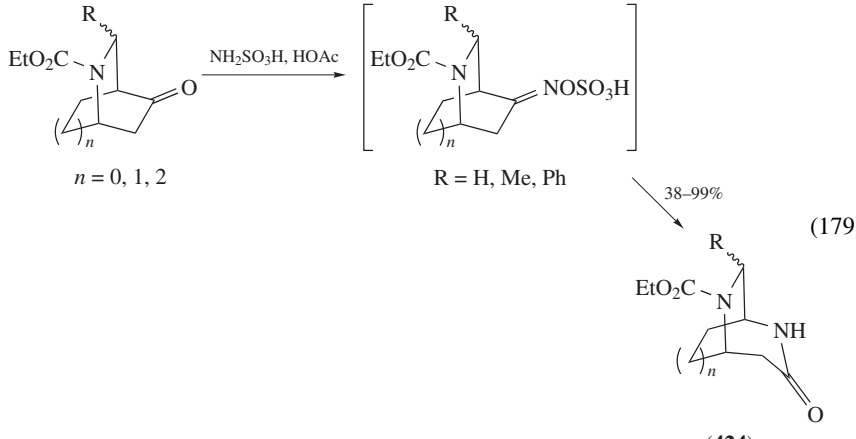

n = 0, 1, 2 R = H, Me, Ph (**424**) (179)

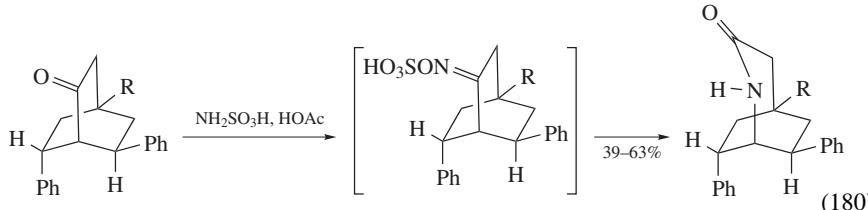

(**425**) R = NMe_2, pyrrolidine, piperidine, morpholine (**426**) (180)

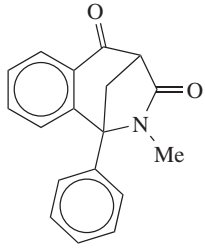

(**427**)

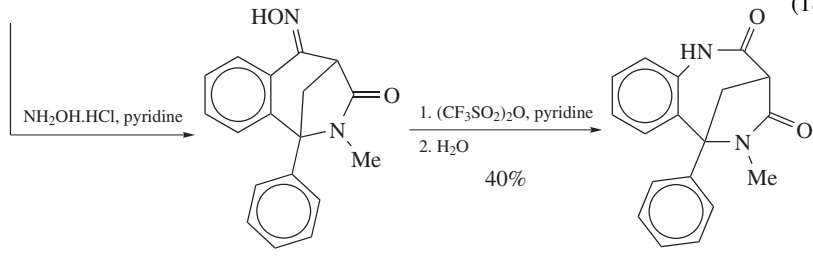

(**428**) (**429**) (181)

The asymmetric synthesis of (+)-Codeine **432** devised by White and colleagues[270] included a Beckmann rearrangement to introduce the nitrogen atom in the carbocyclic structure (equation 182). Even though two isomeric lactams **430** and **431** were obtained as a result of the rearrangement, the preferential migration of the bridgehead carbon atom produced **430** as the predominant isomer. The synthesis of the non-natural enantiomer of Codeine was completed after oxidation, olefin formation and reduction.

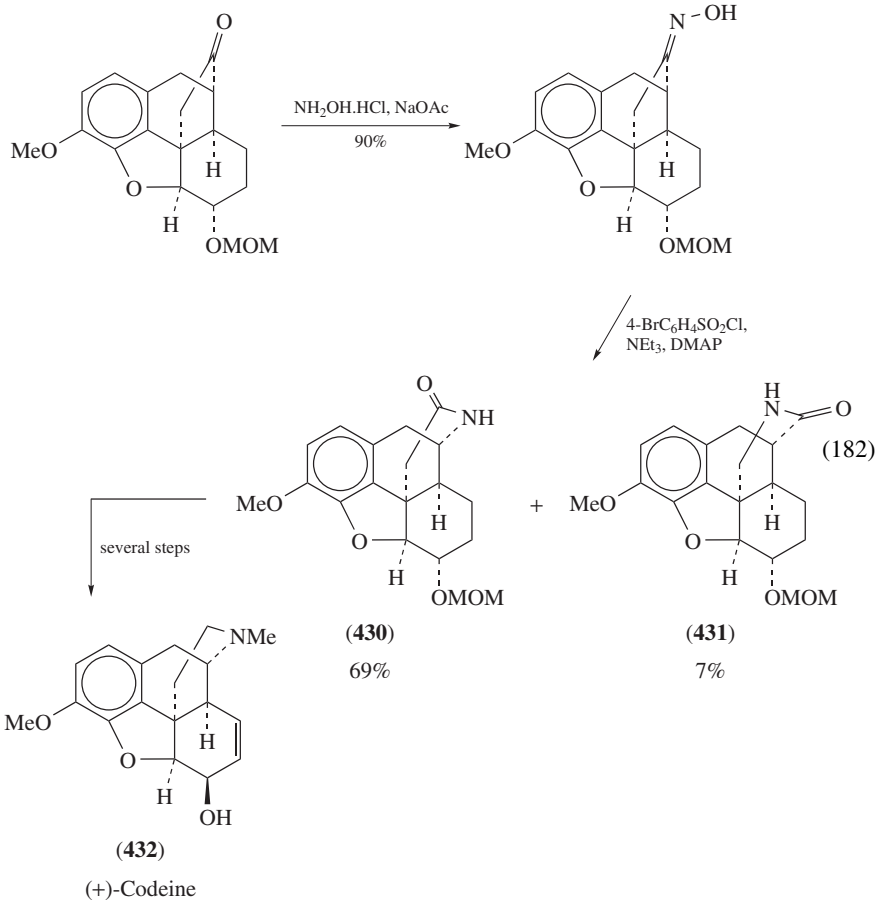

The carbocyclic **434**, precursor of nucleoside analogues, was synthesized from the commercially available (−)-β-pinene **433**[271]. The Beckmann rearrangement was used to cleave the carbocyclic ring and *cis* stereochemistry of the ring substituents is guaranteed (equation 183).

During the synthesis of **436**, Muraoka and colleagues[272, 273] produced the diazobicyclo[4.3.1]decane **435** via the classical ring expansion (equation 184). Huisgen–White rearrangement of the cyclic lactam leads to **436**, a key synthetic intermediate for piperidine alkaloids.

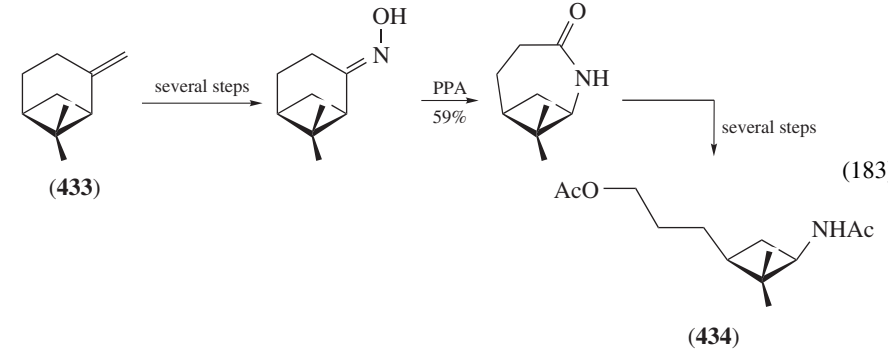

(**433**)

(**434**)

(183)

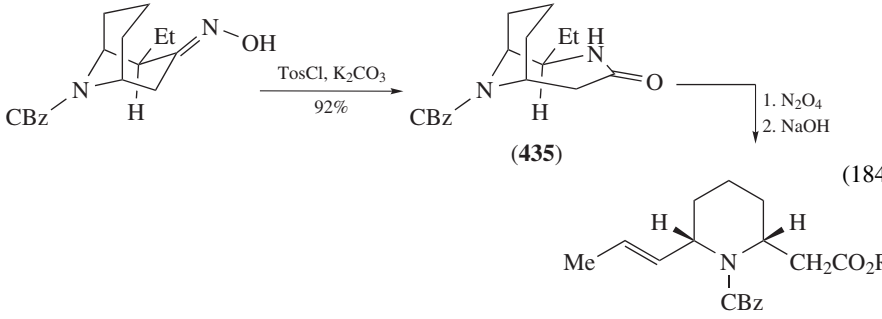

(**435**)

(184)

(**436**)

Recently, racemic 2-azabicyclo[3.2.2]nonanes **437** were synthesized to be tested as β-glycoside inhibitors[274] (equation 185). Once again the Beckmann rearrangement was selected as the method to introduce selectively the nitrogen atom into the carbocyclic structure.

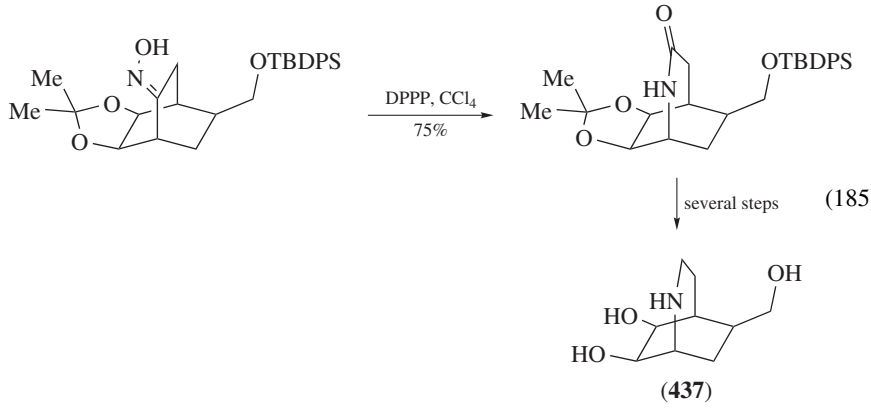

(**437**)

(185)

2. The Beckmann rearrangement–addition process

The electrophilic intermediate formed during the Beckmann rearrangement may be trapped by nucleophiles other than water. Strictly speaking, these reactions do not fit into the classical rearrangement reaction type. However, due to the fact that the carbon framework changes during the course of the reaction and to the similarities with the classical Beckmann rearrangement process, this topic will be analysed in the present chapter.

a. Imidoyl halides. Imidoyl halides (iodides and chlorides) are useful synthetic intermediates that can be obtained via a Beckmann rearrangement–addition process. Some of the compounds produced from imidoyl halides are α-alkylated amines (via imines), amidines, thioimidates, imidoyl cyanides, iminophosphonates and enaminones.

Grignard reagents and other carbon nucleophiles can react with imidoyl halides **438** to produce imines **439**[275] (equation 186). Other nucleophiles may be used to displace successfully the halide.

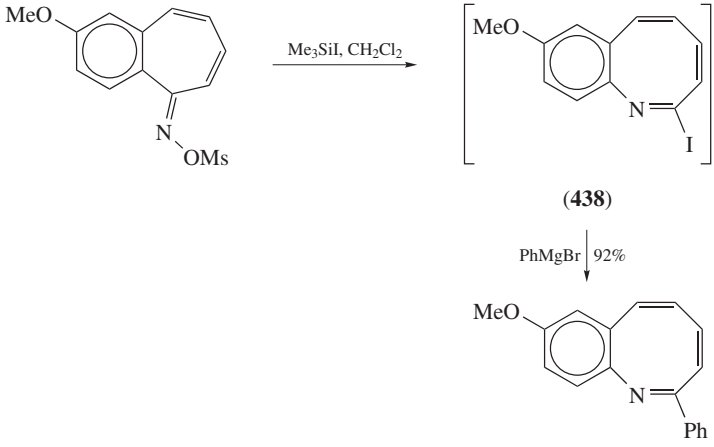

(186)

Grignard reagents may themselves be used to induce the Beckmann rearrangement, trapping the reactive intermediate. A new and highly efficient one-step synthesis of 2-arylated 1-benzocines **440** by a Beckmann rearrangement was recently devised[275] (equation 187).

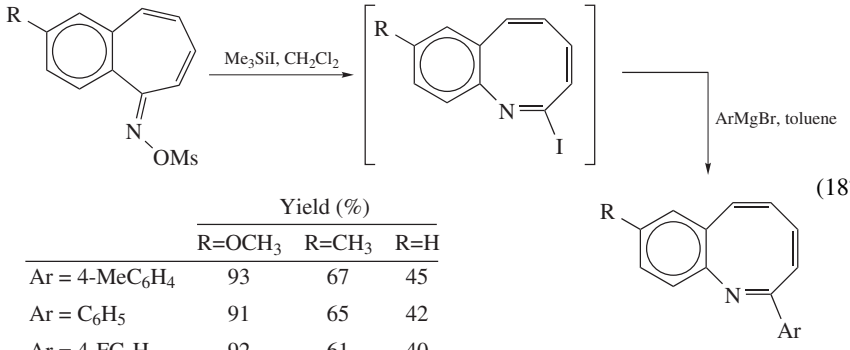

(187)

	Yield (%)		
	R=OCH_3	R=CH_3	R=H
Ar = 4-MeC_6H_4	93	67	45
Ar = C_6H_5	91	65	42
Ar = 4-FC_6H_4	92	61	40

Treatment of *N*-monosubstituted acetamides as well as aryl or alkyl methyl ketoximes **441** with dimethyl(methylene)ammonium chloride **442** in the presence of phosphorus oxychloride offers two promising, straightforward and generally applicable routes to 2-bis(dimethylaminomethyl)acetamides **443** as a result of the formation of imidoyl chlorides as intermediates[276] (equation 188).

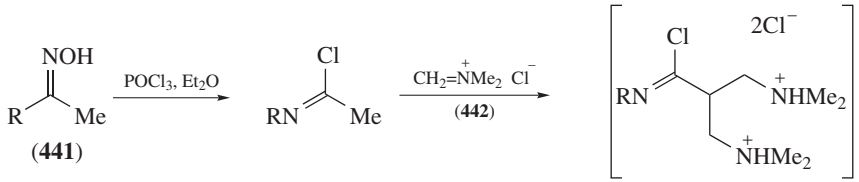

(**441**) (**442**)

(188)

R = Ph, 51%
4-$NO_2C_6H_4$, 53%
4-BrC_6H_4, 48%
4-$CH_3C_6H_4$, 51%
4-$CH_3OC_6H_4$, 42%
CH_3, 45%

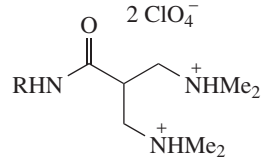

(**443**)

Pyrimidinamine derivatives **446** were produced by Ti^{IV}-mediated reaction of imidoyl chlorides **444** with cyanamides **445**[277] (equation 189).

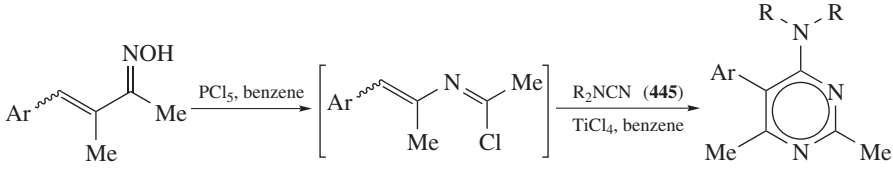

(**444**) (**446**)

Ar = 3-Pyr, R = H, 85%
Ar = 3-Pyr, R = Et, 90%
Ar = 4-Pyr, R = Me, 96%

(189)

b. Nitrogen terminator. Nitrogen nucleophiles may be added directly to the electrophilic intermediate. As an example, *N*-imidoylbenzotriazoles **447** were obtained under mild conditions in variable yields (20–87%) in a one-pot synthesis[278] (equation 190). Compounds **447** are relatively stable and can be useful substitutes for the more reactive imidoyl halides.

Amidines **450** were produced by trapping the cationic intermediate **448** with amines **449**[279] (equation 191).

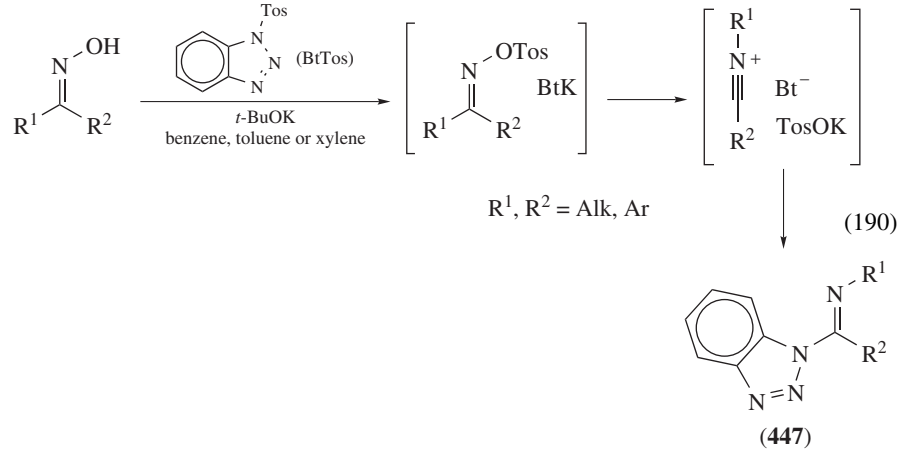

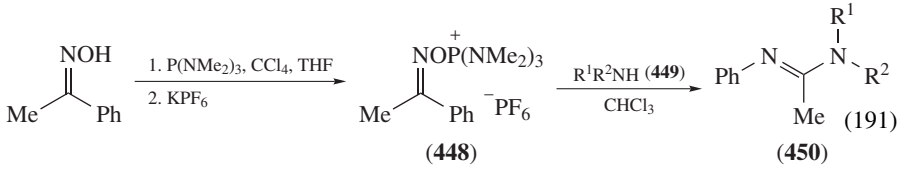

R^1, R^2 = Et, 90%
R^1, R^2 = $(CH_2)_2OMe$, 40%

c. Phosphorus terminator. Phosphorus may be the attacking atom. Aminomethylene *gem*-diphosphonic acids **452** are formed in Beckmann rearrangement of ketoximes in the presence of phosphorus trichloride. The capture of the nitrilium ion intermediate and of the resulting iminophosphonic acids **451** by phosphorus nucleophiles explain these results[280] (equation 192).

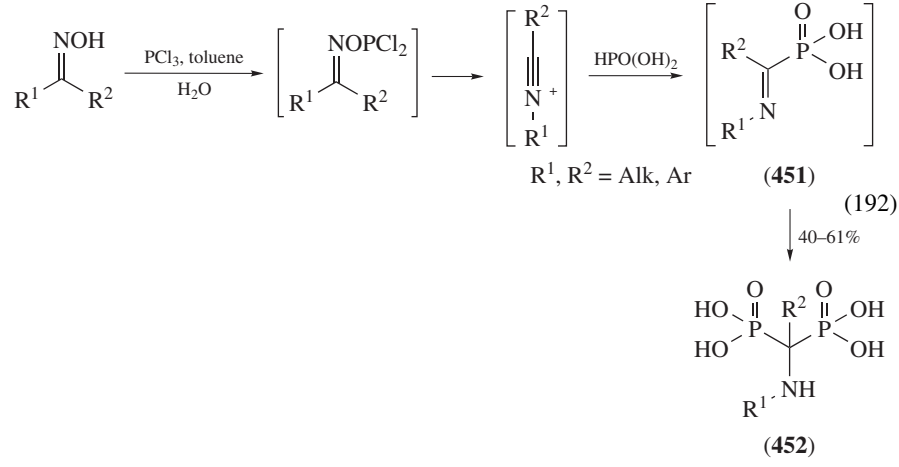

Novel syntheses of α-aminophosphonic acid derivatives (**453** and **454**) were disclosed, using the Beckmann rearrangement as a key synthetic step[281]. The ring size was crucial and only seven-membered cycles could be formed in fair yield (51–62%) (equations 193 and 194).

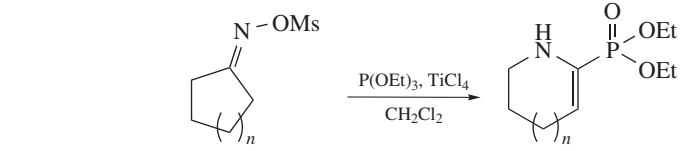

(193)

(**453**) $n = 2$, 51%
$n = 1$, 0%

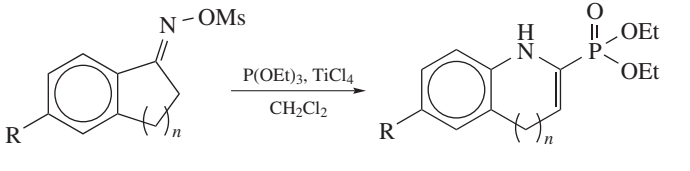

R = H, $n = 2$, 62%
R = OMe, $n = 2$, 55%
R = H, $n = 1$, 0%

(194)

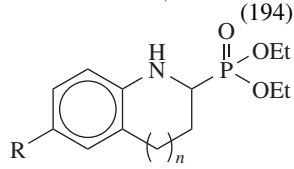

(**454**)

d. Oxygen terminator. Oxygen nucleophiles can trap the nitrilium ion to produce imidates (imine ether). The reaction conditions for the Beckmann rearrangement may be neutral or basic, allowing the use of acid-sensitive precursors. Ring expansion of **455**, containing the acid-sensitive ketal protecting group, was achieved by a sodium-ethoxide-induced Beckmann rearrangement[282] (equation 195).

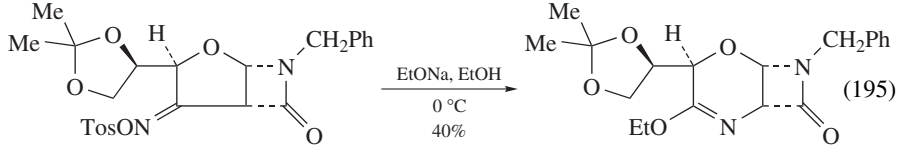

(195)

(**455**)

For cyclic oximes, ring cleavage can take place by hydrolysis of the resulting imidates **456**. This strategy was used to obtain optically pure octanoic acid derivative **457**[283] (equation 196).

When the oxime precursor for the Beckmann rearrangement contains one or more oxygen atoms placed in the appropriate position, a cyclization reaction may occur. One example of a Beckmann rearrangement–cyclization involving an oxygen atom as

terminator was observed by Uncuta and colleagues[284] (equation 197). 2,4,6-Trisubstituted pyrylium salts **459** were obtained from **458**.

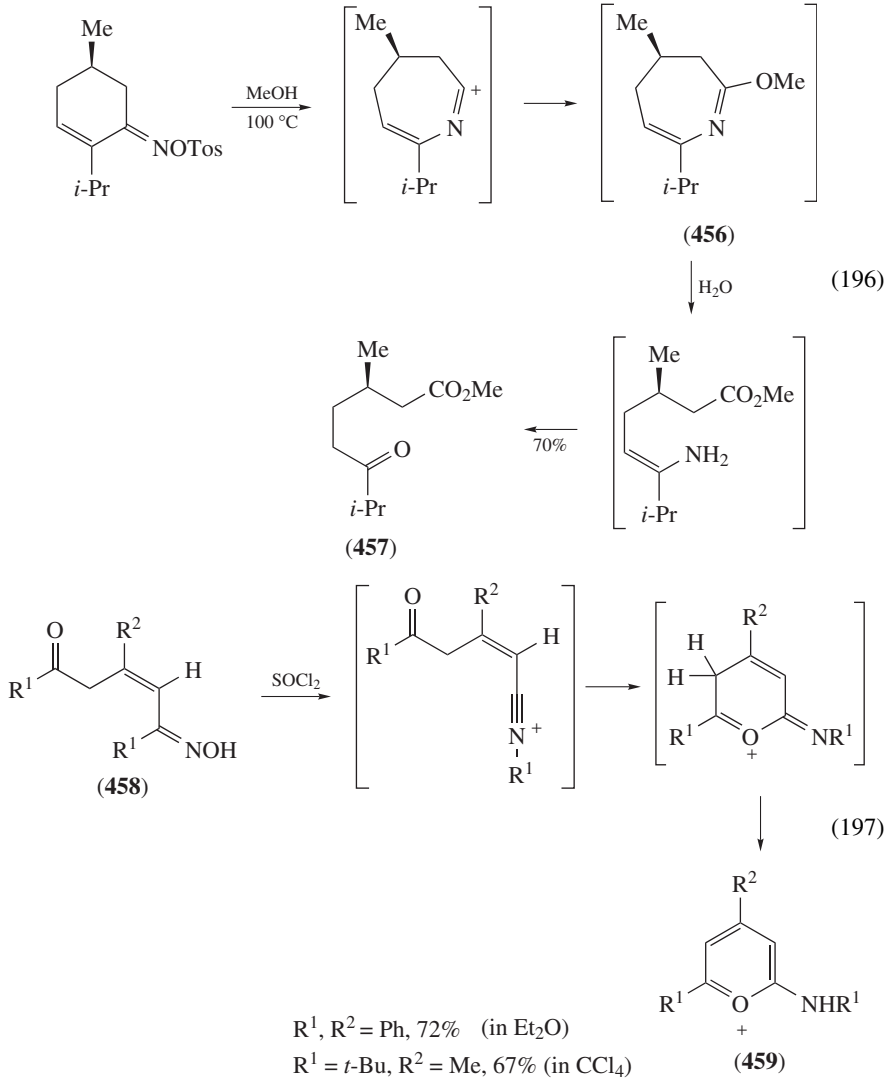

One of the most famous examples of intramolecular attack of oxygen on the nitrilium ion intermediate was observed in the Beckmann rearrangement of Erythromycin oxime derivatives and was used in the discovery and synthesis of the commercial macrolide antibiotic Azithromycin **464**[285]. In fact, the Beckmann rearrangement of Erythromycin A 9(*E*)-oxime **460** produced only small amounts (5%) of the expected amide **463**, along with two isomeric imino ethers (**461** and **462**) in a fair yield (38 and 43%) (equation 198).

Experiments showed that the imino ethers may interconvert under various conditions. Reduction of both imino ethers produced the 15-membered azacyclo compound, which on methylation produced Azithromycin **464**.

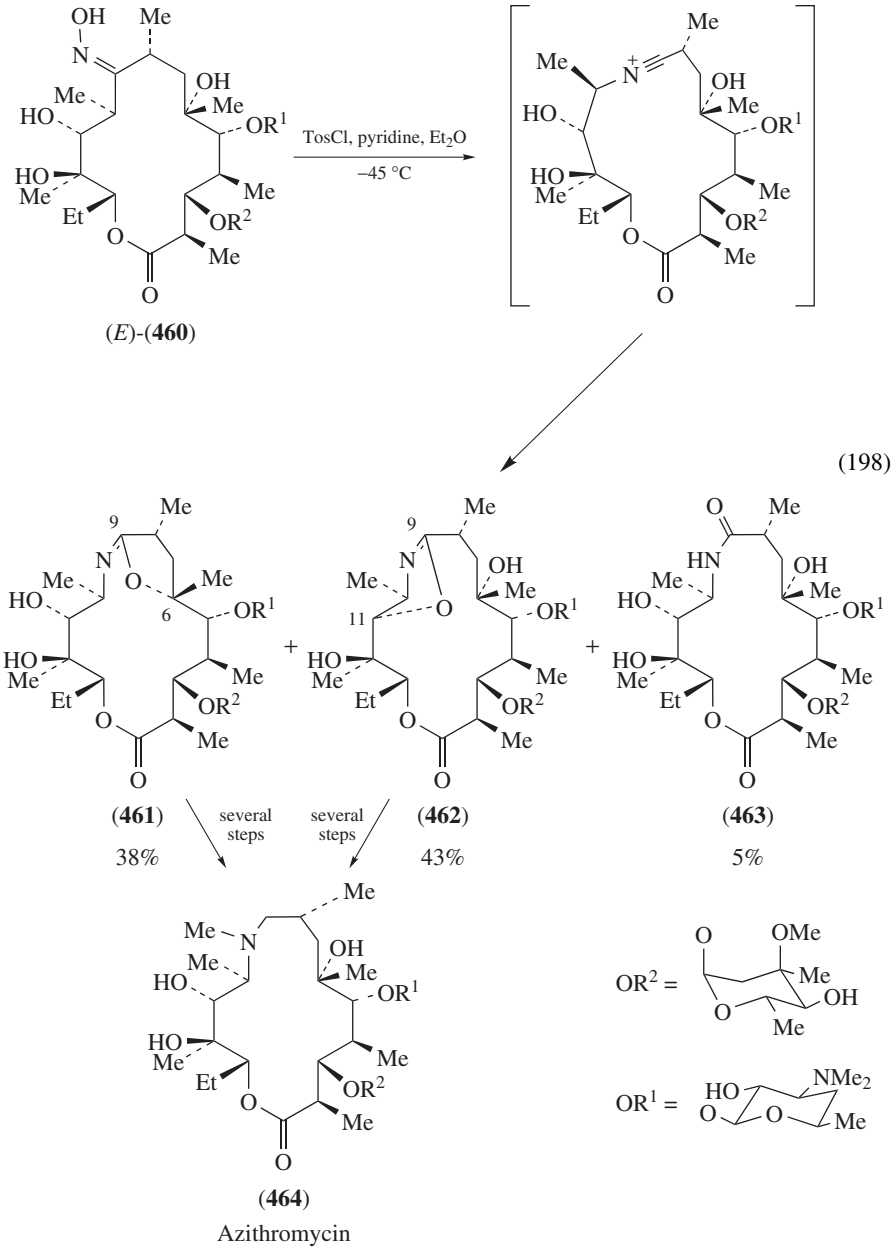

(*E*)-(**460**)

(198)

(**461**) 38%

(**462**) 43%

(**463**) 5%

(**464**)
Azithromycin

In contrast, the isomeric Erythromycin A 9(*Z*)-oxime **460** produced an isomeric nitrilium ion intermediate **465** as the result of different oxime geometry[286] (equation 199). In comparison with the products obtained from the *E*-oxime, isomeric lactam **468** and imino ethers (**466** and **467**) were isolated. Reaction conditions (including solvent polarity and the concentration of the reaction mixture) proved to have a strong influence on the yields of the various products of the rearrangement.

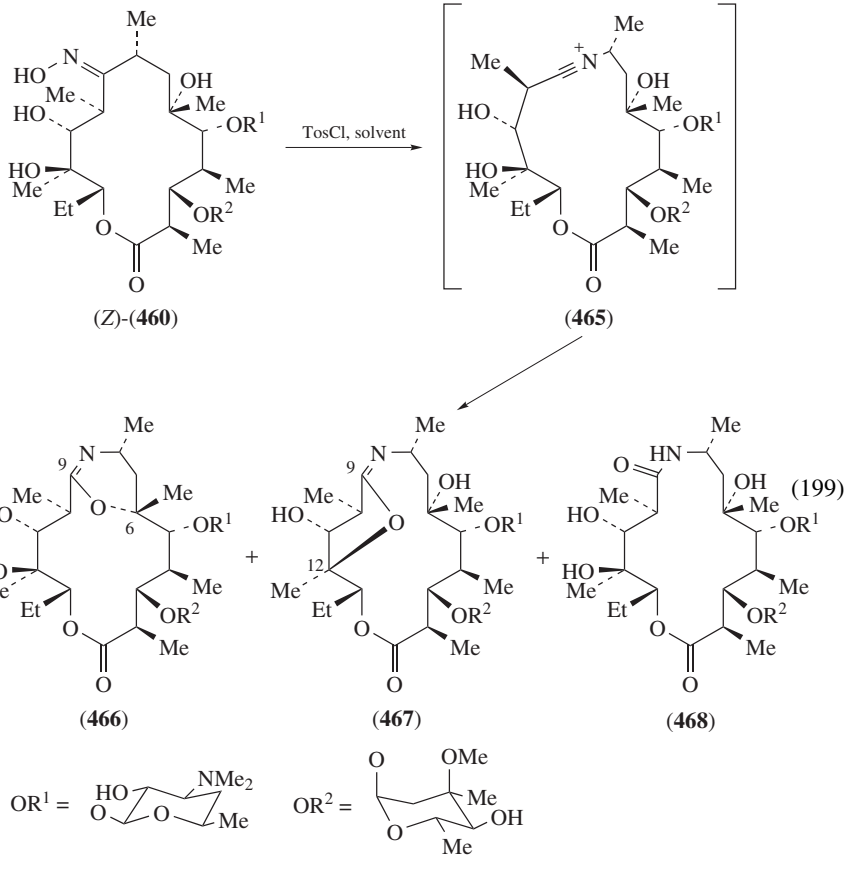

(199)

Reaction conditions	**466**	**467**	**468**
TosCl, $NaHCO_3$, acetone, water	17%	–	48%
TosCl, pyridine	25%	70%	–

Similar rearrangements were conducted with both geometric isomers of Clarithromycin oxime[287]. The structure of Clarithromycin is very similar to Erythromycin, differing only in one methyl group (the hydroxyl group in C(6) is methylated). As the oxygen atom in C(6) is no longer nucleophilic, only the 9,11-imino ether analogue **470** can be formed from Clarithromycin 9(*E*)-oxime **469**. However, and interestingly, the lactam **471** was the only product observed, in fairly good yield (70%), when similar experimental conditions to those applied for Erythromycin were applied in Clarithromycin 9(*E*)-oxime **469**

(equation 200). Changing the solvent to pyridine, no lactam was observed and only the imino ether **470** was obtained[265].

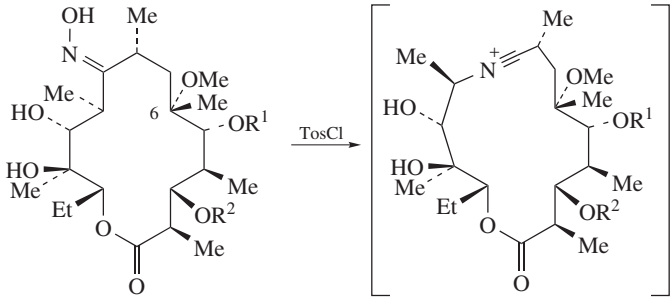

(*E*)-(**469**)

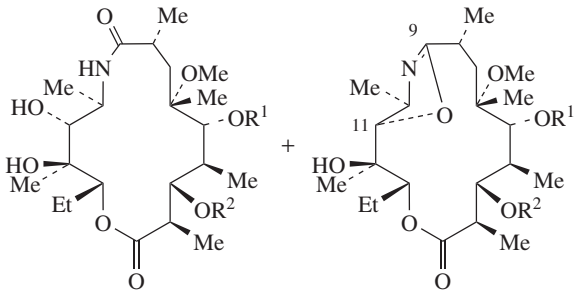

(200)

(**470**) (**471**)

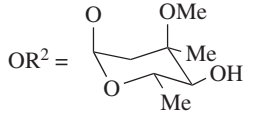

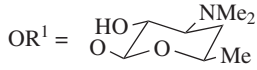

Reaction conditions	**470**	**471**
TosCl, acetone, $NaHCO_3$	70%	-
TosCl, pyridine, ether	-	40%

e. Reductive reagents. Reductive reagents are also used to promote the rearrangement. An efficient route to the chiral tetrahydroquinoline **473** used an organoaluminium-promoted Beckmann rearrangement of the oxime indanone sulfonate **472**[288] (equation 201).

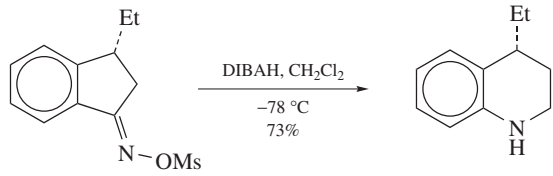

(201)

(**472**) (**473**)

Several other combinations of reagents are possible. Another example is the use of boron trifluoride to induce the rearrangement of *O*-silylated oximes **474**[174] (equation 202).

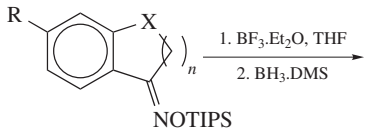

(**474**)

X	*n*	R	Yield (%)
CH_2	1	H	98
CH_2	1	Me	66
CH_2	2	H	81
CH_2	2	OMe	93
O	2	H	62

(202)

Diisobutylaluminium hydride may even be used to promote the rearrangement in *O*-unsubstituted oximes. Several heterocyclic fused azepines **475** were synthesized from the corresponding cyclohexanone oximes[289] (equation 203).

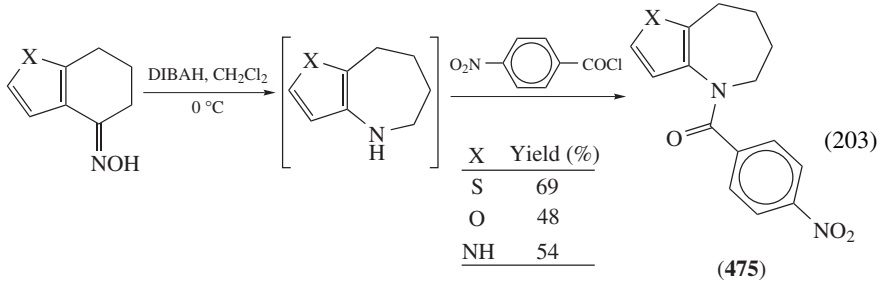

X	Yield (%)
S	69
O	48
NH	54

(203)

(**475**)

f. Aromatic terminator. In some cases, the nitrilium intermediate can be trapped by an aromatic ring (aromatic terminator). Classically, this reaction has been used in the synthesis of isoquinolines with moderate to good yields. An efficient green process of isoquinoline **476** catalysed by various HFAU-Y zeolites has been developed recently[148] (equation 204).

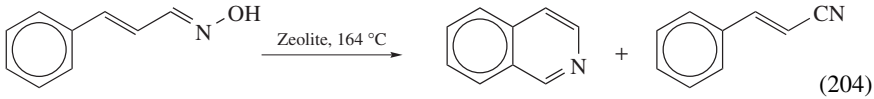

(204)

(**476**) 74–96% 2–8%

Phenethyl ketone oximes have been cyclized by a Beckmann rearrangement to isoquinolines **477** (equation 205), but quinoline derivatives **478** can also be obtained as a result of a formal displacement at the nitrogen atom of the oxime[204, 290] (equation 206).

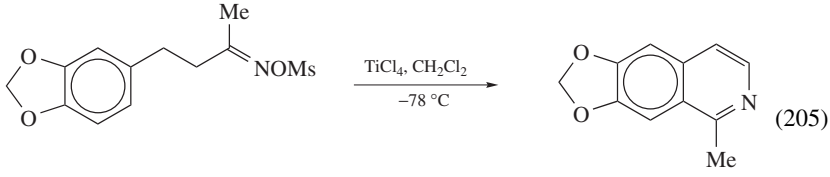

(205)

(**477**) 75%

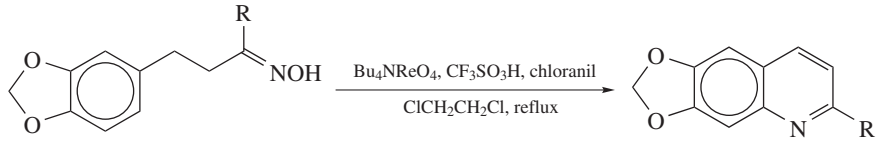

(**478**) (206)

75–89%

R = Me, Et

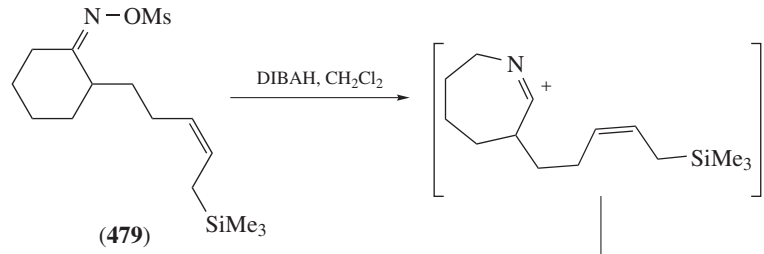

(**479**)

(207)

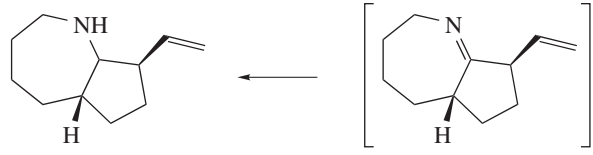

(±)-(**481**)
45%

(**480**)

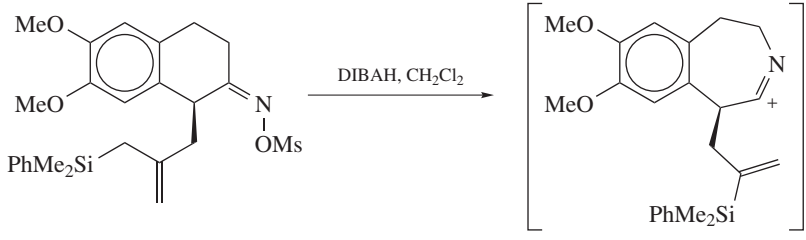

55%
(81% ee)

(208)

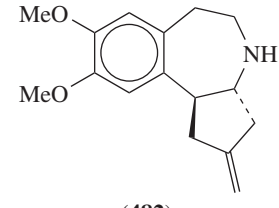

(**482**)

g. Alkene terminator. A very promising method to produce new carbocycles involves the addition of an alkene to the nitrilium intermediate (alkene terminator). Although simple alkenes may act as the nucleophile that traps the nitrilium intermediate, allyl silanes have been used to increase the nucleophilicity of the double bond. DIBAH-induced rearrangement–cyclization of **479** produces initially an imine intermediate **480**, readily reduced by DIBAH to the stable amine **481**[291] (equation 207).

A tandem Beckmann rearrangement/allylsilane was used to produce the optically active cephalotaxine framework **482**[292] (equation 208). Asymmetry could be induced as a result of stereochemical effects.

3. The Beckmann fragmentations

The Beckmann fragmentation may compete seriously with the Beckmann rearrangement. Both reactions may proceed via common intermediates and the observed selectivity strongly depends on the structural features of the starting compound. Reaction conditions can also have a strong influence on the success of the reaction.

In some cases, the 'fragmentation product' is largely predominant, or even the only product observed. The Beckmann fragmentation process will be analysed briefly in this text as it can limit the utility of the Beckmann rearrangement.

Methods that produce the nitrilium ion or the imidate other than the fragmentation of an oxime are beyond the scope of this chapter and will not be analysed.

Fragmentation occurs when the α-carbon–carbon bond breaks (Scheme 12), rather than migrates. When a stable carbocation (R^{1+}) can be formed, the Beckmann fragmentation can be the main reaction. A concerted process may occur (Scheme 12, process a), but a stepwise reaction should occur in the vast majority of cases (Scheme 12, process b).

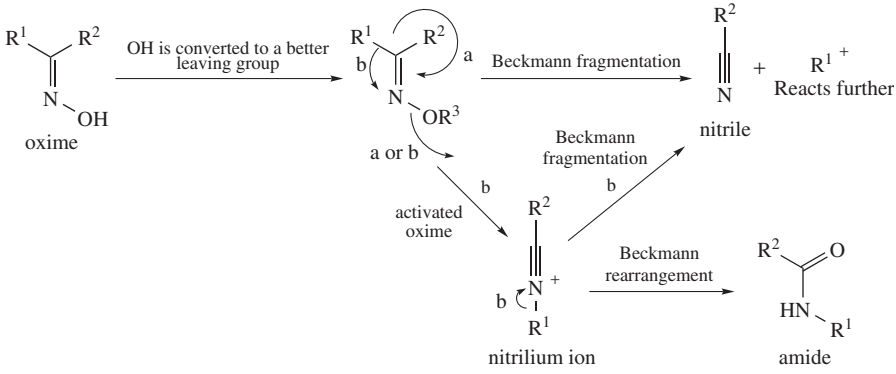

SCHEME 12

Some other mechanisms are possible, but the vast majority of the cases proceed via the imidate or the nitrilium ion.

The Beckmann fragmentation process becomes more important when assisted by neighbouring groups, either by hyperconjugation or by mesomeric donation (note that these effects occur in the migrating group). Examples of oximes that are more prone to fragmentation are collected in Scheme 13. The mechanism and the reaction conditions for the Beckmann fragmentation have been established long ago[293].

Many different reagents and conditions have been reported to produce nitriles from aldoximes. This conversion is very much expected under the presence of dehydrating agents, proton or Lewis acid and is independent of the oxime geometry.

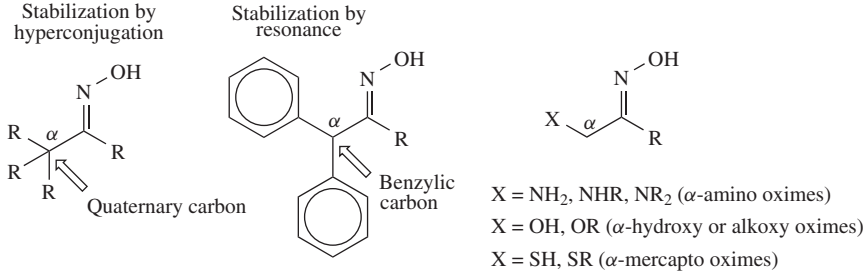

SCHEME 13

Although the Beckmann fragmentation may be regarded as a limitation for the application of the Beckmann rearrangement, it provides a synthetic method to produce nitrile compounds. Some examples from the recent literature are collected in the next section.

a. Beckmann fragmentations. The Beckmann fragmentation yields can be improved by appropriate design of the starting material, providing a useful nitrile synthetic method. The reaction is sometimes used for degradation and structure elucidation of oximes.

As an example, chiral (*E*)-1,3,4-tri-*O*-substituted-6-methoxyhex-5-en-2-one oxime derivatives **483**, available from glycals and glycosyl glycals, gave enantiopure nitriles **484** by treatment with mesyl chloride and triethylamine (equation 209). The C(1)−C(2) heterolytic fragmentation was stereospecific and directed by the adjacent C(1) ether oxygen, which generates a relatively stable carbenium−oxonium ion as an active electrofugal group. The compounds obtained from the Beckmann fragmentation can be used for the synthesis of pure enantiomeric protected pyranosylamines **485**[294].

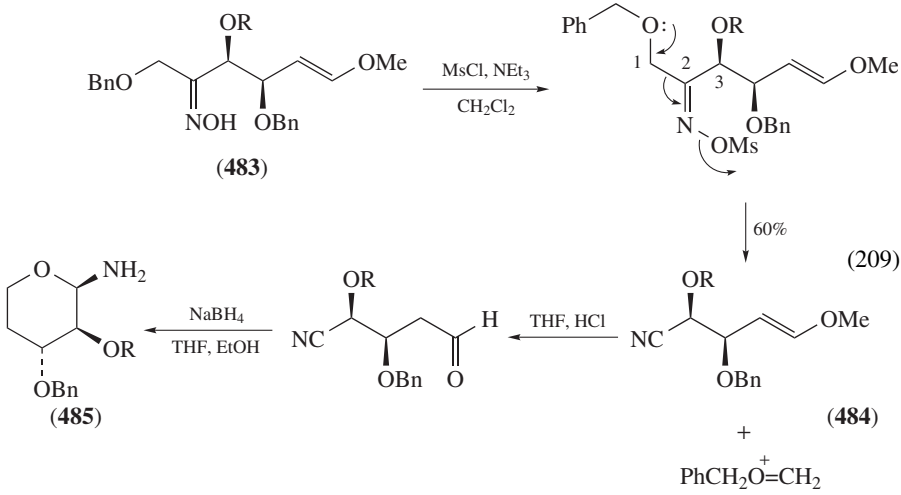

R = Bn, 2',3',4',6'-tetra-*O*-benzyl-*β*-D-galactopyranosyl

Beckmann fragmentation is frequently applied to cyclic oximes resulting in a ring-cleavage reaction. Normally, a nitrile−alkene compound is obtained from the oxime and further transformation is usual.

Perhaps the largest class of structural types that undergo fragmentation are oximes with a quaternary center adjacent to the oxime carbon. 18-Nor-androgens (for example **487**) were produced from 17-ketosteroids **486** by a Beckmann fragmentation of the D-ring followed by a ring-closing metathesis[295] (equation 210). Epoxidation of the unsaturated steroid gives **487**. The fragmentation of the D-ring of **486** was expected to be favourable, as C(13) is a quaternary carbon atom. Even so, reaction conditions had to be developed in order to reduce the lactam formation (normal Beckmann rearrangement) and increase the nitrile yield[296].

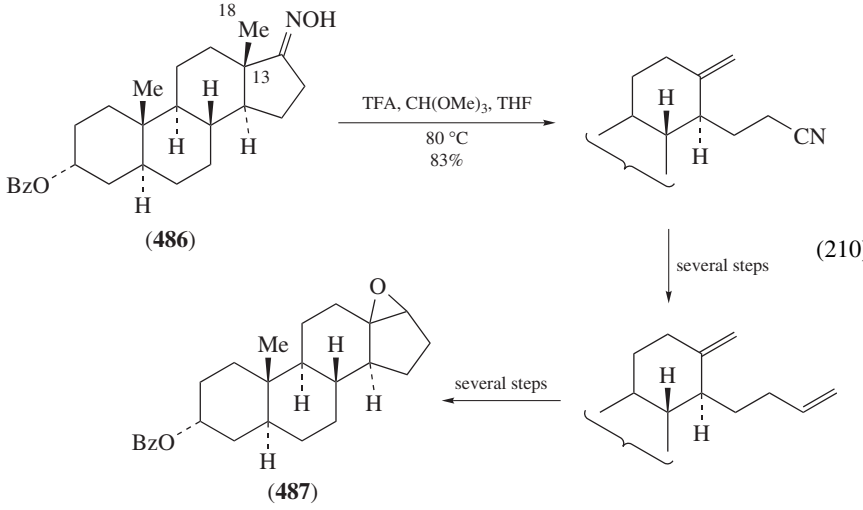

(210)

Due to the ring strain, cyclobutanone oximes are more likely to give high fragmentation yields. A recent example was shown in equations 130 and 131.

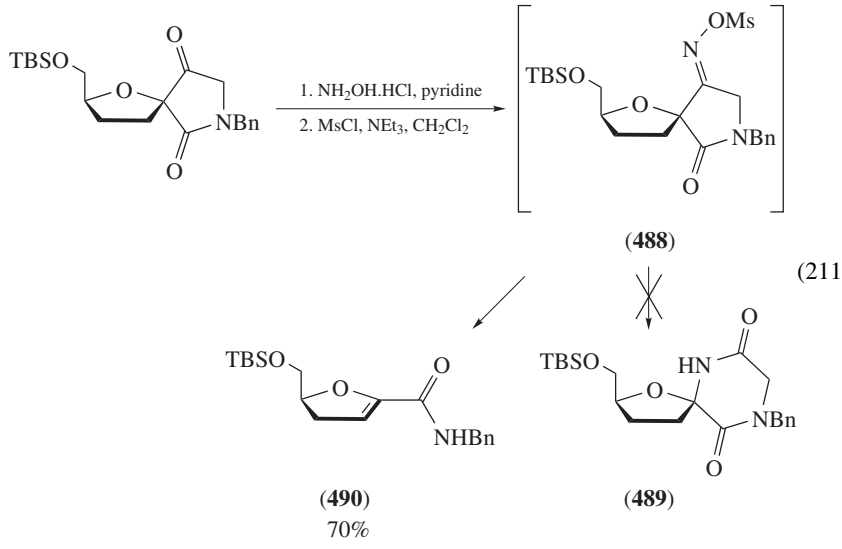

(211)

Ring cleavage assisted by an oxygen atom is very common. Sometimes, fragmentation is too favourable to allow the Beckmann rearrangement to occur. For example, various conditions were tested to obtain **489** from **488** via a Beckmann rearrangement, but all were unsuccessful[297] (equation 211). In this example, the very favourable Beckmann fragmentation produced **490** and turned the lactam formation impossible by this route, and an alternative synthetic strategy had to be devised to produce **489**.

Another recent example of unsuccessful Beckmann rearrangement is shown in equation 212 and produced a benzopyran nitrile **491**[298]. As in the previous example, mesomeric assistance by the oxygen atom turned the fragmentation very favourable.

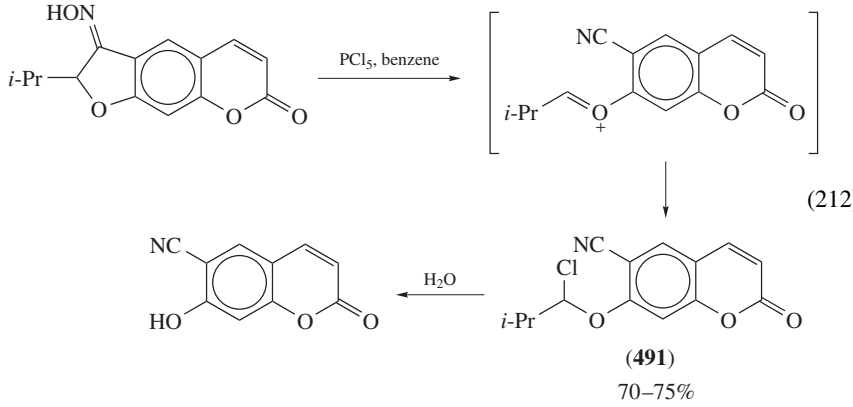

(212)

(**491**)

70–75%

The D-ring of steroids has been cleaved frequently by a Beckmann fragmentation. Typical strategy uses enolate chemistry to introduce an oximino group at the α-carbonyl carbon. Reduction of the carbonyl (or addition of a carbanion) produces an α-hydroxy oxime which serves as good substrate for the fragmentation. Two examples[299–301] of this strategy are shown in equations 213 and 214.

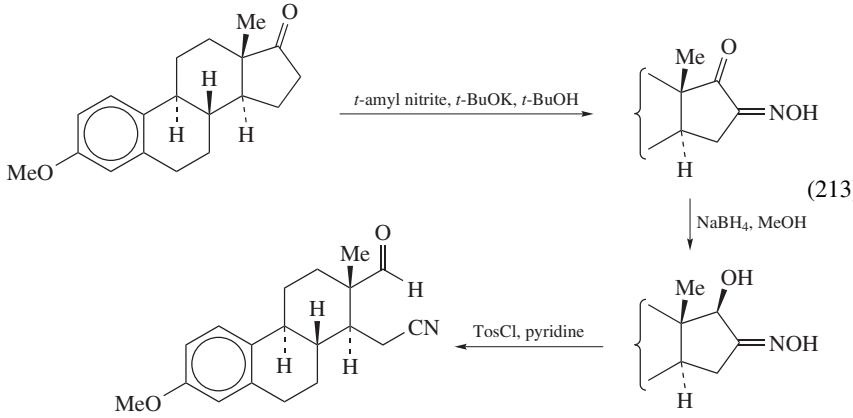

(213)

A similar cleavage was performed in a B-ring steroid **492**[302] (equation 215). In view of the oxime geometry the fragmentation was unexpected. A new mechanism, involving a six-membered cyclic *N*-*O*-sulfite **493**, was proposed to account for the observations.

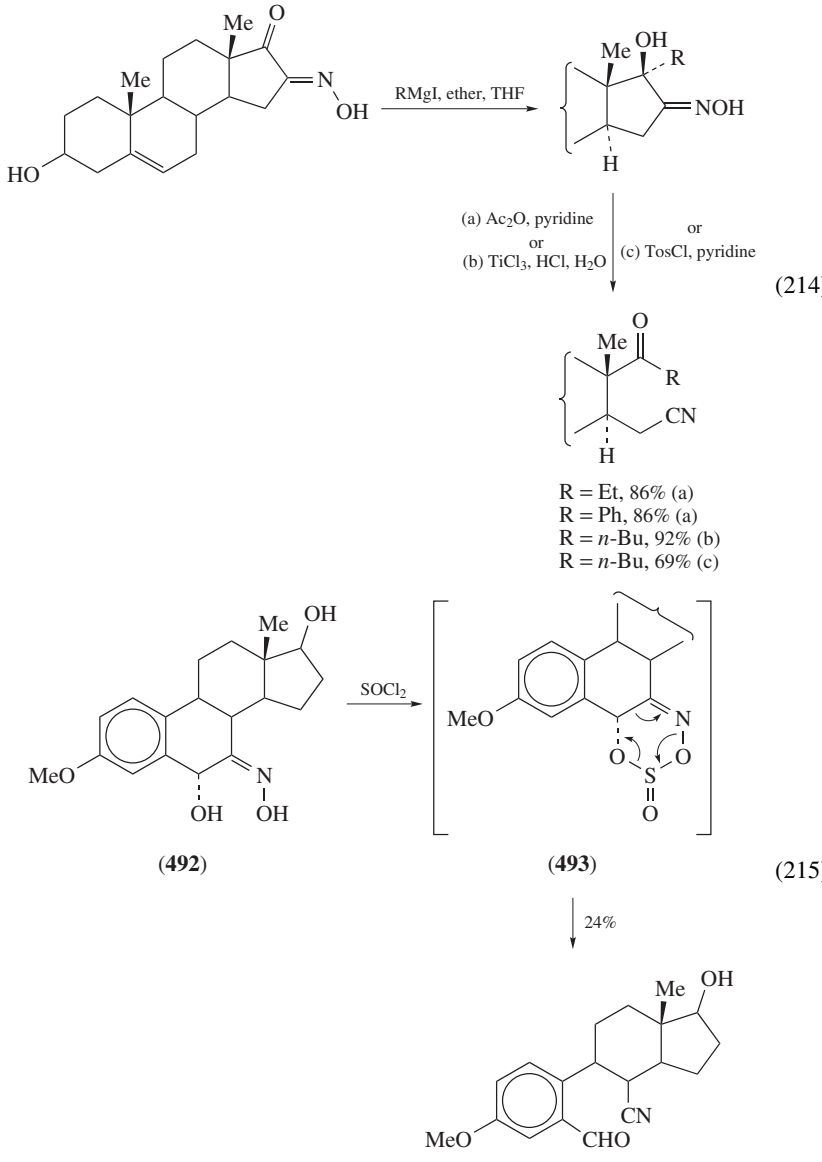

A new transformation of the spiroketal side chain of diosgenin was recently reported[303–305]. Beckmann fragmentation of 23-hydroxyiminosapogenin **494** induced by $POCl_3$ in pyridine produced a mixture of compounds (**496**, **497** and **498**) as a result of the decomposition of the unstable intermediate **495** (equation 216). The observed stereochemistry of the products showed clearly that the cleavage was induced by the mesomeric donation of the two oxygen atoms (attack of chlorine in **495** inverts the configuration while the configuration of C(16) was retained in **497** and **498**).

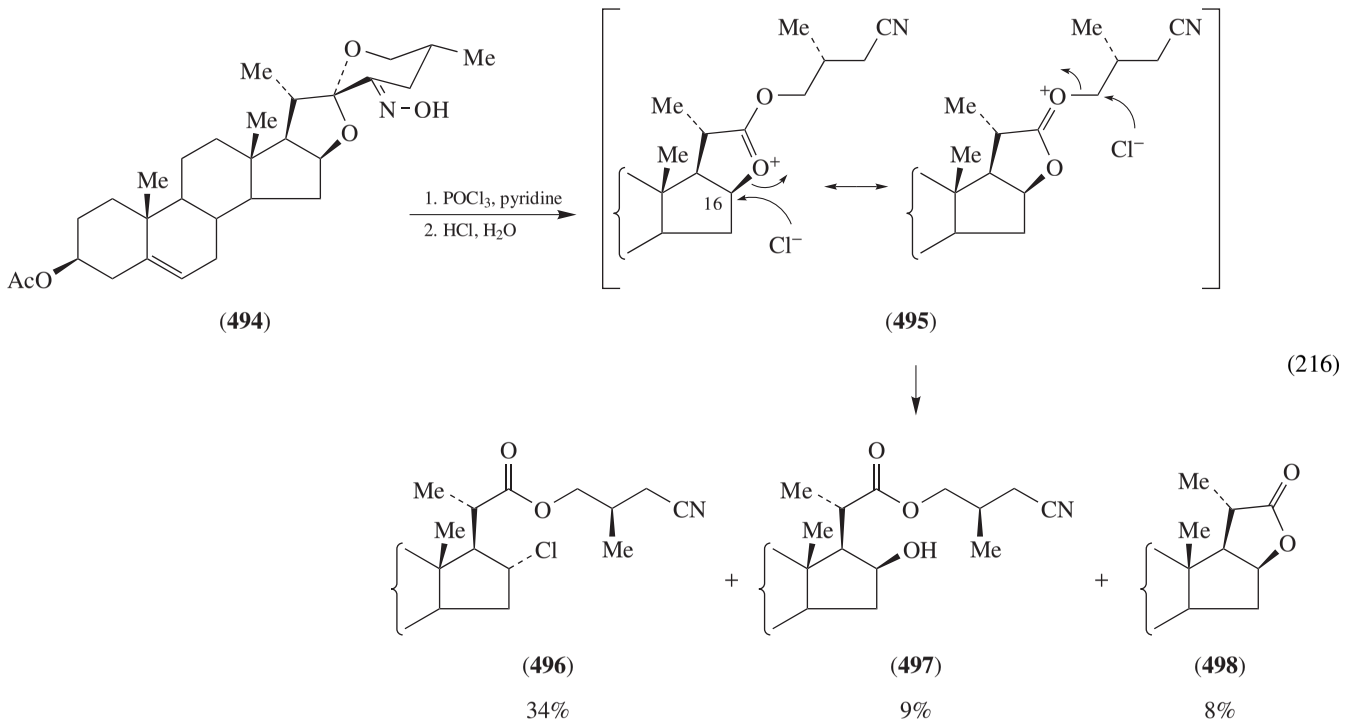

(**494**) (**495**) (216)

(**496**) 34%

(**497**) 9%

(**498**) 8%

Performing the reaction with BF_3/Et_2O in acetic acid, high yield (84%) of the corresponding bisnorcholanic lactone **498** as the sole product was obtained[303].

The key stage of the synthesis to prepare 100 g amounts of a novel anthelmintic drug **500** from the metabolite VM-44866 (**499**) was a Beckmann-type oxime fragmentation[306] (equation 217). A two-step reassembly of the spiroketal moiety efficiently produced the target molecule (30% yield of complete sequence in a 0.5 kg scale).

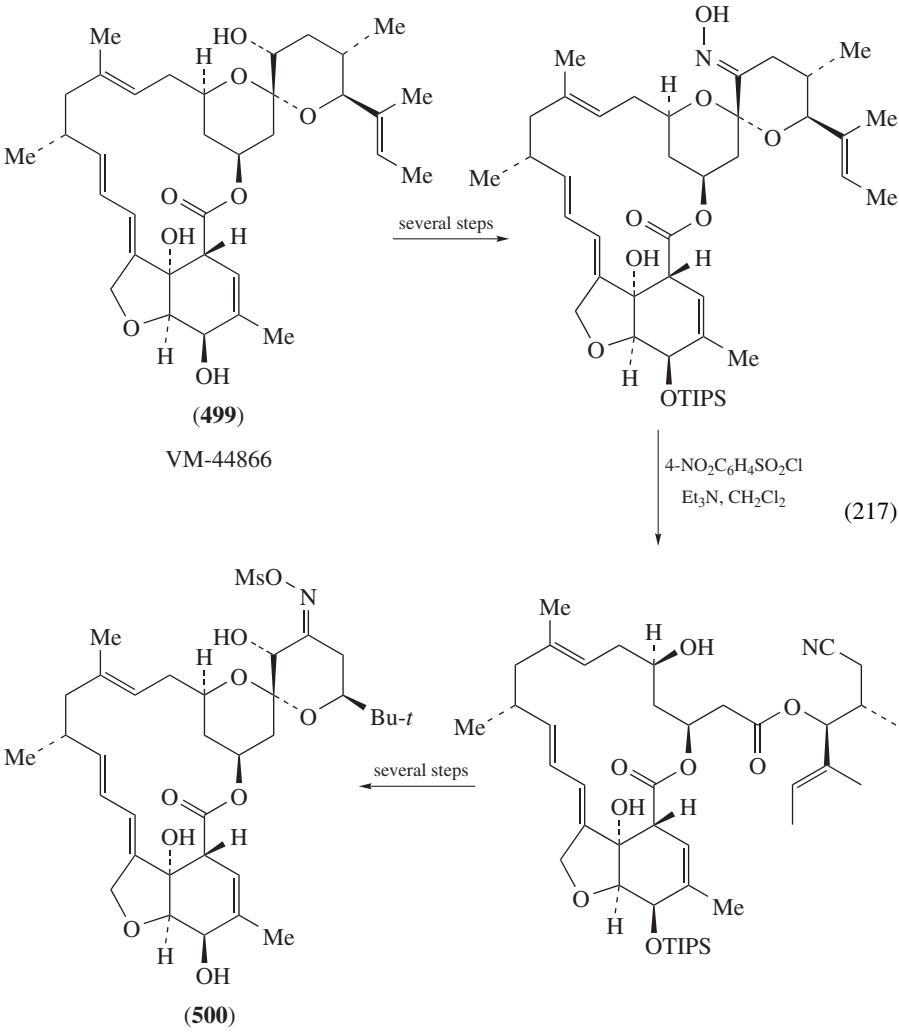

(**499**)

VM-44866

(217)

(**500**)

Fragmentations of oximes of bicyclic compounds, e.g. camphor oxime, have been extensively studied, as the products can be used as chiral intermediates in enantiospecific syntheses.

The *cis*-substituted cyclobutane ester **502** is of interest as intermediate for the synthesis of carbocyclic **503**[307] (equation 218). Ring opening of the bicyclic (+)-Nopinone **501**

provides the cyclobutane **502** with the intended *cis* stereochemistry, converted to **503** by reduction.

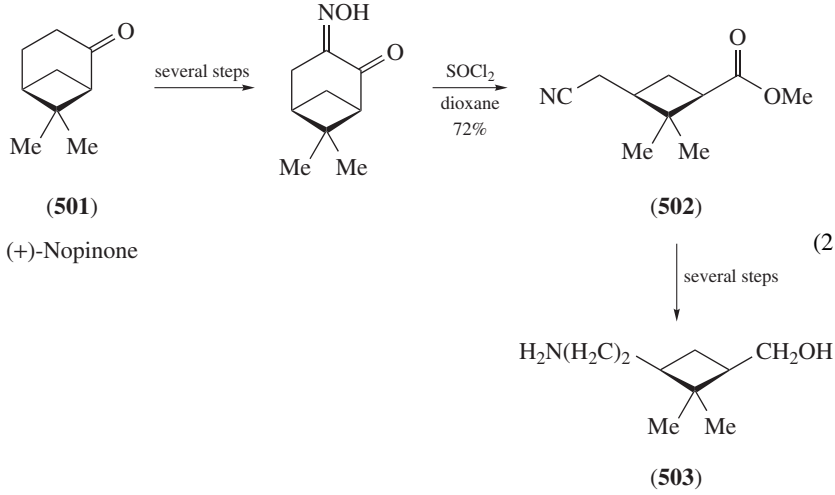

(218)

As expected, champhor oxime **504** fragments at the C(1)−C(2) bond due to the quaternary C(1) carbon atom[308] (equation 219).

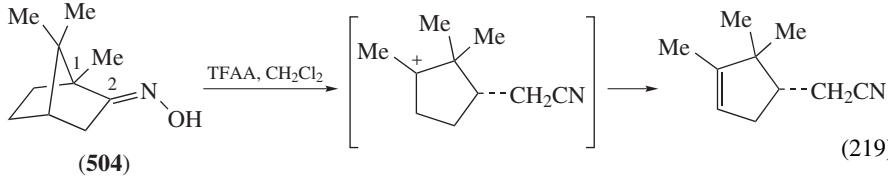

(219)

As an example, this opening was applied to the synthesis of enantiopure 3-substituted cyclopentanones **506** from 2-norbornanones **505**[309] (equation 220). The key step on this synthetic route was the Beckmann fragmentation of the oxime **505**, promoted by Tf_2O/pyridine.

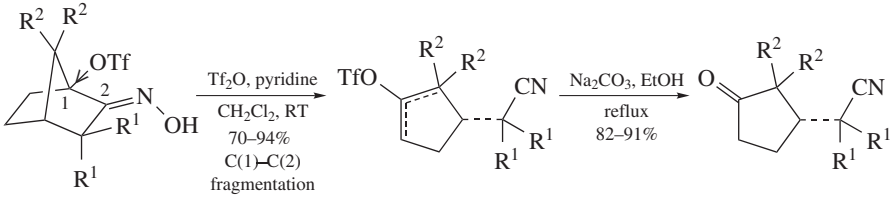

(220)

The fragmentation regioselectivity of substituted bicyclic compounds was investigated and the observed cleavage has a strong correlation with the ability to stabilize a positive charge at the α-carbon atom. The preferred cleavage usually occurs between the oximino carbon and the α-carbon atom more able to sustain and stabilize a positive charge.

The presence of electron-donating (EDG) or electron-withdrawing groups (EWG) clearly influences the place at which the fragmentation takes place. Electron-donating groups increase the stability of a positive charge at C(1) and therefore promote C(1)−C(2) bond cleavage (equation 221). In contrast, electron-withdrawing groups turn a C(1) cation unstable, and cleavage of the C(2)−C(3) bond is more favourable (equation 222).

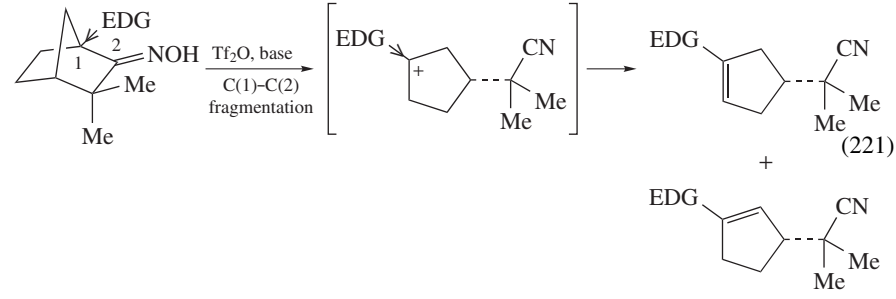

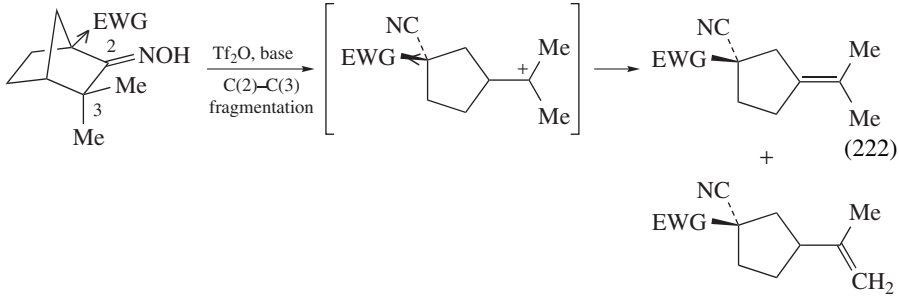

Martínez, Cerero and colleagues[310,311] discovered a useful and unexpected bromine-assisted Beckmann fragmentation of the bornan-2-one **507** (equation 223). When trying to form the oxime **508**, **509** was isolated in high yields. More interestingly, the product obtained was not consistent with the presence of the electron-withdrawing group at C(1). The assistance of the bromine atom at the bridgehead position was regarded as responsible for the unexpected selectivity of the cleavage, and the product of the reaction (**509**) is an interesting synthetic intermediate.

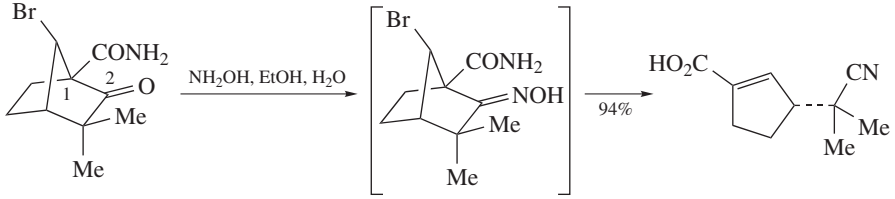

(**507**) (**508**) (**509**) (223)

Beckmann fragmentation of polycyclic structures can be of great utility and was a key step in the two synthetic routes for the synthesis of propellane **510**[312,313] (equation 224). Both fragmentation processes are oxygen assisted.

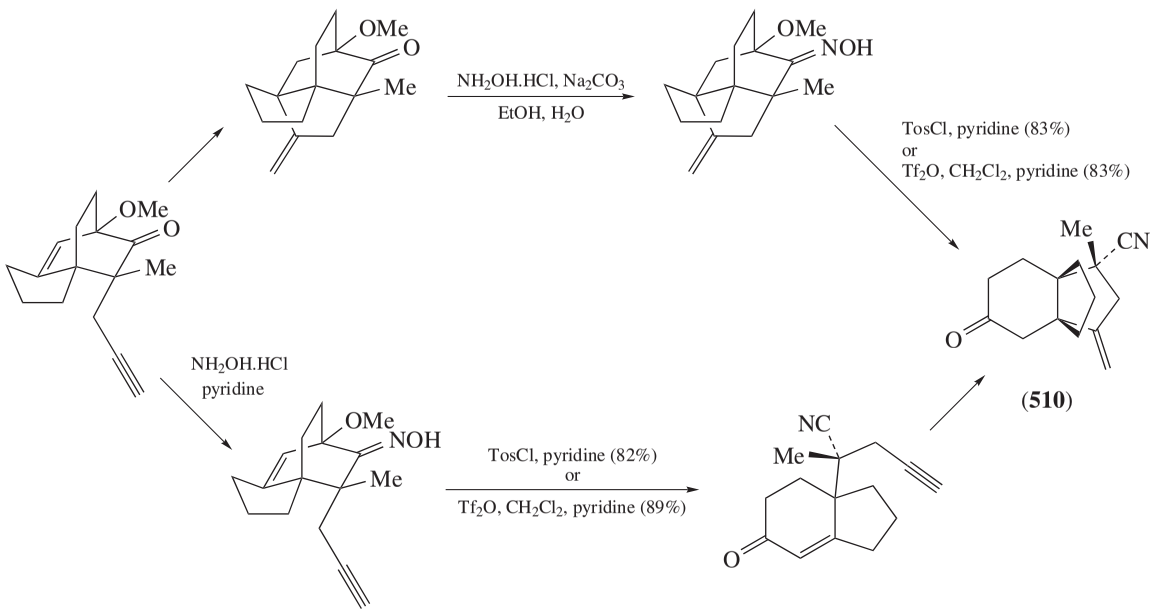
OMe
O
Me
NH2OH.HCl, Na2CO3
EtOH, H2O
OMe
NOH
Me
TosCl, pyridine (83%)
or
Tf2O, CH2Cl2, pyridine (83%)
Me
CN
O
(510)
NH2OH.HCl
pyridine
OMe
NOH
Me
TosCl, pyridine (82%)
or
Tf2O, CH2Cl2, pyridine (89%)
NC
Me
O

(224)

Although they are much less common, the fragmentations can also be assisted by nitrogen or sulfur substituents at the α-carbon atom. An immonium salt has to be an intermediate in the fragmentation of α-amino oximes, which on hydrolysis produce a carbonyl group (ketone or aldehyde).

It was observed that α-amino oximes **511**, when treated with sodium borohydride in boiling acetonitrile, produced the expected fragmentation products **513** in moderate to good yields (31–87%)[314] (equation 225). The use of the hydride-induced fragmentation in cyclic oximes leads to amino nitrile compounds, as a result of the reduction of the immonium salt intermediates **512**. Careful selected oxime structures showed that the reaction time increases when the stability of the immonium intermediate decreases, showing the importance of the mesomeric assistance.

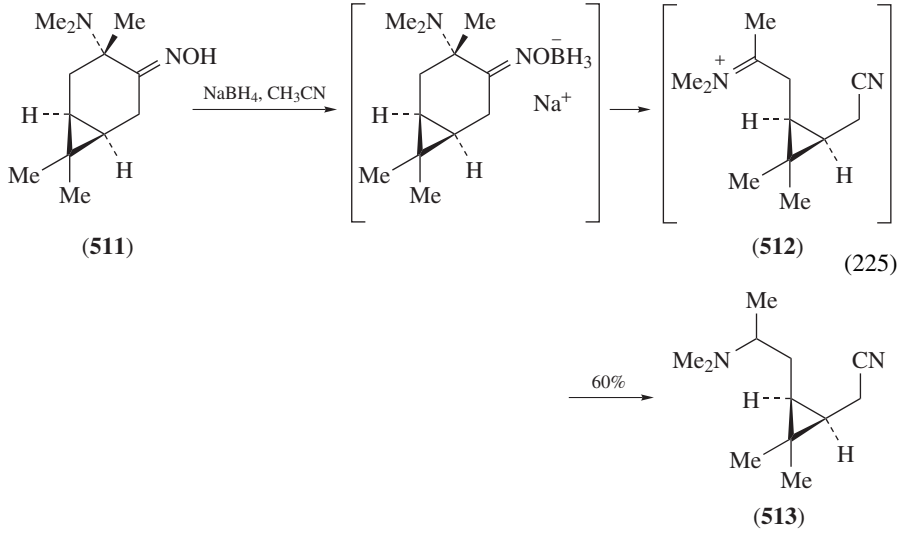

(**511**) (**512**) (225)

(**513**)

Although rare, it is possible to trap the electrophilic intermediate of the Beckmann fragmentation. An example is the fluorinative Beckmann fragmentation discovered by Kirihara and colleagues[315] (equation 226).

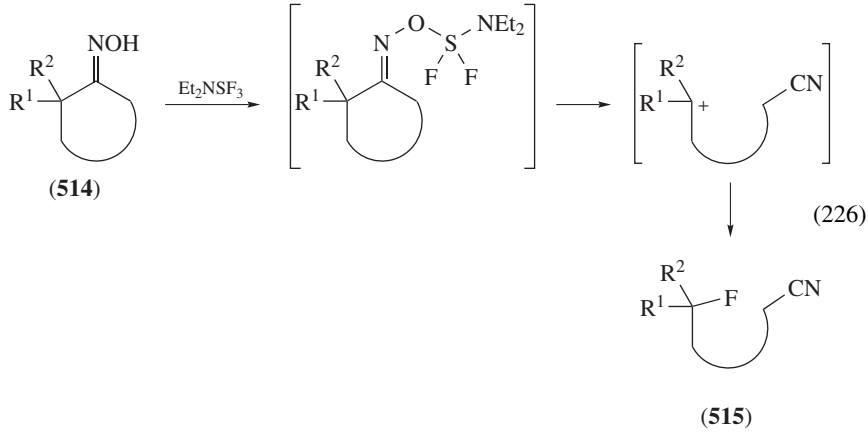

(**514**) (226)

(**515**)

Cyclic ketoximes **514** bearing cation-stabilizing groups produced fluorinated carbonitriles **515** in good yields (63–97%). In substrates with no stabilizing groups such as cyclohexanone oxime, the reaction was unsuccessful. In these cases it is assumed that a Beckmann rearrangement–addition occurs, producing a very unstable imidoyl fluoride that decomposes to a complex mixture. A sulfur-assisted fragmentation was also reported by the same authors (equations 227–229).

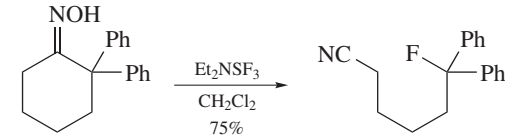

(227)

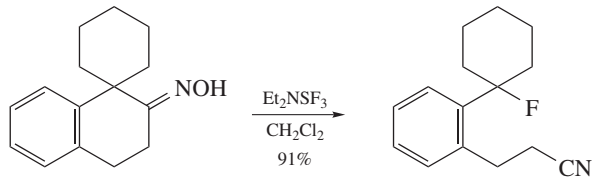

(228)

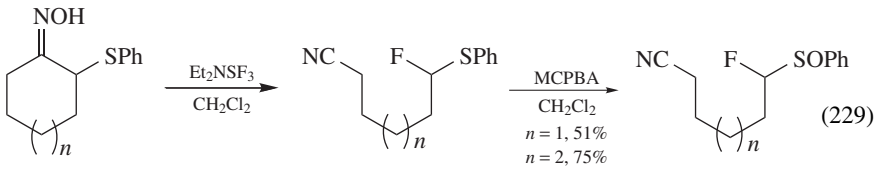

(229)

F. Industrial Uses

The most notable application of the Beckmann rearrangement is in the industrial production of ε-caprolactam from cyclohexanone (or its oxime), which is used as monomer for the polymerization to a polyamide for the production of synthetic fibres (for example, nylon 6).

The production of the nylon precursor ε-caprolactam via the Beckmann rearrangement is one of the largest industrial processes worldwide. There are a large number of synthetic routes to ε-caprolactam, most of which need to be improved because, without exception, all are multistage processes that produce large amounts of by-products, primarily ammonium sulfate. Due to its industrial application, the improvement of the Beckmann rearrangement of ε-caprolactam was the aim of several studies and a lot of scientific papers, patents[138] and book chapters[316,317] have been published on this topic during the last century.

The classical production of ε-caprolactam is based on cyclohexanone oxime and on its Beckmann rearrangement. For this step, all manufacturers use fuming sulfuric acid or oleum, sometimes enriched with more sulfur trioxide than present anyway in the oleum, to increase the rate of the rearrangement process.

The rearrangement was done in similar ways by different caprolactam producers, and the differences can only be found in the purification processes. With the formation of ammonium sulfate being the most important problem for the producers of ε-caprolactam, and due to the rising costs of its removal, many companies searched for new possibilities to produce caprolactam. There are some important industrial processes avoiding the cyclohexanone oxime as an intermediate product.

There is extensive research ongoing for new synthesis processes which are economically favourable due to less expensive reactants or easier processes. One very important point is the avoidance of the production of a large amount of ammonium sulfate, which can be achieved by the prevention of the formation of any salt or by the replacement of ammonium sulfate by another ammonium salt with increased economical value. Recently, studies of Beckmann rearrangement of cyclohexanone oxime in friendly environment conditions have received special attention[192, 318].

The industrial ε-caprolactam processes with cyclohexanone oxime as intermediate product were recently reviewed[138]. The catalytic gas-phase Beckmann rearrangement has great industrial interest. Since the process proposed by DuPont in 1938 the investigation on catalytic gas-phase Beckmann rearrangement has been investigated, and a large variety of catalysts have been tested for the reaction.

The main research objectives to industrial applications are: the relation of the catalyst acidity to the yield, the location of the rearrangement reaction on the catalyst, the catalyst's deactivation, the best reaction conditions, the best solvent and advanced reactor concepts.

Various reactions leading to by-products occur to all catalysts and, especially, the unsaturated nitriles formed by Beckmann fragmentation are easily polymerized.

As the Beckmann rearrangement is believed to be a typical acid-catalysed reaction, many researchers have reported the relationship between the vapour phase reaction catalysis and the acidity of the catalysts tested on non-zeolitic catalysts[121, 122, 125, 128–131, 318–334] and on zeolitic catalysts[142, 335–348]. Another interesting point for the heterogeneous gas-phase Beckmann rearrangement is the location of the reaction on the catalyst and different studies have been published[140, 145, 349–353]. The outer surface of the catalyst particle seems to be the most probable place for the Beckmann rearrangement supported by the traces of reagents, and notable amounts of by-products found only in the outer layers of the zeolite crystal. Development of new and more efficient catalysts have also been reported[123, 354–361].

The deactivation and regeneration of the catalyst are also important processes in the industrial production of the caprolactam by the Beckmann rearrangement and have been studied[143, 362–366].

The best reaction conditions[131, 340, 367–369] and the solvents used are important features in the industrial processes. The use of different solvents has influence on the deactivation time of the catalyst[106, 127, 333, 336, 344, 370–374]. Different groups examined the role of different solvents on the different catalysts used in production of ε-caprolactam by Beckmann rearrangement[142, 330, 356, 369, 375–378]. It can be stated that ethanol seems to be the best choice when using MFI-type zeolites, which are the most common materials used in the Beckmann rearrangement. Using non-MFI materials, especially larger-pore-size materials, 1-hexanol seems to be a good choice.

The reactor systems were also improved, concerning the Beckmann rearrangement of cyclohexanone oxime and the production of the unwanted ammonium salts[138], by-products and contaminants[379].

Recently, the Sumitomo Chemical Co., Ltd. developed the vapour-phase Beckmann rearrangement process for the production of ε-caprolactam. In the process, cyclohexanone oxime is rearranged to ε-caprolactam by using a zeolite as a catalyst instead of sulfuric acid. EniChem in Italy developed the ammoximation process that involves the direct production of cyclohexanone oxime without producing any ammonium sulfate. The Sumitomo Chemical Co., Ltd. commercialized the combined process of vapour-phase Beckmann rearrangement and ammoximation in 2003[142].

Apart from the uses in the production of ε-caprolactam, the Beckmann rearrangement has been used industrially in the synthesis of various APIs (Active Pharmaceutical Ingredient) or other compounds with economical value (essentially monomers for the production of polymers). A survey of the bulk reaction scaled in the GMP facilities at

the Pfizer-Groton site between 1985 and 2002 was carried out[380]. During this period, a dramatic decrease in the use of Beckmann and related rearrangements to form C−N bonds was observed, mainly due to the reduction of investigation in the macrolide antibiotics field, with less Azithromycin analogues produced. The two more famous APIs are without doubt Azithromycin **464** (equation 198) and Paracetamol **516**[381] (acetaminophen) (equation 230).

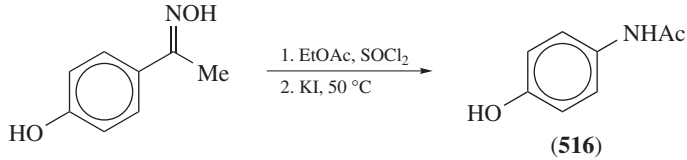

(230)

(**516**)

Paracetamol
(acetaminophen)

VII. THE NEBER REARRANGEMENTS

The Neber rearrangement[382, 383] was discovered in 1926 during the investigation of the Beckmann rearrangement. It was reported that treatment of ketoxime tosylate **517** with potassium ethoxide followed by acetic and hydrochloric acid produced α-amino ketones **518** (equation 231).

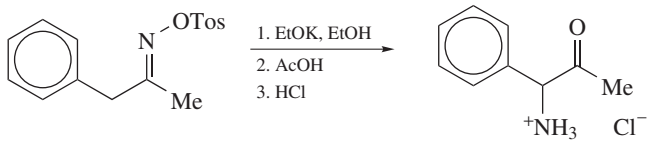

(231)

(**517**) (**518**)

The Neber reaction has found application as an important synthetic tool, particularly in the synthesis of heterocycles.

Although both the Beckmann and Neber reactions can use oxime derivatives as starting materials, *O*-unsubstituted oximes cannot undergo the Neber rearrangement. The latter occurs only in strongly alkaline reaction conditions while the former can also proceed in both acid and basic media. As a consequence, the Neber rearrangement will only be a possible side reaction of base-induced Beckmann rearrangements.

A. Mechanism

The Neber rearrangement is usually performed with ketoxime tosylates but ketone trimethylhydrazonium halides (**519**), *N*,*N*-dichloro-*sec*-alkyl amines (**520**), *N*-chloroimines (**521**) and *N*-chloroimidates (**522**) may also be precursors for the reaction. Only the Neber rearrangement of oxime derivatives will be analysed in this chapter.

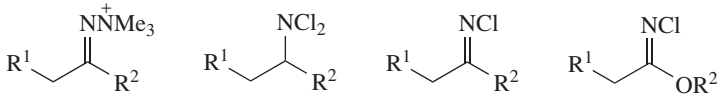

(**519**) (**520**) (**521**) (**522**)

$R^2 \neq H$

Generally, the Neber rearrangement is a base-catalysed conversion of *O*-acylated ketoximes **523** (but not aldoximes) to α-amino ketones **525** via an isolable 2*H*-azirine intermediate **524** (equation 232). The azirine itself may be used as a valuable synthetic tool[384] and the Neber rearrangement is commonly used to produce it.

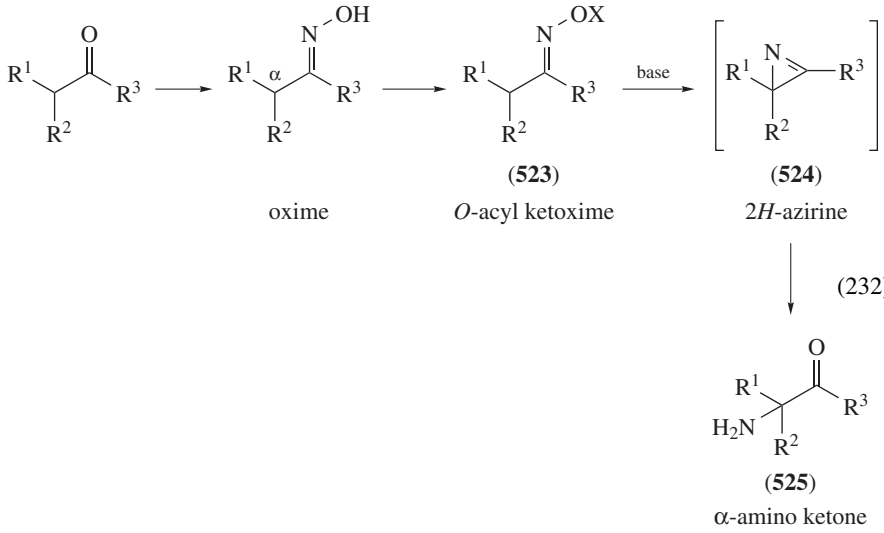

R^1, R^2 = Alk, Ar, H, R^3 = Alk, Ar, *O*-Alk, NH_2, HN-Alk, $R^3 \neq H$, X = Tos, Ms

Apart from the azirine pathway, a vinylnitrene **526** was postulated as a possible intermediate in the reaction (Scheme 14). The nitrene may be formed by a base-promoted elimination of the leaving group on the nitrogen and gives rise to the 2*H*-azirine by electrocyclization (nitrene insertion) and, in view of current data, this pathway cannot be excluded.

Both cyclic and acyclic ketoximes may be used in this transformation and the reaction is usually performed in an alcohol solution containing equimolar quantities of alkoxide. For a successful reaction, the starting material usually contains at least an α-methylene group but the presence of only one α-hydrogen may suffice. When treated with base the *O*-acylated aldoximes do not react via the Neber rearrangement and instead they undergo an E2 elimination to cyanides or isocyanides.

Beckmann rearrangement and fragmentation may be side reactions of the Neber rearrangement. In contrast to the Beckmann rearrangement, the Neber rearrangement is not stereospecific, since the stereochemistry of the starting oxime derivative (*E* or *Z*) does not determine in which α-carbon the amine group will be introduced. When more than one α-methylene group is present, a mixture of products is usually obtained, unless one of the two possible enolates is much more stable. In this case, a Neber reaction will formally result in the substitution of the more acidic hydrogen by an amino group.

As the product amino ketone has a great tendency to dimerize, it is usual to produce the amino ketal from the azirine intermediate by treatment with acidic alcohols.

The Neber rearrangement has been used as a valuable synthetic tool to introduce an α-amino group relative to a ketone and it has been used as a key step in the synthesis of a large array of heterocycles, including imidazoles, oxazoles, isoquinolines and pyrazines and has been reviewed long ago[100, 385].

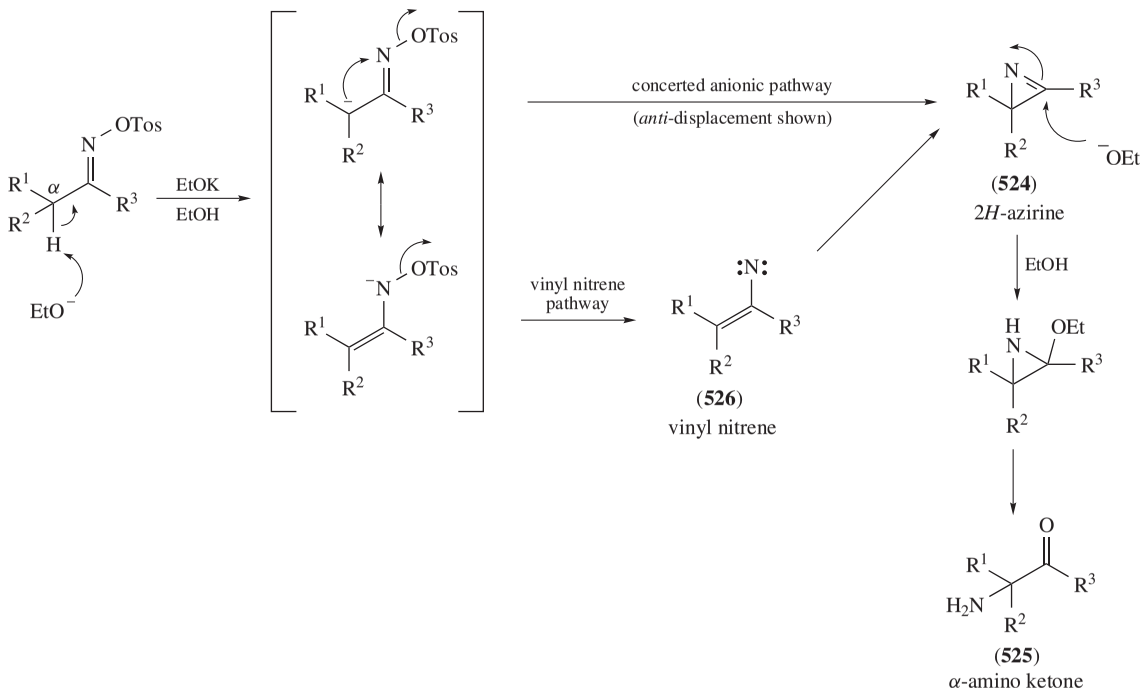
OTos
N
R1
α
R3
R2
H
EtO−
EtOK
EtOH
OTos
N
R1
R3
R2
−N
OTos
R1
R3
R2
concerted anionic pathway
(anti-displacement shown)
vinyl nitrene
pathway
:N:
R1
R3
R2
(526)
vinyl nitrene
N
R1
R3
R2
−OEt
(524)
2H-azirine
EtO
H
OEt
N
R1
R3
R2
O
R1
R3
H2N
R2
(525)
α-amino ketone

SCHEME 14

B. Synthetic Uses

Direct introduction of an amino group at an α-position to the carbonyl carbon atom is of great synthetic value. One example is shown in the synthetic route to a 3-pyridylethanolamino β_3 adrenergic receptor agonist, suitable for large-scale synthesis[386]. The α-amino group was successfully introduced in high yield (82%) providing the projected α-amine ketone subunit (equation 233). As previously noted, it is preferable to obtain an amine ketal **527** as the product of the Neber rearrangement in order to avoid the easy dimerization of the amino ketone. Regeneration of the carbonyl group was performed later in the synthesis.

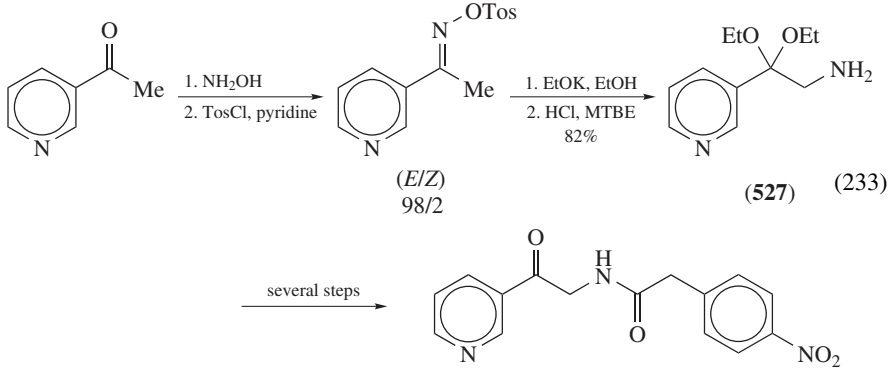

Similar Neber rearrangements were used to produce **528**, an intermediate for an efficient synthesis of 2-imidazol-2-yl acetates **530**[387] (equation 234). Condensation of the α-amino ketals **528** with imidates **529**, followed by cyclization in refluxing acidic dioxane, yielded 2-imidazol-2-yl acetates **530** in a one-pot reaction.

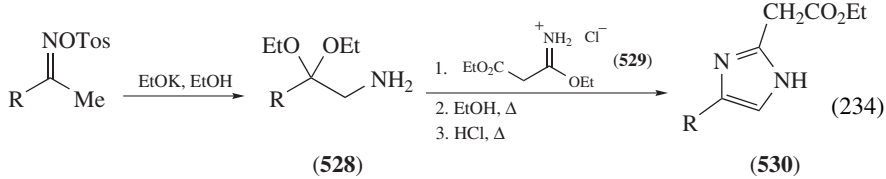

R = Ar, 3- or 4-Pyr

A Neber route to substituted indoles **532**, complementary to the Fischer indole synthesis, was recently developed[388] (equation 235). Formation of azirine **531** from the oxime was smoothly induced, for example using MsCl/DBU or DIAD/Bu_3P or Ph_3P, and the intermediate was isolated. Thermal rearrangement of the azirine (40 to 170 °C, depending on the azirine structure) produced the indoles **532** directly in usually good yields (84–88% from the azirine).

The Neber rearrangement was applied as a key step to produce 3-aminopiperidines **534** and **535**, intermediates for the synthesis of a series of potential Substance P antagonists[389] (equation 236). The 3-aminopiperidines **535** were produced from 4-piperidones **533** based on EtOK treatment of the tosylate of the corresponding oximes. The observed regioselectivity suggests that an *anti* displacement of the tosyl group is preferable (equation 236). Using a chiral *N*-substituted precursor **536** small diatereoselection was observed (equation 237).

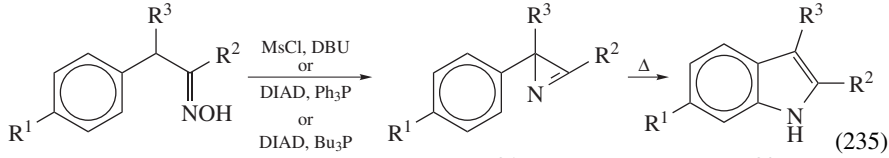

(235)

(**531**) 70–78% (**532**) 84–88%

DIAD = *i*-$PrO_2CN{=}NCO_2Pr$-*i*

R^1 = H, Br, R^2 = CH_3, *n*-C_8H_{17}, R^3 = H, Ph

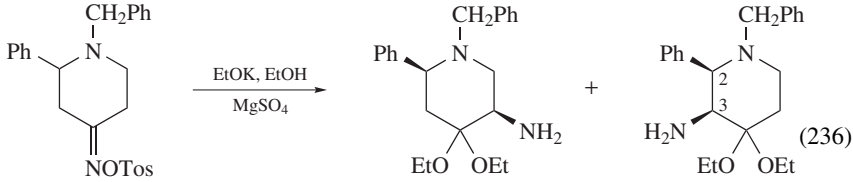

(**533**)

Precursor	(**534**)	(**535**)
(*E*)-**533**	12%	48%
(*Z*)-**533**	43%	9%

(236)

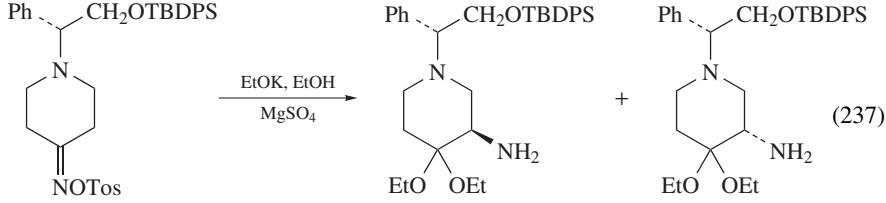

(**536**) 14% 22%

(237)

During the total synthesis of Dragmacidin F (**537**) from quinic acid, Stoltz and colleagues[390, 391] applied a high-yield late-stage Neber rearrangement to introduce in a completely enantioselective manner an amino group into a complex framework (equation 238).

1. The Neber reaction as a 2H-azirine synthetic tool

The 2*H*-azirine intermediate of the Neber rearrangement is a valuable precursor for the preparation of a wide range of polyfunctional acyclic or cyclic compounds. When appropriate reaction conditions are set, the azirine can be isolated during a Neber rearrangement. In fact, the intramolecular displacement on the nitrogen atom is one of the synthetic methods for 2*H*-azirines. The synthetic uses of the 2*H*-azirine are not restricted to the nucleophilic ring opening that occurs in the Neber rearrangement and its synthetic uses have been reviewed recently[384].

The 2*H*-azirine may be optically active and therefore be regarded as a chiral building block for enatioselective synthesis. This opens a wide field of investigation and recently efforts have been made to produce optically pure azirines. Considering the anionic displacement as the main pathway (and not the nitrene pathway), the Neber reaction may be modified to serve as a synthetic tool for the production of optically active 2*H*-azirine intermediates.

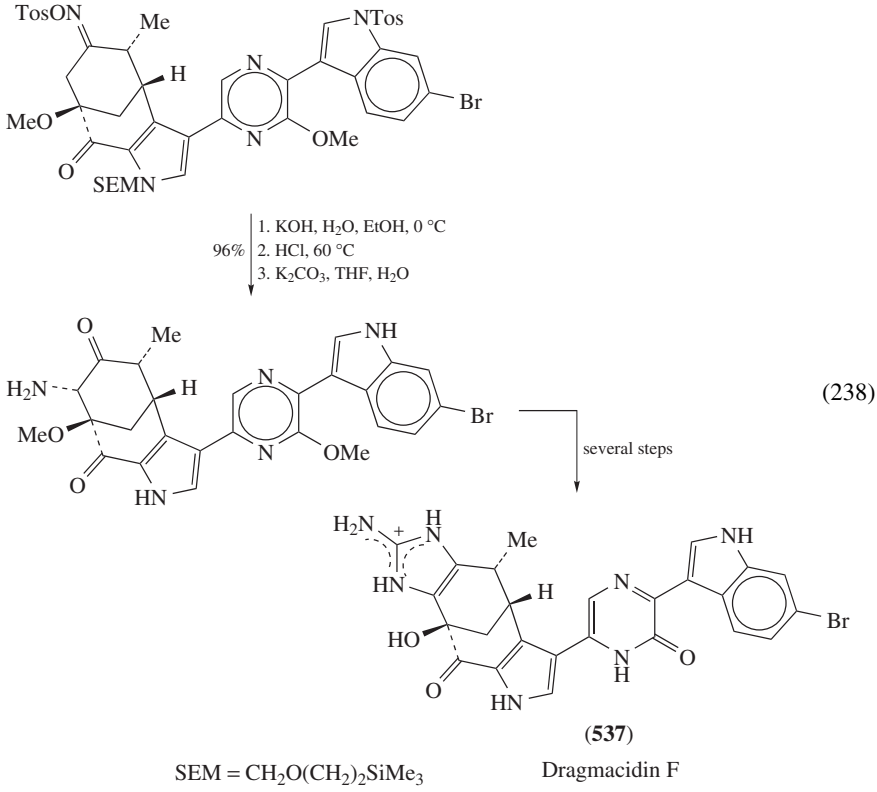

(238)

(**537**)

SEM = $CH_2O(CH_2)_2SiMe_3$ Dragmacidin F

Piskunova and colleagues reported chiral auxiliary mediated asymmetric azirine **538** syntheses in good yields (74–82%) and with a de of 92%[392] (equation 239).

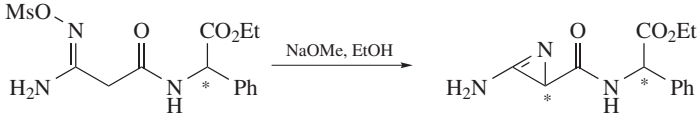

(239)

(*R,R*)-(**538**) 82% (92% de) from (*R*)-precursor

(*S,S*)-(**538**) 74% (93% de) from (*S*)-precursor

The use of compounds with activated methylene protons (doubly activated) enables the use of a mild base during the Neber reaction to 2*H*-azirines. Using ketoxime 4-toluenesulfonates of 3-oxocarboxylic esters **539** as starting materials and a catalytic quantity of chiral tertiary base for the reaction, moderate to high enantioselectivity (44–82% ee) was achieved[393] (equation 240). This asymmetric conversion was observed for the three pairs of Cinchona alkaloids (Cinchonine/Cinchonidine, Quinine/Quinidine and Dihydroquinine/Dihydroquinidine). When the pseudoenantiomers of the alkaloid bases were used, opposite enantioselectivity was observed in the reaction. This fact shows that the absolute configuration of the predominant azirine can be controlled by base selection.

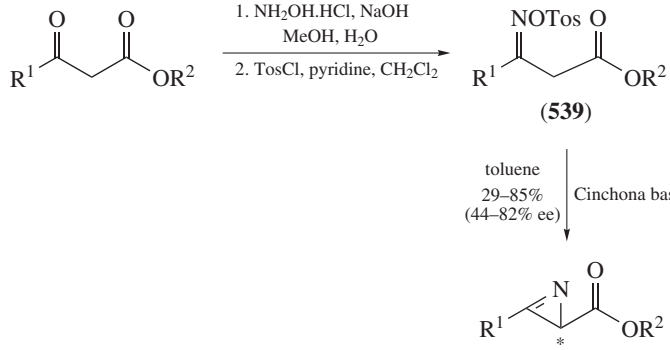

(240)

R^1	R^2	Base	Yield (%)	ee (%)
Me	Et	Quinidine	43	82 (*R*)
Me	Et	Quinine	38	55 (*S*)
Bn	Et	Quinidine	85	80 (*R*)
Br	Et	Quinine	58	57 (*S*)

R^1 = Me, *n*-Pr, Bn, R^2 = Me, Et, *t*-Bu

The previous strategy has been applied to the synthesis of other enantiomerically enriched 2*H*-azirines. Palacios and coworkers[394–396] developed the alkaloid-mediated Neber reaction to produce enantiomerically enriched 2*H*-azirines containing a phosphorus substituent in the C(2) position.

A simple method for asymmetric synthesis of 2*H*-azirine-2-phophonates **540** was described, using various alkaloids as bases[396] (equation 241). Moderate to good asymmetric induction was observed (69–94% yield, 33–72% ee) when quinidine was used as the base (the *S* isomer was obtained). A solid-phase asymmetric synthesis was also performed (**541** and **542** used as bases) and good yields were usually obtained (43–88%) but only low enantioselectivity was achieved (3–11%).

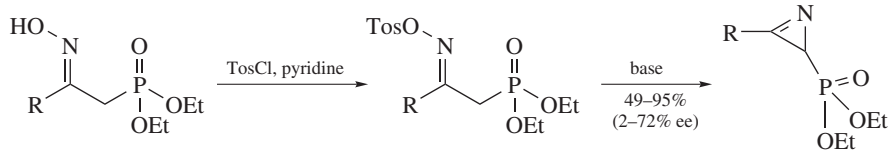

base = Sparteine, Quinidine, Hydroquinidine, Quinine, **541** or **542** (**540**)

R = Me, Et, Ph (241)

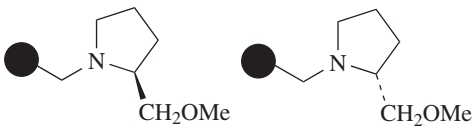

(**541**) (**542**)

R	Base	Yield **540** (%)	ee (%)
Ph	Quinidine	85	65 (*S*)
Ph	Quinine	79	39 (*R*)
Me	Quinidine	72	42 (*S*)
Me	Quinine	93	8 (*R*)

The same research group synthesized also 2*H*-azirine-2-phosphine oxides **543** in a similar manner[395] (equation 242).

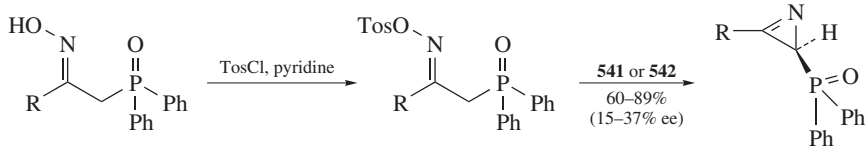

(**543**)

R = Me, Et (242)

Asymmetric induction in the Neber rearrangement was also obtained under phase-transfer conditions with chiral quaternary ammonium bromides **544** as catalysts (equation 243). Moderate enantioselectivities (30–70% ee, 60–95% yield) were observed, but there is still an opportunity for extending the full synthetic utility of this classical rearrangement.

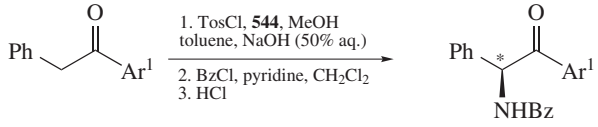

60–95% (30–70% ee)

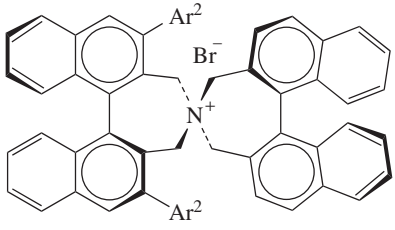

(**544**)

(243)

Ar^1	Ar^2	Yield (%)	ee (%)
Ph	4-$CF_3C_6H_4$	80	51 (*S*)
4-FC_6H_4	4-$CF_3C_6H_4$	81	70 (*S*)

VIII. THE LOSSEN REARRANGEMENT

The Lossen rearrangement, discovered in the 19th century by Lossen[397], provides a practical procedure for replacing the hydroxamic group of a hydroxamic acid (**545**) by an amino group[398,399] (equation 244). Generally, the rearrangement involves nucleophilic migration from a carbon to an electron-deficient nitrogen center. The isocyanate (**546**), the product of hydroxamic acid (**545**) rearrangement, readily reacts with nucleophiles, for example with OH and NH functionalities to give amines (**547**) or ureas (**548**).

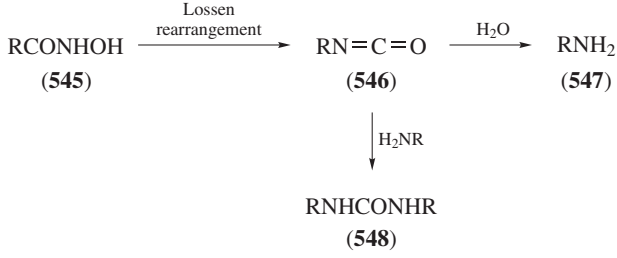

(244)

The Lossen rearrangement has limited synthetic use, since hydroxamic acids are not readily available and there are only few references in the literature concerning this transformation. The reaction is mechanistically similar to the Beckmann rearrangement discussed previously where N−O bond fission with synchronous migration of an alkyl group is involved. Initial attachment of electron-withdrawing groups to the oxygen atom of the hydroxamic acids is essential to conduct the reaction. The rate of the rearrangement is directly proportional to the acidity of these groups, which act as leaving groups[398]. An acyl nitrene species **550** was proposed as an intermediate in Lossen rearrangement of *O*-aroyl hydroxamic acids **549** to explain the mechanism of inactivation of serine proteases by *N*-peptidyl-*O*-aroyl hydroxylamines (equation 245). A nitrene intermediate **552** is also proposed in the Lossen rearrangement in basic medium of the *O*-acyl hydroxylamines **551** to synthesize the spiro-fused (C2)-azirino-(C4)-pyrazolones **553**[400] (equation 246).

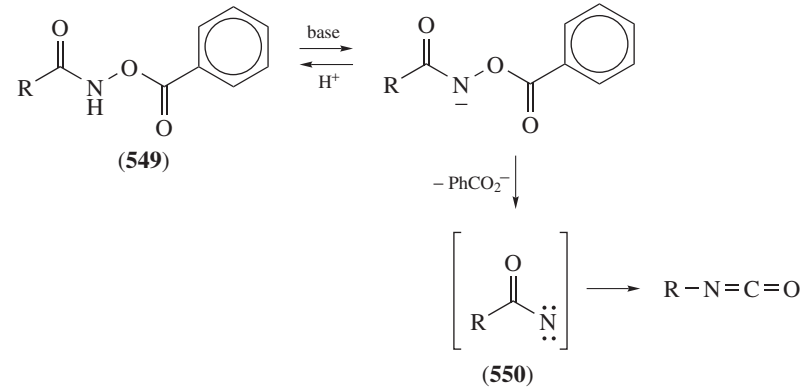

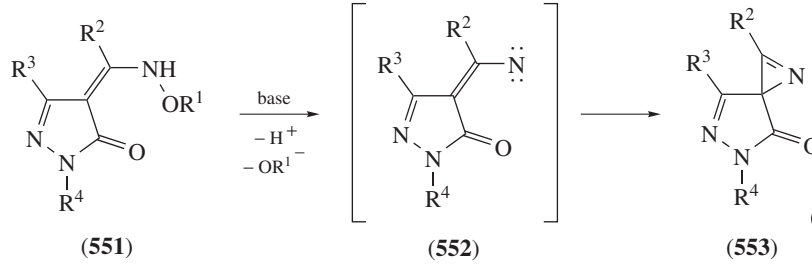

R^1 = CONHCOCCl$_3$, R^2, R^3, R^4 = H, Me, Ph

Rearrangements under basic, neutral and acid conditions have been observed. *O*-Acylhydroxamic acids are most often used though *O*-aryl[401], *O*-alkyl[402], *O*-pyridinium[403], *O*-sulfonyl[403, 404], *O*-phosphoryl and *O*-silyl[405] derivatives may also be employed. As with Beckmann reaction, inorganic acylating agents are extremely effective at inducing N−O bond fission. Adams and colleagues[406] studied the rearrangement process of hydroxamic acid in the gas phase; upon collisional activation the product of Lossen rearrangement was detected, as well as other products resulting from the 1,2-oxygen rearrangement to the carbonyl site.

Lossen rearrangement has been used in the synthesis of compounds with pharmacological interest as an alternative to the explosive Curtius rearrangement as in the synthesis of ONO-6818[407] (**554**) (equation 247).

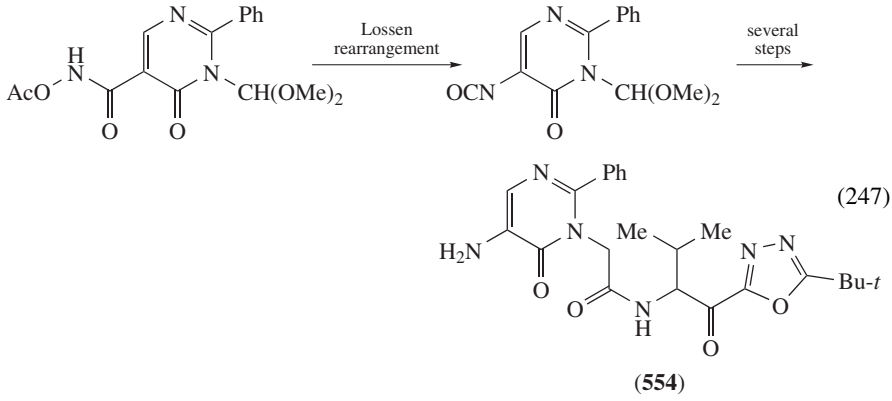

(247)

(**554**)

Determination of pectic structures by specific degradation of pectins, via a carbodiimide **556** mediated Lossen rearrangement on alkaline hydrolysis of galacturonic acid residues **555**, was reported[408] (equation 248).

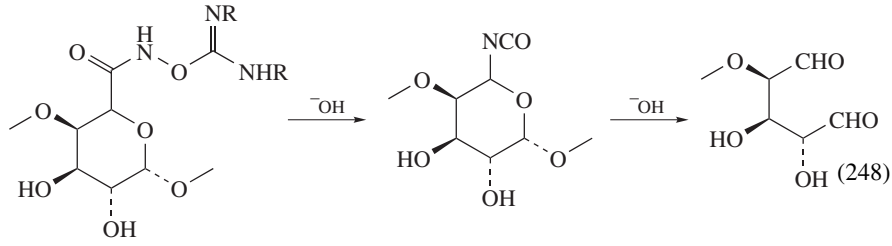

(248)

(**555**) (**556**)

To improve the product yields in Lossen rearrangement, mesyloxycarbamates have been used as alternative reagents[409]. The use of *N*-acyl-*O*-mesylhydroxamic acids (**558**) avoids the competing formation of self-condensation by-products (**560**). These are obtained from the accumulation of isocyanate (**559**) before complete consumption of the hydroxamic acid (**557**) as observed in the classical Lossen rearrangement[403,410] (equation 249).

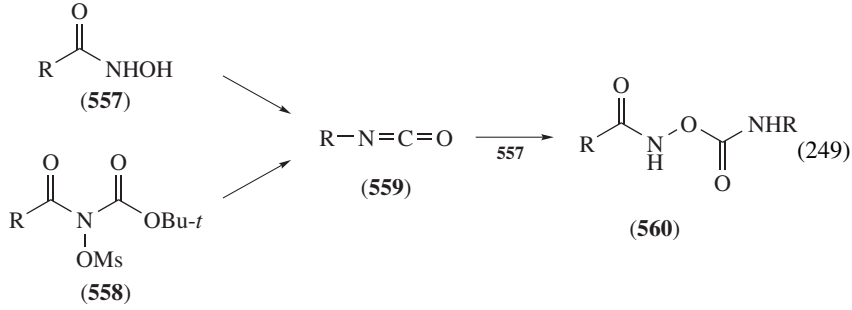

(249)

(**557**) (**558**) (**559**) (**560**)

The migration of the *O*-*t*-butoxy group with concomitant generation of the *O*-*t*-butoxy isocyanate **562** was observed in the Lossen rearrangement of **561** induced by base deprotonation[411] (equation 250).

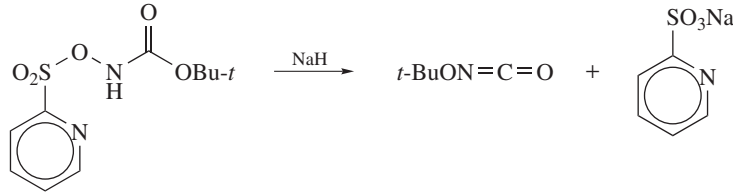

(250)

(**561**) (**562**)

Chandrasekhar and colleagues[412] used *N*-acyl-*N*,*O*-bis(ethoxycarbonyl)hydroxylamines in a similar procedure to prepare amines. Aromatic *N*-hydroxyimide derivatives were used by Marzoni and Varney[413] and Gütschow[414] to synthesize benz[*cd*]indol-2(1*H*)-one and 1-benzoxazin-4-one derivatives, respectively, via Lossen rearrangements. Both *N*-benzyloxy and *N*-mesyloxy derivatives were used.

Lossen rearrangement of alkyl succinimidyl carbonates in basic buffers was reported in protein modification procedures[415]. Recent interest in asymmetric transformations directed the attention to chiral Lossen rearrangement. Chandrasekhar and Sridhar[416] reported a chiral Lossen rearrangement of the activated *O*-(1*S*)-10-camphor sulfonate norbornene-fused *N*-hydroxyimine **563** (equation 251). It has been shown that the rearrangement proceeds with the retention of the configuration of the asymmetric carbon where the migration reaction occurs. The hydroxamic acids formed from amides and hydroxylamines by an Amilase from *Rhodococcus erythropolis* MP50 were subject to Lossen rearrangement to probe the highly enantioselective acyltransferase activity[417]. The synthesis of chiral amines from chiral hydroxamic acids was also reported[418].

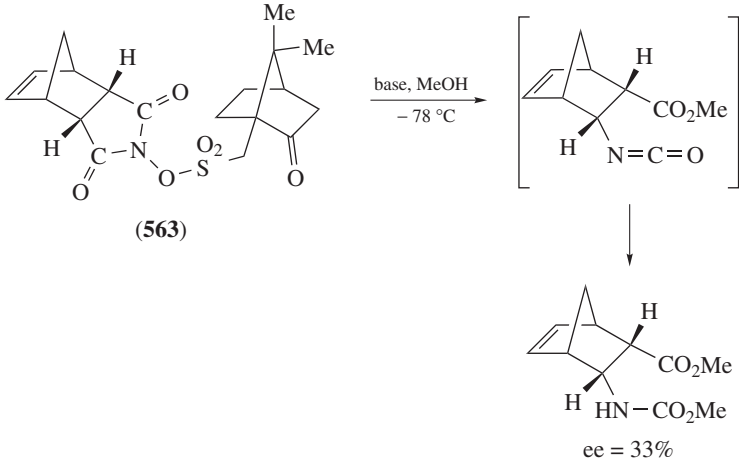

(**563**) (251)

The hydroxamate anion **566** is invoked as intermediate in the formation of urea **568** from the *N*-tosylated *β*-lactam **564** by a Lossen rearrangement in the presence of a secondary amine **565**[404] (equation 252). Apparently, attack of amine in an S_N2 fashion at the C(4) carbon of the *β*-lactam **564** opened the ring to form hydroxamate anion **566**, which then initiated a facile Lossen rearrangement to isocyanate **567** trapped with another molecule of base to give **568**.

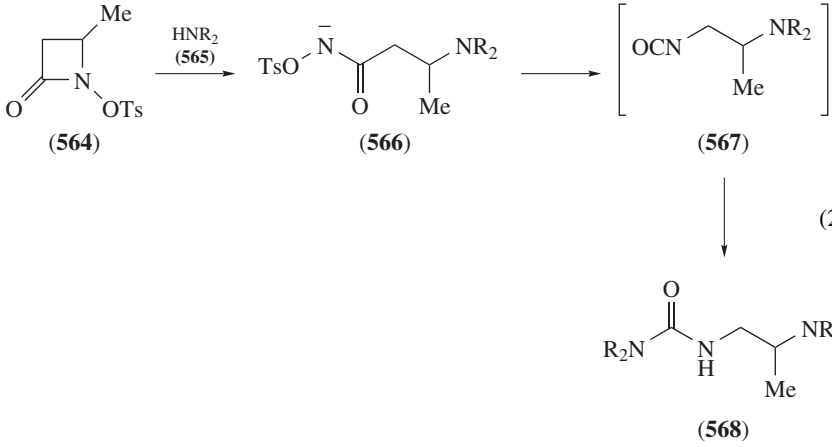

(**564**) (**566**) (**567**) (**568**) (252)

To improve the scope of the Lossen rearrangement, other structural analogous substrates to hydroxamic acids have been tested. *N*-Phosphinoylhydroxylamines are the phosphorus analogues of hydroxamic acids and, when suitably activated, they undergo a Lossen-like rearrangement in the presence of base.

The unusual Lossen rearrangement of free (phosphonoformyl)hydroxamic acid (**569**) providing the dialkoxyphosphinyl isocyanate (**570**) was reported[419] (equation 253). This spontaneous rearrangement is due to the unusually high migratory aptitude of the phosphonyl group with concomitant departure of the OH at room temperature, resembling the Beckmann rearrangement[419]. Alkali metal hydroxamates also rearrange to *N*,*N*′-diarylureas[420].

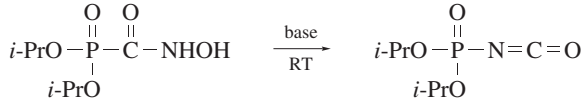

(**569**) (**570**) (253)

Harger[421] has studied the rearrangement of *N*-substituted *N*-phosphinoylhydroxylamines in the presence of base[422–426]. He proposed a concerted mechanism based on the observed retention of the configuration at the phosphorous center during the transposition[427], and on studies with ^{18}O-labelled compounds[428]. Similar cyclic transition states **572** were proposed in the base-induced rearrangement of *N*,*O*-bis(diphenylphosphinoyl)hydroxylamines[429] (**571**) (equation 254). However, in the rearrangement of *O*-benzoyl-*N*-(diphenylphosphinothiol)hydroxylamine where a transposition of O and S atoms occurs, the proposed cyclic transition state has sulfur participation[430].

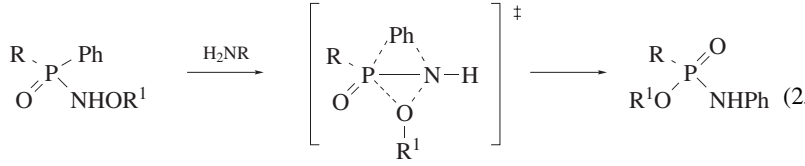

(**571**) (**572**) (254)

IX. OTHER REARRANGEMENTS

The most widely used rearrangement reactions of hydroxylamine, oximes and hydroxamic acids are reported in previous sections of this chapter, but there are other relevant rearrangements which were less exploited.

Thermal rearrangement of *O*-acyl *N*-hydroxycarbamates carrying a cyclopropane substituent was reported[431] (equation 255). When subject to flash vacuum thermolysis at 500 °C the carbamate **573** generates the *N*-acyl imine **574** that rearranges to pyrroline **577** in 21–37% yield. The formation of a biradical intermediate **575** or a polar zwitterionic structure **576** was proposed.

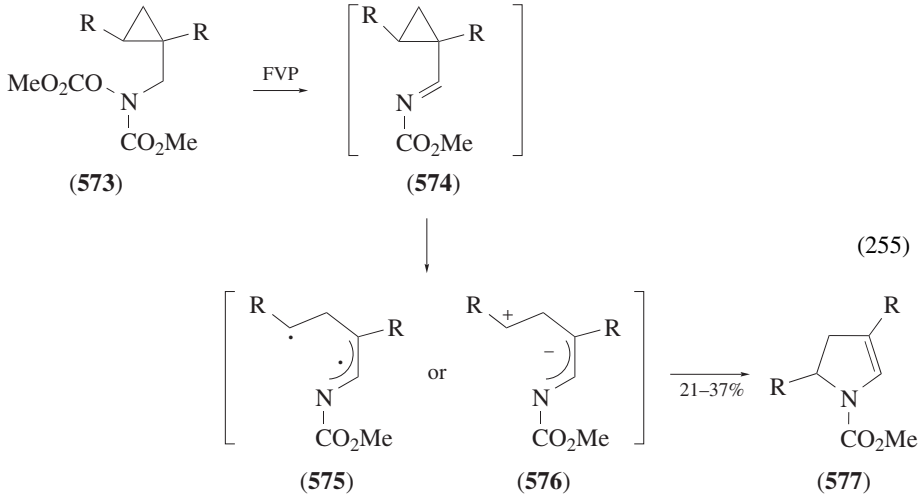

(255)

A new semipinacol rearrangement mediated by Sn(IV) was proposed by Bates and Li[432] to explain the formation of **579** from **578** (equation 256). As stated by the authors, the mechanism of formation of **579** most likely involves an intermediate hydroxylamine **580** (equation 257). Nucleophilic addition of the hydroxylamine to the ketonic carbonyl leads to **581**, which may undergo a tin-mediated pinacol-type rearrangement with preferred migration of the phenyl substituent to produce amide **582**.

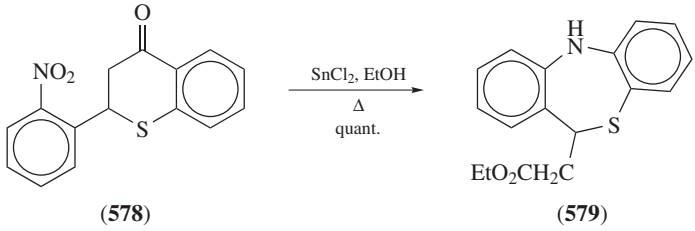

(256)

The unusual rearrangement of *O*-(2-arylphenyl)hydroxylamines **583** to aryldihydroazepinones in moderate yields (43–63%) was reported[433] (equation 258). The rearrangement occurs in the presence of trifluoroacetic acid and an ionic mechanism is proposed. At room temperature the intimate pair **584** gives the stable intermediate **585** that can be trapped with trifluoroacetic anhydride or affords the azepinone **586** by ring enlargement.

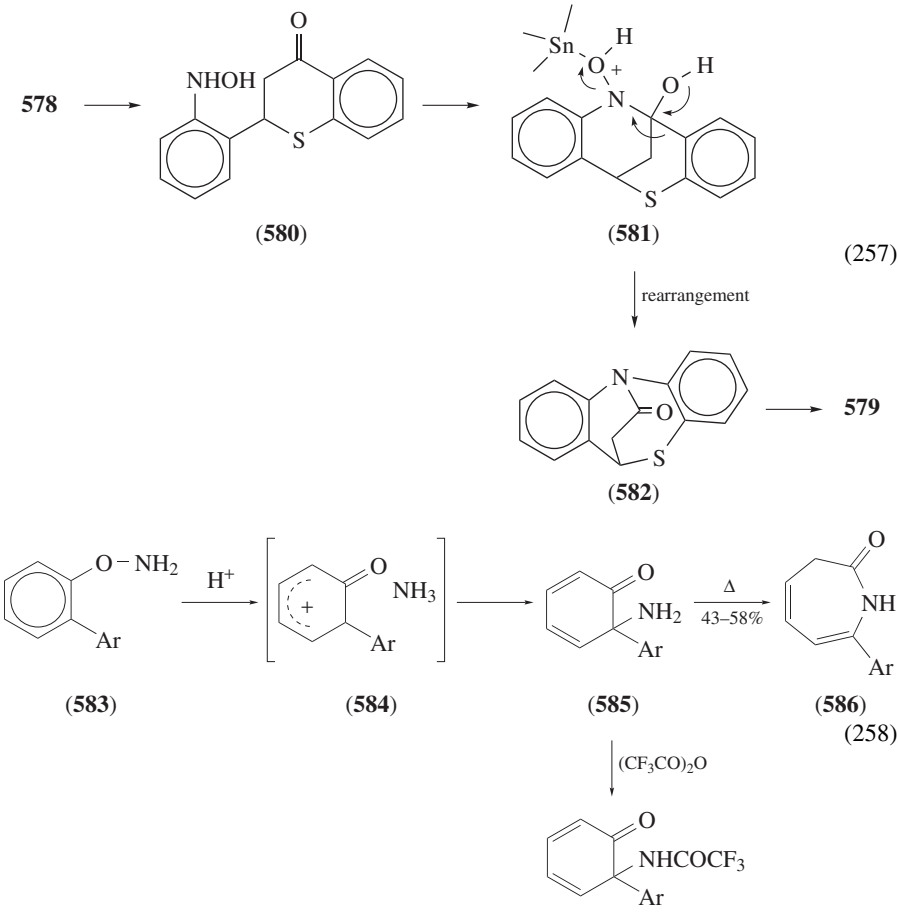

(257)

(258)

Ar = Ph, 4-MeC_6H_4, 4-$NO_2C_6H_4$

As reported by Hoffman and Buntain[434] cyclic *N*-((4-nitrophenyl)sulfonoxy)amines (**587**) rearrange at low temperatures to ring-expanded cyclic imines **588** in fair to good yields (42–82%) (equation 259). A competitive migration of the 1,2 and 2,3 bonds is observed and an ionic pathway is proposed.

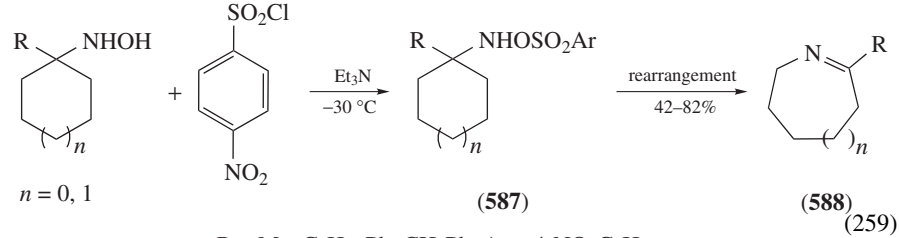

(259)

R = Me, C_4H_9, Ph, CH_2Ph, Ar = 4-$NO_2C_6H_4$

A 2-aminoarylation of heterocyclic rings via a benzidine-like rearrangement of *O*-substituted *N*-arylhydroxamic acid was reported[435] and an ionic pathway was proposed. After heterolysis of the nitrogen–oxygen bond, an aryl oxenium ion and an acyl aniline anion are formed. Charge delocalization in both would involve mainly the *ortho* and *para* positions of the rings. A transition state with two parallel rings favouring the linking between the *para* positions because of special proximity and least hindrance was proposed. The *ortho–ortho* linking occurs if the *para* position is blocked by a substituent.

The conversion of hydroxamic acids **589** to α,β-unsaturated amides **592** reported by Hoffmagn and Madan[436] appears to be a first-order reaction of bis-anion **590** characterized by an intramolecular proton rearrangement to one of the anionic oxygen atoms to give conjugated ion **591** (equation 260).

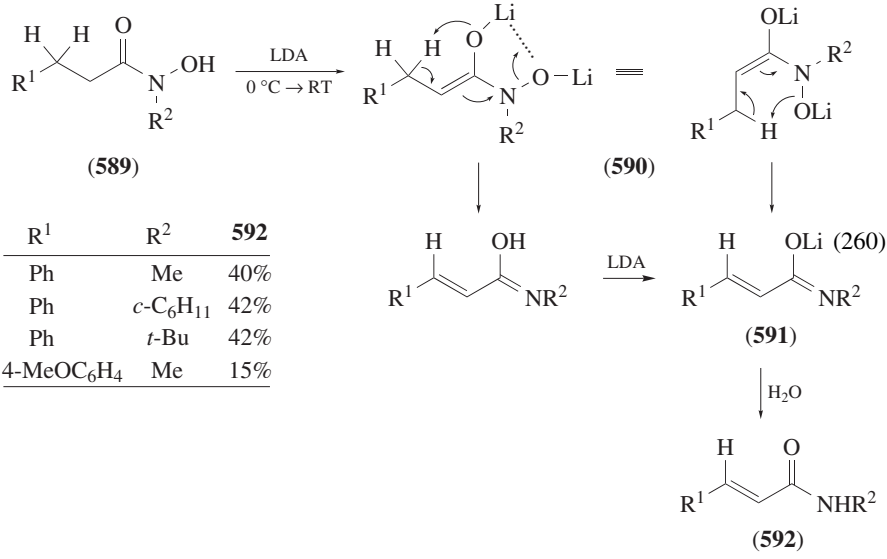

(**589**) (**590**) (**591**) (**592**)

R^1	R^2	**592**
Ph	Me	40%
Ph	*c*-C_6H_{11}	42%
Ph	*t*-Bu	42%
4-$MeOC_6H_4$	Me	15%

A relatively unexplored method to prepare a pyridine ring by thermolysis of *O*-allyl cyclic oximes (**593**) was used in the synthesis of some unsymmetrical bridged terpyridines[437] and in the synthesis of the E-ring in modified steroids[438] (equation 261).

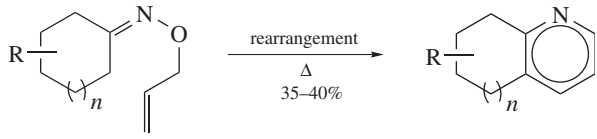

(261)

(**593**)

$n = 0, 1$

X. REFERENCES

1. R. P. Lutz, *Chem. Rev.*, **84**, 205 (1984).
2. S. Blechert, *Synthesis*, 71 (1989).
3. Y. Endo, T. Uchida, S. Hizatate and K. Shudo, *Synthesis*, 1096 (1994).

4. S. Oae and T. Sakurai, *Tetrahedron*, **32**, 2289 (1976).
5. G. R. Cook and J. R. Stille, *Tetrahedron*, **50**, 4105 (1994).
6. J. C. Gilbert and K. R. Cousins, *Tetrahedron*, **50**, 10671 (1994).
7. M. J. S. Gomes, L. Sharma, S. Prabhakar, A. M. Lobo and P. M. C. Glória, *Chem. Commun.*, 746 (2002).
8. T. Sheradsky, E. Nov, S. Segal and A. Frank, *J. Chem. Soc., Perkin Trans. 1*, 1827 (1977).
9. L. V. Reis, A. M. Lobo, S. Prabhakar and M. P. Duarte, *Eur. J. Org. Chem.*, 190 (2003).
10. E. Vedejs, J. D. Little and L. M. Seaney, *J. Org. Chem.*, **69**, 1788 (2004).
11. P. Martin, *Helv. Chim. Acta*, **72**, 1554 (1989).
12. P. Martin, *Helv. Chim. Acta*, **67**, 1647 (1984).
13. P. Martin, *Tetrahedron Lett.*, **28**, 1645 (1987).
14. P. Martin, *Helv. Chim. Acta*, **71**, 344 (1988).
15. S. Blechert, *Helv. Chim. Acta*, **68**, 1835 (1985).
16. F. Saczewski, T. Debowski, M. Gdaniec and Z. Gdaniec, *J. Org. Chem.*, **61**, 5425 (1996).
17. M. M. A. Pereira, S. Prabhakar and A. M. Lobo, *J. Nat. Prod.*, **59**, 744 (1996).
18. J. Hendrick, *Angew. Chem., Int. Ed. Engl.*, **13**, 47 (1974).
19. R. M. Coates and I. M. Said, *J. Am. Chem. Soc.*, **99**, 2355 (1977).
20. K. I. Hirao, K. Mohri, O. Yonemitsu, M. Tabata and J. Sohma, *Tetrahedron Lett.*, **33**, 1459 (1992).
21. Y. Endo and K. Shudo, *Tetrahedron Lett.*, **32**, 4517 (1991).
22. P. S. Almeida, S. Prabhakar, A. M. Lobo and M. J. Marcelocurto, *Tetrahedron Lett.*, **32**, 2671 (1991).
23. Z. Mao and S. W. Baldwin, *Org. Lett.*, **6**, 2425 (2004).
24. J. Wolff and M. Taddei, *Tetrahedron*, **42**, 4267 (1986).
25. P. F. Santos, P. S. Almeida, A. M. Lobo and S. Prabhakar, *Heterocycles*, **55**, 1029 (2001).
26. A. J. Clark, Y. S. S. Al-Faiyz, M. J. Broadhurst, D. Patel and J. L. Peacock, *J. Chem. Soc., Perkin Trans. 1*, 1117 (2000).
27. F. A. Macias, D. Marin, A. Oliveros-Bastidas, D. Chinchilla, A. M. Simonet and J. M. G. Molinillo, *J. Agric. Food Chem.*, **54**, 991 (2006).
28. A. J. Clark, D. Patel and M. J. Broadhurst, *Tetrahedron Lett.*, **44**, 7763 (2003).
29. A. J. Clark, Y. S. S. Al-Faiyz, D. Patel and M. J. Broadhurst, *Tetrahedron Lett.*, **42**, 2007 (2001).
30. A. J. Clark and J. L. Peacock, *Tetrahedron Lett.*, **39**, 1265 (1998).
31. Y. S. S. Al-Faiyz, A. J. Clark, R. P. Filik, J. L. Peacock and G. H. Thomas, *Tetrahedron Lett.*, **39**, 1269 (1998).
32. T. Uchida, Y. Endo, S. Hizatate and K. Shudo, *Chem. Pharm. Bull.*, **42**, 419 (1994).
33. A. V. Varlamov, L. G. Voskresensky, T. N. Borisova, A. I. Chernyshev and A. N. Levov, *Chem. Heterocycl. Compd.*, **35**, 613 (1999).
34. C. A. Marques, M. Selva, P. Tundo and F. Montanari, *J. Org. Chem.*, **58**, 5765 (1993).
35. P. Tundo and M. Selva, *Acc. Chem. Res.*, **35**, 706 (2002).
36. I. Lantos, W. Y. Zhang, X. Q. Shui and D. S. Eggleston, *J. Org. Chem.*, **58**, 7092 (1993).
37. T. Sheradsky, *Tetrahedron Lett.*, 5225 (1966).
38. A. Alemagna, C. Baldoli, P. Delbuttero, E. Licandro and S. Maiorana, *Synthesis*, 192 (1987).
39. P. R. Guzzo, R. N. Buckle, M. Chou, S. R. Dinn, M. E. Flaugh, A. D. Kiefer, K. T. Ryter, A. J. Sampognaro, S. W. Tregay and Y. C. Xu, *J. Org. Chem.*, **68**, 770 (2003).
40. J. Y. Laronze, R. Elboukili, D. Patigny, S. Dridi, D. Cartier and J. Levy, *Tetrahedron*, **47**, 10003 (1991).
41. J. Y. Laronze, R. Elboukili, D. Cartier, J. Laronze and J. Levy, *Tetrahedron Lett.*, **30**, 2229 (1989).
42. Y. Kikugawa, C. Tsuji, E. Miyazawa and T. Sakamoto, *Tetrahedron Lett.*, **42**, 2337 (2001).
43. A. Hall, E. P. Huguet, K. L. Jones, T. C. Jones, N. M. Killeen, S. C. Yau and N. C. O. Tomkinson, *Synlett*, 293 (2007).
44. A. Hall, K. L. Jones, T. C. Jones, N. M. Killeen, R. Porzig, P. H. Taylor, S. C. Yau and N. C. O. Tomkinson, *Synlett*, 3435 (2006).
45. N. Takeda, O. Miyata and T. Naito, *Eur. J. Org. Chem.*, 1491 (2007).
46. O. Miyata, N. Takeda and T. Naito, *Org. Lett.*, **6**, 1761 (2004).
47. E. R. Civitello and H. Rapoport, *J. Org. Chem.*, **59**, 3775 (1994).
48. L. Marx and A. Rassat, *Tetrahedron Lett.*, **43**, 2613 (2002).

49. N. R. Ayyangar, U. R. Kalkote and P. V. Nikrad, *Tetrahedron Lett.*, **23**, 1099 (1982).
50. P. S. Branco, S. Prabhakar, A. M. Lobo and D. J. Williams, *Tetrahedron*, **48**, 6335 (1992).
51. F. Saczewski and T. Debowski, *Phosphorus Sulfur Silicon Relat. Elem.*, **140**, 95 (1998).
52. Y. Endo, K. Shudo and T. Okamoto, *Synthesis*, 471 (1983).
53. T. Yosief, A. Rudi and Y. Kashman, *J. Nat. Prod.*, **63**, 299 (2000).
54. P. S. Almeida, A. M. Lobo and S. Prabhakar, *Heterocycles*, **28**, 653 (1989).
55. F. Saczewski and T. Debowski, *Tetrahedron Lett.*, **34**, 2843 (1993).
56. M. P. Duarte, R. F. Mendonca, S. Prabhakar and A. M. Lobo, *Tetrahedron Lett.*, **47**, 1173 (2006).
57. R. Brückner, in *Comprehensive Organic Synthesis, Selectivity, Strategy and Efficiency in Modern Organic Chemistry*, Vol. 6 (Eds. B. M. Trost and I. Fleming), Chap. 4.6, Pergamon Press, Oxford, 1991, pp. 873–908.
58. R. W. Hoffmann, *Angew. Chem., Int. Ed. Engl.*, **18**, 563 (1979).
59. S. G. Davies, J. F. Fox, S. Jones, A. J. Price, M. A. Sanz, T. G. R. Sellers, A. D. Smith and F. C. Teixeira, *J. Chem. Soc., Perkin Trans. 1*, 1757 (2002).
60. S. G. Davies, S. Jones, M. A. Sanz, F. C. Teixeira and J. F. Fox, *Chem. Commun.*, 2235 (1998).
61. T. Ishikawa, M. Kawakami, M. Fukui, A. Yamashita, J. Urano and S. Saito, *J. Am. Chem. Soc.*, **123**, 7734 (2001).
62. S. D. Bull, S. G. Davies, S. Jones, J. V. A. Ouzman, A. J. Price and D. J. Watkin, *Chem. Commun.*, 2079 (1999).
63. S. D. Bull, S. G. Davies, S. H. Domingez, S. Jones, A. J. Price, T. G. R. Sellers and A. D. Smith, *J. Chem. Soc., Perkin Trans. 1*, 2141 (2002).
64. S. U. Pandya, C. Garcon, P. Y. Chavant, S. Py and Y. Vallee, *Chem. Commun.*, 1806 (2001).
65. M. I. Rodriguez-Franco, I. Dorronsoro and A. Martinez, *Synthesis*, 1711 (2001).
66. L. Pennicott and S. Lindell, *Synlett*, 463 (2006).
67. F. Diedrich, U. Klingebiel and M. Schafer, *J. Organomet. Chem.*, **588**, 242 (1999).
68. S. Schmatz, C. Ebker, T. Labahn, H. Stoll and U. Klingebiel, *Organometallics*, **22**, 490 (2003).
69. R. Wolfgramm, T. Muller and U. Klingebiel, *Organometallics*, **17**, 3222 (1998).
70. N. W. Mitzel, A. J. Blake and D. W. H. Rankin, *J. Am. Chem. Soc.*, **119**, 4143 (1997).
71. F. Duboudin, E. Frainnet, G. Vincon and F. Dabescat, *Acad. Sci., Ser. C, Sci. Chim.*, **276**, 1469 (1973).
72. P. Nowakowski and R. West, *J. Am. Chem. Soc.*, **98**, 5616 (1976).
73. T. Albrecht, G. Elter and A. Meller, *Z. Anorg. Allg. Chem.*, **625**, 1453 (1999).
74. R. Wolfgramm and U. Klingebiel, *Z. Anorg. Allg. Chem.*, **624**, 1031 (1998).
75. R. Wolfgramm and U. Klingebiel, *Z. Anorg. Allg. Chem.*, **624**, 1035 (1998).
76. F. Diedrich, U. Klingebiel, F. Dall'Antonia, C. Lehmann, M. Noltemeyer and T. R. Schneider, *Organometallics*, **19**, 5376 (2000).
77. S. Schmatz, F. Diedrich, C. Ebker and U. Klingebiel, *Eur. J. Inorg. Chem.*, 876 (2002).
78. E. Bamberger, *Chem. Ber.*, **27**, 1347 (1894).
79. T. Sone, Y. Tokuda, T. Sakai, S. Shinkai and O. Manabe, *J. Chem. Soc., Perkin Trans. 2*, 298 (1981).
80. T. Sone, K. Hamamoto, Y. Seiji, S. Shinkai and O. Manabe, *J. Chem. Soc., Perkin Trans. 2*, 1596 (1981).
81. J. S. Roberts, in *Comprehensive Organic Chemistry, The Synthesis and Reactions of Organic Compounds*, Vol. 2 (Eds. D. Barton and W. D. Ollis), Part 6.4, Pergamon Press, Oxford, 1979, pp. 185–218.
82. T. Komatsu and T. Hirose, *Appl. Catal. A*, **276**, 95 (2004).
83. K. P. Naicker, K. Pitchumani and R. S. Varma, *Catal. Lett.*, **54**, 165 (1998).
84. K. P. Naicker, K. Pitchumani and R. S. Varma, *Catal. Lett.*, **58**, 167 (1999).
85. A. Schenzle, H. Lenke, J. C. Spain and H.-J. Knackmuss, *J. Bacteriol.*, **181**, 1444 (1999).
86. S. Q. Huang, P. A. Lindahl, C. Y. Wang, G. N. Bennett, F. B. Rudolph and J. B. Hughes, *Appl. Environ. Microbiol.*, **66**, 1474 (2000).
87. Z. Q. He, L. J. Nadeau and J. C. Spain, *Eur. J. Biochem.*, **267**, 1110 (2000).
88. L. J. Nadeau, Z. Q. He and J. C. Spain, *Appl. Environ. Microbiol.*, **69**, 2786 (2003).
89. J. C. Fishbein and R. A. McClelland, *Can. J. Chem.*, **74**, 1321 (1996).

90. N. Haga, Y. Endo, K. Kataoka, K. Yamaguchi and K. Shudo, *J. Am. Chem. Soc.*, **114**, 9795 (1992).
91. J. C. Fishbein and R. A. McClelland, *J. Chem. Soc., Perkin Trans. 2*, 653 (1995).
92. M. Novak, A. J. VandeWater, A. J. Brown, S. A. Sanzenbacher, L. A. Hunt, B. A. Kolb and M. E. Brooks, *J. Org. Chem.*, **64**, 6023 (1999).
93. L. A. Sternson and R. Chandrasakar, *J. Org. Chem.*, **49**, 4295 (1984).
94. M. Novak, M. J. Kahley, E. Eiger, J. S. Helmick and H. E. Peters, *J. Am. Chem. Soc.*, **115**, 9453 (1993).
95. M. Novak, L. Xu and R. A. Wolf, *J. Am. Chem. Soc.*, **120**, 1643 (1998).
96. M. Novak, M. J. Kahley, J. Lin, S. A. Kennedy and T. G. James, *J. Org. Chem.*, **60**, 8294 (1995).
97. F. P. Guengerich, R. G. Mundkowski, M. Voehler and F. F. Kadlubar, *Chem. Res. Toxicol.*, **12**, 906 (1999).
98. M. Novak, K. Toth, S. Rajagopal, M. Brooks, L. L. Hott and M. Moslener, *J. Am. Chem. Soc.*, **124**, 7972 (2002).
99. E. Beckmann, *Chem. Ber.*, **19**, 988 (1886).
100. C. G. McCarty, in *The Chemistry of Functional Groups. The Chemistry of the Carbon–Nitrogen Double Bond* (Ed. S. Patai), Wiley-Interscience, London, 1970, pp. 409–464.
101. R. E. Gawley, 'The Beckmann reactions: Rearrangements, elimination–additions, fragmentations, and rearrangement–cyclizations', in *Organic Reactions*, Vol. 35 (Ed. A. S. Kende), Wiley-Interscience, London, 1988, pp. 1–415.
102. D. Craig, 'The Beckmann and related reactions', in *Comprehensive Organic Synthesis, Selectivity, Strategy and Efficiency in Modern Organic Chemistry*, Vol. 7 (Eds. B. M. Trost and I. Fleming), Chap. 4.3, Pergamon Press, Oxford, 1991, pp. 689–794.
103. M. Gopalakrishnan, P. Sureshkumar, V. Kanagarajan and J. Thanusu, *Lett. Org. Chem.*, **2**, 444 (2005).
104. N. C. Marziano, L. Ronchin, C. Tortato, O. Tonon and R. Bertani, *Int. J. Chem. Kinet.*, **36**, 417 (2004).
105. M. T. Nguyen, G. Raspoet and L. G. Vanquickenborne, *J. Chem. Soc., Perkin Trans. 2*, 821 (1997).
106. M. T. Nguyen, G. Raspoet and L. G. Vanquickenborne, *J. Am. Chem. Soc.*, **119**, 2552 (1997).
107. S. Yamabe, N. Tsuchida and S. Yamazaki, *J. Org. Chem.*, **70**, 10638 (2005).
108. A. Padwa, *Chem. Rev.*, **77**, 37 (1977).
109. G. Tennant, in *Comprehensive Organic Chemistry, The Synthesis and Reactions of Organic Compounds*, Vol. 2 (Eds. D. Barton and W. D. Ollis), Part 8, Pergamon Press, Oxford, 1979, pp. 383–590.
110. S. Nsikabaka, W. Harb and M. F. Ruiz-Lopez, *J. Mol. Struct. (THEOCHEM)*, **764**, 161 (2006).
111. B. S. Lee, S. Chu, I. Y. Lee, B. S. Lee, C. E. Song and D. Y. Chi, *Bull. Korean Chem. Soc.*, **21**, 860 (2000).
112. M. Kitamura, M. Yoshida, T. Kikuchi and K. Narasaka, *Synthesis*, 2415 (2003).
113. K. Narasaka and M. Kitamura, *Eur. J. Org. Chem.*, 4505 (2005).
114. H. Eshghi and Z. Gordi, *Synth. Commun.*, **33**, 2971 (2003).
115. B. J. Gregory, R. B. Moodie and K. Schofield, *J. Chem. Soc. B*, 338 (1970).
116. K. D. Kopple and J. J. Katz, *J. Org. Chem.*, **24**, 1975 (1959).
117. D. Konwar, M. Boruah, G. K. Sarmah, N. K. Bhattacharyya, N. Borthakur, B. N. Goswami and K. R. Boruah, *J. Chem. Res. (S)*, 490 (2001).
118. M. Ghiaci and G. H. Imanzadeh, *Synth. Commun.*, **28**, 2275 (1998).
119. P. Catsoula, *Chim. Ind. (Milan)*, **5**, 401 (1970).
120. L. W. Castle and T. A. Elmaaty, *J. Heterocycl. Chem.*, **43**, 629 (2006).
121. Y. Izumi, S. Sato and K. Urabe, *Chem. Lett.*, 1649 (1983).
122. S. J. Kim, K. D. Jung, O. S. Joo, E. J. Kim and T. B. Kang, *Appl. Catal. A*, **266**, 173 (2004).
123. Y. H. Ko, M. H. Kim, S. J. Kim, G. Seo, M. Y. Kim and Y. S. Uh, *Chem. Commun.*, 829 (2000).
124. M. K. Dongare, V. V. Bhagwat, C. V. Ramana and M. K. Gurjar, *Tetrahedron Lett.*, **45**, 4759 (2004).
125. D. S. Mao, Q. L. Chen and G. Z. Lu, *Appl. Catal. A*, **244**, 273 (2003).
126. L. X. Dai, R. Hayasaka, Y. Iwaki, K. A. Koyano and T. Tatsumi, *Chem. Commun.*, 1071 (1996).

127. L. X. Dai, K. Koyama, M. Miyamoto and T. Tatsumi, *Appl. Catal. A*, **189**, 237 (1999).
128. R. Maheswari, K. Shanthi, T. Sivakumar and S. Narayanan, *Appl. Catal. A*, **248**, 291 (2003).
129. K. Chaudhari, R. Bal, A. J. Chandwadkar and S. Sivasanker, *J. Mol. Catal. A*, **177**, 247 (2002).
130. G. Dahlhoff, U. Barsnick and W. F. Holderich, *Appl. Catal. A*, **210**, 83 (2001).
131. C. C. Tsai, C. Y. Zhong, I. Wang, S. B. Liu, W. H. Chen and T. C. Tsai, *Appl. Catal. A*, **267**, 87 (2004).
132. P. S. Singh, R. Bandyopadhyay, S. G. Hegde and B. S. Rao, *Appl. Catal. A*, **136**, 249 (1996).
133. R. Raja, G. Sankar and J. M. Thomas, *J. Am. Chem. Soc.*, **123**, 8153 (2001).
134. S. E. Sen, S. M. Smith and K. A. Sullivan, *Tetrahedron*, **55**, 12657 (1999).
135. N. R. Candeias and C. A. M. Afonso, *J. Mol. Catal. A*, **242**, 195 (2005).
136. A. B. Fernández, A. Marinas, T. Blasco, V. Fornes and A. Corma, *J. Catal.*, **243**, 270 (2006).
137. H. Sato, *Catal. Rev., Sci. Eng.*, **39**, 395 (1997).
138. G. Dahlhoff, J. P. M. Niederer and W. F. Hoelderich, *Catal. Rev., Sci. Eng.*, **43**, 381 (2001).
139. A. B. Fernández, M. Boronat, T. Blasco and A. Corma, *Angew. Chem., Int. Ed.*, **44**, 2370 (2005).
140. H. Kath, R. Gläser and J. Weitkamp, *Chem. Eng. Technol.*, **24**, 150 (2001).
141. M. A. Camblor, A. Corma, H. Garcia, V. Semmer-Herledan and S. Valencia, *J. Catal.*, **177**, 267 (1998).
142. H. Ichihashi, M. Ishida, A. Shiga, M. Kitamura, T. Suzuki, K. Suenobu and K. Sugita, *Catal. Surv. Asia*, **7**, 261 (2003).
143. J. Sirijaraensre and J. Limtrakul, *Chem. Phys. Chem.*, **7**, 2424 (2006).
144. A. B. Fernández, M. Boronat, T. Blasco and A. Corma, *Angew. Chem., Int. Ed.*, **44**, 2370 (2005).
145. T. Bucko, J. Hafner and L. Benco, *J. Phys. Chem. A*, **108**, 11388 (2004).
146. J. Sirijaraensre, T. N. Truong and J. Limtrakul, *J. Phys. Chem. B*, **109**, 12099 (2005).
147. B. Thomas and S. Sugunan, *Microporous Mesoporous Mat.*, **96**, 55 (2006).
148. B. Thomas, S. Prathapan and S. Sugunan, *Microporous Mesoporous Mat.*, **84**, 137 (2005).
149. B. Thomas, U. R. Prabhu, S. Prathapan and S. Sugunan, *Microporous Mesoporous Mat.*, **102**, 138 (2007).
150. B. Thomas, S. Prathapan and S. Sugunan, *Microporous Mesoporous Mat.*, **79**, 21 (2005).
151. Y. Tamura, H. Fujiwara, K. Sumoto, M. Ikeda and Y. Kita, *Synthesis*, 215 (1973).
152. B. Wang, Y. L. Gu, C. Luo, T. Yang, L. M. Yang and J. S. Suo, *Tetrahedron Lett.*, **45**, 3369 (2004).
153. S. Chandrasekhar and K. Gopalaiah, *Tetrahedron Lett.*, **44**, 7437 (2003).
154. R. Anilkumar and S. Chandrasekhar, *Tetrahedron Lett.*, **41**, 7235 (2000).
155. L. D. Luca, G. Giacomelli and A. Porcheddu, *J. Org. Chem.*, **67**, 6272 (2002).
156. Y. Furuya, K. Ishihara and H. Yamamoto, *J. Am. Chem. Soc.*, **127**, 11240 (2005).
157. M. Hashimoto, S. Sakaguchi and Y. Ishii, *Chem. Asian J.*, **1**, 712 (2006).
158. M. Z. Zhu, C. T. Cha, W. P. Deng and X. X. Shi, *Tetrahedron Lett.*, **47**, 4861 (2006).
159. N. Iranpoor, H. Firouzabadi and G. Aghapour, *Synth. Commun.*, **32**, 2535 (2002).
160. D. M. Li, F. Shi, S. Guo and Y. Q. Deng, *Tetrahedron Lett.*, **46**, 671 (2005).
161. S. Chandrasekhar and K. Gopalaiah, *Tetrahedron Lett.*, **44**, 755 (2003).
162. T. Mukaiyama and T. Harada, *Chem. Lett.*, 1653 (1991).
163. Y. Izumi, *Chem. Lett.*, 2171 (1990).
164. S. Park, Y. Choi, H. Han, S. H. Yang and S. B. Chang, *Chem. Commun.*, 1936 (2003).
165. N. A. Owston, A. J. Parker and J. M. J. Williams, *Org. Lett.*, **9**, 73 (2007).
166. M. Arisawa and M. Yamaguchi, *Org. Lett.*, **3**, 311 (2001).
167. B. M. Khadilkar and D. J. Upadhyaya, *Synth. Commun.*, **32**, 1867 (2002).
168. P. Yan, P. Batamack, G. K. S. Prakash and G. Olah, *Catal. Lett.*, **103**, 165 (2005).
169. J. S. Yadav, B. V. S. Reddy, A. V. Madhavi and Y. S. S. Ganesh, *J. Chem. Res. (S)*, 236 (2002).
170. M. Boruah and D. Konwar, *J. Org. Chem.*, **67**, 7138 (2002).
171. K. H. Yoo, E. B. Choi, H. K. Lee, G. H. Yeon, H. C. Yang and C. S. Pak, *Synthesis*, 1599 (2006).
172. D. C. Barman, M. Gohain, D. Prajapati and J. S. Sandhu, *Indian J. Chem., Sect. B*, **41**, 154 (2002).
173. R. Anilkumar and S. Chandrasekhar, *Tetrahedron Lett.*, **41**, 5427 (2000).

174. M. Ortiz-Marciales, L. D. Rivera, M. D. Jesus, S. Espinosa, J. A. Benjamin, O. E. Casanova, I. G. Figueroa, S. Rodriguez and W. Correa, *J. Org. Chem.*, **70**, 10132 (2005).
175. V. Simunic-Meznaric, Z. Mihalic and H. Vancik, *J. Chem. Soc., Perkin Trans. 2*, 2154 (2002).
176. O. M. Jürgen, *Angew. Chem., Int. Ed.*, **37**, 2975 (1998).
177. K. Tanaka and F. Toda, *Chem. Rev.*, **100**, 1025 (2000).
178. M. M. Khodaei, F. A. Meybodi, N. Rezai and P. Salehi, *Synth. Commun.*, **31**, 2047 (2001).
179. M. Hosseini-Sarvari and H. Sharghi, *J. Chem. Res. (S)*, 205 (2006).
180. H. Sharghi and M. Hosseini, *Synthesis*, 1057 (2002).
181. S. Chandrasekhar and K. Gopalaiah, *Tetrahedron Lett.*, **43**, 2455 (2002).
182. H. Eshghi and Z. Gordi, *Phosphorus Sulfur Silicon Relat. Elem.*, **180**, 619 (2005).
183. F. M. Moghaddam, A. A. R. Rad and H. Zali-Boinee, *Synth. Commun.*, **34**, 2071 (2004).
184. Z. Li, R. B. Ding, Z. Lu, S. X. Xiao and X. L. Ma, *J. Mol. Catal. A*, **250**, 100 (2006).
185. M. A. Zolfigol and P. Salehi, *J. Mol. Catal. A*, **256**, 346 (2006).
186. M. Gopalakrishnan, P. Sureshkumar, V. Kanagarajan, J. Thanusu and R. Govindaraju, *Arkivoc*, 131 (2006).
187. J. Ranke, S. Stolte, R. Stormann, J. Arning and B. Jastorff, *Chem. Rev.*, **107**, 2183 (2007).
188. N. E. Leadbeater, H. M. Torenius and H. Tye, *Comb. Chem. High Throughput Screen*, **7**, 511 (2004).
189. J. J. Peng and Y. Q. Deng, *Tetrahedron Lett.*, **42**, 403 (2001).
190. S. Guo and Y. Q. Deng, *Catal. Commun.*, **6**, 225 (2005).
191. Z. Li, Z. Lu, R. B. Ding and J. Y. Yang, *J. Chem. Res. (S)*, 668 (2006).
192. R. X. Ren, L. D. Zueva and W. Ou, *Tetrahedron Lett.*, **42**, 8441 (2001).
193. J. K. Lee, D. C. Kim, C. E. Song and S. G. Lee, *Synth. Commun.*, **33**, 2301 (2003).
194. Z. Y. Du, Z. P. Li, Y. L. Gu, J. Zhang and Y. Q. Deng, *J. Mol. Catal. A*, **237**, 80 (2005).
195. H. Z. Gui, Y. Q. Deng, Z. D. Hu and Z. L. Sun, *Tetrahedron Lett.*, **45**, 2681 (2004).
196. Y. Yamaguchi, N. Yasutake and M. Nagaoka, *J. Mol. Struct. (THEOCHEM)*, **639**, 137 (2003).
197. Y. Ikushima, K. Hatakeda, O. Sato, T. Yokoyama and M. Arai, *Angew. Chem., Int. Ed.*, **38**, 2910 (1999).
198. O. Sato, Y. Ikushima and T. Yokoyama, *J. Org. Chem.*, **63**, 9100 (1998).
199. Y. Ikushima, K. Hatakeda, O. Sato, T. Yokoyama and M. Arai, *J. Am. Chem. Soc.*, **122**, 1908 (2000).
200. Y. Ikushima, O. Sato, M. Sato, K. Hatakeda and M. Arai, *Chem. Eng. Sci.*, **58**, 935 (2003).
201. M. Boero, T. Ikeshoji, C. C. Liew, K. Terakura and M. Parrinello, *J. Am. Chem. Soc.*, **126**, 6280 (2004).
202. H. Takahashi, K. Tanabe, M. Aketa, R. Kishi, S. I. Furukawa and M. Nakano, *J. Chem. Phys.*, **126**, 84508 (2007).
203. H. Akimoto, A. Kawai, N. Hashimoto and H. Nomura, *Chem. Pharm. Bull.*, **32**, 2565 (1984).
204. H. Kusama, Y. Yamashita, K. Uchiyama and K. Narasaka, *Bull. Chem. Soc. Jpn.*, **70**, 965 (1997).
205. J. Skarzewski, M. Zielinska-Blajet and I. Turowska-Tyrk, *Tetrahedron: Asymmetry*, **12**, 1923 (2001).
206. G. Loloiu, C. Draghici, T. Loloiu and O. Maior, *Chem. Heterocycl. Compd.*, **34**, 866 (1998).
207. N. Saldabol, V. Slavinskaya, E. Liepinsh, Y. Popelis and I. Mazheika, *Chem. Heterocycl. Compd.*, **35**, 1415 (1999).
208. L. J. Nurkkala, R. O. Steen and S. J. Dunne, *Synthesis*, 1295 (2006).
209. K. Hisaki and M. Munetsugu, EP Patent 1,580,189, 2005.
210. K. Geisler, A. Kunzler, H. Below, E. Bulka, W. D. Pfeiffer and P. Langer, *Synthesis*, 97 (2004).
211. F. M. Avotin'sh, M. V. Petrova, N. N. Tonkikh and A. Strakov, *Chem. Heterocycl. Compd.*, **36**, 1326 (2000).
212. C. Balo, O. Caamano, F. Fernandez and C. Lopez, *Tetrahedron: Asymmetry*, **16**, 2593 (2005).
213. R. P. Frutos and D. M. Spero, *Tetrahedron Lett.*, **39**, 2475 (1998).
214. V. Y. Sosnovskikh, A. Y. Sizov, B. I. Usachev, M. I. Kodess and V. A. Anufriev, *Russ. Chem. Bull., Int. Ed.*, **55**, 535 (2006).
215. V. Y. Sosnovskikh, B. I. Usachev, A. Y. Sizov and M. I. Kodess, *Tetrahedron Lett.*, **45**, 7351 (2004).
216. W. Stadlbauer, W. Fiala, M. Fischer and G. Hojas, *J. Prakt. Chem.*, **342**, 33 (2000).

217. M. Sugimori, A. Ejima, S. Ohsuki, K. Uoto, I. Mitsui, Y. Kawato, Y. Hirota, K. Sato and H. Terasawa, *J. Med. Chem.*, **41**, 2308 (1998).
218. K. Blaszczyk, H. Koenig, K. Mel and Z. Paryzek, *Tetrahedron*, **62**, 1069 (2006).
219. C. Roche, K. Kadlecikova, A. Veyron, P. Delair, C. Philouze, A. E. Greene, D. Flot and M. Burghammer, *J. Org. Chem.*, **70**, 8352 (2005).
220. R. K. Webber, S. Metz, W. M. Moore, J. R. Connor, M. G. Currie, K. F. Fok, T. J. Hagen, D. W. Hansen, G. M. Jerome, P. T. Manning, B. S. Pitzele, M. V. Toth, M. Trivedi, M. E. Zupec and F. S. Tjoeng, *J. Med. Chem.*, **41**, 96 (1998).
221. F. Broeders, J. C. Braekman and D. Daloze, *Bull. Soc. Chim. Belg.*, **106**, 377 (1997).
222. B. Westermann and I. Gedrath, *Synlett*, 665 (1996).
223. N. Diedrichs, R. Krelaus, I. Gedrath and B. Westermann, *Can. J. Chem.*, **80**, 686 (2002).
224. B. Westermann, N. Diedrichs, R. Krelaus, A. Walter and I. Gedrath, *Tetrahedron Lett.*, **45**, 5983 (2004).
225. T. Buttler and I. Fleming, *Chem. Commun.*, 2404 (2004).
226. T. Buttler, I. Fleming, S. Gonsior, B. H. Kim, A. Y. Sung and H. G. Woo, *Org. Biomol. Chem.*, **3**, 1557 (2005).
227. M. Toyota, T. Asoh, M. Matsuura and K. Fukumoto, *J. Org. Chem.*, **61**, 8687 (1996).
228. G. Mehta and M. Praveen, *J. Org. Chem.*, **60**, 279 (1995).
229. S. M. N. Efange, A. B. Khare, R. H. Mach and S. M. Parsons, *J. Med. Chem.*, **42**, 2862 (1999).
230. A. Garcia-Granados, P. E. Lopez, E. Melguizo, J. N. Moliz, A. Parra, Y. Simeo and J. A. Dobado, *J. Org. Chem.*, **68**, 4833 (2003).
231. E. V. Tret'yakova, O. B. Flekhter, F. Z. Galin, I. P. Baikova and G. A. Tolstikov, *Chem. Nat. Compd.*, **39**, 16 (2003).
232. P. Stanetty, M. H. Bahardoust, M. D. Mihovilovic and K. Mereiter, *Monatsh. Chem.*, **130**, 1257 (1999).
233. I. W. Elliott, M. J. Sloan and E. Tate, *Tetrahedron*, **52**, 8063 (1996).
234. C. E. Elliott, D. O. Miller and D. J. Burnell, *J. Chem. Soc., Perkin Trans. 1*, 217 (2002).
235. D. G. Hilmey and L. A. Paquette, *Org. Lett.*, **7**, 2067 (2005).
236. Y. Torisawa, T. Nishi and J. Minamikawa, *Bioorg. Med. Chem. Lett.*, **12**, 387 (2002).
237. L. P. Khanh, P. Dallemagne, A. Alsaidi and S. Rault, *Heterocycles*, **45**, 527 (1997).
238. A. Magyar, B. Schönecker, J. Wolfling, G. Schneider, W. Gunther and H. Gorls, *Tetrahedron: Asymmetry*, **14**, 1925 (2003).
239. W. S. Murphy, B. Sarsam, G. Ferguson and J. E. Gallagher, *J. Chem. Soc., Perkin Trans. 1*, 4121 (1998).
240. K. Bhandari, V. L. Sharma and C. M. Singh, *Indian J. Chem., Sect. B.*, **36**, 352 (1997).
241. X. Jiang, J. Wang, J. X. Hu, Z. M. Ge, Y. F. Hu, H. W. Hu and D. F. Covey, *Steroids*, **66**, 655 (2001).
242. A. Kasal, L. Matyas and M. Budesinsky, *Tetrahedron*, **61**, 2269 (2005).
243. D. W. Hansen, K. B. Peterson, M. Trivedi, S. W. Kramer, R. K. Webber, F. S. Tjoeng, W. M. Moore, G. M. Jerome, C. M. Kornmeier, P. T. Manning, J. R. Connor, T. P. Misko, M. G. Currie and B. S. Pitzele, *J. Med. Chem.*, **41**, 1361 (1998).
244. C. M. Sun, *Lett. Drug Des. Discov.*, **2**, 48 (2005).
245. P. Nesvadba, L. Bugnon and R. Sift, *J. Polym. Sci., Polym. Chem. Ed.*, **42**, 3332 (2004).
246. C.-C. Chang, K. O. Siegenthaler and A. Studer, *Helv. Chim. Acta*, **89**, 2200 (2006).
247. H. Hu, G. E. Jagdmann, P. F. Hughes and J. B. Nichols, *Tetrahedron Lett.*, **36**, 3659 (1995).
248. E. Albertini, A. Barco, S. Benetti, C. DeRisi, G. P. Pollini and V. Zanirato, *Tetrahedron*, **53**, 17177 (1997).
249. E. Albertini, A. Barco, S. Benetti, C. DeRisi, G. P. Pollini and V. Zanirato, *Synlett*, 29 (1996).
250. M. H. Wu and E. N. Jacobsen, *Tetrahedron Lett.*, **38**, 1693 (1997).
251. J. W. Lyga, *J. Heterocycl. Chem.*, **33**, 1631 (1996).
252. M. J. Mphahlele and T. A. Modro, *J. Chem. Res. (S)*, 198 (1998).
253. D. E. Stepanov and E. I. Ivanov, *Russ. J. Gen. Chem.*, **72**, 1829 (2002).
254. A. Cordero-Vargas, B. Quiclet-Sire and S. Z. Zard, *Bioorg. Med. Chem.*, **14**, 6165 (2006).
255. S. V. Tolkunov, A. I. Khyzhan and V. I. Dulenko, *Chem. Heterocycl. Compd.*, **39**, 1627 (2003).
256. S. H. Jung, J. E. Lee, H. J. Joo, S. H. Kim and H. Y. Koh, *Bull. Korean Chem. Soc.*, **21**, 159 (2000).

257. P. A. Grieco and Y. Dai, *J. Am. Chem. Soc.*, **120**, 5128 (1998).
258. U. Berg, H. Bladh, C. Svensson and M. Wallin, *Bioorg. Med. Chem. Lett.*, **7**, 2771 (1997).
259. R. Brecht, G. Seitz, D. Guenard and S. Thoret, *Bioorg. Med. Chem.*, **8**, 557 (2000).
260. S. Bergemann, R. Brecht, F. Buttner, D. Guenard, R. Gust, G. Seitz, M. T. Stubbs and S. Thoret, *Bioorg. Med. Chem.*, **11**, 1269 (2003).
261. V. G. Pawar, S. R. Bhusare, R. P. Pawar and B. M. Bhawal, *Synth. Commun.*, **32**, 1929 (2002).
262. P. Pigeon and B. Decroix, *J. Heterocycl. Chem.*, **34**, 375 (1997).
263. M. G. Constantino, K. T. Oliveira, A. Beatriz and G. V. J. Silva, *Tetrahedron Lett.*, **44**, 2641 (2003).
264. Y. J. Wu, *Curr. Pharm. Design*, **6**, 181 (2000).
265. A. Denis and C. Agouridas, *Bioorg. Med. Chem. Lett.*, **8**, 2427 (1998).
266. G. R. Krow, O. H. Cheung, Z. Hu and Y. B. Lee, *J. Org. Chem.*, **61**, 5574 (1996).
267. G. R. Krow, S. W. Szczepanski, J. Y. Kim, N. Liu, A. Sheikh, Y. S. Xiao and J. Yuan, *J. Org. Chem.*, **64**, 1254 (1999).
268. W. Seebacher, R. Weis, M. Kaiser, R. Brun and R. Saf, *J. Pharm. Pharmaceut. Sci.*, **8**, 578 (2005).
269. P. Herold, J. W. Herzig, P. Wenk, T. Leutert, P. Zbinden, W. Fuhrer, S. Stutz, K. Schenker, M. Meier and G. Rihs, *J. Med. Chem.*, **38**, 2946 (1995).
270. J. D. White, P. Hrnciar and F. Stappenbeck, *J. Org. Chem.*, **64**, 7871 (1999).
271. J. M. Blanco, O. Caamano, F. Fernandez, G. Gomez and I. Nieto, *Synthesis*, 281 (1996).
272. O. Muraoka, B. Z. Zheng, K. Okumura, G. Tanabe, T. Momose and C. H. Eugster, *J. Chem. Soc., Perkin Trans. 1*, 1567 (1996).
273. O. Muraoka, B. Z. Zheng, K. Okumura, E. Tabata, G. Tanabe and M. Kubo, *J. Chem. Soc., Perkin Trans. 1*, 113 (1997).
274. S. Buser and A. Vasella, *Helv. Chim. Acta*, **89**, 416 (2006).
275. Z. B. Ma, S. J. Dai and D. Q. Yu, *Tetrahedron Lett.*, **47**, 4721 (2006).
276. A. Brunschweiger and D. Heber, *Tetrahedron Lett.*, **42**, 2653 (2001).
277. M. Mazik and W. Zielinski, *Monatsh. Chem.*, **127**, 1161 (1996).
278. A. R. Katritzky, D. A. Monteux and D. O. Tymoshenko, *Org. Lett.*, **1**, 577 (1999).
279. S. Thiebaut, C. Gerardin-Charbonnier and C. Selve, *Tetrahedron*, **55**, 1329 (1999).
280. M. S. Wu, R. Y. Chen and Y. Huang, *Synthesis*, 2441 (2004).
281. T. Yokomatsu, T. Minowa, Y. Yoshida and S. Shibuya, *Heterocycles*, **44**, 111 (1997).
282. W. Abramski, K. Urbanczy, Z. Lipkowska and M. Chmielewski, *J. Carbohydr. Chem.*, **16**, 63 (1997).
283. R. Y. Kharisov, E. R. Latypova, R. F. Talipov, R. R. Muslukhov, G. Y. Ishmuratov and G. A. Tolstikov, *Chem. Nat. Compd.*, **39**, 569 (2003).
284. C. Uncuta, A. Tudose, M. T. Caproiu, M. Plaveti and R. Kakou-Yao, *Tetrahedron*, **55**, 15011 (1999).
285. M. Bright, EP Patent 101,186, 1984.
286. R. R. Wilkening, R. W. Ratcliffe, G. A. Doss, K. F. Bartizal, A. C. Graham and C. M. Herbert, *Bioorg. Med. Chem. Lett.*, **3**, 1287 (1993).
287. S. T. Waddell, G. M. Santorelli, T. A. Blizzard, A. Graham and J. Occi, *Bioorg. Med. Chem. Lett.*, **8**, 1321 (1998).
288. N. S. Mani and M. Wu, *Tetrahedron: Asymmetry*, **11**, 4687 (2000).
289. H. Cho, K. Murakami, H. Nakanishi, H. Isoshima, K. Hayakawa and I. Uchida, *Heterocycles*, **48**, 919 (1998).
290. K. Uchiyama, A. Ono, Y. Hayashi and K. Narasaka, *Bull. Chem. Soc. Jpn.*, **71**, 2945 (1998).
291. D. Schinzer and Y. X. Bo, *Angew. Chem., Int. Ed. Engl.*, **30**, 687 (1991).
292. D. Schinzer, U. Abel and P. G. Jones, *Synlett*, 632 (1997).
293. C. A. Grob, *Angew. Chem., Int. Ed. Engl.*, **8**, 535 (1969).
294. P. Passacantilli, C. Centore, E. Ciliberti, G. Piancatelli and F. Leonelli, *Eur. J. Org. Chem.*, 5083 (2004).
295. C. Wang, N. P. Rath and D. F. Covey, *Tetrahedron Lett.*, **47**, 7837 (2006).
296. C. D. Wang, X. Jiang, H. J. Shi, J. Lu, Y. F. Hu and H. W. Hu, *J. Org. Chem.*, **68**, 4579 (2003).
297. L. A. Paquette, S. Brand and C. Behrens, *J. Org. Chem.*, **64**, 2010 (1999).

298. I. Y. Bagryanskaya, Y. V. Gatilov, S. A. Osadchii, A. A. Martynov, M. M. Shakirov, E. E. Shul'ts and G. A. Tolstilkov, *Chem. Nat. Compd.*, **41**, 657 (2005).
299. A. Magyar, B. Schönecker, J. Wolfling, G. Schneider, W. Gunther and H. Gorls, *Tetrahedron: Asymmetry*, **14**, 2705 (2003).
300. K. M. P. Gasi, S. M. Stankovic, J. J. Csanadi, E. A. Djurendic, M. N. Sakac, L. M. Mijacevic, O. N. Arcson, S. Z. Stojanovic, S. Andric, D. M. Gabor and R. Kovacevic, *Steroids*, **66**, 645 (2001).
301. S. Stojanovic, D. M. Gabor, L. Medic-Mijacevic, M. Sakac and K. P. Gasi, *J. Serb. Chem. Soc.*, **66**, 23 (2001).
302. V. M. Pejanovic, J. A. Petrovic, J. J. Csanadi, S. M. Stankovic and D. A. Miljkovic, *Tetrahedron*, **51**, 13379 (1995).
303. M. A. Iglesias-Arteaga and A. A. Alvarado-Nuno, *Tetrahedron Lett.*, **47**, 5351 (2006).
304. M. Flores-Alamo, J. A. Rosiles-Exkiws and M. A. Iglesias-Arteaga, *Acta Crystallogr., Sect. E., Struct. Rep. Online*, **62**, O3774–(2006).
305. M. A. Iglesias-Arteaga, J. Sandoval-Ramirez, M. Y. Mata-Esma, O. Vinas-Bravo and S. Bernes, *Tetrahedron Lett.*, **45**, 4921 (2004).
306. I. P. Andrews, R. J. J. Dorgan, T. Harvey, J. F. Hudner, N. Hussain, D. C. Lathbury, N. J. Lewis, G. S. Macaulay, D. O. Morgan, R. Stockman and C. R. White, *Tetrahedron Lett.*, **37**, 4811 (1996).
307. M. J. Figueira, J. M. Blanco, O. Caamano, F. Fernandez, X. Garcia-Mera and C. Lopez, *Synthesis*, 1459 (2000).
308. P. Weyerstahl and H. Marschall, in *Comprehensive Organic Synthesis, Selectivity, Strategy and Efficiency in Modern Organic Chemistry*, Vol. 6 (Eds. B. M. Trost and I. Fleming), Pergamon Press, Oxford, 1991, pp. 1041–1070.
309. A. G. Martinez, E. T. Vilar, A. G. Fraile, S. D. M. Cerero, P. M. Ruiz and L. R. Subramanian, *Tetrahedron: Asymmetry*, **7**, 2177 (1996).
310. A. G. Martinez, E. T. Vilar, A. G. Fraile, S. D. M. Cerero and B. L. Maroto, *Eur. J. Org. Chem.*, 781 (2002).
311. A. G. Martinez, E. T. Vilar, A. G. Fraile, S. D. M. Cerero and B. L. Maroto, *Tetrahedron*, **60**, 9447 (2004).
312. P. J. Biju, M. S. Laxmisha and G. Rao, *J. Chem. Soc., Perkin Trans. 1*, 4512 (2000).
313. M. S. Laxmisha and G. Rao, *Tetrahedron Lett.*, **41**, 3759 (2000).
314. P. A. Petukhov and A. V. Tkachev, *Tetrahedron*, **53**, 2535 (1997).
315. M. Kirihara, K. Niimi, M. Okumura and T. Momose, *Chem. Pharm. Bull.*, **48**, 220 (2000).
316. V. D. Luedeke, 'Caprolactam', in *Encyclopedia of Chemical Processing and Design*, Vol. 6 (Ed. J. J. McKetta), Marcel Dekker, New York, 1978, pp. 72–95.
317. J. Ritz, H. Fuchs, H. Kieczka and W. C. Moran, 'Caprolactam', in *Ullmann's Encyclopedia of Industrial Chemistry*, Vol. A 5 (Ed. W. Gerhartz), VCH, Weinheim, 1986, pp. 31–50.
318. T. Ushikubo, *Catal. Today*, **57**, 331 (2000).
319. A. Costa, P. M. Deya, J. V. Sinisterra and J. M. Marinas, *Can. J. Chem.*, **58**, 1266 (1980).
320. S. Sato, H. Sakurai, K. Urabe and Y. Izumi, *Chem. Lett.*, 277 (1985).
321. S. Sato, K. Urabe and Y. Izumi, *J. Catal.*, **102**, 99 (1986).
322. T. Curtin, J. B. McMonagle and B. K. Hodnett, *Appl. Catal. A*, **93**, 91 (1992).
323. T. Curtin, J. B. McMonagle and B. K. Hodnett, *Appl. Catal. A*, **93**, 75 (1992).
324. T. Ushikubo and K. Wada, *J. Catal.*, **148**, 138 (1994).
325. N. Katada, T. Tsubouchi, M. Niwa and Y. Murakami, *Appl. Catal. A*, **124**, 1 (1995).
326. D. S. Mao, G. Z. Lu, Q. L. Chen, Z. K. Xie and Y. X. Zhang, *Acta Chim. Sin.*, **59**, 1139 (2001).
327. D. S. Mao, G. Z. Lu, Q. L. Chen, Z. K. Xie and Y. X. Zhang, *Catal. Lett.*, **77**, 119 (2001).
328. R. Bechara, A. D'Huysser, M. Fournier, L. Forni, G. Fornasari, F. Trifiro and A. Vaccari, *Catal. Lett.*, **82**, 59 (2002).
329. D. S. Mao, G. H. Lu and Q. L. Chen, *Appl. Catal. A*, **263**, 83 (2004).
330. D. S. Mao, G. Z. Lu and Q. L. Chen, *Appl. Catal. A*, **279**, 145 (2005).
331. T. D. Conesa, J. M. Hidalgo, R. Luque, J. M. Campelo and A. A. Romero, *Appl. Catal. A*, **299**, 224 (2006).
332. R. Palkovits, C. M. Yang, S. Olejnik and F. Schuth, *J. Catal.*, **243**, 93 (2006).
333. T. D. Conesa, J. M. Campelo, D. Luna, J. M. Marinas and A. A. Romero, *Appl. Catal. B*, **70**, 567 (2007).

334. D. S. Mao and G. Z. Lu, *J. Solid State Chem.*, **180**, 484 (2007).
335. H. Sato and K. Hirose, *Chem. Lett.*, 1765 (1993).
336. T. Yashima, N. Oka and T. Komatsu, *Catal. Today*, **38**, 249 (1997).
337. G. P. Heitmann, G. Dahlhoff, J. P. M. Niederer and W. F. Holderich, *J. Catal.*, **194**, 122 (2000).
338. T. Takahashi, M. N. A. Nasution and T. Kai, *Appl. Catal. A*, **210**, 339 (2001).
339. P. O'Sullivan, L. Forni and B. K. Hodnett, *Ind. Eng. Chem. Res.*, **40**, 1471 (2001).
340. H. Ichihashi and H. Sato, *Appl. Catal. A*, **221**, 359 (2001).
341. R. Anand, R. B. Khomane, B. S. Rao and B. D. Kulkarni, *Catal. Lett.*, **78**, 189 (2002).
342. M. Ishida, T. Suzuki, H. Ichihashi and A. Shiga, *Catal. Today*, **87**, 187 (2003).
343. L. Forni, G. Fornasari, G. Giordano, C. Lucarelli, A. Katovic, E. Trifiro, C. Perri and J. B. Nagy, *Phys. Chem. Chem. Phys.*, **6**, 1842 (2004).
344. C. Ngamcharussrivichai, P. Wu and T. Tatsumi, *J. Catal.*, **227**, 448 (2004).
345. J. C. Chang and A. N. Ko, *React. Kinet. Catal. Lett.*, **83**, 283 (2004).
346. Y. J. Zhang, Y. Q. Wang, Y. F. Bu, Z. T. Mi, W. Wu, E. Min, S. Han and S. B. Fu, *Catal. Commun.*, **6**, 53 (2005).
347. X. G. Wang, C. C. Chen, S. Y. Chen, Y. Mou and S. F. Cheng, *Appl. Catal. A*, **281**, 47 (2005).
348. V. R. R. Marthala, Y. J. Jiang, J. Huang, W. Wang, R. Glaser and M. Hunger, *J. Am. Chem. Soc.*, **128**, 14812 (2006).
349. P. Albers, K. Seibold, T. Haas, G. Prescher and W. F. Holderich, *J. Catal.*, **176**, 561 (1998).
350. D. Shouro, Y. Ohya, S. Mishima and T. Nakajima, *Appl. Catal. A*, **214**, 59 (2001).
351. G. S. Lee, Y. Nakagawa, S. J. Hwang, M. E. Davis, P. Wagner, L. Beck and S. I. Zones, *J. Am. Chem. Soc.*, **124**, 7024 (2002).
352. C. Flego and L. Dalloro, *Microporous Mesoporous Mat.*, **60**, 263 (2003).
353. L. Forni, G. Fornasari, G. Giordano, C. Lucarelli, A. Katovic, F. Trifiro, C. Perri and J. B. Nagy, in *Recent Advances in the Science and Technology of Zeolites and Related Materials, Pts. A–C*, (Eds. E. Steen, L. H. Callanan and M. Claeys), Vol. 154, Elsevier Science Bv, Amsterdam, 2004, pp. 2823–2830.
354. M. H. Kim, Y. Ko, S. J. Kim and Y. S. Uh, *Appl. Catal. A*, **210**, 345 (2001).
355. A. N. Ko, C. C. Hung, C. W. Chen and K. H. Ouyang, *Catal. Lett.*, **71**, 219 (2001).
356. L. Forni, C. Tosi, G. Fornasari, F. Trifiro, A. Vaccari and J. B. Nagy, *J. Mol. Catal. A*, **221**, 97 (2004).
357. W. C. Li, A. H. Lu, R. Palkovits, W. Schmidt, B. Spliethoff and F. Schuth, *J. Am. Chem. Soc.*, **127**, 12595 (2005).
358. X. J. Guo, W. H. Hou, W. P. Ding, Y. N. Fan, Q. J. Yan and Y. Chen, *Microporous Mesoporous Mat.*, **80**, 269 (2005).
359. B. M. Reddy and A. Khan, *Catal. Rev., Sci. Eng.*, **47**, 257 (2005).
360. M. Ghiaci, A. Abbaspur and R. J. Kalbasi, *Appl. Catal. A*, **287**, 83 (2005).
361. J. Hafner, L. Benco and T. Bucko, *Top. Catal.*, **37**, 41 (2006).
362. T. Curtin, J. B. McMonagle, M. Ruwet and B. K. Hodnett, *J. Catal.*, **142**, 172 (1993).
363. D. Shouro, Y. Moriya, T. Nakajima and S. Mishima, *Appl. Catal. A*, **198**, 275 (2000).
364. B. Q. Xu, S. B. Cheng, X. Zhang, S. F. Ying and Q. M. Zhu, *Chem. Commun.*, 1121 (2000).
365. L. Forni, G. Fornasari, C. Tosi, F. Trifiro, A. Vaccari, F. Dumeignil and J. Grimblot, *Appl. Catal. A*, **248**, 47 (2003).
366. T. Takahashi, M. Nakanishi and T. Kai, *J. Jpn. Pet. Inst*, **49**, 301 (2006).
367. A. Romero, P. Yustos and A. Santos, *Ind. Eng. Chem. Res.*, **42**, 3654 (2003).
368. A. Romero, A. Santos and P. Yustos, *Ind. Eng. Chem. Res.*, **43**, 1557 (2004).
369. J. C. Chang and A. N. Ko, *Catal. Today*, **97**, 241 (2004).
370. W. F. Holderich, J. Roseler, G. Heitmann and A. T. Liebens, *Catal. Today*, **37**, 353 (1997).
371. Y. Shinohara, S. Mae, D. Shouro and T. Nakajima, *J. Mol. Struct. (THEOCHEM)*, **497**, 1 (2000).
372. T. Takahashi, T. Kai and E. Nakao, *Appl. Catal. A*, **262**, 137 (2004).
373. T. Takahashi and T. Kai, *J. Jpn. Pet. Inst*, **47**, 190 (2004).
374. C. Ngamcharussrivichai, P. Wu and T. Tatsumi, *Catal. Commun.*, **8**, 135 (2007).
375. Y. M. Chung and H. K. Rhee, *J. Mol. Catal. A*, **175**, 249 (2001).
376. H. Ichihashi and M. Kitamura, *Catal. Today*, **73**, 23 (2002).
377. C. Ngamcharussrivichai, P. Wu and T. Tatsumi, *Appl. Catal. A*, **288**, 158 (2005).

378. C. Ngamcharussrivichai, P. Wu and T. Tatsumi, *J. Catal.*, **235**, 139 (2005).
379. G. Dahlhoff, A. Sbresny and W. F. Holderich, *Chem. Eng. Sci.*, **56**, 6661 (2001).
380. R. W. Dugger, J. A. Ragan and D. H. B. Ripin, *Org. Process Res. Dev.*, **9**, 253 (2005).
381. H. L. Schulmann, F. A. Baron and A. E. Weinberg, GB Patent 1,335,260, 1973.
382. P. W. Neber and A. V. Friedolsheim, *Ann. Chem.*, **449**, 109 (1926).
383. P. W. Neber and A. Uber, *Ann. Chem.*, **467**, 52 (1928).
384. F. Palacios, A. M. O. Retana, E. M. Marigorta and J. M. Santos, *Eur. J. Org. Chem.*, 2401 (2001).
385. C. Obrien, *Chem. Rev.*, **64**, 81 (1964).
386. J. Y. L. Chung, G. J. Ho, M. Chartrain, C. Roberge, D. L. Zhao, J. Leazer, R. Farr, M. Robbins, K. Emerson, D. J. Mathre, J. M. McNamara, D. L. Hughes, E. J. J. Grabowski and P. J. Reider, *Tetrahedron Lett.*, **40**, 6739 (1999).
387. J. D. Ha, S. J. Lee, S. Y. Nam, S. K. Kang, S. Y. Cho, J. H. Ahn and J. K. Choi, *Tetrahedron Lett.*, **47**, 6201 (2006).
388. D. F. Taber and W. W. Tian, *J. Am. Chem. Soc.*, **128**, 1058 (2006).
389. A. Diez, A. Voldoire, I. Lopez, M. Rubiralta, V. Segarra, L. Pages and J. M. Palacios, *Tetrahedron*, **51**, 5143 (1995).
390. N. K. Garg, D. D. Caspi and B. M. Stoltz, *J. Am. Chem. Soc.*, **127**, 5970 (2005).
391. N. K. Garg and B. M. Stoltz, *Chem. Commun.*, 3769 (2006).
392. I. P. Piskunova, A. V. Eremeev, A. F. Mishnev and I. A. Vosekalna, *Tetrahedron*, **49**, 4671 (1993).
393. M. M. H. Verstappen, G. J. A. Ariaans and B. Zwanenburg, *J. Am. Chem. Soc.*, **118**, 8491 (1996).
394. F. Palacios, A. M. O. Retana and J. I. Gil, *Tetrahedron Lett.*, **41**, 5363 (2000).
395. F. Palacios, D. Aparicio, A. M. O. Retana, J. M. Santos, J. I. Gil and J. M. Alonso, *J. Org. Chem.*, **67**, 7283 (2002).
396. F. Palacios, D. Aparicio, A. M. O. Retana, J. M. Santos, J. I. Gil and R. U. Munain, *Tetrahedron: Asymmetry*, **14**, 689 (2003).
397. H. Lossen, *Ann. Chem.*, **150**, 314 (1869).
398. T. Shiori, 'Degradation reactions', in *Comprehensive Organic Synthesis, Selectivity, Strategy and Efficiency in Modern Organic Chemistry*, Vol. 6 (Eds. B. M. Trost and I. Fleming), Chap. 4.4, Pergamon Press, Oxford, 1991, pp. 795–828.
399. G. Boche and J. C. W. Lohrenz, *Chem. Rev.*, **101**, 697 (2001).
400. W. Holzer, R. M. Claramunt, M. Perez-Torralba, D. Guggi and T. H. Brehmer, *J. Org. Chem.*, **68**, 7943 (2003).
401. T. Sheradsky and S. Avramovicigrisaru, *Tetrahedron Lett.*, 2325 (1978).
402. D. Muri, J. W. Bode and E. M. Carreira, *Org. Lett.*, **2**, 539 (2000).
403. J. Pihuleac and L. Bauer, *Synthesis*, 61 (1989).
404. J. R. Bellettini and M. J. Miller, *J. Org. Chem.*, **61**, 7959 (1996).
405. F. D. King, S. Pike and D. R. M. Walton, *J. Chem. Soc., Chem. Commun.*, 351 (1978).
406. G. W. Adams, J. H. Bowie and R. N. Hayes, *J. Chem. Soc., Perkin Trans. 2*, 689 (1991).
407. K. Ohmoto, T. Yamamoto, T. Horiuchi, T. Kojima, K. Hachiya, S. Hashimoto, M. Kawamura, H. Nakai and M. Toda, *Synlett*, 299 (2001).
408. P. W. Needs, N. M. Rigby, S. G. Ring and A. J. MacDougall, *Carbohydr. Res.*, **333**, 47 (2001).
409. J. A. Stafford, S. S. Gonzales, D. G. Barrett, E. M. Suh and P. L. Feldman, *J. Org. Chem.*, **63**, 10040 (1998).
410. D. G. Hoare, A. Olson and D. E. Koshland, *J. Am. Chem. Soc.*, **90**, 1638 (1968).
411. S. Hanessian and S. Johnstone, *J. Org. Chem.*, **64**, 5896 (1999).
412. R. Anilkumar, S. Chandrasekhar and M. Sridhar, *Tetrahedron Lett.*, **41**, 5291 (2000).
413. G. Marzoni and M. D. Varney, *Org. Process Res. Dev.*, **1**, 81 (1997).
414. M. Gütschow, *J. Org. Chem.*, **64**, 5109 (1999).
415. S. Zalipsky, *Chem. Commun.*, 69 (1998).
416. S. Chandrasekhar and M. Sridhar, *Tetrahedron: Asymmetry*, **11**, 3467 (2000).
417. B. Hirrlinger and A. Stolz, *Appl. Environ. Microbiol.*, **63**, 3390 (1997).
418. B. Hirrlinger, A. Stolz and H.-J. Knackmuss, US Patent 6,281,003, 2001.
419. C. J. Salomon and E. Breuer, *J. Org. Chem.*, **62**, 3858 (1997).
420. J. Podlaha, I. Cisarova, L. Soukupova, J. Schraml and O. Exner, *J. Chem. Res. (S)*, 520 (1998).

421. M. J. P. Harger, *Org. Biomol. Chem.*, **1**, 3390 (2003).
422. M. J. P. Harger, *Tetrahedron Lett.*, **31**, 1451 (1990).
423. M. J. P. Harger and P. A. Shimmin, *Tetrahedron Lett.*, **32**, 4769 (1991).
424. J. Fawcett, M. J. P. Harger and R. Sreedharan-Menon, *J. Chem. Soc., Chem. Commun.*, 227 (1992).
425. M. J. P. Harger and P. A. Shimmin, *Tetrahedron*, **48**, 7539 (1992).
426. M. J. P. Harger and R. Sreedharan-Menon, *J. Chem. Soc., Chem. Commun.*, 1619 (1994).
427. M. J. P. Harger and R. Sreedharan-Menon, *J. Chem. Soc., Perkin Trans. 2*, 159 (1999).
428. M. J. P. Harger, *Org. Biomol. Chem.*, **4**, 1863 (2006).
429. M. J. P. Harger, *Chem. Commun.*, 1503 (1997).
430. M. J. P. Harger, *Tetrahedron Lett.*, **39**, 2177 (1998).
431. P. L. Wu and W. S. Wang, *J. Org. Chem.*, **59**, 622 (1994).
432. D. K. Bates and K. Li, *J. Org. Chem.*, **67**, 8662 (2002).
433. Y. Endo, K. Kataoka, N. Haga and K. Shudo, *Tetrahedron Lett.*, **33**, 3339 (1992).
434. R. V. Hoffman and G. A. Buntain, *J. Org. Chem.*, **53**, 3316 (1988).
435. T. Sheradsky, E. Nov and S. Avramovicigrisaru, *J. Chem. Soc., Perkin Trans. 1*, 2902 (1979).
436. R. V. Hoffman and S. Madan, *J. Org. Chem.*, **68**, 4876 (2003).
437. T. R. Kelly and R. L. Lebedev, *J. Org. Chem.*, **67**, 2197 (2002).
438. D. S. Fischer, G. M. Allan, C. Bubert, N. Vicker, A. Smith, H. J. Tutill, A. Purohit, L. Wood, G. Packham, M. F. Mahon, M. J. Reed and B. V. L. Potter, *J. Med. Chem.*, **48**, 5749 (2005).

CHAPTER 10

Electrochemistry of hydroxylamines, oximes and hydroxamic acids

OSAMU ONOMURA

Department of Molecular Medicinal Sciences, Graduate School of Biomedical Sciences, Nagasaki University, 1-14, Bunkyo-machi, Nagasaki 852-8521, Japan
Fax: (+81) 95 819 2476; e-mail: onomura@nagasaki-u.ac.jp

I. INTRODUCTION

This review describes electrochemical reactions of hydroxylamines, oximes and hydroxamic acids. In addition, utilization of hydroxylamines and hydroxamic acids as redox mediators are shown. Since the electroorganic chemistry of hydroxylamines, oximes and hydroxamic acids is rather a minor area in the electrochemistry of organic compounds, the reader is advised to refer to texts[1,2] which are written for organic chemists unfamiliar with the electroorganic chemistry.

The chemistry of hydroxylamines, oximes and hydroxamic acids
Edited by Z. Rappoport and J. F. Liebman

II. CATHODIC REDUCTION

A. Hydroxylamines

Aliphatic hydroxylamines are not easily reduced by direct electrochemical reduction[1]. However, they are reduced indirectly by electrochemically generated low-valent Ti(III) or Fe(II) to afford the corresponding amino compounds (equation 1)[3]. This electrochemical method has certain advantages; it takes place at a less negative potential where hydrogen ions are not reduced and the low concentration of the metal salts facilitates the work-up compared to the reduction by chemical reagents where at least equivalent amounts of reagents must be used.

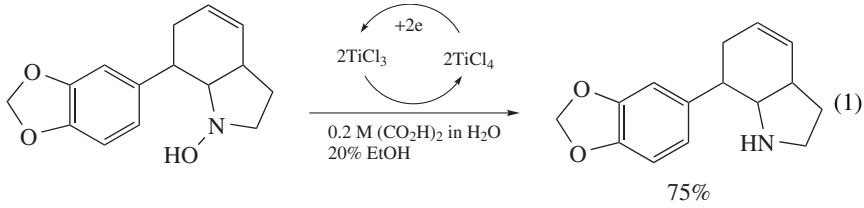

(1)

75%

B. Oximes

Oximes are electrochemically reduced to the corresponding amines in aqueous or aqueous-alcoholic media[1,4]. This method is applicable to the reduction of biologically active complex molecules (equation 2)[5].

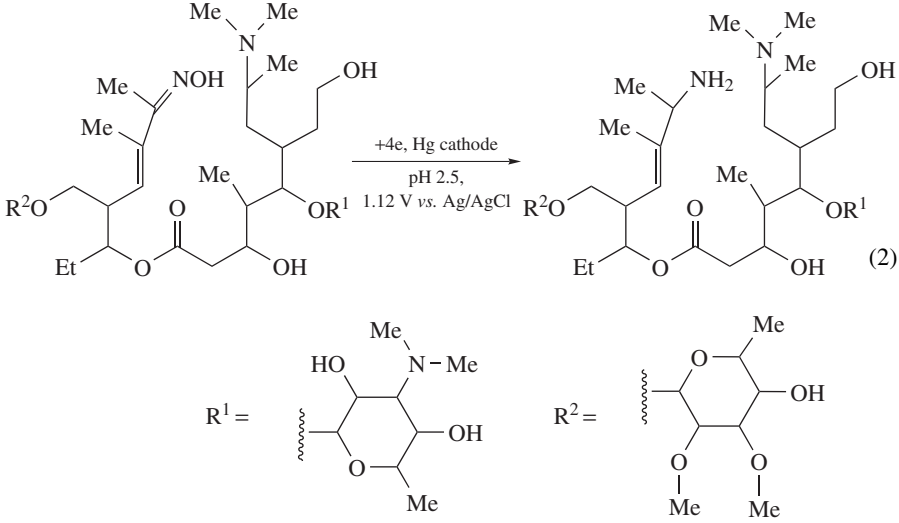

(2)

Electrochemical reductions of camphor oxime (R = Me) and norcamphor oxime (R = H) at a mercury cathode proceed with a high degree of diastereoselectivity (equation 3)[6]. The products are in fact of opposite stereochemistry to those formed in dissolving metal (sodium–ethanol) reductions of the oximes.

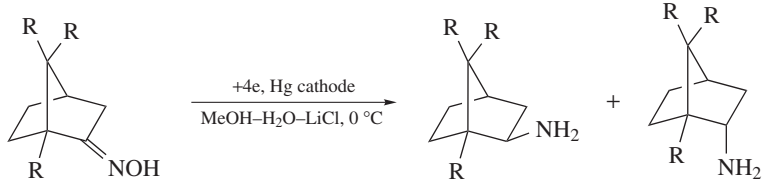

R = Me	99%	1%
(Na-EtOH	4%	96%)
R = H	0%	100%
(Na-EtOH	75%	25%)

(3)

The electrochemical reduction of phenylglyoxylate oxime in the presence of strychnine afforded the corresponding optically active amines (equation 4)[7,8]. Also, the electrochemical reduction of oximes by utilizing poly-L-valine-coated graphite electrode afforded optically active amine[9]. However, in both cases the enantioselectivities were very low.

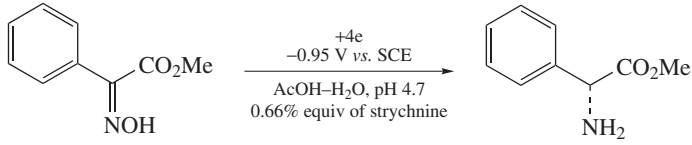

anti 17% ee

(4)

On the other hand, since oxime ethers were electrochemically more inert than ketones under the electroreduction conditions, the electroreductive intra- and inter-molecular coupling of ketones with oxime ethers proceeded via anion radicals in good yields (equations 5 and 6)[10,11]. Moreover, cobaloxime-mediated intramolecular radical addition onto oxime functions in the electrolysis media proceeded to afford the cyclized aminoethers (equation 7)[12].

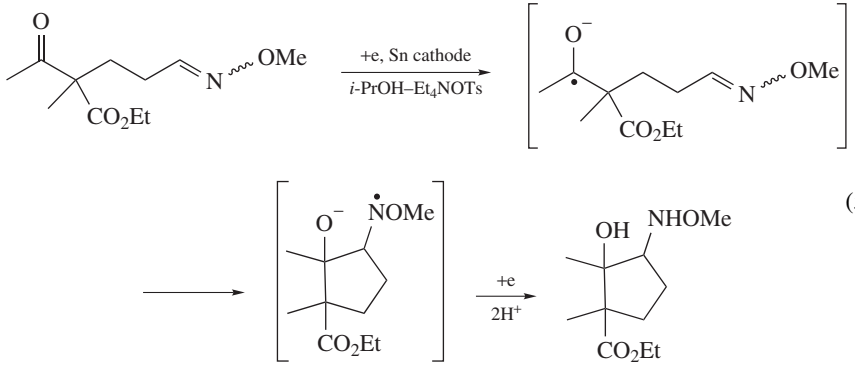

86%

(5)

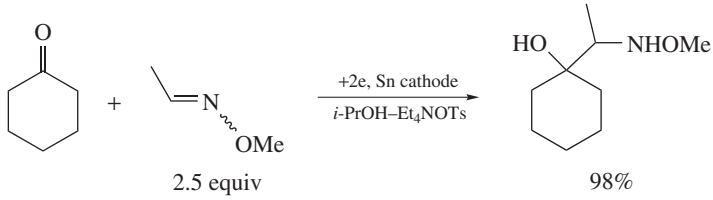

(6)

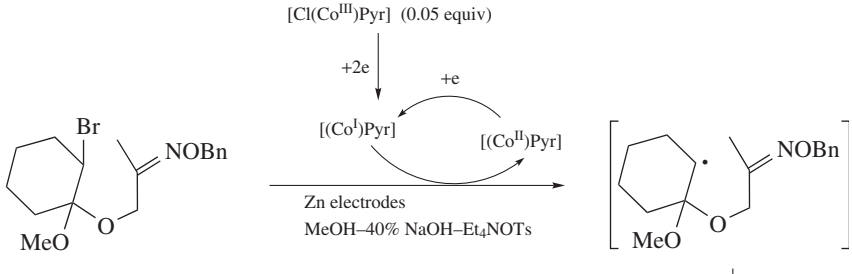

(7)

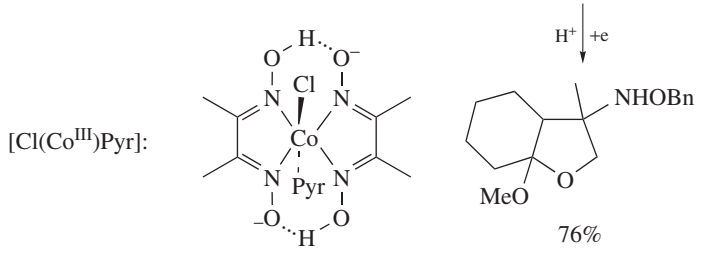

C. Hydroxamic Acids

Electrochemical reduction of hydroxamic acid has hardly been known. The reduction of PhCOCONHOH at a Hg cathode gave $PhCH(OH)CONH_2$ and $[CPh(OH)CONH_2]_2$[13].

III. ANODIC OXIDATION

A. Hydroxylamines

Although electrochemical oxidation of *N*-cyclohexyl-*N*-hydroxylamine in the presence of pyridine afforded the corresponding dimeric nitroso compound with a low yield, *N*-hydroxy *t*-alkylamines were transformed into the corresponding nitroso compounds (equation 8)[14]. Similarly, *N*-phenylhydroxylamine was transformed into nitrosobenzene under similar reaction conditions[15].

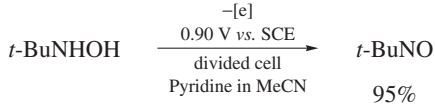

(8)

Also, primary *N*-alkoxyalkylamines afforded the corresponding oxime ethers (equation 9)[16].

$$\mathrm{EtNHOEt} \xrightarrow[\text{1.15 V } \textit{vs.}\text{ SCE}]{-[e]} \underset{\text{divided cell}}{\underset{\text{Pyridine in MeCN}}{}} \mathrm{MeCH{=}NOEt} \quad 70\% \tag{9}$$

Electrochemical oxidation of secondary *N*-hydroxylamines using halide ions as mediators afforded the corresponding nitrones (equation 10)[17]. Among the examined halide salts, NaI was the most effective. The formation of nitrones might have proceeded by the anodically generated 'I^+' from I^- and cathodically generated MeO^- anion from MeOH as shown in Scheme 1. Since I^- is more oxidizable than *N*-hydroxypiperidine [oxidation peak potential of I^- for Et_4NI (0.01 M) = 0.60V *vs*. SCE (SCE: Saturated Calomel Electrode), that of *N*-hydroxypiperidine (0.01 M) = 0.68V *vs*. SCE, in MeOH–0.1M $LiClO_4$–$3H_2O$, 100 mV s^{-1}], the direct oxidation mechanism may be unlikely.

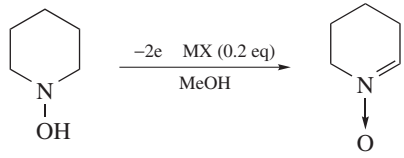

MX = NaI: 92%
MX = KI: 83%
MX = Et_4NI: 80%
MX = NaBr: 54%
MX = NaCl: 16%

(10)

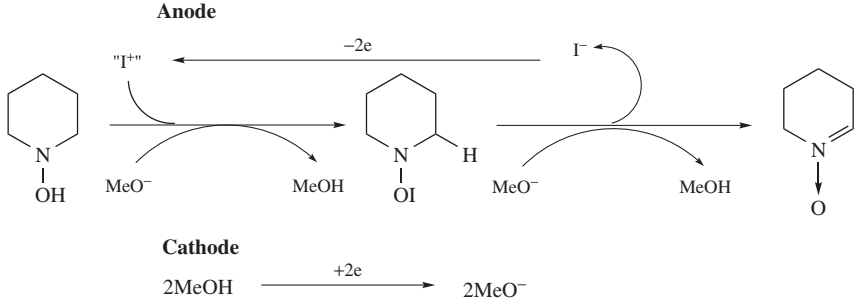

SCHEME 1

Since paired electrosynthesis of nitrones from *N*-hydroxylamines can proceed by both anodic and cathodic oxidation, the current efficiencies are very high[18,19].

β,*N*-Dihydroxy primary amines afforded the corresponding aldehydes and oximes (equation 11)[20].

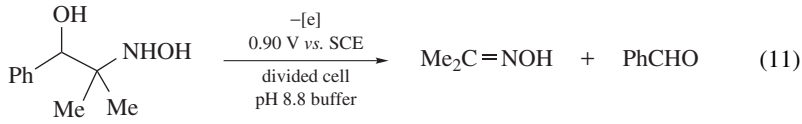

(11)

On the other hand, *N*-alkoxyamines were more stable than styrenes under electrooxidation conditions. As a result, the electrooxidative intramolecular cyclized acetoxyamination product was obtained in good yields (equation 12)[21].

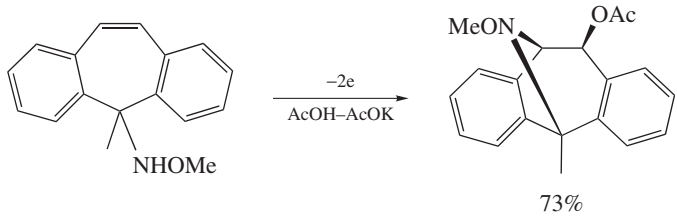

(12)

B. Oximes

Usually, electrochemical oxidative hydrolysis of ketoximes affords the corresponding ketones. Hence, 2-octanone (equation 13) and acetophenone were obtained from the corresponding ketoximes in 90%[22] and 97%[23] yields, respectively. However, camphor oxime was transformed into the ring-cleaved nitrile (equation 14)[22].

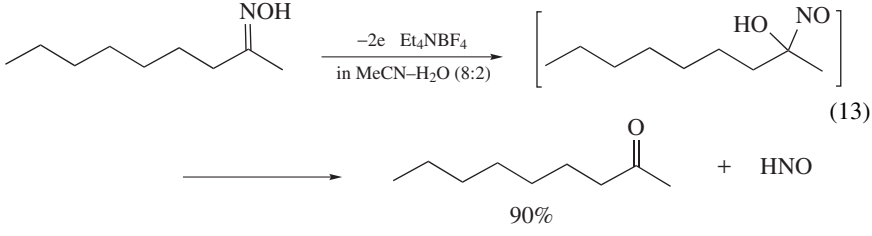

(13)

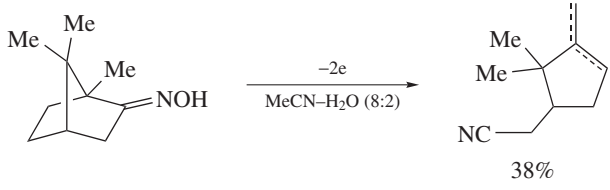

(14)

Electrochemical oxidation of aldoximes using halide ions as mediators afforded the corresponding nitrile oxides in the anode compartment, which were simultaneously reduced to nitriles by cathodic reduction (equation 15)[24]. Sodium chloride affords the best result among the supporting electrolytes ($Cl^- > Br^- > I^- > ClO_4^- > TsO^-$). Accordingly, the electrochemical reaction of oximes carried out in the presence of dipolephiles yielded isooxazolines (equation 16).

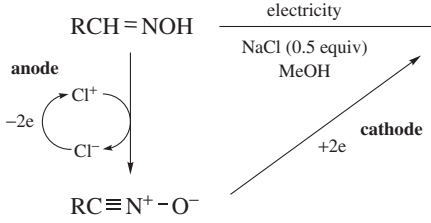

R=Me(CH$_2$)5: 83%
cyclohexyl: 71%
2,4,6-Me$_3$C$_6$H$_2$: 91%

(15)

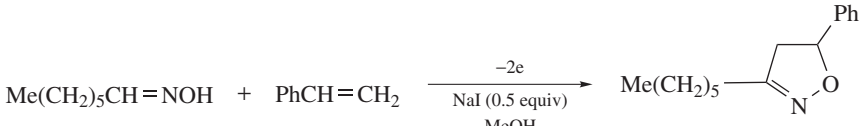

56% yield (16)

Electrolysis of ketoximes using triphenylphosphine as mediator afforded the corresponding rearranged amides (equation 17)[25].

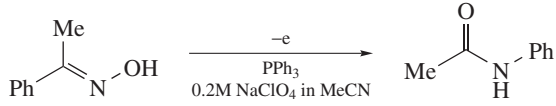

93% (17)

Electrochemical oxidation of phenol substituted by a side chain containing an oxime group afforded a spiro-isoxazole in a quantitative yield (equation 18)[26].

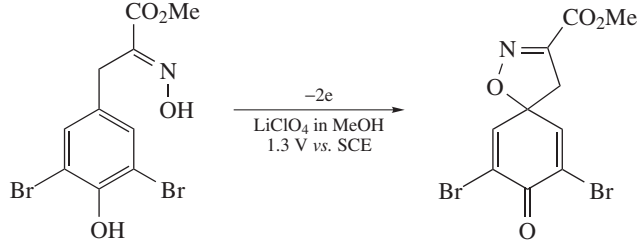

quantitative yield (18)

C. Hydroxamic Acids

Electrochemical oxidation of hydroxamic acids in the presence of amines, alcohols or water afforded the corresponding amides, esters or carboxylic acids (equation 19)[27,28].

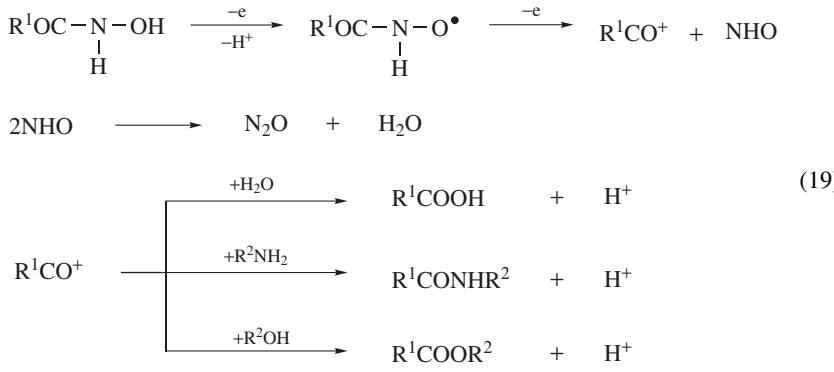

(19)

IV. HYDROXYLAMINES AND HYDROXAMIC ACIDS AS REDOX CATALYSTS

A. Hydroxylamines

Oxidations employing an electrochemically regenerated reagent are finding increasing application in organic synthesis. Oxoammonium ion is easily generated by electrochemical oxidation of hydroxylamine via intermediary formation of nitroxyl radicals (*N*-oxyl)[29]. For example, *N*-hydroxy-2,2,6,6-tetramethylpiperidine and 2,2,6,6-tetramethylpiperidinyl-1-oxy (TEMPO) at +0.33 V (*vs.* Ag/Ag^+) are easily oxidized to the corresponding oxoammonium ion[30]. Semmelhack and coworkers found that highly reactive oxoammonium ion might be a useful oxidant for primary and secondary alcohols (Scheme 2)[30].

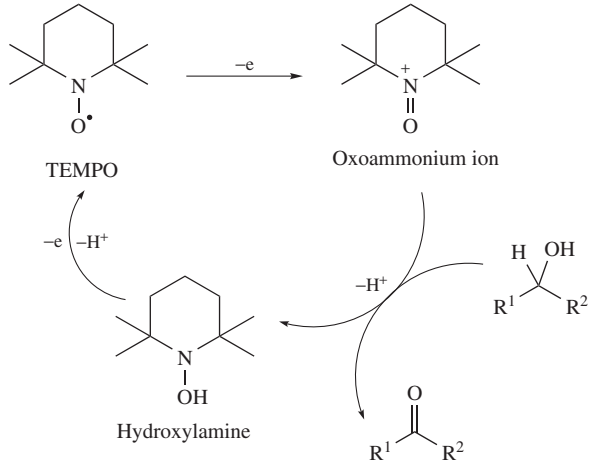

SCHEME 2

The oxidation of alcohols to aldehydes and ketones using catalytic amounts of TEMPO and controlled potential electrolysis has been reported, including the observation of a special selectivity for primary alcohols in the presence of secondary alcohols (equation 20)[30]. The oxidation of secondary alcohol is much slower than that of primary alcohols. This method is especially effective for oxidation of the primary alcohol group in carbohydrates (equations 21 and 22)[31,32].

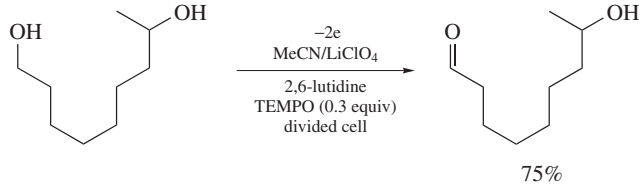

(20)

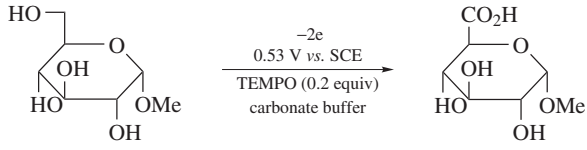

(21)

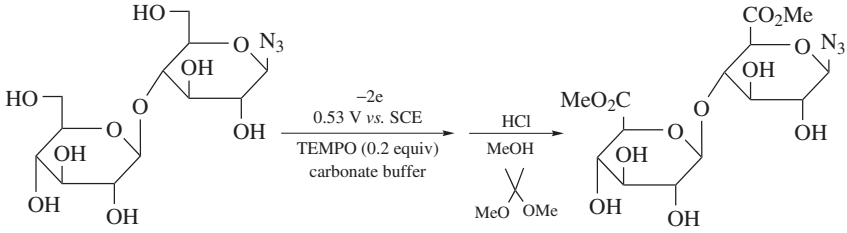

(22)

A double mediatory system consisting of TEMPO and halide ion, which was suitable to obtain aldehyde and had higher current efficiency than a single mediatory system, was also exploited for the oxidation of alcohols (Scheme 3)[33,34].

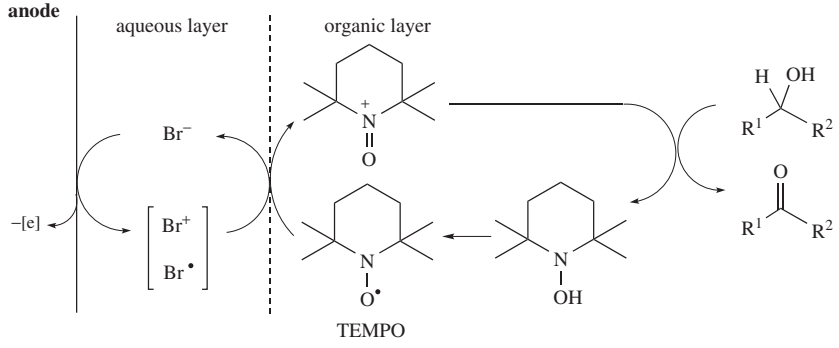

SCHEME 3

TEMPO has been structurally modified to bring about new selectivities. Highly efficient anionic water-soluble TEMPO[35], oil-in-water nanoemulsion containing TEMPO for oxidation of alcohols[36] and a waste-free system were developed[37]. Especially, the sterically less crowded azabicyclo-*N*-oxyls oxidized *l*-menthol to *l*-menthone with much higher efficiencies than TEMPO (equation 23)[38].

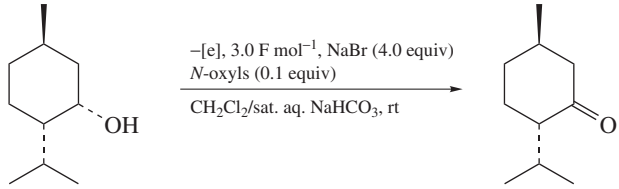

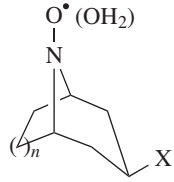

Azabicyclo-*N*-oxyls

TEMPO : 23%
n=1, X=Cl : 99%
n=1, X=H: 86%
n=2, X=Cl : 92%
n=2, X=H: 87%

(23)

Highly enantioselective oxidation of phenylethyl alcohol was achieved by using a TEMPO-modified graphite felt electrode in the presence of (−)-sparteine, where the enantiopurity of the unreacted (*R*)-alcohol was >99% ee and the current efficiency was >90% (equation 24)[39]. However, this selectivity has been questioned[40].

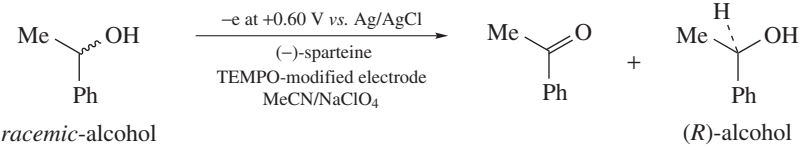

racemic-alcohol (*R*)-alcohol (24)

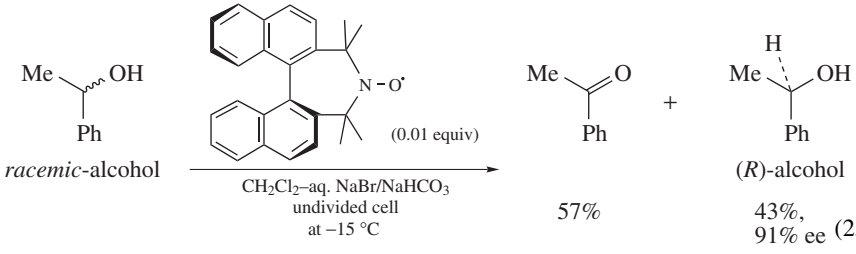

racemic-alcohol (*R*)-alcohol

57% 43%, 91% ee (25)

meso-diol

89%, 74% ee

Oxidative kinetic resolution of *secondary* alcohols mediated with a catalytic amount of optically active binaphthyl-type *N*-oxyl has been performed with high selectivity[41]. Also, it has mediated oxidative asymmetric desymmetrization of primary alcohols with good selectivity (equation 25)[42].

Graphite felt anode modified by spiro-type chiral *N*-oxyl mediated enantioselective oxidation of primary alcohols proceeded with excellent efficiencies (equation 26)[43].

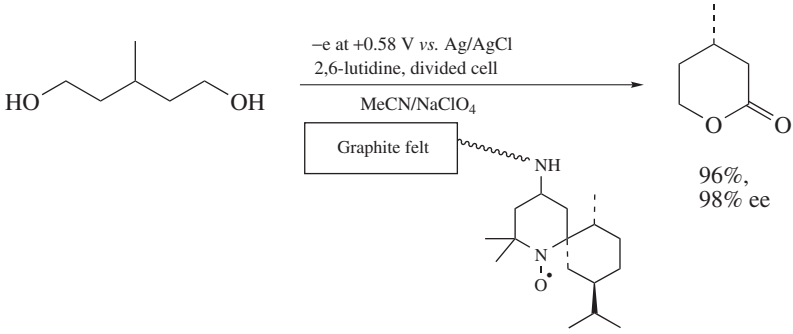

(26)

1,1′-Binaphthol (BINOL) was prepared from 2-naphthol in high current efficiency on a graphite felt electrode coated with a thin poly(acrylic acid) layer immobilizing 4-amino-2,2,6,6-tetramethylpiperidinyl-1-oxyl (4-amino-TEMPO) (equation 27)[44].

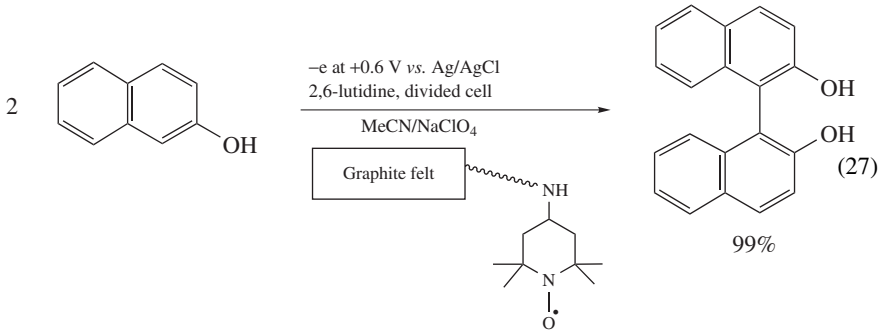

(27)

Furthermore, electrochemical oxidation with TEMPO mediated aromatization of 6-membered cyclic dienes[45] and transformation of alkenes to alkenones also took place[46].

The *N*-oxoammonium ion is theoretically expected to react with an amine, eliminating a proton and forming the hydroxylamine while the amine is converted to imines and/or nitriles (Scheme 4). These were indeed observed by Semmelhack and Schmid (equation 28)[47].

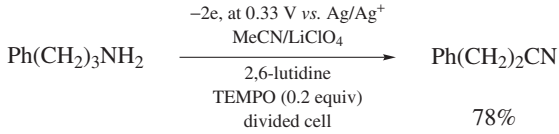

(28)

Recently, a similar reaction has been shown to affect the kinetic resolution of racemic secondary amines. In this example, chiral spiro-type *N*-oxyl radical was utilized as the

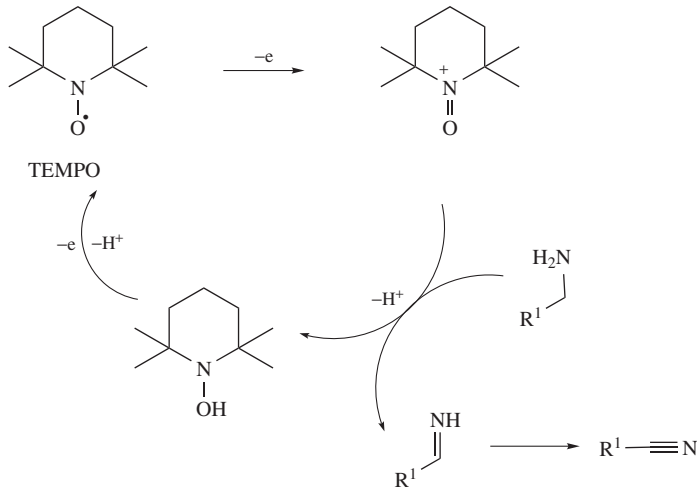

SCHEME 4

mediator (equation 29)[48]. The reactions were run to partial conversion and then the chirality of the recovered amine-starting material was measured. Enantiomeric excesses of 62 to 78% were obtained. The turnover number for the *N*-oxyl radical ranged from 21.7 to 26.7.

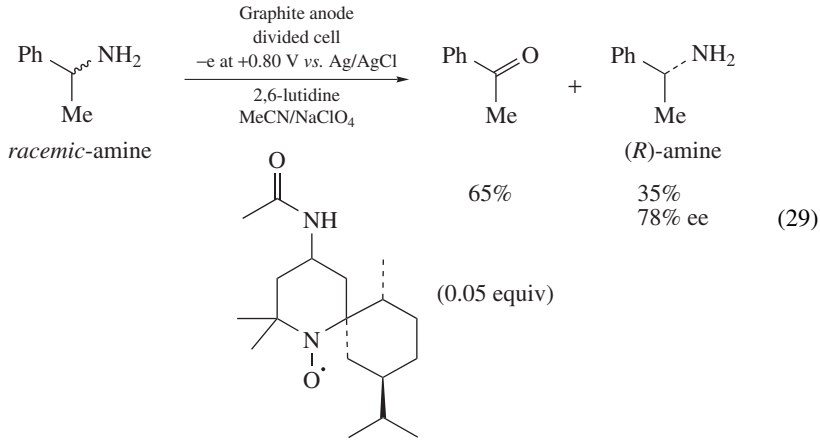

(29)

B. Hydroxamic Acids

Ishii and coworkers have demonstrated that *N*-hydroxyphtalimide (NHPI) is an effective mediator for the oxidation of inactive hydrocarbons, alcohols, olefins and aromatic compounds by molecular oxygen, since the corresponding *N*-oxyl (PINO) generated from NHPI is an active species for their oxidation[49]. Before the aerobic oxidation by Ishii

and coworkers, Masui and coworkers exploited the electrochemical oxidations of various organic compounds with a catalytic amount of NHPI. The oxidation process depicted in equation 30 is suitable for the oxidation of secondary alcohols[50]. A large deuterium isotope effect ($k_H/k_D = 10.6$) was observed in the oxidation of benzhydrol[51]. Recently, tetrafluoro-NHPI was found to be efficient for the oxidation of borneol[52].

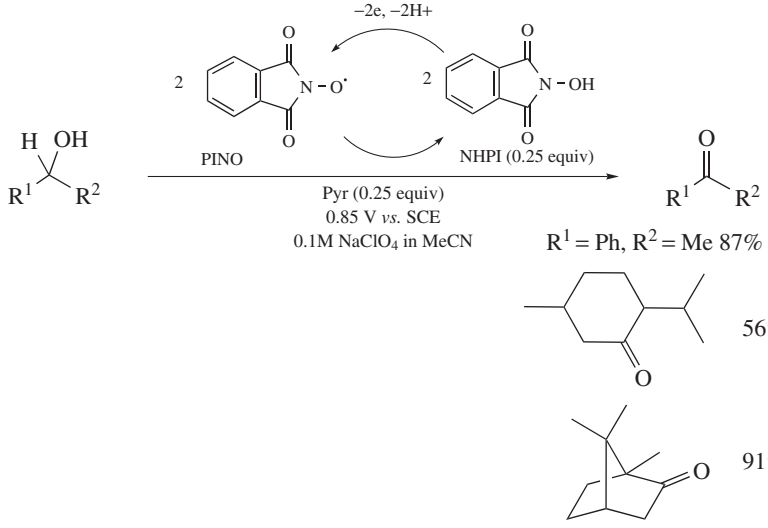

(30)

This electrochemical oxidation mediated by NHPI was applicable to benzylic carbons, allylic carbons, deprotection of acetals, oxidative cleavage of cyclic acetals and amide to afford benzoylated compounds[53], enones[54], carbonyl compounds[55], β-hydroxyethyl esters[56] and imides[57], respectively (equations 31–35).

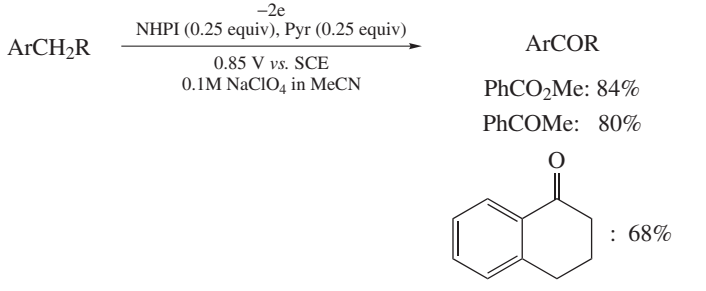

(31)

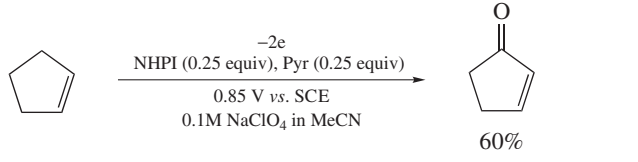

(32)

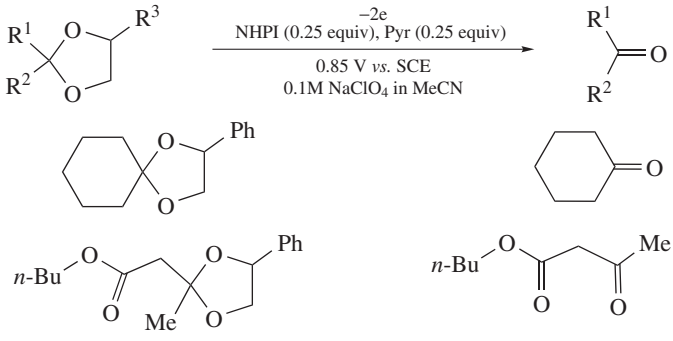

(33)

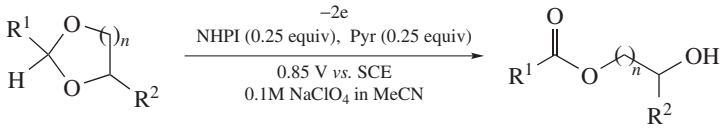

(34)

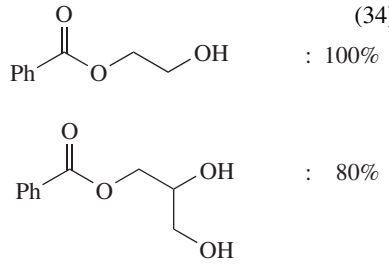

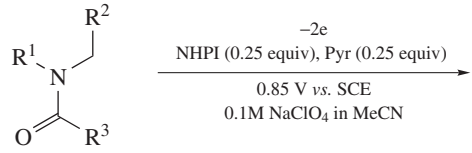

(35)

MeCONHEt

$(MeCO)_2NH$: 60%

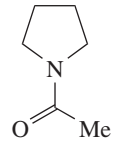
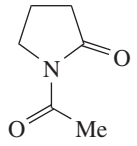

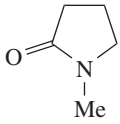
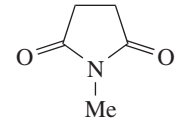

V. REFERENCES

1. H. Lund and M. M. Baizer (Eds.), *Organic Electrochemistry*, Dekker, New York, 1991.
2. H. J. Schäfer (Ed.), *Encyclopedia of Electrochemistry Vol. 8: Organic Electrochemistry*, Wiley-VCH, Weinheim, 2004.
3. G. Feroci and H. Lund, *Acta Chem. Scand., Ser. B*, **30**, 651 (1976).
4. B. Scoucaze-Guillous and H. Lund, *Acta Chem. Scand.*, **52**, 417 (1998).
5. Z. Mandic and N. Lopotar, *Electrochem. Commun.*, **7**, 45 (2005).
6. A. J. Fry and J. H. Newberg, *J. Am. Chem. Soc.*, **89**, 6374 (1967).
7. M. Jubault, E. Raoult, J. Armand and L. Boulares, *J. Chem. Soc., Chem. Commun.*, 250 (1977).
8. M. Jubault, *J. Chem. Soc., Chem. Commun.*, 953 (1980).
9. S. Abe, T. Fuchigami and T. Nonaka, *Chem. Lett.*, 1033 (1983).
10. T. Shono, N. Kise and T. Fujimoto, *Tetrahedron Lett.*, **32**, 525 (1991).
11. T. Shono, N. Kise, T. Fujimoto, A. Yamanami and R. Nomura, *J. Org. Chem.*, **59**, 1730 (1994).
12. T. Inokuchi and H. Kawafuchi, *Synlett*, 421 (2001).
13. J. Armand, P. Souchay and F. Valentini, *C. R. Acad. Sci., Ser. C*, **265**, 1267 (1967).
14. H. Sayo, S. Ozaki and M. Masui, *Chem. Pharm. Bull.*, **21**, 1988 (1973).
15. S. Ozaki and M. Masui, *Chem. Pharm. Bull.*, **26**, 1364 (1978).
16. H. Sayo, S. Ozaki and M. Masui, *Chem. Pharm. Bull.*, **23**, 1702 (1975).
17. T. Shono, Y. Matsumura and K. Inoue, *J. Org. Chem.*, **51**, 549 (1986).
18. W. Li and T. Nonaka, *Chem. Lett.*, 1271 (1997).
19. W. Li and T. Nonaka, *J. Electrochem. Soc.*, **146**, 592 (1999).
20. S. Ozaki, S. Nishiguchi and M. Masui, *Chem. Pharm. Bull.*, **32**, 2609 (1984).
21. S. Karady, E. G. Corley, N. L. Abramson, J. S. Amato and L. M. Weinstock, *Tetrahedron*, **47**, 757 (1991).
22. M. R. Van De Mark and A. M. Scornavacca, *Org. Prep. Proced. Int.*, **13**, 395 (1981).
23. L. Bencharif, A. Tallec and R. Tardival, *Electrochim. Acta*, **42**, 3509 (1997).
24. T. Shono, Y. Matsumura, K. Tsubata, T. Kamada and K. Kishi, *J. Org. Chem.*, **54**, 2249 (1989).
25. H. Ohmori, S. Nakai and M. Masui, *Chem. Pharm. Bull.*, **28**, 2247 (1980).
26. H. Noda, M. Niwa and S. Yamamura, *Tetrahedron Lett.*, **22**, 3247 (1981).
27. S. Ozaki and M. Masui, *Chem. Pharm. Bull.*, **25**, 1179 (1977).
28. M. Masui, T. Ueshima, T. Yamazaki and S. Ozaki, *Chem. Pharm. Bull.*, **31**, 2130 (1983).
29. A. E. J. de Nooy, A. C. Besemer and H. van Bekkum, *Synthesis*, 1153 (1996).
30. M. F. Semmelhack, C. S. Chou and D. A. Cortes, *J. Am. Chem. Soc.*, **105**, 4492 (1983).
31. K. Schatbaum and H. J. Schäfer, *Synthesis*, 864 (1999).
32. M. Schämann and H. J. Schäfer, *Eur. J. Org. Chem.*, 351 (2003).
33. T. Inokuchi, S. Matsumoto, T. Nishiyama and S. Torii, *Synlett*, 57 (1990).
34. T. Inokuchi, S. Matsumoto and S. Torii, *J. Org. Chem.*, **56**, 2416 (1991).
35. K. Mitsudo, H. Kumagai, F. Takabatake, J. Kubota and H. Tanaka, *Tetrahedron Lett.*, **48**, 8994 (2007).
36. T. Yoshida, M. Kuroboshi, J. Oshitani, K. Gotoh and H. J. Schäfer, *Synlett*, 2691 (2007).
37. G. Palmisano, R. Ciriminna and M. Pagliaro, *Adv. Synth. Catal.*, **348**, 2033 (2006).
38. Y. Demizu, H. Shiigi, T. Oda, Y. Matsumura and O. Onomura, *Tetrahedron Lett.*, **49**, 48 (2008).

39. Y. Kashiwagi, Y. Yanagisawa, F. Kurashima, J. Anzai, T. Osa and J. M. Bobbitt, *Chem. Commun.*, 2745 (1996).
40. E. M. Belgsir and H. J. Schäfer, *Chem. Commun.*, 435 (1999).
41. H. Tanaka, Y. Kawakami, K. Goto and M. Kuroboshi, *Tetrahedron Lett.*, **42**, 445 (2001).
42. M. Kuroboshi, H. Yoshihisa, M. N. Cortona, Y. Kawakami, Z. Gao and H. Tanaka, *Tetrahedron Lett.*, **41**, 8131 (2000).
43. Y. Kashiwagi, F. Kurashima, S. Chiba, J. Anzai, T. Osa and J. M. Bobbitt, *Chem. Commun.*, 114 (2003).
44. Y. Kashiwagi, H. Ono and T. Osa, *Chem. Lett.*, 81 (1993).
45. T. Breton, D. Liaigre and E. M. Belgsir, *Electrochem. Commun.*, **7**, 1445 (2005).
46. T. Breton, D. Liaigre and E. M. Belgsir, *Tetrahedron Lett.*, **46**, 2487 (2005).
47. M. F. Semmelhack and C. R. Schmid, *J. Am. Chem. Soc.*, **105**, 6732 (1983).
48. Y. Kashiwagi, F. Kurashima, C. Kikuchi, J. Anzai, T. Osa and J. M. Bobbitt, *Chem. Commun.*, 1983 (1999).
49. Y. Ishii, S. Sakaguchi and T. Iwahama, *Adv. Synth. Catal.*, **343**, 393 (2001).
50. M. Masui, T. Uemura and S. Ozaki, *J. Chem. Soc., Chem. Commun.*, 479 (1983).
51. C. Ueda, M. Noyama, H. Ohmori and M. Masui, *Chem. Pharm. Bull.*, **35**, 1372 (1987).
52. K. Gorgy, J.-C. Lepretre, E. Saint-Aman, C. Einhorn, J. Einhorn, C. Marcadal and J.-L. Pierre, *Electrochim. Acta*, **44**, 385 (1998).
53. M. Masui, S. Hara, T. Ueshima, T. Kawaguchi and S. Ozaki, *Chem. Pharm. Bull.*, **31**, 4209 (1983).
54. M. Masui, K. Hosomi, K. Tsuchida and S. Ozaki, *Chem. Pharm. Bull.*, **33**, 4798 (1985).
55. M. Masui, T. Kawaguchi and S. Ozaki, *J. Chem. Soc., Chem. Commun.*, 1484 (1985).
56. M. Masui, T. Kawaguchi, S. Yoshida and S. Ozaki, *Chem. Pharm. Bull.*, **34**, 1837 (1986).
57. M. Masui, S. Hara and S. Ozaki, *Chem. Pharm. Bull.*, **34**, 976 (1986).

CHAPTER **11**

Use of oximes, hydroxamic acids and related species as reagents in inorganic analytical chemistry*

MAJA PONIKVAR

Department of Inorganic Chemistry and Technology, Jožef Stefan Institute, Jamova 39, SI-1000 Ljubljana, Slovenia
Fax: +386 1 477 31 55; e-mail: maja.ponikvar@ijs.si

and

JOEL F. LIEBMAN

Department of Chemistry and Biochemistry, University of Maryland, Baltimore County, 1000 Hilltop Circle, Baltimore, Maryland 21250, USA
Fax: (+1)410-455-2608; e-mail: jliebman@umbc.edu

* This chapter is dedicated to the memory of Professor Nicholas D. Cheronis, organic chemist and educator who pioneered semimicroanalysis.

The chemistry of hydroxylamines, oximes and hydroxamic acids
Edited by Z. Rappoport and J. F. Liebman

I. INTRODUCTION

Analytical chemistry is a science with applications throughout medicine, industry, environment, and indeed, seemingly all of the sciences. Quoting from the 2007 WebSite of the Division of Analytical Chemistry of the American Chemical Society[1]: 'Analytical Chemistry seeks ever improved means of measuring the chemical composition of natural and artificial materials. The techniques of this science are used to identify the substances which may be present in a material and to determine the exact amounts of the identified substances'.

The components of the sample that are to be determined are often referred to as analytes. While qualitative analysis reveals the chemical identity of the species in the sample, quantitative analysis establishes the relative amount of one or more of these species, the analytes, in numerical terms. Often separation is required as a necessary part of either qualitative or quantitative analysis.

Another definition of the term chemical analysis is also worth mentioning. The dictionary definition as found in Vogel's *Textbook of Quantitative Inorganic Analysis*[2] says that chemical analysis is: 'The resolution of a chemical compound into its proximate or ultimate parts; the determination of its elements or of the foreign substances it may contain'.

Contemporary analytical chemistry relies heavily on instrumental methods. Nonetheless, organic as well as inorganic reagents play an important role throughout each step of the analytical procedure from sampling, preparation of the sample for the analyses to the analysis itself. The *Dictionary of Analytical Reagents* lists the following application areas of analytical reagents[3]: amperometric reagents, buffers (pH), chemiluminiscence generation agents, chromatographic derivatization agents, enzyme substrate co-factors, extractants, fluorescent labels, gravimetric reagents, indicators, masking agents, NMR shift reagents, scintillators, spectrofluorimetric reagents, spectrophotometric reagents, surfactants, titrants.

Many analytical reagents can be characterized as substituted amines and/or imines, i.e. species with trivalent nitrogen with its pair of electrons as $>N-$ and/or $=N-$, and multiple affixed groups. These compounds have been extensively investigated and it is no wonder that an impressive number of this type of compounds have been reported for determination of different analytes. These analytes include not only elements with differing oxidation states but also species with different inorganic or organic groups. Our initial literature search resulted in a huge number of original articles and citations on the use of oximes, hydroxamic acids and related species as analytical reagents. In the name of brevity, we decided that the *Dictionary of Analytical Reagents*[3] dated 1993 will be taken as our most important literature source for listing our overview of the reagents. However,

some additional literature sources were also considered in this chapter when this source provided inadequate citations for a given analyte of interest.

Oximes, hydroxamic acids and related species are usually used to determine metallic elements although some methodologies also exist for determination of the metalloid and nonmetallic elements. For the current chapter, the choice of elements to be considered was limited to the left-hand metallic side of the line in the periodic system which 'divides' metallic elements from nonmetallic; metalloids were generally ignored here along with nonmetals. Additionally, the search was limited to nonradioactive elements with the exception of uranium and thorium because of their exceptionally long (*ca* 10^9 year) half-lives. It should be noted, however, that the use of some of the selected reagents can be extended to determination of CN^-, F^-, PO_4^{3-}, SCN^-, SO_4^{2-}, among other anions.

From the *Dictionary of Analytical Reagents*[3] we find that oximes, hydroxamic acids and related species are frequently used in classical analysis especially for gravimetric and volumetric determinations. Additionally, these reagents are used for preconcentration, separation and derivatization of the analyte and subsequent determination of the analyte using instrumental techniques; among others, spectrophotometric determinations are frequently used. It can be noted that instrumental and classical analyses, although instrumental methods rightfully assume an overwhelming role in analytical laboratory practice, complement each other also and can often be used in tandem to the analyst's advantage in analytical laboratory practice. Consequently, this was also a powerful criterion for the inclusion of a specific reagent in this chapter, the aim of which is to provide an overview on the use of oximes, hydroxamic acids and related species as reagents in inorganic chemical analysis.

II. DEFINITIONS OF REAGENTS — REACTIVE GROUPS OF OXIMES, HYDROXAMIC ACIDS AND RELATED SPECIES

Oximes and hydroxamic acids, together with hydroxylamines, can be generally considered as a class of compounds having a common functional group −NOH−. Additional functional features distinguish these three parent classes of compounds. Some confusion often occurs over a reagent generally called 'oxine'. This is not an oxime (and certainly not a hydroxamic acid) but rather is 8-hydroxyquinoline[4].

A. Oximes

The defining 'active' group in oximes is >C=N−OH. Oximes are often divided into the two groups, aldoximes and ketoximes. Both can be written as $R^1R^2C{=}N{-}OH$ where either or both R^1 and R^2 are H, alkyl or aryl (including heterocyclic) derivatives, i.e. there is a hydrogen or carbon attached to the carbon with the =N−OH group. Should either or both affixed groups be hydrogen, the oxime is an aldoxime (a chemically and etymologically condensed form of 'aldehyde + oxime'); should both affixed groups involve carbon attachment, then the oxime is likewise a ketoxime ('ketone + oxime'). When $R^1 \neq R^2$, as is the general case, there are two isomeric possibilities corresponding to the OH and the 'smaller' R group being on the same side of the C=N double bond, and on opposite sides respectively—the early literature abounds with the prefixes 'syn-' and 'anti-', and 'α' and 'β'. It is very rare in the analytical chemistry literature to distinguish between these two stereoisomeric cases as reagents, or even to specify the predominant isomer in the reagent or resulting complex. Likewise, generally unstated is the observation that oximes can coordinate the metal through either their nitrogen and/or oxygen electron-donating sites, often with accompanying deprotonation, as well as intramolecular complexation

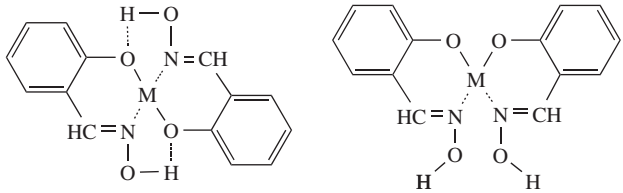

FIGURE 1. Structural formulas of salicylaldoxime chelates: (a) chelates with M = Cu^{II}, Ni^{II} and Pd^{II}; (b) chelates with M = Mn^{II}, Fe^{II}, Co^{II} and Zn^{II}

involving electron-donating sites found on the other groups that compose the oxime to form what is generally called a chelate.

In this chapter, oximes are discussed as simple monoximes (monooximes) with one oxime group and as dioximes with two oxime groups. Within these individual groups, there are other large subclasses of reagents such as ketooximes (oximes with another carbonyl group, not to be confused with ketoximes) as well as reagents that can be considered as belonging to other classes of reagents, for example trioximes. It is important to note that ketomonoximes (and other ketooximes) frequently exhibit tautomerization which can lead to difficulties with nomenclature: are they oximes with an affixed carbonyl group and/or are they enols with nitroso substituents? We ignore this problem both for the oxime reagents themselves as well as for any of their metal derivatives appearing in our text or in its associated tables. Likewise, α-dioximes (i.e. having their two oxime functionalities on adjacent carbons) could be *N*-hydroxy-β-nitrosoenamines, i.e. −C(=NOH)−C(=NOH)− vs. −C(NO)=C(NHOH)−. In fact, this possibility is unlikely as well as irrelevant for the analytically inclined chemist.

We have to acknowledge that in most cases it is not really defined which ligand atoms are in fact involved in the complexation or chelation process.

As a typical example of monoxime reaction products with metal ions, structural formulas of salicylaldoxime, which reacts with several metal ions to give intensively colored complexes insoluble in water, are given in Figure 1[5].

The reaction of aqueous green Ni^{II}, or its blue ammonia complex, with colorless dimethylglyoxime (DMG) to form a vibrantly red precipitate of a 1:2 metal:DMG complex demonstrates an example of precise stereochemistry and oxime deprotonation in what is perhaps the archetypal analytical metal dioxime reaction (equation 1). This transformation certainly intrigued both authors early in their education. It is interesting to note that DMG is an excellent example of highly specific reagent because under the same reaction conditions only yellow palladium chelate is also precipitated.

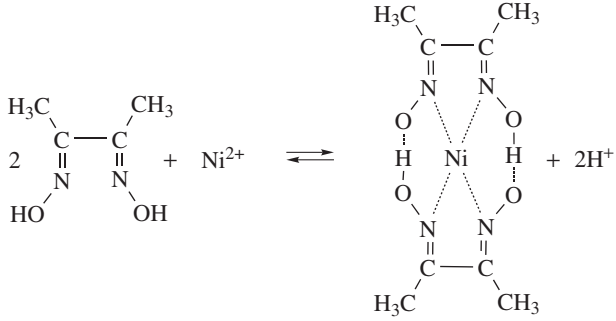

(1)

Numerous other types of compounds can also be regarded as a type of oximes, such as amidoximes (amideoximes), that can be written with the general formula $R^1C(NR^2R^3)$=N−OH and their formal and often indistinguishable isomers, *N*-hydroxyamidines, $R^1C(=NR^2)-NR^3OH$. There are also nitrooximes (= nitrolic acids) with a general formula $RC(NO_2)$=N−OH, and nitrosooximes (= nitrosolic acids) with the general formula RC(NO)=NOH. However, based on our definition of oximes for this chapter, these reagents were excluded from our primary discussion because it is nitrogen, and not only carbon and/or hydrogen, bonded to the oxime >C=N−OH core.

B. Hydroxamic Acids

Hydroxamic acids can be written with a general formula $R^1-CO-N(OH)-R^2$; a −CO− group is attached to the −NOH− group where in a simple way they can be described as carboxylic acids in which an amino group has been inserted allowing for another group to be appended. Perhaps because they are readily associated with both carboxylic acids and hydroxylamines, both structurally and synthetically, hydroxamic acids have been very 'popular' reagents. Indeed, as drawn in their tautomeric form, RC(OH)=NOH, hydroxamic acids are the oximes of carboxylic acids and, as with ketooximes, this tautomeric distinction will not be made in our current study nor which of the nitrogen and two oxygens is involved in complexation.

For hydroxamic acids, it is generally assumed that it is the *N*-hydroxyamide/keto form, as opposed to the hydroximic/hydroxyoxime form, that predominates in acid medium, the environment usually required for most precipitates or colors to form[6,7]. It is in general unknown what is the stoichiometry and structure of most metal hydroxamate complexes in solution. Nevertheless, the reaction of the majority of hydroxamic acids with metal ions can be written schematically as shown in equation 2.

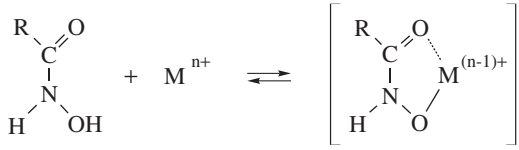

(2)

For example, the specific reaction of yellow Fe^{III} with acetohydroxamic acid to form a purple complex is therefore assumed to correspond to the scheme in equation 3.

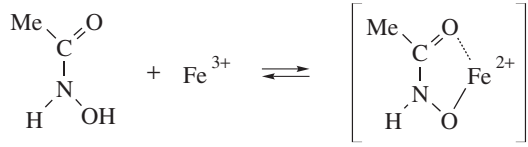

(3)

In this chapter, accompanying hydroxamic acids is a much smaller collection of thiohydroxamic acids with their reactive group −CS−N(OH)−. Comparison of thiohydroxamic acids with their isomeric −CO−N(SH)− seemingly remains unexplored. Then again, as will be documented elsewhere in the current volume, either form of thiohydroxamic acids has been less investigated than hydroxamic acids, much as thiocarboxylic acids, amides and their esters (both *O*- and *S*-isomers) have been investigated less than the oxygenated carboxylic acids, amides and their esters. We welcome, however, further comparison of hydroxamic and thiohydroxamic acids in that there are generally profound differences

between ligating O and S—we recall the general solubility of metal ions in aqueous solution only to be precipitated by added sulfide ion.

C. Some Other Related Species that will be Ignored: Hydroxylamines, Nitrosohydroxylamines, Hydroxytriazenes

Hydroxylamines are among the simplest compounds with the functional group−NOH−. A general formula can be written as $R^1-N(OH)-R^2$, where either or both R^1 and R^2 are H, alkyl or aryl (including heterocycles), i.e. there is a hydrogen or carbon attached to the nitrogen with attached −OH group. The simplest hydroxylamine is H_2NOH itself, which can be considered as a hybrid or composite of ammonia and water due to parallels with each of them. We have already discussed the case where an affixed group is acyl—these are hydroxamic acids. We will neglect the above hydroxylamines affixed solely to H, alkyl or aryl since in comparison to oximes and hydroxamic acids the majority of the activity has involved organic chemical analytes, and furthermore, generally narrowed to carbonyl derivatives (aldehydes, ketones) and carboxylic acid derivatives (e.g. esters) to the near exclusion of other classes of compounds. Some references are given elsewhere[8–10].

Having chosen to neglect amidoximes because they contain nitrogen affixed to the oxime carbon instead of hydrogen or another carbon, we therefore neglect nitrosohydroxylamines (now often called diazenium diolates with the functional group −N(NO)−OH or, more generally, its related anion, $-N(O)=NO^-$) with their nitroso group affixed to the hydroxylamine. We accordingly do not concern ourselves with whether they or their tautomer −N(O)=NOH is more stable. Accordingly, we ignore many important compounds widely used in the past and still used widely during the analytical chemical laboratory practicum that could be regarded as hydroxylamines: the compounds and their uses—precipitation, extraction, separation of a variety of elements—have been multifold. So doing, we do not further discuss rather famous species such as so-called cupferron, PhN(NO)OH, and neocupferron, 1-NpN(NO)OH, generally employed as their ammonium salts. Acknowledging the origin of these trivial names is 'cup + fer' reflecting their historical use in the analysis of copper and iron with their illogical symbols Cu and Fe, these and related reagents have been used in the study of other cations.

Having chosen to ignore amidoximes with the general formula $R^1C(NR^2R^3)=N-OH$ legitimizes our decision to ignore in this chapter *N*-hydroxytriazenes with their functionality $R^1N(OH)-N=N-R^2$ (or are they the tautomeric triazene *N*-oxides, $R^1N(O)=N-NH-R^2$?) because they are all *N*-substituted hydroxylamines.

Some references are given for the curious reader on amidoximes[11,12], on *N*-nitrosohydroxylamines[13,14] and on *N*-hydroxytriazenes[15,16].

III. THE COLLECTION OF THE REAGENTS AND ASSOCIATED ANALYTES

An overview of the use of oximes, hydroxamic acids and related reagents in inorganic analytical chemistry is presented in Tables S1–S6, listed for simplicity at the end of this chapter. The tables were prepared based on data from the *Dictionary of Analytical Reagents*[3] and some other, more recent, primary literature sources. The reagents in the tables were arranged according to the molecular formula based on the Hill sort scheme; the basic rule is that the number of carbons in a certain compound is followed by the number of hydrogens followed by all the other elements in alphabetical order. For each reagent a molecular formula and name next to types of determinations and elements determined with the particular reagent as well as the reference are given. However, details such as the stoichiometry and color of the reagent–analyte complex will not be presented.

The reagents are arranged according to the functional groups into monoximes (aldoximes, ketoximes and related species, Table S1), ketomonoximes (species not to

be confused with ketoximes, Table S2), dioximes including ketodioximes (Table S3), trioximes (Table S4), hydroxamic acids (Table S5) and thio derivatives of hydroxamic acids (Table S6)—structures of some selected reagents from each of 'structural' classes which can work as *specific* reagent for one analyte under certain reaction conditions only or *selective* reagent that work for only a few analytes are presented in Table 1.

In Tables S1–S6, we list the species of interest by class of compound and then by formula within it rather than by the analyte or methodology of analysis. For each species, the methods for which it was used are listed alphabetically and then for each method, the elements are listed alphabetically therein. In this chapter, we have not attempted to discuss regularities as to why a given reagent works better for a given analyte. Indeed, such patterns have scarcely been discussed in the literature—analytical chemistry is generally a rather empirically based discipline and remains so for the current chapter.

IV. PERIODIC TABLES

Tables S1–S6 show a wide diversity of the elements determined within an individual group of reagents. For the purpose of having a better idea on the applicability of these reagents, we decided to now present the number of reagents for the determination of each element in a set of periodic tables (Tables 2 and 3) that show the vast majority of metallic elements of the periodic table can be determined either by the use of oximes and/or hydroxamic acids.

V. A VERY BRIEF REVIEW OF OXIMES, HYDROXAMIC ACIDS AND RELATED SPECIES AS ANALYTICAL REAGENTS FOR THE STUDY OF ORGANIC ANALYTES[3,8–10]

Species of the type $R^1R^2C{=}NOH$, i.e. simple oximes, have long been used to derive the identity of 'unknown' aldehydes and ketones as found in a mixture of organic compounds. In general, oximes are readily formed by reaction of the carbonyl compound with NH_2OH, and then purified to allow for determination of the melting point of the solid derivative. Along with other solid derivatives (very often hydrazones of some persuasion), the unknown could be matched with but one among a long list of parent species and so identified. More recently *O*-functionalized counterparts have been studied including the trimethylsilyl ($(CH_3)_3Si-$) where derivatives other than OH groups have likewise been silylated, pentafluorobenzyl ($C_6F_5CH_2ON{=}$) and anthracenylmethyl ($C_{14}H_9CH_2ON{=}$) derivatives where the affixed groups allow for significantly higher volatility, facile electron capture and fluorescence photodetection, respectively as part of contemporary, and hence more sophisticated, separation and characterization protocols.

As befits the enhanced nucleophilicity of hydroxylamines (cf. the α effect), the reaction of hydroxylamine itself with esters, and a variety of other carboxylic acid derivatives, readily produce the corresponding hydroxamic acid (equation 4),

$$RCOX + NH_2OH \longrightarrow RCONHOH \tag{4}$$

Besides the use of this reaction to synthesize the plethora of species recorded in our table for hydroxamic acids, it provided a simple qualitative test, a resulting purple color, for the carboxylic acid species upon reaction with Fe^{III}. Although this test was not employed to distinguish which compound, the class-dependent wide variety of reactivity allowed for distinguishing esters, amides, anhydrides and occasionally the carboxylic acids themselves (after conversion to their acyl chloride).

Another aspect of organic analytic chemistry resulted from the reaction of aliphatic nitro compounds in alkaline media with 'nitrous acid'. Primary nitro compounds, i.e. species

TABLE 1. Structures of some specific and selective reagents from each of "structural" classes of oximes and hydroxamic acids [a]

Name	Formula	Structure
Monoximes		
Acetaldoxime (Ethylidenehydroxylamine) (**1**)	C_2H_5NO	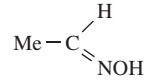
2-Pyridinecarboxaldehyde oxime (**2**)	$C_6H_6N_2O$	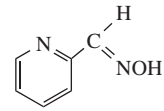
Salicylaldoxime (2-Hydroxybenzaldehyde oxime) (**3**)	$C_7H_7NO_2$	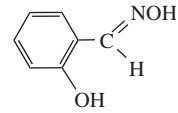
o-Vanillin oxime (2-Hydroxy-3-methoxybenzaldoxime) (**4**)	$C_8H_9NO_3$	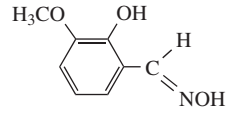
Cobaltone I (Biacetylmonoxime *p*-nitrophenylhydrazone) (**5**)	$C_{10}H_{12}N_4O_3$	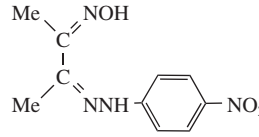
Ketomonoximes		
Violuric acid (2,4,5,6(1*H*,3*H*)-Pyrimidinetetrone 5-oxime) (**6**)	$C_4H_3N_3O_4$	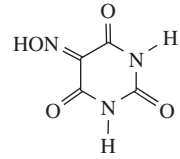
Ammonium violurate (**7**)	$C_4H_6N_4O_4$	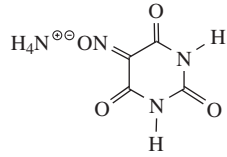
1*H*-Indole-2,3-dione 3-oxime (**8**)	$C_8H_6N_2O_2$	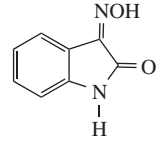

TABLE 1. (*continued*)

Name	Formula	Structure
Cupron ((*E*)-Benzoin oxime) (**9**)	$C_{14}H_{13}NO_2$	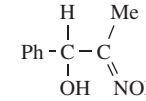
Dioximes including ketodioximes		
Chuagev's reagent (DMG) (Dimethylglyoxime) (**10**)	$C_4H_8N_2O_2$	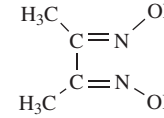
1,2-Cyclopentanedione dioxime (**11**)	$C_5H_8N_2O_2$	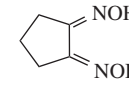
Neonickelone (Di(2-furyl)ethanedione dioxime) (**12**)	$C_{10}H_8N_2O_4$	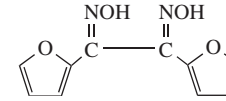
Palladon (1-Phenyl-1,2,3-butanetrione 2,3-dioxime) (**13**)	$C_{10}H_{10}N_2O_3$	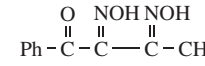
Trioximes		
2,3,4-Pentanetrione trioxime (**14**)	$C_5H_9N_3O_3$	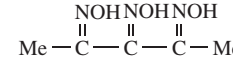
Niconoxime (Nicon) (1,2,3-Cyclohexanetrione trioxime) (**15**)	$C_6H_9N_3O_3$	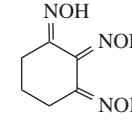
1,2,3-Indanetrione trioxime (**16**)	$C_9H_7N_3O_3$	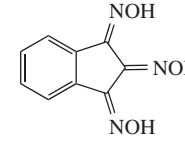
Hydroxamic acids		
Oxalohydroxamic acid (**17**)	$C_2H_4N_2O_4$	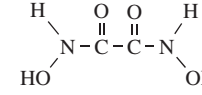
Nicoxamat (Heparit) (Nicotinohydroxamic acid) (**18**)	$C_6H_6N_2O_2$	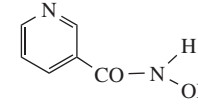

(*continued overleaf*)

TABLE 1. (*continued*)

Name	Formula	Structure
Caprylohydroxamic acid (Octanohydroxamic acid) (**19**)	$C_8H_{17}NO_2$	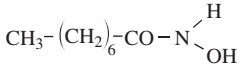
BPHA (*N*-Benzoyl-*N*-phenylhydroxylamine) (**20**)	$C_{13}H_{11}NO_2$	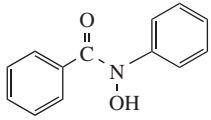
Thio derivatives of hydroxamic acids		
2*H*-1,4-Benzothiazine-2,3(4*H*)dione dioxime (**21**)	$C_8H_7N_3O_2S$	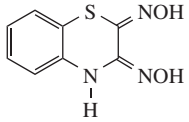
N-Phenylthiobenzohydroxamic acid (**22**)	$C_{13}H_{11}NOS$	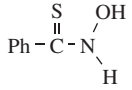
N,*N*′-Diphenylthiocarbamoyl-hydroxamic acid (**23**)	$C_{13}H_{14}N_2OS$	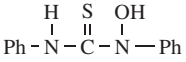

[a] No (*Z*)/(*E*)-stereochemistry is intended to be shown by our stuctures for either the reagent or any complex formed from it.

of the type RCH_2NO_2 and hence $[RCHNO_2]^-$, react to form unstable, but colorimetrically unequivocal, red-brown nitronate salts $[RC(NO)NO_2]^-$. Secondary nitro compounds, i.e. species of the type $R^1R^2CHNO_2$ and hence $[R^1R^2CNO_2]^-$, react to form the blue-green $R^1R^2C(NO)NO_2$ as befits their being monomeric nitroso species (earlier misnamed 'pseudonitroles'). Tertiary nitro compounds, species of the type $R^1R^2R^3CNO_2$, are unreactive here because they cannot form any related, hydrogen-abstracted anion in basic aqueous media. As such, the solution remains colorless and this reaction provides a simple analytical test (the so-called 'red-blue-white' reaction) for distinguishing the three classes of aliphatic nitro compounds.

VI. ANALYTICAL CHEMISTRY: A BRIEF OVERVIEW OF METHODS AND MATERIALS

Oximes, hydroxamic acids and related species are often used as reagents in inorganic analytical chemistry for precipitation, gravimetric and volumetric determinations as well as for preconcentration, extraction, derivatizations and subsequent determination of analyte using instrumental techniques. A brief review of analytical chemistry in general and of these species in particular follows.

The two major divisions of analytical chemistry are *qualitative* analysis, which provides information about the identity of atomic or molecular species or the functional groups in the sample, while *quantitative* analysis provides information on the amount of one or more of these components. Quantitative methods of analysis are often classified according to the

TABLE 2. Periodic system showing the number of reagents from the group of oximes with which a certain element can be determined. Superscripts denote the number of reagents considered as 'monooximes' (aldoximes, ketoximes and ketomonoximes) and subscripts denote the number of elements considered as dioximes

IUPAC Notation

1	2	3	4	5	6	7	8	9	10	11	12	13	14	15	16	17	18
Previous IUPAC Notation																	
IA	**IIA**	**IIIA**	**IVA**	**VA**	**VIA**	**VIIA**	**VIIIA**			**IB**	**IIB**	**IIIB**	**IVB**	**VB**	**VIB**	**VIIB**	**0**
H ^{1}																	**He**
Li ^{3}	**Be** ^{3}											**B**	**C**	**N**	**O**	**F**	**Ne**
Na ^{4}	**Mg** ^{2}											**Al** ^{1}	**Si**	**P**	**S**	**Cl**	**Ar**
K ^{4}	**Ca** ^{2}	**Sc** ^{3}	**Ti** ^{6}	**V** ^{14}	**Cr** $^{6}_{3}$	**Mn** $^{20}_{1}$	**Fe** $^{49}_{17}$	**Co** $^{65}_{16}$	**Ni** $^{55}_{45}$	**Cu** $^{78}_{22}$	**Zn** $^{9}_{1}$	**Ga**	**Ge**	**As**	**Se** ^{1}	**Br**	**Kr**
Rb ^{2}	**Sr** ^{2}	**Y** ^{3}	**Zr** ^{8}	**Nb** ^{3}	**Mo** ^{8}	**Tc***	**Ru** $^{11}_{1}$	**Rh** ^{7}	**Pd** $^{53}_{25}$	**Ag** ^{10}	**Cd** $^{6}_{1}$	**In**	**Sn** $^{2}_{1}$	**Sb** ^{1}	**Te** ^{1}	**I**	**Xe**
Cs ^{2}	**Ba** ^{2}	*	**Hf** ^{4}	**Ta** ^{3}	**W** ^{4}	**Re** $^{6}_{4}$	**Os** $^{9}_{3}$	**Ir** ^{6}	**Pt** $^{7}_{1}$	**Au** $^{8}_{5}$	**Hg** $^{3}_{1}$	**Tl** ^{2}	**Pb** $^{12}_{1}$	**Bi** $^{7}_{4}$	**Po***	**At***	**Rn***
Fr*	**Ra***	**	**Rf***	**Db***	**Sg***	**Bh***	**Hs***	**Mt***	**Ds***	**Rg***							

La ^{3}	**Ce** ^{3}	**Pr** $^{1}_{1}$	**Nd** ^{1}	**Pm***	**Sm** ^{1}	**Eu** ^{1}	**Gd** ^{1}	**Tb** ^{1}	**Dy** ^{1}	**Ho** ^{1}	**Er** ^{1}	**Tm** ^{1}	**Yb** ^{1}	**Lu** ^{1}	***Lanthanides**		
Ac*	**Th*** ^{5}	**Pa***	**U*** ^{10}	**Np***	**Pu***	**Am***	**Cm***	**Bk***	**Cf***	**Es***	**Fm***	**Md***	**No***	**Lr***	****Actinides**		

*Radioactive elements.

TABLE 3. Periodic system showing the number of reagents from the group of hydroxamic acids with which a certain element can be determined. Superscripts denote the number of reagents considered as hydroxamic acids and subscripts denote the number of elements considered as thiohydroxamic acids

IUPAC Notation

1	2	3	4	5	6	7	8	9	10	11	12	13	14	15	16	17	18
Previous IUPAC Notation																	
IA	IIA	IIIA	IVA	VA	VIA	VIIA	VIIIA			IB	IIB	IIIB	IVB	VB	VIB	VIIB	0
H																	He
Li	Be ^{1}											B	C	N	O	F	Ne
Na	Mg											Al ^{16}	Si	P	S	Cl	Ar
K	Ca ^{3}	Sc ^{2}	Ti $^{34}_{1}$	V $^{121}_{1}$	Cr ^{1}	Mn $^{17}_{1}$	Fe $^{35}_{2}$	Co ^{9}	Ni $^{5}_{3}$	Cu $^{25}_{5}$	Zn ^{2}	Ga ^{1}	Ge $^{2}_{13}$	As	Se	Br	Kr
Rb	Sr ^{1}	Y	Zr ^{10}	Nb $^{10}_{1}$	Mo $^{7}_{2}$	Tc* $_{1}$	Ru $_{3}$	Rh	Pd ^{3}	Ag	Cd ^{3}	In ^{2}	Sn ^{1}	Sb ^{1}	Te	I	Xe
Cs	Ba ^{1}	*	Hf ^{6}	Ta ^{6}	W ^{1}	Re	Os	Ir	Pt	Au	Hg ^{1}	Tl ^{1}	Pb ^{8}	Bi $^{2}_{1}$	Po*	At*	Rn*
Fr*	Ra*	**	Rf*	Db*	Sg*	Bh*	Hs*	Mt*	Ds*	Rg*							

La ^{13}	Ce ^{15}	Pr ^{8}	Nd ^{8}	Pm*	Sm ^{8}	Eu ^{7}	Gd ^{8}	Tb ^{7}	Dy ^{7}	Ho ^{7}	Er ^{7}	Tm ^{7}	Yb ^{7}	Lu ^{7}	*Lanthanides
Ac*	Th* ^{6}	Pa*	U* ^{17}	Np*	Pu*	Am*	Cm*	Bk*	Cf*	Es*	Fm*	Md*	No*	Lr*	**Actinides

*Radioactive elements.

nature of the final measurement as being *classical* or *instrumental*. This classification is largely historical and/or pedagogical with the introduction of classical methods preceding instrumental by a century or more.

A. Classification of Analytical Methods

1. Classical methods

In the early years of chemistry, most analyses were carried out by decomposing the samples and/or separating the components from the sample by ignition, fusion, precipitation or extraction. The sample or separated components were then treated with reagents that yielded products that could be recognized, and thereby distinguished, by color, boiling or melting point, solubility, odor, optical activity, refractive index or crystalline form. The amount of *analyte* was quantitatively determined by *gravimetric* or by *titrimetric* (also often called volumetric) methods which are now considered as classical methods—the calculations for classical analysis require no more information than experimentally measured weights (or weights and volumes), definite chemical reactions and atomic weights. Classical analysis is most useful for highly accurate and precise elemental determination at major levels (from about 1% up to essentially 100%) where instrumental analysis generally does not assure results with high accuracy and precision.

2. Instrumental methods

Early in the 20th century chemists began to research and exploit physical properties of the analyte properties, such as conductivity, electrode potential, light absorption or emission, mass-to-charge ratio and fluorescence for solving analytical problems. Classical principles remain useful in modern analytical instruments and methods. In comparison to classical methods the output of instrumental methods is a signal from which the result of the analyses is calculated. Instrumental analysis is most useful for elemental determinations at minor and trace levels (about 1% all the way down to 1 atom)—in this range classical analysis does not perform well.

The field of instrumental methods is being continuously expanded. Different methods can be combined into 'hybrid' or 'hyphenated' and 'multidimensional' methods. Methods can be divided according to the characteristic properties into methods based on:

(i) the interaction of analyte with electromagnetic radiation (over much of the known frequency/wavelength range) such as absorption, fluorescence, phosphorescence, luminescence and chemiluminescence spectroscopy,
(ii) electrical potential, charge, current or resistance,
(iii) mass,
(iv) mass-to-charge ratio,
(v) rate of reaction,
(vi) thermal characteristics such as thermal gravimetry and titrimetry, differential scanning colorimetry, differential thermal analysis and thermal conductometric methods,
(vii) radioactivity.

In addition to these methods there is also a group of instrumental methods used for separation and resolution of related compounds which are usually based on chromatography or electrophoresis. The final quantification of the analyte is conducted using one of the above methods.

B. Analytical Methods Based on the Use of Oximes and Hydroxamic Acids

Our review on the use of oximes and hydroxamic acids in inorganic analytical chemistry showed that these reagents are/were most frequently used for gravimetric determinations, determinations based on complexation, spectrophotometric determinations and separations, while their use for column separations, as electrode sensors, as supporting electrolytes or compounds that enhance sensitivity of determination is less common. Additionally, it was noticed that the analytical chemistry of anions is less advanced than that of cations and for this reason this chapter was limited to analytical chemistry of metallic cations.

1. Gravimetric methods

Gravimetric methods are based upon weight measurement. In principle we can distinguish between two basic types:

(i) *Precipitation methods* are based on the precipitation of analyte to form a poorly soluble precipitate which is filtered, washed and converted by heating to a product of known composition which is then weighed. Precipitation reactions are also frequently used in qualitative analysis or for separation of analyte or interfering components.

(ii) *Volatilization methods* are based on volatilization of analyte or its decomposition products at suitable temperature. The weight of volatile product or weight loss of the sample is then determined.

2. Determinations based on complexation

Complexation or chelation is a reaction of complexing agent, also called ligand or chelating agent (or chelator), with a metal ion during which metal complex or chelate is formed. A complexing agent is an ion or molecule that forms a covalent (dative) bond with a cation by donating a pair of electrons which are then shared by the ligand and the cation. The word 'ligand' is generic; the word 'chelating agent' is applied to bi-, tri- or multidentate species that multiply bind or tie the cation with its claws, to give the etymological origins of the mode of activity of these compounds.

Oximes and hydroxamic acids are frequently used as titrants, for masking, as metallochromic or chromogenic indicators as well as for spectrophotometric determinations.

3. Molecular absorption spectroscopy

Molecular absorption spectroscopy deals with measurement of the ultraviolet-visible spectrum of electromagnetic radiation transmitted or reflected by a sample as a function of the wavelength. Ordinarily, the intensity of the energy transmitted is compared to that transmitted by some other system that serves as a standard.

Beer's law serves as the basis for quantitative analyses and can be written as equation 5:

$$A = -\log T = -\log(\Phi/\Phi_0) = abc \tag{5}$$

where A is called the absorbance, T is the transmittance, a is the absorptivity, b is the pathlength of the absorption and c is the concentration of the absorbing species. Typical detection limits for molecular absorption spectroscopy range from 10^{-4} to 10^{-5} mol l^{-1}; however, with certain modifications this range can be even lower.

In comparison to UV-visible spectroscopy, IR absorption bands can be of great assistance in determining the molecular structure of a compound and of less importance for quantitative analysis.

4. Extraction of metal ions as chelates

Extraction can be used for separation or isolation of the analyte from the sample matrix or vice versa as well as a preconcentration method. Extraction of metal ions is based on the reaction of weak organic acids with metal ions that give uncharged complexes that are highly soluble in organic solvents as ethers, hydrocarbons, ketones and polychlorinated species (generally chloroform and carbon tetrachloride). The efficacy of the extraction is mainly dependent on the extent to which solutes distribute themselves between two immiscible solvents. The amounts of analyte can be determined spectrophotometrically as well as with other available analytical methods.

TABLE S1. Examples of monoximes used for determination of various elements

Molecular formula	Name	Type of determination	Elements	Reference
CH_3NO	Formaldoxime	Photometric	Ce, Fe, Mn, Ni, V	3
C_2H_5NO	Acetaldoxime (Ethylidenehydroxylamine) (**1**)	Colorimetric	Co, Cu, Ni	3
C_3H_7NO	Acetone oxime	Photometric	Pt	3
C_3H_7NO	Propanal oxime	Colorimetric	Pd	3
C_4H_9NO	Butanone oxime	Extraction	Ag	3
$C_5H_4BrNO_2$	5-Bromofurfural oxime	Extraction-spectrophotometric	Pd	17
$C_5H_4INO_2$	5-Iodofurfural oxime	Extraction-spectrophotometric	Pd	18
$C_5H_5NO_2$	3-Furancarboxaldehyde oxime	Extraction-photometric	Pd	3
C_5H_5NOSe	2-Selenophenecarboxaldehyde oxime	Amperometric-polarographic; Gravimetric	Pd; Pd	3
C_5H_5NOS	2-Thiophenecarboxaldehyde oxime	Gravimetric	Pd	3
$C_5H_{10}N_4OS$	2,3-Butanedione oxime thiosemicarbazone	Photometric	Bi, Co, Cu, Mn, Ni	3
$C_5H_{10}N_4O_2$	2,3-Butanedione oxime semicarbazone	Extraction-photometric	Co, Cu, Ni, Pd	3
$C_6H_6N_2O$	2-Pyridinecarboxaldehyde oxime (**2**)	Titrimetric	Fe	3
$C_6H_{10}N_2O_3$	*N*-[2-(Hydroxyimino)-1-methylpropylidene]glycine	Extraction-photometric; Gravimetric	Pd; Pd	3
$C_7H_5N_3O$	2-Pyridylcyanoxime	Extraction-photometric	Cu, Fe	3
$C_7H_6ClNO_2$	5-Chloro-2-hydroxybenzaldehyde oxime	Determination	Bi, Cu, Fe, Ni, Pb	3
$C_7H_6N_2O_4$	2-Hydroxy-5-nitrobenzaldehyde oxime	Determination; Gravimetric; Photometric	Bi, Cu, Ni, Pb; Ag, Cu, Pd; Ag, Pd	3
C_7H_7NO	α-Benzaldoxime ((*E*)-Benzaldoxime)	Precipitation	Co, Ni	3
$C_7H_7NO_2$	Furanylacroleinoxime	Extraction-photometric	Pd	19
$C_7H_7NO_2$	Salicylaldoxime (2-Hydroxybenzaldehyde oxime) (**3**)	Amperometric; Gravimetric; Nephelometric; Spectrophotometric; Volumetric	Cu, Pd; Bi, Cu, Fe, Ni, Pb, Pd, Zn; Cu, Pd; Fe, V; Cu, Pd	3, 5

(*continued overleaf*)

TABLE S1. (*continued*)

Molecular formula	Name	Type of determination	Elements	Reference
$C_7H_7NO_3$	Resorcylaldoxime (2,4-Dihydroxybenzaldehyde oxime)	Metallochromic indicator	Fe	3
$C_7H_7NO_3$	2,5-Dihydroxybenzaldehyde oxime	Gravimetric	Cu, Ni, Pd	3
$C_7H_8N_2O$	Acepox (2-Acetylpyridine monoxime)	Photometric	Re	3
$C_7H_{12}N_4OS$	Cyclohexane-1,2-dione oxime thiosemicarbazone	Spectrophotometric	Cu, Fe, Mn	20–22
$C_7H_{15}NO$	4-Heptanone oxime	Extraction-separation; Photometric	Ag, Au, Pd; Pd	3
$C_7H_{15}NO$	2,4-Dimethyl-3-pentanone oxime	Extraction-photometric	Pd	3
$C_8H_7Cl_2NO_2$	3′,5′-Dichloro-2′-hydroxy-acetophenone oxime	Complexing agent; Extraction-photometric; Gravimetric; Photometric	Be, Cd, Co, Mn, Ni, U, V, Zn; Co, V; Pd; Mn, U	3
$C_8H_7NO_4$	3-Oximinomethylsalicylic acid	Color reaction; Gravimetric; Precipitation	Co, Fe, Mo, U, Fe; Th; Ag, Bi, Cd, Cu, Hg, Ni, Pb, Th, Zn, Zr	23, 24
$C_8H_7NO_4$	5-Oximinomethylsalicylic acid	Precipitation	Th, Zr	24
$C_8H_8N_2O_4$	2-Nitro-*p*-anisaldoxime	Gravimetric; Photometric	Ag, Cu, Pd; Ag, Pd	3
$C_8H_8N_2O_4$	4-Nitro-*o*-anisaldoxime	Gravimetric; Photometric	Ag, Cu, Pd; Ag, Pd	3
C_8H_9NO	4-Methylbenzaldehyde oxime	Extraction-spectrophotometric	Pd	25
$C_8H_9NO_2$	2′-Hydroxyacetophenone oxime	Gravimetric; Metallochromic indicator	V; Fe	3
$C_8H_9NO_2$	4′-Hydroxyacetophenone oxime	Extraction-photometric; Simultaneous	Ni; Cu, Ni	3
$C_8H_9NO_2$	4-Methylsalicylaldoxime	Gravimetric	Cu	3
$C_8H_9NO_3$	2′,4′-Dihydroxyacetophenone oxime	Amperometric; Metallochromic indicator; Photometric	Cu, Ni; Fe; Au, Co, Fe	3, 26
$C_8H_9NO_3$	2′,5′-Dihydroxyacetophenone oxime	Amperometric	Cu, Ni, Pd	3
$C_8H_9NO_3$	2-Hydroxy-5-anisaldoxime	Gravimetric; Photometric	Cu, Ni, Pd; Mo	3
$C_8H_9NO_3$	3-Methoxy-4-hydroxybenzaldoxime	Gravimetric; Precipitation	Ni, Pd; Ni, Pd	3
$C_8H_9NO_3$	*o*-Vanillin oxime (2-Hydroxy-3-methoxybenzaldoxime) (**4**)	Spraying	Be, Co, Cr, Cu, Fe, Mn, Ni, Pd, Se, Th, Ti, U, V	27
$C_8H_9N_3O_2$	2-Oximinodimedone dithiosemicarbazone	Spectrophotometric	Fe	28
$C_8H_{10}N_2O$	(*E*)-2-Acetyl-4-methylpyridine monoxime	Photometric	Cu	3
$C_8H_{10}N_2O$	(*E*)-2-Acetyl-6-methylpyridine monoxime	Extraction-photometric; Photometric	Fe; Co, Cu	3
$C_8H_{10}N_2O_2$	(*Z*)-2-Acetyl-4-methoxypyridine monoxime	Extraction-photometric; Photometric	Fe; Co, Cu	3

TABLE S1. (*continued*)

Molecular formula	Name	Type of determination	Elements	Reference
$C_9H_7NOS_2$	Di(2-thienyl)ketoxime	Gravimetric; Nephelometric	Au, Pd; Pd	3
$C_9H_8N_2O_4$	*N*-Glyoxyloylanthranilic acid oxime	Photometric	Co	3
$C_9H_9N_5O$	2-[[1-(Hydroxyimino) ethyl]azo]-1*H*-benzimidazole	Photometric	Co, Cu	3
$C_9H_{10}ClNO_2$	5-Chloro-2-hydroxy-4-methylacetophenone oxime	Extraction-photometric; Gravimetric	V; V	3
$C_9H_{10}ClNO_2$	2-Hydroxy-4-chloro-5-methylacetophenone oxime	Extraction-spectrophotometric	Co, Cu, Ni	29
$C_9H_{10}N_2O_5$	2,4-Dihydroxy-5-nitropropiophenone	Gravimetric; Spectrophotometric	Co; Co	30
$C_9H_{10}N_4OS$	1-Phenyl-1,2-propanedione-2-oxime thiosemicarbazone	Spectrophotometric	Cu, Ni	31
$C_9H_{11}NO_2$	1-(2-Hydroxyphenyl)-1-propanone oxime	Gravimetric; Precipitation	Ti; Ti	3
$C_9H_{12}N_2O$	(*Z*)-2-Acetyl-4-ethylpyridine monoxime	Extraction-photometric; Photometric	Fe; Co, Cu	3
$C_9H_{12}N_4O$	2,3-Butanedione oxime 2-pyridylhydrazone	Extraction-photometric	Co, Pd	3
$C_9H_{13}NO_3$	1-(2,4-Dihydroxyphenyl)-1-propanone oxime	Metallochromic indicator; Photometric	Fe; Fe	3
$C_{10}H_8N_2OS$	2-Pyridyl-2-thienyl-β-ketoxime	Photometric	Co	3
$C_{10}H_9NO_4$	α-Furoinoxime (1,2-Di(2-furanyl)-2-hydroxyethanone oxime)	Photometric	Fe	3
$C_{10}H_{10}N_3O_4$	Biacetylmonoxime benzoylhydrazone	Spectrophotometric	Cu, Ni	32
$C_{10}H_{12}N_4OS$	1-Phenyl-1,2-propanedione-2-oxime thiosemicarbazone	Spectrophotometric	Ni	33
$C_{10}H_{12}N_4O_2$	3-Pyridine-[2-(hydroxyimino)-1-methylpropylidene]carboxylic acid	Fluorimetric	Hf, Ti, Zr	3
$C_{10}H_{12}N_4O_3$	Cobaltone I (Biacetylmonoxime *p*-nitrophenylhydrazone) (**5**)	Photometric	Co	3
$C_{10}H_{13}NO_2$	1-(2-Hydroxyphenyl)-1-butanone oxime	Extraction-photometric	Fe	3
$C_{10}H_{13}NO_3$	1-(2,4-Dihydroxyphenyl)-1-butanone oxime	Metallochromic indicator; Photometric	Fe; Fe	3
$C_{10}H_{13}NO_3$	2-Hydroxy-4-ethoxy-acetophenone oxime	Gravimetric	Zr	34
$C_{10}H_{13}NO_3$	2,4-Dihydroxy-5-ethyl-acetophenone oxime	Gravimetric	Te	35
$C_{10}H_{15}NOS$	3-Thioxocamphor oxime	Extraction-photometric	Pb	36
$C_{10}H_{16}ClNO_2$	2-Hydroxy-4-chloro-5-methylpropiophenone oxime	Spectrophotometric	U	37
$C_{10}H_{17}N_7OS_2$	5,5-Dimethyl-1,2,3-cyclohexanetrione 2-oxime 1,3-bis(thiosemicarbazone)	Photometric	Co, Cr, Fe, Ni	3
$C_{11}H_7N_3O$	2-Quinolylcyanoxime	Extraction-photometric	Cu, Fe	3

(*continued overleaf*)

TABLE S1. (*continued*)

Molecular formula	Name	Type of determination	Elements	Reference
$C_{11}H_9NO$	1-Naphthaldehyde oxime	Gravimetric	Pd	3
$C_{11}H_9NO_2$	2-Hydroxy-1-naphthaldehyde oxime	Complexing agent; Gravimetric; Extraction; Extraction-photometric	Ce; V; Mn; Ni, U	3, 38, 39
$C_{11}H_9N_3O$	Di-2-pyridinylmethanone oxime	Determination	Co, Fe, Pd	3
$C_{11}H_{10}N_4O$	α-(Hydroxyimino)-1,5-dimethyl-1*H*-benzimidazole-2-acetonitrile	Extraction-photometric	Fe	3
$C_{11}H_{11}N_3O_3S$	4-(2′-Thiazolylazo) resacetophenone oxime	Complexing agent; Photometric	Cu, Ni, Os, Pd, V; Th, U	40–42
$C_{11}H_{14}BrNO_3$	2,4-Dihydroxy-5-bromo-valerophenone oxime	Gravimetric; Photometric	Cu, Mn, Ni, Pd; Ni	43–45
$C_{11}H_{14}N_4O_3$	2,3-Pentanedione 3-oxime 2-nitrophenylhydrazone	Determination	Co	3
$C_{11}H_{14}N_4OS$	2-[2-(Hydroxyimino)-1-methylpropylidene-*N*-phenylhydrazinecarbothioamide (2,3-Butanedione oxime phenylthiosemicarbazone)	Photometric	Co, Mn	3
$C_{11}H_{15}NO_3$	1-(2,4-Dihydroxyphenyl)-1-pentanone oxime	Gravimetric	Cu, Ni	3
$C_{11}H_{15}NO_3$	2-Hydroxy-4-isopropoxy-acetophenone oxime	Gravimetric; Spectrophotometric	Mn; Mn	46
$C_{11}H_{16}N_2O$	1-(2-Pyridyl)-1-hexanone oxime	Extraction-photometric	Cu	3
$C_{12}H_{10}N_2O$	(*Z*)-2-Benzoylpyridine oxime	Extraction-photometric; Photometric	Au, Pd; Fe, Re	3
$C_{12}H_{11}NO_2$	1-Acetyl-2-naphthol oxime	Determination; Gravimetric	Cu; Mn, Ni, Pd	3
$C_{12}H_{11}NO_2$	2-Acetyl-1-naphthol oxime	Gravimetric	Cu, Mn, Ni, Pd	3
$C_{12}H_{11}NO_3$	Benzfuroin oxime (1-(2-Furanyl)-2-hydroxy-2-phenylethanone oxime)	Photometric	U	3
$C_{12}H_{11}N_3O$	3,4-Dihydro-1(2*H*)-phenazinone oxime	Photometric	Cu	3
$C_{12}H_{16}N_2O_5$	2-Hydroxy-4-*n*-butoxy-5-nitroacetophenone oxime	Gravimetric; Spectrophotometric	Ni; Ni	47
$C_{12}H_{17}NO_3$	2-Hydroxy-4-ethoxy-butyrophenone oxime	Gravimetric; Photometric	Pd; Pd	48
$C_{12}H_{17}NO_3$	2-Hydroxy-4-*n*-butoxy-acetophenone oxime	Gravimetric; Extraction-spectrophotometric	Cu; Cu	49, 50
$C_{12}H_{17}NO_3$	2-Hydroxy-4-isopropoxypro-piophenone oxime	Spectrophotometric	Fe	51
$C_{12}H_{19}NO_4$	1-(2-Oxocyclohexyl)-1,2-cyclohexanediol oxime	Electrode sensor	Co	52
$C_{13}H_9NO_3$	Dibenzo[b,e][1,4]dioxin-2-carboxaldehyde oxime	Extraction-photometric	Pd	3
$C_{13}H_9NO_2S$	2-Phenoxathiincarboxaldehyde oxime	Extraction-photometric	Pd	3
$C_{13}H_{11}NO_3$	2,4-Dihydroxybenzophenone oxime	Extraction-photometric	Pd	53
$C_{13}H_{12}N_2O$	(*E*)-2-Acetyl-4-phenylpyridine oxime	Photometric; Extraction-photometric	Co, Cu; Fe	3
$C_{13}H_{12}N_2O$	(*E*)-2-Acetyl-6-phenylpyridine oxime	Photometric	Cu	3
$C_{13}H_{12}N_2O$	(*E*)-2-Benzoyl-4-methylpyridine oxime	Photometric; Extraction-photometric	Co, Cu; Fe	3

TABLE S1. (*continued*)

Molecular formula	Name	Type of determination	Elements	Reference
$C_{13}H_{12}N_2O$	(*E*)-2-Benzoyl-6-methylpyridine oxime	Photometric	Cu	3
$C_{13}H_{13}NO_2$	2-Propanoyl-1-naphthol oxime	Gravimetric; Precipitation	Cu, Pd; Pd	3
$C_{13}H_{13}N_3O_2$	2-(4-Methoxyphenylazo) benzaldoxime	Photometric	Co	3
$C_{13}H_{19}NO_3$	2-Hydroxy-4-*n*-butoxy-propiophenone oxime	Spectrophotometric	Fe	44
$C_{13}H_{19}NO_3$	2-Hydroxy-4-ethoxy-valerophenone oxime	Spectrophotometric	Mo	54
$C_{14}H_{11}ClN_2O_3$	5-(*p*-Chlorophenylazo) resacetophenone	Chelating agent	Cu, Ni, Zn	55
$C_{14}H_{11}N_5O$	2-[[(Hydroxyimino) phenylmethyl]azo]-1*H*-benzimidazole	Photometric	Co, Cu, Mn, Ni	3
$C_{14}H_{11}N_5O_5$	Phenylglyoxal 2-oxime 1-(2,4-dinitrophenylhydrazone)	Photometric	Co	3
$C_{14}H_{12}N_4O_3$	Phenylglyoxal 2-oxime 1-(*p*-nitrophenylhydrazone)	Photometric	Co	3
$C_{14}H_{13}NO$	2-Hydroxy-5-methyl-benzophenone oxime	Photometric	Mo	56
$C_{14}H_{14}N_2O$	(*E*)-2-Benzoyl-4-ethylpyridine oxime	Extraction-photometric; Photometric	Fe; Co, Cu	3
$C_{14}H_{20}N_2O_2$	3-(Dimethylamino)-4-(2,5-dimethylphenyl)-2-butanone oxime	Extraction-spectrophotometric	Cu	57
$C_{14}H_{21}NO_2$	2-Hydroxy-4-*n*-butoxy-butyrophenone oxime	Gravimetric; Photometric	Ni; Ni	58
$C_{14}H_{21}N_3O_3S$	1-Phenylpropanone-1-pentylsulfonylhydrazone-2-oxime	Complexing agent	Cd, Co, Cu, Ni, Pb	59
$C_{15}H_{11}N_3O_2$	*O*-Methyl 9,10-Phenanthraquinone dioxime	Metallochromic indicator; Photometric	Cu; Cu, Os	3
$C_{15}H_{13}N_3O$	1-(Phenylmethyl)-1*H*-benzimidazole-2-carbox-aldehyde oxime	Extraction-photometric	Co, Cu	3
$C_{16}H_{13}N_7O$	Pyrazinyl-2-pyridinyl-ethanedione 2-(2-pyridinyl-hydrazone) 1-oxime	Photometric	Co, Cu, Fe, Ni	3
$C_{16}H_{13}N_7O$	2-Pyridinyl-4-pyrimidinylethanedione 2-oxime 1-(2-pyridinylhydrazone)	Photometric	Co, Cu, Fe, Ni	3
$C_{16}H_{15}N_5O$	2-[[1-(Hydroxyimino) ethyl]azo]-1-(phenylmethyl)-1*H*-benzimidazole	Photometric	Co, Cu, Mn, Ni	3
$C_{17}H_{14}ClNO_3$	2-Chloro-2′-hydroxy-4′-ethoxychalcone oxime	Gravimetric; Spectrophotometric	Cu; Cu	60
$C_{17}H_{14}N_6O$	Di-2-pyridinylethanedione oxime 2-pyridinylhydrazone	Photometric	Co, Cu, Fe, Ni	3
$C_{17}H_{15}NO$	1,5-diphenyl-1,4-pentadien-3-one oxime	Extraction-photometric	Cu	61
$C_{17}H_{17}NO_3$	1-(2-Hydroxy-5-methylphenyl)-3-(4-methoxyphenyl)-2-propen-1-one oxime	Gravimetric; Extraction-photometric	Cu, Ni, Pd; Cu, V	3
$C_{18}H_{14}N_2O$	(*E*)-2-Benzoyl-4-phenylpyridine oxime	Extraction-photometric; Photometric	Fe; Co, Cu	3

(*continued overleaf*)

TABLE S1. (*continued*)

Molecular formula	Name	Type of determination	Elements	Reference
$C_{18}H_{14}N_2O$	(*E*)-2-Benzoyl-6-phenylpyridine oxime	Photometric	Cu	3
$C_{18}H_{15}N_5O$	Di-2-pyridylethanedione monoxime phenylhydrazone	Photometric	Fe	3
$C_{18}H_{17}NO_3$	2′-Hydroxy-4′-ethoxy-4-methoxychalcone oxime	Gravimetric; Spectrophotometric	Cu; Cu	62
$C_{18}H_{19}N_5O$	2-[[1-(Hydroxyimino)-2-methylpropyl]azo]-1-(phenylmethyl)-1*H*-benzimidazole	Photometric	Co, Cu, Ni	3
$C_{19}H_{13}N_3O$	2,2′-Diquinolylketoxime	Extraction-photometric	Co	3
$C_{21}H_{17}N_5O$	2-[[(Hydroxyimino) phenylmethyl]azo]-1-(phenylmethyl)-1*H*-benzimidazole	Photometric	Co, Cu, Mn, Ni, Pb	3

TABLE S2. Examples of ketomonoximes used for determination of various elements

Molecular formula	Name	Type of determination	Elements	Reference
$C_3H_5NO_2$	MNA (Methylglyoxal 1-oxime) (Isonitrosoacetone)	Determination	Cd, Co, Cu, Fe, Hg, Mn, Pb, Sn, Zn	3
$C_4H_3N_3O_4$	Violuric acid (2,4,5,6(1*H*,3*H*)-Pyrimidinetetrone 5-oxime) (**6**)	Colorimetric; Complexing agent; Extraction-photometric; Gravimetric; Precipitation; Separation; Spectrophotometric; Spot test	Ca, K, Li, Mg, Na, Sr; Co, Cu, Fe; Co; Pd; Fe, Pb; K, Na; Co, Fe, Na, Ni; Ba, Ca, Cd, Co, Cs, Li, Pb, Rb, Sr, Tl, U, Zn	63–76
$C_4H_3N_3O_3S$	Thiovioluric acid (Dihydro-2-thioxo-4,5,6(1*H*)-pyrimidinetrione 5-oxime)	Photometric	Co, Fe	3
$C_4H_4N_4O_4$	Isonitrosomalonylguanidine (2-Amino-4,5,6-(1*H*)-pyrimidinetrione 5-oxime)	Photometric	Co	3
$C_4H_6N_4O_4$	Ammonium violurate (**7**)	Metallochromic indicator	Co, Ni	77, 78
$C_4H_7NO_2$	2,3-Butanedione monoxime	Photometric	Re	3
$C_5H_7NO_3$	2,3,4-Pentanetrione 3-oxime	Color reactions; Extraction-photometric	Co, Cu, Fe, Ni; Pd	3
$C_6H_5NO_2$	2-Nitrosophenol (*o*-Benzoquinone monoxime)	Acid-base indicator; Metallochromic indicator	H; Co, Cu, Fe, Ni, Zn	3
$C_6H_5NO_3$	2-Hydroxy-1,4-benzoquinone 1-oxime (4-Hydroxy-1,2-benzoquinone 1-oxime)	Photometric	Ag	3

TABLE S2. (*continued*)

Molecular formula	Name	Type of determination	Elements	Reference
$C_6H_7N_3O_4$	Dimethylvioluric acid (2,4,5,6(1*H*,3*H*)-Pyrimidinetetrone 1,3-dimethyl 5-oxime)	Titration	Be, Cs, K, Li, Mg, Na, Rb	79
$C_6H_9NO_4$	2,3-Dioxobutanoic acid 2-oxime ethyl ester	Extraction-photometric	Pd, Ru	3
$C_7H_7NO_3$	3-Methoxy-4-nitrosophenol	Photometric	Co, Fe	3
$C_8H_6N_2O_2$	1*H*-Indole-2,3-dione 3-oxime (**8**)	Electrode sensor; Photometric	Li, Tl; Transition metals	3, 80
$C_8H_7NO_2$	Phenylglyoxal 1-oxime (α-Isonitrosoacetophenone)	Determination	Co, Mn, Ni, Pb	3
$C_8H_7NO_3$	2-Oxo-4′-hydroxyphenyl-acetaldehyde oxime	Complexing agent; Extraction-photometric	Co, Ni, Pd; Pd	81, 82
$C_8H_9NO_4$	3-Acetyl-6-methyl-2*H*-pyran-2,4(3*H*)-dione oxime (Dehydracetic acid oxime)	Spectrophotometric	Co, Cu	83, 84
$C_8H_{11}NO_3$	5,5-Dimethyl-1,2,3-cyclohexanetrione 2-oxime (Isonitrosodimedone)	Gravimetric; Extraction-photometric	Co; Co	3
$C_9H_5NO_4$	Oximidobenzotetronic acid (3-Nitroso-4-hydroxycoumarin) (2*H*-1-Benzopyran-2,3,4-trione 3-oxime)	Gravimetric; Metallochromic indicator; Separation and determination; Spectrophotometric; Spot test	Fe; Fe; Pd, Ru; Cu, Ir, Os, Pt, Th; Co, Cu, Fe	85–90
$C_9H_6N_2O_2$	8-Hydroxy-5-nitrosoquinoline (5,8-Quinolinedione 5-oxime)	Photometric	Zn	3
$C_9H_6N_2O_3$	5-Oxo-4-oximino-3-phenylisoxazoline	Separation	K, Na	70
$C_9H_6N_2O_3$	2,3,4(1*H*)-Quinolinetrione 3-oxime	Photometric	Os	3
$C_9H_7NO_2$	1,2-Indanedione 2-oxime	Extraction-photometric; Precipitation	Pt; Pd	3, 91
$C_9H_7N_3O_2$	3-Phenyl-1*H*-pyrazole-4,5-dione 4-oxime	Gravimetric	Cu	3
$C_9H_{14}N_4O_2S$	5,5-Dimethyl-1,2,3-cyclohexanetrione 2-oxime 3-thiosemicarbazone	Photometric	Cu, Fe	3
$C_{10}H_6ClNO_2$	4-Chloro-1,2-naphthoquinone 2-oxime	Determination; Extraction-photometric	Fe; Ni	3
$C_{10}H_7NO_2$	1,2-Naphthoquinone 1-oxime (1-Nitroso-2-naphthol)	Complexing agent; Extraction-photometric; Gravimetric; Separation	Transition and rare earth metals; Co, Fe, Mo, U; Co; U	3
$C_{10}H_7NO_2$	1,2-Naphthoquinone 2-oxime (2-Nitroso-1-naphthol)	Complexing agent; Extraction-photometric	Transition metals; Co, Ni, Pd, Ru	3
$C_{10}H_7NO_4$	Di(2-furyl)ethanedione monoxime (Furil monoxime)	Photometric	Co, Ru	3

(*continued overleaf*)

TABLE S2. (*continued*)

Molecular formula	Name	Type of determination	Elements	Reference
$C_{10}H_9N_3O_2$	3-Methyl-1-phenyl-1*H*-pyrazole-4,5-dione 4-oxime	Gravimetric; Precipitation	Cu; Bi, Co, Cu, Fe, Sb	3
$C_{10}H_{10}BrNO_2$	1-(4-Bromophenyl)-1,3-butanedione 3-oxime	Extraction-photometric	Pd, Ru	3
$C_{10}H_{10}ClNO_2$	1-(4-Chlorophenyl)-1,3-butanedione 3-oxime	Extraction-photometric	Pd, Ru	3
$C_{11}H_9NO_3$	2-Hydroxy-3-methyl-1,4-naphthoquinone monoxime	Extraction-photometric; Photometric	Rh; Ni	3, 92
$C_{11}H_9NO_3$	3-Hydroxy-2-methyl-1,4-naphthoquinone 4-oxime	Photometric	Ir, Rh	93
$C_{12}H_7NO_2$	Acenaphthenequinone monoxime	Photometric	Ir, Os, Pt, Rh, Ru	3, 94
$C_{12}H_9N_3O_2$	Di-2-pyridylethanedione monoxime	Photometric	Co	3
$C_{14}H_9NO_2$	9,10-Phenanthraquinone monoxime	Photometric	Co, Os, Rh, Ru	3
$C_{14}H_{13}NO_2$	Cupron ((*E*)-Benzoin oxime) (**9**)	Complexing; Electrode material; Extraction-separation; Photometric; Precipitation	Mo; Pb; Mo, V, W; Cr, Pd; Au, Bi, Cu, Pd	3, 95–99
$C_{15}H_{11}N_3O_3$	3-Phenylquinazolin-4(3*H*)-one-2-carboxaldoxime	Complexing agent; Gravimetric	Cu, Ni, Pd; Cu, Ni, Pd	100, 101
$C_{16}H_{11}N_3O_3S$	Diphenylthiovioluric acid (Dihydro-2-thioxo-4,5,6(1*H*)-pyrimidinetrione 5-oxime)	Extraction-photometric	Co, Ru	3
$C_{16}H_{11}N_3O_4$	Diphenylvioluric acid (1,3-Diphenyl-5-nitrosobarbituric acid) (1,3-Diphenyl-2,4,5,6(1*H*,3*H*)-pyrimidinetetrone 5-oxime)	Photometric; Spraying	Co; Al, Ba, Ca, Cd, Co, Cu, Hg, K, Na, Mn, Ni, Pb, Sr, Sn, U, Zn, Zr	3, 102
$C_{16}H_{16}N_2O_2$	α-Oximinobenzoyl-*m*-methylacetanilide	Metallochromic indicator	Cu	103
$C_{16}H_{16}N_2O_2$	α-Oximinobenzoyl-*p*-methylacetanilide	Metallochromic indicator	Cu	103
$C_{17}H_{12}N_2O_2$	1-(2-Quinolyl)-2-phenylglyoxal-2-oxime	Electrode sensor	Cu	104
$C_{17}H_{16}N_4O_3$	α-Oximinoacetoacetanilide benzoylhydrazone	Spectrophotometric	Co, Ni, Pd	105, 106
$C_{17}H_{16}N_4O_4$	α-Oximinoacetoacetanilide	Spectrophotometric	Pd	107
$C_{18}H_{15}N_3O_3S$	2-Thio-1,3-di-*o*-tolylalloxan 5-oxime	Spot test	Fe	108
$C_{18}H_{15}N_3O_3S$	2-Thio-1,3-di-*p*-tolylalloxan 5-oxime	Spot test	Fe	108
$C_{18}H_{18}N_4O_4$	α-Oximinoacet-*o*-toluidide	Spectrophotometric	Pd	107
$C_{21}H_{16}N_6O_3$	1-Benzyl-2-(α-hydroxyimino-4-nitrobenzyl)-1*H*-imidazole	Photometric	Co, Cu, Ni	3
$C_{22}H_{15}NO_2$	1,2-Di(1-naphthalenyl)-1,2-ethanedione monoxime	Extraction-photometric	Co	3

TABLE S3. Examples of dioximes used for determination of various elements

Molecular formula	Name	Type of determination	Elements	Reference
$C_2H_4N_2O_2$	Glyoxime (Ethanedialdoxime)	Determination; Separation and determination	Ni; Pd	3
$C_3H_4N_2O_3$	2-Oxopropanedial 1,3-dioxime	Color reaction	Fe	3
$C_3H_6N_2O_2$	2-Oxopropanal dioxime	Photometric	Cd, Co, Cu, Fe, Hg, Mn, Ni, Pb, Re, Sn, Zn	3
$C_4H_8N_2O_2$	Chuagev's reagent (DMG) (Dimethylglyoxime) (**10**)	Gravimetric; Photometric; Separation by extraction or precipitation	Ni, Pd; Co, Cu, Fe, Ni, Pd, Re; Ni, Pd, Pt	3, 109
$C_5H_8N_2O_2$	1,2-Cyclopentanedione dioxime (**11**)	Gravimetric	Ni	3
$C_5H_{10}N_2O_2$	Ethylmethylglyoxime (2,3-Pentanedione dioxime)	Extraction-photometric	Ni	3
$C_5H_{10}N_2O_2$	2,4-Pentanedione dioxime	Photometric	Cu	3
$C_6H_{10}N_2O_2$	Nioxime (1,2-Cyclohexanedione dioxime)	Extraction-photometric	Fe, Ni	3
$C_6H_{12}N_2O_2$	(*E*,*Z*)-2,5-Hexanedione dioxime	Color reactions	Ni, Pd	3
$C_7H_{10}N_2O_4$	4-Carboxynioxime (3,4-Dioxocyclohexanecarboxylic acid dioxime)	Extraction-photometric	Ni	3
$C_7H_{12}N_2O_2$	1,2-Cycloheptanedione dioxime	Gravimetric	Bi, Ni, Pd	3
$C_7H_{12}N_2O_2$	3-Methylnioxime (3-Methyl-1,2-cyclohexanedione dioxime)	Gravimetric; Extraction-photometric	Bi, Ni, Pd; Ni	3
$C_7H_{12}N_2O_2$	4-Methylnioxime (4-Methyl-1,2-cyclohexanedione dioxime)	Extraction-photometric; Gravimetric; Photometric	Pd; Bi, Ni, Pd; Re	3
$C_8H_8N_2O_2$	Phenylglyoxime	Photometric	Co	3
$C_8H_{14}N_2O_2$	1,2-Cyclooctanedione dioxime	Gravimetric	Bi, Ni, Pd	3
$C_8H_{14}N_2O_2$	5,5-Dimethyl-1,3-cyclo-hexanedione dioxime	Photometric	Co	3
$C_8H_{16}N_2O_2$	4,5-Octanedione dioxime	Color reactions	Ni, Pd	3
$C_9H_7N_3O_2$	5,8-Quinolinedione dioxime	Extraction-photometric	Co	3
$C_9H_{11}N_3O_2$	2,6-Diacetylpyridine dioxime	Photometric	Cu, Fe	
$C_9H_{11}N_3O_2$	2,6-Pyridinediacetaldehyde dioxime	Photometric	Cu, Fe, Ni	
$C_9H_{15}N_5O_2S$	2-[2,3-Bis(hydroxyimino)-5,5-dimethylcyclohexylidene] hydrazinecarbothioamide	Extraction-photometric	Fe	3
$C_9H_{16}N_2O_2$	1,2-Cyclononanedione dioxime	Gravimetric	Bi, Ni, Pd	3
$C_9H_{16}N_2O_2$	4-Isopropyl-1,2-cyclohex-anedione dioxime	Extraction-photometric	Ni	3
$C_{10}H_7BrN_2O_2$	6-Bromo-1,2-naphthoquinone dioxime	Extraction-photometric	Ni	3
$C_{10}H_7ClN_2O_2$	4-Chloro-1,2-naphthoquinone dioxime	Extraction-photometric	Ni	3
$C_{10}H_7ClN_2O_2$	6-Chloro-1,2-naphthoquinone dioxime	Extraction-photometric	Ni	3
$C_{10}H_8N_2O_2$	1,2-Naphthoquinone dioxime	Extraction-photometric	Co, Fe, Ni	3
$C_{10}H_8N_2O_3$	5-Hydroxy-1,2-naphthoquinone dioxime	Extraction-photometric	Ni	3
$C_{10}H_8N_2O_4$	Neonickelone (Di(2-furyl)ethanedione dioxime) (**12**)	Extraction-photometric	Co, Ni, Pd, Re	3

(*continued overleaf*)

TABLE S3. (*continued*)

Molecular formula	Name	Type of determination	Elements	Reference
$C_{10}H_8N_2O_5S$	1,2-Naphthoquinone-4-sulfonic acid dioxime	Extraction-photometric	Co, Cu, Fe, Ni	3
$C_{10}H_8N_2O_5S$	1,2-Naphthoquinone-5-sulfonic acid dioxime	Extraction-photometric	Ni	3
$C_{10}H_8N_2O_5S$	1,2-Naphthoquinone-6-sulfonic acid dioxime	Extraction-photometric	Ni	3
$C_{10}H_8N_2O_5S$	1,2-Naphthoquinone-7-sulfonic acid dioxime	Extraction-photometric	Ni	3
$C_{10}H_{10}N_2O_2$	3-Methyl-1,2-indanedione dioxime	Precipitation	Au, Co, Cu, Fe, Pd	3
$C_{10}H_{10}N_2O_3$	Palladon (1-Phenyl-1,2,3-butanetrione 2,3-dioxime) (**13**)	Gravimetric	Pd	3
$C_{10}H_{12}N_2O_2$	1-Phenyl-1,3-butanedione dioxime	Determination	Ni, Pd	3
$C_{10}H_{18}N_2O_2$	4-*tert*-Butylnioxime (4-*tert*-Butyl-1,2-cyclohexanedione dioxime)	Extraction-photometric; Gravimetric	Ni; Bi, Ni, Pd	3
$C_{10}H_{18}N_2O_2$	1,2-Cyclodecanedione dioxime	Extraction-photometric; Gravimetric	Ni; Bi, Co, Cu, Pd	3
$C_{10}H_{18}N_4O_2$	3,3′-(1,2-Ethanediyldinitrilo) bis-2-butanone dioxime	Gravimetric	Ni, Pd	3
$C_{11}H_{12}N_2O_2$	3,3-Dimethyl-1,2-indanedione dioxime	Precipitation	Au, Cu, Ni, Os, Pd	3
$C_{11}H_{20}N_2O_2$	1,2-Cycloundecanedione dioxime	Gravimetric	Bi, Ni, Pd	3
$C_{12}H_7N_3O_4$	5-Nitro-1,2-acenaphthyl-enedione dioxime	Extraction-photometric	Co, Cu, Fe	3
$C_{12}H_8N_2O_2$	Acenaphthenequinone dioxime	Extraction-photometric	Co, Cu, Ni	3
$C_{12}H_{10}N_4O_2$	Di-2-pyridinylethanedione dioxime	Extraction-photometric	Au, Fe	3
$C_{12}H_{22}N_2O_2$	1,2-Cyclododecanedione dioxime	Gravimetric	Bi, Ni, Pd	3
$C_{12}H_{23}N_5O_2$	3-{[2-(2-Hydroxyimino-1-methylpropylideneamino)-ethylamino]-ethylimino}-butan-2-one oxime	Spectrophotometric	Cu	110
$C_{13}H_{28}N_4O_2$	*meso*-3,6,6,9-Tetramethyl-4,8-diazaundecane-2,10-dione dioxime	Spectrophotometric	Cu	111
$C_{14}H_{10}Cl_2N_2O_2$	Bis(4-chlorophenyl)ethanedione dioxime	Extraction-photometric	Co, Cu, Ni	3
$C_{14}H_{10}N_2O_2$	9,10-Phenanthraquinone dioxime	Photometric	Co, Cu, Fe, Ni	3
$C_{14}H_{10}N_4O_6$	Bis(4-nitrophenyl)ethanedione dioxime	Extraction-photometric	Cu, Ni	3
$C_{14}H_{11}BrN_2O_2$	4-Bromobenzil dioxime	Extraction-photometric	Cu, Fe, Ni	3
$C_{14}H_{11}ClN_2O_2$	(4-Chlorophenyl)phenyl-ethanedione dioxime	Extraction-photometric	Cu, Fe, Ni	3
$C_{14}H_{11}N_3O_4$	(4-Nitrophenyl)phenyl-ethanedione dioxime	Extraction-photometric	Cu, Ni	3
$C_{14}H_{12}N_2O_2$	(*E*,*E*)-Diphenylglyoxime (α-Benzil dioxime)	Extraction-photometric	Fe, Ni	3
$C_{14}H_{18}N_4O_2$	Bis(2-hydroxyimino-3-butylidene)-*o*-phenylenediimine	Gravimetric	Ni, Pd	3
$C_{15}H_{12}N_2O_2$	3-Phenyl-1,2-indanedione dioxime	Precipitation	Au, Co, Cu, Ni, Os, Pd	3
$C_{15}H_{14}N_2O_2$	1,3-Diphenyl-1,3-propanedione dioxime	Extraction-photometric	Pd, Ru	3

TABLE S3. (*continued*)

Molecular formula	Name	Type of determination	Elements	Reference
$C_{16}H_{12}N_2O_6$	*o*,*o*′-Oxaloxybis(benzaldoxime)	Electrode sensor	Cr	112
$C_{16}H_{14}N_2O_2$	3-Methyl-3-phenyl-1,2-indanedione dioxime	Precipitation	Au, Co, Cu, Fe, Ni, Os, Pd, Pr	3
$C_{16}H_{18}N_4O_4$	*N*,*N*′-Ethylenebis(4-methoxy-1,2-benzoquinone 2-imine) dioxime	Extraction-photometric	Pd	3
$C_{18}H_{20}N_4O_2$	3-[(8-{[(*E*)-2-hydroxyimino-1-methylpropylidene]amino}-1-naphthyl)imino]-2-butanone oxime	Extraction	Cu, Ni	113
$C_{20}H_{16}N_2O_6$	*o*,*o*′-Succinyloxybis (benzaldoxime)	Electrode sensor	Cr	112
$C_{21}H_{16}N_2O_2$	3,3-Diphenyl-1,2-indanedione dioxime	Precipitation	Pd	3
$C_{22}H_{16}N_2O_6$	*o*,*o*′-Isophthaloxybis (benzaldoxime)	Electrode sensor	Cr	112

TABLE S4. Examples of trioximes used for determination of various elements

Molecular formula	Name	Type of determination	Elements	Reference
$C_5H_9N_3O_3$	2,3,4-Pentanetrione trioxime (**14**)	Photometric	Fe	3
$C_6H_9N_3O_3$	Niconoxime (Nicon) (1,2,3-Cyclohexanetrione trioxime) (**15**)	Photometric	Co, Ni	3
$C_9H_7N_3O_3$	1,2,3-Indanetrione trioxime (**16**)	Photometric	Co, Pd	3, 114

TABLE S5. Examples of hydroxamic acids used for determination of various elements

Molecular formula	Name	Type of determination	Elements	Reference
CH_3NO_2	Formohydroxamic acid	Photometric	Fe	115
$C_2H_2Cl_3NO_2$	2,2,2-Trichloroacetohydroxamic acid	Extraction-photometric	Mo	3
$C_2H_4N_2O_4$	Oxalohydroxamic acid (**17**)	Colorimetric; Complexing agent	Ca, Fe, Th, U, Zr; Th, Zr	3, 116–120
$C_2H_5NO_2$	Acetohydroxamic acid	Photometric	Fe	121
$C_4H_5NO_4K_2$	*N*-Hydroxysuccinamic acid, potassium salt	Photometric	Fe, Mn, Ti, V	3
$C_4H_9NO_2$	Butyrohydroxamic acid	Photometric	V	3
$C_5H_5N_3O_2$	Pyrazinohydroxamic acid	Gravimetric	La	122
$C_5H_{11}NO_2$	Trimethylacetohydroxamic acid	Color reactions	Cu, Fe, U, V, Ti	3
$C_6H_6N_2O_2$	Nicoxamat (Heparit) (Nicotinohydroxamic acid) (**18**)	Color reactions; Extraction-photometric	Fe, Mo, V; Mn, V	3
$C_6H_9NO_2$	Sorbohydroxamic acid	Photometric	V	3
$C_6H_{13}NO_2$	Hexanohydroxamic acid	Photometric	V	3
$C_7H_6BrNO_2$	*p*-Bromophenylhydroxamic acid	Column separation	Cu, Ni from Co, U from Cr	3

(*continued overleaf*)

TABLE S5. (*continued*)

Molecular formula	Name	Type of determination	Elements	Reference
$C_7H_6BrNO_3$	5-Bromosalicylhydroxamic acid	Extraction-photometric	V	3
$C_7H_6ClNO_2$	4-Chlorobenzohydroxamic acid	Photometric	V	3
$C_7H_6N_2O_4$	*p*-Nitrobenzohydroxamic acid	Photometric	V	3
$C_7H_7NO_2$	Benzohydroxamic acid	Extraction-photometric; Precipitation	Co, Mo, Ni, V; Al, Cd, Cu, In, Th, Zr	3
$C_7H_7NO_3$	Salicylhydroxamic acid	Extraction-photometric	Ce, Ti, V	3, 123
$C_7H_8N_2O_2$	Anthranilohydroxamic acid	Extraction-photometric	Re	124
$C_7H_8N_2O_2$	Anilinohydroxamic acid	Color reactions	Fe, Os, U	3
$C_8H_9NO_2$	*N*-Hydroxy-*N*-phenylacetamide	Precipitation	Nb	3
$C_8H_9NO_3$	*p*-Methoxybenzohydroxamic acid	Extraction-photometric	V	3
$C_8H_9NO_3$	Mandelohydroxamic acid, ±-form	Photometric	Fe	3
$C_8H_{10}N_2O$	*N*-Hydroxy-4-methylbenzene-carboximidamide	Extraction-photometric	Co	3
$C_8H_{17}NO_2$	Caprylohydroxamic acid (Octanohydroxamic acid) (**19**)	Photometric	V	3
$C_9H_9NO_2$	Cinnamohydroxamic acid	Complexing agent; Gravimetric	Fe; Fe	3
$C_{10}H_{10}ClNO_2$	*N*-(*p*-Chlorophenyl) crotonohydroxamic acid	Extraction-photometric	V	3
$C_{10}H_{10}N_2O_2$	3-Indoleacetohydroxamic acid	Extraction-photometric	V	125
$C_{10}H_{11}NO_2$	*N*-Phenylcrotonohydroxamic acid	Extraction-photometric	V	3
$C_{11}H_8ClNO_2S$	*N*-3-Chlorophenyl-2-thenoylhydroxamic acid	Extraction-photometric	Sn, U	3
$C_{11}H_8ClNO_2S$	*N*-4-Chlorophenyl-2-thenoylhydroxamic acid	Extraction-photometric	Sn, V	3
$C_{11}H_8ClNO_3$	*N*-*p*-Chlorophenyl-2-furohydroxamic acid	Extraction-photometric	Ge, Sn, Tl	3, 126
$C_{11}H_8ClNO_3$	*N*-(3-Chlorophenyl)-*N*-hydroxy-2-furancarboxamide	Extraction-photometric	Sn	3
$C_{11}H_9NO_2$	2-Naphthohydroxamic acid	Photometric	V	3
$C_{11}H_9NO_2S$	*N*-Phenyl-2-thenoylhydroxamic acid	Extraction-photometric	V	3
$C_{11}H_9NO_3$	3-Hydroxy-2-naphtho-hydroxamic acid	Photometric	V	3
$C_{11}H_9NO_3$	*N*-Furoyl-*N*-phenyl-hydroxylamine	Gravimetric; Extraction-photometric; Photometric	Cu, Fe, Ni, V; V; Ti	3, 127
$C_{11}H_{13}NO_2$	*N*-Hydroxy-*N*-(4-methylphenyl)-2-butenamide	Extraction-photometric	V	3
$C_{11}H_{15}NO_2$	*N*-Phenyl-*n*-valerohydroxamic acid	Extraction-photometric	V	3
$C_{12}H_7NO_3$	Naphthalhydroxamic acid	Photometric	Ca	3
$C_{12}H_{11}NO_2$	1-Naphthoacetohydroxamic acid	Color reactions	Cu, Fe, Os, Ti, U, V	3
$C_{12}H_{11}NO_3$	*N*-(4-Methylphenyl)-*N*-hydroxy-2-furancarboxamide	Extraction-photometric	Ce, V	3
$C_{12}H_{11}NO_2S$	*N*-*p*-tolyl-2-thenoylhydroxamic acid	Extraction-photometric	V	3
$C_{12}H_{12}ClNO_2$	*N*-(4-Chlorophenyl)-*N*-hydroxy-2,4-hexadienamide	Extraction-photometric	V	3
$C_{12}H_{13}NO_2$	*N*-Phenylsorbohydroxamic acid	Extraction-photometric	Ti, V	3
$C_{12}H_{17}NO_2$	*N*-Phenylhexanohydroxamic acid	Extraction-separation; Photometric	Co, Ni, Pb, Zn; V	3

TABLE S5. (*continued*)

Molecular formula	Name	Type of determination	Elements	Reference
$C_{12}H_{25}NO_2$	Laurohydroxamic acid	Photometric	V	3
$C_{13}H_8ClN_3O_6$	*N*-(4-Chlorophenyl)-*N*-hydroxy-3,5-dinitrobenzamide	Extraction-photometric	Co, Cu, Fe, Ti, V	3
$C_{13}H_9Cl_2NO_2$	*N*-(2,4-Dichlorobenzoyl) phenylhydroxylamine	Precipitation	Al, Cu, Fe, Hf, Mn, Pb, Sn, Ti, Zr	3
$C_{13}H_9N_3O_6$	*N*-Hydroxy-3,5-dinitro-*N*-phenylbenzamide	Photometric; Precipitation	U; Al, Cu, Fe, Hf, Mn, Pb, Sn, Ti, Zr	3
$C_{13}H_{10}BrNO_2S$	*N*-*p*-Bromophenyl-2-thienylacrylohydroxamic acid	Extraction-photometric	V	3
$C_{13}H_{10}BrNO_3$	*N*-*p*-Bromophenyl-2-furylacrylohydroxamic acid	Photometric	Ge	128
$C_{13}H_{10}ClNO_2$	*N*-(2-Chlorophenyl)-*N*-hydroxybenzamide	Gravimetric	Fe	3
$C_{13}H_{10}ClNO_2$	*N*-(3-Chlorophenyl)-*N*-hydroxybenzamide	Extraction-photometric	Sn	3
$C_{13}H_{10}ClNO_2$	*N*-(4-Chlorophenyl)-*N*-hydroxybenzamide	Extraction-photometric	Co, Cu, Fe, Nb, Sn, Ti, V	3
$C_{13}H_{10}ClNO_3$	*N*-(*p*-Chlorophenyl)-2-furanacrylohydroxamic acid	Extraction-photometric	V	3
$C_{13}H_{10}ClNO_3$	*N*-(4-Chlorophenyl)-3-(2-furanyl)-*N*-hydroxy-2-propenamide	Amperometric	Sc	3
$C_{13}H_{10}ClNO_2$	*o*-Chloro-*N*-phenylbenzohydroxamic acid	Photometric	V	3
$C_{13}H_{10}ClNO_2S$	*N*-*p*-Chlorophenyl-2-thienylacrylohydroxamic acid	Extraction-photometric	V	3
$C_{13}H_{10}INO_2$	*N*-(*o*-Iodobenzoyl) phenylhydroxylamine	Precipitation	Al, Cu, Fe, Hf, Mn, Pb, Sn, Ti, Zr	3
$C_{13}H_{10}N_2O_4$	*N*-Hydroxy-3-nitro-*N*-phenylbenzamide	Extraction-photometric	V	3
$C_{13}H_{10}NO_5NaS$	*N*-(2-Sulfobenzoyl)-*N*-phenylhydroxylamine, sodium salt	Photometric	Fe	3
$C_{13}H_{10}N_2O_4S$	*N*-*p*-Nitrophenyl-2-thienylacrylohydroxamic acid	Extraction-photometric	V	3
$C_{13}H_{11}NO_2$	BPHA (*N*-Benzoyl-*N*-phenylhydroxylamine) (**20**)	Gravimetric; Extraction-separation; Extraction-photometric	Cu, Fe, Pd, Ni, Ti; Al, Bi, Ca, Mo, Nb, Sb, Sn, Sr, Ta, U; Ce, Fe, Ti, V	3, 127, 129
$C_{13}H_{11}NO_3$	*N*-Phenyl-2-furanacrylohydroxamic acid	Extraction-photometric	Ti	3
$C_{13}H_{11}NO_2S$	*N*-Phenyl-2-thiopheneacrylohydroxamic acid	Extraction-photometric	V	3
$C_{13}H_{12}N_2O_2S$	*N*-*m*-Aminophenyl-2-thienylacrylohydroxamic acid	Extraction-photometric	V	3

(*continued overleaf*)

TABLE S5. (*continued*)

Molecular formula	Name	Type of determination	Elements	Reference
$C_{13}H_{12}N_2O_2S$	*N*-*p*-Aminophenyl-2-thienylacrylohydroxamic acid	Extraction-photometric	V	3
$C_{13}H_{13}Cl_2NO_3$	2-(2,4-Dichlorophenoxy)-*N*-(4-methylphenyl)acetohydroxamic acid	Extraction-photometric	V	3
$C_{13}H_{15}NO_2$	*N*-Hydroxy-*N*-(3-methylphenyl)-2,4-hexadienamide	Extraction-photometric	V	3
$C_{13}H_{17}NO_2$	Cyclohexanoylphenyl-hydroxylamine	Color reaction	V	3
$C_{14}H_{10}F_3NO_2$	*N*-*m*-Trifluoromethylbenzoyl-*N*-phenylhydroxylamine	Extraction-separation	Al, Cu, Fe, Mn, V	3
$C_{14}H_{11}Cl_2NO_3$	2-(2,4-Dichlorophenoxy)-*N*-phenylacetohydroxamic acid	Extraction-photometric	V	3
$C_{14}H_{11}N_3O_6$	*N*-Hydroxy-*N*-(4-methylphenyl)-3,5-dinitrobenzamide	Extraction-photometric	Co, Cu, Fe, Ti, V	3
$C_{14}H_{12}ClNO_2$	*N*-*o*-Tolyl-*p*-chlorobenzo-hydroxamic acid	Extraction-photometric	V	3
$C_{14}H_{12}ClNO_2$	*N*-*m*-Tolyl-*p*-chlorobenzo-hydroxamic acid	Extraction-photometric	Bi	3
$C_{14}H_{12}ClNO_2$	4-Chloro-*N*-hydroxy-*N*-(4-methylphenyl)benzamide	Extraction-photometric	Ce	3
$C_{14}H_{12}ClNO_2$	*N*-*o*-Tolyl-*o*-chlorobenzo-hydroxamic acid	Extraction-photometric	V	3
$C_{14}H_{12}ClNO_2$	*N*-*m*-Tolyl-*o*-chlorobenzo-hydroxamic acid	Extraction-photometric	V	3, 130
$C_{14}H_{12}ClNO_3$	*N*-*m*-Chlorophenyl-*p*-methoxybenzohydroxamic acid	Extraction-photometric	Pd	131
$C_{14}H_{12}INO_2$	*N*-*o*-Tolyl-*o*-iodobenzo-hydroxamic acid	Extraction-photometric	V	3
$C_{14}H_{12}INO_2$	*N*-*m*-Tolyl-*o*-iodobenzo-hydroxamic acid	Extraction-photometric	V	3
$C_{14}H_{12}N_2O_4$	*N*-Hydroxy-*N*-(3-methyl-phenyl)-2-nitrobenzamide	Gravimetric	Ce, Gd, La, Nd, Pr, Sm	3
$C_{14}H_{12}N_2O_4$	*N*-Hydroxy-*N*-(4-methyl-phenyl)-3-nitrobenzamide	Extraction-photometric	V	3
$C_{14}H_{12}N_2O_4$	*N*-*m*-Tolyl-3-nitrobenzo-hydroxamic acid	Extraction-photometric; Gravimetric	U; Ba, Be, Sm, and other lanthanides	3, 132, 133
$C_{14}H_{12}N_2O_6S_2$	5,5′-Dithiodisalicylhydroxamic acid	Extraction-photometric	Mn	3
$C_{14}H_{13}NO_2$	*N*-Benzylbenzohydroxamic acid	Extraction-photometric	V	3
$C_{14}H_{13}NO_2$	*N*-*o*-Tolylbenzohydroxamic acid	Extraction-photometric; Extraction-separation; Gravimetric	Cu, Fe, Mo, Ti, V; Al, Cu, Fe, Mn, V; U	3
$C_{14}H_{13}NO_2$	*N*-*m*-Tolylbenzohydroxamic acid	Extraction-photometric	Cu, Fe, Mn, V	3
$C_{14}H_{13}NO_2$	*N*-Hydroxy-*N*-(4-methyl-phenyl)benzamide	Extraction-photometric	Ce, Ti	3
$C_{14}H_{13}NO_2$	*N*-*p*-Methylbenzoyl-*N*-phenyl-hydroxylamine	Extraction separation	Al, Cu, Fe, Mn, V	3

TABLE S5. (*continued*)

Molecular formula	Name	Type of determination	Elements	Reference
$C_{14}H_{13}NO_2$	*N*-Phenylacetylphenyl-hydroxylamine	Extraction-photometric	Ti	3
$C_{14}H_{13}NO_2$	*N*-Benzoyl-*o*-tolylhydroxyl-amine	Gravimetric; Photometric	Ga, In; Os	134, 135
$C_{14}H_{13}NO_2S$	*N*-*m*-Tolyl-2-thiophenyl-acrylohydroxamic acid	Extraction-photometric	V	3
$C_{14}H_{13}NO_2S$	*N*-Hydroxy-*N*-(4-methyl-phenyl)-3-(2-thienyl)-2-propenamide	Extraction-photometric	V	3
$C_{14}H_{13}NO_3$	3-(2-Furanyl)-*N*-hydroxy-*N*-(4-methylphenyl)-2-propenamide	Extraction-photometric	Ti	3
$C_{14}H_{13}NO_3$	*N*-Hydroxy-2-methoxy-*N*-phenylbenzamide	Extraction-photometric	V	3
$C_{14}H_{13}NO_3$	*N*-Phenyl-*p*-anisohydroxamic acid	Extraction-separation	Al, Cu, Fe, Mn, V	3
$C_{14}H_{13}NO_3S$	*N*-*m*-Methoxyphenyl-2-thienylacrylohydroxamic acid	Extraction-photometric	V	3
$C_{14}H_{13}NO_3S$	*N*-*p*-Methoxyphenyl-2-thienylacrylohydroxamic acid	Extraction-photometric	V	3
$C_{14}H_{13}NO_4$	*N*-*p*-Methoxyphenyl-2-furylacrylohydroxamic acid	Extraction-photometric	Pd	136
$C_{14}H_{21}NO_2$	*N*-Phenyloctanohydroxamic acid	Extraction-separation	Pb, Zn, lanthanides	3
$C_{14}H_{21}NO_2$	*N*-(2-Propylpentanoyl)-*N*-phenylhydroxylamine	Extraction-separation	Lanthanides	3
$C_{14}H_{29}NO_2$	Tributylacetohydroxamic acid	Extraction-separation	Zr	3
$C_{15}H_{11}N_3O_8$	4-[(3,5-Dinitrobenzoyl) hydroxyamino]benzoic acid methyl ester	Extraction-photometric	Co, Cu, Fe, Ti, V	3
$C_{15}H_{12}ClNO_2$	*N*-(*p*-Chlorophenyl) cinnamohydroxamic acid	Extraction-photometric	V	3
$C_{15}H_{12}F_3NO_2$	*N*-*p*-Methylbenzoyl-*N*-*m*-trifluoromethylphenyl-hydroxylamine	Extraction-separation	Mo, W	3
$C_{15}H_{12}N_2O_4$	*N*-(*m*-Nitrocinnamoyl) phenylhydroxylamine	Amperometric	La	3
$C_{15}H_{13}NO_2$	*N*-Cinnamoylphenyl-hydroxylamine	Gravimetric; Extraction-photometric; Extraction-separation	Nb, Ta; Fe, U, V; Hg	3, 137
$C_{15}H_{13}NO_4$	*N*-Phenyl-2-acetatosalicylo-hydroxamic acid	Photometric	Nb, Ti	3
$C_{15}H_{13}NO_4$	Methyl 4-(Benzoylhydroxy-amino)benzoate	Extraction-photometric	Co, Cu, Fe, Ti, V	3
$C_{15}H_{14}N_2O_6$	5,5′-Methylenebis(salicylo-hydroxamic acid)	Photometric	V	3
$C_{15}H_{15}NO_2$	*N*-Hydroxy-2-methyl-*N*-(2-methylphenyl)benzamide	Extraction-photometric	V	3
$C_{15}H_{15}NO_2$	*N*-Hydroxy-2-methyl-*N*-(3-methylphenyl)benzamide	Extraction-photometric	V	3
$C_{15}H_{15}NO_2$	*N*-Hydroxy-4-methyl-*N*-(3-methylphenyl)benzamide	Extraction-photometric	V	3

(*continued overleaf*)

TABLE S5. (*continued*)

Molecular formula	Name	Type of determination	Elements	Reference
$C_{15}H_{15}NO_2$	*N*-Hydroxy-4-methyl-*N*-(4-methylphenyl)benzamide	Extraction-photometric	V	3
$C_{15}H_{15}NO_2$	*N*-(*o*-Ethoxybenzoyl) phenylhydroxylamine	Precipitation	Al, Cu, Fe, Hf, Mn, Pb, Sn, Ti, Zr	3
$C_{15}H_{15}NO_2$	*N*-*p*-Ethylbenzoyl-*N*-phenylhydroxylamine	Extraction-separation	Al, Cd, Cu, Fe, U, V	3
$C_{15}H_{15}NO_3$	*N*-Hydroxy-2-methoxy-*N*-(2-methylphenyl)benzamide	Extraction-photometric	V	3
$C_{15}H_{15}NO_3$	*N*-Hydroxy-2-methoxy-*N*-(3-methylphenyl)benzamide	Extraction-photometric	V	3
$C_{15}H_{15}NO_3$	*N*-Hydroxy-2-methoxy-*N*-(4-methylphenyl)benzamide	Extraction-photometric	U	3
$C_{15}H_{15}NO_3$	*N*-(4-Methylphenyl)-2-phenoxyacetohydroxamic acid	Extraction-photometric	V	3
$C_{15}H_{17}NO_2$	*N*-1-Naphthylvalerohydroxamic acid	Extraction-photometric	V	3
$C_{15}H_{23}NO_2$	*N*-*p*-Tolyloctanohydroxamic acid	Extraction-photometric	V	3
$C_{15}H_{23}NO_2$	*N*-Phenyl-*N*-(3,5,5-trimethyl-hexanoyl)hydroxylamine	Extraction-separation	Lanthanides	3
$C_{16}H_{12}ClNO_4$	*N*-(*p*-Chlorophenyl)-3,4-(methylenedioxy)cinnamo-hydroxamic acid	Extraction-photometric	V	3
$C_{16}H_{13}NO_4$	3-(1,3-Benzodioxol-5-yl)-*N*-hydroxy-*N*-phenyl-2-propenamide	Extraction-photometric	Ti, V	3
$C_{16}H_{14}ClNO_3$	*N*-(*p*-Chlorophenyl)-*p*-methoxycinnamohydroxamic acid	Extraction-photometric	V	3
$C_{16}H_{15}NO_2$	*N*-*o*-Tolylcinnamohydroxamic acid (*N*-Hydroxy-3-phenyl-2-propenamide)	Extraction-photometric	Ti, V	3
$C_{16}H_{15}NO_2$	*N*-*m*-Tolylcinnamohydroxamic acid	Extraction-photometric	V	3
$C_{16}H_{15}NO_2$	*N*-*p*-Tolylcinnamohydroxamic acid	Extraction-photometric	V	3
$C_{16}H_{15}NO_3$	*p*-Methoxy-*N*-phenylcinn-amohydroxamic acid	Extraction-photometric	Ti, V	3
$C_{16}H_{19}NO_2$	*N*-1-Naphthylcaprohydroxamic acid	Extraction-photometric	V	3
$C_{16}H_{25}NO_2$	*N*-Phenyldecanohydroxamic acid	Extraction-photometric	V	3
$C_{17}H_7F_{12}NO_2$	*N*-(3,5-Bis(trifluoromethyl) phenyl)-3,5-bis(trifluoromethyl) benzohydroxamic acid	Extraction-separation	Al, Cu, Fe, Mn, V	3
$C_{17}H_{12}ClNO_2$	*N*-1-Naphthyl-*p*-chlorobenzo-hydroxamic acid	Extraction-photometric	V	3
$C_{17}H_{12}N_2O_4$	*N*-1-Naphthyl-*p*-nitrobenzo-hydroxamic acid	Extraction-photometric	V	3
$C_{17}H_{13}NO_2$	*N*-Phenyl-2-naphthohydroxamic acid	Extraction-photometric	V	3
$C_{17}H_{13}NO_2$	*N*-Benzoyl-*N*-(1-naphthyl) hydroxylamine	Precipitation	Al, Cu, Fe, Hf, Mn, Pb, Sn, Ti, Zr	3

TABLE S5. (*continued*)

Molecular formula	Name	Type of determination	Elements	Reference
$C_{17}H_{13}NO_2$	*N*-(1-Naphthoyl)phenyl-hydroxylamine	Precipitation	Al, Cu, Fe, Hf, Mn, Pb, Sn, Ti, Zr	3
$C_{17}H_{13}N_3O_3$	1-Phenylazo-2-hydroxy-3-naphthylhydroxamic acid	Extraction-photometric	V	3
$C_{17}H_{14}ClNO_2$	PCPPASAHA (*N*-*p*-Chlorophenyl-α-phenylstyrylacrylohydroxamic acid)	Extraction	Mo, Nb	138, 139
$C_{17}H_{15}NO_2$	*N*-Phenyl-3-styrylacrylo-hydroxamic acid	Extraction-photometric; Amperometric	V; Sc	3
$C_{17}H_{15}NO_4$	3-(1,3-Benzodioxol-5-yl)-*N*-hydroxy-*N*-(3-methylphenyl)-2-propenamide	Extraction-photometric	V	3
$C_{17}H_{15}NO_4$	3-(1,3-Benzodioxol-5-yl)-*N*-hydroxy-*N*-(4-methylphenyl)-2-propenamide	Extraction-photometric	V	3
$C_{17}H_{17}Cl_2NO_3$	*N*-(4-Chlorophenyl)-4-chlorophenoxyisobutyro-hydroxamic acid	Extraction-photometric	Nb, Ta, Ti	3
$C_{17}H_{17}NO_2$	*N*-Cinnamoyl-*N*-(2,3-xylyl)hydroxylamine	Extraction-photometric	V	3
$C_{17}H_{17}NO_3$	*N*-*m*-tolyl-4-Methoxycinnamo-hydroxamic acid	Extraction-photometric	V	3
$C_{17}H_{17}NO_3$	*N*-*p*-tolyl-4-Methoxycinnamo-hydroxamic acid	Extraction-photometric	V	3
$C_{17}H_{18}ClNO_3$	4-Butoxy-*N*-(4-chlorophenyl) benzohydroxamic acid	Extraction-photometric	Nb, Ta, Ti	3
$C_{17}H_{19}NO_2$	*N*-(4-Butylbenzoyl)-*N*-phenylhydroxylamine	Extraction-separation	Lanthanides	3
$C_{17}H_{19}NO_2$	4-(1,1-Dimethylethyl)-*N*-hydroxy-*N*-phenylbenzamide	Extraction-separation	Al, Cd, Cu, Fe, Mn, V	3
$C_{17}H_{19}NO_3$	*N*-Phenyl-4-butoxybenzo-hydroxamic acid	Extraction-photometric	Nb, Ta, Ti	3
$C_{17}H_{25}NO_2$	*N*-(4-Butylcyclohexanoyl)-*N*-phenylhydroxylamine	Extraction-separation	Lanthanides	3
$C_{17}H_{27}NO_2$	*N*-Hydroxy-*N*-(3-methylphenyl)decanamide	Extraction-photometric	V	3
$C_{17}H_{27}NO_2$	*N*-Hydroxy-*N*-(4-methylphenyl)decanamide	Extraction-photometric	V	3
$C_{18}H_{15}NO_2$	*N*-Benzyl-2-naphthohydroxamic acid	Extraction-photometric	V	3
$C_{18}H_{15}NO_2$	*N*-1-Naphthyl-*o*-methylbenzo-hydroxamic acid	Extraction-photometric	V	3
$C_{18}H_{15}NO_2$	*N*-1-Naphthyl-*p*-methylbenzo-hydroxamic acid	Extraction-photometric	V	3
$C_{18}H_{15}NO_2$	*N*-1-Naphthylphenylaceto-hydroxamic acid	Extraction-photometric	V	3
$C_{18}H_{15}NO_3$	*N*-1-Naphthyl-*o*-methoxybenzo-hydroxamic acid	Extraction-photometric	V	3
$C_{18}H_{15}NO_3$	*N*-1-Naphthyl-*p*-methoxybenzohydroxamic acid	Extraction-photometric	V	3
$C_{18}H_{18}ClNO_5$	*N*-(4-Chlorophenyl)-3,4,5-trimethoxycinnamohydroxamic acid	Extraction-photometric	Nb, Ta, Ti	3

(*continued overleaf*)

TABLE S5. (*continued*)

Molecular formula	Name	Type of determination	Elements	Reference
$C_{18}H_{21}NO_2$	4-(1,1-Dimethylethyl)-*N*-hydroxy-*N*-(2-methylphenyl)benzamide	Extraction	Al, Fe, Mn, V	3
$C_{18}H_{29}NO_2$	*N*-Phenyllaurohydroxamic acid	Extraction-photometric	Ti	3
$C_{19}H_{15}N_3O_2$	*N*-Phenyl-4-(phenylazo) benzohydroxamic acid	Color reaction	V	3
$C_{19}H_{22}N_2O_4$	*N*,*N*′-Dihydroxy-*N*,*N*′-diphenylheptanediamide	Extraction-photometric	Ti	3
$C_{20}H_{15}NO_2$	*N*-Fluoren-1-ylbenzo-hydroxamic acid	Colorimetric	V	3
$C_{20}H_{17}NO_2$	*p*-(Diphenylmethyl) benzohydroxamic acid	Photometric	V	3
$C_{20}H_{20}N_2O_3$	*N*-(*p*-*N*,*N*-Dimethylanilino)-3-methoxy-2-naphthohydroxamic acid	Extraction-photometric	V	3
$C_{20}H_{27}NO_2$	*N*-1-Naphthylcaprihydrox-amic acid	Extraction-photometric	V	3
$C_{20}H_{33}NO_2$	*N*-Phenyltetradecano-hydroxamic acid	Extraction-photometric	V	3
$C_{21}H_{27}NO_3$	*N*-*p*-Octyloxybenzoyl-*N*-phenylhydroxylamine	Extraction-photometric	Ti, V	3
$C_{21}H_{35}NO_2$	*N*-(4-Methylphenyl)tetrade-canohydroxamic acid	Extraction-photometric	V	3
$C_{22}H_{31}NO_2$	*N*-1-Naphthyllaurohydroxamic acid	Extraction-photometric	V	3
$C_{22}H_{37}NO_2$	*N*-(2-Hexyldecanoyl)-*N*-phenylhydroxylamine	Extraction separation	Lanthanides	3
$C_{23}H_{29}NO_8$	PBCHA (*N*-phenylbenzo-18-crown-6-hydroxamic acid)	Extraction	Ce, La, Th, U	140–142
$C_{24}H_{35}NO_2$	*N*-1-Naphthylmyristo-hydroxamic acid	Extraction-photometric	V	3
$C_{30}H_{44}N_4O_8$	5,14-*N*,*N*′-hydroxyphenyl-4,15-dioxo-1,5,14,18-tetraazahexacosane	Extraction	La, Th, V	143–145
$C_{67}H_7NO_2$	PMFFHA (*N*-Phenyl-(1,2-methanofullerene C60)61-formohydroxamic acid)	Extraction	Ce, La, U, V	146–148
$C_{80}H_{56}Cl_4N_4O_{12}$	CPCHA (25,26,27,28-tetrahydroxy-5,11,17,23-tetrakis(*N*-*p*-chlorophenyl)calix[4]arene-*p*,*p*′,*p*″,*p*‴-tetrakis(amino-bis(acetohydroxamic acid)))	Extraction	Th, U, Zr	149–151
$C_{96}H_{88}N_8O_{24}$	2,2′,2″,2‴,2⁗,2⁗′,2⁗″,2⁗‴-[(2,8,14,20-tetramethyl-pentacyclo [19.3.1.1 (3,7).1(9,13).1(15,19)]octacosa-1(25),3,5,7(28),9,11,13(27),15, 17,19(26),21,23-dodecaene-4,6,10,12,16,18,22,24-octayl)octakis(oxy)]octakis[*N*-hydroxy-*N*-phenylacetamide]	Extraction	Th, U	152, 153

TABLE S6. Examples of thiohydroxamic acids used for determination of various elements

Molecular formula	Name	Type of determination	Elements	Reference
$C_8H_7N_3O_2S$	2*H*-1,4-Benzothiazine-2,3(4*H*)dione dioxime (**21**)	Complexing agent	Cu, Ni	154
$C_8H_9NO_2S$	*p*-Methoxybenzothiohydroxamic acid	Extraction-photometric	Bi, Fe, Mn, Mo, Nb, Sn, Ti, V	3
$C_8H_{10}N_2OS$	*N*-Methylaminothioformyl-*N*′-phenylhydroxylamine	Gravimetric; Extraction-photometric; Photometric	Cu; Ni; Cu	3
$C_{13}H_{10}BrN_2OS$	*N*-(*p*-Bromophenyl)-*N*′-phenylthiocarbonylhydroxamic acid	Extraction-photometric	Cu	3
$C_{13}H_{11}NOS$	*N*-Phenylthiobenzohydroxamic acid (**22**)	Gravimetric	Cu, Fe	3
$C_{13}H_{14}N_2OS$	*N*,*N*′-Diphenylthiocarbamoylhydroxamic acid (**23**)	Complexing agent; Extraction-photometric; Photometric	Mo; Cu, Mo; Ni	3, 155

VII. REFERENCES

1. http://www.acs-analytical.duq.edu/whatisanalyticalchem.html
2. A. I. Vogel, *Vogel's Textbook of Quantitative Inorganic Analysis: Including Elementary Instrumental Analysis*, 4th edn., Longman, London, 1978.
3. A. Townshend, D. T. Burns, R. Łobiński, E. J. Newman, G. G. Guilbault, Z. Marczenko and H. Onishi, *Dictionary of Analytical Reagents*, 1st edn., Chapman & Hall, London, 1993.
4. P. R. Loconto and J. Pavelock, *Am. Lab.*, **17**, 172 (1985).
5. K. Burger, *Organic Metals in Metal Analysis*, Pergamon Press, Oxford, 1973.
6. A. E. Harvey and D. L. Manning, *J. Am. Chem. Soc.*, **72**, 4488 (1950).
7. V. C. Bass and J. H. Yoe, *Talanta*, **13**, 735 (1966).
8. R. C. Shriner, R. L. Fuson and D. Y. Curtin, *Systematic Identification of Organic Compounds*, 4th edn., Wiley, New York, 1956.
9. N. D. Cheronis and J. B. Entrikin, *Semimicro Qualitative Analysis*, 2nd edn., Interscience, New York, 1957.
10. N. D. Cheronis, *Semimicro Experimental Organic Chemistry: A Laboratory Manual*, John De Groff, New York, 1958.
11. (a) N. Kabay and H. Egawa, *Turk. J. Chem.*, **17**, 62 (1993).
    (b) R. A. Beauvais and S. D. Alexandratos, *React. Funct. Polym.*, **36**, 113 (1998).
12. (a) C. Agarwal, K. S. Patel and R. K. Mishra, *Ind. Asian Env.*, **12**, 29 (1990).
    (b) M. K. Deb and R. K. Mishra, *Int. J. Environ. Anal. Chem.*, **48**, 151 (1992).
    (c) S. Chakravarty, M. K. Deb and R. K. Mishra, *J. AOAC Int.*, **76**, 604 (1993).
    (d) S. C. Tiwari and H. Mohabey Hemlata, *Asian J. Chem.*, **17**, 2565 (2005).
13. (a) N. H. Furman, W. B. Mason and J. S. Pekola, *Anal. Chem.*, **21**, 1325 (1949).
    (b) A. I. Popov and W. W. Wendlandt, *Anal. Chem.*, **26**, 883 (1954).
14. (a) H. M. Liu, S. Y. Chen, P. H. Chang and S. J. J. Tsai, *Anal. Chim. Acta*, **459**, 161 (2002).
    (b) N. Öztekin and F. B. Erim, *J. Chromatogr. A*, **895**, 263 (2000).
    (c) J. A. Hrabie and L. K. Keefer, *Chem. Rev.*, **102**, 1135 (2002).
    (d) G. Kefala, A. Economou and M. Sofoniou, *Talanta*, **68**, 1013 (2006).
    (e) M. Korolczuk, K. Tyszczuk and M. Grabarczyk, *Talanta*, **72**, 957 (2007).
15. (a) D. K. Gorji, R. S. Chauhan, A. K. Goswami and D. N. Purohit, *Rev. Anal. Chem.*, **17**, 223 (1998).
    (b) S. Kumar, A. K. Goswami and D. N. Purohit, *Rev. Anal. Chem.*, **22**, 73 (2003).

16. (a) J. C. Sharma, M. Upadhyay, C. P. Jain and R. Dashora, *Asian J. Chem.*, **18**, 3151 (2006). (b) A. R. Ghiasvand, B. Rezaei and G. A. Masroor, *Asian J. Chem.*, **18**, 2185 (2006).
17. J. A. Silva and F. F. Vidal, *Afinidad*, **53**, 35 (1996); *Chem. Abstr.*, **124**, 249061 (1996).
18. C. Silva, A. Jose, G. P. Andreu and L. S. Orozco, *Afinidad*, **58**, 367 (2001); *Chem. Abstr.*, **136**, 144308 (2001).
19. C. Silva, A. Jose and R. Rodriguez-Hernandez, *Ecletica Quimica*, **20**, 89 (1995); *Chem. Abstr.*, **124**, 277091 (1996).
20. L. F. Salinas, J. C. Jimenez Sanchez and T. Galeano Diaz, *Microchem. J.*, **36**, 285 (1987).
21. F. Salinas, J. C. Jimenez Sanchez and M. M. Lozano Ruiz, *Bull. Soc. Chim. Belg.*, **96**, 73 (1987).
22. F. Salinas, J. C. Jimenez Sanchez, T. Galeano Diaz and V. Lopez-Arza, *Ann. Chim. (Rome)*, **76**, 387 (1986).
23. A. K. Ray, *Anal. Chim. Acta*, **28**, 580 (1963).
24. R. A. Kumar and R. Priyadaranjan, *Indian Assoc. Cultivation Sci.*, **21**, 547 (1956).
25. R. S. Lokhande and U. Patil, *Asian J. Chem.*, **19**, 165 (2007).
26. V. K. Reddy, S. M. Reddy, P. R. Reddy and T. S. Reddy, *Ind. J. Chem. A*, **39**, 557 (2000).
27. M. L. Dhar, S. M. Jain and R. Ravinder, *J. Chromatogr.*, **129**, 488 (1976).
28. F. Salinas, J. C. Jimenez Sanchez and J. M. Lemus Gallego, *Microchem. J.*, **35**, 157 (1987).
29. P. S. Bharadwaj and H. B. Naik, *Asian J. Chem.*, **11**, 45 (1999).
30. N. K. B. Patel and K. K. Desai, *Asian J. Chem.*, **14**, 1769 (2002).
31. K. H. Reddy, N. B. L. Prasad and T. S. Reddy, *Talanta*, **59**, 425 (2003).
32. K. H. Reddy and K. B. Chandrasekhar, *Ind. J. Chem. A*, **40**, 727 (2001).
33. N. B. L. Prasad and K. H. Reddy, *J. Ind. Chem. Soc.*, **81**, 794 (2004).
34. K. L. Soni and K. K. Desai, *J. Inst. Chem. (India)*, **65**, 144 (1993).
35. H. D. Tayal, P. C. Pachauri and S. Kumar, *Acta Cienc. Ind. Chem.*, **6**, 115 (1980).
36. S. Ninan, A. Varadarajan, S. B. Jadhav, A. J. Kulkarni and S. P. Malve, *Spectrochim. Acta A*, **55**, 825 (1999).
37. P. S. Bharadwaj and H. B. Naik, *Asian J. Chem.*, **11**, 243 (1999).
38. J. Dutta and S. Basu, *J. Radioanal. Nucl. Chem.*, **221**, 221 (1997).
39. J. Dutta and S. Basu, *Radiochim. Acta*, **79**, 191 (1997).
40. A. Ramesh, *Indian J. Chem. A*, **32**, 829 (1993).
41. A. Ramesh, *Talanta*, **41**, 355 (1994).
42. A. Ramesh, J. Krishnamacharyulu, L. K. Ravindranath and S. B. Rao, *J. Radioan. Nucl. Ch. Ar.*, **170**, 181 (1993).
43. N. B. Patel and K. K. Desai, *Asian J. Chem.*, **11**, 1080 (1999).
44. N. B. Patel and K. K. Desai, *Asian J. Chem.*, **11**, 1083 (1999).
45. J. D. Talati and K. S. Parikh, *Asian J. Chem.*, **6**, 581 (1994).
46. V. K. Desai and K. K. Desai, *Orient. J. Chem.*, **12**, 215 (1996).
47. J. D. Talati and K. S. Parikh, *J. Inst. Chem. (India),* **67**, 83 (1995).
48. G. R. Desai and K. K. Desai, *Orient. J. Chem.*, **11**, 197 (1995).
49. J. D. Talati and P. K. Patel, *Asian J. Chem.*, **7**, 389 (1995).
50. G. R. Desai and K. K. Desai, *Asian J. Chem.,* **7**, 592 (1995).
51. P. A. Kahar and K. K. Desai, *Asian J. Chem.*, **10**, 910 (1998).
52. M. R. Ganjali, F. Mizani, M. Emami, M. Darjezini, M. R. Darvich and M. Yousefi, *Anal. Sci.*, **20**, 531 (2004).
53. R. S. Lokhande, U. Patil and S. S. Dapale, *Res. J. Chem. Environ.*, **8**, 59 (2004).
54. B. R. Naik and K. K. Desai, *Asian J. Chem.*, **18**, 3176 (2006).
55. I. Bhattacharya, *Asian J. Chem.*, **13**, 581 (2001).
56. S. K. Shingadia and K. K. Desai, *Orient. J. Chem.*, **22**, 703 (2006).
57. S. V. Vartanyan, S. A. Ovakimyan, A. V. Babakhanyan and S. T. Kocharyan, *Haya. Kim. Hand.*, **57**, 66 (2004); *Chem. Abstr.*, **142**, 168373 (2004).
58. J. D. Talati and K. S. Parikh, *Asian J. Chem.*, **6**, 581 (1994).
59. E. N. Iliadou, S. T. Girousi, U. Dietze, M. Otto, A. N. Voulgaropoulos and C. G. Papadopoulos, *Analyst*, **122**, 597 (1997).
60. J. J. Desai, P. G. Desai and A. G. Mehta, *Asian J. Chem.*, **12**, 399 (2000).
61. N. Y. Sreedhar and Y. Jyothi, *J. Ind. Chem. Soc.*, **82**, 1038 (2005).
62. J. J. Desai, P. G. Desai and A. G. Mehta, *Asian J. Chem.*, **11**, 519 (1999).
63. J. Beltran and J. Faus, *Inf. Quim. Anal.*, **26**, 63 (1972); *Chem. Abstr.*, **77**, 83159 (1972).

64. H. Erlenmeyer, H. V. Hahn and E. Sorkin, *Helv. Chim. Acta*, **34**, 1419 (1951).
65. P. A. Leermakers and W. A. Hoffman, *J. Am. Chem. Soc.*, **80**, 5663 (1958).
66. K. Matsusaki, *Yamaguchi Daigaku Kogakubu Kenkyu Hokoku*, **28**, 249 (1978); *Chem. Abstr.*, **89**, 70378 (1978).
67. A. S. Bogonostsev, *Izv. Vys. Ucheb. Zav. Khim. Khim. Tekhn.*, **6**, 1046 (1963); *Chem. Abstr.*, **61**, 7821 (1964).
68. M. Ziegler and O. Glemser, *Mikrochim. Acta*, **44**, 1152 (1956).
69. S. Saracoglu, M. Soylak, D. S. K. Peker, L. Elci, W. N. L. dos Santos, V. A. Lemos and S. L. C. Ferreira, *Anal. Chim. Acta*, **575**, 133 (2006).
70. G. W. Robinson, *Metallurgia*, **37**, 107 (1947).
71. Y. Yan, G. Zhao and X. Lu, *Yejin Fenxi*, **23**, 9 (2003); *Chem. Abstr.*, **142**, 106047 (2004).
72. S. R. Kaza and U. Muralikrishna, *Acta Cienc. Ind., Chem.*, **10**, 20 (1984).
73. L. V. Ershova, V. M. Ivanov, A. I. Busev and M. V. Lomonosov, *Zh. Anal. Khim.*, **29**, 1367 (1974); *Chem. Abstr.*, **81**, 180919 (1974).
74. L. V. Ershova, V. V. Noskov and G. I. Nosov, *Zh. Anal. Khim.*, **26**, 2406 (1971); *Chem. Abstr.*, **76**, 80634 (1972).
75. R. F. Muraca and J. P. Bonsack, *Chemist-Analyst*, **44**, 38 (1955).
76. J. W. L. van Ligten and H. van Velthuyzen, *Mikrochim. Acta*, **52**, 759 (1964).
77. S. Yu, G. Wang, Z. Zhou, S. Li, Y. Wang and S. Wang, *Yejin Fenxi*, **12**, 45 (1992); *Chem. Abstr.*, **120**, 234939 (1994).
78. P. Wang, *Guangxi Huagong*, **26**, 47 (1997); *Chem. Abstr.*, **128**, 303408 (1998).
79. M. E. Taylor and R. J. Robinson, *Anal. Chem.*, **34**, 533 (1962).
80. E. Jansons, K. Puke and D. Cedere, *Latv. Kim. Zur.*, **6**, 680 (1992); *Chem. Abstr.*, **118**, 246373 (1992).
81. S. B. Jadhav, S. P. Tandel and S. P. Malve, *J. Ind. Counc. Chem.*, **18**, 70 (2001).
82. S. S. Utekar, S. B. Jadhav and S. P. Malve, *Ind. J. Chem. Technol.*, **9**, 424 (2002).
83. M. Aminuddin, J. Iqbal and J. I. Gill, *J. Chem. Soc. Pakistan*, **21**, 20 (1999).
84. J. Iqbal, F. H. Wattoo, S. A. Tirmizi, M. H. S. Wattoo, N. Ishrat and A. N. Memon, *J. Chem. Soc. Pakistan*, **29**, 136 (2007).
85. G. S. Manku, A. N. Bhat and B. D. Jain, *Proc. Ind. Sci. A*, **68**, 88 (1968).
86. G. S. Manku, *Fresenius Z. Anal. Chem.,* **258**, 365 (1972).
87. G. S. Manku, A. N. Bhat and B. D. Jain, *Talanta*, **16**, 1421 (1969).
88. G. S. Manku, R. D. Gupta, A. N. Bhat and B. D. Jain, *Mikrochim. Acta*, **58**, 836 (1970).
89. G. S. Manku, *Mikrochim. Acta*, **60**, 811 (1972).
90. G. S. Manku, A. N. Bhat and B. D. Jain, *Mikrochim. Acta*, **58**, 1101 (1970).
91. J. C. Kim, M. K. You, M. S. Won, Y. B. Shim and Y. S. Koh, *Yakhak Hoechi*, **28**, 61 (1984); *Chem. Abstr.*, **101**, 143018 (1984).
92. M. S. El-Shahawi and M. Almehdi, *J. Chromatogr. A*, **697**, 185 (1995).
93. K. Shravah and S. K. Sindhwani, *Bull. Chem. Soc. Jpn.,* **58**, 3560 (1985).
94. S. K. Sindhwani and R. P. Singh, *Fresenius Z. Anal. Chem.,* **268**, 31 (1974).
95. A. R. Ghiasvand, S. Shadabi, E. Mohagheghzadeh and P. Hashemi, *Talanta*, **66**, 912 (2005).
96. T. Peng, T. Zhe, G. Wang and B. Shen, *Electroanalysis*, **6**, 597 (1994).
97. A. N. Sierra, J. S. D. Alegria and A. C. Martin, *Fresenius J. Anal. Chem.,* **345**, 437 (1993).
98. M. Ghaedi, E. Asadpour and A. Vafaie, *Spectrochim. Acta A*, **63**, 182 (2006).
99. A. Dakshinamoorthy, R. K. Singh and R. H. Iyer, *J. Radioanal. Nucl. Ch. Ar.*, **177**, 327 (1994).
100. K. M. Singh and B. K. Pandey, *Asian J. Chem.*, **11**, 840 (1999).
101. A. Rani, B. D. Singh and K. M. Singh, *Himalayan Chem. Pharm. Bull.*, **13**, 34 (1996); *Chem. Asbtr.*, **125**, 346408 (1996).
102. R. P. Singh and V. Purshottam, *Proc. Symp. Chem. Coord. Compounds, Agra, India*, 262 (1960); *Chem. Abstr.*, **61**, 50 (1964).
103. R. N. Thakor, N. F. Mody, G. C. Desai and A. G. Mehta, *J. Inst. Chem. (India)*, **60**, 182 (1988).
104. A. R. Firooz, M. Mazloum, J. Safari and M. K. Amini, *Anal. Bioanal. Chem.*, **372**, 718 (2002).
105. M. N. Naik and N. V. Thakkar, *Ind. J. Chem. A*, **34**, 410 (1995).
106. P. V. Jagasia and D. P. Dave, *J. Ind. Chem. Soc.*, **80**, 145 (2003).
107. M. M. Patel, M. R. Patel and B. N. Mankad, *J. Ind. Chem. Soc.*, **52**, 773 (1975).
108. R. P. Singh, *J. Indian Chem. Soc.*, **37**, 442 (1960).

109. H. Fu and B. Wang, *Huaxue Gongye Yu Gongcheng Jishu*, **23**, 46 (2002); *Chem. Abstr.*, **138**, 313485 (2003).
110. O. Dalman, M. Tufekci, S. Nohut, S. Guner and S. Karabocek, *J. Pharm. Biomed.*, **27**, 183 (2002).
111. K. Thipyapong and C. Suksai, *Bull. Korean Chem. Soc.*, **24**, 1767 (2003).
112. M. Shamsipur, A. Soleymanpour, M. Akhond, H. Sharghi and M. H. Sarvari, *Electroanalysis*, **17**, 776 (2005).
113. F. Shemirani, M. R. Jamali, R. R. Kozani and M. Salavati-Niasari, *Sep. Sci. Technol.*, **41**, 3065 (2006).
114. D. M. Rao, K. H. Reddy and D. V. Reddy, *Ind. J. Chem. A*, **26**, 363 (1987).
115. E. E. Vonesch, O. A. Guagnini and S. V. Guagnini, *Anal. Assoc. Quim. Argent.*, **41**, 162 (1953); *Chem. Abstr.*, **48**, 17717 (1954).
116. S. K. Dhar and A. K. Das Gupta, *J. Sci. Indus. Res. B*, **11**, 520 (1952).
117. D. Monnier and C. Jegge, *Helv. Chim. Acta*, **40**, 513 (1957).
118. S. K. Dhar and A. K. Das Gupta, *J. Sci. Indus. Res. B*, **12**, 518 (1953).
119. A. K. Dasgupta and J. Gupta, *J. Sci. Ind. Res. B*, **9**, 237 (1950).
120. S. K. Dhar and A. K. Das Gupta, *J. Sci. Ind. Res. B*, **11**, 500 (1952).
121. A. T. Senior and J. D. Glennon, *Anal. Chim. Acta*, **196**, 333 (1987).
122. V. K. Bishimbaev, S. P. Nazarbekova, K. T. Sharipov and N. K. Sarypbekova, *Izv. Nat. Akad. Nauk Respub. Kazak., Ser. Khim.*, **2**, 31 (2006); *Chem. Abstr.*, **146**, 197132 (2006).
123. M. Hassiruzzaman, A. S. Kamal, G. M. M. Rahman, S. M. R. Ullah, M. A. Hossain, A. I. Mustafa and A. Ismail, *J. Bengladesh Chem. Soc.*, **10**, 25 (1997); *Chem. Abstr.*, **131**, 345847 (1999).
124. I. Sharma and A. K. Chakraburtty, *Ind. J. Chem. A*, **27**, 271 (1988).
125. G. C. Caro, G. P. Valiente, A. M. Jimenez Arrabal, M. V. Lopez-Arza and M. A. Sanchez, *Fresenius Z. Anal. Chem.*, **340**, 169 (1991).
126. Y. K. Agrawal and V. J. Bhatt, *Analyst*, **111**, 761 (1986).
127. M. I. Roushdy, Y. M. Issa, S. M. El-Zein and F. M. El-Deen Harb, *Asian J. Chem.*, **11**, 1231 (1999).
128. S. A. Abbasi, *Int. J. Environ. Anal. Chem.*, **33**, 113 (1988).
129. I. P. Alimarin, I. V. Sokolova and E. V. Smolina, *Vest. Mosk. Univ., Ser. 2, Khim.*, **23**, 67 (1968); *Chem. Abstr.*, **69**, 54761 (1968).
130. P. Vijayavani and P. M. Dhadke, *Chem. Environ. Chem.*, **4**, 311 (1995).
131. Y. K. Agrawal and P. C. Parekh, *J. Ind. Chem. Soc.*, **63**, 230 (1986).
132. Y. K. Agrawal, *J. Ind. Chem. Soc.*, **55**, 180 (1978).
133. P. C. Verma, P. V. Khadikar and Y. K. Agrawal, *Ind. J. Chem. A,* **14**, 637 (1976).
134. S. P. Bag and S. Lahiri, *Ind. J. Chem.*, **13**, 415 (1975).
135. V. V. Yeole, P. S. Patil and V. M. Shinde, *Fresenius Z. Anal. Chem.*, **294**, 46 (1979).
136. S. A. Abbasi, *Anal. Lett.*, **20**, 1013 (1987).
137. Y. K. Agrawal and T. A. Desai, *Anal. Lett.*, **18**, 2521 (1985).
138. Y. K. Agrawal, S. K. Menon and K. R. Patel, *Mikrochim. Acta*, **122**, 259 (1996).
139. K. Patel, S. K. Menon and Y. K. Agrawal, *Microchem. J.*, **53**, 158 (1966).
140. Y. K. Agrawal, S. B. Vora and G. Shah, *Ind. J. Chem. A*, **44**, 497 (2005).
141. Y. K. Agrawal and S. B. Vora, *Mikrochim. Acta*, **142**, 255 (2003).
142. Y. K. Agrawal, G. Shah and S. B. Vora, *J. Radioanal. Nucl. Chem.*, **270**, 453 (2006).
143. Y. K. Agrawal and P. Shrivastav, *Talanta*, **44**, 1307 (1997).
144. P. Shrivastav, S. K. Menon and Y. K. Agrawal, *J. Radioanal. Nucl. Chem.*, **250**, 459 (2001).
145. P. Shrivastav and Y. K. Agrawal, *Analusis*, **24**, 13 (1996).
146. Y. K. Agrawal, *Fuller. Nanotub. Car. N.*, **12**, 545 (2004).
147. Y. K. Agrawal, *Fuller. Nanotub. Car. N.*, **11**, 135 (2003).
148. Y. K. Agrawal, *Fuller. Nanotub. Car. N.*, **14**, 621 (2006).
149. Y. K. Agrawal and M. Sanyal, *Analyst*, **120**, 2759 (1995).
150. Y. K. Agrawal and M. Sanyal, *J. Radioanal. Nucl. Chem.*, **198**, 349 (1995).

151. Y. K. Agrawal, M. Sanyal, P. Shrivastav and S. K. Menon, *Talanta*, **46**, 1041 (1998).
152. V. K. Jain, S. G. Pillai, R. A. Pandya, Y. K. Agrawal and P. S. Shrivastav, *Anal. Sci.,* **21**, 129 (2005).
153. V. K. Jain, S. G. Pillai, R. A. Pandya, Y. K. Agrawal and P. S. Shrivastav, *Talanta*, **65**, 466 (2005).
154. A. R. Ghiasvand, S. Shadabi and A. Kakanejadifard, *Chem. Anal. (Warsaw)*, **52**, 125 (2007).
155. O. S. Panwar and S. P. Mathur, *J. Ind. Chem. Soc.*, **72**, 563 (1995).

CHAPTER **12**

Structural effects on reactivity and properties of oximes and hydroxamic acids

MARVIN CHARTON

Chemistry Department, School of Liberal Arts and Sciences, Pratt Institute, Brooklyn, New York 11205, USA
Fax: 718-722-7706; email: mcharton@pratt.edu

The chemistry of hydroxylamines, oximes and hydroxamic acids
Edited by Z. Rappoport and J. F. Liebman

I. THE NATURE OF STRUCTURAL EFFECTS

A. Introduction

Models for the quantitative description of the structural effects of substituents are described in this work. Also described are substituent effects of NO, −C=NOH, C(O) NHOH and NHOH substituents.

The structural theory of organic chemistry was developed in the last half of the nineteenth century. It led to the concept that chemical, physical and biological properties of all kinds must be a function of structural change. The earliest structure−property relationships (SPR) were qualitative. Examples are the directional effect of substituents on the benzene ring with respect to electrophilic aromatic substitution and orientation in

hydrogen halide addition to substituted double bonds.[1,2] With the development of methods of quantitative measurement of chemical reactivities such as ionization constants for acids and bases and rate constants for reactions, and phase change properties such as melting and boiling points and solubilities, data accumulated. Attempts were then made to develop quantitative models for the structural dependence of these properties. It is these methods for the quantitative description of structural effects that will now be described.

B. Structure–Property Quantitative Relationships (SPQR)

Quantitative descriptions for the structural dependence of properties are called structure–property quantitative relationships (SPQR). There are four types of these relationships:

1. *Quantitative structure–chemical reactivity relationships* (QSRR). Chemical reactivities involve the formation and/or cleavage of chemical bonds. Equilibrium constants, rate constants, polarographic half-wave potentials and oxidation–reduction potentials are examples of chemical reactivity data.
2. *Quantitative structure–chemical property relationships* (QSCR). Chemical properties involve a difference in intermolecular forces between an initial and a final state. Equilibrium constants for hydrogen bonding; charge transfer complex formation, conformational equilibria, partition coefficients; chromatographic properties such as capacity factors in high performance liquid chromatography, retention times in gas chromatography, and R_F values in thin layer and paper chromatography; melting and boiling points; solvent effects on equilibrium or rate constants; and solubilities are examples of chemical property data.
3. *Quantitative structure–physical property relationships* (QSPR). Physical properties are either ground state properties or properties which depend on the difference in energy between the ground state and an excited state. Bond lengths, bond angles and dipole moments are ground state properties, infrared, ultraviolet, nuclear magnetic resonance and other types of spectra, ionization potentials and electron affinities are properties which depend on the energy difference between states.
4. *Quantitative structure–bioactivity relationships* (QSAR). Any property associated directly or indirectly with a living organism is a bioactivity. The bioactive substrates studied include pure enzymes, tissue homogenates, single cell organisms, whole tissues and multi-cellular organisms. The data for organisms may be obtained *in vitro* or *in vivo*; that for other substrates is obtained only *in vitro*. They include rate and equilibrium constants for enzyme reactivity and for binding to receptor sites, various kinds of toxicity determinations such as lethal dose and lethal concentration, and minimum effective concentrations, a measure of activity used for a wide range of bioactivity type.

1. The nature of SPQR

There are several different types of chemical species, including molecules, ions, radicals, carbenes; nitrenes, benzynes and so on, for which SPQR can be determined. Four kinds of structure are possible:

1. Species with the structure XGY, where X is a variable substituent, Y is a constant active site (an atom or group of atoms at which a measurable phenomenon takes place) and G is a constant skeletal group to which X and Y are bonded. An example

is a set of 4-substituted bicyclo[2.2.2]octane-1-carboxylic acids in which the bicyclo [2.2.2]octanylene segment is the skeletal group to which the substituent and the carboxyl group are bonded.
2. Species with the structure XY in which the variable substituent X is directly attached to the constant active site Y. An example is the set of XNH_2 where the amino group is the active site.
3. Species with the structure XG_Y in which the active site is part of the skeletal group. An example is a set of 3-substituted pyridinium ions in which the pyridine ring is the skeletal group and the N atom in the ring is the active site.
4. Species in which substituent and active site are the same, the entire species is the active site and it varies. These species are designated X_Y. Solvent effects fall into this category.

SPQR are intended to provide a quantitative description of the change in some measurable quantity Q that occurs when a change is made in the structure of the species by varying the substituent X. All of the other pertinent variables, such as the conditions of the measurement and the structural features G and Y, are not varied. Then equation 1 applies:

$$(\partial Q/\partial X)_{G,Y,T,P,Sv,I,\ldots} = Q_X \tag{1}$$

where Q_X is the measured quantity when the substituent is X, G is the skeletal group, Y the active site, T the temperature, P the pressure, Sv the solvent and I is the ionic strength, all of which are constant throughout the data set.

We *assume* that Q_X will be a linear function of some number of parameters which represent the effects of the structural variation of X. Equations 2a and 2b then apply:

$$Q_X = a_1 p_{1X} + a_2 p_{2X} + a_3 p_{3X} + \cdots + a_0 \tag{2a}$$

$$= \sum_{i=1}^{n} a_i p_{iX} + a_0 \tag{2b}$$

where the p_i are the parameters which account for the structural effect of X on Q. These parameters have been obtained in various ways:

1. From quantum chemical calculations[3]. This method is most suitable for electrical effect parameters.
2. From molecular mechanics calculations[4] for steric effect parameters.
3. From some property of a reference set by definition (primary values). This method assumes that structural effects on the data set to be studied are a linear function of those which occur in the reference set. Secondary values of these parameters can be estimated by various methods.
4. From comparative molecular field analysis (COMFA)[5]. This method can be used for electrical, steric and polarizability parameters.
5. From molecular geometry for steric parameters.
6. From topological algorithms[6]. This method is best restricted to steric effects and polarizability parameters. The nature of topological parameters has been described. They are composite parameters and result from a count of structural features[7].

When suitable parameters are available, the values of Q can be correlated with them by means of either simple linear regression analysis if the model requires only a single

variable, or multiple linear regression analysis if it requires two or more variables. Such a correlation results in a SPQR. In this work we consider only those parameters that are defined directly or indirectly from suitable reference sets or, in the case of steric parameters, calculated from molecular geometries.

An alternative method for obtaining SPQR is based on the use of neural networks[8].

2. The Uses of SPQR

SPQR have three major uses:

1. *Mechanistic.* QSRR and those QSAR which involve enzyme reactivity can provide information about the sensitivity of a reaction to electrical effects, its electronic demand, the composition of the electrical effect and the sensitivity to steric effects. QSAR which involve binding to receptor sites on proteins can provide information about the nature of the receptor site. Other QSAR can shed light on the bioactivity-determining step.
2. *Predictive.* All SPQR can be used to predict reactivities, chemical and physical properties and bioactivities. There are many practical applications of such predictions. Particular examples include the design of bioactive molecules such as medicinal drugs and pesticides. In addition to the maximization of activity and minimization of side effects, desirable pharmaceutical properties such as improved solubility, longer shelf life and controlled release can be developed. Also significant is their use in the development of prodrugs. They are also of great importance in environmental science, where they can be used to predict toxicities, biodegradabilities, solubilities and other properties of environmental interest. They may also be useful in materials science for the design of materials with specific properties.
3. *Archival.* SPQR provide a concise, efficient and convenient method for storing the results of experimental studies on the effect of structural changes upon chemical reactivities and properties, physical properties and bioactivities.

C. The Types of Structural Effects

Structural effects may be divided into three categories:

1. *Electrical effects.* These effects cause a variation in the electron density at the active site. They account for the ability of a substituent to stabilize or destabilize a cation, anion, radical, carbene or other chemical species.
2. *Steric effects.* These effects result from the repulsion between valence electrons in orbitals on atoms which are in close proximity but not bonded to each other, or by shielding an active site from a reactant or solvent.
3. *Inter- and intramolecular force effects.* These effects result either from the interactions between the substituent and its immediate surroundings such as the medium, a surface or a receptor site, or from the effect of the substituent on the interactions of the skeletal group G and the active site Y with their surroundings.

Electrical effects are the major factor in chemical reactivities and physical properties. Intermolecular forces are usually the major factor in bioactivities. Either electrical effects or intermolecular forces may be the predominant factor in chemical properties. Steric effects only occur when the substituent and the active site are in close proximity to each other and even then rarely account for more than twenty-five percent of the overall substituent effect.

II. ELECTRICAL EFFECTS

A. Introduction

The earliest successful parameterization of electrical effects is due to Hammett[9–11]. Though Burkhardt reported the existence of QSRR two years before Hammett, he did not develop a general relationship[12]. Hammett defined the σ_m and σ_p constants using the ionization constants $K_{A,X}$ of 3- and 4-substituted benzoic acids in water at 25 °C as the reference set and hydrogen as the reference substituent (K_H) to which all others are compared. For hydrogen, the values of the σ_m and σ_p constants were defined as zero (equation 3):

$$\sigma_X \equiv \log \frac{K_X}{K_H} \tag{3}$$

These parameters were intended to apply to XGY systems in which the skeletal group is 3- or 4-phenylene. Hammett found it necessary to define an additional set of parameters, σ_p^-, in order to account for substituent effects in 4-substituted benzene systems with an active site that has a lone pair on the atom adjacent to the benzene ring. The reference set was the ionization constants of 4-substituted phenols in water at 25 °C. Brown and his coworkers[13,14] later defined another set of constants, σ_p^+, to account for substituent effects in benzene derivatives with electronically deficient active sites. The reference set was the rate constants for the solvolysis of 4-substituted cumyl chlorides in 90% aqueous acetone at 25 °C. Finally, Wepster and coworkers[15] and Taft[16] both independently proposed constants intended to represent substituent effects in benzene derivatives with minimal delocalized effect. Using the Taft notation these constants are written as σ_p°. The reference systems had a methylene group inserted between the benzene ring and the active site ($XGCH_2Y$, where G is 1,4-phenylene) as it was argued that the methylene group acted as an insulator preventing conjugation between X and Y. These parameters all differ in electronic demand. They are used in the Hammett equation, which may be written in the form of equation 4:

$$Q_X = \rho\sigma_X + h \tag{4}$$

where Q_X is the value of the quantity of interest when the substituent is X, and σ_X is either σ_{mX}, σ_{pX}, ${\sigma_p}^{\circ}{}_X$, ${\sigma_p}^{+}{}_X$ or ${\sigma_p}^{-}{}_X$; ρ and h are the slope and intercept of the line. In using the Hammett equation it is necessary to make an *a priori* choice of parameters based on the location of the substituent and knowledge of the electronic demand in the data set which is to be modeled. If such knowledge is unavailable, as is often the case, it is necessary to correlate the data set with each different parameter. The parameter which gives the best fit is then assumed to be the proper choice and the electronic demand associated with it is that of the data set.

Taft and his coworkers[17–19] developed a diparametric model that separates the electrical effect into contributions from the 'inductive' (actually the field) effect and the resonance effect. This separation depends on the difference in the extent of electron delocalization when a substituent is bonded to an sp^3 hybridized carbon atom in one reference system and to an sp^2 hybridized carbon atom in another. As the first case represents minimal delocalization and the second extensive delocalization, we have referred to the two effects as the localized and delocalized electrical effects. This diparametric electrical effect model can be written as equation 5:

$$\mathrm{Q}_X = L\sigma_{LX} + D\sigma_{DX} + h \tag{5}$$

where σ_L and σ_D are the localized and delocalized electrical effect parameters, respectively, L and D are their coefficients and h is the intercept. Taft and coworkers[19] stated that four σ_D constants are required in order to account for all types of electronic demand, namely σ_{RX}, ${\sigma_R}^{o}{}_X$, ${\sigma_R}^{+}{}_X$ and ${\sigma_R}^{-}{}_X$. They correspond to the σ_p constants described above. Charton noted that in cases of very large electron demand two additional σ_D constants were required, $\sigma_R^{\oplus}$ for highly electron-deficient (positive) active sites[20] and $\sigma_R^{\ominus}$ for active sites that have a large electron excess (negative)[21].

An alternative diparametric model was proposed by Yukawa and Tsuno[22] for use with electron-deficient active sites and was originally written as equation 6:

$$Q_X = \rho\sigma_X + \rho r({\sigma_X}^{+} - \sigma_X) \tag{6}$$

A later version has the form of equation 7[23]:

$$Q_X = \rho\sigma_X + \rho r({\sigma_X}^{+} - \sigma_X^{\circ}) \tag{7}$$

Equation 8 is a similar relationship:

$$Q_X = \rho\sigma_X + \rho r({\sigma_X}^{-} - \sigma_X) \tag{8}$$

and has been proposed for active sites with an electron excess[24]. These relationships are termed the YT equations. They resemble the Hammett equation in being able to include both *meta*- and *para*-substituted compounds in the same data set. To do this it must be assumed that ρ_m is equal to ρ_p. This assumption is a reasonable approximation when the geometry of the data set of interest resembles that of the reference set from which σ_m and σ_p were defined, but in some cases the difference between ρ_m and ρ_p ($\Delta\rho$) is significant. The Yukawa–Tsuno and related models are therefore limited in scope.

Like the case of the Hammett equation, the use of the LD equation for the description of chemical reactivities required either an *a priori* knowledge of the type of σ_D substituent constant required or a comparison of the results obtained with correlations using each of the available σ_D constants. The use of the YT equation has generally been restricted to electronically deficient active sites. Clearly there was a need for a more general model of electrical effects that would avoid the *a priori* parameter choice. A triparametric model of the electrical effect has been introduced[25] that can account for the complete range of electrical effects on chemical reactivities of closed-shell species (carbenium and carbanions), namely reactions which do not involve radical intermediates. The basis of this model was the observation that the σ_D constants differ in their electronic demand. On the assumption that they are generally separated by an order of magnitude in this variable, it is possible to assign to each σ_D type a corresponding value of the electronic demand, η. Thus, equation 9 is obeyed:

$$\sigma_{DX} = a_1\eta + a_0 = \sigma_e\eta + \sigma_d \tag{9}$$

The intercept of this linear relationship represents the intrinsic delocalized (resonance) effect, σ_{dX}. This is the delocalized effect observed when the electronic demand of the data set studied is zero. The slope represents the sensitivity of the X group to the electronic demand of the active site. On substituting equation 9 into the LD equation (equation 10) we obtain the triparametric LDR equation:

$$Q_X = L\sigma_{lX} + D\sigma_{dX} + R\sigma_{eX} + h \tag{10}$$

The σ_l values are identical to the σ_I constants. The symbol was changed in order to be consistent with the other symbols used in the equation.

It is useful to describe the composition of the electrical effect for a particular case by the quantity P_D, which is defined by equation 11:

$$P_D \equiv 100|D|/(|L| + |D|) \tag{11}$$

When P_D is held constant, the LDR equation simplifies to the CR equation (equation 12):

$$Q_X = C\sigma_{ldX} + R\sigma_{eX} + h \tag{12}$$

where σ_{ld} is a composite parameter representing the localized and delocalized electrical effects. It is defined by equation 13:

$$\sigma_{ldX} = l\sigma_{lX} + d\sigma_{dX} \tag{13}$$

Lowercase letters are used for the coefficients in equations that represent a substituent constant as a function of other substituent constants. The difference between pure and composite parameters is that the former represent a single effect while the latter represent a combination of two or more. The percent composition of these parameters is given by equation 14:

$$P_D = \frac{100d}{l + d} \tag{14}$$

If the constant value of P_D is written as k', then the σ_{ldX} parameter for a given value of k' is given by equation 15:

$$\sigma_{ldXk'} = \sigma_{lX} + [k'/100 - k']\sigma_{DX} \tag{15}$$

Writing equation 16:

$$k^* = k'/(100 - k') \tag{16}$$

gives equation 17:

$$\sigma_{ldXk'} = \sigma_{lX} + k^*\sigma_{dX} \tag{17}$$

The Yukawa–Tsuno equation for 4-substituted benzene derivatives is approximately equivalent to the CR equation[26,27]. This observation has led to the development of a modified Yukawa–Tsuno (MYT) equation (equation 18) which has the form:

$$Q_X = \rho\sigma_X + R\sigma_{eX} + h \tag{18}$$

with σ taking the value σ_m for 3-substituted benzene derivatives and σ_{50} for 4-substituted benzene derivatives, while σ_{eX} for 3-substituted benzene derivatives is 0. The σ_{50} constants have k' equal to 50 and η equal to zero; they are therefore equal to the sum of the σ_l and σ_d values.

If the sensitivity to electronic demand is held constant, the LDR equation reverts to the LD equation (equation 5). An equation analogous to the MYT equation, the modified LD (MLD) equation (equation 19), can be written:

$$Q_X = \rho'\sigma_X + D\sigma_{DX} + h \tag{19}$$

In the MLD equation, σ is σ_m for 3-substituents and σ_l for 4-substituents while σ_D is 0 for 3-substituents; 3- and 4-substituted benzene derivatives can be combined into a single

data set. Again, use of the MLD equation is restricted to systems for which $\Delta\rho$ is not significant.

When both the electronic demand and the composition of the electrical effect are held constant, a set of composite parameters is described by equation 20:

$$\sigma_{k'/kX} = l\sigma_{lX} + d\sigma_{dX} + r\sigma_{eX} \tag{20}$$

where P_D and η are given by equations 21a and 21b, respectively:

$$k' = P_D = \frac{100d}{(l+d)} \tag{21a}$$

$$k = \eta = r/d \tag{21b}$$

The Hammett substituent constants are special cases of these parameters.

The $\sigma_{k'/k}$ values describe the overall electrical effect of the X group. They are obtained from equations 22a and 22b:

$$\sigma_{k'/kX} = \sigma_{lX} + [P_D/(100 - P_D)](\sigma_{dX} + \eta\sigma_{eX}) \tag{22a}$$

$$= \sigma_{lX} + k^*(\sigma_{dX} + k\sigma_{eX}) \tag{22b}$$

A plot of the $\sigma_{k'/kX}$ values for a group with P_D on the x-axis, η on the y-axis and $\sigma_{k'/k}$ on the z-axis produces a surface that characterizes the electrical effect of the X group.

B. Electrical Effects of Oxime, Hydroxamic Acid, Hydroxylamino and Related Substituents

Values of electrical effect substituent constants for oxime and hydroxylamino groups have been reported[25,28–30]; their values are set forth in Tables 1a–c. No value for the acid group, CO(NHOH), was available. We have estimated values for it; they are given in Tables 1a–c. Also in Tables 1a–c are values for some other types of substituents[25,28–30] either for purposes of comparison or because they were used in correlations in this work.

1. Classification of substituent electrical effects

Substituents are frequently classified as either electron acceptor (electron withdrawing, electron sink), EA; or electron donor (electron releasing, electron source), ED. There is a small third category as well that consists of groups whose electrical effect is not significantly different from zero (NS groups). Groups vary in the nature of their electrical effect to a greater or lesser extent depending on the electronic demand of the phenomenon being studied, the skeletal group, if any, to which they are bonded and the experimental conditions. Very few groups are in the same category throughout the entire range of P_D and η normally encountered. We have noted earlier that a plot of the $\sigma_{k'/k,X}$ values for a group with $X = P_D$, $Y = \eta$ and $Z = \sigma_{k'/k}$ produces a surface that characterizes the electrical effect of the X group[31]. A matrix of these values can be obtained by calculating them for values of P_D in the range 10 to 90 in increments of 10 and values of η in the range -6 to 6 in increments of 1. The resulting 9 by 13 matrix has 117 values. We define $\sigma_{k'/k,X}$ values greater than 0.05 as EA, $\sigma_{k'/k,X}$ values less than -0.05 as ED and $\sigma_{k'/k,X}$ values between 0.05 and -0.05 as NS. The variability of the electrical effect of a group can be quantitatively described by the percent of the matrix area in the P_D–η plane in

TABLE 1a. Electrical effect substituent constants for common substituents[a]

	σ_l	σ_d	σ_e	$\sigma_{c14.3}$	$\sigma_{c16.7}$	σ_{c50}	σ_{c60}
Ak, *c*-Ak							
Me	−0.01	−0.14	−0.03	−0.03	−0.04	−0.15	−0.22
Et	−0.01	−0.12	−0.04	−0.03	−0.03	−0.13	−0.19
c-Pr	0.01	−0.17	−0.07	−0.02	−0.02	−0.16	−0.25
Pr	−0.01	−0.15	−0.04	−0.04	−0.04	−0.16	−0.24
i-Pr	0.01	−0.16	−0.04	−0.02	−0.02	−0.15	−0.22
c-Bu	−0.01	−0.13	−0.05				
Bu	−0.01	−0.15	−0.04	−0.04	−0.04	−0.16	−0.24
i-Bu	−0.01	−0.14	−0.04	−0.03	−0.04	−0.15	−0.22
s-Bu	−0.01	−0.14	−0.04	−0.03	−0.04	−0.15	−0.22
t-Bu	−0.01	−0.15	−0.04	−0.04	−0.04	−0.16	−0.24
c-Pe	−0.01	−0.14	−0.04				
Pe	−0.01	−0.14	−0.04	−0.03	−0.04	−0.15	−0.22
CH_2Bu-*t*	0	−0.16	−0.04	−0.03	−0.03	−0.16	−0.24
c-Hx	0	−0.14	−0.04	−0.02	−0.03	−0.14	−0.21
1-Ad	−0.01	−0.12	−0.06	−0.03	−0.03	−0.13	−0.19
CH_2Z							
CH_2Br	0.2	−0.08	−0.03	0.19	0.18	0.12	0.08
CH_2OH	0.11	−0.1	−0.03	0.09	0.09	0.01	−0.04
CH_2Cl	0.17	−0.06	−0.02	0.16	0.16	0.11	−0.08
CH_2CN	0.2	−0.01	−0.01	0.2	0.2	0.19	0.18
CH_2OMe	0.11	−0.1	−0.04	0.09	0.09	0.01	−0.04
CH_2Vi	0.02	−0.16	−0.04	−0.01	−0.01	−0.14	−0.22
CH_2OEt	0.11	−0.1	−0.04	0.09	0.09	0.01	−0.04
CH_2NEt_2	0.03	−0.12	−0.04	0.01	0.01	−0.09	−0.15
CH_2Ph	0.03	−0.13	−0.06	0.01	0	−0.1	−0.17
CZ_3							
CF_3	0.4	0.13	−0.03	0.42	0.43	0.53	0.6
CCl_3	0.36	0.1	−0.02	0.38	0.38	0.46	0.51
VnX							
Vi	0.11	−0.08	−0.12	0.1	0.09	0.03	−0.01
C_2Z							
C_2H	0.29	−0.02	−0.1	0.29	0.29	0.27	0.26
C_2Me	0.3	−0.29	−0.09			0.01	
Ar							
Ph	0.12	−0.12	−0.12	0.1	0.1	0	−0.06
PnZ							
4-PnNMe$_2$	0.09	−0.32	−0.12	0.04	0.03	−0.23	−0.39
4-PnNEt$_2$	0.08	−0.27	−0.12	0.04	0.03	−0.19	−0.34
4-PnCl	0.15	−0.01	−0.07	0.15		0.14	
4-PnMe	0.1	−0.12	−0.04	0.08		−0.02	
4-PnOMe	0.11	−0.15	−0.06	0.08		−0.04	
4-PnNO$_2$	0.23	−0.01	−0.05	0.23		0.22	
Har							
2-Fr	0.17	−0.18	−0.13	0.14	0.13	−0.01	−0.1
3-Fr	0.09	−0.13	−0.12	0.07	0.06	−0.04	−0.11
(CO)Z							
CHO	0.3	0.27	−0.1	0.35	0.35	0.57	0.71
CO_2H	0.3	0.17	−0.04	0.33	0.33	0.47	0.56

TABLE 1a. (*continued*)

	σ_I	σ_d	σ_e	$\sigma_{c14.3}$	$\sigma_{c16.7}$	σ_{c50}	σ_{c60}
Ac	0.3	0.25	−0.1	0.34	0.35	0.55	0.68
CO_2Me	0.32	0.16	−0.07	0.35	0.35	0.48	0.56
CO_2Et	0.3	0.18	−0.06	0.33	0.34	0.48	0.57
$CONH_2$	0.28	0.12	−0.06			0.4	
CONHOH	**0**.29	**0.17**	**−0.07**			**0.46**	
$CONMe_2$	0.28	0.05	−0.06			0.33	
Bz	0.3	0.22	−0.11			0.52	
CN	0.57	0.12	−0.06	0.59	0.59	0.69	0.75
CH=NH	**0.16**	**0.09**	**−0.060**			**0.25**	
CH=NPh	**0.31**	**0.17**	**−0.060**			**0.48**	
CH=NOH	**0.20**	**0.12**	**−0.020**			**0.32**	
CH=NOMe							0.09
CMe=NOH	***0.20***	***0.12***	***−0.020***			***0.32***	
N							
N_3	0.43	−0.27	−0.12	0.38	0.38	0.16	0.02
NH_2	0.17	−0.68	−0.13	0.06	0.03	−0.51	−0.85
NHOH	0.15	−0.39	−0.10				
NHMe	0.13	−0.67	−0.18	0.02	0	−0.54	−0.88
NHAc	0.28	−0.35	−0.09			−0.07	
NMe_2	0.17	−0.66	−0.24	0.06	0.04	−0.49	−0.82
NEt_2	0.15	−0.65	−0.18	0.04	0.02	−0.5	−0.83
NO	0.37	0.31	−0.06	0.42	0.43	0.68	0.84
NO_2	0.67	0.18	−0.08	0.7	0.71	0.85	0.94
O							
OH	0.35	−0.57	−0.04	0.25	0.24	−0.22	−0.51
OMe	0.3	−0.55	−0.06	0.21	0.19	−0.25	−0.53
OAc	0.38	−0.24	0	0.34	0.33	0.14	0.02
OEt	0.28	−0.55	−0.07	0.19	0.17	−0.27	−0.55
OPr-*i*	0.27	−0.55	−0.07	0.18	0.16	−0.28	−0.56
OBu	0.28	−0.55	−0.07	0.19	0.17	−0.27	−0.55
OPh	0.4	−0.51	−0.08	0.31	0.3	−0.11	−0.37
S							
SH	0.27	−0.4	−0.1	0.2	0.19	−0.13	−0.33
SMe	0.3	−0.38	−0.13	0.24	0.22	−0.08	−0.27
SAc	0.39	−0.08	−0.06			0.31	
SEt	0.26	−0.39	−0.12	0.19	0.18	−0.13	−0.33
SPh	0.31	−0.34	−0.17	0.25	0.24	−0.03	−0.2
SOMe	0.54	−0.01	−0.04			0.53	
SOPh	0.51	−0.02	−0.05			0.49	
SO_2Me	0.59	0.13	−0.05	0.31	0.62	0.72	0.79
SO_2Ph	0.56	0.08	−0.08	0.57	0.58	0.64	0.68
Other							
H	0	0	0	0	0	0	0
Br	0.47	−0.27	−0.03	0.42	0.42	0.2	0.06
Cl	0.47	−0.28	−0.01	0.42	0.41	0.19	0.05
F	0.54	−0.48	0.041	0.46	0.44	−0.06	−0.18
I	0.4	−0.2	−0.06	0.37	0.36	−0.2	0.1

[a] Values are from References 24, 25 and 27 unless otherwise noted. Those in italics are estimates. Abbreviations will be found in Section VIII.B.

TABLE 1b. Values of F_D for common substituents[a]

X	σ_R^-	σ_R^-	σ_R^o	σ_R	σ_R^+	σ_R^+
Ak, *c*-Ak						
Me	−0.03	−0.1	−0.16	−0.16	−0.2	−0.25
Et	−0.01	−0.1	−0.14	−0.14	−0.1	−0.28
c-Pr	0.01	*−0.08*	*−0.15*	−0.19	−0.3	−0.43
Pr				−0.16		
i-Pr	*−0.04*	−0.1	−0.16	−0.16	−0.2	−0.34
Bu				−0.16		
i-Bu				−0.16		
s-Bu				−0.16		
t-Bu	*−0.05*	−0.11	−0.18	−0.18	−0.2	−0.33
Pe				−0.16		
CH_2Bu-*t*				−0.17		
c-Hx				−0.15		
Oc				−0.16		
Vinyl						
$CH{=}CH_2$	0.45	−0.1	−0.15	−0.15	−0.2	−0.56
Ethynyl						
C≡CH	0.28	0.13	−0.04	−0.04	−0.1	−0.45
Aryl						
Ph	0.28	0	−0.11	−0.11	−0.2	−0.69
PnZ						
4-PnCl	0.05	0	−0.07	−0.03	−0.2	−0.3
4-PnMe	0	−0.1	−0.12	−0.13	−0.2	−0.32
4-PnOMe		0		−0.19	−0.3	
4-PnNO_2	0.29	0.04	−0.03	0.03	−0.2	−0.21
CH_2Z						
CH_2Br				−0.1		
CH_2OH				−0.07	−0.2	
CH_2Cl				−0.08		
CH_2CN				−0.04		
CH_2OMe				−0.1		
CH_2Vi				−0.14		
CH_2NEt_2						
CH_2Ph				−0.13		
CZ_3						
CCl_3				0.08		
CF_3	*0.2*	0.18	0.11	0.11	0.15	0
Carbonyl						
CHO	*0.57*	0.53	0.15	0.15	0.15	−0.04
Ac	0.56	0.41	0.2	0.2	0.1	−0.05
$CONH_2$	*0.28*	0.23	0.08	0.08	0.1	−0.1
CONHOH						
CO_2Me	*0.37*	0.3	0.11	0.11	0.11	−0.12
CO_2Et	*0.37*	0.31	0.11	0.11	0.11	*−0.06*
CH=NOH					**−0.12**	
CMe=NOH					***0.12***	
CN	0.26	0.26	0.08	0.08	0.1	−0.1

TABLE 1b. (*continued*)

X	σ_R^-	σ_R^-	σ_R^o	σ_R	σ_R^+	σ_R^+
N						
NH_2	*−0.30*	−0.55	−0.42	−0.8	−1.1	−1.05
NHAc	*−0.09*	−0.28	−0.25	−0.35	−0.5	−0.75
NMe_2	*0.05*	−0.3	−0.44	−0.88	−1.2	−1.38
NO_2	0.41	0.37	0.1	0.1	0.1	−0.08
N_3	*0.08*	*−0.11*	*−0.21*	−0.31	*−0.47*	−0.67
O						
OH	*−0.45*	−0.45	−0.46	−0.62	−0.6	−0.71
OMe	−0.36	−0.51	−0.44	−0.58	−0.7	−0.83
OEt	*−0.35*	−0.51	−0.44	−0.57	−0.7	−0.86
OAc	*−0.23*	−0.16	*−0.22*	−0.23	−0.3	*−0.32*
OPh	*−0.27*	*−0.44*	−0.42	−0.48	*−0.64*	−0.96
S						
SH	*−0.11*	*−0.29*	*−0.32*	*−0.41*	*−0.56*	−0.81
SMe	0.01	−0.24	−0.31	−0.38	−0.6	−0.97
SAc	*0.09*	*0.00*	−0.08	*−0.09*	*−0.13*	*−0.34*
SEt	*−0.04*	−0.1	−0.3	−0.3	*−0.59*	−0.99
SPh	*0.16*	−0.11	−0.24	−0.34	*−0.65*	−1.00
SOMe	0.13	0.05	0	0	−0.1	−0.7
SOPh	*0.03*	*0.06*	−0.07	−0.07	*−0.21*	−0.81
SO_2Me	0.18	0.35	0.11	0.11	0.11	−0.12
SO_2Ph	*0.32*	*0.22*	0.12	0.12	*−0.16*	−0.42
Other						
F	*−0.61*	−0.58	−0.44	−0.48	−0.4	*−0.25*
Cl	*−0.25*	−0.3	−0.25	−0.25	−0.2	−0.41
Br	−0.21	−0.28	−0.25	−0.25	−0.2	−0.44
I	*−0.06*	−0.18	−0.16	−0.16	−0.2	−0.57
H	0	0	0	0	0	0

[a] Values are from References 24, 25 and 27 unless otherwise noted. Those in italics are estimates. Abbreviations will be found in Section VIII. B.

TABLE 1c. Values of Hammett substituent constants [a]

X	σ_m	σ_p^-	σ_p^o	σ_p	σ_p^+
Ak, *c*-Ak					
Me	−0.06	−0.15	−0.15	−0.17	−0.3
Et	−0.06	−0.1	−0.12	−0.15	−0.3
c-Pr	−0.08	−0.1	−0.15	−0.22	−0.5
Pr	−0.06			−0.17	
i-Pr	*−0.04*	*−0.12*	*−0.12*	−0.15	−0.3
s-Bu					
t-Bu	0	*−0.15*	*−0.14*	−0.19	−0.3
CH_2Bu-*t*	−0.05			−0.17	
c-Hx	−0.05			−0.17	
Vinyl					
$CH{=}CH_2$	0.02	0.21	0.02	−0.05	−0.3

(*continued overleaf*)

TABLE 1c. (*continued*)

X	σ_m	σ_p^-	σ_p^o	σ_p	σ_p^+
Ethynyl					
C≡CH	0.24	0.5	0.26	0.21	0.10
Aryl					
Ph	0.09	0.08	0	0.01	−0.50
CH_2Z					
CH_2Br	0.17			0.1	
CH_2OH	0.1			0.04	
CH_2Cl	0.15			0.09	
CH_2CN	0.2			0.16	
CH_2OMe	0.08			0.01	
CH_2Ph	−0.01			−0.1	
CX_3					
CF_3	0.46	0.74	0.52	0.53	0.61
CCl_3	0.4			0.44	
Carbonyl					
CHO	0.36	0.91	0.5	0.45	0.53
Ac	0.38	0.82	0.46	0.5	0.51
$CONH_2$	0.31	0.62	0.37	0.37	0.39
CONHOH					
$CONMe_2$	0.31	0.62	0.37	0.37	0.39
CO_2Me	0.36	0.74	0.46	0.44	0.49
CO_2Et	0.35	0.74	0.46	0.44	0.49
Bz	0.36			0.41	
CN	0.61	1.02	0.69	0.65	0.66
CH=NOH	**0.22**			**0.10**	
CH=NOMe	**0.37**			**0.30**	
CMe=NOH	**0.49**	**0.61**			**0.16**
N					
NH_2	−0.21	−0.51	*−0.40*	−0.63	−1.3
NHAc	0.11	0.03	0	−0.12	−0.5
NMe_2	−0.22	−0.35	−0.44	−0.67	−1.5
NO_2	0.74	1.29	0.82	0.77	0.79
N_3	0.27	0.38	0.2	0.08	−0.3
O					
OH	0.13	*−0.24*	−0.1	−0.38	*−0.6*
OMe	0.11	−0.25	−0.12	−0.28	−0.8
OEt	*0.07*	*−0.27*	−0.16	*−0.29*	*−0.73*
OAc	0.31	0.2	0.21	0.16	0.1
OPh	*0.23*	*−0.04*	*−0.01*	*−0.08*	*−0.6*
S					
SH	*0.07*	*−0.04*	*−0.06*	−0.19	−0.58
SMe	0.09	0.04	−0.02	−0.17	−0.6
SAc	0.34	0.5	0.33	0.28	0.18
SEt	*0.16*	*−0.01*	*−0.07*	*−0.04*	*−0.63*
SPh	*0.23*	0.18	*0.01*	−0.15	*−0.64*
SOMe	0.47	0.74	0.47	0.54	0.21
SOPh	*0.50*	*0.75*	*0.51*	*0.44*	*0.44*
SO_2Me	0.63	1.13	0.71	0.7	0.75
SO_2Ph	*0.62*	0.95	*0.68*	*0.68*	*0.48*

TABLE 1c. (*continued*)

X	σ_m	σ_p^-	σ_p^o	σ_p	σ_p^+
Other					
F	0.34	0.03	0.17	0.06	0
Cl	0.37	0.28	0.27	0.22	0.11
Br	0.34	0.3	0.26	0.22	0.15
I	0.35	0.35	0.27	0.24	0.13
H	0	0	0	0	0

[a] Values are from References 24, 25 and 27 unless otherwise noted. Those in italics are estimates. Abbreviations will be found in Section VIII.B.

which the group is in each category (P_{EA}, P_{ED} and P_0). Approximate measures of these quantities are given by equation 23:

$$P_{EA} = \frac{n_{EA}}{n_T}, \quad P_0 = \frac{n_{NS}}{n_T}, \quad P_{ED} = \frac{n_{ED}}{n_T} \tag{23}$$

where n_{EA}, n_{NS}, n_{ED} and n_T are the number of EA, the number of NS, the number of ED and the total number of values in the matrix. Substituent electrical effects can be classified as follows:

1. Entirely electron acceptor (**EA**) ($P_{EA} = 100$). Examples: CF_3, $PO(OMe)_2$, $POPh_2$.
2. Predominantly electron acceptor (**PA**) ($100 > P_{EA} \geqslant 75$). Examples: NO_2, HCO, CN.
3. Largely electron acceptor (**LA**) ($75 > P_{EA} \geqslant 50$). Examples: Cl, C_2Ph, OCN, OAc.
4. Ambielectronic (**AM**) ($50 > P_{EA}$ or P_{ED}). Examples: SH, CH_2Ph, $SiMe_3$.
5. Largely electron donor (**LD**) ($75 > P_{ED} \geqslant 50$). Examples: Me, OH, NH_2.
6. Predominantly electron donor (**PD**) ($100 > P_{ED} \geqslant 75$). Examples: $P = PMe$, $P = POMe$.
7. Entirely electron donor (**ED**) ($P_{ED} = 100$). Example: $P = PNMe_2$

The values in italics are based on estimated substituent constants.

2. The nature of substituent electrical effects

The overall electrical effect of a substituent as noted above is a function of its σ_l, σ_d and σ_e values. It depends on the nature of the skeletal group G, the active site Y, the type of phenomenon studied, the medium and the reagent, if any. These are the factors that control the values of P_D and η, which in turn determine the contributions of σ_l, σ_d and σ_e.

3. The mode of transmission of substituent electrical effects

The mode of transmission of a substituent electrical effect is the way in which a substituent bonded to the i-th atom of a skeletal group G exerts an electrical effect on an active site bonded to the j-th atom of G. For almost a century there has been disagreement about the manner of transmission of substituent electrical effects. Derick[32] in 1911 proposed two possible modes of transmission:

1. An inductive effect which involves the successive polarization of the bonds between X and Y. The decrease in the effect with increasing number of bonds is due to a falloff factor f, which decreases the effect for each successive polarization. The value of f is 0.33–0.36[33–35]. This is the classical inductive effect (CIE) model.

2. A through-space electrostatic effect (field effect) due to the charge on X. This model was developed by Kirkwood and Westheimer[36,37] who applied classical electrostatics to the problem. They showed that this model, the classical field effect (CFE), depended on the distance d between X and Y, the cosine of the angle θ between d and the X−G bond, the effective dielectric constant and the bond moment of X.

Exner and Fiedler[38] have proposed a modified inductive effect (MIE). The MIE model represents transmission through two or more paths by an expression analogous to Kirchhoff's Law for the resistance of parallel resistors.

When the conditions under which the reactivity or property that is measured are held constant and L is chosen as the measure of the extent of electrical-effect transmission, the classical inductive effect is given by equation 24[39]:

$$L = \text{Ç} \sum_{i=1}^{k} f^n \tag{24}$$

where Ç is a constant, f is the falloff factor, k is the number of paths between X and Y and n is the number of bonds in each path.

The available data are best fit by the modied field effect (MFE) model, which can be written as either equation 25 or equation 26:

$$L = \check{C} \cos\theta n^m \tag{25}$$

$$\log|L| = \log\cos\theta + m\log n + \log\check{C} \tag{26}$$

Quantum chemical calculations on substituted alkanes are in agreement with a through-space (field) transmission of substituent electrical effects[40]. In view of the ever-increasing evidence for through-space transmission of electrical effects, it is time to make a conclusive statement. *There is no inductive-effect component in electrical-effect transmission!*

III. STERIC EFFECTS

A. Introduction

The concept of steric effects was introduced by Kehrmann[41] over a century ago. V. Meyer[42] and Sudborough and Lloyd[43] shortly thereafter presented kinetic results supporting the steric effect as an explanation of rate retardation in the esterification of 2-substituted and 2,6-disubstituted benzoic and 3-*cis*-substituted acrylic acids. Major early reviews of steric effects were given by Stewart[44] and Wittig[45]. Somewhat later reviews are those by Wheland[46] and contributors to a volume edited by Newman[47].

B. The Nature of Steric Effects

1. Primary steric effects

Primary steric effects are due to repulsions between electrons in valence orbitals on adjacent atoms which are not bonded to each other. They are believed to result from the interpenetration of occupied orbitals on one atom by electrons on the other, resulting in a violation of the Pauli exclusion principle. *All steric interactions raise the energy of the system in which they occur*. Their effect on chemical reactivity is to either decrease or increase a rate or equilibrium constant depending on whether steric repulsions are greater in the reactant or in the product (equilibria) or transition state (rate).

2. Secondary steric effects

Secondary steric effects on chemical reactivity can result from the shielding of an active site from the attack of a reagent, from solvation, or both. Alternatively they may be due to a steric effect on the reacting conformation of a chemical species that determines its concentration.

3. Direct steric effects

These effects can occur when the active site at which a measurable phenomenon occurs is in close proximity to the substituent. Among the many systems that can exhibit direct steric effects are *ortho*-substituted benzenes, **1**, *cis*-substituted ethenes, **2**, and polycyclic aromatic hydrocarbons with *ortho* or *peri* substituents such as the *ortho*- (1,2-; 2,1-; and 2,3-) and *peri*- (1,8-) substituted naphthalenes, **3**, **4**, **5** and **6**, respectively. Other examples are alicyclic systems such as *cis*-1,2-disubstituted cyclopropanes, *cis*-2,3-disubstituted norbornanes and *cis*-2,3-disubstituted [2.2.2]bicyclooctanes, **7**, **8** and **9**, respectively. Some systems with substituents adjacent to active sites generally do not show steric effects. Geminally substituted systems such as disubstituted methanes, **10**, and 1,1-disubstituted ethenes, **11**, are examples; 2,3-, 3,2- and 3,4-disubstituted heteroarenes with five-membered rings, such as furans, pyrroles, thiophenes and selenophenes, **12**, **13** and **14**, respectively, are also generally free of steric effects (Ht is the heteroatom). This is probably due to the larger XCC angle in these systems as compared with benzenoid systems. Heteroarenes with six-membered rings, such as 2,3-disubstituted pyridines **15**, can exhibit steric effects.

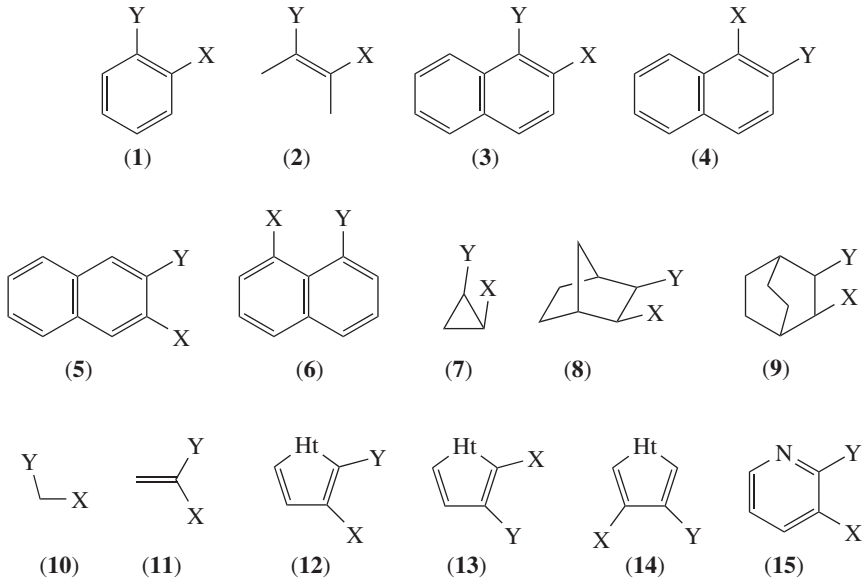

4. Indirect steric effects

These effects are observed when the steric effect of the variable substituent is relayed by a constant substituent between it and the active site, as in **16** where Y is the active site,

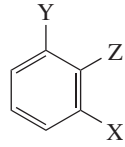

(**16**)

Z is the constant substituent and X is the variable substituent. This is a type of buttressing effect.

5. The directed nature of steric effects

There is a regrettable tendency to regard steric effects as being related to 'bulk'. Unfortunately, the word bulk is invariably used without a precise definition of its meaning. The usual form of this error is the use of the phrase 'steric bulk', generally accompanied by verbal hand waving. Presumably, this is intended to imply group size in some undefined way. Steric effects are vector quantities. This is easily shown by considering, for example, the ratio r of the steric parameter υ for any five-carbon alkyl group to that for 1-pentyl. Values of r are: 1-Pe, 1; 2-Pe, 1.54; 3-Pe, 2.22; CH_2Bu-*s*, 1.47; CH_2Bu-*i*, 1.00; CH_2Bu-*t*, 1.97; CMe_2Et, 2.40; CHMePr-*i*, 1.90. All of these groups have the same volume and therefore the same bulk and the same polarizability but they differ in steric effect. In order to account for this it is necessary to consider what happens when a nonsymmetric substituent is in contact with an active site. Take as an example the simple case of a spherical active site Y in contact with a nonsymmetric substituent, $MZ^LZ^MZ^S$, where the superscripts L, M and S represent the largest, the medium sized and the smallest Z groups respectively. There are three possible conformations of this system. They are shown in Figure 1. As all steric repulsions raise the energy of the system, the preferred conformation will be the one that results in the lowest energy increase. This is the conformation which presents the smallest face to the active site, conformation **A**. This observation results in the minimum steric interaction (MSI) principle which states:

A nonsymmetric substituent prefers that conformation which minimizes steric interactions.

The directed nature of primary steric effects results in a conclusion of vital importance, that in general:

The volume of a substituent is not an acceptable measure of its steric effect[48–50].

There are still some workers who are unable to comprehend this point. It is nevertheless true that group volumes are not useful as steric parameters. They are actually

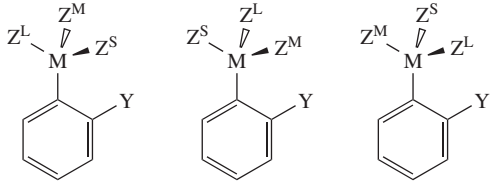

(**A**) (**B**) (**C**)

FIGURE 1. Possible conformations of an *ortho*-substituted benzene having a spherical reaction site Y in contact with a tetrahedral substituent consisting of a central atom M bonded to large (Z^L), medium (Z^M) and small (Z^S) groups. The energy of the conformations is A < B < C. Analogous systems are those in which substituent and reaction site are in contact

measures of group polarizability. In short, for a range of different substituent shapes in a data set:

Steric effects are not *directly related to bulk, polarizability is.*

C. The Monoparametric Model of Steric Effects

Stewart[44] proposed a parallel between the rate of esterification of 2-substituted benzoic acids and the molecular weights of the substituents. The nitro group deviated strongly from this relationship. It is the first work to attempt to relate the steric effect of a group to some property that might at least in part be a measure of size. Kindler[51] made the first attempt at defining a set of steric parameters. These parameters were later shown to be a function of electrical effects. The first successful parameterization of the steric effect is due to Taft[35], who defined the steric parameter E_S for aliphatic systems by equation 27:

$$E_{S,X} \equiv \delta \log \frac{k_X}{k_{Me}} \tag{27}$$

where k_X and k_{Me} are the rate constants for the acid-catalyzed hydrolysis of the corresponding esters XCO_2Ak and $MeCO_2Ak$, respectively. The value of δ is taken as 1.000 for this purpose; $E_{So,X}$ parameters intended to represent the steric effects of substituents in the *ortho* position of a benzene derivative were defined for a few groups from the rates of acid-catalyzed hydrolysis of 2-substituted alkyl benzoates. These parameters are a mix of electrical and steric effects with the former predominating and are therefore of no use as steric parameters.

The original Taft $E_{S,X}$ values suffered from several deficiencies:

1. Their validity as measures of steric effects was unproven.
2. They were determined from average values of rate constants obtained under varying experimental conditions, often in different laboratories.
3. They were available only for those groups in which the atom bonded to G or Y (the first atom of the substituent) is an sp^3 hybridized carbon atom, and for hydrogen. Values were therefore unavailable for many if not most of the substituents generally encountered.
4. The use of the methyl group as the reference substituent meant that they were not compatible with electrical-effect substituent constants for which the reference substituent is hydrogen.

The first problem was resolved when it was shown that the E_S values for symmetric groups are a linear function of van der Waals radii[52]. The latter have long been held to be an effective measure of atomic size. The second and third problems were solved by Charton, who proposed the use of the van der Waals radius as a steric parameter[53] and developed a method for the calculation of group van der Waals radii for tetracoordinate symmetric top substituents MZ_3, such as the methyl and trifluoromethyl groups[54]. In later work the hydrogen atom was chosen as the reference substituent and the steric parameter υ was defined in equation 28:

$$\upsilon_X \equiv r_{VX} - r_{VH} = r_{VX} - 1.20 \tag{28}$$

where r_{VX} and r_{VH} are the van der Waals radii of the X and H groups in Angstrom units[55]. Expressing r_V in these units is preferable to the use of picometers, because the coefficient of the steric parameter is then comparable in magnitude to the coefficients of the electrical-effect parameters in correlation equations containing both types of parameters. Whenever possible, υ parameters are obtained directly from van der Waals radii or

calculated from them. An equation has been derived which makes possible the calculation of υ values for nonsymmetric tetrahedral groups of the types $MZ_2^SZ^L$ and $MZ^SZ^MZ^L$ in which the Z groups are symmetric. These are considered to be primary values[56]. For the greater number of substituents however, υ parameters must be calculated from the regression equations obtained for correlations of rate constants with primary values. The values obtained in this manner are considered to be secondary υ values. All other measures of atomic size are a linear function of van der Waals radii. There is, therefore, no reason for preferring one measure of atomic size over another. As values of υ were developed for a wide range of substituent types with central atoms including oxygen, nitrogen, sulfur and phosphorus as well as carbon, these parameters provide the widest structural range of substituents for which a measure of the steric effect is available.

1. Steric classification of substituents

Substituents may be divided into three categories based on the degree of conformational dependence of their steric effects:

1. No conformational dependence (NCD). Groups of this type include monatomic substituents such as hydrogen and the halogens, cylindrical substituents such as the ethynyl and cyano groups, and tetracoordinate symmetric top substituents such as the methyl, trifluoromethyl and silyl groups.
2. Minimal conformational dependence (MCD). Among these groups are:
   a. Nonsymmetric substituents with the structure $MH_n(lp)_{3-n}$ such as the hydroxyl and amino groups (lp is a lone pair).
   b. Nonsymmetric substituents with the structure $MZ_2^SZ^L$ where S stands for small and L for large.
3. Strong conformational dependence (SCD). These groups have the structures:
   a. $MZ_2^LZ^S$ and $MZ^LZ^MZ^S$, where the superscript M indicates medium.
   b. Planar π-bonded groups MZ^LZ^S where M and either or both Z^S are sp^2 hybridized, such as phenyl, acetyl, nitro ($X_{p\pi}$ groups) (Figure 2).
   c. Quasi planar π-bonded groups such as dimethylamino and cyclopropyl.

The steric parameter for NCD groups can be obtained directly from van der Waals radii, or calculated from them. The values for MCD groups are often obtainable from van der Waals radii although in some cases they must be derived as secondary values from regression equations obtained by correlating rate constants with known values of the steric parameter. Steric parameters for SCD groups of the nonsymmetric type are usually obtainable only from regression equations. In the case of planar π-bonded groups the maximum and minimum values of the steric parameter are available from the van der Waals radii. These groups are sufficiently common and important to require a more detailed discussion.

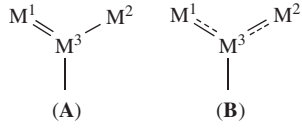

FIGURE 2. Examples of planar π-bonded groups. (A) M^1, any atom that can have sp^2 hybridization; M^3, C or N; M^2, any substituent. Examples of doubly bonded groups are ZC=O, ZC=S, C=C, N=N, ZN=O, $Z^1C{=}NZ^2$. (B) M^1, M^2, M^3, any atom that can undergo sp^2 hybridization e.g. aryl, heteroaryl, nitro, carboxylate. M^1 and M^2 are atoms of Z^S and Z^L

2. Planar π-bonded groups

These $X_{p\pi}$ groups represent an especially difficult problem because their delocalized electrical effect depends on the steric effect when they are bonded to planar π-bonded skeletal groups, $G_{p\pi}$. An approach to the problem has been developed[57,58]. The σ_d and σ_e electrical-effect parameters are a function of the dihedral angle formed by $X_{p\pi}$ and $G_{p\pi}$. The relationship generally used is equation 29:

$$P = P_0 \cos^2 \theta \tag{29}$$

where P is the property of interest and P_0 is its value when the dihedral angle, θ, is zero. Thus for $\sigma_{X,\theta}$ equation 29 becomes equations 30 and 31:

$$\sigma_{dX,\theta} = \sigma_{dX,0} \cos^2 \theta \tag{30}$$

$$\sigma_{eX,\theta} = \sigma_{eX,0} \cos^2 \theta \tag{31}$$

where $\sigma_{dX,0}$ and $\sigma_{eX,0}$ are the values of σ_d and σ_e when the substituent and skeletal group are coplanar ($\theta = 0$). The steric parameter does not depend on equation 31; the effective value of υ, which is derived from the geometry of the system, is given by equation 32:

$$\upsilon = d' \cos\theta + r_{VZS} - 1.20 \tag{32}$$

where Z^S is the smaller of the two Z groups attached to the central atom, M, of the $X_{p\pi}$ group and d' is the distance between the center of Z^S and the perpendicular to the line joining that center with the group axis. There is no simple *a priori* way to determine θ. It could conceivably be estimated by molecular mechanics calculations, but there is some reason to believe that θ is a function of the medium. Alternatively, the $X_{p\pi}$ group can be included in the data set by means of an iteration procedure. The method requires an initial correlation of the data set with all $X_{p\pi}$ and other SCD groups excluded. This constitutes the basis set. The correlation equation used for this purpose is the LDRS equation, which takes the form of equation 33:

$$Q_X = L\sigma_{lX} + D\sigma_{dX} + R\sigma_{eX} + S\upsilon + h \tag{33}$$

The correlation is then repeated for each $X_{p\pi}$ group using υ values increasing incrementally by some convenient amount from the minimum which represents the half-thickness of the group, to the maximum which occurs when $X_{p\pi}$ is nearly perpendicular to $G_{p\pi}$. The proper value of θ is that which:

1. Results in the best fit of the data to the correlation equation. The best fit is indicated by the minimal value of the S_{est} and S^o statistics, and the maximal value of the F and $100R^2$ statistics. The statistics used in this work are described in Section VIII. A.
2. Has the L, D, R, S and h values that are in best agreement with those of the basis set.

This method has the advantage of providing an estimate of θ under the reaction conditions.

D. Bond Length Difference as a Factor in Steric Effects

The steric effect exerted by some group X is a function of the lengths of the substituent-skeletal group (X−G) and active site-skeletal group (Y−G) bonds[58]. The steric parameters described above function best when they are of comparable length. In that case the contact between X and Y is that shown in Figure 3A. If the YG bond is much shorter than the XG bond the contact is as shown in Figure 3B. In that case the distance from Y to the

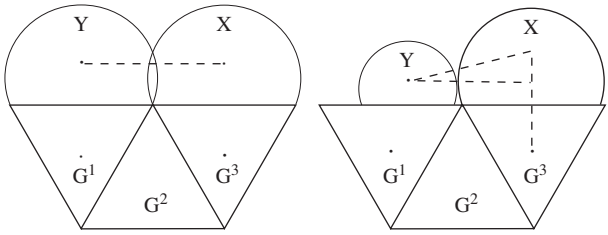

G^1, G^2 and G^3 consecutive atoms of the skeletal group G,
X is a substituent and Y is an active site.

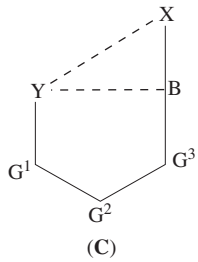

FIGURE 3. The effect of the major substituent on the reaction-site bond-length difference. (A) GX and GY are of comparable length (G is the skeletal group to which X and Y are bonded). (B, C) There is a major difference between XG and YG

X−G bond is less in Figure 3B than it is in Figure 3A although the XY distance in both Figures 3A and 3B is the sum of the van der Waals radii, r_{VX} and r_{VY}. The effective size of the van der Waals radius of X is reduced. Steric parameters were originally derived for systems like that in Figure 3A. In a system like that in Figure 3B, corrected steric parameters are needed. An approximate value of the effective van der Waals radius of X, r^c_{VX}, can be calculated for the case in which the X−G and Y−G bonds are parallel to each other from a consideration of Figure 3C and Scheme 1, where l_{XG} and l_{YG} are the lengths of the X−G and Y−G bonds, respectively.

Values of steric effect substituent constants for typical groups are set forth in Table 2.

$$\overline{XY} = r_{VX} + r_{VY}$$
$$\overline{XB} = l_{XG} - l_{YG}$$
$$\overline{BY} = [(\overline{XY})^2 - (\overline{XB})^2]^{1/2}$$
$$\overline{BY} = [(r_{VX} + r_{VY})^2 - (l_{XG} - l_{YG})^2]^{1/2}$$
$$\overline{BY} = r_{VY} + r^c_{VX}$$
$$r^c_{VX} = [(r_{VX} + r_{VY})^2 - (l_{XG} - l_{YG})^2]^{1/2} - r_{VY}$$

SCHEME 1

TABLE 2. Steric-effect parameters for common substituents[a]

X	υ	υ_1	υ_2	n_1	n_2
Ak, *c*-Ak					
Me	0.52	0.52	0	0	0
Et	0.56	0.52	0.25	1	0
Pr	0.68	0.52	0.52	1	1
i-Pr	0.78	0.78	0	2	0
Bu	0.68	0.52	0.52	1	1
i-Bu	0.98	0.52	0.78	1	2
s-Bu	1.02	0.78	0.52	2	1
t-Bu	1.24	1.24	0.52	3	0
Pe	0.68	0.52	0.52	1	1
s-Pe	0.68	0.52	0.52	1	1
c-Hx	0.87			1.5	0.74
Hx	0.73	0.52	0.52	1	1
Oc	0.68	0.52	0.52	1	1
1-Ad	1.33	1.33			
CH_2Z					
CH_2Br	0.64	0.52	0.65		
CH_2Cl	0.6	0.52	0.55		
CH_2OMe	0.63				
CH_2-2-Fr	0.7	0.52	0.57		
CH_2NEt_2		0.52	0.63		
Vn					
Vi	0.57	0.57	0.57		
Ar					
Ph	0.57	0.57	0.57		
PnZ					
4-$PnNMe_2$	0.57	0.57	0.57		
4-$PnNEt_2$	0.57	0.57	0.57		
4-PnCl	0.57	0.57	0.57		
4-PnMe	0.57	0.57	0.57		
4-PnOMe	0.57	0.57	0.57		
4-$PnNO_2$	0.57	0.57	0.57		
Har					
2-Fr	0.57	0.57	0.57		
3-Fr	0.57	0.57	0.57		
COZ, CNZ					
CHO	0.50	0.50	0.32		
Ac	0.50	0.50	0.32		
$CONH_2$	0.50	0.50	0.32		
CONHOH	**0.50**	**0.50**	**0.32**		
$CONMe_2$	0.50	0.50	0.32		
CO_2Me	0.50	0.50	0.32		
CO_2Et	0.50	0.50	0.32		
Bz	0.50	0.50	0.32		
CN	0.40	0.40	0.40		
CH=NH	**0.50**	**0.50**	**0.35**		
CH=NOH	**0.50**	**0.50**	**0.35**		

(*continued overleaf*)

TABLE 2. (*continued*)

X	υ	υ_1	υ_2	n_1	n_2
CH=NOMe	**0.50**	**0.50**	**0.35**		
CMe=NOH	**0.50**	**0.50**	**0.35**		
CH=NPh	**0.50**	**0.50**	**0.35**		
N					
NH_2	0.35	0.35			
NHOH	0.35	0.35	0.32		
NHMe	0.35	0.35	0.52		
NHAc	0.35	*0.50*	0.32		
NMe_2	0.35	0.52	0		
NO_2	0.35	0.32	0.35		
N_3	0.35	0.35	0.35		
O					
OH	0.32	0			
OMe	0.32	0.32	0.52		
OEt	0.36	0.32	0.52		
OAc	0.48	0.32	*0.52*		
$OSiMe_3$	0.5	0.32	1.4		
OPh	0.57	0.32	*0.57*		
S					
SH	0.6	0.6	0		
SMe	0.64	0.6	0.52		
SAc	1.09	0.6	*0.50*		
SEt	0.94	0.6	0.52		
SPh	1	0.6	*0.57*		
SOMe	0.76	0.74	0.52		
SOPh	1.1	0.74	*0.57*		
SO_2Me	1.13	1.03	0.52		
SO_2Ph		1.03	*0.57*		
Other					
H	0	0	0		
F	0.27	0.27	0		
Cl	0.55	0.55	0		
Br	0.65	0.65	0		
I	0.78	0.78	0		

[a] Values in italics are estimates. Abbreviations will be found in Section VIII. B.

E. Multiparametric Models of Steric Effects

In some cases a simple monoparametric model of the steric effect is insufficient. Examples are when the active site is itself large and nonsymmetric, or alternatively when the phenomenon studied is some form of bioactivity in which binding to a receptor is the key step. The failure of the monoparametric model is due to the fact that a single steric parameter cannot account for the variation of the steric effect at various points in the substituent. The use of a multiparametric model of steric effects that can represent the steric effect at different segments of the substituent is required. Five multiparametric models are available: that of Verloop and coworkers[59], the simple branching model, the expanded branching model, the segmental model and the composite model. The Verloop model suffers from the fact that its parameters measure maximum and minimum distances perpendicular to the group axis for each group. These maxima and minima may occur

at any point in the group skeleton (the longest chain in the group). The steric effect, however, may be very large at one segment of the chain and negligible at others. If a data set is large, as it must be if a multiparametric model is to be used, the likelihood that:

1. the maximum and minimum distances of all groups are located at the same segment,
2. that it is this segment at which the steric effect is important,

is very small. The Verloop model will therefore not be discussed further.

1. The branching equations

The simple branching model[56, 58, 60] for the steric effect is given by equation 34:

$$S\psi = \sum_{i=1}^{m} a_i n_i + a_b n_b \tag{34}$$

where $S\psi$ represents the steric effect parameterization, a_i and a_b are coefficients, n_i is the number of branches attached to the i-th atom and n_b is the number of bonds between the first and last atoms of the group skeleton. It follows that n_b is a measure of group length. Unfortunately, it is frequently highly collinear in group polarizability, which greatly limits its utility. For saturated cyclic substituents it is necessary to determine values of n_i from an appropriate regression equation[61]. For planar π-bonded groups n_i is taken to be 1 for each atom in the group skeleton. For other groups n_i is obtained simply by counting branches. The model makes the assumption that all of the branches attached to a skeleton atom are equivalent. This is at best only a rough approximation. Distinguishing between branches results in an improved model, called the expanded branching equation (equation 35):

$$S\psi = \sum_{i=1}^{m} \sum_{j=1}^{3} a_{ij} n_{ij} + a_b n_b \tag{35}$$

which allows for the difference in steric effect that results from the order of branching[56, 61]. This difference follows from the MSI principle. The first branch has the smallest steric effect because a conformation in which it is rotated out of the way of the active site is preferred. In this conformation the active site is in contact with two hydrogen atoms. The preferred conformation in the case of a second branch has the larger of the two branches directed out of the way. The smaller branch and a hydrogen atom are in contact with the active site. When there are three branches, the largest will be directed out of the way and the other two will be in contact with the active site.

The problem with the expanded branching method is that it requires a large number of parameters. Data sets large enough to permit its use are seldom seen. It has been applied to a number of studies in which only alkyl groups are substituents that are varying. In this case electrical effects are constant, thus only steric effects need be considered.

2. The segmental model

As both branching methods have problems associated with them, the segmental method[61] is often the simplest and most effective of the multiparametric models. In this model each atom of the group skeleton together with the atoms attached to it constitutes a segment of the substituent. Applying the MSI principle, the segment is considered to have that conformation which presents its smallest face to the active site. The segment is assigned the υ value of the group which it most resembles. Values of the segmental

steric parameters υ_i, where i designates the segment number, are also given in Table 2. Numbering starts from the first atom of the group skeleton which is the atom that is attached to the rest of the system. The segmental model is given by equation 36.

$$S\psi = \sum_{i=1}^{m} S_i \upsilon_i \tag{36}$$

When only steric effects are present, equation 37 applies:

$$Q_X = S\psi_X \tag{37}$$

In the general case, electrical effects are also present and the general form of the LDRS equation (equation 38) applies:

$$Q_X = L\sigma_{DX} + D\sigma_{dX} + R\sigma_{eX} + S\psi_X + h \tag{38}$$

3. The composite model

The composite model is a combination of the monoparametric υ model with the simple branching model. This method has proven useful in modeling amino acid, peptide and protein properties[62]. It is an improvement over the simple branching model and requires only one additional parameter.

IV. INTERMOLECULAR FORCES

A. Introduction

Inter- and intramolecular forces (imf) are of vital importance in the quantitative description of structural effects on bioactivities and chemical properties. They can make a significant contribution to chemical reactivities and some physical properties as well. Types of intermolecular forces and their present parameterization are listed in Table 3[63, 64].

TABLE 3. Intermolecular forces and the quantities upon which they depend[5a]

Intermolecular force	Quantity
Molecule–molecule	
Hydrogen bonding (hb)	q_{MH}, q_{ME}, orbital type
Dipole–dipole (dd)	dipole moment
Dipole–induced dipole (di)	dipole moment, polarizability
Induced dipole–induced dipole (ii)	Polarizability
Charge transfer (ct)	ionization potential, electron affinity
Ion–molecule	
Ion–dipole (Id)	ionic charge, dipole moment
Ion–induced dipole (Ii)	ionic charge, polarizability

[a] Abbreviations are in parentheses. dd interactions are also known as Keesom interactions; di interactions are also known as Debye interactions; ii interactions are also known as London or dispersion interactions. Collectively, dd, di and ii interactions are known as van der Waals interactions. Charge transfer interactions are also known as donor–acceptor interactions.

B. Parameterization of Intermolecular Forces

1. Hydrogen bonding

Hydrogen bonding requires two parameters for its description:

1. one to account for the hydrogen atom donating capacity of a substituent,
2. another to account for its hydrogen atom accepting capacity.

A simple approach is the use of n_H, the number of OH and/or NH bonds in the substituent, and n_n, the number of lone pairs on oxygen and/or nitrogen atoms as parameters[62]. The use of these parameters is based on the argument that if one of the phases involved in the phenomenon studied includes a protonic solvent, particularly water, then all of the hydrogen bonds that the substituent is capable of forming will indeed form. For such a system, hydrogen bond parameters defined from equilibria in highly dilute solution in an 'inert' solvent are unlikely to be a suitable model. This parameterization accounts only for the number of hydrogen-donor and hydrogen-acceptor sites in a group. It does not take into account differences in hydrogen bond energy. A more sophisticated parameterization than that described above would be the use of the hydrogen bond energy for each type of hydrogen bond formed[63]. Thus for each substituent the parameter E_{hbX} would be given by equation 39:

$$E_{hbX} = \sum_{i=1}^{m} n_{hbi} E_{hbi} \tag{39}$$

where E_{hbX} is the hydrogen bonding parameter, E_{hbi} is the energy of the i-th type of hydrogen bond formed by the substituent X and n_{hbi} is the number of such hydrogen bonds. The validity of this parameterization is as yet untested. In any event the site number parameterization suffers from the fact that, though it accounts for the number of hydrogen bonds formed, it does not differentiate between their energies and can therefore be only an approximation. A definition of a scale of hydrogen bond acceptor values from 1-octanol–water partition coefficients of substituted alkanes shows that the site number method strongly overestimates the hydrogen-acceptor capability of the nitro group and seriously underestimates that of the methylsulfoxy group[65]. It is now apparent that there are many weak types of H donors and H acceptors that are capable of contributing significantly to the intermolecular forces that are responsible for many properties involving a change of phase. Green reported[66] evidence many years ago for the H donor activity of CH groups, and in a more recent work Nishio, Hirota and Urezama have reviewed evidence for CH-π interactions[67]. No really satisfactory parameterization of hydrogen bonding is available at present.

2. Van der Waals interactions

These interactions (dd, di, ii) are a function of dipole moment and polarizability. It has been shown that the dipole moment cannot be replaced entirely by the use of electrical-effect substituent constants as parameters[68]. This is because the dipole moment has no sign. Either an overall electron-donor group or an overall electron-acceptor group may have the same value of μ. It has also been shown that the bond moment rather than the molecular dipole moment is the parameter of choice. The dipole moments of MeX and PhX were taken as measures of the bond moments of substituents bonded to sp^3 and sp^2 hybridized carbon atoms, respectively, of a skeletal group. Application to substituents bonded to sp hybridized carbon atoms should require a set of dipole moments for substituted ethynes.

The polarizability parameter used in this work, α, is given by equation 40:

$$\alpha \equiv \frac{MR_X - MR_H}{100} = \frac{MR_X}{100} - 0.0103 \tag{40}$$

where MR_X and MR_H are the group molar refractivities of X and H, respectively[61,63]. The factor 1/100 is introduced to scale the α parameter so that its coefficients in the regression equation are roughly comparable to those obtained for the other parameters used. There are many other polarizability parameters including parachor, group molar volumes of various kinds, van der Waals volumes and accessible surface areas, any of which will do as well as they are all highly collinear in each other[69]. Proposing other polarizability parameters was a popular occupation in the past.

Values of α can be estimated by additivity from the values for fragments or from group molar refractivities calculated from equation 41:

$$MR_X = 0.320n_c + 0.682n_b - 0.0825n_n + 0.991 \tag{41}$$

where n_c, n_b and n_n are the number of core, bonding and nonbonding electrons, respectively, in the group X[48,69].

For alkyl and cycloalkyl groups, the number of carbon atoms in the group is a good polarizability parameter when no other type of substituent is present in the data set. Improved results are obtained on using corrected values of n_C for cycloalkyl groups[60].

3. Charge transfer interactions

These interactions can be roughly parameterized by the indicator variables n_A and n_D. Here, n_A takes the value 1 when the substituent is a charge transfer acceptor and 0 when it is not, and n_D takes the value 1 when the substituent is a charge transfer donor and 0 when it is not. An alternative parameterization would use the first ionization potential of MeX (ip_{MeX}) as the electron-donor parameter and the electron affinity of MeX as the electron-acceptor parameter if these values were available. Usually, the indicator variables n_A and n_D are sufficient. This parameterization accounts for charge transfer interactions directly involving the substituent. If the substituent is attached to a π-bonded skeletal group, then the skeletal group is capable of charge transfer interaction the extent of which is modified by the substituent. This is accounted for by the electrical-effect parameters of the substituent.

4. The intermolecular force (IMF) equation

A general relationship for the quantitative description of intermolecular forces, called the intermolecular force (IMF) equation, is equation 42:

$$\begin{aligned} Q_X = {} & L\sigma_{lX} + D\sigma_{dX} + R\sigma_{eX} + M\mu_X + A\alpha_X + H_1 n_{HX} \\ & + H_2 n_{nX} + Ii_X + B_{DX} n_{DX} + B_{AX} n_{AX} + S\psi_X + B^o \end{aligned} \tag{42}$$

Some values of the IMF parameters for nitroso, oxime and hydroxamic acid groups and other commonly encountered groups are given in Table 4.

5. Solvent effects

Solvent effects are due to intermolecular forces. A number of different correlation equations have been proposed for modeling the effect of varying solvent on chemical

TABLE 4. Intermolecular force substituent constants [a]

X	α	$\mu(sp^2)$	$\mu(sp^3)$	n_H	n_n
Ak, *c*-Ak					
Me	0.046	0.37	0	0	0
Et	0.093	0.37	0	0	0
c-Pr	0.125	0.48		0	0
Pr	0.139	0.37	0	0	0
i-Pr	0.14	0.4	0	0	0
Bu	0.186	0.37	0	0	0
i-Bu	0.186		0	0	0
s-Bu	0.186		0	0	0
t-Bu	0.186	0.52	0	0	0
Pe	0.232		0	0	0
CH_2Bu-*t*	0.232		0	0	0
c-Hx	0.257		0	0	0
Hx	0.278		0	0	0
Oc	0.372		0	0	0
1-Ad	0.396		0	0	0
CH_2Z					
CH_2Br	0.124	1.87	2.069	0	0
CH_2Cl	0.095	1.83	1.895	0	0
CH_2OH	0.062	1.71	1.58	1	2
CH_2CN	0.091	3.43	3.53	0	0
CH_2OMe	0.114			0	2
CH_2Vi	0.135	0.364	0.438	0	0
CH_2OEt	0.16			0	2
CH_2-Fr-2	0.215		0.65	0	2
CH_2NEt_2	0.278		0.612	0	1
CH_2Ph	0.29	0.22	0.37	0	0
CZ_3					
CF_3	0.04	2.86	2.321	0	0
CCl_3	0.191		1.95	0	0
VnX					
Vi	0.1	0.13	0.364	0	0
C_2Z					
C_2H	0.085	0.7	0.7809	1	0
C_2Me	0.131			0	0
Ar					
Ph	0.243	0	0.37	0	0
PnZ					
4-$PnNMe_2$	0.388		1.6	0	1
4-$PnNEt_2$	0.475		1.81	0	1
Har					
2-Fr	0.169		0.65	0	1
3-Fr	0.169		1.03	0	1
(CO)Z					
CHO	0.059	2.92	2.69	0	2
CO_2H	0.059	1.86	1.7	1	4

(*continued overleaf*)

TABLE 4. (*continued*)

X	α	$\mu(sp^2)$	$\mu(sp^3)$	n_H	n_n
Ac	0.102	2.88	2.93	0	2
CO_2Me	0.118	1.92	1.706	0	4
CO_2Et	0.164	1.846	1.84	0	4
$CONH_2$	0.088				
CONHOH	**0.112**				
CONHMe	0.134				
$CONMe_2$	0.204				
Bz	0.293				
CN	0.053	4.14	3.9185	0	0
CH=NH	**0.093**		**1.60**		
CH=NPh	**0.336**		**1.46**		
CH=NOH	**0.111**	**0.87**	**0.75**		
CH=NOMe	**0.157**				
CMe=NOH	**0.157**		**0.89**		
N					
N_3	0.092	1.56	2.17	0	1
NH_2	0.044	1.49	1.296	2	1
NHMe	0.093	1.77	1.01	1	1
NHAc	0.139	3.75	3.71	1	3
NMe_2	0.145	1.6	0.612	0	1
NEt_2	0.232	1.81		0	1
NO_2	0.063	4.28	3.56	0	4
O					
OH	0.018	1.4	1.77	1	2
OMe	0.068	1.36	1.31	0	2
OAc	0.114	1.69	1.706	0	4
OEt	0.114	1.38	1.22	0	2
OPr-*i*	0.16			0	2
OBu	0.206			0	2
OPh	0.267	1.13	1.36	0	2
S					
SH	0.082	1.21	1.52	0	0
SMe	0.128	1.29	1.06	0	0
SAc	0.174			0	2
SEt	0.174			0	0
SPh	0.333	1.37	1.5	0	0
SOMe	0.127	3.98	3.96	0	2
SOPh	0.32	4.02		0	2
SO_2Me	0.125	4.73		0	4
SO_2Ph	0.322	5	4.73	0	4
Other					
H	0	0	0	0	0
Br	0.079	1.7	1.84	0	0
Cl	0.05	1.7	1.895	0	0
F	0	1.66	1.8549	0	0
I	0.129	1.71	1.618	0	0

[a] Abbreviations will be found in Section VIII.B.

reactivity and physical properties. Of the many monoparametric equations proposed, two are so often used that they are worth describing here. The Winstein–Grunwald[70] equation was intended for nucleophilic solvolysis and was originally written as equation 43:

$$\log k_{Sv} = mY_{Sv} + lN_{Nu} + \log k^{o} \tag{43}$$

where Y_{Sv} is the solvent parameter, N_{Nu} is the solvent nucleophilicity parameter, m and l are the coefficients of Y_{Sv} and N_{Nu}, respectively, $\log k^{o}$ is the intercept and $\log k$ is the rate of solvolysis in the solvent Sv. t-BuCl was chosen as the reference substrate and 80% (v/v) aqueous ethanol as the reference solvent; m was defined as 1.000 for the solvolysis of the reference substrate. In practice, the term in lN was dropped, thereby converting equation 43 into a monoparametric relationship. In recent years 2-adamantyl tosylate has been used as the reference substrate.

Dimroth and Reichardt[71,72] defined the E_T parameter on the basis of the solvatochromism of the pyridinium betaine **17** as equation 44:

$$E_{T,Sv} = hc/\lambda_{max} = 28590/\lambda_{max} \tag{44}$$

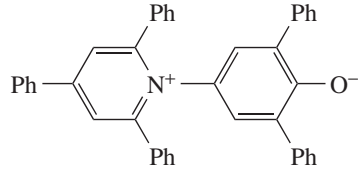

(**17**)

where E_T is the transition energy and serves as the solvent parameter, λ_{max} is the maximum absorbence, while h and c are Planck's constant and the velocity of light in a vacuum, respectively.

Solvatochromic species have a solvent-dependent electronic transition. This method is inapplicable to acidic solvents that would protonate the O^- of the betaine. Thus the correlation equation is equation 45:

$$Q_{Sv} = sE_{T,Sv} + s_o \tag{45}$$

Multiparametric models of solvent effects are the IMF and the Kamlet–Taft–Abraham equations.

V. APPLICATION METHODS

A. Introduction

Examples of the application of correlation analysis to oxime and hydroxamic acid pK_a data sets are considered below. In the best of all possible worlds all data sets have a sufficient number of substituents and cover a wide enough range of substituent electronic demand, steric effect and intermolecular forces to provide a clear reliable description of the kind and magnitude of structural effects on the property of interest. In the real world this is often not the case. We will therefore try to show how the maximum amount of information can be extracted from small data sets.

1. The choice of correlation equations

In choosing a correlation equation there are several factors that must be considered. They include the number of data points in the set to be studied, the experimental conditions, the type of data to be correlated and the types of structural effects that are expected.

a. The number of data points. The number of data points, N_{DP}, and the number of independent variables, N_V, determine the number of degrees of freedom, N_{DF}, as in equation 46:

$$N_{DF} = N_{DP} - N_V - 1 \tag{46}$$

In order to obtain reliable models (minimize the probability of chance correlations) it is necessary to consider the ratio $r_{DF/V}$ (equation 47):

$$r_{DF/V} = \frac{N_{DF}}{N_V} \tag{47}$$

The minimum value of $r_{DF/V}$ required for a reliable model depends on the quality of the determination of the data to be correlated. The smaller the experimental error in the data, the smaller the value of $r_{DF/V}$ required for dependable results. Experience indicates that in the case of chemical reactivity data $r_{DF/V}$ should be not less than three. For bioactivity studies $r_{DF/V}$ depends heavily on the type of data, for rate and equilibrium constants obtained from enzyme kinetics a value of not less than three is reasonable, while for toxicity studies on mammals at least seven is required.

b. Steric effects. If substituent and active site are proximal, then steric effects may occur. In that event it is necessary to include a steric effect parameterization in the correlation equation. The choice of parameterization depends on the number of data points in the set. If N_{DF} is sufficiently large, then the segmental method is a good choice for parameterization. If this is not the case, then it is best to use a monoparametric method.

c. Intermolecular forces. If intermolecular forces are likely to be significant, as is the case with bioactivity data and many types of chemical properties, then it is necessary to use the intermolecular force equation or some relationship derived from it. If N_{DF} is too small, it may be necessary to use composite parameters such as the partition coefficient in order to get a reliable model.

d. Small chemical reactivity data sets. Chemical reactivity data sets which involve only electrical effects are best modeled by the LDR equation. Although data sets are often encountered which are too small to give reliable results with the LDR equation, it is still possible to extract from them useful information regarding structural effects. There are two ways to handle this problem. The best approach is to combine two or more small data sets into a single large data set. This can be done if all of the data sets to be combined have been studied under experimental conditions such that all but one are kept constant and the variation in that one can be parameterized. Consider, for example, the case in which the data are rate constants that have been determined at various temperatures. Addition to the correlation equation of the term $T\tau$ where t is the absolute temperature gives equation 48:

$$\tau \equiv \frac{100}{t} \tag{48}$$

This makes possible the combination of rate constants at different temperatures into a single data set. Thus, the LDR equation becomes the LDRT equation (equation 49):

$$Q_X = L\sigma_{lX} + D\sigma_{dX} + R\sigma_{eX} + T\tau_X + h \tag{49}$$

If the data sets were studied in aqueous organic solvents, they can be combined into a single large set by the addition of the term $F\phi$, where ϕ is the mole fraction of organic solvent in the medium. Thus, the LDR equation becomes the LDRF equation (equation 50):

$$Q_X = L\sigma_{lX} + D\sigma_{dX} + R\sigma_{eX} + F\phi_X + h \tag{50}$$

A structural feature W which is present in some members and absent in others can be represented by an indicator variable n_W, which takes the value 1 when W is present and 0 when it is not. The resulting correlation equation is equation 51:

$$Q_X = L\sigma_{lX} + D\sigma_{dX} + R\sigma_{eX} + Nn_w + h \tag{51}$$

In the general case, if the resulting data set has a large enough value of $r_{dp/iv}$ a number of additional variables may be introduced, giving equation 52:

$$Q_X = L\sigma_{lX} + D\sigma_{dX} + R\sigma_{eX} + \Sigma N_i v_i + h \tag{52}$$

where v_i is the i-th indicator variable and N_i is its coefficient; v_i is a composite parameter representing the sum of all possible effects of the feature W.

e. Data sources. When the data points in a set are taken from the results of different laboratories, the probability that some part of the experimental error will be constant is significantly reduced. This must be taken into account when discussing the results of correlations.

VI. APPLICATIONS OF CORRELATION ANALYSIS TO ACIDITY

In order to illustrate the application of the methods described above, they will be applied to the acidities of oximes and hydroxamic acids.

A. Substituent Effects on Oxime Acidity

The data used in these correlations are set forth in Table 5 and results of correlations are reported in Table 6. The pK_a values of all data sets were determined in water at 25° unless otherwise noted.

In any discussion of oxime acidities the configuration of the members of the data set must be considered. In this work the *syn* configuration has the constant substituent Z *cis* to the OH group, while in the *anti* configuration Z is *trans* to OH.

The pK_a values of *syn* substituted aldoximes XCH=NOH (set OX1) were best correlated by the LD equation. The range of substituent type and the value of $r_{df/iv}$ imply that the results are suspect, although the goodness of fit is acceptable. For the *anti* substituted aldoximes (set OX2), again the best results were obtained with the LD equation. The much larger L value is due to the configuration in which X and OH are *cis* to each other. The goodness of fit, range of substituent type and value of $r_{df/iv}$ are all acceptable, especially so in view of the fact that the pK_a values are from several sources. For XMeC=NOH and XPnC=NOH (sets OX3 and OX4) the best fit was with the C equation using the σ_{50} constants. For both sets the fit was excellent, the $r_{df/iv}$ values acceptable and the range of substituent type too small. Surprisingly, the set of XCH_2COCMe=NOH (set OX5) was

TABLE 5. Oxime acidity data sets[a]

OX1. *syn*-XCH=NOH, aq., 25 °C, X, pK_a: H, 11.78; CF_3, 8.9; Hx, 11.60; Ph, 11.33; PhCH=CH, 10.80; 3-O_2NPn, 10.16; 2-Fn, 11.16; 2-Tn, 10.76.

OX2. *anti*-XCH=NOH, aq., 25 °C, X, pK_a: H, 11.78; Ac, 8.30; 3-O_2NPn, 10.16; 4-O_2NPn, 9.96; 4-MeOPn, 10.92; Ph, 10.68; PhCH=CH, 10.55; 2-Fn, 10.85; CH=NOH, 9.32[b]; Bz, 8.40[30].

OX3. XMeC=NOH, aq., 25 °C, X, pK_a: Me, 12.42; Et, 12.45; Ac, 9.30; NO_2, 7.4; Ph, 11.35; Bz, 9.25.

OX4. XPnC=NOH, aq., 25 °C, X, pK_a: H, 11.33; Ac, 8.85; $CONH_2$, 9.55; CO_2Et, 8.95; CO_2Me, 8.87; 4-O_2NPn, 10.47; Ph, 11.18; Bz, 8.80.

OX5. XCH_2COCMe=NOH, aq., 25 °C, X, pK_a: H, 9.35; Cl, 8.80; Br, 8.75; I, 8.78; OH, 9.16; CO_2Me, 8.72.

OX6. 4-XPnCH=NOH, aq., 25 °C, X, pK_a: H, 10.68; OMe, 10.92; NMe_2, 11.25; NO_2, 7.96.

OX7. 3-XPn-N=N−CH=NOH, aq., 25 °C, X, pK_a: H, 8.48; Me, 8.56; Cl, 8,27; Br, 8.33; NO_2, 8.10.

OX8. 4-XPn-N=N−CH=NOH, aq., 25 °C, X, pK_a: H, 8.48; Me, 8.60; Cl, 8.44; Br, 8.41; OMe, 8.70; OEt, 8.67; Ac, 8.21; CO_2Et, 8.22.

OX9. 4-XPnCH=NOH, 10% v/v aq. dioxane, 35 °C, X, pK_a: H, 11.01; Me, 11.05; CF_3, 10.51; F, 10.96; Cl, 10.66; Br, 10.79; OMe, 11.16; NMe_2, 11.56; CO_2Me, 10.48; CN, 10.27; NO_2, 10.28.

OX10. pK_a[c]. 4-XPnCH=NOH in DMSO, 25 °C, X, pK_a: OMe, 20.80; Me, 20.62; H, 20.21; Cl, 19.25; Br, 19.20; CF_3, 18.61; CN, 18.07; NO_2, 17.30.

OX11. pK_a[c]. 4-XPnCMe=NOH in DMSO, 25 °C, X, pK_a: OMe, 21.98; Me, 21.71; H, 21.05; Cl, 20.48; Br, 20.48; CF_3, 9.50; CN, 18.88; NO_2, 18.18.

OX12. AcXC=NOH, aq., I=0.1, 25 °C, X, pK_a: H, 8.30[21]; CO_2Et, 7.20; Ac, 7.58[21]; Me, 9.30[21]; Et, 9.38[21]; *i*-Pr, 9.50[21]; Cl, 7.9[21].

OX13. *anti*-Ak−*syn*-X−C=NOH, aq. 25 °C, Ak, X, pK_a: Me,Me, 12.42; Me,Et, 12.45; Me,CMe=NOH, 10.72; Me,Ac, 9.30[21]; Me,NO_2, 7.4[21]; Me,Ph, 11.35; Et,Et, 12.60; Et,Ac, 9.38[21]; Et,CEt=NOH, 10.67

OX14. pK_a. 3-X-5-methyl-1,2-benzoquinones1-oximines. X, pK_a: Me, 6.76; *t*-Bu, 7.64; CEt_2Me, 7.66; CEt_3, 7.78; *c*-Hx, 7.07; CMe_2Ph, 7.41; CH_2Ph, 6.84.

OX15.[d]. pK_a. 4-XPnC(NH_2)=NOH in MeOH, 25 °C, X, pK_a: H, 16.67; Cl, 16.48; OMe, 16.83; Me; 16.73, NO_2, 16.10.

[a] All data sets are from V. Palm (Ed.), *Tables of Rate and Equilibrium Constants of Heterolytic Organic Reactions, Vol. I(I), VINITI, Moscow, 1975*, unless otherwise noted. Superscript numbers indicate temperature other than 25 °C. I is ionic strength.
[b] Tn = thienylene; Fn = Furanylidene; sf indicates inclusion of statistical factor.
[c] F. G. Bordwell, Y.-Y. Zhao and J.-P. Cheng, *J. Phys. Org. Chem.*, **11**, 10 (1988).
[d] L. Dusek, J. Kavalek and V, Sterba, *Collect. Czech. Chem. Commun.*, **84**, 265 (1999).

best fit by the LD equation. The value of D is significant at the 99.5% confidence level. It is tempting to ascribe this dependence to the enolic tautomer XCH=C(OH)−CMe=NOH. This is unjustified as the range of substituent type is too small, and so is the value of $r_{df/iv}$. Set OX6, 4-XPnCH=NOH, is best correlated by composite σ_{50} substituent constants. The range of substituent type is again too small, and again so is the value of $r_{df/iv}$. No conclusions can be drawn from this data set. Sets OX7 and OX8, 3- and 4-XPn−N=N−CH=NOH, are both best fit by the C equation, the former with the σ_m constants and the latter with the σ_{50} constants. As the values of ρ and h for these sets

TABLE 6. Oxime acidity correlation results [a]

Set	Eq.	L/C	$S_{L/C}$	D	S_D	R	S_R	h	S_h	$100R^2$	$A100R^2$	F	S_{est}
OX1	LD	−5.90	0.891	−2.18	1.00	—	—	11.57	0.206	95.32	94.39	40.77	0.266
OX2	LD	−9.11	1.42	−2.01	0.711	—	—	11.69	0.275	94.38	93.68	58.81	0.305
OX3	C	−4.80	0.261	—	—	—	—	11.67	0.123	98.83	—	337.8	0.246
OX4	C	−4.71	0.248	—	—	—	—	11.31	0.0975	98.37	—	362.6	0.149
OX5	LD	−1.64	0.0959	−0.677	0.0666	—	—	9.35	0.0319	99.02	98.77	151.1	0.0336
OX6	C	−0.933	0.0659	—	—	—	—	10.73	0.0334	99.01	—	200.3	0.0667
OX7	C	−0.554	0.0422	—	—	—	—	8.50	0.0169	98.29	—	172.6	0.0272
OX8	C	−0.587	0.0326	—	—	—	—	8.52	0.0101	98.19	—	324.7	0.0272
OX9	LD	−0.919	0.124	−0.965	0.0912	—	—	10.96	0.0556	96.24	95.82	102.3	0.0867
OX10	LD	−3.52	0.211	−2.67	0.207	—	—	20.25	0.0962	99.15	99.01	293.0	0.135
OX11	LD	−3.38	0.151	−3.34	0.148	—	—	21.16	0.0687	99.63	99.57	672.6	0.0965
OX12	LDR	−3.81	0.105	−4.46	0.162	−14.0	0.998	8.28	0.0472	99.87	99.81	777.6	0.0495
OX13	LDR	−5.99	0.297	−2.78	0.402	3.91	1.51	12.21	0.114	99.85	99.77	662.2	0.111
OX14	S_1	1.05 [a]	0.225	—	—	—	—	6.28	0.228	81.25	—	21.67	0.197
OX15	LD	−0.674	0.0616	−0.638	0.0658	—	—	16.65	0.0271	99.22	98.95	12.65	0.0361

Set	S_0	N_{dp}	$R_{df/iv}$	P_D	$C_{L/C}$	C_D	C_R	S_{PD}	r_{ld}	r_{le}	r_{de}	r_{ce}
OX1	0.286	7	2	26.9	96.4	3.56	—	13.20	0.484	0.165	0.625	—
OX2	0.283	10	3.5	18.1	81.9	18.1	—	6.90	0.625	0.358	0.278	—
OX3	0.143	6	4	50	100	—	—	—	—	—	—	0.475
OX4	0.147	8	6	50	100	—	—	—	—	—	—	0.331
OX5	0.140	6	15	29.2	70.8	29.2	—	3.22	0.484	—	—	—
OX6	0.141	4	1	50	100	—	—	—	—	—	—	0.439
OX7	0.169	5	30	—	100	—	—	—	—	—	—	—
OX8	0.155	8	6	50	100	—	—	—	—	—	—	0.218
OX9	0.228	11	4	51.2	48.8	51.2	—	6.40	0.1694	0.173	0.279	—
OX10	0.116	8	2.5	43.1	56.9	43.1	—	3.92	0.246	0.526	0.102	—
OX11	0.0770	8	2.5	49.7	50.3	49.7	—	3.11	0.246	0.526	0.102	—
OX12	0.0547	7	2	53.4	39.4	46.1	14.5	2.33	0.165	0.281	0.758	—
OX13	0.0593	7	2	31.7	65.4	30.3	4.27	4.92	0.787	0.499	0.528	—
OX14	0.512	7	5	—	—	—	—	—	0.156	0.599	0.004	—
OX15	0.140	5	1	48.6	51.4	4836	—	6.02	0.156	0.599	0.003	—

[a] The column headings are as follows: Eq. denotes the correlation equation; L, C, D, R, S, T, F, ... are regression coefficients; S_L, S_C, S_D, ... are standard errors of the regression coefficients; $100R^2$, percent of the data accounted for by the regression equation; $A100R^2$, adjusted for the number of independent variables in the regression equation; F, F test; S_{est}, standard error of the estimste; S^o, standard error of the estimate divided by the root mean square of the data; N_{dp}, the number of data points in the set; $r_{df/nV}$, the ratio of the number of degrees of freedom in the data set to the number of independent variables in the best regression equation; P_D, the percent delocalized effect of the total electrical effect; S_{PD}, the standard error of P_D; η, the electronic demand of the active site Y; S_η, the standard error of η; r_{ij}, the zeroth order partial correlation coefficient of the i-th independent on the j-th independent variable; C_i, the percent contribution of the i-th independent variable to the regression equation.

show no significant difference, it is safe to combine them into a single data set. The resulting combined data set (set OX7/8) meets all the requirements for reliability. Set OX9, 4-XPnCH=NOH in 10% aqueous dioxane at 25 °C, was best fit by the LD equation. This set has a full range of substituent types and a good value for $r_{df/iv}$. The results are reliable.

Set OX10, 4-XPnCH=NOH in DMSO at 25 °C, and Set OX11, 4-XPnCMe=NOH, under the same conditions, were both best fit by the LD equation. The goodness of fit was excellent and the range of substituent type good. The value of $r_{df/iv}$ was somewhat less than desired. Set OX12, AcXC=NOH, in water with ionic strength $I = 0.1$ gave best fit with the LDR equation. The range of substituent type is poor and the $r_{df/iv}$ value unacceptably low. No trust can be put in the results of this correlation.

On the condition that two subsets have a structural feature whose parameterization is essentially the same, they can be combined into a single data set. As an example consider set OX13, *anti*-Ak−*syn*-X−C=NOH, where Ak is either Me or Et. The electrical effects of these groups for Me and Et, respectively, are σ_l, −.01, −,01; σ_d, −.14, −.12; σ_e, −.030, −.036; the values of the steric parameter υ are .52 and .56. A significant difference is found only in the polarizability parameter α, where the values for Me and Et are .046 and .093, respectively. Combination of oxime pK_a values for Ak = Me or Et results in set OX13; the best correlation was with the LDR equation. As only three substituent types are present in this data set and $r_{df/iv}$ is 0.33, this data set cannot be considered as proof of anything. The only acceptable conclusion is that it is in accord with the combination of the two subsets.

Set OX14, 1-oximino-3-X-5-methyl-1,2-benzoquinones, is of interest because the substituents in this data set do not differ significantly from each other in electrical effects. As chemical reactivities in water normally do not depend on polarizability, it would seem that the variations in pK_a in this data set should be a function of steric effects. Correlation with the two parameter segmental steric effect equation gave best fit with the υ_l parameters. The correlation is significant at the 99.0% confidence level and $r_{df/iv}$ is good. It seems probable that the pK_a values of these compounds are dependent on steric effects.

For pK_a values of 4-XPnC(NH_2)=NOH in MeOH at 25 °C, set OX15, best fit was obtained with the LD equation. The range of substituent type is good but the $r_{df/iv}$ value is too small for reliability. The correlation is significant at the 99.0% confidence level.

B. Hydroxamic Acid Acidity

Hydroxamic acids are biocides and lipogenase inhibitors. They are also of interest as reagents in analytical chemistry. Of first importance is the dependence of their acidity on structure.

1. The acid site in hydroxamic acids

There has been considerable interest in the last two decades in the site of acidity of hydroxamic acids. There are two possible acidity sites: the NH and OH fragments in the C(O)NHOH group. It was originally assumed that these compounds were acidic due to the OH group. Since then, much effort has been expended on the determination of the site of proton transfer under various conditions by both experimental and computational studies. The proton transfer leads to the following possible products:

$$X(C{=}O)N^-(OH) + H_3O^+ \leftrightharpoons X(C{=}O)NHOH + H_2O \leftrightharpoons X(C{=}O)NHO^- + H_3O^+$$

The experimental results suggest that the acidity site depends on medium and substituent effects. These results are summarized in Table 7. The computational results show that the

TABLE 7. Experimental determination of the acid site in hydroxamic acids

Medium	Method	Hydroxamic acid	Acid site	Reference
Acidic and basic aq.	UV spectra	4-XPnCONHOH, 4-XPnCONHOMe, 4-XPnCON(Me)OH	N, O	*a*, *b*
aq.	pKa	MeCONHOH, MeCON(Me)OH	O	*c*
aq.	pKa	MeCONHOH, MeCON(Ph)OH	O	*d*
aq. 2 M in $NaNO_3$	ΔHa vs. ΔSa	MeCONHOH, MeCON(Me)OH, MeCON(Ar)OH	O	*e*
Dioxane	IR, UV, pKa	XCONHOH	N	*f*
aq. MCS (methyl cellosolve)	IR, UV, pKa	XCONHOH	N	*f*
aq., aq. dioxane	pKa	XCONHOH	O	*g*
MeOH	^{17}O NMR	XCONHOH	N	*h*
Solid state	XPS	XCONHOH	N	*i*
DMSO	pKa	MeCONHOH, PhCONHOH	N	*j*
DMSO	Eox	MeCONHOH, PhCONHOH	N, O	*j*
Gas	ΔH(g)	MeCONHOH, MeCON(Me)OH, MeCON(Me)OMe	N	*k*
aq. MeOH	^{14}N, ^{15}N, ^{17}O NMR, NOE	XCONHOH, X = Me, Ph	Me: O in H_2O. Ph: N in MeOH	*l*

[a] R. E. Paplinger, *J. Org. Chem.*, **24**, 802 (1959).
[b] G. M. Steinberg and R. Swidler, *J. Org. Chem.*, **30**, 2362 (1965).
[c] J. Gerstein and W. P. Jencks, *J. Am. Chem. Soc.*, **86**, 4655 (1964).
[d] W.M. Wise and W.W. Brant, *J. Am. Chem. Soc.*, **77**, 1058 (1955); A. R. Fields, B. M. Daye and R. Christian, *Talanta*, **13**, 929 (1966).
[e] B. Monzyk and A. L. Crumbliss, *J. Org. Chem.*, **45**, 4670 (1980); C. P. Brink and A. L. Crumbliss, *J. Org. Chem.*, **47**,1171 (1982); C.P. Brink, L. L. Fish and A. L. Crumbliss, *J. Org. Chem.*, **50**, 2277 (1985).
[f] L. Bauer and O. Exner, *Angew. Chem., Int. Ed. Eng.*, **13**, 376 (1974); O. Exner and W. Simon, *Collect. Czech. Chem. Commun.*, **30**, 4078 (1965); O. Exner and R. Kakac, *Collect. Czech. Chem. Commun.*, **28**, 1656 (1965); O. Exner, *Collect. Czech. Chem. Commun.*, **28**, 2933 (1965); O. Exner and J. Holubek, *Collect. Czech. Chem. Commun.*, **30**, 940 (1965).
[g] A. E. Fazary, *J. Chem. Eng. Data*, **50**, 888 (2005).
[h] E. Lipczynska-Kochany and H. Iwamura, *J. Org. Chem.*, **47**, 5277 (1982).
[i] B. Lindberg, A. Berndtsson, R. Nilsson, R. Nyholm and O. Exner, *Acta Chim. Scand., Ser. A*, **32**, 353 (1978).
[j] F. G. Bordwell, H. E. Fried, D. L. Hughes, T.-Y. Lynch, A. V. Datish and Y. E. Whang, *J. Org. Chem.*, **55**, 3330 (1990).
[k] M. Decouzon, O. Exner, J.-F. Gal and P.-C. Maria, *J. Org. Chem.*, **55**, 3980 (1990).
[l] A. Bagno, C. Comuzzi and G. Scorrano, *J. Am. Chem. Soc.*, **116**, 916 (1994).

NH fragment is the acidic site in the gas phase and in media of lower polarity than water. The results are presented in Table 8.

A hydroxamic acid may be written as:

$$X^{C}C(O)NX^{N2}OX^{O2}$$

TABLE 8. Computational determination of acid site and conformation of hydroxamic acids

Method	Basis sets	Hydroxamic acids	Acid site	Reference
SCF	3-21G	XCONHOH, X = H, Me	N in (g)	*a*
AM1, PM3, HF, MP2	3-21G, 3-21G(d), 6-31G(d,p), 6-311G(d,p)	HCONHOH	N in (g)	*b*
AM1, MP2	6-311++G(2d,2p)	$XCONHO^-$, X = H, Me	N in (g), nonprotic solvents, O in protic solvents	*c*
SCF, MP2, MP4	6-311++G(2d,2p)	HCONHOH	N in (g)	*d*
ONIOM	(B3LYP/6-311G+(d,p): AM1)	$XCONHO^-$, X = H, Me, CF_3, Ph	N in (g)	*e*
HF	3-21G, 6-311G**, 6-311++G**	XCONHOH, X = H, Me, Ph	N in (g)	*f*
MP	6-311++G**			

[a] N. J. Fitzpatrick and R. Mageswaran, *Polyhedron*, **8**, 2255 (1989).
[b] L. Turi, J. J. Dannenberg, J. B. Rama and O. N. Ventura, *J. Phys. Chem.*, **96**, 3709 (1992).
[c] O. N. Ventura, J. B. Rama, L. Turi and J. J. Dannenberg, *J. Am. Chem. Soc.*, **115**, 5754 (1993).
[d] O. N. Ventura, J. B. Rama, L. Turi and J. J. Dannenberg, *J. Phys. Chem.*, **99**, 131 (1995).
[e] M. Remko, *J. Phys. Chem. A*, **106**, 5005 (2002).
[f] Reference l, Table 7.

Thus, taking benzohydroxamic acid, PhC(O)NHOH, as an example, X^C is Ph, X^{N1} is PhC(O) and X^{O1} is PhC(O)NH; X^{N2} and X^{O2} are H in hydroxamic acids. The pK_a values of NH acids were calculated from equation 53:

$$pK_{a_N} = -21.0(\sigma_{l,XN1} + \sigma_{l,XN2}) + 22.76 \tag{53}$$

where XN1 is X^CC(O) and XN2 is OX. The pK_a values of OH acids were calculated from equation 54:

$$pK_{a_N} = -20.0\sigma_{lX} - 7.68\sigma_{dX} + 35.0\sigma_{eX} + 15.56 \tag{54}$$

The calculated pK_a values for both the NH and the OH acids are in fairly good agreement with the experimental values.

There is a means of determining the acidity site based on the extent of transmission of the electrical effect. We have shown that electrical-effect transmission in a data set is dependent on L, the coefficient of σ_l; L is a function of the number of bonds, n, intervening between the nearest atom of the substituent and the atom losing the proton. For 2nd period elements in a number of acidic functional groups, the average values of L are:

$$n, \text{average } L; 2, 9.18(\pm 1.19); 3, 4.57(\pm 0.604); 4, 2.21(\pm 0.431)$$

Correlation of the pK_a values of XCONHOH with the LDR equation (set HA12) gave the regression equation 55:

$$pK_{a_{XC}} = -3.50(\pm 0.406)\sigma_{lX} - 3.28(\pm 0.192)\sigma_{dX} + 8.90(\pm 0.0562) \tag{55}$$

$100R^2$, 97.23; $A100R^2$, 96.98; F, 175.6; S_{est}, 0.118; S^{o}, 0.190; N_{dp}, 11;

$r_{df/iv}$, 4; P_D, 48.4(±4.28); range of pK_{a}, 2.5 log units; range of σ_l, −0.01 to 0.23;

range of σ_d, 0 to −0.68; range of substituent type, limited.

In XC(O)NHOH for NH acidity $n = 2$, for OH acidity $n = 3$. Clearly, best agreement is with $n = 3$. This suggests that in water, hydroxamic acids are oxygen acids. Also examined were the $XCH_2C(O)NHOH$ (set HA13) for which the n values of the NH and OH sites are 3 and 4, respectively. Correlation of the pK_{a} values for these acids with the LDR equation gave the regression equation 56:

$$\text{p}K_{\text{aXC}} = -1.92(\pm 0.358)\sigma_{lX} + 9.39(\pm 0.0689) \tag{56}$$

$100R^2$, 85.16; F, 28.68, S_{est}, 0.151; S^{o}, 0.456; N_{dp}, 7; $r_{df/iv}$, 5; range of pK_{a},

0.95 log units; range of σ_l, −0.01 to 0.47; range of substituent type, limited.

On dropping the point for 4-ClPn the fit is considerably improved. The regression equation is equation 57:

$$\text{pKa}_{\text{Xc}} = -1.85(\pm 0.242)\sigma_{lX} + 9.42(\pm 0.0480) \tag{57}$$

$100R^2$, 93.5; F, 58.41; S_{est}, 0.102; S^{o}, 0.310; N_{dp}, 6; $r_{df/iv}$, 4; range of pK_{a},

0.95 log units; range of σ_l, −0.01 to 0.47; range of substituent type, limited.

The coefficients of equation 57 are not significantly different from those of equation 56. Unfortunately, 5 of the 6 points in the data set lie in the range 9.22 to 9.48, thus there is significant clustering. While the L value is about what is expected for $n = 4$, indicating that in water, hydroxamic acids in the range of σ_l studied are oxygen acids, it does not constitute proof.

2. Hydroxamic acid pK_{a} values

The data used in the following correlations are reported in Table 9, the results of the correlations in Table 10.

The pK_{a} values of 3-substituted benzohydroxamic acids in water at 25 °C were correlated with the σ_m constants with good results. Although the fit is excellent the number of data points is the minimal acceptable, as is the range of substituent type. The pK_{a} values of 4-substituted benzohydroxamic acids in aqueous ethanol ($\phi = 0.0405$, ϕ represents the mole fraction of ethanol) at various temperatures (set HA4) on correlation with the LDRT equation (equation 49) gave best results on dropping σ_e as a variable. The goodness of fit is excellent. The range of substituent type is too small. Set HA5 was excluded from the correlations because two of the data points did not fit into the overall pattern of substituent behavior. In set HA6, 2-substituted benzohydroxamic acids in aqueous dioxane of variable mole fraction at 25 °C, required the LDRSF equation, to account for possible steric effects and variation in solvent composition. The goodness of fit is excellent. The most important factor in determining acid strength is solvent composition, the overall electrical effect ($C_L + C_D + C_R$) is next in magnitude and the steric effect, though

TABLE 9. Hydroxamic acid pK_a values[a]

HA1. 4-XPnC=O(NHOH), aq., 25 °C, $I = 0$.[b] X, pK_a: H, 8.91; Me, 9.05; F, 8.81; Cl, 8.70; Br, 8.57; OMe, 9.15; CN, 8.26; NO_2, 8.13.

HA2. 4-XPnC=O(NHOH), aq., 20.5 °C, $I = 0$.[c] X, pK_a: H, 8.80; Me, 8.93; F, 8.70; OMe, 9.03; CN, 8.16; NO_2, 8.01.

HA3. 3-XPnC=O(NHOH), aq., 25 °C, $I = 0.01$.[d] X, pK_a: H, 8.80; Me, 8.93; Cl, 8.42; Br, 8.43; NO_2, 8.10.

HA4. 4-XPnC=O(NHOH), aq. EtOH ($\phi = 0.0405$), $I = 0.08$ KCl[e]. X, pK_a at $T = 5.0$, 15.0, 25.0, 35.0 45.0 °C: H, 9.27, 9.06, 8.84, 8.78, 8.60; Cl, 9.07, 8.89, 8.60, 8.55, 8.43; OMe, 9.51, 9.26, 9.05, 8.89, 8.72; NO_2, 8.47, 8.28, 8.03, 7.96, 7.84.

HA5. 4-XPnCH=CHC=O(NHOH), aq. EtOH ($\phi = 0.0405$), $I = 0.08$ KCl[e]. X, pK_a at $T = 5.0$, 15.0, 25.0, 35.0 45.0 °C: H, 9.02, 8.91, 8.74, 8.66, 8.57; Cl, 8.89, 8.78, *8.49*, 8.64, 8.47; OMe, 9.14, 8.96, 8.85, 8.70, 8.60; NO_2, 8.49, 8.35, *7.97*, 8.05, 7.94.

HA6. 2-XPn(C=O)NPhOH, aq. dioxane at 25 °C[f], X, pK_a at $\phi = 0.0203$, 0.0503, 0.0832, 0.124, 0.148, 0.174, 0.240[g], 0.330[g]: H, 8.84, 9.23, 9.76, 10.30, 10.63, 11.04; 12.04, 13.39; Me, —, 9.12, 9.61, 10.18, —, 10.90; F, 8.51, 8.92, 9.42, 10.00, 10.34, 10.74; Cl, 8.43, 8.85, 9.35, 9.93, 10.28, 10.67; Br, 8.45, 8.86, 9.36, 9.96, 10.30, 10.66; I, —, 8.92, 9.91, 10.00, 10.35, 10.75; OMe, 8.84, 9.24, 9.81, 10.36, 10.70, 11.09; NO_2, —, 8.87, 9.39, 10.01, 10.37, 10.80.

HA7.[h] 2-XPn(C=O)NPhOH, aq. dioxane at 35 °C[e], X, pK_a at $\phi = 0.0203$, 0.0503, 0.0832, 0.124, 0.148, 0.174, 0.240[g], 0.330[g]: H, 8.58, 9.07, 9.45, 10.12, 10.40, 10.82, 11.95, 13.28; Me, —, 9.02; 9.48, 10.04, —, 10.71; F, 8.43, 8.83, 9.32, 9.89, 10.26, 10.67; Cl, 8.31, 8.79, 9.23, 9.81, 10.14, 10.56; Br, 8.34, 8.76, 9.26, 9.84, 10.20, 10.58; I, —, 8.80, 9.30, 9.90, 10.25, 10.63; OMe, 8.78, 9.21, 9.70, 10.27, 10.66, 11.03, NO_2, —, 8.78, 9.29, 9.95, 10.29, 10.65.

HA8.[h] 4-XPn(C=O)N(3′-Pn)OH, aq. dioxane at 25 °C, $I = 0$, X, pK_a at $\phi = 0.0230$, 0.0503, 0.0832, 0.124, 0.148, 0.174, 0.240[f], 0.330[g]: H, 9.02, 9.38, 9.84, 10.38, 10.78, 11.12, 12.11, 13.38; Me, —, —, 9.93, 10.56, 10.91, 11.33, 12.28, 13.66; F, 8.93, 9.32, 9.83, 10.46, 10.85, 11.20, 12.30, 13.63; Cl, 8.81, 9.22, 9.73, 10.34, 10.70, 11.12, 12.15, 13.53; Br, 8.80, 9.21, 9.73, 10.33, 10.69, 11.10, 12.14, 13.52; OMe, 9.22, 9.53, 10.03, 10.64, 11.01, 11.42, 12.42, 13.79; NO_2, 8.45, 8.87, 9.38, 10.00, 10.37, 10.79, 11.71, 13.09.

HA9.[h] 4-XPn(C=O)N(3′-MePn)OH, aq. dioxane at 35 °C, $I = 0$. X, pK_a at $\phi = 0.0230$, 0.0503, 0.0832, 0.124, 0.148, 0.174, 0.240[g], 0.330[g]: H, 8.86, 9.25, 9.75, 10.34, 10.65, 11.07, 11.96, 13.23; Me, —, —, 9.82, 10.46, 10.80, 11.23, 12.20, 13.55; F, 8.78, 9.20, 9.72, 10.32, 10.63, 11.06, 12.06, 13.42; Cl, 8.66, 9.08, 9.53, 10.18, 10.56, 10.92, 11.96, 13.38; Br, 8.64, 9.07, 9.52, 10.16, 10.56, 10.92, 11.94, 13.37; OMe, 9.00, 9.43, 9.92, 10.53, 10.90, 11.30, 12.30, 13.67; NO_2, 8.25, 8.68, 9.18, 9.80, 10.18, 10.59, 11.50, 12.90.

HA10. 4-XPn(C=O)N(4′-Pn)OH, aq. dioxane at 25 °C, $I = 0$, X, pK_a at $\phi = 0.0230$, 0.0503, 0.0832, 0.124, 0.148, 0.174, 0.240[f], 0.330[g]: H, 9.03, 9.37, 9.82, 10.36, 10.68, 11.05, 11.94, 13.15; Me, —, —, 10.06, 10.57, 10.88, 11.24, 12.06, 13.21; F, 9.04, 9.39, 9.81, 10.32, 10.63, 10.99, 11.81, 12.96; Cl, 8.83, 9.18, 9.60, 10.11, 10.42, 10.78, 11.60, 12.75; Br, 8.81, 9.16, 9.58, 10.09, 10.40, 10.76, 11.56, 12.78; OMe, 9.32, 9.68, 10.10, 10.62, 10.93, 11.30, 12.13, 13.28; NO_2, —, —, —, —, —, 10.24, —, —.

TABLE 9. (*continued*)

HA11. 4-XPn(C=O)N(4′-Pn)OH, aq. dioxane at 35 °C, $I = 0$, X, pK_a at $\phi = 0.0230$, 0.0503, 0.0832, 0.124, 0.148, 0.174, 0.240[f], 0.330[g]: H, 8.93, 9.26, 9.72, 10.25, 10.57, 10.96, 11.84, 13.05; Me, —, —, 9.86, 10.36, 10.67, 11.05, 11.86, 13.06; F, 8.93, 9.28, 9.70, 10.21, 10.52, 10.88, 11.70, 12.85; Cl, 8.71, 9.06, 9.48, 9.99, 10.30, 10.66, 11.48, 12.63; Br, 8.70, 9.05, 9.47, 9.98, 10.28, 10.64, 11.47, 12.62; OMe, 9.10, 9.47, 9.87, 10.40, 10.70, 11.08, 11.87, 13.10; NO_2, —, —, —, —, —, 10.04, —, —.

HA12. XCONHOH,[i,j] aq. at 25 °C, X, pK_a: H, 8.78; Pe, 9.88; *c*-Hx, 9.92; CH_2Cl, 8.53; Ph, 8.89; CH_2Ph, 9.33; CH_2CH_2Ph, 9.22; 4-O_2NPn, 8.02; NH_2, 10.5; 2-MeCH=CH, 8.90; 3-O_2NPn, 8.10.

HA13. $XCH_2CONHOH$,[i,j] aq. at 25 °C, X, pK_a: H, 9.40; Ph, 9.33; Cl, 8.53; CH_2Ph, 9.72; Et, 9.46; Pr, 9.48; 4-ClPn, 8.85.

[a] Values in italics are uncertain.
[b] Y. K. Agrawal and J. P. Shukla, *Z. Phys. Chem. (DDR)*, **255**, 889 (1974).
[c] R. Swidler, R. E. Plapinger and G. M. Steinberg, *J. Am. Chem. Soc.*, **81**, 3271 (1959).
[d] A. Ahmad, J. Sucha and M. Vecera, *Collect. Czech. Chem. Commun.*, **39**, 3293 (1974).
[e] M. Dessolin and M. Laloi-Diard, *Bull. Soc. Chim. Fr.*, 2946 (1971); M. Dessolin, M. Laloi-Diard, and M. Vilkas, *Bull. Soc. Chim. France* 2573 (1970)
[f] Y. K. Agrawal and S. G. Tandon, *Ind. J. Chem.*, **10**, 552 (1972); Y. K. Agrawal and S. G. Tandon, *Talanta*, **19**, 700 (1972); Y. K. Agrawal and H. Kapoor, *J. Chem. Eng. Data*, **22**, 159 (1977); J. P. Shukla and S. G. Tandon, *Ind. J. Chem.*, **9**, 279 (1971); J. P. Shukla and S. G. Tandon, *J. Inorg. Nucl. Chem.*, **33**, 1681 (1971).
[g] Y. K. Agrawal, *Thermochimica Acta*, **18**, 250 (1972).
[h] Values of pK_a for $\phi = 0.240$ or 0.340 are available only for X = H.
[i] Y. K. Agrawal and V. P. Khare, *Rocz. Chem.*, **50**, 795 (1976); Y. K. Agrawal, V. P. Khare, and A. S. Kapur, *J. Fluor. Chem.*, **8**, 447 (1976); Y. K. Agrawal and V. P. Khare, *Bull. Soc. Chim. Fr.*, 873 (1977); Y. K. Agrawal and H. Kapoor, *J. Chem. Eng. Data*, **22**, 159 (1977).
[j] V. Palm, Ed., *Tables of Rate and Equilibrium Constants of Heterolytic Organic Reactions, Vol. 1(1)*, Moscow, 1975; *Suppl. Vol. 1(1,2)*, Tartu, 1984.

significant, has the least effect. The results for set HA7 in which the pK_a values were determined at 35 °C, are fully in accord with those obtained for set HA6. The pK_a values of 4-substituted-*N*-(3'-methylphenyl)benzohydroxamic acids at 25 and 35 °C in aqueous dioxane of variable Φ (sets HA8 and HA9) required the LDRF equation (equation 50) for correlation. Excellent results were obtained for both data sets. Correlation of pK_a values for 4-substituted-*N*-(4'-methylphenyl)benzohydroxamic acids at 25 and 35 °C in aqueous dioxane of variable Φ (sets HA10 and HA11) were also carried out with the LDRF equation, again with excellent results.

Sets HA6 and HA7, HA8 and HA9, and HA10 and HA11 can be combined with sets HA6.7, HA8.9 and HA10.11 by adding the term $T\tau$ to the correlation equation. Sets HA8.9 and HA10.11 can be further combined to give set HA8.9.10.11 by adding a term in $\rho\sigma$ to account for the effect of the 3′- or 4′-Me group.

VII. FURTHER APPLICATIONS TO REACTIVITIES AND PROPERTIES

The application of correlation analysis to oximes and hydroxamic acid acidity has been taken as an illustration of how it can be applied to a wide range of properties and reactivities. It does not need further discussion. In the Tables below data sets and results of correlations that exemplify these applications to various types of data are presented.

TABLE 10. Results of hydroxamic acid pK_a correlations [a]

Set	Eq.	L/C	$S_{L/C}$	D	S_D	R	S_R	$S/T/F$	$S_S/T/F$	h	S_h
HA1	LD	−0.988	0.0874	−0.866	0.0844	—	—	—	—	8.92	
HA2	C	−0.917	0.0187	−0.917	—	—	—	—	—	8.79	0.00865
HA3	LD	−1.00	0.0598	−0.333	—	—	—	—	—	8.81	0.0240
HA4	LDT	−0.951	0.0416	−0.849	0.0369	—	—	14.9	0.619	3.89	0.209
HA6	LDRSF	−0.462	0.0605	−0.295	0.0624	−2.71	0.400	−0.402 −14.6	0.0645 0.203	8.50	0.0398
HA7	LDRSF	−0.325	0.0311	−0.436	0.0321	−3.11	0.206	−0.482 −14.8	0.0312 0.104	8.29	0.0209
HA8	LDRF	−0.511	0.0262	−0.684	0.0274	−0.340	0.179	15.1	0.0660	8.55	0.0170
HA9	LDRF	−0.64	0.0305	−0.702	0.0317	−0.521	0.206	15.1	0.521	8.44	0.0196
HA10	L	−1.18	0.0337	−1.11	0.0364	0.351	0.186	13.0	0.0629	8.78	0.0155
HA11	LDRF	−1.12	0.0279	−0.994	0.0300	1.36	0.153	13.0	0.0520	8.67	0.0128
HA12	LD	−4.81	0.718	−3.37	0.336	—	—	—	—	9.09	0.0998
HA13	L	−1.85	0.24							9.4	0.05

Set	$100R^2$	$A100R^2$	F	S_{est}	S^0	N_{dp}	$r_{df/nV}$	P_D	S_{PD}	η	S_η
HA1	98.08	97.76	127.5	0.0594	0.175	8	1.67	46.7	5.49	—	
HA2	99.83	—	2418.	0.0191	0.0498	6	4	—	—	99.83	
HA3	98.95	—	282.6	0.0392	0.132	5	3	—	—	—	—
HA4	99.17	99.08	639.9	0.0447	0.102	20	5.33	47.2	2.51	—	—
HA6	99.33	99.27	1193.	0.0843	0.0875	46	8	39.0	9.37	9.18	—
HA7	99.82	99.81	4543	0.0434	0.0450	46	8	57.3	5.40	7.13	—
HA8	99.91	99.90	13520.	0.0456	0.0316	54	12.3	57.2	2.93	0.542	0.261
HA9	99.88	99.87	10170.	0.0527	0.0364	54	12.3	52.5	2.93	0.742	0.292
HA10	99.91	99.90	11150	0.0401	0.0324	47	10.5	48.3	1.90	−0.316	0.167
HA11	99.94	99.93	16210	0.03	0.03	47	10.5	47.1	1.69	—	—
HA12	94.51	93.9	68.88	0.2	0.28	12	4.5	41.2	5.72	—	—
HA13	93.5	—	58.41	0.1	0.31	6	4	—	—	—	—

[a] See footnote *a*, Table 6, for column headings.

A. Chemical Reactivities

1. Oximes

TABLE 11. Oxime reactivities and formation

OX31. 4-XPnCH=NOH, X, $10^5 K_{TH1H}$ (mol^{-1})[a]:
H, 2.34; Me, 2.79; CF_3, 3.90; F, 2.47; Cl, 3.52; Br, 2.89; OMe, 2.01; NMe_2, 1.40; CO_2Me, 3.77; CN, 4.55; NO_2, 5.35.

OX32. 4-XPnCH=NOH, X, 10^2 Ka_{TH1H} (s^{-1})[a]: H, 1.25; Me, 1.20; CF_3, 1.63; F, 1.68; Cl, 1.25; Br, 1.39; OMe, 1.10; NMe_2, 1.14; CO_2Me, 1.61; CN, 2.15; NO_2, 1.96.

OX33. 4-XPnCH=NOH, X, $10^{10} K_3$, K_{aTH1H} (s^{-1} l mol^{-1})[a]: H, 8.82; Me, 8.07; CF_3, 18.5; F, 7.44; Cl, 10.9; Br, 12.4; OMe, 4.64; NMe_2, 5.32; CO_2Me, 20.9; CN, 31.2; NO_2, 42.2.

OX34. 4-XPnCHO + H_2NOH, aq., $I = 0.5$, 30 °C. X, K_{ad} (l mol^{-1})[b]: NMe_2, 0.15; OMe, 1.8; H, 17.6; Cl, 24; NO_2, 152.5[b].

OX35. 4-XPnCHO + H_2NOH, aq., $I = 0.5$, 30 °C. X, 10^7 k_2 (l mol^{-1} min^{-1})[b]: NMe_2, 1060; OMe, 466; H, 15.8; Cl, 23.1; NO_2, 1.43.

OX36. 4-XPnCHO + H_2NOH, aq., $I = 0.5$, 30 °C. X, 10^7 k_{deh} (l mol^{-1} min^{-1})[b]: NMe_2, 2.26; OMe, 1.05; H, 50.7; Cl, 33.3; NO_2, 830.

OX37. XPnC(NH_2)=$NOCO_2$PnNO_2-4′, X, K_{i1}[c]: OMe, 25.73; Me, 31.31; H, 44.60; Cl, 45.94; NO_2, 111.80.

OX38. XPnC(NH_2)=$NOCO_2$PnNO_2-4′, X, k_{ip1}[c]: OMe, 324.1; Me, 359.2; H, 566.2; Cl, 894.6; NO_2, 1731.

OX39. XPnC(NH_2)=$NOCO_2$PnNO_2-4′, X, k_{ipC18}[c]: OMe, 24.58; Me, 32.61; H, 40.51; Cl, 47.27; NO_2, 133.93.

OX40. XPnC(NH_2)=$NOCO_2$Me, X, k_{i2}[c]: OMe, 0.17; Me, 0.22; H, 0.29; Cl, 0.38; NO_2, 0.86.

OX41. XPnC(NH_2)=$NOCO_2$Me, X, k_{ip2}[c]: OMe, 4.66; Me, 5.39; H, 5.96; Cl, 7.77; NO_2, 11.49.

OX42. XPnC(NH_2)=$NOCO_2$Me, MeOH, 25 °C. X, $k_{iC18,2}$[c]: OMe, 0.20; Me, 0.25; H, 0.31; Cl, 0.42; NO_2, 0.81.

OX43. XPnC(NH_2)=$NOCO_2$Ph, MeOH, 25 °C. X, k_{iC18}[c]: OMe, 0.92; Me, 1.45; H, 2.00; Cl, 2.18; NO_2, 6.90.

OX44. XPnC(NH_2)=$NOCO_2$PnNO_2-4′, MeOH, 25 °C. X, k_{OH} (l mol^{-1} s^{-1})[d]: OMe, 114; Me, 121; H, 143; Cl, 184; NO_2, 370.

[a] J. Picha, R. Cibulka, F. Hampl, F. Liska, P. Parik and O. Pytela, *Collect. Czech. Chem. Commun.*, **69**, 397 (2004).
[b] M. Calzadilla, M. Malpica and T. Cordova, *J. Phys. Org. Chem.*, **12**, 708 (1999).
[c] L. Dusek, J. Kavalek and V. Sterba, *Collect. Czech. Chem. Commun.*, **64**, 265 (1999).
[d] d. J. Mjndl, J. Kavalek and V. Sterba, *Collect. Czech. Chem. Commun.*, **64**, 1641 (1999).

TABLE 12. Results of correlations of oxime reactivities and formation[a]

Set	Eq.	L	S_L	D	S_D	R	S_R	h
OX31	LD	0.346	0.0741	0.417	0.0544	—	—	0.419
OX32	LD	0.294	0.0596	0.158	1.1435	—	—	0.0916
OX33	LDR	0.654	0.0745	0.834	0.0562	−0.852	0.238	0.948
OX34	LD	1.33	0.0616	2.00	—	4.27	0.431	1.28
OX35	LD	−0.945	0.411	−2.94	0.300	—	—	1.22
OX36	LD	0.957	0.827	2.84	0.605	—	—	1.14
OX37	LD	0.468	0.0504	0.650	0.0538	—	—	1.62
OX38	CR	0.887	0.0185	0.591	—	2.67	0.208	2.74
OX39	LD	0.567	0.0126	0.719	0.00134	—	—	1.61
OX40	CR	0.650	0.00749	—	—	1.11	0.0983	−0.533
OX41	C	0.363	0.0322	—	—	—	—	0.781
OX42	CR	0.554	0.0249	—	—	1.10	0.326	−0.490
OX43	LDR	0.615	0.0106	0.894	0.00904	0.488	0.0931	0.304
OX44	LD	0.501	0.00458	0.447	0.00489	—	—	2.15

Set	S_h	$100R^2$	$A100R^2$	F	S_{est}	S^0	N_{dp}	$r_{df/nV}$	P_D
OX31	0.0332	92.45	91.61	48.97	0.0517	0.322	11	4	54.6
OX32	0.0262	87.23	85.63	23.92	0.0408	0.427	10	3.5	35.0
OX33	0.0356	98.04	97.55	116.8	0.0516	0.175	11	4	56.0
OX34	0.0452	99.81	99.74	519.7	0.0718	0.0693	5	1	60.
OX35	0.198	98.54	98.06	67.72	0.199	0.11	5	1	75.7
OX36	0.398	94.01	92.01	15.69	0.401	0.387	5	1	74.7
OX37	0.0222	99.28	99.03	137.0	0.0295	0.135	5	1	58.1
OX38	0.00862	99.92	99.89	1214.	0.0121	0.0454	5	1	40.
OX39	0.00554	99.97	99.95	2907.	0.00734	0.0293	5	1	55.8
OX40	0.00425	99.98	99.97	4122	0.00597	0.0246	5	1	50.
OX41	0.0132	97.79	—	127.2	0.0281	0.196	5	1.5	50.
OX42	0.0141	99.63	99.50	267.7	0.0198	0.0965	5	1	50.
OX43	0.00396	99.99	99.99	5807.	0.00492	0.0169	5	1	59.3
OX44	0.00202	99.99	99.99	12030	0.00258	0.0144	5	1	47.2

Set	S_{PD}	C_L	C_D	C_R	r_{ld}	r_{le}	r_{de}	η	S_η
OX31	9.71	45.4	54.6	—	0.194	0.173	0.279	—	—
OX32	11.2	65.0	35.0	—	0.220	—	—	—	—
OX33	5.16	41.6	53.0	5.41	0.194	0.173	0.279	−1.02	0.277
OX34	—	23.8	—	76.2	—	0.500 *ce*	—	2.14	0.192
OX35	12.6	24.3	75.7	—	0.361	0.095	0.586	—	—
OX36	25.7	25.2	74.7	—	0.361	0.095	0.586	—	—
OX37	6.15	41.9	58.1	—	0.16	0.599	0.004	—	—
OX38	—	7608		23.2	—	0.477 *ce*	—	4.52	0.340
OX39	1.31	44.2	55.8	—	0.156	0.599	0.004	—	—
OX40	—	85.5 *c*	—	14.5	—	0.404 *ce*	—	1.70	0.150
OX41	—	100	—	—	—	—	—	—	—
OX42	—	83.4	—	16.6	—	0.409 *ce*	—	1.99	0.583
OX43	0.811	39.5	57.4	3.14	0.156	0.599	0.004	0.546	0.104
OX44	0.614	52.8	47.2	—	0.156	0.599	0.004	—	—

[a] See footnote *a*, Table 6, for column headings. *ce* indicates that the partial correlation coefficient is that for σ_c with σ_e.

2. Hydroxamic acids

TABLE 13. Hydroxamic acid reactivities

HA21. Reaction rates of X(C=O)NHOH with $K_2(SO_3)_2NO$ [a], X, $t_{1/2}$: NH_2, <5; H, 36; Me, 23; OEt, <5; Ph, 29; H_2NCH_2, 27; H_2NCO, 72; MeNH, <5; $PhCH_2$, 24; Et, 25.

HA22. Reaction rates of X(C=O)NHOH with $K_2(SO_3)_2NO$ [a], X, $t_{1/2}$: Me, 26; Pe, 41; Bu, 27; Et, 25; *i*-$Pr(CH_2)_2$, 38; *i*-Bu, 452; *i*-Pr, 27; *t*-Bu, 31; *c*-Hx, 40.

HA23. (4-$XPnCO_2$)($PhCH_2O$)NBz, 10^2k_2, acid-catalyzed solvolysis (H_2SO_4) in 3.81:1 CD_3CN:H_2O, 35 °C [b], X, 10^2k_2: MeO, 0.395; Me, 0.369; H, 0.411; Cl, 0.424; CHO, 0.578; CF_3, 0.689; CN, 0.630; NO_2, 0.863.

HA24. (4-$XPnCO_2$)($PhCH_2O$)NBz, k_2, OH^- in 25% aq. MeCN, 25 °C [b], X, k_2: Me, 2.27; H, 3.16; Cl, 3.82; CHO, 4.91; CN, 6.97; NO_2, 8.14.

[a] I. K. Larsen, B. M. Sjöberg and L. Thelander, in *Chemistry and Biology of Hydroxamic Acids* (Ed. E. Kiehl), S. Karger, Basel, 1982, pp. 83–93.
[b] S. A. Glover, G. P. Hammond and A. M. Bonin, *J. Org. Chem.*, **63**, 9684 (1998).

TABLE 14. Results of correlations for chemical reactivities of hydroxamic acids [a]

Set	Eq.	$L/a_{1/c}$	$S_{L/a1}$	D/a_1	$S_{D/a2}$	R/a_L	$S_R/_{ac}$	h
HA21	LD	0.51	0.0588	1.33	0.0330	—	—	1.56
HA22	SB	—	—	0.0574	0.0326	0.0359	0.0155	1.34
HA23	LD	0.444	0.127	0.348	0.114	—	—	0.407
HA24	CR	6.16	0.788	—	—	—	—	2.73

Set	S_h	$100R^2$	$100R^2$	F	S_{est}	S^0	N_{dp}	$N_{P/nV}$
HA21	0.00887	99.76	99	853.9	0.0103	0.0639	7	2
HA22	0.0517	76.58	72.23	9.807	0.0527	0.593	9	3
HA23	0.0525	85.08	82.59	14.25	0.0803	0.489	8	2.5
HA24	0.376	93.86		61.14	0.630	0.303	6	4

Set	P_D	S_{PD}	$C_{L/a1}$	$C_{D/a2}$	r_{ld}	r_{le}	r_{de}
HA21	72.2		27.8	72.2	0.733	—	
HA22	—	—	—	—	0.574	—	—
HA23	43.9		56.1	43.9	0.249	0.42	0.31
HA24			100		—	—	—

[a] See footnote *a*, Table 6, for column headings.

B. Single Electron Transfer

1. Oximes

TABLE 15. Oxime electron transfer data

OX21. 4-XPnCH=NOH in DMSO, X, E_{OX} (A^-) [a]: OMe, −0.608; Me, −0.585; H, −0.559; Cl, −0.520; Br, −0.520; CF_3, −0.471; CN, −0.440; NO_2, −0.371.

OX22. 4-XPnCMe=NOH in DMSO, X, E_{OX} (A^-) [a]: OMe, −0.629; Me, −0.609; H, −0.598; Cl, −0.539; Br, −0.537; CF_3, −0.483; CN, −0.450; NO_2, −0.407.

OX23. 4-XPnCMe=NOH, X, E_p (V) [b]: OMe, 1.46; Me, 1.60; F, 1.77; H, 1.87; Cl, 1.73; NO_2, 2.18; CN, 2.19; CF_3, 2.13.

(*continued overleaf*)

TABLE 15. (*continued*)

OX24. 3-XPnCMe=NOH, X, E_p (V)[b]: OMe, 1.65; Me, 1.66; H, 1.87; NO_2, 2.24; CN, 2.15; CF_3, 2.13.

OX25. 4-XPnCMe=NOH, X, IP (kcal mol^{-1})[b]: OMe, 163.36; Me, 172.32; F, 177.53; H, 177.70; Cl, 178.47; NO_2, 192.74; CN, 188.05; CF_3, 186.00.

OX26. 3-XPnCMe=NOH, X, IP(kcal mol^{-1})[b]: OMe, 168.61; Me, 174.47; F, 177.53; H, 177.70; Cl, 182.00; NO_2, 191.21; CN, 189.38; CF_3, 185.24.

[a] F. G. Bordwell, Y.-Y. Zhao and J.-P. Cheng, *J. Phys. Org. Chem.*, **11**, 10 (1988).
[b] A. Park, N. M. Kosareff, J. S. Kim and H. J. P. de Lijser, *Photochem. Photobiol.*, **82**, 110 (2006).

TABLE 16. Oxime electron transfer quantities[a]

Set	Eq.	r_{ld}	r_{le}	r_{de}	η	S_η	F	S_{est}	S^0
OX21	LD	0.246	0.526	0.102			109.9	0.0139	0.189
OX22	LD	0.246	0.526	0.102			517.2	0.00654	0.0877
OX23	LDR	0.121	0.200	0.385	1.69	0.826	38.12	0.0613	0.260
OX24	LDR	0.414	0.772	0.119	7.46	2.71	84.41	0.0363	0.153
OX25	LDR	0.121	0.200	0.385	2.16	0.475	12.05	1.29	0.148
OX26	LDR	0.121	0.200	0.385	2.66	0.674	74.38	1.33	0.188

Set	N_{dp}	$r_{df/hV}$	P_D	S_{PD}	C_L	C_D	C_R	L	S_L
OX21	8	2.5	48.8	6.62	51.2	48.36	—	0.201	0.0217
OX22	8	2.5	45.6	2.99	54.4	45.6	—	0.217	0.0102
OX23	8	1.33	62.9	9.60	33.6	56.8	9.61	0.509	0.102
OX24	6	0.67	34.8	9.62	51.7	27.4	20.63	0.803	0.151
OX25	8	1.33	58.7	5.09	36.6	52.1	11.2	19.9	1.96
OX26	8	1.33	50.0	5.93	44.1	44.1	11.8	20.0	2.01

Set	D	S_D	R	S_R	h	S_h	$100R^2$	$A100R^2$
OX21	0.191	0.0213	—	—	−0.562	0.00990	97.98	97.41
OX22	0.182	0.0100	—	—	−0.591	0.00465	99.52	99.44
OX23	0.861	0.0972	1.46	0.730	1.83	0.0501	96.62	95.27
OX24	0.430	0.100	3.21	1.39	1.84	0.0282	99.22	98.69
OX25	28.3	1.87	61.0	14.0	1757.5	0.962	98.91	98.47
OX26	20.0	1.92	53.2	14.4	179.9	0.988	98.24	97.53

[a] See footnote *a*, Table 6, for column headings.

C. NMR Chemical Shifts

1. Oximes

TABLE 17. Oxime NMR chemical shifts

OX27. $\delta^{13}C^{\beta}$, $XCH_2CH{=}NOH$[a], X, $\delta^{13}C^{\beta}$, X, $\delta^{13}C$: H, 0.00; F, −1.31; Cl, −1.08; Br, −0.99; I, −0.21; OMe, 0.01; SEt, −0.02; NMe_2, 0.30.

OX28. $\delta^{13}C^{\alpha}$, $XCH_2CH{=}NOH$[a], X, $\delta^{13}C^{\alpha}$: H, 0.00; F, 61.40; Cl, 23.80; Br, 10.98; I, −16.56; OMe, 51.75; SEt, 14.29; NMe_2, 41.88.

TABLE 17. (*continued*)

OX61. *Syn*-XCH=NOH, NMR in DMSO[b]. X, δ_{OH}: OMe, 10.80; Me, 10.28; MeSO, 11.22; $MeSO_2$, 11.40; CN, 11.16; NO_2, 11.43; Et, 10.30; *i*-Pr, 10.32; *i*-Bu, 10.35; SPh, 10.66; SMe, 10.61; Ph, 11.19; 1-MeVn-1-, 10.99; CCl_3, 12.17.

OX62. XCMe=NOH, NMR in DMSO[b], X, δ_{OH}: H_2N, 8.86; OMe, 9.28; OEt, 9.27; Me, 10.12; MeSO, 11.72; H, 10.28; $MeSO_2$, 12.50; CN, 11.09; NO_2, 11.31; $CHCl_2$, 11.02; *t*-Bu, 10.21; SEt, 10.50; SMe, 10.66; Ph, 11.15.

OX64. *Syn*-4-XPnCH=NOH, NMR in DMSO[b], X, δ_{OH}: Me_2N, 9.12; OMe, 9.37; Me, 9.45; H, 9.57; Cl, 9.67; Br, 9.66; NO_2, 10.07.

OX65. NMR, 4-XPnCH=NOMe, X, NMR in CCl_4[c], δ^1 H(OMe): NO_2, 6; CN, 4; CO_2Me, 3; Cl, 1; I, 1; H, 0; Me, −1; OMe, −2; Me_2N, −3.

OX66. NMR, 4-XPnCH=NOMe, X, NMR in PhH[c], δ^1 H(OMe): NO_2, −4; CN, −3; CO_2Me, −1; Cl, −2; I, −2; H, 0; Me, 2; OMe, 3; Me_2N, 7.

OX67. NMR, 4-XPnCH=NOMe, X, NMR in CCl_4[c], δ^1 H(αH): NO_2, 5; CN, 3; CO_2Me, 3; Cl, −1; I, −3; H, 0; Me, −2; OMe, −3; Me_2N, −6.

OX68. NMR, 4-XPnCH=NOMe, X, NMR in PhH[c], δ^1 H(αH): NO_2, −23; CO_2Me, −11; I, −18; H, 0; OMe, 0, Me_2N, 9.

[a] L. Tasic and R. R. Rittner, *J. Mol. Struct.*, **616**, 49 (2002).
[b] A. P. Kurtx and T. D. J. D' Silva, *J. Pharm. Sci.*, **76**, 599 (1987).
[c] N. E. Alexandrov and A. G. Varroglis, *Org. Magn. Res.*, **3**, 293 (1971).

TABLE 18. Oxime NMR chemical shift results[a]

Set	Eq.	L	S_L	D	S_D	R	S_R	h	S_h
OX27	LA	−2.64	0.522	4.31[b]	1.45	—	—	0.104	0.233
OX28	LDR	−65.0	22.4	−1.9	21.2	283.	55.1	−1.98	7.60
OX61	L	1.72	0.113	—	—	—	—	10.28	0.0444
OX62	LDR	−0.344	0.152	2.87	0.138	−11.7	0.818	10.22	0.0578
OX64	CR	0.641	1.1240			0.512	0.0725	0.0956	0.00704
OX65	LD	538	0.539	6.65	0.419	—	—	−3.62	0.233
OX66	LDR	−7.71	1.40	−4.69	1.27	−21.1	5.21	0.345	0.609
OX67	LD	4.21	1.92	9.58	1.49	—	—	−0.339	0.829
OX68	C	−34.2	6.26	—	—	—	—	0.357	2.36

Set	$100R^2$	$A100R^2$	F	S_{est}	S^0	N_{dp}	$r_{df/nv}$	P_D	S_{PD}
OX27	88.32	96.37	18.91	0.248	0.432	8	2.5	—	—
OX28	95.18	93.25	36.30	7.74	0.311	8	1.33	73.3	12.7
OX61	96.29	—	233.4	0.0965	0.213	11	9	—	—
OX62	98.69	98.36	175.8	0.0928	0.143	11	2.33	89.3	7.16
OX64	99.86	99.84	1459.	0.0134	0.0489	7	1	50	—
OX65	98.98	98.83	291.1	0.340	0.124	9	3	51.0	
OX66	96.13	94.84	41.40	0.862	0.264	9	1.67	37.8	11.8
OX67	91.23	89.98	31.20	1.21	0.363	9	3	69.5	
OX68	88.19	—	29.8	4.70	0.421	6	4	40	—

(*continued overleaf*)

TABLE 18. (*continued*)

Set	C_L	C_D	C_R	r_{ld}	r_{le}	r_{de}	η	$S_{\lambda\eta}$
OX27	75.4	24.6	—	0.699 [a]	—	—	—	—
OX28	23.9	65.7	10.4	0.2	0.43	0.57	−1.58	0.25
OX61	100	—	—	—	—	—	—	—
OX62	7.86	65.4	26.8	0.25	0.31	0.39	−4.09	0.21
OX64	9.26	—	7.39	0.42	—	—	0.8	0.11
OX65	51.0	49.0	—	0.34	0.01	0.52	—	—
OX66	53.1	32.3	14.6	34	0.01	0.52	4.5	ind [d]
OX67	30.5	69.5	—	0.34	0.01	0.52	—	—
OX68	100 [c]	—	—	—	—	—	—	—

[a] See footnote *a*, Table 6, for column headings.
[b] C_A represents the contribution of the polarizability parameter α to the regression equation; r is the partial correlation coefficient of σ_I with α.
[c] C_C represents the contribution of the composite substituent constant σ_C to the regression equation; r is the partial correlation coefficient of σ_I with σ_e.
[d] ind = independent.

2. Hydroxamic acids

TABLE 19. Hydroxamic acid NMR chemical shifts

HA41. 4-XPn(C=O)NHOH, X, δ^1H(NH) [a]: Me_2N, 10.845; H_2N, 10.730; MeO, 11.063; Me, 11.132; H, 11.215; F, 11.240; Cl, 11.301; CF_3, 11.452; NO_2, 11.588.

HA42. 4-XPn(C=O)NHOH, X, δ^1H(OH) [a]: Me_2N, 8.700; H_2N, 8.643; MeO, 8.899; Me, 8.955; H, 9.027; F, 9.060; Cl, 9.107; CF_3, 9.230; NO_2, 9.315.

HA43. 4-XPn(C=O)NHOH, X, δ^{15}N(NH) [a]: Me_2N, −218.9; H_2N, −218.3; MeO, −216.8; Me, −215.6; H, −215.1; F, −215.8; Cl, −215.3; CF_3, −214.1; NO_2, −213.2.

HA44. 4-XPn(C=O)NHOH, X, δ^{13}C(CO) [a]: Me_2N, 164.84; H_2N, 165.26; MeO, 164.21; Me, 164.38; H, 164.42; F, 163.42; Cl, 163.34; CF_3, 162.85; NO_2, 162.54.

HA45. 4-XPn(C=O)NHOH, X, δ^{13}C(C^1) [a]: Me_2N, 119.26; H_2N, 119.36; MeO, 125.05; Me, 130.12; H, 132.97; F, 129.41; Cl, 131.70; CF_3, 136.63; NO_2, 138.71.

HA46. 4-XPnC($OSiMe_2$Bu-*t*)=N$OSiMe_2$Bu-*t* in $CDCl_3$, X, δ^{29}Si(CN) [b]: Me_2N, 26.15; OMe, 26.88; CF_3, 28.34; NO_2, 29.10; H, 27.33; Me, 27.05; F, 27.51; Cl, 27.79.

HA47. 4-XPnC($OSiMe_2$Bu-*t*)=N$OSiMe_2$Bu-*t* in $CDCl_3$, X, δ^{29}Si(CO) [b]: Me_2N, 22.09; OMe, 22.83; CF_3, 24.33; NO_2, 25.10; H, 23.17; Me, 22.92; F, 23.57; Cl, 23.82.

HA48. 4-XPnC($OSiMe_2$Bu-*t*)=N$OSiMe_2$Bu-*t* in $CDCl_3$, X, δ^{13}C(C=N) [b]: Me_2N, 153.36; OMe, 152.71; CF_3, 151.95; NO_2, 151.53; H, 152.92; Me, 153.05; F, 152.23; Cl, 152.73.

HA49. 4-XPnC($OSiMe_2$Bu-*t*)=N$OSiMe_2$Bu-*t* in $CDCl_3$, X, δ^{13}C(C^1) [b]: Me_2N, 120.85; OMe, 125.71; CF_3, 136.72; NO_2, 139.44; H, 133.18; Me, 130.37; F, 129.32; Cl, 131.73.

HA50. 4-XPnC($OSiMe_3$)=N$OSiMe_3$ in $CDCl_3$, X, δ^{29}Si(CN) [c]: Me_2N, 24.48; OMe, 25.24; CF_3, 22.51; NO_2, 23.26; H, 21.38; Me, 21.10; F, 21.72; Cl, 21.97.

HA51. 4-XPnC($OSiMe_2$Bu-*t*)=N$OSiMe_2$Bu-*t* in $CDCl_3$, X, δ^{29}Si(CO) [c]: Me_2N, 20.3; OMe, 21.00; CF_3, 22.51; NO_2, 23.26; H, 21.38; Me, 21.10; F, 21.72; Cl, 21.97.

HA52. 4-XPnC($OSiMe_2$Bu-*t*)=N$OSiMe_2$Bu-*t* in $CDCl_3$, X, δ^{13}C(C=N) [c]: Me_2N, 154.38; OMe, 153.74; CF_3, 152.76; NO_2, 152.26; H, 153.82; Me, 153.96; F, 153.07; Cl, 153.05.

TABLE 19. (*continued*)

HA53. 4-XPnC(OSiMe$_2$Bu-*t*)=NOSiMe$_2$Bu-*t* in $CDCl_3$, X, $\delta^{13}C(C^1)$ [c]: Me_2N, 120.47; OMe, 126.35; CF_3, 136.32; NO_2, 139.03; H, 132.80; Me, 130.01; F, 128.90; Cl, 131.36.

[a] J. Schraml, M. Tvicalova, S. Pataridis, L. Soukupova, V. Plechta, J. Roithova and O. Exner, *Magn. Reson. Chem.,* **43**, 535 (2005).
[b] J. Schraml, M. Tvicalova, L. Soukupova, V. Plechta and O. Exner, *J. Phys. Org. Chem.*, **12**, 668 (1999).
[c] J. Schraml, M. Tvicalova, L. Soukupova, V. Plechta and O. Exner, *J. Organomet. Chem.*, **597**, 200 (2000).

TABLE 20. Hydroxamic acid NMR chemical shifts [a]

Set	Eq.	L/C	$S_{L/C}$	D	S_D	R	S_R	h	S_h
HA41	C	0.646	0.521					11.17	0.0202
HA42	LDR	0.402	0.0645	0.422	0.0507	0.596	0.203	9.03	0.0300
HA43	LDR	2.00	0.372	4.12	0.292	5.78	1.17	−2.5	0.173
HA44	LD	−2.68	0.383	−1.53	0.273	—	—	16.43	0.172
HA45	LDR	6.63	1.02	16.2	0.801	18.96	3.207	132.8	0.475
HA46	LDR	2.11	0.980	2.00	0.0817	0.804	0.308	27.33	0.0454
HA47	LDR	2.40	0.0757	0.91	0.0631	0.940	0.238	23.20	0.0351
HA48	LDR	−1.95	0.142	−0.870	0.119	−0.945	0.448	157.9	0.0659
HA49	LDR	6.43	0.564	15.5	0.471	11.9	1.78	133.0	0.261
HA50	LDR	2.28	0.0982	2.16	0.0819	0.869	0.309	25.76	0.0454
HA51	LDR	2.33	0.0592	1.93	0.0493	0.798	0.186	21.39	0.0274
HA52	LDR	−2.17	0.0623	−1.02	0.0519	−1.20	0.196	−0.0426	0.0288
HA53	LDR	6.37	0.561	15.5	0.468	11.9	1.77	132.6	0.260

Set	$100R^2$	$A100R^2$	F	S_{est}	S^0	N_{dp}	$r_{df/nV}$	P_D
HA41	95.64		153.5	0.0606	0.237	9	35	50
HA42	97.77	97.03	73.23	0.0420	0.200	9	1.67	52.4
HA43	98.12	98.56	152.8	0.242	0.139	9	1.67	67.3
HA44	94.43	93.63	50.84	0.252	0.289	9	3	36.3
HA45	99.42	99.23	285.6	0.644	0.102	9	1.67	71.0
HA46	99.72	99.61	480.1	0.0634	0.0744	8	1.33	48.7
HA47	99.85	99.78	863.7	0.0990	0.0535	8	1.33	44.4
HA48	98.76	98.26	106.1	0.0921	0.158	8	1.33	30.9
HA49	99.78	99.69	606.6	0.365	0.0662	8	1.33	70.7
HA50	99.76	99.67	556.9	0.0635	0.0691	8	1.33	4837
HA51	99.90	99.86	1376.	0.0383	0.0440	8	1.33	45.4
HA52	99.81	99.74	717.3	−0.0403	−0.0609	8	1.33	32.0
HA53	99.78	99.70	610.8	0.363	0.0660	8	1.33	70.9

Set	S_{PD}	η	S_η	$C_{L/C}$	C_D	C_R	r_{ld}	r_{le}	r_{ce}
HA41	—	—	—	100			—	—	—
HA42	7.88	1.35	0.433	44.5	48.9	6.60	0.215	0.219	0.467
HA43	7.06	1.40	0.266	29.8	61.5	8.63	0.215	0.219	0.467
HA44	7.66	—	—	63.7	36.3		0.215	—	—
HA45	5.34	1.17	0.189	50.3	47.8	1.92	0.140	0.166	0.383
HA46	2.49	0.401	0.153	50.3	47.8	1.95	0.140	0.166	0.383
HA47	1.78	0.491	0.12	54.4	43.5	2.13			
HA48	4.68	1.09	0.493	66.9	29.9	3.24			
HA49	3.19	0.769	0.112	77.8	67.0	5.16			
HA50	2.32	0.402	0.142	50.3	47.8	1.92			
HA51	1.42	0.413	0.0957	53.6	44.6	1.84			
HA52	1.82	1.17	0.183	65.5	30.9	3.62			
HA53	31.9	0.769	0.111	27.6	67.2	5.17			

[a] See footnote *a*, Table 6, for column headings.

VIII. APPENDICES

A. Glossary

This appendix is an updated, corrected and slightly modified version of one we have published elsewhere[50].

General

X A variable substituent.

Y An active site. The atom or group of atoms at which a measurable phenomenon occurs.

G A skeletal group to which X and Y may be attached.

W A variable group of atoms which can form two or more bonds to a skeletal group and/or an active site (a variable fragment).

Parameter An independent variable.

Pure parameter A parameter which represents a single effect.

Composite parameter A parameter which represents two or more effects.

Modified composite parameter A composite parameter whose composition has been altered by some mathematical operation.

Monoparametric equation A relationship in which the effect of structure on a property is represented by a single, generally composite parameter. Examples are the Hammett and Taft equations.

Diparametric equation A relationship in which the effect of structure on a property is represented by two parameters, one of which is generally composite. Examples discussed in this work include the LD, CR and MYT equations. Other examples are the Taft, Eherenson and Brownlee DSP (dual substituent parameter), Yukawa–Tsuno YT, and the Swain, Unger, Rosenquist and Swain SURS equations[74]. The DSP equation is a special case of the LDR equation with the intercept set equal to zero. It is inconvenient to use and has no advantages. The SURS equation uses composite parameters which are of poorer quality than those used with the LDR and DSP equations. The MYT equation has all the advantages of the YT equation and gives results which are easier to interpret.

Multiparametric equation An equation which uses three or more parameters all of which may be either pure or composite. The LDR equation used in this work is an example of a triparametric equation. The Taft–Topsom equation is an alternative triparametric equation[75].

Electrical effect parameterization

σ_1 The localized (field) electrical-effect parameter. It is identical to σ_I. Though other localized electrical effect parameters such as σ_I^q and σ_F have been proposed there is no advantage to their use. The σ^* parameter has sometimes been used as a localized electrical-effect parameter; such use is generally incorrect. The available evidence is strongly in favor of an electric field model for transmission of the effect.

σ_d The intrinsic delocalized (resonance) electrical-effect parameter. It represents the delocalized electrical effect in a system with zero electronic demand.

σ_e The electronic demand sensitivity parameter. It adjusts the delocalized effect of a group to meet the electronic demand of the system.

σ_D A composite delocalized electrical-effect parameter which is a function of σ_d and σ_e. Examples of σ_D constants are the σ_R^+ and σ_R^- constants. The $\sigma_{R,k}$ constants, where k designates the value of the electronic demand η, are also examples of σ_D constants.

σ_R A composite delocalized electrical-effect parameter of the σ_D type with η equal to 0.380. It is derived from 4-substituted benzoic acid pK_a values.

σ_R^o A composite delocalized electrical-effect parameter of the σ_D type with η equal to -0.376. It is derived from 4-substituted phenylacetic acid pK_a values.

σ_R^+ A composite delocalized electrical-effect parameter of the σ_D type with η equal to 2.04. It is derived from rate constants for the solvolysis of 4-substituted cumyl chlorides.

σ_R^ρ A composite delocalized electrical-effect parameter of the σ_D type with η equal to 3.31. It is derived from ionization potentials of the lowest energy π orbital in substituted benzenes.

σ_R^σ A composite delocalized electrical-effect parameter of the σ_D type with η equal to -2.98. It is derived from pK_a values of substituted nitriles.

σ_R^- A composite delocalized electrical-effect parameter of the σ_D type with η equal to -1.40. It is derived from pK_a values of substituted anilinium ions.

$\sigma_{k'/k}$ A composite parameter which is a function of σ_l, σ_d and σ_e. Its composition is determined by the values of k and k'. The Hammett σ_m and σ_p constants are of this type.

$\sigma_{Ck'}$ A composite constant that is a function of σ_l and σ_d; its composition is determined by the value of k'.

$\sigma^\blacklozenge$ An electrical-effect modified composite parameter.

σ Any electrical-effect parameter.

η The electronic demand of a system or of a composite electrical-effect parameter that is a function of both σ_d and σ_e. It is represented in subscripts as k. It is a descriptor of the nature of the electrical effect. It is given by R/D where R and D are the coefficients of σ_e and σ_d respectively.

$\mathbf{P}_D$ The percent delocalized effect. It too is a descriptor of the nature of the electrical effect. It is represented in subscripts as k'.

LDR equation A triparametric model of the electrical effect.

$\mathbf{P}_{EA}$ The percent of the $\sigma_{k'/k}$ values in a substituent matrix which exhibit an electron-acceptor electrical effect.

$\mathbf{P}_{ED}$ The percent of the $\sigma_{k'/k}$ values in a substituent matrix which exhibit an electron-donor electrical effect.

$\mathbf{P}_0$ The percent of the $\sigma_{k'/k}$ values in a substituent matrix which do not exhibit a significant electrical effect.

Steric effect parameterization

$\mathbf{r}_V$ The van der Waals radius. A useful measure of group size. The internuclear distance between two nonbonded atoms in contact is equal to the sum of their van der Waals radii.

υ A composite steric parameter based on van der Waals radii. For groups whose steric effect is at most minimally dependent on conformation, it represents the steric effect due to the first atom of the longest chain in the group and the branches attached to that atom. The only alternative monoparametric method for describing steric effects is that of Taft which uses the E_S parameter. This was originally developed only for alkyl and substituted alkyl groups and for hydrogen. Hansch and Kutter[73] have estimated E_S values for other groups from the υ values using a method which in many cases disregards the MSI principle. It is best to avoid their use.

Simple branching equation (SB) A topological method for describing steric effects which takes into account the order of branching by using as parameters n_i, the number of atoms other than H that are bonded to the i-th atoms of the substituent.

$\mathbf{n}_i$ The number of branches on the i-th atoms of a substituent. These are the steric parameters used in the SB equation.

Expanded branching equation (XB) A topological method for describing steric effects which takes into account the order of branching by using as parameters n_{ij}, the number of j-th branching atoms bonded to the i-th atoms of the substituent.

$\mathbf{n}_{ij}$ The number of j-th branches on the i-th atoms of a substituent. These are the steric parameters used in the XB model of steric effects.

$\mathbf{n}_b$ The number of bonds in the longest chain of a substituent. It is a steric parameter which serves as a measure of the length of a group along the group axis.

Segmental equation A steric-effect model that separately parameterizes each segment of a substituent. It requires fewer parameters than the XB equation and is generally more effective than the SB equation.

υ_i A steric parameter based on van der Waals radii that is a measure of the steric effect of the i-th segment of a substituent. The i-th segment consists of the i-th atom of the longest chain in the substituent and the groups attached to it. The MSI principle is assumed to apply and the segment is assigned the conformation that gives it the smallest possible steric effect.

MSI principle The principle of minimal steric interaction which states that the preferred conformation of a group is that which results in the smallest possible steric effect.

Intermolecular force parameterization

α A polarizability parameter defined as the difference between the group molar refractivities for the group X and for H divided by 100. Many other polarizability parameters, such as the van der Waals volume, the group molar volume and the parachor, can be used in its place. All of these polarizability parameters are very highly linear in each other.

$\mathbf{n}_H$ A hydrogen-bonding parameter which represents the lone-pair acceptor (proton donor) capability of a group. It is defined as the number of OH and/or NH bonds in the group.

$\mathbf{n}_n$ A hydrogen-bonding parameter which represents the lone-pair donor (proton acceptor) capability of the group. It is defined as the number of lone pairs on O and/or N atoms in the group.

i A parameter which represents ion–dipole and ion-induced dipole interactions. It is defined as 1 for ionic groups and 0 for nonionic groups.

n_D A charge transfer donor parameter which takes the value 1 when the substituent can act as a charge transfer donor and 0 when it cannot.

n_A A charge transfer acceptor parameter which takes the value 1 when the substituent can act as a charge transfer acceptor and 0 when it cannot.

IMF equation A multiparametric equation which models phenomena that are a function of the difference in intermolecular forces between an initial and a final state.

Solvent effect parameterization

Winstein–Grunwald equation An equation which accounts for the effect of solvent on nucleophilic solvolysis.

Y_{sv} The solvent parameter in the Winstein–Grunwald equation.

N_{Nu} The solvent nucleophilicity parameter.

Dimroth–Reichart equation Monoparametric equation for solvent effects.

$E_{T,Sv}$ A solvent parameter defined as the transition energy for the pyridinium betaine **17** in the solvent Sv.

Statistics

Correlation equation An equation with a data set is correlated by simple (one parameter) or multiple (two or more parameters) linear regression analysis.

Regression equation The equation obtained by the correlation of a data set with a correlation equation.

N_{dp} The number of data points in a data set.

N_{iv} The number of independent variables in a data set.

Degrees of freedom (N_{df}) Defined as the number of data points, N_{dp}, minus the number of parameters (N_{iv}) plus 1 [$N_{df} = N_{dp} - (N_{iv} + 1)$].

F statistic A statistic which is used as a measure of the goodness of fit of a data set to a correlation equation. The larger the value of F the better the fit. Confidence levels can be assigned by comparing the F value calculated with the values in an F table for the N_{iv} and DF values of the data set.

$100R^2$ A statistic which represents the percent of the variance of the data accounted for by the regression equation. It is a measure of the goodness of fit.

A$100R^2$ A statistic that corrects $100R^2$ for the number of independant variables.

S_{est} The standard error of the estimate. It is a measure of the error to be expected in predicting a value of the dependent variable from the appropriate parameter values.

S^o Defined as the ratio of S_{est} to the root mean square of the data. It is a measure of the goodness of fit. The smaller the value of S^o the better the fit.

$\mathbf{r}_{df/iv}$ Defined as the ratio of N_{df} to N_{iv}. It is a measure of the reliability of the data set in the absence of clustering.

B. Abbreviations

Ac	acetyl	C_2H	ethynyl	Ph	phenyl
Ad	adamantyl	Et	ethyl	Pn	phenylene
Ak	alkyl	Har	heteroaromatic	Pr	1-propyl
c-Ak	cycloalkyl	Hp	heptyl	*c*-Pr	cyclopropyl
Bs	4-bromobenzene-sulfonyl	Hx	hexyl	*i*-Pr	2-propyl
		c-Hx	cyclohexyl	1-*c*-Prn	cyclopropylidene
Bu	butyl	Me	methyl	2-*E*-*c*-Prn	*trans*-cyclo-propylene
c-Bu	cyclobutyl	*neo*-Pe	3,3-dimethylpropyl		
i-Bu	2-methyl-1-propyl	*c*-Pe	cyclopentyl	2-*Z*-*c*-Prn	*cis*-cyclopropylene
s-Bu	1-methyl-1-propyl	*i*-Pe	3-methylbutyl	Py	pyridyl
t-Bu	2-methyl-2-propyl	*t*-Pe	2,2-dimethylpropyl	Ts	4-toluenesulfonyl
		1-Pe	1-pentyl	Vi	vinyl
Bz	benzoyl	2-Pe	2-pentyl	1-Vn	1-vinylene
C_2	ethynylene	3-Pe	3-pentyl	2-Vn	2-vinylene

IX. REFERENCES

1. M. Charton, in *Chemistry of the Alkenes*, Vol. 2 (Ed. J. Zabicky), John Wiley & Sons, Inc., New York, 1970, p. 511.
2. A. Greenberg and J. F. Liebman, *Strained Organic Molecules*, Academic Press, New York, 1978.
3. M. R. Saunders and D. Livingstone, in *Advances in Quantitative Structure Property Relationships*, Vol. 1 (Ed. M. Charton), JAI Press, Greenwich, Conn., 1996, p. 56.
4. U. Burkert and N. L. Allinger, *Molecular Mechanics*, American Chemical Society, Washington D.C., 1982.
5. Y. C. Martin and Ki-H. Kim, in *Advances in Quantitative Structure Property Relationships*, Vol. 1 (Ed. M. Charton), JAI Press, Greenwich, Conn., 1996, p. 1.
6. L. B. Kier and L. H. Hall, *Molecular Connectivity in Chemistry and Drug Research*, Academic Press, New York, 1976; R. E. Merrifield and H. E. Simmons, *Topological Methods in Chemistry*, Wiley-Interscience, New York, 1989; A. T. Balaban (Ed), *From Chemical Topology to Three-Dimensional Geometry*, Plenum Press, New York, 1997.
7. M. Charton, *J. Computer-Aided Mol. Design*, **17**, 197 (2003); M. Charton and B. l. Charton, *J. Computer-Aided Mol. Design*, **17**, 211 (2003); M. Charton, in *Designing Drugs and Crop Protectants: Processes, Problems and Solutions*, Proc. 14th Eur. QSAR Conf. (Eds. M. Ford, D. Livingstone, J. Dearden and H. Van de Waterbeemd), Kluwer, Amsterdam, 2003, p. 122.
8. J. Devillers (Ed), *Neural Networks in QSAR and Drug Design,* Academic Press, London, 1996; S. Haykin, *Neural Networks*, Macmillan, New York, 1994; R. Neal, *Bayesian Learning for Neural Networks*, Springer, New York, 1996.
9. L. P. Hammett, *J. Am. Chem. Soc.*, **59**, 96 (1937).
10. L. P. Hammett, *Trans. Faraday Soc.*, **34**, 156 (1938).
11. L. P. Hammett, *Physical Organic Chemistry*, 1st edn., McGraw-Hill, New York, 1940, p. 184.
12. G. N. Burkhardt, *Nature*, **136**, 684 (1935).
13. H. C. Brown and Y. Okamoto, *J. Am. Chem. Soc.*, **79**, 1913 (1957).
14. L. M. Stock and H. C. Brown, *Adv. Phys. Org. Chem.*, **1**, 35 (1963).
15. H. van Bekkum, P. E. Verkade and B. M. Wepster, *Rec. Trav. Chim. Pays-Bas*, **78**, 815 (1959).
16. R. W. Taft, *J. Phys. Chem.*, **64**, 1805 (1960).
17. R. W. Taft, *J. Am. Chem. Soc.*, **79**, 1045 (1957).
18. R. W. Taft and I. C. Lewis, *J. Am. Chem. Soc.*, **80**, 2436 (1958).
19. S. Ehrenson, R. T. C. Brownlee and R. W. Taft, *Prog. Phys. Org. Chem.*, **10**, 1 (1973).

20. M. Charton, in *Molecular Structures and Energetics*, Vol. 4 (Eds A. Greenberg and J. F. Liebman), VCH Publ., Weinheim, 1987, p. 261.
21. M. Charton, *Bull. Soc. Chim. Belg.*, **91**, 374 (1982).
22. Y. Yukawa and Y. Tsuno, *Bull. Chem. Soc. Jpn.*, **32**, 965, 971 (1959).
23. Y. Yukawa, Y. Tsuno and M. Sawada, *Bull. Chem. Soc. Jpn.*, **39**, 2274 (1966).
24. M. Yoshioka, M. Hamamoto and T. Kabota, *Bull. Chem. Soc. Jpn.*, **35**, 1723 (1962).
25. M. Charton, *Prog. Phys. Org. Chem.*, **16**, 287 (1987).
26. M. Charton and B. I. Charton, *Abstr. 10th Int. Conf. Phys. Org. Chem.*, Haifa, 1990, p. 24.
27. M. Charton, in *The Chemistry of Arsenic, Antimony and Bismuth* (Ed. S. Patai), John Wiley & Sons, Inc., New York, 1994, p. 367.
28. M. Charton, in *The Chemistry of the Functional Groups. Supplement A, The Chemistry of Double Bonded Functional Groups*, Vol. 2, Part 1 (Eds S. Patai and Z. Rappoport), John Wiley & Sons, Inc., New York, 1989, p. 239.
29. M. Charton, *Prog. Phys. Org. Chem.*, **13**, 119 (1981).
30. C. Hansch, A. Leo and D. Hoekman, *Exploring QSAR. Hydrophobic, Electronic and Steric Constants*, American Chemical Society, Washington D.C., 1995.
31. M. Charton, *Advances in Quantitative Structure Property Relationships*, **1**, 171 (1996).
32. C. G. Derick, *J. Am. Chem. Soc.*, **33**, 1152 (1911).
33. C. G. Derick, *J. Am. Chem. Soc.*, **33**, 1181 (1911).
34. G. K. Branch and M. Calvin, *The Theory of Organic Chemistry*, Prentice-Hall, New York, 1941, p. 211.
35. R. W. Taft, in *Steric Effects in Organic Chemistry* (Ed. M. S. Newman), John Wiley & Sons, Inc., New York, 1956, p. 556.
36. J. G. Kirkwood, *J. Chem. Phys.*, **2**, 351 (1934).
37. J. G. Kirkwood and F. H. Westheimer, *J. Chem. Phys.*, **6**, 506 (1938); F. H. Westheimer and J. G. Kirkwood, *J. Chem. Phys.*, **6**, 513 (1938); F. H. Westheimer and M. W. Shookhoff, *J. Am. Chem. Soc.*, **61**, 555 (1939); F. H. Westheimer, *J. Am. Chem. Soc.*, **61**, 1977 (1939); J. N. Sarmousakis, *J. Chem. Phys.*, **12**, 277 (1944).
38. O. Exner and P. Fiedler, *Collect. Czech. Chem. Commun.*, **45**, 1251 (1980).
39. M. Charton, *J. Phys. Org. Chem.*, **12**, 275 (1999); M. Charton and B. I. Charton, *J. Chem. Soc., Perkin Trans. 2*, 2203 (1999); M. Charton, *Collect. Czech. Chem. Commun.*, **64**, 1849 (1999); M. Charton and B. I. Charton, *J. Phys. Org. Chem.*, **14**, 832 (2001).
40. E. M. Nolan and R. G. Linck, *J. Am. Chem. Soc.*, **122**, 11497 (2000); *J. Phys. Chem. A*, **105**, 7297 (2001); *J. Phys. Chem. A*, **106**, 533 (2002).
41. F. Kehrmann, *Ber.*, **21**, 3315 (1888); **23**, 130 (1890); *J. prakt. chem.*, [2] **40**, 188, 257 (1889); [2] **42**, 134 (1890).
42. V. Meyer, *Ber.*, **27**, 510 (1894); **28**, 1254, 2773, 3197 (1895); V. Meyer and J. J. Sudborough, *Ber.*, **27**, 1580, 3146 (1894); V. Meyer and A. M. Kellas, *Z. physik. chem.*, **24**, 219 (1897).
43. J. J. Sudborough and L. L. Lloyd, *Trans. Chem. Soc.*, **73**, 81 (1898); J. J. Sudborough and L. L. Lloyd, *Trans. Chem. Soc.*, **75**, 407 (1899).
44. A. W. Stewart, *Stereochemistry*, Longmans and Green, London, 1907, p. 314; *ibid*, 2nd edn., 1919, p. 184.
45. G. Wittig, *Stereochemie*, Akademische Verlagsgesellschaft, Leipzig, 1930, p. 333.
46. G. W. Wheland, *Advanced Organic Chemistry*, 3rd edn., John Wiley & Sons, Inc., New York, 1960, p. 498.
47. M. S. Newman (Ed.), *Steric Effects in Organic Chemistry*, John Wiley & Sons, Inc., New York, 1956.
48. M. Charton and B. I. Charton, *J. Org. Chem.*, **44**, 2284 (1979).
49. M. Charton, *Top. Curr. Chem.*, **114**, 107 (1983).
50. M. Charton, in *Rational Approaches to the Synthesis of Pesticides* (Eds P. S. Magee, J. J. Menn and G. K. Koan), American Chemical Society, Washington D.C., 1984, p. 247.
51. K. Kindler, *Ann. Chem.*, **464**, 278 (1928).
52. M. Charton, *J. Am. Chem. Soc.*, **91**, 615 (1969).
53. M. Charton, *Prog. Phys. Org. Chem.*, **8**, 235 (1971).
54. M. Charton, *Prog. Phys. Org. Chem.*, **10**, 81 (1973).
55. M. Charton, *Top. Curr. Chem.*, **114**, 57 (1983).
56. M. Charton and C. Sirovich, *Abstr. 27th Mid-Atlantic Regional Meeting*, American Chemical Society, New York, 1993, p. 129.

57. M. Charton, *J. Org. Chem.*, **48**, 1011 (1983); M. Charton, *J. Org. Chem.*, **48**, 1016 (1983).
58. M. Charton, *Advances in Molecular Structure Research*, **5**, 25 (1999).
59. A. Verloop, W. Hoogenstraaten and J. Tipker, *Drug Design*, **7**, 165 (1976).
60. M. Charton, in *Proceedings of the Third Congress of the Hungarian Pharmacological Society, Budapest, 1979*, Akademiaj Kiado, Budapest, 1980, p. 211.
61. M. Charton, *Stud. Org. Chem.*, **42**, 629 (1992).
62. M. Charton and B. I. Charton, *J. Theor. Biol.*, **99**, 629 (1982); M. Charton, *Prog. Phys. Org. Chem.*, **18**, 163 (1990); M. Charton, in *Trends in Medicinal Chemistry '88* (Eds. H. van der Goot, G. Domany, L. Pallos and H. Timmerman), Elsevier, Amsterdam, 1989, p. 89; M. Charton and B. I. Charton, *J. Phys. Org. Chem.*, **7**, 196 (1994).
63. M. Charton, in *The Chemistry of Organic Germanium, Tin and Lead Compounds* (Ed. S. Patai) Wiley, Chichester, 1996, p. 603.
64. M. Charton, *Advances in Quantitative Structure Property Relationships*, **3**, 137, (2002).
65. M. Charton and B. I. Charton, *Collect. Czech. Chem. Commun.*, **69**, 2147 (2004); M. Charton, *Current Computer-Aided Drug Design*, **2**, 353 (2006).
66. R. D. Green, *Hydrogen Bonding by C−H Groups*, Wiley, New York, 1974.
67. M. Nishio, M. Hirota and Y. Urezama, *The CH/π Interaction. Evidence, Nature, and Consequences*, Wiley-VCH, New York, 1998.
68. M. Charton, in *Classical and 3-D QSAR in Agrochemistry and Toxicology* (Eds. C. Hansch and T. Fujita) American Chemical Society, Washington D.C., 1995, p. 75.
69. M. Charton, in *The Chemistry of Organolithium Compounds* (Ed. Z. Rappoport), Wiley, Chichester, 2004, p. 267.
70. S. Winstein and N. J. Holness *J. Am. Chem. Soc.*, **70**, 846 (1955).
71. K. Dimroth, C. Reichardt, T. Siepmann and F. Bohlmann, *Ann. Chem.*, **661**, 1 (1963).
72. C. Reichardt, *Solvents and Solvent Effects in Organic Chemistry*, 3rd edn., Wiley-VCH, Weinheim, 2003.
73. E. Kutter and C. Hansch, *J. Med. Chem.*, **12**, 647 (1969).
74. C. G. Swain, S. H. Unger, R. N. Rosenquist and M. S. Swain, *J. Am. Chem. Soc.*, **105**, 492 (1983).
75. R. W. Taft and R. D. Topsom, *Prog. Phys. Org. Chem.*, **16**, 1 (1987).

CHAPTER 13

Hydroxylamines and oximes: Biological properties and potential uses as therapeutic agents

YACOV ASHANI and ISRAEL SILMAN

Department of Neurobiology, The Weizmann Institute of Science, Rehovot 76100, Israel
Fax: +972-8-9346017; e-mail: yaacov.ashani@weizmann.ac.il and israel.silman@weizmann.ac.il

The chemistry of hydroxylamines, oximes and hydroxamic acids
Edited by Z. Rappoport and J. F. Liebman

I. INTRODUCTION

A. Background

Hydroxylamines (R^1R^2NOH, **1**; HA) and their two major derivatives, oximes ($R^1R^2C{=}NOH$, **2**) and hydroxamic acids ($RCONR^3OH$, **3**), where R represents an H, an alkyl, a cycloalkyl or an aromatic moiety, are characterized by an oxygen-containing core that is linked directly to an electronegative nitrogen with an unshared electron pair. In general, −NR−OH-containing molecules appear to be amenable to biotransformations such as reduction, oxidation, hydrolysis and conjugations with organic and inorganic molecules. The unshared electrons on the α-neighboring atom can be recruited by all three classes of compounds to enhance reactions that involve nucleophilic displacements by the anionic form $N{-}O^-$, a phenomenon that is known as the α-effect (discussed in Chapter 17 of the present volume). In addition, the ability of oximes and hydroxamic acids to form strong complexes with a variety of metals, and the tendency of the NH−OH function to form the nitroxide radical, $-NH-O^{\bullet}$ determines largely, but not exclusively, the biological and toxicological behavior of **1**, **2** and **3**. Hydroxylamine is also thought to be a precursor of nitric oxide (NO), which is a bioactive endogenous metabolite in various biological systems. These properties have been exploited by numerous investigators to design and develop novel therapeutic agents that can display acyl group transfer capabilities and/or serve as specific inhibitors of a variety of metalloenzymes. The isolation of stable molecules and identification of labile intermediates containing the N−OH

group in plants, marine sponges, microorganisms and mammals, and elucidation of their physiological and biochemical roles, gave considerable impetus to the synthesis and evaluation of novel candidate drugs for the treatment of various diseases. For example, HA was proposed both as part of a treatment regimen for cyanide toxicity in humans and as a donor of NO, and HA derivatives were demonstrated to show promise in the treatment of sickle cell anemia, as scavengers of reactive oxygen species, as anticancer drugs and in conferring protection against ionizing radiation. N−OH-containing compounds were further reported to be effective antimalarial, antimicrobial and anticancer drugs, to possess antioxidant and anti-inflammatory activity, to serve as efficient drugs in nonabsorbed iron chelating therapy and to be potential agents for treatment of osteoarthritis. Heteroaromatic and aliphatic oximes are used as antidotes to treat organophosphate intoxication caused by nerve agents and commercial pesticides, and some oxime ligands have been shown to possess antimicrobial activity, potential digitalis-like properties, antitumor activity, ability to relax blood vessels and the capacity to initiate oxidative DNA cleavage. Thus, both the increasing synthetic effort and the growing body of scientific information with respect to N−OH compounds hold great promise for the development of novel therapeutic drugs in various fields of medicine.

B. Scope

This chapter summarizes the biological properties of naturally occurring and synthetic N−OH-containing compounds represented by **1** and **2**, and their potential therapeutic applications. For each class of compounds the following issues will be reviewed:

1. Natural occurrence, biosynthesis and possible physiological function.
2. Biochemical characteristics and physiological effects.
3. Toxicity.
4. Current and potential therapeutic applications.

II. HYDROXYLAMINES (HAs)

A. Natural Occurrence

The first to suggest the natural occurrence of hydroxylamine, NH_2OH (HA), was Blom who, already in 1928–1931, proposed that it is generated in microorganisms during nitrogen fixation[1,2]. Since then, numerous studies have provided evidence that HA occurs in both prokaryotes and eukaryotes. It was reported to occur as an intermediate in a wide spectrum of bacteria capable of oxidizing ammonia or reducing nitrates[3–12]. Jason and coworkers recently reviewed the molecular diversity of bacterial nitrite reductase genes[13]. In 1985, Gross reviewed the biological activity of HA, mostly in terms of toxicity, and highlighted the *in vivo* formation of the N−OH function as part of an intracellular detoxification system[14a].

There is now a wide consensus that HA is a product of normal metabolism, and that its toxicity, and that of substituted HAs, is manifested only at concentrations well above those expected when HA is produced as a result of normal cell metabolism. However, despite the fact that *N*-hydroxylation is a key detoxification reaction for various drugs, the lack of convincing direct *in vivo* measurements of HA itself in healthy individuals does not permit a definitive conclusion as to its normal endogenous levels as a harmless species in mammalian cells.

HA may be found in water, soil, plants and mammalian tissues. The fact that diverse microorganisms are capable of producing HA via metabolic reactions suggests that in mammals its natural occurrence may stem, at least in part, from production by normal

bacterial flora. For example, Lewis suggested the formation of HA as an intermediate in the reduction of nitrates by a suspension of sheep rumen bacteria[15].

The involvement of isobutylhydroxylamine, $(CH_3)_2CHCH_2NH{-}OH$ (**4**), and of HA (NH_2OH) in the biosynthesis of the antibiotics valanimycin[16] (**5**) and nebularine[7] (**6**), respectively, has been demonstrated in *Streptomyces* species (see Section II.B). In the case of nebularine, HA is released in the final step of its production by enzymatically induced deamination of adenosine, while the isobutylhydroxylamine is a precursor for the biosynthesis of valanimycin. In cyanobacterium, the presence of free and bound HA was demonstrated to be a product of enzyme-mediated glutamine oxidation[17–19].

Since HA is unstable *in vivo*[14a], and is known to rapidly associate with the heme part of heme proteins[20,21], and possibly also with a variety of biological oxidants, such as the superoxide anion that is produced by many mammalian cells[22], it is difficult to demonstrate its accumulation *in vivo*. Already in 1932 Lindsey and Rhines[3] discussed some analytical difficulties in the detection of HA, since when added externally, it disappeared rapidly from bacterial cultures; this led to the conclusion that even if it is produced as an intermediate, its consumption is too fast to allow the accumulation of sufficient quantities for analytical demonstration. Compelling indirect evidence for the presence of HA as an intermediate in the enzymatically catalyzed reduction of nitrite (NO_2^-) to NH_3 was provided by Einsle and colleagues[10], who characterized the crystal structure of the complex obtained by soaking cytochrome *c*-nitrite reductase with NH_2OH[23].

Despite the scarcity of direct evidence, HA is generally believed to be present as a metabolic intermediate in mammalian tissues[14a,22,24–26]. Recent studies on the reductive detoxification of HAs both by human NADH-cytochrome *b*5 reductase and by human cytochrome *b*5 may be considered as additional supporting evidence for the *in vivo* formation of HA in mammalian cells that needs to be controlled in order to avoid the toxic effects of an excess of endogenously produced HA, as well as of HA produced by detoxification of xenobiotic HA derivatives[27–29].

Substituted HAs have been shown to be metabolic intermediates in the *N*-oxygenation of biogenic amines such as phenethylamine and amphetamine, and have been detected in the urine of experimental animals. The end products of these metabolic pathways are oximes, and will be discussed at length in Section III.

B. Biosynthesis

HA can be produced by catalytic oxidation of ammonia with hydrogen peroxide[30] or by catalytic reduction of nitrates with hydrogen[31]. Analogously, oxidative and reductive enzymic pathways in which HA is produced from either ammonia or nitrate have been identified in a variety of biological systems.

1. Oxidation of ammonia

Studies on nitrogen cycle enzymology in microorganisms that use ammonia as a major source of energy for growth suggest that HA serves as an intermediate in its oxidation to nitrite[8,9,13], as depicted in equations 1 and 2:

$$NH_3 + 2H^+ + O_2 \xrightarrow{+2e^-} NH_2OH + H_2O \quad (1)$$

$$NH_2OH + H_2O \longrightarrow NO_2^- + 5H^+ + 4e^- \quad (2)$$

The first reaction (equation 1), which is catalyzed by ammonium monooxygenase (AMO), increases the oxidation state from −3 in NH_3 to −1 in HA. The conversion of HA to nitrite (equation 2) is performed by HA oxyreductase (HAO), and is accompanied by an increase in the oxidation state from −1 in HA to +3 in nitrite. Schmidt and colleagues provided evidence for the existence of active transport of HA in bacteria that permitted them to demonstrate its binding to HAO[32]. As seen, 4 electrons are released in the second step, and 2 of them are utilized by AMO for the conversion of NH_3 to HA. The remaining 2 electrons are taken up by components of the respiratory chain, resulting in enhanced bacterial growth. In the case of *Nitrosomonas europea*, this step is believed to be carried out by the tetraheme cytochrome c_{554}[12]. The ubiquitous occurrence of AMO-containing bacteria in both soils and aqueous environments[9] suggests that, depending upon the relative activities of AMO and HAO and upon the environmental conditions (e.g. pH, temperature, availability of oxygen), HA may accumulate transiently in both environments. In this context, it is of interest to mention the study of Tanaka who, already in 1953, demonstrated bacterially induced changes in HA levels in lake water as a function of the depth, the temperature and the concentration of dissolved oxygen[6].

2. Reduction of nitrates and nitrites

Production of HA from nitrate as the sole nitrogen source by unknown soil bacteria was demonstrated as early as 1928[1] and 1931[2], and was confirmed in 1932 by the use of known pure bacterial cultures[3]. Later, HA was suggested to be an intermediate in the *in vitro* reduction of nitrate by sheep rumen bacteria[15].

The involvement of HA during bacterial conversion of nitrate to NH_3 (known also as the 'nitrate ammonification' phase of the nitrogen cycle) has been studied at the molecular level as part of an effort to delineate the mechanism of conversion of nitrite to NH_3 by a group of multiheme cytochromes of bacterial origin. The overall reduction reaction is depicted in equation 3 for cytochrome *c*-nitrite reductase[10, 23, 33]:

$$NO_2^- + 8H^+ + 6e^- \longrightarrow NH_4^+ + 2H_2O \qquad (3)$$

Based on crystallographic observations it was suggested that the HA intermediate is bound to the cytochrome reductase via the iron atom, Fe(II)−NH_2OH, and undergoes subsequent reduction to produce the NH_3 that then dissociates from the protein[10]. It is of interest that the specific activity of cytochrome *c*-nitrite reductase from *S. deleyianum* in the conversion of NO_2^- to NH_3 is only 2-fold greater than that recorded for the conversion of HA to ammonia by the same enzyme, an observation that strongly supports the involvement of HA as an intermediate in the catalytic reduction of nitrite to NH_3[23].

3. Conversion of L-arginine to nitric oxide (NO)

Guanylate cyclase, the enzyme that catalyzes the biosynthesis of cyclic GMP from GTP, has been shown to be activated in rat-brain slices by HA, resulting in increased accumulation of cyclic GMP[34, 35]. In addition, HA was demonstrated to possess vasodilatory properties[36–38]. Since these properties resemble the activation of guanylate cyclase by nitric oxide (NO) and its vasodilatory activity[39], it was suggested that the vasorelaxant properties of HA are probably due to the release of NO, not to direct action of HA itself[22, 24, 37]. Based on these correlations, DeMaster and colleagues[38] proposed a pathway for the conversion of L-arginine to NO via the formation of HA (equation 4).

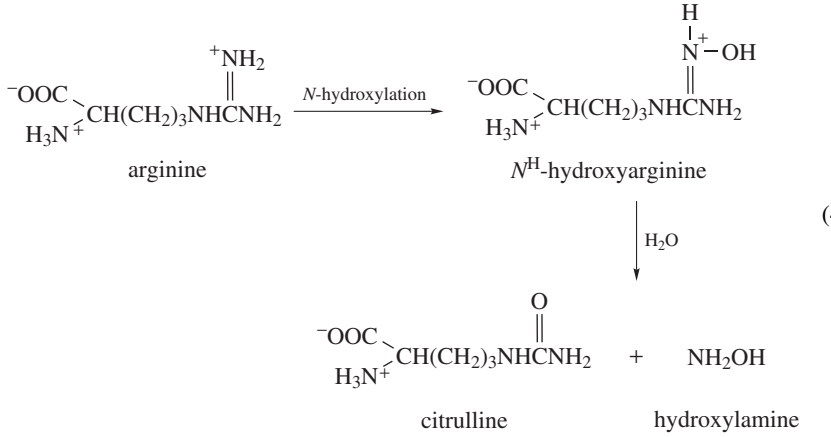

(4)

Thus, HA may be a natural product in mammalian cells that stems, in part, from the oxidative conversion of arginine to nitric oxide[25, 34, 40–42].

4. Involvement of HAs in biosynthesis of naturally occurring antibiotics

Parry and Wenying[16] provided evidence for the pathway (shown in equation 5) for biosynthesis of the antibiotic and antitumor agent, valanimycin (**5**), in streptomyces by isolation and partial purification of an HA-forming enzyme.

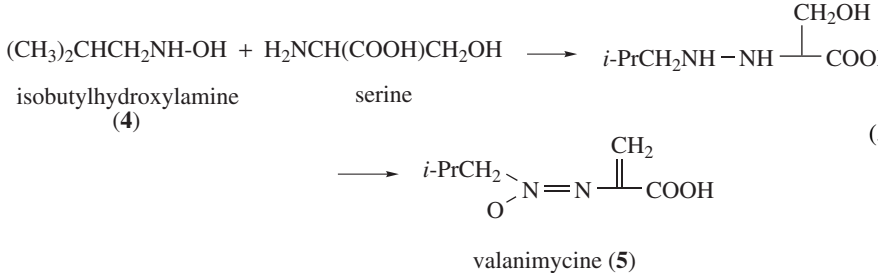

(5)

The enzymatic formation of **4** from isobutylamine, which is derived from valine, during the biosynthesis of valanimycin, was confirmed by high-resolution MS analysis[16, 43]. The importance of the pathway shown in equation 5 is the notion that naturally occurring N−N bond products are likely to involve the condensation of HA and an amine to yield a hydrazine that is subsequently transformed to an azoxy moiety such as that occurring in valanimycin.

Production of HA during the biosynthesis of the antibiotic nebularine (**6**) was demonstrated in another *Streptomyces* species[7]. The formation of HA was confirmed both by chemical reactions designed to detect it and by MS analysis. An unusual enzymic deamination of adenosine was suggested, which resulted in release of HA, rather than of NH_3, as a key step in the production of nebularine (equation 6).

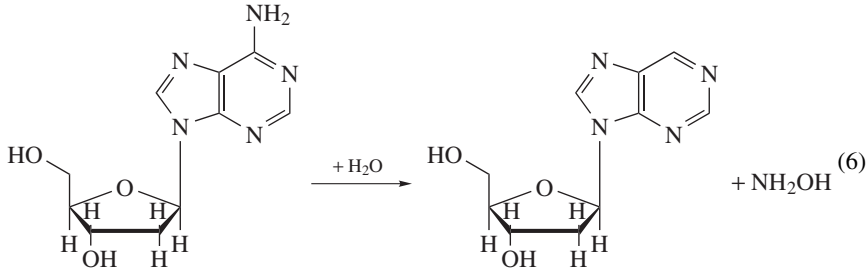

(6)

nebularine (**6**)

5. In vivo conversions of arylamines to substituted HAs

Substituted HAs were shown to stem *in vivo* from bio-activation of numerous arylamines and heterocyclic arylamines (HAA) of commercial and industrial importance. HAAs are also known to be present in grilled meats and tobacco smoke. Bio-activation of HAAs occurs via cytochrome P450-induced *N*-hydroxylation that leads to the formation of carcinogenic substituted HAs in both animals and humans[44]. HAAs can also be oxidized *in vivo* to substituted HAs by peroxidases and flavin monooxygenases. Equation 7 exemplifies a general biochemical pathway for the bio-activation of an HAA, via an *N*-hydroxylated intermediate, to an activated *N*-acetoxy ester (**7**) that is even more reactive than the HA intermediate with respect to covalent conjugation with DNA (see structure **13**, in Section II.D.1.d). This biological pathway probably underlies the etiology of several HAA-induced human cancers.

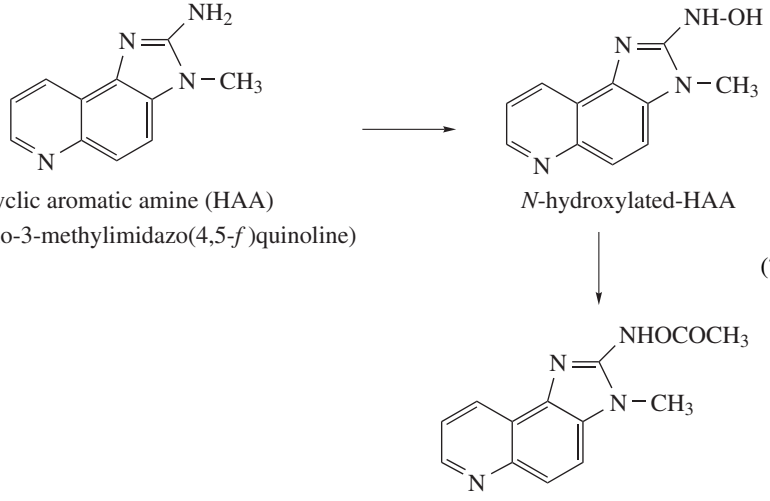

(7)

C. Possible Physiological Role of Naturally Occurring HA

The presence of HA reductase and oxygenase in multicellular organisms, together with the large body of indirect evidence for its occurrence as a metabolic intermediate in mammalian cells, and the identification of the arginine-to-NO pathway, suggest that HA may be involved to some extent in several physiological functions that are affected by NO, such as[45]: (a) control of relaxation of smooth muscle cells via the release of NO; (b) enhancement of NO activity as a neurotransmitter in the brain, presumably due to increased NO levels; (c) regulation of gastrointestinal and respiratory functions; (d) control of platelet aggregation; (e) cell respiration. The idea that HA is a putative intermediate in the arginine-to-NO pathway points to the possibility that, like acetylcholine, endogenous HA can induce vasodilation; however, unlike acetylcholine, its effect is independent of an endothelium-derived relaxing factor (i.e. NO), an observation that appears to be valid for many nitrovasodilators that are known to serve as NO donors[37,39]. It was suggested that HA generates NO exclusively intracellularly, probably due to the fact that it is a small neutral molecule that can rapidly penetrate the cell and be utilized by the intracellular metabolic machinery. By contrast, sodium nitroprusside ($Na_2[Fe(CN)_5NO]$), a charged inorganic NO donor, releases NO mainly in the extracellular space[46]. Tang and colleagues[25] showed that *in vitro* vasorelaxation activity of HA on vascular smooth muscle cells ($EC_{50} = 54\ \mu M$) is induced by NO in the presence of H_2O_2. Thus, HA is thought to manifest its physiological effects (e.g. hypotension) via production of free radicals that affect ATP-sensitive potassium currents and membrane polarization. Based on a recent *in vivo* study in rats, Vidrio and Medina[26] suggested that, in addition to the release of NO, the observed HA-induced hypotension could be attributed in part to its inhibition of the enzyme semicarbazide-sensitive amine oxidase (SSAO). SSAO is abundant in vascular smooth muscle, and is involved in the production of H_2O_2 that causes vasoconstriction. It can, therefore, be hypothesized that maintaining normal endogenous concentrations of HA and H_2O_2 might be important for safeguarding normal blood pressure. The lowest HA dose that elicited a threshold response in rat blood pressure was reported to be $25\ \mu g\,kg^{-1}\,min^{-1}$ over a 1-hour period of intravenous infusion[26]. This value is more than 100-fold lower than the reported LD_{50} for HA in rats[14a]. Thus, better understanding of the biochemical events that link HA with vasorelaxation of smooth muscles may offer new therapeutic approaches to the treatment of vascular diseases.

HA is an important intermediate in some reactions of the nitrogen cycle that occur in several bacteria, and appears to be associated with electron transport systems and with bacterial growth energetics. Thus, in the nitrification of NH_3 to nitrate, ammonia monooxygenase generates HA from NH_3, and the subsequent oxidation of HA to nitrite provides electrons that are required for the activity of the ammonia monooxygenase. For further details of the enzymatic reactions of the nitrogen cycle the reader is referred to the review of Ferguson[47]. The importance of the HA pathway in ammonia-oxidizing bacteria is not limited to understanding the energy-generating source for metabolism and growth. Ammonia-oxidizing bacteria have been demonstrated to release large amounts of the 'greenhouse' gas, nitrous oxide (N_2O), which can be produced, among other sources, by the autooxidation of HA or as a result of its enzymatic conversion to N_2O by several oxidoreductases[13]. Although N_2O accounts for only 5% of the greenhouse gases released into the atmosphere, understanding the parameters that regulate N_2O emission, including the formation and degradation of HA, may help in the development of strategies for decreasing global warming.

Bagchi and Kleiner[18] suggested that endogenous HA can undergo dismutation by the action of a cyanobacterial hydroxylamine dismutase, thereby providing a detoxification mechanism for excess hydrogen peroxide, as well as for an excess of HA itself. This

reaction (equation 8) is accompanied by release of ammonia and nitrite, both excreted as stable end products:

$$NH_2OH + H_2O_2 \xrightarrow{\text{hydroxylamine dismutase}} NH_4^+ + NO_2^- \quad (8)$$

Thus, in some cases HA may serve physiologically as a biological detoxifier.

Finally, HA derivatives may be utilized as potential precursors for the biosynthesis of naturally occurring oximes (**2**) and hydroxamates (**3**) (see Section III).

D. Biochemical and Physiological Characteristics

The abundance of HA derivatives in plants and living organisms, either as normal metabolic intermediates or as products of detoxification, together with their reported biological effects and toxicity[14a], suggest that this class of compounds is likely to interact with a wide spectrum of enzymes and receptors, as either substrates, inhibitors or activators. Table 1 summarizes data on the interaction of HA and its derivatives with enzymes.

1. Biochemical properties

In a review article published in 1985[14a], HA was cited as inhibiting a large variety of enzymes, both *in vivo* (e.g. monoamine oxidase, catalase, cytochrome oxidase) and *in vitro* (e.g. hepatic phosphatase, succinate oxidase, diamine oxidase, human cytochrome P450 and several transaminases). In long-term monitored reactions HA enhanced the activity of monoamine oxidase, and was also reported to activate guanyl cyclase. Table 1 lists studies reported during the last two decades on the enzyme-induced production/degradation of HA, and on additional enzymes that are affected by HA. These investigations, that include recent molecular biology approaches together with 3D structural analyses, provide new information that offers a better understanding of the mechanisms underlying the relevant enzymic transformations of HA and its derivatives.

a. Oxidation. Since HA is a toxic metabolite in eukaryotes[14a, 28, 44, 59], and an important intermediate in the generation of energy by prokaryotes that utilize ammonia as their source of energy[8, 47], it undergoes rapid oxidation by several enzymes that change the oxidation state of the nitrogen atom from -1 in HA to $+1$, $+2$, $+3$ or $+5$ in N_2O, NO, NO_2^- and NO_3^-, respectively. The end result of such oxidation is twofold: (a) Detoxification aimed at abolishing the N$-$OH function that can form adducts with DNA[28, 59] or may enhance oxidative stress by forming reactive oxygen species in eukaryotes[60]. (b) The second outcome is to serve as an intermediate in the oxidation of ammonia that is being utilized to provide energy for bacterial growth. However, in both prokaryotes and eukaryotes these oxidative transformations can also produce a variety of toxic reactive oxygen species (ROS).

In recent years a large number of multi-heme cytochromes have been reported that are capable of catalyzing the oxidation of HA to NO_2^- (equation 2). The gene encoding hydroxylamine oxidoreductase (HAO) from *Nitrosomonas europea* has been characterized[61], and its 3D structure and mechanism of action have been reviewed by several authors[8, 9, 33, 47, 62]. HAO is believed to be responsible for the greater part of ammonia oxidation in the biosphere[9], and its isolation from *Nitrosomonas europea* provided a valuable protein model for the oxidation of HA. It is a 63–67 kDa protein containing seven *c*-type heme groups and a heme P460 moiety. The latter is thought to be responsible

TABLE 1. Interaction of hydroxylamine (NH_2OH, HA) and its derivativegs (R^1R^2N-OH) with enzymes

Enzyme	Substrates/Inhibitors/Products	References
Semicarbazide-sensitive amine oxidase (SSAO) (*rat*)	SSAO can generate vasoactive H_2O_2. HA (1 mM) inhibits staining of SSAO in rat aorta, and is thought to antagonize H_2O_2-induced vasoconstriction	26, 48
Hydroxylamine oxidoreductase (HAO) (*bacteria*)	*c*-type cytochrome heme-containing enzyme. Oxidizes HA to nitrite (NO_2^-)	8, 33, 47
Cytochrome *c* nitrite reductase (*bacteria*)	Reduces HA and NH_2OCH_3 to ammonia (NH_3)	10, 23
Hydroxylamine reductase of hybrid cluster protein (*bacteria*)	Reduces HA to ammonia with K_m values of 38.9 mM (pH 7.5) and 2.5 mM (pH 9.0). Maximal V_{max} value (pH 9.0): HA reduced at 458 units mg^{-1} protein	49
Cytochrome b_5/NADH cytochrome b_5 reductase (*human*)	Reductive detoxification of substituted hydroxylamine carcinogens ($K_m = 200–400$ μM)	27–29, 50
Ornithine decarboxylase (ODC, *human)*	NH_2O-R (R = 3-aminopropyl) inhibits ODC with $IC_{50} = 0.1$ mM (at 60 min, 37 °C)	51
Hydroxylamine dismutase *(cyanobacterium)*	Conversion of HA by H_2O_2 to NH_3 and nitrite	17, 18
S-adenosylmethionine decarboxylase (SAMDC, *human*)	Substituted HA inhibits SAMDC with $IC_{50} = 0.1$ mM (at 60 min, 37 °C)	51
Amidase (*bacteria*)	HA at 10–30 mM is an activator of amidase-induced hydrolysis of acetamide (enhancing k_{cat})	52, 53
Glyceraldehyde-3-phosphate dehydrogenase (*bacteria*)	HA inhibits ($K_I = 4.7$ mM) the oxidation of glyceraldehyde-3-phosphate to 3-phosphoglycerate	54
Glutathione-*S*-transferase (GST, *human*)	HA and NH_2O-Et inhibit GST in the mM range. Inhibition is linked to lipid peroxidation and to formation of active oxygen radicals	55
NADPH methemoglobin reductase (*human*)	HA and NH_2O-Et inhibit enzyme activity in mM range	55
Glucose-6-phosphate dehydrogenase (G6PDH) (*human*)	Inhibited by *O*,*N*-dimethyl-HA, but not by HA	55
Cytochrome P450 (*human*)	Bioactivation of arylamines via *N*-hydroxylation	44
Catalase (*fungal*)	HA inhibits decomposition of H_2O_2 with IC_{50} values ranging from 25 to 260 nM	56

TABLE 1. (*continued*)

Enzyme	Substrates/Inhibitors/Products	References
Urease (*jack bean*)	Hypothesized to convert hydroxyurea to HA	57
Acid glucan-1,4-α-glucosidase (*mouse*)	Inhibition of enzyme activity by 0.3 mM HA with parallel inhibition of glucose-stimulated insulin release	58

for the catalytic activity of the enzyme, whereas the other 7 *c*-type heme groups transfer the electrons generated from the active center to cytochrome c_{554}, which serves as the physiological acceptor. Tetra-heme cytochrome c_{554} from *Nitrosomonas europea* was also demonstrated to possess NO reductase activity, and it was suggested that the *N*-oxide that is formed as an intermediate in the HAO-induced oxidation of HA is bound to cytochrome c_{554}, permitting the latter to regulate the concentration of free NO in *Nitrosomonas*[12].

Cytochrome P460 is the only heme known to withdraw electrons from an iron-bound ligand[63]. The crystal structure of HAO revealed that the enzyme is organized as a trimer, with a unique arrangement of the 3×8 heme groups, and the active-site heme, like many other *c*-type hemes, is attached to the protein via a CXXCH binding motif. The conversion of HA to nitrite (equation 2) by HAO is accompanied by release of two electrons that reduce the enzyme, ammonium monooxygenase (AMO), which converts NH_3 to HA, together with two electrons that are transferred to the respiratory chain of the bacterium via a sequence of heme groups within the three different subunits of HAO. More recently, a solution of the crystal structure of *Nitrosomonas europea* cytochrome P460, which is analogous in its spectral properties to the P460 of HAO, permitted the clarification of subtle structural features that are characteristic of HAO, and explain its functional profile[63].

$$2NH_2OH + 4Fe^{3+} \longrightarrow N_2O + H_2O + 4H^+ + 4Fe^{2+} \quad (9)$$

The oxidation of HA to N_2O by Fe^{3+} (equation 9) is a well-established chemical reaction that is used for the quantitative determination of HA in pharmaceutical preparations[64]. The only enzyme-bound intermediate, HNO, that is produced during the HAO-induced oxidation of HA to nitrite must be rapidly oxidized to avoid the potential side-reaction of heme-containing metal centers, viz. formation of N_2O in accordance with equation 9, which will initiate denitrification rather than nitrifying to NO_2^-. The latter step is necessary for completion of the nitrification of NH_3. This is achieved by the unique structure of the HAO protein that permits electron transfer between the P460 and other heme moieties of the enzyme[33]. The crystallographic analysis of a fungal peroxidase complex with HA provided evidence that HA interacts directly with the heme via coordination of the nitrogen atom to the heme iron[65,66]. The binding mode of HA was suggested by the authors to simulate the binding of the natural substrate H_2O_2 to peroxidase, which is consistent with the observation that HA is a competitive inhibitor of hydrogen peroxide[65].

Myoglobin (Mb) and hemoglobin are both O_2-binding proteins that contain iron porphyrins, and have been reported to be involved in the oxidation of HA. The *in vitro* oxidation of HA by H_2O_2 and Mb demonstrated a possible pathway for NO generation; it is not, however, clear whether such a route exists, which can account for NO formation in mammal tissues[24]. In this context, it is of interest to point out that in cyanobacterium that produces H_2O_2, the latter is consumed both by enzymic formation of HA from glutamine and by oxidation of HA[19]. These biological pathways could be involved in detoxification of either HA or H_2O_2, in addition to the commonly accepted enzymic degradation of

H_2O_2 by catalase. Kulys and colleagues[56] provided kinetic evidence for the inhibition of fungal catalase by concentrations of HA as low as 25 nM. HA was postulated (like other catalase inhibitors) to introduce biphasic behavior that slows the decomposition of H_2O_2 by forming a NO-ferrocatalase intermediate in the presence of H_2O_2. The importance of these findings is in the understanding of the mechanism of catalase inhibition.

In an attempt to understand the production of iron nitrosyl hemoglobin (HbNO) from hydroxyurea ($NH_2C(O)NH-OH$, HU), which is employed in the therapy of sickle cell disease, and taking into consideration the fact that HA reacts with a variety of heme proteins to produce NO[67], Lockamy and colleagues studied the reaction of HA with oxy-, deoxy- and methemoglobin[68]. Using electron paramagnetic resonance, they demonstrated the production of HbNO via the oxidation of HA by the various oxygenated states of hemoglobin, and substantiated their previous contention[57] concerning the potential involvement of HA in the *in vivo* biological action of hydroxyurea by the use of urease to enhance the conversion of HU to HA. The hematological toxicity of HA was reviewed extensively by Gross[14a] in 1985, and briefly by Evelo and colleagues[55]. Two mechanisms were offered by Evelo and colleagues for the hematoxic effects, such as induction of hemolytic anemia, of HA and HA derivatives: (a) production of methemoglobin accompanied by production of ROS, that initiate lipid oxidation, mostly by HA and its *O*-alkylated derivatives; (b) inhibition of glucose-6-phosphate dehydrogenase and gluthatione reductase by *N*-alkylated HA. Both these enzymes are required for protection from oxidative stress.

b. HAs and reactive oxygen species (ROS). Radical and nonradical ROS in living organisms are being investigated extensively with respect to their physiological and pathological roles. The reaction of HAs with ROS to convert the diamagnetic HAs to their paramagnetic nitroxide derivatives that can be detected by electron spin resonance spectroscopy was proposed, as exemplified in equation 10, for superoxide and peroxynitrite[69].

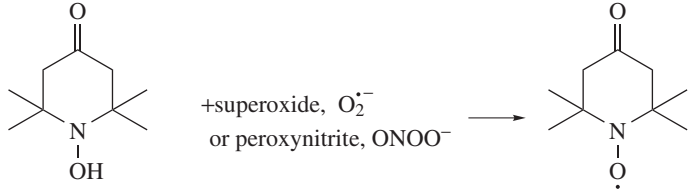

(10)

HA derivative, Tempon-H nitroxide Tempon

The occurrence of the same biological reaction prototype was demonstrated by Taira and colleagues[24], who provided experimental evidence for the formation of hydronitroxide radical ($H_2NO^{\bullet}$) from HA in the presence of Mb and H_2O_2. The conversion of HA to $H_2NO^{\bullet}$ is induced by the ferryl-Mb species ($^{\bullet}MbFe^{+4}=O$), a radical generated by the interaction of H_2O_2 with Mb. This pathway of nitroxide radical formation was also demonstrated for substituted HAs such as the *N*-methyl and *N*,*N*-dimethyl analogs, though only HA resulted in the release of NO (and consequently the $^{\bullet}MbFe^{+4}=O$ species was reduced to $MbFe^{2+}$). Thus, the nitroxide-type ROS radicals can react with a variety of biological substrates. The same hydronitroxide radical was shown to be generated as an intermediate in the conversion of hemoglobin to methemoglobin following the reaction of HA with intact erythrocytes or with oxyhemoglobin[70]. The formation of ROS from HA can initiate lipid peroxidation that can give rise to general protein damage.

c. Reduction. HA can undergo both chemical and biological reduction, with the oxidation state of the N atom being reduced from -1 to -3, resulting in formation of ammonia.

Blom was the first to demonstrate, in 1928, the formation of HA by an unknown mixture of bacteria which utilized nitrate as their sole nitrogen source to produce ammonia[1], an observation substantiated by Lindsey and Rhines who generalized this reaction to a diverse set of microorganisms capable of producing NH_3 by reduction of both nitrites and nitrates[3]. The mechanism of the 6-electron reduction of nitrite to ammonia (i.e. conversion of the $[N^{(+3)}O_2]^-$ species to $N^{(-3)}H_3$) by bacterial cytochrome *c* nitrite reductase (ccNiR, a multiheme *c* enzyme) was proposed by Einsle and colleagues[10], who employed crystallographic monitoring of intermediates along the reduction pathway. The authors could not detect the release of HA; however, they demonstrated that ccNiR could reduce HA to ammonia with a specific activity of only half of that for nitrite as substrate, and suggested its formation as depicted in equation 11.

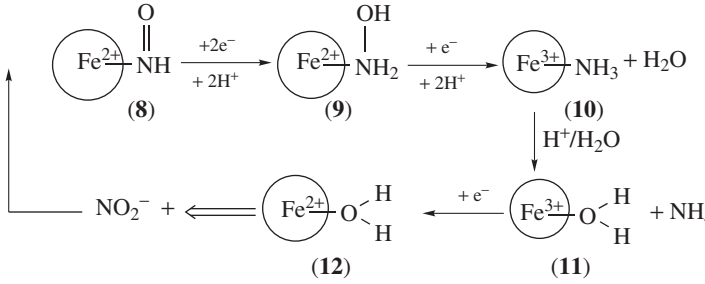

(11)

The proposed reaction scheme suggests that following the binding of nitrite, it is reduced by two one-electron reduction steps (not shown), and that protonation then produces intermediate **8**, which is further reduced by 2 electrons to HA that remains bound via the nitrogen to the heme iron, **9**. Subsequent reduction of **9** yields an ammonia complex (**10**) from which the ammonia dissociates as the ammonium ion, leaving behind the oxidized (and hydrated) form of ccNiR, **11**. The reduced form of the enzyme, **12**, is then again ready to bind nitrite, and thus to renew the enzymic cycle. Similarly, Wolfe and colleagues[49] demonstrated the ability of hybrid cluster protein (HCP) purified from *Escherichia coli* to reduce HA to ammonia and water. HCP also reduces CH_3NHOH. Thus, it seems that the heme center metal is capable of conjugating HA(s) to form the Michaelis–Menten complex and to reduce the HA nitrogen atom by electron transfer.

In humans, a variety of HA derivatives that are obtained by bioactivation of arylamine drugs (i.e. *N*-hydroxylation) or of pro-drugs that contain the NH−OH function, and whose activation requires the reduction of the hydroxylamine nitrogen atom, have been shown to undergo enzymatic reduction by the cytochrome *b*5/NADH cytochrome *b*5 reductase system[27].

In view of the importance of microsomal reduction of drugs and xenobiotic HAs, in both a pharmacological context and with respect to detoxification, Kurian and colleagues[29] recently reported the results that they obtained in a screen aimed at the discovery of genetic variants of human cytochrome *b*5 displaying differences in their capacity to reduce the HN−OH function. One naturally occurring variant that they isolated (T60A) showed *ca* 2-fold reduction in substrate affinity for HAs relative to wild-type cyt *b*5; V_{max} was less affected. However, a substantial decrease was observed in the levels of expression of the variant. This important finding provides a new approach to understanding how genetic variations can influence a major route for xenobiotic detoxification of the HA family in humans.

d. Conjugations with DNA. HA induces a variety of chromosomal abnormalities; its mutagenicity and possible carcinogenicity were reviewed extensively in 1985 by Gross[14a].

HA was found to be mutagenic in bacteria, and it was reported that plant chromosomes break in the presence of HA, but it was found to be noncarcinogenic to mice. However, Gross did cite some *N*-hydroxy compounds (i.e. HA derivatives) as carcinogens[14a]. The mechanism of mutagenesis of HA was found to involve primarily interaction with the pyrimidine bases of the cytidine–guanosine pairs.

The carcinogenicity of HA derivatives was reviewed recently by Kim and Guengerich[44], who summarized the properties and toxicity of heterocyclic arylamines, including their bioactivation by cytochrome P450 to the corresponding *N*-hydroxylamine derivatives, and their subsequent activation to produce guanine adducts that are capable of initiating mutagenic and carcinogenic events[71]. An example of such an adduct is the conjugate of guanosine with a heterocyclic amine, **13**, formed subsequent to activation of the amine as shown in equation 7.

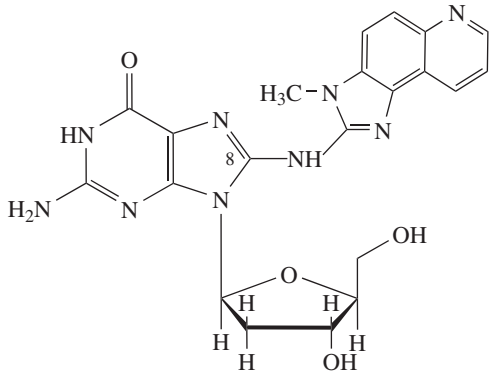

(**13**) *N*-(deoxyguanosin-8-yl) adduct with 2-amino-3-methylimidazo(4,5-*f*)quinoline

2. Physiological characteristics

In his 1985 review, Gross summarized the toxic effects of HA at doses well above the concentrations that are assumed to be produced *in vivo* as a result of normal metabolic processes. LD_{50} values for rodents range from 30 to 200 mg kg^{-1} [14a]. Briefly, HA affects the status of hemoglobin, causes anemia, relaxes nonvascular smooth muscles, activates guanyl cyclase in brain tissues, and has been reported both to trigger convulsant behavior and to serve as an anticonvulsant. It is also reported to elevate GABA levels in the brain, and to cause chromosomal abnormalities at doses approaching the LD_{50} in mice, viz. 50 mg kg^{-1}. It has also been reported to be a skin irritant, and to serve as a potent mutagenic drug *in vitro* (but not *in vivo*)[14a]. During the last two decades, several investigations have highlighted physiological pathways that are affected directly by HA, and have provided an explanation at the molecular level for the responses observed.

a. Blood, erythrocytes and hemoglobin. The antithrombotic activity of HA *in vitro* is considered relatively low ($IC_{50} = 62.5$ μM); but in the presence of H_2O_2, the IC_{50} is decreased to 2.5 μM, an observation that led to the conclusion that NO production is increased by enhanced oxidation of HA in the presence of the peroxide[72]. The effect of HA and of its derivatives was studied in human blood cells *in vitro*, and shown to produce a high percentage of methemoglobin, accompanied by hemolysis and by production of Heinz bodies (cellular inclusions within an erythrocyte that consist of damaged

and aggregated hemoglobin)[55]. The no-effect hematological level of HA in rats was set at 10 ppm. The formation of methemoglobin by HA and its *O*-ethyl and *N*,*N*-dimethyl derivatives involves generation of ROS[20,55,70] that can cause oxidation of thiol groups, release of iron, membranal damage and hemolysis. Indeed, upon addition of HA either to erythrocytes or to an oxyhemoglobin, ESR measurements revealed the transient formation of the $NH_2O^{\bullet}$ radical in accordance with equation 12:

$$NH_2OH + HbO_2 \longrightarrow NH_2O^{\bullet} + [MetHb(III) - O - O - H] \qquad (12)$$

The formation of nitrosyl hemoglobin (HbNO) by direct reaction with HA, or indirectly with hydroxyurea that produces HA, was also demonstrated concomitantly with the formation of methemoglobin[57,68].

An interesting cycle was proposed for the antileprotic-anti-inflammatory drug, dapsone (**14**) which undergoes *N*-hydroxylation by hepatic enzymes to yield hematotoxic dapsone-HA that generates methemoglobin. It turns out that the methemoglobin formed within the erythrocytes regenerates the parent drug, dapsone, from dapsone-HA, thereby recycling the drug for a fresh round of conversion of hemoglobin to methemoglobin[73]. The overall effect anticipated is an increase in the half-life of dapsone *in vivo*. More recently, Clement and colleagues established the enzymic *N*-hydroxylation of dapsone by cytochrome P450, and the *N*-reduction by the cytochrome *b*5/NADH–cytochrome *b*5 reductase system, to regenerate the parent dapsone[50]. These biotransformations of the oxidation state of the *N* atom of dapsone are depicted in equation 13.

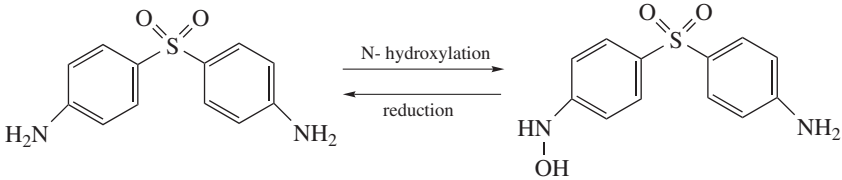

(13)

dapsone (**14**) dapsone hydroxylamine

Finally, it should be mentioned that HA is effective as an antidote against cyanide poisoning by virtue of converting *ca* 20% of the hemoglobin to methemoglobin. This will be discussed at length in Section II.F.

b. Vascular relaxation and blood pressure. HA has been shown by many investigators to cause vasodilation both *in vitro* and *in vivo*, due to relaxation of smooth vascular muscles, a physiological response that is accompanied by hypotension[26,37,74]. This activity is generally attributed to generation of NO rather than to direct action of HA itself[38,42,46]. NO generation from HA was demonstrated in the presence of superoxide ion and also suggested to be induced by NO synthase[75]. As mentioned earlier (see equation 4) HA is a possible intermediate in the conversion of arginine to NO, via its catalase/H_2O_2 oxidation[38]. The NO so generated activates guanylate cyclase, thereby increasing intracellular levels of cyclic GMP, which has been postulated to promote contraction of smooth muscles[76]. The *in vivo* blockade of HA-induced hypotension by methylene blue supports the involvement of guanylate cyclase activation in the observed hypotension[26].

Tang and colleagues proposed that HA increases ATP-sensitive K^+ channel currents, which may underlie the observed HA vasorelaxation, and suggested that enhanced production of free radicals is involved in this physiological response[25]. These results are consistent with the observations of Huang, who suggested that HA-induced relaxation of

rat aortic rings could be inhibited by K^+ channel blockers[77]. It is, however, not unlikely that generation of NO is responsible for these observations.

The linkage HA-NO-blood pressure was also demonstrated in rats that had been administered HA intracerebroventricularly into a particular forebrain area, in doses ranging from 0.01 to 0.5 mg[78,79]. A dose-dependent increase in NO release and a concomitant decrease in arterial blood pressure promoted the understanding of the role of NO in central regulation of blood pressure, and further substantiated the contention that endogenous HA may serve as a source of NO. The intracranial administration of HA into rats was also used to demonstrate the existence of an NO-dopamine pathway that is likely to be involved in control of blood pressure[9].

c. Suppression of insulin secretion. Mosen and colleagues[58] showed that 0.3 mM HA inhibited lysosomal acid glucan-1,4-α-glucosidase activity in isolated mice pancreatic islets, presumably via intracellular donation of NO. The physiological consequence of this inhibition was suppression of glucose-stimulated insulin release from isolated pancreatic islets.

d. The hypothesis of 'percussion chemistry', muscle function and HA. In 2002, Robertson presented a hypothesis that explained initiation of muscle contraction on the basis of 'percussion chemical reactions' that occur very rapidly[80]. According to the author, these percussion reactions produce temporary intracellular precipitates which produce changes in cell volume that trigger muscle contraction. Resolubilization of these precipitates initiates the next cycle of contraction. It was suggested that HA, which is produced in all cells, can act, depending on the pH, as either an oxidizing and reducing agent, and is a key component in the percussion chemistry' that drives muscle activity[80]. However, rigorous experimental data will be needed to support the hypothesis and especially the involvement of HA in such activities as walking and arm movement.

E. Toxicity

The diverse chemical reactivity of HAs makes them potential toxic compounds, either directly, by chemical modification of functional groups of a variety of biological systems, or indirectly, by their conversion to toxic metabolites. In some cases their metabolites are considered to be toxic in humans, animals and plants even at relatively modest levels of exposure.

The toxicity of unsubstituted HA, following exposure of experimental animals to acute or long-term administration of $NH_2OH.HCl$, was reviewed in 1985, and the median lethal dose (LD_{50}) in mice, rats, guinea pigs and dogs was tabulated for various routes of administration[14a]. The LD_{50} values range from *ca* 30 mg kg^{-1} for intraperitoneal injection to *ca* 200 mg kg^{-1} for per-os administration. The major and immediate toxic signs of large doses of HA in rodents are hematological effects, such as anaemia and methemoglobinemia, accompanied by a 55–73% reduction in the RBC count, and a significant elevation of white blood cells in the circulation. Chronic exposure of rats (90 days) to 250 ppm HA caused hematological damage and increased spleen weight, whereas 10–50 ppm were defined as a no-effect level (for additional references see Evelo and colleagues[55a]).

Gross cited a single article concerning HA intoxication in humans, in which a woman accidentally consumed the chemical per os (dose unknown)[14a]. The case report described development of hemolytic anemia, accompanied by leukocytosis and enhanced sedimentation rate. The patient recovered after 5 weeks, and no abnormalities were found

with respect to platelet count, bleeding or coagulation time. The development of severe hemolytic anemia (lowered hemoglobin and increase in serum iron) among laboratory employees who were exposed to *O*-methyl, *N*,*O*-dimethyl, *N*,*N*-dimethyl and trimethyl HA suggested possible mechanisms for development of hematotoxicity in humans due to exposure to *O*-alkylated and *N*-alkylated HA derivatives[55a,b]. Other reports concerning humans affected by HA described the irritation and inflammatory reactions following skin contact with HA[14a].

A large volume of evidence suggests that the mutagenic activity of HA is largely mediated via reaction with cytosine–guanosine pairs of DNA[14a]. Uracil that replaces thymine in RNA also reacts with HA, however to a minor extent, with concomitant ring opening; thus, in the latter case HA is an inactivating agent rather than mutagenic[14a]. In 1985 it was stated by Gross that mutagenic activity of HA occurs only *in vitro*, and apparently no convincing evidence was provided until 1985 to demonstrate its *in vivo* potency as a genotoxic chemical in experimental animals[14a]. Chromosomal aberrations induced by HA and by some of its derivatives were demonstrated in mouse embryo and hamster cell cultures, an observation that was attributed to direct interaction of HA and DNA[14b,c]. HA can affect viruses, bacteria, fungi and phages, and is also toxic to aquatic life, presumably due to its mutagenicity[14a,d]. However, intracellular accumulation of HA in ammonia-oxidizing bacteria, such as *Nitrosomonas europea*, was reported to reach *ca* 0.8 M without any apparent effect on viability[11]. In contrast with 'naked' HA, substituted HAs, such as the biological *N*-hydroxylation products of heterocyclic amines (see equations 7 and 13, and Section II.D.1.d), were found to be cytotoxic in human mammary epithelial cells incubated for 2 h with 1 μM *N*-hydroxylated amine[59]. This suggests that the products of *in vivo* *N*-hydroxylation of heterocyclic amines present in various food products, but not the parent amine compounds themselves, may initiate carcinogenic responses in humans[28,59,81a,b]. Stiborova and colleagues[81b] suggested a genotoxic mechanism for the carcinogenicity of *o*-anisidine in rodents following its *in vivo* conversion to an HA derivative by enzymic *N*-hydroxylation of *o*-anisidine, and proposed a similar mechanism for its potential carcinogenicity in humans. The *N*-hydroxylated metabolite of the antiprostate cancer drug, flutamide, exhibits strong inhibition of the growth of primary cultures of rat hepatocytes[82], suggesting that *N*-hydroxylated heterocyclic and aromatic amines may be hepatoxic in addition to being potential carcinogens. Another mechanism suggested for toxicity of *N*-hydroxylated heterocyclic amines is the generation of ROS such as $ONOO^-$, $O_2^{\bullet -}$, H_2O_2 and $OH^{\bullet}$, that may produce severe oxidative stress[60].

F. Current and Potential Medical Applications

1. Treatment of cyanide poisoning

Intoxication by cyanide (either as inhaled HCN or due to per-os intake of cyanide salts) is manifested as a rapid blockade of oxygen transfer to tissues due to formation of a strong complex between mitochondrial cytochrome oxidase iron atoms and the CN^- anion[83]. Since HA causes methemoglobinemia, and taking into account the fact that CN^- has a higher affinity for methemoglobin than for cytochrome oxidase, several attempts have been made to counteract cyanide intoxication by administration of methemoglobin promoters such as sodium nitrite, *p*-dimethylaminophenol (DMAP) and HA[83]. Injectible preparations of HA were patented in 1981, and claimed to be a suitable antidote for treatment both of animals (veterinary use) and of humans (e.g. suicide and homicide attempts, and accidental intoxication during use) poisoned by cyanide, using 5–10 mg kg^{-1} of HA per body weight[84]. Over the past three decades, combinations of sodium nitrite and DMAP, or of sodium nitrite and HA, followed by sodium thiosulfate to detoxify circulating CN^-,

or to pull it off the cyanomethemoglobin complex by conversion of the free CN^- to the thiocyanate anion, SCN^-, were repeatedly demonstrated to confer good protection against cyanide poisoning[83,85,86]. Thus, via rapid production of sufficient amounts of a relatively long-lived sufficient endogenous scavenger (by conversion of *ca* 20% of the hemoglobin to methemoglobin), HA appears to provide a reasonable pre- and post-treatment therapeutic approach to medically counteract cyanide intoxication in humans. Sarnoff suggested that, in addition to its role in the induction of formation of methemoglobin, HA may also act as a respiratory stimulant in cyanide poisoning, but offered no mechanism to explain how this might occur[84]. Since HA was demonstrated to bind directly to the iron atom of a peroxidase, as does cyanide[65,66], it may compete out cyanide from cytochrome oxidase, and thus contribute to its overall antidotal activity.

2. *N*-hydroxyurea and therapy of sickle cell disease

N-hydroxyurea (HU; $H_2NC(O)NH-OH$) is a derivative of HA that was found to be an effective anticancer and antipsoriasis drug whose biological activity is attributed to the N−OH function attached directly to the carbon atom of a carbonyl group. HU has also been tested in recent years as a novel treatment for sickle cell anaemia[22], which is caused by a mutation in the hemoglobin gene that produces sickle cell hemoglobin that tends to polymerize, and thus to cause damage to the red blood cells that is accompanied by severe painful crises. Treatment with HU has been shown to reduce the number of these painful crises, and to decrease mortality[57,68]. Patients treated with HU showed an increase in levels of nitrosyl hemoglobin (HbNO) and of other NO derivatives, which could be correlated with the improvement in their clinical condition[57,68,87]. Lockamy and colleagues provided evidence that formation of NO derivatives *in vivo* stems in part from the metabolic conversion of HU to HA, and that the reaction of the latter with hemoglobin produces HbNO[68]. The authors proposed a mechanism involving pharmacologically induced regeneration of fetal hemoglobin, which has higher affinity for oxygen than adult hemoglobin, and that regeneration is triggered by HU, presumably via production of NO derivatives. It is thought that the presence of fetal hemoglobin reduces the polymerization of the mutant hemoglobin in sickle cell anemia patients. For further discussion of the biological properties of HU the reader is referred to the review of Wang and colleagues[22].

3. HA derivatives as antiplatelet and antithrombotic drugs

NO donors have been demonstrated to be potential drugs for the treatment of cardiovascular and related diseases, and some have been reported to prevent myocardial ischemia, to possess antiplatelet activity and to affect blood pressure[22]. HA was demonstrated to inhibit aggregation of blood platelets *in vitro*[88]. Since HA is an NO donor, a group of pro-drugs with the structure $R^1R^2NOR^3$ were generated, where the substituents R^1, R^2 and R^3 alternate between ethoxycarbonyl (C(O)OEt), phenyl, phenylsulfonyl, ($PhSO_2$) and H. The rationale behind their synthesis was both to reduce HA toxicity and to decrease its hydrophilicity, so as to allow improved absorption from the gastrointestinal tract[72]. The monoethoxycarbonyl derivative, [EtO(O)C]NH-OH, and the homologous derivative of phenylhydroxylamine, [EtO(O)C]N(Ph)OH, inhibited thrombus formation in rats about 4- and 6-fold better, respectively, than HA itself. However, no influence on blood pressure was recorded for either of the two derivatives, presumably due to the inability of the blood vessel endothelium to convert the pro-drugs to the corresponding HA. The authors concluded that this series of HA derivatives offers a clear separation between

antithrombotic and antihypertensive effects, which is important for the treatment and prevention of thrombosis in cases in which lowering of the blood pressure is undesirable. Thus, HA pro-drugs may find useful medical application in cardiovascular diseases, with a specific activity being targeted to tissues that are capable of hydrolyzing the pro-drug.

4. Bioscavengers of ROS

ROS, such as the radicals $O_2^{\bullet -}$ and $^{\bullet}OH$, and nonparamagnetic species, such as H_2O_2, are known to cause tissue damage, and have been implicated in several pathogeneses resulting from oxidative stress. One of the problems in applying antioxidants to reduce ROS levels is their inability to cross the cell membrane, and thus to quench the ROS intracellularly. Consequently, more effective ROS scavengers are being sought. Several HAs were demonstrated to be able to scavenge ROS due to the unique chemistry of the N-OH group. For example, scavenging of various lipid radicals by the HA derivative, OXANOH (see below), prevented microsomal lipid peroxidation[89]. Similarly, the cyclic HA derivative, TPL-H, protected cultured cardiomyocytes against oxidative damage induced by $O_2^{\bullet -}$ and by H_2O_2[90]. In both cases, it was suggested that donation of the HA hydrogen atom, N-OH, to a lipid radical or to a lipid peroxide, with concomitant formation of a cyclic nitroxide radical, $R^1R^2N{-}O^{\bullet}$, quenches the oxidative chain reaction. A clear advantage of such antioxidant drugs is the ability of both OXANOH and TPL-H to continuously regenerate themselves to the active form of the cyclic N-OH function. This implies that HA derivatives can prevent oxidative stress damage by a catalytic mode of action as opposed to other scavengers that are stoichiometric.

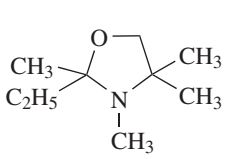

OXANOH

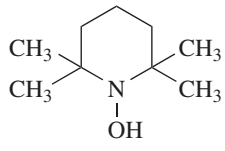

TPL-H

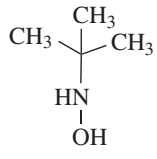

N*t*BHA

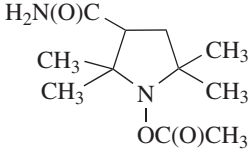

ACP

N-*t*-butyl hydroxylamine (N*t*BHA) was demonstrated to protect both cultured cells and mice from ionizing radiation damage that is attributed to production of ROS[91], and to retard the process of aging (i.e. senescence) of normal human lung fibroblasts, probably due to its antioxidant effect on mitochondria[92]. N*t*BHA was also demonstrated to be capable of protecting U937 cells from heat-shock-induced apoptosis, presumably via scavenging of ROS[93]. However, it is not clear whether, like OXANOH and TPL-H, N*t*BHA acts as a catalytic scavenger of ROS.

The potential of HAs as ROS scavengers is further highlighted by the use of an acyl-protected hydroxylamine function, ACP, that was developed as a spin-radical reagent to probe intracellular oxidative stress. ACP does not react with ROS outside the cells; however, once it penetrates into the cell, the protecting acyl group is removed by esterase action, thus exposing the pyrrolidine N-OH function, which reacts with ROS, and is converted into a stable nitroxide radical that can be detected by electron paramagnetic resonance measurements. This technique allowed the detection and quantification of ROS in an experimental rat model of human nephrosis[94]. The successful use of ACP suggests that a pro-drug approach for converting a variety of HA derivatives to useful antioxidants should be further explored.

5. Inhibition of cancer cell proliferation by O-ether derivatives of HA

Aminooxy compounds can be viewed as *O*-ethers of HA and are discussed here in terms of their potential anticancer activity. Thus, 1-aminooxy-3-aminopropane (APA) is a potent reversible inhibitor of mammalian ornithine decarboxylase (ODC) and of *S*-adenosylmethionine decarboxylase (SAMDC)[95], and *S*-(5′-deoxy-5′-adenosyl)methylsulfonium *O*-ethylhydroxylamine (AMA) was reported to be an efficient reversible inhibitor of the latter enzyme[96].

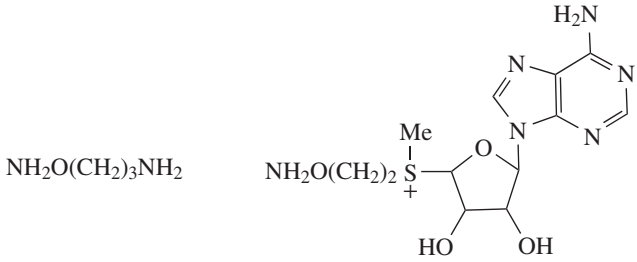

APA AMA

Both ODC and SAMDC are involved in regulating the level of intracellular polyamines (i.e. putrescine, spermidine and spermine), and are present in high concentrations in neoplastic cells. It was suggested that because of the involvement of polyamines in rapid cell proliferation, their depletion by means of simultaneous inhibition of ODC and SAMDC by nontoxic ligands could impair the growth of cancer cells. Milovic and colleagues demonstrated, using colon cancer cell lines, that the combined application of APA, AMA and 5-fluorouracil prevented cell proliferation and highlighted their potential therapeutic value in treatment of colorectal cancer[97]. It should be pointed out that the HA function is not being utilized here in its classical role as a source of an oxidation–reduction moiety, but rather as a complementary structural residue attached to the corresponding substrates of ODC and SAMDC, which converts them to inhibitors that compete out the natural substrates of the two enzymes. Aminooxy derivatives of polyamines are promising, relatively nontoxic anticancer drugs.

III. OXIMES

A. Natural Occurrence and Possible Physiological Role

The abundance of diverse oximes as naturally occurring products is attributed, in general, to complicated metabolic processes that include enzyme-induced oxidation of either amino acids or biogenic amines, as well as to the relatively low reactivity of oximes compared to HA. The co-occurrence of HA and a variety of carbonyl-containing molecules in plants and animals may also contribute to the formation of the oxime bond in nature.

Mahadevan reviewed research up to 1973, with respect to the pathways of oxime metabolism in plants, and evaluated a series of aliphatic and aromatic oximes that are precursors for the biosynthesis of plant secondary metabolites (as opposed to basic metabolism products that are essential for cell survival), such as cyanogenic glycosides, glucosinolates and certain phytohormones[98]. Some of these oximes are shown below.

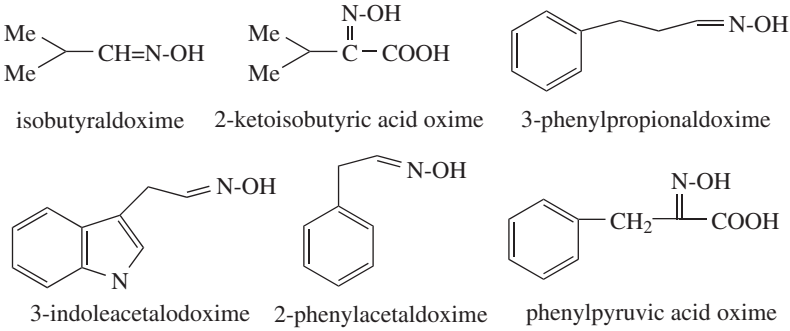

isobutyraldoxime 2-ketoisobutyric acid oxime 3-phenylpropionaldoxime

3-indoleacetalodoxime 2-phenylacetaldoxime phenylpyruvic acid oxime

A relatively large body of scientific data on the structure and biosynthesis of cyanogenic glycosides and glucosinolates, as well as concerning the presence and importance of various acetaldoximes as intermediates in the production of other secondary metabolites (e.g. indole-3-acetic acid), has been published in the last 18 years[99–106]. The oxime function is retained in the end products of glucosinolates (**15**) as a thioester bond, while in cyanogenic glycosides the aldoxime moiety is ultimately dehydrated to form nitriles such as **16**.

Both **15** and **16** are involved in plant defense, they may have a role in the flavor spectrum, and their concentration can influence the nutritional safety and quality of food crops. For example, Soledade and colleagues[99] demonstrated the crucial role of indole-3-aldoxime in the biogenesis of cruciferous defense against fungi-induced plant diseases. This is achieved by inserting the indolyl moiety via indole-3-aldoxime, which is a precursor of several secondary chemical defense metabolites of cruciferae.

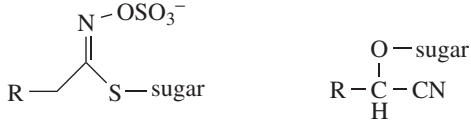

glucosinolates (**15**) cyanogenic glycosides (**16**)

Many secondary metabolites that contain the oxime bond have been isolated from marine sponges, such as **17**, a histamine H_3 receptor antagonist[107], and from actinomyces, such as **18**, an antibiotic[108]. These structures became targets for the synthesis of compounds with a variety of biological activities such as potent histamine H_3 receptor antagonists[109]. Both **17** and **18** originate from tyrosine, which undergoes both ring and *N*-oxidation and subsequent reactions, to produce the multiring structures. Bromotyrosine-derived metabolites (purpuramines) that contain a phenylpyruvic amide oxime building block (as in **17**), and phenylpyruvic acid oxime itself, were also isolated from marine sponges[107,110].

The discovery of a *Bacillus* sp. strain capable of degrading aldoximes via their conversion to nitriles prompted the isolation and purification of an enzyme capable of producing the *syn* geometrical isomer of phenylacetaldoxime from *N*-hydroxy-L-phenylalanine, suggesting that amino acid-derived aldoximes are biosynthesized and metabolized in microorganisms like in plants[111].

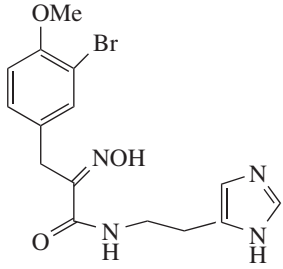

Verongamine (**17**)

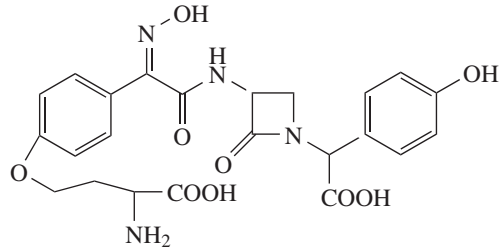

Nocardicin A (**18**)

Oximes were identified in the sternal gland of male koalas. Thus, a mixture of *syn* and *anti* phenylacetaldoxime and the *syn* and *anti* forms of 3-methylthiopropanal oxime, **19**, $MeS(CH_2)_2CH{=}N\text{-}OH$, were found in the sternal secretion, and are thought to be involved in the scent territorial marking of koalas[112]; *syn* and *anti* phenylacetaldoximes were also observed in the urine of male guinea pigs by Smith and colleagues, who attributed to the oxime a repellent effect on the approach of other male guinea pigs[113]. It should be noted that aldoximes, in general, can readily dehydrate to form the corresponding nitriles that may be utilized for olfactory communication between animals, as is attributed to benzyl cyanide[112].

Using pig and human microsomes and *c*DNA-expressed human flavin-containing monooxygenase, Lin and Cashman demonstrated a metabolic detoxification pathway that converts tyramine into the HA derivative, **20**, and the *anti* oxime, **21**, which was sufficiently stable to permit its chemical characterization[114].

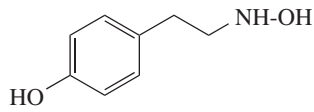

(4-hydroxyphenylethyl)hydroxylamine (**20**)

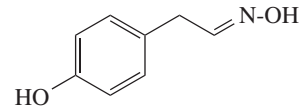

(4-hydroxyphenylethyl)acetaldoxime (**21**)

Similarly, the formation of phenethylhydroxylamine and phenethyl oxime (i.e. phenylacetaldoxime) from phenethylamine[115], and the conversion of amphetamine to its corresponding HA and oxime derivatives[116], were demonstrated *in vitro* in the presence of human liver microsomes. The authors suggested that these biological *N*-oxygenations by hepatic human flavin-containing monooxygenase (FMO) serve to detoxify the untoward physiological effects of biogenic amines. Thus, despite a scarcity of direct evidence, the presence of oximes in mammalian tissues may be ascribed to their being the end products of detoxification pathways of certain biological amines[114].

B. Biosynthesis

Mahadevan, in his 1973 review, proposed a scheme for the formation of diverse oximes from amino acids that involves *N*-hydroxylation of the amino group, to form the corresponding HA derivative, which is then further converted to the corresponding more stable oxime function[98]. According to this scheme, the *N*-hydroxylation of amino acids leads to the unstable intermediate, **22**, that is converted to the aldoxime, **23**, or to the less stable

carboxylic acid ketoxime, **24** (equation 14); both **23** and **24** are then further transformed to a variety of cyanogenic glycosides, glucosinolates, aldehydes, nitriles and HCN, or accumulate as free oximes.

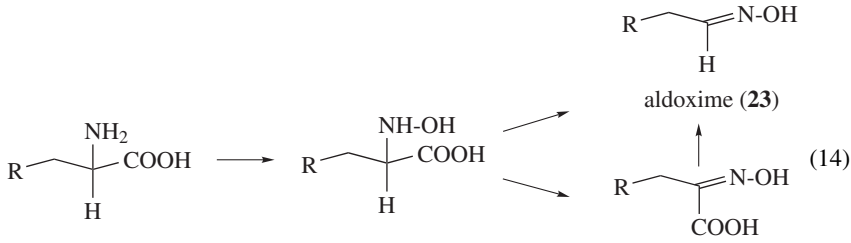

For example, the *anti* (**25**) and *syn* (4-hydroxyphenyl)acetaldoximes, **26**, are established intermediates in the biosynthesis of the cyanogenic glucoside of sorghum, dhurrin, **27**, and the biochemical pathway for its production in the plant was shown to originate in the *N*-hydroxylation of tyrosine, in the presence of NADPH/O_2, as outlined in equation 15[117]. It was further suggested that the *Z* (*syn*) isomer, **26**, is utilized preferentially over *E*(*anti*)-**25** in the subsequent biosynthesis of dhurrin, **27**. The same authors provided evidence that the biosynthesis of the aldoxime, **25**, proceeds via an *aci*-nitro containing intermediate, $R^1R^2C{=}N(O)OH$, that is positioned between *N*-hydroxytyrosine and *anti*-**25** in the biosynthetic pathway[10].

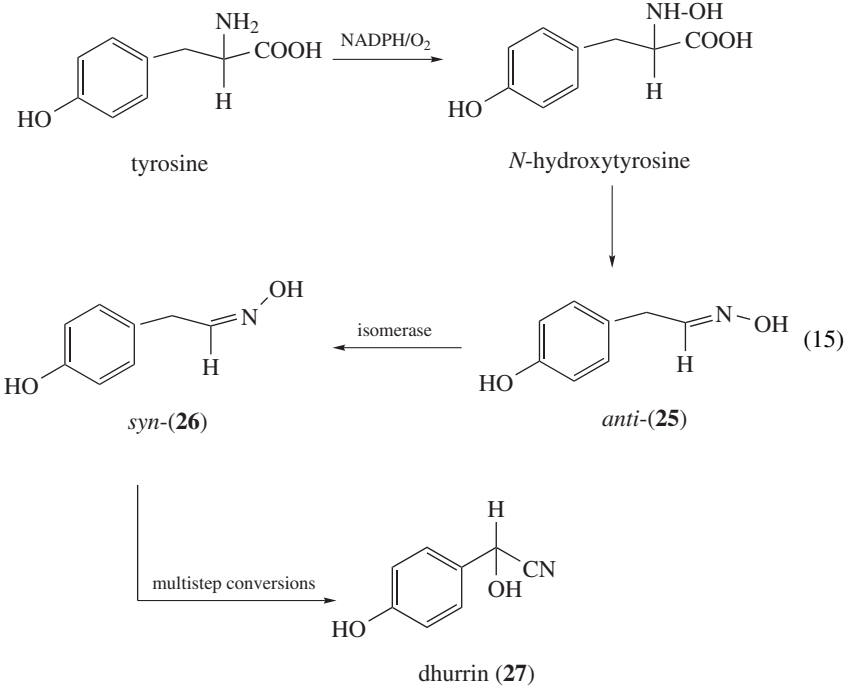

The enzymes that are involved in the conversion of tyrosine to the aldoximes, **25** and **26**[102, 105], of tryptophan[102], phenylalanine[104], valine and isoleucine[103] to the corresponding aldoximes are the multifunction cytochrome P450. CYP79A1, that hydroxylates tyrosine, was isolated from *Sorghum bichlor* and subsequently cloned[118]. These oximes are the building blocks of plant glucosinolates, **15**, and glycosides, **16**.

From the biosynthetic point of view, the secondary metabolites, **15** and **16**, are interrelated via the common intermediate aldoximes that originate from natural amino acids, and the *anti*-isomer of the corresponding aldoxime was suggested to be the branch point between the biochemical pathways that lead to **15** and **16**. However, the biosynthesis pathway involved is not limited to natural amino acids, and was also demonstrated to be capable of producing oximes from nonprotein amino acids[98], such as short- and long-chain elongated methionines with the general structure $MeS(CH_2)_{2\text{-}8}CH(NH_2)COOH$. The corresponding oximes, $MeS(CH_2)_{2\text{-}8}CH{=}N\text{-}OH$, are utilized to biosynthesize short- and long-chain aliphatic glucosinolates[100]. As mentioned above, the P450 that is responsible for converting tyrosine to *anti*-**25** in sorghum by its multifunctional *N*-hydroxylase activity has been cloned and sequenced[118].

The production of the *anti* oxime, **21**, from tyramine, in the presence of pig or human liver microsomes, was attributed to *N*-oxygenation of tyramine by NADPH and FMO, and is similar to the conversion of tyrosine in plants to the same aldoxime by P450[114]. The authors suggested that the same biochemical pathway that leads to oxime formation is responsible for mammalian detoxification of biogenic amines such as phenethylamine[115], amphetamine, methamphetamine[116] and tyramine[114]. In the case of *N*-methylamphetamine (methamphetamine), due to the absence of the NH moiety on the oxygenated amine, as is the case for amphetamine, the end-product of the FMO-induced oxygenation is phenylpropanone rather than the oxime function[116]. Although HA was not isolated, indirect experiments supported the notion that it is the first metabolite in the conversion of biogenic amines, such as phenethylamine, to the corresponding *trans* aldoxime, **29**, as depicted in equation 16. Notably, although the labile *N*,*N*-dihydroxy intermediate, **28**, can be dehydrated spontaneously to form **29**, it was suggested that the FMO serves as a template to accelerate the formation of the *anti* oxime[115].

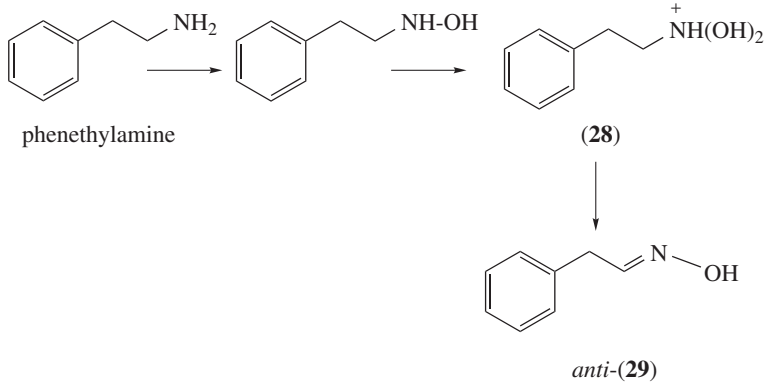

phenethylamine (**28**)

anti-(**29**) (16)

By analogy with the biogenesis of oximes via oxidation of amino acids or biogenic amines, the biosynthetic pathway for insertion of the ketoxime function into the antibiotic, nocardicin A (**18**), was shown to be dependent on the oxidation of the corresponding primary amine precursor of **18** by cytochrome P450[108]. Similarly, the formation of the ketoxime bond of verongamine (**17**) is attributed to the oxidation of a primary amine precursor[107].

In conclusion, oximes are produced in nature mostly, but not exclusively, as intermediates of secondary metabolites by enzymic oxidation of an amine function. The oxygenation is mediated by cytochrome P450 complex enzymes and FMOs. However, their formation via condensation of a carbonyl moiety with HA cannot be excluded.

C. Biochemical and Physiological Characteristics

Over the last 30 years an ever increasing amount of information on the biosynthesis of oxime intermediates in plant metabolism and on interactions of oximes with enzymes has accumulated. Enzymatic reactions that were characterized with respect to oximes as products, substrates or inhibitors are listed in Table 2.

1. Biochemical properties

a. Biochemical transformations of the C=N−OH function. Despite the difficulties encountered in demonstrating the natural occurrence of aldoximes as intermediates, Mahadevan constructed a branched pathway for oxime metabolism in plants, on the basis of studies carried out up to 1973, together with the structures that had been elucidated by then of about 70 glucosinolates and cyanogenic glycosides (**15** and **16**, respectively)[98]. Briefly, numerous aldoximes were shown, using isotope labeling, to be precursors of **15** and **16**, of other nitrogen-containing compounds (e.g. amines, hydrocyanic acid, nitriles, thiocyanates) and of nonnitrogenous metabolic products in plants (e.g. organic acids, aldehydes, alcohols). In more recent research, compelling evidence has been presented for the pivotal role of aldoximes as intermediates in plant nitrogen metabolism. For example, by use of a genetic-engineering approach, the two cytochrome P450 enzymes encoded by CYP79B2 and CYP79B3, that have been shown to convert tryptophan to indole-3-acetaldoxime (**30**) *in vitro*, have been demonstrated to be critical in the *in planta* (*Arabidopsis)* biosynthesis of the plant metabolite, **31**, and of the plant growth hormone auxin (indole-3-acetic acid, **32**, equation 17)[119].

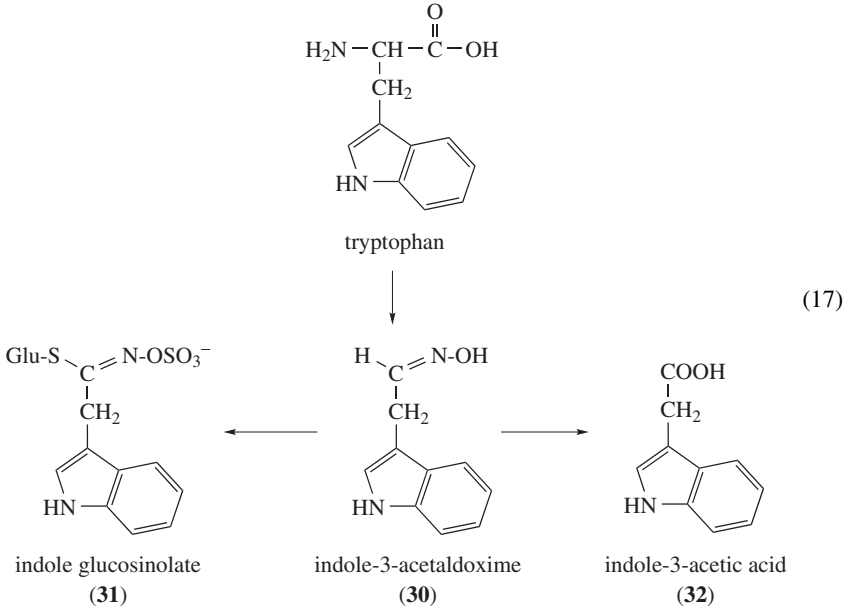

(17)

TABLE 2. Interactions of oximes ($R^1R^2C{=}N{-}OH$) and their derivatives ($R^1R^2C{=}N{-}OR^3$) with enzymes

Enzyme	Substrates/Inhibitors/Products	References
Sorghum microsomal enzyme system	Production of **25** from tyrosine, isomerization of oxime **25** to **26**, and its conversion to hydroxymandelonitrile	106, 117
Sorghum microsomal enzyme system	1-Nitro-2-(*p*-hydroxyphenyl)ethane is a precursor of oxime **25**: $K_m = 0.05$ mM and $V_{max} = 14$ nmol mg^{-1} h^{-1}	106
Sorghum cytochrome $P450_{Tyr}$(CYP79A1)	Catalyzes conversion of tyrosine to oxime **25**. For the reconstituted system, $K_m = 0.21$ mM and turnover is 228 min^{-1}	105
Sorghum $P450_{ox}$ (CYP71E1)	Conversion of aldoxime **26** to *p*-hydroxymandelonitrile *en route* to formation of dhurrin	120
Arabidopsis cytochrome P450 (CYP83A1, CYP83B1)	Conversion of aromatic and aliphatic oximes to glucosinolates	101
Arabidopsis cytochrome P450 (CYP79B2 and CYP79B3)	Conversion of tryptophan to indole acetaldoxime	119
Arabidopsis cytochrome P450 (CYP71A13)	Conversion of indole acetaldoxime to indole-3-acetonitrile	121
Synapis alba cytochrome P450	Catalyzes conversion of tyrosine to oxime **25**. $K_m = 034$ mM and $V_{max} = 0.54$ nmol mg^{-1} h^{-1}	122
Tropaeolum majus cytochrome P450	Conversion of phenylalanine to phenylacetaldoxime	104
Manihot esculenta cytochrome P450	Conversion of valine and isoleucine to aliphatic aldoximes	103
Nocardia uniformis NocI oxidase	A cytochrome P450 enzyme that converts an amine to an oxime in noncaridicin A	108
cDNA-expressed *human* FMO3	*N*- and *C*-hydroxylation of tyramine into oximes **25** and **26** ($K_m = 0.95$ mM; $V_{max} = 0.89$ nmol mg^{-1} min^{-1})	114
cDNA-expressed *human* FMO3	Conversion of phenethylamine into oxime **29**; $V = 17.4$ nmol mg^{-1} min^{-1} at 1.2 mM substrate	115
cDNA-expressed *human* FMO3	*N*-oxygenation of amphetamine and methamphetamine to the corresponding aldoxime and keto compounds, respectively	116
Bovine aldose reductase	Inhibited by aliphatic, cyclic and aromatic oximes, using benzyl alcohol as substrate	123
Horse liver alcohol dehydrogenase	Inhibited by aliphatic, cyclic and aromatic oximes using ethanol as substrate	123
Human lipoxygenase	Inhibition of leukotriene synthesis by oximes of diphenyl sulfides with IC_{50} *ca* 50 nM	124
Human glycogen synthase kinase-3	Inhibited by indigoid oxime with $IC_{50} = 5{-}13$ nM	125

TABLE 2. (*continued*)

Enzyme	Substrates/Inhibitors/Products	References
Mouse lanosterol 14α-Me demethylase (P 450DM)	A steroidal oxime that inhibits cholesterol biosynthesis	126
Cholinesterases from various sources	Quaternary heterocyclic oximes inhibit enzyme activity reversibly	127–131
Bacillus sp. *N*-hydroxy-L-phenylalanine decarboxylase/ oxidase	Catalyzes the formation of *Z*-phenylacetaldoxime from *N*-hydroxy-L-phenylalanine	111
Rat, bovine NO synthase	Oxime inhibits NOS activity with $IC_{50} = 0.2$ mM	132
Starfish and human cycline-dependent kinases (CDKs)	Indirubin-3′-monoxime inhibits CDKs with $IC_{50} = 0.18$ μM	133
Glycogen synthase kinase-3 (GSK-3)	Indigoid oximes inhibit GSK-3 and CDK with $IC_{50} = 5–33$ nM	125

Indole-3-acetaldoxime (**30**) and 4-hydroxyphenylacetaldoxime were shown to be metabolized by plant and pest fungi to **32** and to other related indole- and 4-hydroxyphenyl carboxylic acids, however, the biochemical transformation differed between the two fungi. These biochemical transformations may be relevant to the ability of certain fungi to cause plant diseases[100]. Compound **30** has been shown to be a key intermediate in the biosynthesis of camalexin, 3-thiazolyl-2′-yl-indole, a member of the family of phytoalexins that are produced in response to pathogen attack. It was demonstrated that CYP71A13 catalyzes the conversion of **30** to indole-3-acetonitrile, which is essential for the biosynthesis of camalexin[121]. Thus, the literature supplies a large body of evidence for the existence of a set of enzymes dedicated to the production of the auxin, **32**, from tryptophan via indole-3-acetaldoxime (**30**).

Based on kinetic analyses, Bak and Feyereisen[134] and Naur and colleagues[101] demonstrated that the pair of recombinant enzymes, CYP83A1 and CYP83B1, cloned and expressed from *Arabidopsis*, are involved in the conversion of a variety of acetaldoximes to the corresponding glycosinolates, and that the two enzymes are characterized by different affinities for aliphatic and aromatic aldoximes (K_m) and by different turnover efficiencies (k_{cat}) toward them. As shown in equation 17, since **30** is a branch point between the two biochemical pathways depicted, the relative levels of the two enzymes might affect the oxime-derived metabolite profile of the *Arabidopsis* plants and regulate auxin (**32**) levels. For example, the monooxygenase activity of CYP83B1 catalyzes the conversion of **30** (with K_m and k_{cat} values of 3 μM and 53 min^{-1}, respectively) to **33**, followed by the nonenzymic reaction of this active intermediate with an RSH molecule to give **34** (equation 18)[135]. Inhibition of the *N*-hydroxylation of **30** by CYP83B1 (e.g. by tryptamine)[135] might, therefore, result in the accumulation of **30** which, in turn, can be shifted to production of elevated levels of the plant auxin hormone, **32**. The importance of understanding the role of plant aldoximes, such as indole acetaldoxime (**30**), and of the enzymes involved in their metabolic pathways offers possibilities of genetic engineering of glucosinolates that may improve plant nutritional values and increase resistance to pathogens and pests.

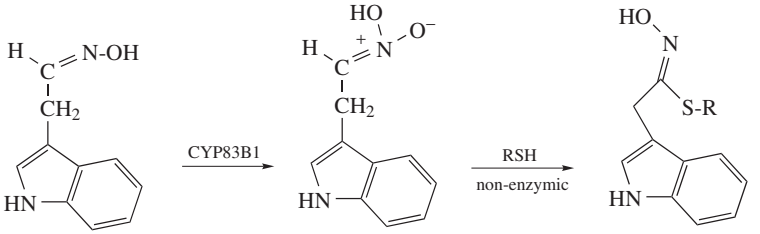

indole-3-acetaldoxime (**30**) | 1-*aci*-nitro-2-(3-indolyl)ethane (**33**) | *S*-alkylthiohydroximate (**34**)

(18)

The oxime, **34**, is glycosylated by a UDPG-thiohydroximate glucosyltransferase, and subsequently sulfonated by sulfotransferase to yield a glucosinolate of the type **15**[136, 137]. Thus, aldoximes generated by initial oxygenation of amino acids are found to serve as substrates of a wide variety of plant enzymes that act directly at the hydroximino function.

The biosynthesis of cyanogenic glucosides (**16**) also occurs via the formation of aldoxime intermediates. In this case, however, dehydration to produce **35**, and subsequent *C*-hydroxylation to the corresponding mandelonitrile (dhurrin, **27**), is required and proposed to be mediated by the P450 enzyme CYP71E1, as illustrated in equation 19 for the accumulation of dhurrin, **27**, in sorghum. The oxime, **21**, has the *syn* geometry, and glycosylation of **27** to produce **36** is catalyzed by UDP-glucose: 4-hydroxymandelonitrile-*O*-glucosyltransferase. The cytochrome P450 CY79A1 and CY71E1 enzymes that are involved in the production and biotransformation of plant aldoximes have been cloned, expressed and their function verified[102, 138].

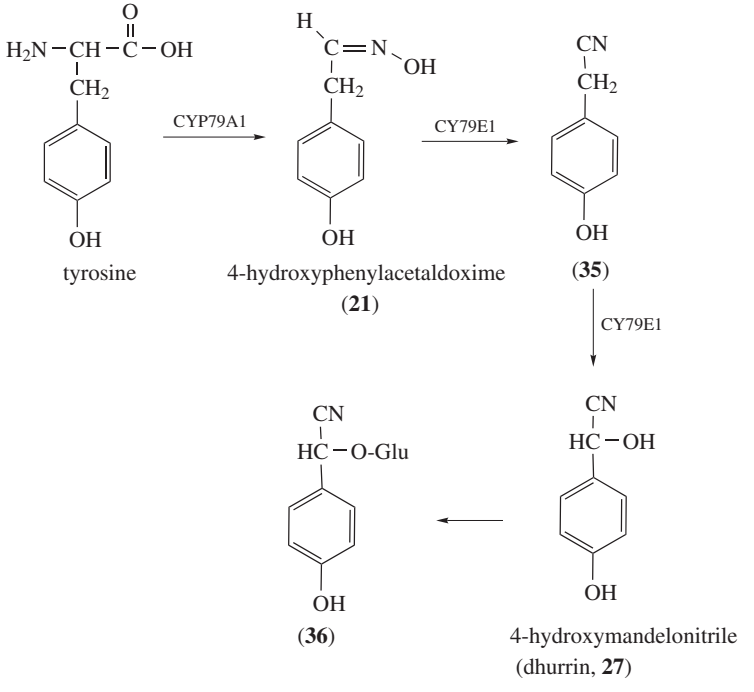

tyrosine | 4-hydroxyphenylacetaldoxime (**21**) | (**35**)

(**36**) | 4-hydroxymandelonitrile (dhurrin, **27**)

(19)

Notably, nitrile-degrading enzymes (e.g. nitrilase that converts the CN group to carboxylic acid, and nitrile hydratase that produces an amide function) have been described, and they co-exist with aldoxime-degrading enzymes in bacteria (Reference 111 and references cited therein). Studies in this area led to the proposal that the 'aldoxime-nitrile' pathway, which is implemented in synthesis of drugs and fine chemicals, occurs as a natural enzymic pathway. It is of interest that the enzyme responsible for bacterial conversion of *N*-hydroxy-L-phenylalanine to phenacetylaldoxime, an oxidative decarboxylation reaction, lacks heme or flavin groups which are found in plant or human enzymes that catalyze the same reaction. Its dependency on pyridoxal phosphate raised the possibility that similar systems may also be present in plants[111].

An oxime derivative of indirubin (a natural bis-indole alkaloid used in traditional Chinese medicine to treat chronic myelocytic leukemia), indirubin-3′-monoxime (**37**), was found to be a potent inhibitor of cyclin-dependent kinases (CDKs), and of the proliferation of myeloid leukemia cells via inhibition of a tyrosine kinase[133, 139]. The 3D structure of the complex of **37** with CDK revealed that the oxime function is intact, and that it occupies the ATP-ribose site of the CDK-ATP structure[133]. While the specific role of the oxime group in the biological activity of **37** is not clear, it was proposed that its reactivity may be utilized for further drug design[133].

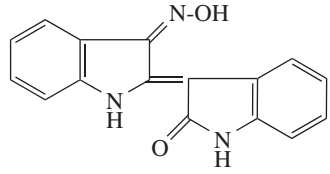

indirubin-3′-monoxime (**37**)

Biochemical transformations of the −C=N−OH function of synthetic drugs to an NO[132] and to nitroso intermediates[140] were recently demonstrated as a new pathway for metabolic activation of oxime-containing molecules. These reactions were recently explored in detail, and may underlie possible biochemical transformations of the −C=N−OH moiety in mammalian tissues, which are likely to be catalyzed by cytochrome P450 and by flavin-containing monooxygenase[141].

b. Nucleophilic properties of −C=N−OH in biological systems. Organophosphate (OP)-based pesticides and nerve agents are potent anticholinesterases, and their acute cholinergic syndromes are attributed to accumulation of acetylcholine. Death in severe poisoning is attributed to respiratory failure. The commonly employed therapeutic drug regimen consists of atropine (an antimuscarinic drug), diazepam (anticonvulsant) and quaternary *N*-alkyl pyridinium-based aldoximes that serve as reactivators of the phosphylated acetylcholinesterase (AChE)[142].

In 1951, Wilson reported a dramatic HA-induced *in vitro* regeneration of AChE that had been inhibited by the OP, tetraethyl pyrophosphate; 50% of baseline activity was recovered after 1 h in the presence of 1.2 M NH_2OH[143]. This observation, together with experimental evidence for the presence of an anionic site at the active center of AChE, that apparently remained intact following phosphoylation of the enzyme, led Wilson and colleagues to the first site-directed drug design of an oxime antidote against OP intoxication, *N*-methyl-2-pyridine aldoxime iodide (2-PAM, **38**)[127, 144, 145]. Thus, the correct molecular combination of an oxime moiety with enhanced nucleophilicity due to the α-effect (i.e. an α-nucleophile) and a quaternary template that could interact with the anionic site of

AChE and direct the oximate anion toward the P atom, proved to be extremely efficient in terms of rate of displacement of the enzyme-bound phosphoryl group (i.e. reactivation) and, consequently, as an antidote. The pioneering work of Wilson and colleagues in the early 1950s served as the scientific foundation for the synthesis and evaluation of more than 1000 oxime-containing reactivators over the past 50 years, that have been described in hundreds of publications. 2-PAM and several bis-quaternary oximes **39**[146], **40**[147] and **41**[148] are in clinical use in various countries, and constitute the reactivation component of their therapeutic doctrines against OP intoxications. The oxime HLo-7, **42**, is currently regarded as the most potent *in vitro* reactivator of nerve-agent-inhibited human AChE and is, in general, a superior antidote to the currently employed oximes[149–152]. Some recent reviews and research articles survey the relevant literature[130, 152, 153–156].

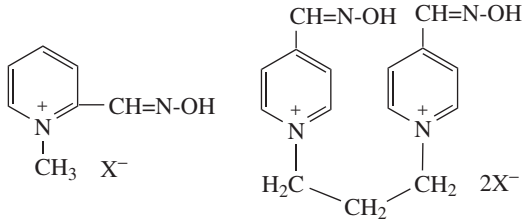

2-PAM (pralidoxime, **38**) TMB-4 (trimedoxime, **39**) LuH-6 (toxogonin, obidoxime, **40**)

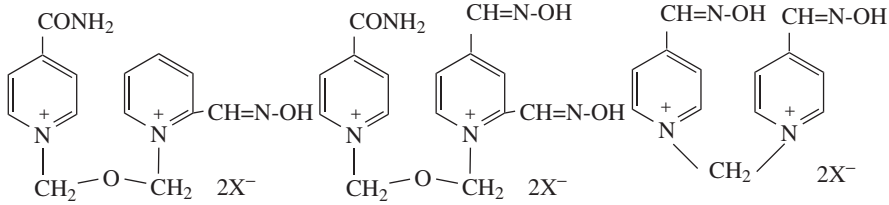

HI-6 (**41**) HLo-7 (**42**) MMB-4 (methoxime, **43**)

The kinetic scheme for the reactivation of OP-inhibited AChE is depicted in equation 20 for pyridinium-based aldoximes, where $R^1 = CH_3$ or an alkoxy group, and R^2 = alkyl or aryl. The nerve agents that generate the covalent OP-AChE conjugates are those with $R^1 = CH_3$ and R^2 = ethyl(VX), isopropyl (sarin), cyclohexyl (cyclosarin) and pinacolyl (soman). For tabun-inhibited AChE, R^1 = *N*,*N*-dimethylamido and R^2 = ethyl.

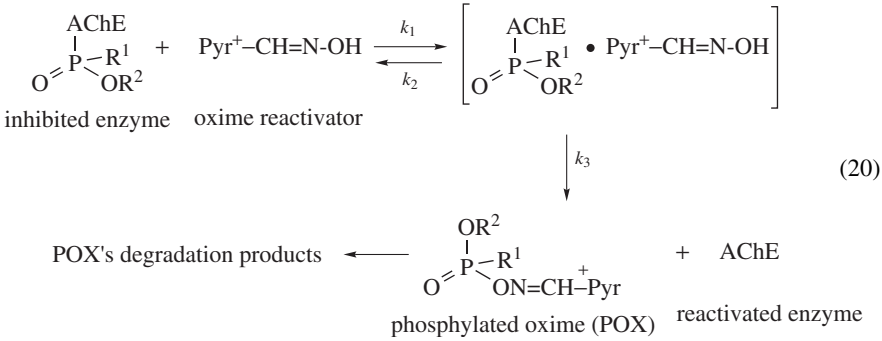

inhibited enzyme oxime reactivator phosphylated oxime (POX) reactivated enzyme (20)

A simplified mathematical solution of the reactivation scheme shown in equation 20 is equation 21:

$$k_{obs} = k_3(1 + K_{ox}/[\text{reactivator}])^{-1} \quad (21)$$

where the Michaelis constant for the reversible complex between the inhibited enzyme and the reactivator is $K_{ox} = (k_2 + k_3)/k_1$. Assuming that the dissociation of the Michaelis complex (k_2) is significantly faster than the unimolecular rate of OP displacement (k_3), K_{ox} is approximated by k_2/k_1, and is the dissociation constant of the Michaelis complex expressed in terms of molar concentration, M. For $K_{ox} \gg$ [reactivator], k_{obs} becomes k_3/K_{ox}, which is the bimolecular second-order rate constant for conversion of the OP conjugate to the free enzyme. When the inhibited enzyme is saturated by the reactivator ([reactivator] $\gg K_{ox}$), k_{obs} becomes k_3, which is the maximal unimolecular rate of OP displacement. The site-directed quaternary oximes of the type **38**–**43** encompass two important features that contribute to their reactivation potency: nucleophilicity toward the P atom that is reflected formally in equation 20 by k_3, and structural complementarity in the catalytic gorge of phosphylated AChEs, that corresponds to the affinity parameter, K_{ox}. In the following, the relative contribution of the two parameters to the overall reactivation properties will be analyzed in some detail, so as to highlight structural features of oximes that might be modified by drug design in order to improve reactivation.

It is accepted that the actual nucleophile in the reactions of oximes with OPs is the oximate anion, Pyr^+-CH=N-O^-, and the availability of the unshared electrons on the α-N neighboring atom enhances reactions that involve nucleophilic displacements at tetravalent OP compounds (known also as the α-effect). In view of the fact that the concentration of the oximate ion depends on the oxime's pK_a and on the reaction pH, and since the pK_a also reflects the affinity of the oximate ion for the electrophile, such as tetravalent OP, the theoretical relationship between the pK_a and the nucleophilicity parameter was analyzed by Wilson and Froede[127b]. They proposed that for each type of OP, at a given pH, there is an optimum pK_a value of an oxime nucleophile that will provide a maximal reaction rate. The dissociation constants of potent reactivators, such as **38**–**43** (with pK_a values of 7.0–8.5), are close to this optimum pK_a, and can be calculated, at pH = 7.4, from: $pK_{a_{opt}} = -\log[1/\beta - 1] + 7.4$, where β is the OP electrophile susceptibility factor, known as the Brønsted coefficient. If the above relationship holds also for the reactivation kinetics of the tetravalent OP-AChE conjugate (see equation 20), it would be important to estimate the magnitude of the effect of changes in oxime pK_a on the rate of reactivation, and to address two questions: (a) How do changes in the dissociation constants of oximes affect the rate of reactivation? (b) What is the impact of the β value, that ranges from 0.1 to 0.9 for the various OPs, on the relationship between the pK_a and the rate of reactivation? To this end, Table 3 summarizes some theoretical calculations for the pK_a

TABLE 3. Relative reduction in the optimal rate of reactivation of OP-inhibited AChE at pH = 7.4 for oximes with various pK_a values and OPs with various β values

β [a]	Optimum pK_a [b]	Relative rates of reactivation at pH 7.4 for a specified oxime pK_a [c]					
		6.0	7.0	7.4	8.0	9.0	10.0
0.3	7.0	0.67	1.00	0.88	0.68	0.14	0.03
0.5	7.4	0.39	0.90	1.00	0.80	0.31	0.10
0.8	8.0	0.12	0.22	0.82	1.00	0.77	0.49

[a] The slope of the Brønsted plot for a given OP, $\log k = \beta\ pK_a + \log A$.
[b] The optimum pK_a at pH 7.4 for the specified β.
[c] Calculated in accordance with the rate equation suggested by Wilson and Froede[127b].

range of 6 to 10, that illustrate the dependency of the reactivation rate on the pK_a and on the β values at pH = 7.4.

These calculations assumed that the Brønsted linear equation holds for the kinetic scheme for reactivation shown in equation 20. It should be noted, however, that a recent study showed that above $pK_a = 9$ the corresponding Brønsted plot deviates from linearity for nucleophilic displacements of oximates at the P atom of a variety of OPs, a behavior that was attributed by the authors to an increase in solvation[158]. Yet, the observed break in the linear curve could also be explained by a change in the rate-limiting step of the addition–elimination S_N2 reaction. Regardless of the detailed mechanism, Table 3 provides reasonable information showing that for oximes with pK_a values of 6–9, and for a wide range of β values that represent different susceptibilities of OPs to nucleophilic displacement by oximes (i.e. different OP inhibitors), deviation of 1 pK_a unit from the optimum pK_a is envisaged as producing a minor reduction in $k_{reactivation}$. It should be noted that the pK_a of the 3-PAM analogs is >9, and that they are poor reactivators[127b]. This can be attributed either to the low concentration of the corresponding oximate ion at physiological pH, or to poor orientation of the nucleophile toward the P atom of the phosphylated enzyme, or to a combination of the two factors.

Drug design efforts to improve the pK_a values of existing reactivators, such as **38**–**43**, so as to push them toward the optimal pK_a, are likely to result in relatively small improvements in the *in vitro* rate of reactivation. The theoretical analysis summarized in Table 3 also suggests that the nucleophilicities of the two oxime functions in the leading reactivators, such as TMB-4 (**39**), toxogonin (**40**) and a TMB-4 analog in which the trimethylene bridge is replaced by a single methylene group, MMB-4 (**43**)[159], seem to be similar. Within a given molecule, the two ionizable groups of **39**, **40** and **43** are separated by less than 1 pK_a unit[160], and in the case of HLo-7, **42**, the pK_a values of the 2- and 4-aldoximes are expected to be 7.3 and 8.8, respectively[149]. Thus, the two nucleophiles of a given dioxime in different positions can equally be utilized for reactivation provided that they are directed properly toward the P atom of the OP-inhibited enzyme. In terms of drug design considerations, in symmetrical bisquaternary dioximes such as **39**, **40** and **43**, one −C=N−OH group can be replaced by a nonnucleophilic moiety, as in the case of HI-6 (**41**), with relatively small changes in the overall rate of reactivation obtained compared to analogous dioximes. The observed changes in the bimolecular rate constant of reactivation by HI-6 compared to toxogonin, **40**[156], or to MMB4, **43**[152, 156], strongly depend on the OP used, and in the case of the nerve-agent-inhibited enzyme, $CH_3P(O)OR$-AChE, the nature of the R substituent determines the reactivatability of the inhibited enzyme, and dictates the choice of the oxime for reactivation. It is also apparent that one cannot attribute these changes to a single parameter; the combination of both the affinity, K_{ox}, and the unimolecular rate constant, k_3, are responsible for the observed differences. These observations suggest that: (1) the ground-state affinity, K_{ox}, may not adequately reflect the transition state stabilization of the OP-AChE-oxime complex which is the driving force for reactivation; (2) the positioning of the attacking oximate anions toward the P atom is different for each reactivator, and the higher its affinity for the inhibited enzyme in the proper orientation, the greater is the probability of a productive interaction leading to reactivation. Thus, perhaps it is the bimolecular rate constant of reactivation (i.e. the ratio k_3/K_{ox}) that needs to be compared, rather than the traditionally dissected individual constants, K_{ox} and k_3.

It should be emphasized that subsequent to the introduction of 2-PAM in the mid-1950s, the development of the bisquaternary oximes between the 1960s and the early 1990s provided reactivators that, depending on the OP structure and the enzyme source, displayed enhancements of 10–200-fold in k_3/K_{ox} compared to 2-PAM. These drug design achievements occurred before the elucidation of the 3D structure of AChE in 1991[161], studies on the reactivation of OP-conjugates of engineered mutant AChEs in

the mid-1990s[128, 129, 162] and the crystallographic analysis of both covalent OP-AChE conjugates[163–165] and oxime-AChE complexes[166, 167]. It is therefore envisaged that the crystal structures of oxime-AChE complexes, with and without the OP moiety attached to the catalytic serine, together with mutations of the relevant AChEs, will provide a new and improved generation of reactivators that may well turn out to be far more effective as antidotes than the currently employed oximes. Future drug design approaches aimed at administration of a mixture of an AChE variant and a reactivator, for rapid catalytic hydrolysis of OPs in the blood by a low dose of exogenously administered enzyme, before they reach physiologically important targets, require that k_3/K_{ox} of the corresponding reactivator be greater than 100-fold that of the most potent reactivators known, in order to provide meaningful turnover of OP hydrolysis in the circulation, and to convert AChE from a stoichiometric to a 'pseudo-catalytic scavenger'. This might, perhaps, be achieved by synthesis of the reactivator inside the the active-site gorge of the OP-AChE conjugate, thereby conferring tight binding together with optimal orientation of the oxime function toward the P atom[157].

Of all oximes, HLo-7, **42**, displays the greatest bimolecular rate constant for reactivation of human AChE inhibited by most nerve agents[152, 156]. However, in the cases of paraoxon- and tabun-inhibited human AChE, toxogonin (**40**) regenerates enzyme activity 3-fold faster than HLo-7[156]. On the basis of animal model studies, Clement and colleagues[150] concluded that HLo-7, **42**, is superior to other oximes in terms of being a broad spectrum antidote, presumably due to its distinctive wide range of reactivation of a variety of OP-inhibited human AChEs. Thus, in general, the antidotal capacity of some bis-quaternary oximes is correlated with their rate of reactivation of OP-inhibited enzymes. The generalization that a plasma concentration of oxime greater than 4 $\mu g\,ml^{-1}$ plasma is needed to counteract OP intoxication has been recently challenged; it appears that, depending both on the OP and on the animal used, each oxime will have a different threshold of effectiveness[130].

As mentioned earlier, the nucleophilicities of the two oxime groups of **42** are expected to be similar, and it is therefore speculated that one −CH=N−OH group might enhance reactivation by way of intramolecular anchimeric assistance of the displacement of the covalently-bound OP moiety from the active-site serine. More kinetic and product analysis studies will be required to explain the exceptional reactivity of **42**.

In contrast to the beneficial effects of treatment with oximes in cases of OP intoxication, reports in the literature suggest that treatment of poisoning with certain anticholinesterase carbamates with some oximes should be avoided because they may actually potentiate carbamate action. Other oximes decrease carbamate toxicity. The effects observed are, in general, correlated with changes in the rates of carbamylation and decarbamylation in the presence of the various oximes[168].

Although the major research and development effort on oxime reactivators has focused on the positively charged pyridinium ring, the poor ability of the charged oximes to cross the blood–brain barrier (BBB) has prompted several studies on noncharged aliphatic oximes in an effort to increase reactivation of OP-inhibited AChE in the central nervous system. The most studied noncharged oximes are mono isonitrosoacetone (MINA, **44**) and diacetyl monoxime (DAM, **45**)[169–173].

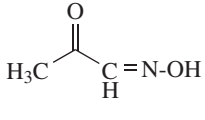

MINA (**44**)

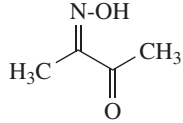

DAM (**45**)

The pK_a (6.5–8.2) and nucleophilicity of MINA, **44**, and of a series of aliphatic oximes derived from it, were found to be consistent with their ability to reactivate AChE inhibited by the nerve agents, sarin and VX[174]. Yet, despite their ability to significantly reactivate AChE in the brains of sarin-intoxicated rats[171], these aliphatic oximes are not used as antidotes for treatment of OP poisoning in humans; this is presumably due to their poor stability in aqueous solution and to their rapid clearance from the circulation.

Finally, the phosphylated oximes (POXs), that are formed transiently during the reactivation process (equation 20), although relatively unstable and thus able to reach only low concentrations, are extremely potent anticholinesterase intermediates[175], and might thus slow down the rate of reactivation. POXs need to be taken into account in the kinetic evaluation *in vitro* of existing oxime reactivators and in the development of new antidotal drugs. In terms of stability at physiological pH values, POXs of aldoximes are less stable than the ketoxime analogs, and the 2-pyridine-based POXs (e.g. those generated from 2-PAM) hydrolyze with $t_{1/2}$ values of *ca* 1 min, 50–100-fold faster than those generated by 4-PAM-based POXs (the 4-pyridinium aldoximes)[175]. Thus, reactivation with oximes such as **38**, **41** and **42**, in which the oxime function is *ortho* to the positively charged pyridinium nitrogen, have the advantage over **39**, **40** and **43** that their corresponding POXs are less likely to impede the regeneration of OP-inhibited AChEs. It should be pointed out that POXs are good substrates of OP-hydrolyzing enzymes, such as bacterial phosphotriesterases[176] and mammalian paraoxonase[177]; thus, their accumulation *in vivo* may not reach levels high enough to interfere with the overall rate of reactivation.

2. Physiological properties

By contrast to the pharmacologically active HA(s), the oxime function is a significantly less reactive moiety, and there are only few reports on interactions with biological systems that trigger physiological events that can be attributed directly to the −C=N−OH function. In fact, the conversion of biogenic amines such as phenethylamine to the corresponding phenethyl oxime was claimed to be a detoxification process that terminates the biological activity of phenethylamine[115]. This conclusion was based on the fact that the IC_{50} values of phenethyl oxime for interaction with the receptors for the biogenic amines, 5-HT and dopamine, were above 10 μM, a value that is above the physiological concentration of the corresponding oxime metabolites; phenethyl oxime would not, therefore, be expected to exert a physiological effect on these receptors. Similar conclusions were reached with respect to both amphetamine oxime[116] and tyramine oxime[114]. It should be pointed out that in mice, large doses (25–150 mg kg^{-1}) of oximes such as indole-3-aldehyde oxime produced hypothermia and depression of locomotor activity that could be antagonized by amphetamine. This observation led the authors to suggest that oximes of this type may be useful tools for studying central motor functions and mood control, as well as serving as lead compounds for new drugs in this area[178].

The relatively lack of pharmacological activity of the −CH=N−OH group is further illustrated by the work of Cerri and colleagues, who substituted the unsaturated butyrolactone moiety of the digitalis cardiac glycosides with an unsaturation introduced by the double bond of an aldoxime function (i.e. −C=N−)[179]. This modification reduced 200-fold (IC_{50} = 100 μM) the inhibition of Na^+, K^+-ATPase by digoxin (IC_{50} = 0.5 μM). However, etherification of the oxime function with aminopropanol to produce −C=N−O−$(CH_2)_3NH_2$ resulted in 25-fold (IC_{50} = 0.02 μM) enhancement of the anti-ATPase activity relative to digoxin. Thus, a polarizable oxime double bond, together with a basic amino group, were shown to be an efficient pharmacophore for improving the cardiotonic properties of the digitalis glycosides. It should be mentioned, however, that oximes that

bear an NH_2 group on the α carbon, such as amidoximes ($H_2N-C(R)=N\text{-}OH$) and N^H-hydroxyarginine (see Section II.B.3), can produce NO via oxidative cleavage of the C=N bond, thus affecting cGMP accumulation and, consequently, vascular relaxation[180].

The naturally occurring verongamine (**17**) ($IC_{50} = 0.5\ \mu M$), and a closely related analog that also contains an oxime function ($K_I = 7$ nM), are potent histamine H_3 receptor antagonists. **17** is being used as a structural template for drug design aimed at the development of improved and selective histamine H_3 receptor antagonists. Yet, the oxime function is not essential, and its replacement with different spacer residues between the important two structural extremities was found to maintain, and even improve, the pharmacological properties of these drug series, such as increased blood–brain barrier penetration[109].

Bisquaternary oxime reactivators, such as HI-6 (**41**) and HLo-7 (**42**), serve as ganglionic blockers, and interfere with peripheral cholinergic systems[149,151,181]. Jokanovic and Stojiljkovic recently reviewed literature data on the physiological effects of quaternary oximes that might enhance their antidotal capacity over and above their capacity to reactivate phosphorylated AChEs[155]. Thus, observed direct pharmacological reduction of the toxic effects of acetylcholine at the level of muscarinic and nicotinic receptors in the presence of these oximes is likely to contribute to the overall therapeutic capacity of oxime antidotes. These pharmacological properties can probably be ascribed to the bisquaternary pharmacophore, that produces a curaremimetic response, rather than to the presence of the oxime function. Depending on the route of administration and on the dose consumed, quaternary oximes have been shown to exert cardiovascular and gastrointestinal effects, and the reader is referred to a most comprehensive review published in 1984 on possible health effects of oxime reactivators by a panel of the USA National Research Council[182]. This review includes 171 references and data from human volunteer testing of oxime reactivators, and covers numerous studies on the pharmacology, toxicology, pharmacokinetics and metabolism of oximes **38**, **39** and **40**, both in experimental animals and in humans.

Metabolic activation of α,β-unsaturated oximes, such as **46**, leads to the conclusion that this class of unsaturated oximes are pro-haptens. They can undergo epoxidation that eventually produces reactive nitroso intermediates which act as strong contact sensitizers[140]. Here, the oxime function plays a major role in the chemical activation that results in the reactive nitrosoalkenes. It was further pointed by the authors that oximes can be hydrolyzed *in vivo* to the corresponding carbonyl compounds which are potential allergens.

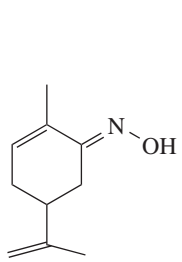

(**46**)

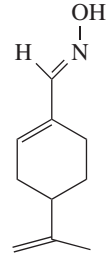

(**47**)

It is of interest to point out in this context that a closely related analog of **46**, perillartine (**47**)[183], is used in Japan as artificial sweetner[140], and apparently is devoid of the physiological untoward effects of **46**. Perillartine was used as a lead substance for systematic study of numerous combinations of an α,β-unsaturation group and an aldoxime

function as sweeteners or bitter molecules[183,184]. The α,β-unsaturated aldoxime template fits the electronic and shape requirements modeled for binding of low molecular weight compounds to the human sweet taste receptor[185].

Bimoclomol, **48**, is a nontoxic *O*-alkyl ether derivative of a pyridine carboxaldoxime, and was demonstrated to be a heat shock protein coinducer that is capable of conferring multilateral cell protection against various manifestations of stress injuries and pathophysiological conditions by increasing the expression of heat shock genes. For example, it was shown to significantly ameliorate cardiovascular conditions associated with diabetes mellitus[186]. Bimoclomol maleate has a biphasic effect on the amplitude of intracellular systolic and diastolic calcium transients.

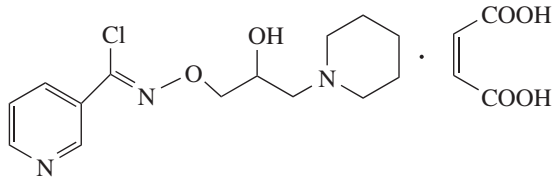

bimoclomol maleate (**48**)

D. Toxicity

The most extensive reports concerning oxime toxicity relate to the mono- and bispyridinium aldoxime reactivators of OP-inhibited cholinesterases, viz. **38**, **39**, **40**, **41** and **42**. However, it should be clarified that the reported toxic signs are mostly attributed to the positively charged pairs of pyridinium moieties, that display curare-like pharmacological behavior, rather than to the oxime function. In rodents, the toxicity of toxogonin (**40**) in terms of intravenous LD_{50} values is in the range of 200–400 mg kg^{-1}, while both the homologous bisquaternary oximes, HI-6 (**41**) and HLo-7 (**42**), and the monoquaternary oxime, 2-PAM (**38**), are 2–5-fold less toxic. MMB-4 (**43**) was reported to be the least toxic of the oximes examined, with an LD_{50} of 1950 mg kg^{-1} (reviewed by Kassa[130] and by Dawson[187]), while TMB-4 (**39**) is the most toxic bisquaternary oxime among **39**–**43**[155]. A quantitative evaluation of dose-related toxic symptoms of toxogonin, HI-6 and HLo-7 was made by Chen and colleagues, who ranked a list of oxime-induced toxic signs in dogs and monkeys[188]. They estimated the dose that affected 10% of the treated monkeys to be 133, 296 and 616 μmol kg^{-1} for toxogonin, HLo-7 and HI-6 , respectively, which is consistent with the relative toxicity reported in rodents. At near-lethal doses, the most common toxic signs are vomiting, salivation, loss of reflexes and convulsions. Aliphatic noncharged oxime reactivators, such as DAM (**45**), produce mainly CNS depression, in contrast to the charged pyridinium oximes, high doses of which primarily affect cardiac muscle[182].

The human intravenous bolus dose of oximes in nerve agent treatment ranges between 250 and 500 mg[130]. Side effects of oxime treatment in humans were monitored in 750 volunteers, and the main adverse effects reported were changes in blood pressure, pulse rate, dizziness, nausea and blurred vision[182,189]. Oral administration of oximes produces gastrointestinal distress[182].

Toxicity studies with noncharged oximes, such as methyl ethyl ketoxime, showed that 300–900 mg kg^{-1} produced reversible neurobehavioral changes that were attributed to CNS depression[190]. Significant depression of locomotor activity was reported already with 30 mg kg^{-1} of indole-3-aldoxime, and increasing the dose to 120 mg kg^{-1} produced

complete immobility. However, it was not accompanied by the anticonvulsant activity produced by many other depressants of locomotor activity[191]. Bisbenzamidoximes that were tested as anti-*pneumocystis* in rats produced ataxia and severe hypoactivity only when administered i.v. at a dose of >30 mg kg^{-1}, with complete recovery within 5 min post injection[192]. These reports, taken together with the toxic effects of DAM (**45**), suggest that the oxime functions of compounds that can cross the blood–brain barrier have a depressive activity in the CNS.

E. Current and Potential Medical Applications

The therapeutic efficacy of diverse mono and bis-quaternary pyridine aldoximes as antidotes against OP poisoning has been established in hundreds of publications, and three of them, 2-PAM (**38**), toxogonin (**40**) and HI-6 (**41**), are available in autoinjectors for post-exposure self-treatment or treatment by medical staff. For further information on the clinical use and potential side effects of these oximes the reader is referred to the reviews of Kassa[130], Eyer[153] and of Marrs and colleagues[193].

The broad spectrum of biological activities, including insecticidal and herbicidal applications, of diverse molecular species containing the oxime function is discussed in several reviews published between 2001 and 2005 by Abele and colleagues[194–198]. Many of these oximes are potential candidates for drugs with a number of applications as outlined in the following.

1. Cardiovascular system

Abele and colleagues reviewed the biological activity of various heterocyclic oximes on the cardiovascular system. Oximes (and their *O*-ether derivatives) of furan and thiophene[194], pyridine[195], indole and isatin[196], pyrrole[197] and quinoline[198] are characterized by vasodilating and cardiotonic activities, and they were proposed as potential anticoagulant and antihypertensive drugs. *O*-aminoalkyl oximes with structures resembling that of digitogenin were reported as potential substitutes for the digitalis cardiac glycosides in the treatment of congestive heart failure[179,199]. Another *O*-aminoalkyl oxime, bimoclomol maleate, is considered to be a promising drug for treatment of abnormal vascular reactivity[186].

2. Antidepressants and CNS activity

Heterocyclic oximes were reported as antidepressant and anticonvulsive drugs that can act as tranquilizers and antimigraine compounds. Some heterocyclic oximes have been studied as potential drugs for the treatment of Alzheimer's disease, and they have a general potential for treating neurodegenerative diseases[178,194–198]. A recent review describes the analgesic potential of oxo-morphinane oximes, some of which also prevent the respiratory depression activity of morphin-derived analgesics such as fentanyl[200].

3. Anti-inflammatory agents

Oxime derivatives of heterocyclic compounds, such as pyrrole and quinoline, were proposed as anti-inflammatory agents, probably due to their ability to inhibit the biosynthesis of leukotrienes[196–198]. Inhibition of 5-lipogenase by oximes of biphenyl sulfides[201], and by *O*-alkylcarboxylate oximes of indole[202], were suggested as key leads for the development of efficient anti-inflammatory drugs.

4. Antitumor activity

The antitumor activities of indole and isatin oximes[196] and of furan oximes[194] were studied by several investigators. Furan oximes were found to inhibit DNA, RNA and protein synthesis in lipoid leukemia cells. Derivatives of quinoline oximes were also shown to possess antitumor activity[198], and glucosinolates, **15**, were suggested as cancer-preventive agents[101].

The stability of oxime complexes with various metals has been shown to result in promising metallodrugs with antitumor activity, such as *cis* and *trans* platinum complexes[203] and homo- and heteronuclear Cu(II) and Mn(II) oxime complexes[204]. The bidentate oxime–metal complexes exhibit nucleolytic activity and induce DNA cleavage. Huang and colleagues described the inhibitory activity of 4-aminopyrimidine-5-carboxaldehyde oxime derivatives on factors that play an important role in angiogenesis[205]. The oxime derivative of the bis-indole alkaloid, indirubin, has low toxicity and is being considered as an antitumor drug[133,139]. A complex of ^{99}technetium with hexamethylpropyleneamine oxime was used to monitor photodynamic therapy of prostate tumors[206].

5. Antiviral agents, bactericides and fungicides

The cytotoxic activity of many heterocyclic oxime derivatives confers on them antiviral, antibacterial and antifungal properties[194–198,207]. The oxime function was utilized to synthesize and evaluate prodrugs of bisbenzamidines with excellent oral and intravenous anti-*Pneumocystis* activities in a rat model of the disease[192]. Bromotyrosine derivatives isolated from a marine sponge that contain the oxime function have been shown to possess antibacterial activity against *Staphylococcus aureus*[193]. Series of 5-keto-5-oxime derivatives of the antehelmintic and insecticidal milbemycins exhibited high activity as antimicrofilariae in dogs[208]. Transition metal complexes with bidentate oximes were shown to exhibit antibacterial activity[209,210].

6. Miscellaneous

The oxime bond has been suggested as a chemical tool for targeted intracellular delivery of synthetic oligonucleotides via conjugation to cell-penetrating peptides. Such hybrid conjugates have the potential to serve as therapeutic agents acting at the level of inhibition of gene expression[211].

Oximes of certain sterols were examined as inhibitors of cholesterol biosynthesis, by suppressing two enzymes that are involved in the biochemical pathway of cholesterol biosynthesis. This dual activity indicates a promising series of biologically reactive oximes (and oxime ethers) capable of reducing cholesterol levels[212].

IV. REFERENCES

1. J. Blom, *Biochem. Z.*, **194**, 392 (1928).
2. J. Blom, *Zentralbl. Bakteriol. Parasitenkd. Infektionskr.*, **II 84**, 60 (1931).
3. G. A. Lindsey and C. M. Rhines, *J. Bacteriol.*, **24**, 489 (1932).
4. D. D. Woods, *Biochem. J.*, **32**, 2000 (1938).
5. H. Lees, *Nature*, **169**, 156 (1952).
6. M. Tanaka, *Nature*, **171**, 1160 (1953).
7. E. G. Brown and M. Konuk, *Phytochemistry*, **38**, 61 (1995).
8. D. J. Richardson and N. J. Watmough, *Curr. Opin. Chem. Biol.*, **3**, 207 (1999).
9. G. A. Kowalchuk and J. R. Stephen, *Annu. Rev. Microbiol.*, **55**, 485 (2001).
10. O. Einsle, A. Messerschmidt, R. Huber, P. M. H. Kroneck and F. Neese, *J. Am. Chem. Soc.*, **124**, 11737 (2002).

11. I. Schmidt, C. Look, E. Bock and M. S. M. Jetten, *Microbiology*, **150**, 1405 (2004).
12. A. K. Upadhyay, A. B. Hooper and M. P. Hendrich, *J. Am. Chem. Soc.*, **128**, 4330 (2006).
13. J. Jason, L. Cantera and L. Y. Stein, *Environ. Microbiol.*, **9**, 765 (2007).
14. (a) P. Gross, *CRC Crit. Rev. Toxicol.*, **14**, 87 (1985).
    (b) A. Bendich, E. Borenfreund, G. C. Korngold and M. Krim, *Fed. Proc.*, **22**, 582 (1963).
    (c) E. Borenfreund, M. Krim and A. Bendich, *J. Natl. Cancer. Inst.*, **32**, 667 (1964).
    (d) H. S. Rosenkranz and A. J. Bendich, *Biochim. Biophys. Acta*, **87**, 40 (1964).
15. D. Lewis, *Biochem. J.*, **49**, 149 (1951).
16. R. J. Parry and L. Wenying, *J. Chem. Soc., Chem. Commun.*, 995 (1994).
17. S. N. Bagchi and D. Kleiner, *Biochim. Biophys. Acta*, **1041**, 9 (1990).
18. S. N. Bagchi and D. Kleiner, *Arch. Microbiol.*, **156**, 367 (1991).
19. T. M. Shakila, N. S. Rao and S. N. Bagchi, *Arch. Microbiol.*, **162**, 282 (1994).
20. K. Stolze and H. Nohl, *Biochem. Pharmacol.*, **38**, 3055 (1989).
21. K. Stolze and H. Nohl, *Biochem. Pharmacol.*, **49**, 1261 (1995).
22. P. G. Wang, M. Xian, X. Tang, X. Wu, Z. Wen, T. Cai and A. J. Janczuk, *Chem. Rev.*, **102**, 1091 (2002).
23. P. Stach, O. Einsle, W. Schumacher, E. Kurum and P. M. H. Kroneck, *J. Inorg. Biochem.*, **79**, 381 (2000).
24. J. Taira, V. Misik and P. Riesz, *Biochim. Biophys. Acta*, **1336**, 502 (1997).
25. G. Tang, L. Wu and R. Wang, *Mol. Pharmacol.*, **67**, 1723 (2005).
26. H. Vidrio and M. Medina, *J. Neural Transm.*, **114**, 863 (2007).
27. J. Kurian, S. Bajad, J. Miller, N. Chin and L. Trepanier, *J. Pharmacol. Exp. Ther.*, **311**, 1171 (2004).
28. J. R. Kurian, N. A. Chin, B. J. Longalis, K. L. Hayes and L. A. Trepanier, *Chem. Res. Toxicol.*, **19**, 1366 (2006).
29. J. R. Kurian, B. J. Longalis and L. A. Trepanier, *Pharmacogenetics and Genomics*, **17**, 597 (2007).
30. H. Munakata, Y. Oumi and A. Miyamoto, *J. Phys. Chem. B*, **105**, 3493 (2001).
31. H. J. H. Rouhof, G. M. Van Dortmont and M. W. M. Boesten, US Patent 5364609 (1994); *Chem. Abstr.*, **120**, 110923 (1994).
32. I. Schmidt, C. Look, E. Bock and M. S. M. Jetten, *Microbiology*, **150**, 1405 (2004).
33. C. G. Mowat and S. K. Chapman, *Dalton Trans.*, **21**, 3381 (2005).
34. H. Kimura, C. K. Mittal and F. Murad, *Nature*, **257**, 700 (1975).
35. T. Deguchi, *J. Biol. Chem.*, **252**, 596 (1977).
36. R. M. Rapoport and F. Murad, *Eur. J. Pharmacol.*, **104**, 61 (1984).
37. P. K. Moore, L. Burrows and R. Bhardwai, *J. Pharm. Pharmacol.* **41**, 426 (1989).
38. E. G. DeMaster, L. Raij, S. L. Archer and E. K. Weir, *Biochem. Biophys. Res. Commun.*, **163**, 527 (1989).
39. S. A. Waldman and F. Murad, *J. Cardiovas., Pharmacol.*, **12**, S115 (1988).
40. G. Thomas and P. W. Ramwell, *Biochim. Biophys. Res. Commun.*, **164**, 889 (1989).
41. H. H. Schmidt, B. Zernikow, S. Baeblich and E. Bohme, *J. Pharmacol. Exp. Ther.*, **254**, 591 (1990).
42. P. Beranova, K. Chalupsky, A. L. Kleschyov, C. Schott, J.-L. Boucher, D. Mansuy, T. Munzel, B. Muller and J.-L. Stoclet, *Eur. J. Pharmacol.*, **516**, 260 (2005).
43. R. J. Parry, Y. Li and F. L. Lii, *J. Am. Chem. Soc.*, **114**, 10062 (1992).
44. D. Kim and P. Guengerich, *Annu. Rev. Pharmacol.*, **45**, 27 (2005) and references cited therein.
45. H. M. H. van Eijk, Y. C. Luiking and N. E. P. Deutz, *J. Chromatogr. B*, **851**, 172 (2007).
46. K. Ohta, G. Rosner and R. Graf, *NeuroReport*, **8**, 2229 (1997).
47. S. J. Ferguson, *Curr. Opin. Chem. Biol.*, **2**, 182 (1998).
48. G. A. Lyles and I. Singh, *J. Pharm. Pharmacol.*, **37**, 637 (1985).
49. M. T. Wolfe, J. Heo, J. S. Garavelli and P. W. Ludden, *J. Bacteriol.*, **184**, 5898 (2002).
50. B. Clement, D. Behrens, J. Amschler, K. Matschke, S. Wolf and A. Havemeyer, *Life Sci.*, **77**, 205 (2005).
51. V. Milovic, L. Turchanowa, A. R. Khomutov, R. K. Khomotov, W. F. Caspary and J. Stein, *Biochem. Pharmacol.*, **61**, 199 (2001).
52. R. Tata, P. Marsh and P. B. Brown, *Biochim. Biophys. Acta*, **1205**, 139 (1994).
53. M. S. Martins, A. Karmali and M. L. Serralheiro, *Anal. Biochem.*, **355**, 232 (2006).
54. S. Marchal and G. Branlant, *Eur. J. Biochem.*, **268**, 5764 (2001).

55. (a) C. Evelo, A. Spooren, R. Bisschops, L. Baars and J. M. Neis, *Blood Cell. Mol. Dis.*, **15**, 280 (1998).
    (b) A. Spooren and C. Evelo, *Blood Cell. Mol. Dis.*, **26**, 373 (2000).
56. J. Kulys, K. Kriauciunas and R. Vidziunaite, *J. Mol. Catal. B: Enzymatic*, **26**, 79 (2003).
57. V. L. Lockamy, J. Huang, H. Shields, S. K. Ballas, S. B. King and D. B. Kim-Shapiro, *Biochim. Biophys. Acta*, **1622**, 199 (2003).
58. H. Mosen, A. Salehi and I. Lundquist, *J. Endocrinol.*, **165**, 293 (2000).
59. L. Fan, H. A. Schut and E. G. Snyderwine, *Carcinogenesis*, **16**, 775 (1995).
60. P. M. Vyas, S. Roychowdhury, P. M. Woster and C. G. Svensson, *Biochem. Pharmacol.*, **70**, 275 (2005).
61. L. A. Sayavedra-Soto, N. G. Hommes and D. J. Arp, *J. Bacteriol.*, **176**, 504 (1994).
62. D. J. Arp and L. Y. Stein, *Crit. Rev. Biochem. Mol. Biol.*, **38**, 471 (2003).
63. A. R. Pearson, B. O. Elmore, C. Yang, J. D. Ferrara, A. B. Hooper and C. M. Wilmot, *Biochemistry*, **46**, 8340 (2007).
64. J. P. Guzowski, C. Golanski and E. R. Montgomery, *J. Pharm. Biomed. Anal.*, **33**, 963 (2003).
65. H. Wariishi, D. Nonaka, T. Jojima, N. Nakamura, Y. Naruta, S. Kubo and K. Fukuyama, *J. Biol. Chem.*, **275**, 32919 (2000).
66. K. Fukuyama and T. Okada, *Acta Crystallegr., Sect. D*, **63**, 472 (2007).
67. S. B. King, *Free Radic. Biol. Med.*, **37**, 737 (2004) and references cited therein.
68. V. L. Lockamy, H. Shields, D. B. Kim-Shapiro and S. B. King, *Biochim. Biophys. Acta*, **1674**, 260 (2004).
69. G. Bartosz, *Clin. Chim. Acta*, **368**, 53 (2006).
70. K. Stolze, A. Dadak, Y. Liu and H. Nohl, *Biochem. Pharmacol.*, **52**, 1821 (1996).
71. H. A. Schut and E. G. Snyderwine, *Carcinogenesis*, **20**, 353 (1999).
72. K. Rehse and T. Shahrouri, *Arch. Pharm.*, **331**, 365 (1998).
73. M. D. Coleman and D. P. Jacobus, *Biochem. Pharmacol.*, **45**, 1027 (1993).
74. R. Kruszyna, H. Kruszyna, P. A. Doherty and R. P. Smith, *Arch. Toxicol.*, **55**, 203 (1984).
75. M. Klink, A. Swierzko and Z. Sulowska, *Acta Pattologica, Microbiologica, and Immunologica Scandinavica*, **109**, 493 (2001).
76. K. D. Schultz, K. Schultz and G. Schultz, *Nature*, **265**, 750 (1977).
77. Y. Huang, *Eur. J. Pharmacol.*, **349**, 53 (1998).
78. M. T. Lin, S. P. Pan, J. H. Lin and Y. L. Yang, *Br. J. Pharmacol.*, **127**, 1511 (1999).
79. C. P. Chang, S. P. Pan and M. T. Lin, *Br. J. Pharmacol.*, **132**, 1524 (2001).
80. D. S. Robertson, *Med. Hypotheses*, **59**, 140 (2002).
81. (a) R. J. Turesky, *Curr. Drug Metab.*, **5**, 169 (2004).
    (b) M. Stiborova, M. Mikosanova, M. Sulc, H. Rydlova, H. H. Schmeise and E. Frei, *Int. J. Cancer*, **116**, 667 (2005)
82. R. Goda, D. Nagai, Y. Akiyama, K. Nishikawa, I. Ikemoto, Y. Aizawa, K. Nagata and Y. Yamazoe, *Drug Metab. Dispos.*, **34**, 828 (2006).
83. R. Bhattacharya, *Indian J. Pharmacol.*, **32**, 94 (2000).
84. S. J. Sarnoff, US Patent 4292311 (1981); *Chem. Abstr.*, **95**, 198824 (1981).
85. R. Bhattacharya, *Hum. Exp. Toxicol.*, **14**, 29 (1995).
86. J. A. Vick and J. D. Von Bredow, *J. Appl. Toxicol.*, **16**, 509 (1996).
87. S. B. King, *Curr. Top. Med. Chem.*, **5**, 665 (2005).
88. K. Iizuka and K. Kikugawa, *Chem. Pharm. Bull.*, **20**, 614 (1972).
89. U. A. Nilsson, L-I. Olsson, G. Carlin and A-C. Bylund-Fellenius, *J. Biol. Chem.*, **264**, 11131 (1989).
90. R. Zhang, A. Pinson and A. Samuni, *Free Radic. Biol. Med.*, **24**, 66 (1998).
91. J. H. Lee, I. S. Kim and J-W. Park, *Carcinogenesis*, **25**, 1435 (2004).
92. H. Atamna, A. Paler-Martinez and B. N. Ames, *J. Biol. Chem.*, **275**, 6741 (2000).
93. H.-J. Kim, S-W. Shin, C-J. Oh, M-Y. Lee, C-H. Yang and J-W. Park, *Redox Rep.*, **10**, 287 (2005).
94. A. Ueda, A. Hirayama, S. Nagase, M. Inoue, T. Oteki, M. Aoyama and H. Yokoyama, *Free Radic. Res.*, **41**, 823 (2000).
95. T. Hyvonen, L. Alakuijala, L. Andersson, A. R. Khomutov, R. M. Khomutov and T. O. Eloranta, *J. Biol. Chem.*, **263**, 11138 (1988) and references cited therein.
96. D. L. Kramer, R. M. Khomutov, Y. V. Bukin, A. R. Khomutov and C. W. Porter, *Biochem. J.*, **259**, 325 (1989).

97. V. Milovic, L. Turchanowa, A. R. Khomutov, R. M. Khomutov, W. F. Caspary and J. Stein, *Biochem. Pharmacol.*, **61**, 199 (2001).
98. S. Mahadevan, *Annu. Rev. Plant Physiol.*, **24**, 69 (1973).
99. M. Soledade, C. Pedras and S. Montaut, *Bioorg. Med. Chem.*, **11**, 3115 (2003).
100. S. Chen, E. Glawischnig, K. Jorgensen, P. Naur, B. Jorgensen, C. E. Olsen, C. H. Hansen, H. Rasmussen, J. A. Pickett and B. A. Halkier, *Plant J.*, **33**, 923 (2003).
101. P. Naur, B. L. Petersen. M. D. Mikkelsen, S. Bak, H. Rasmussen, C. E. Olsen and B. A. Halkier, *Plant Physiol.*, **133**, 63 (2003).
102. J. L. Celenza, *Curr. Opin. Plant Biol.*, **4**, 234 (2001).
103. M. D. Andersen, P. K. Busk, I. Svendsen and B. L. Moller, *J. Biol. Chem.*, **275**, 1966 (2000).
104. L. Du and B. A. Halkier, *Plant Physiol.*, **111**, 831 (1996).
105. O. Sibbesen, B. Koch, B. A. Halkier and B. L. Moller, *J. Mol. Biol.*, **270**, 3506 (1995).
106. B. A. Halkier and B. L. Moller, *J. Biol. Chem.*, **265**, 21114 (1990).
107. T. R. Boehlow, J. J. Harburn and C. D. Spilling, *J. Org. Chem.*, **66**, 3111, (2001).
108. W. L. Kelly and C. A. Townsend, *J. Am. Chem. Soc.*, **124**, 8186 (2002).
109. S. M. Ali, C. E. Tedford, R. Gregory, S. L. Yates and J. G. Phillips, *Bioorg. Med. Chem. Lett.*, **8**, 1133 (1998).
110. H. Yagi, S. Matsunaga and N. Fusetani, *Tetrahedron*, **49**, 3749 (1993).
111. Y. Kato, T. Tsuda and Y. Asano, *Biochim. Biophys. Acta*, **1774**, 856 (2007) and references cited therein.
112. M. Salamon and N. W. Davies, *J. Chem. Ecol.*, **24**, 1659 (1998).
113. A. B. Smith, K. J. Byrne and G. K. Beauchamp, *J. Chem. Ecol.*, **3**, 309 (1977).
114. J. Lin and J. R. Cashman, *Chem. Res. Toxicol*, **10**, 842 (1997).
115. J. Lin and J. R. Cashman, *J. Pharmacol. Exp. Ther.*, **282**, 1269 (1997).
116. J. R. Cashman, Y. N. Xiong, L. Xu and A. Janowsky, *J. Pharmacol., Exp. Ther.*, **288**, 1251 (1999).
117. B. A. Halkier, C. E. Olsen and B. L. Moller, *J. Biol. Chem.*, **264**, 19487 (1989).
118. B. M. Koch, O. Sibbesen, B. A. Halkier, I. Svendsen and B. L. Moller, *Arch. Biochem. Biophys.*, **323**, 177 (1995).
119. Y. Zhao, A. K. Hull, N. R. Gupta, K. A. Goss, J. Alonso, J. R. Ecker, J. Normanly, J. Chory and J. L. Calenza, *Genes Dev.*, **16**, 3100 (2002).
120. R. A. Kahn, S. Bak, L. B. Svendsen, B. A. Halkier and B. L. Moller, *Plant Physiol.*, **115**, 1661 (1997).
121. M. Nafisi, S. Goregaoker, C. J. Botanga, E. Glawisching, C. E. Olsen, B. A. Halkier and J. Glazebrook, *The Plant Cell*, **19**, 2039 (2007).
122. L. Du, J. Lykkesfeldt, C. E. Olsen and B. A. Halkier, *Proc. Natl. Acad. Sci. USA*, **92**, 12505 (1995).
123. C. Shen and D. S. Sigman, *Arch. Biochem. Biophys.*, **286**, 596 (1991).
124. P. A. Ple, T. Geoffrey and C. Bird, *Bioorg. Med. Chem. Lett.*, **6**, 127 (1996).
125. Z-L. Wu, P. Aryal, O. Lozach, L. Meijer and F. P. Guengerich, *Chem. Biodiver.*, **2**, 51 (2005).
126. D. A. Leonard and J. A. Anderson, *J. Lipid Res.*, **35**, 1333 (1994).
127. (a) I. B. Wilson and S. Ginzburg, *Biochim. Biophys. Acta*, **18**, 168 (1955).
(b) I. B. Wilson and H. C. Froede, in *Drug Design, Vol. II* (Ed. E. J. Ariens), Academic Press, New York, 1971, pp. 213–229.
128. Y. Ashani, Z. Radic, I. Tsigelny, D. C. Vellom, N. A. Pickering, D. M. Quinn, B. P. Doctor and P. Taylor, *J. Biol. Chem.*, **270**, 6370 (1995).
129. M. Grosfeld, D. Barak, A. Ordentlich, B. Velan and A. Schafferman, *Mol. Pharmacol.*, **50**, 639 (1996).
130. J. Kassa, *Clin. Toxicol.*, **40**, 803 (2002).
131. R. Odzak, M. Calic, T. Hrenar, I. Primozic and Z. Kovarik, *Toxicology*, **233**, 85 (2007).
132. N. Sjakste, V. G. Andrianov, J.-L. Boucher, I. Shestakova, L. Baumane, M. Dzintare, D. Meirena and I. Kalvinsh, *Nitric Oxide*, **17**, 107 (2007).
133. R. Hoessel, S. Leclerc, J. A. Endicott, M. E. M. Nobel, A. Lawrie, P. Tunnah, M. Leost, E. Damiens, D. Marie, D. Marko, E. Niederberger, W. Tang, G. Eisenbrand and L. Meijer, *Nat. Cell Biol.*, **1**, 60 (1999).
134. S. Bak and R. Feyereisen, *Plant Physiol.*, **127**, 108 (2001).
135. S. Bak, F. E. Tax, K. A. Feldman, D. W. Galbraith and R. Feyereisen, *The Plant Cell*, **13**, 101 (2001).

136. J. C. Jain, J. W. D. GrootWassink, A. D. Kolenovsky and E. W. Underhill, *Phytochemistry*, **29**, 1425 (1990).
137. D. Liangcheng and B. A. Halkier, *Plant Physiol.*, **111**, 831 (1996) and references cited therein.
138. P. R. Jones, B. L. Moller and P. B. Hoj, *J. Biol. Chem.*, **274**, 35483 (1999).
139. Y. Zhen, V. Sorensen, Y. Jin, Z. Suo and A. Wiedlocha, *Oncogene*, **26**, 6372 (2007).
140. M. A. Bergstrom, K. Luthman and A-T. Karlberg, *Chem. Res. Toxicol.*, **20**, 927 (2007).
141. J. R. Cashman and J. Zhang, *Annu. Rev. Pharmacol. Toxicol.*, **46**, 65 (2006).
142. T. C. Marrs, *Pharmac. Ther.*, **58**, 51 (1993).
143. I. B. Wilson, *J. Biol. Chem.*, **190**, 11 (1951).
144. I. B. Wilson and S. Ginsburg, *Arch. Biochem. Biophys.*, **54**, 569 (1955).
145. H. Kewitz and I. B. Wilson, *Arch. Biochem. Biophys.*, **60**, 261 (1956).
146. F. Hobbiger, D. G. O'Sullivan and P. W. Sadler, *Nature*, **182**, 1498 (1958).
147. A. Lutringhaus and I. Hagedorn, *Arzneim.-Forsch.*, **14**, 1 (1964).
148. I. Hagedorn, W. H. Gundel and K. Schoene, *Arzneim.-Forsch.*, **19**, 603 (1969).
149. P. Eyer, I. Hagedorn, R. Klimmek, P. Lippstreu, M. Loffler, H. Oldiges, U. Spohrer, I. Steidl, L. Szinicz and F. Worek, *Arch. Toxicol.*, **66**, 603 (1992).
150. J. G. Clement, A. S. Hansen and C. A. Boulet, *Arch. Toxicol.*, **66**, 216 (1992).
151. F. Worek, P. Eyer, N. Aurbek, L. Szinicz and H. Thiermann, *Toxicol. Appl. Pharmacol.*, **219**, 226 (2007).
152. C. Luo, M. Tong, N. Chilukuri, K. Brecht, D. M. Maxwell and A. Saxena, *Biochemistry*, **46**, 11771 (2007).
153. P. Eyer, *Toxicol. Rev.*, **22**, 165 (2003).
154. P. Lundy, L. Raveh and G. Amitai, *Toxicol. Rev.*, **25**, 231 (2006).
155. M. Jokanovic and M. P. Stojiljkovic, *Eur. J. Pharmacol.*, **553**, 10 (2006).
156. F. Worek, P. Eyer, N. Aurbek, L. Szinicz and H. Thiermann, *Toxicol. Appl. Pharmacol.*, **219**, 226 (2007).
157. P. Taylor, Z. Kovarik, E. Reiner and Z. Radic, *Toxicology*, **233**, 70 (2007).
158. F. Terrier, P. Rodriguez-Dafonte, E. Le Guevel and G. Moutiers, *Org. Biomol. Chem.*, **4**, 4352 (2006).
159. F. Hobbiger and P. W. Sadler, *Br. J. Pharmacol.*, **40**, 2677 (1959).
160. K. Schoene and E. M. Starke, *Biochem. Pharmacol.*, **20**, 1041 (1971).
161. J. L. Sussman, M. Harel, F. Frolow, C. Oefner, A. Golsman, L. Toker and I. Silman, *Science*, **253**, 872 (1991).
162. Z. Kovarik, Z. Radic, H. A. Berman, V. Simeon-Rudolf, E. Reiner and P. Taylor, *Biochemistry*, **43**, 3222 (2004).
163. C. B. Millard, G. Kryger, A. Ordentlich, H. M. Greenblatt, M. Harel, M. Raves, Y. Segall, D. Barak, A. Shafferman, I. Silman and J. L. Sussman, *Biochemistrty*, **38**, 7032 (1999).
164. C. B. Millard, G. Koellner, A. Ordentlich, A. Shafferman, I. Silman and J. L. Sussman, *J. Am. Chem. Soc.*, **121**, 9883 (1999).
165. F. Ekstrom, C. Akfur, A-K. Tunemalm and S. Lundberg, *Biochemistry*, **45**, 74 (2006).
166. F. J. Ekstrom, Y. Pang, M. Boman, E. Artursson, C. Akfur and S. Borjegren, *Biochem. Pharmacol.*, **72**, 497 (2006).
167. F. J. Ekstrom, C. Astot and Y-P. Pang, *Clin. Pharmacol. Ther.*, **82**, 282 (2007).
168. R. D. Dawson, *Neurochem. Int.*, **26**, 643 (1995).
169. M. V. Rajapurkar, G. B. Koelle and P. Smart, *J. Pharmacol. Exp. Ther.*, **123**, 247 (1958).
170. E. M. Cohen and H. Wiersinga, *Acta Physiol. Pharmacol. Neerlandica*, **8**, 40 (1959).
171. J. H. Fleisher, L. W. Harris and P. T. Berkowitz, *Biochem. Pharmacol.*, **19**, 421 (1970).
172. D. J. Ecobichon, *Can. J. Physiol. Pharmacol.*, **54**, 86 (1976).
173. A. K. Srivastava and J. K. Malik, *Indian. Vet. Med. J.*, **25**, 49 (2001).
174. F. Degorre, D. Kiffer and F. Terrier, *J. Med. Chem.*, **31**, 757 (1988).
175. Y. Ashani, A. K. Bhattacharjee, H. Leader, A. Saxena and B. P. Doctor, *Biochem. Pharamcol.*, **66**, 191 (2003).
176. H. Leader, A. Vincze, B. Manisterski, N. Rothchild, C. Dosoretz and Y. Ashani, *Biochem. Pharmacol.*, **58**, 503 (1999).
177. J. Stenzel, F. Worek and P. Eyer, *Biochem. Pharmacol.*, **74**, 1390 (2007).
178. N. R. Banna and C. W. T. Pilcher, *Neuropharmacology*, **19**, 103 (1980).

179. A. Cerri, N. Almirante, P. Barrasi, A. Benicchio, G. Fedrizzi, P. Ferrari, R. Michelletti, L. Quadri, E. Ragg, R. Rossi, M. Santagostino, A. Schiavone, F. Serra, M. P. Zappavigna and P. Melloni, *J. Med. Chem.*, **43**, 2332 (2000).
180. P. Vetrovsky, J.-L. Boucher, C. Scott, P. Beranova, K. Chalupsky, N. Callizot, B. Muller, G. Entlicher, D. Mansu and J.-L. Stoclet, *J. Pharmacol. Exp. Ther.*, **303**, 823 (2002).
181. H. P. M. van Helden, R. W. Busker, B. P. C. Melchers and P. L. B. Bruijnzeel, *Arch. Toxicol.*, **70**, 779 (1996).
182. *Possible Long-term Health Effects of Short-term Exposure to Chemical Agents*, Vol. 2, National Academy Press, Washington D.C., 1984; http://books.nap.edu/openbook.php?record_id=91368&page=331)
183. E. M. Acton and H. Stone, *Science*, **193**, 584 (1976).
184. Y. Takahashi, Y. Miyashita, Y. Tanaka, H. Abe and S. Sasaki, *J. Med. Chem.*, **25**, 1245 (1982).
185. G. Morini, A. Bassoni and P. A. Temussi, *J. Med. Chem.*, **48**, 5520 (2005).
186. P. P. Nanasi and A. Jednakovits, *Cardiovasc. Drug Rev.*, **19**, 133 (2001).
187. R. M. Dawson, *J. Appl. Toxicol.*, **14**, 317 (1994).
188. R. Chen, L. Raveh, G. Zomber, I. Rabinovitz, G. Cohen, R. Adani and G. Amitai, *J. Appl. Toxicol.*, **21**, 285 (2001).
189. B. Ballantyne, *Vet. Human Toxicol.*, **33**, 151 (1991).
190. G. E. Schulze and M. J. Derelanko, *Fundam. Appl. Toxicol.*, **21**, 476 (1993).
191. N. R. Bana and C. W. T. Pilcher, *Neuropharmacology*, **19**, 103 (1979).
192. J. E. Hall, J. E. Kerrigan, K. Ramachandran, B. C. Bender, J. P. Stanko, S. K. Jones, D. A. Patrick and R. R. Tidwell, *Antimicrob. Agents Chemother.*, **42**, 666 (1998).
193. T. Marrs, P. Rice and J. A. Vale, *Toxicol. Rev.*, **25**, 297 (2006).
194. E. Abele and E. Lukevics, *Chem. Heterocycl. Compd.*, **37**, 141 (2001).
195. E. Abele, R. Abele and E. Lukevics, *Chem. Heterocycl. Compd.*, **39**, 825 (2003).
196. E. Abele, R. Abele, O. Dzenitis and E. Lukevics, *Chem. Heterocycl. Compd.*, **39**, 3 (2003).
197. E. Abele, R. Abele and E. Lukevics, *Chem. Heterocycl. Compd.*, **40**, 1 (2004).
198. E. Abele, R. Abele, K. Rubina and E. Lukevics, *Chem. Heterocycl. Compd.*, **41**, 137 (2005).
199. M. Gobbini and A. Cerri, *Curr. Med. Chem.*, **12**, 2343 (2005).
200. A. Gergely, K. Gyimesi-Forrás, P. Horváth, S. Hosztafi, J. Kökösi, P. I. Nagy, G. Szász and A. Szentesi, *Curr. Med. Chem.*, **11**, 2555 (2004).
201. P. A. Ple, T. Geoffrey and C. Bird, *Bioorg. Med. Chem. Lett.*, **6**, 127 (1996).
202. K. W. Woods, C. D. W. Brooks, R. G. Maki, K. E. Rodriques, J. B. Bouska, P. Young, R. L. Bell and G. W. Carter, *Bioorg. Med. Chem. Lett.*, **6**, 1547 (1996).
203. A. G. Quiroga, L. Cubo, E. de Blas, P. Aller and C. Navarro-Ranninger, *J. Inorg. Biochem.*, **101**, 104 (2007).
204. N. Saglem, A. Colak, K. Serbest, S. Dulger, S. Guner, S. Karabocek and A. O. Belduz, *BioMetals*, **15**, 357 (2002).
205. S. Huang, R. Li, P. J. Connolly, G. Xu, M. D. Gaul, S. L. Emanuel, K. R. LaMontagne and L. M. Greenberger, *Bioorg. Med. Chem. Lett.*, **16**, 6063 (2006).
206. R. B. Moore, J. D. Chapman, A. D. Mokrzanowski, M. R. Arnfield, M. S. McPhee and A. J. McEwen, *Br. J. Cancer*, **65**, 491 (1992).
207. C. Kirilmis, M. Ahmedzade, S. Servi, M. Koca, A. Kizirgil and C. Kazaz, *Eur. J. Med. Chem.*, **43**, 300 (2008).
208. Y. Tsukamoto, K. Sato, S. Mio, S. Sugai, T. Yanai, N. Kitano, S. Muramatsu, Y. Nakada and J. Ide, *Agric. Biol. Chem.*, **55**, 2615 (1991).
209. M. Kurtoglu, M. M. Dagdelen and S. Toroglu, *Transition Metal Chem.*, **31**, 382 (2006).
210. M. Kurtoglu and S. A. Ayse, *J. Coord. Chem.*, **60**, 655 (2007).
211. Y. Singh, O. P. Edupuganti, M. Villien, E. Defrancq and P. Dumy, *C.R. Chemie*, **8**, 789 (2005).
212. L. L. Frye, K. P. Cusack, D. A. Leonard and J. A. Anderson, *J. Lipid Res.*, **35**, 1333 (1994).

CHAPTER **14**

Nitrosomethanides and their acids: Synthesis, structure and bonding

AXEL SCHULZ

Universität Rostock, Institut für Chemie, Abteilung Anorganische Chemie, Albert-Einstein-Straße 3a, 18059 Rostock, Germany and Leibniz-Institut für Katalyse e.V. an der Universität Rostock, Albert-Einstein-Str. 29a, 18059 Rostock, Germany
Fax: +49 (0)381/498-6382; e-mail: Axel.Schulz@uni-rostock.de

HARALD BRAND

LMU Munich, Butenandt-Str. 5-13, 81377 München, Germany
E-mail: Harald.Brand@cup.uni-muenchen.de

and

ALEXANDER VILLINGER

Universität Rostock, Institut für Chemie, Abteilung Anorganische Chemie, Albert-Einstein-Straße 3a, 18059 Rostock, Germany
E-mail: Alexander.Villinger@uni-rostock.de

The chemistry of hydroxylamines, oximes and hydroxamic acids
Edited by Z. Rappoport and J. F. Liebman

I. INTRODUCTION

The growing interest in the chemistry of monomeric nitrosomethanide compounds and their corresponding oxime acids is due in part to the recognition of their participation in various metabolic processes of nitrogen-containing compounds. In general, C-nitroso compounds have a rich organic chemistry displaying interesting intra- and intermolecular dimerization processes. Furthermore, they have a fascinating coordination chemistry. While most of the attention has been directed towards C-nitroso compounds (mostly containing a single NO moiety), this chapter focuses on functionalized nitrosomethanides and their acids. Synthetic routes and properties of these relatively unexplored nitrosomethanides and their acids is presented and discussed combined with quantum chemical considerations.

A. General Considerations

The quintessential C-nitroso compound nitrosomethane, CH_3-NO (**1**), was first isolated by Coe and Doumani[1] in 1948 while already in 1936 Staveley and Hinshelwood[2] found that addition of small quantities of nitric oxide to the reaction vessel during the

pyrolytic decomposition of diethyl ether brought about a considerable reduction of the decomposition reaction rate (by trapping of radicals with NO). Although no experimental detection of nitrosomethane or formaldoxime was presented, the authors assumed the intermediate formation of nitrosomethane. Hence, the first isolation of (dimeric) nitrosomethane can be attributed to Coe and Doumani who carried out a photolysis of gaseous *tert*-butyl nitrite, followed by deposition of the dimeric nitrosomethane at the unirradiated wall of the reaction vessel.

Five isomers of **1** with a different connectivity are relevant: the tautomers formaldehyde oxime (**2**) with one hydrogen atom attached to the oxygen atom and formaldonitrone (**3**) with one hydrogen atom attached to the nitrogen atom. Investigations of the potential energy surface displayed two further high-energy isomers $CH_2{-}O{-}NH$ (**4**) and the cyclic oxaziridine (**5**) (Scheme 1). For the formaldehyde oxime (**2**) two isomers, *syn* and *anti* configuration, are known.

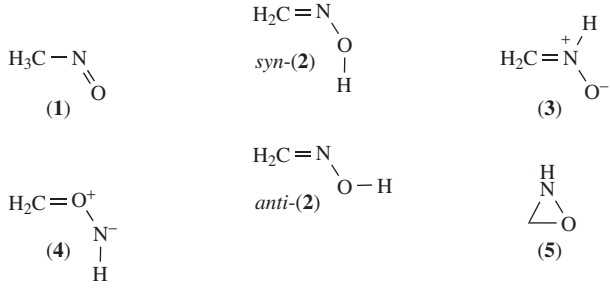

SCHEME 1. Isomers of nitrosomethane. Besides **4** and **5** deprotonation of **1**, **2** and **3** would lead to the formation of a nitrosomethanide, while in case of **4** and **5** only an isomerization process following the deprotonation can give nitrosomethanide

While highly reactive formaldonitrone (**3**) was detected only recently[3], both the nitrosomethane (**1**) and the formaldehyde oxime (**2**) are also reactive compounds in the condensed phase; **2** undergoes facile oligomerization[4–6], whereas **1** forms a dimer[1] and isomerizes to **2**[6]. Deprotonation of any of these isomers (**1**, **2**, **3**) would result in the corresponding simplest nitrosomethanide anion: $[H_2C{=}N{-}O]^-$.

To be precise the potential surface of the [C, H_3, N, O] displays further isomers such as formamide $HC(O){-}NH_2$ or the *Z* and *E* imidic isomers HC(OH)=NH (including four rotamers).

Interestingly, the 'oldest' experimentally known isomer is 'formoxime' (**2**), nowadays better known as formaldoxime (the oxime of formaldehyde—formaldehyde oxime), which was first synthesized as early as 1891[5]. Scholl already reported that **2** is unstable with respect to slow polymerization, while Dunstan and Bossi were able to stabilize **2** as its hydrochloride salt and described its properties in 1898[6]. Dunstan and Bossi also reported the reaction of **2**•HCl with alkali metals yielding the sodium salt of **2**, Na^+ $[H_2C{=}NO]^-$, which 'explodes when heated'. Probably, this 'explosive' statement was one of the first descriptions of a nitrosomethanide.

Pioneering work in Germany (Bamberger, Wieland, Scholl), England (Dunstan, Bossi, Gowenlock) and the USA (Coe, Doumani), especially between 1890–1960, uncovered a rich chemistry for nitrosomethanide-based systems. Their early efforts were notable because of the unavailability of many modern physical techniques for structural characterization that are commonplace today. Two excellent review articles by Gowenlock and Richter-Addo should be mentioned as they are exclusively devoted to the chemistry of nitroso and polynitroso compounds[7].

The chemistry of NO-based methanides has progressed slowly but, in the last ten years, there have been numerous developments in these areas also, as a result of the creative contributions of both inorganic and organic synthetic chemists. This chapter is not intended to cover comprehensively the primary literature. Rather it provides an overview of the field with the emphasis on the pseudohalide concept—a concept which can nicely be applied to the group of resonance stabilized nitrosomethanides $[R^1R^2C{-}NO]^-$ (R^1, R^2 = functional groups). This chapter is designed to be self-contained with a strong focus on resonance stabilized nitrosomethanides, $[R^1R^2C{-}NO]^-$. The only functional groups that are discussed are those which are capable of delocalization of π-electron density such as R^1, R^2 = CN, NO_2. The discussion starts with nitrosomethane, with the formal R^1, R^2 = H. Subsequent substitution leads to all species to be discussed. By the use of selected examples (limited to the above functional group), it is hoped that the reader, who is unfamiliar with or new to the field, will be able to gain an appreciation of the subtleties of nitrosomethanide chemistry. The literature is covered up to mid-2007.

Computational quantum chemistry has emerged in recent years as a viable tool for the elucidation of molecular structure and molecular properties, especially for the prediction of geometrical parameters, kinetics and thermodynamics of highly labile compounds such as nitrosomethanides. However, they are difficult objects for both experimental (high toxicity, redox lability, high reactivity, explosive character etc.) and computational studies, even with today's sophisticated techniques (e.g. NO compounds are often species with open-shell biradical character which requires the application of multi-configuration methods).

This chapter details the chemistry of nitrosomethanides and their corresponding acids and is primarily devoted to the subject as a whole and to its basic concepts, ranging from molecules to polymers, from synthesis to reaction mechanisms and from molecular to solid state structures, topics which are often aided by computational results.

B. Resonance Stabilized Methanides — A New Class of Pseudohalides

Halogens are important since these elements form compounds with the vast majority of the other elements in the periodic table. By means of easy concepts such as the pseudohalogen concept, correlation between structure, bonding and properties can be predicted for unknown compounds.

The term *pseudohalogen* was first introduced by Birckenbach and Kellermann[8a] in 1925 and further developed and justified in a series of papers of the Birckenbach group in the following years[8b–d]. Anions such as CN^-, CNO^-, N_3^-, OCN^- and SCN^- are regarded as *classical linear pseudohalides*. A small species can be classified as a classical pseudohalogen X when it fulfills the following criteria with respect to a halogen-like chemical behavior[9,10]. A pseudohalogen (X) forms

(i) a strongly bound (linear) univalent radical ($X^\bullet$),
(ii) a singly charged anion (X^-),
(iii) a pseudohalogen hydrogen acid of the type HX,
(iv) salts of the type $M(X)_n$ with silver, lead and mercuric salts of low solubility,
(v) a neutral dipseudohalogen compound (X–X) which disproportionates in water and can be added to double bonds, and
(vi) interpseudohalogen species (X–Y) with pseudohalogen Y.

However, not all criteria are always met. While many linear pseudohalogens (e.g. CN, OCN, CNO, N_3, SCN) are known, often the corresponding pseudohalide acids, dipseudohalogens and interpseudohalogens are thermodynamically highly unstable (e.g. HN_3, OCN–NCO, NC–SCN) with respect to N_2/CO elimination or polymerization or, indeed, remain unknown (e.g. $N_3{-}N_3$).

1. Classical linear and nonlinear pseudohalides

Starting from the binary nonmetal hydrides CH_4, NH_3, H_2O etc. a simple approach can be utilized to derive the hydrogen acids of the classical linear pseudohalides by combining or substituting isolobal (e.g. HC≡/≡N in HCN, HN=/=N=N in HN_3, HO−/−CN in HOCN), isosteric (e.g. N_2/CO in HN_3/HNCO) or isoelectronic fragments (e.g. CO/CS in HOCN/HSCN)[9].

Nonlinear resonance-stabilized pseudohalides can be derived with the help of the Grimm hydride displacement law, a pseudoelement concept established as early as 1925[11]. This law describes the formation of a new pseudoelement $^{\bullet}AH_n$ when nH ($n = 1–4$) atoms are formally added to the element A. The new complexes $^{\bullet}AH_n$ (e.g. $^{\bullet}OH$, $^{\bullet}NH_2$ and $^{\bullet}CH_3$) behave like pseudoatoms (in this case like halogens) similar to elements of the group n positions to the right in the periodic table (e.g. they form single charge anions: HO^-, H_2N^- and H_3C^-, or neutral dimers: HO−OH, $H_2N–NH_2$ and $H_3C–CH_3$). However, chemically there is a significant difference in the basicity (see Section VII) between these pseudohalides and the halides as the latter represent only very weak bases while these pseudohalides are strong bases. Only the successive substitution of the hydrogen atoms in $^{\bullet}CH_3$ (CH_3^-) and $^{\bullet}NH_2$ (NH_2^-) by electron-withdrawing groups such as CN, NO and NO_2 leads to the class of resonance-stabilized, nonlinear pseudohalogens (pseudohalides). Important also is the capability of the electron-withdrawing groups to delocalize the single p-AO-type lone pair (AO = atomic orbital) of the C and N atom in $^{\bullet}CH_3$ (CH_3^-) and $^{\bullet}NH_2$ (NH_2^-), respectively, and hence to decrease the basicity into the range of the halides. A compilation of all resonance-stabilized nitroso-methanides, $[R^1R^2C–NO]^-$ (R^1, R^2 = H, NO_2, NO and CN), is displayed in Table 1. With respect to feature (iii) of the characteristics of a pseudohalogen, the acid strengths of protonated resonance-stabilized methanides are in the range between medium and strong. Hence the corresponding acid (oxime, Scheme 1) should 'easily' be prepared by protonation of the methanides and *vice versa*.

2. Generalization

Substitution of H by electron-withdrawing groups (R) in CH_3/NH_2/OH resulting in new pseudohalogens CR_3^-, NR_2^- and OR^- is not limited to R = CN, NO or NO_2. All electron-withdrawing groups R which are capable of delocalization of the central carbon/nitrogen lone pair can be used (OR^-, $R'NR^-$, $R'CR_2^-$, $(R')_2CR^-$ with R = NO, NO_2, R′CO, $R'SO_2$, $(R')_2PO$, R′R″PO, C_6F_5, CF_3 etc; and R′, R″ = H, alkyl or aryl); additional variation and permutation of different groups also results in the formation of a pseudohalide (e.g. $NR'R''^-$, $CR'(R'')_2^-$, $C(R')_2R''^-$ and $CR'R''R'''^-$). More complex pseudohalides can also be constructed when linear or nonlinear pseudohalides are utilized, e.g. $HC(N_3)_2^-$, $C(N_3)_3^-$, $HC(C(CN)_3)_2^-$, $C(C(CN)_3)_3^-$, $C(NO)_3^-$ etc[12].

3. Extension of the pseudohalogen concept

The pseudohalogen concept can be extended (i) to some special nonplanar anions such as CF_3^-, (ii) to heavier elements (isovalence electronic exchange of O by S, Se, Te; of N by P etc. in SCN^-, $SeCN^-$, $TeCN^-$, $P(CN)_2^-$)[9,13] and (iii) to derivatives such as the five-membered ring anion $[CS_2N_3]^-$[14,15], which can be obtained in the reaction of carbon disulfide and sodium azide as shown by Sommer[16] as early as 1915. The introduction of heavier elements, however, results in weaker delocalization effects due to the formation of weaker π-bonds.

All species discussed in detail in the following sections represent *C*-nitroso compounds of the type $[R^1R^2C–NO]^-$ (R^1, R^2 = H, NO_2, NO and CN).

TABLE 1. Nitrosomethanides of the type $[R^1R^2C{-}NO]^-$ with R^1, R^2 = H, CN, NO, NO_2[17]

Acid[a]	Anion	Anion structure[b]	Reference	Abbreviation
$CH_3(NO)$	$[CH_2(NO)]^-$		6, 18	NM^-
$CH_2(NO)_2$	$[CH(NO)_2]^-$	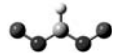	19	DNM^-
$CH(NO)_3$	$[C(NO)_3]^-$		not known	TNM^-
$CH_2(CN)(NO)$	$[CH(CN)(NO)]^-$	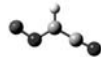	20	NCM^-
$CH_2(NO)(NO_2)$	$[CH(NO)(NO_2)]^-$		21	$NNtM^-$
$CH(CN)_2(NO)$	$[C(CN)_2(NO)]^-$		22	$NDCM^-$
$CH(CN)(NO)_2$	$[C(CN)(NO)_2]^-$		not known	$DNCM^-$
$CH(NO)(NO_2)_2$	$[C(NO)(NO_2)_2]^-$		23[c]	$NDNtM^-$
$CH(CN)(NO)(NO_2)$	$[C(CN)(NO)(NO_2)]^-$		24	$NNtCM^-$

[a] Formula displays no connectivity (!), we note for NO- and NO_2-substituted methanides protonation occurs preferentially at the O atom instead at the C atom leading to the formation of an oxime[25,26].
[b] Calculated structure at B3LYP/cc-aug-pvTZ level.
[c] $C(NO)_2(NO_2)^-$ is not known.

C. General Procedure for the Synthesis of Nitrosomethanides and Their Corresponding Acids

The classic synthetic approach to methanides involves the preparation of the free hydrogen acid which often is only generated *in situ*. Neutralization or a slightly basic work-up of the acid yields the corresponding methanide salt. In any case a nitrosation step is necessary. The method used depends on the chemical system (Figure 1)[7a]: (i) hydrocarbons and compounds with activated CH groups can be nitrosated by direct substitution of H in CH by NO[27], (ii) nitrosation of organometallic compounds is often carried out by substitution of a functional group by the nitroso group[28], (iii) addition reaction to −C=C−double bonds (e.g. addition of nitrosyl halides or oxides of nitrogen) is a useful way to introduce a nitroso group[29] and (iv) oxidation of other nitrogen-containing functional groups such as amino ($R{-}NH_2$)[30] or hydroxylamino groups ($R{-}NOH$)[31] also leads to *C*-nitroso compounds. Moreover, (v) *C*−NO compounds can be prepared from nitro

species ($R-NO_2$)[32] by direct reduction or (vi) in the reaction of free radicals with nitric oxide[1]. A short summary of nitrosation methods and reagents is given in Figure 1.

Most of the simplest formaldoximes are very labile at ambient temperature (often they are stable only at low temperatures) while their alkali and silver salts are stable in bulk due to kinetic stabilization. However, ***caution***: Although alkali and silver nitro- and nitrosomethanides are kinetically stable compounds, they are nonetheless energetic materials and appropriate safety precautions (e.g. a protection shield when dried substances are used, preparation of small quantities (<2 g), keeping these salts wet when stored) should be taken, especially when these compounds are prepared on a larger scale.

II. NITROSOMETHANIDES AND THEIR ACIDS

A. Mononitrosomethanide

1. Synthesis

As early as 1898 Dunstan and Bossi[6] described the formation of sodium mononitrosomethanide (sodium formaldoximate, $Na^+[H_2C{=}N{-}O]^-$) (**6**) in the reaction of the formaldoxime **2** with sodium metal in a dry ether solution (equation 1). The sodium salt of **6** is crystalline, very readily loses water forming sodium cyanide ($[H_2C{=}N{-}O]^- \rightarrow H_2O + CN^-$) and explodes when heated. Eight decades later Andersen and Jensen[18] prepared some unique transition metal complexes of the type $[M^{IV}(H_2CN{-}O)_6]^{2-}$ (M = Ni, Fe, Mn, V) via complexes of M^{2+} with trimeric **2** by oxidation with O_2 in strongly alkaline solution. According to their IR results, salts with trimeric anions of **2** ($[H_2CN{-}O]_3^{3-}$) are formed at the beginning, and then depolymerize into the anion of monomeric **2**. To the best of our knowledge these two papers are the only ones dealing with the synthesis and properties of mononitrosomethanide.

$$Na + H_2C{=}N{-}OH \xrightarrow{ether} {}^1/_2H_2 + Na^+[H_2C{=}N{-}O]^- \quad (1)$$
(**6**)

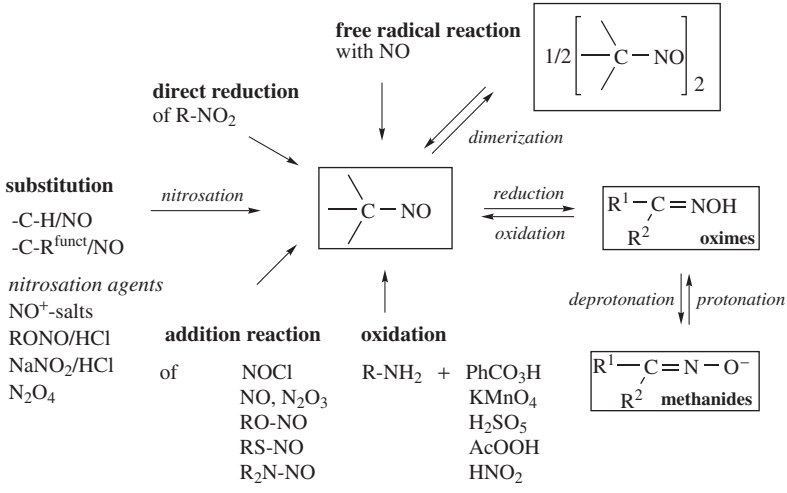

FIGURE 1. Synthetic routes to C-nitroso compounds

2. Structure and bonding[17,33]

So far no structural data of salts of **6** are available. A summary of the IR data in comparison with theoretically obtained data of salts is listed along with approximate assignments of the frequencies in Table 2. Two structural isomers of **6** were found at the potential energy surface of **6**, both planar with C_s symmetry: (i) $H_2C{=}NO^-$ (Figure 2A) and (ii) $[HC{=}N{-}OH]^-$ (Figure 2B). Since deprotonation at the oxygen is energetically preferred in **6**, $H_2C{=}NO^-$ represents the global minimum, 83.2 kJ mol^{-1} lower in energy than $[HC{=}N{-}OH]^-$ in which resonance of the π-electron density is much less pronounced. According to natural population analysis (NBO)[34] the best description of $H_2C{=}NO^-$ in the Lewis picture is the resonance of the four π-electrons as displayed in Figure 2A, in accord with the MO description as illustrated in Figure 3. The calculated partial charges are -0.67 at the oxygen, -0.14 at nitrogen and -0.45 *e* at the carbon atom. Hence, also

TABLE 2. Experimental[18] and calculated[33] vibrational frequencies (cm^{-1}) of **6**, IR intensities in parentheses (km mol^{-1})

	Approximate assignment of vibration	$[H_2C{=}N{-}O]^-$ calc [a]	$[H_2C{=}N{-}O]^-$ exp [b]	$[D_2C{=}N{-}O]^-$ exp	ν^H/ν^D
ν_1	C−H asym.	3149(55)	3064 m	2305 m	1.33
ν_2	C−H sym.	3079(117)	2943 m	2171 m	1.36
ν_3	C−N + CH_2 bending	1491(118)	1540 m	1493 m	1.03
ν_4	CH_2 bending + C−N	1358(282)	1373 s	1027 m	1.34
ν_5	N−O + CH_2 rocking	1212(112)	1196 s	1107 s	1.08
ν_6	CH_2rocking + N−O	1069(185)	998 vs,br	896 s,br	1.11
ν_7	CH_2 twisting	779(11)	876 s	711 m	1.23
ν_8	CH_2 waging	652(74)	752 w	578 w	1.30
ν_9	C−N−O bending	567(6)	574 w	505 w	1.14

[a] B3LYP/aug-pvTZ.
[b] The assignment has been changed in comparison with the calculated data set.

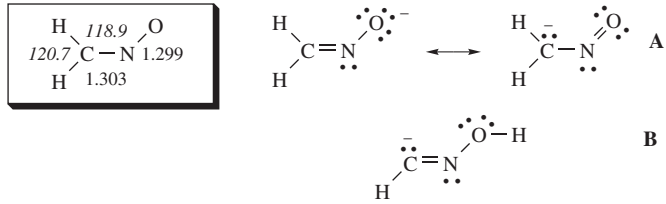

FIGURE 2. Structure (B3LYP/aug-cc-pvTZ) and bonding (VB) in isomers of **6** (distances in Å, angles in deg)

FIGURE 3. Calculated π-MOs (A'' symmetry) of **6** displaying the delocalization of four π-electrons

from the electrostatic point of view protonation at the oxygen in **6** is energetically preferred at the oxygen leading to formaldoxime, whereas protonation at the carbon would give nitrosomethane (Scheme 1).

B. Acids of Mononitrosomethanide

1. Synthesis

Formally, protonation of **6** might lead to five different acids according to Scheme 1. The most stable acid is formaldoxime. All tautomeric isomers can formally be derived from either 1,3- or 1,2-hydrogen shifts (pathway A or B, Scheme 2)[35].

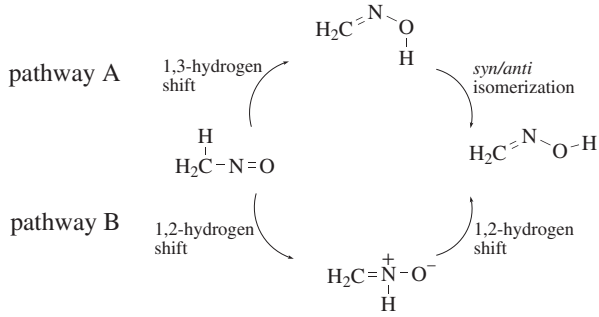

SCHEME 2. Hydrogen shifts on the potential energy surface of $H_3C{-}NO$ resulting in four tautomers

Formaldoxime (**2**), $H_2C{=}NOH$, the simplest member of the oxime family and a rare example of a small molecule containing a C=N bond, was first reported in 1891 by Scholl[5]. He succeeded in isolating **2** in the condensation reaction of formaldehyde and hydroxylamine leading to white, amorphous solid $(H_2CNOH)_n$. Furthermore, he speculated that this polymer is composed of trimeric **2**. By gentle heating (100–134 °C) of polymeric **2** Scholl obtained monomeric **2** as a vapor and also in solution, while at high temperatures instantaneous decomposition $H_2C{=}NOH \rightarrow H_2O + HCN$ took place. From the properties of the solution he could show that **2** acts as a powerful reducing agent in solution of many metallic salts: silver, gold and mercury being precipitated as metals. Formaldehyde and hydroxylamine are formed upon hydrolysis.

Pure monomeric **2**, isolated by extraction with ether shortly after combining aqueous solutions of formaldehyde and hydroxylamine, is a liquid with a boiling point of 83–85 °C which burns with a livid flame, producing considerable quantities of hydrogen cyanide (see equation above)[6]. This liquid very rapidly polymerizes, yielding a white amorphous solid which could not be re-crystallized. In the absence of water **2** combines with mineral acids to form salts of the type $(H_2CNOH)_3{\bullet}HX$ (X = e.g. halogen), which are substantially more stable. These hydrohalides of trimeric **2** can be used to generate pure **2** when dissolved in water and exactly neutralized. Jensen and Holm pointed out that trimeric formaldehyde oxime ('triformoxime') is actually a chain polymer analogous to paraformaldehyde[36], while the acetyl and benzoyl derivatives of **2** are derivatives of cyclic trimers. Cyclic trimeric **2** exists only as the hydrochloride and depolymerizes on neutralization to give monomeric **2**. NMR studies showed that the hydrochloride of cyclic trimeric **2** dissociates and an equilibrium exists between monomeric and trimeric **2** which, at higher pH values, is shifted towards the monomeric form. Hence, monomeric **2** can be extracted with ether at pH = *ca* 8 but in HCl only the trimer is formed as hydrochloride (Scheme 3)[37].

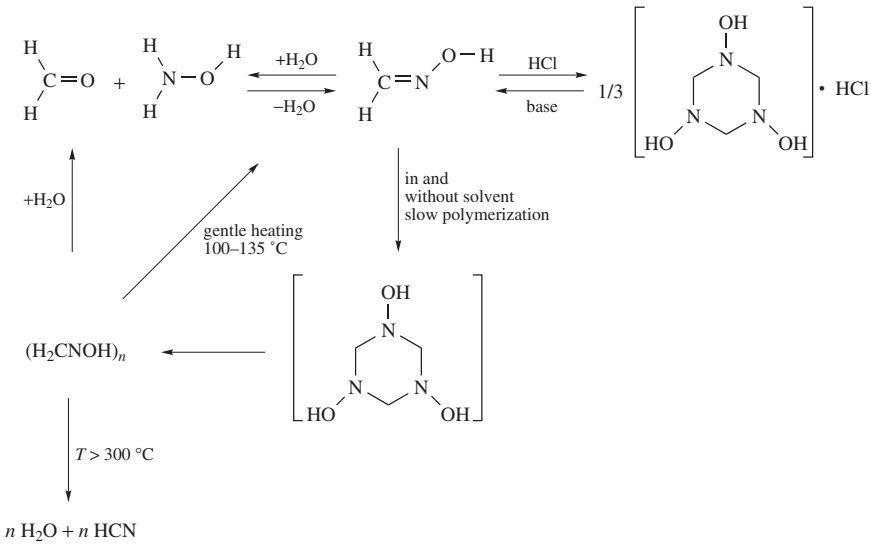

SCHEME 3. Synthesis of monomeric and polymeric **2**

TABLE 3. Experimental and calculated vibrational frequencies (cm^{-1}) of monomeric *anti*-**2** (see Figure 4), IR intensities in parentheses ($km\,mol^{-1}$)

	Approximate assignment of vibration	exp[42]	BLYP/ 6-311+G(d)[43]	B3LYP/ aug-cc-pvTZ[33]	MP2/ 6-311+G(d)[43]
$\nu_1(A')$	O−H	3646	3678(78)	3811(92)	3880(103)
$\nu_2(A')$	CH_2 asym.	3106	3138(4)	3221(3)	3296(2)
$\nu_3(A')$	CH_2 sym.	2969	3013(8)	3094(6)	3155(3)
$\nu_4(A')$	C−N	1647	1625(8)	1712(6)	1671(5)
$\nu_5(A')$	CH_2 bending	1410	1402(10)	1451(14)	1463(10)
$\nu_6(A')$	O−H bending	1318	1294(86)	1349(81)	1351(87)
$\nu_7(A')$	CH_2 rocking	1166	1131(7)	1178(11)	1189(6)
$\nu_8(A')$	N−O	888	823(129)	909(128)	939(107)
$\nu_9(A')$	C−N−O bending	530	514(7)	536(7)	537(6)
$\nu_{10}(A'')$	CH_2 waging	950	931(39)	986(34)	967(42)
$\nu_{11}(A'')$	CH_2 torsion	769	767(10)	800(7)	800(6)
$\nu_{12}(A'')$	O−H torsion	400	421(136)	438(125)	370(148)

The existence of monomeric **2** has been proven unequivocally by microwave studies and vibrational spectroscopy. The IR and Raman data are listed in Table 3. The *anti* configuration is the energetically preferred isomer (see Figure 4 below).

Oxime **2** has been extensively used only as an analytical reagent (determination of manganese by photometry)[38], jet-fuel additive[39] and more recently in polymer synthesis[40].

Schorpp and Beck reacted formaldoxime with $Pt(PPh_3)_4$ yielding, analogous to the reaction with nitromethane, a cyano complex as depicted in Scheme 4[41]. The Pt−H complex that is involved in the first reaction step was identified by its IR spectrum with the help of the ν_{Pt-H} vibrational mode at 2220 cm^{-1}.

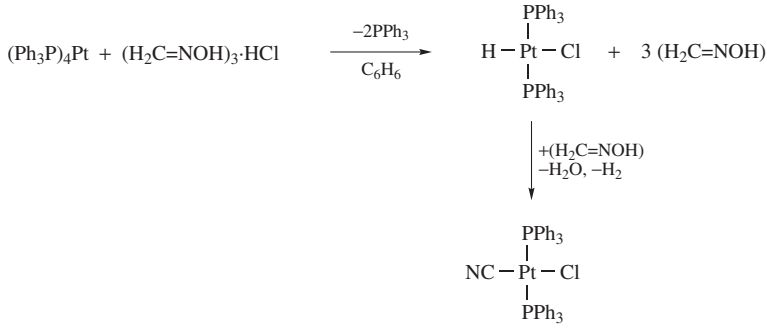

SCHEME 4. Reaction of $Pt(PPh_3)_4$ with formaldoxime

Nitrosomethane (**1**) is known to be less stable than its isomer formaldoxime **2** and original attempts to isolate this species failed owing to its facile isomerization to the oxime **2**. Already Bamberger and Seligman considered in 1903 that it would be difficult to isolate nitrosomethane after oxidation of methylamine due to its rapid isomerization to **2**[44]. Hence, **2** is always present in the synthesis of the nitrosomethane. Nitrosomethane is produced in the pyrolysis or photolysis of *tert*-butyl nitrite and by the reaction of methyl radicals with nitric oxide. Early results were confusing since the final product obtained is dimeric nitrosomethane. It was first isolated in 1948 by Coe and Doumani[1] from the photolysis of gaseous *tert*-butyl nitrite according to the overall reaction shown in equation 2.

Batt, Gowenlock and Trotman carried out a detailed study of the pyrolysis and photolysis of *tert*-butyl nitrite and established that dimeric nitrosomethane exists in two isomeric forms, *cis* and *trans* (Scheme 5). Monomeric nitrosomethane could be generated by heating the dimer in the gas phase (the activation energy for dissociation was found to be *ca* 90 kJ mol^{-1})[45]. Also ultraviolet irradiation dissociates the dimer, leaving monomeric **1**. Vibrational analysis of monomeric **1** is summarized in Table 4.

$$(CH_3)_3CONO \xrightarrow{h\nu} (CH_3)_2CO + CH_3NO \qquad (2)$$

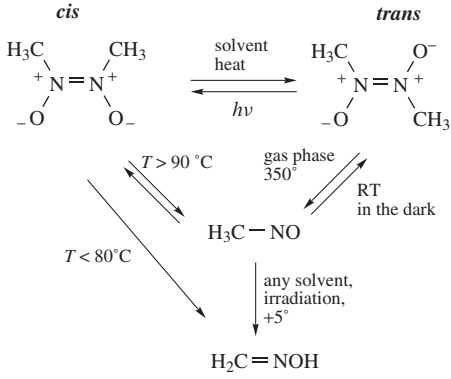

SCHEME 5. Reactions of nitrosomethane

TABLE 4. Experimental and calculated vibrational frequencies (cm^{-1}) of monomeric nitrosomethane, IR intensities in parentheses ($km\,mol^{-1}$)

	Approximate assignment of vibration	Exp[48]	B3LYP/ aug-cc-pvTZ[33]
$\nu_1(A')$	C−H asym.	2991 m	3126(11)
$\nu_2(A'')$	C−H asym.	2955 m	3095(2)
$\nu_3(A')$	C−H sym.	2901 m	3019(2)
$\nu_4(A')$	N−O	1549 s[a]	1654(85)
$\nu_5(A')$	CH_3 asym. deformation	1410 s	1453(27)
$\nu_6(A'')$	CH_3 asym. deformation	1410 s	1450(12)
$\nu_7(A')$	CH_3 sym. deformation	1348 s	1371(26)
$\nu_8(A')$	CH_3 deformation	967 w	1152(19)
$\nu_9(A'')$	CH_3 deformation	916 m	971(2)
$\nu_{10}(A')$	C−N	870 m	842(28)
$\nu_{11}(A')$	C−N−O bending	574 m	577(1)
$\nu_{12}(A'')$	Torsion	146	167(1)

[a] 1564 cm^{-1} according to Shimanouchi[46]; value taken from Reference[47].

For the photolysis of *tert*-butyl nitrite a possible reaction mechanism (Scheme 6) consists of the production of *tert*-butoxy radicals (equation 3), followed by their decomposition to give acetone and methyl radicals (equation 4). The latter are trapped by the nitric oxide liberated in the first step (equation 5). However, the absence of ethane production in the actual experiments suggested that an intramolecular formation of nitrosomethane is unlikely[6,48].

$$(CH_3)_3CONO \xrightarrow{h\nu} (CH_3)_3CO^{\bullet} + {}^{\bullet}NO \tag{3}$$

$$(CH_3)_3CO^{\bullet} \longrightarrow (CH_3)_2CO + CH_3^{\bullet} \tag{4}$$

$$CH_3^{\bullet} + {}^{\bullet}NO \longrightarrow CH_3{-}NO \longrightarrow 1/2(CH_3{-}NO)_2 \tag{5}$$

SCHEME 6. Possible reaction mechanism for the formation of nitrosomethane in a free radical reaction

Formaldonitrone[3], $CH_2{=}N(H){-}O$ (**3**), the elusive simplest organic nitrone, has been prepared transiently in the gas phase by femtosecond collisional neutralization of its cation radical, $CH_2{-}N(H){-}O^{+\bullet}$. The latter was generated by dissociative ionization of 1,2-oxazolidine. Nitrone **3** showed negligible dissociation upon collisional neutralization and was distinguished from its tautomers formaldoxime **2** and nitrosomethane **1** that gave different NR mass spectra. The enthalpy of formation was calculated from enthalpies of atomization and two isodesmic reactions as $\Delta_f H_{298}(\mathbf{3}) = 58 \pm 1\ kJ\,mol^{-1}$. The calculated, large activation barriers for isomerization of **3** (179 and 212 $kJ\,mol^{-1}$ for $\mathbf{3} \rightarrow$ *anti*-**2** and $\mathbf{3} \rightarrow \mathbf{1}$, respectively)[49] indicate that once **3** is formed and diluted in the gas phase it should not isomerize unimolecularly to either **1** or (*syn*/*anti*) **2**.

2. Structure and bonding[17,33]

Since formaldoxime **2** is stable in the gas phase it is more easily studied experimentally than nitrosomethane. Experimental structural data are only available for formaldoxime **2**

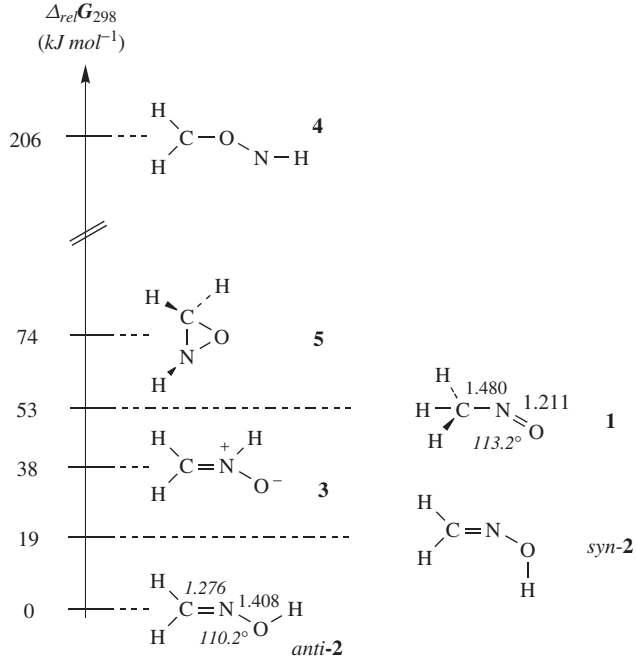

FIGURE 4. Relative energies of CH_3NO isomers along with experimental structural data (distances in Å) of microwave studies

and monomeric and dimeric nitrosomethane **1**. Exploration of the potential energy surface displayed that the formaldonitrone, CH_2=N(H)–O (**3**), is close in energy to **1** (Figure 4). However, experimental access to **3** is rather difficult, preventing an experimental structural analysis[3]. Based on a series of *ab initio* and DFT calculations[3,49,50], formaldoxime represents the lowest-lying isomer in its *anti* conformation followed by the *syn* structure. Some papers predicted the nitrone **3** to be less stable than nitrosomethane, whereas recent papers indicated that **1** and **3** were comparable in energy, with **3** slightly more stable[3,49,50]. Other N–O bonds containing isomers (e.g. isonitrosomethane **4** and oxaziridine **5**, Figure 4) were calculated to be substantially less stable. There have been several other theoretical studies[51] but for reasons of consistency only the B3LYP/aug-cc-pvTZ level will be discussed in comparison with the experimental data[33].

Formaldoxime (**2**) has been shown to have a planar structure with C_s symmetry (Figures 1 and 4). Experimental and theoretical studies found the *anti* conformer (*anti*-**2**) to have the lower energy (with $\Delta_{syn-anti}E = ca\ 24.2$ kJ mol^{-1}), which may reflect the lone-pair–lone-pair repulsion between oxygen and nitrogen atoms. The *anti–syn* internal rotational barrier is about 38–42 kJ mol^{-1} depending on the level of theory applied[33,43,52].

The gas-phase structure was determined by Levine[53] using microwave spectroscopy. In agreement with a double bond localized along the CN moiety, a short CN distance of 1.276 Å was determined, while the N–O distance of 1.408 Å is rather long displaying a single bond, with a small amount of π-bonding (cf. Σr_{cov}(N–O) = 1.45 Å vs. Σr_{cov}(N=O) = 1.17 Å)[54]. In agreement with these structural features NBO analysis[34] localizes a double bond between carbon and nitrogen in the best Lewis representation of

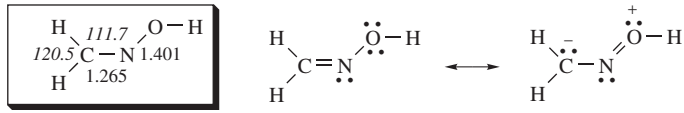

FIGURE 5. Structure (B3LYP/aug-cc-pvTZ) and bonding (VB) in isomers of *anti*-**2** (distances in Å, angles in deg)

2. Inspection of delocalization effects shows the interaction of one lone pair at oxygen (localized perpendicular to the molecule plane) with the antibonding π^*-bond orbital of the CN bond (estimated energy gain *ca* 84 kJ mol^{-1}) corresponding to the resonance hybrid shown in Figure 5.

A most interesting feature of the experimentally determined structure in *anti*-**2** is the 6.2° difference between the *cis*- and *trans*-H−C−N angles (*cis*-H−C−N 121.5°, *trans*-H−C−N 115.3°, *cis* and *trans* refer to the position of an H atom of the CH_2 group relative to the O atom). Structural analyses of oximes have given 10° or even 15° between *cis* and *trans* CCN bond angles in oximes. The large difference in acetoxime, for instance, was attributed to steric repulsion between the *cis* methyl group and the oxygen atom[55]. Although the distance between the *cis* hydrogen and the oxygen in **2** is about 0.2 Å less than the sum of the van der Waals radii, it is quite unlikely that steric repulsion is solely responsible for the 6.2° angle difference.

Upon deprotonation, the CN distance (**2**: 1.265 vs. **6**: 1.303 Å) increases while the NO distance decreases (**2**: 1.401 vs. **6**: 1.299 Å) due to a better delocalization of the four π-electrons (cf. Figures 2 and 3, and 5 and 6) in the anion. However, even in the protonated species, in the oxime **2**, there is still a considerable amount of delocalization of the π-electrons as depicted in Figures 5 and 6. The calculated NPA overall charges are $q_C = -0.19$, $q_N = -0.13$ and $q_O = -0.59$ *e*.

Monomeric nitrosomethane (**1**). The gas-phase structure of **1** as determined by Turner and Cox is shown in Figure 4. The microwave spectra of ten isotopic species of nitrosomethane have been measured, enabling structures of CH_3−NO and CD_3−NO to be determined independently[56]. This study established the methyl group conformation as eclipsing, the nitrosyl bond with rather short NO bonds [d(N−O) = 1.211 Å vs. 1.408 Å in **2**] and a long CN bond [d(C−N) = 1.480 Å vs. 1.276 Å in **2**] contrary to **2**. The value of the NO distance corresponds to a bond order for a strong double bond. Thus, strong delocalization as found in **2** is not possible, being one of the reasons for dimerization and isomerization. Indeed, the CN bond is destabilized by hyperconjugation (Figure 7). As indicated by NBO analysis[34], there is a significant interaction of the in-plane lone pair on the oxygen atom with the unoccupied, antibonding σ^*-orbital of the C−N bond. This n(O) → σ^*(N−C) donor–acceptor interaction (energy gain of 72.7 kJ mol^{-1}) accounts for the rather long N–C bond and the eclipsed conformation as well as the strengthening of the NO bond.

FIGURE 6. Calculated π-MOs (A'' symmetry) of *anti*-**2** displaying the delocalization of four π-electrons

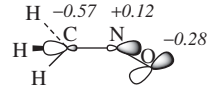

FIGURE 7. $n(O) \rightarrow \sigma^*(N-C)$ donor–acceptor interaction in **1** and calculated NPA charges

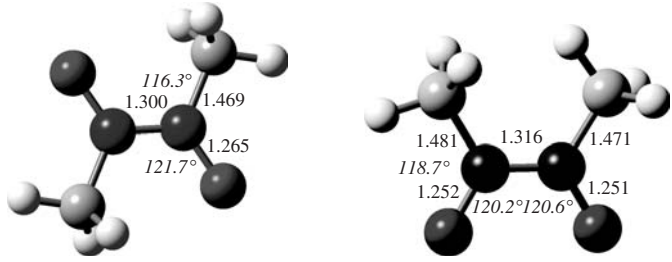

FIGURE 8. Calculated structures of *trans* (C_{2h}) and *cis* (C_s) dimer of CH_3NO (distances in Å)

The *dimer of nitrosomethane* (azo-dioxide), $(CH_3NO)_2$, exists at ambient temperatures in two isomeric forms, *cis* and *trans* (Figure 8), which undergo isomerization relatively easily. *Trans*-$(CH_3-NO)_2$, having a planar azo-dioxide moiety, crystallizes in the orthorhombic space group *C*mcm with $Z = 4$. The experimentally determined bond lengths are $d(N-O) = 1.25$ and $d(N-C) = 1.57$ Å, respectively (calculated data, see Figure 8)[57].

Comparison with other dimers, RN(O)−N(O)R, of substituted nitrosomethanes shows generally that the central *trans*-dimeric framework, as judged from the N−N and N−O bond lengths, is perturbed to only a minor extent by changes in the nature of the substituent R. It is also apparent that the ease of dissociation to monomer is not reflected in the N−N lengths in the dimer, as would be expected from consideration of theoretical studies of the dissociation reaction[58]. For the values of N−N distance in $(CH_3NO)_2$, Gowenlock and coworkers reported two different values, 1.31 and 1.22 Å[59]. The latter value determined by van Meerssche and Germain[57] seems to be too short while 1.31 Å is in the range of other N−N distances found in dimers of substituted nitrosomethanes RN(O)−N(O)R (e.g. 1.309 Å for R = *t*-Bu). In any case N−N distances in the range 1.22–1.32 Å indicate a bond order between a double and single bond in agreement with NBO analysis (Figure 9)[34]. Kinetic investigations of nitrosomethane and nitrosoethane show that the dissociation energy in the gas phase is as low as 66.9 kJ mol^{-1} for the former and 62.7 kJ mol^{-1} for the latter compound[60].

The *trans* isomer turned out to be favored over the *cis* isomer by 41.8 kJ mol^{-1} at B3LYP/aug-cc-pvTZ level of theory. In both isomers the C−N−O moiety is strongly polarized. The charges are +0.24 *e* for both nitrogens and −0.50 and 0.51 *e* for both

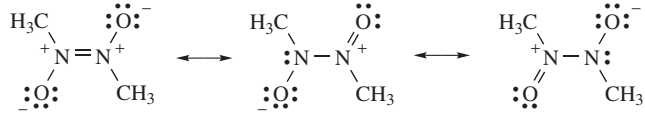

FIGURE 9. Resonance scheme for dimeric *trans* nitrosomethane

carbon and oxygen atoms, respectively (charges of the *trans* isomer). According to NBO analysis, the bonding is best described by resonance of 6π-electrons according to Figure 9[34].

C. Dinitrosomethanides (7)

1. Synthesis

In a series of papers almost a century ago, Wieland and coworkers described the synthesis of alkali and silver nitrosolates (M[RC(NO)$_2$], M = metal, R = organic substituent)[61]. These nitrosolates can be obtained from unstable *N*,*N*′-dihydroxyamidines by disproportionation in ammonia (Scheme 7) or by oxidation (KIO_4) in basic solution[62,63]. For R = H these procedures result in the formation of, e.g., potassium dinitrosomethanide, the simplest nitrosolate, when potassium hydroxide is used as base.

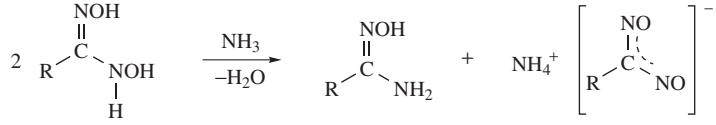

SCHEME 7. Nitrosolate synthesis of Wieland and coworkers

A recently published new synthesis of dinitrosomethanides salts (DNM = *din*itroso*m*ethanide) starts from formamidinium nitrate (**8**), which represents an easily accessible source for an NC(H)N unit[19]. Treating a methanolic solution of **8** and hydroxylammonium nitrate (two equivalents) with a methanolic solution of KOBu-*t* (two equivalents) results in the formation of the labile intermediate *N*,*N*′-dihydroxyformamidinium nitrate (**9**) (Scheme 8). The reaction of **9** with MOBu-*t* (two equivalents, M = alkali metal) in the presence of oxygen yields the deep blue alkali DNM salt (**7**), which can easily be purified by recrystallization from methanol (yield 60–70%)[19].

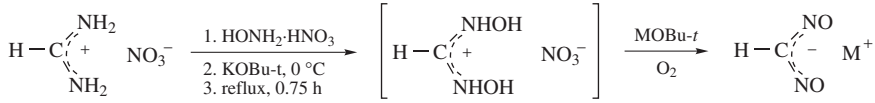

(**8**) (**9**) (**7**)

SCHEME 8. Synthesis of DNM salts (M = alkali metal)[19]

Via pure KDNM, all other alkali (or ammonium) DNM^- salts can be obtained (i) by ion exchange or (ii) by release of the methyl nitrosolic acid when a water solution of KDNM is buffered with H_3PO_4 (pH = 6.5) followed by low-temperature extraction with diethyl ether and a basic work-up (equations 6 and 7):

$$KHC(NO)_2 + H_3PO_4 \longrightarrow HON{=}C(NO)H + KH_2PO_4 \qquad (6)$$

$$HON{=}C(NO)H + [N(CH_3)_4][OH] \bullet (H_2O)_5 \longrightarrow [N(CH_3)_4][HC(NO)_2] + 6\ H_2O \qquad (7)$$

Pure dry alkali DNM salts are stable at ambient temperature, are heat and shock sensitive, and decompose slowly in polar solvents releasing N_2O gas. Small amounts of impurities (e.g. KNO_3) considerably decrease the shock and heat sensitivity. Combined IR and MS

TABLE 5. Calculated and experimental (Raman, IR in cm^{-1}) data of DNM anion (**w_*C*$_{2v}$**-isomer, see Figure 12)

Approx. assign.	B3LYP/ Aug-cc-pvTZ [a]	Na[HC(NO)$_2$]		K[HC(NO)$_2$]		Cs[HC(NO)$_2$]	
		Raman [b]	IR [c]	Raman [b]	IR [c]	Raman [b]	IR [c]
ν_{CH}	3036(71,115)	3025(2)	2990(w)	2990(1)	2989(w)	2971(1)	2980(w)
$\nu_{s,NO}$	1431(0,104)	1404(4)	—	1390(3)	—	1381(4)	—
$\nu_{as,CN}(+\delta_{CH})$	1412(83,0)	—	1402(sh)	—	1400(sh)	—	1405(sh)
$\nu_{as,NO}$	1326(827,0)	—	1386(s)	—	1384(s)	—	1386(s)
$\nu_{s,CN}$	1309(10,30)	1305(9)	1291(s)	1306(10)	1293(s)	1302(9)	1290(s)
		—	1276(vs)	—	1271(s)	—	1273(s)
		—	1245(s)	—	1244(vs)	—	1245(vs)
δ_{CH}	1174(398,12)	1188(0.8)	1183(s)	—	1185(s)	—	—
		—	1164(s)	—	—	1141(1)	1168(s)
		1111(0.8)	1133(vs)	1132(2)	1130(vs)	1119(2)	1133(vs)
γ_{CH}	864(17,2)	856(0.2)	858(s)	860(0.5)	858(s)	872(0.3)	858(m)
δ_{ONCNO} (rocking)	631(50,0)	—	629(m)	—	628(m)	—	629(m)
δ_{NCN} (bending)	573(1,26)	581(10)	—	577(8)	—	572(10)	—
γ_{NCN}	424(0,0)	—	—	—	—	—	—
δ_{ONCNO} (bending)	291(7,1)	141(3)	—	144(2)	—	148(1)	—
γ_{ONCNO}	200(10,1)	117(2)	—	120(3)	—	124(1)	—

[a] In parentheses: (IR intensities in km mol^{-1}, Raman activities in $Å^4$ AMU^{-1}).
[b] Raman intensity scaled (1–10).
[c] vs, very strong; s, strong; m, medium; w, weak; vw, very weak; sh, shoulder.

pyrolysis experiments revealed that the only gaseous products formed are N_2O, NO and HCN.

KDNM undergoes an exothermic decomposition (explosion, $\Delta H = -233.2$ kJ mol^{-1}) with an onset of 168.56 °C ($\beta = 5$ °C/min) in a temperature range of 168–186 °C and an estimated activation energy of *ca* 200.6 kJ mol^{-1}. It is assumed that the presence of a delocalized π-system probably accounts for the remarkable kinetic stability of **7** (see below). Introduction of bulky cations such as R_4N^+ or imidazolium cations significantly stabilizes DNM salts.

Especially Raman and IR spectroscopy are suitable to identify DNM salts very rapidly with the help of the in-phase and out-of-phase NO stretching mode at roughly 1400 and 1390 cm^{-1}, respectively (Table 5); the C−H stretch can be observed at *ca* 3000 cm^{-1}. The ^{13}C and ^{1}H NMR spectra show a singlet resonance at 190 ppm and 8.7 ppm, respectively. The ^{14}N NMR spectrum displays a resonance at 332 ppm, which is the typical range of NO compounds (e.g. K[(ON)C(CN)$_2$]: 381 ppm)[64].

As shown in the introduction, the DNM anion can be regarded as a resonance stabilized, nonlinear planar pseudohalide, which forms an insoluble, highly explosive brownish silver salt upon addition of silver nitrate to an aqueous solution of **7**. The DNM anion is related to the linear fulminate ion (CNO^-) and can formally be regarded as the addition product of NO^- to fulminic acid (HCNO). Starting from CH_4, NO containing nonlinear pseudohalides can be derived by successive substitution of H by NO, e.g. $H_3C(NO)/H_2C(NO)^-$, $H_2C(NO)_2/HC(NO)_2^-$ and $HC(NO)_3/C(NO)_3^-$, whereas the linear pseudohalide CNO^- is formally formed by replacing three H atoms by one NO unit and deprotonation.

2. Structure and bonding

All alkali and ammonium DNM salts have been prepared and characterized. Solid state structures of the potassium, cesium, tetramethylammonium and a potassium crown-ether complex of DNM are available[12, 19].

KDNM crystallizes in beautiful Prussian blue octahedra in the tetragonal space group $I\bar{4}\ 2d$ with eight units per cell. The structure consists of an infinite three-dimensional network of repeating $K[HC(NO)_2]$ units. Each anion is bonded to seven potassium cations and *vice versa* (Figure 10). The oxygen atom is coordinated to three potassium cations with K−O bond distances of 2.803(1), 2.849(1) and 2.887(2) Å. The nitrogen atom is coordinated to two neighboring potassium ions with K−N bond distances of 3.070(2) and 3.148(2) Å. Three types of coordination modes are found: (i) monodentate via the O atom, (ii) bidentate via NO and (iii) bidentate via the two N atoms (N,N' coordination of the NCN unit). As shown in Figure 10, each potassium ion is surrounded by four nitrogen and six oxygen atoms. The bonding interaction of the anion with seven neighboring potassium ions leads to the three-dimensional network arrangement of the ions. Changing the coordination environment on potassium by introducing a crown ether (18-crown-6), linear chains of repeating K(18-crown-6)$[HC(NO)_2]$ units are observed in the solid state instead of the three-dimensional network (Figure 11). The cesium salt crystallizes in the monoclinic space group $P2_1/c$ and also exhibits a three-dimensional network arrangement. The anion is also bonded to seven Cs ions, whereas the cesium is surrounded by 13 donor atoms (5 times bidentate via NO, one N,N' coordination of the NCN unit and one monodentate O atom).

In principle, three different planar structures of DNM^- are possible: (i) the *anti/anti* arrangement (as shown in Figure 10), (ii) the *syn/anti* and (iii) the *syn/syn* arrangement (Figure 12)[19]. In agreement with the experiment B3LYP/aug-cc-pvTZ calculation revealed that the *anti/anti* form represents the most stable isomer followed by the *syn/anti* ($+31.4\ kJ\,mol^{-1}$) and the *syn/syn* isomer ($+54.8\ kJ\,mol^{-1}$), in accord with increasing electrostatic repulsion between lone pairs localized on the oxygen atoms. As expected, the N−O distances [KDNM: 1.264(2); CsDNM: 1.277(3), 1.268(3) Å] are significantly smaller than the C−N distances [KDNM: 1.321(2); CsDNM: 1.333(4), 1.338(4) Å].

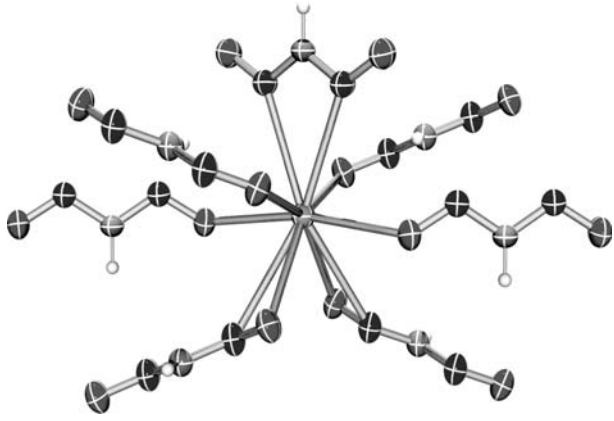

FIGURE 10. View of K^+ coordination environment in KDNM (N black, O gray, C dark gray, K central atom, H light gray)

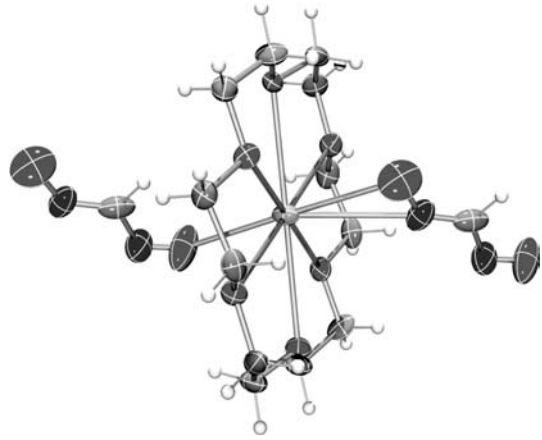

FIGURE 11. View at a small section of the linear chains in K(18-crown-6)[$HC(NO)_2$] (N black, O gray, C dark gray, K central atom, H light gray)

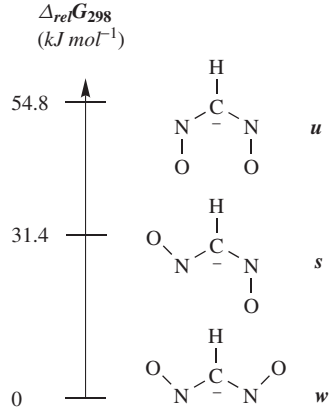

FIGURE 12. Isomers (***s***: C_s symmetric *syn/anti,* ***u***: C_{2v} symmetric *syn/syn*, ***w***: C_{2v} symmetric *anti/anti* arrangement) of the DNM anion

These bond lengths together with the planarity indicate the presence of delocalization of a double bond over the whole anionic species. MO and NBO calculation revealed the existence of a 6π-electron 5-center bond unit (Figures 13 and 14)[34].

In Figure 14, formulae **A** and **B** represent the energetically preferred Lewis representations of DNM according to NBO analysis[34]. Investigation of the intramolecular donor–acceptor interactions, utilizing the NBO partitioning scheme, clearly indicates a highly delocalized 6π-electron system according to resonance between Lewis representations **A** ↔ **B** ↔ **C**. The calculated natural atomic orbital population (NAO) net charges are $q(O) = -0.524$, $q(N) = -0.043$, $q(C) = 0.008$ and $q(H) = 0.126$ e, which means that the negative charge is mainly found on both oxygen atoms.

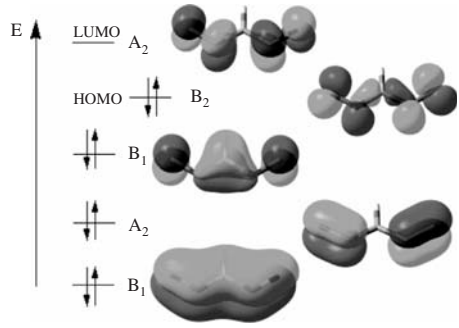

FIGURE 13. Schematic MO diagram of DNM

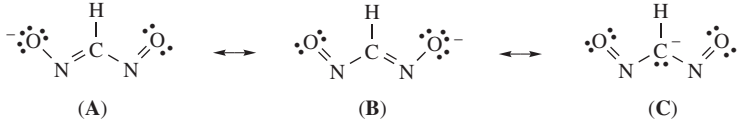

FIGURE 14. Lewis representation of DNM according to NBO analysis[34]

TABLE 6. Experimental (λ_{max} [ε in $cm^2\,mmol^{-1}$]) and calculated (B3LYP/6-311G(3df,2p)) electronic transitions of the C_{2v} (*anti/anti*) isomer (including solvent effects, methanol)

Excitation energies (λ_{max} in nm)		eV	Oscillator strengths	Excited state	Ground → excited state	Coefficient	
exp	calc						
679 [37]	681.50	1.8193	$f = 0.0005$	$^1B_1$	19 → 20	0.65295	$n \rightarrow \pi^*$
503 [32]	568.41	2.1812	$f = 0.0000$	$^1A_2$	18 → 20	0.66089	$n/\sigma \rightarrow \pi^*$
331 [1503]	254.55	4.8709	$f = 0.4224$	$^1B_2$	17 → 20	0.54099	$\pi \rightarrow \pi^*$
					19 → 22	0.15224	
—	239.38	5.1793	$f = 0.0000$	$^1A_2$	19 → 21	0.69084	$n \rightarrow \pi^*$
224 [118]	222.81	5.5644	$f = 0.0002$	$^1B_1$	18 → 21	0.69085	$n/\sigma \rightarrow \pi^*$

The UV-Vis spectra of the deep purple methanolic solution of alkali DNM salts exhibit one very strong characteristic $\pi \rightarrow \pi^*$ and two weak $n \rightarrow \pi^*$ electronic transitions at *ca* 331, 503 and 679 nm, respectively, which could be assigned on the basis of TD-B3LYP calculation (Figure 13, Table 6). The purple color arises from the two weak $n \rightarrow \pi^*$ electronic transitions[63].

D. Acids of Dinitrosomethanides

1. Synthesis

Wieland was the first who studied nitrosolic acids[61]. He was especially interested in the simplest member of this group, the methylnitrosolic acid, ON−C(H)=NOH (**10**), because he already thought of the dioxime of carbon dioxide, HO−N=C=N−OH, which is an intriguing isomer of methylnitrosolic acid. Wieland tried first the reaction sequence in

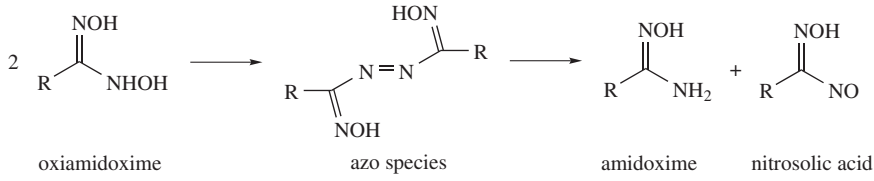

SCHEME 9. Mechanism for the synthesis of nitrosolic acids proposed by Wieland[61]

Scheme 9 to synthesize **10** which, however, did not work although successfully utilized for the generation of other nitrosolic acids.

Since the direct oxidation failed, Wieland used Nef's methods[65] to synthesize 'oxyisuretin' (formoxyamidoxime), which is generated *in situ* when formamidoxime, $HC(=NOH)NH_2$, is gently heated with hydroxylamine hydrochloride in methanol (Scheme 10). Oxyisuretin is only stable in solution and gives methylnitrosolic acid and formamidoxime (Scheme 11) upon treatment with an alcoholic solution of KOH.

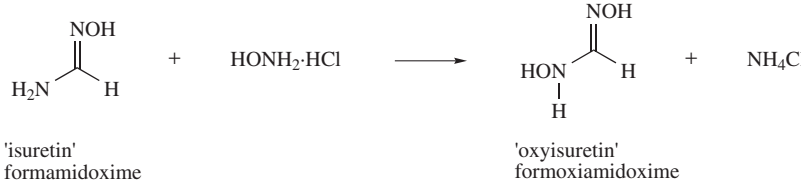

SCHEME 10. Synthesis of 'oxyisuretin' starting from 'isuretin'

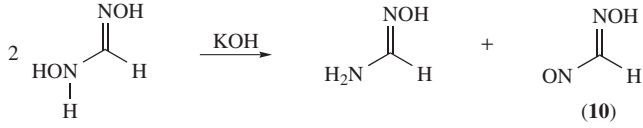

SCHEME 11. Decomposition of 'oxyisuretin' in alkaline solution

The easiest way to **10** goes via the synthesis of KDNM (see Section II.C). Acidification of an aqueous solution of KDNM, which should be buffered with H_3PO_4 (pH = 6.5), followed by low-temperature extraction with diethyl ether, gives the monomeric emerald-green nitrosolic acid **10** dissolved in the ether phase. Slow removal of the solvent yields the yellowish dimeric form of **10**. The acid (**10**) is only poorly characterized. It is known to slowly decompose into HCN and HNO_2 in basic solution (decomposition of the anion DNM), while the free acid (**10**) rapidly decomposes to give fulminic acid, HCNO and hyponitrous acid, HON=NOH. It should be noted that both the free acid and its metal DNM salts are *highly explosive*.

2. Structure and bonding

Protonation of DNM might lead to three different tautomers: (i) dinitrosomethane ($H_2C(NO)_2$) when the protonation occurs at the carbon (ketonic isomer)[66], (ii) methylnitrosolic acid (**10**) when one of the oxygen atoms of the nitroso groups forms an oxime (enolic isomer) and (iii) a dioxime (HON=C=NOH) of CO_2 if a 1,3-hydrogen shift

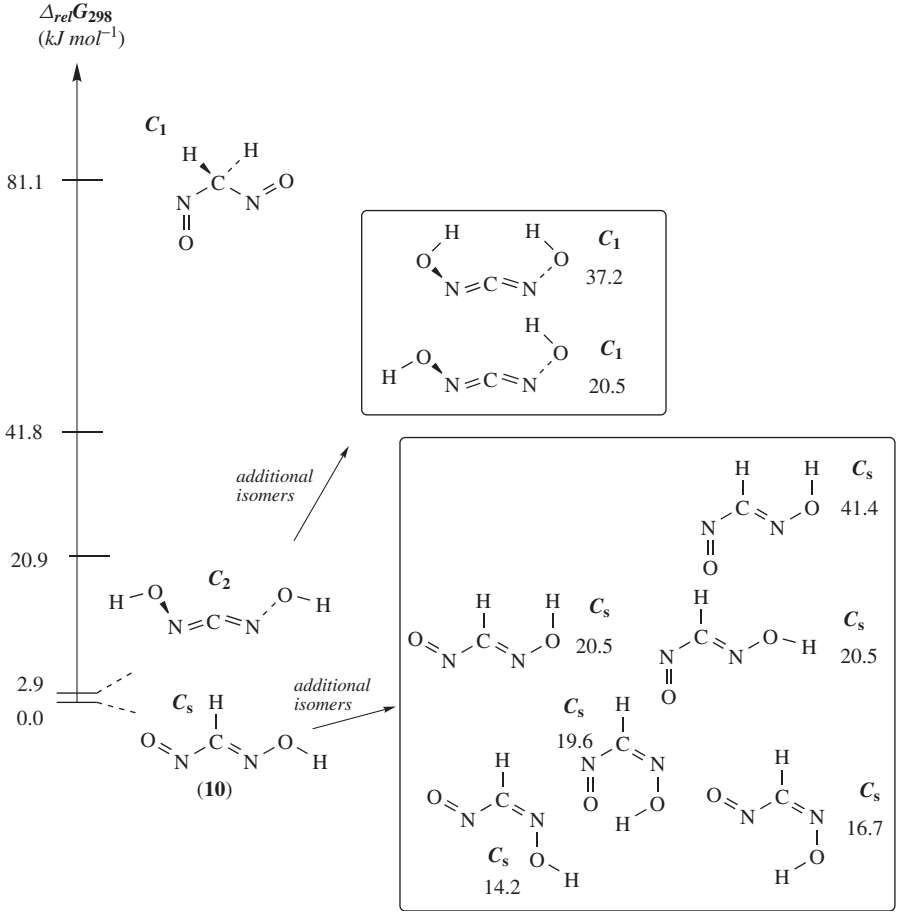

FIGURE 15. Tautomers and conformers of protonated DNM (relative energies of additional conformers in the boxes are in kJ mol^{-1} and point groups are in italics)

of the hydrogen atom attached to the carbon follows protonation in methyl nitrosolic acid (Figure 15). Experimental structural data of **10** or any other isomer of **10** are not known yet.

Stationary points were found for all possible tautomers at the potential energy surface that were characterized as minima by frequency analyses. Seven conformers of **10** and three for the dioxime were calculated (Figure 15). Compound **10** turned out to be favored over dinitrosomethane by 81.1 kJ mol^{-1} at the aug-cc-pvTZ level of theory. Hence, it can be concluded that protonation occurs exclusively on the oxygen atoms of the nitroso group in DNM. Interestingly, the dioxime is only 2.9 kJ mol^{-1} less stable than **10**; however, the formation of the dioxime (besides **10**) in solution is rather unrealistic due to a very large activation barrier of *ca* 200 kJ mol^{-1} for an intrinsic 1,3-hydrogen shift. Thus,

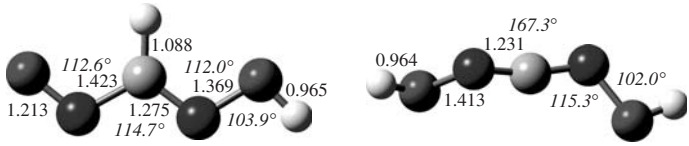

FIGURE 16. Calculated structures of the mono- and dioxime (bond lengths in Å)

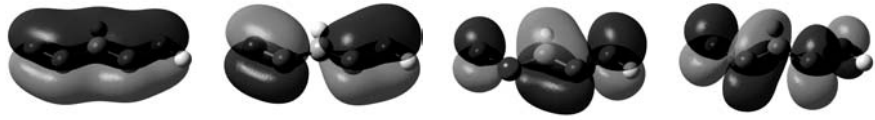

FIGURE 17. π-MOs displaying 6π-electrons delocalized over the entire oxime (**10**)

preparation of the dioxime species needs a different synthetic approach, starting from a −N=C=N− precursor.

Computed structural data of **10** and the dioxime are given in Figure 16. The planar C_s symmetric structure of **10** displays two significantly different NO and CN bond lengths with alternating bonds with respect to the bond lengths [d(NO) = 1.21, d(CN) = 1.42, d(CN) = 1.27, d(NO) = 1.37 Å, Figure 16]. Inspection of the π-MOs revealed three occupied MOs (Figure 17) containing six electrons. However, due to symmetry decrease, the overall π-electron density is not symmetrically distributed, leading to the mentioned alternating bond situation. According to NBO analysis the NCN unit is almost not polarized ($q_N = -0.07$, $q_C = 0.10$, $q_N = +0.07$ e) in contrast to the NO bonds ($q_{O(NO)} = -0.54$, $q_{O(NOH)} = -0.28$ e)[34].

The calculated structural data obtained for the dioxime display a nonplanar C_2 symmetric species for the lowest-lying isomer (dihedral angles: HONC = 180.0°, ONCN = 135.1°) with two short CN bonds (1.231 Å) and two long NO bonds (1.413 Å), which is in contrast to the situation in the monoxime (**10**) (Figure 16) with one longer NO and CN and one shorter NO and CN bond, respectively. Albeit there is a strong π-type bond situation along the NCN unit; the NCN angle with 167.3° is far from an ideal 180° angle, which might be attributed to a considerable weight of Lewis representation **A** and **C** in the VB resonance scheme of the dioxime, as shown in Figure 18. NBO analysis supports this idea since strong delocalization is found for one of the lone pairs on the oxygen atoms (p-AO type) which interacts with the π^* CN bond describing resonance, as depicted in Figure 18[34].

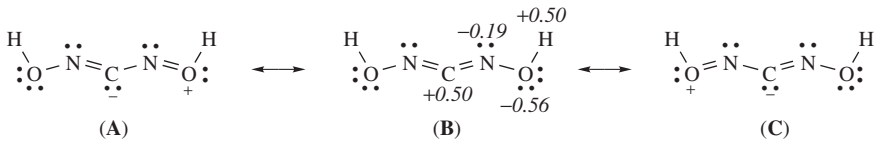

FIGURE 18. VB representation of the dioxime along with NPA partial charges

E. Trinitrosomethanides (TNM)

Trinitrosomethanides, $C(NO)_3^-$, are not known yet. However, access to this class of nitrosomethanides should similarly be possible as for dinitrosomethanides, if the preparation of $[C(NHOH)_3]^+[NO_3]^-$ succeeds. (It should be noted that as starting material for the synthesis of $[C(NHOH)_3]^+[NO_3]^-$, triaminoguanidinium salts $[C(NHNH_2)_3]^+$ $[X]^-$ (X = e.g. halogen), which are well-known, may be used.) A basic work-up in the presence of molecular oxygen should lead to trinitrosomethanides, which are assumed to be even more labile than DNM salts.

Albeit experimentally not known, quantum mechanical investigations of the potential energy surface displayed four stationary points on a very flat surface (Figure 19), two planar and two nonplanar conformers[17]. Interestingly, in contrast to DNM, only the nonplanar structures were found to be minima while the planar C_{3h} and C_s symmetric conformers represent transition states (NIMAG = 1, $\Delta_{rel}E$ = 6.3 and 1.3 kJ mol^{-1}). The C_1 symmetric species turned out to be favored over the propeller-like C_3 isomer by only 2.5 kJ mol^{-1} at the B3LYP/aug-cc-pvTZ level of theory[33]. Obviously, resonance stabilization prefers a planar arrangement of the atoms in the TNM anion, whereas a nonplanar arrangement is caused by minimization of the Coulomb repulsion[17].

F. Acids of Trinitrosomethanides (HTNM)[33]

According to computations at the B3LYP/aug-cc-pvTZ level of theory, six stationary points were found on the potential energy surface of HTNM. Protonation might occur at the central carbon atom leading to the trinitrosomethane or at one of the oxygen atoms of the NO groups leading to oximes (Figure 20). The C_1-symmetric trinitrosomethane was calculated to be the less stable isomer lying 55.2 kJ mol^{-1} above the most stable C_1-symmetric oxime (*u*-C(NOH)$(NO)_2$ Figure 20) species, in accord with simple charge consideration (negative charge sits on the oxygen atoms). All other found minima represent planar C_s-symmetic oximes which differ in the arrangement of the two nitroso groups and the position of the hydrogen atom attached to one oxygen (see isomers of the corresponding TNM and DNM, see also Figure 12). The hydrogen atom can be directed towards a neighboring O atom (*endo-w*) which stabilizes the conformation due to the formation of an intramolecular hydrogen bridge (formal formation of a six-membered ring) or towards a neighboring N atom (*endo-s*). All five oxime isomers of HTNM are within a range of 12.5 kJ mol^{-1}, indicating a very flat potential energy surface, and hence they may be observed in acidic solutions of TNM salts.

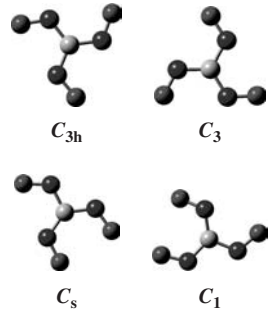

FIGURE 19. Stationary points at the potential energy surface of TNM

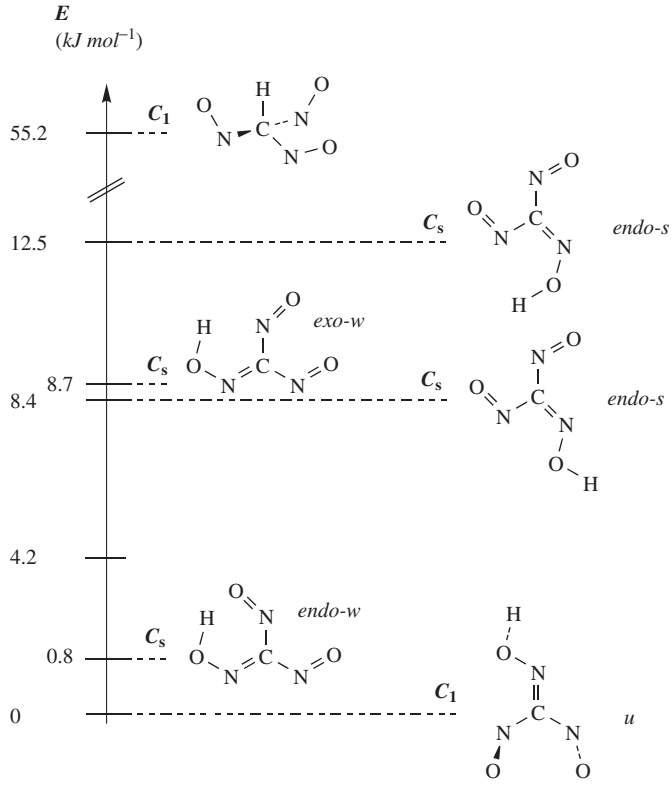

FIGURE 20. Isomers of HTNM

G. Methane(diazene-*N*-oxide-*N*′-hydroxylates)

Methanebis(diazene-N-oxide-N′-hydroxylate), $H_2C(N_2O_2)_2^{2-}$ (**11**), and *methanetris (diazene-N-oxide-N′-hydroxylate)*, $HC(N_2O_2)_3^{3-}$ (**12**)[67]. Over a century ago, Traube[68] reported the reaction of four nitric oxides with acetone and sodium ethoxide to yield the sodium salt of **11** and sodium acetate (Scheme 12). However, when this reaction is carried out in the presence of nitric oxide at slightly elevated pressures (35–40 psi), a product corresponding to the addition of six nitric oxide molecules, the sodium salt of **12**, forms as the main product in addition to a trace of the sodium salt of **11** and sodium acetate. Interestingly, the product distribution between **11** and **12** strongly depends on the base used, which is attributed to competing hydrolytic reactions of the acetyl and trimethylacetyl group-containing intermediates. The dianion **11** can be regarded as the product of the formal addition of HNO and NO^- to $HC(NO)_2^-$, while the triple anion **12** can be derived from trinitrosomethanide $C(NO)_3^-$, by formal addition of HNO and two NO^-.

Up to six nitric oxides readily add to ketoenolates when they are treated with strong base in methanol. This sequential addition is stereospecific, generating *Z*-configured products. The tris(diazene-*N*-oxide-*N*′-hydroxylates) are an intriguing type of molecular propeller (Figure 21) with relatively low energy barriers for rotation of the three N_2O_2 'blades' around the C−N bond.

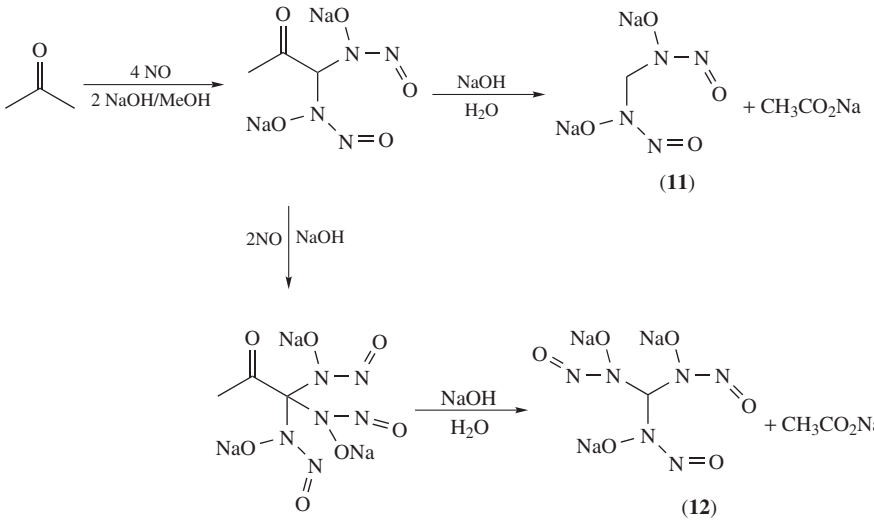

SCHEME 12. Synthesis of **11** and **12**

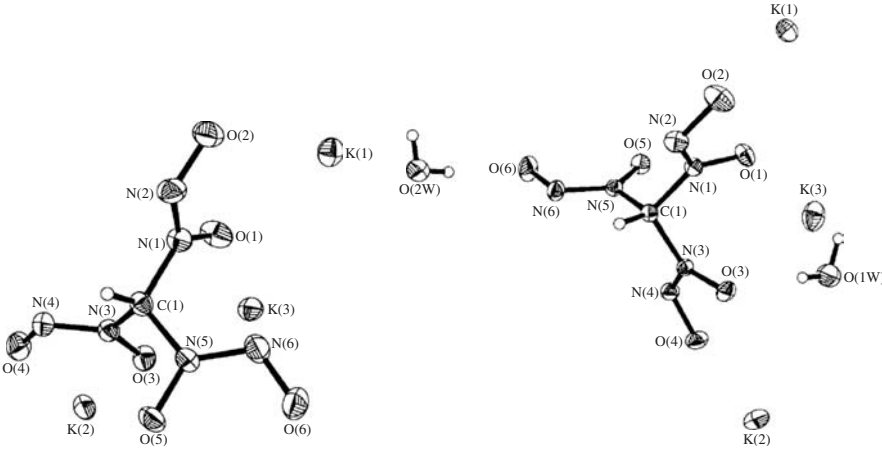

FIGURE 21. ORTEP representations of tripotassium methanetris(diazene-*N*-oxide-*N′*-hydroxylate), as the anhydrous form (left) and as the dihydrate (right). Reprinted with permission from Arulsamy and Bohle, *J. Am. Chem. Soc.*, **123**, 10860. Copyright (2001) American Chemical Society

The sodium and potassium salts of **11** and **12** and their hydrates have been synthesized and characterized[67]. The solid state structures of anhydrous potassium salt of **12** and its hydrate have been determined by single-crystal X-ray diffraction (Figure 21). Each structure has nearly planar N_2O_2 groups arranged as blades of a propeller around the main C–H axis. The three blades have similar helicities, or relative orientations. Helicity can be viewed as the relative orientation of the oxygen of the carbon-bound nitrogen with respect to the plane defined by the HCN atoms for the individual blades[67].

TABLE 7. Selected structural data from X-ray diffraction of $[HC(N_2O_2)_3]^{3-}$ (distance in Å, angles in deg). Reprinted with permission from Arulsamy and Bohle, *J. Am. Chem. Soc.*, **123**, 10860. Copyright (2001) American Chemical Society

Parameters	$K_3HC(N_2O_2)_3$	$K_3HC(N_2O_2)_3 \bullet 2H_2O$
C−N	1.450(3), 1.465(2), 1.460(3)	1.457(2), 1.453(2), 1.466(2)
N−N	1.300(2), 1.300(2), 1.295(2)	1.305(2), 1.298(2), 1.291(2)
$N_\alpha-O_\alpha$	1.295(2), 1.302(2), 1.304(2)	1.303(2), 1.314(2), 1.318(2)
$N_\beta-O_\beta$	1.272(2), 1.281(2), 1.289(3)	1.279(2), 1.279(2), 1.282(2)
C−N−N	112.2(2), 112.7(2), 119.0(2)	113.3(1), 112.9(1), 118.3(1)
$C-N_\alpha-O_\alpha$	122.3(2), 120.6(2), 114.4(2)	120.4(1), 121.4(1), 115.3(1)
$N_\beta-N_\alpha-O_\alpha$	125.4(2), 126.6(2), 126.5(2)	126.2(1), 125.8(1), 125.7(1)
$N_\alpha-N_\beta-O_\beta$	114.4(2), 114.3(2), 113.2(2)	113.4(1), 113.6(1), 113.6(1)

$N_\alpha-O_\alpha$ corresponds to N(1)−O(1), N(3)−O(3) and N(5)−O(5), while $N_\beta-O_\beta$ corresponds to N(2)−O(2), N(4)−O(4) and N(6)−O(6) in Figure 21

In terms of the bonding in the individual N_2O_2 groups, the observed N−N and N−O bond distances are in the range 1.272(2)–1.304(2) Å and lie between the ranges typically found for the corresponding single or double bonds (Table 7). This is consistent with prior structural data for these groups and is also indicative of considerable electron delocalization over the four atoms, as has been found in the structures of $CH_2(N_2O_2K)_2$ and $CH_2(N_2O_2Na)_2 \bullet H_2O$[69]. In Figure 21 in both structures, each of the potassium ions is surrounded by six oxygen atoms of four neighboring anions, and one or two nitrogen atoms of the neighboring anions. The K−O and K−N ionic interaction leads to an infinite three-dimensional network of the ions.

III. NITROSOCYANOMETHANIDES AND THEIR ACIDS

A. Nitrosocyanomethanides

1. Synthesis

Nitrosocyanomethanides (NCM) are easily prepared from furazane (stable liquid with b.p. 98 °C), which can be obtained by melting glyoxime with succinic anhydride and allowing the heterocycle to distil from the mixture (Scheme 13)[20]. It is interesting to note that early attempts to synthesize furazane failed as an alkaline solution was used, conditions under which furazane would not survive if formed, since furazane undergoes rapid, base-induced ring scission to crystalline, unstable and explosive nitrosocyanomethanide (α-oximinoacetonitrile), $Na^+HC(CN)NO^-$. Hence, first pure furazane needs to be synthesized and a basic work-up yields sodium nitrosocyanomethanide. The kinetics of the base-induced ring scission of furazane to the sodium salt of cyanomethanide has been studied. This facile reaction has a half-life of only 4.3 min at 25.0 °C in aqueous sodium hydroxide at pH 11.97[20].

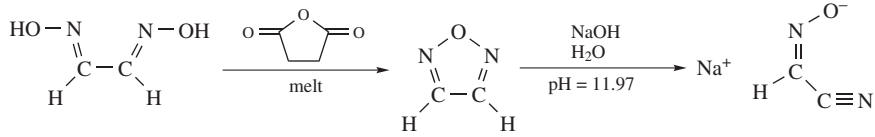

SCHEME 13. Synthesis of cyanonitrosomethanides

While dinitrosocyanomethanides (DNCM) have not been synthesized yet, nitrosodicyanomethanides (NDCM) have been studied extensively[22,70]. There are three ways to synthesize NDCM salts: (i) synthesis of silver nitrosodicyanomethanide from malononitrile, sodium nitrite and silver nitrate in acetic acid/sodium acetate buffer medium (*ca* pH 3)[71], (ii) synthesis of alkali NDCM salts by adding alkali nitrite to malononitrile dissolved in pH 2.75–3 acetic acid/alkali acetate buffer solution[22a] and (iii) the metathesis reaction of AgNDCM with MX (M = alkali metal, X = halogen) in aqueous media (Scheme 14)[22c]. Already Longo reported in 1931 that malononitrile undergoes nitrosation in diluted acid solution to give the dicyano oxime, which in the presence of silver ions yields AgNDCM (equation 8)[72]. In the absence of catalysts, the reaction is slow and competes with the spontaneous decomposition of nitrous acid.

$$CH_2(CN)_2 + HNO_2 \xrightarrow{H^+} (CN)_2C{=}NOH + H_2O \xrightarrow{Ag^+} Ag^+[C(CN)_2(NO)]^- + H^+ \quad (8)$$

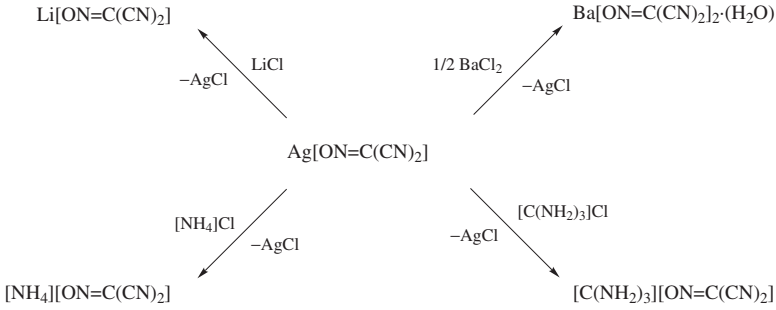

SCHEME 14. Synthesis of NDCM salts via a metathesis reaction

The IR spectra of NDCM salts exhibit cyanide stretching absorption bands in the 2250–2210 cm^{-1} region and three broad absorption bands associated with the coupling of the ν(NO) and ν(CC) modes in the 1375–1210 cm^{-1} region (Table 8). The electronic spectra of the NDCM salts exhibit characteristic $\pi \rightarrow \pi^*$ and $n \rightarrow \pi^*$ electronic transitions at *ca* 300 and 480 nm, respectively[73]. In aqueous solution the UV-vis spectra of, e.g., the lithium and barium salts exhibit an additional absorption at 401 nm, which can be attributed to the solvatochromic effect of water.

2. Structure and bonding

Experimental structural data for NCM and DNCM salts are not available whereas X-ray elucidations of several alkali, alkaline earth and different ammonium NDCM salts have been carried out.

TABLE 8. Crystallographic and vibrational spectroscopic data for NDCM salts. Reprinted with permission from Arulsamy *et al.*, *Inorg. Chem.*, **38**, 2709. Copyright (1999) American Chemical Society

Compound	d(O−N) (Å)	d(N−C) (Å)	ν(C≡N)	ν_a, ν_s(ONC)
[K][ONC(CN)$_2$]	1.287(1)	1.324(2)	2229, 2218	1325, 1275
[Ag][ONC(CN)$_2$]	1.18	1.44	2246, 2232	1322, 1270
[NH$_4$][ONC(CN)$_2$]	1.286(2)	1.314(2)	2230, 2222	1325, 1274
Ba[(ONC(CN)$_2$)$_2$]•(H$_2$O)	1.292(2)[a]	1.313(5)[a]	2239, 2228	1345, 1263

[a] Average distance.

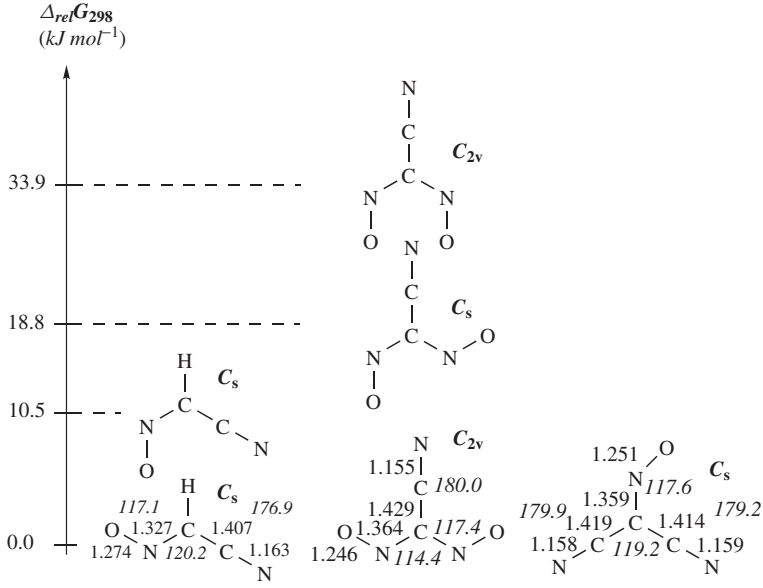

FIGURE 22. Calculated structural data and relative energies of nitrosocyanomethanides (bond lengths in Å, angles in deg)[33]

According to DFT computations at the B3LYP/aug-cc-pvTZ level of theory, two C_s-symmetric isomers of NCM, an *anti* and a *syn* isomer, are found (Figure 22). Both are planar with an energy difference of 10.5 kJ mol^{-1} in favor of the *anti* conformation. Similar to DNM, three planar isomers with an *anti*/*anti, anti*/*syn* and *syn*/*syn* arrangement of the two NO groups with respect to CN group are found to be minima (cf. Figures 12 and 22). The lowest-lying C_{2v}-symmetric *anti*/*anti* isomer corresponds to the *anti*/*anti* isomer of DNM with the H atom substituted by CN. Both higher-lying isomers can be derived in the same way, being 4.5 (*anti*/*syn*) and 33.9 kJ mol^{-1} (*syn*/*syn*) less stable. Only one planar C_s-symmetric isomer was computed for NCM, in accord with experiment.

Solid state X-ray studies of NDCM salts reveal that the NDCM anion possesses comparable structural features irrespective of the nature of the cation. For instance, the N−O distances in $[NH_4][NDCM]$ and $Ba[NDCM]_2 \bullet (H_2O)$ are similar at 1.286(2) and 1.292(4) Å, respectively, and the anion possesses a nearly planar geometry (Figures 23 and 24). In $Ba[NDCM]_2 \bullet (H_2O)$, the nitrosodicyanomethanide anion binds a single metal center through the nitrogen and oxygen atoms of the nitroso group while also binding two other metal centers through the cyano nitrogen atoms (Figure 24). These structural features indicate that the negative charge is not exclusively localized on the nitroso group, but rather it is delocalized over the whole anion. Structural data obtained for different NDCM (alkali, alkaline earth, ammonium and silver) salts reveal that in both anions the distances between the nitroso nitrogen atom and the dicyanomethanide carbon atom are larger than the typical C−N double bond distance and the C−C bond distances are considerably smaller than the typical C−C single bond. These bond distances together with the observed planarity of the NDCM anion indicate the presence of delocalization of a double bond over the whole anionic species, and these results correlate with predictions from quantum mechanical calculations.

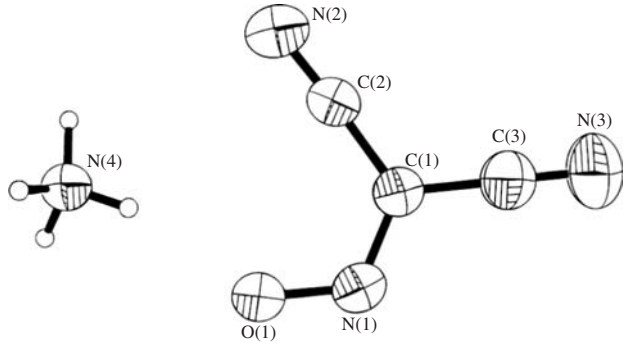

FIGURE 23. View of NDCM anion and ammonium cation in the crystals of $[NH_4][NDCM]$ (50% thermal ellipsoids of the atoms are shown)

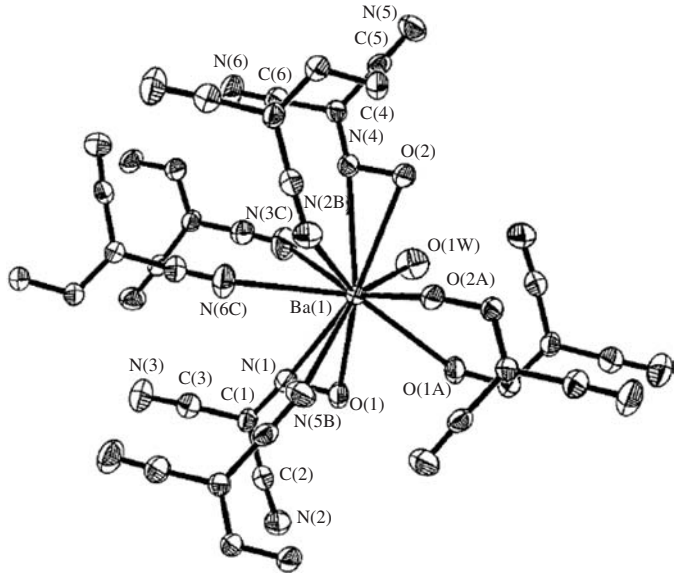

FIGURE 24. View of barium coordination environment in $Ba[NDCM]_2 \bullet (H_2O)$. Symmetrically generated atoms, except those coordinated to Ba(1), are not labeled (50% thermal ellipsoids of the atoms are shown)

Recently, ammonium salts with a discrete 12-coordinate Ln trianion (Ln = lanthanide) containing six identical NDCM ligands have been reported, which bind through a highly unusual symmetrical μ^2-nitroso group of the nitrosodicyanomethanide ion (Figure 25)[70d]. The isostructural complexes $[Et_4N]_3[Ln(NDCM)_6]$ (Ln = La, Ce, Nd, Gd) were obtained by reaction of tetraethylammonium nitrosodicyanomethanide and the corresponding rare earth chloride in methanol:

$$LnCl_3 \bullet x H_2O + 3[Et_4N][NDCM] + 3[Ag][NDCM] \rightarrow [Et_4N]_3[Ln(NDCM)_6] + 3\ AgCl$$

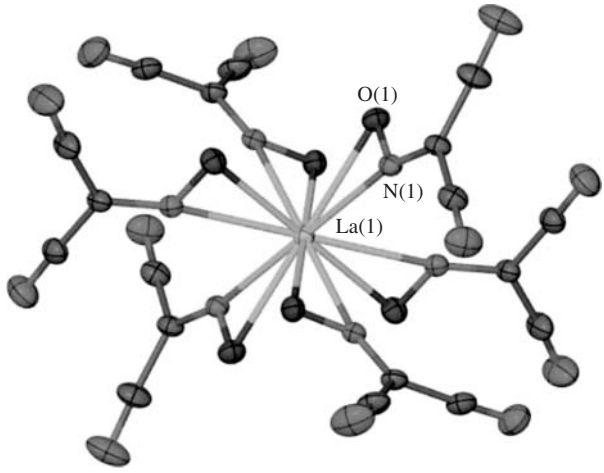

FIGURE 25. X-ray crystal structure of the discrete species $[La(NDCM)_6]^{3-}$; ellipsoids shown at 50% probability. Et_4N^+ counteractions were omitted for clarity. The Ce, Nd and Gd complexes are isostructural. From Chesman *et al.*, *Dalton Trans.*, 1371 (2007). Reproduced by permission of The Royal Society of Chemistry

The complexes crystallize in the cubic space group $Ia\ \overline{3}$. The six NDCM ligands are octahedrally arranged around the metal ion, forming a trianionic complex with the formula $[Ln(NDCM)_6]^{3-}$. The NDCM ligand is attached to the metal through a 'side-on' symmetrical μ^2-interaction involving both the oxygen and nitrogen atoms of the nitroso group.

B. Acids of Cyanonitrosomethanides

1. Synthesis

Acids of NCM. Formally, three tautomeric forms can be regarded as corresponding acids of NCM upon protonation: (i) the cyanoformaldoxime when protonation occurs at the oxygen, (ii) nitrosocyanomethane if a proton is added to the central carbon and (iii) nitrosovinylideneamine upon addition of a proton to the nitrogen atom of the cyano group (Figure 26). Furthermore, if a 1,3-hydrogen shift follows protonation of the NO group, an iminoethenone oxime could be formed. Furazane represents a constitutional isomer which is used as precursor in the synthesis of NCM salts.

Cyanoformaldoxime was first described by Grundmann and Fulton in the decarboxylation reaction of isonitrosocyanoacetic acid (Scheme 15)[74]. Cyanoformaldoxime is very sensitive with respect to base. Catalytic amounts of bases immediately trigger a highly exothermic decomposition into cyanogen and water. Moreover, cyanoformaldoxime is unstable at ambient temperatures and hence needs to be prepared and stored at low temperatures. According to Grundmann, synthesis of cyanoformaldoxime results in the formation of a mixture of a *syn* and *anti* isomer (m.p. 33–35 and 83 °C, respectively). Above 0 °C both isomers decompose slowly to cyanogen and water, while below 0 °C a very slow (several months) Beckmann rearrangement[75] to cyanoformamide occurs (Scheme 15).

Another synthetic route to cyanoformaldoxime involves the decarboxylation of furazane dicarboxylic acid (Scheme 16). Interestingly, Grundmann's intention was the synthesis of the (in those days) unknown furazane which, however, isomerizes immediately to

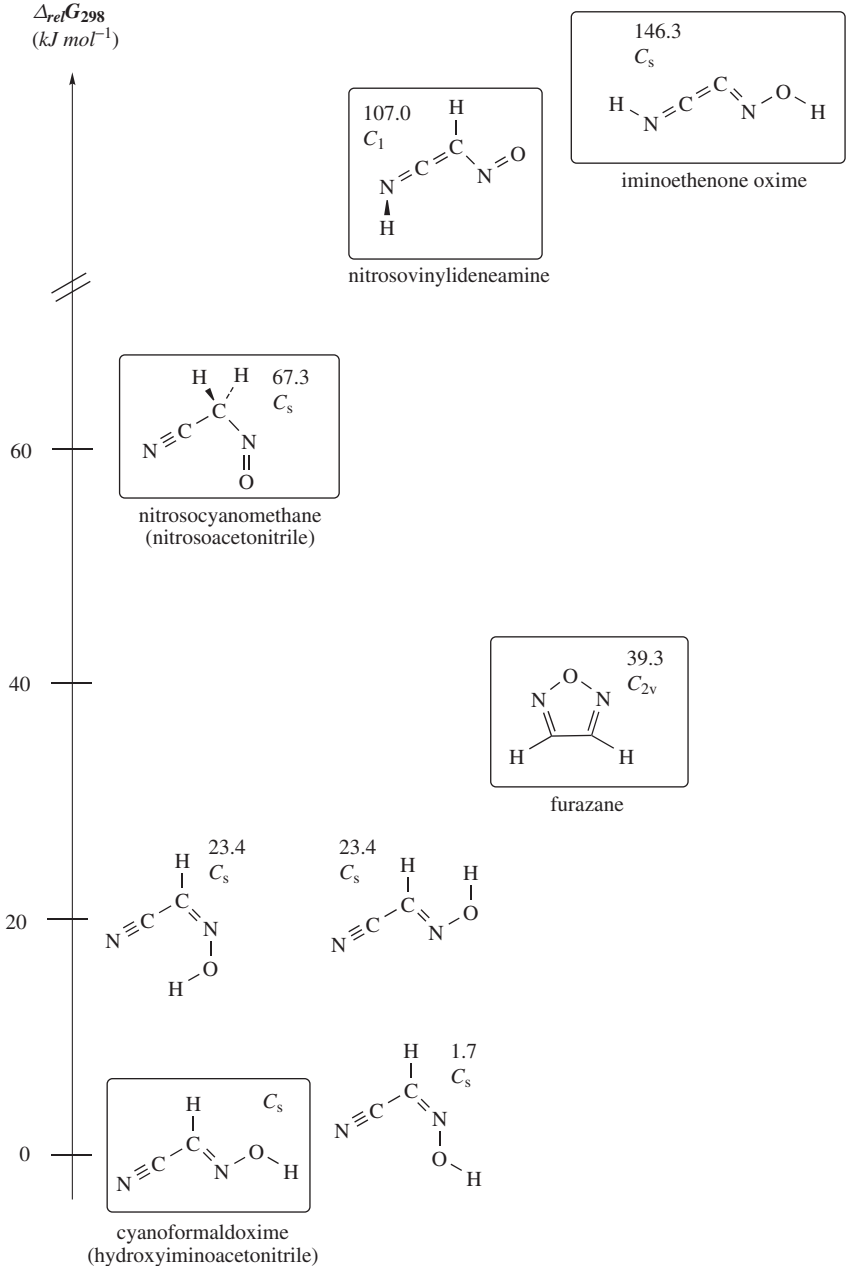

FIGURE 26. Acids of NCM (constitution isomers of cyanoformaldoxime are shown in boxes)

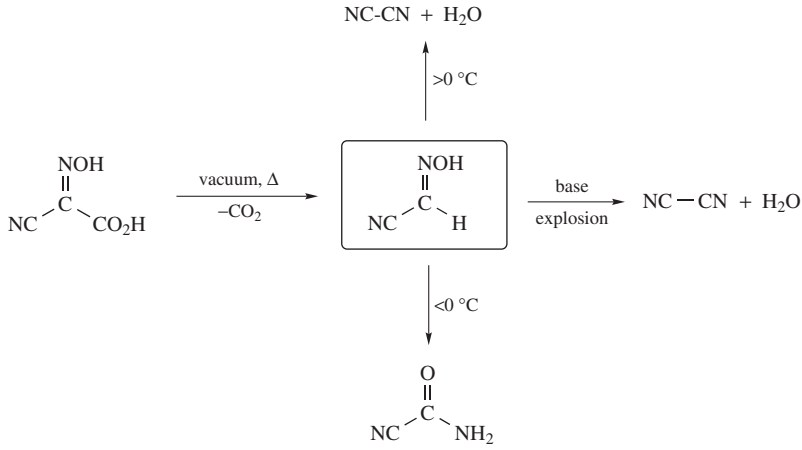

SCHEME 15. Synthesis and reaction of cyanoformaldoxime

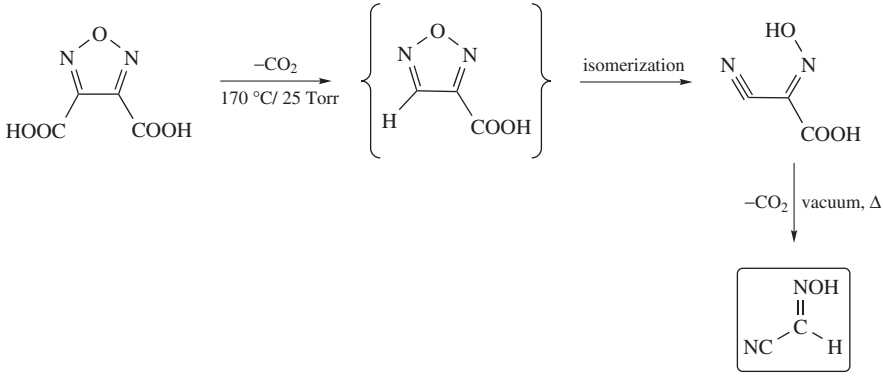

SCHEME 16. Synthesis of cyanoformaldoxime from furazane dicarboxylic acid

isonitrosocyano acetic acid. Upon increasing the temperature a release of CO_2 is observed, resulting in the formation of cyanoformaldoxime (cf. Scheme 15)[76].

Beside Grundmann, many scientists (e.g. Wieland and coworkers[77], Hantzsch[78] and Lach[79]) tried to prepare furazane (1,2,5-oxadiazole), but it took the synthetic effort of organic chemists for more than 80 years to isolate furazane. The problem was to choose the proper dehydration conditions of glyoxime, the simplest precursor for the synthesis of furazane. Olofson and Michelman solved these problems (e.g. avoiding alkaline solutions) by a high-temperature dehydration of glyoxime in a mildly acidic medium under conditions in which furazane is removed from the reaction mixture as it is generated (Scheme 13)[20]. They melted glyoxime with succinic anhydride and encouraged the product to distil from the reaction mixture as formed. By this procedure furazane is obtained as stable liquid (m.p. −28 °C, b.p. 98 °C).

Acids of NDCM. Formally, three tautomeric forms can be regarded as the corresponding acids of DNCM according to quantum chemical studies (Figure 27). Again, protonation might occur at the oxygen of the nitroso group leading to an oxime, at the central carbon

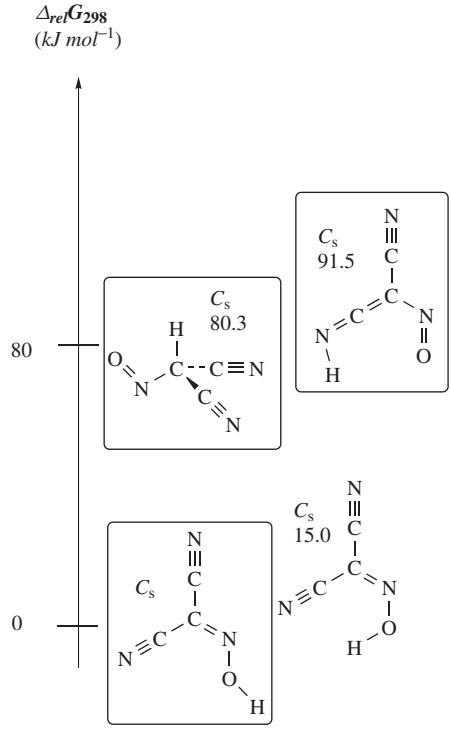

FIGURE 27. Acids of NDCM

forming a methane derivative, and at the nitrogen of the cyano group. Experimentally known is only the most stable tautomeric isomer, the dicyanooxime (Figure 27), which can be prepared by nitrosation of malononitrile. Malononitrile reacts readily with nitrous acid in aqueous acid buffer solutions, particularly in the presence of nucleophilic catalysts (e.g. Br^-, SCN^- etc.) to give the corresponding oxime product $(NC)_2C{=}NOH$ (equation 5)[71]. Kinetic measurements showed that only the carbanion is the reactive species and not the tautomeric form of the nitrile itself, i.e. the keteneimine HC(CN)=C=NH.

Acids of DNCM. The most stable form of DNCM acids is the oxime (Figure 28), while all other species, protonated either at the central C atom (dinitrosocyanomethane; dinitrosoacetonitrile) or at the nitrogen of the cyano group, represent high-lying tautomeric isomers. Neither of the acids of DNCM is experimentally known.

2. Structure and bonding

Comparison of all isomers of NCM, DNCM and NDCM illustrates that the oxime form is always the most stable tautomer (see Figures 26–28). Protonation at the central carbon of the methanide dramatically increases the total energy relative to the oxime species (NCM: 67.3, NDCM: 80.3 and DNCM: 81.1 kJ mol^{-1}) whereas protonation at the cyano group is even less favored (NCM: 107.0, NDCM: 91.5 and DNCM: 92.0 kJ mol^{-1}). Hence, it can be concluded that protonation of NCM, DNCM and NDCM salts always occurs exclusively at the oxygen of the nitroso group generating firstly an oxime[33].

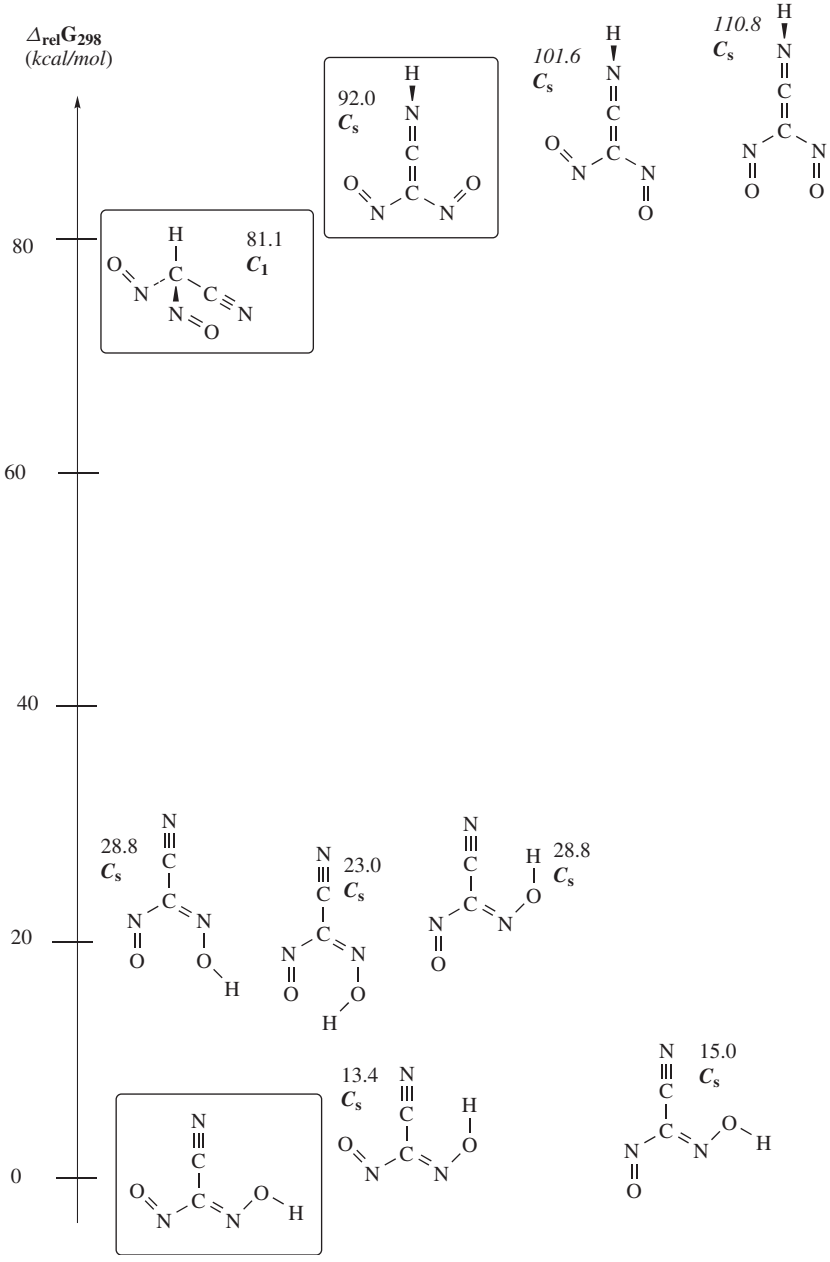

FIGURE 28. Acids of DNCM

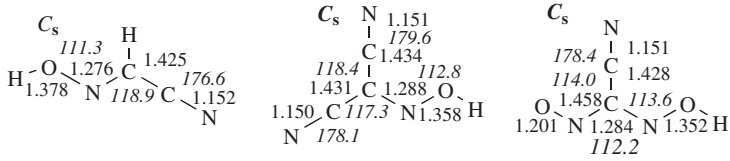

FIGURE 29. Selected bond lengths (Å) and angles (deg) of the oximes of NCM, NDCM and DNCM

All three oximes are planar (C_s symmetry) and several isomers (*syn* and *anti* isomers) are computed (see Figures 26, 27 and 28). Planar structures are favored due to the presence of a highly delocalized π-system as discussed before. Selected structural data are given for all oximes in Figure 29. As expected, the NO distance (HNCM: 1.378, HNDCM: 1.358, HDNCM: 1.352 Å) decreases upon protonation while the CN bond length remains almost unchanged (HNCM: 1.152, HNDCM: 1.150, HDNCM: 1.151 Å). The C−C≡N moiety reveals a slight deviation from linearity due to symmetry constraints (HNCM: 176.6°, HNDCM: 178.1°, HDNCM: 178.4°).

IV. NITROSONITROMETHANIDES AND THEIR ACIDS

A. Synthesis of Nitrosonitromethanides and Their Acids

Three types of nitrosonitromethanides can be derived from the general formula $[R^1(NO_2)C{=}NO]^-$ (R^1 = H, NO, NO_2, Table 1): nitrosonitromethanide (NNtM), dinitrosonitromethanide (DNNtM) and nitrosodinitromethanide (NDNtM). Experimentally known are only the sodium and potassium salts of the nitrolic acids. The nitrosonitromethanides, however, were only generated *in situ* in aqueous solutions[21].

The class of nitrolic acids (nitro-oximes) was introduced by Victor Mayer as early as 1873 with the simplest representative methylnitrolic acid ($HC(NO_2){=}NOH$)[80]. Tscherniak, a student of Mayer, was the first to isolate the very labile methylnitrolic acid at low temperatures[81], while Wieland improved the synthesis by detailing the exact reaction conditions to increase the low yields[82]. Methylnitrolic acid can be prepared as crystalline solid from nitromethane and KNO_2/H_2SO_4 (*in situ* generation of nitrous acid) in water at low temperatures, followed by extraction from this weak acidic solution into ether (Scheme 17). Removal of ether yields the pure, highly unstable free acid. Salts of methylnitrolic acid, NNtM, can be generated by extracting the acid into sodium carbonate solution[83].

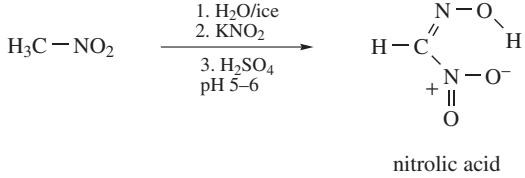

SCHEME 17. Synthesis of nitrolic acid

Another method for the preparation of nitrolic acids was introduced by Ponzio[84]: Methylnitrolic acid was prepared by the action of an ether solution of nitrogen dioxide on the isonitrosoacetic acid. The resulting solution is afterwards washed with a little

water and the nitrolic acid is then extracted as potassium salt by treatment with potassium hydroxide solution. Methylnitrolic acid, prepared in this way from isonitrosoacetic acid, crystallizes from a mixture of ether and light petroleum in long flattened needles, melting and decomposing at 68 °C. Methylnitrolic acid explodes when heated, releasing NO_2, or when touched with a glass rod covered with NaOH.

According to Tscherniak methylnitrolic acid decomposes in water to give formic acid and N_2O, while Wieland found that when methylnitrolic acid $O_2NCH{=}NOH$ is boiled in aqueous solution, with or without the addition of a mineral acid it yields formic acid, nitrous oxide and fulminic acid, which is precipitated as the silver or mercuric salt if silver or mercuric nitrate is added to the above mixture (equation 9)[85]. The yield of fulminate is increased by the presence of mineral acid and by boiling, but it is also formed at ambient temperatures.

$$O_2NCH{=}NOH \xrightarrow{H_2O} HNO_2 + HCNO \xrightarrow{H_2O} HCOOH + N_2O \qquad (9)$$

Schorpp and Beck studied the reaction of $M(PPh_3)_4$ (M = Pd and Pt) with methylnitrolic acid in order to isolate mixed fulminato–nitro complexes, since methylnitrolic acid is considered to possess fleeting existence in the mercury fulminate preparation reaction (Hg, C_2H_5OH and HNO_3). However, only mixtures of $(Ph_3P)_2M(NCO)_2$, $(Ph_3P)_2M(NCO)NO_2$ and $(PPh_3)_2M(NO_2)_2$ were observed[41].

Radical mono- and dianions of nitrosonitromethanides have been generated by addition of nitric oxide and nitrogen dioxide to anions of nitromethane and formaldoxime. The electron transfer was established by EPR experiments and the fleeting existence of $[C(NO_2)_2NO]^{\bullet 2-}$, $[H_2C(NO)_2]^{\bullet -}$, $[HC(NO)_2]^{\bullet 2-}$ and $[HC(NO_2)NO]^{\bullet -}$ was proven[86,87].

B. Structure and Bonding of Nitrosonitromethanides and Their Acids

Methanides. Both isomers of NNtM are planar, the difference in energy (23.4 kJ mol^{-1}) between both arises from unfavorable electrostatic interactions between the lone pairs on the oxygens in the higher-lying isomer (Figure 30), while two stabilizing intramolecular H bridges are established in the lower-lying isomer. For DNNtM and NDNtM, nonplanar structures are found to be the most stable isomers although the central CN_3 unit remains always planar. Obviously, balance between electrostatic repulsion due to the increasing number of lone pairs, and energy gain due to resonance stabilization, forces these anions to rotate one NO or NO_2 group out of the CN_3 plane.

Selected computed structural data at the B3LYP/aug-cc-pvTZ level of theory are given in Figure 31. With respect to resonance stabilization, it is interesting to compare the C–N distances. Two things are worthy of discussion: (i) the $C{-}NO$ distance is always smaller compared to the $C{-}NO_2$ (e.g. NNtM: 1.320 vs. 1.399; DNNtM: 1.342 vs. 1.489; NDNtM: 1.318 vs. 1.399/1.476 Å), and (ii) the smallest C–N distance is found in DNNtM, displaying the best resonance along the ON–C–NO unit (cf. DNM).

Acids. For the acids of nitrosonitromethanides, a similar situation is found with respect to the energetic order compared to the nitroso- and nitrosocyanomethanide. Protonation at the nitroso group leading to oxime species is always energetically preferred (Figure 32). Less favorable with 59.8 and 61.0 kJ mol^{-1} is the formation of C_s-symmetric nitrosonitromethane (protonation at the central carbon atom) and a species with a protonated nitro species, respectively (Figure 32). For DNNtM- and NDNtM-based acids, similar energy differences are found: 43.9 vs. 72.3 and 54.8 vs. 79.0 kJ mol^{-1}.

Four different isomers of *aci*-nitrosonitromethane have been found, all within an energy difference of 25 kJ mol^{-1} and planar. Interestingly, in contrast to DNM the *syn* conforma-

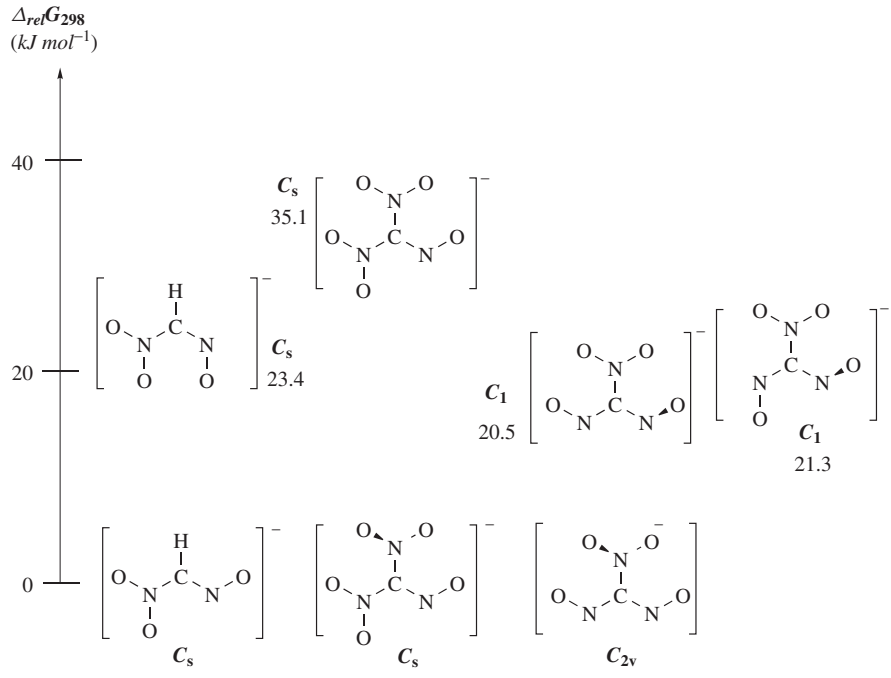

FIGURE 30. Isomers of NNtM, NDNtM and DNNtM

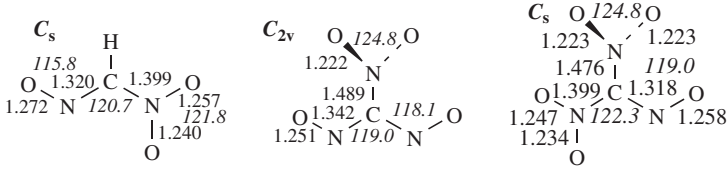

FIGURE 31. Selected bond lengths (Å) and angles (deg, italics) of NNtM, DNNtM and NDNtM

tion is energetically preferred due to the existence of an intramolecular hydrogen bridge between the nitroso and nitro groups (−N=O−H•••O−NO), closing a six-membered ring. For the protonated nitro species, this kind of H-bridged species results always in a proton transfer leading to the most stable oxime species: −N=O•••H−O−NO → −N=O−H•••O−NO. Stabilization of the oxime species by formation of an intramolecular H bridge is also found for DNNtM- and NDNtM-based acids for the energetically preferred isomer, as shown in Figure 32.

Selected computed structural data on the three tautomeric forms of protonated NNtM, DNNtM and NDNtM are depicted in Figure 33. Only the most stable oxime isomers are presented. As long as only two functional groups are attached to the central methanide carbon, the entire molecule remains planar due to resonance stabilization, whereas introduction of a third group, either NO or NO_2, results in rotation of at least one group, preferably the nitro group. However, the CN_3 moiety in the nonplanar species remains

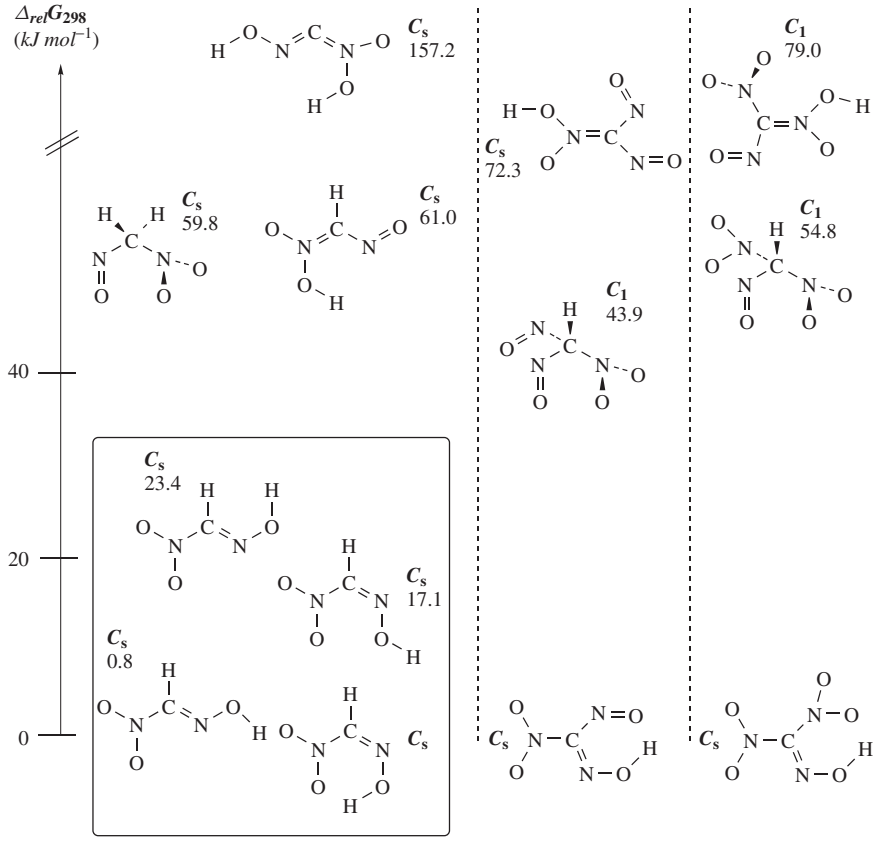

FIGURE 32. Tautomers and isomers of nitrosonitromethanides

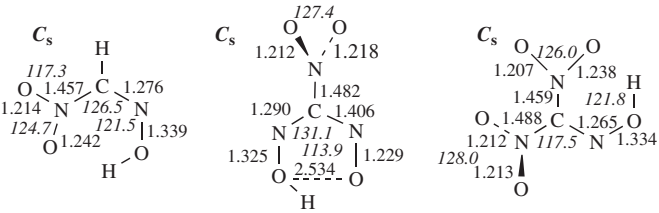

FIGURE 33. Selected bond length (Å) and angles (deg, italics)

nearly planar; only the oxygen atom leaves the molecular plane (dihedral angles close to 90°). As already discussed above, the C−N distances display bond orders between 1 and 2 for both the *C*−NO and *C*−NO_2 bonds. However, the C−NO bonds are always significantly shorter (NNtM: 1.276 vs. 1.457, DNNtM: 1.290/1.406 vs. 1.482 and NDNtM: 1.265 vs. 1.459/1.488 Å; Figure 33).

V. NITROSONITROCYANOMETHANIDES AND NITROLIC ACIDS[24]

A. Synthesis of Nitrosonitrocyanomethanides and Their Acids

Nitrosonitrocyanomethanides (NNtCM) can easily be synthesized in a two-step reaction (Scheme 18): (i) formation of the metastable cyanomethylnitrolic acid by nitrosation of nitroacetonitrile in water and extracting the cyanomethylnitrolic acid with ether, (ii) treating the dried ether solution of cyanomethylnitrolic acid with a solution of MOR (M = alkali metal, NR_4; R = H, alkyl) in isopropanol results in a red precipitate of MNNtCM. The beautiful red alkali NNtCM salts can easily be purified by re-crystallization from methanol (yield 50–60%).

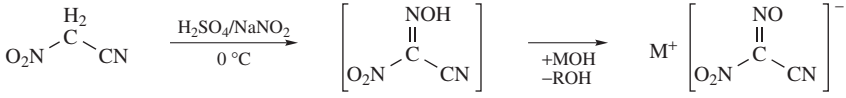

SCHEME 18. Synthesis of alkali NNtCM salts (M = alkali metal, NR_4; R = H, alkyl)

Metastable cyanomethylnitrolic acid and its red color in basic water solution have already been observed by Steinkopf[88]. Moreover, he postulated the existence of the silver salt AgNNtCM. The intermediate formation of the silver salt has also been postulated by Pillai and Boyer in the reaction of ICH_2CN with $AgNO_2$ which finally gave $NC{-}CH_2{-}O{-}N{=}C(NO_2)CN$, the only product which could be isolated[89].

Crystals of LiNNtCM and NaNNtCM are very hygroscopic (they deliquesce within seconds) while crystals of KNNtCM and CsNNtCM can be handled without inert gas for some minutes. Interestingly, the red color of the NNtCM salts darkens, the heavier the alkali counterion is: LiNNtCM exhibits a bright orange-red color while CsNNtCM displays a purple color. It can be assumed that small lattice effects, such as a different electrostatic environment for the anion, slightly changes the $n \rightarrow \pi^*$ gap for the electronic excitation process responsible for the color of the anion (see below). Similar to the alkali dinitrosomethanides, pure dry alkali NNtCM salts are stable at ambient temperature, are heat and shock sensitive, and decompose slowly in polar solvents, releasing N_2O gas. To determine the explosion gases of MNNtCM, combined IR and HR-MS pyrolysis experiments were carried out. The only gaseous products observed were $NC{-}CNO$, N_2O, CO_2, NO and CO. An intriguing feature of NNtCM salts is the liberation of cyanogen N-oxide ($NC{-}CNO$)[90] upon gentle heating (e.g. for KNNtCM at $80\,^{\circ}C < T < T_{onset}$) and the formation of MNO_2 in the solid state as well as in solution (Scheme 19)[91]. Differential scanning calorimetry experiments revealed that MNNtCM (M = K, Cs, NMe_4) undergo an exothermic decomposition [explosion, e.g. for KNNtCM: $\Delta H = -155.7\ kJ\,mol^{-1}$ with an onset of 101.7 °C ($\beta = 5\,^{\circ}C\,min^{-1}$ in a temperature range of 90–117 °C) and an estimated activation energy of *ca* 133 (± 2) $kJ\,mol^{-1}$][92]. It is assumed that the presence of a delocalized π-system over the entire anion probably accounts for the remarkable kinetic stability of NNtCM salts (see below). Compared to MNNtCM, nitro-, nitrosodicyanomethanide and dinitrosomethanide salts possess a higher thermal stability.

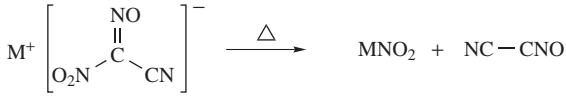

SCHEME 19. Decomposition of MNNtCM (M = alkali metal) upon gentle heating

Solution ^{14}N NMR studies of the NNtCM anion in DMSO display three resonances in the typical range of C−NO (265 ppm, cf. 332 ppm for $[HC(NO_2)_2]^-$), C−NO_2 (−15 ppm, cf. −25 ppm for $H_2C(NO_2)_2$)[64] and C−CN species (−107 ppm, cf. −105 ppm for $[C(NO)(CN)_2]^-$). The ^{13}C spectrum shows two singlet resonances at 149.6 (C−CN, cf. 150.3 ppm for $[C(NO_2)_3]^-$)[93] and 119.5 ppm (C−CN, cf. 117.2 ppm for $[C(NO_2)(CN)_2]^-$), respectively. The characteristic group frequency of the NO (1380–1400 cm^{-1}), NO_2 (1490–1510 cm^{-1}) and CN (2210–2230 cm^{-1}) groups can be detected in the Raman and IR spectra of all MNNtCM salts (M = alkali metal, Me_4N).

B. Structure and Bonding of Nitrosonitrocyanomethanides and Their Acids

KNNtCM crystallizes in red rods in the monoclinic space group $P2_1/c$ with four units per cell[24]. The structure consists of an infinite three-dimensional network of repeating K[$C(NO_2)(NO)(CN)$] units. Each anion is bonded to six potassium cations and *vice versa* (Figure 34). Specifically, the oxygen atoms of the nitro group are bonded to three potassium centers with K−O distances of 2.790(2) to 3.586(2) Å while the oxygen of the NO group is attached to two potassium centers [d(K−O) = 2.814(2) and 2.744(2) Å]. Additionally, two K−N interactions are found for the N atom of the NO group [3.003(2) and 3.276(2) Å]. The nitrogen atom of the CN group coordinates to two neighboring potassium centers with K−N distances of 2.832(2) and 3.275(3) Å. Hence, as shown in Figure 34, each potassium center is surrounded by four nitrogen and five oxygen atoms. The potassium coordination sphere consists of six NNtCN ligands, leading to the interesting three-dimensional network arrangement of the ions (Figure 35). A view along the a-axis reveals chains of K^+ and $NNCM^-$ stacked one upon the other.

As depicted in Figure 34, the NNCM anion is planar within experimental error (Σ < (C1) = 359.9°) like most of the known NO, NO_2 and CN substituted methanide anions (except from trinitromethanide, in which the balance between resonance stabilization

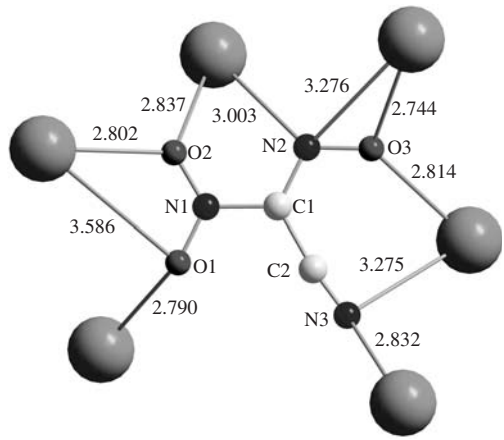

FIGURE 34. View of NNCM coordination environment in KNNCM; bond lengths (Å): C1−N1 1.418(3), C1−N2 1.323(3), C1−C2 1.422(4), C2−N3 1.138(3), N1−O1 1.233(3), N1−O2 1.236(3), N2−O3 1.273(3); bond angles (deg): C1−C2−N3 173.2(3), C1−N1−O1 117.5(2), C1−N1−O2 119.7(2), C1−N2−O3 115.6(2), N1−C1−N2 117.4(2), N1−C1−C2 117.7(2), N2−C1−C2 124.9(2). Reproduced with permission from Brand *et al.*, *Angew. Chem.*, (2005), **117**, 3998. Copyright Wiley-VCH Verlag GmbH & Co.

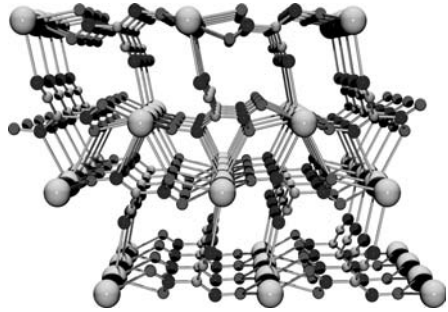

FIGURE 35. Stacking diagram of KNNCM (view along 100)

and steric repulsion results in a torsion of one NO_2 group out of plane)[94]. Inspection of the conformational space at the B3LYP/aug-cc-pvTZ level displayed two different planar structures of the NNCM ion: (i) a *cis* isomer (as shown in Figure 34, O3 in *cis* position to C2) and (ii) a *trans* arrangement. In agreement with experiment, our calculation revealed that the *cis* form represents the most stable isomer [$\Delta E^{tot}(cis-trans) = +19.2\ kJ\,mol^{-1}$][17,24]. As expected, all N−O bonds [KNNCM: 1.233(3), 1.236(3), and

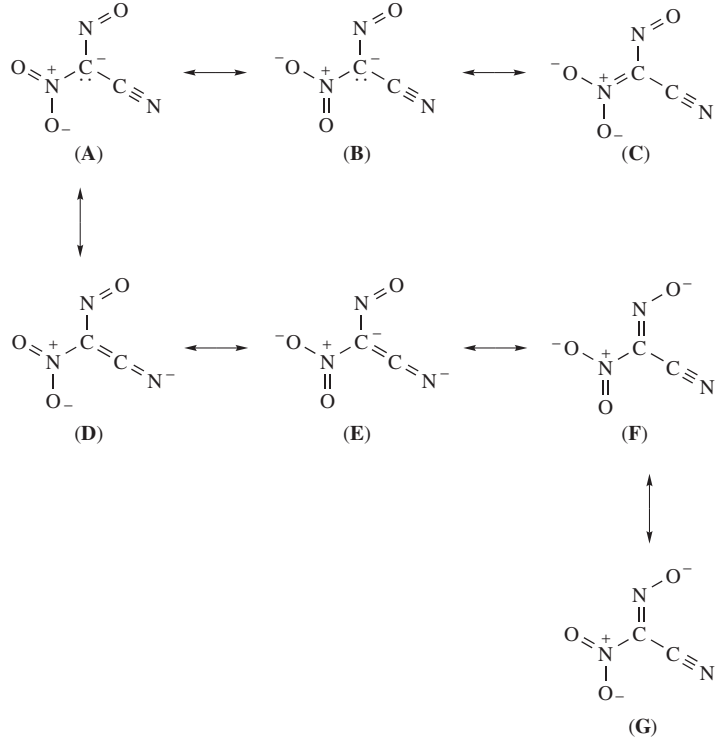

FIGURE 36. Lewis representations of NNCM according to NBO analysis[34]

1.273(3) Å] are significantly shorter than the C1−N1, C1−N2 and C1−C2 bonds [KNNtCM: 1.418(3), 1.323(3) and 1.422(4) Å], which is comparable to the situation found in the structure of the dinitrosomethanide, nitroso- and nitrodicyanomethanides. The $C-N_{nitroso}$ bond length is significantly shorter than the $C-N_{nitro}$ bond length, indicating a stronger π-interaction along the $C-N_{nitroso}-O$ moiety. These bond lengths, together with the planarity indicate the presence of delocalization of π-bonds over the whole anionic species—a typical feature of all resonance-stabilized methanides. MO and NBO[34] calculations displayed the existence of a 10π-electron, 8-center bond unit (Figures 36 and 37). In Figure 36, **A** and **B** are the energetically preferred Lewis representations of NNCM according to NBO analysis. Investigation of the intramolecular donor–acceptor interactions utilizing the NBO partitioning scheme clearly indicates a highly delocalized 10π-system according to resonance between Lewis representations **A**–**G**. The calculated natural atomic orbital population (NAO) net charges are $q(O) = -0.459$ (O1), -0.430 (O2), -0.464 (O3); $q(N) = 0.475$ (N1), 0.022 (N2), -0.382 (N3); $q(C) = -0.025$ (C1) and 0.263 e (C2), which means that the negative charge is mainly found on the three O atoms and the N atom of the CN group.

The UV-Vis spectra of the red methanolic solution of alkali NNCM salts exhibit one very strong characteristic $\pi \rightarrow \pi^*$ and one weak $n \rightarrow \pi^*$ electronic transition at *ca* 328 and 489 nm, respectively, which could be assigned on the basis of time-dependent B3LYP calculations (Figure 37)[24]. The red color arises from the weak $n \rightarrow \pi^*$ HOMO–LUMO electronic transition in the anion. The HOMO describes a lone pair which lies in the anion plane. A closer inspection of the orbital coefficients composing the HOMO shows rather large coefficients for the nitroso group; hence it can be concluded that the nitroso group is mainly responsible for the red color.

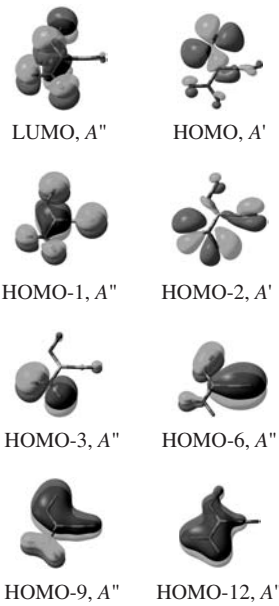

FIGURE 37. Selected molecular orbitals (B3LYP/aug-cc-pvTZ) of *cis* NNCM (the five occupied π-MOs are those with A'' symmetry)

VI. RESONANCE STABILIZATION

Carbanions of the type $[H_2CR^1]^-$, $[HCR^1R^2]^-$ and $[CR^1R^2R^3]^-$ (R^1 = NO and R^2, R^3 = CN, NO, NO_2) can be considered to be resonance-stabilized, nonlinear pseudohalides. All experimentally known resonance-stabilized methanides are reported to be planar or nearly planar (Table 1). While the parent ion, the methanide anion H_3C^-, adopts a pyramidal structure [$\Delta E_{\text{planar-pyramidal}} = 9.8$ kJ mol^{-1}; d(CH) = 1.099 Å, <(HCH) = 109.7°; cf. d(CH) = 1.093 Å, <(HCH) = 109.6°] due to the lack of delocalization (no resonance for the p-AO-type lone pair possible)[95], substitution of one H atom by NO results in a planar anion since the empty π^*-orbitals of the NO group are perfectly suitable to delocalize the carbon lone pair. Further substitution of the second H atom again results in planar anions, and the same holds for the third substitution in case of R = CN. In case of R = NO and NO_2, the third substitution leads either to a propeller-type structure with only a small distortion from planarity or one NO_2 group is twisted by 90°, nevertheless leaving the central carbon in an almost trigonal planar environment[94].

Computational data display that obviously only two NO or NO_2 groups fit into a planar structure in a methanide as long as the third R group is either H or CN. However, when a third NO or NO_2 group is introduced into the methanides (TNM, NDNtM, DNNtM), the larger electrostatic repulsion forces the anion into a nonplanar geometry. Here, the balance between resonance stabilization and steric repulsion results in the twisting of one NO_2 or NO group out of the anion plane.

Structural parameters, such as the fairly short C−NO, C−NO_2 and C−CN bond lengths, together with the planarity, indicate the presence of delocalized π-bonds over the whole anion. MO and NBO[34] calculations displayed the existence of an $n\pi$-electron, m-center bond unit in all methanides (Scheme 20, with $n = 2 + 4x + 2y + 2z$ and $m = 1 + 3x + 2y + 2z$; x = number of NO_2 groups, y = number of NO groups and z = number of CN groups in the anion plane).

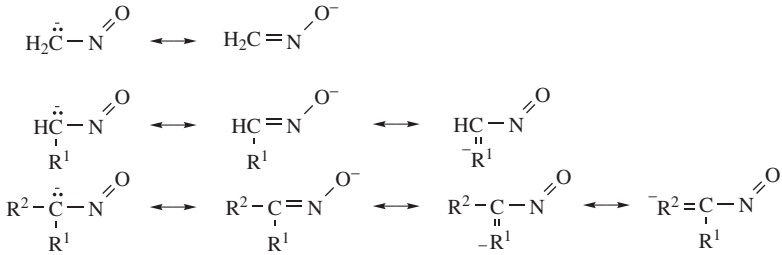

SCHEME 20. Resonance scheme for nitrosomethanides (R^1, R^2 = NO, NO_2 and CN)

To gain a quantitative view of the delocalization of the p-type lone pair (LP) localized at the central C atom, the partial charges, occupancies of the p-type LP (occ(LP(C)p_z)) and the charge transfer upon substitution have been listed in Table 9. The overall charge transfer ($q_{CT}(\pi + \sigma)$) was divided into a π ($q_{CT}(\pi)$) and σ contribution ($q_{CT}(\sigma)$, Table 9). The delocalization of the p-type lone pair, $q_{CT}(\pi)$, increases along the series CN < NO_2 < NO for all substitution patterns whereas the σ contribution increases along CN < NO < NO_2. Introduction of the second NO group results once again in an increase of both the π and σ contribution, although the magnitude strongly decreases, especially for the π contribution (e.g. CH_2NO^-: −0.75 and −0.15 e for the second NO group in $CH(NO)_2^-$ resulting in an

TABLE 9. NPA charges (q), occupancies (occ) and charge transfers (q_{CT}) in e

	q(C) (in e)	occ(LP(C)p_z)	$q_{CT}(\pi)$	$q_{CT}(\sigma)$	$q_{CT}(\pi+\sigma)$	% C[a]
CH_3^-	−1.45	2.00	0.00	+0.45	+0.45	99.7
CH_2NO^-	−0.40	1.25	−0.75	−0.31	−1.06	55.4
$CH(NO)_2^-$	−0.03	1.10	−0.90	−0.52	−1.42	50.3
$C(NO)_3^-$	0.14	1.15	−0.85	−0.74	−1.59	66.7
$C(CN)(NO)(NO_2)^-$	−0.03	1.25	−0.75	−0.67	−1.43	61.9

[a] Percent of localization of the methanide lone pair on the carbon atom according to the calculated NLMO (natural localized molecular orbital).

overall $q_{CT}(\pi) = -0.90\ e$). Upon introducing a third NO group, the π contribution actually decreases in TNM. However, the σ contribution increases significantly. The dramatic decrease of the partial charge on the C atom (cf. −1.45 in CH_3^- vs. +0.15 e in TNM) in the methanides is mainly attributed to the delocalization of the p-LP (π contribution) and the increase of the polarization in the σ bonds upon substitution. The σ contribution increases relatively to the π contribution the larger the degree of substitution. The best delocalization of the p-type LP is found in DNM with $q_{CT}(\pi) = -0.90\ e$. Molecular orbital theory, classical VB resonance structures and electron charge arguments suggest that most of the negative charge in the NO- and NO_2-substituted methanides is located on the oxygen atom, which is also the more electronegative element.

To estimate the resonance stabilization energy, the reaction energies of a series of isodesmic reactions[96] according to equations 10–12 (Table 10) have been computed. The computed resonance-stabilization energies reveal a similar picture to the charge transfer/delocalization consideration: The largest resonance energy is gained for monosubstitution in $[H_2C{-}NO]^-$ (−289.3 kJ mol^{-1}), while the second and third substitution give only −184.6 and −31.0 kJ mol^{-1}, displaying a dramatic decrease.

$$[H_3C]^- + H_3C{-}R^1 \longrightarrow [H_2CR^1]^- + H_3C{-}H \tag{10}$$

$$[H_2CR^1]^- + H_2CR^1R^2 \longrightarrow [HCR^1R^2]^- + H_3C{-}R^1 \tag{11}$$

$$[HCR^1R^2]^- + HCR^1R^2R^3 \longrightarrow [CR^1R^2R^3]^- + H_2CR^1R^2 \tag{12}$$

Also, the NBO approach[34] can be used to study delocalization effects quantitatively. The NLMO (natural localized molecular orbitals) are especially suitable to display delocalization of a localized natural bond orbital. Here, the contributions of the antibonds represent the delocalization of the bonding orbital, φ_{AB}, from an idealized, strictly-localized Lewis structure, over antibonding orbitals due to noncovalent, hyperconjungative interactions. Thus, the localized MOs offer a direct description of delocalization. Again, the inspection of the delocalization effects in the NLMO describing the methanide lone pair displays similar trends as discussed for the charge transfer, nicely corresponding to the resonance energies (Tables 9 and 10). While the localization of the p-type lone pair on the methanide C atom steadily decreases for the first and second substitution (55.4% and 50.3%; only a small decrease is found for the second substitution), an increase is found for the third substitution (66.7%).

In summary, as shown by different theoretical approaches (charge transfer, resonance energies and NLMO delocalization) resonance effects occur in all three classes of methanides. However, the magnitude of such effects strongly differs depending on the degree of substitution.

TABLE 10. Resonance energies according to equations 10–12 in kJ mol^{-1}

$\Delta_{res}E$	$R^1 = R^2 = R^3 = NO$
$\Delta_{res}E$(eq. 10)	−289.2
$\Delta_{res}E$(eq. 11)	−184.6
$\Delta_{res}E$(eq. 12)	−31.0
$\Delta_{res}E$(eq. 10 + eq. 11)	−474.1
$\Delta_{res}E$(eq. 10 + eq. 11 + eq. 12)	−504.7
$\Delta_{res}E$	$R^1 = NO$, $R^2 = NO_2$, $R^3 = CN$
$\Delta_{res}E$(eq. 12)	−91.0

VII. GAS-PHASE ACIDITIES

Gas-phase acidities ($\Delta G_{(gas,\ 298\ K)}$) describe the energetics of the deprotonation reaction of an acid in the gas phase at 298 K, and small gas-phase acidities in comparison with that of unsubstituted methane, $CH_4 \rightarrow CH_3^- + H^+$, can be regarded as a measure of the resonance stabilization in substituted methanides. Furthermore, with the help of gas-phase acidities it is possible to calculate absolute pK_a value if solvation can be estimated, as illustrated in Figure 38 (p$K_a = \Delta G_{aq}$/2.303 RT)[97–99]. On the basis of DFT calculation at the B3LYP/aug-cc-pvTZ level of theory, gas-phase acidities are easily calculated with sufficient accuracy while theoretical estimation of solvation effects with acceptable accuracy (±5 kJ mol^{-1}) remains an unsolved problem. Hence, only gas-phase acidities have been calculated due to the lack of experimental data. Since for all considered substituted methane derivatives the oxime ($R^1R^2C{=}NOH$ with R^1, R^2 = H, NO, NO_2, CN) represents the most stable species, gas-phase acidities listed in Figure 39 refer always to the most stable isomer of the oxime species.

The calculated gas-phase acidity of methane is 1704.4 kJ mol^{-1}, which is nicely in agreement with the experimental value 1709.0 ± 3.3 kJ mol^{-1}[100]. Substitution of one hydrogen atom by one nitroso group dramatically increases the acid strength as displayed by the decrease in the $\Delta G_{(gas,\ 298\ K)}$ value (by 224.5 kJ mol^{-1}) down to 1479.9 kJ mol^{-1}. Double and triple substitution further increases the acid strength of the corresponding oxime acids to 1333.4 and 1272.2 kJ mol^{-1} for *aci*-dinitroso and trinitrosomethane (Figure 39); however, the difference for the gas-phase acidity between double and triple substitution is much smaller (146.5 and 61.2 kJ mol^{-1}). Interestingly, the gas-phase acidity of HC(NOH)R (R = NO, NO_2 or CN) does not depend much on whether R = NO or NO_2, but R = CN gives an acidity which is *ca* 32 kJ mol^{-1} larger. For the triply substituted methane derivative $HC(NOH)R^1R^2$ (R = NO, NO_2 or CN) the difference between NO and NO_2 is more pronounced [1272.2 for $C(NOH)(NO)_2$ vs. 1236.6 for $C(NOH)(NO)(NO_2)$]. Nevertheless, two distinct ranges can be established: (i) the gas-phase acidities for the doubly substituted oximes lie in the range between 1333 and

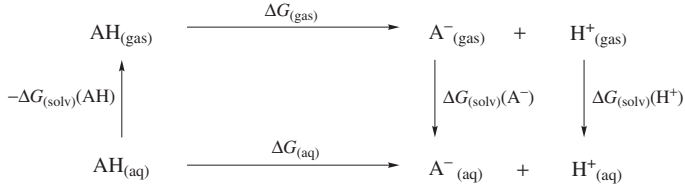

FIGURE 38. Thermodynamic cycle for the estimation of pK_a values

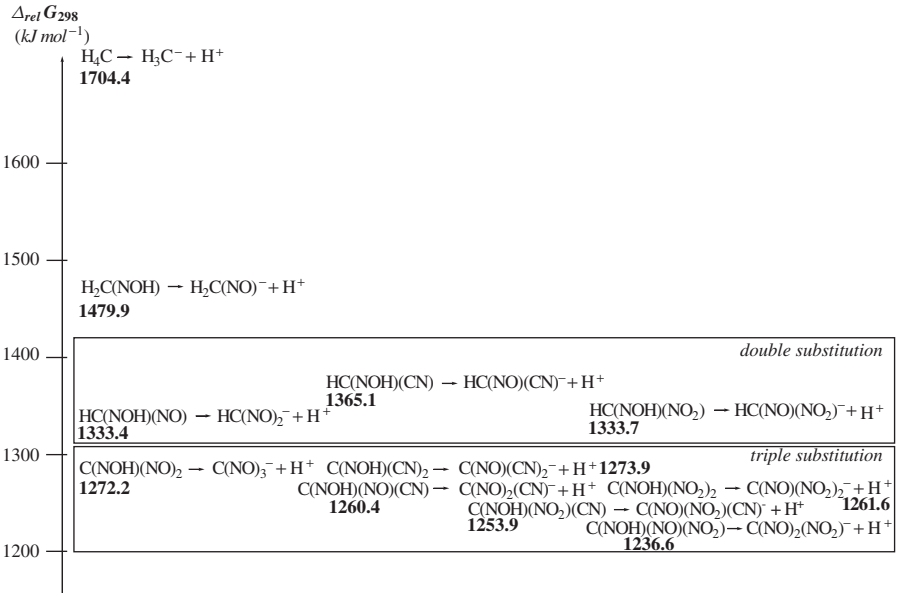

FIGURE 39. Calculated gas-phase acidities ($\Delta G_{(\text{gas, 298 K})}$) of substituted oxime acids

1365 kJ mol^{-1} (cf. $CH_4 \rightarrow CH_3^- + H^+$1704.4 kJ mol^{-1}), and (ii) for the triply substituted oximes between 1236 and 1274 kJ mol^{-1}.

VIII. APPLICATION–SUMMARY–OUTLOOK

All nitrosomethanides represent resonance-stabilized anions, which are stable at ambient temperatures. However, their alkali and silver salts are energetic materials and hence most of them are explosive. The reason for this thermodynamic instability lies in the smaller CN and NO bond energies compared to those of N_2 and CO (in CO_2).

Protonation always preferably occurs at the nitroso group, leading to oxime species which are very labile and must be prepared at low temperatures. Intramolecular hydrogen bonding often stabilizes isomers. For instance, two intramolecular hydrogen bonds are found in the lowest-lying w-shaped isomer of DNM, $HC(NO)_2^-$, while for the isoelectronic dinitrosoamide a nonplanar structure is assumed due to the lack of such hydrogen bonding.

Application may be found for ionic liquids of resonance-stabilized methanides which can easily be prepared from the alkali salts. The first synthetic step includes the formation of the nearly insoluble silver salts in water (AgX, X = methanide). Since the silver salts dissolve in 2N aqueous NH_3, adding ethyl(methyl)imidazolium bromide (EMI^+Br^-) results in the formation of a water-soluble ethyl(methyl)imidazolium methanide (EMI^+X^-) which can be separated from the AgBr precipitate by filtration[12].

In contrast to most of the high energy-density alkali and silver (NO- and NO_2-substituted) methanides, the ionic liquids of these methanides with a bulky organic cation are neither heat nor shock sensitive, and hence can be prepared and stored in large scale. Nevertheless, this type of methanide-based ionic liquids can also be considered ‘energetic ionic liquids’ since the thermodynamically unstable methanide anion is only kinetically

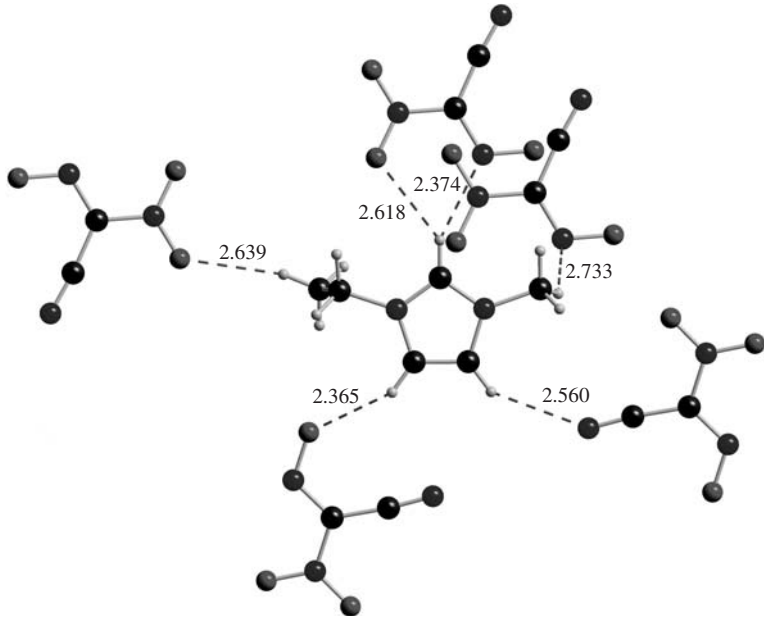

FIGURE 40. Cation–anion interactions in ethyl(methyl)imidazolium NNtCM salt–ionic liquid with a m.p. of 35 °C. (distances are in Å)

TABLE 11. Properties of methanide based ionic liquids [RMI^+X^-] (R organic group, M = methyl, I = imidazolium; X = resonance-stabilized nitrosomethanide)

Methanide	R	Mol. Weight ($g\,mol^{-1}$)	T_m/T_g (°C) [a]	T_{dec} (°C) [a]	λ_{max} (nm) [b]	Color
$NtNCM^-$	Ethyl	225.2	35	52	489	red
$NtNCM^-$	*n*-butyl	253.3	−4	65	489	red
DNM^-	Ethyl	184.2	−6	180	679	blue-violet

[a] T_m = melting point, T_g = phase-transition temperature, T_{dec} = decomposition onset temperature.
[b] UV-Vis in water solution.

stabilized by bulky organic cations such as EMI^+ or BMI^+ [BMI^+ = butyl(methyl) imidazolium]. Nitrosomethanide-based ionic liquids are very hygroscopic and immediately absorb water when exposed to air. The experimentally determined melting points vary between −4 °C and 35 °C (Figure 40, Table 11), with the BMI^+ salts always possessing the lower melting point[17].

In summary, resonance effects occur in all three classes (CN-, NO- and NO_2-substituted) of methanides; however, the magnitude of such effects strongly differs depending on the degree of substitution. In contrast to the parent species CH_3^-, most methanides are planar as long as the carbon lone pair is stabilized by resonance; however, for triply substituted NO_2 and NO methanides, the balance between electrostatic repulsion and resonance effects results in deviation from planarity. TNM^- salts are not known yet, but it can be assumed according to theory (B3LYP/aug-cc-pvTZ) that the TNM^- anion adopts a non-planar geometry similar to those of $TNtM^-$ salts. On the other hand, good delocalization

results is a low basicity of the anion or in an increased acidity of the oxime acid expressed by small $\Delta G_{(\text{gas, 298 K})}$ values.

'Energetic ionic liquids', such as NO_2- and NO-substituted methanide-based ionic liquids, are kinetically stabilized by bulky organic cations. Both the alkali salts and the ionic liquids represent good precursors for further synthesis and can be used as interesting ligands in organometallic chemistry. Interesting physical properties can be expected from such metal complexes.

IX. REFERENCES

1. C. L. Coe and T. F. Doumani, *J. Am. Chem. Soc.*, **70**, 1516 (1948).
2. (a) L. A. K. Staveley and C. N. Hinshelwood, *Nature (London)*, **137**, 29 (1936).
   (b) L. A. K. Staveley and C. N. Hinshelwood, *J. Chem. Soc.*, 812 (1936).
   (c) L. A. K. Staveley and C. N. Hinshelwood, *Proc. R. Soc. London, Ser. A*, **154**, 335 (1936).
3. M. Polasek and F. Turecek, *J. Am. Chem. Soc.*, **122**, 525 (2000).
4. H. A. Taylor and H. Bender, *J. Chem. Phys.*, **9**, 761 (1941).
5. R. Scholl, *Chem. Ber.*, **24**, 573 (1891).
6. W. R. Dunstan and A. L. Bossi, *J. Chem. Soc. Trans.*, **73**, 353 (1898).
7. (a) B. G. Gowenlock and G. B. Richter-Addo, *Chem. Rev.*, **104**, 3315 (2004).
   (b) B. G. Gowenlock and G. B. Richter-Addo, *Chem. Soc. Rev.*, **34**, 797 (2005).
8. (a) L. Birckenbach and K. Kellermann, *Chem. Ber.*, **58B**, 786 (1925).
   (b) L. Birckenbach and K. Kellermann, *Chem. Ber.*, **58B**, 2377 (1925).
   (c) L. Birckenbach, K. Huttner and W. Stein, *Chem. Ber.*, **62B**, 2065, 2261 (1929).
   (d) L. Birckenbach and M. Linhard, *Chem. Ber.*, **63B**, 2528, 2544, 2588 (1930).
9. A. M. Golub and H. Köhler, *Chemie der Pseudohalogenide*, VEB Deutscher Verlag der Wissenschaften, Berlin, 1979.
10. (a) A. Schulz, *Habilitationsschrift*, LMU, München, 2001.
    (b) A. M. Golub, H. Köhler and V. V. Stopenko, *Chemistry of Pseudohalides*, Elsevier, Amsterdam, 1986.
11. H. Grimm, *Z. Elektrochem.*, **31**, 474 (1925).
12. H. Brand, A. Schulz and A. Villinger, *Z. Anorg. Allg. Chem.*, **633**, 22 (2007).
13. (a) E. Kessenich, K. Polborn and A. Schulz, *Z. Anorg. Allg. Chem.*, **627**, 2506 (2001).
    (b) E. Kessenich, A. Schulz and K. Polborn, *Acta Crystallogr.*, **E58**, i15 (2002).
14. A. W. Browne and A. B. Hoel, *J. Am. Chem. Soc.*, **44**, 2106 (1922).
15. E. Lieber, E. Offentdahl and C. N. R. Rao, *J. Org. Chem.*, **22**, 1750 (1957).
16. F. Sommer, *Chem. Ber.*, **48**, 1833 (1915).
17. H. Brand, J. F. Liebman, A. Schulz and A. Villinger, *Eur. J. Inorg. Chem.*, 4294 (2006).
18. F. A. Andersen and K. A. Jensen, *J. Mol. Struct.*, **60**, 165 (1980).
19. H. Brand, P. Mayer, K. Polborn, A. Schulz and J. J. Weigand, *J. Am. Chem. Soc.*, **127**, 1360 (2005).
20. (a) R. A. Olofson and J. S. Michelman, *J. Am. Chem. Soc.*, **86**, 1863 (1964).
    (b) R. A. Olofson and J. S. Michelman, *J. Org. Chem.*, **30**, 1854 (1965).
21. (a) D. Mulvey and W. A. Waters, *J. Chem. Soc., Perkin Trans. 2*, 666 (1974).
    (b) V. V. Paramonov, V. A. Petrosyan and V. I. Slovetskii, *Bull. Acad. Sci. USSR, Div. Chem. Sci.*, **27**, 678 (1978).
22. (a) H. Köhler and G. Lux, *Inorg. Nucl. Chem. Lett.*, **4**, 133 (1968).
    (b) H. Köhler, V. F. Bolelij and V. V. Skopenko, *Z. Anorg. Allg. Chem.*, **468**, 179 (1980).
    (c) N. Arulsamy, D. S. Bohle and B. G. Doletski, *Inorg. Chem.*, **38**, 2709 (1999).
23. (a) V. A. Petrosyan, V. V. Paramonov, *Bull. Acad. Sci. USSR, Div. Chem. Sci.*, **25**, 1863 (1976).
    (b) V. V. Paramonov, V. A. Petrosyan and V. I. Slovetskii, *Bull. Izv. Akad. Nauk SSSR, Ser. Khim.*, **4**, 786 (1978); *Chem. Abstr.*, **89**, 119661 (1978).
24. H. Brand, P. Mayer, A. Schulz and J. J. Weigand, *Angew. Chem.*, **117**, 3998 (2005); *Angew. Chem. Int. Ed.*, **44**, 3929 (2005).
25. V. A. Petrosyan, V. V. Paramonov and V. I. Slovetskii, *Bull. Izv. Akad. Nauk SSSR, Ser. Khim.*, **9**, 1983 (1976); *Chem. Abstr.*, **86**, 162765 (1976).

26. K. Lammertsma and B. Prasad, *J. Am. Chem. Soc.*, **115**, 2348 (1993).
27. For instance: (a) E. Bosch and J. K. Kochi, *J. Org. Chem.*, **59**, 5573 (1994).
(b) J. H. Atherton, R. B. Moodie and D. R. Noble, *J. Chem. Soc., Perkin Trans. 2*, 699 (1999).
28. For instance: (a) A. Baeyer, *Chem. Ber.*, **7**, 1638 (1874).
(b) B. Oddo, *Gazz. Chim. Ital.*, **39**, 659 (1911).
(c) W. L. Waters and P. G. Marsh, *J. Org. Chem.*, **40**, 3344 (1975).
(d) L. I. Smith and F. L. Taylor, *J. Am. Chem. Soc.*, **57**, 2460 (1935).
(e) E. Robson, J. M. Tedder and D. J. Woodcock, *J. Chem. Soc., C*, 1324 (1968).
(f) J. C. Motte and H. G. Viehe, *Chimia*, **29**, 515 (1975).
29. For instance: (a) O. Wallach, *Terpene und Campher*; 2nd edn., Veit and Co., Leipzig, 1914.
(b) L. J. Beckham, W. A. Fessler and M. A. Kise, *Chem. Rev.*, **48**, 319 (1951).
(c) P. P. Kadzyauskas and N. S. Zefirov, *Russ. Chem. Rev.*, **37**, 543 (1968).
(d) M. A. Samartsev and K. A. Ogloblin, *J. Org. Chem. USSR*, **1**, 29 (1965).
(e) K. A. Ogloblin and M. A. J. Samartsev, *J. Org. Chem. USSR*, **1**, 864 (1965).
30. (a) H. Z. Caro, *Angew. Chem.*, **11**, 845 (1898).
(b) W. J. Mijs, S. E. Hoeskstra, R. M. Ulmann and E. Havinga, *Recl. Trav. Chim. Pays-Bas*, **77**, 746 (1958).
(c) W. J. Mijs, Ph.D. Thesis, University of Leiden, Leiden, 1959.
(d) A. Schors, A. Kraaijeveld and E. Havinga, *Recl. Trav. Chim. Pays-Bas*, **74**, 1243 (1955).
(e) R. R. Holmes, R. P. Bayer, L. A. Errede, H. R. Davis, A. W. Wiesenfeld, P. M. Bergman and D. L. Nicholas, *J. Org. Chem.*, **30**, 3837 (1965).
31. (a) F. J. Alway, *Chem. Ber.*, **36**, 2303 (1903).
(b) H. Pechmann and A. Nold, *Chem. Ber.*, **31**, 557 (1898).
(c) R. D. Haworth and A. Lapworth, *J. Chem. Soc.*, **119**, 768 (1921).
(d) D. Vorländer, *Chem. Ber.*, **58**, 1893 (1925).
(e) E. Bamberger, *Chem. Ber.*, **28**, 1218 (1895).
(f) F. J. Always and A. B. Walker, *Chem. Ber.*, **36**, 2312 (1903).
32. (a) A. Maltha, H. F. Kist, T. L. F. Favre, H. G. Karge, F. Asmussen, H. Onishi, Y. Iwasawa and V. Ponec, *Appl. Catal. A: Gen.*, **115**, 85 (1994).
(b) A. Maltha, M. Muhler and V. Ponec, *Appl. Catal. A: Gen.*, **115**, 69 (1995).
(c) A. Maltha, T. L. F. Favre, B. Brunet, C. Gaudin and V. Ponec, *Catal. Lett.*, **28**, 17 (1994).
(d) A. Meijers, T. P. P. van der Hoeven, V. Ponec, J. P. Jacobs and H. H. Brongersma, *J. Catal.*, **161**, 459 (1996).
33. N. Strauch, Diploma Thesis, Munich, 2006.
34. (a) E. D. Glendening, A. E. Reed, J. E. Carpenter and F. Weinhold, *NBO Version 3.1*.
(b) J. E. Carpenter and F. Weinhold, *J. Mol. Struct. (THEOCHEM)*, **169**, 41 (1988).
(c) F. Weinhold and J. E. Carpenter, *The Structure of Small Molecules and Ions*, Plenum Press, New York, 1988, p. 227.
(d) F. Weinhold and C. Landis, *Valency and Bonding. A Natural Bond Orbital Donor–Acceptor Perspective*, Cambridge University Press, 2005 and references therein.
35. P. D. Adeney, W. J. Bouma, L. Radom and W. R. Rodewell, *J. Am. Chem. Soc.*, **102**, 4069 (1980).
36. K. A. Jensen and A. Holm, *Den. Matem.-Fys. Med.—Kong. Danske Vid. Sel.*, **40**, 24 (1978); *Chem. Abstr.*, **89**, 110480 (1978).
37. K. A. Jensen, *Angew. Chem., Int. Ed. Engl.*, **13**, 348 (1974).
38. (a) A. P. Argekar and A. K. Shelty, *Anal. Sci.*, **13**, 131 (1997).
(b) M. Dogutan, H. Filik and R. Apak, *Anal. Chim. Acta*, **485**, 205 (2003).
39. T. F. Doumani, C. S. Coe, US Patent 19610509 (1961).
40. D. Dallas, A. B. Padias and H. K. Hall, *J. Polym. Sci., Part A: Polym. Chem.*, **40b**, 181 (2001).
41. K. Schorpp and W. Beck, *Chem. Ber.*, **107**, 1371 (1974).
42. A. Azman, D. Hazi, J. Kidric, B. Orel and C. Trampuz, *Spectrochim. Acta*, **27A**, 2499 (1971)
43. Y. Umar, T. Jimoh and M. A. Morsy, *J. Mol. Struct. (THEOCHEM)*, **725**, 157 (2005).
44. E. Bamberger and R. Seligman, *Chem. Ber.*, **36**, 685 (1903).
45. L. Batt, B. G. Gowenlock and J. Trotman, *J. Chem. Soc.*, 2222 (1960).
46. T. Shimanouchi, *Tables of Molecular Vibrational Frequencies* (NSRDS-NBS 39, 1972).
47. P. H. Turner and A. P. Cox, *J. Chem. Soc., Faraday Trans. 2*, **74**, 533 (1978).
48. A. J. Barnes, H. E. Hallam, S. Waring and J. R. Armstrong, *J. Chem. Soc., Faraday Trans. 2*, **72**, 1 (1976).

49. (a) M. Alcami, O. Mo, M. Yáñez, A. Luna, J.-P. Morizur and J. Tortajada, *J. Phys. Chem., A*, **102**, 10120 (1998).
    (b) T. Vladimiroff, *J. Mol. Struct. (THEOCHEM)*, **401**, 141 (1997).
50. D. C. Frost, W. M. Lau, C. A. McDowell and N. P. C. Westwood, *J. Phys. Chem.*, **86**, 3577 (1982).
51. For instance: (a) J. A. Altmann and H. S. Rzepa, *J. Mol. Struct. (THEOCHEM)*, **33**, 149 (1987).
    (b) M. Alcami, O. Mo and M. Yáñez, *J. Comput. Chem.*, **109**, 1072 (1998).
52. J. A. Long, N. J. Harris and K. Lammertsma, *J. Org. Chem.*, **66**, 6762 (2001).
53. I. N. Levine, *J. Chem. Phys.*, **38**, 2326 (1963)
54. N. Wiberg, *Lehrbuch der Anorganischen Chemie*, 102. Aufl., Walter de Gruyter, Berlin, 2007.
55. T. K. Bierlein and E. C. Lingafelter, *Acta Crystallogr.*, **4**, 450 (1951).
56. P. H. Turner and A. P. Cox, *J. Chem. Soc., Fraday Trans. 2*, **74**, 533 (1978).
57. M. van Meerssche and G. Germain, *Bull. Soc. Chim. Belg.*, **68**, 244 (1957).
58. (a) R. Hoffman, R. Gleiter and F. B. Mallory, *J. Am. Chem. Soc.*, **72**, 1460 (1970).
    (b) A. B. Heiberg, *Chem. Phys.*, **26**, 309 (1977).
    (c) J. Bentley and K. P. Madden, *J. Am. Chem. Soc.*, **116**, 11397 (1994).
59. B. G. Gowenlock, K. J. McCullough and R. B. Manson, *J. Chem. Soc., Perkin Trans. 2*, 701 (1988).
60. M. I. Christie, J. S. Frost and M. A. Voisey, *Trans. Fraday Soc.*, **61**, 674 (1965).
61. (a) H. Wieland, *Chem. Ber.*, **38**, 1445 (1905).
    (b) H. Wieland and H. Bauer, *Chem. Ber.*, **39**, 1480 (1906).
    (c) H. Wieland, *Justus Liebigs Ann. Chem.*, **353**, 65 (1907).
    (d) H. Wieland and H. Hess, *Chem. Ber.*, **42**, 4175 (1909).
62. (a) J. Armand and R.-M. Minvielle, *C. R. Hebd. Seances Acad. Sci.*, **258**, 207 (1964).
    (b) J. Armand and R.-M. Minvielle, *C. R. Hebd. Seances Acad. Sci.*, **260**, 2512 (1965).
63. (a) G. Vetter and G. Klar, *Z. Naturforsch.*, **28b**, 287 (1973).
    (b) G. Vetter, J. Kopf and G. Klar, *Z. Naturforsch.*, **28b**, 293 (1973).
    (c) F. Olbrich, B. Zimmer, M. Kastner, C. von Schlabrendorff, G. Vetter and G. Klar, *Z. Naturforsch.*, **47b**, 1571 (1992).
64. M. Witanowski, L. Stefaniak and G. A. Webb, *Annu. Rep. NMR Spectrosc. (Nitrogen NMR Spectroscopy)*, **25**, 1 (1993).
65. J. U. Nef, *Justus Liebigs Ann. Chem*, **280**, 338 (1894).
66. A. C. Fantoni and W. Caminati, *J. Mol. Struct.*, **376**, 33 (1996).
67. N. Arulsamy and D. S. Bohle, *J. Am. Chem. Soc.*, **123**, 10860 (2001).
68. W. Traube, *Justus Liebigs Ann. Chem.*, **300**, 81 (1898).
69. (a) J. H. Bryden, *Acta Crystallogr.*, **12**, 581 (1959).
    (b) V. D. Cherepinskii-Malov, A. S. Mukhametzyanov, V. G. Andrianov and G. A. Marchenko, *Russ. J. Org. Chem.*, **24**, 157 (1983).
70. (a) Y. M. Chow and D. Britton, *Acta Crystallogr.*, **B30**, 1117 (1974).
    (b) M. Hvastijova, K. Kohout, J. Kozisek and I. Svoboda, *J. Coord. Chem.*, **47**, 573 (1999).
    (c) D. J. Price, S. R. Batten, K. J. Berry, B. Moubaraki and K. S. Murray, *Polyhedron*, **22**, 165 (2003).
    (d) A. S. R. Chesman, D. R. Turner, E. I. Izgorodina, S. R. Batten and G. B. Deacon, *Dalton Trans.*, 1371 (2007).
71. E. Iglesias and D. L. H. Williams, *J. Chem. Soc., Perkin Trans. 2*, 343 (1989).
72. G. Longo, *Gazz. Chim. Ital.*, **61**, 578 (1931).
73. D. S. Bohle, B. J. Conklin and C.-H. Hung, *Inorg. Chem.*, **34**, 2569 (1995).
74. C. Grundmann and M. Fulton, *Chem. Ber.*, **97**, 566 (1964).
75. E. Beckmann and E. Bark, *J. Prakt. Chem.*, **105**, 327 (1923).
76. C. Grundmann, *Chem. Ber.*, **97**, 575 (1964).
77. H. Wieland, L. Semper and E. Gmelin, *Justus Liebigs Ann. Chem.*, **367**, 52 (1909).
78. S. v. Hantzsch, *Chem. Ber.*, **25**, 705 (1892).
79. B. Lach, *Chem. Ber.*, **17**, 1571 (1884).
80. (a) V. Mayer, *Chem. Ber.*, **6**, 1492 (1873).
    (b) V. Mayer, *Justus Liebigs Ann. Chem.*, **214**, 328 (1882).
81. J. Tscherniak, *Chem. Ber.*, **8**, 114 (1875).

82. (a) H. Wieland, *Chem. Ber.*, **42**, 803 (1909).
(b) H. Wieland, *Chem. Ber.*, **40**, 418 (1907).
83. D. Mulvey and W. A. Waters, *J. Chem. Soc., Perkin Trans. 2*, 666 (1974).
84. G. Ponzio, *Mat. e Naturali*, **38**, 201 (1903).
85. H. Wieland, *Chem. Ber.*, **40**, 418 (1907).
86. K. J. Reszka, C. F. Chignell and P. Bilski, *J. Am. Chem. Soc.*, **116**, 4119 (1994).
87. G. A. Russel, R. K. Norris and A. R. Metcalfe, *J. Am. Chem. Soc.*, **94**, 4959 (1972).
88. W. Steinkopf, *Chem. Ber.*, **42**, 617 (1909).
89. P. Pillai and J. H. Boyer, *Org. Prep. Proced. Int.*, **14**, 365 (1982).
90. (a) Ch. Grundmann and H. D. Frommeld, *J. Org. Chem.*, **31**, 4235 (1966).
(b) B. Guo, T. Pasinszki, N. P. C. Westwood, K. Zhang and P. F. Bernath, *J. Chem. Phys.*, **105**, 4457 (1996).
(c) T. Pasinszki and N. P. C. Westwood, *J. Phys. Chem.*, **100**, 16856 (1996).
(d) T. Pasinszki and N. P. C. Westwood, *J. Chem. Soc., Chem. Commun.*, **18**, 1901 (1995).
(e) G. Maier and J. H. Teles, *Angew. Chem.*, **99**, 152 (1987).
91. Ch. Grundmann and P. Günanger, *The Nitrile Oxides*, Springer-Verlag, New York, 1971.
92. (a) T. Ozawa, *Bull. Chem. Soc. Jpn.*, **38**, 1881 (1965).
(b) H. E. Kissinger, *Anal. Chem.*, **29**, 1702 (1957).
(c) Standard Test Method for Arrhenius Kinetic Constants for Thermally Unstable Materials, ASTM Designation E698-99, 1999.
93. A. A. Gakh, J. C. Bryan, M. N. Burnett and P. V. Bonnesen, *J. Mol. Struct.*, **520**, 221 (2000).
94. J. Cioslowski, S. T. Mixon and E. D. Fleischmann, *J. Am. Chem. Soc.*, **113**, 4751 (1991).
95. (a) HF/TZ+2p+d level; T. J. Lee and H. F. Schaefer III, *J. Chem. Phys.*, **83**, 1784 (1985).
(b) U. Salzner and P. v. R. Schleyer, *Chem. Phys. Lett.*, **199**, 267 (1992).
96. (a) W. J. Hehre, L. Radom, P. v. R. Schleyer and J. Pople, *Ab Initio Molecular Orbital Theory*, Wiley, New York, 1986.
(b) T. M. Klapötke and A. Schulz, *Quantenmechanische Methoden in der Hauptgruppenchemie*, Spektrum, Heidelberg, 1996.
97. I. A. Topol, G. J. Tawa, S. K. Burt and A. A. Rashin, *J. Phys. Chem., A*, **101**, 10075 (1997).
98. M. D. Liptak and G. C. Shields, *Int. J. Quantum Chem.*, **85**, 727 (2001).
99. A. M. Toth, M. D. Liptak, D. L. Phillips and G. C. Shields, *J. Chem. Phys.*, **114**, 4595 (2001).
100. G. B. Ellison, P. C. Engelking and W. C. Lineberger, *J. Am. Chem. Soc.*, **100**, 2556 (1978).

CHAPTER **15**

Nitroxyl radicals

CARLO GALLI

Dipartimento di Chimica, Università 'La Sapienza', and IMC-CNR Sezione Meccanismi di Reazione, 00185 Roma, Italy
Fax: +0039 06 490421; e-mail: carlo.galli@uniroma1.it

The chemistry of hydroxylamines, oximes and hydroxamic acids
Edited by Z. Rappoport and J. F. Liebman

I. INTRODUCTION

A. Abbreviations

Shorthand notations such as ET (electron transfer), HAT (hydrogen atom transfer), BDE (bond dissociation energy), NHE (normal hydrogen electrode), CV (cyclic voltammetry), LFP (laser flash photolysis), EPR (electron paramagnetic resonance) and KIE (kinetic isotope effect) will be used throughout the chapter. In addition, recurring chemical compounds such as TEMPO (2,2,6,6-tetramethylpiperidine-*N*-oxyl), HBT (1-hydroxybenzotriazole), BTNO (benzotriazole-*N*-oxyl), HPI (*N*-hydroxyphthalimide), PINO (phthalimide-*N*-oxyl), NHA (*N*-hydroxyacetanilide) and a few others will be referred to by means of the capital-letter acronym.

B. General Remarks

The recent 'IUPAC Compendium of Chemical Terminology—The Gold Book'[1] recommends that the name of compounds having the structure $R_2N{-}O^{\bullet} \leftrightarrow R_2N^{\bullet+}{-}O^{-}$ is more appropriately that of 'aminoxyl radicals'. The synonymous terms 'nitroxyl radical' or 'nitroxide' are accordingly not desirable, even though quite popular in various fields of science and technology. This chapter follows a previous chapter of the series[2] and, for this historical reason, retains the old terminology of the compounds in the title, but this use will be discontinued from now on in the text.

The aminoxyl radicals derive from hydroxylamines by removal of hydrogen atom from the hydroxyl group[2]. The interest in this class of compounds stems from the numerous applications. In many cases these paramagnetic species are stable and isolable, at variance with other free radicals[3], and the persistency grants an important practical role. Stable aminoxyl radicals have found use as both promoters of polymerization reactions and inhibitors of free radical processes or autooxidation[4–8]. They are useful as spin probes in EPR investigations[9–13] both in medical science and in more remote fields[14], for example for tracing the migration of underground fluids in the oil industry[4,15], or as antioxidants in the food industry[3] or for the preparation of novel magnetic materials[16,17]. The aminoxyl radicals are popular in biological media as spin-label and spin-trapping agents[13,18,19], as inhibitors of the metabolism of enzymes or else as inhibitors of the development of certain malignant formations[20]. These points have been dealt with before[2,11]. The present chapter will survey a specific and more recent application of the aminoxyl radicals, where the role of persistency is not so crucial. I refer to their use as catalysts in chemical transformations, and particularly in oxidation reactions endowed with low environmental impact ('green chemistry')[21,22]. In this context, the aminoxyl radical ($R_2NO^{\bullet}$) removes hydrogen atom from a substrate, enabling subsequent interaction with O_2 and therefore an oxidation outcome (Scheme 1).

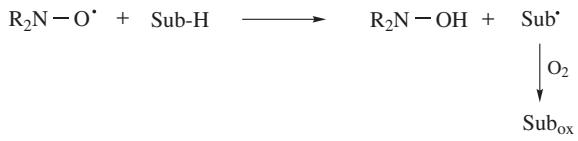

SCHEME 1. Oxidation of a substrate (Sub-H) induced by the use of an aminoxyl radical

Besides this hydrogen atom transfer (HAT) route, the aminoxyl radical may also take part in oxidation procedures where, through a preliminary monoelectronic step, it is converted into an oxoammonium ion ($R_2N{=}O^{+}$), or variations of this route. Examples of

synthetic application of these oxidation procedures will be considered, but first salient properties and reactivity features of the aminoxyl radicals are commented on in Sections II and III.

II. PHYSICOCHEMICAL PROPERTIES OF THE AMINOXYL RADICALS

A. General Features

It is appropriate to summarize here relevant data of both the aminoxyl radicals and their precursors that are useful for the ensuing discussion. Hydroxylamine (H_2NOH) is the precursor of the archetypal aminoxyl radical ($H_2NO^{\bullet}$)[23]. Upon one-electron oxidation of H_2NOH by a suitable oxidant, e.g. Ce^{4+}, the formation of $H_2NO^{\bullet}$ (plus one proton) has been documented by EPR[24,25], the first step being the formation of the transient radical cation $H_2NOH^{\bullet+}$ [26]; the same radical $H_2NO^{\bullet}$ is alternatively formed from H_2NOH by a suitable H-atom abstractor[23]. This underlines the possible dichotomy of generation of an aminoxyl radical from the parent hydroxylamine, by either H-abstraction or electron abstraction/deprotonation (Scheme 2).

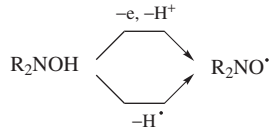

SCHEME 2. Possible pathways for the generation of aminoxyl radicals

In principle, aminoxyl radicals ($R_2N-O^{\bullet}$) might abstract hydrogen atom from the C–H bond of a hydrogen donor, thereby enabling subsequent oxidative transformation of the latter (Scheme 1). This represents one of the main issues of the present review; key points to discuss will be: (i) the H-abstraction reactivity of the $R_2NO^{\bullet}$ species, (ii) the needed match in bond dissociation energy (BDE) between the breaking C–H bond and the forming O–H bond in the two reacting partners, (iii) the incursion of competing routes.

1. Structural information

The UV spectrum of $H_2NO^{\bullet}$ shows an absorption maximum at 217 nm in alkaline water solution; this radical is unstable and decays by either dimerisation/cleavage or reaction with other species, with rate constants in the 10^8-10^9 M^{-1} s^{-1} range[23]. Whereas $H_2NO^{\bullet}$ is a typical reactive intermediate endowed with short lifetime, aminoxyl radicals deriving from secondary amines may instead be stable whenever complying with the general structure **1** ($R \neq H$), in which there are no hydrogens attached to the α-carbon atoms.

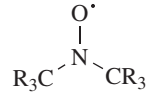

(**1**)

TEMPO (2,2,6,6-tetramethylpiperidine-*N*-oxyl) and its cognates (4-OH, 4-oxo, 4-OMe substituted derivatives; TMIO etc.) belong to a group of sterically hindered aminoxyl radicals (Chart 1) and, in view of the long lifetimes, are said to be 'persistent'[27,28] and

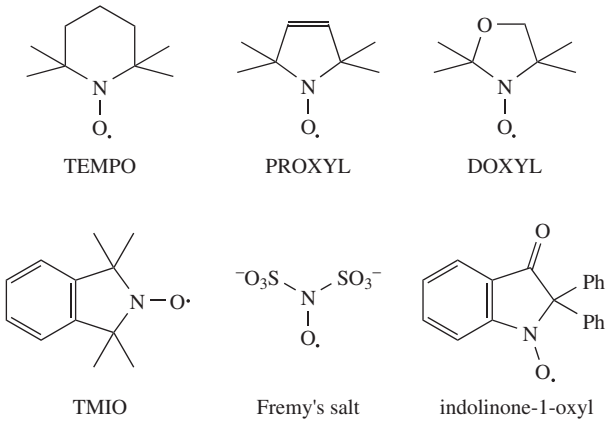

CHART 1. Structure of typical aminoxyl radicals

can be isolated and stored for many months[29]. The stability of these species, as well as that of the analogous PROXYL (2,2,5,5-tetramethylpyrroline-*N*-oxyl), DOXYL (4,4-dimethyloxazolidine-*N*-oxyl) derivatives[9,10,30–32], or di-*tert*-butyl nitroxide[33] and many more[3,34,35] is the bonus that enables use in spin-labelling studies[11].

The Fremy's salt (nitrosodisulfonate), whose properties as a selective oxidant have been reviewed[36], and bis(trifluoromethyl)aminoxyl radical, $(CF_3)_2N{-}O^{\bullet}$ [37–40], which has been mainly investigated from a kinetic viewpoint, are accordingly stable as aminoxyl radicals owing to the lack of α-hydrogens. Indole-derived aminoxyl radicals can analogously display stability due to the lack of H-atoms in α and to conjugation with the benzenoid ring[15,41–43]. Finally, conjugation and lack of α-H-atoms make both $Ph_2N{-}O^{\bullet}$ and *t*-Bu(Ph)N$-$O$^{\bullet}$ moderately stable[44–47].

In contrast to the persistency of compounds having the structure of **1**, aminoxyl radicals having one or more hydrogen atoms attached to the α-carbons typically disproportionate (Scheme 3), producing a nitrone **2** and the parent hydroxylamine **1H,** which may undergo further reaction[48]. The rate of this disproportionation strongly depends on the degree of α-substitution and on the solvent[11], typical examples being provided by the short-living dialkl nitroxides, e.g. $Et_2NO^{\bullet}$ [49]. A reasonable exception to this rule is represented by bicyclic aminoxyl radicals (e.g. **3**), that are made stable because Bredt's rule prevents the α-H abstraction and consequently any disproportionation to the nitrone[46].

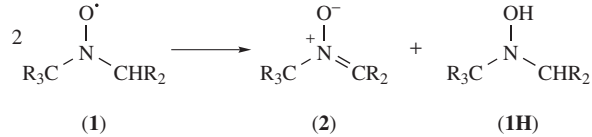

SCHEME 3. Disproportionation of an aminoxyl radical

In general, dialkyl aminoxyl radicals show an intense absorption band in the 220–260 nm range, and a yellow colour due to a weaker absorption band in the 410–450 nm region[23]. α-Electron-withdrawing or α-conjugating groups shift λ_{max} towards 290–300 nm, and the weaker absorption band towards 480–510 nm[15,50]. Factors affecting

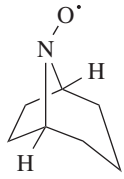

(**3**)

the geometry of the aminoxyl radicals (pyramidal vs. planar) have been addressed by computational studies[51].

A few hints about methods of generation of non-persistent aminoxyl radicals, which will be quoted a few times later in the chapter, are now given. The dichotomy of generation of an aminoxyl radical from the parent hydroxylamine has already been outlined in Scheme 2.

a. One-electron abstraction. Monoelectronic oxidation of a hydroxylamine to the aminoxyl radical can be achieved by electrochemical methods, such as cyclic voltammetry[52]. The redox potential measured in this way is often irreversible (an E^p value), unless a fast sweep scan of the potential is used[53], because the initially formed radical cation $R_2NOH^{\bullet+}$ deprotonates quickly (Scheme 4, path a). Full reversibility (E° values) can be achieved if the hydroxylamine is preliminarily deprotonated at the appropriate pH (Scheme 4, path b)[54,55].

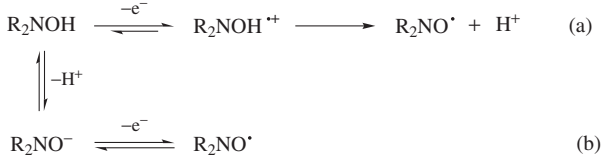

SCHEME 4. One-electron oxidation of the hydroxylamine (path a) or of its conjugate base (path b)

Characterization of the $R_2NO^\bullet$ transient species becomes then possible through the EPR[56]. As an alternative to the electrochemical one-electron abstraction, chemical oxidants such as $Pb(OAc)_4$ or Ce^{4+} salts have been analogously employed in order to generate the $R_2NO^\bullet$ species[57–59].

b. H-atom abstraction. A clean approach to the generation of an aminoxyl radical entails use of laser flash photolysis via photoinduced cleavage of an appropriate peroxide. For example, the cumyloxyl radical, generated from dicumyl peroxide by laser pulse at 355 nm (Scheme 5), gives rise to the $R_2NO^\bullet$ species from a hydroxylamine precursor, allowing UV-Vis spectral characterization[59,60].

SCHEME 5. Generation of an aminoxyl radical by H-abstraction, ensuing laser flash photolysis of an appropriate peroxide. Redrawn with permission from Reference 134. Copyright (2005) American Chemical Society

2. Bond dissociation energy BDE_{NO-H}

The redox potential of the couple ($H_2NO^{\bullet}$,H^+/H_2NOH) is reported[23] as $E^\circ = 0.90$ V vs. NHE (all the redox potentials will be referred to the normal hydrogen electrode throughout the paper) in water (cf. Scheme 4), and this value explains why Ce^{4+}, having $E^\circ = 1.3$ V[61], can oxidize H_2NOH quantitatively. One-electron reduction of $H_2NO^{\bullet}$ yields instead H_2NO^- ($E^\circ = 0.09$ V)[23], i.e. the conjugate base of H_2NOH. Because the pK_a of hydroxylamine is 13.7 in water[23,62], a thermochemical cycle (equation 1)[23,63] provides the NO−H bond dissociation energy for H_2NOH as 75 kcal mol^{-1}. A previous BDE_{NO-H} determination, based on a $E^\circ = -0.1$ V for the $H_2NO^{\bullet} \rightarrow H_2NO^-$ reduction, gave a 72 kcal mol^{-1} value[13].

$$BDE(H_2NO{-}H) = pK_a(H_2NOH) + E^\circ(H_2NO^{\bullet}/H_2NO^-) + E(H^+/H^{\bullet}) \qquad (1)$$

The N−H bond energy, i.e. BDE(H−NHOH), is instead larger and equal to 81–82 kcal mol^{-1}, thereby explaining why H-atom removal from H_2NOH yields $H_2NO^{\bullet}$ and not the isomeric $^{\bullet}NHOH$ radical[23,64]. These two BDE values are well matched by quantum chemical computations[64].

α-Substituents affect the dissociation energy of the NO−H bond in the parent hydroxylamine $R_2NO{-}H$. A few experimental BDE($R_2NO{-}H$) data are listed in Table 1 for significant structures[13,30,58,63,65–68]. Moving from the archetypal hydroxylamine (R = H)[13,23] towards α-substituted derivatives having R = electron-withdrawing group, we observe that the energy of the NO−H bond increases appreciably.

TABLE 1. Experimentally available BDE($R_2NO{-}H$) data

R_2NOH	BDE($R_2NO{-}H$) (kcal mol^{-1})
H_2NOH	75 (or 72)
Et_2NOH	73
t-Bu_2NOH[a]	68
Ar_2NOH	72
$(CF_3)_2NOH$	84
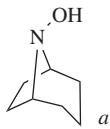 *a*	77
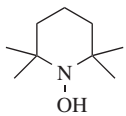 *a*	69
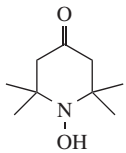 *a*	71

TABLE 1. (*continued*)

R_2NOH	BDE(R_2NO-H) (kcal mol^{-1})
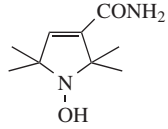 *a*	70
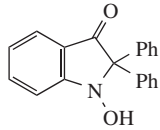 *a*	71
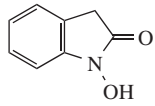	79
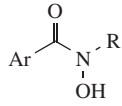	80
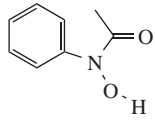 (NHA)	*ca* 80
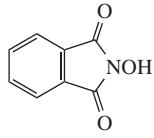 (HPI)	88
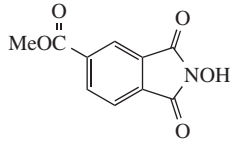	89
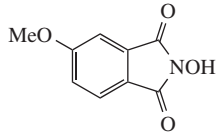	87

[a] Stable as the aminoxyl radical.

Additional BDE_{NO-H} data for a few other R_2NOH compounds were calculated in compliance with the thermochemical cycle reported in equation 1[63,69], on the basis of available pK_a (R_2NOH)[70] and E° ($R_2NO^\bullet/R_2NO^-$)[54] data (cf. Scheme 4), and are listed in Table 2. The thermochemical calculation reproduces the experimental BDE_{NO-H} value (i.e. 88.1 kcal mol^{-1})[58] of *N*-hydroxyphthalimide (HPI) exactly, so that these calculated values can be confidently compared with the experimental ones in Table 1. DFT calculations of BDE_{NO-H} also provide reliable results[71,72].

There is an obvious expectation that the larger the BDE_{NO-H} value, the more efficiently the aminoxyl radical will abstract H-atom from a substrate (cf. Scheme 1). We will see in Section III how this expectation finds reasonable experimental support, and how the BDE data of Tables 1 and 2 provide a guideline to foresee H-abstraction proficiency. However, before proceeding to Section III, more important information needs to be added.

TABLE 2. Data relevant for the calculation of BDE(R_2NO-H) values

R_2NO-H	pK_a in H_2O	E° (V/NHE) ($R_2NO^\bullet/R_2NO^-$)	Calculated (from equation 1) BDE(R_2NO-H) (in kcal mol^{-1})
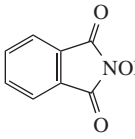 (HPI)	6.3	1.09	88
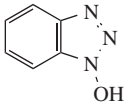 (NBT)	4.6	1.08	85
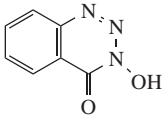	4.0	1.2	85–87
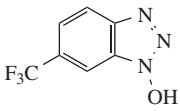	3.8	1.1	83–85
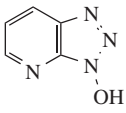	3.5	1.1	83–85
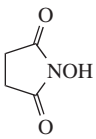	6.1	1.3	92–93

B. Oxidation to the Oxoammonium Ion

Persistent or moderately stable aminoxyl radicals (**1**, in Scheme 6) lend themselves to one-electron oxidation to yield an oxoammonium ion (**4**) at a redox potential that depends on the structure of the hydroxylamine precursor (**1H**)[13,55,73,74]. Calculation methods have been developed to predict the redox potential in this one-electron oxidation[75].

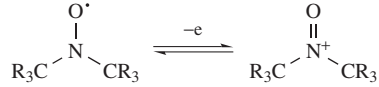

(**1**) (**4**)

4 + RCH_2OH ⟶ **1H** + RCHO + H^+

SCHEME 6. Oxidation of an alcohol by the oxoammonium ion **4** derived from an aminoxyl radical **1**

This **1** → **4** redox event has importance both in reactivity studies and in synthetic procedures because, for example, the oxoammonium ion **4** brings about the oxidation of primary or secondary alcohols into carbonyl compounds[74,76] (Scheme 6). The chemistry of ion **4** represents the other main issue of the present review. Table 3 collects redox data for the $R_2N{=}O^+/R_2NO^\bullet$ one-electron reduction, which can be reversible or irreversible (E° or E^p data, respectively)[63,74] because ion **4** may present either moderate or low stability[77].

Besides electrochemical techniques, appropriate oxidants endowed with the needed redox potential, such as $PhI(OAc)_2$, cupric salts, Mn−Co salts or Ce^{4+} salts[63,74,76,78–80], are employed to perform the oxidation of **1** to **4**, and the use of the multicopper oxidase enzyme laccase for this purpose is also described[81]. The lower the redox potential required for the **1** → **4** conversion, the easier and more convenient the subsequent oxidation of an alcohol (in Scheme 6) will be; this plays against the use of the Fremy's salt[36] in this particular contest. Conversely, the easy oxidation of $t\text{-}Bu_2NO^\bullet$ (or DOXYL) gives rise to oxoammonium ions that are not stable and undergo cleavage[82], thereby hampering any practical use as oxidation catalysts according to Scheme 6. Summing it up, TEMPO comes out as the most convenient aminoxyl radical for yielding the oxoammonium ion **4** (i.e. $TEMPO^+$), and consequently for catalysing the oxidation of alcohols. The tetrafluoroborate of $TEMPO^+$ can be obtained as a stable salt by electrochemical oxidation of TEMPO[83], and used for synthetic purposes[84]. Mechanistic details upon the synthetically useful route delineated in Scheme 6 will be provided later.

III. REACTIVITY STUDIES

A. H-abstraction by Persistent Aminoxyl Radicals

As a rule of thumb, one would expect that the more stable the aminoxyl radical, the lower its overall reactivity. This matches the above reported expectation (cf. Scheme 1) that the lower the BDE_{NO-H} value, the less efficiently the aminoxyl radical will abstract H-atom from a substrate. These two statements are indeed corroborated by a few literature examples. TEMPO (Chart 1), a persistent aminoxyl radical[29], upon H-abstraction forms one of the weakest NO−H bonds among those reported in Table 1[63,85]. It is no wonder

TABLE 3. Redox data for the monoelectronic oxidation of aminoxyl radicals

$R_2NO^{\bullet}$	E (V/NHE) $R_2N{=}O^+/R_2NO^{\bullet}$
t-$Bu_2NO^{\bullet}$	0.7
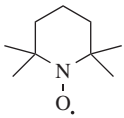 (TEMPO)	0.8
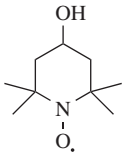	0.9
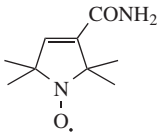	1.0
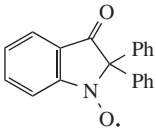	1.2
$(^{-}O_3S)_2NO^{\bullet}$ (Fremy's salt)	1.4

then that the H-abstraction reactivity reported for TEMPO is uniformly low[30], because the process is enthalpically disfavoured. For example, among a series of oxygen-centred radicals (BDE_{O-H} in parentheses, in kcal mol^{-1})[85,86], $HO^{\bullet}$ (119), t-$BuO^{\bullet}$ (104), t-$BuOO^{\bullet}$ (89), $(CF_3)_2NO^{\bullet}$ (84) and TEMPO (69), the reactivity of abstraction (k_H, in M^{-1} s^{-1}, at 300 ± 5 K) of the benzylic hydrogen from ethylbenzene (BDE_{C-H} 85.5 kcal mol^{-1})[85] is 2×10^9, 1×10^6, 0.2, 0.3 and *ca* 10^{-9}, respectively[3,86,87]. In another study, comparison of k_H values for H-abstraction from the benzylic position in a lactone substrate shows t-$BuO^{\bullet}$ to be more reactive than a TEMPO derivative by a factor of 10^7, in different solvents[88]. Clearly, steric hindrance in TEMPO[15,89] may play an additional role in lowering its reactivity, apart from the low value of the BDE_{O-H}. Consistently, the rate constant of H-abstraction from the N−H bond of an aniline derivative (BDE_{N-H} *ca* 85–87 kcal mol^{-1})[85] is 50 times lower for TEMPO than for the indolinone-1-oxyl shown in Chart 1[15], i.e. a less hindered radical, despite the very comparable BDE_{NO-H} (Table 1)[63,90]. Finally, the dipolar character of an aminoxyl radical must also be taken into consideration, and the entropy of desolvation of the $R_2N^{\bullet+}-O^-$ charge-separated canonical structure, which is a preliminary requisite for spin localization onto the aminoxyl O-atom (in the $R_2N-O^{\bullet}$ canonical structure) and ensuing H-abstraction, depresses TEMPO reactivity in hydrogen-bonding solvents[89,91]. As a final point, the oxidation of phenols and aromatic amines to quinones by the relatively stable Fremy's salt has been also described to proceed through H-abstraction[36,92].

The reactivity of TEMPO, and of other aminoxyl radicals, in the scavenging of carbon- or sulfur-centred radicals (equation 2)[42,91,93–95],

$$R_2NO^{\bullet} + R'^{\bullet} \longrightarrow R_2NO{-}R' \quad \text{(scavenging)} \tag{2}$$

or towards electron donors (ED) (equation 3)[96–98],

$$R_2NO^{\bullet} + ED \longrightarrow R_2NO^{-} \quad \text{(reduction)} \tag{3}$$

or in the addition to double bonds[7,99–101], or in reaction with molecular oxygen[102] or superoxide anion[41], will not be dealt with in the present chapter. Nor will the use of aminoxyl radicals as spin probes in EPR study, either *per se*[103–108] or in biological media[109–115], be considered.

B. H-abstraction by Transient Aminoxyl Radicals

Table 1 shows that *N*-hydroxyphthalimide (HPI) presents features almost opposite to those of TEMPO. In fact, the dissociation energy of the NO−H bond in HPI (88 kcal mol^{-1})[58,63,90], accessible through EPR measurements[116,117], is much higher than that of the corresponding NO−H bond in the hydroxylamine moiety of TEMPO (viz. TEMPOH, 69 kcal mol^{-1})[85]. TEMPO is a persistent aminoxyl radical[27–29], whereas the aminoxyl radical of HPI, dubbed PINO (phthalimide-*N*-oxyl)[118], is not stable but endowed with a half-life of *ca* 8000 s in AcOH solution at 25 °C[57]. By using an oxidant such as a $Pb(OAc)_4$[57], or a Co(III) salt[58,118,119], HPI can be oxidized into PINO, and the H-abstraction reactivity of the latter subsequently exploited in the catalytic oxidation of appropriate H-donor substrates (RH) (Scheme 7).

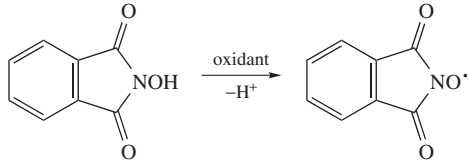

SCHEME 7. The hydrogen atom transfer (HAT) pathway of an aminoxyl radical

As opposed to TEMPO, PINO is a powerful H-abstracting radical because it forms a strong NO−H bond (in HPI). Accordingly, the synthetic proficiency of PINO as a catalyst in oxidation procedures endowed with low environmental impact has been investigated, and will be reported later. The reactivity features of PINO in the H-abstraction route are now commented on.

1. PINO generated electrochemically

A pioneering electrochemical investigation was undertaken by Masui and coworkers[52]. They showed that HPI is an efficient electron carrier (viz. mediator) in the electrochemical oxidation of alcohols to the corresponding carbonyl compounds. The anodic one-electron

oxidation of HPI to PINO (plus one H^+) takes place at 1.5 V/NHE in MeCN solution (Scheme 4, path a). Upon addition of two molar equivalents of pyridine, HPI deprotonates (Scheme 4, path b) to its >N−O$^-$ conjugate base that gives rise to a fully reversible oxidation wave at a lower E° value, namely 1.1 V/NHE[120]. Under these conditions, and by the use of a spectro-electrochemical cell, the anodic oxidation of HPI to PINO could be followed, and a UV-Vis spectrum acquired in MeCN solution. It presented an absorption maximum at $\lambda = 400$ nm ($\varepsilon = 1400\ M^{-1}\ cm^{-1}$), undergoing second-order self-decomposition with $k_d = 24\ M^{-1}s^{-1}$ at 25 °C and [PINO] = 0.5 mM. An EPR spectrum of PINO could be obtained from this solution[52]. Upon addition of a H-donor substrate into the spectro-electrochemical cell solution, Masui and coworkers could monitor the fast decay of the anodically generated PINO, and determine the rate constants of H-abstraction (k_H) from appropriate RH substrates[52]. The process was first order both in PINO and in the H-donor, selected examples of substrates being reported in Table 4. These RH compounds have one or more H-atoms at a benzylic or allylic position, or on a C-atom adjacent to a heteroatom, and the rate constant values (k_H) determined are larger than the self-decomposition of PINO. By comparing the rate constants of Ph_2CHOH and Ph_2CDOH, a k_H/k_D ratio of 11 was obtained, in keeping with a rate-determining H-abstraction by PINO[52].

More recently, the soundness of the electrochemical approach for the generation of PINO from HPI has been confirmed by using cyclic voltammetry at a rotating disk electrode[121]. Anodic oxidation had been also employed for the generation of the aminoxyl radical from hydroxamic acids[122].

TABLE 4. Rate constants of H-abstraction (k_H) obtained with the PINO radical in different studies, and compared with similar results obtained in the case of the $(CF_3)_2NO^\bullet$ species

Substrate, RH (BDE_{C-H}, in kcal mol^{-1})[85]	k_H ($M^{-1}\ s^{-1}$) by PINO,[a] at 25 °C in MeCN	k_H ($M^{-1}\ s^{-1}$) by PINO,[b] at 25 °C in AcOH	k_H ($M^{-1}\ s^{-1}$) by $(CF_3)_2NO^\bullet$, at 25 °C in Freons[c]
Cyclohexanol (92)	4.5	—	—
$PhCH_2OH$ (80)	16	12	—
p-$MeOC_6H_4CH_2OH$ (*ca* 79)	52	45	—
$PhCH_2CH_2OH$ (*ca* 85)	0.78	—	—
$PhCH_3$ (89)	—	0.62	8.8×10^{-3}
$PhCH_2CH_3$ (85)	—	5.4	0.3
$PhCHMe_2$ (84)	—	27	0.3
Ph_2CHOH (79)	37	58	—
Ph_2CH_2 (84)	—	13	0.48
Ph_3CH (81)	—	59	8.8
Fluorene (82)	26	40	—
Tetralin (83)	43	—	—
Cyclohexene (81)	20	—	—
Tetrahydrofuran (92)	2.9	—	0.35
Isochroman (*ca* 84)	156	—	—
N-acetylpyrrolidine (*ca* 88)	48	—	—
PhCHO (87)	—	11	1.8

[a] Generated by electrochemical oxidation[52]; [PINO] = 0.5 mM.
[b] Generated by oxidation with $Pb(OAc)_4$[57,124]; [PINO] = 0.2 mM.
[c] From Reference 86; Freons = CF_2Cl_2 and $CF_2ClCFCl_2$.

2. PINO generated by $Pb(OAc)_4$

A different approach to the generation of the PINO reactive intermediate for kinetic purposes has been described by Espenson and coworkers[57], through the oxidation of HPI by $Pb(OAc)_4$ in AcOH solution at 25 °C (Scheme 4). The absorption maximum recorded at 382 nm ($\varepsilon = 1360\ M^{-1}\,cm^{-1}$) in AcOH solution is very comparable with that found for PINO in MeCN by Masui and coworkers[52]. PINO undergoes a second-order self-decomposition (k_d 0.6 $M^{-1}\,s^{-1}$ at 25 °C)[57, 123] in AcOH slower than that described in MeCN solution[52], the first half-life being 2.2 h at [PINO] = 0.2 mM. Under these experimental conditions[57], a kinetic study of H-abstraction from a number of H-donor substrates was run (cf. Scheme 7), and selected results are given in Table 4[57, 124]. It can be verified that, for the same RH, good agreement exists between this set of reactivity data and the one previously reported by Masui and coworkers[52], thus supporting the intermediacy of the same reactive intermediate (i.e. PINO) in both cases, even though generated by different procedures. A k_H/k_D ratio of 27 was determined by comparing the rate constants of toluene and toluene-d_8[57], thereby indicating a strong relevance of tunneling. On measuring the H-abstraction rate constants for a set of *p*-substituted benzyl alcohols, analysis by the Hammett equation gave $\rho = -0.41$ (vs. σ^+)[57]. All this body of experimental evidence is in favour of a radical process with a rate-determining H-abstraction from the substrate by the PINO reactive intermediate. The k_H data correlate reasonably well with the energy trend of the C–H bond that is cleaved in RH[124], keeping in mind the experimental uncertainty of some of the BDE thermochemical data[85]. The H-abstraction reactivity of PINO is therefore dominated by enthalpic factors, as expected for a radical process. Finally, the higher reactivity of PINO as compared with that of $(CF_3)_2NO^\bullet$ (in Table 4)[86] is consistently ascribable to enthalpic factors, as supported by the BDE_{NO-H} value of the two corresponding hydroxylamines, which is larger (i.e. 88 vs. 84 kcal mol^{-1})[86, 90] for the more reactive HPI.

3. PINO generated by Co(III)

A third approach to the generation of PINO from HPI is the one first described by Ishii and coworkers[118, 125, 126], and subsequently followed by Minisci and coworkers[119, 127], for synthetically useful transformations of alcohols or other H-donor substrates into carbonyl derivatives. It entails the use of catalytic amounts of a Co(II) salt, usually $Co(OAc)_2$, with O_2 in the presence of *m*-Cl-benzoic acid (MCBA)[118]. The synthetic scope of this procedure will be commented on later, but it is sufficient to point out here that PINO is produced from HPI in a catalytic cycle through a short-living Co(III) oxidizing intermediate[68, 119, 128–130]. MCBA enhances the solubility of the cobalt salts in MeCN solution, thereby ensuring better efficiency to a needed redox decomposition of the hydroperoxide intermediate of the substrate *en route* to the products[127]. By using the HPI/Co(II)/MCBA/O_2 system in MeCN solution at 25 °C, competitive oxidations of *p*-X-substituted benzyl alcohols were run pairwise (Scheme 8)[58]. From the amount of the aldehydes produced, the relative reactivity (k_X/k_H) could be reckoned, and the acquired data provided a $\rho = -0.68$ in a Hammett plot vs. σ^+[58].

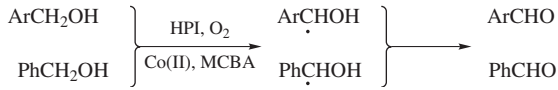

SCHEME 8. Competitive HAT oxidation of benzyl alcohols by the use of PINO

The latter result is remarkably well confirmed by another investigation where a $\rho = -0.69$ was obtained vs. σ^+ from competition experiments performed with a larger set of *m*- and *p*-X-substituted benzyl alcohols, on employing the same HPI/Co(II)/MCBA/O_2 system[68, 129]. In this case, the direct rate constants of H-abstraction could be determined by EPR spectroscopy, by monitoring the decay of the PINO radical in the presence of a few substrates ($PhCH_3$, $PhCH_2CH_3$, $PhCHMe_2$, $PhCH_2OH$), and the acquired k_H data[90, 128] compare favourably with those of the other studies[52, 57, 124] reported in Table 4. The competitive oxidation of $PhCH_2OH$ and $PhCD_2OH$ by HPI/Co(II)/MCBA/O_2 was also investigated, and GC-MS determination with integration of the intensities of the molecular ions of products PhCHO and PhCDO gave the intermolecular primary isotope effect $k_H/k_D = 16$[58]. This oxidation study was expanded through the use of six X-aryl-substituted-*N*-hydroxyphthalimides (X-HPIs), containing electron-withdrawing (4-MeOCO, 3-F) and electron-donating (4-Me, 4-MeO, 3-MeO, 3,6-$(MeO)_2$) X-groups[58]. The BDE_{O-H} of the X-HPIs was determined by the EPR radical equilibration technique (Table 5)[58, 90, 117], and the Hammett correlations for the oxidation of substituted benzyl alcohols, as well as the KIE, were appraised (in Table 5) for each X-HPI according to the experimental procedure employed for the unsubstituted HPI[58].

Once again, the sizeable k_H/k_D values obtained indicate a rate-determining H-atom transfer from the benzylic alcohol to the X-HPIs. According to the negative ρ value of the Hammett correlations vs. σ^+, polar effects play a role in this radical process, because PINO is an electrophilic radical[119, 127, 131, 132]. A novel method must be finally quoted for the generation of PINO from HPI, by the use of the heterogeneous oxidizing system $NaIO_4$/wet silica gel in CH_2Cl_2[133].

4. BTNO from HBT

Another transient aminoxyl radical has been generated[59], and employed in H-abstraction reactivity determinations[134]. Precursor 1-hydroxybenzotriazole (HBT, Table 2) has been oxidized by cyclic voltammetry (CV) to the corresponding $>N-O^{\bullet}$ species, dubbed BTNO[59] (Scheme 9). A redox potential comparable to that of the HPI $\rightarrow$ PINO oxidation, i.e. E° 1.08 V/NHE, has been obtained in 0.01 M sodium acetate buffered solution at pH 4.7, containing 4% MeCN[135]. Oxidation of HBT by either $Pb(OAc)_4$ in AcOH, or cerium(IV) ammonium nitrate (CAN; E° 1.35 V/NHE)[61] in MeCN, has been monitored by spectrophotometry[59], providing a broad UV-Vis absorption band with λ_{max} at 474 nm and $\varepsilon = 1840\ M^{-1}\ cm^{-1}$. As in the case of PINO from HPI, the absorption spectrum of aminoxyl radical BTNO is not stable, but decays faster (half-life of 110 s at [HBT] = 0.5 mM)[59, 134] than that of PINO[57]. An EPR spectrum consistent with the structure of BTNO was obtained from equimolar amounts of CAN and HBT in MeCN solution[59]. Finally, laser flash photolysis (LFP) of an Ar-saturated MeCN solution of dicumyl peroxide and HBT at 355 nm gave rise to a species whose absorption spectrum, recorded 1.4 ms after the laser pulse, had the same absorption maximum (*ca* 474 nm) of the spectrum recorded by conventional spectrophotometry (Scheme 9)[59, 134].

An extensive kinetic study of the H-abstraction reactivity (k_H) from appropriate substrates (RH) has been undertaken by spectrophotometry in MeCN solution at 25 °C, by using CAN for the generation of BTNO from HBT[134]. The rate constants, which are first order in both BTNO and the H-donor, are faster than the self-decomposition of BTNO for the substrates reported in Table 6, but uniformly slower than those determined with PINO (cf. Table 4) for equal substrate by at least one order of magnitude.

Once again the oxidized RH compounds are examples of benzylic or allylic alcohols or hydrocarbons, expected to have an energy of the scissile C–H bond accessible to the H-abstraction power of BTNO. However, the BDE_{NO-H} of HBT was not known[85], and

TABLE 5. NO−H bond dissociation energy values of X-aryl-substituted *N*-hydroxyphthalimides (X-HPIs), listed with the Hammett ρ values (vs. σ^+) and k_H/k_D ratios obtained in the oxidation of substituted benzyl alcohols using the X-HPIs/Co(II)/MCBA/O_2 system in MeCN solution at 25 °C

Precursor	BDE_{O-H} (kcal mol^{-1}) [a]	ρ	k_H/k_D
HPI	88.1	−0.68	16
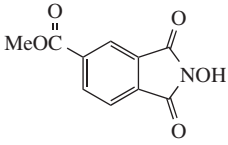	88.9	−0.70	14
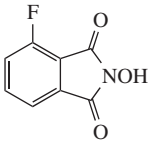	88.6	−0.69	—
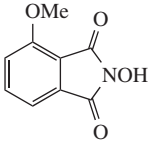	87.9	−0.60	—
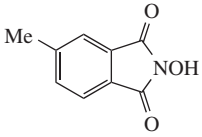	88.2	−0.67	—
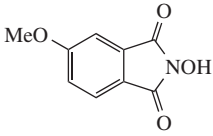	87.3	−0.60	18
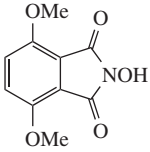	87.1	−0.54	20

[a] Determined at −10 °C in MeCN[58] by the EPR radical equilibration technique[117].

experimental problems made its determination by the EPR equilibration technique impossible. Anyhow, Table 2 shows that this BDE value could be attained (as 85 kcal mol^{-1})[63] by resorting to thermochemical calculation according to equation 1. This lower BDE_{NO-H} of HBT with respect to HPI (88 kcal mol^{-1})[63,90] is in keeping with the lower H-abstraction reactivity measured for the former (cf. Tables 6 and 4), the difference in BDE_{NO-H} representing a crucial point in a radical H-abstraction process.

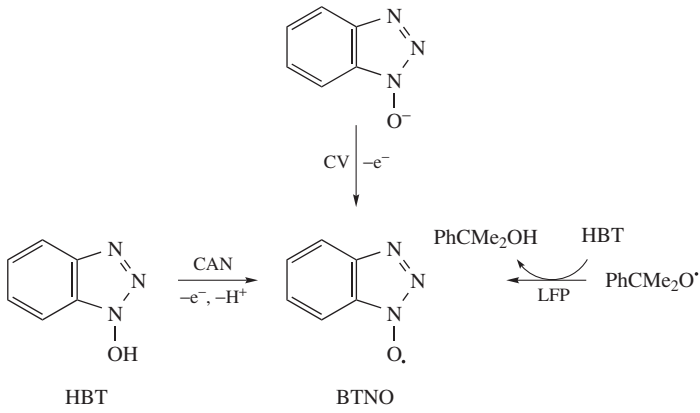

SCHEME 9. Generation of BTNO from HBT by means of different experimental approaches. Reprinted with permission from Reference 134. Copyright (2005) American Chemical Society

TABLE 6. Second-order rate constants of H-abstraction (k_H) from H-donor substrates RH by BTNO at 25 °C[a]. The radical was generated from HBT with CAN in MeCN solution. Literature BDE_{C-H} data of the substrates are given

Substrate, RH	k_H ($M^{-1}\,s^{-1}$) at 25 °C in MeCN	BDE_{C-H} of RH (kcal mol^{-1})[b]
$C_6H_5CH_2OH$	1.9	83–85
4-$MeOC_6H_4CH_2OH$	6.2	82–84
Decanol	0.22	93
Cyclohexanol	0.33	92
4-MeO-toluene	0.27	89–90
4-MeO-ethylbenzene	0.70	85–87
4-MeO-*i*-propylbenzene	0.55	83–85
1-(4-$MeOC_6H_4$)ethanol	5.9	82–84
$PhCH{=}CHCH_2OH$	36	80–83
Geraniol	22	82
Ph_2CHOH	3.2	79
Fluorene	3.8	82
Ph_3CH	2.3	81
Ph_2CH_2	0.72	84

[a] Conditions: [BTNO] 0.5 mM, [RH] 5–25 mM in MeCN solution. Determinations in triplicate, errors ±3%; followed at 474 nm by spectrophotometry[134].
[b] From Reference 85.

Additional clues confirm the radical nature of the reaction of BTNO with RH substrates. A Hammett correlation, obtained on plotting log k_H for reaction of BTNO with *p*-substituted benzyl alcohols, gave a ρ value of -0.55[59] vs. σ^+. This small value, which is reasonable for a radical reaction, compares well with the ρ values ranging from -0.54 to -0.70 and obtained vs. the same substrates with the aminoxyl radicals generated from X-aryl-substituted HPIs (Table 5)[58]. In all cases better Hammett correlations were obtained vs. the σ^+ values. Hence, a uniform pattern of selectivity emerges among these electrophilic $>N-O^{\bullet}$ species[136] in H-abstraction reactions.

The intramolecular kinetic isotope effect determined in reaction of BTNO with *p*-MeO-$C_6H_4CH(D)OH$ gave a k_H/k_D ratio of 5.6 in MeCN[59], consistent with a rate-determining H-abstraction step. Additional determinations gave a k_H/k_D of 7 with PhCH(D)OH, and 12 for the intermolecular competition of fluorene vs. 9,9-dideuteriofluorene[134]. The latter value supports the contribution of tunnelling already commented on for reaction of PINO with various C−H donors (k_H/k_D values in the 11−27 range)[52,57,58].

Some remarks on the rate constants of Table 6[134] are possible. Abstraction of hydrogen by BTNO becomes increasingly faster on going from an aliphatic to a benzyl and further on to an allyl alcohol, thus reflecting the BDE_{C-H} values undergoing cleavage in RH[85]. Analogously, by increasing the number of Ph substituents on the C−H group undertaking cleavage, i.e. $ArCH_3$, Ph_2CH_2, Ph_3CH, an increase of k_H value in line with the decreasing trend of the BDE_{C-H} is found. Finally, the *relative reactivity* of abstraction of a primary vs. secondary vs. tertiary benzylic hydrogen by BTNO, reckoned as 1:4:6 from comparing 4-MeO-toluene vs. 4-MeO-ethylbenzene vs. 4-MeO-*i*-propylbenzene, is consistent with the BDE_{C-H} values (88, 85 and 84 kcal mol^{-1}, respectively)[85], and with the relative rates of 1:3:7 reported[137] for the analogous HAT reactions by *t*-Bu$O^{\bullet}$, an exemplary oxygen-centred radical[138]. All this body of evidence supports a rate-determining HAT process[137] by BTNO towards C−H donor substrates.

The expectation that the k_H rate constants correlate with thermochemical bond-energy data in this radical process has indeed found quantitative support through the determination of the activation parameters, on running the H-abstraction experiments by BTNO from selected substrates at various temperatures[134]. From the Arrhenius equation ($\log k_H = \log A - E_a/RT$), log A and E_a were obtained (Table 7).

Correlation of H-abstraction reactivity vs. C−H bond-energy data was attempted according to the Evans–Polanyi equation, $E_a = \alpha BDE_{C-H} + \text{const}$. Figure 1 confirms that the reactivity of H-abstraction scales with the C−H bond energies linearly. The reactivity of BTNO is increasingly lower (i.e. higher E_a value) towards increasingly stronger C−H bonds, and the slope of the correlation is $\alpha = 0.44$[134].

From this linear correlation, and entering the experimental E_a value determined for 4-$MeOC_6H_4CH_2OH$ (Table 7), a BDE value of 77 ± 1 kcal mol^{-1} could be extrapolated for the benzylic C−H bond[134] bearing a geminal OH group. As a matter of fact, the BDE_{C-H} of benzyl alcohols was not experimentally available or reported with reasonable confidence[85]; the extrapolated value compares well with a BDE_{C-H} of 81 ± 1 kcal mol^{-1} that could be extrapolated for $PhCH_2OH$ from data of Espenson and coworkers[124]. Because the BDE_{C-H} of toluene is 88.5 kcal mol^{-1} [85], the extrapolated value

TABLE 7. Activation parameters for H-abstraction by BTNO from selected RH substrates[a]

Substrate, RH	E_a (kcal mol^{-1}) (±0.15)	log A (M^{-1} s^{-1}) (±0.5)
4-$MeOC_6H_4CH_2OH$	6.8	13
Ph_2CHOH	6.7	12
FL[b]	8.9	16
9-OH-FL[b]	5.1	11
Ph_2CH_2	10.6	17
Ph_3CH	8.8	16

[a] From Reference 134.
[b] FL stands for fluorene.

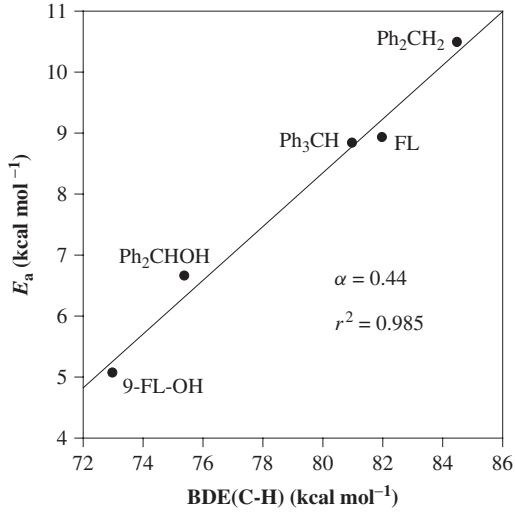

FIGURE 1. Evans–Polanyi plot for the H-abstraction reaction by BTNO with selected substrates (FL stands for fluorene). Reprinted with permission from Reference 134. Copyright (2005) American Chemical Society

of $ArCH_2OH$ (averaged here as 79 ± 2 kcal mol^{-1}) points to a significant weakening (by *ca* 9 kcal mol^{-1}) of a benzylic C–H bond bearing a geminal OH group.

It will be useful to evaluate and compare the reactivity of additional aminoxyl radicals in the H-abstraction reaction in future investigations.

C. Aminoxyl Radicals as One-electron Oxidants

Another facet of the reactivity of aminoxyl radicals has been brought to attention by recent studies of the oxidation of substrates endowed with low redox potential. Some aminoxyl radicals, depending on the reduction potential value of the couple $>N-O^{\bullet}/>N-O^{-}$, can behave as moderate one-electron abstractor towards substrates endowed with appropriate oxidation potential. This rather unprecedented[139,140] reactivity feature, outlined in Scheme 10, has been substantiated by the oxidation of aniline or phenol derivatives, whose redox potential is conveniently located in the 0.4–1.0 V/NHE range[141].

$$>N-O^{\bullet} + \text{sub} \longrightarrow >N-O^{-} + \text{sub}^{\bullet+}$$

SCHEME 10. Monoelectronic oxidation by an aminoxyl radical

For example, PINO (i.e. $>N-O^{\bullet}$), generated from HPI by oxidation with $Pb(OAc)_4$ (cf. Scheme 7) or by laser flash photolysis of $(t\text{-BuO})_2$ (cf. Scheme 5) at 266 nm, has been investigated in the oxidative *N*-demethylation of 4-X-substituted-*N*,*N*-dimethylanilines (X-DMAs) (Scheme 11)[142].

$$\text{PINO} + \text{ArNMe}_2 \xrightarrow[\text{MeCN}]{} \text{HPI} + \text{ArNHMe} + \text{CH}_2\text{O}$$

SCHEME 11. *N*-Demethylation induced by PINO

TABLE 8. Substrate oxidation potentials and kinetic data for the reaction of PINO with 4-X-substituted-*N*,*N*-dimethylanilines (X-DMAs), at 25 °C in MeCN solution [a]

X in X-DMA	E° (V/NHE) in MeCN [a]	k ($M^{-1}\,s^{-1}$)
CN	1.29	4.5×10^2
CF_3	1.25	1.4×10^3
CO_2Et	1.21	3.5×10^3
OPh	0.80	3.0×10^5
OMe	0.69	3.7×10^6

[a] From Reference 142.

The kinetic study has been performed by following the decay of PINO absorption at 380 nm in the presence of X-DMAs at 25 °C in MeCN solution, and the oxidation products have been independently examined. The oxidation rate constants were very sensitive to the electron-donating power of the X-substituents ($\rho = -2.5$ vs. σ^+) (Table 8), as well as to the oxidation potential of the substrates. An intermolecular kinetic isotope effect $k_H/k_D = 1$ was determined with an appropriately deuteriated *p*-MeO-*N*,*N*-dimethylaniline[142]. These experimental findings differ strongly from those acquired for the radical HAT route of oxidation of X-substituted benzyl alcohols by PINO or PINO congeners (cf. Table 5). They are instead compatible with a two-step mechanism involving the reversible electron transfer (ET) from the DMAs to PINO (cf. Scheme 10), followed by fast proton loss from the N−(α)C−H bond of an anilinium radical-cation intermediate, leading to an α-amino carbon radical and ultimately to the *N*-demethylation product (cf. Scheme 11). In line with this conclusion, the reactivity data exhibited a good fit with the Marcus equation, a quite large reorganization energy (>60 kcal mol^{-1}) being estimated for the PINO/R_2N-O^- self-exchange reaction. Because the reduction potential of PINO is 0.92 V/NHE in MeCN, electron abstraction from the various DMAs (E° data in Table 8) is exoergonic or moderately endorgonic, and therefore feasible[142].

Besides having smaller oxidation potential values than substituted benzyl alcohols ($E^\circ > 1.4$ V/NHE)[143], the DMAs have larger energy values (90–92 kcal mol^{-1})[85] for the NC−H bond with respect to C−H bond energies around 75–85 kcal mol^{-1} of the benzyl alcohols[85] (Scheme 12). Both factors disfavour the operation of the radical HAT route for PINO with the DMAs, and cause a mechanistic changeover to the ET route, as opposed to the reactions with the benzylic substrates listed in Table 4.

Consistent with the results of this study is the outcome of the oxidation of 4-X-substituted phenols by use of PINO, generated from HPI with $Pb(OAc)_4$ at 25 °C in MeCN containing 1% AcOH[144]. The reactivity (k_H) of PINO towards phenolic O−H bonds (BDE 85–90 kcal mol^{-1})[85] was about one order of magnitude higher than that measured towards the C−H bond of benzyl alcohols (cf. Table 4). A ρ value of −3.1 was obtained from plotting log k_H vs. σ^+ for this reaction[144], where removal of H-atom from the phenolic O−H bond (which is weaker than the O−H bond of aliphatic or benzyl alcohols)[85] induces an oxidative phenolic coupling with the PINO moiety. In view of the low redox potential of the substituted phenols (in the 0.8–1.1 V/NHE range)[141], and of the substantial value of the kinetic isotope effect $k_H/k_D = 3.1–3.7$ measured[144], operation of a proton-coupled electron transfer (PCET) mechanism[145, 146] was suggested, the transition state structure of which is outlined in Figure 2.

Investigation of other easily oxidizable substrates with PINO, or other aminoxyl radicals, will possibly confirm the soundness of the mechanism delineated in Scheme 10[147].

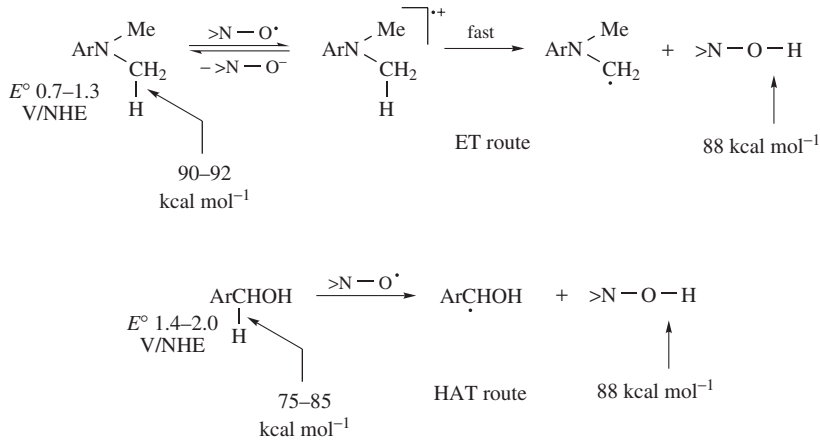

SCHEME 12. Mechanistic dichotomy of ET vs. HAT for PINO

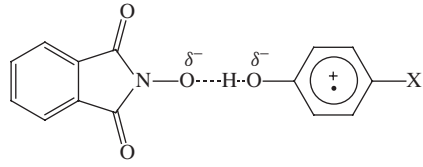

FIGURE 2. Transition state structure for the reaction of PINO with X-substituted phenols. Reprinted with permission from Reference 144. Copyright (2004) American Chemical Society

D. Enzymatic Generation of Transient Aminoxyl Radicals

We have seen that the generation of an aminoxyl radical from the hydroxylamine precursor (cf. Scheme 2) is viable through the use of a monoelectronic oxidant having appropriate redox potential, such as CAN (i.e. Ce^{4+})[59, 134], or by the use of the inner-sphere $Pb(OAc)_4$ oxidant[57]: the case of PINO and BTNO from HPI and HBT, respectively, has been underpinned above. It is of no wonder, then, that the generation of PINO and BTNO, and of additional aminoxyl radicals as well[63, 148, 149], has been achieved through the use of enzymes having a redox potential that matches the one of the hydroxylamine precursors, thereby behaving as alternative oxidants (Scheme 13).

$$\text{Enz} + \text{R}_2\text{NOH} \xrightarrow[-\text{e}, -\text{H}^+]{} \text{R}_2\text{NO}^{\bullet} + \text{Enz}_{\text{red}}$$

SCHEME 13. Redox generation of an aminoxyl radical from the hydroxylamine by an enzyme

Laccase is perhaps the metallo-enzyme most widely used for this aim. Laccases are a family of multicopper ('blue copper') oxidases widely distributed in nature[150, 151]. Many laccases have fungal origin, while others are produced in plants. They contain four Cu(II) ions, and catalyse the one-electron oxidation of four molecules of a reducing substrate with the concomitant four-electron reduction of oxygen to water[150–152]. In view of their low redox potential, which is in the range of 0.5–0.8 V vs. NHE depending on the fungal source[150, 153], laccases typically oxidize phenols (*phenoloxidase* activity) or anilines.

However, suitable compounds, often referred to as redox mediators[63, 135, 150, 154, 155], enable laccase to oxidize indirectly non-phenolic benzylic substrates having a redox potential too high ($E^\circ > 1.4$ V)[143] for the enzyme. The reason is that laccase performs the monoelectronic oxidation of the mediator[63, 135, 156], and subsequently the oxidized mediator (Med_{ox} in Scheme 14)[69] reacts with the non-phenolic substrate, e.g. benzylic alcohols or ethers, according to a mechanism unattainable to laccase. This mechanism can be the radical HAT route (cf. Scheme 7), which clearly enables one to by-pass any redox inadequacy of the enzyme towards the substrate. Hydroxylamines such as HPI or HBT or NHA (i.e. *N*-hydroxyacetanilide), having a redox potential compatible (1.08, 1.09 and 0.83 V/NHE, respectively)[63, 157] with that of laccase from *Trametes villosa* (0.78 V/NHE)[153], are accordingly converted into the respective aminoxyl radicals ($R_2N{-}O^\bullet$), and the H-abstraction route discussed before opens up for the enzyme as well[156]. The catalytic oxidation reactions occur smoothly at 25 °C in buffered (pH = 4.5) water solution, thereby presenting also synthetic interest, as will be commented on below. It must be added that many hydroxylamines are extensively deprotonated ($R_2N{-}O^-$) at the pH of these experiments, in view of their pK_a values (cf. Table 2)[63]; the anionic form undergoes one-electron oxidation to the $R_2N{-}O^\bullet$ form more readily[54, 55, 120], thereby making the role of laccase as an oxidant easier (cf. Scheme 4).

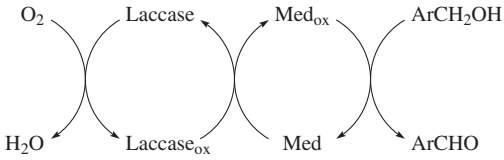

SCHEME 14. The oxidation cycle of a laccase/mediator system with non-phenolic substrates. Redrawn from Reference 69 by permission of The Royal Society of Chemistry on behalf of the Centre National de la Recherche Scientifique

What is the evidence that aminoxyl radicals are indeed the reactive intermediates in the oxidation of non-phenolic benzylic substrates catalysed by laccase with $R_2NO{-}H$ mediators? An extensive investigation of the reactivity features of laccase/mediator systems has been performed, based upon the determination of the Hammett ρ parameter for the oxidation of pairs of X-substituted benzyl alcohols in competition experiments, or upon the measurement of the KIE with appropriately deuteriated substrates[63, 156, 158]. The results are reported in Table 9, and compared with analogous results of PINO and BTNO once independently generated by the use of 'chemical' oxidants (Table 5 and Sections III.B.3 and III.B.4). The agreement of the data obtained in the oxidations with laccase/mediators versus those obtained with the *bona fide* aminoxyl radicals is quite satisfactory, keeping in mind the different experimental conditions used. The consistency of the results uniformly supports a rate-determining H-abstraction route of oxidation by radical reactive intermediates having electrophilic character[136]. The agreement is particularly good for HBT, thereby supporting the intermediacy of the BTNO species under both generating conditions (i.e. chemical and chemo-enzymatic).

The use of laccase in combination with mediators is also synthetically valuable for environmental benign oxidations[21, 22, 159, 160], and details will be provided later.

E. Oxidations by Means of the 'Oxoammonium Ion' of TEMPO

As anticipated in Section II.B (Scheme 6), monoelectronic oxidation of $R_2N{-}O^\bullet$ may afford a stable oxoammonium ion ($R_2N{=}O^+$), the case of TEMPO being exemplary.

TABLE 9. Oxidation of X-substituted benzyl alcohols with *Trametes villosa* laccase and R_2NO-H mediators in buffered (pH = 4.5) water solution at 25 °C. Comparison of ρ (vs. σ^+) and KIE ratios with those obtained for PINO and BTNO independently generated in MeCN solution at 25 °C

R_2NO-H mediator of laccase	ρ [a]	k_H/k_D [b]
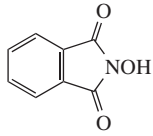 (HPI)	−0.89	6.2
PINO generated from oxidation of HPI [c]	−0.68	16
PINO generated from oxidation of HPI [d]	−0.41	27
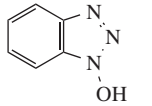 (HBT)	−0.64	6.4
BTNO generated from oxidation of HBT [e]	−0.55	5.6
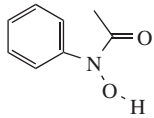 (NHA)	−0.42 [f]	5.2 [f]

[a] Oxidation of $XC_6H_4CH_2OH$ substrates[158].
[b] Oxidation of $XC_6H_4CH(D)OH$ substrates[158].
[c] Oxidation by means of the Co(II)/MCBA/O_2 system[58].
[d] Oxidation by means of $Pb(OAc)_4$ in AcOH[57].
[e] Oxidation by means of Ce(IV) in MeCN[59].
[f] From Reference 69.

Although this point has been known for many years[74, 76], and despite the important synthetic applications of TEMPO-oxoammonium that will be summarized later, the nature of the involved reactive species and the ensuing mechanism of oxidation are still a matter of debate, and this is why the term 'oxoammonium ion' is put within quotation marks in the title of the present section. The reactivity subtleties will be summarized here.

The basic features are delineated in a fundamental review[76], where the alleged $R_2N{=}O^+$ species is reported to be generated *in situ* by a suitable 'primary' oxidant from precursor $R_2N-O^\bullet$ (i.e. TEMPO). The substrate to be oxidized, e.g. an alcohol, attacks the oxoammonium ion as a nucleophile (Scheme 15)[63], giving an adduct that, by α-elimination, yields the carbonyl end product, while the primary oxidant regenerates the reactive $R_2N{=}O^+$ ion from the reduced R_2NO-H (viz. TEMPOH) in a catalytic cycle.

Good selectivity for the oxidation of primary alcohols in the presence of secondary ones can be achieved. By appropriate choice of the reaction conditions, overoxidation of the aldehyde from a primary alcohol to carboxylic acid can be minimized. Kinetic isotope effects in the range of 2 to 3 testify about the relevance of the H^+-elimination step upon the overall reactivity[76]. In general, the efficiency of oxidation of alkanols is slightly lower

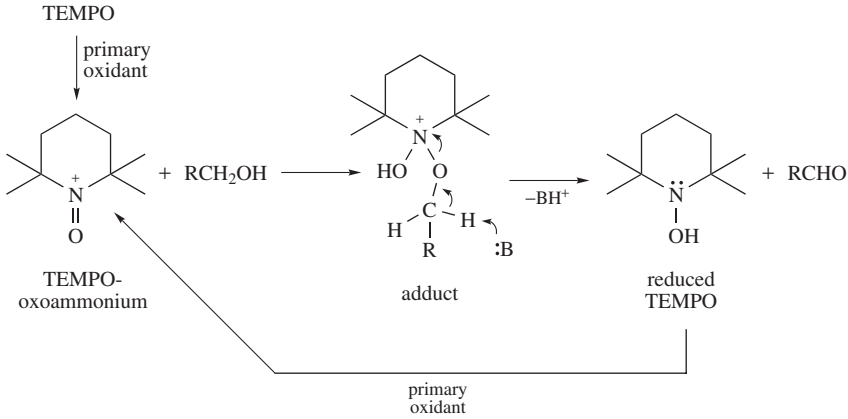

SCHEME 15. Ionic mechanism of oxidation of alcohols by TEMPO-oxoammonium ion. Redrawn from Reference 63 by permission of The Royal Society of Chemistry on behalf of the Centre National de la Recherche Scientifique

than that of benzylic or allylic alcohols, but still significant. Alkylarenes are unsuitable substrates, owing to the lack of a lone-pair for the required nucleophilic attack outlined in Scheme 15.

However, the rationalization of this matter is made more complex by the possible equilibration among various forms deriving from catalyst TEMPO. For example, and depending on the pH of the reaction, either disproportionation of TEMPO or of TEMPOH (viz. R_2NO-H) can occur (Scheme 16)[76], making it difficult to evaluate the extent of participation of the alleged 'oxoammonium ion' in some cases.

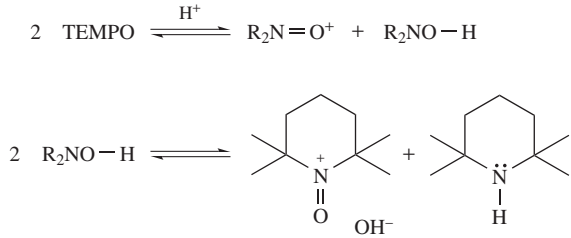

SCHEME 16. Side-reactions of TEMPO or TEMPOH

Studies by Sheldon's group raised doubts about the intermediacy of TEMPO-oxoammonium in synthetic procedures based on a few 'primary' oxidants[161–163]. For example, the first method employed to initiate the reaction was that of Semmelhack, by the use of CuCl in combination with TEMPO[164]. The rationalization offered to explain the good results obtained was that one-electron oxidation of TEMPO by Cu(II) (formed *in situ* by interaction of CuCl with O_2) gave rise to TEMPO-oxoammonium, which oxidized benzylic or allylic alcohols according to the ionic route of Scheme 15[164]. Strangely enough, the method was barely efficient towards aliphatic alcohols. New investigation of the procedure led Sheldon and coworkers to rather postulate the copper-mediated H-abstraction mechanism sketched in Scheme 17[161–163], in keeping with the fact that

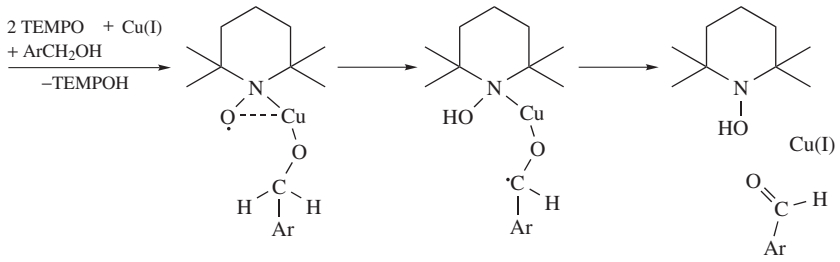

SCHEME 17. Sheldon's mechanism[161–163] of an aerobic copper-centred oxidation of alcohols by TEMPO

benzylic C−H bonds are weaker and therefore easier to remove in a radical route than aliphatic ones.

Consistently, a large KIE of 5.4 and a small $\rho = -0.16$ were measured. These numbers appear more consonant with a rate-determining HAT route rather than with the 'ionic' mechanism of Scheme 15. In support of the hypothesis embodied by Scheme 17, Sheldon and coworkers set forth[161] the exemplary cases of the oxidation of alcohols by Cu(II) and a salen-ligand[165], or the oxidation of alcohols with the enzyme *Galactose oxidase*[166]. In both cases, reported to proceed through a radical HAT route, large values of the KIE (5.3 and 5.0, respectively) and small ρ values (−0.14 and −0.09) were found, in analogy with the results of the Sheldon-revisited CuCl-TEMPO procedure[161–163] (Table 10). Even the oxidation of alcohols catalysed by $RuCl_2(PPh_3)$/TEMPO does not involve an 'oxoammonium' mechanism, but rather a hydridometal route[161,167], characterized by a KIE of 5.1 and by a somewhat larger ρ value (i.e. −0.58). Moreover, this particular oxidation procedure occurs at 100 °C rather than at room temperature, as the previous ones.

An extended series of primary oxidants of TEMPO was investigated by Sheldon and coworkers[161,162], but we do not report on all of them; suffice it to observe that the selectivity of oxidation of primary vs. secondary alcohols varies substantially among the procedures, as well as the efficiency of oxidation of primary aliphatic alcohols, thereby concurring to make the matter complex.

Another method capable of inducing a TEMPO-catalysed oxidation is the one reported by Minisci and coworkers, which exploits Mn(II)−Co(II) nitrates in AcOH solution at 20–40 °C in the presence of O_2[80]. Primary and secondary alcohols, including aliphatic ones, are oxidized very efficiently. This procedure gave a good Hammett correlation vs. σ in the oxidation of X-substituted benzyl alcohols with a large ρ value of −1.44

TABLE 10. Summary of Hammett ρ values and kinetic isotope effects in the oxidation of benzylic alcohols[a]

System	ρ[b]	k_H/k_D
CuCl/TEMPO/O_2	−0.16	5.4
Cu(II)-salen/O_2	−0.14	5.3
Galactose oxidase	−0.09	5.0
$RuCl_2(PPh_3)$/TEMPO/O_2	−0.58	5.1
Mn(II)-Co(II)/TEMPO/O_2	−1.44	—
Laccase/TEMPO/O_2	cf. Figure 4	2.3

[a] Values taken from References 161–167.
[b] Obtained vs. σ.

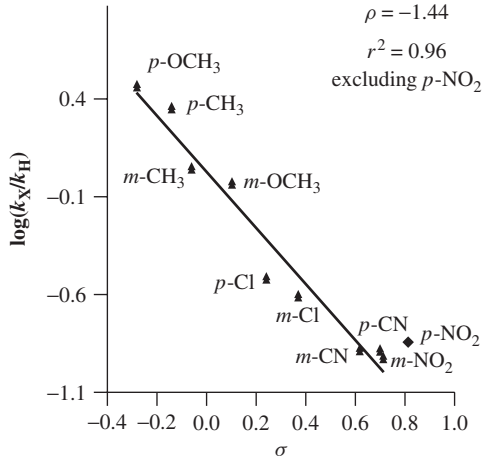

FIGURE 3. Hammett plot for the aerobic oxidation of X-substituted benzyl alcohols with Mn(II)–Co(II) nitrates and TEMPO in AcOH, in competition experiments. Reprinted with permission from Reference 129. Copyright (2004) Wiley-VCH

(Figure 3)[129], which is too large for being attributable to a radical process, and perhaps more fitting to the ionic oxoammonium route of Scheme 15.

Operation of the latter mechanism has also been invoked for the oxidation of X-substituted benzyl alcohols with TEMPO and the enzyme laccase[156, 168], because the redox potential of the enzyme (0.78 V)[150, 153] is adequate for the oxidation of TEMPO to oxoammonium ion (0.8 V)[63, 74]. Strangely enough, no linear correlation of the log k_X/k_H ratios was obtained in this case vs. either σ or σ^+ parameters. The log k_X/k_H data could instead be fitted to the σ_I parameters to yield a bell-shaped plot[156, 168] (Figure 4).

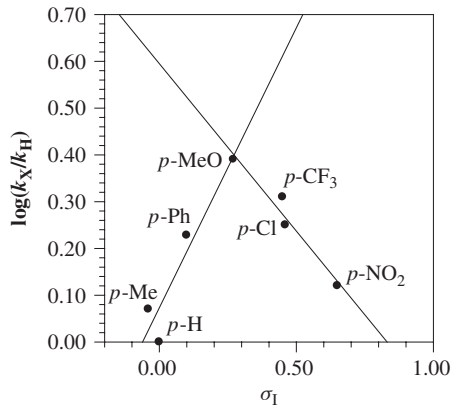

FIGURE 4. Hammett plot for the oxidation of 4-X-substituted benzyl alcohols with the laccase/TEMPO system, in competition experiments vs. benzyl alcohol. Reprinted with permission from Reference 156. Copyright (2004) John Wiley & Sons Limited

An explanation of this peculiar finding was offered on the basis of a change in the rate-determining step within the frame of the oxoammonium route (Scheme 15), attributable to a shift from a rate-determining adduct formation with electron-withdrawing substituents to a rate-determining elimination with electron-participating ones[156,168]. Consistently, an intramolecular KIE of 2.3 was measured for X = Ph. In this particular example, the agreement between the enzymatic method and the chemical method(s) for the generation of the reactive intermediate is not as good as in the cases listed in Table 9. It would appear peculiar if the difference in behaviour between a bell-shaped Hammett plot (Figure 4) and a linear one having a large ρ value (Figure 3)[129] depends only on the different solvent employed, i.e. water for the laccase-induced procedure[168] vs. AcOH for the one induced by Mn(II)–Co(II) nitrates[129]. This contrasting evidence certainly does not contribute to clarify the 'oxoammonium' story.

F. Concluding Remarks

A consolidated mechanistic tenet has been followed here, that the Hammett correlation and the KIE can provide a reliable tool with which to assess the reactivity features of the process under investigation. Accordingly, we have seen that the features displayed by the reactive intermediates arising from a few hydroxylamines, despite the variety of methods of generation followed, comply with the frame of an aminoxyl radical performing a H-abstraction step (Sections III.A, B and D; Schemes 1 and 7). EPR and spectroscopic evidence, when available, supports this conclusion. Reacting substrates, such as benzyl alcohols or alkylarenes, are discriminated in H-donation reactivity depending on the relative energy of the C–H bond that is cleaved in the rate-determining step upon the intervention of the aminoxyl radical: the weaker the C–H bond of the substrate, the faster the H-abstraction. The value of the k_H/k_D ratio is invariably in keeping with a rate-determining H-abstraction. The Hammett ρ parameter is small in value, as expected for a radical step, and its negative sign endorses the electrophilic character of the aminoxyl radical. Whenever the comparison is possible, the increasing reactivity of various aminoxyl radicals scales with the increasing energy of the NO–H bond they form in the rate-determining H-abstraction step. The reliability of the latter trend can be somewhat subverted by the diverse experimental conditions under which the various $R_2NO^{\bullet}$ species reacted, as well as by the limited stability of these reactive intermediates, or by the small number of studies available for proper comparison. Future research activity in this field will certainly provide additional keys of interpretation, capable for reconciling persisting discrepancies. The associated but novel field (Section III.C) where the aminoxyl radical behaves as a one-electron oxidant of reducing substrates is the object of current investigation.

As opposed to such a consistent body of evidence in favour of the H-abstraction route with aminoxyl radical intermediates, the reactivity features of the 'oxoammonium ion', as a derivative of the aminoxyl radical (TEMPO), are somewhat baffling (Section III.E). In spite of the many studies from the literature, a lack of uniformity emerges whenever the Hammett and KIE parameters are investigated and compared. The possible interplay of different mechanistic routes has been suggested, and more experimental work is needed before satisfactory conclusions can be drawn. Certainly, this does not undermine the synthetic value of the procedure, as we will see below, even though care must be exerted when comparing results obtained by the use of different primary oxidants.

IV. SYNTHETIC APPLICATIONS

Following the discussion on the reactivity features of exemplary aminoxyl radicals, it is now time to deal with applications of those concepts to valuable oxidative

transformations[21,159]. The ensuing discussion will focus on two fields. The first pertains to the realm of radical chemistry, and concerns the use of an appropriate aminoxyl radical in selective H-abstraction from a substrate, bound to afford an intermediate radical which eventually yields the desired oxidation product upon further interaction with O_2 (cf. Scheme 1)[21,159,163,169–171]. The most profitable player in this synthetic scheme is certainly PINO, generated according to procedures of Ishii and coworkers[126] and Minisci and coworkers[68,128] featuring the use of the Co(II)/O_2 oxidizing system. The second field, instead, concerns the one-electron oxidation of a suitable aminoxyl radical, most commonly TEMPO, to the corresponding oxoammonium ion (cf. Schemes 6 and 15, and previous Section III.E)[21,76,172,173]. The latter ion enables turning a substrate into the desired oxidation product through a route that may be ionic. Both of these experimental approaches testify to the efforts made by chemists to develop new synthetic strategies that are environmental friendly, and/or that exploit oxygen (or other oxygen donors) rather than more conventional but polluting inorganic oxidants[21,161,169,170].

A. Use of PINO in Oxidations of Synthetic Relevance

In the first reports by Ishii and coworkers[125,174], catalytic amounts of both HPI and Co(II)acetylacetonate, Co(acac)$_2$, were employed for the oxidation of alkanes in AcOH at 100 °C, dioxygen being the terminal oxidant. The appeal of this procedure for the oxidative transformation of simple hydrocarbons into carbonyl derivatives is clear. Cycloalkanes were converted into a mixture of cyclic ketones plus open-chain α,ω-dicarboxylic acids (Table 11), while linear alkanes yielded the corresponding alcohols plus ketones in significant amounts (40–80%), and alkylbenzenes could be oxidized in almost quantitative yields[126,175].

In the absence of either HPI or Co(acac)$_2$, no appreciable conversion into products was obtained. EPR evidence for the formation of an aminoxyl radical intermediate was acquired, and a KIE of 3.8 determined[125]. Generation of PINO *in situ* as the reactive intermediate was postulated[125,126,175]. A subtle alternative enables the functionalization of hydrocarbons through the formation of carbocations as transient intermediates whenever PINO is formed and reacts in the presence of NO (e.g. 1 atm)[176].

By employing the HPI/Co(acac)$_2$/O_2 system in $PhCF_3$ solution at 80 °C, the group of Sheldon obtained results comparable to those of the group of Ishii in the radical oxidation of hydrocarbons or cycloalkanes to mixtures of alcohol and ketone, or also in the oxidation of alkylarenes, while cyclohexylbenzene could be oxidized to phenol[177]. Moreover, *N*-hydroxysaccharin could successfully substitute HPI[163,173], and lead to the corresponding aminoxyl radical SINO (saccharin *N*-oxyl) as the reactive intermediate, particularly for the oxidation of cycloalkanes[178]. The group of Ishii serendipitously found (Table 11) that the addition of small amounts of an additive, such as *m*-chlorobenzoic acid (MCBA), to the HPI/Co(acac)$_2$/O_2 system enabled one to run the oxidation of alcohols to carbonyl compounds at room temperature in over 75% yields[118,126]. Diols gave either ketoalcohols or dicarbonyl products, or even the one-carbon-less carboxylic acid depending on the structure of the precursor. Good selectivity for the oxidation of a secondary alcohol in the presence of a primary one was achieved[118].

Minisci and coworkers followed Ishii's procedure, and implemented it in the oxidation of benzylic alcohols to benzaldehydes in almost quantitative yields[119,128] (Table 12). *N*,*N*-dimethylbenzylamines were converted into aldehydes in good yields, by using catalytic amounts of either HPI or *N*-hydroxysuccinimide (HSI) for the formation of the corresponding aminoxyl radical intermediates. Because the attempted oxidation of primary and secondary amines caused the degradation of catalyst HPI, protection of the amino group in those substrates by acetylation was considered. This led one to develop

TABLE 11. Selected examples of PINO-depending oxidations from the Ishii group[126, 175]

Reaction system	Reference	Substrate	Product(s) (% yield)
HPI/$Co(acac)_2$/O_2 at 100 °C in AcOH solution	125	cyclohexane	cyclohexanone (30) and adipic acid (35)
HPI/$Co(acac)_2$/O_2 at 100 °C in AcOH solution	125	octane	octanols (55) and octanones (15)
HPI/$Co(acac)_2$/O_2 at 100 °C in AcOH solution	125	toluene	benzoic acid (90)
HPI/$Co(acac)_2$/O_2 at 100 °C in AcOH solution	125	ethylbenzene	acetophenone (85)
HPI/$Co(acac)_2$/MCBA/O_2 at r.t. in AcOEt or MeCN solution	118	2-octanol	2-octanone (80)
HPI/$Co(acac)_2$/MCBA/O_2 at r.t. in AcOEt or MeCN solution	118	$CH_3CH(Ph)OH$	acetophenone (98)
HPI/$Co(acac)_2$/*m*-CPBA/O_2 at r.t. in AcOEt or MeCN solution	118	1-octanol	octanoic acid (75)[a]
HPI/$Co(acac)_2$/MCBA/O_2 at r.t. in AcOEt or MeCN solution	118	2,3-octanediol	2,3-octanedione (70) and hexanoic acid (15)
HPI/$Co(acac)_2$/MCBA/O_2 at r.t. in AcOEt or MeCN solution	118	1,2-butanediol	propanoic acid (70)
HPI/$Co(acac)_2$/MCBA/O_2 at r.t. in AcOEt or MeCN solution	118	PhCH(OH)CH(OH)Ph	benzyl (80) and benzoin (10)
HPI/$Co(acac)_2$/MCBA/O_2 at r.t. in AcOEt or MeCN solution	118	1,2-cyclohexanediol	1,2-cyclohexanedione (25) and adipic acid (30)
HPI/$Co(acac)_2$/MCBA/O_2 at r.t. in AcOEt or MeCN solution	118	1,3-cyclohexanediol	3-OH-cyclohexanone (80)
HPI/$Co(acac)_2$/MCBA/O_2 at r.t. in AcOEt or MeCN solution	118	1,5-pentanediol	glutaric acid (65)
HPI/$Co(acac)_2$/MCBA/O_2 at r.t. in AcOEt or MeCN solution	118	1,3-butanediol	4-OH-2-butanone (60)

[a] MCBA was replaced by *m*-Cl-perbenzoic acid[118].

the aerobic oxidation of *N*-alkyl- or benzylamides or even lactams under mild conditions, affording carbonyl products in good yields as mixtures of imides, carboxylic acids or aldehydes[128]. Finally, silanes (R_3SiH) were oxidized to silanols (R_3SiOH), a transformation of considerable industrial interest in the field of polymeric materials (polysiloxanes, silicones)[127, 128].

The electrocatalytic oxidation of several secondary and primary alcohols has been also described, in keeping with the original work by Masui and coworkers[52]; it resorts to HPI or to X-substituted HPIs as electron carriers[179]. The tetrafluoroaryl-substituted HPI was the most efficient among these catalysts. Secondary alcohols gave carbonyl compounds; primary alcohols gave the corresponding aldehyde exclusively under anaerobic conditions, whereas a mixture of aldehyde plus carboxylic acid was formed in the presence of O_2[179].

TABLE 12. Selected examples of oxidation through PINO from the Minisci group[119, 128]

Reaction system	Substrate	Product(s) (% yield)
HPI/$Co(OAc)_2$/O_2 at r.t. in MeCN solution	benzyl alcohol	benzaldehyde (95)
HPI/$Co(OAc)_2$/O_2 at 35 °C in MeCN solution	$PhCH_2NMe_2$	benzaldehyde (60)
HSI/$Co(OAc)_2$/O_2 at 35 °C in MeCN solution[a]	$PhCH_2NMe_2$	benzaldehyde (40)
HPI/$Co(OAc)_2$/MCBA/O_2 at r.t. in MeCN solution	$PhCH_2NHCOCH_3$	benzaldehyde (20) and $PhCONHCOCH_3$ (75)
HPI/$Co(OAc)_2$/MCBA/O_2 at 100 °C in AcOH solution		benzoic acid (95) and $PhCONHCOCH_3$ (5)
HPI/$Co(OAc)_2$/MCBA/O_2 at 80 °C in MeCN solution	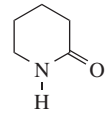	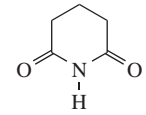 (85)
HPI/$Co(OAc)_2$/MCBA/O_2 at 80 °C in MeCN solution	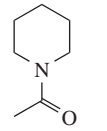	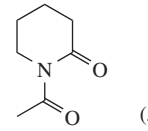 (55)
HPI/$Co(OAc)_2$/MCBA/O_2 at 80 °C in MeCN solution	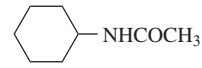	cyclohexanone (60)

[a] *N*-hydroxysuccinimide (HSI).

B. Use of TEMPO in Oxidations of Synthetic Relevance

Three fundamental review papers enlist examples of oxidation of a number of substrates by TEMPO-oxoammonium[74, 76, 171], and a summary of the accessible transformations is given in graphic form in Scheme 18[171].

Only a few examples will be summarized in Table 13; it is apt to remind the reader that a variety of primary oxidants have been used in the literature in order to produce the alleged oxoammonium ion (see Section III.E), and this might lie at the basis of some of the contrasting results experienced.

In one of the earlier cases, Ma and Bobbitt[180] oxidized allylic alcohols to aldehydes selectively and in good yields (entry 1, Table 13) in CH_2Cl_2 solution at 0 °C, in the presence of 2 molar equivalents of both TEMPO and *p*-toluenesulfonic acid (*p*-TSA) vs. the substrate. The formation of TEMPO-oxoammonium *in situ* by no other means than the acid-promoted disproportionation of TEMPO (cf. Scheme 16) was implied. Substantial retention of the *E* configuration of the allylic group in the starting alcohol was observed. The oxidation of aliphatic alcohols or glycols was instead sluggish, with the exception of *cis*-1,2-cyclohexanedimethanol (entry 2), which gave cyclization to a lactone in 89% yield.

The most convenient and commonly employed method for promoting the generation of TEMPO-oxoammonium is instead the so-called 'Anelli procedure'[181–184]. It resorts to NaClO as the regenerating oxidant in 1:1 molar ratio with the substrate, under co-catalysis by KBr. In a two-phase CH_2Cl_2–water system at 0 °C, the oxidation of a primary alkanol does take place, to give the aldehyde selectively and in good yields (entry 3) after a few minutes. In contrast, if the reaction is run in aqueous solution with 2 molar equivalents of

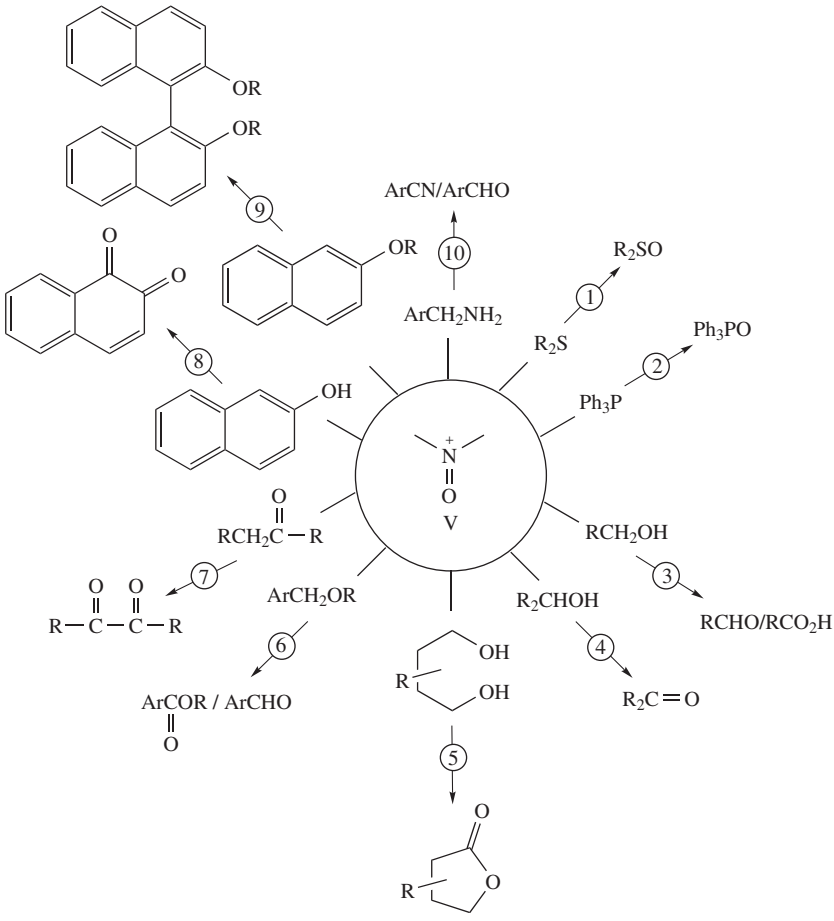

SCHEME 18. Organic transformations accessible to the oxoammonium-ion system. Reprinted with permission from Reference 171. Copyright (2001) American Chemical Society

NaClO, or else in the two-phase system but with a quaternary ammonium (viz. Aliquat) ion as a phase-transfer catalyst, overoxidation to the corresponding carboxylic acid is obtained (entry 4). Therefore, by proper choice of the experimental conditions, a synthetically useful distinction in products formation can be made for the oxidation of primary alcohols, even though we are far from a satisfactory understanding of the reason behind this different behaviour. In fact TEMPO, as a well-known inhibitor of free-radical processes[4,5], is allegedly responsible for the lack of overoxidation of an aldehyde to carboxylic acid (entry 3)[181]; this notwithstanding, TEMPO is also present under those conditions where the overoxidation does occur (entry 4). Moreover, a common tenet is that the formation of the hydrated form of an aldehyde (in water solution) prevents further oxidation to the carboxylic acid; however, both entries 3 and 4 refer to water–organic solutions, and their

contrasting outcome is therefore baffling. As an alternative to the Anelli method, the use of *N*-chlorosuccinimide (NCS) as a co-oxidant in CH_2Cl_2–water stops the overoxidation and affords the aldehyde exclusively (entry 5)[185]. The selective oxidation of benzylic or allylic alcohols is clearly very effective under the Anelli conditions (entry 6), but overoxidation can also be obtained on using $NaClO_2$ in a mixed H_2O–MeCN solvent (entry 7). Secondary alcohols afford the ketone in good yields (entry 8). Vicinal internal diols give the diketone derivative (entry 9), while appropriate α,ω-diols give the 5- or 6-membered ring lactone (entry 10). With cyclohexanol derivatives (entries 11 and 12) the treatment of 2,2,6,6-tetramethylpiperidine (TMP) with *m*-chloroperbenzoic acid (*m*-CPBA; 2 equivalents) generates TEMPO-oxoammonium *in situ*, and a Baeyer–Villiger-like oxidation of the substrate takes place in CH_2Cl_2 solution[186,187] in addition to the 'normal' oxidation route. Going back to the Anelli procedure, there is a substantial preference for the oxidation of a primary vs. secondary alcohol (entry 13), and a diol can be in part or fully oxidized depending on the amount (1 or 2 equivalents) of NaClO employed (entry 14). Finally, the primary alcohol of a protected aldohexose can be oxidized to carboxylic acid (entry 15) in water medium[188], and the conversion is particularly good at pH = 10. Even cellulosic material has been oxidized at the primary alcohol group to yield the carboxylate derivative by the use of the TEMPO/NaBr/NaClO catalytic system[189].

Another convenient procedure is the one described by the group of Piancatelli when resorting to TEMPO in the presence of [bis(acetoxy)iodo]benzene, $PhI(OAc)_2$ (viz. BAIB), as the regenerating oxidant, in CH_2Cl_2 solution at room temperature[78]. Both primary and secondary alcohols are oxidized in high yield (entries 16 and 17), and a very high selectivity is observed for the oxidation of the primary alcohol (without overoxidation) in the presence of the secondary one. The EPR spectrum of TEMPO has been found to fade out during the reaction, but to return to the initial value at its end[78], in keeping with the oxidation cycle of Scheme 15. The selective oxidation of one OH group in diols can be efficiently achieved (entry 18), as well as the conversion of the primary alcohol group of a protected aldohexose into the aldehyde (entry 19). The same result with an unprotected carbohydrate has been recently reported by the use of TEMPO-oxoammonium BF_4^-, independently generated by anodic oxidation of TEMPO in DMF[190].

A successful oxidant of TEMPO is the polyoxometalate $H_5PV_2Mo_{10}O_{40}$ (i.e. POM) in acetone solution[191]. This system gives excellent yields of oxidation with primary and secondary alcohols, both aliphatic and benzylic ones, without overoxidation (entries 20 and 21). Practical disadvantages are that it requires an overpressure of 2 atm of O_2 and reaction temperature of 100 °C, and therefore the use of a pressure tube, in addition to reaction times in the 6–20 h range[192]. The active oxidant is suggested to be the TEMPO-oxoammonium, which would be generated *in situ* by the POM in a catalytic cycle. In keeping with this hypothesis, no EPR spectrum of TEMPO could be recorded during the reaction time[192]. The reduced form of TEMPO, i.e. the hydroxylamine TEMPOH, would be re-oxidized to TEMPO-oxoammonium by POM in the rate-determining step, while O_2 would regenerate the oxidized form of the POM in a fast step. Accordingly, no kinetic isotope effect ($k_H/k_D = 1$) was determined in a competitive oxidation of benzyl and benzyl-d_7 alcohols[192].

The ruthenium–TEMPO catalytic system analogously requires a high temperature (100 °C) and long (3–24 h) reaction times, besides the use of an expensive noble metal[161,167]. However, it gives quantitative conversion with all kinds of alcohols, without overoxidation. The true active oxidant is the $RuCl_2(PPh_3)_3$ complex, and the role of TEMPO is simply to regenerate the ruthenium catalyst ($RuCl_2L_3$, L being the ligand) by abstracting H-atom from its spent hydride form (RuH_2L_3). Consistent with a metal-centred

dehydrogenation of the substrate are both the sizeable KIE ($k_H/k_D = 5.1$) and the Hammett ρ value (i.e. -0.58) determined vs. σ[161, 167].

We now come to the CuCl/TEMPO procedure, as the one first encountered[79]. Actually, the experimental approach of Semmelhack was inspired by earlier evidence acquired by his group, and based on the unambiguous anodic oxidation of TEMPO to TEMPO-oxoammonium. Addition of the substrate to this electrogenerated species led to the oxidation of both primary and secondary benzylic and allylic alcohols to carbonyl products in high yields. Primary aliphatic alcohols gave 80% conversion to the aldehyde, while secondary ones gave about 30% of the ketone[193]. The same electrochemical procedure was applied to the oxidation of amines, RCH_2NH_2[194]; in anhydrous MeCN solution, the nitrile (RCN) was obtained in 60–90% yields, whereas in aqueous media the oxidation afforded the aldehyde (RCHO) in 80–90% yields. Amines having the R_2CHNH_2 structure gave the ketone (85%), while those of the $PhCH_2NHR$ kind produced PhCHO in 89% yield[194]. Based on this experience, the group of Semmelhack moved on to use CuCl in equimolar amount with TEMPO for the aerobic oxidation of alcohols at room temperature in DMF[79]. The rationale was that the formation *in situ* of the oxidizing Cu(II) species, from interaction of Cu(I) with O_2, would enable conversion of TEMPO into the oxoammonium reactive intermediate. For sure, Cu(II) is a rather weak monoelectronic oxidant. Nevertheless, primary benzylic and allylic alcohols were turned into the corresponding aldehydes in 90–95% yields (entry 22) without overoxidation, and with retention of the original configuration of the double bond in the case of allylic precursors[79]. The KIE of *ca* 2 was taken as evidence supporting the oxoammonium mechanism (Scheme 15)[195]. However, primary alkanols gave only partial conversion into the aldehyde, and strangely enough 2-cyclohexenol was recovered unreacted (entry 23)[79]. The use of $CuCl_2$ and CaH_2, rather than CuCl, in a 10 times molar excess with respect to TEMPO, gave 75–85% conversion of primary aliphatic alcohols into aldehydes in MeCN solution, while 2-hexanol afforded 21% of 2-hexanone (entries 24 and 25). According to the authors, this outcome confirms that Cu(II) is the needed oxidant of TEMPO *en route* to TEMPO-oxoammonium because, whenever $CuCl_2$ is available in large amounts since the early stages of the reaction, a more efficient oxidation takes place[79]. Whether this may alternatively be caused by the operation of a different and radical mechanism, as later suggested by the group of Sheldon, or by some other interference is hard to say.

As anticipated, Sheldon and coworkers attempted to revise the Cu/TEMPO system, and suggested that a piperidinyloxycopper(II) adduct, rather than the oxoammonium ion, is instead formed as an intermediate species[161]; that adduct would be responsible for turning the alcohol into the carbonyl product. Sheldon and coworkers proposed the radical mechanism outlined in Scheme 17, and supported it with a Hammett ρ value of -0.16 (vs. σ) and with a KIE of 5.4[161, 162]. They also suggested that steric hindrance arising from interaction of secondary alcohols with the active-TEMPO species, whatever it can be, are possibly responsible for the lower, or lack of, reactivity displayed by these substrates[163]. Accordingly, a novel TEMPO-like system has been recently developed in order to specifically bypass this steric interference[196], as we are going to see below.

At the end of this long list of procedures, a few additional data from the recent literature are commented on. First of all, it is a common notion that a supported catalyst is easier to separate from the end products, and its re-use is facilitated. Accordingly, several reports deal with TEMPO immobilized on appropriate polymeric supports (i.e. PIPO)[129, 163, 173, 197–199], or similar heterogeneous devices. Apart from the above anticipated advantages, the immobilized TEMPO leads to the same reactive intermediate (i.e. the oxoammonium) and gives the same reaction products seen before, thereby presenting no additional synthetic or mechanistic value. Then, some 'specialized' TEMPO-like aminoxyl radicals begin to appear in the literature, in order to tackle specific needs.

For example, 2-azaadamantane *N*-oxyl (AZADO) is an aminoxyl radical considered to be structurally less hindered than TEMPO, due to the expanded accessibility that the 'folded-back' adamantyl structure grants to the corresponding oxoammonium form. As a matter of fact, AZADO shows an enhanced catalytic efficiency in the oxidation of structurally hindered secondary alcohols[196], by using either the 'Anelli'[181] or the 'Piancatelli'[78] oxidizing systems. An oxidative kinetic resolution of racemic alcohols has also been attempted and achieved by using a chiral binaphthyl-derived TEMPO-like catalyst[200]. Finally, a seemingly very convenient procedure is the one recently described by a Chinese team, even though not many hints about the involved mechanism were provided[201]. By means of the catalytic system $O_2/FeCl_3$/TEMPO/$NaNO_2$ in $PhCF_3$ solution, benzylic and allylic alcohols are quantitatively oxidized at room temperature without overoxidation (entries 26–28). Secondary aliphatic alcohols are quantitatively converted into ketones (entry 29), whereas primary alkanols give lower conversion and evidence of overoxidation[201]. It is plausible that TEMPO-oxoammonium is the crucial reactive intermediate, but the authors do not address this point explicitly[201,202].

In conclusion, TEMPO is an aminoxyl radical very valuable for synthetic purposes, not just as such but in its oxidized form, most likely the TEMPO-oxoammonium ion. Many 'recipes' are available (Table 13), which allow synthetic transformations endowed with high efficiency and mild operating conditions. One needs to search and choose the one recipe that most likely fits the specific needs, without indulging too much in mechanistic considerations that are perhaps still far from a fully exhaustive assessment.

C. Chemo-enzymatic Methods of Oxidation

In Section III.D it has been anticipated that the copper-enzyme laccase is able to generate aminoxyl radicals by one-electron oxidation of the parent R_2NOH species (Schemes 4 and 13), as well as to produce TEMPO-oxoammonium from TEMPO[156,158]. The redox potential of fungal laccases, being in the 0.70–0.80 V/NHE range[150,151,153], is in fact adequate for these monoelectronic oxidations[135], thereby enabling an 'enzymatic' generation of the reactive intermediates[156] $R_2N{-}O^{\bullet}$ and $R_2N{=}O^{+}$, respectively, as an alternative to those commented on in Sections IV.A and IV.B. Either the hydroxylamines or TEMPO play the role of mediators in this context[135,154,156], and are represented as Med in Scheme 14. Once oxidized by laccase to their corresponding $R_2N{-}O^{\bullet}$ and $R_2N{=}O^{+}$ species (Med_{ox}), respectively, they undertake the 'chemical' oxidation of primary and secondary alcohols[81] or ethers[168,203], and in a few cases even of alkylarenes[204], according to the radical or ionic routes delineated in Schemes 1 or 15. Laccase replenishes the Med_{ox} form in a catalytic cycle relying on O_2 as the terminal oxidant[156,158], and enables one to develop chemo-enzymatic strategies of environmentally benign oxidations[81,160,205]. Fungal laccases are easily available as well as robust enzymes, capable of enduring reaction temperatures approaching 50 °C[150], or operating in water/organic mixtures containing up to 30–50% of an organic co-solvent without extensive denaturation[206]. There are therefore good chances of industrial application of the chemo-enzymatic procedures. A few cases of synthetically useful transformations with laccase/mediator systems have been documented, and will be commented on here.

The most profitable is certainly the use of laccase (Lc) with TEMPO[81]. It enables the almost quantitative conversion of primary benzylic and allylic alcohols to aldehydes without overoxidation under mild conditions (Table 14, entries 1 and 2), that is, 25 °C and pH = 4.5 in the presence of atmospheric O_2, for a reaction time of 24 h. The successful enzyme is the one obtained from the fungus *Trametes villosa*.

Ketones are obtained in good yields from secondary benzylic alcohols (entry 3), whereas the oxidation is less satisfactory with aliphatic alcohols (entries 4 and 5)[81]. This is a

TABLE 13. Selected examples of TEMPO-dependent oxidations

Entry	Substrate	Method	Product(s)	Yield (%)	Reference
1	Geraniol (E)	TEMPO/*p*-TSA/CH_2Cl_2	geranial (*E*): neral (*Z*) (4:1)	90	180
2	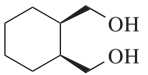	TEMPO/*p*-TSA/CH_2Cl_2	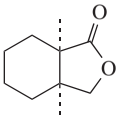	89	180
3	1-Octanol	TEMPO/NaClO/KBr/ CH_2Cl_2–water, 0 °C	octanal	90	76, 181, 182
4	1-Octanol	TEMPO/NaClO/KBr/ CH_2Cl_2–water/Aliquat [a]	octanoic acid	95	76, 181, 182
5	1-Octanol	TEMPO/NaClO/NCS/ CH_2Cl_2–water, 0 °C	octanal	85	185
6	$PhCH_2OH$	TEMPO/NaClO/KBr/ CH_2Cl_2–water, 0 °C	PhCHO	90	76, 181, 182
7	$PhCH_2OH$	TEMPO/$NaClO_2$/KBr/ H_2O–MeCN	$PhCO_2H$	98	76
8	Cyclohexanol	TEMPO/NaClO/KBr/ CH_2Cl_2–water, 0 °C	cyclohexanone	90	76, 181, 182
9	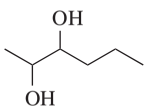	TEMPO/NaClO/KBr/ CH_2Cl_2–water, 0 °C	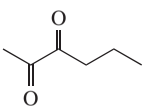	90	76, 181, 182
10	$HO(CH_2)_5OH$	TEMPO/NaClO/KBr/ CH_2Cl_2–water, 0 °C	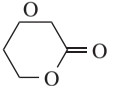	100	76, 181, 182
11	Cyclohexanol	TMP/*m*-CPBA/CH_2Cl_2 [b]	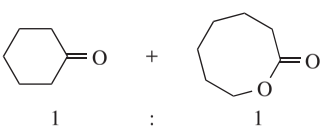 1 : 1	90	186, 187

12	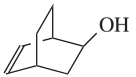	TMP/*m*-CPBA/CH_2Cl_2 [b]	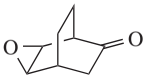	60	187
13	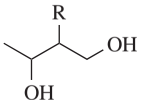	TEMPO/NaClO/KBr/ CH_2Cl_2–water/Aliquat [a]	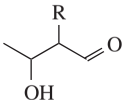	98	76, 181, 182
14	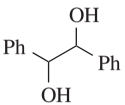	TEMPO/KBr/ CH_2Cl_2–water/1 or 2 eq. NaClO	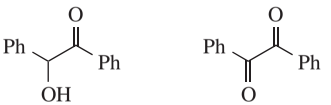 85% or 97%	76, 181, 182	
15	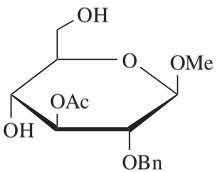	TEMPO/NaClO/ KBr/water (pH = 10)	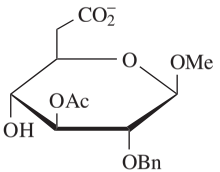	70	76, 188
16	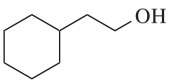	TEMPO/BAIB/ CH_2Cl_2 [c]	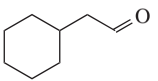	89	78
17	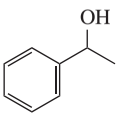	TEMPO/BAIB/ CH_2Cl_2 [c]	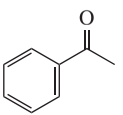	95	78

(*continued overleaf*)

TABLE 13. (*continued*)

Entry	Substrate	Method	Product(s)	Yield (%)	Reference
18	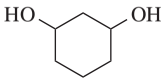	TEMPO/BAIB/CH_2Cl_2 [c]	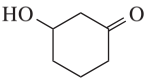	90	78
19	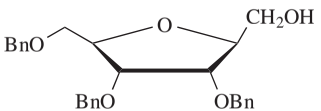	TEMPO/BAIB/CH_2Cl_2 [c]	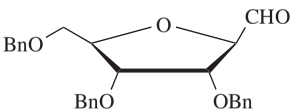	75	78, 190
20	1-Octanol	TEMPO/O_2/POM [d]	octanal	98	191, 192
21	2-Octanol	TEMPO/O_2/POM [d]	2-octanone	96	191, 192
22	$PhCH_2OH$	CuCl/TEMPO/O_2/DMF	PhCHO	94	79
23	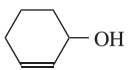	CuCl/TEMPO/O_2/DMF	no oxidation	0	79
24	$Ph(CH_2)_2CH_2OH$	$CuCl_2$/CaH_2/TEMPO/O_2/MeCN	$Ph(CH_2)_2CHO$	85	79
25	$CH_3CH(OH)C_4H_9$	$CuCl_2$/CaH_2/TEMPO/O_2/MeCN	$CH_3C(O)C_4H_9$	21	79
26	$PhCH_2OH$	$FeCl_3$/TEMPO/$NaNO_2$/O_2/$PhCF_3$	PhCHO	99	201
27	$PhCH{=}CHCH_2OH$	$FeCl_3$/TEMPO/$NaNO_2$/O_2/$PhCF_3$	PhCH=CHCHO	99	201
28	PhCH(OH)Me	$FeCl_3$/TEMPO/$NaNO_2$/O_2/$PhCF_3$	PhC(O)Me	99	201
29	2-Octanol	$FeCl_3$/TEMPO/$NaNO_2$/O_2/$PhCF_3$	2-octanone	99	201

[a] Aliquat = trioctylmethyl ammonium chloride.
[b] 2,2,6,6-Tetramethylpiperidine (TMP).
[c] Bis(acetoxy)iodobenzene, $PhI(OAc)_2$ (viz. BAIB).
[d] Polyoxometalate $H_5PV_2Mo_{10}O_{40}$ (i.e. POM).

TABLE 14. Aerobic oxidations with the Lc/TEMPO system, at room temperature

Entry	Substrate	Method	Product(s)	Yield (%)	Reference
1	$PhCH_2OH$	Lc/TEMPO/O_2/ pH = 5 or 3.5	PhCHO	92	81, 135
2	geraniol	Lc/TEMPO/O_2/ pH = 5	geranial	96	81
3	ArCH(OH)R	Lc/TEMPO/O_2/ pH = 5	ArCOR	90	81
4	1-decanol	Lc/TEMPO/O_2/ pH = 5	decanal	55	81
5	cyclohexanol	Lc/TEMPO/O_2/ pH = 5	cyclohexanone	35	81
6	$(PhCH_2)_2O$	Lc/TEMPO/O_2/ pH = 5	PhCHO + $PhCO_2CH_2Ph$	16 + 3	168, 203
7	$PhCH_2NMe_2$	Lc/TEMPO/O_2/ pH = 5	PhCHO	99	81
8	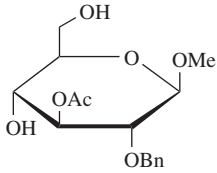	Lc/TEMPO/O_2	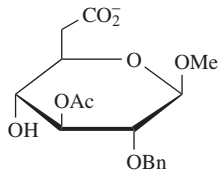	—	160

reactivity trend in common with the TEMPO-oxoammonium procedures listed in Table 13. Benzyl ethers give a mixture of carbonyl products in low yields (entry 6)[168], while benzyl amines are quantitatively oxidized to benzaldehyde (entry 7)[81]. Due to the high selectivity of oxidation of primary vs. secondary alcohols, the regioselective catalytic oxidation of the primary hydroxyl group of glycosides has been achieved with *Trametes pubescens* laccase and TEMPO, to give uronate salt (entry 8)[160]. Both the wild-type and an Eupergit®-supported enzyme showed significant activity here, and the partial oxidation of water-soluble cellulose samples has also been successfully achieved[207, 208].

Other examples of chemo-enzymatic oxidations useful for synthetic purposes rely on the use of laccase in combination with the hydroxylamines (Scheme 1). Fungal laccases, due to their higher redox potential with respect to those from plants[150], are able to oxidize R_2NOH mediators, such as HPI, HBT, NHA (or others), to their $R_2NO^{\bullet}$ form[63, 69, 135, 156, 158], *Trametes villosa* laccase providing a good case. Oxidation with the latter is favoured by the pH (4–5) operating conditions, which are not only suitable for the enzyme metabolism but also cause extensive deprotonation of the hydroxylamine into the easier-to-oxidize R_2NO^- form[63, 120]. The chemical transformations described before (in Tables 11 and 12), and depending on the use of PINO or similar aminoxyl radicals, become in this way accessible to the laccase/R_2NOH oxidizing systems. Not many examples of synthetic relevance have been reported, however, because the conversion into product(s) is often low or moderate, and this chemo-enzymatic method does not compare favourably with the chemical ones described before (Tables 11 and 12). Table 15 offers significant cases.

Primary benzylic alcohols are oxidized to aldehydes in good yields without overoxidation (entry 1); lowering the pH from 5 to 3.5 increases the conversion, for reasons not fully understood yet (entry 2)[135]. The aminoxyl radical is an electrophilic species[119, 127]

TABLE 15. Aerobic oxidations with *Trametes villosa* laccase (Lc) and R_2NOH mediators [a]

Entry	Substrate	Method	Product(s)	Yield (%)	Reference
1	*p*-$MeOC_6H_4CH_2OH$	Lc/HBT/O_2/pH = 5/r.t.	*p*-$MeOC_6H_4CHO$	76	135
2	*p*-$MeOC_6H_4CH_2OH$	Lc/HBT/O_2/pH = 3.5/r.t.	*p*-$MeOC_6H_4CHO$	95	135
3	$PhCH_2OH$	Lc/HBT/O_2/pH = 5/r.t.	PhCHO	30	135
4	*p*-$MeOC_6H_4CH_2OH$	Lc/HPI/O_2/pH = 5/r.t.	*p*-$MeOC_6H_4CHO$	70	135
5	*p*-$MeOC_6H_4CH(OH)CH_3$	Lc/HBT/O_2/pH = 5/r.t.	*p*-$MeOC_6H_4COCH_3$	49	158
6	$ArCH_2OMe$ Ar = 3, 4-$(MeO)_2C_6H_3$	Lc/HBT/O_2/pH = 5/r.t.	ArCHO + $ArCO_2Me$	60 + 25	158
7	$PhCH_2OCH_2Ph$	Lc/HBT/O_2/pH = 5/r.t.	PhCHO + $PhCO_2CH_2Ph$	21 + 8	203
8	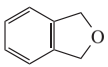	Lc/HBT/O_2/pH = 5/r.t.	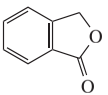	62	203
9	$ArCH_2CH_3$ Ar = *p*-$MeOC_6H_4$	Lc/HBT/O_2/pH = 5/r.t.	$ArCH(OH)CH_3$ + $ArCOCH_3$	8 + 20	158
10	1-Me-naphthalene	Lc/HPI/O_2/pH = 5/r.t.	1-Naph-CH_2OH + 1-Naph-CHO	8 + 5	204
11	$ArCH_3$ Ar = 3,4-$(MeO)_2C_6H_3$	Lc/HBT/O_2/pH = 4.5/45 °C.	$ArCH_2OH$ + ArCHO	3 + 20 − 76 [b,c]	210
12	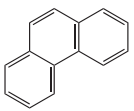	Lc/HBT/O_2/Tween/pH = 5/r.t.[b]	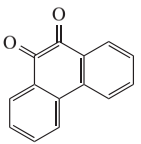 + 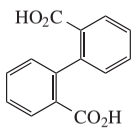	6 + 10	211
13	$PhCH=CHCH_2OH$	Lc/HBT/O_2/pH = 4.5/r.t.	PhCH=CHCHO + PhCHO	40 + 43	212
14	*cis*-2-Hexen-1-ol	Lc/HBT/O_2/pH = 4.5/r.t.	*trans*-2-hexenal + *cis*-2-hexenal	34 + 3	212
15	Cyclohexene	Lc/HBT/O_2/pH = 4.5/r.t.	2-cyclohexen-1-one	4	212
16	α-Pinene	Lc/HBT/O_2/pH = 4.5/r.t.	mixture of enones and enols	*ca* 30	212

[a] Reaction time of 24 h, unless otherwise given.
[b] Increasing the amount of laccase by 10-fold.
[c] Reaction times of 60–180 h.

and, as such, is sensitive to the presence of electron-donor substituents; accordingly, a lower conversion is obtained with plain benzyl alcohol (compare entry 3 with 1). Mediator HPI is slightly less efficient than HBT (entry 4)[135]. Secondary benzylic alcohols give ketones in fair yields (entry 5)[158]. Benzyl ethers are oxidatively cleaved to the aldehyde plus the ester derivative (entries 6 and 7)[203]. Cyclic benzylic ethers are more efficiently oxidized than open-chain counterparts (cf. entry 8 vs. 7) due to the operation of a stereoelectronic effect[209]. Alkylarenes are oxidizxed at the benzylic C−H bond to give the corresponding alcohol plus carbonyl derivatives in modest yields (entries 9 and 10)[204]. These yields become more interesting on increasing the reaction temperature and the amount of enzyme (entry 11)[210]. The oxidation of phenanthrene has been described to occur in modest yield with the Lc/HBT system in the presence of the surfactant Tween 80 (entry 12), but the incursion of peroxidation cannot be excluded in this case[211]. The use of *Trametes hirsuta* laccase at 20 °C, in the presence of HBT, has allowed one to oxidize allyl alcohols in relatively good yields after a reaction time of 20 h (entries 13 and 14), even though partial cleavage of the chain also occurred[212]. Cyclic alkenes give low conversion to the enones (entries 15 and 16)[212]. Finally, a series of polycyclic aromatic hydrocarbons has been oxidized by *Trametes versicolor* laccase in the presence of HBT as the mediator, at pH = 4.5 (temperature not given)[213]. Conversion of the reagents was described to vary from 0 to 100%, and found proportional to the redox potential of the starting material, product analysis being carried out only occasionally. It is somewhat odd that the 'mediator' had to be employed in unbelievably high molar ratios, ranging from 40:1 up to 200:1 with respect to the 'substrate'[213]. It is therefore difficult to assess the nature of the process that actually took place under these conditions.

Considerable efforts have been made towards the oxidation of lignin-model compounds by laccase and mediators. The rationale was to find chemo-enzymatic procedures suitable to replace existing industrial methods of oxidation bound to remove lignin from wood pulp for paper manufacturing[150,154,214]. Successful replacement of the industrial methods, which use polluting oxidizing agents based upon chlorine or its derivatives, would be an example of 'green chemistry', mimicking what occurs in nature through the oxidizing enzymes produced by ligninolytic fungi. In fact, oxidation of lignin in rotten wood by fungi is a remarkable example of 'cold combustion', carried out by a consortium of enzymes including *Lignin peroxidase, Manganese peroxidase* and laccase[150,214]. While the first two enzymes are stronger oxidants, laccase is weaker but has the advantage of using atmospheric oxygen as the terminal oxidant, besides being a much more robust and heat-tolerant enzyme. In addition, the phenoloxidase laccase becomes able to oxidize indirectly benzylic alcohol or ether functional groups by the use of mediators (Scheme 14)[154,214], as noted above (Tables 14 and 15). This is a key advantage in the perspective of the industrial delignification of wood pulp. In fact, benzylic alcohols and ethers are residues much more abundant in lignin than phenolic groups[215], although being endowed with a redox potential too high ($E^\circ > 1.4$ V)[143] for being directly accessible to the redox capacity of fungal laccases. Because the chemo-enzymatic oxidation of benzylic groups by laccase and mediators is feasible[156], extension of the laccase/mediator approach to the oxidation of model compounds of lignin, or even of lignin itself, has been actively sought, in the hope of causing the oxidative collapse of the covalent network of this polymer (Scheme 19)[63].

Adlerol, i.e. 1-(3,4-dimethoxyphenyl)-3-hydroxy-2-(2-methoxyphenoxy)propan-1-ol, is a well-established dimeric model compound of lignin[155] and, as such, its oxidation to the ketone-derivative Adlerone, i.e. 1-(3,4-dimethoxyphenyl)-3-hydroxy-2-(2-methoxyphenoxy)propan-1-one, has been taken as a benchmark reaction (Scheme 20) to evaluate the efficiency of several chemo-enzymatic procedures.

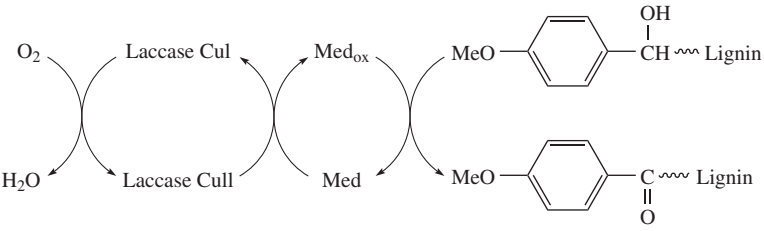

SCHEME 19. The redox cycle of a laccase/mediator system towards lignin. Reprinted from Reference 63 by permission of The Royal Society of Chemistry on behalf of the Centre National de la Recherche Scientifique

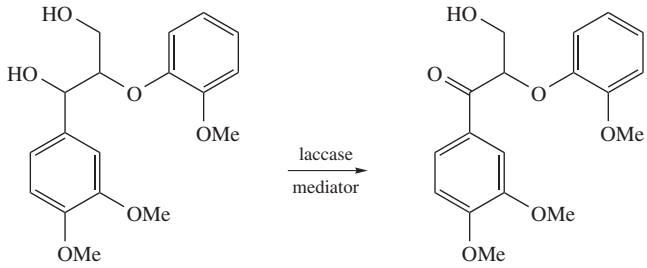

Adlerol Adlerone

SCHEME 20. Chemo-enzymatic oxidation of Adlerol

Many attempts at oxidation of this (or similar) model have been published, by using laccase and either HBT or HPI as the most common mediators, and present variable extents of success[69,155,216–221]. In some cases, the same procedures have been applied to the oxidative degradation of samples of lignin itself, or even of wood pulp[219,222–226]. The results show a potential proficiency of the laccase/mediator concept for an effective lignin degradation that selectively spares cellulose for paper making. Problems of insufficient removal of all traces of lignin, summed up to the cost of the mediators and to the occasional development of coloured by-products from the mediator, or anyhow the slight environmental endanger of some of these by-products, have so far hampered full industrial application of the laccase/mediator strategy.

D. Concluding Remarks

The aminoxyl radicals lend themselves to synthetically interesting procedures of oxidation, both in the radical form itself and in the oxoammonium form (from TEMPO). Major advantages appear to be the mild operating conditions, the range of substrates susceptible to transformation and the selectivity in the oxidation of specific structural motifs.

V. REFERENCES

1. Electronic version 2005, http://goldbook.iupac.org/A00285.html.
2. H. G. Aurich, in E. Breuer, H. G. Aurich and A. Nielsen, *Nitrones, Nitronates and Nitroxides*, updates from 'The Chemistry of Functional Groups' (Eds.), S. Patai and Z. Rappoport, Wiley, Chichester, 1989, p. 313.

3. O. I. Aruoma and B. Halliwell (Eds.), *Free Radicals and Food Additives*, Taylor & Francis, London, 1991.
4. E. G. Rozantsev, *Pure Appl. Chem.*, **62**, 311 (1990).
5. J. Antosiewicz, J. Popinigis, M. Wozniak, E. Damiani, P. Carloni and L. Greci, *Free Radical Biol. Med.*, **18**, 913 (1995).
6. L. Eberson and O. Persson, *Acta Chem. Scand.*, **53**, 680 (1999).
7. L. Eberson, O. Persson, H. K. Hall, A. Buyle Padias and P. J. Steel, *Macromolecules*, **33**, 2021 (2000).
8. C. Jargstorff and U. Wille, *Eur. J. Org. Chem.*, 3173 (2003).
9. E. G. Rozantsev, *Free Nitroxyl Radicals*, Plenum Press, New York, 1970.
10. L. J. Berliner (Ed.), *Spin Labeling: Theory and Applications*, Academic Press, New York, 1976.
11. J. F. W. Keana, *Chem. Rev.*, **78**, 37 (1978).
12. M. J. Perkins, *Adv. Phys. Org. Chem.*, **17**, 1 (1980).
13. L. Eberson, *Adv. Phys. Org. Chem.*, **31**, 91 (1998).
14. Y. Nosaka, H. Natsui, M. Sasagawa and A. Y. Nosaka, *J. Phys. Chem. B*, **110**, 12993 (2006).
15. E. Damiani, P. Astolfi, M. Benaglia, A. Alberti and L. Greci, *Free Radical Res.*, **38**, 67 (2004).
16. S. Nakatsuji, H. Ikemoto, H. Akutsu, J. Yamada and A. Mori, *J. Org. Chem.*, **68**, 1708 (2003).
17. S. Nakatsuji, M. Fujino, S. Hasegawa, H. Akutsu, J. Yamada, V. S. Gurman and A. Kh. Vorobiev, *J. Org. Chem.*, **72**, 2021 (2007).
18. C. J. Rhodes, *Annu. Rep. Prog. Chem., Sect. C: Phys. Chem.*, **100**, 149 (2004).
19. R. Basosi, G. Della Lunga and R. Pogni, *Biomedical EPR*, Kluwer, New York, 2005.
20. V. P. Gubskaya, L. Sh. Berezhnaya, A. T. Gubaidullin, I. I. Faingold, R. A. Kotelnikova, N. P. Konovalova, V. I. Morozov, I. A. Litvinov and I. A. Nuretdinov, *Org. Biom. Chem.*, **5**, 976 (2007).
21. I. W. C. E. Arends and R. A. Sheldon, Chap. 4, in *Modern Oxidation Methods* (Ed. J.-E. Bäckvall), Wiley-VCH, Weinheim, 2004, p. 83.
22. (a) D. Rochefort, D. Leech and R. Bourbonnais, *Green Chem.*, **6**, 14 (2004).
(b) A full issue of *Chem. Rev.*, **107**, 2167–2820 (2007) deals with 'green chemistry'.
23. J. Lind and G. Merényi, *J. Phys. Chem. A*, **110**, 192 (2006).
24. O. P. Chawla and R. W. Fessenden, *J. Phys. Chem.*, **79**, 2693 (1975).
25. H. Takase and O. Kikuchi, *J. Phys. Chem.*, **98**, 5160 (1994).
26. M.-L. Hung, M. L. McKee and D. M. Stanbury, *Inorg. Chem.*, **33**, 5108 (1994).
27. D. Griller and K. U. Ingold, *Acc. Chem. Res.*, **9**, 13 (1976).
28. T. Kothe, S. Marque, R. Martschke, M. Popov and H. Fischer, *J. Chem. Soc., Perkin Trans. 2*, 1553 (1998).
29. A. F. Parsons, *An Introduction to Free Radical Chemistry*, Blackwell Science, Oxford, 2000.
30. E. Denisov, *Handbook of Antioxidants*, CRC Press, Boca Raton, 1995.
31. K. E. Hammel, M. Tien, B. Kalyanaraman and T. K. Kirk, *J. Biol. Chem.*, **260**, 8348 (1985).
32. A. Kuliopulos, P. Talalay and A. S. Mildvan, *Biochemistry*, **29**, 10271 (1990).
33. R. Chiarelli and A. Rassat, *Tetrahedron*, **29**, 3639 (1973).
34. L. Volodarsky, *Imidazolines Nitroxides*, CRC Press, Boca Raton, 1988.
35. F. A. Villamena, A. Rockenbauer, J. Gallucci, M. Velayutham, C. M. Hadad and J. L. Zweier, *J. Org. Chem.*, **69**, 7994 (2004).
36. H. Zimmer, D. C. Lankin and S. W. Horgan, *Chem. Rev.*, **71**, 229 (1971).
37. W. D. Blackley and R. R. Reinhard, *J. Am. Chem. Soc.,* **87**, 802 (1965).
38. R. E. Banks, R. N. Haszeldine and M. J. Stevenson, *J. Chem. Soc. C*, 901 (1966).
39. V. Malatesta and K. U. Ingold, *J. Am. Chem. Soc.,* **103**, 3094 (1981).
40. A. I. Kokorin and I. A. Grigorev, *Mendeleev Commun.*, 195 (2006).
41. P. Carloni, E. Damiani, L. Greci, P. Stipa, G. Marrosu, R. Petrucci and A. Trazza, *Tetrahedron*, **52**, 11257 (1996).
42. E. Damiani, R. Castagna, P. Astolfi and L. Greci, *Free Radical Res.*, **39**, 325 (2005).
43. D. Gigmes, A. Gaudel-Siri, S. R. A. Marque, D. Bertin, P. Tordo, P. Astolfi, L. Greci and C. Rizzoli, *Helv. Chim. Acta*, **89**, 2312 (2006).
44. H. Wieland and K. Roth, *Chem. Ber.*, **53B**, 210 (1920).
45. G. Chapelet-Letourneux, H. Lemaire and A. Rassat, *Bull. Soc. Chim. Fr.*, 444 (1965).
46. R.-M. Dupeyre and A. Rassat, *J. Am. Chem. Soc.*, **88**, 3180 (1966).

47. A. R. Forrester and R. H. Thomson, *Nature*, **203**, 74 (1964).
48. G. D. Mendenhall and K. U. Ingold, *J. Am. Chem. Soc.*, **95**, 6395 (1973).
49. G. Chapelet-Letourneux, H. Lemaire and A. Rassat, *Bull. Soc. Chim. Fr.*, 3283 (1965).
50. P. Wautelet, J. Le Moigne, V. Videva and P. Turek, *J. Org. Chem.*, **68**, 8025 (2003).
51. I. Komaromi and J. M. J. Tronchet, *J. Phys. Chem.*, **99**, 10213 (1995).
52. C. Ueda, M. Noyama, H. Ohmori and M. Masui, *Chem. Pharm. Bull.*, **35**, 1372 (1987).
53. A. J. Bard and L. R. Faulkner, *Electrochemical Methods: Fundamentals and Applications*, Wiley, New York, 1980.
54. S. Kishioka and A. Yamada, *Electrochim. Acta*, **51**, 4582 (2006).
55. L. Marx and B. Schöllhorn, *New J. Chem.*, **30**, 430 (2006).
56. H.-C. Kim, M. Mickel and N. Hampp, *Chem. Phys. Lett.*, **371**, 410 (2003).
57. K. Nobuyoshi, B. Saha and J. H. Espenson, *J. Org. Chem.*, **68**, 9364 (2003).
58. C. Annunziatini, M. F. Gerini, O. Lanzalunga and M. Lucarini, *J. Org. Chem.*, **69**, 3431 (2004).
59. C. Galli, P. Gentili, O. Lanzalunga, M. Lucarini and G. F. Pedulli, *Chem. Commun.*, 2356 (2004).
60. E. Baciocchi, M. Bietti, M. F. Gerini and O. Lanzalunga, *J. Org. Chem.*, **70**, 5144 (2005).
61. G. Prabhakar Rao and A. R. Vasudeva Murthy, *J. Phys. Chem.*, **68**, 1573 (1964).
62. M. N. Hughes, H. G. Nicklin and K. Shrimanker, *J. Chem. Soc. A*, 3485 (1971).
63. P. Astolfi, P. Brandi, C. Galli, P. Gentili, M. F. Gerini, L. Greci and O. Lanzalunga, *New J. Chem.*, **29**, 1308 (2005).
64. D. A. Dixon, J. S. Francisco and Y. Alexeev, *J. Phys. Chem. A*, **110**, 185 (2006).
65. L. R. Mahoney, G. D. Mendenhall and K. U. Ingold, *J. Am. Chem. Soc.*, **95**, 8610 (1973).
66. F. G. Bordwell and W.-Z. Liu, *J. Am. Chem. Soc.*, **118**, 10819 (1996).
67. P. Mulder, H.-G. Korth, D. A. Pratt, G. A. DiLabio, L. Valgimigli, G. F. Pedulli and K. U. Ingold, *J. Phys. Chem. A*, **109**, 2647 (2005).
68. F. Minisci, C. Punta and F. Recupero, *J. Mol. Catal. A: Chem.*, **251**, 129 (2006).
69. G. Cantarella, C. Galli and P. Gentili, *New J. Chem.*, **28**, 366 (2004).
70. I. Koppel, J. Koppel, I. Leito, V. Pihl, L. Grehn and U. Ragnarsson, *J. Chem. Res. (S)*, 446 (1993).
71. W. van Scheppingen, E. Dorrestijn, I. Arends, P. Mulder and H.-G. Korth, *J. Phys. Chem. A*, **101**, 5404 (1997).
72. J. S. Wright, D. J. Carpenter, D. J. McKay and K. U. Ingold, *J. Am. Chem. Soc.*, **119**, 4245 (1997).
73. Z. B. Alfassi (Ed.), *General Aspects of the Chemistry of Radicals*, in the series *The Chemistry of Free Radicals*, Wiley, Chichester, 1999.
74. J. M. Bobbitt and M. C. L. Flores, *Heterocycles*, **27**, 509 (1988).
75. S. D. Rychnovsky, R. Vaidyanathan, T. Beauchamp, R. Lin and P. J. Farmer, *J. Org. Chem.*, **64**, 6745 (1999).
76. A. E. J. de Nooy, A. C. Besemer and H. van Bekkum, *Synthesis*, 1153 (1996).
77. M. Yamaguchi, T. Miyazawa, T. Takata and T. Endo, *Pure Appl. Chem.*, **62**, 217 (1990).
78. A. De Mico, R. Margarita, L. Parlanti, A. Vescovi and G. Piancatelli, *J. Org. Chem.*, **62**, 6974 (1997).
79. M. F. Semmelhack, C. R. Schmid, D. A. Cortes and C. S. Chou, *J. Am. Chem. Soc.*, **106**, 3374 (1984).
80. A. Cecchetto, F. Fontana, F. Minisci and F. Recupero, *Tetrahedron Lett.*, **42**, 6651 (2001).
81. M. Fabbrini, C. Galli, P. Gentili and D. Macchitella, *Tetrahedron Lett.*, **42**, 7551 (2001).
82. J. A. Cella, J. A. Kelley and E. F. Kenehan, *Tetrahedron Lett.*, 2869 (1975).
83. J. M. Bobbit, M. C. Flores, M. Zhenkum and T. Huitong, *Heterocycles*, **30**, 1131 (1990).
84. T. Breton, G. Bashiardes, J.-M. Léger and K. B. Kokoh, *Eur. J. Org. Chem.*, 1567 (2007).
85. Y.-R. Luo, *Handbook of Bond Dissociation Energies in Organic Compounds*, CRC Press, Boca Raton, 2003.
86. T. Doba and K. U. Ingold, *J. Am. Chem. Soc.*, **106**, 3958 (1984).
87. I. A. Opeida, A. G. Matvienko and O. Z. Ostrovskaya, *Kinet. Catal.*, **36**, 441 (1995).
88. C. Aliaga, D. R. Stuart, A. Aspée and J. C. Scaiano, *Org. Lett.*, **7**, 3665 (2005).
89. A. L. J. Beckwith, V. W. Bowry and K. U. Ingold, *J. Am. Chem. Soc.*, **114**, 4983 (1992).
90. R. Amorati, M. Lucarini, V. Mugnaini, G. F. Pedulli, F. Minisci, F. Recupero, F. Fontana, P. Astolfi and L. Greci, *J. Org. Chem.*, **68**, 1747 (2003).

91. I. W. C. E. Arends, P. Mulder, K. B. Clark and D. D. M. Wayner, *J. Phys. Chem.*, **99**, 8182 (1995).
92. B. Koch and W. Steglich, *Eur. J. Org. Chem.*, 1631 (2007).
93. N. V. Lebedeva, D. P. Zubenko, E. G. Bagryanskaya, R. Z. Sagdeev, G. S. Ananchenko, S. Marque, D. Bertin and P. Tordo, *Phys. Chem. Chem. Phys.*, **6**, 2254 (2004).
94. E. Damiani, P. Carloni, M. Iacussi, P. Stipa and L. Greci, *Eur. J. Org. Chem.*, 2405 (1999).
95. A. L. J. Beckwith and J. S. Poole, *J. Am. Chem. Soc.*, **124**, 9489 (2002).
96. G. Ananchenko and H. Fischer, *J. Chem. Soc., Perkin Trans. 2*, 1887 (2001).
97. L. Marx, R. Chiarelli, T. Guiberteau and A. Rassat, *J. Chem. Soc., Perkin Trans. 1*, 1181 (2000).
98. A. Alberti, P. Carloni, L. Eberson, L. Greci and P. Stipa, *J. Chem. Soc., Perkin Trans. 2*, 887 (1997).
99. L. Eberson, *J. Chem. Soc., Perkin Trans. 2*, 1865 (1999).
100. T. T. Tidwell and M. H. Fenwick, *Eur. J. Org. Chem.*, 3415 (2001).
101. S. Coseri, G. D. Mendenhall and K. U. Ingold, *J. Org. Chem.*, **70**, 4629 (2005).
102. H. A. Göttinger, V. E. Zubarev and O. Brede, *J. Chem. Soc., Perkin Trans. 2*, 2167 (1997).
103. L. Eberson, *Acta Chem. Scand.*, **53**, 584 (1999).
104. E. Sartori, A. Toffoletti, C. Corvaja, L. Garlaschelli, M. Maggini and G. Scorrano, *Chem. Commun.*, 311 (2001).
105. R. Owenius, G. E. Terry, M. J. Williams, S. S. Eaton and G. R. Eaton, *J. Phys. Chem. B*, **108**, 9475 (2004).
106. G. M. Rosen, A. Beselman, P. Tsai, S. Pou, C. Mailer, K. Ichikawa, B. H. Robinson, R. Nielsen, H. J. Halpern and A. D. MacKerell, *J. Org. Chem.*, **69**, 1321 (2004).
107. I. El Hassan, R. Lauricella and B. Tuccio, *Mendeleev Commun.*, 149 (2006).
108. H. Utsumi, K. Yamada, K. Ichikawa, K. Sakai, Y. Kinoshita, S. Matsumoto and M. Nagai, *Proc. Natl. Acad. Sci. U.S.A.*, **103**, 1463 (2006).
109. C. Mathieu, B. Tuccio, R. Lauricella, A. Mercier and P. Tordo, *J. Chem. Soc., Perkin Trans. 2*, 2501 (1997).
110. C. Rizzi, C. Mathieu, B. Tuccio, R. Lauricella, J.-C. Bouteiller and P. Tordo, *J. Chem. Soc., Perkin Trans. 2*, 2777 (1999).
111. M. Aso, T. Ikeno, K. Norihisa, M. Tanaka, N. Koga and H. Suemune, *J. Org. Chem.*, **66**, 3513 (2001).
112. K. D. Welch, T. Z. Davis and S. D. Aust, *Arch. Biochem. Biophys.*, **397**, 360 (2002).
113. H. Utsumi and K. Yamada, *Arch. Biochem. Biophys.*, **416**, 1 (2003).
114. S. Shimakawa, Y. Yoshida and E. Niki, *Lipids*, **38**, 225 (2003).
115. I. Koshiishi, K. Tsuchida, T. Takajo and M. Komatsu, *J. Lipid Res.*, **46**, 2506 (2005).
116. M. Lucarini, P. Pedrielli, G. F. Pedulli, L. Valgimigli, D. Gigmes and P. Tordo, *J. Am. Chem. Soc.*, **121**, 11546 (1999).
117. G. Brigati, M. Lucarini, V. Mugnain and G. F. Pedulli, *J. Org. Chem.*, **67**, 4828 (2002).
118. T. Iwahama, Y. Yoshino, T. Keitoku, S. Sakaguchi and Y. Ishii, *J. Org. Chem.*, **65**, 6502 (2000).
119. F. Minisci, C. Punta, F. Recupero, F. Fontana and G. F. Pedulli, *Chem. Commun.*, 688 (2002).
120. M. Masui, T. Ueshima and S. Ozaki, *J. Chem. Soc., Chem. Commun.*, 479 (1983).
121. S. Kishioka and A. Yamada, *J. Electroanal. Chem.*, **578**, 71 (2005).
122. S. Ozaki and M. Masui, *Chem. Pharm. Bull.*, **25**, 1179 (1977).
123. Y. Cai, N. Koshino, B. Saha and J. H. Espenson, *J. Org. Chem.*, **70**, 238 (2005).
124. N. Koshino, Y. Cai and J. H. Espenson, *J. Phys. Chem. A*, **107**, 4262 (2003).
125. Y. Ishii, T. Iwahama, S. Sakaguchi, K. Nakayama and Y. Nishiyama, *J. Org. Chem.*, **61**, 4520 (1996).
126. Y. Ishii, S. Sakaguchi and T. Iwahama, *Adv. Synth. Catal.*, **343**, 393 (2001).
127. F. Minisci, C. Punta, F. Recupero, F. Fontana and G. F. Pedulli, *J. Org. Chem.*, **67**, 2671 (2002).
128. F. Minisci, F. Recupero, G. F. Pedulli and M. Lucarini, *J. Mol. Catal. A: Chem.*, **204–205**, 63 (2003).
129. F. Minisci, F. Recupero, A. Cecchetto, C. Gambarotti, C. Punta, R. Faletti, R. Paganelli and G. F. Pedulli, *Eur. J. Org. Chem.*, 109 (2004).
130. B. Saha, N. Koshino and J. H. Espenson, *J. Phys. Chem. A*, **108**, 425 (2004).

131. A. Pross, *Theoretical & Physical Principles of Organic Reactivity*, Wiley-Interscience, New York, 1995.
132. B. P. Roberts, *Chem. Soc. Rev.*, **28**, 25 (1999).
133. S. Coseri, *Eur. J. Org. Chem.*, 1725 (2007).
134. P. Brandi, C. Galli and P. Gentili, *J. Org. Chem.*, **70**, 9521 (2005).
135. M. Fabbrini, C. Galli and P. Gentili, *J. Mol. Catal. B: Enzym.*, **16**, 231 (2002).
136. F. d'Acunzo, P. Baiocco, M. Fabbrini, C. Galli and P. Gentili, *New J. Chem.*, **26**, 1791 (2002).
137. E. Baciocchi, F. d'Acunzo, C. Galli and O. Lanzalunga, *J. Chem. Soc., Perkin Trans. 2*, 133 (1996).
138. G. A. Russell and C. De Boer, *J. Am. Chem. Soc.*, **85**, 3130 (1963).
139. C. M. Paleos and P. Dais, *J. Chem. Soc., Chem. Commun.*, 345 (1977).
140. T. D. Lee and J. F. W. Keana, *J. Org. Chem.*, **40**, 3145 (1975).
141. J. C. Suatoni, R. E. Snyder and R. O. Clark, *Anal. Chem.*, **33**, 1894 (1961).
142. E. Baciocchi, M. Bietti, M. F. Gerini and O. Lanzalunga, *J. Org. Chem.*, **70**, 5144 (2005).
143. B. Branchi, C. Galli and P. Gentili, *Org. Biomol. Chem.*, **3**, 2604 (2005).
144. E. Baciocchi, O. Lanzalunga and M. F. Gerini, *J. Org. Chem.*, **69**, 8963 (2004).
145. J. M. Mayer, D. A. Hrovat, J. L. Thomas and W. T. Borden, *J. Am. Chem. Soc.*, **124**, 11142 (2002).
146. J. M. Mayer, *Annu. Rev. Phys. Chem.*, **55**, 363 (2004).
147. E. Baciocchi, M. Bietti, M. Di Fusco and O. Lanzalunga, *J. Org. Chem.*, **72**, 8748 (2007).
148. F. Xu, H.-J. W. Deussen, B. Lopez, L. Lam and K. Li, *Eur. J. Biochem.*, **268**, 4169 (2001).
149. F. Xu, J. J. Kulys, K. Duke, K. Li, K. Krikstopaitis, H.-J. W. Deussen, E. Abbate, V. Galinyte and P. Schneider, *Appl. Environ. Microbiol.*, **66**, 2052 (2000).
150. A. Messerschmidt, *Multi-Copper Oxidases*, World Scientific, Singapore, 1997.
151. E. I. Solomon, U. M. Sundaram and T. E. Machonkin, *Chem. Rev.*, **96**, 2563 (1996).
152. C. Bukh, M. Lund and M. J. Bjerrum, *J. Inorg. Biochem.*, **100**, 1547 (2006).
153. F. Xu, A. E. Palmer, D. S. Yaver, R. M. Berka, G. A. Gambetta, S. H. Brown and E. I. Solomon, *J. Biol. Chem.*, **274**, 12372 (1999).
154. R. Bourbonnais and M. G. Paice, *FEBS Lett.*, **267**, 99 (1990).
155. K. Li, F. Xu and K. E. L. Eriksson, *Appl. Environ. Microbiol.*, **65**, 2654 (1999).
156. C. Galli and P. Gentili, *J. Phys. Org. Chem.*, **17**, 973 (2004).
157. J. Kulys, H.-J. Deussen, K. Krikstopaitis, R. Lolck, P. Schneider and A. Ziemys, *Eur. J. Org. Chem.*, 3475 (2001).
158. P. Baiocco, A. M. Barreca, M. Fabbrini, C. Galli and P. Gentili, *Org. Biomol. Chem.*, **1**, 191 (2003).
159. For a recent review, see: *Adv. Synth. Catal.*, **346** (Special Issue: Oxidations), 107–375 (2004).
160. S. Riva, *Trends Biotechnol.*, **24**, 219 (2006).
161. R. A. Sheldon, I. W. C. E. Arends, G.-J. Ten Brink and A. Dijksman, *Acc. Chem. Res.*, **35**, 774 (2002).
162. A. Dijksman, I. W. C. E. Arends and R. A. Sheldon, *Org. Biomol. Chem.*, **1**, 3232 (2003).
163. R. A. Sheldon and I. W. C. E. Arends, *J. Mol. Catal. A: Chem.*, **251**, 200 (2006).
164. M. F. Semmelhack, C. R. Schmid and D. A. Cortes, *Tetrahedron Lett.*, **27**, 1119 (1986).
165. Y. Wang, J. L. DuBois, B. Hedman, K. O. Hodgson and T. D. P. Stack, *Science*, **279**, 537 (1998).
166. M. M. Whittaker and J. M. Whittaker, *Biochemistry*, **40**, 7140 (2001).
167. A. Dijksman, A. Marino-Gonzalez, A. Mairata i Payeras, I. W. C. E. Arends and R. A. Sheldon, *J. Am. Chem. Soc.*, **123**, 6826 (2001).
168. F. d'Acunzo, P. Baiocco, M. Fabbrini, C. Galli and P. Gentili, *Eur. J. Org. Chem.*, 4195 (2002).
169. L. L. Simandi, *Dioxygen Activation and Homogeneous Catalytic Oxidations*, Elsevier, Amsterdam, 1991.
170. D. H. R. Barton, A. E. Martell and D. T. Sawyer (Eds.), *The Activation of Dioxygen and Homogeneous Catalytic Oxidations*, Plenum Press, New York, 1993.
171. W. Adam, C. R. Saha-Möller and P. A. Ganeshpure, *Chem. Rev.*, **101**, 3499 (2001).
172. J. B. Arterburn, *Tetrahedron*, **57**, 9765 (2001).
173. R. A. Sheldon and I. W. C. E. Arends, *Adv. Synth. Catal.*, **346**, 1051 (2004).
174. Y. Ishii, K. Nakayama, M. Takeno, S. Sakaguchi, T. Iwahama and Y. Nishiyama, *J. Org. Chem.*, **60**, 3934 (1995).

175. Y. Ishii and S. Sakaguchi, Chap. 5, in *Modern Oxidation Methods* (Ed. J.-E. Bäckvall), Wiley-VCH, Weinheim, 2004, p. 119.
176. S. Sakaguchi, M. Eikawa and Y. Ishii, *Tetrahedron Lett.*, **38**, 7075 (1997).
177. I. W. C. E. Arends, M. Sasidharan, A. Kühnle, M. Duda, C. Jost and R. A. Sheldon, *Tetrahedron*, **58**, 9055 (2002).
178. X. Baucherel, L. Gonsalvi, I. W. C. E. Arends, S. Ellwood and R. A. Sheldon, *Adv. Synth. Catal.*, **346**, 286 (2004).
179. K. Gorgy, J.-C. Lepretre, E. Saint-Aman, C. Einhorn, J. Einhorn, C. Marcadal and J.-L. Pierre, *Electrochim. Acta*, **44**, 385 (1998).
180. Z. Ma and J. M. Bobbitt, *J. Org. Chem.*, **56**, 6110 (1991).
181. P. L. Anelli, C. Biffi, F. Montanari and S. Quici, *J. Org. Chem.*, **52**, 2559 (1987).
182. P. L. Anelli, F. Montanari and S. Quici, *J. Org. Chem.*, **54**, 2970 (1989).
183. P. L. Anelli, F. Montanari and S. Quici, *Org. Synth.*, **69**, 212 (1990); in Coll. Vol. VIII, 367 (1993).
184. T. Fey, H. Fischer, S. Bachmann, K. Albert and C. Bolm, *J. Org. Chem.*, **66**, 8154 (2001).
185. J. Einhorn, C. Einhorn, F. Ratajczak and J.-L. Pierre, *J. Org. Chem.*, **61**, 7452 (1996).
186. B. Ganem, *J. Org. Chem.*, **40**, 1998 (1975).
187. J. A. Cella, J. A. Kelley and E. F. Kenehan, *J. Org. Chem.*, **40**, 1860 (1975).
188. P. L. Bragd, A. C. Besemer and H. van Bekkum, *J. Mol. Catal. A: Chem.*, **170**, 35 (2001).
189. A. Isogai, C. Kitaoka and F. Onabe, *J. Pulp Paper Sci.*, **23**, J215 (1997); *Chem. Abstr.*, **126**, 306465 (1997).
190. T. Breton, G. Bashiardes, J.-M. Léger and K. B. Kokoh, *Eur. J. Org. Chem.*, 1567 (2007).
191. R. Neumann, Chap. 8, in *Modern Oxidation Methods* (Ed. J.-E. Bäckvall), Wiley-VCH, Weinheim, 2004, p. 223.
192. R. Ben-Daniel, P. Alsters and R. Neumann, *J. Org. Chem.*, **66**, 8650 (2001).
193. M. F. Semmelhack, C. S. Chou and D. A. Cortes, *J. Am. Chem. Soc.*, **105**, 4492 (1983).
194. M. F. Semmelhack and C. R. Schmid, *J. Am. Chem. Soc.*, **105**, 6732 (1983).
195. M. F. Semmelhack, C. R. Schmid and D. A. Cortes, *Tetrahedron Lett.*, **27**, 1119 (1986).
196. M. Shibuya, M. Tomizawa, I. Suzuki and Y. Iwabuchi, *J. Am. Chem. Soc.*, **128**, 8412 (2006).
197. P. Ferreira, E. Phillips, D. Rippon, S. C. Tsang and W. Hayes, *J. Org. Chem.*, **69**, 6851 (2004).
198. D. Brunel, F. Fajula, J. B. Nagy, B. Deroide, M. J. Verhoef, L. Veum, J. A. Peters and H. van Bekkum, *Appl. Catal. A: General*, **213**, 73 (2001).
199. D. J. Vugts, L. Veum, K. Al-Mafraji, R. Lemmens, R. F. Schmitz, F. J. J. de Kanter, M. B. Groen, U. Hanefeld and R. V. A. Orru, *Eur. J. Org. Chem.*, 1672 (2006).
200. S. D. Rychnovsky, T. L. McLernon and H. Rajapakse, *J. Org. Chem.*, **61**, 1194 (1996).
201. (a) N. Wang, R. Liu, J. Chen and X. Liang, *Chem. Commun.*, 5322 (2005).
(b) Y. Xie, W. Mo, D. Xu, Z. Shen, N. Sun, B. Hu and X. Hu, *J. Org. Chem.*, **72**, 4288 (2007).
202. R. Liu, X. Liang, C. Dong and X. Hu, *J. Am. Chem. Soc.*, **126**, 4112 (2004).
203. F. d'Acunzo, P. Baiocco and C. Galli, *New J. Chem.*, **27**, 329 (2003).
204. G. Cantarella, C. Galli and P. Gentili, *J. Mol. Catal. B: Enzym.*, **22**, 135 (2003).
205. W. Kroutil, H. Mang, K. Edegger and K. Faber, *Adv. Synth. Catal.*, **346**, 125 (2004).
206. F. d'Acunzo, A. M. Barreca and C. Galli, *J. Mol. Catal. B: Enzym.*, **31**, 25 (2004).
207. M. Marzorati, B. Danieli, D. Haltrich and S. Riva, *Green Chem.*, **7**, 310 (2005).
208. L. Baratto, A. Candido, M. Marzorati, F. Sagui, S. Riva and B. Danieli, *J. Mol. Catal. B: Enzym.*, **39**, 3 (2006).
209. P. Brandi, C. Galli and P. Gentili, *J. Phys. Org. Chem.*, **19**, 552 (2006).
210. E. Fritz-Langhals and B. Kunath, *Tetrahedron Lett.*, **39**, 5955 (1998).
211. S. Böhmer, K. Messner and E. Srebotnik, *Biochem. Biophys. Res. Commun.*, **244**, 233 (1998).
212. M.-L. Niku-Paavola and L. Viikari, *J. Mol. Catal. B: Enzym.*, **10**, 435 (2000).
213. C. Johannes and A. Majcherczyk, *Appl. Environ. Microbiol.*, **66**, 524 (2000).
214. R. ten Have and P. J. M. Teunissen, *Chem. Rev.*, **101**, 3397 (2001).
215. T. Higuchi, *Biochemistry and Molecular Biology of Wood*, Springer-Verlag, London, 1997.
216. A. M. Barreca, M. Fabbrini, C. Galli, P. Gentili and S. Ljunggren, *J. Mol. Catal. B: Enzym.*, **26**, 105 (2003).
217. F. d'Acunzo, A. M. Barreca and C. Galli, *J. Mol. Catal. B: Enzym.*, **31**, 25 (2004).
218. S. Kawai, M. Nakagawa and H. Ohashi, *Enz. Microbiol. Technol.*, **30**, 482 (2002).

219. R. Bourbonnais, M. G. Paice, B. Freiermuth, E. Bodie and S. Borneman, *Appl. Environ. Microbiol.*, **63**, 4627 (1997).
220. K. Li, R. F. Helm and K. E. L. Eriksson, *Biotechnol. Appl. Biochem.*, **27**, 239 (1998).
221. C. Crestini and D. S. Argyropoulos, *Bioorg. Med. Chem.*, **6**, 2161 (1998).
222. S. Shleev, P. Persson, G. Shumakovich, Y. Mazhugo, A. Yaropolov, T. Ruzgas and L. Gorton, *Enz. Microbiol. Technol.*, **39**, 841 (2006).
223. C. Annunziatini, P. Baiocco, M. F. Gerini, O. Lanzalunga and B. Sjögren, *J. Mol. Catal. B: Enzym.*, **32**, 89 (2005).
224. A. M. Barreca, B. Sjögren, M. Fabbrini, C. Galli and P. Gentili, *Biocatal. Biotransfor.*, **22**, 105 (2004).
225. X. Geng, K. Li and F. Xu, *Appl. Microbiol. Biotechnol.*, **64**, 493 (2004).
226. J. Sealey, A. J. Ragauskas and T. J. Elder, *Holzforschung*, **53**, 498 (1999); *Chem. Abstr.*, **131**, 287899 (1999).

CHAPTER **16**

Natural and biomimetic hydroxamic acid based siderophores

ABRAHAM SHANZER, CLIFFORD E. FELDER and YANIV BARDA

Department of Organic Chemistry, Weizmann Institute of Science, P.O. Box 26, Rehovot 76100, Israel
Fax: +972-8-9342917; e-mail: abraham.shanzer@weizmann.ac.il, clifford.felder@weizmann.ac.il and yaniv.barda@weizmann.ac.il

The chemistry of hydroxylamines, oximes and hydroxamic acids
Edited by Z. Rappoport and J. F. Liebman

I. INTRODUCTION

Siderophores (Greek for iron bearers) are low molecular weight, iron-chelating molecules secreted by microorganisms to extract and internalize scarce ferric ions with high affinity and specificity from their environment. The intricate mechanisms operating in microbial iron-transport include various iron-carriers, their receptors and numerous additional proteins acting in concert. The role of the various proteins involved in microbial Fe(III) metabolism has been established by applying the tools of molecular biology[1–5]. However, the structural requirements for recognition of iron-carriers by the membrane receptors and the nature of the interactions between the siderophores and the receptor proteins are much less understood. Successes in this area have been achieved by numerous, well-defined synthetic model compounds, frequently designed by the use of biomimetic approaches. Many model compounds showed bioactivity in mimicking iron(III) transport into microbial cells and inducing growth and proliferation, while others, frequently very closely related structures, were either able to recognize the target receptors, but failed to transport iron(III) into the cells, or were completely inactive. A comparison between the various analogs led to the deduction of key factors essential for recognition and transport.

The recently resolved X-ray structures of several siderophore receptors with and without their natural siderophores, from *Escherichia coli* and *Pseudomonas aeruginosa*, allows one to pinpoint with atomic resolution some of the previously hypothesized interactions derived from model studies but could not be quantified and exposed new interactions not identified previously. In addition, X-ray structures, although limited in numbers, provided an ideal 'sounding board' for theoretical docking studies to identify potential improved model compounds prior to their synthesis. As the number of 3-dimensional receptor-siderophore structures from different microorganisms will increase, examining their interaction with biomimetic analogs is expected to shed light not only on siderophore-receptor recognition, but also on the yet unknown mechanism of siderophores transported across the receptors. Site-specific mutational studies to resolve the transport mechanism have recently been addressed[6].

For a comprehensive review of current knowledge of this field of microbial iron metabolism and possible therapeutic applications of siderophores, the reader should consult some recent, excellent books[7–12] and reviews[13–20].

The high specificity of siderophore iron coordination has been extensively explored in iron-chelation therapy for various medical applications, including iron overload diseases[21], control of iron in specific brain tissues[22,23], arresting the growth and proliferation of malaria parasite within their host[24,25], as well as arresting the proliferation of cancer cells[26]. Other directions for metal ligation involve enzyme inhibition, which have been demonstrated by the inhibition of urease by coordination of hydroxamate ligand to nickel ions[27] and zinc coordination in matrix metalloprotease (MMP) inhibition by primary hydroxamates[28].

Natural siderophores are primarily hexadentate chelators composed of bidentate ligands such as hydroxamates, catecholates or both, that form complexes of the tris-bidentate type, with a high affinity for iron(III) ions. In this review we focus on the principal design of simplified biomimetic hydroxamate siderophore analogs as selective iron-carriers. Model compounds that can be fine-tuned to target specific iron-uptake receptors, either as growth promoters or inhibitors, provide integrated probes capable of tracing iron-uptake routes for microbial identification and diagnostics, as well as potential delivery systems for drugs or toxic substances addressing essential cellular targets for antimicrobial therapeutics. Special attention will be devoted to identify structural and functional motifs governing receptor-substrate recognition and transport events.

II. PHYSICAL AND CHEMICAL PROPERTIES OF HYDROXAMATE-BASED SIDEROPHORES

The physical and coordination chemistry of hydroxamate-based iron chelators, their thermodynamic, kinetic, structural, spectroscopic and surface properties, have been extensively reviewed[29–36]. Therefore, only selective aspects that are relevant for the design of biomimetic siderophore analogs will be discussed.

A. Ligands and Chelators and Their Iron(III) Complexes

The majority of natural siderophores are hexadentate chelators, frequently constructed from three bidentate ligands arranged in different topologies. Upon iron(III) binding they show many similarities in complex characteristics, electronic configuration and preferential selectivity for iron(III). The two most common ferric ligating groups, i.e. catecholates (as catecholic acid derivatives) and hydroxamates, possess several chemical properties that make them particularly suitable as microbial iron-carriers. They are small, hydrophilic and intrinsically unsymmetrical. Hydroxamates and catecholates form five-membered chelation rings through charged oxygen-donor atoms, hard Lewis bases with high affinity for hard Lewis acids like the small and highly charged ferric ion (in contrast to the soft ferrous ion with affinity for polarizable ligands, such as nitrogen). Coordination of siderophores with Fe(III) leads to the formation of thermodynamically stable ferri-siderophore complexes with high-spin ferric ion. Since high-spin d^5 configuration is spherically symmetric and has no crystal-field stabilization energy, the energy in forming stable complexes is obtained from columbic interactions between the positively charged iron(III) and the negatively charged oxygen atoms. The geometry of iron(III) complexes results from a delicate balance between electrical attraction and repulsion, and can therefore deviate substantially from perfect octahedral geometry, depending on the structural and electronic effects originating from the chelators. It is also the origin for the high selectivity of the siderophores toward ferric ions with respect to other triply charged metal ions. Fe(III) is a

harder Lewis acid than the much more abundant Al(III), with greater electronegativity and stronger affinity for OH^-. The smaller size of Al(III) compared to Fe(III) increases the electronic repulsion between the oxygen ligating atoms and consequently decreases the Al(III)-siderophore complex stability and effectively increases the thermodynamic selectivity toward Fe(III)[34,35]. The binding to nonspherical transition metals such as Cu(II), Ni(II) and Zn(II) is much weaker and their hydroxamate complex stability decreases correspondingly.

In this chapter, we will concentrate mainly on hydroxamate-based siderophores. However, the most representative example of the catechol-based siderophore family is enterobactin[19], a highly C_3-symmetric molecule based on a trilactone ring system derived from three L-serine amino acids. The serine amino groups are extended with three catecholic acid units. Enterobactin binds iron(III) in an octahedral coordination of preferred Δ-*cis* configuration (see Figure 1 in Section II.C).

Hydroxamic acids are weak organic acids, where the mono-deprotonation of the N−OH group (pK_a *ca* 9 for the N−OH proton) forms the hydroxamate functional group. Hydroxamates may be described by several resonance structures; the most relevant are the two canonical forms presented in Scheme 1. In structure **(a)** all the negative charge is localized on one of the oxygens, whereas in form **(b)** the negative charge is distributed over both oxygen atoms. The metal coordination properties are governed by the nature of the substituents at R_C and R_N. Complex stability can be enhanced by an electron-donating group at R_C and R_N, as well as conjugation at R_C.

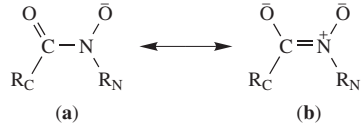

SCHEME 1. Two main resonance forms of hydroxamic acid based ligands

In contrast to the tris-catecholate siderophores, which form charged iron(III) complexes, the hydroxamate-based ferri-siderophore complexes are electrically neutral, which may influence their transport through biological membranes.

Since the hydroxamate group −N(OH)−CO is intrinsically unsymmetrical, its coordination characteristics do not change when positioned in the reverse direction −CO−N(OH) (in which the positions of the hydroxamate nitrogen and carbon are interchanged). The relationship between these different structures is referred to as retro-hydroxamate isomers. The 'retro' prefix is generally preserved for structures that are reversed to that of the naturally occurring structure.

Upon iron(III) binding, hydroxamate ligands can form both *fac* (*cis*) and *mer* (*trans*) isomers with a 3:1 molar ratio. In tripodal topology, when the hydroxamate bidentate ligands are covalently bound to a template, they form exclusively *fac* isomers; a second *fac* isomer is formed from the 'retro' isomer. The different isomers can exhibit minor changes in metal binding and solubility properties. In the linear topology, the bidentate hydroxamates are generally separated by a spacer and together they form a hexadentate chelator. Iron complexes, in this topology, depend on the chemical nature and the length of the spacers between the ligating groups. Long and extended spacers favor the formation of a large number of various combinations of geometrical as well as optical isomers (see Section V.C.1).

B. The Multiple Roles of the Siderophore Backbone

Like the geometry around the metal center, the geometry in the backbone can also be important in receptor recognition. This has been extensively probed by synthetic

analogs, for example in the case of enterobactin[37] and ferrichromes[38–41]. The backbone affects water solubility of the chelator and its complex, it dictates the intricate interactions with the receptor and, as will be demonstrated later, it also serves as a platform to carry task-oriented additional functional groups and asymmetric centers. To ensure water solubility, natural siderophores had to introduce backbone entities that adjust hydrophilic/hydrophobic balance to guarantee their complex solubility. They do so by introducing appropriate moieties to the siderophore backbone, e.g. the peptide template (as in ferrichrome) and amide bonds (as in ferrioxamine), or by introducing externally positioned carboxylic acid moieties as in aerobactin. This presents an elegant demonstration for the delicate interplay between function and structure. We will discuss this subject in further detail as we describe the design of biomimetic siderophore analogs. The free siderophores are more hydrophilic than their metal complexes due to the strong interaction of the acidic hydroxamic acid chelating unit with the highly charged iron(III). Metal complexation exposes the backbone toward interactions with the receptor. It is these interactions that determine the adjustability of the siderophores to a given receptor. The interactions are generally hydrogen bonding, consequently controlled by the distance and the angles between the proton-donor and the proton-acceptor and therefore very sensitive to a small deviation in siderophore structure.

In order to use the siderophores as targeting agents for task-oriented applications, it is essential to identify sites that do not interfere with iron chelation or receptor recognition, to which additional functional groups can be attached. In natural siderophores, sites suitable for substitution are rare. By preparing biomimetic analogs, such sites can be identified only by extensive trial and error attempts. Once identified, these sites may be utilized to bind various functional groups as fluorescent markers and surface adhesive functionalities for diagnostics, or for the incorporation of drugs or toxins to generate an antimicrobial delivery system for therapeutics.

C. Importance of Chiral Centers in Biomimetic Siderophores

Chelation of three bidentate ligands to ferric ions forms octahedral complexes in which the iron acts as an asymmetric center. Therefore, it is sufficient to form racemic mixtures of enantiomeric pairs with right-handed Δ-*cis* or left-handed Λ-*cis* configuration, e.g. two opposite helical twists about the iron center are possible (Figure 1, top). These structures are energetically indistinguishable and therefore equally populated. When a chiral center is introduced these become diastereomers (Figure 1, bottom) energetically nonequivalent, and therefore one configuration predominates. Since most receptors show stereospecificity for one helical twist over the other, only that diastereomer with the preferred handedness will be selected or bound. For example, the biologically active iron(III) complex of enterobactin assumes a right-handed Δ-configuration, that of ferrichrome a left-handed Λ-configuration, coprogen assumes a right-handed Δ-configuration and ferrioxamines lack chiral centers altogether. In an attempt to obtain enantiopure biomimetic siderophore–iron(III) complexes of specified Δ-(right-handed) or Λ-(left-handed) configuration, it is necessary to incorporate chiral centers into the synthetic analog, either as part of the template structure, the extending arms, or within the ligating functional groups.

III. IRON METABOLISM

Iron is an essential trace metal nutrient required by practically[42,43] all living organisms for a wide variety of fundamental cell functions ranging from oxygen metabolism and electron transfer processes to DNA and RNA synthesis[3,18,31,44,45].

In an oxidizing earth atmosphere, iron exists in its ferric state forming insoluble ferric hydroxide. Under aqueous aerobic conditions and neutral pH, the total concentration of

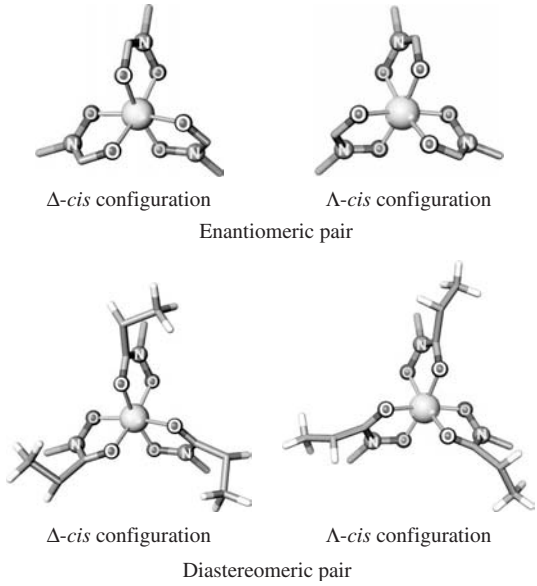

FIGURE 1. Schematic representation of octahedral coordination isomers. Top: two enantiomers formed by iron(III) complexation by a nonchiral chelator. Bottom: incorporation of chiral centers to the ligating groups generates two diastereomers

soluble iron is as low as 10^{-18} M[18,46]. Microorganisms, which need higher iron concentrations for optimal growth (*ca* 10^{-6} M)[4], developed specific mechanisms for iron uptake and accumulation to ensure growth and proliferation[20]. Yet, just as a shortage of iron is problematic, a surplus of iron induces oxidative damage[47] through the classical Fenton reaction[48], where iron(II) oxidizes H_2O_2, leading to the generation of hydroxyl radicals, which are highly cytotoxic.

$$Fe^{2+} + H_2O_2 \longrightarrow Fe^{3+} + {}^{\bullet}OH + {}^{-}OH$$

Hydroxyl radicals and other reactive oxygen species (ROS) cause oxidative damage to DNA and lipids, beyond the ability of cellular defense mechanisms to withstand[49].

A. Siderophores-mediated Iron Metabolism

To cope with their need for iron, microorganisms possess remarkably sophisticated mechanisms to scavenge iron from its plentiful, yet biologically inaccessible, environmental sources. Among the various mechanisms for iron uptake[2,50–56], the most general is the use of iron sequestering agents.

When deficient in iron, bacteria and fungi produce and excrete to the extracellular medium low molecular weight, specific iron-carrier molecules, called siderophores. These siderophores bind ferric ions, to form soluble complexes. The complexed ferric ions are transported into the cell through high-affinity and energy-dependent receptor proteins located on the outer membrane. In Gram-negative bacteria, such as *E. coli*, the most studied system, siderophore–iron complexes are transported initially to the periplasm.

The uptake of the chelated ferric ion through the cytoplasmic membrane depends on ATP-binding cassette (ABC) transporters. The energy for the transport is supplied by the TonB-ExbB-ExbD protein cluster, located on the cytoplasmatic membrane.

Once the siderophore–iron complexes are inside the bacteria, the iron is released and utilized for vital cell functions. The iron-free hydroxamate siderophores are commonly re-excreted to bring in an additional iron 'load' (Enterobactin is at least partially degraded by a cytoplasmic esterase[19, 57, 58]). This cycle is repeated until specific intracellular ferric uptake regulation proteins (Fur proteins)[59] bind iron, and signal that the intracellular iron level is satisfactory, at which point new siderophore and siderophore-receptor biosynthesis are halted and the iron-uptake process stops. This intricate feedback mechanism allows a meticulous control over iron(III) uptake and accumulation against an unfavorable concentration gradient so as to maintain the intracellular iron(III) level within the required narrow window. Several excellent reviews concerning siderophore–iron transport mechanisms have been recently published [1, 3, 16, 18, 40, 45, 60–62].

Each microorganism produces its own unique siderophore (endogenous siderophores) to be picked up by its specific transmembranal siderophore receptor. However, most microorganisms have additional membrane siderophore receptors, due to horizontal gene transfer, that enable them to exploit other microorganisms' siderophores (exogenous siderophores or xenosiderophores). For example, *E. coli* K-12 typically produces only the siderophore enterobactin, but has five different membrane receptors, namely FepA, FhuA, FhuE, FecA and IutA for recognizing enterobactin, ferrichrome, coprogen, ferric citrate and aerobactin, respectively[63].

The multiple iron transport systems exemplify not only microbial diversity in utilizing different ways of sequestering essential iron, but also provide an array of potential targets unique to each species that could be utilized, separately or in concert, for species-specific identification, for diagnosis or as targeting agents for drug delivery and therapeutics.

The several hundred natural siderophores that have been isolated and identified to date present a diversity of chemical compositions and topological arrangements. The majority can be classified according to their iron-binding ligating group into two main categories: catecholates and hydroxamates (Figure 2). Other iron ligating groups such as phenol oxazolines, phenol thiazolines, α- and β-hydroxy acids and α-keto acids are known to form mixed-type siderophores by integrating at least two distinctly different classes of ligating groups into a single molecule. Alternatively, the siderophores can be classified by the topological arrangements of the ligands, including tripodal (enterobactin and ferrichrome), macrocyclic (ferrioxamine G) and linear (ferrioxamine B and coprogen).

Regardless of their composition and topology, siderophores are generally hydrophilic species, although hydrophobic species in both marine siderophores[64] and some pathogenic bacteria[65, 66] have been isolated and identified. All siderophores function by a similar principle: They bind iron(III) effectively by embedding the metal into an octahedral binding cavity, thus generating a molecular 'envelope' that shields the iron, and complements the respective microbial outer-membrane receptor.

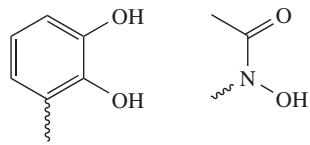

FIGURE 2. The most common iron(III) bidentate ligating groups: catechol and hydroxamic acid

IV. BIOMIMETIC CHEMISTRY

Biomimetic chemistry[67] represents a conceptual approach for a rational design of simplified model compounds that reproduce or imitate the function and biological activity of intricate natural compounds. The basic underlying principle is to reproduce the function of natural products without necessarily incorporating their full, detailed structures. The methodology of biomimetics design relies on identifying the minimal essential elements or components of a complex biochemical system, and incorporating these very features into the simplest possible synthetic molecular structures.

Biomimetic analogs can be utilized for understanding the correlation between structure and function, and identifying structural and functional motifs governing receptor-substrate recognition events. By analyzing the biological properties of different analogs, together with theoretical tools, key structural elements can be refined, leading to new synthetic siderophores with improved desired properties (e.g. selectivity, stability, solubility, permeability etc.). The biomimetic approach is a continuous iterative process in which each new generation of analogs profits from previous successes or failures alike, until an ultimate model is finally reached.

Model building with synthetic structures is a valuable method to examine biological phenomena at a molecular level and to deduce the underlying principles. Models can serve as 'sounding boards' to differentiate between the essential and the superfluous, between the understood and the still obscured. They enable systematic development of ever superior synthetic analogs.

A. Methodology

The biomimetic methodology involves several iterative steps: (i) A natural siderophore family is inspected, analyzed and divided into *functional* and *structural* domains. The relative locations and orientations of these essential components are then determined. (ii) These components are then incorporated into a highly modular, simplified chemical skeleton that allows considering several, closely related alternatives, which differ in linker size, the nature of the ligating group and sites for the incorporation of asymmetric centers and the location of additional side chains. (iii) Each of these possible alternatives is carefully analyzed for steric repulsions, structural strain and possible noncovalent interactions, in addition to computational analysis, searching for the lowest-energy conformations of the iron complex. (iv) The best model compounds are selected for synthesis. (v) Once prepared, the compounds are submitted for extensive chemical and biological testing, aimed at establishing their bioactivity, the nature of the receptor they target and species specificity. (vi) The results are evaluated, and the next series of compounds to be studied determined.

This stepwise approach helps in selecting from the many possible structures the most promising for synthesis, provides a coherent way to interpret the experimental findings and suggests improved structures for further reiteration processes.

B. Considerations in the Design of Biomimetic Siderophore Analogs

In the design of potential biomimetic analogs the following principles were followed:

1. *Modular design.* Synthetic molecules were constructed of multiple, closely related nonsymmetric repeat units that can be covalently attached from either end. This approach allows rational design of various congeners, controlling their physical properties, such as iron-binding capacities and partition coefficients (lipophilic/hydrophilic

ratios), increases structural diversity in building-up structures with gradually increased complexity, as well as their structural adjustability to specific receptors and simplified synthesis. It also facilitates the theoretical conformational scanning and allows rapid examination of a variety of related structures.

2. *Simplicity.* The simplest building blocks suitable for the given task can be efficiently condensed within themselves or with related building units with complementary functionalities, leading to complex structures, analogous to fragment condensation in peptide synthesis[68].
3. *Symmetry.* Symmetry is not an essential property, but contributes greatly to the economy of effort, both in the synthesis and in the interpretation of the observed properties of the products. Structures possessing C_3-rotational symmetry facilitate a symmetric arrangement of the ligating groups, favoring a less distorted octahedral coordination geometry that should bind iron with greater affinity, and also facilitates conformational scanning and energy minimization by symmetry constraint.
4. *Chirality.* Asymmetric centers were generally introduced by incorporating amino acid residues as variable building blocks, enabling systematic modification of the molecule's envelope by varying the side chains of the amino acid residues and imparting chiral preference of choice by using either L- or D-amino acids. These defined conformational handednesses of the iron complexes have been demonstrated to be critical for chiral discrimination of siderophore receptors[3,69,70]. In this chapter, the three-letter symbols for the 22 proteinogenic amino acids are used according to the IUPAC-IUB conventions[71,72]. To discriminate between natural amino acids and their enantiomers, lowercase letters are used for D-amino acids.
5. *Fast testing.* Assessing biomimetic analogs with live bacteria provides fast screening to establish transport and microbial growth, allows identifying receptor involvement and species specificity. The large variety of transmembranal receptors for siderophore–iron (III) complexes present in the outer membranes of microorganisms provides a versatile bioassay to probe receptor–complex interactions.
6. *Theoretical computations.* Molecular mechanical force-field calculations were carried out using the Empirical Force Field method (EFF)[73,74]. These calculations were performed on a routine basis: (i) in the design, to help in selecting the most appropriate candidates for synthesis, (ii) in result analysis, to aid in constructing a coherent picture from spectroscopic data and biological results and (iii) in reiteration, planning the next generation of compounds to be prepared.

Symmetric molecules with short strand between the ligating groups facilitated rapid calculations and easy comparison of a number of related structures[75]. Together with extensive spectroscopic analysis including NMR, IR, UV and CD measurements, they allowed the determination of the preferred sense of helical twist about the iron, left- or right-handed.

V. NATURAL AND BIOMIMETIC HYDROXAMIC ACID BASED SIDEROPHORES

A. The Major Hydroxamate Siderophore Families and Their Analogs

The hydroxamate-based siderophores discussed in this review represent a large and structurally diversified family (cyclic, tripodal and linear structures). This family includes (i) trihydroxamate siderophores, forming electrically neutral octahedral iron complexes, (ii) mixed siderophores, integrating at least two distinctly different classes of ligating groups, thus forming octahedral complexes of varying net charges, and (iii) dihydroxamate siderophores forming binuclear iron complexes with a 3:2 ligand-to-metal ratio. The most common siderophores are hexadentate chelators, generally as a tris-bidentate ligand,

optimally arranged in an octahedral geometry around the ferric ion. Many of these siderophores have been reviewed in the past[32,76,77]. Representative examples of hydroxamate-based siderophores are illustrated in Figure 3.

The only clinically approved and therefore most studied natural siderophore is desferrioxamine B (DFO), and hence it serves as a reference compound in evaluating new biomimetic siderophores. The following discussion will include a short description of several natural hydroxamate siderophore families in separate tables, followed by the various attempts to prepare novel simplified structures that reproduce biological activity. These tables are not intended to cover the entire archive of known siderophores, but merely to allow the reader to observe structural variations, their chemical composition and location as well as conserved domains.

B. The Ferrichrome Family

1. Natural ferrichromes

Ferrichrome was the first siderophore to be isolated and characterized from the fungi *Ustilago sphaerogena* in 1952[78]. It is a cyclic hexapeptide with the sequence *cyclo*[$(Gly)_3$-(N^{δ}-acetyl-N^{δ}-hydroxy-L-ornithine)$_3$] (**1**)[79]. The biologically active ferrichromes form iron(III) complexes with a left-handed Λ-*cis* helical twist.

Structurally, ferrichrome is composed of a hexapeptide ring nonsymmetrically substituted by three identical side chains each bearing a bidentate hydroxamate group. In this structure, the hexapeptide serves as a template or platform, while the three side chains create the octahedral cavity suitable for binding iron(III). Over the years, variant forms of ferrichrome have been isolated and their structure elucidated (Table 1). The cyclic hexapeptide may contain different combinations of glycine, alanine and serine residues as occur in the ferrichrome siderophore analog ferrichrome C **2**, ferricrocin **5** or ferrichrysin **6**. These are the main exogenous sites available in the natural ferrichrome family for chemical modifications. Indeed, these sites have been utilized for the preparation of ferrichrome-drug conjugates[80]. The acetyl hydroxamate moiety, terminating each of the side arms, is considered conserved, although variations have been observed (structures **3**, **4** and **7**–**13** in Table 1). These variations are less common and are important in receptor recognition of selected strains and therefore less attractive for incorporation in biomimetic models.

Since siderophore receptors, being membrane-bound, are hard to crystallize, there are to date few structures in the Protein Data Bank (PDB). One such structure is the *E. coli* FhuA entries 1by5[81], with and without ferrichrome, 1fcp and 2fcp[82], respectively[83].

The FhuA receptor, composed of a β-barrel and *N*-terminal globular domains, serves as a 'cork' that plugs the barrel, separating the receptor's interior space into inner and outer cavities. The ferrichrome complex forms hydrogen bonding and van der Waals interactions with the outer cavity.

It is beyond the scope of this review to describe in detail the structure and interactions that take place between the FhuA receptor and the ferrichrome siderophore. Nevertheless, a brief summery may explain some of the biological ambiguities in which closely related synthetic analogs exhibit totally different microbial uptake characteristics[84]. The X-ray study of ferrichrome in the FhuA[81,82] showed two types of interactions between ferrichrome and its receptor: one set of interactions is directed to the oxygens at the iron–hydroxamate binding site (first coordination sphere), and these interactions are expected to be sensitive to stereochemical discrimination, while a second set of interactions is directed to several amide groups on the ferrichrome peptide backbone ring (second coordination sphere). It is therefore not surprising that synthetic ferrichrome analogs that do not possess amide groups or related functional groups on their arms

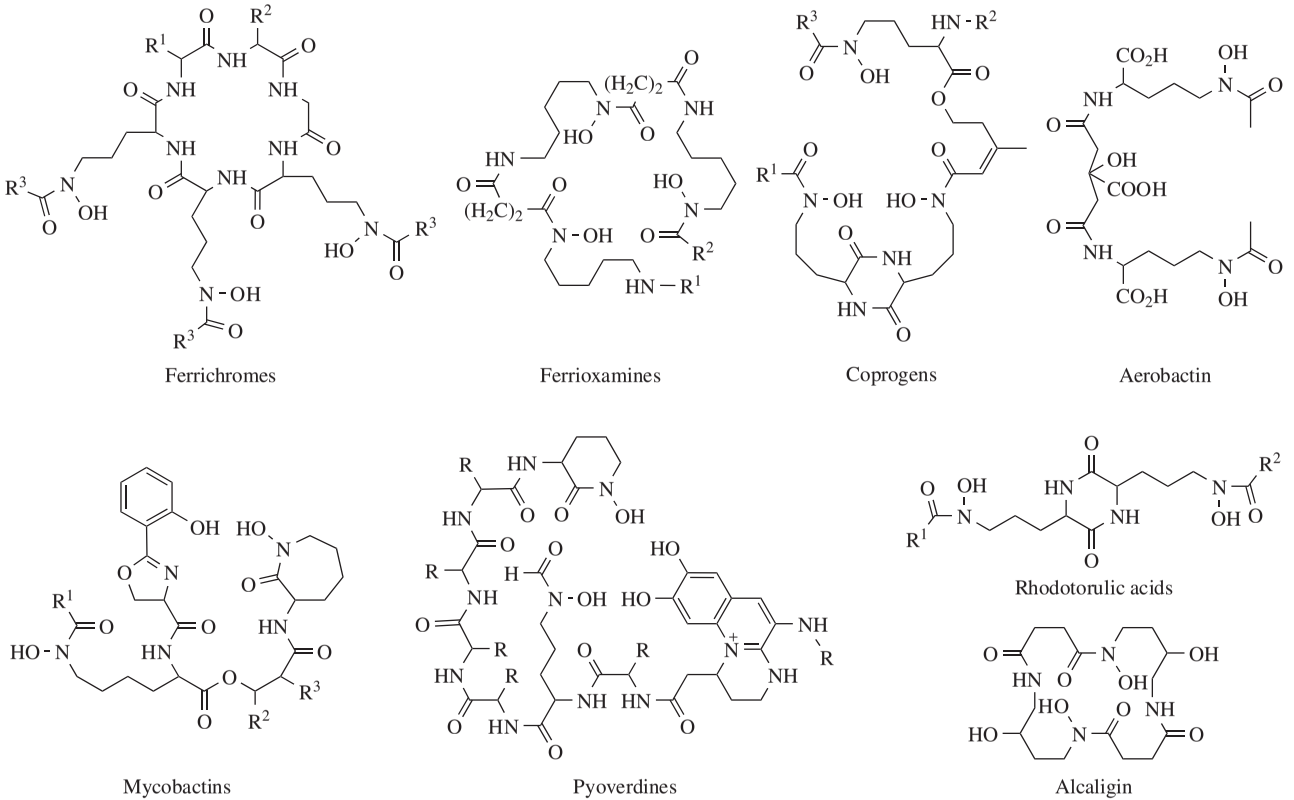

FIGURE 3. Selected examples of natural siderophores based on hydroxamic acid. Siderophores containing three hydroxamate groups (Ferrichromes, ferrioxamines and coprogens). Mixed siderophores, utilizing different iron-binding groups (Aerobactin, mycobactins and pyoverdines). Siderophores that form binuclear iron complexes (Rhodotorulic acids and alcaligin)

TABLE 1. Natural ferrichromes and their structural variations [a]

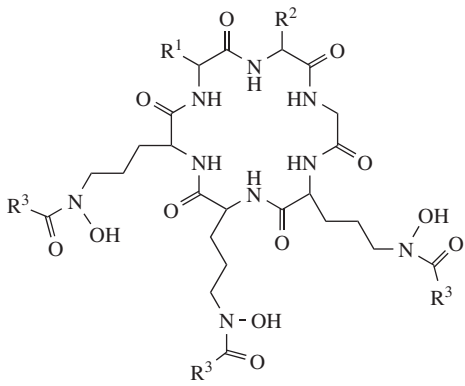

(**A**)

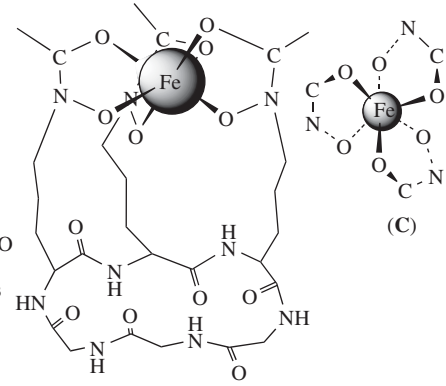

(**B**)

(**C**)

	R^1	R^2	R^3 [b]	Reference
Ferrichrome **1**	H	H	CH_3	78, 85
Ferrichrome C **2**	H	CH_3	CH_3	85, 86
Malonichrome **3**	H	CH_3	CH_2COOH	87
Ferrichrome A **4**	H	H	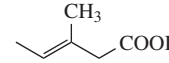	88, 89
Ferricrocin **5**	H	CH_2OH	CH_3	85, 90
Ferrichrysin **6**	CH_2OH	CH_2OH	CH_3	90
Ferrirubin **7**	CH_2OH	CH_2OH	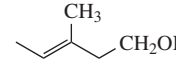	88
Ferrirhodin **8**	CH_2OH	CH_2OH	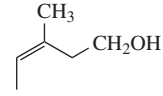	88
Asperchrome A **9**	CH_2OH	CH_3	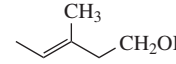	91
Asperchrome (B1-B3) **10**	CH_2OH	CH_2OH	CH_3 and 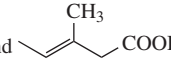	91
Asperchrome (D1-D3) **11**	CH_2OH	CH_2OH	CH_3 and 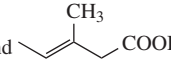	91
Asperchrome C **12**	CH_2OH	CH_2OH	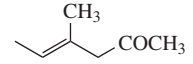 and 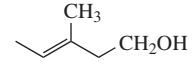	91

TABLE 1. (*continued*)

	R^1	R^2	$R^{3\,b}$	Reference
Asperchrome E **13**	CH_2OH	CH_2OH	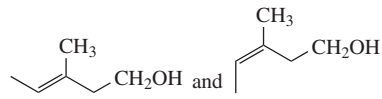	91

[a] Structure *A* represents the desferrichrome structures, *B* represents its metal complex and *C* is a Newman projection indicating the helicity generated by the metal ion. For the sake of clarity, the metal was not introduced in the structures throughout the chapter.
[b] The point of attachment of R^3 is from the vinylic position to the hydroxamate carbon.

would exhibit lower, if any, recognition than those that possess them. Hydrogen bonding is also very sensitive to the distance and orientation between the proton-donor and the proton-acceptor. The relevance of these interactions may well explain the different biological activity between two very closely related structures in which the amide groups (in the arms) adopt different geometrical orientations[84].

2. Biomimetic ferrichromes

Over the years, a great variety of analogs to the natural ferrichrome **1** have been prepared. A common theme in most synthetic ferrichrome analogs was to replace the nonsymmetric cyclic hexapeptide ring system by a simpler, symmetric, generally tripodal template, to which three identical arms carrying hydroxamate groups are attached, since such structures are much easier to synthesize and calculate. In this topological arrangement, bidentate ligands form hexadentate chelators, which delineate an internal space suitable to host an octahedral metal ion. The nature of the template and its chemical composition in addition to the length of the arms and their rigidity control the cavity size, the conformational symmetry, chelator flexibility and complex stability. In this topological arrangement (tripodal), unsymmetrical bidentate ligands (hydroxamates) adopt a *fac* orientation upon coordination, leading to exclusive formation of the *cis*-isomers.

As explained above in Section II, incorporation of chiral amino acids in the linker arms between the template and the ligating hydroxamate groups not only allows one to determine the directionality of the helical twist, but also permits one to modify the chelator properties such as bulkiness, hydrophobicity and receptor selectivity.

Emery and coworkers[92] were the first to realize that the hydroxamic acid group does not change its coordination characteristics when positioned in the reverse direction, and prepared the first retro-hydroxamate ferrichrome siderophore analog **14**, in which the position of the hydroxamate nitrogen and carbon are interchanged relative to their position in the natural siderophore. Except for a minor reduction in its iron(III) binding constant and some solubility alterations, the retro-ferrichrome showed practically identical uptake and growth promotion activity in fungi *Ustilago sphaerogena* and *Arthrobacter JG*, and its potency in antagonizing albomycin was indistinguishable from that of natural ferrichrome. These findings and the relative ease of the synthesis of retro-hydroxamates encouraged their utilization in the design of model compounds.

On the other hand, desmethyl-retro-hydroxamate ferrichrome **15**, where the terminal methyl groups were replaced by hydrogen, showed no significant growth promotion activity toward *Arthrobacter flavescence*, and only one third of the iron(III) transport efficiency toward *U. sphaerogena*, which confirms the importance of the methyl groups

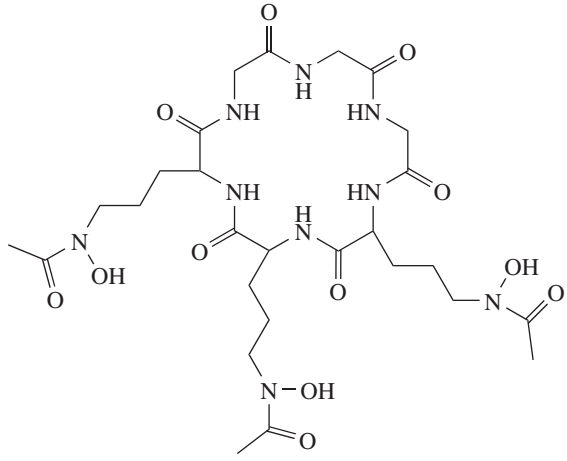

(**1**)

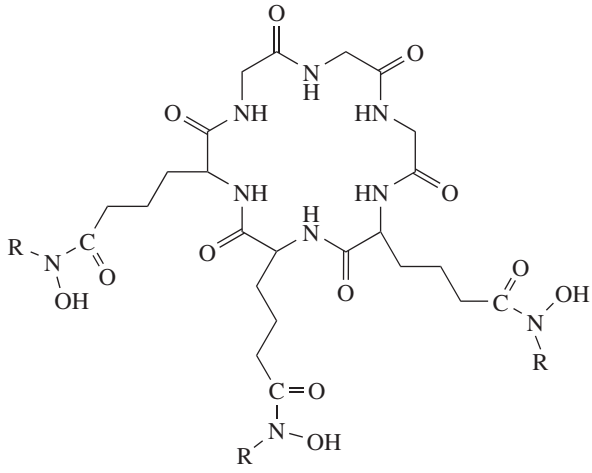

(**14**) R = Me
(**15**) R = H

at the chelation center for cellular recognition[93]. These observations demonstrate that the directionality of the hydroxamate groups does not play a major role in receptor recognition, while replacement of the terminal methyl groups by hydrogen may drastically reduce activity.

a. Special considerations in the design of biomimetic ferrichromes. In the design and synthesis of ferrichrome analogs, major consideration should be given to the nature of possible noncovalent interactions between the ferrichrome analog and the relevant receptor. The specificity of ferrichrome analogs is determined by its shape, charge, hydrophobic/

hydrophilic balance and complementarities to the receptor. The biomimetic compounds can be classified according to their stability in the free and complexed form and with respect to their binding affinity to the receptor. Thus, the 1st order of biomimetic ferrichrome analogs are compounds in which the ligands are bound directly or via a non-functionalized spacer to the template, thus forming symmetric compounds capable of chelating iron(III). Upon iron binding, they form racemic mixtures composed of Δ-right- and Λ-left-handed configurations. The high lability of the iron(III) allows fast interconversion between these configurations (cf. Section II). The receptor may select the appropriate configuration, shifting the equilibrium between closely energetically related species. Further, being conformationally flexible, they are likely to be adaptable to bind a number of different receptors, thus showing relatively low species and receptor specificity. The need to select one of a large mixture of conformations leads to a significant entropy cost that probably lowers receptor affinity.

Biomimetic analogs with conformational restrained iron(III) complexes represent the 2nd-order biomimetic analogs. These structures are characterized by the presence of non-covalent interactions, such as hydrogen bonds and van der Waals interactions, between the arms. Consequently, the conformational space is restricted to one or a very small number of rapidly interconverting states that are well characterized, and probably specific for a single or a small number of closely related receptors, thus showing much higher species and receptor specificity. The binding entropy is also lower, leading to stronger binding affinities.

Introducing chiral centers forms 3rd-order structures. The relationship between the Δ-right- and Λ-left-handed configurations become diastereomeric (composed of two types of asymmetric elements: the chirality of the side chain and the helical twist about the metal upon complexation). The diastereomers are energetically nonequivalent and therefore one of them will be preferentially populated. These systems provide a clear way to identify receptor stereospecificity.

In the following, we describe the various ferrichrome analogs according to their order.

b. Simple ferrichrome analogs (1st order). Initial approaches for mimicking ferrichrome utilized symmetric tripodal templates, to which three identical hydroxamates were attached via three identical spacers or linkers. Tris(aminoethyl)amine (TREN) based analog **16** and the retro-hydroxamate derivative **17** were found to bind iron(III) in a 1:1 stoichiometry and showed no growth promotion in *Arthrobacter flavescens*[38]. The analogous TRENDROX **18** was found to be a slightly stronger chelating agent than natural trihydroxamate siderophore[94].

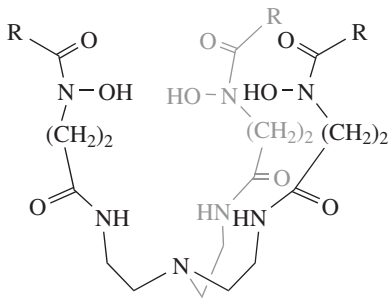

(**16**) R = *p*-$C_6H_4OCH_3$

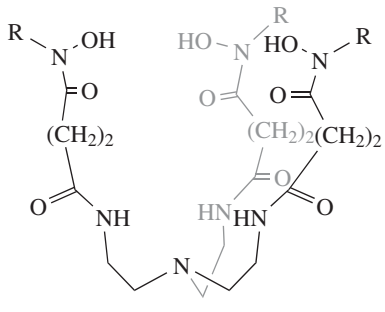

(**17**) R = H
(**18**) R = *p*-$C_6H_4CH_3$ (TRENDROX)

Attaching cyclic, bidentate 1-hydroxy-1*H*-pyridin-2-thione, 1-hydroxy-1*H*-pyridin-2-one (1,2-HOPO) and 2-hydroxy-2*H*-isoquinolin-1-one (1,2-HOIQO) ligating units via their C-6 carbon to TREN template produced **19**[95], **20**[96] and **21**[96], respectively.

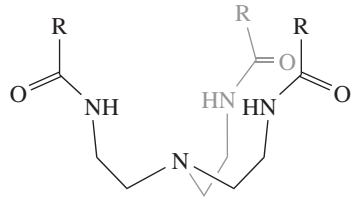

(**19**) R = 1-hydroxy-1*H*-pyridin-2-thione
(**20**) R = 1,2-HOPO
(**21**) R = 1,2-HOIQO

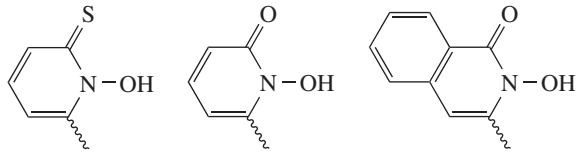

1-hydroxy-1*H*-pyridin-2-thione

1,2-HOPO

1,2-HOIQO

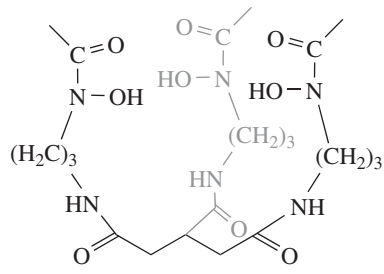

(**22**)

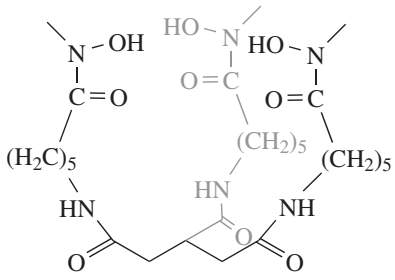

(**23**)

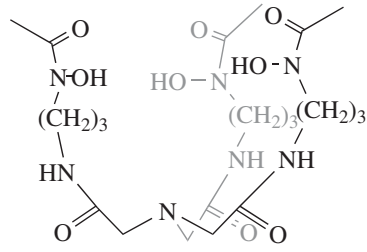

(**24**)

Propane-1,2,3-tricarboxylic acid was also used as template for the preparation of artificial siderophores **22** and **23**. A structurally similar template, bis(carboxymethylamino) acetic acid, was used to prepare **24**. All three showed identical growth promotion of several strains of *E. coli*[97].

Several trisubstituted aromatic compounds were used as a tripodal template, usually substituted on the 1,3 and 5 positions of the benzene ring. An interesting example is BTAMGH **25**[98], which showed 10% potency compared to DFO in rodent studies of iron removal, while its isomer, with the more rigid template, BAMTPH **26**[99], showed no biological activity. Extending the spacer of BAMTPH **26** with a single methylene group resulted in BZCO3MHA **27**[98], which showed 20% potency compared to DFO. In addition, methylation of the hydroxamic acid helped prevent degradation of the ligand and increased its donor properties[98].

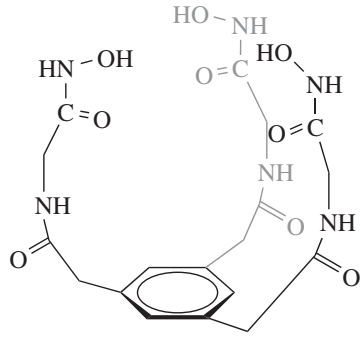

(**25**) BTAMGH

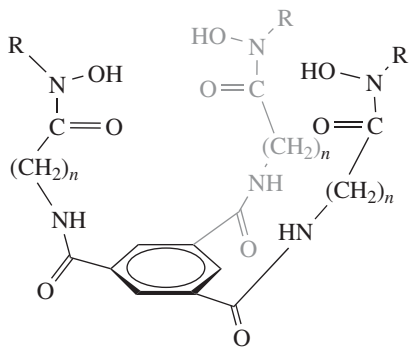

(**26**) n = 2, R = H (BAMTPH)
(**27**) n = 3, R = Me (BZC03MHA)

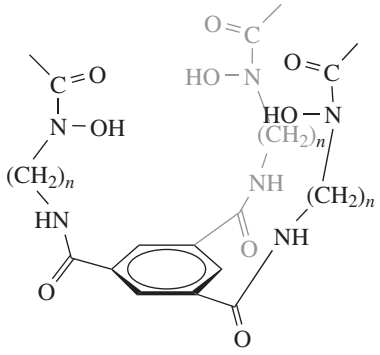

(**28**) n = 3
(**29**) n = 5

Two 1,3,5-trisubstituted benzenes, *N*,*N*′,*N*″-tris[3-(acetylhydroxyamino)propyl]-1,3,5-benzenetricarboxamide (**28**) and *N*,*N*′,*N*″-tris[5-(acetylhydroxyamino)pentyl]-1,3,5-benzenetricarboxamide (**29**), were prepared by Lee and coworkers [97]. Both analogs did not promote growth in various strains of *E. coli*.

Additional template, utilizing 2,4,6-trisubstituted cyanurates, containing side arms with varying chain lengths (**30**–**32**), along with the retro-hydroxamate analog **33**, were synthesized in order to study the effect of structural modifications on biological activity[100]. All compounds **30**–**33** promoted growth of *E. coli* RW 193. Further, compound **33** and possibly **30** were taken up by the ferrichrome receptor. Moreover, **31** promoted growth of *E. coli* AN 193, which can transport rhodotorulic acid and dimerum acid but lacks the ferrichrome receptor on the outer membrane.

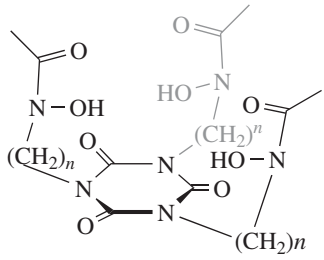

(**30**) $n = 3$
(**31**) $n = 4$
(**32**) $n = 5$

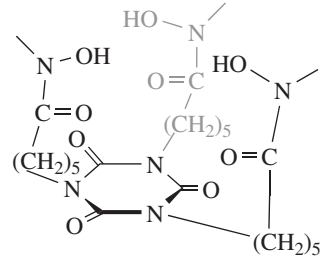

(**33**)

An elegant approach by the Miller group was to use trimelamol, which is structurally similar to cyanurates, as a template for tripodal siderophores **34** and **35**[101]. Trimelamol **36** is a nitrogen mustard used extensively in cancer chemotherapy[102]. Ramuthy and Miller[101] expected that after active transport to the cell, the trimelamol-like framework of the siderophore analog will generate highly reactive iminium ions, causing damage by interacting covalently with DNA and formaldehyde, leading to cytotoxic damage[103]. Compound **34** was unstable and decomposed to the corresponding alcohol and trimelamol. Hence, only **35** was assessed for antimicrobial activity against *Escherichia coli* X580 and *Candida albicans*. At 5 μM, compound **35** delayed growth of *E. coli* X580, indicating that the iron complex of **35** could be recognized by its outer membrane receptors.

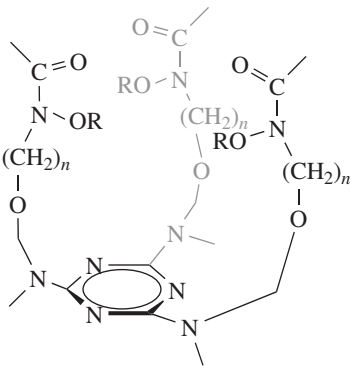

(**34**) $n = 3$, R = H unstable
(**35**) $n = 4$, R = H

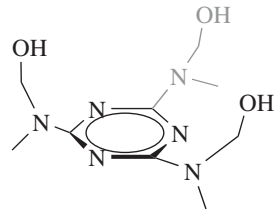

(**36**) Trimelamol

Two macrocyclic templates, 1,5,9-triazacyclododecane and 1,4,8,11-tetraazacyclotetradecane, were used to prepare 1,5,9-triazacyclododecane-*N*,*N*′,*N*″-tris(*N*-methylacetohydroxamic acid) (DOTRMAHA) **37**[104] and 1,4,8,11-tetraazacyclotetradecane, *N*,*N*′,*N*″-tris(*N*-methylacetohydroxamic acid) (TETMAHA) **38**[105], respectively. Both analogs possess very short arms compared to other active biomimetic siderophores; nevertheless, their iron(III) complexes were stable. Both analogs required very high concentrations to promote growth of several transport-defective mutants of *E. coli* strains[106], indicating that the transport was not specific, probably due to the short arms, the too flexible templates that lead to a broad conformational space of the 'envelope' around the metal ion, but most probably to the lack of functional groups on the arms that preclude interaction with the receptor. (See the discussion on the FhuA receptor with ferrichrome as derived from X-ray crystallography, toward the end of this section.)

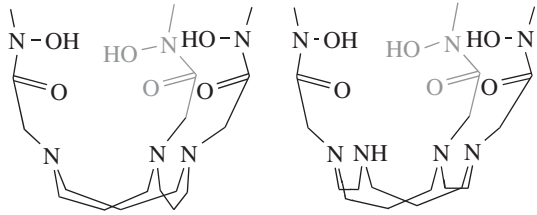

(**37**) (**38**)

Spermidine-based trihydroxamates, spermexatins **39** and **40**[107], showed similar behavior as vibriobactin in stimulating growth of wild type and siderophore mutants of *V. cholerae* and *E. coli*. Calixarenes were also used as templates for tetrahydroxamates, with spectacular metal chelating properties (**41–43**)[108–110]. 1,3,5-OMe-2,4,6-$OCH_2CONHOH$-*p*-*tert*-butylcalix[6]arene with alternating hydroxamate groups was also prepared to chelate plutonium Pu(IV) and separate it from U(VI)[111–113].

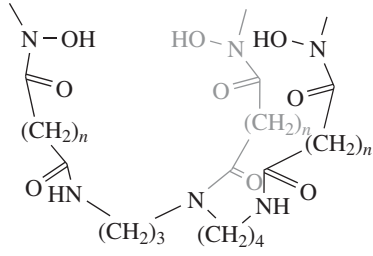

(**39**) $n = 2$ Spermexatin [2,2,2]
(**40**) $n = 3$ Spermexatin [3,3,3]

Despite their simplified structures, most of the tripodal based chelators exhibit iron binding with pronounced affinity, facilitate synthesis and allow fast screening of a variety of related structures with a number of bacterial types in a relatively short time. There is, however, a clear distinction between the flexible and the rigid templates. While the former generally exhibit broad spectrum microbial activity, the latter are generally less active and frequently show no biological activity at all.

Since the metal complexes can assume a number of closely related conformational structures and form racemic mixtures containing both right- and left-handed enantiomers in

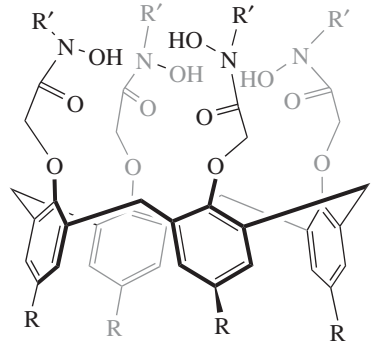

(**41**) R = *t*-Bu, R′ = H
(**42**) R = $(CH_2)_3S(CH_2)_2(CF_2)_7CF_3$, R′ = H
(**43**) R = $(CH_2)_3S(CH_2)_3Si(OEt)_3$, R′ = H

equilibrium, the probability to match a receptor is quite high. Indeed, synthetic ferrichrome analogs prepared from various flexible templates show high adjustability in generating analogs that could match a receptor and induce microbial growth. Therefore, scientists interested in broad-range microbial activity can be quite satisfied with 1st-order tripodal ferrichrome analogs. On the other hand, those interested in addressing specific receptors will find it necessary to explore systems that would form more constrained iron complexes, frequently stabilized by noncovalent interactions.

c. Constrained iron complexes via noncovalent interactions (2nd order). An additional TREN-based analog, tris[2-{(*N*-acetyl-*N*-hydroxy)glycylamino}ethyl]amine (TAGE) **44**[114], was synthesized as a ligand with intra- and interstrand hydrogen-bonding networks, which contributed to the tight binding and shielding of the iron(III) ion. Tris[2-{(*N*-acetyl-*N*-hydroxy)propylamido}ethyl]amine (TAPE) **45**[115] was synthesized as a ligand with poor hydrogen bonds between the amide hydrogen and amino hydroxyl oxygen, and indeed could not form a stable tris(hydroxamato)iron(III) complex. Matsumoto and coworkers[116] also prepared the tris(3-aminopropyl)amine (TRPN) based siderophore tris[{3-(*N*-acetyl-*N*-hydroxy)glycylamino}propyl]amine (TAGP) **46**, where the alkyl chains are one

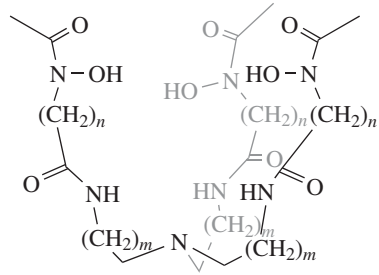

(**44**) $n = 1$, $m = 1$ (TAGE)
(**45**) $n = 2$, $m = 1$ (TAPE)
(**46**) $n = 1$, $m = 2$ (TAGP)

methylene group longer than in TAPE. Both TAGE and TAGP promoted the growth of *Microbacterium flavescens*[117], suggesting that TRPN can also serve as a template for biomimetic siderophores.

A more complex set of 1,3,5-benzenetricarboxamids, composed of mono- di- and tritopic iron chelating groups, prepared by Tsubouchi and coworkers[118], showed that tripodal hydroxamates **47** and **48** were able to form tripodal interstrand complexes with one and two iron(III) ions. The tritopic hydroxamate **49** formed preferably ferrioxamine-like intrastrand structures, where each arm binds an iron(III) ion independently. No microbial activity was reported for **47**–**49**.

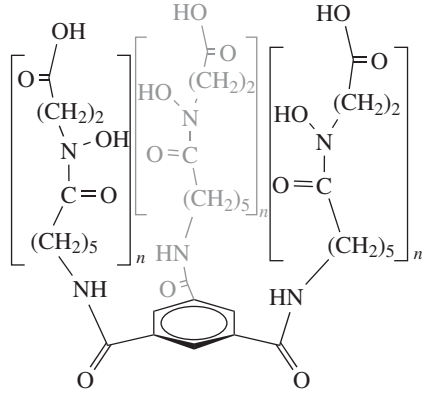

(**47**) $n = 1$
(**48**) $n = 2$
(**49**) $n = 3$

A comparison between the high formation constant observed for the TREN-based ferrichrome analog, TRENDROX **18**, having a flexible nitrogen-based template, and the 1,3,5-tris(aminomethyl)benzene-based analog, MEDROX **50**[94], showed the advantage of a flexible template versus an aromatic, more rigid template. The high formation constant of **18** may be in line with the observation of Matsumoto and coworkers[114] with a similar compound **44** in which stabilization by forming inter/intrastrand H-bonding interactions was observed.

These initial efforts established the basic prerequisites in organizing a tripodal system when forming a preferred helical twist by utilizing noncovalent interactions, mainly H-bonding, and in rare cases possible contributions from the backbone by van der Waals interactions. The limited number of conformations in the rigid tripodal arrangements allows the implementation of theoretical computation tools to screen through the conformational space of the analogs for candidates with improved complex stability and selectivity.

However, this approach still produces racemic mixtures that preclude assessing chiral recognition events taking place between siderophore mimics and their bacterial outer-membrane receptors. Since many siderophore receptors were shown to exhibit high enantioselectivity[69, 70, 119], it was anticipated that pure enantiomeric siderophore analogs would allow one to identify the preferred directionality of the helical twist about the iron for the specific receptors.

d. Chiral ferrichrome analogs (3rd order). A simple and effective approach to overcome these limitations and obtain pure enantiomeric complexes of defined handedness was the

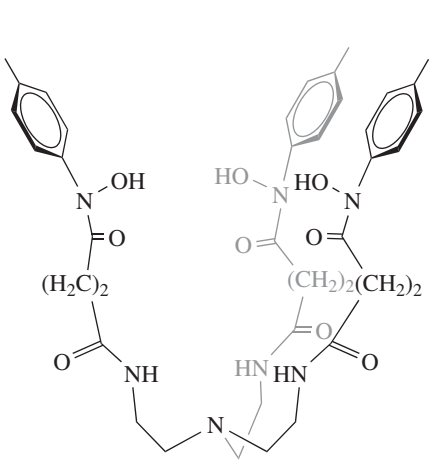

(**18**) TRENDROX

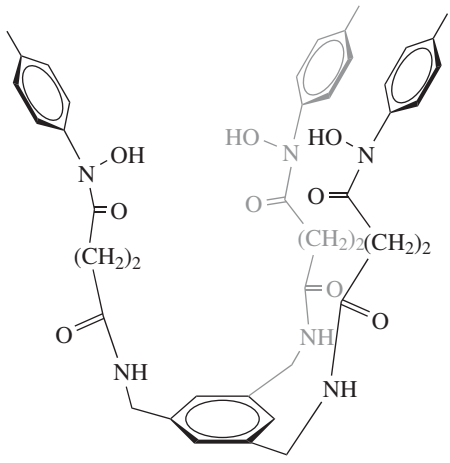

(**50**) MEDROX

development of models that incorporate chiral centers in the vicinity of the metal binding site. Indeed, such analogs provided the ability to assess the stereochemical specificity of different receptors or the same receptor in different bacteria.

Chirality can be introduced at two possible sites on the basic tripodal structures: replacing the tripodal template by a chiral template or modifying each arm with a chiral component, usually as amino acids, between the template and the ligating groups. Incorporation of amino acids inevitably introduced an amide bond known to promote intricate H-bonding networks. The latter can be applied to the various templates described so far.

Initial studies aimed at isolating the contribution of noncovalent interactions were pursued by constructing templates with extended arms containing chiral amino acids, but lacking the metal binding moiety, to be introduced at a later stage. The approach toward biomimetic ferrichrome analogs relied on replacing the nonsymmetric structure of the natural ferrichrome by 1,3,5-tris(*N*-Boc-leucy1amido)benzene (TRAM) **51**[120], a symmetric tripod that exhibits a cage-like structure and generates propeller-type conformations of defined chiral sense by virtue of an interstrand hydrogen-bond network. In the interstrand hydrogen bonds in **51**, the carbamate nitrogen may bond to the carbonyl on either the right or the left handedness. Because the chains are chiral, these two alternatives are energetically nonequivalent diastereomers. The calculations performed[120] predicted that the most stable conformation is counterclockwise, as seen for **52**, while the next most stable conformation, 4 kcal mol^{-1} more strained, is clockwise. Structure **52** presents the most stable conformation as well as two types of stabilizing H-bonded interactions.

These hydrogen bonds between nonidentical amides of adjacent chains create a chiral organized structure in both polar and nonpolar solvents. In a later work, Tor and coworkers found that interstrand hydrogen bonding generating propeller-type conformations can be similarly formed with a series of amino-acid-substituted (Leu, Ile, Val and Ala) 1,3,5-tris(aminomethyl)benzene (TRAM), **51** and **53**–**55**, and TREN-based templates **56**[121], again without ligating groups.

Substitution of the terminal amine with ligating groups, such as catecholate[122], hydroxamate[123] or diketonate[124], lead to the formation of Δ-*cis* chiral complexes. In these structures the chiral information content is located in the amino acid bridges, instead of the macrocyclic peptide ring structure used in ferrichrome. It should be emphasized

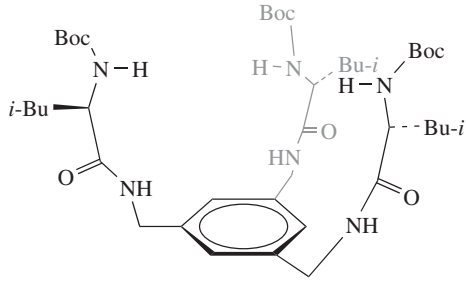

(**51**)

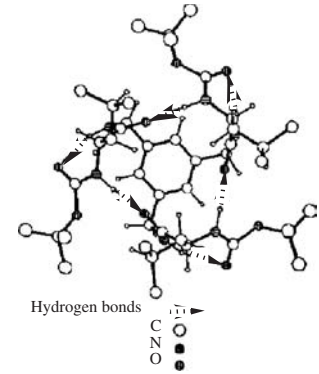

(**52**)

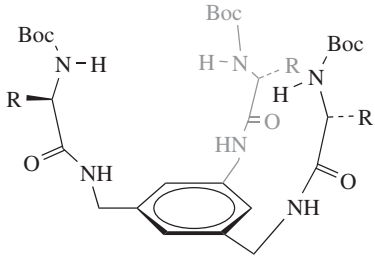

(**51**) R = *i*-Bu
(**53**) R = *sec*-Bu
(**54**) R = *i*-Pr
(**55**) R = Me

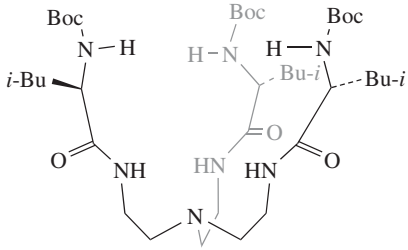

(**56**)

that the use of amino acids in these structures not only induces helicity of preferred chiral sense, but also allows systematic modifications of the molecule's 'envelope' and shape by incorporating different amino acids residues.

In order to prepare ligands forming complexes of a predominant Λ-*cis* configuration like in ferrichrome, rather than a Δ-configuration, tris-carboxylate-based templates were selected as a template whose three arms were extended by attachment of amino acids via their amino termini rather than via their carboxy termini.

To assess the relevance of H-bonds in shaping the structure and the absolute configuration in chiral tris-carboxylate-based templates, several compounds with and without hydrogen-bonding capabilities were prepared. When the terminal amide in **57** was replaced by a methyl ester in **58**, weaker H-bonds were formed, indicated by ^{1}H NMR signals for the diastereotopic protons $-CH_2-O$ and $-CH_2-CO$ in $CDCl_3$[123]. Further, the NMR pattern of Ga(III) complexes of the chiral **59** (Leu) showed a single set of signals confirming the presence of a single conformational isomer, while the Ga(III) complex with the proline derivative **60** showed the formation of isomeric mixtures[123]. A range of spectroscopic measurements (IR, NMR, CD) and behavior in polar and apolar aprotic media and temperature effects on their Mössbauer spectra all confirmed complex stabilization derived from interstrand and intrastrand hydrogen networks[123].

In addition, EFF calculations also yielded single, threefold symmetric conformations for the iron(III) complex of **59**[74].

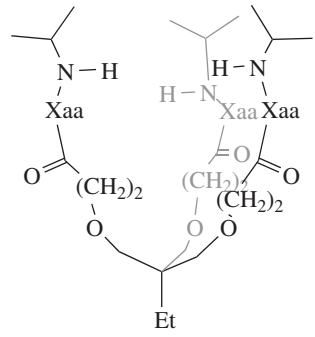

(**57**) Xaa = Leu

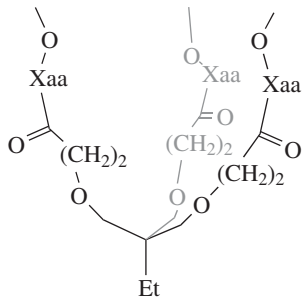

(**58**) Xaa = Leu

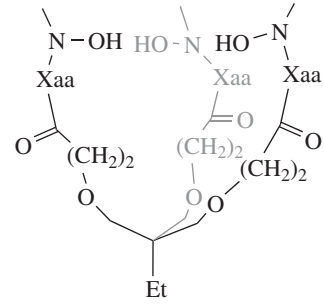

(**59**) Xaa = Leu
(**60**) Xaa = Pro

Following this principle of design, two homologous families of tris carboxylate templates were prepared, where type 2 has an additional methylene group in the template backbone compared to type 1. Both templates were extended with various amino acids, varying in the bulkiness and hydrophobic characteristics, and their structures were examined in detail[125]. It was demonstrated that both families form networks of inter- and intrastrand H-bonds that shape the conformations of the free ligands toward propeller-like arrangements (Scheme 2). When loaded with metal ions, H-bonds and van der Waals forces stabilize the complexes formed, and thereby promote the formation of well-defined 1:1 complexes of high isometric and optical purity[84, 125].

Some of the hydrophilic type 2 analogs, but none of type 1 (**61**–**65**), exerted quite remarkable microbial activity[39, 125, 126]. Microbial activity was tested on *Arthrobacter flavescens* in comparison to natural ferrichrome. Reducing the bulkiness of the amino acid side chain showed gradual increase in growth promotion in the following order: Ile **66** (0%), Leu **59** (1%), Pro **60** (80%), Sarcosine (Sar) **67** (85%) and Ala **68** (100%), practically indistinguishable from the native ferrichrome[38, 41, 127]. Moreover, the biomimetic chelator activity differed from organism to organism. Thus, the L-Ala derivative **68** that acted as iron(III)-carrier and growth promoter in *Arthrobacter flavescens*[38] was found to act as an inhibitor in *Pseudomonas putida*[41]. On the other hand, the Gly derivative **69** acted as iron(III)-carrier in *Pseudomonas putida*[41, 125] in close analogy to the natural

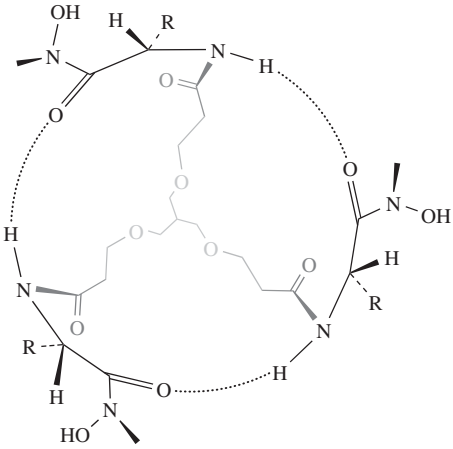

SCHEME 2. A schematic top view presentation of tris-carboxylate template and the stabilizing 'belt' of interstrand hydrogen bonding

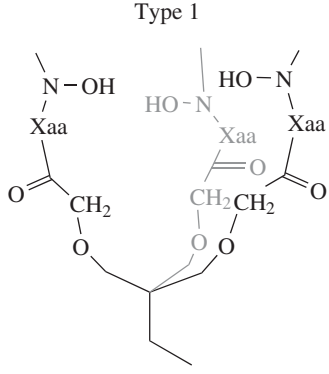

(**61**) Xaa = none
(**62**) Xaa = Ala
(**63**) Xaa = Val
(**64**) Xaa = Leu
(**65**) Xaa = Ile

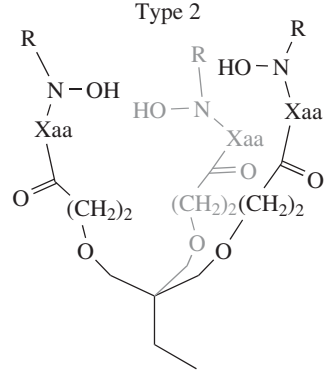

(**66**) R = Me, Xaa = Ile
(**67**) R = Me, Xaa = Sarcosine
(**68**) R = Me, Xaa = Ala
(**69**) R = Me, Xaa = Gly
(**70**) R = Me, Xaa = D-Ala
(**71**) R = H, Xaa = Ala

siderophore[92]. (The achiral glycyl forms racemic mixtures of complexes, where the Λ-*cis* isomer is believed to be taken up and constantly replenished by fast equilibrium in the medium.) The enantiomeric D-Ala derivative **70** and the desmethyl-retro-hydroxamate analog **71**, in which the terminal methyl group was replaced by hydrogen, did not show ferrichrome-like activity in any of the organisms examined.

The EFF calculations yielded a single C_3-symmetric conformation for each type of ferrichrome analog (Figure 4), both with a Λ-*cis* configuration of the hydroxamates about the metal when L-amino acids were used[84]. Taken together with the spectroscopic data[125], pronounced differences were observed for the conformations of these iron complexes. Inspection of the calculated conformations showed that the backbone amide groups may

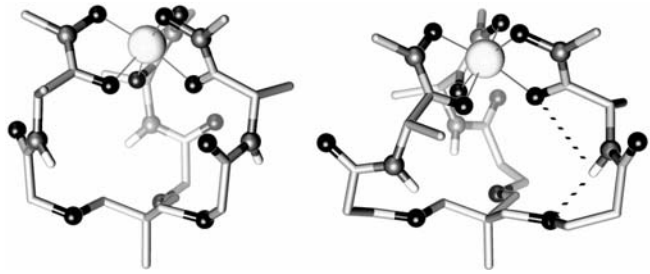

(**62**) Type 1 (**68**) Type 2

FIGURE 4. Calculated lowest-energy conformations of ferrichrome analogs (Type 1, left; Type 2, right). Nitrogens are light gray, oxygens black and iron is a bright ball. Hydrogen bonds are indicated as dotted lines

adopt different orientations with respect to the 3-fold symmetry of the molecule. The three amide nitrogen atoms on the identical linker arms together define a circle whose center is the 3-fold axis and is perpendicular to it. Any substituents pointing along a radius from the axis to the circumference is axial. Any substituents in the circle's plane and perpendicular to the radius is tangential. While in type 1 complexes, the amides are positioned tangentially to the molecules' cross section, in type 2 complexes they are oriented radially with the amide-NH groups pointing inward. In the latter arrangement these groups can form intramolecular hydrogen bonds.

The closely related structures show completely different microbial uptake characteristics. The 3D structures described above show distinct different orientation of the backbone amide (tangental in type 1 versus radial in type 2), which can be explained by the interactions that take place between the FhuA receptor and the ferrichrome siderophore[81,82]. As mentioned, the second coordination sphere of natural ferrichrome in FhuA receptor is very sensitive to the distance and orientation between a proton donor and the proton acceptor, therefore the orientation of the amide groups in the biomimetic siderophore plays a crucial role in receptor recognition.

Recently, crystal structures of chiral and nonchiral siderophore analogs with such H-bonds have been reported by Matsumoto and coworkers in a triple-stranded helix with both intra- and interstrand hydrogen-bonding networks[114,117]. These confirm the suggested relevance of noncovalent interactions in shaping the complex structure and inducing the proper helical sense. This analogous approach incorporates amino acid residues into TREN-based templates. The chiral, TREN-based siderophore, R-TAAE **72**, was crystallized and subjected to single-crystal X-ray diffraction analysis. Together with anomalous diffraction studies the absolute configuration of **72** was established. It indeed showed the formation of a Λ-*cis* helical structure containing both *intra-* and *interstrand* hydrogen-bonding networks[117], thus supporting the proposal of Shanzer and coworkers[37,121,128] that these noncovalent interactions shape molecular chiral preference and stabilize the complexes formed. Additional chiral siderophores were prepared by attaching the tripeptide Ala-Ala-β-(N-hydroxy)Ala to TREN-based templates[129]. Two TREN based analogs, **73** and **74**, preferred the Δ-*cis* configuration, where the additional Ala unit in **74** did not affect the chiral tendency.

In contrast to the TREN template, **75** with the NTA template preferred the Λ-*cis* configuration[129]. This could be caused either due to the inverse directionality of the hydroxamate group, or, more plausibly, because the tripeptide is connected through the amino end, leading to opposite orientation of the hydrogen-bonding network[126].

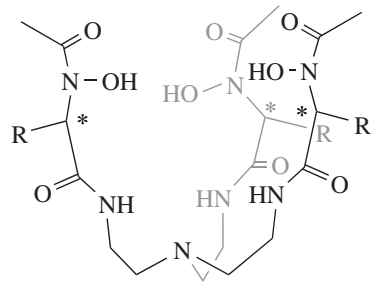

(**72**) R = Me (D-Ala); R-TAAE

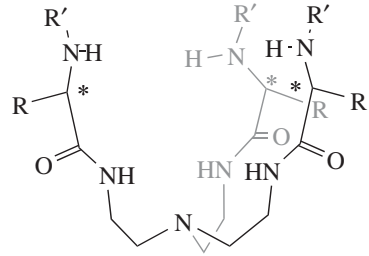

(**73**) R = Me (L-Ala), R′ = Ac-Ala-Ala-β(NOH)-Ala-Ala-
(**74**) R = Me (L-Ala), R′ = Boc-Ala-Ala-β(NOH)-Ala-

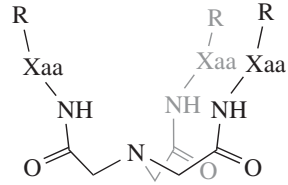

(**75**) R = CO-Ala-β-(NOH)Ala-OMe, Xaa = L-Ala
(**76**) R = CO-Ala-β-(NOH)Ala-OMe, Xaa = D-Ala
(**77**) R = CO-β-(NOH)Ala-OMe, Xaa = L-Ala
(**78**) R = CO-β-(NOH)Ala-OMe, Xaa = D-Ala
(**79**) R = CO-Ala-Ala-β-(NOH)Ala-OMe, Xaa = L-Ala

In a later work, the iron(III) complex stability and structure of **75** was compared to other NTA-based analogs **76**, **77**, **78** and **79**[130]. Complex stability was in the order **75** > **79** ⩾ **76** > **77** = **78**. CD spectra revealed that the enantiomeric pair **77** and **78** gave Δ- and Λ-configurations, respectively, by reference to the assignment for ferrichrome[79, 131]. Both **75** and its diastereomer **76** showed preference for the Λ-*cis* configuration.

Similiar to albomycin and ferrichromes, the linear tripeptide of N^{δ}-hydroxy-N^{δ}-acetyl-ornithine can be used as the simplest chiral template for artificial siderophores. It can be used alone as a tripeptide like for **80**[132], can be conjugated to a hydrophobic fatty acid **81**[132] or as part of a longer peptide **82**, **83**, **84**[133, 134] and **85**[135].

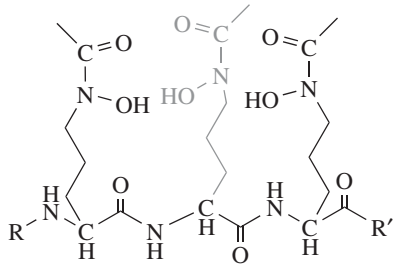

(**80**) R = H, R′ = OH
(**81**) R = $C_{15}H_{31}CO$, R′ = OH
(**82**) R = H, R′ = Phe
(**83**) R = H, R′ = Tyr
(**84**) R = H, R′ = Ser
(**85**) R = H, R′ = Peptide

A unique feature of the biomimetic approach is the ability to construct model compounds that combine all the required parameters gained over time in a single molecule and to examine to which extent the new structures sustain bioactivity. Motifs that have not been incorporated in the assembled structures will be exposed, either by reduced bioactivity or by the lack of it altogether, thus providing an indication that some parameters have been omitted, and should be searched for and introduced.

An example of this ability, performed on a chiral template, was described by Weizman and Shanzer[136] by the synthesis of two symmetrically substituted enantiomeric trilactones, with 1,2-HOPO moiety (1-hydroxy-2-oxo-6-pyridyl). The chiral ring structure derived from three L-serine-generated iron(III) complexes of a Δ-configuration **86**, an aromatic hydroxamate analog of enterobactin, while starting from D-serine, generated its enantiomeric complex possessing the Λ-configuration, **87**, the required handedness of ferrichrome. Since the 1,2-HOPO ligating functionalities are isoelectronic with the catechol[137] the first should be recognized by the enterobactin receptor (FepA) in *E. coli*, while the enantiomeric iron complex with a Λ-configuration resembling ferrichrome should therefore be recognized by the ferrichrome receptor (FhuA) in *E. coli* or *P. putida*.

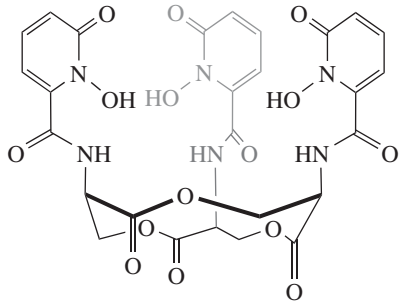

(**86**)

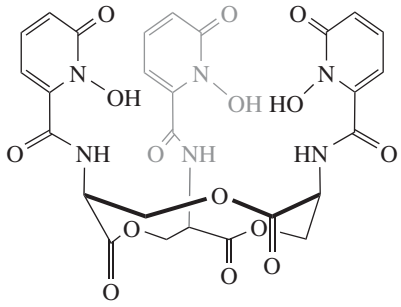

(**87**)

Surprisingly, although the complexes preferentially form stable enantiomer complexes as indicative from their CD spectra, negative iron uptake was observed for both enantiomers. No growth promotion was identified with the enterobactin analog with *E. coli*

and no growth promotion was observed for the ferrichrome analog in both *E. coli* and *P. putida*, although both possessed the appropriate stereochemical requirements.

Since the 1,2-HOPO chelators form neutral complexes while the catecholates form charged complexes, it is reasonable to assume that charged species are essential for the enterobactin receptor recognition. The lack of recognition by the ferrichrome analog may well be attributed to the bulky substituents on the hydroxamate moiety in agreement with early observations by Emery and Emery[93] and others[98, 138, 139].

These results imply that additional factors, such as charge and bulkiness, in addition to those described above, affect receptor recognition and should be taken into consideration during the design of improved siderophore mimics.

An interesting departure from traditional approaches was introduced[140, 141], utilizing carbohydrate building blocks as the chiral templates. Some advantages of the saccharide-based siderophore analogs are water solubility and hydrogen-bonding capabilities, which can provide favorable receptor recognition, synthetic versatility and the availability of additional functional groups for future modifications. Siderophore analogs based on sugar backbones substituted at the 2,3,4 or 2,3,6 positions with hydroxamic acid or retro-hydroxamic acid chelating units with varying hydrophilic and hydrophobic terminal groups were prepared[142–145], analyzed[146] and tested for biological activity.

Recently, a ferrichrome analog based on α-D-glucopyranose backbone substituted at the 2,3,4 positions with retro-hydroxamic acid chelating units, **88**, was prepared by Heggemann and coworkers[147, 148]. An additional α-D-glucopyranose based ferrichrome analog, **89**, substituted at the 2,3,6 positions with hydroxamic acid chelating arms was also reported[146]. A broad activity spectrum was observed for these ferrichrome analogs in growth promotion bioassays of Gram-positive and Gram-negative bacteria including *Mycobacterium smegmatis, Pseudomonas aeruginosa, Salmonella typhimurium* and *Escherchia coli* comprising wild-type strains and mutants, including siderophore biosynthesis, siderophore receptor and general iron-transport mutants[146]. Both **88** and **89** promoted the growth of *M. smegmatis*. In contrast to the excellent activity of the retro-hydroxamic acid derivative, **88**, which was actively taken up by ferrichrome receptor FhuA and to a lesser extent by the FhuE receptor, **89** did not promote growth of *E. coli*.

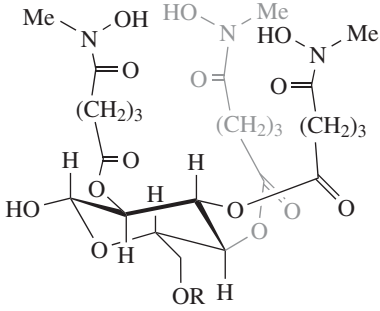

(**88**) R = CH_3

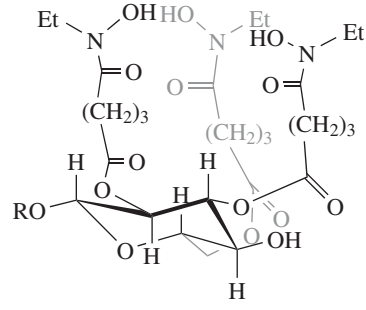

(**89**) R = CH_3

In the biological activity on *Mycobacterium smegmatis* wild-type strains and mutants, observed growth promotion activity seems to depend on the lipophilicity rather than on siderophore-mediated uptake[144]. Nevertheless, from the overall characteristics (very high pFe values, broad spectrum of biological activity and the potential for incorporating various drugs) the future of ferrichrome mimics based on the saccharide template seems very promising.

Template **90**, derived from 1,3,5-tris benzyl esters, was capable of orienting ligand strands with chiral spacer (L-alanine) in the same direction[149]. Once complexed with an inert Cr(III) ion through its hydroxamic acid groups, a diastereomeric mixture dominated by the Δ isomer was formed. This tripodal template can be removed by hydrogenolysis to obtain pure chiral unidirectional chromium tris hydroxamate complexes. The CD spectrum of complexed **90** was identical to that of the template-free complex. This 'cleavable template' approach represents a general way for controlling the ligand's mutual orientation.

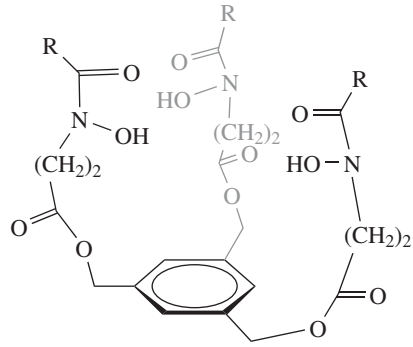

(**90**) R = $CH(CH_3)NHBoc$

In summary, the feasibility of preparing active biomimetic ferrichrome analogs was demonstrated utilizing simplified tripodal structures with variable degrees of molecular complexity. There is a clear advantage for: (i) flexible templates that increase receptor adjustability, (ii) medium size spacers capable in forming intramolecular hydrogen-bond networks that stabilize complex formation (by reducing entropy loss) and interacting with the receptor and (iii) methyl terminated hydroxamate groups. It is of particular interest to note that receptor recognition is tolerated by both the natural and the retro isomers utilizing similar structural motifs.

The degeneracy of the non-chiral complexes can be removed by incorporating chiral centers, usually as resolved amino acids, into the arms at close vicinity to the hydroxamate iron binding sites. Thus, only one of the energetically non-equivalent diastereomers predominates, leading to pure enantiomeric iron(III) complexes with defined helicity that allows assessing stereospecific recognition by the ferrichrome receptor.

Templates based on tetrahedral carbon provide an additional advantage as they can be further extended with additional functional groups (see Section VI).

C. The Ferrioxamine Family

1. Natural ferrioxamines

The ferrioxamines, produced by both Gram-negative and Gram-positive bacteria[76, 150] and similar to the ferrichromes described above, make use solely of the hydroxamate group as their iron-binding sites. Yet, at variance with the ferrichromes, the ferrioxamine family contains both cyclic (**95**, **96**, **104**–**108**) and linear (**91**–**94**, **97**–**103**, **109**) structures that lack chiral centers. They all possess two or three hydroxamate groups bridged by amide bonds, assembled from α-amino-ω-hydroxaminoalkane and succinic or acetic acid[151–153].

TABLE 2. Natural ferrioxamines and their structural variations

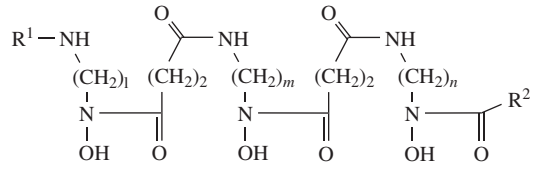

Desferrioxamine	$R^{1\,b}$	R^2	*l*	*m*	*n*	Reference
A_1 **91**	H	CH_3	5	5	4	164
A_2 **92**	H	CH_3	5	4	4	164
B **93**	H	CH_3	5	5	5	163, 165
D_1 **94**	Ac	CH_3	5	5	5	151
D_2**95**	Cyclic	$-(CH_2)_2CO-$	4	5	5	166, 167
E **96**	Cyclic	$-(CH_2)_2CO-$	5	5	5	167–169
G_1 **97**	H	$(CH_2)_2COOH$	5	5	5	167, 168
G_{1t} **98**	H	H	5	5	5	167
G_{2a} **99**	H	$(CH_2)_2COOH$	5	5	4	167, 168
G_{2b} **100**	H	$(CH_2)_2COOH$	5	4	5	167
G_{2bt} **101**	H	H	5	4	5	167
G_{2c} **102**	H	$(CH_2)_2COOH$	4	5	5	167
G_{2ct} **103**	H	H	4	5	5	167
$^aX_1$ **104**	Cyclic	$-(CH_2)_2CO-$	4	4	5	167, 170
$^aX_2$ **105**	Cyclic	$-(CH_2)_2CO-$	4	4	4	167, 170
$^aX_3$ **106**	Cyclic	$-(CH_2)_2CO-$	5	5	6	170
$^aX_4$ **107**	Cyclic	$-(CH_2)_2CO-$	5	6	6	170
X_7 **108**	Cyclic	$-(CH_2)_2CO-$	3	5	5	171
Tanacibactin D **109**	H	$CH_2CH(CH_3)_2$	5	5	5	172

[a] Obtained by directed fermentation.
[b] Cyclic hydroxamines are obtained when $R^2 = -CH_2CH_2CO-$ and the carbonyl group form an amide bond with the terminal amine (replacing R^1).

The most studied member of this family is desferrioxamine B **93** (DFO), a linear hexadentate containing three hydroxamate groups as iron-binding sites bridged alternatively by amide groups. DFO-B is produced by fermentation of *streptomyces pilosus* strain A 21748 and isolated in crystalline form as its methanesulfonate (mesylate) salt (Desferal). Desferal is the only clinically used siderophore for the treatment of iron overload diseases. Although Desferal is an excellent drug, successfully used for many years, some limitations (such as slow onset of acting, short plasma half-life, poor cell permeation and prolonged parental administration of extensive dosages) triggered an extensive search for developing improved iron Fe(III) chelators[139, 154–157]. When binding trivalent metal ions, ferrioxamine B forms a total of five conformational isomers, each within enantiomeric pairs, as demonstrated elegantly by Raymond and coworkers[158].

The crystal structure of five members of the ferrioxamine family has been determined: ferrioxamine D_1[159], ferrioxamine E[160], desferrioxamine E[161], the retro-isomer of ferrichrome E[162] and ferrioxamine B[163]. While all of the Fe(III)–ferrioxamine structures (Table 2) crystallize as racemic mixtures of Δ- and Λ-*cis* isomers[163], the configuration of the binary ferrioxamine-B in FhuD complex (2.0 Å resolution) is Λ-*C-trans,cis*, indicating that the interaction between ferrioxamine-B and FhuD is enantioselective, and also exhibits geometric selectivity.

2. Biomimetic ferrioxamines

Though desferal is being used successfully for the treatment of iron overload, it has several drawbacks, such as the need for daily subcutaneous infusions due to lack of oral bioavailability, its low cell internalization and its metabolic instability that limit its clinical use[173]. Much synthetic effort was invested in developing alternatives to DFO. In addition to its clinical use in iron-overload treatment, several other therapeutic targets are actively pursued for the following reasons: (i) antimalarial activity of DFO and other iron chelators have been demonstrated under both *in vitro* and *in vivo* conditions[25, 174]; (ii) there is evidence that iron chelators has antitumor activity and can act as an antiproliferative agent against tumor cells[175]; (iii) biomimetic ferrioxamines targeted to ferrioxamine receptors[39] on microorganism membranes are important in the understanding of ferrioxamine receptor recognition events and for the development of antibiotics and diagnostic kits. The need for an efficient, stable and orally effective iron chelator resulted in the design and synthesis of many ferrioxamine analogs[176, 177]. Examples for such ferrioxamine analogs will be given in this section, with a discussion of the considerations in their development.

One approach in preparing ferrioxamine analogs was to substitute the primary amine, trying to achieve stability and enhanced solubility. In contrast to the heptyl analog, **110**, which was found to be insoluble[178], improved permeability to tissue iron stores could be gained by incorporation of lipophilic substituents. Two polyether-containing DFO analogs, **111** and **112**, prepared by Bergeron and coworkers[179], showed excellent ability to clear iron in rats compared to DFO when given subcutaneously. However, when administered orally, both analogs were less active than DFO.

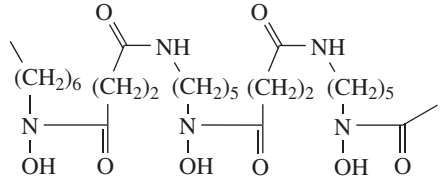

(**110**)

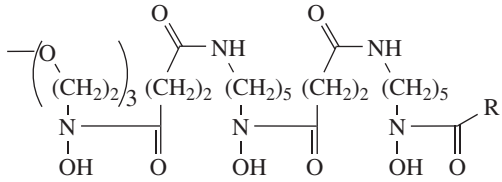

(**111**) R = Me
(**112**) R = $CH_2O(CH_2)_2O(CH_2)_2OCH_3$

Ihnat and coworkers[180] substituted the primary amine group with a series of gradually increasing alkyl amides **113**–**119**, aromatic amides **120** and **121**, succinamide **122** and methylsulfonamide **123** with a systematic increase in partition coefficient (octanol/water), to increase permeability while retaining iron-chelating ability. The formamide derivative

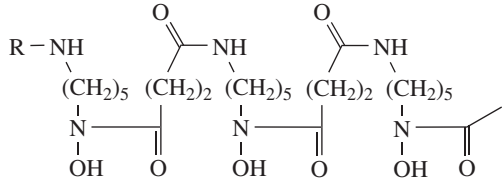

(**113**) R = CHO
(**114**) R = $COCH_3$
(**115**) R = COC_2H_5
(**116**) R = COC_3H_7-*n*
(**117**) R = COC_4H_9-*n*
(**118**) R = COC_5H_{11}-*n*
(**119**) R = COC_7H_{15}-*n*
(**120**) R = COC_6H_5
(**121**) R = $COCH_2C_6H_5$
(**122**) R = $CO(CH_2)_2COOH$
(**123**) R = SO_2CH_3

113 had partition coefficient 200-fold higher than ferrioxamine-B and reduced water solubility by approximately 2000-fold. In a homologous series of the aliphatic amides, each additional methylene group decreased water solubility 2-fold.

Bergeron and coworkers[181] studied several sites that can be modified in the desferrioxamine backbone in order to prepare low molecular weight analogs with enhanced stability to proteolytic enzymes. First, monohydroxamates **124** and **125** showed no iron excretion at all, indicating that for effective iron clearance, the three hydroxamate groups must be connected covalently. Second, 'amideless' DFO analogs, **126**, **127** and especially **128**, were as effective as DFO in iron-clearing properties, meaning that the spacer which links the hydroxamate groups can be replaced by alkyl chains.

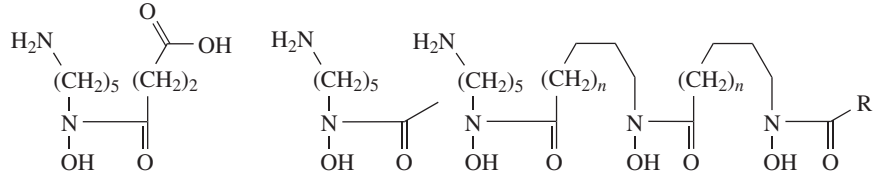

(**124**)

(**125**)

(**126**) *n* = 1, R = Me
(**127**) *n* = 1, R = Nonyl
(**128**) *n* = 4, R = Me

In accordance with Emery's retro-hydroxamate ferrichrome, mentioned above, two retro analogs of the linear ferrioxamine G and cyclic desferrioxamine E (**129** and **130**, respectively) were prepared. The iron-chelating properties were compared to DFO, showing that the linear retro-desferrioxamine G (**131**) binds iron faster and the cyclic retro desferrioxamine E (**132**) has improved affinity to iron, compared to the linear DFO[182]. Based on these results, many retro-hydroxamate ferrioxamines were prepared. In a later paper, Akiyama and coworkers[183] reported the attachment of β-cyclodextrin, a cyclic oligosaccharide, composed of seven α-D-glucopyranoside units, linked from position 1 to position 4, to linear retro-hydroxamate ferrioxamines (**133** and **134**), which formed 1:1 iron(III) complexes. Influenced by the chiral β-cyclodextrin group, **133** and **134** formed Δ-selective coordination around the metal ion. In addition, Akiyama proposed that the

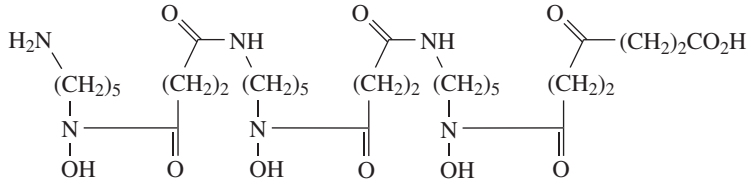

(**129**)

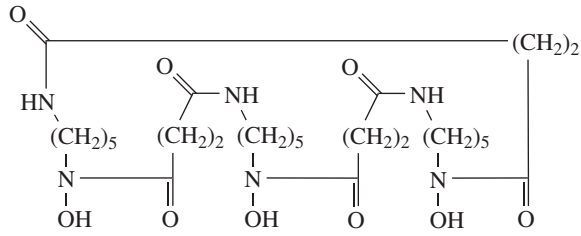

(**130**)

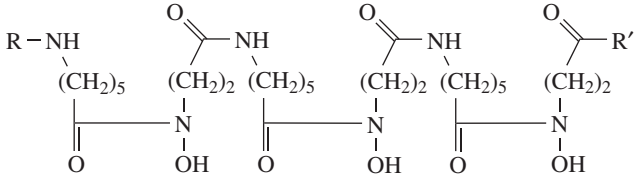

(**131**) R = H, R′ = OH
(**133**) R = Boc, R′ = NH-β-cyclodextrin
(**134**) R = Ac, R′ = NH-β-cyclodextrin

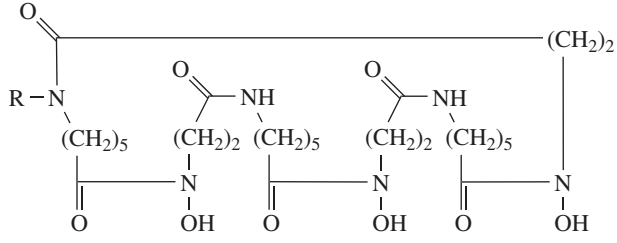

(**132**)

β-cyclodextrin cavity hosts the hydrophobic *t*-butyl group to form a pseudo-cyclic structure. Though β-cyclodextrin does not pass the cell membrane, both analogs exhibited 10% growth promotion of *Aureobacterium flavescens* compared with ferrioxamine B.

N-hydroxy hexapeptide **135**, with alternating *N*-hydroxy amide units, introduced by Akiyama and coworkers[184], is an additional fragment for introducing chirality to ferriox-

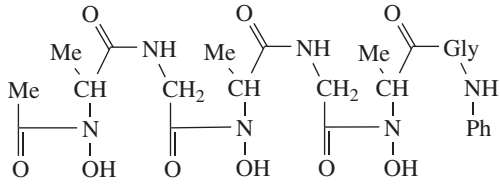

(**135**) R = Me

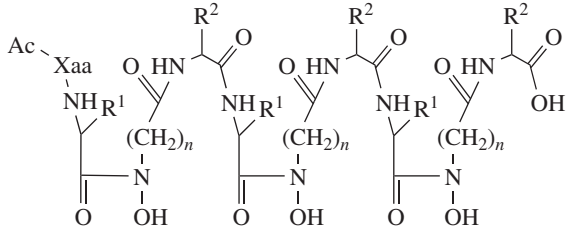

(**136**) Xaa = none, R^1 = Me, n = 1, R^2 = Me

(**137**) Xaa = Ala, n = 2, R^1 = Me, R^2 = Me

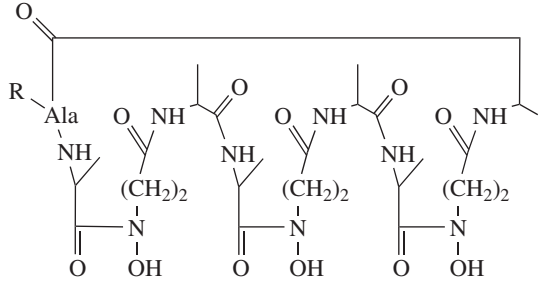

(**138**)

amine analogs. However, it appears that due to its rigid peptidic structure, unstable 1:1 complexes with iron(III) are formed. With the assumption that addition of amino acid residue will increase the degrees of freedom of the linker, the nonapeptide **136** with tripeptide spacers between the hydroxamate groups was synthesized. A Δ-*N-cis,cis* configuration was proposed for the chiral complex of low stability formed with iron(III)[185]. Additional flexibility was introduced by incorporating β-alanine residues instead of the glycine residues in **136**, in order to obtain a linear and a cyclic peptide-based ligand, **137** and **138**[186]. These ligands were much more flexible and formed more stable complexes with iron(III) compared to **136**, with Δ-*C-cis,cis* configuration.

Recently, the power of solid-phase synthesis and combinatorial chemistry was employed for the synthesis of several libraries of structurally modified DFO analogs **139** (R^1–R^6 = alkyl, cycloalkyl, aryl), in addition to nonamide analogs **140** (m, n, p = 1, 3, 5), C-terminal modified nonamide analogs **141** (R = alkyl, aryl, aminoalkyl, m, n, p = 1, 3, 5, a = 0, 1), as well as reverse-amide analogs **142** (R^1–R^4 = alkyl, aminoalkyl, car-

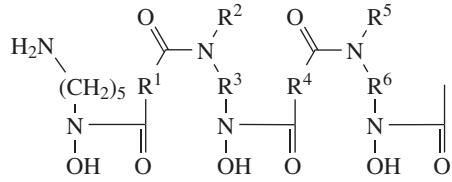

(**139**)

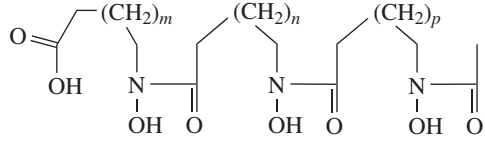

(**140**)

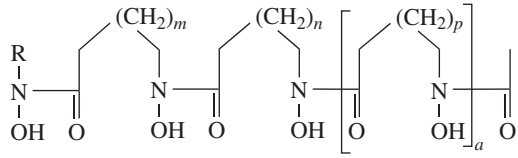

(**141**)

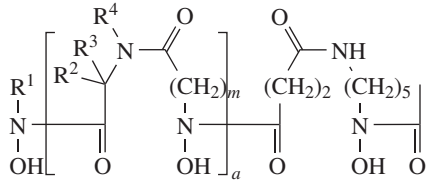

(**142**)

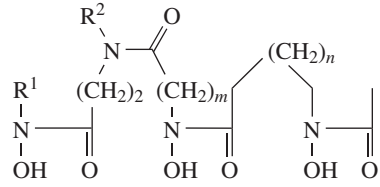

(**143**)

boxyalkyl, $m = 1, 3, 5$, $a = 0, 1$) and hybrid analogs **143** (R^1, R^2 = alkyl, aminoalkyl, carboxyalkyl, $m, n = 1, 3, 5$)[187]. High throughput screening assay was developed to assess the iron-binding affinities of these compounds and to establish the structure–activity correlation of DFO. In each of these libraries, several compounds were found with promising iron-chelating properties.

In the search for cytotoxic DFO analogs, a set of constrained trihydroxamate-containing peptides, including linear **144** and its cyclic analog **145**, were synthesized via fragment condensation of hydroxamate-containing oligopeptides and the correlation between three-dimentional structure and metal binding coordination was studied[188]. Despite their lower affinity for iron, the cyclic analogs, **145**, showed higher cytotoxicity than DFO (69% (**145**) compared to 25% (DFO) death rate in Hela cells at 50 μM), attributed to its increased lipophilicity and improved cell penetration.

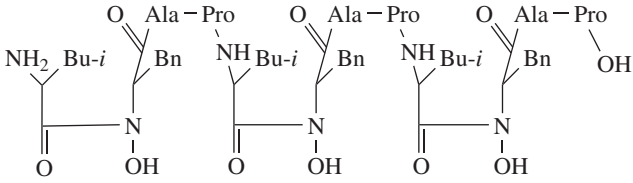

(**144**)

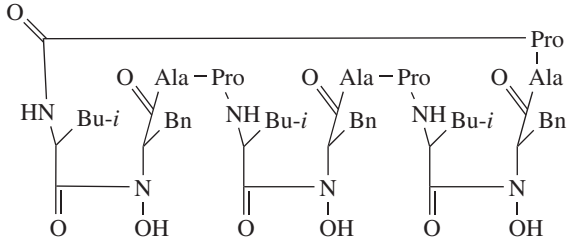

(**145**)

Unlike desferrioxamine analogs designed for specific therapeutic purposes described above, chiral DFO analogs that form conformationally unique complexes with iron(III) were designed to serve as chemical probes of microbial iron(III) uptake processes. As mentioned above, ferrioxamine B can form a total of five isomers when binding trivalent metal ions, each as a racemic mixture[158]. Muller and Raymond[189] studied three separate, kinetically inert chromium complexes of desferrioxamine B (*N-cis,cis*, *C-cis,cis* and *trans* isomers), which showed the same inhibition of ^{55}Fe-ferrioxamine B uptake by *Streptomyces pilosus*. This result may indicate either that (i) ferrioxamine B receptor in this microorganism does not discriminate between geometrical isomers, or that (ii) ferrioxamine B complexes are conformationally poorly defined and are not optimal to serve as probes.

In an attempt to form a smaller number of configurational isomers when binding iron(III) and provide sensitive probes for assessing the structural requirements of ferrioxamine B receptor, a set of linear, chiral ferrioxamine B analogs, with reduced flexibility, forming conformationally unique complexes with iron(III) was designed[190]. Reversing the directionality of the hydroxamate group eases the synthesis and allows the introduction of various amino acids with the appropriate chirality, thus the 'retro' derivatives are formed. This reversal is tolerated by biological receptors, since earlier studies had shown that retro-ferrichromes have equal activity and growth promotion of the parent ferrichrome as an iron(III)-carrier[38, 92, 123]. Toward this goal, the spacers between the hydroxamates ligating groups were shortened, so as to cause preferential formation of *cisoidal* complexes and to minimize conformational freedom. In addition, chiral centers were introduced to direct the handedness to either the left- or right-handed chiral sense[190, 191]. The compounds were examined by physicochemical methods to assess iron(III) release kinetics as a sensitive indicator of their coordination properties. Iron(III) release was shown to occur in two rate-limiting processes: a bimolecular ligand exchange step and a monomolecular one which measures the inertness of the complex under given acidic conditions. Both processes showed pronounced dependence on the nature of the amino acid and chain length. The bulkier the side chain and the longer the chain length, the slower the complex dissociation constant and iron(III) exchange rate. The decisive parameter is the transport of siderophore complexes across the membrane.

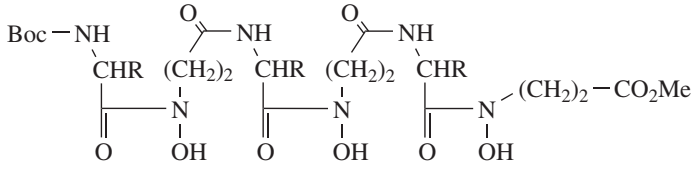

(**146**) R = Me (**148**) R = *i*-Bu (D)
(**147**) R = *i*-Bu (**149**) R = CH_2CONEt_2

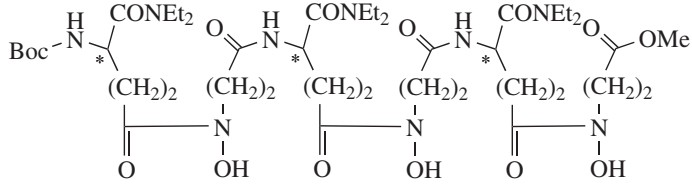

(**150**) L-Glu derivative
(**151**) D-Glu derivative

Compounds **146**–**149** were examined for their iron-transport properties in a series of microorganisms including *P. agglomerans, Hafnia* and *E. coli*. All compounds were active; however, they behaved as ferrioxamine in *H. alvi*, as coprogen in *E. coli* and both as ferrioxamine and coprogen in *P. agglomerans*[192]. In order to increase the differential

selectivity, two additional compounds were prepared: L-Glu (**150**) and D-Glu (**151**). All compounds **146**–**151** were tested for growth promotion in *Pseudomonas putida*[190,191]. Some of the analogs **146**–**149**, derived from alanine, *L*-leucine *D*-leucine and aspartic acid, respectively, showed growth promotion of *Erwinia herbicola* and *Pseudomonas putida*. The higher homologs, however, the L-Glu (**150**) and D-Glu (**151**), showed different behavior in the two organisms. In *Erwinia herbicola*, **150** and **151** simulated ferrioxamine B, while in *Pseudomonas putida* they inhibited ferrioxamine B promoted iron(III) uptake, although with different efficacy. Quite remarkably, **151** adopts the Λ configuration when binding iron(III), and proved more effective than its enantiomer **150**, which forms the Δ configuration as an iron(III) complex. The latter results demonstrate that the ferrioxamine receptor exhibits chiral preference for the Λ-*cis* configuration, in spite of the fact that the natural ferrioxamine B lacks chiral centers.

Based on the results described above, the chiral ferrioxamine analogs can be classified according to their uptake routes. The analogs that act both as ferrioxamine B and coprogen represent broad-range iron(III)-carriers, while others, such as the Glu derivatives, discriminating between different bacteria, correspond to narrow-range iron(III)-carriers.

Attempting to narrow down the range of activity to a specific receptor (FoxA receptor in *Yersinia enterocolitica*), an additional set of chiral ferrioxamine analogs **152**–**155**, modified at the vicinity of the terminal amine, suspected to be involved in receptor recognition was prepared[193]. Of particular interest is the observation that **152** was utilized by the uptake system of ferrioxamine B in *Yersinia enterocolitica* but failed to use the ferrioxamine uptake route in *Pseudomonas putida*, exhibiting therefore species specificity.

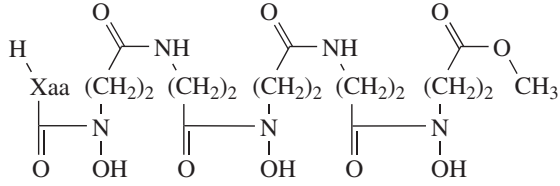

(**152**) Xaa = β-Ala (**154**) Xaa = Cha (Cyclohexyl alanine)
(**153**) Xaa = Phe (**155**) Xaa = Gly

Biomimetic analogs can therefore distinguish between related uptake systems in different microorganisms. A similar trend was described previously with biomimetic ferrichrome analogs (see Section V.B.2.)

The majority of modifications in the linear hydroxamate structures concentrated on modifying the chemical composition and the length of the spacers between the hydroxamate groups. Although accompanied with reduced Fe(III) binding affinities, some analogs showed promising biological activity.

The spacer length between the hydroxamate ligating groups in the natural ferrioxamines seems to present a case of optimal adjustment. Shortening the spacer reduced binding affinities by several orders of magnitude compared to the DFO[190]. When the spacer length and chemical composition are ideal, the backbone amides are optimally oriented for effective interaction with the receptor.

As has been observed, the terminal amine was found to be essential for interaction with the receptor and many modifications on this site lead to either reduced recognition or transport (See Section VI.B. for additional information).

D. The Coprogens

1. Natural coprogens

Coprogen is a linear trihydroxamate produced by *Penicillium* species and *Neurospora crassa* and was first isolated and characterized by Hesseltine and coworkers[194]. Coprogens are predominantly produced by fungi species and frequently several coprogens are produced by the same species. Coprogen is composed of N^{δ}-acyl-N^{δ}-hydroxy-L-ornithine, anhydromevalonic acid and acetic acid.

The coprogens share some similarities and many differences with the ferrioxamines. Like the ferrioxamines they are linear molecules composed of three hydroxamate binding sites that are separated from each other by aliphatic, flexible spacers. Both siderophores form 1:1 octahedral complexes with Fe(III). Yet, coprogens differ from the ferrioxamines by the directionality of the hydroxamate groups, the uneven length and composition of the spacers and the fact that coprogens, being chiral molecules, form well-defined chiral ferric complexes of defined Δ-configuration.

A selected number of coprogens (**156**–**167**), isolated and characterized, are listed in Table 3.

2. Biomimetic coprogens

The coprogen structure can be viewed as an unsymmetrically substituted dipodal diketopiperazine template with one arm containing a single hydroxamate ligating group and the second arm composed of two hydroxamate groups, separated by an extended spacer. Binding Fe(III) to form octahedral complexes requires folding of the terminal hydroxamate inward to the dipodal anchor, toward the binding cavity, thus forming a well-defined geometrical *mer* isomer (Figure 5).

While in the ferrioxamine biomimetics the aim was to reduce the conformational freedom by shortening the length of the spacers to prevent formation of *mer* (*trans*) isomers and favor instead the exclusive formation of the *fac* (*cis*) isomers, in preparing coprogen analogs the *mer* isomers are pursued.

Attempts to prepare biomimetic analogs to coprogen centered on preserving the relative directionality of the hydroxamate groups and mimicking the *mer* geometry around the ferric ion. This can be achieved by utilizing the isopentyl group as a dipodal template and exploiting the folding motif taken from collagen by introducing Gly-Pro or Pro-Gly dipeptide or other β-turn formation building blocks between the two hydroxamate groups on the extended arm. The isopentyl group was shown in related studies to assist in membrane crossing[201,202].

Following this line of design, several biomimetic analogs (**168**–**170**) to coprogen were prepared[203]. While several biomimetic ferrioxamine analogs exhibit coprogen activity in different microorganisms[192] (see Section V.C.2), these coprogen analogs did not show similar microbial activity, neither in *Pseudomonas putida* nor in *Yersinia enterocolitica*.

The low molecular weight and the liphophilic nature of these analogs suggest that they could potentially serve as drugs capable of crossing the Blood Brain Barrier (BBB).

TABLE 3. Natural coprogens and their structural variations

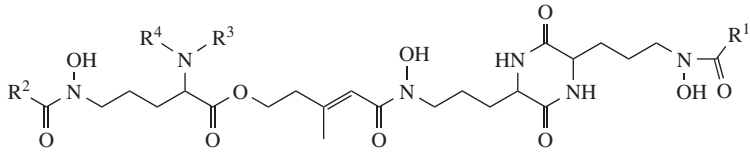

	R^1	R^2	R^3	R^4	Reference
Coprogen **156**	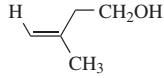	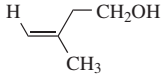	H	Ac	194
Coprogen B **157**	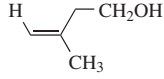	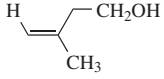	H	H	195
Neocoprogen I (triornicin) **158**	CH_3	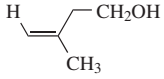	H	Ac	196, 197
Isoneocoprogen I (isotriornicin) **159**	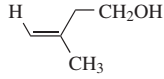	CH_3	H	Ac	196, 197
Neocoprogen II **160**	CH_3	CH_3	H	Ac	197
N^{α}-Dimethyl coprogen **161**	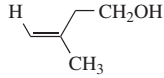	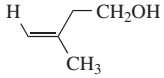	CH_3	CH_3	198
N^{α}-Dimethyl neocoprogen I **162**	CH_3	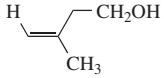	CH_3	CH_3	198
N^{α}-Dimethyl isoneocoprogen I **163**	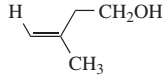	CH_3	CH_3	CH_3	198
Hydroxycoprogen **164**	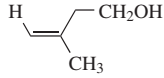	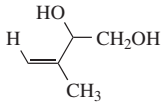	H	Ac	199
Hydroxyneocoprogen I **165**	CH_3	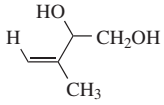	H	Ac	199
Hydroxyisoneo-coprogen I **166**	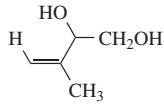	CH_3	H	Ac	199
Palmitoylcoprogen **167**	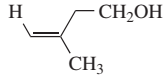	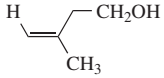	H	*n*-$C_{15}H_{31}CO$ (Palmitoyl)	200

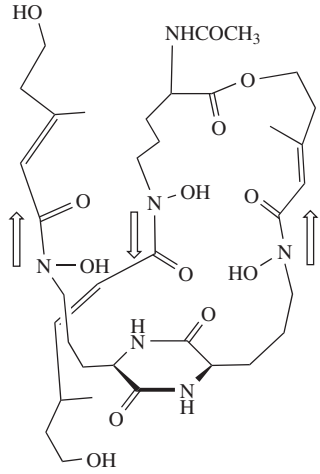

FIGURE 5. Schematic presentation of coprogen structure. The arrows indicate the relative directionality of the hydroxamate ligating groups in forming *mer* (*trans*) configurational isomers

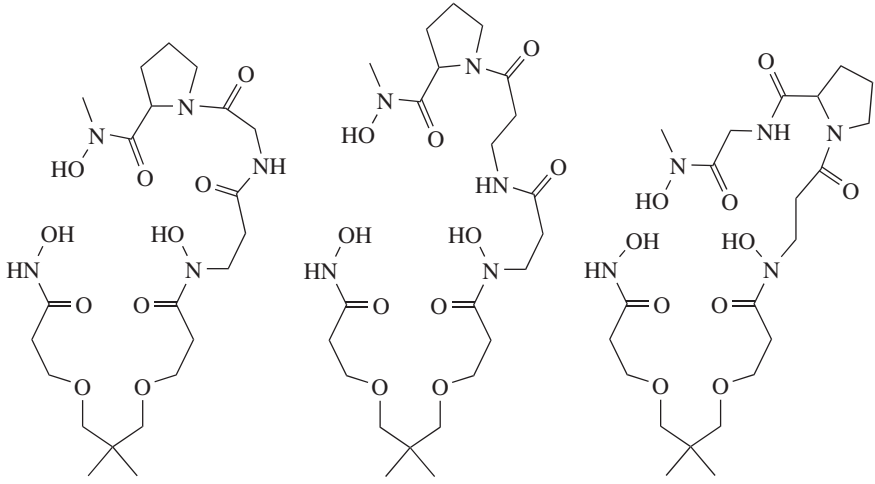

(**168**)
Gly-Pro

(**169**)
β-Ala-Pro

(**170**)
Pro-Gly

Achieving cell permeation may, in turn, reduce the free Fe(III) pool, shifting the cellular equilibrium Fe(II)/Fe(III) toward Fe(III), thereby reducing the level of Fe(II) free to participate in the Fenton reaction (see Section III).

In addition, such chelators, based on the hydroxamic acid bidentate ligand, may diminish the toxic effect of Reactive Oxygen Species (ROS), such as hydroxyl and superoxide radicals, by generating relatively stable nitroxyl radicals[204].

To assess the protective abilities of these chelators, a spontaneously transformed cell line of oligodendroglia origin (OLN 93) was chosen as a model for neural cells. These cells were previously used to demonstrate a remarkable sensitivity to genotoxic stress, culminating in cell death when both divalent iron and H_2O_2 were added to cells[205].

The most potent analog **168** has a protective effect 25-fold higher in oligodendrial cells that were exposed to oxidative stress (Fe(II) and H_2O_2) in comparison to DFO[203]. While analog **168** almost fully protects the cells from oxidative stress (77% increase in cell survival), DFO has a negligible effect (7.5% increase in cell survival). We attribute these differences to the lipophilic character of these synthetic analogs in comparison to the relatively hydrophilic character of DFO. (Partition coefficients of analog **168** and DFO (as free ligands) were determined in water–octanol as 14.5 and 0.8, respectively.)

It is unlikely that the observed protection of analogs **168**–**170** in comparison to DFO is based solely on Fe(III) binding, as the binding constants of all compounds are expected to lie within the same range. Instead, we suggest that the lipophilic character is the key element of these analogs, allowing them to cross the cell membrane and to protect the cells from oxidative stress.

Preliminary studies of compound **168** on a Parkinson animal model showed encouraging results[206].

VI. SIDEROPHORE CONJUGATES

Within each family of biomimetic siderophores it was possible to identify members that have a broad spectrum of microbial activity, members with high species specificity that act either as agonists mimicking the iron transport and promoting microbial growth, or antagonists that specifically target appropriate membrane receptors, binding to them reversibly, but neither transfer iron nor promote microbial growth. (Here we use the term 'agonist' for a siderophore analog that fully mimics the natural compound by acting as a microbial iron(III)-carrier, and the term 'antagonist' for a siderophore analog that competitively binds to the receptor.)

In addition, within each family of synthetic siderophores, it was possible to identify sites suitable for chemical modifications, without altering iron binding or receptor recognition. These sites are appropriate for covalently binding auxiliary functional groups such as fluorescent markers, surface-adhesive functional groups or drugs, thus forming functional, integrated, siderophore conjugates. These biomimetic siderophore conjugates acting as microbial cell-targeting agents open new opportunities in developing novel tools for studying microbial iron uptake, and may find potential application to microbial diagnostics and innovative microbial delivery systems for therapeutics.

The following discussion will concentrate on fluorophore conjugates of ferrichrome and ferrioxamine analogs followed by siderophore surface-adhesive conjugates, presenting alternative, yet complementary approaches to diagnostic methodologies. Finally, several recent directions in siderophore-drug conjugates will be outlined.

A. Natural Fluorescent Siderophores

Pyoverdins and Azotobactin are known examples of natural fluorescent siderophores that have been isolated from *Pseudomonas aeruginosa* and *Azotobacter vinelandii*, respectively[207–209]. Pyoverdin Pa (**171**)[210] and pyoverdin Pa TII (**172**)[211] are members of the pyoverdin family, which are peptide based hexadentate mixed siderophores that consist of a fluorescent chromophore dihydroxyquinoline, which provides a catecholate ligand for Fe(III) coordination in addition to two bidentate hydroxamate ligating groups.

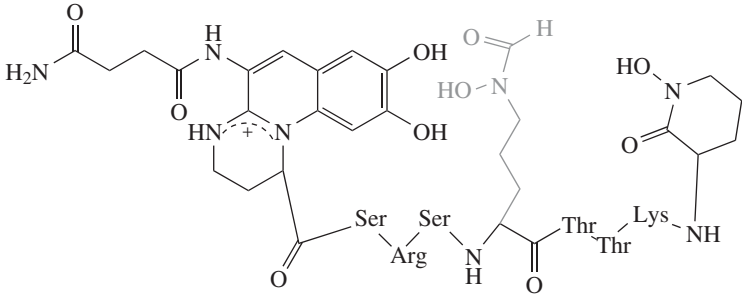

(**171**) Pyoverdin Pa

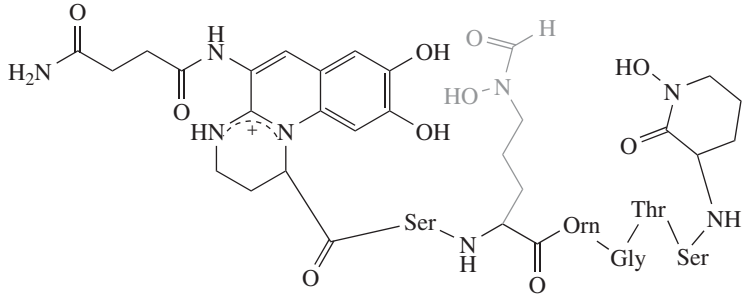

(**172**) Pyoverdin (Pa TII)

Azotobactin is a highly fluorescent hexadentate mixed siderophore containing a pyoverdin-like bidentate ligating chromophore, derived from 2,3-diamino-6,7-dihydroxyquinoline, a hydroxamate and a α-hydroxycarboxylic acid for Fe(III) coordination[212].

B. Biomimetic Siderophore–Fluorophore Conjugates

The observation that the fluorescence of the siderophore–fluorophore conjugate is quenched when binding Fe(III) and restored when iron is removed by a competitive chelator[213–216] prompt their use in monitoring microbial iron(III) uptake, where the appearance of intense fluorescence indicates that the siderophore–fluorophore iron complex (quenched) entered the bacterial cell, delivered its iron, and the iron free fluorescent labeled desferrisiderophore (fluorescent) was excreted back into the medium. Coupling microbial iron uptake with fluorescent signaling provides a rapid and powerful tool in identifying microbial receptors and may have diagnostic potential for detecting and identifying pathogenic microorganisms.

Fluorescence quenching of anthracene by the iron(III) could occur by heavy-atom-induced intersystem crossing, energy transfer or electron transfer. The quenching process follows the Perrin model, for static quenching in compliance with an intramolecular processes involving electron transfer[217–220]. Indeed, close contact between the fluorescent moiety and iron complex is advantageous for electron transfer[221]. For example, the quenching efficiency is higher in **173**, where the fluorophore attached to an extended spacer can

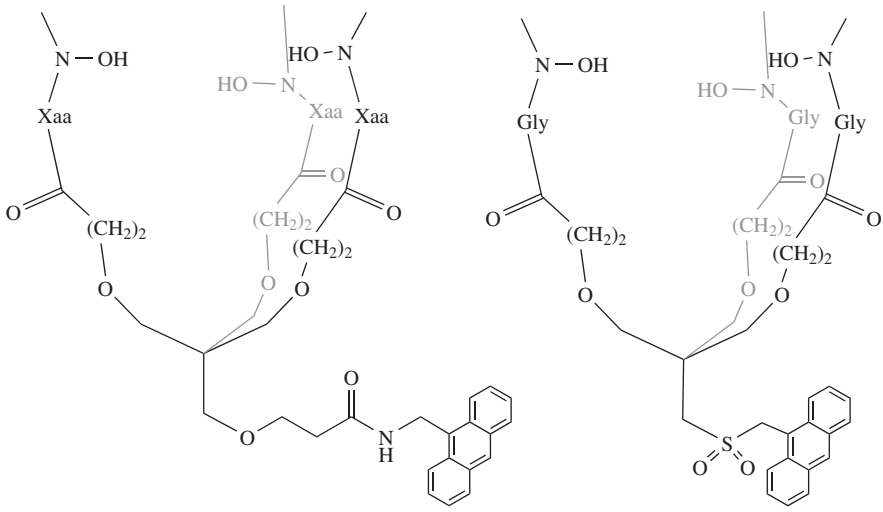

FIGURE 6. Ferrichrome–fluorophore conjugates with an extended spacer (left) and a short spacer (right)

reach the iron(III) center, than in **175** which had only 50% of **173**'s fluorescence even with excess iron.

Biomimetic ferrichrome analogs (precursor of **173** and **174**) contain several potential sites for incorporating a fluorescent marker: (i) the template, (ii) the arms carrying the ligating groups or their projecting side groups. (iii) sometimes the ligating group, as in the natural fluorescent siderophores described above.

Since modifications at the hydroxamate termini or the projecting side groups on the linking arms were not tolerated by the ferrichrome receptor, most of the modifications were carried out at the epical template site (Figure 6).

1. Biological testing

Incubation of *Pseudomonas putida* with anthracene-labeled carbon-base ferrichrome analog Fe(III) complex **173** resulted in cellular iron uptake and the appearance of anthracene fluorescence in the culture medium identical to the ^{55}Fe-ferrichrome uptake. Incubation with the alanyl analog **174** failed to show any significant iron uptake or fluorescence. This is consistent with the tests described above on the unlabeled analogs. Remarkably, other strains such as *Pseudomonas fluorescens* S680 or WCS3742 also did not show any iron uptake or culture fluorescence.

2. Probe selection

A series of analogs with probes of varying size and polarity was prepared to determine the effect on siderophore receptor transport. These include 7-nitrobenz-2-oxa-1,3-diazole (NBD) (**176**–**179**), fluorescein-5-isothiocyanate methyl ether methyl ester (diMe-FITC)

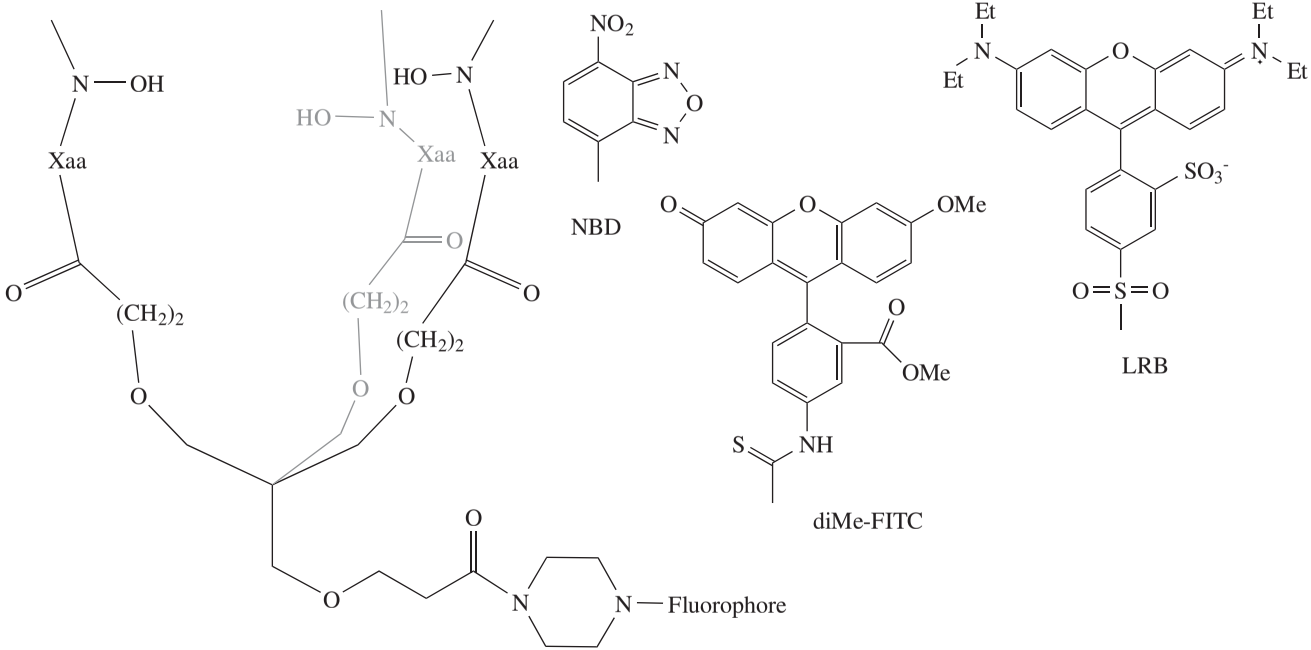

(**176**) Xaa = Gly, Fluorophore = NBD
(**177**) Xaa = Ala, Fluorophore = NBD
(**178**) Xaa = Leu, Fluorophore = NBD
(**179**) Xaa = Phe, Fluorophore = NBD

(**180**) Xaa = Gly, Fluorophore = FITC
(**181**) Xaa = Ala, Fluorophore = FITC

(**182**) Xaa = Gly, Fluorophore = LRB
(**183**) Xaa = Ala, Fluorophore = LRB
(**184**) Xaa = Leu, Fluorophore = LRB

(**180** and **181**) and lissamine rhodamine B (LRB) (**182**–**184**). While NBD and the fluorescein derivative diMe-FITC have similar optical properties but differ in size, the LRB and diMe-FITC are of similar size but differ in polarity (LRB is positively charged). Analogous compounds were prepared by linking various fluorescent probes to the tetrahedral carbon of ferrichrome analogs, via piperazine as a bifunctional linker. This methodology facilitated the insertion of a great variety of fluorescent probes. The fluorescence intensity of these probes was found to be stronger than the autofluorescence of the bacterial culture. The probes' different quenching properties were also examined. The fluorescence emission of NBD and of diMe-FITC are quenched in the presence of iron(III), whereas that of LRB is not. These optical properties enabled both *in vitro* monitoring of iron(III) binding and *in vivo* follow-up of the microbial iron(III) uptake process. The fate of the iron-carriers after iron delivery could be monitored optically by using the quenchable probes, and the iron-uptake pathway in eukaryote cells could be followed using the nonquenchable probe LRB[222].

All the synthesized compounds, regardless of their probe's size or charge, display microbial activity in *P. putida* similar to that of the biomimetic analogs lacking the probe[222]. These results provide an indication that the epical site in the tetrahedral carbon-based templates is available for attachment of chemical moieties without hampering iron(III) coordination and receptor recognition.

In the ferrioxamine family, two approaches were followed: one, based on modifying the amine at the end of the extended tail in the natural ferrioxamine B with an appropriate fluorophore; the second, substituting biomimetic analogs **146**–**155** on either their amino or carboxy termini, to assess their chemical and biological differences. Both approaches were followed and two classes of compounds were prepared with various fluorescent tags.

In the first class, different fluorophores were bound to the amino terminus of ferrioxamine B including NBD, *N*-methylanthranilic acid (MA) and 1-cyanobenz[*f*]isoindole (CBI) to form **185**, **186** and **187**, respectively. The NBD-DFO was examined for the determination of Fe(III) under physiological conditions[223] and monitoring the interaction with ferritin and transferrin.

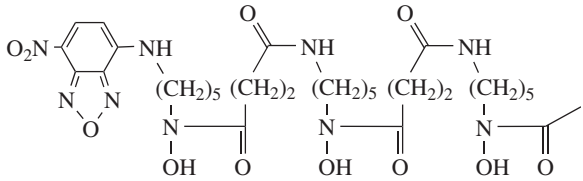

(**185**) NBD-DFO

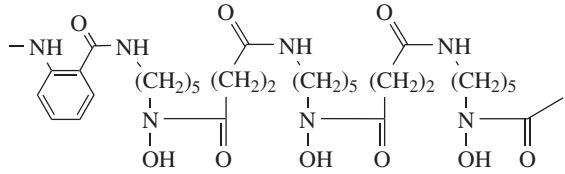

(**186**) MA-DFO

In the second series, the fluorophore NBD was linked to the carboxy terminus via a piperazine spacer as in **188**[224] or via 6-(ethylamino)-*N*-butyl-1,8-naphthalimides and yielded the fluorescently labeled compound **189**[193].

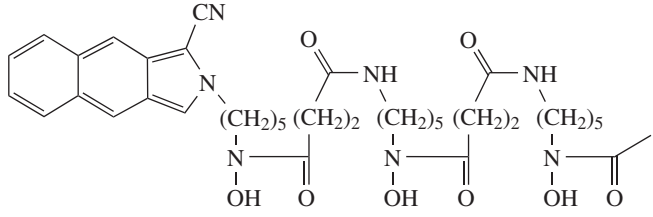

(**187**) NCP-DFO

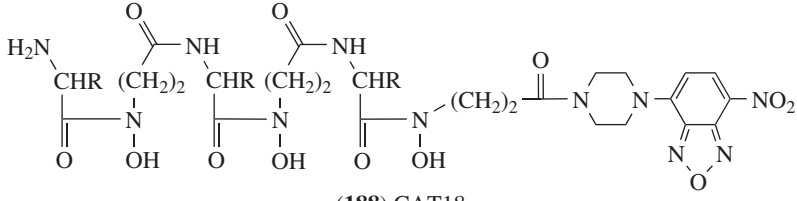

(**188**) CAT18

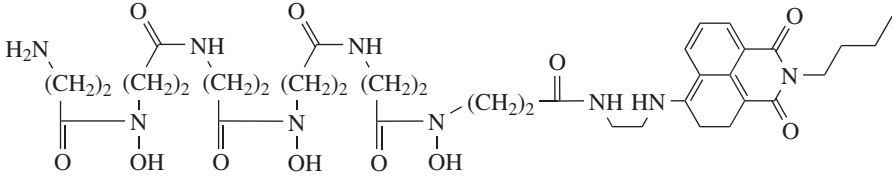

(**189**)

Analogs **185–189** showed similar fluorescent characteristics and fluorescence quenching by binding iron(III), which could be restored by iron removal with a competitor chelator. In contrast, *in vivo* radioactive uptake experiments in *Yersinia enterocolitica* (via FoxA receptor) were greatly altered with a clear advantage for the analogs substituted at the carboxy terminus. Consequently, it was suggested that the amino terminus is essential for recognition and transport, which was verified with X-ray structures of the ferrioxamine B bound to the *E. coli* periplasmic receptor FhuD (PDB entry 1k2v)[83], where this terminal amine is hydrogen-bonded to a receptor residue near the binding site.

Two fluorescent siderophore analogs, one based on ferrichrome **173** and the second on ferrioxamine **188**, were used to study iron transport in the fungus *Ustilago maydis* that has an uptake system for ferrichrome but lacks a defined ferrioxamine receptor. Nevertheless, ferrioxamine can be utilized by the fungus albeit at a slower rate.

Combining fluorescence spectroscopy with fluorescence microscopy, confocal microscopy could be used to elucidate the pathway of siderophore-mediated iron uptake in the fungus *Ustilago maydis,* and visualize this pathway by providing unique fluorescent microscopic images[224]. Using these techniques, clear images of two independent iron-uptake mechanisms have become visualized as well as their cellular compartment localized.

Using fluorescently labeled siderophore analogs, allowed to monitor the time course, as well as the localization, of iron-uptake processes within the fungal cells. A fluorescently labeled ferrichrome analog **182**, which does not exhibit fluorescence quenching upon iron binding, was used to monitor the entry of the labeled ferrichrome analog into the fungal cells. The fluorescence was found intracellularly and later was found concentrated

in two to three vesicles within each cell. The fluorescence of the fluorescently labeled ferrioxamine (FOB) analog CAT18, which is quenched by iron, was visualized around the cell membrane. This fluorescence intensity increased with time, demonstrating that fungal iron uptake from the siderophores involves an extracellular ferric reduction mechanism. Therefore, a biomimetic siderophore–fluorophore conjugate provides powerful tools for direct tracking and discriminating between different pathways of iron uptake in real time and spatial resolution.

A new class of highly sensitive and selective fluorescent molecular systems based on a tripodal carbon structure utilizing tripyrenyl trihydroxamate fluorescent ligand has been prepared (**190**)[225] for environmental monitoring of iron(III). Binding of iron(III) was shown to induce quasi-total fluorescence of the pyrene fluorescence.

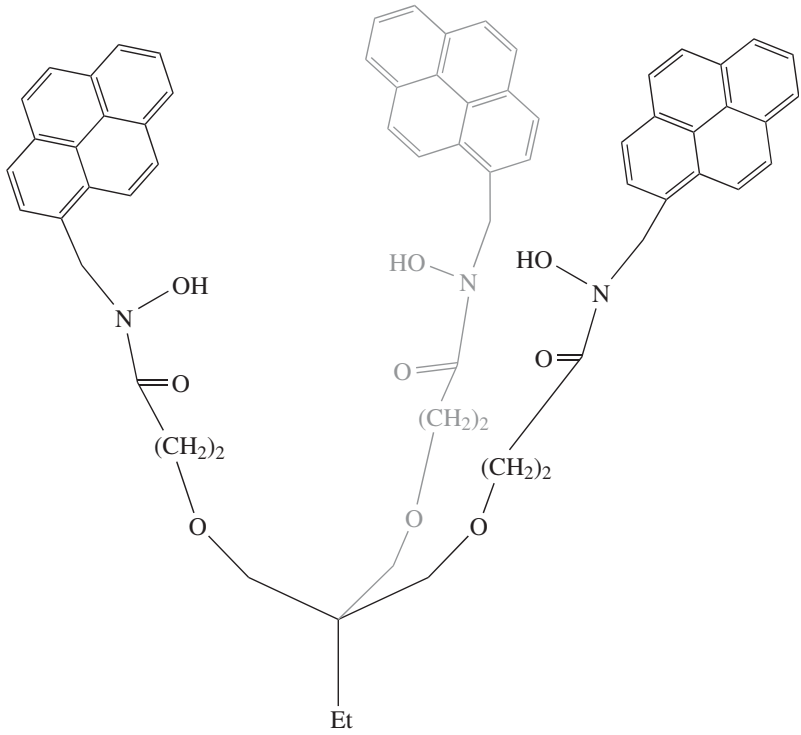

(**190**)

Siderophore–fluorophore conjugates of both ferrichrome and ferrioxamine have been successfully applied to the study of iron transport in a variety of microbial species[224], in transport of iron to plants[226, 227] and in mammalian targets for effective permeation into red blood[214, 223] and liver[228] cells infected with malaria parasite. They have also found application as selective iron sensors, both qualitative and quantitative, for the determination of environmental iron concentration[216]. Recently, double-labeled ferrioxamine analogs were applied to information technology for molecular algebraic computation[229] and molecular logical gates with decision-making capabilities[230].

C. Siderophore Surface-adhesive Conjugates

Siderophore analogs with species-specific properties were covalently attached, via a spacer, to a surface-adhesive functional group, such as thiol, carboxylic acid or biotin, and anchor onto solid surfaces, such as gold[231], glass[232, 233] or polymeric substrates. Upon immersing the coated/modified slide into a solution containing different bacterial strains, only bacteria possessing matching receptors to the tethered siderophore will adhere to the surface, while the other weakly binding strains will be easily washed off. The captured bacteria can be visualized and identified using dyes that stain the cell membrane, fluorescently labeled siderophores (see above) or fluorescently labeled antibodies.

The efficiency of the surface bound siderophores in capturing bacteria was found to depend on the surface-adhesive functional groups, the length of the spacer, the ability to form defined surface layers or monolayers and the topology of the siderophore.

While the thiol groups were found to be suitable for gold surfaces[231], cyclic disulfide systems were preferred[234]. The spacer length was also found to be a critical parameter, as very short linkers produce ill defined layers that improve considerably with increased length. On the other hand, highly organized layers tend to limit the number of bacteria bound to them, whereby extended spacers form a 'brush'-like surface coat and increase bacterial trapping[233, 235].

While tripodal structures were well adjusted in forming trapping layers, the linear ferrioxamine derivative failed to do so, probably due to their need to fold-up when binding iron thereby disrupting the formed layers.

D. Siderophore Drug Conjugates

The most challenging endeavor is the development of siderophore drug conjugates in which a specific siderophore acts as a microbial cell-targeting agent carrying a broad spectrum of active antibiotic into microbial targets within a host. Approaches using siderophore drug conjugates, for developing novel antibiotics, have been extensively explored[236, 237] with increasing successes.

Those siderophores with low molecular weight, nonpeptidal structures are anticipated to be stable to proteolytic enzymatic degradation, and less likely to evoke an immune response. The antibiotic can be selected from commercial sources or from a large arsenal of potential antibiotics with low solubility that were overlooked, or never underwent extensive clinical investigations.

The chemical nature of the linker, its size and bulkiness will determine whether the drug remains attached to the siderophore or is released enzymatically into the cell. The synthesis of conjugates can proceed by derivatization of natural siderophores or by total synthesis.

Today, the limitations are very stringent, including the need to avoid not only potential side effects to the patient, but also resistance-induced influences of antibiotics on patient microbial flora and on those of the surrounding environment. Nevertheless, the feasibility of the siderophore drug-conjugation approach has been verified by the existence of highly powerful antibiotics in nature with albomycin (**191**), salmycin (**192**) and ferrimycin (**193**). Although their mechanism of action is not completely resolved, progress is being made rapidly.

Albomycin, for example, is constructed from a tripeptide iron binding moiety structurally related to ferrichrome that is covalently linked through a serine spacer to a thioribosyl pyrimidine antibiotic[238, 239]. Albomycin exhibits a broad range of antibacterial activity against both Gram-negative and Gram-positive bacteria in exceedingly low MIC values[240]. It is actively transported across the outer membrane of Gram-negative bacteria, into the cytoplasm, where the antibiotic is cleaved off by a peptidase[241, 242].

1. Natural siderophore antibiotics

As reviewed earlier, bacteria have specific transport systems for siderophore–iron complexes. This system can be utilized to internalize molecules that structurally resemble siderophores. In nature, there are several siderophore-based compounds with antibiotic properties, called sideromycins, acting by various routes: (i) causing iron starvation by blocking the iron-transport receptors, (ii) complexing other metals which are metabolically less useful and cause iron starvation and (iii) in conjugation of a toxic compound to a siderophore, leading to its accumulation inside the microbial target cell. The latter group of natural antibiotic siderophores includes albomycins, salmycins and ferrimycins, which are conjugated to toxic compounds.

Albomycins (**191**), based on a linear tripeptide, N^{δ}-hydroxy-N^{δ}-acetylornithine, such as found in ferrichrome, is attached to a toxic moiety, thioribosyl pyrimidine antibiotic, that is believed to inhibit *t*RNA synthetase[238,239] through a serine spacer. Salmycins A to D (**192**) consist of the natural siderophore danoxamine ($n = 5$), a close analog to DFO, conjugated to aminoglycoside moieties and are known to be active against staphylococci and streptococci[243]. Ferrimycin (**193**) mimics the transport properties of ferrioxamine B by its attachment to an antibiotic moiety by an amide bond[244].

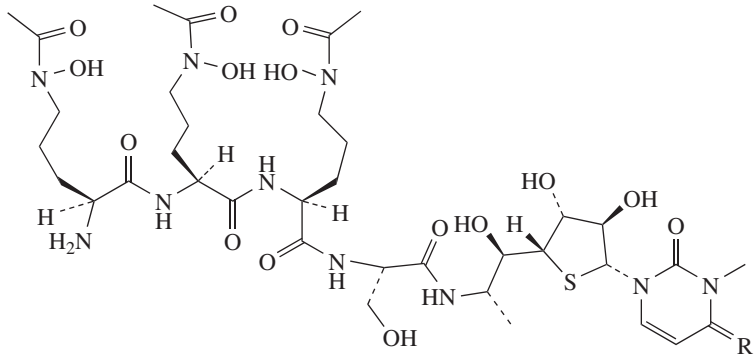

(**191**) Albomycins, R=O, NH or $NCONH_2$

These compounds have not found extensive use in medicine because the exact mode of action is not known and due to the rapid resistance developed against them by microorganisms. It was shown that they select nonpathogenic strains that cannot efficiently compete for iron, though albomycin was found recently to be effective against enterobacteriaceae in mouse models[245].

These conjugated natural antibiotics prompted the search for novel synthetic siderophores that contain a variety of drugs[16,209].

2. Biomimetic siderophore antibiotics

Two distinct approaches can be envisioned in the development of siderophore–drug conjugates. A strategy of drug delivery utilizing the pathogen's own iron-transport system to act as a delivery system has been referred to as the 'Trojan Horse' approach. Examples in which sulfonamides **194**[246], penicillins[247], cephalosporins[135] and other antibiotics[248] attached to DFO which exhibit antibacterial activity were reported.

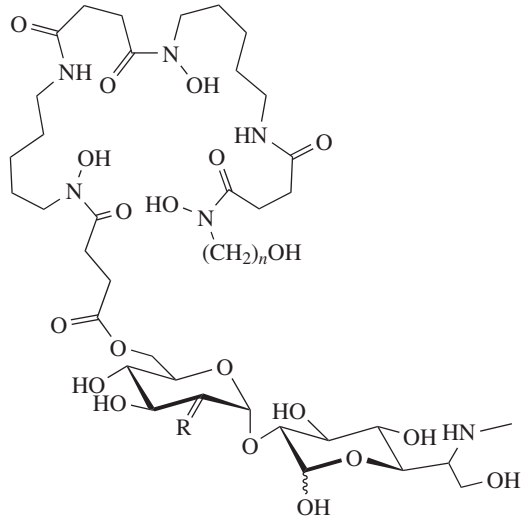

(**192**) Salmycin A–D R = NOH, O or $(OH)_2$, n = 4 or 5

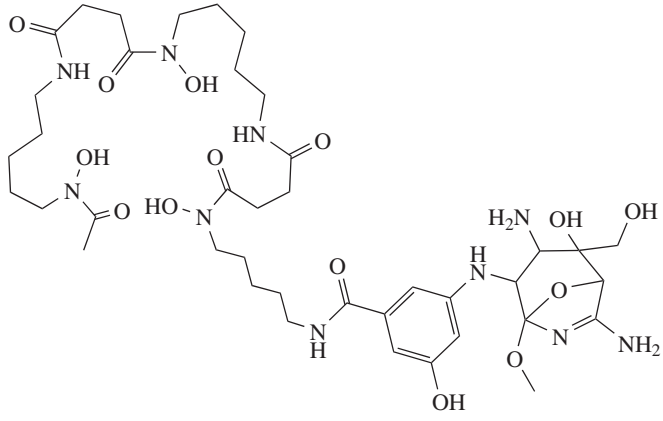

(**193**) Ferrimycin

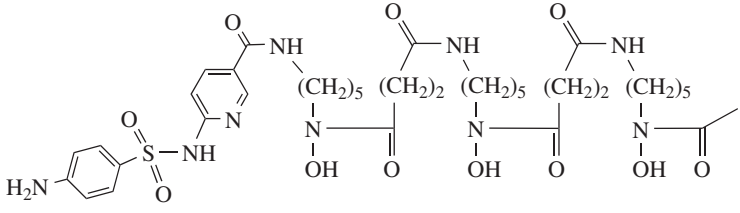

(**194**)

The traditional approach, encouraged and rewarded by pharmaceutical companies, aims toward the development of antimicrobial drugs affecting the broadest range of bacteria possible. On the other hand, there is a persistent request for highly species-specific antimicrobial agents addressing directly microorganisms causing infection. Although advantages and limitations exist for each approach, the latter may considerably slow down the emergence of drug-resistant bacteria strains, where antibiotic overuse was recognized to be the main cause for their development.

Siderophore drug conjugates can be utilized for both approaches. While the natural siderophores show generally low specificity, biomimetic analogs have been consistently improved to exhibit enhanced species specificity.

One of the major difficulties that hampered the development of this field to its full potential is the need to cleave the drug from the siderophore carrier while still in the cell interior. Counting on enzymatic cleavage of sensitive bonds, such as esters, amides or urea linkages, did not meet expectations by being either too slow or insufficiently specific. Alternative approaches, using drugs that are active while bound to the siderophore carrier, were more successful, as was shown in early studies with sulfonamide drugs and many β-lactam antibiotics. However, only a small portion of the antibiotic siderophore conjugates showed stronger activity than the unconjugated drug. The recent elegant approach adopted by Miller and coworkers in utilizing succinyl linkers, as in the natural antibiotic salmolycin, to facilitate internal cleavage as soon as iron is released, is a welcome new direction with great potential. The success in controlled release of the active 5-fluorouridine (5-FU) **195**–**197** by this method was demonstrated by Lu and Miller[249].

The close proximity of the drug to the iron coordination site, and hence to the receptor recognition domain, casts some doubts as to the generality of this approach and to the scope of utilizable drugs.

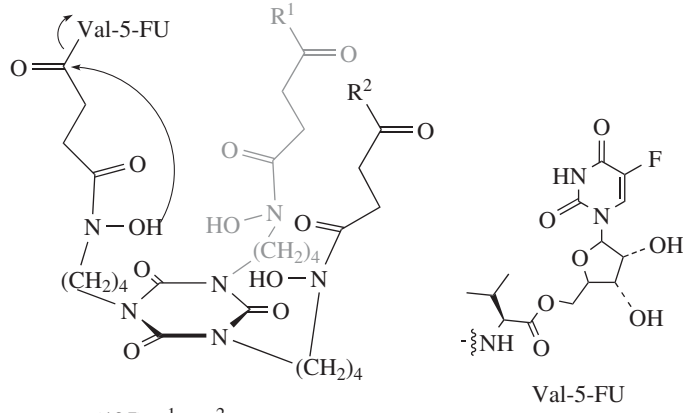

(**195**) $R^1 = R^2 = H$
(**196**) R^1 = Val-5-FU, $R^2 = H$
(**197**) $R^2 = R^3$ = Val-5-FU

VII. BIOMIMETIC SIDEROPHORES IN HEALTH AND DISEASE

The high efficiency and selectivity of the natural siderophores in binding iron(III) inspired attempts to develop siderophore analogs with improved iron-scavenging properties amenable for chelation therapy. A most pertinent example is desferrioxamine B (DFO), where low patient compliance generates the need for developing oral means of administration for

therapeutics associated with iron-overload diseases. These attempts have recently scored several successes with the approval of new drugs and several others in progress. Chelation therapy was also applied to eradicate malaria, a disease causing the greatest threat to tropical populations with great morbidity and mortality, and in which emerging drug-resistant strains have arisen.

Although no remedy has yet been developed, many concentrated efforts are providing profound understanding of the major factors affecting parasite growth and proliferation and means to address the parasite in its erythrocyte host.

A. Iron Overload

Desferrioxamine (DFO-B), the natural siderophore initially isolated from *Streptomyces pilosus*[165], is the only iron chelator currently used for clinical treatment of iron-overload disease such as thalassemia, sickle cell anemia and hemochromatosis[250–252].

Due to their capacity to specifically chelate ferric iron, siderophores have been used for chelation therapy to treat iron overload diseases[253, 254].

Several trisubstituted aromatic compounds were used as a tripodal platform. An interesting example, 1,3,5-benzenetri(acetamidoglycylhydroxamic acid) (BTAMGH) **25**[98], with retro-hydroxamate groups, compared to ferrichrome, showed 10% potency in iron elimination in mice compared to DFO, while its more rigid structural isomer, *N*,*N*′,*N*″-tris[2-(*N*-hydroxycarbamoyl)ethyl]-1,3,5-benzenetricarboxamide (BAMTPH) **26**[99], showed no activity whatsoever. Extending **26** with one methylene group resulted in **27**[98], which showed 20% potency compared to DFO. In addition, methylation of the hydroxamic acid helped prevent degradation of the ligand and increased its donor properties[98].

B. Malaria

Malaria is the cause for approximately 20% of child deaths in Africa and for more than 1 million deaths around the world each year. The appearance and spread of drug resistance of the *Plasmodium falciparum* parasites to common antimalarial drugs, such as chloroquine and hydroxychloroquine, have posed the urgent challenge of developing effective, safe and affordable antimalarial drugs.

Like practically all living organisms, malaria parasites depend on iron for their growth and replication. This property makes them susceptible to iron deprivation, which can be induced by treatment with iron chelators[24, 255], as shown in *in vitro* cultures of *P. falciparum*[215, 256, 257], in animal models of malaria[258–260] and in human trials[261–263] with the clinically approved agent desferrioxamine (DFO). However, despite its activity, DFO lacks the requisite speed of action and therapeutic efficacy to serve as a reliable substitute or additive for the treatment of severe cases of malaria, in particular, multi-drug-resistant strains[264].

One of the major disadvantages of DFO as an antimalarial agent is its slow permeability into parasitized red cells. To overcome this limitation, two classes of compounds with increased lipophilicity were prepared and found to dramatically improve permeability properties[215, 255, 265, 266]. The first group of chelators consists of modified DFO, in which its *N*-terminal was coupled with various hydrophobic moieties. These derivatives showed practically no decrease in the iron(III) binding capacity[214, 266] but greatly improved membrane permeability and affect the growth and replication of intra-erythrocytic parasites. Methylanthranilic-DFO **186**, the least hydrophilic and most membrane-permeable member of the group, reduces parasite proliferation with an IC_{50} of 4 ± 1 μM, while the parent natural DFO-B **93**, the most hydrophilic member of the series, displays the greatest IC_{50} (21 ± 7 μM). Cyclic-DFO (DFO-E) **96** and nitrilo-DFO **198**, *N*-terminal derivatives

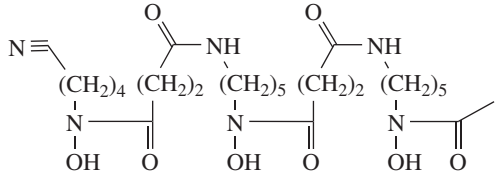

(**198**) Nitrilo-DFO

with intermediate hydrophilicity, have intermediate IC_{50} of 7 ± 2 μM and 17 ± 3 μM, respectively[266].

The second group of hydroxamate-based chelators consists of biomimetic ferrichrome analogs modified by introducing hydrophobic amino acids between the template and the hydroxamic acid binding sites **59**, **60**, **66**, **68**, **70**, **199** and **200**. Since they function to withhold iron from cells in contrast to their original function of iron delivery, they were named 'reversed siderophores' (RSF)[265,267].

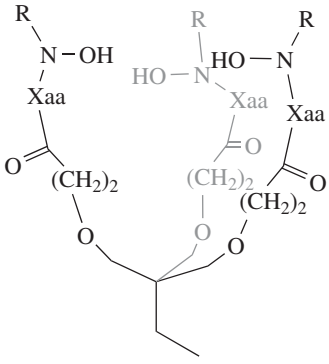

(**59**) R = Me, Xaa = Leu (**68**) R = Me, Xaa = Ala
(**60**) R = Me, Xaa = Pro (**70**) R = Me, Xaa = D-Ala
(**66**) R = Me, Xaa = Ile (**199**) R = Me, Xaa = Phe
(**200**) R = CH_2CH_2COOH, Xaa = None

The antimalarial activity of the synthetic ferrichrome analogs correlated with their lipophilicity, and this antimalarial activity was averted when the chelators were applied as iron(III) complexes. The sites of synthetic ferrichrome action reside in the intra-erythrocytic parasite and not in serum or on normal erythrocyte components. The agents were effective against all stages of parasite growth and against a variety of multi-drug-resistant strains of *Plasmodium falciparum*. The most potent agent of this synthetic ferrichrome series **66** was not toxic to mammalian cells in culture and was 15-fold more potent and 20-fold faster acting than desferrioxamine. The antimalarial activity of the more hydrophobic Phe derivative **199** was found to be 5-fold more effective ($IC_{50} = 0.6$ μM) than **66**[138] (Table 4). Taken in total, these agents constitute a series of promising candidates for future use in malaria chemotherapy.

There is a considerable difference in the antimalarial action of desferrioxamine B (DFO) and the hydrophobic chelators based on ferrichrome analogs. While the former is limited to mature forms in the life cycle of *P. falciparum* (trophozoites and schizonts), the latter effects to a greater extent early developing stages (ring). Therefore, studies explored

TABLE 4. Partition coefficient and antimalarial activity of various RSF derivatives

Compound	Partition coefficient octanol:water [a]	IC_{50} (μM) [b]
DFO	0.74	46
60 (Pro)	0.65	>100
68 (L-Ala)	0.53	62
70 (D-Ala)	0.53	70
59 (Leu)	12.5	22
66 (Ile)	14.0	3
199 (Phe)	40	0.6
200 (Propionic acid)	0.12	275

[a] Partition coefficients were obtained by overnight equilibration of the free RSFs between equal volumes of 1-octanol and saline. Concentrations of ligands in each phase were determined by adding excess iron(III) and measuring the ferric complexes at 430 nm.
[b] IC_{50} values were determined at 48 h by nonlinear least-square fit to sigmoidal functions[268].

the possibility of improving the antimalarial efficacy of iron chelators by using them in various combinations of iron chelators with different speeds of action, stage dependences and degrees of reversibility of effects[269–271].

Experiments performed *in vitro* revealed that in contrast to DFO, which has a major cytotoxic effect only on trophozoites and early schizonts of *P. falciparum*, reversed siderophores have a cytotoxic effect on ring-stage and cytostatic effects on trophozoites and schizonts[215,272]. These observations provided the basis for studying combinations of iron chelators for antimalarial therapy. When DFO is added to malaria parasites cultured in erythrocytes in combination with the more lipophilic and more permeate reversed siderophore **66**, a strong synergistic inhibitory effect on parasite growth is observed[272]. This effect may result from the different speeds of permeation of the two chelators

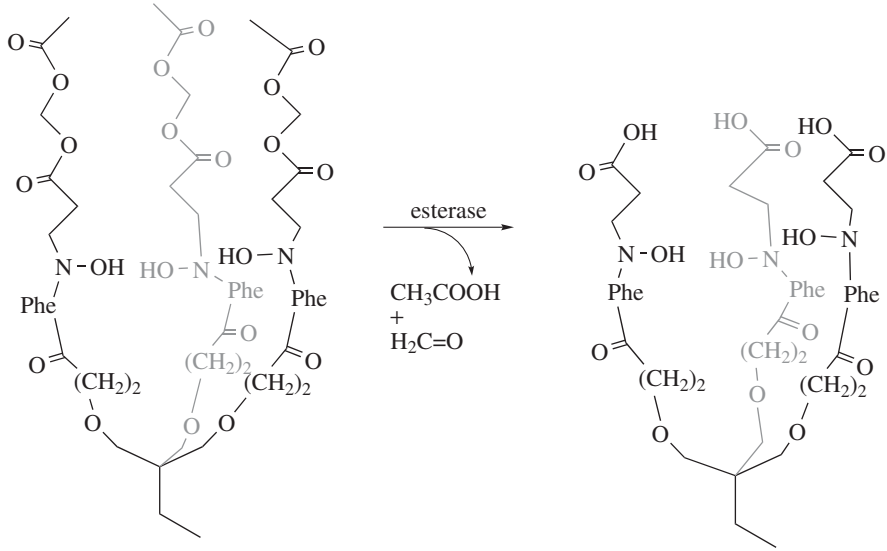

(**201**) (**202**)

through the host and parasite cell membranes. The rapidly permeating lipophilic agent **66** irreversibly affects ring-stage parasites, whereas the slowly permeating but persistent DFO mainly arrests the development of mature parasite stages[272]. It seems, therefore, that with the combination of DFO and reversed siderophores, the parasite is vulnerable at all stages of growth and the antimalarial potential of the drugs increases to beyond the theoretical additive effects[267, 269, 272].

A possible limitation of the RSF is their fast egress from erythrocyte cells. Attempts to extend their duration within the erythrocyte cell were pursued by developing analogs that can convert intracellularly from hydrophobic to hydrophilic congeners. Lipophilic ferrichrome analogs carrying acetoxymethyl ester moieties **201** indeed turn highly hydrophilic (**202**) upon esterase-mediated hydrolysis of the lipophilic termini in laboratory experiments as well as inhibition of parasitemia caused by *Plasmodium falciparum* infection of erythrocyte cells ($IC_{50} = 10\ \mu M$)[228].

A new class of lipophilic ferrichrome analogs carrying acetoxymethyl ester moieties **203** has been synthesized and shown to penetrate rapidly through cell membranes. Intracellular esterase mediated hydrolysis transformed the lipophilic termini from hydrophobic to hydrophilic. The intracellular retention was visualized in hepatoma cells by labeling these analogs with a fluorescent naphthy-imide probe[228]. Their fluorescence analogs retained their fluorescent properties for extended periods in comparison to hydrophobic derivatives **204** lacking the cleavable substituents.

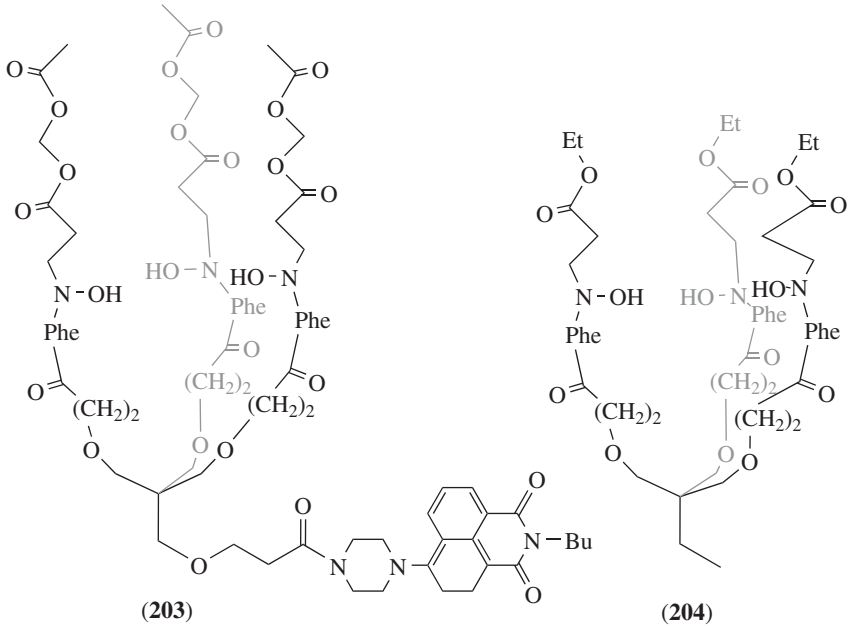

(**203**) (**204**)

VIII. ACKNOWLEDGMENTS

The authors thank Miss Jenny Kolsenik for her skillful artwork. Financial support from the G. M. J. Schmidt Minnerva Center on supermolecular architecture, the Israel Science Foundation, the Helen and Martin Kimmel center for molecular design and the Kimmelman Center for Macromolecular Assemblies are greatly acknowledged. A. S. Holds the Siegfried and Irma Ullman Professorial Chair.

IX. REFERENCES

1. V. Braun, *Contrib. Microbiol.*, **12**, 210 (2005).
2. C. Ratledge and L. G. Dover, *Annu. Rev. Microbiol.*, **54**, 881 (2000).
3. G. Winkelmann, D. van der Helm and J. B. Neilands, *Iron Transport in Microbes, Plants, and Animals*, VCH, Weinheim, New York, 1987.
4. J. B. Neilands, *Annu. Rev. Nutr.*, **1**, 27 (1981).
5. C. F. Earhart, in *The Desk Encyclopedia of Microbiology* (Eds M. Schaechter and J. Lederberg), Elsevier, Academic Press, San Diego, 2003, p. 637.
6. R. Chakraborty, E. Storey and D. van der Helm, *Biometals*, **20**, 263 (2007).
7. J. H. Crosa, A. R. Mey and S. M. Payne, *Iron Transport in Bacteria*, 1st edn, American Society for Microbiology, Washington, DC, 2004.
8. L. L. Barton and J. Abadia, *Iron Nutrition in Plants and Rhizospheric Microorganisms*, Springer, Dordrecht, 2006, p. 477.
9. C. Hershko, *Iron Chelation Therapy*, Kluwer Academic/Plenum, New York, 2002.
10. D. M. Templeton, *Molecular and Cellular Iron Transport*, CRC Press, New York, 2002, p. 848.
11. R. Crichton and J. R. Boelaert, *Inorganic biochemistry of iron metabolism : from molecular mechanisms to clinical consequences*, Second Edition, John Wiley & Sons, Ltd., Chichester, 2001.
12. G. Winkelmann, *Microbial Transport Systems*, Wiley-VCH, Weinheim, 2001.
13. H. Drechsel and G. Jung, *J. Pept. Sci.*, **4**, 147 (1998).
14. A. Butler, *Biometals,* **18**, 369 (2005).
15. J. B. Neilands, *J. Biol. Chem.*, **270**, 26723 (1995).
16. J. M. Roosenberg, Y.-M. Lin, Y. Lu and M. J. Miller, *Curr. Med. Chem.*, **7**, 159 (2000).
17. J. H. Crosa and C. T. Walsh, *Microbiol. Mol. Biol. Rev.*, **66**, 223 (2002).
18. H. Boukhalfa and A. L. Crumbliss, *Biometals,* **15**, 325 (2002).
19. K. N. Raymond, E. A. Dertz and S. S. Kim, *Proc. Natl. Acad. Sci. U.S.A.*, **100**, 3584 (2003).
20. V. Braun and H. Killmann, *Trends Biochem. Sci.*, **24**, 104 (1999).
21. D. S. Kalinowski and D. R. Richardson, *Pharmacol. Rev.*, **57**, 547 (2005).
22. J. A. Gaasch, P. R. Lockman, W. J. Geldenhuys, D. D. Allen and C. J. van der Schyf, *Neurochem. Res.*, **32**, 1196 (2007).
23. P. Ponka, *Ann. N. Y. Acad. Sci.*, **1012**, 267 (2004).
24. Z. I. Cabantchik, H. Glickstein, J. Golenser, M. Loyevsky and A. Tsafack, *Acta Haematol.*, **95**, 70 (1996).
25. G. F. Mabeza, M. Loyevsky, V. R. Gordeuk and G. Weiss, *Pharmacol. Ther.*, **81**, 53 (1999).
26. J. D. Kemp, *Histol. Histopathol.*, **12**, 291 (1997).
27. S. Benini, W. R. Rypniewski, K. S. Wilson, S. Miletti, S. Ciurli and S. Mangani, *J. Biol. Inorg. Chem.*, **5**, 110 (2000).
28. R. Gendron, D. Grenier, T. Sorsa, V. J. Uitto and D. Mayrand, *J. Periodont. Res.*, **34**, 50 (1999).
29. B. Kurzak, H. Kozlowski and E. Farkas, *Coord. Chem. Rev.*, **114**, 169 (1992).
30. A. L. Crumbliss, in *Handbook of Microbial Iron Chelates* (Ed. G. Winkelmann), CRC Press, Boca Raton, 1991, p. 177.
31. B. F. Matzanke, G. Mueller-Matzanke and K. N. Raymond, in *Iron Carriers and Iron Proteins, Vol. 5* (Ed. T. M. Loehr), VCH, New York, 1989, p. 1.
32. K. N. Raymond, G. Muller and B. F. Matzanke, in *Topics in Current Chemistry* (Ed. F. L. Boschk), Springer-Verlag, Berlin, 1984, p. 49.
33. R. C. Hider, in *Structure and Bonding (Siderophores from microorganisms and plants), Vol. 58* (Eds M. J. Clarke, J. A. Ibers, D. M. P. Mingos, G. A. Palmer, P. J. Sadler and R. J. P. Williams), Springer-Verlag, Berlin, 1984, p. 25.
34. D. van der Helm and G. Winkelmann, in *Metal Ions in Fungi* (Eds G. Winkelmann and D. R. Winge), CRC Press, Boca Raton, 1994, p. 39.
35. A. M. Albrecht-Gary and A. L. Crumbliss, *Met. Ions Biol. Syst.*, **35**, 239 (1998).
36. R. Codd, *Coord. Chem. Rev.*, **252**, 1387 (2008).

37. Y. Tor, J. Libman, A. Shanzer, C. E. Felder and S. Lifson, *J. Am. Chem. Soc.*, **114**, 6661 (1992).
38. A. Shanzer, J. Libman, R. Lazar, Y. Tor and T. Emery, *Biochem. Biophys. Res. Commun.*, **157**, 389 (1988).
39. A. Shanzer, J. Libman, P. Yakirevitch, Y. Hadar, Y. Chen and E. Jurkevitch, *Chirality,* **5**, 359 (1993).
40. G. Winkelmann, *Handbook of Microbial Iron Chelates*, 1st edn, CRC Press, Boca Raton, 1991.
41. E. Jurkevitch, Y. Hadar, Y. Chen, J. Libman and A. Shanzer, *J. Bacteriol.*, **174**, 78 (1992).
42. J. B. Neilands, *Annu. Rev. Biochem.*, **50**, 715 (1981).
43. J. DiGuiseppi and I. Fridovich, *J. Biol. Chem.*, **257**, 4046 (1982).
44. J. B. Neilands, in *Structure and Bonding (Siderophores from microorganisms and plants), Vol. 58* (Eds M. J. Clarke, J. A. Ibers, D. M. P. Mingos, G. A. Palmer, P. J. Sadler and R. J. P. Williams), Springer-Verlag, Berlin, 1984, p. 1.
45. G. Winkelmann, *Biochem. Soc. Trans.*, **30**, 691 (2002).
46. J. R. Chipperfield and C. Ratledge, *Biometals,* **13**, 165 (2000).
47. P. T. Lieu, M. Heiskala, P. A. Peterson and Y. Yang, *Mol. Aspects Med.*, **22**, 1 (2001).
48. H. J. H. Fenton, *J. Chem. Soc., Trans.*, **65**, 899 (1894).
49. D. R. Lloyd and D. H. Phillips, *Mutat. Res.*, **424**, 23 (1999).
50. V. Coulanges, P. Andre, O. Ziegler, L. Buchheit and D. J. M. Vidon, *Infect. Immun.*, **65**, 2778 (1997).
51. C. N. Cornelissen and P. F. Sparling, *Methods Enzymol.*, **235**, 356 (1994).
52. A. G. Torres and S. M. Payne, *Mol. Microbiol.*, **23**, 825 (1997).
53. A. H. T. Hissen, J. M. T. Chow, L. J. Pinto and M. M. Moore, *Infect. Immun.*, **72**, 1402 (2004).
54. M. J. Bjorn, B. H. Iglewski, S. K. Ives, J. C. Sadoff and M. L. Vasil, *Infect. Immun.*, **19**, 785 (1978).
55. S. B. Calderwood and J. J. Mekalanos, *J. Bacteriol.*, **169**, 4759 (1987).
56. C. Wolz, K. Hohloch, A. Ocaktan, K. Poole, R. W. Evans, N. Rochel, A. M. Albrecht-Gary, M. A. Abdallah and G. Doring, *Infect. Immun.*, **62**, 4021 (1994).
57. I. G. Obrien, G. B. Cox and F. Gibson, *Biochim. Biophys. Acta,* **237**, 537 (1971).
58. T. J. Brickman and M. A. Mcintosh, *J. Biol. Chem.*, **267**, 12350 (1992).
59. L. Escolar, J. Perez-Martin and V. De Lorenzo, *J. Bacteriol.*, **181**, 6223 (1999).
60. K. Postle, *J. Bioenerg. Biomembr.*, **25**, 591 (1993).
61. V. Braun, *FEMS Microbiol. Rev.*, **16**, 295 (1995).
62. M. Miethke and M. A. Marahiel, *Microbiol. Mol. Biol. Rev.*, **71**, 413 (2007).
63. V. Braun and K. Hantke, in *Handbook of Microbial Iron Chelates*, 1st edn (Ed. G. Winkelmann), CRC Press, Boca Raton, 1991, p. 107.
64. J. S. Martinez, G. P. Zhang, P. D. Holt, H. T. Jung, C. J. Carrano, M. G. Haygood and A. Butler, *Science,* **287**, 1245 (2000).
65. A. F. Vergne, A. J. Walz and M. J. Miller, *Nat. Prod. Rep.*, **17**, 99 (2000).
66. M. A. Fischbach, H. N. Lin, D. R. Liu and C. T. Walsh, *Nat. Chem. Biol.*, **2**, 132 (2006).
67. R. Breslow, *Chem. Soc. Rev.*, **1**, 553 (1972).
68. M. Fridkin and A. Patchornik, *Annu. Rev. Biochem.*, **43**, 419 (1974).
69. G. Winkelmann and V. Braun, *FEMS Microbiol. Lett.*, **11**, 237 (1981).
70. J. B. Neilands, T. J. Erickson and W. H. Rastetter, *J. Biol. Chem.*, **256**, 3831 (1981).
71. IUPAC-IUB Joint Commission on Biochemical Nomenclature (JCBN), *Eur. J. Biochem.*, **138**, 9 (1984).
72. J. H. Jones, *J. Pept. Sci.*, **5**, 465 (1999).
73. S. Lifson, *NATO Adv. Stud. Inst., Ser. A: Life Sci.*, **45**, 359 (1982).
74. C. E. Felder and A. Shanzer, *Biopolymers,* **68**, 407 (2003).
75. C. E. Felder, A. Shanzer and S. Lifson, *J. Comput. Chem.*, **5**, 170 (1984).
76. D. van der Helm, M. A. F. Jalal and M. B. Hossain, in *Iron Transport in Microbes, Plants, and Animals* (Eds G. Winkelmann, D. van der Helm and J. B. Neilands), VCH Verlagsgesellschaft mbH, Weinheim, 1987, p. 135.
77. A. L. Crumbliss, *Coord. Chem. Rev.*, **105**, 155 (1990).

78. J. B. Neilands, *J. Am. Chem. Soc.*, **74**, 4846 (1952).
79. D. van der Helm, J. R. Baker, D. L. Engwilmot, M. B. Hossain and R. A. Loghry, *J. Am. Chem. Soc.*, **102**, 4224 (1980).
80. M. J. Miller, J. A. Mckee, A. A. Minnick and E. K. Dolence, *Biol. Met.*, **4**, 62 (1991).
81. K. P. Locher, B. Rees, R. Koebnik, A. Mitschler, L. Moulinier, J. P. Rosenbusch and D. Moras, *Cell,* **95**, 771 (1998).
82. A. D. Ferguson, E. Hofmann, J. W. Coulton, K. Diederichs and W. Welte, *Science,* **282**, 2215 (1998).
83. http://www.rcsb.org/pdb.
84. S. Lifson, C. E. Felder, J. Libman and A. Shanzer, *NATO Adv. Stud. Inst., Ser. C. Math. Phys. Sci.*, **426**, 349 (1994).
85. H. Mor, Y. Kashman, G. Winkelmann and I. Barash, *Biometals,* **5**, 213 (1992).
86. M. Llinas and J. B. Neilands, *Biophys. Struct. Mech.*, **2**, 105 (1976).
87. T. Emery, *Biochim. Biophys. Acta,* **629**, 382 (1980).
88. W. Keller-Schierlein, *Helv. Chim. Acta,* **46**, 1920 (1963).
89. A. Zalkin, J. D. Forrester and D. H. Templeton, *Science,* **146**, 261 (1964).
90. M. Llinas, M. P. Klein and J. B. Neilands, *Int. J. Pept. Protein Res.*, **4**, 157 (1972).
91. M. A. Jalal, R. Mocharla, C. L. Barnes, M. B. Hossain, D. R. Powell, D. L. Eng-Wilmot, S. L. Grayson, B. A. Benson and D. van der Helm, *J. Bacteriol.*, **158**, 683 (1984).
92. T. Emery, L. Emery and R. K. Olsen, *Biochem. Biophys. Res. Commun.*, **119**, 1191 (1984).
93. T. Emery and L. Emery, *Biochem. Biophys. Res. Commun.*, **50**, 670 (1973).
94. C. Y. Ng, S. J. Rodgers and K. N. Raymond, *Inorg. Chem.*, **28**, 2062 (1989).
95. K. Abudari and K. N. Raymond, *Inorg. Chem.*, **30**, 519 (1991).
96. M. Seitz, M. D. Pluth and K. N. Raymond, *Inorg. Chem.*, **46**, 351 (2007).
97. B. H. Lee, M. J. Miller, C. A. Prody and J. B. Neilands, *J. Med. Chem.*, **28**, 317 (1985).
98. A. E. Martell, R. J. Motekaitis, I. Murase, L. F. Sala, R. Stoldt, C. Y. Ng, H. Rosenkrantz and J. J. Metterville, *Inorg. Chim. Acta*, **138**, 215 (1987).
99. I. Yoshida, I. Murase, R. J. Motekaitis and A. E. Martell, *Can. J. Chem.*, **61**, 2740 (1983).
100. B. H. Lee, M. J. Miller, C. A. Prody and J. B. Neilands, *J. Med. Chem.*, **28**, 323 (1985).
101. S. Ramurthy and M. J. Miller, *J. Org. Chem.*, **61**, 4120 (1996).
102. A. J. Cumber and W. C. J. Ross, *Chem. Biol. Interact.*, **17**, 349 (1977).
103. H. M. Coley, N. Brooks, D. H. Phillips, A. Hewer, T. C. Jenkins, M. Jarman and I. R. Judson, *Biochem. Pharmacol.*, **49**, 1203 (1995).
104. M. A. Esteves, M. C. T. Vaz, M. L. S. S. Goncalves, E. Farkas and M. A. Santos, *J. Chem. Soc., Dalton Trans.*, 2565 (1995).
105. M. Gaspar, R. Grazina, A. Bodor, E. Farkas and M. A. Santos, *J. Chem. Soc., Dalton Trans.*, 799 (1999).
106. M. Gaspar, M. A. Santos, K. Krauter and G. Winkelmann, *Biometals,* **12**, 209 (1999).
107. S. K. Sharma, M. J. Miller and S. M. Payne, *J. Med. Chem.*, **32**, 357 (1989).
108. J. D. Glennon, S. Hutchinson, S. J. Harris, A. Walker, M. A. McKervey and C. C. McSweeney, *Anal. Chem.*, **69**, 2207 (1997).
109. S. Hutchinson, G. A. Kearney, E. Horne, B. Lynch, J. D. Glennon, M. A. Mckervey and S. J. Harris, *Anal. Chim. Acta,* **291**, 269 (1994).
110. U. Lesinska and M. Bochenska, *Synthesis (Stuttg.),* 2671 (2006).
111. B. Boulet, C. Bouvier-Capely, C. Cossonnet and G. Cote, *Solvent Extr. Ion Exc.*, **24**, 319 (2006).
112. B. Boulet, C. Bouvier-Capely, G. Cote, L. Poriel and C. Cossonnet, *J. Alloy Compd.*, **444**, 526 (2007).
113. B. Boulet, L. Joubert, G. Cote, C. Bouvier-Capely, C. Cossonnet and C. Adamo, *J. Phys. Chem. A,* **110**, 5782 (2006).
114. K. Matsumoto, T. Ozawa, K. Jitsukawa, H. Einaga and H. Masuda, *Inorg. Chem.*, **40**, 190 (2001).
115. K. Matsumoto, T. Ozawa, K. Jitsukawa and H. Masuda, *Inorg. Chem.*, **43**, 8538 (2004).
116. K. Matsumoto, N. Suzuki, T. Ozawa, K. Jitsukawa and H. Masuda, *Eur. J. Inorg. Chem.*, 2481 (2001).

117. K. Matsumoto, T. Ozawa, K. Jitsukawa, H. Einaga and H. Masuda, *Chem. Commun.*, 978 (2001).
118. A. Tsubouchi, L. Shen, Y. Hara and M. Akiyama, *New J. Chem.*, **25**, 275 (2001).
119. A. Bagg and J. B. Neilands, *Microbiol. Rev.*, **51**, 509 (1987).
120. Y. Tor, J. Libman, A. Shanzer, C. E. Felder and S. Lifson, *J. Chem. Soc., Chem. Commun.*, 749 (1987).
121. Y. Tor, J. Libman, A. Shanzer, C. E. Felder and S. Lifson, *J. Am. Chem. Soc.*, **114**, 6653 (1992).
122. Y. Tor, J. Libman, A. Shanzer and S. Lifson, *J. Am. Chem. Soc.*, **109**, 6517 (1987).
123. Y. Tor, J. Libman and A. Shanzer, *J. Am. Chem. Soc.*, **109**, 6518 (1987).
124. Y. Tor, A. Shanzer and A. Scherz, *Inorg. Chem.*, **29**, 4096 (1990).
125. I. Dayan, J. Libman, Y. Agi and A. Shanzer, *Inorg. Chem.*, **32**, 1467 (1993).
126. A. Shanzer, J. Libman and S. Lifson, *Pure Appl. Chem.*, **64**, 1421 (1992).
127. A. Shanzer, J. Libman, R. Lazar and Y. Tor, *Pure Appl. Chem.*, **61**, 1529 (1989).
128. J. Libman, Y. Tor and A. Shanzer, *J. Am. Chem. Soc.*, **109**, 5880 (1987).
129. M. Akiyama, Y. Hara and H. Gunji, *Chem. Lett.*, 225 (1995).
130. Y. Hara, L. T. Shen, A. Tsubouchi, M. Akiyama and K. Umemoto, *Inorg. Chem.*, **39**, 5074 (2000).
131. A. Zalkin, J. D. Forrester and D. H. Templeton, *J. Am. Chem. Soc.*, **88**, 1810 (1966).
132. Y.-M. Lin, M. J. Miller and U. Mollmann, *Biometals,* **14**, 153 (2001).
133. E. K. Dolence, A. A. Minnick, C. E. Lin, M. J. Miller and S. M. Payne, *J. Med. Chem.*, **34**, 968 (1991).
134. E. K. Dolence, C. E. Lin, M. J. Miller and S. M. Payne, *J. Med. Chem.*, **34**, 956 (1991).
135. A. A. Minnick, J. A. Mckee, E. K. Dolence and M. J. Miller, *Antimicrob. Agents Chemother.*, **36**, 840 (1992).
136. H. Weizman and A. Shanzer, *Chem. Commun.*, 2013 (2000).
137. R. C. Scarrow, D. L. White and K. N. Raymond, *J. Am. Chem. Soc.*, **107**, 6540 (1985).
138. A. Tsafack, J. Libman, A. Shanzer and Z. I. Cabantchik, *Antimicrob. Agents Chemother.*, **40**, 2160 (1996).
139. G. Zanninelli, H. Glickstein, W. Breuer, P. Milgram, P. Brissot, R. C. Hider, A. M. Konijn, J. Libman, A. Shanzer and Z. I. Cabantchik, *Mol. Pharmacol.*, **51**, 842 (1997).
140. B. Tse and Y. Kishi, *J. Am. Chem. Soc.*, **115**, 7892 (1993).
141. M. Schnabelrauch, D. A. M. Egbe, L. Heinisch, R. Reissbrodt and U. Mollmann, *Biometals,* **11**, 243 (1998).
142. S. Dhungana, S. Heggemann, L. Heinisch, U. Mollmann, H. Boukhalfa and A. L. Crumbliss, *Inorg. Chem.*, **40**, 7079 (2001).
143. S. Heggemann, M. Schnabelrauch, D. Klemm, U. Mollmann, R. Reissbrodt and L. Heinisch, *Biometals,* **14**, 1 (2001).
144. P. Gebhardt, A. L. Crumbliss, M. J. Miller and U. Mollmann, *Biometals,* **21**, 41 (2008).
145. K. A. Mies, P. Gebhardt, U. Mollmann and A. L. Crumbliss, *J. Inorg. Biochem.*, **102**, 850 (2008).
146. S. Dhungana, J. M. Harrington, P. Geblhardt, U. Mollmann and A. L. Crumbliss, *Inorg. Chem.*, **46**, 8362 (2007).
147. S. Heggemann, U. Mollmann, P. Gebhardt and L. Heinisch, *Biometals,* **16**, 539 (2003).
148. S. Dhungana, S. Heggemann, P. Gebhardt, U. Mollmann and A. L. Crumbliss, *Inorg. Chem.*, **42**, 42 (2003).
149. H. Weizman, J. Libman and A. Shanzer, *J. Am. Chem. Soc.*, **120**, 2188 (1998).
150. G. Winkelmann, in *Iron Transport in Bacteria*, 1st edn (Eds J. H. Crosa, A. R. Mey and S. M. Payne), American Society for Microbiology, Washington, DC, 2004, p. 437.
151. H. Bickel, R. Bosshardt, E. Gaumann, P. Reusser, E. Vischer, W. Vofser, A. Wettstein and H. Zahner, *Helv. Chim. Acta,* **43**, 2118 (1960).
152. G. W. Keller-Schierlein and V. Prelog, *Helv. Chim. Acta,* **45**, 590 (1962).
153. R. Kachadourian, S. Chuilon, C. Merienne, G. Kunesch and A. Deroussent, *Supramol. Chem.*, **8**, 301 (1997).
154. R. C. Hider, S. Singh and J. B. Porter, *Proc. R. Soc. Edinburgh, Sect. B*, **99**, 137 (1992).

155. P. Baret, C. G. Beguin, H. Boukhalfa, C. Caris, J. P. Laulhere, J.-L. Pierre and G. Serratrice, *J. Am. Chem. Soc.*, **117**, 9760 (1995).
156. G. Faa and G. Crisponi, *Coord. Chem. Rev.*, **184**, 291 (1999).
157. J. B. Galey, O. Destree, J. Dumats, S. Genard and P. Tachon, *J. Med. Chem.*, **43**, 1418 (2000).
158. J. Leong and N. Raymond, *J. Am. Chem. Soc.*, **97**, 293 (1975).
159. M. B. Hossain, M. A. F. Jalal and D. van der Helm, *Acta Crystallogr., Sect. C,* **42**, 1305 (1986).
160. D. van der Helm and M. Poling, *J. Am. Chem. Soc.*, **98**, 82 (1976).
161. M. B. Hossain, D. van der Helm and M. Poling, *Acta Crystallogr., Sect. B,* **39**, 258 (1983).
162. M. B. Hossain, M. A. F. Jalal, D. van der Helm, K. Shimizu and M. Akiyama, *J. Chem. Crystallogr.*, **28**, 53 (1998).
163. S. Dhungana, P. S. White and A. L. Crumbliss, *J. Biol. Inorg. Chem.*, **6**, 810 (2001).
164. W. Keller-Schierlein, V. Prelog and H. Zahner, *Fortschr. Chem. Org. Naturst.*, **22**, 279 (1964).
165. H. Bickel, G. E. Hall, W. Keller-Schierlein, V. Prelog, E. Vischer and A. Wettstein, *Helv. Chim. Acta,* **43**, 2129 (1960).
166. W. Keller-Schierlein, P. Mertens, V. Prelog and A. Walser, *Helv. Chim. Acta,* **48**, 710 (1965).
167. A. M. Zawadzka, F. P. J. Vandecasteele, R. L. Crawford and A. J. Paszczynski, *Can. J. Microbiol.*, **52**, 1164 (2006).
168. R. Reissbrodt, W. Rabsch, A. Chapeaurouge, G. Jung and G. Winkelmann, *Biol. Met.*, **3**, 54 (1990).
169. I. Berner, S. Konetschny-Rapp, G. Jung and G. Winkelmann, *Biol. Met.*, **1**, 51 (1988).
170. J. Meiwes, H. P. Fiedler, H. Zahner, S. Konetschnyrapp and G. Jung, *Appl. Microbiol. Biotechnol.*, **32**, 505 (1990).
171. G. J. Feistner, D. C. Stahl and A. H. Gabrik, *Org. Mass Spectrom.*, **28**, 163 (1993).
172. J. H. Jang, K. Kanoh, K. Adachi, S. Matsuda and Y. Shizuri, *J. Nat. Prod.*, **70**, 563 (2007).
173. Z. D. Liu and R. C. Hider, *Med. Res. Rev.*, **22**, 26 (2002).
174. V. R. Gordeuk, P. E. Thuma, G. M. Brittenham, S. Zulu, G. Simwanza, A. Mhangu, G. Flesch and D. Parry, *Blood,* **79**, 308 (1992).
175. D. R. Richardson, *Crit. Rev. Oncol. Hematol.*, **42**, 267 (2002).
176. R. J. Bergeron, J. Wiegand, J. S. McManis and N. Bharti, *J. Med. Chem.*, **49**, 7032 (2006).
177. R. C. Hider and T. Zhou, *Ann. N. Y. Acad. Sci.*, **1054**, 141 (2005).
178. R. J. Bergeron and J. J. Pegram, *J. Org. Chem.*, **53**, 3131 (1988).
179. R. J. Bergeron, J. Wiegand, J. S. Mcmanis and P. T. Perumal, *J. Med. Chem.*, **34**, 3182 (1991).
180. P. M. Ihnat, J. L. Vennerstrom and D. H. Robinson, *J. Pharm. Sci.*, **89**, 1525 (2000).
181. R. J. Bergeron, Z. R. Liu, J. S. McManis and J. Wiegand, *J. Med. Chem.*, **35**, 4739 (1992).
182. K. Shimizu and M. Akiyama, *J. Chem. Soc., Chem. Commun.*, 183 (1985).
183. M. Akiyama, A. Katoh, J. Kato, K. Takahashi and K. Hattori, *Chem. Lett.*, 1189 (1991).
184. K. Shimizu, K. Nakayama and M. Akiyama, *Bull. Chem. Soc. Jpn.*, **57**, 2456 (1984).
185. M. Akiyama, A. Katoh, M. Iijima, T. Takagi, K. Natori and T. Kojima, *Bull. Chem. Soc. Jpn.*, **65**, 1356 (1992).
186. Y. Hara and M. Akiyama, *Inorg. Chem.*, **35**, 5173 (1996).
187. A. R. Poreddy, O. F. Schall, T. A. Osiek, J. R. Wheatley, D. D. Beusen, G. R. Marshall and U. Slomczynska, *J. Comb. Chem.*, **6**, 239 (2004).
188. Y. Ye, M. Liu, J. L. F. Kao and G. R. Marshall, *Biopolymers,* **84**, 472 (2006).
189. G. Muller and K. N. Raymond, *J. Bacteriol.*, **160**, 304 (1984).
190. P. Yakirevitch, N. Rochel, A. M. Albrecht-Gary, J. Libman and A. Shanzer, *Inorg. Chem.*, **32**, 1779 (1993).
191. E. Jurkevitch, Y. Hadar, Y. Chen, P. Yakirevitch, J. Libman and A. Shanzer, *Microbiol.-UK,* **140**, 1697 (1994).
192. I. Berner, P. Yakirevitch, J. Libman, A. Shanzer and G. Winkelmann, *Biol. Met.*, **4**, 186 (1991).
193. H. Kornreich-Leshem, C. Ziv, E. Gumienna-Kontecka, R. Arad-Yellin, Y. Chen, M. Elhabiri, A. M. Albrecht-Gary, Y. Hadar and A. Shanzer, *J. Am. Chem. Soc.*, **127**, 1137 (2005).
194. C. W. Hesseltine, C. Pidacks, A. R. Whitehill, N. Bohonos, B. L. Hutchings and J. H. Williams, *J. Am. Chem. Soc.*, **74**, 1362 (1952).

195. H. Diekmann, *Arch. Mikrobiol.*, **73**, 65 (1970).
196. C. B. Frederick, M. D. Bentley and W. Shive, *Biochemistry,* **20**, 2436 (1981).
197. M. B. Hossain, M. A. F. Jalal, B. A. Benson, C. L. Barnes and D. van der Helm, *J. Am. Chem. Soc.*, **109**, 4948 (1987).
198. M. A. F. Jalal, M. B. Hossain, D. van der Helm and C. L. Barnes, *Biol. Met.*, **1**, 77 (1988).
199. M. A. F. Jalal and D. van der Helm, *Biol. Met.*, **2**, 11 (1989).
200. H. Anke, J. Kinn, K. E. Bergquist and O. Sterner, *Biol. Met.*, **4**, 176 (1991).
201. R. Margalit and A. Shanzer, *Biochim. Biophys. Acta,* **649**, 441 (1981).
202. Y. Shechter, A. Shisheva, R. Lazar, J. Libman and A. Shanzer, *Biochemistry,* **31**, 2063 (1992).
203. E. Yavin, R. Kikkiri, S. Gil, R. Arad-Yellin, E. Yavin and A. Shanzer, *Org. Biomol. Chem.*, **3**, 2685 (2005).
204. E. Yavin, L. Weiner, R. Arad-Yellin and A. Shanzer, *J. Phys. Chem. A,* **105**, 8018 (2001).
205. A. Brand, S. Gil and E. Yavin, *J. Neurochem.*, **74**, 1596 (2000).
206. D. Dexter, personal communication.
207. M. A. Abdallah, in *Handbook of Microbial Iron Chelates*, 1st edn (Ed. G. Winkelmann), CRC Press, Boca Raton, 1991, p. 139.
208. H. Budzikiewicz, *FEMS Microbiol. Rev.*, **104**, 209 (1993).
209. H. Budzikiewicz, *Curr. Top. Med. Chem.*, **1**, 73 (2001).
210. S. Wendenbaum, P. Demange, A. Dell, J. M. Meyer and M. A. Abdallah, *Tetrahedron Lett.*, **24**, 4877 (1983).
211. R. Tappe, K. Taraz, H. Budzikiewicz, J. M. Meyer and J. F. Lefevre, *J. Prak. Chem.-Chem. Ztg.*, **335**, 83 (1993).
212. T. Palanche, S. Blanc, C. Hennard, M. A. Abdallah and A. M. Albrecht-Gary, *Inorg. Chem.*, **43**, 1137 (2004).
213. H. Weizman, O. Ardon, B. Mester, J. Libman, O. Dwir, Y. Hadar, Y. Chen and A. Shanzer, *J. Am. Chem. Soc.*, **118**, 12368 (1996).
214. S. D. Lytton, Z. I. Cabantchik, J. Libman and A. Shanzer, *Mol. Pharmacol.*, **40**, 584 (1991).
215. M. Loyevsky, S. D. Lytton, B. Mester, J. Libman, A. Shanzer and Z. I. Cabantchik, *J. Clin. Invest.*, **91**, 218 (1993).
216. T. Palanche, F. Marmolle, M. A. Abdallah, A. Shanzer and A. M. Albrecht-Gary, *J. Biol. Inorg. Chem.*, **4**, 188 (1999).
217. R. A. Bissell, A. P. Desilva, H. Q. N. Gunaratne, P. L. M. Lynch, G. E. M. Maguire and K. R. A. S. Sandanayake, *Chem. Soc. Rev.*, **21**, 187 (1992).
218. L. Fabbrizzi, M. Licchelli, P. Pallavicini, A. Perotti and D. Sacchi, *Angew. Chem., Int. Ed. Engl.*, **33**, 1975 (1994).
219. T. Nakamura, A. Kira and M. Imamura, *J. Phys. Chem.*, **87**, 3122 (1983).
220. H. Weizman, PhD thesis, The Weizmann Institute of Science (Rehovot), 1993.
221. E. van der Donckt and C. Van Vooren, *J. Chem. Soc., Faraday Trans. 1,* **74**, 827 (1978).
222. R. Nudelman, O. Ardon, Y. Hadar, Y. N. Chen, J. Libman and A. Shanzer, *J. Med. Chem.*, **41**, 1671 (1998).
223. S. D. Lytton, B. Mester, J. Libman, A. Shanzer and Z. I. Cabantchik, *Anal. Biochem.*, **205**, 326 (1992).
224. O. Ardon, R. Nudelman, C. Caris, J. Libman, A. Shanzer, Y. N. Chen and Y. Hadar, *J. Bacteriol.*, **180**, 2021 (1998).
225. F. Fages, B. Bodenant and T. Weil, *J. Org. Chem.*, **61**, 3956 (1996).
226. E. Bar Ness, Y. Hadar, Y. Chen, A. Shanzer and J. Libman, *Plant Physiol.*, **99**, 1329 (1992).
227. R. Ganmore-Neumann, B. Bar-Yosef, A. Shanzer and J. Libman, *J. Plant Nutr.*, **15**, 1027 (1992).
228. M. M. Meijler, R. Arad-Yellin, Z. I. Cabantchik and A. Shanzer, *J. Am. Chem. Soc.*, **124**, 12666 (2002).
229. D. Margulies, G. Melman, C. E. Felder, R. Arad-Yellin and A. Shanzer, *J. Am. Chem. Soc.*, **126**, 15400 (2004).
230. D. Margulies, C. E. Felder, G. Melman and A. Shanzer, *J. Am. Chem. Soc.*, **129**, 347 (2007).
231. I. Rubinstein, S. Steinberg, Y. Tor, A. Shanzer and J. Sagiv, *Nature,* **332**, 426 (1988).

232. C. Estes, A. Duncan, B. Wade, C. Lloyd, W. Ellis and L. Powers, *Biosens. Bioelectron.*, **18**, 511 (2003).
233. H. Y. Mason, C. Lloyd, M. Dice, R. Sinclair, W. Ellis and L. Powers, *Biosens. Bioelectron.*, **18**, 521 (2003).
234. T. Moav, A. Hatzor, H. Cohen, J. Libman, I. Rubinstein and A. Shanzer, *Chem.-Eur. J.*, **4**, 502 (1998).
235. C. R. Lloyd, F. C. Cleary, H. Y. Kim, C. R. Estes, A. G. Duncan, B. D. Wade, W. R. Ellis and L. S. Powers, *Proc. Ieee,* **91**, 908 (2003).
236. R. J. Bergeron and J. S. McManis, in *The development of iron chelators for clinical use* (Eds R. J. Bergeron and G. M. Brittenham), CRC Press, Boca Raton, 1996, p. 237.
237. V. Girijavallabhan and M. J. Miller, in *Iron Transport in Bacteria*, 1st edn (Eds J. H. Crosa, A. R. Mey and S. M. Payne), American Society for Microbiology, Washington, DC, 2004, p. 413.
238. A. L. Stefanska, M. Fulston, C. S. Houge-Frydrych, J. J. Jones and S. R. Warr, *J. Antibiot.*, **53**, 1346 (2000).
239. G. Benz, T. Schroder, J. Kurz, C. Wunsche, W. Karl, G. Steffens, J. Pfitzner and D. Schmidt, *Angew. Chem., Int. Ed. Engl.*, **21**, 527 (1982).
240. V. Braun, K. Hantke and W. Koster, *Met. Ions Biol. Syst.*, **35**, 67 (1998).
241. V. Braun, K. Gunthner, K. Hantke and L. Zimmermann, *J. Bacteriol.*, **156**, 308 (1983).
242. A. Hartmann, H. P. Fiedler and V. Braun, *Eur. J. Biochem.*, **99**, 517 (1979).
243. L. Vertesy, W. Aretz, H. W. Fehlhaber and H. Kogler, *Helv. Chim. Acta,* **78**, 46 (1995).
244. H. Bickel, P. Mertens, V. Prelog, J. Seibl and A. Walser, *Tetrahedron Suppl.*, 171 (1966).
245. A. Pramanik and V. Braun, *J. Bacteriol.*, **188**, 3878 (2006).
246. H. Zahner, H. Diddens, W. Keller-Schierlein and H. U. Nageli, *Jpn. J. Antibiot.*, **30 Suppl.**, 201 (1977).
247. H. Bruckner and G. Jung, *Liebigs Ann. Chem.*, 37 (1980).
248. M. Ghosh, L. J. Lambert, P. W. Huber and M. J. Miller, *Bioorg. Med. Chem. Lett.*, **5**, 2337 (1995).
249. Y. Lu and M. J. Miller, *Bioorg. Med. Chem.*, **7**, 3025 (1999).
250. T. B. Chaston and D. R. Richardson, *Am. J. Hematol.*, **73**, 200 (2003).
251. C. Hershko, G. Link, A. M. Konijn and Z. I. Cabantchik, *Hematology,* **10**, 171 (2005).
252. C. Hershko, G. Link, A. M. Konijn and Z. I. Cabantchik, *Ann. N. Y. Acad. Sci.*, **1054**, 124 (2005).
253. M. Franchini, *Am. J. Hematol.*, **81**, 202 (2006).
254. M. Franchini and D. Veneri, *Ann. Hematol.*, **84**, 347 (2005).
255. Z. I. Cabantchik, *Parasitol. Today*, **11**, 74 (1995).
256. C. Raventos Suarez, S. Pollack and R. L. Nagel, *Am. J. Trop. Med. Hyg.*, **31**, 919 (1982).
257. M. D. Scott, A. Ranz, F. A. Kuypers, B. H. Lubin and S. R. Meshnick, *Br. J. Haematol.*, **75**, 598 (1990).
258. G. Fritsch, J. Treumer, D. T. Spira and A. Jung, *Exp. Parasitol.*, **60**, 171 (1985).
259. S. D. Lytton, M. Loyevsky, B. Mester, J. Libman, I. Landau, A. Shanzer and Z.I. Cabantchik, *Am. J. Hematol.*, **43**, 217 (1993).
260. S. Pollack, R. N. Rossan, D. E. Davidson and A. Escajadillo, *Proc. Soc. Exp. Biol. Med.*, **184**, 162 (1987).
261. D. Bunnag, A. A. Poltera, C. Viravan, S. Looareesuwan, K. T. Harinasuta and C. Schindlery, *Acta Trop.*, **52**, 59 (1992).
262. V. R. Gordeuk, G. M. Brittenham and P. E. Thuma, in *The Development of Iron Chelators for Clinical Use* (Eds R. J. Bergeron and G. M. Brittenham), CRC Press, Boca Raton, 1994, p. 111.
263. O. Traore, P. Carnevale, L. Kaptuenoche, J. Mbede, M. Desfontaine, J. Elion, D. Labie and R. L. Nagel, *Am. J. Hematol.*, **37**, 206 (1991).
264. D. J. Wyler, *N. Engl. J. Med.*, **327**, 1519 (1992).
265. A. Shanzer, J. Libman, S. D. Lytton, H. Glickstein and Z. I. Cabantchik, *Proc. Natl. Acad. Sci. U.S.A.*, **88**, 6585 (1991).
266. H. Glickstein, W. Breuer, M. Loyevsky, A. M. Konijn, J. Libman, A. Shanzer and Z. I. Cabantchik, *Blood,* **87**, 4871 (1996).
267. S. D. Lytton, B. Mester, I. Dayan, H. Glickstein, J. Libman, A. Shanzer and Z. I. Cabantchik, *Blood,* **81**, 214 (1993).

268. R. E. Desjardins, C. J. Canfield, J. D. Haynes and J. D. Chulay, *Antimicrob. Agents Chemother.*, **16**, 710 (1979).
269. J. Golenser, A. Tsafack, Y. Amichai, J. Libman, A. Shanzer and Z. I. Cabantchik, *Antimicrob. Agents Chemother.*, **39**, 61 (1995).
270. A. Tsafack, J. Golenser, J. Libman, A. Shanzer and Z. I. Cabantchik, *Mol. Pharmacol.*, **47**, 403 (1995).
271. A. Tsafack, M. Loyevsky, P. Ponka and Z. I. Cabantchik, *J. Lab. Clin. Med.*, **127**, 574 (1996).
272. S. D. Lytton, B. Mester, J. Libman, A. Shanzer and Z. I. Cabantchik, *Blood,* **84**, 910 (1994).

CHAPTER 17

Hydroxylamine, oximate and hydroxamate as α-nucleophiles in dephosphorylation

ERWIN BUNCEL

Department of Chemistry, Queen's University, Kingston, Ontario K7L 3N6, Canada
Fax: +1-613-533-6669; e-mail: buncele@chem.queensu.ca

IK HWAN UM

Division of Nano Sciences and Department of Chemistry, Ewha Womans University, Seoul 120-750, Korea
Fax: +82-2-3277-2844; e-mail: ihum@ewha.ac.kr

and

FRANÇOIS TERRIER

Institut Lavoisier, UMR 8180, Université de Versailles, 45 Avenue des Etats-Unis 78035, Versailles Cedex, France
Fax: +33-01-3925-4452; e-mail: terrier@chimie.uvsq.fr

The chemistry of hydroxylamines, oximes and hydroxamic acids
Edited by Z. Rappoport and J. F. Liebman

I. INTRODUCTION

Hydroxylamines, oximes and hydroxamic acids have found great utility in diverse areas of chemistry as is readily seen on glancing at the contents page of this volume. In the present chapter we focus on reactivities of these classes of compounds, especially in substitution reactions at carbon, phosphorus and sulfur centers. The C, P and S centers act as electrophilic sites while the hydroxylamine, oxime and hydroxamic acids or their conjugate bases serve as nucleophilic agents by virtue of the oxygen and nitrogen centers possessing excessive electron densities.

With each of the C, P and S centers, compounds with several oxidation states are possible, thus multiplying the types of nucleophilic reactions extant. Importantly, the types of compounds cover a variety of classes each with its characteristic behaviors and reactivities, each defining a specific area in chemistry. Since the C, P and S reactive centers are incorporated in the majority of molecules in living systems it follows that the chemistry to be considered in this chapter is closely tied with the chemistry of life, i.e. bioorganic reaction mechanisms. It is known in fact that many organophosphorus and organosulfur compounds are toxic toward mammalian organisms which renders their destruction under mild conditions of critical importance.

It is in the realm of detoxification that the hydroxylamines/oximes/hydroxamic acids and their conjugate bases are of direct use, since a number of these compounds have been found to be especially reactive in the destruction of toxins. The fundamental reasons underlying such enhanced reactivity is an important part of this chapter.

II. THE α-EFFECT OF HYDROXYLAMINES, OXIMES AND HYDROXAMIC ACIDS

Scheme 1 illustrates the structures of typical members of this group of compounds. Importantly, each of these compounds contains the structural feature

with the adjacent N and O atoms containing one or more nonbonding electron pairs. It is this structural feature that has led to their naming as α-nucleophiles when dealing with nucleophilic substitution[1].

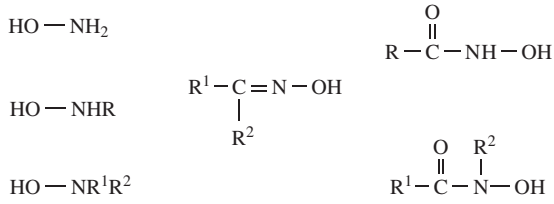

SCHEME 1

Other common α-nucleophiles include the following:

HOO^-, CH_3OO^-, $CH_3C(O)OO^-$,
ClO^-, BrO^-,
HSO_3^-,
NH_2NH_2, $MeONH_2$.

Quantitatively, the enhanced reactivity of hydroxylamine, as well as oximate and hydroxamate ions and also other α-nucleophiles, is expressed as a positive deviation on a Brønsted-type rate–basicity (pK_a) plot, i.e. log k vs pK_a[2]. This is illustrated in Figure 1 for oxygen nucleophiles and in Figure 2 for nitrogen nucleophiles. It is important to note that the reactivity of the α-nucleophile is considered relative to a 'normal' nucleophile of the same Brønsted basicity[3].

A. The Origin of the α-Effect

Several reviews concerning the α-effect phenomenon, such as factors affecting α-nucleophilicity, have been published previously[2a–d]. The topic remains controversial with

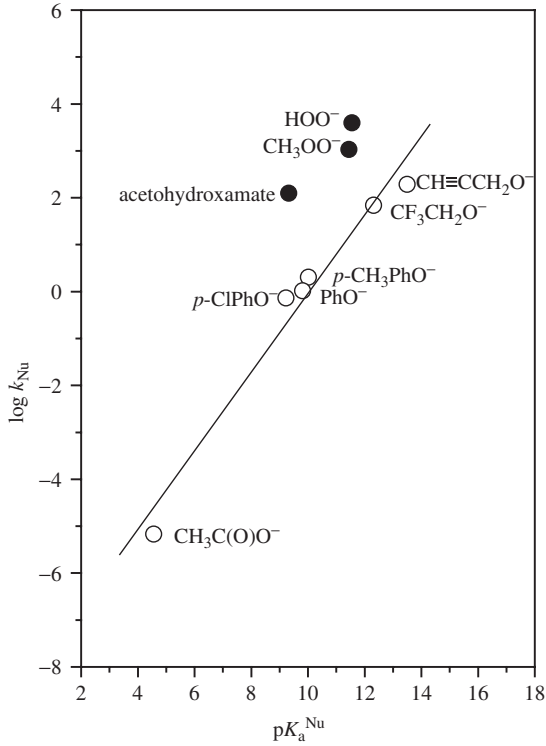

FIGURE 1. Brønsted-type plot for reactions of p-nitrophenyl acetate (PNPA) with anionic oxygen nucleophiles. The α-nucleophiles are shown as solid circles. Data taken from Jencks and Gilchrist, *J. Am. Chem. Soc.*, **90**, 2622 and reprinted with permission. Copyright (1968) American Chemical Society

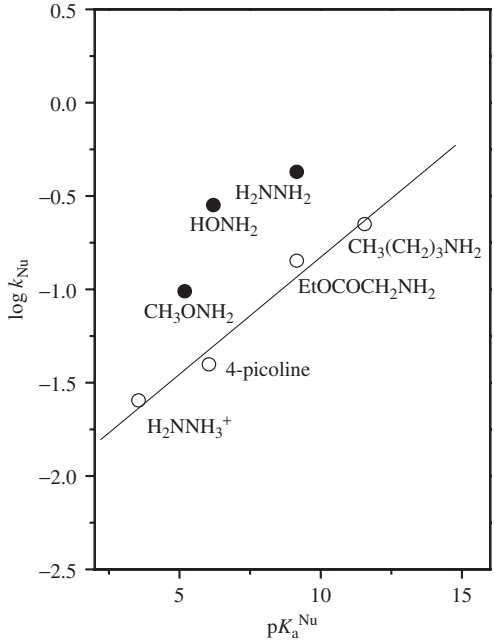

FIGURE 2. Brønsted-type plot for reactions of methyl *p*-nitrophenyl sulfate with amines. The α-nucleophiles are shown as solid circles. Data taken from Buncel, Chuaqui and Wilson, *J. Org. Chem.*, **45**, 3621 and reprinted with permission. Copyright (1980) American Chemical Society

publications contributing to the origin of the phenomenon continuing to appear. There is no single factor that is generally agreed upon as chiefly determining the magnitude or even the existence of the α-effect. Here we mention briefly some of the key factors:

1. Hybridization of substrate at the electrophilic center undergoing reaction—small at sp^3 centers[4b–e], large α-effects have been reported for reactions at sp and sp^2 hybridized centers[4f,g].
2. β_{nuc} values—small α-effects have generally been observed for reactions with small β_{nuc} values, and vice versa[2a, 4b, 5a]
3. Solvent effects—highly unusual kinetic effects have been found to accompany solvent change, such as bell-shaped kinetic profiles in DMSO–H_2O mixtures[2a].
4. Single Electron Transfer (SET) character for α-nucleophile reactions[5b].
5. Ground-state vs transition-state vs thermodynamic stabilization and destabilization[2a, 5c, d].

Clearly, the α-effect phenomenon remains an exciting topic for investigation.

III. AMBIDENT NATURE OF HYDROXYLAMINES AND HYDROXAMATES

Hydroxylamines, as potentially ambident nucleophiles, can utilize either the basic N atom or the O atom in nucleophilic reaction with a variety of electrophilic centers[6,7]. This is illustrated in Scheme 2 through the box on the left hand side of the diagram. Also shown in Scheme 2 are the dissociation equilibria K_{a1}, K_{a2}, and K'_{a2}. The equilibrium denoted as

K_e, while not quantified experimentally, was recently introduced by Kirby and coworkers on the basis of product formation from O-attack at electrophilic P and C centers, as well as MO calculations incorporating the novel species, ammonia oxide, $NH_3^+-O^-$ [6a]. In common with other ambident nucleophiles, factors such as electronic, steric, kinetic and thermodynamic effects will determine actual extant pathways in a given system. *N*-substituted hydroxylamines (see Scheme 1) can in principle partake of the equilibria shown in Scheme 2. Again, actual outcomes will be influenced by the aforementioned criteria.

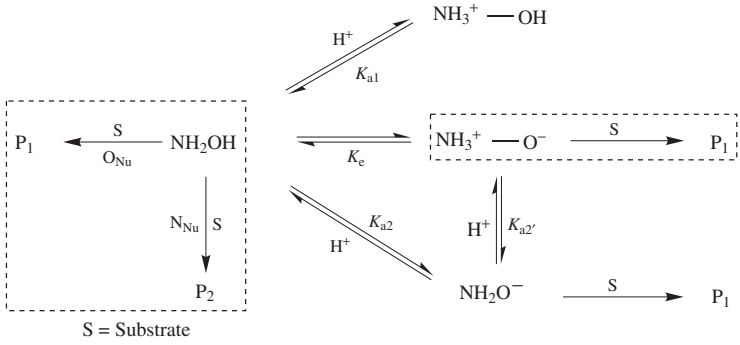

SCHEME 2

Hydroxamic acids **1** (Scheme 1) present both N- and O-centers in their reactions with electrophilic centers. However, commonly alkylation/acylation/phosphorylation occur via the O-center. The ionized hydroxamate is of course more reactive than the unionized form, as is the case with oximes and the corresponding oximates.

pK_a values of hydroxamic acids are generally in the range 8–9. Depending on the solvent, hydroxamic acids behave either as NH or OH acids[8–12], according to the tautomeric equilibrium (Scheme 3).

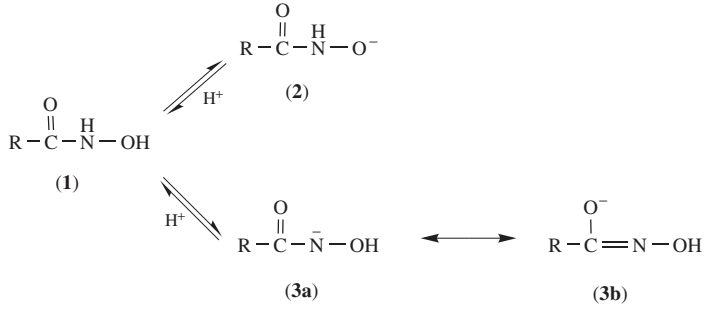

SCHEME 3

Some interesting solvent effects have been observed as a function of medium change in the acetonitrile–water system[13]. Benzohydroxamate (BHA^-, pK_a = 8.8) has been shown to be more reactive than its reference nucleophile, 3-chlorophenoxide (3-$ClC_6H_4O^-$, pK_a = 9.02) toward 4-nitrophenyl acetate (PNPA)[13a] as shown in Figure 3; BHA^- is *ca* 160-fold more reactive than 3-$ClC_6H_4O^-$ in pure water but the reactivity ratio,

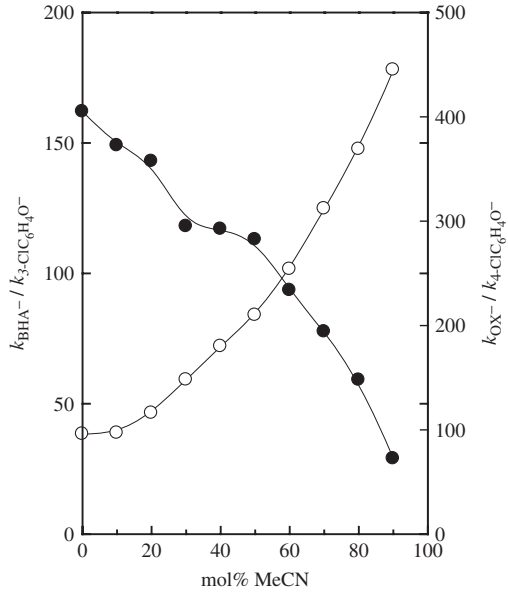

FIGURE 3. Plots showing dependence of the α-effect on the solvent MeCN–H_2O composition for reactions of PNPA with BHA^-/3-$ClC_6H_4O^-$ (●), and with Ox^-/4-$ClC_6H_4O^-$ (○) at 25.0 °C. Reproduced from Um, Yoon and Kwon, *Bull. Korean Chem. Soc.*, **14**, 425 (1993) with permission

$k_{BHA^-}/k_{3\text{-}ClC_6H_4O^-}$, decreases as the mol% acetonitrile increases in the reaction medium. The α-effect profile found for the reactions of PNPA with BHA^-/3-$ClC_6H_4O^-$ is opposite to that found for the corresponding reactions with 2,3-butanedione monoximate (Ox^-)/4-chlorophenoxide (4-$ClC_6H_4O^-$) in the same solvent system[13a]. The tautomerization shown in Scheme 3 has been proposed to account for the decreasing α-effect profile $k_{BHA^-}/k_{3\text{-}ClC_6H_4O^-}$[13b]. However, product analysis revealed that only the *O*-acylated product is produced from the reaction of PNPA with BHA^- under kinetic conditions for all solvent mixtures studied. This is in accord with tautomer **3a/3b** being less reactive than **2**, i.e. the equilibrium shift from **2** to **3a/3b** is responsible for the decreasing α-effect in media with increasing MeCN content.

IV. LEVELING EFFECT OF α-NUCLEOPHILICITY: BRØNSTED-TYPE PLOTS

Brønsted-type studies with oximate α-nucleophiles have led to the unexpected discovery that plots of log rate for oximate nucleophiles reacting with 4-nitrophenyl acetate showed a distinct leveling effect or saturation behavior. In contrast, the corresponding plot for aryloxide nucleophiles remained linear over the same pK_a range (Figure 4).[14] An important consequence of this behavior follows in detoxification through destruction of toxic organophosphorus compounds (to be considered in detail subsequently), that increasing oximate basicity beyond a certain point would not lead to increasing reactivity[15].

Interestingly, on changing from a purely aqueous medium to 70% DMSO–30% H_2O, the leveling effect was no longer observed (Figure 5)[16]. Other important manifestations of solvent effects are considered further below.

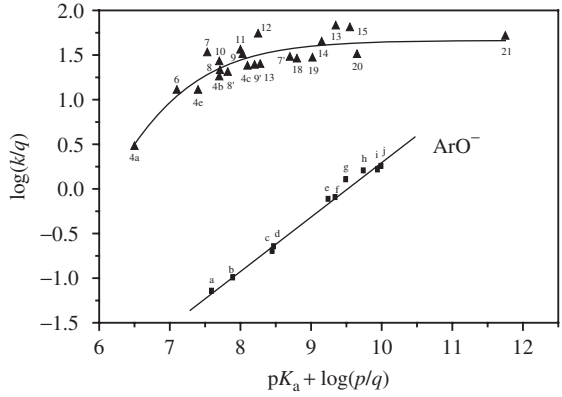

FIGURE 4. Brønsted-type plots for reactions of oximates and phenoxides with PNPA at 25 °C in aqueous solution showing the saturation behavior of oximates (k in $M^{-1}\,s^{-1}$); see Scheme 4 for the identification of the oxime structures[15]. a: 2,4-$Cl_2C_6H_3O^-$, b: 4-CN $C_6H_4O^-$, c: 2-$BrC_6H_4O^-$, d: 3,4-$Cl_2C_6H_3O^-$, e: 4-$ClC_6H_4O^-$, f: 4-$CH_3C(O)NHC_6H_4O^-$, g: 3-$CH_3OC_6H_4O^-$, h: $C_6H_5O^-$, i: 4-$CH_3C_6H_4O^-$), j: 4-$CH_3OC_6H_4O^-$. The plot for the reactions of oximates is statistically corrected using p and q, i.e. $p = q = 1$ except $p = q = 2$ for oximates **6**, **7**, **8** and **9**. From Terrier *et al.*, *Org. Biomol. Chem.*, **4**, 4352 (2006). Reproduced by permission of The Royal Society of Chemistry

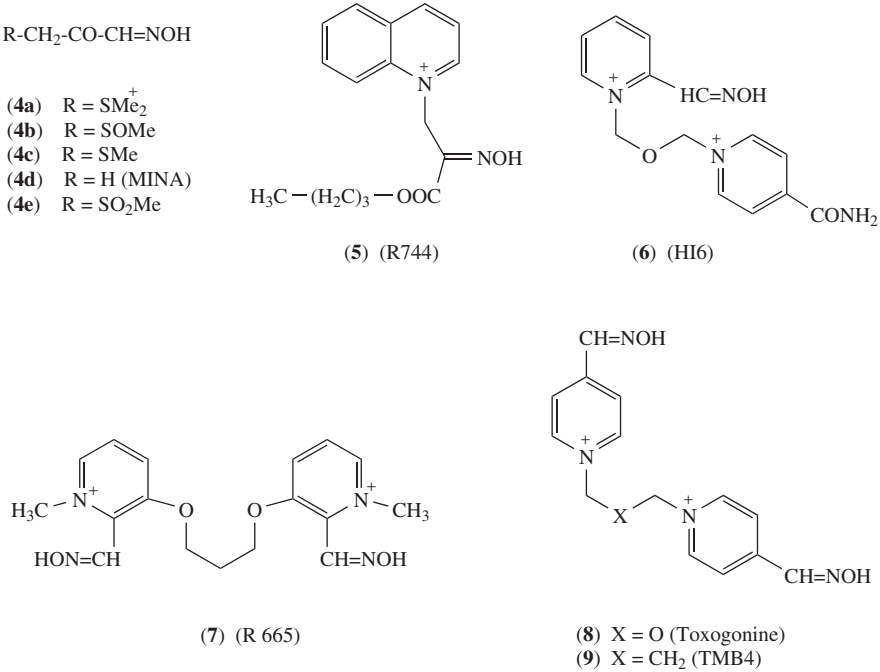

SCHEME 4. Structures and numbering of oximes. From Terrier *et al.*, *Org. Biomol. Chem.*, **4**, 4352 (2006). Reproduced by permission of The Royal Society of Chemistry

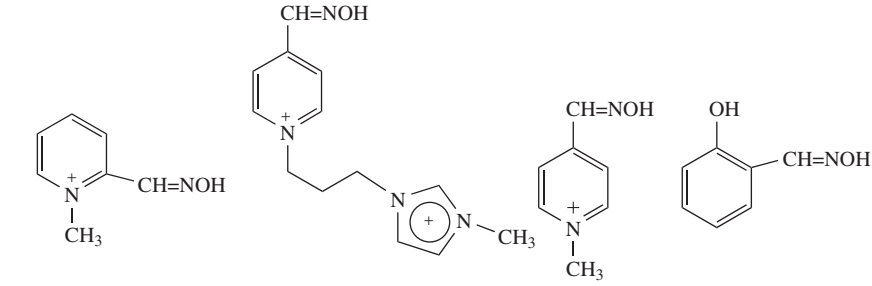

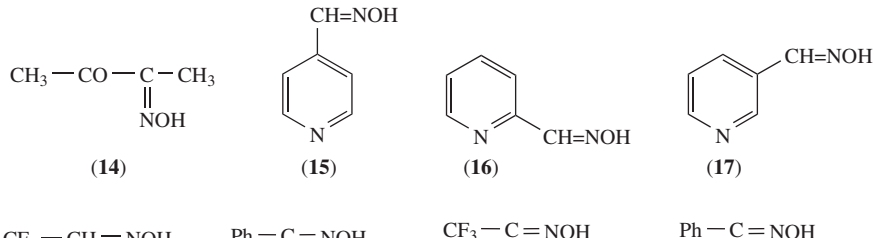

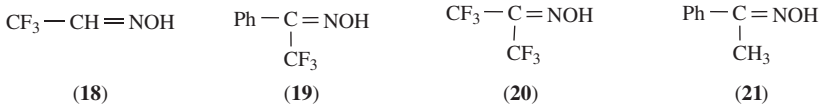

SCHEME 4. (*continued*)

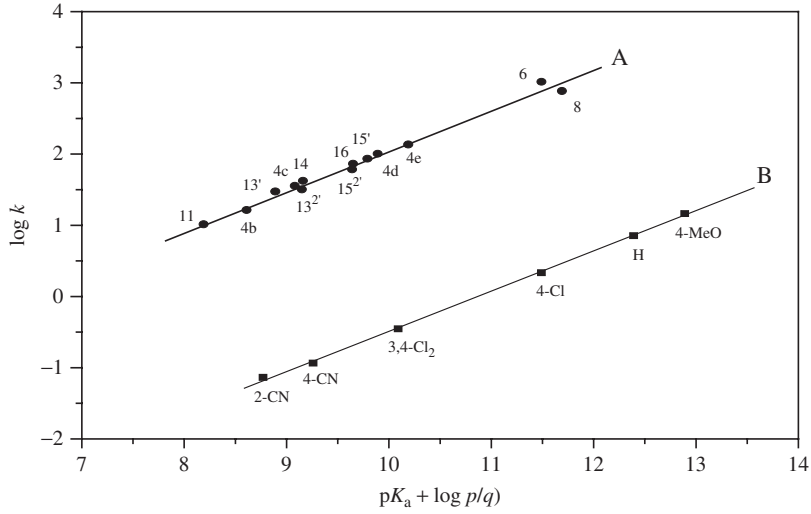

FIGURE 5. Plot A illustrating the metamorphosis (with respect to Figure 4) in Brønsted-type reactivity for PNPA-oximates systems at 25 °C in 30% H_2O–70% DMSO (v/v) with reference to ArO^- reactivities (plot B). Reprinted with permission from Buncel *et al.*, *J. Am. Chem. Soc.*, **124**, 8766. Copyright (2002) American Chemical Society

V. SOLVENT EFFECT ON α-NUCLEOPHILICITY

The effect on oximate reactivity of adding DMSO to an aqueous medium was first investigated by the authors in the 1980s[17,18]. While in the first study a leveling effect on reactivity was observed when the DMSO content reached *ca* 50 mol%[17], in the subsequent study, increasing the DMSO content to 90 mol%, a maximum in the α-effect could be readily discerned, i.e. bell-shaped behavior[18].

It was later shown that one could reformat the log *k* vs mol% DMSO plot as a log *k* vs pK_a plot[19], i.e. a Brønsted-type plot. This transformation was effected through the effect of DMSO composition on pK_a values, i.e. a novel Brønsted-type plot[20], as illustrated in Figure 6 for the reaction of the Ox^-/4-$ClC_6H_4O^-$ pair with 4-nitrophenyl diphenylphosphinate in the DMSO–H_2O system.

A different type of solvent effect on reactivity was observed by Terrier and coworkers for the reaction of oximates with the bis(4-nitrophenyl) phenylphosphonate (BPNPPP)[21]. As shown in Figure 7, the Brønsted-type plot is bell-shaped, i.e. oximates with pK_a > 9 exhibiting lower reactivity than more weakly basic oximates[21].

That this is a manifestation of a specific solvent effect is further demonstrated through Figures 8A and 8B, which show that on going from 20 mol% DMSO to 90 mol% DMSO there is a reversal in reactivity behavior[22]. Comparison of Figures 8A and 8B reveals an appreciable overall rate enhancement on changing the medium from 20 to 90 mol% DMSO. The Hammett plots (Figure 8A) are linear for the reactions performed in 20 mol% DMSO with ρ values of −1.86 and +0.20 for the reactions of PNPB with the aryloxides and oximates, respectively. The ρ value of +0.20 is quite unusual, since it corresponds to a decrease in reactivity of the oximates with increasing a base-strengthening substituent. The positive ρ value for the reactions of PNPB with the oximates in 20 mol% DMSO has

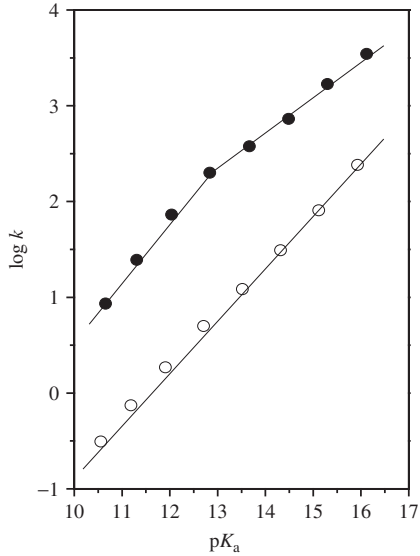

FIGURE 6. Novel Brønsted-type plots: log *k* vs pK_a for the reaction of butane-2,3-dione monoximate (Ox^-, ●) and 4-chlorophenoxide (4-$ClC_6H_4O^-$, ○) with 4-nitrophenyl diphenylphosphinate (PNPDPP) at 25.0 °C. Reprinted with permission from Tarkka and Buncel, *J. Am. Chem. Soc.*, **117**, 1503. Copyright (1995) American Chemical Society

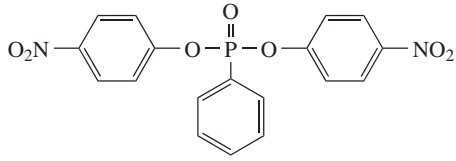

BPNPPP

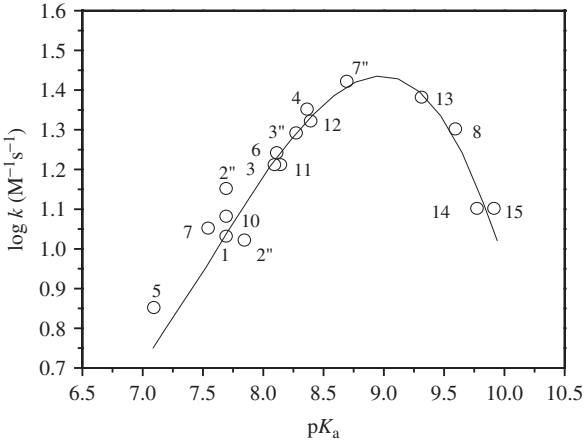

FIGURE 7. Brønsted-type plot for the reaction of the oximates with the bis(4-nitrophenyl) phenylphosphonate at 25 °C in aqueous solution. From Terrier *et al.*, *Chem. Commun.*, **600** (2003). Reproduced by permission of The Royal Society of Chemistry

been attributed to stronger solvation of the more basic oximate by water molecules in the medium[22]. This argument can be supported from the negative ρ value (i.e. -0.15) found for the corresponding reactions in 90 mol% DMSO in which no free water molecules would be available to form H-bonding with the oximate anions (Figure 8B).

These types of 'reverse Brønsted' behaviors further emphasize the direct relationship between fundamental physicochemical studies and the utility of the oximate nucleophiles in detoxification (*vide infra*).

To conclude this section on the effect of solvent on α-nucleophilicity, we refer to the current, rather controversial, situation pertaining to gas-phase studies and the α-effect. As reported in our review on the α-effect and its modulation by solvent[2a] the gas-phase reaction of methyl formate with HOO^- and HO^-, which proceeds via three competitive pathways: proton abstraction, nucleophilic addition to the carbonyl group and S_N2 displacement on the methyl group, showed no enhanced nucleophilic reactivity for HOO^- relative to HO^- [23a]. This was consistent with gas-phase calculational work at the 4-31G level and HOMO–LUMO considerations[23b]. However, recently reported computations using the high-level G2(+) method on 22 gas-phase nucleophilic reactions $Nu^- + R{-}Cl \rightarrow R{-}Nu + Cl^-$ (R = Me, Et, *i*-Pr with a variety of normal and α-Nu reagents) indicate the existence of an α-effect whose size varies depending on the R group and the α-atom[23c]. Among their conclusions one can highlight that the TS structures for α-nucleophiles are associated with less advanced C–X bond cleavage, leading

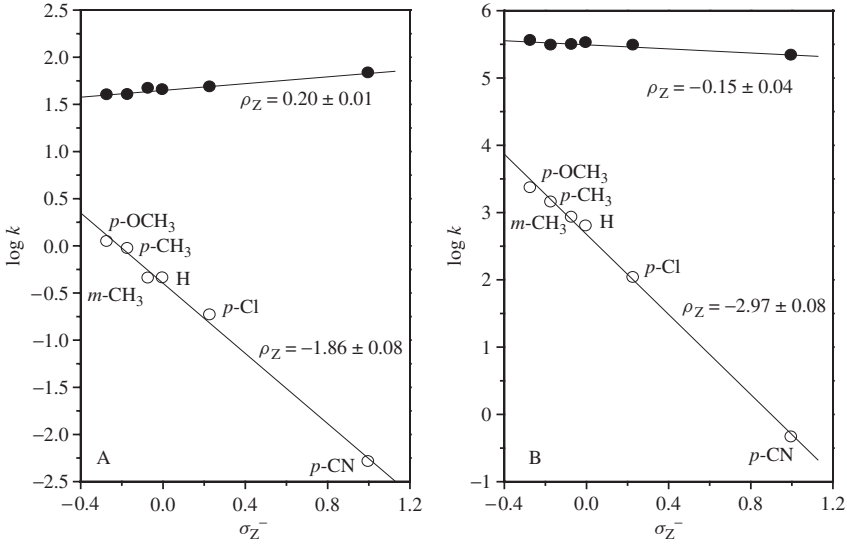

FIGURE 8. Hammett plots for reactions of 4-nitrophenyl benzoate (PNPB) with Z-substituted acetophenone oximates (●) and phenoxides (○) in 20 mol% DMSO (A) and 90 mol% DMSO (B) at 25.0 ± 0.1 °C. Reprinted from *Tetrahedron Lett.*, **36**, Um, Oh and Kwon, 6903, Copyright (1995), with permission from Elsevier

to smaller deformation energies and energy barriers[23c–e]. This calculational study is in accord with earlier solution kinetic work on the existence of the α-effect at sp^3 centers[4b–e].

VI. ACETONITRILE–WATER VERSUS DMSO–WATER BINARY MIXTURES

The need to understand the causes of changing the nature of the solvent medium on reactivity is further emphasized through a study by Um and coworkers, who found that nucleophilic reactivities, including of α-nucleophiles, are radically influenced on changing solvent medium, from DMSO–H_2O to MeCN–H_2O mixtures[24]. An illustrative study is displayed in Figure 9 on the α-effect for reactions of PNPA in MeCN–H_2O and DMSO–H_2O. The α-effect for the reactions in DMSO–H_2O exhibits a bell-shaped profile, while that for the reactions in MeCN–H_2O shows no bell-shaped profile, rather a steadily increasing rate constant ratio, k_{Ox^-}/k_{ArO^-}, as the MeCN content in the medium increases. The pK_a values of the conjugate acids of Ox^- and 4-$ClC_6H_4O^-$ have been reported to vary in a similar manner on changing the DMSO–H_2O composition. However, Um and coworkers have shown that Ox^- becomes more basic than 4-$ClC_6H_4O^-$ as the content of MeCN in the medium increases. Thus, the origin of this contrasting behavior is found in a differential pK_a behavior, Ox^- vs 4-$ClC_6H_4O^-$, in the MeCN–H_2O solvent system as opposed to DMSO–H_2O.

VII. IMBALANCED TRANSITION STATE

Current understanding of the leveling in reactivity of oximate α-nucleophiles, relative to aryloxide nucleophiles, with change in solvent medium, rests on ideas first proposed by Jencks[25], then developed by Bernasconi[26] and subsequently applied to detoxification of

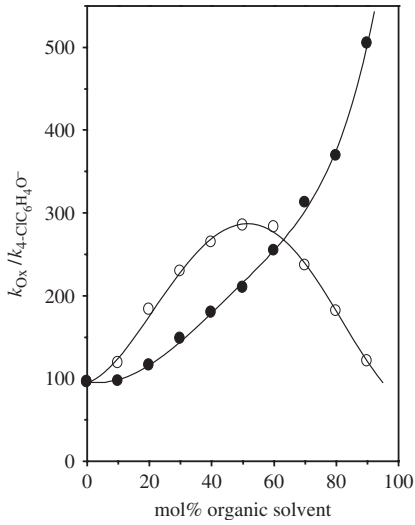

FIGURE 9. Plots showing the effect of solvent on the α-effect for the reactions of PNPA at 25.0 $\pm$ 0.1 °C: $k_{Ox^-}/k_{4\text{-}ClC_6H_4O^-}$ in MeCN–H_2O (●), $k_{Ox^-}/k_{4\text{-}ClC_6H_4O^-}$ in DMSO–H_2O (○). From Um, Park and Buncel, *Chem. Commun.*, 1917 (2000). Reproduced by permission of The Royal Society of Chemistry

organophosphorus toxics by Terrier and coworkers[21]. Basically, it was visualized in the 1930s, 1940s[27] and subsequently that the act of bond formation between the nucleophile and the electrophilic center would require prior shedding of one or more molecules of solvent. The degree of correspondence, or lack thereof, i.e. an imbalance between nucleophile desolvation and bond formation, forms the basis of the principle of nonperfect synchronization (PNS) put forward by Bernasconi[26]. Cogent arguments were presented by Terrier and coworkers that the leveling, or saturation behavior, in Brønsted-type plots by oximate α-nucleophiles (Figure 4) was intimately related to the idea of asynchronicity between nucleophile desolvation and bond formation, discussed above[15,21].

VIII. HYDROXYLAMINES, HYDROXAMATES AND OXIMATES AS ANTIDOTES FOR INTOXICATION BY ORGANOPHOSPHORUS TOXINS (CHEMICAL WARFARE AGENTS) AND ORGANOPHOSPHORUS INSECTICIDES

The discovery in the early years of the 20th century that certain phosphate esters possess mammalian toxicity and insecticidal properties heightened interest in this class of compounds, both in agriculture and as potential agents in chemical warfare[28]. Parathion became the practical choice as a broad-spectrum insecticide because of its greater stability and lower mammalian toxicity compared to its P=O analogue, paraoxon[29].

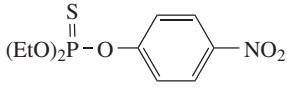

Parathion

LD_{50} = 10–12 mg kg^{-1}

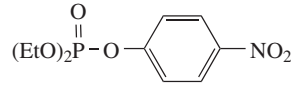

Paraoxon

LD_{50} = 0.6–0.8 mg kg^{-1}

Subsequent work on understanding drug action[30] has shown that parathion and paraoxon belong to the class of organophosphorus compounds that act as acetylcholinesterase (AChE) inhibitors, that can be removed from the active site of the enzyme through nucleophilic attack by oximates. Several reviews of oximes as antidotal agents in poisoning by organophosphorus nerve agents have been published. Selected studies are presented in various References 31–38.

In the search of antidotes for these cholinesterase inhibitors, oximates as well as hydroxylamines and hydroxamates have become paramount, since these are 100- or greater-fold more reactive under mild conditions than the common base, hydroxide[2,15,39]. Structures of commonly studied oximes including pyridinium aldoximes are given in Scheme 4[15]. The pyridinium moiety confers advantages of solubility as well as in lowering the oxime pK_a, thus effecting higher reactivity under milder conditions of pH.

A related series of cholinesterase inhibitors as antidotes, with certain advantages over the pyridinium series, contains the diazolyl ring system, with X = O or X = S (**22**, **23**, **24** and **25**)[39a].

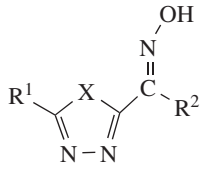

(**22**) X = O
(**23**) X = S

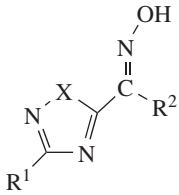

(**24**) X = O
(**25**) X = S

Synthetic studies for the discovery of effective antidotes for cholinesterase inhibitors are continuing[39–41]. Various reactivity studies of oximates with different functional organophosphorus compounds, such as phosphinates, phosphonates, phosphates and thiono analogues (shown in Scheme 5), have been reported[19,21,42–45].

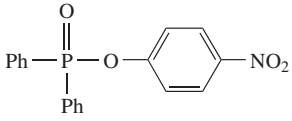

PNPDPP

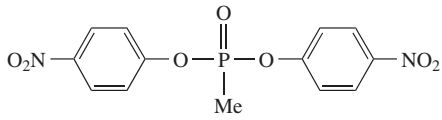

BNPMP

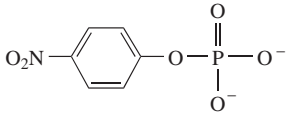

PNPP

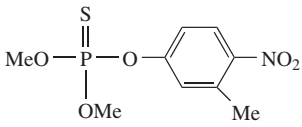

Fenitrothion

SCHEME 5

Other important series of chemical warfare (CW) agents include fluoride-containing organophosphorus compounds that possess extremely high toxicity (Scheme 6).

A recent study has revisited[43] the reactivity of oximate nucleophiles toward detoxification of sarin, soman and DFP[15], using a fluoride-selective electrode to kinetically monitor decomposition of the neurotoxin[46a]. Results are shown in Table 1.

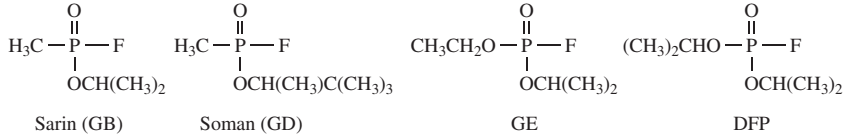

SCHEME 6

TABLE 1. Second-order rate constants for nucleophilic substitution of sarin, soman and DFP by oximates in aqueous solution at 25.0 °C. From Terrier *et al.*, *Org. Biomol. Chem.*, **4**, 4352 (2006). Reproduced by permission of The Royal Society of Chemistry

		Sarin	Soman	DFP
Oxime	$pK_a^{H_2O}$	$k^{Ox}(M^{-1}\,s^{-1})$	$k^{Ox}(M^{-1}\,s^{-1})$	$k^{Ox}(M^{-1}\,s^{-1})$
4a	6.54	0.32	0.14	—
5	6.98	—	0.25	0.050
6	7.13	1.47	0.43	0.062
7	7.33	2.39	—	0.125
	9.02	20.20	—	1.000
8	7.46	—	—	0.13
	8.17	—	—	0.30
10	7.75	4.75	1.42	0.14
9	7.79	5.90	1.65	0.25
	8.55	10.05	3.60	0.40
11	8.05	8.00	2.20	0.30
12	8.27	6.45	—	—
4d	8.30	5.00	1.90	0.28
14	9.30	8.80	4.35	0.60
15	9.55	13.40	5.59	0.64
16	9.85	14.70	5.50	0.64
17	9.95	13.10	—	—
OH^-	15.74	23.70	10.15	0.31

The oxime-induced reactivation of organophosphorus-inhibited AChE has been modeled recently through the Density Functional Theory (DFT) approach. Two possible computed reactivation pathways of Sarin-inhibited AChE adduct by formoximate anion are shown in Scheme 7[46b]. The two-step mechanism (Scheme 7B) is favored by the authors.

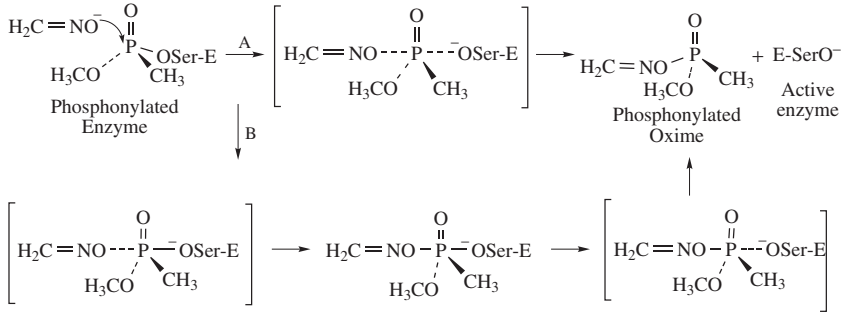

SCHEME 7. Reprinted with permission from Wang *et al.*, *J. Phys. Chem. B*, **111**, 2404, Copyright (2007) American Chemical Society

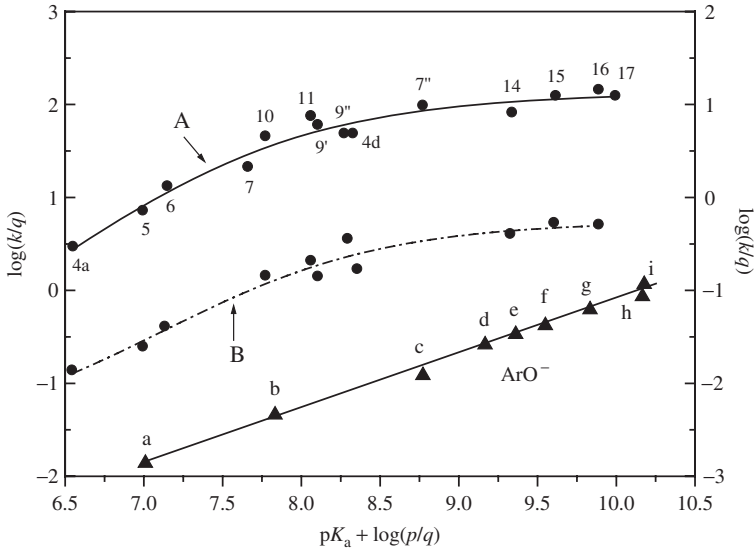

FIGURE 10. Brønsted-type plots for the reactions of oximates with sarin (graph **A**, right Y axis) and soman (graph **B**, left Y axis) at 25 °C in aqueous solution (k in $M^{-1}\,s^{-1}$). The structures of oximates are given in Scheme 4. The lower line refers to the reactions of phenoxides with sarin (left Y axis). a: 4-$NO_2C_6H_4O^-$, b: 2,4-$Cl_2C_6H_3O^-$, c: 2-$FC_6H_4O^-$, d: 3-$CH_3C(O)C_6H_4O^-$, e: 4-$ClC_6H_4O^-$, f: 3-$CH_3OC_6H_4O^-$, g: 4-$HOCH_2C_6H_4O^-$, h: 4-$CH_3C_6H_4O^-$, i: 4-$CH_3OC_6H_4O^-$. Data taken from Terrier *et al.*, *Org. Biomol. Chem.*, **4**, 4352 (2006). Reproduced by permission of The Royal Society of Chemistry

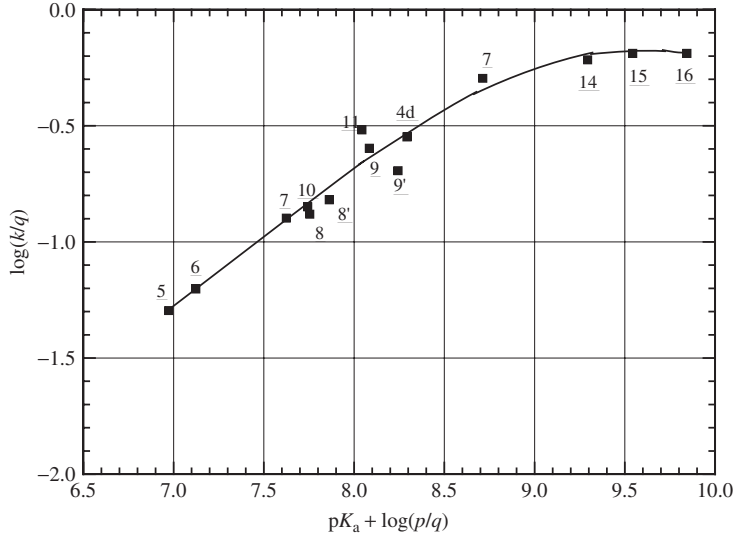

FIGURE 11. Brønsted-type nucleophilicity plot for the reaction of oximates with DFP at 25 °C in aqueous solution (k in $M^{-1}\,s^{-1}$). From Terrier *et al.*, *Org. Biomol. Chem.*, **4**, 4352 (2006). Reproduced by permission of The Royal Society of Chemistry. Structures of the oximates are given in Scheme 4

It is important to note that the computed potential energy surface reveals a facile reactivation via Scheme 7, with low energy barriers both in the gas phase and in aqueous solution[46b]. This accords with experimental findings on oximates as reactivators following poisoning by organophosphorus toxics.

As discussed above, mechanistic insight on oximate reactivity is provided by the nature of Brønsted-type plots. Figure 10 displays the Brønsted-type plot for sarin and soman relative to phenoxide reactivity while Figure 11 provides the Brønsted-type plot for DFP. The higher nucleophilicity of the nucleophiles toward sarin compared with soman is clearly seen in Figure 10; however, the respective plots clearly display the leveling in reactivity with oximate nucleophiles in contrast to the linear plot for aryloxides. The plot for DFP (Figure 11) displays similar saturation behavior. Previously, this type of saturation was observed at acyl carbon, as in *p*-nitrophenyl acetate (see Figure 4)[15]. Clearly, the observation of saturation behavior with the organophosphorus CW agents sarin, soman and DFP is of practical consequence, since detoxification becomes equally effective with relatively weakly basic oximate nucleophiles.

IX. REACTIONS OF OXIMATE AND HYDROXAMATE NUCLEOPHILES IN SURFACTANT SYSTEMS

In connection with research on oximes as reactivators of phosphorylated acetylcholine esterase, a number of studies have shown that introduction of cationic micelles such

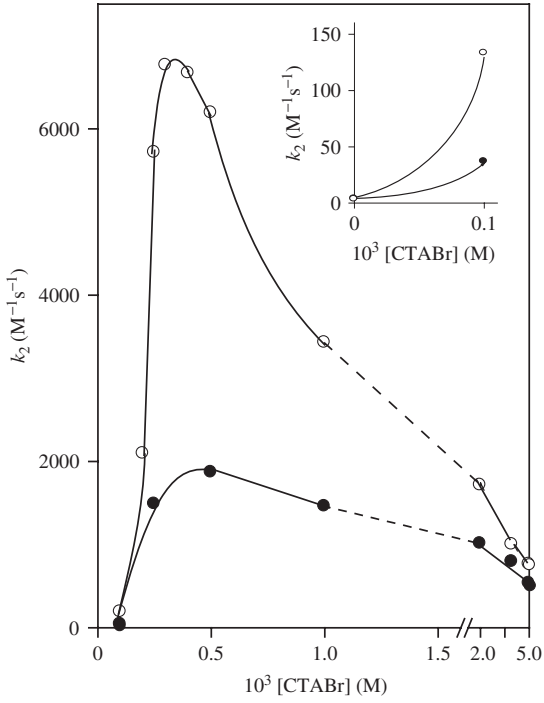

FIGURE 12. Effect of CTABr on reactivity for reactions of 4-nitrophenyl diphenyl phosphate with 4-nitrobenzaldoximate (●) and 2-quinolinealdoximate (○) ions. Reprinted with permission from Bunton and Ihara, *J. Org. Chem.*, **42**, 2865. Copyright (1977) American Chemical Society

as cetyltrimethylammonium with anionic counter partners (CTA^+X^-) could significantly enhance the rate of decomposition of the phosphorylated derivatives[45,48–52]. A typical rate profile, presented in Figure 12 for reaction of oximates with 4-nitrophenyl diphenyl phosphate, shows an initial rate increase up to the critical micelle concentration (cmc) of CTABr, reaching a rate maximum which is then followed by a rate decline. Other

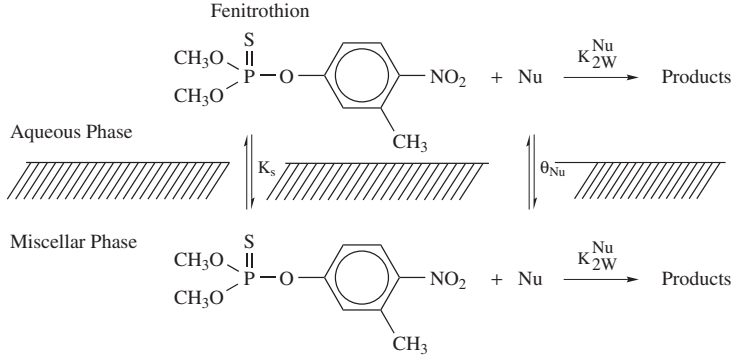

SCHEME 8. Reprinted with permission from Han *et al.*, *Langmuir*, **22**, 9009 Copyright (2006) American Chemical Society

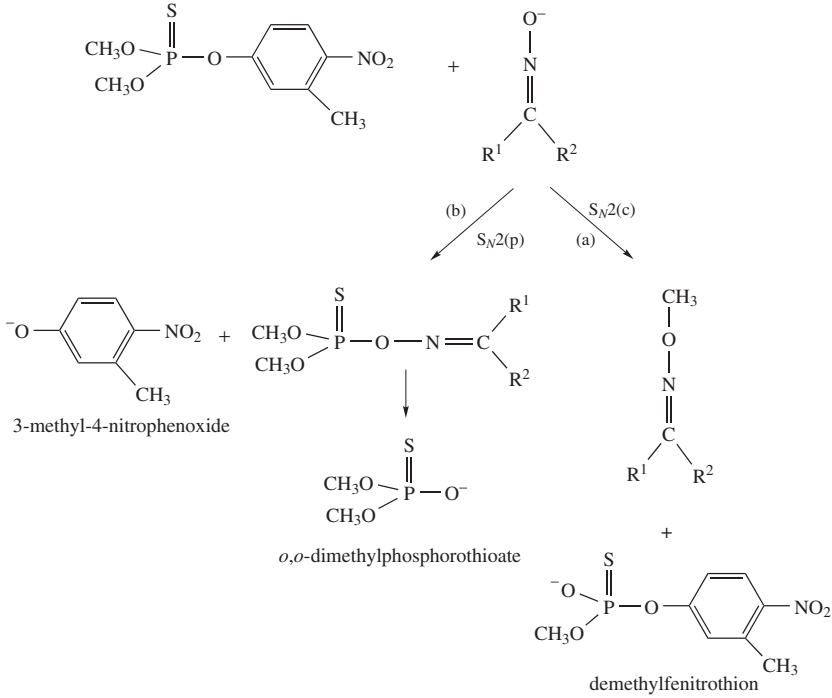

SCHEME 9. Reprinted with permission from Han *et al.*, *Langmuir*, **22**, 9009 Copyright (2006) American Chemical Society

studies have employed micelles with reactive anions such as HO^-, HOO^-, oximate, hydroxamate etc.

Rate enhancement in micellar systems may be discussed in terms of a model that was first proposed by Menger and Portnoy, known as the pseudophase ion exchange (PPIE) model[49]. This is illustrated in Scheme 8 for the decomposition of the organophosphorus pesticide fenitrothion[45]. The organophosphorus substrate will be preferentially situated in the hydrophobic interior of the micelle. Compared with the highly solvated hydroxide anion in the aqueous medium, the oximate anion is less strongly solvated in H_2O and its partitioning through the Stern layer into the micelle interior is more favorable. Thus, the concentrations of substrate and oximate in the micellar pseudophase are both enhanced. This may be described as a concentration effect rather than true catalysis.

Interestingly, in some systems micelles have been found to alter the reaction pathway, as illustrated in Scheme 9 for fenitrothion reacting at the P and CH_3 centers, i.e. S_N2(P) and S_N2(C), respectively[45b].

Current work on dephosphorylation includes the use of different micellar systems. Scheme 10 illustrates dephosphorylation via novel functional detergents which contain an imidazole ring substituted with an oxime or hydroxamic acid moiety[53].

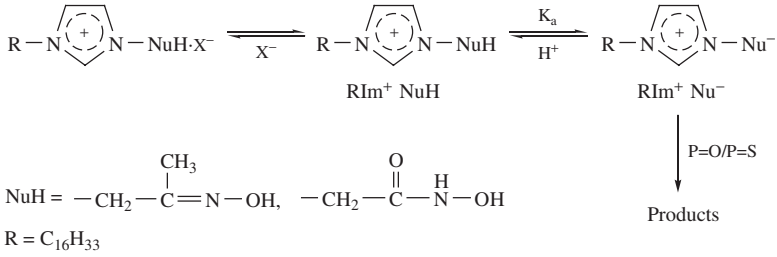

SCHEME 10

X. ACKNOWLEDGMENT

Research in the area covered in this chapter is supported by grants from the Natural Sciences and Engineering Research Council of Canada (NSERC, E.B.), Korea Research Foundation (KRF 2005-015-C00256, I.H.U.), and C.N.R.S. (F.T.).

XI. REFERENCES

1. J. O. Edwards and R. G. Pearson, *J. Am. Chem. Soc.*, **84**, 16 (1962).
2. Reviews:
   (a) E. Buncel and I. H. Um, *Tetrahedron*, **60**, 7801 (2004).
   (b) S. Hoz and E. Buncel, *Isr. J. Chem.*, **26**, 313 (1985).
   (c) N. J. Fina and J. O. Edwards, *Int. J. Chem. Kinet.*, **5**, 1 (1973).
   (d) A. P. Grekov and V. Y. Veselov, *Russ. Chem. Rev.*, **47**, 631 (1978).
3. S. Hoz and E. Buncel, *Tetrahedron Lett.*, **25**, 3411 (1984).
4. (a) W. P. Jencks and M. Gilchrist, *J. Am. Chem. Soc.*, **90**, 2622 (1968).
   (b) E. Buncel, C. Chuaqui and H. Wilson, *J. Org. Chem.*, **45**, 3621 (1980).
   (c) E. Buncel, H. Wilson and C. Chuaqui, *J. Am. Chem. Soc.*, **104**, 4896 (1982).
   (d) K. R. Fountain, D. B. Tad-y, T. W. Paul and M. V. Golynskiy, *J. Org. Chem.*, **64**, 6547 (1999).
   (e) K. R. Fountain, T. W. Dunkin and K. D. Patel, *J. Org. Chem.*, **62**, 2738 (1997).

(f) K. B. Wiberg, *J. Am. Chem. Soc.*, **77**, 2519 (1955).
(g) J. E. Mclssac Jr., J. Subbaraman, H. A. Mulhausen and E. J. Behrman, *J. Org. Chem.*, **37**, 1037 (1972).
5. (a) J. E. Dixon and T. C. Bruice, *J. Am. Chem. Soc.*, **94**, 2052 (1972).
(b) S. Hoz, *J. Org. Chem.*, **47**, 3545 (1982).
(c) C. F. Bernasconi and C. J. Murray, *J. Am. Chem. Soc.*, **108**, 5251 (1986).
(d) C. F. Bernasconi, A. E. Leyes, I. Eventova and Z. Rappoport, *J. Am. Chem. Soc.*, **117**, 1703 (1995).
6. (a) A. J. Kirby, J. E. Davies, T. A. S. Brandao, P. F. da Silva, W. R. Rocha and F. Nome, *J. Am. Chem. Soc.*, **128**, 12374 (2006).
(b) A. J. Kirby, F. Marcelo, D. da Silva, C. D. Roussev and F. Nome, *J. Am. Chem. Soc.*, **128**, 16944 (2006).
(c) A. J. Kirby, N. Dutta-Roy, D. da Silva, J. M. Goodman, M. F. Lima, C. D. Roussev and F. Nome, *J. Am. Chem. Soc.*, **127**, 7033 (2005).
7. (a) J. B. Domingos, E. Longhinotti, T. A. S. Brandao, C. A. Bunton, L. S. Santos, M. N. Eberlin and F. Nome, *J. Org. Chem.*, **69**, 6024 (2004).
(b) J. B. Domingos, E. Longhinotti, C. A. Bunton and F. Nome, *J. Org. Chem.*, **68**, 7051 (2003).
(c) H. Miyabe, K. Yoshida, M. Yamauchi and Y. Takemoto, *J. Org. Chem.*, **70**, 2148 (2005).
8. (a) O. Exner, M. Haradil and J. Mollin, *Collect. Czech. Chem. Commun.*, **58**, 1109 (1993).
(b) M. Decouzon, O. Exner, J. F. Gal and P. C. Maria, *J. Org. Chem.*, **55**, 3980 (1990).
9. (a) C. P. Brink and A. L. Crumbliss, *J. Org. Chem.*, **47**, 1171 (1982).
(b) C. P. Brink, L. L. Fish and A. L. Crumbliss, *J. Org. Chem.*, **50**, 2277 (1985).
10. A. Bagno, C. Comuzzi and G. Scorrano, *J. Am. Chem. Soc.*, **116**, 916 (1994).
11. F. G. Bordwell, H. E. Fried, D. L. Hughes, T. Y. Lynch, A. V. Satish and Y. E. Whang, *J. Org. Chem.*, **55**, 3330 (1990).
12. M. K. Chantoni and I. M. Kolthoff, *J. Phys. Chem.*, **80**, 1306 (1976).
13. (a) I. H. Um, H. W. Yoon and D. S. Kwon, *Bull. Korean Chem. Soc.*, **14**, 425 (1993).
(b) I. H. Um, H. W. Yoon, J. S. Lee, H. J. Moon and D. S. Kwon, *J. Org. Chem.*, **62**, 5939 (1997).
14. (a) F. Terrier, F. Degorre, D. Kiffer and M. Laloi, *Bull. Soc. Chim. Fr.*, 415 (1988).
(b) F. Terrier, P. MacCormack, E. Kizlian, J. C. Halle, P. Demerserman, F. Guir and C. Lion, *J. Chem. Soc., Perkin Trans. 2*, 153 (1991).
(c) G. Moutiers, E. Le Guevel, L. Villien and F. Terrier, *J. Chem. Soc., Perkin Trans. 2*, 7 (1997).
(d) F. Terrier, G. Moutiers, S. Pelet and E. Buncel, *Eur. J. Org. Chem.*, 1771 (1999).
(e) F. Mancin, P. Tecilla and U. Tonellato, *Eur. J. Org. Chem.* 1045 (2000).
15. F. Terrier, P. Rodriguez-Dafonte, E. Le Guevel and G. Moutiers, *Org. Biomol. Chem.*, **4**, 4352 (2006).
16. E. Buncel, C. Cannes, A. P. Chatrousse and F. Terrier, *J. Am. Chem. Soc.*, **124**, 8766 (2002).
17. M. Laloi-Diard, J. F. Verchere, P. Gosselin and F. Terrier, *Tetrahedron Lett.*, **25**, 1267 (1984).
18. E. Buncel and I. H. Um, *J. Chem. Soc., Chem. Commun.*, 595 (1986).
19. R. Tarkka and E. Buncel, *J. Am. Chem. Soc.*, **117**, 1503 (1995).
20. E. Buncel, I. H. Um and S. Hoz, *J. Am. Chem. Soc.*, **111**, 971 (1989).
21. F. Terrier, E. Le Guevel, A. P. Chatrousse, G. Moutiers and E. Buncel, *Chem. Commun.*, 600 (2003).
22. I. H. Um, S. J. Oh and D. S. Kwon, *Tetrahedron Lett.*, **36**, 6903 (1995).
23. (a) C. H. DePuy, E. W. Della, J. Filley, J. J. Grabowski and V. M. Bierbaum, *J. Am. Chem. Soc.*, **105**, 2481 (1983).
(b) S. Wolfe, D. J. Mitchell, H. B. Schlegel, C. Minot and O. Eisenstein, *Tetrahedron Lett.*, **23**, 615 (1982).
(c) Y. Ren and H. Yamataka, *J. Org. Chem.*, **72**, 5660 (2007).
(d) Y. Ren and H. Yamataka, *Org. Lett.*, **8**, 119 (2006).
(e) Y. Ren and H. Yamataka, *Chem. Eur. J.*, **13**, 677 (2007).
24. I. H. Um, Y. M. Park and E. Buncel, *Chem. Commun.*, 1917 (2000).
25. W. P. Jencks, *Chem. Rev.*, **85**, 511 (1985).

26. (a) C. F. Bernasconi, *Adv. Phys. Org. Chem.*, **27**, 119 (1992).
(b) C. F. Bernasconi, *Acc. Chem. Res.*, **25**, 9 (1992).
(c) C. F. Bernasconi, *Acc. Chem. Res.* **20**, 301 (1987).
27. (a) E. A. Moelwyn-Hughes, *The Kinetics of Reactions in Solution*, 2nd edn., Oxford University Press, London, 1947.
(b) E. D. Hughes and C. K. Ingold, *J. Chem. Soc.*, 244 (1935).
28. D. F. Heath, *Organophosphorus Poisons*, Pergamon Press, Oxford, 1961.
29. (a) C. Fest and K. J. Schmidt, *The Chemistry of Organophosphorus Pesticides*, Springer-Verlag, New York, 1971.
(b) B. Holmstedt, *Pharmacol. Rev.*, **11**, 567 (1959).
30. A. Goldstein, L. Arnow and S. M. Kalman, *Principles of Drug Action: The Basis of Pharmacology*, 2nd edn., Wiley, New York, 1974.
31. (a) E. Buncel, G. W. vanLoon, V. Balakrishnan, E. Chambers, D. Churchill, A. Esbata, W. Fang, E. Kiepek, O. Oketunde, E. Omakor and S. Shirin, *Can. Chem. News*, **57**, 18 (2005).
(b) R. S. Brown, T. C. Lumleg and K. Volchek, *Can. Chem. News*, **59**, 12 (2007).
32. (a) J. E. Casida and G. B. Quistad, *Chem. Res. Toxicol.*, **17**, 983 (2004).
(b) J. Kassa, *J. Toxicol. Clinic. Toxicol.*, **40**, 803 (2002).
(c) F. R. Sidell and J. Borak, *Ann. Emerg. Med.*, **21**, 865 (1992).
33. (a) G. Wagner and Y. C. Yang, *Int. Eng. Chem. Res.*, **41**, 1925 (2002).
(b) Y. C. Yang, *Acc. Chem. Res.*, **32**, 109 (1999).
(c) Y. C. Yang, J. A. Baker and J. R. Ward, *Chem. Rev.*, **92**, 1729 (1992).
34. (a) Y. Ashani, N. Dinar and S. Cohen, *J. Med. Chem.*, **11**, 967 (1968).
(b) Y. Ashani and S. Cohen, *J. Med. Chem.*, **13**, 471 (1970).
(c) R. L. Salvador, M. Saucier, D. Simon and R. Goyer, *J. Med. Chem.*, **15**, 646 (1972).
35. L. Bromberg and T. A. Hatton, *Ind. Eng. Chem. Res.*, **44**, 7991 (2005).
36. (a) L. M. Schopfer, T. Voelker, C. F. Barthels, C. M. Thompson and O. Lockridge, *Chem. Res. Toxicol.*, **18**, 747 (2005).
(b) D. M. Maxwell, A. Savena, R. K. Gordon and B. P. Doctor, *Chem. Biol. Int.*, **119–120**, 419 (1999).
37. (a) K. J. Wallace, R. I. Fagbemi, F. J. Folmer-Andersen, J. Morey, V. M. Lynth and E. V. Anslyn, *Chem. Commun.*, 3886 (2006).
(b) B. C. Singer, A. T. Hodgson, H. Destaillats, T. Hotchi, K. L. Revzan and R. G. Sextro, *Environ. Sci. Tech.*, **39**, 3203 (2005).
38. J. Wang, J. Gu, J. Leszczynski, M. Feliks and W. A. Sokalski, *J. Phys. Chem. B*, **111**, 2404 (2007).
39. (a) R. A. Kenley, C. D. Bedford, O. D. Dailey, Jr., R. A. Howd and A. Miller, *J. Med. Chem.*, **27**, 1201 (1984).
(b) C. D. Bedford, R. N. Harris, III, R. A. Howd, A. Miller, H. W. Nolen and R. A. Kenley, *J. Med. Chem.*, **27**, 1431 (1984).
40. P. Demerseman, D. Kiffer, L. Debussche, C. Lion, R. Royer and H. Sentenac-Roumanou, *Eur. J. Med. Chem.*, **23**, 63 (1988).
41. (a) F. Joic, L. Louise, C. Mioskowski and P-Y. Renard, *Tetrahedron Lett.*, **46**, 6809 (2005).
(b) J. Kassa and J. Karasova, *Toxicol. Lett.*, **229**, 136 (2007).
42. F. Degorre, D. Kiffer and F. Terrier, *J. Med. Chem.*, **31**, 757 (1988).
43. A. L. Green and B. Saville, *J. Chem. Soc.*, 3887 (1956).
44. (a) F. Worek, H. Thiermann, L. Szinicz and P. Eyer, *Biochem. Pharmacol.*, **68**, 2237 (2004).
(b) A. T. M. Prokop'eva, Y. S. Simanenko, E. A. Karpichev, V. A. Savelova and A. F. Popov, *Russ. J. Org. Chem.*, **40**, 1617 (2004).
(c) I. Koplovitz and J. R. Stewart, *Toxicol. Lett.*, **70**, 269 (1994).
45. (a) X. Han, V. K. Balakrishnan and E. Buncel, *Langmuir*, **23**, 6519 (2007).
(b) X. Han, V. K. Balakrishnan, G. W. vanLoon and E. Buncel, *Langmuir*, **22**, 9009 (2006).
(c) V. K. Balakrishnan, E. Buncel and G. W. VanLoon, *Environ. Sci. Technol.*, **39**, 5824 (2005).
(d) V. K. Balakrishnan, X. Han, G. W. VanLoon, J. M. Dust, J. Toullec and E. Buncel, *Langmuir*, **20**, 6586 (2004).
(e) J. E. Omakor, I. Onyido, G. W. vanLoon and E. Buncel, *J. Chem. Soc., Perkin Trans. 2*, 324 (2001).
46. (a) G. Moutiers, E. Le Guevel, L. Villien and F. Terrier, *Electroanalysis*, **12**, 1403 (2000).
(b) J. Wang, J. Leszczynski, M. Feliks and W. A. Sokalski, *J. Phys. Chem. B*, **111**, 2404 (2007).

47. (a) J. Epstein, V. E. Bauer, M. Saxe and M. M. Demek, *J. Am. Chem. Soc.*, **78**, 4068 (1956).
(b) J. Epstein, P. L. Cannon, H. O. Michel, B. E. Hackley and W. A. Mosher, *J. Am. Chem. Soc.*, **89**, 2937 (1967).
48. C. A. Bunton and Y. Ihara, *J. Org. Chem.*, **42**, 2865 (1977).
49. (a) F. M. Menger and C. A. Portnoy, *J. Am. Chem. Soc.*, **89**, 4698 (1967).
(b) C. A. Bunton and G. Savelli, *Adv. Phys. Org. Chem.*, **22**, 213 (1986).
50. (a) S. Couderc and J. Toullec, *Langmuir*, **17**, 3819 (2001).
(b) N. Ouarti, A. Marques, I. Blagoeva and M.-F. Ruasse, *Langmuir*, **16**, 2157 (2000).
51. H. Kotoucova, R. Cibulka, F. Hampl and F. Liska, *J. Mol. Catal. A: Chemical*, **174**, 59 (2001).
52. (a) K. K. Ghosh, D. Sinha, M. L. Satnami, D. K. Dubey, P. Rodriguez-Dafonte and G. L. Mundhara, *Langmuir*, **21**, 8664 (2005).
(b) K. K. Ghosh, M. L. Satnami and D. Sinha, *Tetrahedron Lett.*, **45**, 9103 (2004).
53. (a) Y. S. Simanenko, E. A. Karpichev, T. M. Prokop'eva, A. Lattes, A. F. Popov, V. A. Savelova and I. A. Belousova, *Russ. J. Org. Chem.*, **40**, 206 (2004).
(b) A. F. Popov, Y. S. Simanenko, T. M. Prokop'eva, E. A. Karpichev, A. A. Matveev, V. N. Matvienko, I. A. Belousova and V. A. Savelova, *Theor. Exp. Chem.*, **39**, 15 (2003).

CHAPTER **18**

N-Heteroatom-substituted hydroxamic esters

STEPHEN A. GLOVER

Division of Chemistry, School of Science and Technology, University of New England, Armidale, NSW 2351, Australia
Fax: +61-2-67733268; e-mail: Stephen.Glover@une.edu.au

The chemistry of hydroxylamines, oximes and hydroxamic acids
Edited by Z. Rappoport and J. F. Liebman

I. INTRODUCTION

The properties of amides are determinants of the structure and characteristics of a wide range of molecules and particularly those of peptides and proteins[1]. Hydroxamic esters, as a subset of the amide functionality, possess many structural features in common with the more abundant linkage. Amide linkages in hydroxamic esters and amides are characterized by a nitrogen that is essentially sp^2 hybridized and a lone pair that resides in a $2p_z$ orbital. As a consequence there is a strong interaction between the amide nitrogen and the carbonyl, which has been described as a resonance delocalization involving **I** and **II** (Figure 1a). However, contemporary views strongly favour a third resonance contributor **III** in which there is σ back-donation from carbon to the sp^2-hybridized nitrogen. According to Wiberg, amide resonance is best described as a HOMO–LUMO interaction and there is little charge transfer to oxygen since this contributes weakly to the LUMO of carbonyls (Figure 1b)[2,3]. This interaction between the nitrogen lone pair and the carbon of the carbonyl bond and the double bond character that ensues, may also be termed as conjugation, and is the prime cause of both planarity at nitrogen and the restricted rotation

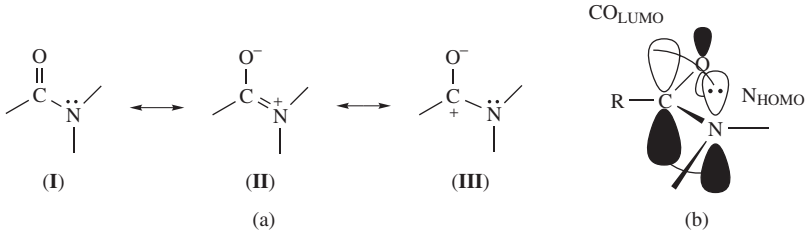

FIGURE 1. (a) Resonance and (b) HOMO–LUMO interaction in simple amides

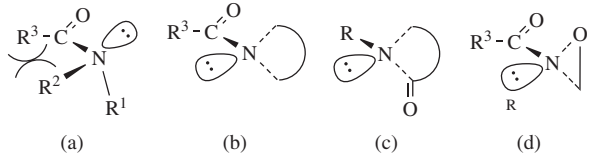

FIGURE 2. (a) A sterically twisted amide; (b) an angularly constrained amide; (c) a twisted lactam; (d) an angularly constrained hydroxamic ester

about $C-N$ bonds in amides and hydroxamic esters. The attachment of one oxygen to the amide nitrogen does not dramatically alter the degree of pyramidality at nitrogen or the extent of lone-pair delocalization/interaction with the carbonyl as evidenced by barriers to isomerism and IR carbonyl stretch frequencies, which are very similar in both amides and hydroxamic esters[1,4–17].

A good number of amides are not planar at nitrogen because of twisting due to steric interactions (Figure 2a)[18–26], configurational properties that close the angles at nitrogen (Figure 2b)[20,27–30] or lactams that lock the nitrogen lone pair out of alignment with the carbonyl carbon $2p_z$ orbital (Figure 2c)[31–37]. Similarly, a number of pyramidal *N*-acyloxaziridines (Figure 2d) have been described and their IR carbonyl stretch frequencies are in the region of 1730–1740 cm^{-1} [38–41] and much higher than those of simple hydroxamic esters, whose carbonyls are typically between 1660 and 1685 cm^{-1} [13]. The result in all cases is a disconnection between the nitrogen lone pair and the amide carbonyl; the amide nitrogens tend towards sp^3 hybridization and the $C-N$ bonds assume greater single-bond character. All these amides constitute the class of 'twisted amides', although in (b) and (d) (Figure 2), twisting may be the result of lone-pair disconnection rather than the cause thereof. Twisted amides undergo rapid hydrolysis or reduction[32,42–47] and exhibit enhanced reactivity[48].

The bourgeoning interest in twisted or atypical amide linkages has resulted in a need to better understand the chemical and physical consequences of disconnection between the amide nitrogen lone pair and its carbonyl. To this end, Mucsi and coworkers recently defined a new 'amidity' index, which shows some promise in quantifying relative amide character[49].

Another class of amides, many of which are hydroxamic esters, possess pyramidal nitrogens but are devoid of any steric or configurational imposition that results in enforced twisting about the amide linkage. These are 'anomeric amides' (**1**), defined as amides that bear two heteroatoms at the amide nitrogen[50]. There is ample evidence of pyramidality in some *N*-alkoxy-*N*-chloroamides (**1a**, X = Cl), *N*-acyloxy-*N*-alkoxyamides (**1b**), *N*,*N*-dialkoxyamides (**1c**), *N*-amino-*N*-alkoxyamides (**1d**) and *N*,*N*-dihaloamides (**1f**). In all of these, the amide nitrogen responds to the collective electronegativity of the substituents

by rehybridizing from sp^2 to sp^3. This facilitates an electron density distribution that better satisfies the electron demand of the nitrogen substituents, *X* and *Y*. The configurational change results in smaller angles at nitrogen and reduced p-character of the lone-pair orbital with attendant disconnection from the amide carbonyl, as evidenced by spectroscopic properties, radically reduced amide isomerization barriers, reactivity patterns and theoretical attributes. In effect the contribution of structure **II** (Figure 1a) to the resonance hybrid is reduced. *N*-Alkoxy-*N*-thioalkylamides (**1e**) appear to be exceptions to **1a–d** and experimental and theoretical evidence suggests they possess more usual amide characteristics.

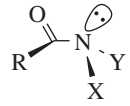

(**1**)

(**a**) X = Cl , Br, I, Y = OR
(**b**) X = OAcyl, Y = OR
(**c**) X = Y = OR
(**d**) X = NR_2, Y = OR
(**e**) X = SR, Y = OR
(**f**) X = Y = Halogen

While the term '*anomeric amides*' may be used to describe all systems bearing two heteroatoms at nitrogen and thus capable of displaying anomeric effects, not all properties exhibited by these amides may be attributed solely to the operation of such effects[10].

This chapter will cover the synthesis, structure and chemical reactivity of various *N*-heteroatom-substituted hydroxamic esters, anomeric amides in which at least one of the heteroatom substituents at nitrogen is an alkoxyl group. Throughout this review, these will either be referred to as *N*-substituted hydroxamic esters or as *N*-substituted-*N*-alkoxyamides.

To date only a few classes of such compounds have been reported. *N*-Chlorohydroxamic esters have been used as precursors to other anomeric amides and extensively as *N*-alkoxynitrenium ion sources[51–61]. The chemistry of a large number of *N*-acyloxy-*N*-alkoxyamides has been described on account of their role as direct-acting chemical mutagens[13] but only a limited number of *N*,*N*-dialkoxyamides have been reported[62–64]. The chemistry of carbamate and urea analogues of all three classes have been reported[65–69]. There have been several reports of amides geminally substituted at nitrogen with both an oxygen and a nitrogen, but these have either dealt with such configurations as reactive intermediates or with *N*,*N*′-dialkoxy-*N*,*N*′-diacylhydrazines as the only stable forms[63,70–73].

Some of the properties of bisheteroatom-substituted hydroxamic esters were described in an earlier review[50] and this chapter will further focus attention on the unique characteristics and reactivity patterns that this configuration imparts to such amides. In short, they display quite different physical and chemical properties to normal hydroxamic esters.

II. UNUSUAL CHARACTERISTICS OF *N*-HETEROATOM-SUBSTITUTED HYDROXAMIC ESTERS

N-Heteroatom-substituted hydroxamic esters can be expected to have different properties to those displayed by simple hydroxamic esters in two respects. On the one hand, bisheteroatom substitution at nitrogen impacts strongly upon the nitrogen hybridization

and amide resonance. On the other, the lone-pair synergy, as a consequence of anomeric effects operating through the nitrogen, influences both conformational preferences and the reactivity of various congeners.

A. Amide Properties in *N*-Heteroatom-substituted Hydroxamic Esters

Like other atoms geminally substituted with two heteroatoms, anomeric amide nitrogens deviate substantially from planarity or sp^2 hybridization, a consequence of a critical combined electronegativity of both substituents on nitrogen. At total electronegativities below this critical value, the situation that pertains where only one heteroatom is present, stabilization through conjugation of the p-type nitrogen lone pair is sufficient to sustain the planar or near-planar conformation at nitrogen. Substitution with a second heteroatom results in a shift of p-character from the lone pair to the $N-X$ and $N-Y$ σ-bonds thereby reducing resonance stabilization. The electron demand of both heteroatoms is best accommodated if nitrogen assumes pure sp^3 or near sp^3 hybridization (Figure 3a). The increased s-character of the lone pair should drastically reduce lone-pair delocalization onto the carbonyl and, with this, the intrinsic barrier to rotation about the $N-C(O)$ bonds, a barrier that is significant in unhindered amides[1,4–9] and hydroxamic esters[10–12] and which often leads to dynamic effects in their room-temperature ^1H NMR spectra. Such amides should have longer than normal $N-C(O)$ bonds. However, this elongation is not matched by a commensurate shortening of the carbonyl double bonds, a fact nicely accounted for by Wiberg's recent theories; the LUMO of carbonyls is strongly biased towards the carbon atom with which there is strongest interaction[2,3]. Nonetheless, the much smaller reduction in $C=O$ bond length results in some stiffening of carbonyl bonds and higher than normal IR carbonyl stretch frequencies. This is observed in the IR spectra of all stable *N*-heteroatom-substituted hydroxamic esters (**1a–d**).

The barrier to inversion at nitrogen in *N*-heteroatom-substituted hydroxamic esters should be greater than that found for hydroxamic esters or simple amides. However, it is likely to be substantially reduced in anomeric amides relative to amines since the planar transition state in which nitrogen is sp^2 hybridized, can benefit from π-overlap with the carbonyl (Figure 3b) and this has been verified experimentally; Rudchenko has measured an inversion barrier for *N*,*N*-dialkoxyureas at $\Delta G^{\ddagger} = 9-11$ kcal mol^{-1} and those of acyclic dialkoxyamines typically at $\Delta G^{\ddagger} = 20-22$ kcal mol^{-1} [74].

In amines, dialkoxyl substitution results in much higher barriers to inversion than in alkylamines[74,75], a fact that has also been explained in terms of an electronegativity effect; increased p-character in the σ bonds results in more s-character for the electron pair on nitrogen. The planar-inversion transition state is therefore destabilized since, in it, the lone pair must develop pure p-character. This transition state is also destabilized by a six-electron anti-bonding interaction between heteroatom lone pairs and, additionally, the better anomeric overlap that is possible in sp^3 rather than sp^2 systems may also play a role (Figure 4)[76]. These phenomena have also been rationalized theoretically[77,78].

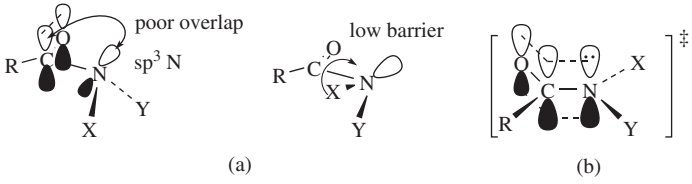

FIGURE 3. (a) Facile amide isomerism in anomeric amides; (b) stabilization of inversion transition state

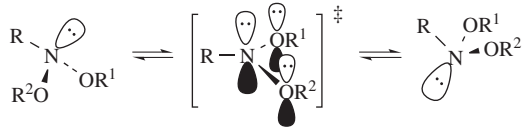

FIGURE 4. Inversion in *N*,*N*-dialkoxyamines

B. The Anomeric Interaction in *N*-Heteroatom-substituted Hydroxamic Esters

By definition, a generalized anomeric effect is observed at carbon of an *XCY* system when a molecule preferentially adopts a conformation that optimizes a secondary, stabilizing electronic interaction involving overlap between the lone pair on one heteroatom with the σ^* orbital of the bond between the central carbon atom and the second heteroatom[79–81]. Figure 5a illustrates that in *XNY* systems, as with anomeric carbon centres, two anomeric interactions are possible and involve either an $n_Y-\sigma^*_{NX}$ or an $n_X-\sigma^*_{NY}$ overlap where n_X and n_Y represent the p-type lone pairs on *X* and *Y* and σ^*_{NX} and σ^*_{NY} represent the $N-X$ and $N-Y$ σ^* orbitals. In either case, the result is a net stabilization of the lone pair of electrons (Figure 5b). Except where the nitrogen is symmetrically substituted, one of these interactions will be strongest.

The degree of lone-pair stabilization is affected by the relative energies of n_Y and σ^*_{NX} and electronegativity of substituents *X* and *Y* influences these in opposite senses; while σ^*_{NX} would be lowered in energy (together with the σ_{NX}) as *X* becomes more electronegative along the same p-block row[81,82], n_Y is higher in energy on less electronegative atoms (Figure 6a). $N-X$ σ^* orbitals reduce in energy as one proceeds down the periodic table and the reduced orbital overlap dominates the energy. As is the case for carbon systems, optimal anomeric stabilization is developed when *Y* is an early p-block element and *X* belongs to the p-block group to the right of the periodic table[77,80]. For instance, in an *NNO* system the $n_N-\sigma^*_{NO}$ anomeric interaction would prevail over the $n_O-\sigma^*_{NN}$ stabilization.

Anomeric interactions are also affected by the sizes of the interacting orbitals and will be best where the *Y* has orbitals of similar size to *N*. Thus, in an *ONCl* system, the similarity in size of orbitals on *N* and *O* and lower energy of the $N-Cl$ σ^* orbital favours the $n_O-\sigma^*_{NCl}$ anomeric effect over the alternative $n_{Cl}-\sigma^*_{NO}$ interaction (Figure 6b).

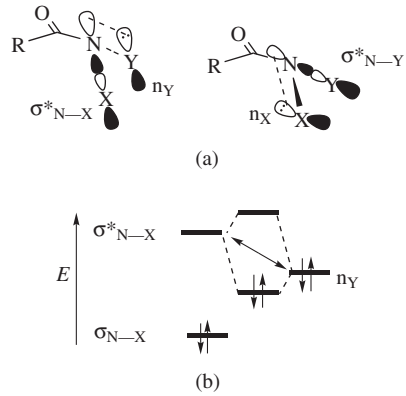

FIGURE 5. (a) Anomeric interactions in bisheteroatom-substituted amides; (b) lone-pair stabilization through an $n_Y-\sigma^*_{NX}$ anomeric interaction

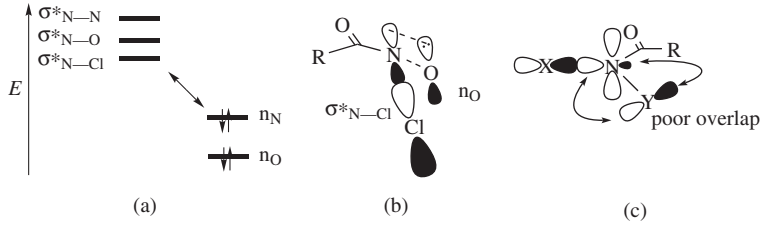

FIGURE 6. (a) Energetics governing anomeric effects; (b) orbitals of similar size favouring anomeric overlap in an *ONCl* system; (c) weak anomeric effect with sp^2 hybridization at the central nitrogen

Hybridization at the central atom is also important; with sp^2 hybridization at nitrogen, edge-on overlap with a p-orbital lone pair on *Y* would be less effective on geometrical grounds (Figure 6c)[50], and since sp^2 nitrogen would be more electronegative than sp^3 nitrogen, its contribution to the $N-X$ σ^* orbital would be reduced, relative to sp^3 $N-X$ σ^*, further weakening any anomeric overlap.

Where one of the anomeric interactions at nitrogen, say the $n_Y-\sigma^*_{NX}$, is significantly stronger, the ground-state structures should facilitate overlap between a lone-pair orbital on heteroatom, *Y*, with a σ^*_{NX} orbital (Figure 7). Depending upon the strength of the anomeric overlap, barriers to rotation about the $N-Y$ bond can be expected to be greater than predicted by steric effects alone and anomeric overlap should also result in shorter than normal $N-Y$ bonds and longer than normal $N-X$ bonds. Operation of the anomeric interaction in one direction will tend to disfavour the reverse anomeric effect for two reasons: firstly, the longer $N-X$ bond disfavours π donation from a lone pair on *X*, and secondly, the shorter $N-Y$ bond raises the energy of the $N-Y$ antibonding orbital.

In an *XNY* system, another consequence of a strong $n_Y-\sigma^*_{NX}$ anomeric interaction should be polarization as shown in Figure 8a. Where *Y* is a strong electron pair donor and *X* a strongly electron affinic atom or group, elimination might be expected, yielding a stabilized nitrenium ion. Work in the author's laboratories and elsewhere has established that nitrenium ions are strongly stabilized by neighbouring heteroatoms including oxygen[51,52,54–56,83,84]. Such a process would be promoted by polar solvents, as well as acid or Lewis acid complexation with *X*. Thus unimolecular decomposition would be expected to be more significant in strongly anomeric amides.

In S_N2 reactions, substituents at the central atom that can stabilize cationic character will also stabilize the S_N2 transition state leading to longer bonds to both the nucleophile and the leaving group[82,85,86]. Thus in systems with moderate anomeric overlap, this together with negative hyperconjugation and anchimeric assisted weakening of the $N-X$ bond should promote S_N2 reactions at nitrogen leading to loss of X^- (Figure 8b).

Where *X* is a poor leaving group, anomeric destabilization of the NX bond can lead to a novel rearrangement. The HERON (from **He**teroatom **R**earrangements **O**n **N**itrogen) reaction of anomeric amides was discovered in the mid-1990s and involves a concerted

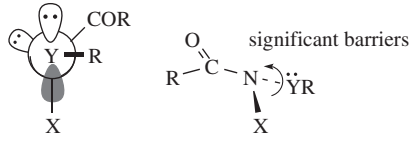

FIGURE 7. Conformational preference in anomeric amides with a dominant $n_Y-\sigma^*_{NX}$ interaction

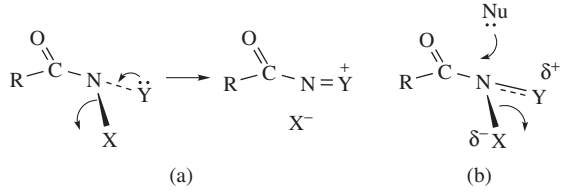

FIGURE 8. (a) Anomerically induced elimination; (b) S_N2 reaction at nitrogen

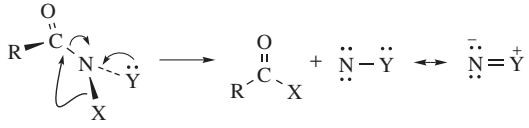

FIGURE 9. HERON reaction of an anomeric amide

migration of the *X* atom or group from the amide nitrogen to the carbonyl carbon with expulsion of a *Y*-stabilized nitrene (Figure 9)[87]. To date, numerous examples of HERON reactivity have been observed in the reactions of both *ONO* and *NNO* anomeric systems[50,63,73,87–91].

This chapter will address the synthesis, theoretical and physical properties and reactivity of a number of different classes of anomeric hydroxamic esters. Principal categories include *N*-alkoxy-*N*-haloamides (*XNO* systems), *N*-acyloxy-*N*-alkoxyamides and *N*,*N*-dialkoxyamides (*ONO* systems), *N*-alkoxy-*N*-aminoamides (*ONN* systems) and *N*-alkoxy-*N*-thioalkylamides (*ONS* systems).

III. *N*-ALKOXY-*N*-HALOAMIDES

N-Alkoxy-*N*-chloroamides (**2a**) constitute the main examples of the class of *N*-halohydroxamic esters (**1a**), and a good number have been reported in the literature[15,50–56,90,92–99]. Shtamburg and coworkers formed the closely related ureas (**3a**) and carbamates (**3b**)[65–69,100]. Some sulfonamide[66,101] and phosphoramidate[102] analogues are also known but have been described in an earlier review and will not be dealt with here[50].

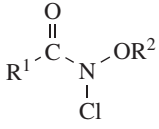

(**2**)

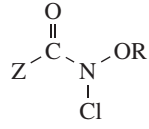

(**3**)

(**a**) R^1 = alkyl, aryl, R^2 = alkyl
(**b**) R^1 = H, R^2 = Me
(**c**) R^1 = Ph, R^2 = benzyl

(**a**) Z = R^2N, RNH, NH_2
(**b**) Z = RO

A. Synthesis of *N*-Alkoxy-*N*-haloamides

N-Chlorohydroxamic esters (**2**) are universally synthesized from the parent hydroxamic esters (**4**) using the positive halogenation source, *tert*-butyl hypochlorite[103]. Reactions are

most easily performed with a 2–3 molar excess of reagent in an organic solvent such as CH_2Cl_2, benzene, ether or even in neat hypochlorite at RT or below (equation 1)[52,55,68]. The low-boiling hypochlorite and *tert*-butanol are readily removed, along with solvent, under reduced pressure, usually with modest heat, leaving chlorinated product in quantitative yields. Most reactions can be conveniently monitored by TLC and reactions are complete within 20 min, though reaction times of several hours have been needed where R^1 and R^2 are bulky groups[99]. Products can be quantified by iodometry but, in almost all applications, the chlorinated hydroxamic esters can be used without further purification.

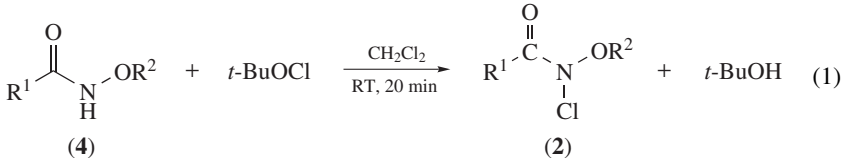

(1)

In certain cases, where the reaction with *tert*-butyl hypochlorite is tardy, reaction in the light with the addition of a trace of molecular bromine has been used[51,52,104].

The attempted formation of *N*-bromo- and *N*-iodohydroxamic esters using *tert*-butyl hypobromite or *tert*-butyl hypoiodite resulted in formation of *N*,*N*′-diacyl-*N*,*N*′-dialkoxyhydrazines as well as nitrenium-derived products (see Section III.C)[51].

B. Properties of *N*-Alkoxy-*N*-haloamides

1. Structural properties

Anomeric effects in *ONCl* systems are $n_O-\sigma^*_{NCl}$ even though oxygen is more electronegative than chlorine; *N* and *O* orbitals are similar in size and chlorine is a 3p element, thus favouring overlap between the p-type lone pair on *O* with the low-energy *N*–*Cl* σ^* orbital. In *XNY* systems, σ^*_{NX} occupation by n_Y leads to transfer of electron density to the *X* substituent and the substantially higher electron affinity of chlorine will also favour this anomeric interaction rather than an $n_{Cl}-\sigma^*_{NO}$ overlap.

Ab initio calculations at the B3LYP/6-31G* level support an $n_O-\sigma^*_{NCl}$ interaction[10,50]. Ground-state structures of *N*-chloro-*N*-methoxyformamide (**2b**), which are *Z* and *E* with respect to the *N*–*C*(*O*) bond (Figure 10a and b), differ in energy by only 0.6 kcal mol^{-1} and possess strongly pyramidal nitrogens (average angles at nitrogen of 113.2° and 112.0°, respectively). The *C*–*N* bond in the lowest-energy *Z*-form (Figure 10a, 1.41 Å) is significantly lengthened relative to formamide (1.362 Å) and *N*-methoxyformamide (1.380 Å) calculated at the same level[10], reflecting a smaller degree of lone-pair interaction with the carbonyl. Accordingly, the computed barrier to amide isomerism is only 7.7 kcal mol^{-1}, much lower than that computed for formamide (17.5 kcal mol^{-1}), which is in the region of the 18 kcal mol^{-1} measured experimentally[5,105,106], *N*-methoxyformamide

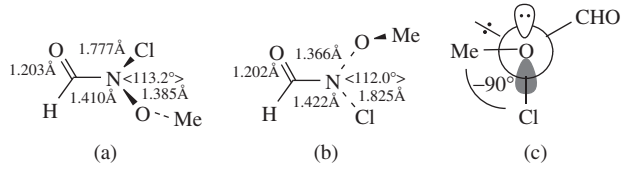

FIGURE 10. (a) *Z*-Form and (b) *E*-form of *N*-chloro-*N*-methoxyformamide computed at B3LYP/6-31G* level; (c) Newman projection along the *O*–*N* bond in (a)

(15.5 kcal mol^{-1}) and *N*-chloroformamide (between 16 and 18 kcal mol^{-1}), all of which are computed to be close to planar at nitrogen[10]. The barrier to inversion at nitrogen in the *ONCl* system was computed to be only 2.5 kcal mol^{-1}, reflecting stabilization of the planar transition state by the carbonyl.

The *Cl*−*N*−*O*−*Me* dihedral angle in the lowest-energy *Z*-form (Figure 10c) is almost 90°, reflecting the optimum anomeric interaction between the p-type lone pair on oxygen and the *N*−*Cl* σ^* orbital. The *N*−*Cl* bond (1.777 Å) is longer than that calculated for *N*-chloroformamide (1.735 Å), although this is in part attributable to sp^3 hybridization at nitrogen. However, the *N*−*O* bond (1.385 Å) is much shorter than that in *N*-methoxyformamide (1.405 Å) despite the change in hybridization and there is a considerable barrier of 10.7 kcal mol^{-1} to rotation about the *N*−*O* bond.

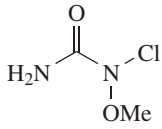

(**5**)

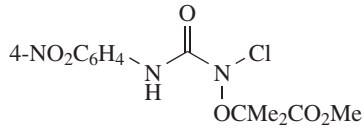

(**6**)

There are no X-ray structures for *N*-alkoxy-*N*-chloroamides. However, structures for two related ureas, **5** and **6**, have been published, which confirm the predicted properties for this class of amides (Figure 11, Table 1)[100]. The average angles at nitrogen, $\langle\beta\rangle$, and respective Winkler–Dunitz distortion parameters[107, 108], χ_N, a measure of pyramidality at nitrogen and which is optimally 60° (Figure 12), indicate pure sp^3 hybridization at nitrogen. The conformation of **5** (Figure 11a) is very similar to that of the theoretical model *N*-chloro-*N*-methoxyformamide (Figure 10a) although the nitrogen in the formamide is predicted to be less pyramidal and the *N*−*C*(*O*) bond is shorter. In **5**, conjugation of the sp^2 urea nitrogen $N_{(2)}$ with the carbonyl would be expected to further reduce residual conjugative interaction between the carbonyl and $N_{(1)}$. Furthermore, as predicted for **2b**

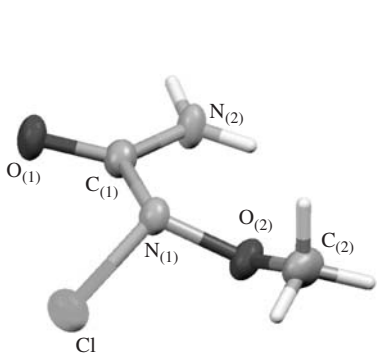

(a)

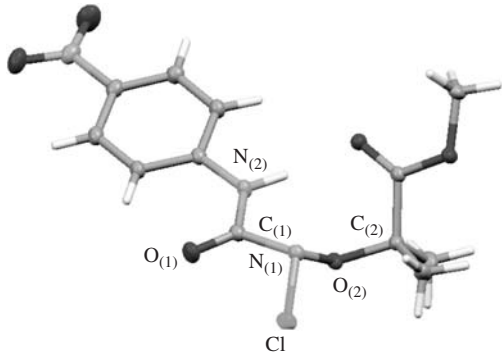

(b)

FIGURE 11. X-ray structure of (a) *N*-chloro-*N*-methoxyurea (**5**) and (b) *N*-chloro-*N*-(2-methoxycarbonyl)propyl-2-oxy-*N*′-(4-nitrophenyl)urea (**6**) with displacement ellipsoids shown at the 50% level. Bond lengths and angles are given in Table 1

TABLE 1. Selected structural properties of *N*-alkoxy-*N*-chloroamides **5** and **6**

Parameter	**5**	**6**
$r_{C(1)O(1)}$ (Å)	1.2264	1.2103
$r_{C(1)N(1)}$ (Å)	1.4429	1.4719
$r_{N(1)O(2)}$ (Å)	1.3984	1.4204
$r_{N(1)Cl}$ (Å)	1.7563	1.7572
$r_{N(2)C(1)}$ (Å)	1.3202	1.3520
$C_{(1)}-N_{(1)}-O_{(2)}$ (deg)	109.9	108.4
$Cl-N_{(1)}-O_{(2)}$ (deg)	109.1	109.0
$Cl-N_{(1)}-C_{(1)}$ (deg)	110.0	108.51
$\langle\beta\rangle$ (deg)[a]	109.7	108.6
τ(deg)[b]	8.2	−13.4
χ_N (deg)[c]	59.9	61.9
$C_{(2)}-O_{(2)}-N_{(1)}-Cl$ (deg)	−90.9	−100.1

[a] $\langle\beta\rangle = \Sigma(\beta)/3$.
[b] Angle subtended by the axes of the nitrogen lone pair and the carbonyl carbon $2p_z$ orbital.
[c] Amide distortion parameters defined in accordance with Winkler–Dunitz[107, 108].

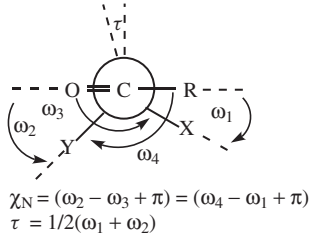

FIGURE 12. The Winkler–Dunitz convention for quantifying pyramidality at nitrogen (χ_N) and twist about the $C-N$ bond (τ) as functions of torsion angles $\omega_1 - \omega_4$ in an RCON(X)Y amide

the $C_{(2)}-O_{(2)}-N_{(1)}-Cl$ torsion angle in **5** is close to ideal for an $n_O-\sigma^*_{NCl}$ anomeric interaction. The amide group of urea **6** (Figure 11b) is similar to that of **5**. The $N_{(2)}-C(O)$ amide bond is much shorter than the $N_{(1)}-C(O)$ bond in both X-ray structures. The small degree of twisting about the $N-C(O)$ bonds in **5** and **6** as indicated by τ (Table 1), the angle between the axes of the nitrogen lone-pair orbital and the neighbouring $C2p_z$ orbital (Figure 12), is likely to be the result of steric demands of the nitrogen substituents rather than any resonance interaction.

2. Spectroscopic properties

In *N*-alkoxy-*N*-chloroamides the extent to which lone-pair delocalization is reduced is reflected in the high IR carbonyl absorption frequencies. These are uniformly in a band at 1720–1745 cm^{-1} and are on average about 40 wavenumbers higher than those of their hydroxamic ester precursors, reflecting much higher double-bond character (Table 2). As is the case for amides themselves, aryl hydroxamic esters (entries 22–41) are at the lower end of the range (1718–1727 cm^{-1}) in keeping with conjugative effects while the alkylamides

TABLE 2. IR carbonyl absorption frequencies ($CHCl_3$) and selected ^{13}C NMR chemical shifts ($CDCl_3$) for *N*-alkoxy-*N*-chloroamides ($R^1CON(Cl)OR^2$) and precursor hydroxamic esters

Entry	R^1	R^2	Amide ν (cm^{-1}) ($\delta^{13}C$)	Hydroxamic ester ν (cm^{-1}) ($\delta^{13}C$)
1[51]	Me	$PhCH_2CH_2$	1735	1695
2[94]	Et	$PhCH_2CH_2$	1744(179.2)	1693(172.2)
3[94]	Bu	$PhCH_2CH_2$	1739(178.3)	1685
4[94]	*i*-Bu	$PhCH_2CH_2$	1720(181.6)	1685(175.1)
5[94]	2-Bu	$PhCH_2CH_2$	1730(181.1)	1693(174.4)
6[94]	3-Pen	$PhCH_2CH_2$	1731(180.5)	1689(173.6)
7[94]	*t*-Bu	$PhCH_2CH_2$	1720(181.9)	1686(176.1)
8[113]	Me	Benzyl	1732(175.3)	1690(168.0)
9[113]	Me	CH_2Naph-2	1733(175.5)	1691(168.2)
10[113]	Me	$(CH_2)_2$Naph-2	1733(175.6)	1695(168.1)
11[113]	Me	$(CH_2)_3$Naph-2	1732(175.5)	1694(168.0)
12[113]	Me	Bu	1740[a] (175.3)	1678[a] (167.9)
13[99]	Et	Bu	1742(179.2)	1664(171.8)
14[99]	*i*-Bu	Bu	1735(181.6)	1657(174.9)
15[99]	1-Ad	Bu	1721(181.5)	1681(175.4)
16[99]	*t*-Bu	Bu	1727(182.1)	1683(176.2)
17[99]	Neopentyl	Bu	1742(171.8)	1653(169.5)
18[97]	*t*-Bu	*t*-Bu	1732	1690
19[97]	1-Ad	*t*-Bu	1740(186.1)	1682(186.6)
20[72]	Cyclohexyl	Me	1718	—
21[97]	*t*-Bu	Cyclohexyl	1715(183.7)	1686(176.4)
22[52]	Ph	4-$MeOC_6H_4(CH_2)_3$	1725	1690
23[51]	2-Biphen	Me	1720	1675
24[50]	Ph	Me	1722	1683
25[50]	4-$MeOC_6H_4$	Me	1719	1687
26[50]	4-ClC_6H_4	Me	1727	1687
27[50]	4-MeC_6H_4	Me	1723	1685
28[114]	4-Biphenlyl	Bu	1718	1684
29[114]	4-*t*-BuC_6H_4	Bu	1724	1679
30[96]	3-$NO_2C_6H_4$	Bu	1723	1694
31[114]	Ph	Et	1719	1679
32[96]	Ph	*n*-Pr	1720	1678
33[114]	Ph	*i*-Bu	1723	1684
34[114]	Ph	Bu	1719(174.2)	1654(165.7)
35[114]	Ph	*i*-Bu	1718	1684
36[97]	Ph	*t*-Bu	1723	1684
37[96]	Ph	*n*-Octyl	1719	1684
38[115]	Ph	4-$C_6H_5C_6H_4CH_2$	1720	1674
39[95,113]	Ph	Benzyl	1718(174.1)	1682(166.3)
40[96]	2-Naph	Bu	1722	1684
41[113]	Ph, Ph	$-CH_2(CH_2)_4CH_2-$	1718(174.2)	1662(166.0)
42[a 116]	NH_2	Me	1720	1685
43[a 116]	NH_2	Et	1725	1680
44[a 116]	NH_2	*n*-Bu	1740	1680
45[a 116]	NH_2	Benzyl	1720	1645
46[a 116]	NH_2	*n*-Octyl	1745	1680
47[a 116]	NH_2	*n*-$C_{12}H_{25}$	1750	1680
48[a 116]	Me_2N	*n*-Pr	1757	1695
49[a 116]	MeO	Me	1785	1765
50[a 116]	MeO	Et	1795	1740
51[a 116]	MeO	*i*-Bu	1780	1745
52[a 116]	EtO	Me	1770	1745

[a] Neat or in paraffin oil.

(entries 1–21) are in the range of 1715–1744 cm^{-1} and straight-chain hydroxamic esters are as high as 1744 cm^{-1} (entries 1–3, 8–13). While carbonyl stretch frequencies are strongly dependent upon solvent and are generally lower in polar solvents[109], the IR stretch frequency of *N*-chloroformamide in chloroform is at 1690 cm^{-1} [110] and those for *N*-chloroacetamide, *N*-chlorophenylacetamide and *N*-chlorobenzamide in chloroform are at 1709, 1699 and 1696 cm^{-1}, respectively[109, 111, 112]. It is clear that the presence of a single electronegative heteroatom at an amide nitrogen has a relatively small influence upon amide properties. However, combined oxygen and chlorine substitution results in significant changes to the amide configuration. The IR carbonyl absorption frequencies become more 'ester-like'; the dipolar form of the carbonyl (Figure 1a, **III**) is further destabilized by the negative inductive effect of the *ONCl* group resulting in a greater $C-O$ π-bond order than that found in simple ketones and aldehydes.

Branched *N*-chlorohydroxamic esters exhibit much lower carbonyl frequencies in their IR spectra. Series of *N*-(phenylethyloxy)amides (Table 2, entries 1–7) and *N*-butoxyamides (Table 2, entries 12–16) show a clear movement to lower carbonyl stretch frequencies with branching alpha to the carbonyl, in accord with greater inductive stabilization of the polar resonance form **III** of the carbonyl (Figure 1a). Neopentyl (entry 17) is a special case. While the group should contribute much more inductive stabilization than ethyl, its carbonyl stretch frequency is higher. Similar changes have been noted in the IR spectra of branched ketones and have been ascribed to a degree of steric hindrance to solvation and therefore destabilization of the polar resonance form **III**[117].

Pyramidalization at nitrogen upon chlorination of ureas (**3a**, Table 2, entries 42–48) and carbamates (**3b**, Table 2, entries 49–52) results in similarly elevated frequencies relative to the parent amides[116]. However, as available data were from either thin-film or solid-state IR spectra, differences cannot be compared directly with the amide data.

^{13}C NMR data for a limited number of *N*-chlorohydroxamic esters are available. The carbonyl chemical shifts support the IR findings. With the exception of two substrates (Table 2, entries 17 and 19), average carbonyls resonate some 7.1 ppm downfield of their precursor hydroxamic esters, presumably due to loss of nitrogen lone-pair overlap with carbon and the electronegative *ONCl* group. Branching at the α-carbon results in a downfield shift relative to methyl and straight-chain hydroxamic esters in the phenylethyloxy series (Table 2, entries 2–7) and the butoxy series (Table 2, entries 12–16) in accordance with increased inductive stabilization of the polar resonance form **III**. However, shifts of *tert*-butyl and 1-adamantyl acyl groups are smaller than expected. This is even more pronounced with the neopentyl side chain (Table 2, entry17) where the carbonyl is at a lower chemical shift than methyl or ethyl acyl side chains despite its greater inductive effect. Similar effects are known to operate with branched ketones. Streck and coworkers showed that in a range of solvents, the ^{13}C carbonyl shifts of dialkyl ketones were affected similarly by branching at the α-position[117]. In chloroform, the carbonyl carbons of di-*tert*-butyl ketone and diisopropyl ketone resonated 11–12 ppm downfield of that of acetone, which they attributed to a mixture of inductive and steric effects. With tertiary systems and neopentyl, particularly in dipolar solvents, hindrance to solvent stabilization of the polar, basic form **III** of the carbonyl offsets the inductive stabilization of the branched alkyl. ^{13}C NMR data presented here, and in Section IV.B.2 for *N*-acyloxy-*N*-alkoxyamides, support this.

Anomeric effects are evident from dynamic NMR studies on at least one substrate, *N*-benzyloxy-*N*-chlorobenzamide (**2c**)[50]. In acetone-d_6 the benzyl aromatic signal (δ 7.85) de-coalesced into two signals (ratio 2:1) close to 200 K, corresponding to a free energy barrier of *ca* 10–11 kcal mol^{-1} [118]. Amide isomerization appeared to be faster than $N-O$ rotation since benzoyl resonances were largely unaffected.

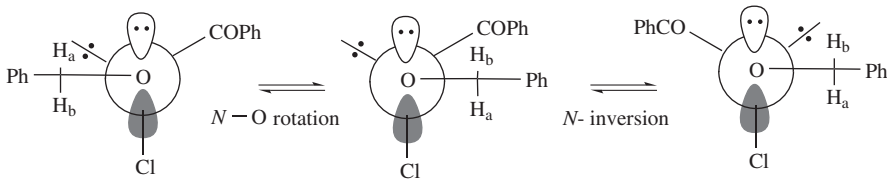

FIGURE 13. Topomerization of benzylic protons in *N*-benzyloxy-*N*-chlorobenzamide (**2c**)

In toluene-d_8, below 217 K, the benzyl aromatic signal resolved into two and the benzylic protons became diastereotopic. The exchange process, which was characterized by $k_{217} = 246\ s^{-1}$ and $\Delta G^{\ddagger} = 10.2$ kcal mol^{-1}, is a complex process involving both rotation around the $O-N$ bond and inversion at nitrogen, but since barriers to the former process are small[10] the barrier best reflects that for rotation away from the anomeric conformation (Figure 13). The amide isomerization barrier is even lower and both energies are in accordance with theoretical calculations (10.7 and 7.7 kcal mol^{-1}, respectively, for $N-O$ rotation and amide isomerism in *N*-chloro-*N*-methoxyformamide)[10].

C. Reactions of *N*-Alkoxy-*N*-haloamides

N-Chlorohydroxamic esters are intrinsically reactive at the amide nitrogen owing to:

(i) the sp^3 character of the nitrogen itself, which results in reactivity akin to sp^3 carbon;
(ii) the substitution pattern, which strongly favours an $n_O-\sigma^*_{NCl}$ anomeric effect resulting in a weakened $N-Cl$ bond.

Anchimeric assistance by the alkoxyl oxygen lone pair promotes heterolytic S_N1 and S_N2 reactions at nitrogen as well as homolysis of the $N-Cl$ bond. *N*-Haloamides are also amidyl radical sources[119,120] but their heterolytic reactivity is known to involve positive, rather than negative, halogen[121,122].

1. Radical reactions

N-Alkoxy-*N*-chloroamides (**2**) are photochemically and thermally unstable compounds. Under photolytic conditions they have been found to be excellent sources of *N*-alkoxyamidyl radicals (**7**) through homolysis of labile $N-Cl$ bonds[123,124]. Both amidyl and alkoxyamidyl radicals reside in the π-state[123–129]. However, unlike amidyl radicals, which are electrophilic in nature[119,127,130–132], alkoxyamidyls (**7**) are strongly resonance-stabilized leading to long lifetimes in solution and a propensity to dimerize to *N*,*N*′-diacyl-*N*,*N*′-dialkoxyhydrazines (**8**)[123,128]. As outlined in Section VI, **8** are themselves a class of anomeric amides, which can be isolated at room temperature and are known to rearrange by the HERON reaction to esters (**9**) and nitrogen (equation 2)[63,70–73,133]. Thermolysis of *N*-alkoxy-*N*-chloroamides almost always leads to the formation of the corresponding esters through homolysis of the $N-Cl$ bonds and intermediacy of the hydrazines.

One-electron reduction of *N*-chlorohydroxamic esters to give alkoxyamidyls, which dimerize to **8**, has been observed in ethanol with triethylamine as reductant[134]. Carbamyl derivatives (**3b**) react analogously in methanol[69] as do *N*-alkoxy-*N*-chloroureas (**3a**) in benzene[65].

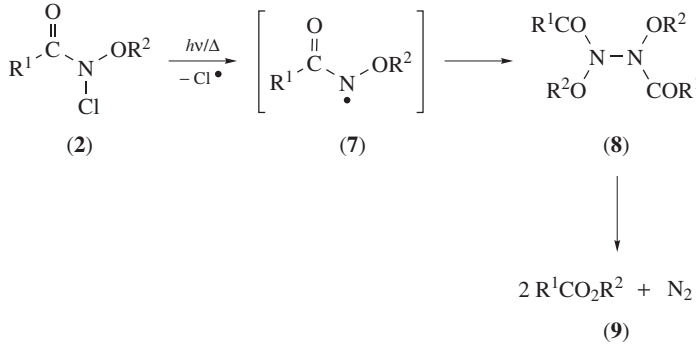

(2)

2. S_N1 reactions

Heterolytic reactivity of *N*-alkoxy-*N*-chloroamides is influenced in a predictable fashion by the anomeric overlap $n_O - \sigma^*_{NCl}$. While this configuration at amide nitrogen is stable at room temperature in non-polar solvents, in polar media S_N1-type reactivity leading to the formation of *N*-alkoxynitrenium ion intermediates is found. *N*-Acyl-*N*-alkoxynitrenium ions are strongly resonance-stabilized through the p-type lone pair of the oxygen atom (Figure 14). *Ab initio* calculations (HF/6-31G*) predict that oxygen and other heteroatoms will stabilize the singlet ground state relative to the triplet and estimates predict strong $N{=}O$ double-bond character with a π-bond order around 0.9[83]. A rotational barrier for hydroxynitrenium ion of some 38 kcal mol^{-1} has been determined at MP4/6-311G** level[84].

Thus in alcoholic or aqueous alcoholic media, *N*-alkoxy-*N*-chlorobenzamides (**10**) are solvolysed to *N*,*N*-dialkoxyamides (**12**) in modest yields[62,63] (equation 3). Evidence for S_N1 solvolysis involving **11** lies in the fact that in mixed aqueous/alcoholic solutions, the rates of solvolysis are linearly dependent upon the percentage composition, and therefore solvent polarity, but otherwise independent of the alcohol concentration[64]. Both symmetrical and unsymmetrical dialkoxyamides can be synthesized, although it was not possible to form *N*-alkoxy-*N*-*tert*-butoxyamides by this method.

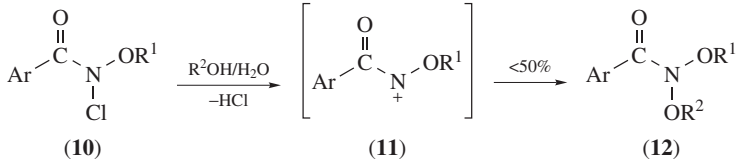

(3)

Incipient *N*-alkoxynitrenium ion character has enabled unusual α-ethoxylation when *N*-alkoxy-*N*-chloroarylacetamides (**13**) were treated with triethylamine in ethanol

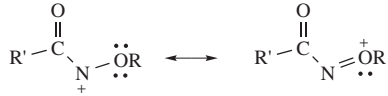

FIGURE 14. Resonance forms of *N*-acyl-*N*-alkoxynitrenium ions

(equation 4). Kikugawa and coworkers proposed loss of HCl to form the zwitterion intermediate (**14**), which is quenched by solvent at the α-carbon rather than at nitrogen to give **15**. Substrates without acidic α-hydrogens, such as 3-phenylpropionamide, formed the alkoxyamidyl radical, which dimerized to the *N*,*N*′-diacyl-*N*,*N*′-dialkoxyhydrazine according to equation 2. With highly acidic α-hydrogens (e.g. Ar = 4-nitrophenyl) α-chlorination occurred instead[134]. Analogous processes are known for α-haloketones[135].

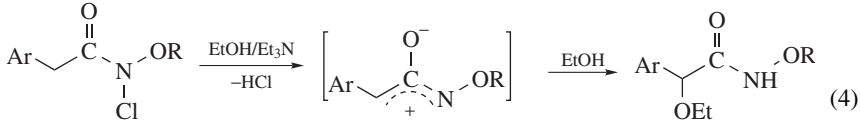

(**13**) (**14**) (**15**) (4)

20–50%

Rudchenko and coworkers have found that upon prolonged standing in CCl_4, *N*-chloro-*N*-methoxy-*N*′,*N*′-dimethylurea (**16**) forms the corresponding urethane (**20**) and have suggested initial unimolecular decomposition to alkoxynitrenium chloride (**17**) leading to the acyl chloride (**18**) and methoxynitrene (**19**). Dimerization of **19** and radical decomposition could generate methanol, which could form the urethane with acid chloride (**18**) (Scheme 1)[66]. However, the formation of **18** and **19** might also be via a HERON reaction by analogy with other anomeric amides (Figure 9, R = Me_2N, X = Cl, Y = OMe).

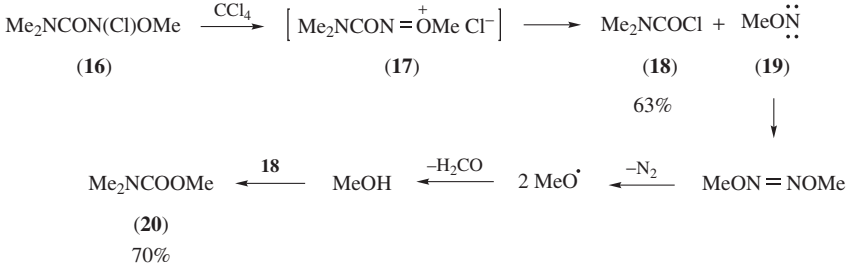

SCHEME 1

3. Lewis acid-catalysed heterolysis reactions

Alkoxynitrenium ion formation in hydroxylic and non-hydroxylic organic solvents has been effected by treating *N*-alkoxy-*N*-chloroamides with Lewis acids, typically silver and zinc ions[51,52,54–56]. Metal ion complexation with the chlorine lowers the energy of the σ^*_{NCl} orbital resulting in elimination of metal chloride. If silver acetate is utilized, the alkoxynitrenium ion can be scavenged by acetate to yield *N*-acetoxy-*N*-alkoxybenzamides (**21**) (equation 5)[62,92].

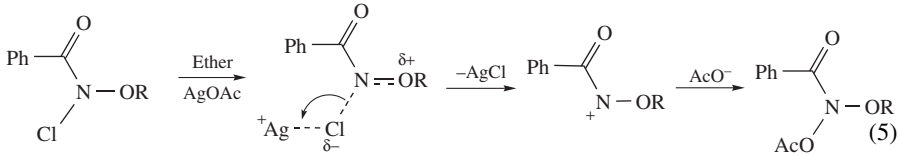

(**21**) (5)

Alkoxynitrenium ions formed by the Lewis acid method have also been shown to be efficient electrophiles towards aromatic ring systems, and two groups in particular have fashioned this reaction as an excellent source of heterocycles and benzolactams[51–56].

Quantitative cyclization of *N*-chloro-*N*-methoxybiphenyl-2-carboxamide (**22**, X = Cl) to *N*-methoxyphenanthridone (**23**) using $AgBF_4$ in benzene was the first example of such chemistry (equation 6)[51]. The cyclization could also be effected thermally in refluxing benzene or catalysed by molecular iodine in the dark. The corresponding *N*-bromo- and *N*-iodoamides, formed *in situ*, reacted at room temperature[51].

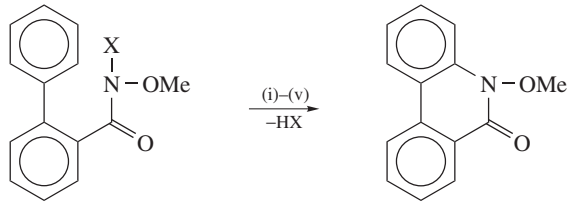

(**22**) (**23**) (6)

(i) X = Cl; $AgBF_4$, benzene, RT, 100%
(ii) X = Cl; Δ, dark, benzene, 50%
(iii) X = Cl; I_2, dark, benzene, RT,58%
(iv) X = Br; dark, benzene, RT, 12%
(v) X = I; dark, *tert*-butanol, RT, 31%

The $AgBF_4$ method was extended to cyclizations onto the alkoxyl side chain. Novel heterocycles *N*-acyl-3,4-dihydro-1*H*-2,1-benzoxazines (**25**) and *N*-acyl-4,5-dihydro-1*H*,3*H*-2,1-benzoxazepines (**26**) were synthesized by the treatment of open-chain *N*-chloro-*N*-(2-phenylethyloxy)- and *N*-chloro-*N*-(3-phenylpropyloxy)amides (**24**, *n* = 2, 3) with silver tetrafluoroborate in benzene (Scheme 2). Optimal yields of **25** were ultimately obtained with $AgBF_4$ in ether or THF[52].

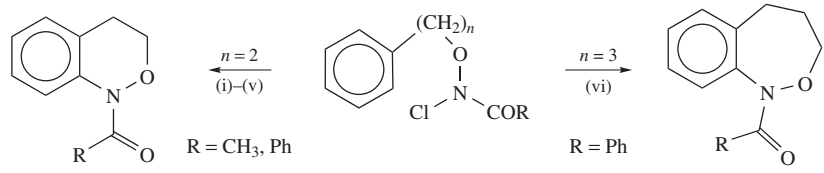

(**25**) (**24**) (**26**)

(i) $AgBF_4/C_6H_6$, 67%; (ii) $AgClO_4/C_6H_6$, 81%; (iii) HgO/C_6H_6, 26%;
(iv) $Hg(OAc)_2/C_6H_6$, 24%; (v) $AgBF_4/Et_2O$ or THF, >90% (vi) $AgBF_4/C_6H_6$, 35%

SCHEME 2

Subsequent deuterium-labelling studies showed that benzoxazines (**25**) were formed by direct Ar_2-6 cyclization of nitrenium ion **27** onto the *ortho* position on the aromatic ring giving intermediate **28**, whereas the benzoxazepines (**26**) were generated mainly by Ar_1-6 cyclization onto the *ipso* position giving **29** followed by carbon migration to give **30** (Scheme 3). The same mechanism in the formation of **25** by Ar_1-5 attack of the nitrenium ion would invoke a strained five-membered transition state with an endocyclic *N*=O π-bond. For a similar reason, benzoxazoles cannot be formed from **27** (*n* = 1) by Ar_2-5 cyclization[52,53].

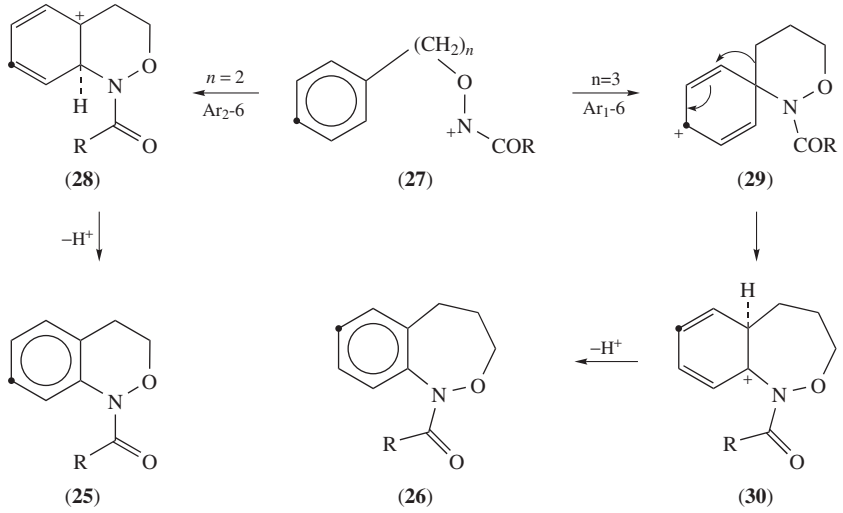

SCHEME 3

The presence of a 4-methoxy substituent on the 2-phenylethyloxyl or 3-phenylpropyloxyl side chains radically altered the course of these cyclizations (Scheme 4). **31a** and **31b** afforded the spiro-fused ring systems **32** and **33** in 26 and 69% yields, respectively, as the only cyclization products. With this substituent, cyclization onto the activated *ipso* positions was favoured over direct attack, even where the strained transition state for Ar_1-5 cyclization of **31a** to **32** was involved. Demethylation of the intermediate spirocyclohexadienyl cation is favoured over rearrangement in these cases. Kikugawa and coworkers effected the formation of **32** (82%) and **33** (39%) with reverse efficiencies using Ag_2CO_3 in TFA[56].

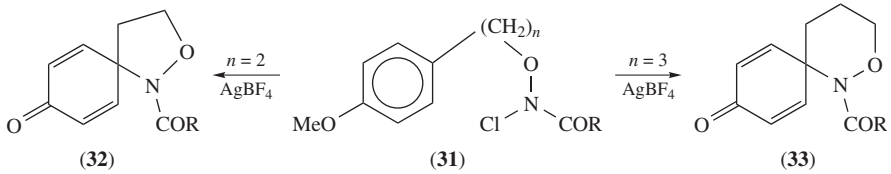

(**a**) $n = 2$
(**b**) $n = 3$

SCHEME 4

The synthesis of a range of benzoxazines (**35**) from **34** using $AgBF_4$ in anhydrous ether has been described[94]. Thermolysis of these in a melt resulted in a retro-Diels–Alder reaction with loss of formaldehyde giving the azaxylylenes (**36**), which undergo spontaneous electrocyclization to give the 2-alkyl-4*H*-3,1-benzoxazines (**37**) in excellent yields (Scheme 5).

Kikugawa and coworkers utilized silver carbonate in TFA and zinc acetate in nitromethane in the synthesis of a variety of benzolactams (**39**, $n = 1,2,3$), in excellent yields, by cyclization onto aryl rings on the acyl side chain of **38** (Scheme 6)[54–56]. $AgBF_4$ was also effective but typically afforded lower yields[52].

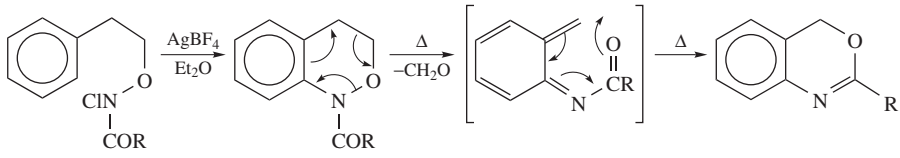

(**34**) (**35**) (**36**) (**37**)

R = Ph, Me, *t*-Bu, *i*-Pr , Et, Bu, 2-Bu, 3-Pen

SCHEME 5

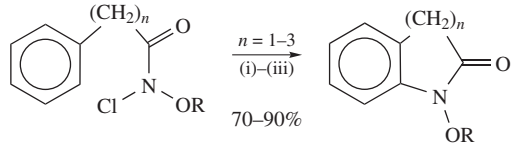

(**38**) (**39**)

(i) Ag_2CO_3/TFA; (ii) $Zn(OAc)_2/CH_3NO_2$; (iii) $AgBF_4/Et_2O$

SCHEME 6

The versatility of lactam formation was demonstrated in the synthesis of the antibacterial agent 3-amino-3,4-dihydrocarbostyril (**41**), starting with a derivatized L-phenylalanine (**40**) (equation 7)[56].

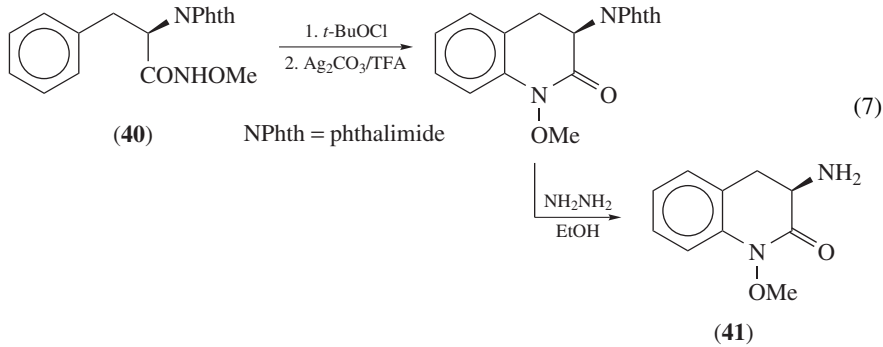

(**40**) NPhth = phthalimide (**41**) (7)

Similarly, Kikugawa and coworkers demonstrated the efficient synthesis of eupolauramine (**44**) in which the critical step involved cyclization of (**42**) via the alkoxynitrenium ion onto a naphthalene skeleton giving intermediate **43** (Scheme 7)[136].

In another early application to natural product synthesis, Fleming and coworkers utilized this approach in the efficient formation of the gelsemine model (**47**) from **45** according to Scheme 8[137]. The cyclization step to form the spiro-oxindole (**46**) proceeded in 85% yield and provided a means of generating the spiro-fused quaternary carbon without the need for carbenium ion or carbanion chemistry.

More recently Wege and coworkers synthesized the Nifedipine analogue *N*-hydroxyphenanthridone (**50**) from *N*-benzyloxybiphenyl-2-carboxamide (**48**) by cyclization to *N*-benzyloxyphenanthridone (**49**) followed by catalytic reductive removal of the benzyl group (Scheme 9)[138].

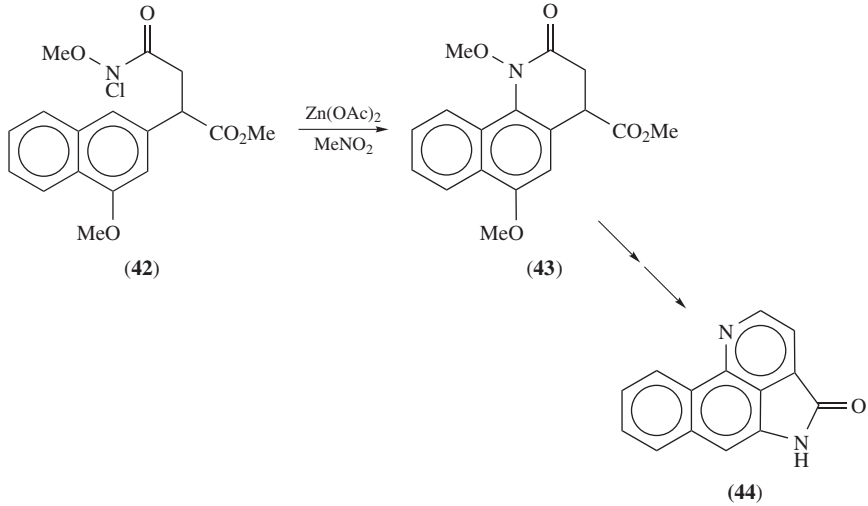

(**42**) (**43**) (**44**)

SCHEME 7

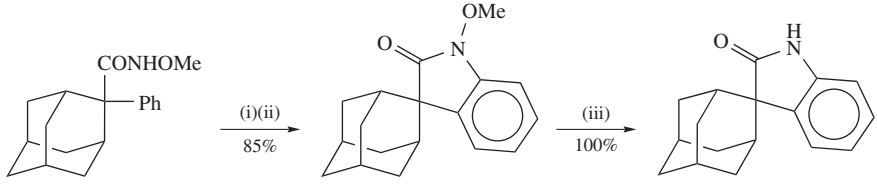

(**45**) (**46**) (**47**)

(i) *t*-BuOCl/CH_2Cl_2
(ii) $Zn(OAc)_2$/$MeNO_2$
(iii) Na-Hg/MeOH-Et_2O

SCHEME 8

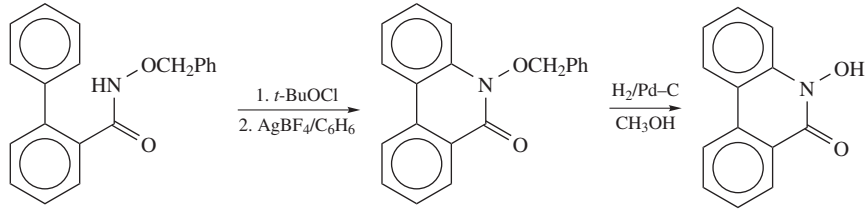

(**48**) (**49**) (**50**)

SCHEME 9

Cyclization of alkoxynitrenium ions onto a (4-methoxyphenyl)alkylamide side chain has been found to produce excellent yields of spiro-fused bicyclic lactams. Kikugawa and coworkers pioneered this approach using **51** and Ag_2CO_3/TFA and showed that formation of four-, five- and six-membered spirolactams (**53a–c**) was possible in 70–80% yield (Scheme 10)[56]. Glover produced lactams (**53a–c**) in lower yields with $AgBF_4$ and both results demonstrated that where the alkoxynitrenium ion π-bond is exocyclic to the transition state, *ipso* cyclization giving **52** was possible even when small rings are formed[52].

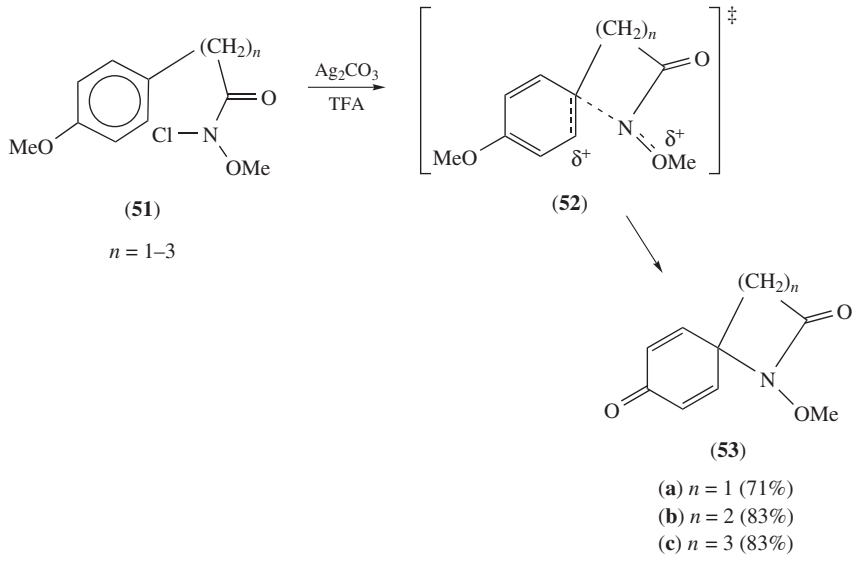

SCHEME 10

While the silver and zinc salts were effective Lewis acids for these cyclizations, Kikugawa and coworkers reported that the alkoxynitrenium ions could be generated directly from hydroxamic esters (**4**) using hypervalent iodine oxidants such as hydroxy(tosyloxy) iodobenzene (HTIB) and phenyliodine(III)bis(trifluoroacetate) (PIFA)[139]. Presumably, with such reagents the reactions proceed through *N*-(oxoiodobenzene) intermediates (**54**), which can themselves be regarded as anomeric hydroxamic esters and sources of alkoxynitrenium ions (**55**) (Scheme 11).

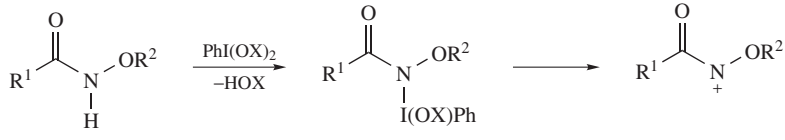

(**4**) (**54**) (**55**)

SCHEME 11

The formation of numerous ring-substituted spirolactams (**53b**) employed this methodology, which to date has also found application in a number of natural product syntheses. For example, the critical spirane junction-forming step in the synthesis of the muscarinic M_1 receptor antagonist (−)-TAN1251A (**58**) from L-tyrosine involves PIFA-induced cyclization of the hydroxamic ester **56** to **57** according to Scheme 12[140].

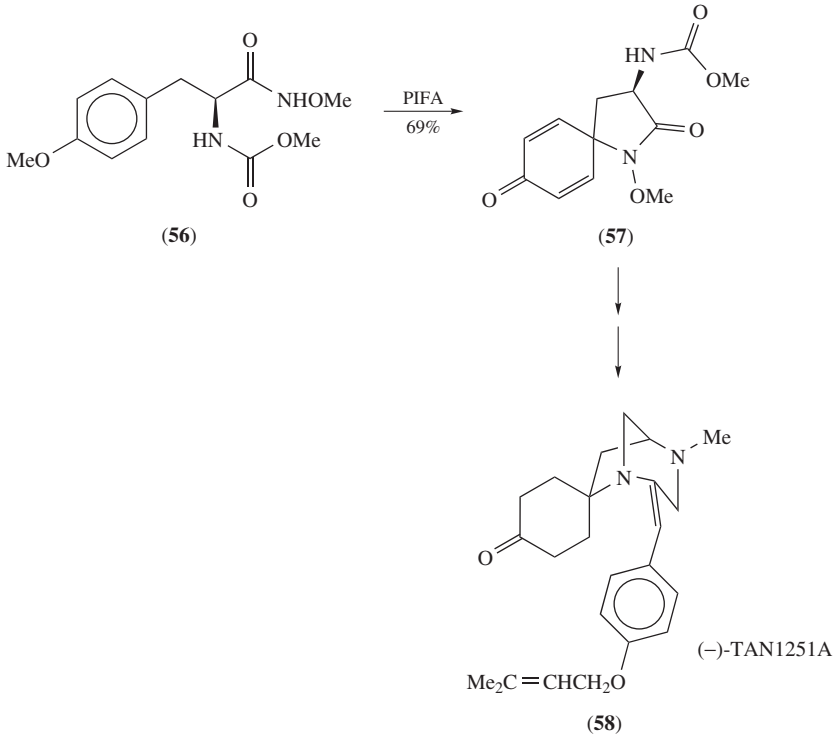

(**56**) (**57**) (**58**)

SCHEME 12

Similarly, the geminally alkylated carbon in the piperidine Coccinellid alkaloid (±)-Adalinine (**61**) was generated from **60**, which was formed through spiro cyclization of **59** with 90% conversion (Scheme 13)[141].

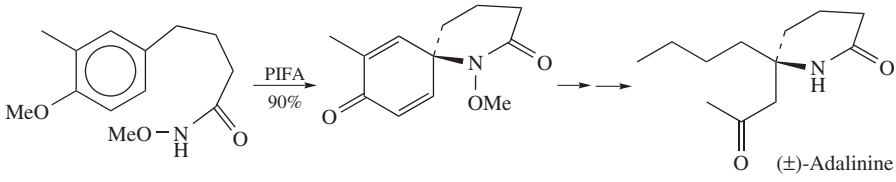

(**59**) (**60**) (**61**)

SCHEME 13

Romero and coworkers employed PIFA, in the synthesis of PNU-95666E, a selective high-affinity agonist at the dopamine D_2 receptor, by successive nitrenium ion cyclizations (Scheme 14). Nitrenium ion cyclizations converted **62** to the lactam **63** which, after reductive demethoxylation to **64**, protection as **65** and *N*-functionalization, afforded the hydroxamic ester (**66**). A second cyclization with PIFA afforded the benzimidazolinone (**67**), which was readily reduced to the product **68** in overall yield of 26%[142].

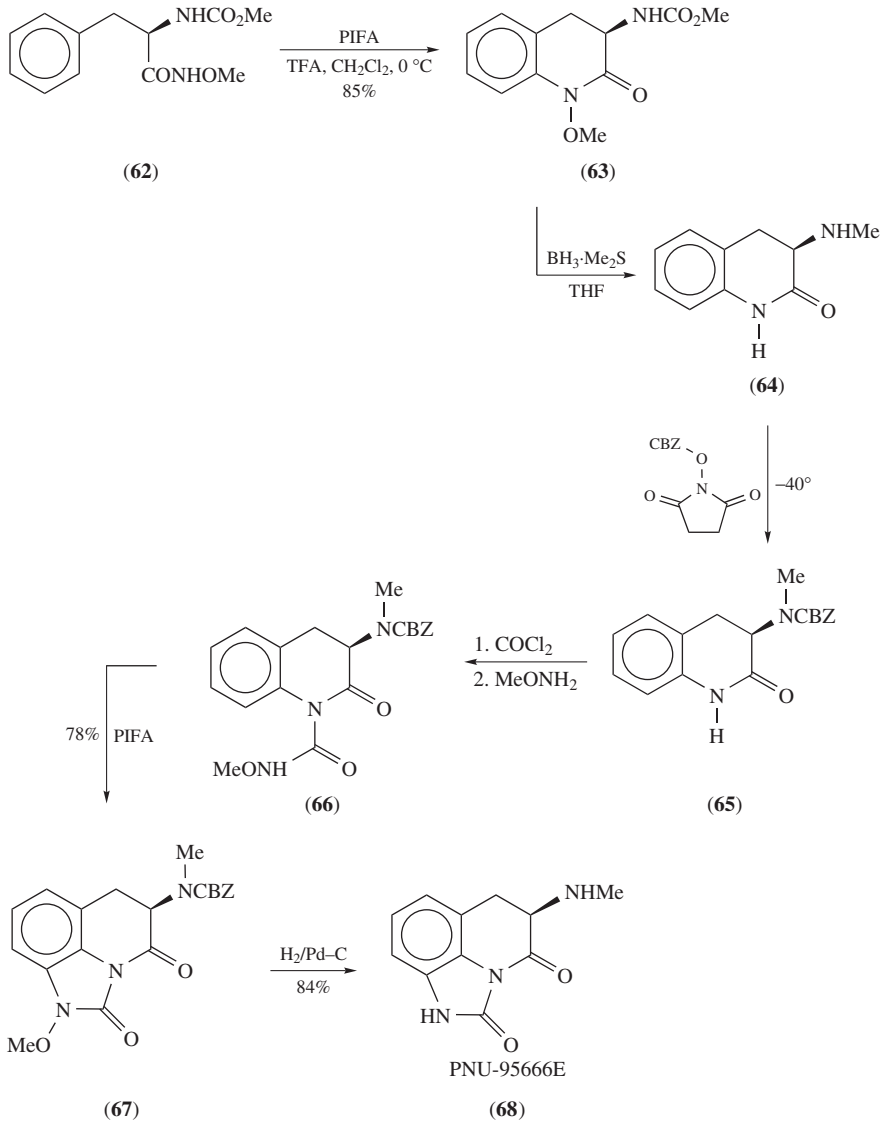

SCHEME 14

Similarly, syntheses of optically pure pyrrolobenzodiazepines (**70**) were effected with PIFA using the proline-derived hydroxamic esters (**69**) (equation 8)[143].

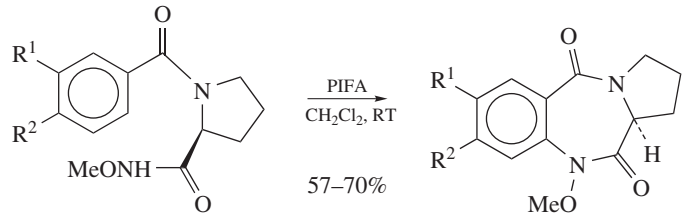

(**69**) (**70**) (8)

(**a**) $R^1 = R^2 = OMe$
(**b**) $R^1 = OMe$, $R^2 = H$
(**c**) $R^1R^2 = C_4H_4$

Finally, starting with suitable *N*-chlorohydroxamic esters, efficient cyclization of *N*-acyl-*N*-alkoxynitrenium ions onto the naphthalene skeleton, giving **71**–**73**, has been reported using $Zn(OAc)_2$ in nitromethane[57].

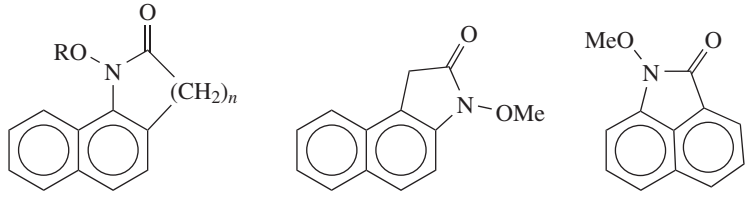

(**71**) (**72**) (**73**)

(**a**) $n = 1$, R = Me
(**b**) $n = 2$, R = Me, Et, allyl

60–95% 70% 26%

Silver or zinc salts could also effect intermolecular addition of *N*-acyl-*N*-alkoxynitrenium ions generated from *N*-chlorohydroxamic esters to arenes[52, 56, 57].

4. S_N2 reactions at nitrogen

In addition to solvolysis and nitrenium ion formation, *N*-alkoxy-*N*-chloroamides (**2**) also undergo bimolecular reactions with nucleophiles at nitrogen. Not only is the configuration destabilized by the anomeric effect, it also parallels that of α-halo ketones, where halogen on an sp^3 carbon is activated towards S_N2 reactions by the adjacent carbonyl. This rate-enhancing effect on S_N2 processes at carbon is well-known, and has been attributed to conjugation of the p-orbital on carbon with the carbonyl π-bond in the S_N2 transition state[82, 135, 144–146], stabilization of ionic character at the central carbon as outlined by Pross[82, 147] as well as electrostatic attraction to the carbonyl carbon[145]. The transition states are also affected by the nature of the nucleophile[148].

Though more widely studied with the class of *N*-acyloxy-*N*-alkoxyamides (**1b**) (see Section IV.C.3), S_N2 reactions at the amide nitrogen of *N*-alkoxy-*N*-chloroamides leads

to replacement of chlorine by a range of nucleophiles, in polar and non-polar solvents. For example, treatment with sodium carboxylates in anhydrous acetone affords *N*-acyloxy-*N*-alkoxyamides (**74**) by S_N2 displacement of chloride by carboxylate ions (equation 9). This reaction has been utilized in the synthesis of a wide variety of *N*-acyloxy-*N*-alkoxyamides[62, 90, 92, 93, 95, 96, 98, 99, 114, 149]. Almost all such compounds are mutagenic and they display all the characteristics of anomeric amides. Details of their synthesis, properties and reactivity are described in Section IV.

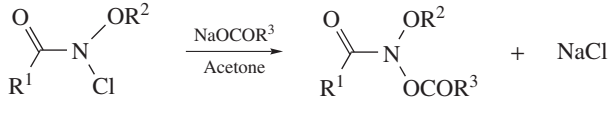

(9)

(**2**) (**74**)

R^1 = alkyl, aryl, RO, NR_2; R^2 = alkyl, benzyl; R^3 = alkyl, aryl

N-Acyloxy-*N*-alkoxyureas and carbamates (equation 9, $R^1 = NR_2$, RO) have been generated similarly in MeCN[68]. Earlier, the same group described the synthesis of *N*,*N*-dialkoxyureas (**76**) from the reaction of *N*-alkoxy-*N*-chloroureas (**75**) with sodium alkoxides in the corresponding alcohol (equation 10)[66, 74]. Properties of *N*,*N*-dialkoxyamides and -ureas and -carbamates are described in Section V.

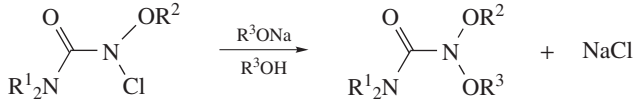

(10)

(**75**) (**76**)

40–85%

N-Alkoxy-*N*-chloroureas (**77**) have also been reacted with nitrogen nucleophiles resulting in S_N2 displacement of chloride. The products suggest that the reaction proceeds via an unstable *N*-alkoxy-*N*-amino intermediate (**78**), which under the influence of hydrochloric acid formed in the reaction, decomposed as illustrated to diaminomethane (**79**) and urea (**80**) (Scheme 15), although the exact mechanism is unclear[65].

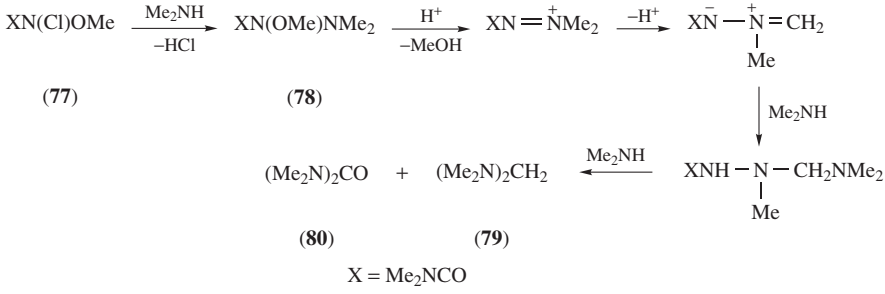

(**77**) (**78**) (**80**) (**79**)

X = Me_2NCO

SCHEME 15

Sodium azide has been shown to react rapidly at the amide nitrogen of *N*-chlorohydroxamic esters (**2a**) in aqueous MeCN in an S_N2 fashion giving excellent conversions to

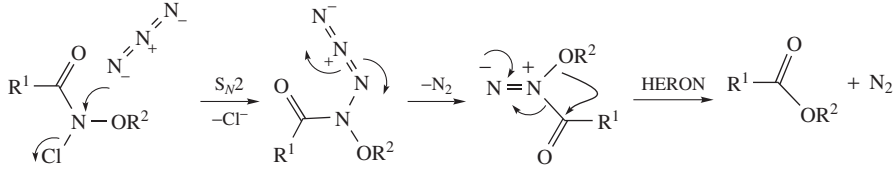

(**2**) (**81**) (**82**) (**83**)

(**a**) R^1 = alkyl, aryl, R^2 = alkyl
(**b**) R^1 = H, R^2 = Me
(**c**) $R^1 = R^2$ = Me

SCHEME 16

non-crossover esters derived from the acyl and alkoxyl substituents and two equivalents of nitrogen according to Scheme 16[97,150]. Theoretical studies suggested that the intermediate *N*-alkoxy-*N*-azidoamide (**81a**) reacts by loss of nitrogen to give a 1-acyl-1-alkoxydiazene (**82a**), which in turn forms ester (**83a**) and a second molecule of nitrogen. The same intermediate is formed in the stepwise decomposition of *N*,*N*′-diacyl-*N*,*N*′-dialkoxyhydrazines (see Section VI.C)[63,72].

A detailed B3LYP/6-31G* study of reaction pathways of the model *N*-azido-*N*-methoxyformamide (**81b**) showed that the most favourable decomposition process by initial loss of nitrogen to afford **82b** was exothermic by 42–44 kcal mol^{-1} with an E_A of only 5.3 kcal mol^{-1} [151]. Subsequent thermal decomposition of **82b** to methyl formate (**83b**) and nitrogen, a type of HERON reaction[87], has an E_A of only 2.9 kcal mol^{-1} and is exothermic by a further 95 kcal mol^{-1}, making overall conversion of **81b** to methyl formate and two molecules of nitrogen exothermic by 137–139 kcal mol^{-1}. Thomson and Hall predicted a similar exothermicity of 95 kcal mol^{-1} and an activation energy of 2.4 kcal mol^{-1} for formation of N_2 and **83c** from **82c**[133].

The reaction of azide with *N*-chlorohydroxamic esters has proved to be an excellent source of highly hindered esters[97]. The rearrangement of **82** to **83** (Scheme 16), apart from being highly favourable energetically, is characterized by an early transition state with little disruption to the carbonyl. In these HERON reactions, the *N*–*C*(*O*) bond

TABLE 3. Ester (R^1COOR^2) formation from the reaction of *N*-alkoxy-*N*-chloroamides ($R^1CON(Cl)OR^2$) with sodium azide in aqueous MeCN

R^1	R^2	Yield (%)[97,150]
Ph	*t*-Bu	87
t-Bu	*t*-Bu	30[a]
1-Ad	*t*-Bu	82[b]
t-Bu	Cyclohexyl	97
Ph	*i*-Bu	92
Ph	Benzyl	93
Me	Benzyl	92
4-$NO_2C_6H_4$	Et	94
Ph	Et	94

[a] GLC analysis; reaction accompanied by formation of 29% pivalic acid.
[b] Traces of adamantane carboxylic acid also detected.

breaks in concert with the $RO-C(O)$ bond formation after the transition state along the reaction coordinate and the process is akin to an S_N2 reaction on an acyl carbon. Accordingly, ester formation is not restricted by the normal constraints in Fischer esterification, where formation of the tetrahedral intermediate is destabilized by bulky alcohol and acyl groups[152–154]. Yields of esters produced by this method are given in Table 3[97,150].

N-Chloro-*N*-methoxy-*N′*-arylureas (**84**) have been reported to cyclize in good yield to 2-benzimidazolinones (**85**) upon treatment with NaH. *N′*-Alkylation prevented the reaction and the process involves anilide formation by hydrogen abstraction and an intramolecular S_N2 displacement of chlorine by the electron-rich *ortho* carbon (equation 11)[142,155].

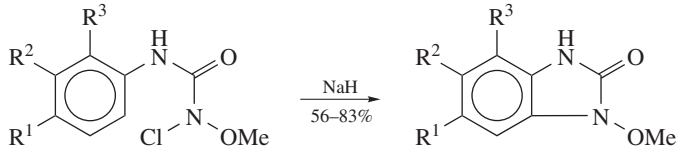

(**84**) (**85**) (11)

R^1 = H, Cl, CF_3
R^2 = H, Cl, NO_2, CN, SO_2Me, Me
R^3 = H, Cl, CF_3

IV. *N*-ACYLOXY-*N*-ALKOXYAMIDES

N-Acyloxy-*N*-alkoxyamides (**1b**) exhibit all the structural and spectroscopic characteristics of anomeric amides and their transformations embrace a range of reactions at the amide nitrogen[13,15,89,90,92,93,95,97,99,114,156,157]. They are mutagenic as well as DNA-damaging agents that have anticancer capability[13,62,92,93,95,96,98,99,149,156] and therefore a wide range of compounds **1b** have been synthesized for structure–activity studies. In addition, a range of urea and carbamate analogues of **1b** have also been reported[67,68,100,158,159].

N-Acyloxy-*N*-alkoxyamides were originally designed as analogues of metabolites formed from arylamines (**86**), namely *N*-acetoxy-*N*-acetylarylamines (**87**)[160–171], which solvolyse to resonance-stabilized arylnitrenium ions (**88**) that can damage DNA (Scheme 17)[172–181]. Based on computational studies, *N*-alkoxynitrenium ions and arylnitrenium ions were expected to have similar stability and ease of formation due to their similar degree of resonance stabilization (see Figure 14, Section III.C.2)[83] and the precursor *N*-acyloxy-*N*-alkoxyamides were initially synthesized to test whether, like **87**, they would solvolyse to *N*-acyl-*N*-alkoxynitrenium ions that react with DNA. However, while they were found to be mutagenic DNA damaging agents, their biological activity is understood not to involve nitrenium ions, and they react directly with DNA through an S_N2 displacement of carboxylate[13,98,113]. Nonetheless, reactivity studies showed that they generate

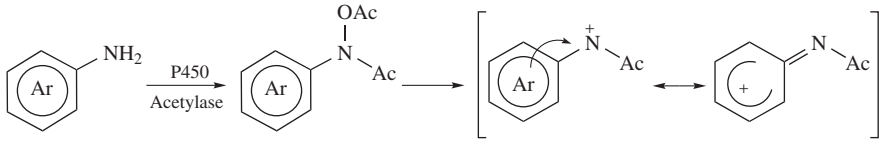

(**86**) (**87**) (**88**)

SCHEME 17

N-acyl-*N*-alkoxynitrenium ions under conditions of acid catalysis[92,93,95,113], and their discovery has led to a rich array of new chemistry at the amide nitrogen that in some ways parallels that of *N*-chlorohydroxamic esters, described in Section III, and saturated carbons bearing leaving groups.

An extensive review on this class of anomeric hydroxamic esters has been published in which, along with structural and reactivity data, their biological activity is discussed[13].

A. Synthesis of *N*-Acyloxy-*N*-alkoxyamides

N-Acyloxy-*N*-alkoxyamides (**90**) have been synthesized from *N*-chlorohydroxamic esters (**89**) by substitution of chlorine with a carboxyl group using silver acetate in anhydrous ether[62] or sodium carboxylates in dry acetone by analogy with Finkelstein chemistry (equation 12)[15,89,90,92,93,95,96,98,99,113]. Yields vary depending upon the stability of the *N*-acyloxy-*N*-alkoxyamide to secondary reactions, but in most instances conversion is clean and in good yield. They are stable on silica gel and are readily separated from minor impurities using centrifugal or column chromatography.

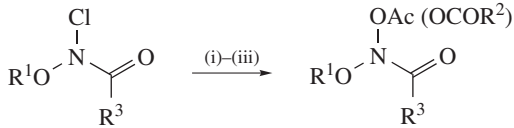

(**89**) (**90**) (12)

(i) AgOAc, anhydrous diethyl ether, R^3 = aryl, alkyl
(ii) NaOAc (NaOCOR^2), anhydrous acetone, R^3 = aryl, alkyl
(iii) NaOAc (NaOCOR^2), MeCN, $R^3 = NR_2$, OR

Selection of appropriate hydroxamic esters and carboxylic acid salts has enabled synthesis of a wide range of *N*-acyloxy-*N*-alkoxyamides in which R^2 and R^3 can be alkyl or aryl but, to date, only alkoxyl or arylalkoxyl groups have been present at R^1 [13].

Shtamburg and coworkers have synthesized a variety of *N*-acyloxy-*N*-alkoxyureas (**90**, $R^3 = NR_2$) and *N*-acyloxy-*N*-alkoxycarbamates (**90**, $R^3 = OR$) by an analogous procedure using appropriate sodium carboxylates in MeCN[67,68,100,158].

B. Properties of *N*-Acyloxy-*N*-alkoxyamides

1. Structural properties

Like *N*-chlorohydroxamic esters, *N*-acyloxy-*N*-alkoxyamides are archetypal anomeric amides. The combined electronegativity of the alkoxyl and acyloxyl oxygens strongly alters the geometry at the nitrogen to give a pyramidal amide with radically reduced or negligible amide conjugation. Alkoxyl and acyloxyl substitution and the sp^3 hybridization at nitrogen also result in a strong $n_O - \sigma^*_{NOAcyl}$ anomeric interaction (Figure 15a). This is likely to be the stronger of the two possible anomeric effects since the σ^*_{NOAcyl} is lower in energy than σ^*_{NOR} while the p-type lone pair of the alkoxyl oxygen would be higher in energy than that of the acyloxyl ether oxygen (Figure 15b). As illustrated in Figure 15c, to maximize such interactions, the optimum twist angle about the donor $N-O$ bond should be around 90°.

These qualitative arguments are supported by both theoretical and X-ray structural data.

Ab initio HF/6-31G* calculations on *N*-formyloxy-*N*-methoxyformamide (**91**)[15,157] predicted a strongly pyramidal nitrogen with an average angle of 110.3° (Figure 16).

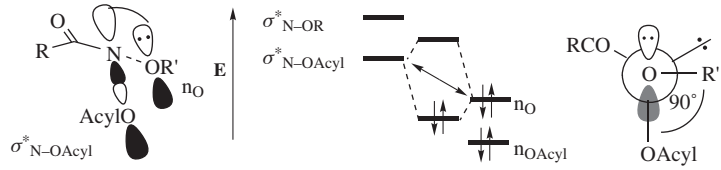

FIGURE 15. (a) Anomeric overlap in *N*-acyloxy-*N*-alkoxyamides; (b) lone-pair stabilization through an $n_O - \sigma^*_{NOAcyl}$ interaction; (c) optimum conformation for anomeric overlap in *N*-acyloxy-*N*-alkoxyamides

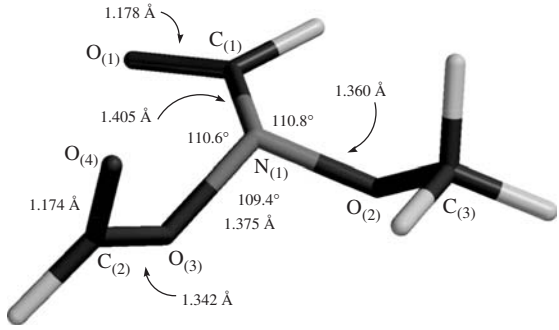

FIGURE 16. HF/6-31G* lowest-energy conformation of *N*-formyloxy-*N*-methoxyformamide (**91**)

In its lowest-energy conformation the amide carbonyl and the formyloxy groups are *syn* and both methyl and formyloxyl carbonyl groups are *exo* to the nitrogen pyramid. The $C_{(1)}-N_{(1)}$ bond (1.405 Å) is very long when compared to *N*-methoxyformamide (**92**, 1.373 Å) or formamide (**93**, 1.348 Å) computed at the same level. In contrast to the 23% $C-N$ bond lengthening, the carbonyl bond of **91** ($C_{(1)}-O_{(1)} = 1.178$ Å) is computed to be shorter than that of **92** by only 0.01 Å (8%).

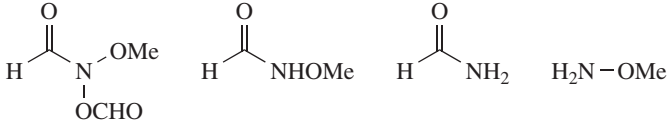

(**91**) (**92**) (**93**) (**94**)

The dihedral angles gave a Winkler–Dunitz amide distortion index of $\chi_N = 58.5$[107, 108]. The $C_{(3)}-O_{(2)}-N_{(1)}-O_{(3)}$ dihedral angle was 102.1° at the HF/6-31G* level reflecting a strong $n_O - \sigma^*_{NOCHO}$ anomeric overlap in this direction. The result of this is a shorter $MeO-N$ bond in **91** ($O_{(2)}-N_{(1)}$ 1.360 Å) than that calculated for methoxyformamide (**92**, 1.373 Å), despite the reduced sp^3 character in the latter, or *O*-methylhydroxylamine (**94**, 1.399 Å), which like **91**, at the HF/6-31G* level, is sp^3 hybridized at nitrogen.

Scaled carbonyl vibrational frequencies[182, 183] for the ground-state HF/6-31G*-optimized geometries of **91**, **92** and **93** were 1828 cm^{-1} (average of symmetrical

(1838 cm^{-1}) and asymmetrical (1819 cm^{-1}) stretch), 1796 and 1784 cm^{-1}, respectively, in support of a measurable stiffening of the carbonyl in *N*-formyloxy-*N*-methoxyformamide as a result of the loss of nitrogen lone-pair interaction[13]. In addition, in contrast to formamide and *N*-methoxyformamide, the *C*=*O* and *C*−*N* vibrational frequencies of **91** were shown to be largely insensitive to rotation about the *C*−*N* bond[13].

In amides, the extent of nitrogen lone-pair–carbonyl overlap is reflected in the height of the barriers to *E*–*Z* isomerization. B3LYP/6-31G*//HF/6-31G* barriers to rotation in formamide (**93**, 18.0 kcal mol^{-1}) and methoxyformamide (**92**, 15.6 kcal mol^{-1}) were found to be similar[10, 13]. However, both barriers were very significantly higher than the smallest barrier of 7.5 kcal mol^{-1} for isomerization of formyloxymethoxyformamide. Interestingly, although the nitrogen of the hydroxamic ester (**92**) is computed to be significantly pyramidal ($\chi_N = 49.6$), the similarity in IR stretch frequencies and isomerization barriers to those of the formamide confirm that the impact of one oxygen substituent upon amide characteristics is far smaller than that brought about by dual substitution with oxygen.

The barrier to inversion at nitrogen was 3.5 kcal mol^{-1} at the B3LYP/6-31G* level in line with that of the *N*-chloro model, **2b** (2.5 kcal mol^{-1}, Section III.B.1).

Predicted theoretical properties have been verified from X-ray structures of several *N*-acyloxy-*N*-alkoxy systems. The geometries of *para*–*tert*-butylated amides **95a** (Figure 17a) and **95b**[15], the *N*-acyloxy-*N*-alkoxyureas **96a** (Figure 17b)[67] and **96b**[159] and an *N*-acyloxy-*N*-alkoxycarbamate **97** (Figure 17c)[67] are dominated by pyramidality at the amide nitrogen. While amides are typically planar or close to planar with average angles at nitrogen around 120° in the overwhelming majority of structures studied[15], these species have nitrogen atoms that are highly sp^3 hybridized. Principal bond lengths, angles at nitrogen, Winkler–Dunitz amide distortion parameters and twist angles are listed in Table 4.

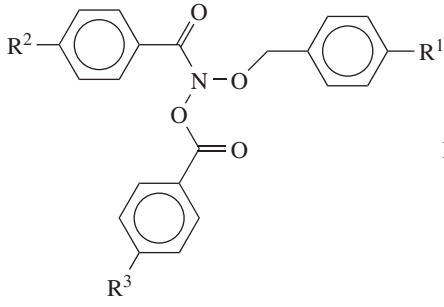

(**95**)

(**a**) R^1 = *t*-Bu, $R^2 = R^3$ = H
(**b**) $R^1 = R^2 = R^3$ = *t*-Bu

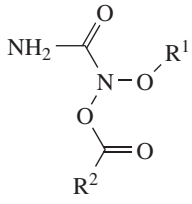

(**96**)

(**a**) R^1 = Et, R^2 = Me
(**b**) R^1 = Bu, R^2 = 4-ClC_6H_4

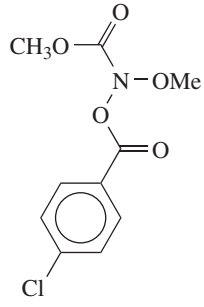

(**97**)

While amides **95a** and **95b** ($|\chi_N| = 65.6°$ and 65.3°, respectively) are more pyramidal than the ureas **96a** and **96b** and carbamate **71** ($|\chi_N| = 57.1°$, 64.6° and 56.3°, respectively), all four possess strongly sp^3-hybridized nitrogens. Average angles at nitrogen, $\langle\beta\rangle$, for the two amides and urea **96b** are smaller than that required by pure tetrahedral geometry. In all cases the high degree of pyramidality that is attributable to the presence of two electronegative oxygen atoms at nitrogen confirms the predictions of HF/6-31G* calculations[13, 15]. On the basis of geometries for all acyclic amides in the Cambridge Structural Database[184] Glover and coworkers reported that amides **95a** and **95b** were the

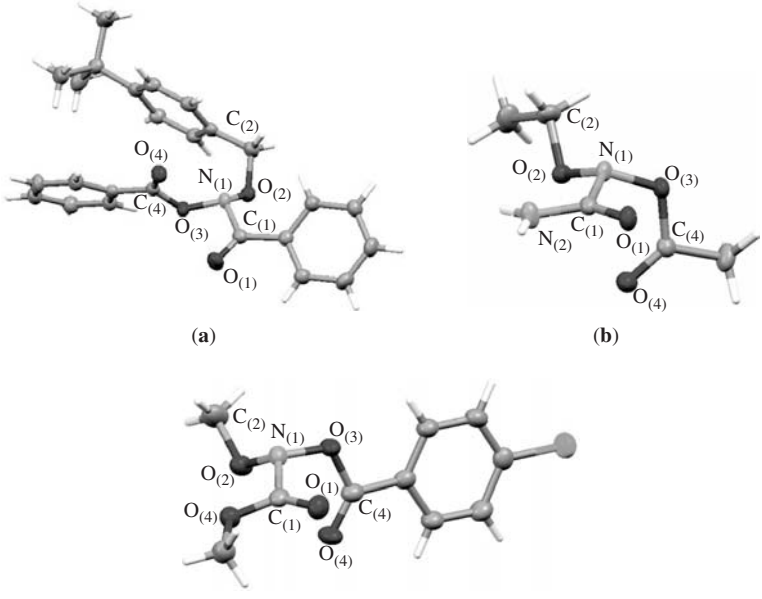

FIGURE 17. X-ray structures of (a) *N*-benzoyloxy-*N*-(4-*tert*-butylbenzyloxy)benzamide (**95a**), (b) *N*-acetoxy-*N*-ethoxyurea (**96a**) and (c) methyl *N*-(4-chlorobenzoyloxy)-*N*-methoxycarbamate (**97**) with displacement ellipsoids shown at the 50% level. Bond lengths and angles are given in Table 4

TABLE 4. Selected structural properties of *N*-acyloxy-*N*-alkoxyamides **95a** and **95b**, -ureas **96a** and **96b**, and -carbamate **97**[13]

Parameter	**95a**	**95b**	**96a**	**96b**	**97**
$r_{C(1)O(1)}$ (Å)	1.207	1.205	1.222	1.233	1.198
$r_{C(1)N(1)}$ (Å)	1.441	1.439	1.426	1.441	1.424
$r_{N(1)O(2)}$ (Å)	1.402	1.401	1.398	1.396	1.396
$r_{N(1)O(3)}$ (Å)	1.440	1.441	1.426	1.447	1.474
$r_{C(1)N(2)}/r_{C(1)O(4)}$ (Å)	—	—	1.330	1.321	1.322
$C_{(1)}-N_{(1)}-O_{(2)}$ (deg)	110.6	109.4	113.5	111.4	113.4
$O_{(3)}-N_{(1)}-C_{(1)}$ (deg)	109.0	108.6	111.6	105.9	111.4
$O_{(3)}-N_{(1)}-O_{(2)}$ (deg)	104.5	105.5	108.5	106.4	109.3
$\langle\beta\rangle$(deg)[a]	108.0	107.8	111.2	107.9	111.4
τ (deg)[b]	13.9	15.5	−6.8	11.8	2.9
χ_N (deg)[c]	−65.6	−65.3	−57.1	64.6	−56.3
$C_{(2)}-O_{(2)}-N_{(1)}-O_{(3)}$ (deg)	96.7	96.2	−104.0	−98.2	−95.5
$C_{(4)}-O_{(3)}-N_{(1)}-O_{(2)}$ (deg)	−137.6	−141.6	−69.0	119.3	−67.1

[a] $\langle\beta\rangle = \Sigma(\beta)/3$.
[b] Angle subtended by the axes of the nitrogen lone pair and the carbonyl carbon $2p_z$ orbital.
[c] Amide distortion parameters defined in accordance with Winkler–Dunitz[107, 108].

most pyramidal acyclic amides[15]. Shtamburg and coworker's urea **96b** is similarly highly pyramidal at nitrogen[159].

Sp^3 hybridization at nitrogen corresponds to decreased lone-pair $2p_z$ character, which manifests itself in three ways:

(i) Poor collinearity between nitrogen lone pair and carbonyl carbon $2p_z$ orbitals;
(ii) Long $N-C$ bond lengths;
(iii) Low $E-Z$ isomerization barriers.

X-ray structures bear testimony to these facts. The more pyramidal substrates **95a**, **95b** and **96b** exhibit a significant degree of twisting around the $N-C(O)$ bond ($\tau = 13.9°$, 15.5° and 11.8°, respectively). In *N*-acyloxy-*N*-alkoxyamides this is in accordance with the experimental barrier to $E-Z$ isomerization, which has been estimated to be below 8–9 kcal mol^{-1} [50] in line with the theoretical barrier for **91** (7.5 kcal mol^{-1}). Since the lone pair on nitrogen resides in an sp^3 hybrid orbital, twisting angles are likely to arise more from steric interactions or crystal packing rather than any significant π-orbital overlap considerations. Nitrogen lone pairs in the less pyramidal urea **96a** and carbamate **97** are closer to the carbonyl carbon $2p_z$ orbital (Table 4).

The $N-C(O)$ bonds in all five structures ($r_{C(1)N(1)}$, Table 4) are very long when compared to normal, acyclic amides (average bond length of 1.359 Å, median 1.353 Å[15]), although they cannot be compared directly with tertiary *N*,*N*-dialkylamides on account of the different hybridization at nitrogen. Even though the twist angles are relatively small (τ, Table 4) these bonds are only slightly shorter than the corresponding bond in the fully twisted lactam, 1-aza-2-adamantanone (**98**) (1.455 Å), a completely non-conjugated amide with an sp^3 nitrogen[31–33,42].

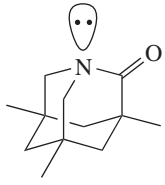

(**98**)

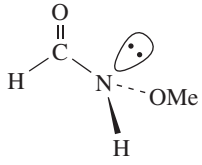

(**99**)

The crystallographic carbonyl bond lengths in the amides **95a** and **95b** and 1-aza-2-adamantanone **98** (1.210 Å) are also similar and only marginally shortened in line with the recent understanding that, when compared to $N-C(O)$ bonds, there is much less variation in carbonyl bond lengths between planar and twisted amides[34]. In further support of Wiberg's theory of amide resonance[2,3], $C=O$ bonds are relatively insensitive to loss of π-overlap through pyramidalization at nitrogen whether it is the consequence of twisting or bisheteroatom substitution.

Geometries of all four amides in the solid state indicate a preference for a conformation in which the alkoxyl oxygen p-type lone pair, n_{OR}, is largely collinear with the σ^*_{NOAcyl} bond. Dihedral angles $C_{(2)}-O_{(2)}-N_{(1)}-O_{(3)}$ in Table 4 are all close to 90°. This anomeric interaction is clearly predominant as the alternative, $C_{(4)}-O_{(3)}-N_{(1)}-O_{(2)}$ dihedral angles indicate poor $n_{OAcyl}-\sigma^*_{NOR}$ interactions. As a consequence, $N_{(1)}-O_{(2)}$ bonds should be shorter than normal. As with the theoretical models, a comparison between experimental $N-OR$ bond lengths in *N*-acyloxy-*N*-alkoxyamides and the parent hydroxamic esters is inappropriate on account of differences in hybridization at nitrogen. However, a comparison can be made with the experimental bond length in hydroxylamines, which are typically of the order of 1.44–1.46 Å. Values in this range have also been computed

for the fully twisted hydroxamic ester **99** where the nitrogen also assumes a pyramidal geometry[10]. Thus the $r_{N(1)O(2)}$ distances of 1.402 Å (**95a**), 1.401 Å (**95b**), 1.398 Å (**96a**), 1.396 Å (**96b**) and 1.396 Å (**97**) represent very significant shortening, presumably on account of an effective $n_O-\sigma^*_{NOAcyl}$ anomeric interaction.

2. Spectroscopic properties

Carbonyl stretch frequencies, carbonyl ^{13}C and amide ^{15}N NMR chemical shifts for a wide range of *N*-acyloxy-*N*-alkoxyamides are collated in Table 5 together with those of the precursor hydroxamic esters. Spectroscopically, mutagens can be categorized into six types:

(i) *N*-Alkanoyloxy-*N*-alkoxyarylamides (entries 1–41);
(ii) *N*-Alkoxy-*N*-aroyloxyarylamides (entries 42–52);
(iii) *N*-Alkanoyloxy-*N*-alkoxyalkylamides (entries 53–58);
(iv) *N*-Alkoxy-*N*-aroyloxyalkylamides (entries 59–68);
(v) *N*-Acyloxy-*N*-alkoxyureas (entries 69–72);
(vi) *N*-Acyloxy-*N*-alkoxycarbamates (entries 73–77).

N-Acyloxy-*N*-alkoxyamides are characterized by two high frequency double-bond absorptions corresponding to the stretching modes of the ester and amide carbonyls.

The acyloxyl substituents are ester groups but the bonding to nitrogen results in higher than normal $C=O$ stretch frequencies. For aliphatic groups (R^2 = alkyl, Table 5, entries 1–41 and 53–58) these are all in the range of 1767 cm^{-1} through to 1800 cm^{-1} whereas carbonyls of saturated esters are generally found between 1735 and 1750 cm^{-1} [191, 192]. Carbonyls of aroyloxyl groups (R^2 = aryl, Table 5, entries 42–52 and 59–68) range from 1750 to 1767 and are similarly increased relative to normal aromatic esters (1715–1730 cm^{-1}). Thus hydroxamic ester substitution through nitrogen at the ester oxygen raises the ester carbonyls into the range for acid chlorides and acid anhydrides[191].

Arylamides (R^3 = aryl, Table 5, entries 1–52) exhibit amide carbonyls in the range of 1718–1742 cm^{-1}, 51 ± 13 cm^{-1} higher than their precursor hydroxamic esters. *N*-Acyloxy-*N*-alkoxyalkanamides (R^3 = alkyl, Table 5, entries 53–68) exhibit carbonyls on average 57 ± 15 cm^{-1} higher than the hydroxamic esters from which they are derived and their amide absorptions appear about seven wave numbers higher than their arylamide counterparts. Clearly most, if not all, sp^2 character at nitrogen is lost upon substitution with two oxygens and the extent of nitrogen lone-pair interaction with the amide carbonyl is radically altered. As a consequence, the carbonyl stiffens measurably. In contrast to $C=O$ bond lengths, $C=O$ vibrational frequencies are very much more sensitive to the extent of lone-pair overlap in amides. In these and in *N*-chlorohydroxamic esters, increasing combined electronegativity of substituents at nitrogen and the attendant pyramidalization and electronic effects result in a marked increase in the $\nu_{C=O}$ values although, relative to the difference between pure $C-O$ and pure $C=O$, the changes reflect only small variations in force constants.

The amide carbonyl vibrational frequencies of *N*-acyloxy-*N*-alkoxyamides are similar to that observed for the twisted 1-aza-2-adamantanone (**98**, 1731 cm^{-1})[31, 33]. It is apparent from the extensive data available for both *N*-chlorohydroxamic esters (Table 2, Section III.B.2) and *N*-acyloxy-*N*-alkoxyamides that when an amide nitrogen lone pair loses conjugation with the carbonyl (either through twisting/pyramidalization or, in the case of anomeric amides, pyramidalization alone), the configuration is analogous to an ester rather than a ketone. As with esters, acid halides and anhydrides or diacyl peroxides[191], the carbonyl stretch frequency is higher than that of ketones and aldehydes

TABLE 5. IR carbonyl absorption frequencies ($CHCl_3$), ^{13}C NMR and selected ^{15}N NMR chemical shifts[a] ($CDCl_3$) for *N*-acyloxy-*N*-alkoxyamides ($R^1ON(OCOR^2)COR^3$) and precursor hydroxamic esters

Entry	R^1	R^2	R^3	Amide ν (cm^{-1}) ($\delta^{13}C$)[$\delta^{15}N$]	Ester ν (cm^{-1}) ($\delta^{13}C$)[$\delta^{15}N$]	Hydroxamic ester ν (cm^{-1}) ($\delta^{13}C$)[$\delta^{15}N$]
1[92]	Bu	Me	4-Biphenyl	1721(173.01)	1794(166.24)	1684(166.38)
2[92]	Bu	Me	4-BrC_6H_4	1731(173.12)	1791(167.94)	1696(165.45)
3[92]	Bu	Me	4-ClC_6H_4	1728(172.85)	1792(167.82)	1695(165.29)
4[92]	Bu	Me	4-MeC_6H_4	1730(173.93)	1790(168.01)	1695(166.44)
5[92]	Bu	Me	4-$NO_2C_6H_4$	1730(172.15)	1790(167.83)	1695(164.14)
6[92]	Bu	Me	4-$MeOC_6H_4$	1728(173.18)	1790(168.02)	1692(166.12)
7[92]	Bu	Me	4-*t*-BuC_6H_4	1721(173.70)	1794(168.08)	1679(166.42)
8[115]	Bu	Me	3-$NO_2C_6H_4$	1727(171.39)	1794(167.71)	1693(164.00)
9[96]	Bu	Me	2-Naph	1724(174.03)	1792(167.98)	1684(166.70)
10[185]	Bu	Me	1-Fluorenyl	1742[b]	1785[b]	1681(167.10)
11[185]	Bu	Me	Anthraquinone-2-yl	1726[b]	1792[b]	1672(182.40)
12[185]	Bu	Pr	Ph	1721(174.4)	1774(170.49)	1654(165.65)
13[186]	Bu	1-Hexyl	Ph	1723(174.2)[-124]	1782(171.10)	1654(165.65)[-197]
14[186]	Bu	5-Hexen-1-yl	Ph	1730(174.4)	1783(171.0)	1654(165.65)
15[185]	Bu	*i*-Bu	Ph	1721(174.3)	1775(174.5)	1654(165.65)
16[185]	Bu	(*S*)-2-Bu	Ph	1725(174.5)	1774(173.9)	1654(165.65)
17[185]	Bu	Neopentyl	Ph	1721(174.4)	1778(169.5)	1654(165.65)
18[185]	Bu	1-Ad	Ph	1723(174.4)	1767(174.4)	1654(165.65)
19[185]	Bu	*t*-Bu	Ph	1722(174.7)	1771(175.7)	1654(165.65)
20[92]	Et	Me	Ph	1724(174.25)[-124]	1789(166.18)	1679(166.50)[-200]
21[96]	*n*-Pr	Me	Ph	1724(174.30)	1789(168.18)	1678(166.42)
22[92]	*i*-Bu	Me	Ph	1724(174.68)[-127]	1788(166.21)	1684(166.77)
23[62]	Bu	Me	Ph	1732(173.90)	1795(167.80)	1654(166.65)
24[92]	*i*-Bu	Me	Ph	1724(174.15)	1790(166.05)	1684(166.54)
25[187]	2-Bu	Me	Ph	1719(174.90)[-127]	1790(168.30)	1685(166.90)[-200]
26[187]	*t*-Bu	Me	Ph	1707(174.9)	1786(168.40)	1686(167.90)

27[62, 96]	*n*-Octyl	Me	Ph	1728(174.29)	1798(168.21)	1684(166.51)
28[62]	Benzyl	Me	Ph	1728(174.12)	1798(168.08)	1678(166.26)
29[92]	4-Br-benzyl	Me	Ph	1731(174.04)	1791(168.02)	1680(166.50)
30[92]	4-Cl-benzyl	Me	Ph	1731(174.08)	1793(168.02)	1687(166.68)[-203]
31[92]	4-NO_2-benzyl	Me	Ph	1732(174.20)	1793(168.19)	1691(166.59)
32[92]	4-Biphenylmethyl	Me	Ph	1729(174.14)	1791(166.10)	1674(164.91)
33[92]	4-*t*-Bu-benzyl	Me	Ph	1725(173.94)	1790(167.89)	1685(167.89)
34[92]	4-Me-benzyl	Me	Ph	1729(174.14)	1791(168.10)	1681(166.24)
35[92]	4-PhO-benzyl	Me	Ph	1725(174.17)[-124]	1795(168.15)	1690(157.97)[-196]
36[92]	4-MeO-benzyl	Me	Ph	1725(174.17)[-124]	1795(168.15)	1684(159.93)[-203]
37[187]	2,6-Me_2-benzyl	Me	Ph	1727(174.20)[-124]	1791(168.20)	1684(166.70)[-202]
38[187]	3,5-Me_2-benzyl	Me	Ph	1728(174.10)	1791(168.10)	1686(166.00)
39[187]	3-Me-benzyl	Me	Ph	1729(174.20)[-124]	1792(168.10)	1684(165.60)[-196]
40[187]	2-Me-benzyl	Me	Ph	1726(174.20)	1792(168.10)	1650(166.20)
41[113]	$-(CH_2)_6-$	Me, Me	Ph, Ph	1724(174.3)	1789(168.20)	1662(166.00)
42[98]	Bu	Ph	Ph	1728(174.50)	1758(164.00)	1654(165.50)
43[95]	Benzyl	4-$MeOC_6H_4$	Ph	1718(174.25)	1750(164.04)	1678(166.26)
44[95]	Benzyl	4-*t*-BuC_6H_4	Ph	1738(174.36)	1756(164.21)	1678(166.26)
45[95]	Benzyl	4-MeC_6H_4	Ph	1733(174.36)	1756(164.21)	1678(166.26)
46[95]	Benzyl	Ph	Ph	1731(174.28)[-123]	1758(164.13)	1678(166.26)[-197]
47[95]	Benzyl	4-ClC_6H_4	Ph	1734(174.20)	1759(163.25)	1678(166.26)
48[95]	Benzyl	4-$CHOC_6H_4$	Ph	1735(174.07)	1761(163.21)	1678(166.26)
49[95]	Benzyl	4-$CF_3C_6H_4$	Ph	1734(174.12)	1765(163.07)	1678(166.26)
50[95]	Benzyl	4-NCC_6H_4	Ph	1732(174.04)	1763(162.70)	1678(166.26)
51[95]	Benzyl	4-$NO_2C_6H_4$	Ph	1733(173.93)	1764(162.37)	1678(166.26)
52[185]	Benzyl	4-Biphenyl	Ph	1729(174.40)[-123]	1757(164.20)	1678(166.26)[-197]
53[186]	Bu	1-Hexyl	*t*-Bu	1718(182.50)	1779(170.70)	1683(176.00)
54[186]	Bu	5-Hexen-1-yl	*t*-Bu	1719(182.50)	1785(170.50)	1683(176.00)

(*continued overleaf*)

TABLE 5. (*continued*)

Entry	R^1	R^2	R^3	Amide ν (cm^{-1}) ($\delta^{13}C$)[$\delta^{15}N$]	Ester ν (cm^{-1}) ($\delta^{13}C$)[$\delta^{15}N$]	Hydroxamic ester ν (cm^{-1}) ($\delta^{13}C$)[$\delta^{15}N$]
55[113]	Bu	Me	Me	1746(176.20)	1797(167.70)	1678(167.90)
56[113]	Benzyl	Me	Me	1736(176.30)	1793(167.90)	1690(168.00)[-196]
57[188]	Benzyl, Benzyl	Me, Me	$-(CH_2)_7-$	1742 [b]	1794 [b]	1689(154.50)
58[188]	Benzyl, Benzyl	Me, Me	$-(CH_2)_8-$	1741(178.48)	1791(167.43)	1690 [b]
59[113]	Benzyl	Ph	Me	1738(176.50)	1762(164.10)	1690(168.00)
60[113]	Bu	Ph	Me	1738(176.50)	1765(164.10)	1678(167.90)
61[99]	Bu	Ph	Et	1745(180.10)	1766(164.10)	1664(171.80)
62[99]	Bu	Ph	*i*-Bu	1736(182.60)	1767(164.10)	1657(174.90)
63[99]	Bu	Ph	*t*-Bu	1728(182.80)	1763(164.00)	1683(176.20)
64[99]	Bu	Ph	Neopent	1735(177.20)	1763(163.80)	1653(169.50)
65[99]	Bu	Ph	1-Ad	1721(182.20)	1755(164.10)	1681(175.40)
66[113]	Bu	2-Naph	Me	1737(176.5)	1757(164.30)	1678(167.90)
67[189]	Bu	1-Fluorenyl	Me	1746(176.5)	1756(164.10)	1678(167.90)
68[189]	Bu	1-Pyrenyl	Me	1743(176.70)	1751(165.20)	1678(167.90)
69[68]	*n*-Pr	Me	NMe_2	1732 [b,c]	1784 [b,c]	1695 [b,c]
70[68]	Pr	Me	NHMe	1730 [b,c]	1795 [b,c]	1685 [b,c]
71[68]	Bu	Me	NH_2	1730 [b,c]	1790 [b,c]	1680 [b,c]
72[67]	Et	Me	NH_2	1720 [b,c]	1798 [b,c]	1680 [b,c]
73[68]	Me	Me	OMe	1780 [b,c]	1805 [b,c]	1765 [b,c]
74[68]	*n*-Octyl	Me	OMe	1780 [b]	1805 [b,c]	[b]
75[68]	Me	Me	OEt	1755 [b,c]	1780 [b,c]	1745 [b,c]
76[67]	Me	4-ClC_6H_4	OEt	1785 [c](158.5)	1780(163.7)	1765
77[190]	Bu	Ph	OEt	1762 [d](158.2)	1772 [d](164.3)	1724 [d](157.7)

[a] ^{15}N shift relative to nitromethane 0 ppm.
[b] ^{13}C carbonyl shift not recorded.
[c] Solid state or thin film IR.
[d] Thin film IR.

on account of destabilization of the polar form of the carbonyl (Figure 1a (**III**), Section I) by the strongly negative inductive effect of the bisheteroatom-substituted nitrogen.

N-Acetoxy-*N*-*tert*-butoxybenzamide (entry 26, Table 5) has an anomalously low carbonyl vibrational frequency (1707 cm^{-1}) that may suggest a smaller degree of pyramidality in this substrate due to steric hindrance. Steric effects on the amide side chain parallel *N*-chlorohydroxamic esters. *Tert*-butyl and adamantyl groups (Table 5, entries 53 and 54, 63 and 65) cause lower stretch frequencies that, on average, are only 40 cm^{-1} higher than their precursor hydroxamic esters.

When comparing the series of (*para*-substituted benzoyloxy)benzyloxybenzamides (Table 5, entries 42–52), one notable exception is the 4-methoxy analogue (entry 43), which exhibits a much lower carbonyl stretch at 1718 cm^{-1}. The through-resonance of the methoxyl lone pair presumably reduces the electron-withdrawing effect of the acyloxyl substituent, resulting in a lesser degree of pyramidality at the amide nitrogen and some lone-pair resonance into the amide carbonyl. The carbonyl resonance frequencies in *N*-acyloxy-*N*-alkoxyamides are very sensitive to steric and electronic effects of remote substituents at nitrogen.

The carbonyl vibrational frequencies of *N*-acyloxy-*N*-alkoxyamides are influenced strongly by an adjacent amino or alkoxyl group. Reported IR data were mostly obtained by liquid film or in the condensed phase (KBr/nujol mull) but the limited data for *N*-acyloxy-*N*-alkoxyureas (Table 5, entries 69–72) gives amide carbonyl frequencies of *ca* 1730 cm^{-1} that are raised by some 37–40 cm^{-1} relative to their precursor ureas. Values for carbamates (Table 5, entries 73–77), *ca* 1780 cm^{-1}, are raised to a lesser extent (10–20 cm^{-1}) relative to the parent compounds[68, 116].

^{13}C NMR resonances for both carbonyls of *N*-acyloxy-*N*-alkoxyamides and that of the parent hydroxamic ester are given for most compounds in Table 5. With the exception of *para*-substituted benzyloxy-*N*-acyloxy-*N*-alkoxyamides, amide carbonyl ^{13}C NMR shifts differ from those of their precursor hydroxamic esters by on average +8.0 (±0.6) ppm. Steric and electronic effects influence hydroxamic esters and *N*-acyloxy-*N*-alkoxyamides similarly. This includes substrates with branching alpha to the amide carbonyl.

For mutagens with benzyloxy and *para*-substituted benzyloxy side chains (Table 5, entries 28–36) carbonyl shifts differ by between 6–16 ppm relative to their parent alkoxyamides. In this subset, this variation is almost entirely due to changes in the carbonyl chemical shift of the hydroxamic ester (δ 168–158) since the *N*-acyloxy-*N*-alkoxyamides chemical shifts are all very close to δ 174. This may be explained as another manifestation of pyramidality at nitrogen in *N*-acyloxy-*N*-alkoxyamides. Hydroxamic esters are largely sp^2 hybridized at nitrogen and lone-pair overlap with the carbonyl carbon is facilitated by electron-donor groups, and disfavoured by electron-withdrawing substituents on the alkoxyl group. In the analogous *N*-acyloxy-*N*-alkoxyamides, where nitrogen is strongly sp^3 hybridized and there is little or no lone pair overlap, amide carbonyl chemical shifts are insensitive to the electronic effect of alkoxyl substituents at nitrogen.

Amide carbonyl vibrational frequencies for the series behave similarly; while those of the hydroxamic esters in this subset vary between 1678 and 1698 cm^{-1}, the *N*-acyloxy-*N*-alkoxyamide carbonyl frequencies span only six wave numbers.

Following the trend towards lower carbonyl IR stretch frequencies, branching alpha to the amide carbonyl (Table 5, entries 53, 54, 62, 63 and 65) affects the shifts for mutagens and hydroxamic esters similarly and causes a marked downfield shift of up to 6 ppm relative to the acetamide substrate (Table 5, entry 60). These effects, as well as the smaller than expected downfield shift with *tert*-butyl and neopentyl side chains are, as with the *N*-chlorohydroxamic esters, due to the combined influence of a stabilizing alkyl inductive effect together with destabilizing desolvation of the polar form of the amide carbonyl[117].

Though the amide resonance interaction is mostly absent, the carbonyl shifts are not ketonic and appear some 20 ppm upfield of aryl/alkyl ketones. The origin of this upfield shift from that of ketones parallels that of esters, anhydrides and acid chlorides. Electron-withdrawing nitrogen in pyramidal *N*-acyloxy-*N*-alkoxyamides, like in *N*-chlorohydroxamic esters, destabilizes the polar resonance form (Figure 1a (**III**), Section I) relative to ketones. These carbonyls have greater double-bond character resulting in higher electron density at carbon, higher field carbonyl chemical shifts and higher carbonyl vibrational frequencies. The observations are in line with those of Neuvonen and coworkers, whose systematic study of ^{13}C NMR shift data for ester carbonyls showed that electron density is actually greater at such carbons: reactivity enhancement of ester carbonyls relative to ketones is actually due to destabilization of the ground states of the esters by the electron-withdrawing substituents rather than positive polarization at carbon[193, 194].

^{15}N NMR data have been obtained for a limited number of *N*-acyloxy-*N*-alkoxyamides and hydroxamic esters and chemical shifts are presented in Table 5. Secondary and tertiary amide nitrogens generally resonate in the region of −200 to −250 ppm relative to nitromethane[195]. Formamide resonates at −267.5 ppm and *N*,*N*-dimethyl-4-toluamide resonates at −282.6 ppm[196]. ^{15}N in *N*-butoxybenzamide (Table 5, entry 13) resonates much further downfield at −197 ppm relative to nitromethane and that of other hydroxamic esters in this study all resonate between −196 and −203 ppm. The large shift to higher frequency of *ca* 87 ppm relative to *N*,*N*-dimethyl-4-toluamide represents a significant impact of electronegative oxygen on the electron density at an amide nitrogen. Acyloxylation would be expected to produce a downfield shift of at least 100 ppm since the acyloxyl group would be expected to be more strongly electron-withdrawing than an alkoxyl group. Ethoxylation of isobutoxyamine to give *N*-ethoxyisobutoxyamine resulted in a ^{15}N downfield shift of 96 ppm[197]. However, for *N*-butoxy-*N*-heptanoyloxybenzamide (Table 5, entry 13) acyloxyl substitution resulted in a significantly smaller downfield shift of about 73 ppm and shifts for other *N*-acyloxy-*N*-alkoxyamides were similar. This smaller than expected shift and increased electron density at nitrogen has been rationalized on the basis of localization of the lone pair through pyramidalization, as well as $n_O-\sigma*_{NOAcyl}$ overlap in these anomeric amides[13].

Alkoxyl and acetoxyl protons in *N*-acetoxy-*N*-alkoxybenzamides give rise to sharp signals well below room temperature. In contrast, hydroxamic esters usually exhibit line broadened alkoxyl group resonances in their ^1H NMR spectra at or even significantly above room temperature[11, 12]. In toluene-d_8, the benzylic and acetoxyl methyl resonances of *N*-acetoxy-*N*-benzyloxybenzamide (**100**) showed significant line broadening below 250 K but remained isochronous down to 190 K.

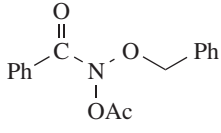

(**100**)

These results indicate that barriers to all isomerization processes in *N*-acyloxy-*N*-alkoxyamides are likely to be less than about 8 kcal mol^{-1}. Like that for its *N*-chloro analogue, the amide isomerization barrier in **100** is too low to be observed by ^1H NMR. While there is definitive X-ray and theoretical evidence for anomeric effects in *N*-acyloxy-*N*-alkoxyamides, in the case of **100** the barrier to isomerization about the *N*−*O*Bn bond must be lower than 10.3 kcal mol^{-1}, the barrier in the corresponding *N*-chlorohydroxamic ester (Section III.B.2). The $n_O-\sigma^*_{NCl}$ anomeric interaction in *N*-chloroadducts is predicted to be stronger than the $n_O-\sigma^*_{NOAcyl}$ interaction on perturbation arguments[50].

C. Reactions of *N*-Acyloxy-*N*-alkoxyamides

Like *N*-chlorohydroxamic esters, *N*-acyloxy-*N*-alkoxyamides are intrinsically reactive at the amide nitrogen owing to the sp^3 character of the nitrogen and the substitution pattern, which strongly favours an $n_O-\sigma*_{NOAcyl}$ anomeric effect resulting in weakening of the $N-O$Acyl bond.

In this configuration, the alkoxyl oxygen lone-pair involvement promotes not only heterolytic S_N1 and S_N2 reactions at nitrogen and homolysis of the $N-O$Acyl bond, but molecular rearrangements.

N-Acyloxy-*N*-alkoxyamides have been shown to undergo acid-catalysed solvolysis reactions producing alkoxynitrenium ions[92, 93, 95, 113, 156], S_N2 reactions with a range of organic and inorganic nucleophiles[13, 89, 90, 95, 97, 99, 114, 157], homolysis reactions that produce alkoxyamidyl radicals[13] and the HERON rearrangement[13, 87]. Urea and carbamate analogues undergo alcoholysis to give *N*,*N*-dialkoxyamides[68] and acyloxyl group exchange[158].

1. Solvolysis studies — $A_{Al}1$ reactivity

N-Acetoxy-*N*-butoxybenzamides (**101**) react in aqueous acetonitrile by an autocatalytic process. In the presence of added mineral acid, they undergo acid-catalysed $A_{Al}1$ solvolysis forming *N*-aroyl-*N*-butoxynitrenium ions (**102**), which are trapped by water. The hydroxamic acid product (**103**) reacted under the conditions to give a range of products that included, *n*-butanol, butanal, benzoic acids, benzohydroxamic acids and butyl benzoates (Scheme 18)[92, 93, 95, 113, 156].

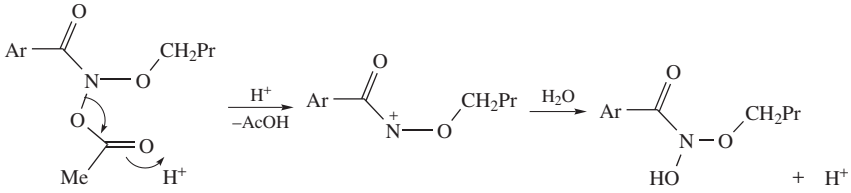

(**101**) (**102**) (**103**)

SCHEME 18

The reactions obeyed pseudo-first-order kinetics consistent with a rapid reversible protonation of the substrate, S, at the ester carbonyl followed by a rate-determining decomposition to acetic acid and nitrenium ion according to Scheme 19. In accordance with equation 13, the pseudo-first-order rate constant, k', was shown to be proportional to acid concentration and inversely proportional to the activity of the water/acetonitrile solvent[92, 156].

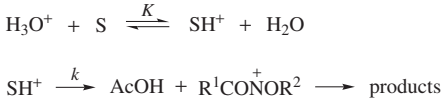

SCHEME 19

$$-\frac{d[S]}{dt} = \frac{d[AcOH]}{dt} = k[SH^+] = k.K.\frac{[S][H_3O^+]}{[H_2O]} = k'[S] \qquad (13)$$

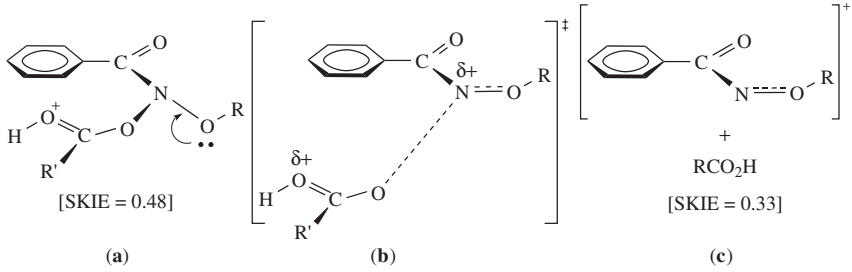

FIGURE 18. (a) Anomerically destabilized protonated intermediate (b) transition state and (c) products from $A_{Al}1$ reaction of *N*-acyloxy-*N*-alkoxybenzamides; predicted SKIE values in parentheses

Formation of *N*-acyl-*N*-alkoxynitrenium ions has been demonstrated by solvent kinetic isotope studies, Arrhenius activation parameters and substituent effects as well as product studies.

A solvent kinetic isotope effect (SKIE) of 0.44 from solvolysis in $CD_3CN–H_2O$ versus $CD_3CN–D_2O$ mixtures was in line with predicted values for the protonation–dissociation mechanism for which the SKIE should be between 0.48 and 0.33 (Figure 18a and c)[13, 92, 156].

Arrhenius E_A values for acid-catalysed solvolysis of a wide range of *N*-acyloxy-*N*-alkoxyamides were between 13 and 31 kcal mol^{-1} and $\Delta S^{\ddagger}$ values were between 15 and 30 cal K^{-1} mol^{-1}, reflecting a dissociative rate-determining step[13, 92, 93, 95, 156]. In contrast, normal $A_{Ac}2$ hydrolysis of esters has a strongly negative $\Delta S^{\ddagger}$ of between −24 and −36 cal K^{-1} mol^{-1} [198]. The activation energies were also in the region of those cited for the $A_{Al}1$ acid-catalysed hydrolysis of tertiary alkyl, diphenylmethyl and α-methylallyl esters, namely *ca* 29 kcal mol^{-1} [199]. However, entropies of activation were more positive than obtained for these esters (*ca* 9.5 cal K^{-1} mol^{-1}) in accord with much looser and later transition states with substantial alkoxynitrenium ion character (Figure 18b).

For a series of *para*-substituted *N*-acetoxy-*N*-butoxybenzamides (**104**), rate constants correlated with Hammett σ^+ with a ρ-value of −1.4[92], which is also consistent with nitrenium ion formation and a build-up of charge beta to the aromatic ring. Rate enhancement by electron-releasing substituents can best be ascribed to a diminution of positive charge at the amide carbonyl carbon in **105**, thereby facilitating the development of positive charge at nitrogen.

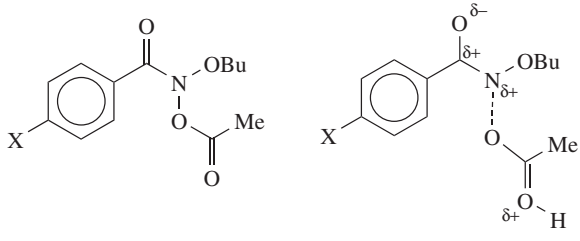

(**104**) (**105**)

Thus *N*-acyloxy-*N*-alkoxyamides undergo acid-catalysed solvolysis forming *N*-acyl-*N*-alkoxynitrenium ions. However, the rate of uncatalysed reaction was shown to be negligible under the same conditions and anomeric weakening of the *N*−*O* bond in the neutral species is insufficient to promote heterolysis[92]. Upon protonation, the acyloxyl group becomes more electronegative (Figure 18a) and population of the lower-energy *N*−*O*Acyl σ^* orbital by the p-type lone pair on the neighbouring oxygen results in dissociation to a resonance-stabilized nitrenium ion (Figure 18c).

All the products resulting from acid-catalysed solvolysis of *N*-acetoxy-*N*-butoxybenzamides in acetonitrile–water mixtures were derived from the *N*-butoxy-*N*-hydroxybenzamide intermediate (**103**), which is itself an anomeric amide and is the amide equivalent of a hemi-acetal[92,93]. Decomposition reactions of **103** under acidic conditions are presented in Scheme 20.

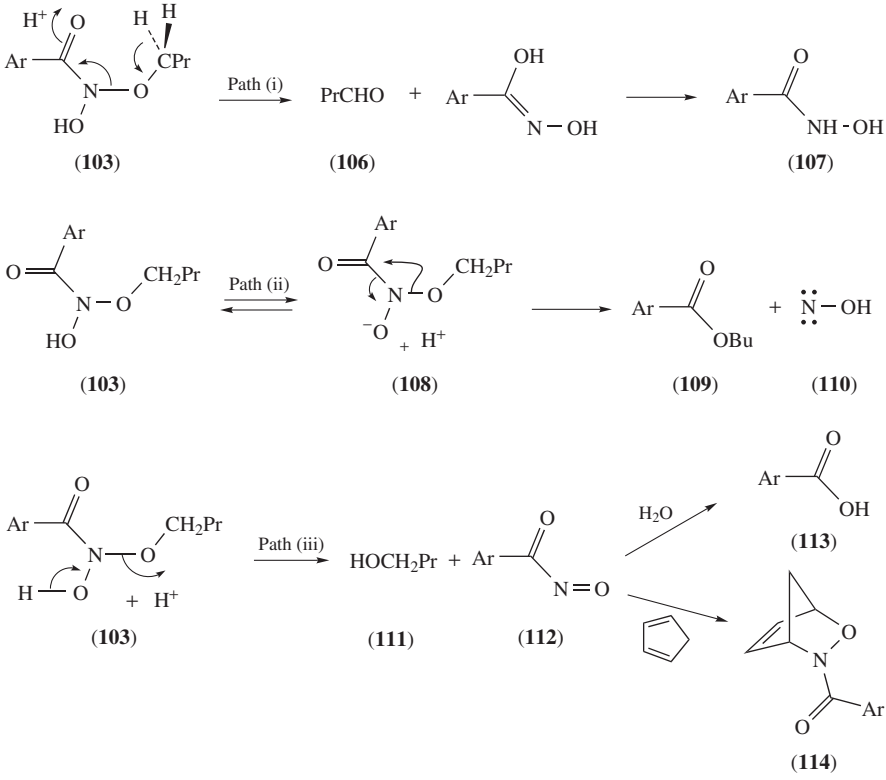

SCHEME 20

Aldehyde (**106**) and the hydroxamic acids (**107**) were generated together in an acid-catalysed elimination reaction (Scheme 20, pathway (i)).

A crossover experiment indicated that esters (**109**) were formed in a concerted HERON rearrangement concomitant with the likely formation of the hydroxynitrene (**110**) (Scheme 20, pathway (ii)). Joint solvolysis of equimolar quantities of *N*-acetoxy-*N*-

butoxy-4-chlorobenzamide (**104**, X = Cl) and *N*-acetoxy-*N*-benzyloxybenzamide (**115**, Y = H) afforded significant quantities of butyl 4-chlorobenzoate (36%) and benzyl benzoate (54%) as the only esters[92]. Since ester formation was shown to predominate in neutral or low acid concentrations, it could involve the conjugate anion of the hydroxamic acid, **108** (see Section IV.C.3.c)[87,95].

The source of alcohol (**111**) was acid-catalysed hydrolysis of **103** to the nitrosocarbonylarene intermediates (**112**), which, like acid chlorides, react with water to give benzoic acids **113** (Scheme 20, pathway (iii))[200]. **112** were trapped as the Diels–Alder adducts (**114**) in reactions in MeCN/H_2O and in the presence of cyclopentadiene. In MeCN/10% $H_2{}^{18}O$, **114** was enriched in ^{18}O providing unequivocal evidence for both the trapping of the nitrenium ion intermediate, **102**, by solvent water molecules and subsequent hemiacetal-like hydrolysis to the nitrosocarbonylarene (**112**)[93].

Studies at different acid strengths indicated that pathways (i) and (iii) in Scheme 20 were favoured over the non-acid-catalysed HERON reaction pathway (ii) at higher acid concentrations[93].

A series of *N*-benzoyloxy-*N*-benzyloxybenzamides (**116**) reacted with similarly positive $\Delta S^{\ddagger}$ (25–29 cal K^{-1} mol^{-1}) but with lower E_A values of between 11 and 21 kcal mol^{-1}. Rate constants at 308 K gave a positive Hammett σ correlation but with a much smaller ρ-value of 0.32 in accordance with the opposing influences of *para* substituents, Z, on the pre-equilibrium protonation and heterolysis steps[95].

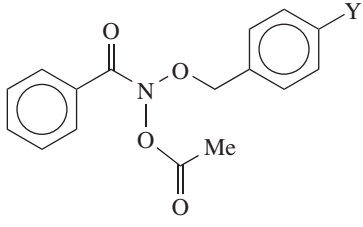

(**115**)

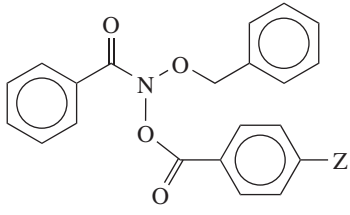

(**116**)

Substituted *N*-acetoxy-*N*-benzyloxybenzamides (**115**) also reacted similarly. However, with resonance-stabilizing substituents on the *para* position of the benzyloxy ring (**115**, Y = OMe, Ph, OPh), acid catalysis resulted in a concerted E1 decomposition of the protonated intermediate (**117**) and release of benzyl cation in the rate-determining step according to Scheme 21.

The reaction exhibited second-order kinetic isotope effects of $k_H^H/k_H^D = 1.32$ for **115**, Y = OMe and 1.18 for **115**, Y = Ph, in accordance with the change in hybridization at the benzylic position in the transition state (**118**). Furthermore, in $H_2{}^{18}O$, the Diels–Alder product (**120**) from cyclopentadiene and **119** was unlabelled while benzyl alcohol (**122**), formed from **121** and water, was enriched in ^{18}O. Methyl and nitro analogues (**115**, Y = Me, NO_2) exhibited no deuterium isotope effect.

2. Alcoholysis

Kostyanovsky and coworkers demonstrated that keeping *N*-acyloxy-*N*-alkoxyureas (**123a**) in neat alcohols for prolonged reaction times (sometimes months) resulted in

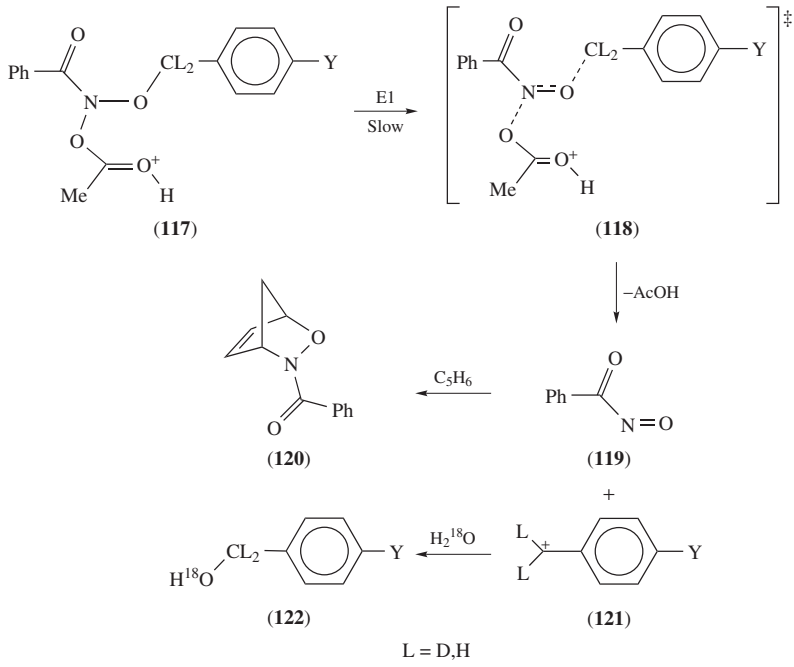

SCHEME 21

formation of symmetrical and mixed *N*,*N*-dialkoxyureas **124a** (equation 14)[68]. The reactions worked with primary alcohols (MeOH, EtOH and PrOH) but 2-propanol required longer reaction times, which is indicative of a bimolecular reaction. Furthermore, *tert*-butanol was unreactive.

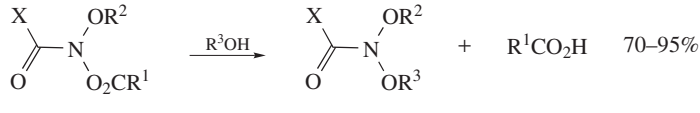

(123) (124) (14)

(**a**) X = NR_2
(**b**) X = OR

The corresponding carbamates **123b** reacted similarly giving **124b**, but methanolysis of ethyl *N*-acetoxy-*N*-methoxycarbamate (**125**) afforded ethyl methyl carbonate (**127**) and the dimethoxy product (**126**) in 44% and 34% yields, respectively. Shtamburg and coworkers accounted for the formation of the carbonate by an S_N1 reaction to give the alkoxynitrenium ion, **128**, that undergoes loss of alkoxynitrene to form the alkoxycarbonyl cation **129** (Scheme 22, pathway (ii))[68]. It is possible that this reaction proceeds by a HERON rearrangement of **126**, which, while slow, is probably energetically more feasible (Scheme 22, pathway (i)).

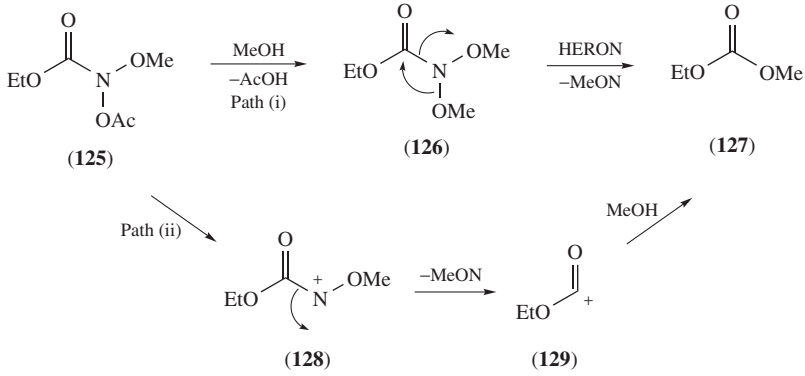

(**125**) (**126**) (**127**) (**128**) (**129**)

SCHEME 22

3. S_N2 reactions at nitrogen

N-Acyloxy-*N*-alkoxyamides undergo S_N2 reactions with a number of organic and inorganic nucleophiles including anilines, thiols, hydroxide and azide. Products from all of these processes are themselves anomeric amides, which undergo secondary reactions.

By analogy with vinyl systems, normal amide nitrogens do not undergo classical S_N2 reactions. However, *N*-acyloxy-*N*-alkoxyamides, which possess a tetrahedral nitrogen bearing a good leaving group, readily undergo S_N2 reactions at the amide nitrogen; nucleophiles react at nitrogen rather than at the amide carbonyl. This is directly attributable to negative hyperconjugation and anchimeric-assisted weakening of the $N-O$Acyl bond. Furthermore, resonance stabilization of nitrenium ions by alkoxy substituents, described in Section III.C.2, also influences the ease of the S_N2 reaction. The E_A is reduced and the S_N2 saddle points are moved in the direction of cationic species, resulting in incipient nitrenium ion character in the transition structure and longer bonds to both the nucleophile and the leaving group (Figure 19)[82, 85, 86, 201].

Like *N*-alkoxy-*N*-chloroamides, the S_N2 reactivity of *N*-acyloxy-*N*-alkoxyamides is directly analogous to the S_N2 reactions of α-haloketones[135, 144] where the α-carbonyl groups are well known to enhance S_N2 reactivity[82, 135, 144–148]. Although there are no comparative rate data for reactions of amines or alkoxyamines, these arguments should apply to substitution at the amide nitrogen in *N*-acyloxy-*N*-alkoxyamides.

a. Reaction with aromatic amines. *N*-Acyloxy-*N*-alkoxyamides are mutagenic towards TA100 and TA98 strains of *Salmonella typhimurium* without metabolic activation and

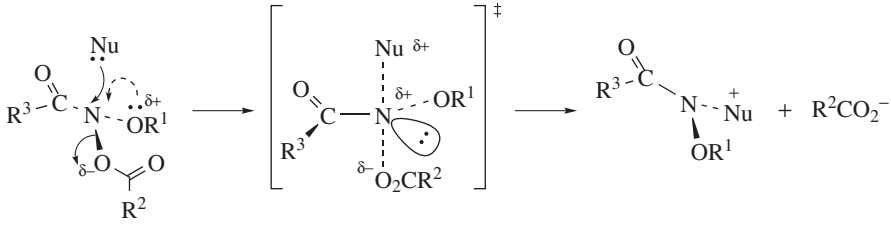

FIGURE 19. Ground state, transition state and products for the S_N2 reaction of nucleophiles and *N*-acyloxy-*N*-alkoxyamides

react as electrophiles directly with nucleophilic centres, principally N7 of Guanine (G-N7), in DNA[62,92,93,95,96,99,149]. DNA damage studies point to an S_N2 displacement of carboxylate by G-N7[13,98,113]. The relative potential of *N*-acyloxy-*N*-alkoxyamides to interact with DNA as such has been evaluated from studies of their reactivity with the aromatic base *N*-methylaniline[89,90,99,114].

Reactions of *N*-acyloxy-*N*-alkoxyamides (**90**) with *N*-methylaniline in methanol or aqueous acetonitrile afforded quantitative yields of esters (**130**), carboxylic acid (**132**) and half an equivalent of *N*,*N*′-dimethyl-*N*,*N*′-diphenyltetrazene (**131**) (equation 15). The reaction is promoted by polar solvents and ester formation was shown to involve an intramolecular process; a crossover experiment using a mixture of *N*-acetoxy-*N*-butoxy-4-toluamide (**90**, R^1 = Bu, R^2 = Me, R^3 = 4-MeC_6H_4) and *N*-acetoxy-*N*-ethoxybenzamide (**90**, R^1 = Et, R^2 = Me, R^3 = Ph) afforded clean yields of butyl 4-toluate (**130**, R^1 = Bu, R^3 = 4-MeC_6H_4) and ethyl benzoate (**130**, R^1 = Et, R^3 = Ph)[114].

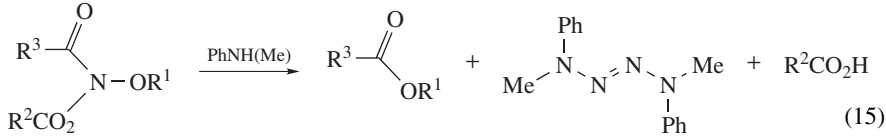

(15)

(**90**) (**130**) (**131**) (**132**)

The mechanism (Scheme 23) involves an S_N2 displacement of the acyloxyl group from **90** and formation of intermediate *N*-alkoxy-*N*-(*N*′-methylanilino)amides (**133**). These are strongly anomeric on account of a high-energy lone pair on nitrogen and the electronegative oxygen of the alkoxyl group. Anomeric weakening of the *N*−*O* bond in **133** results not in heterolysis to alkoxide ion, which would be energetically unfavourable, but in a HERON process whereby the alkoxyl group migrates from the amide nitrogen to the carbonyl carbon with heterolysis of the *C*−*N* bond. Along with ester **130** this results in the formation of 1-methyl-1-phenyldiazene **134** which, under the reaction conditions, dimerizes to the tetrazene **131**.

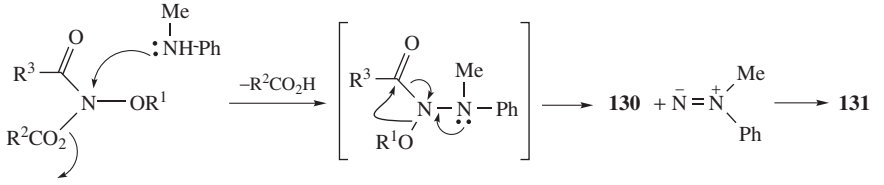

(**90**) (**133**) (**134**)

SCHEME 23

This was the first-discovered HERON reaction but such reactions appear to be common to most *N*-heteroatom-substituted hydroxamic esters[13,87,88,91], and will be described in detail in Section VI.C, which deals more fully with the reactions of *N*-aminohydroxamic esters.

Bimolecular rate constants at 308 K have been determined for a wide range of *N*-acyloxy-*N*-alkoxyamides in methanol-d_4 and are in the range of 10^{-2}–10^{-3} l mol^{-1} s^{-1} in the absence of steric effects (Table 6). E_A values ranged between 6–15 kcal mol^{-1} while $\Delta S^{\ddagger}$ were strongly negative (−20 to −30 cal K^{-1} mol^{-1}) in keeping with both a bimolecular process and increased solvation at the charge-separated transition state (Figure 19)[13,89,90,99,113]. S_N2 reactions of aniline and substituted pyridines with phenacyl

bromides have similar Arrhenius activation energies and entropies of activation in methanol ($E_A = 14–16$ kcal mol^{-1}, $\Delta S^{\ddagger} = -27$ to -31 cal K^{-1} mol^{-1})[144].

The reaction has also been modelled computationally at the HF/6-31G* level using *N*-formyloxy-*N*-methoxyformamide (**91**) and ammonia according to equation 16[157].

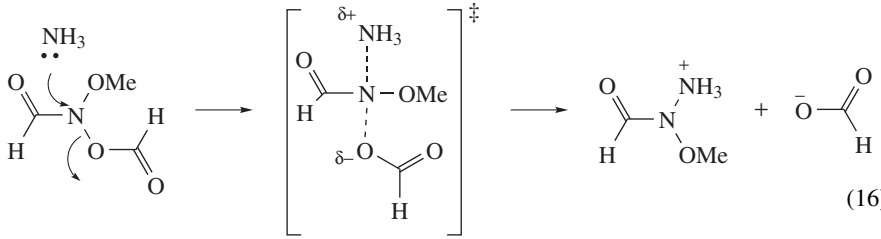

(16)

(**91**) (**135**) (**136**)

The computed structure of transition state **135** leading to product **136** is early along the reaction coordinate and the nucleophile and leaving group are approaching collinearity (Figure 20). The amide nitrogen lone pair, the methoxyl group and the amide formyl substituent are approximately coplanar. The methoxyl group is oriented to maximize alignment of the p-type lone pair on $O_{(5)}$ with the $N_{(2)}-O_{(3)}$ bond and therefore the σ^*_{NO} orbital, suggesting it plays a negative hyperconjugative role even at the transition state. The reaction is concerted, the formyloxyl group departing as $N-N$ bond formation occurs.

Analysis of the group electrostatic charges in the ground state of the reactants and the transition state supported the attribution of the strongly negative $\Delta S^{\ddagger}$ values observed to solvation effects. Figure 20 gives the changes in total charge on the nucleophile ($\Delta q = +0.34$) and the formyloxyl leaving group ($\Delta q = -0.67$). The greater accrual of negative charge in the formyloxyl group compared to positive charge on the nucleophile

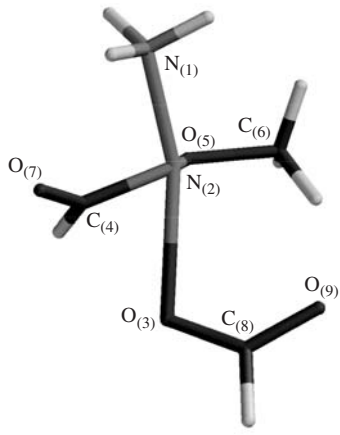

$N_{(1)}$-$N_{(2)}$ = 1.898 Å
$N_{(2)}$-$O_{(3)}$ = 2.316 Å
$N_{(2)}$-$C_{(4)}$ = 1.490 Å
$N_{(2)}$-$O_{(5)}$ = 1.276 Å
$N_{(1)}$-$N_{(2)}$-$O_{(3)}$ = 155.1°
$C_{(4)}$-$N_{(2)}$-$O_{(5)}$ = 108.7°
$C_{(4)}$-$N_{(2)}$-$O_{(3)}$ = 65.1°
$C_{(4)}$-$N_{(2)}$-$N_{(1)}$ = 96.6°
$O_{(5)}$-$N_{(2)}$-$O_{(3)}$ = 98.1°
$O_{(5)}$-$N_{(2)}$-$N_{(1)}$ = 104.1°
$O_{(3)}$-$N_{(2)}$-$O_{(5)}$-$C_{(6)}$ = –95.1°
$O_{(7)}$-$C_{(4)}$-$N_{(2)}$-$O_{(5)}$ = 154.9°

Δq(OCHO) = −0.67
Δq(NH_3) = +0.34
Δq(CHO) = +0.03
Δq(N) = +0.23
Δq(OCH_3) = +0.07

FIGURE 20. HF/6-31G* optimized geometry and changes in group charges (relative to reactants) at the transition state (**135**) for S_N2 displacement of formate from *N*-formyloxy-*N*-methoxyformamide (**91**) by ammonia

is indicative of a non-synchronous process and of partial nitrenium ion character in the transition state [$\Delta q(\mathrm{N}) + \Delta q(\mathrm{OCH_3}) + \Delta q(\mathrm{CHO}) = +0.33$].

B3LYP/6-31G*//HF/6-31G* energies, including aqueous solvation effects, predicted this reaction to be exothermic by 5.1 kcal mol^{-1} with an E_A of just 4.4 kcal mol^{-1}, which is lower than the experimental values for substitution by *N*-methylaniline in methanol[13,157]. With the likely degree of charge separation in the transition state, it is reasonable to suppose that E_A in aqueous solution ($\varepsilon = 80$) would be lower than the E_A in methanol ($\varepsilon = 33$).

Nucleophilic attack by *N*-methylaniline is favoured by electron-withdrawing groups on the amide and acyloxyl side chains. A series of *para*-substituted *N*-acetoxy-*N*-butoxybenzamides (**138**) (Table 6) gave a weak but positive Hammett correlation with σ constants ($\rho = 0.13$, $r = 0.86$)[89,90]. The analogous reactions of pyridine with *para*-substituted phenacyl halides in methanol afforded a similar Hammett correlation (σ, $\rho = 0.25$)[144]. The bimolecular rate constants for the limited series of *N*-benzoyloxy-*N*-benzyloxybenzamides (**139**) in Table 6 correlated strongly with Hammett σ constants ($\rho = 1.7$, $r = 0.97$)[89,90]. Stabilization of developing carboxylate character supported the computed charge redistribution in the transition state[157].

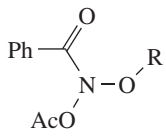

(**137**)

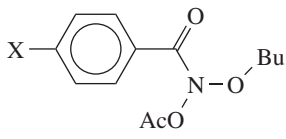

(**138**)

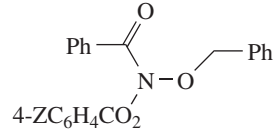

(**139**)

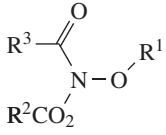

(**90**)

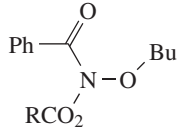

(**140**)

TABLE 6. Bimolecular rate constants for reaction of *N*-acyloxy-*N*-alkoxyamides **90** and **137**–**140** with *N*-methylaniline in methanol-d_4[13,89,90,99,113,185,187]

137 R	$10^4\ k_2^{308}$ (l mol^{-1} s^{-1})	**138** X	$10^4\ k_2^{308}$ (l mol^{-1} s^{-1})	**139** Z	$10^4\ k_2^{308}$ (l mol^{-1} s^{-1})	**90** R^1, R^2, R^3	$10^4\ k_2^{308}$ (l mol^{-1} s^{-1})	**140** R	$10^4\ k_2^{303}$ (l mol^{-1} s^{-1})
Et	276.5	OMe	481.5	H	260.8	Bn, Me, Ph	155.6	Pr	122.0
Pr	628.4	Ph	559.3	OMe	87.7	Bu, Ph, Ph	2550.0	*i*-Bu	91.0
Bu	581.5	Me	222.3	Me	109.8	Bu, Me, Me	16.9	(*S*)-2-Bu	97.0
Pen	643.3	Cl	678.3	Cl	881.2	Bu, Ph, Me	87.5	t-$BuCH_2$	78.0
Oct	363.0	Br	609.4	*t*-Bu	177.0	Bu, Ph, Et	5.3	1-Ad	61.0
i-Pr	96.7	NO_2	693.9			Bu, Ph, *t*-$BuCH_2$	2.2[a]	*t*-Bu	33.8
i-Bu	239.3	*t*-Bu	585.4			3,5-Me_2-benzyl, Me, Ph	214.5	Ph	1844.0
i-Pen	581.5					2,6-Me_2-benzyl, Me, Ph	36.3	4-$MeOC_6H_4$	466.0
								4-MeC_6H_4	816.0

[a] R^3 = neopentyl (*t*-$BuCH_2$), rate constant at 313 K.

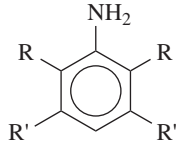

(**141**)

(**a**) R = Me, R' = H
(**b**) R = Et, R' = H
(**c**) R = H, R' = Me

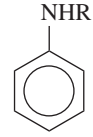

(**142**)

(**a**) R = Me
(**b**) R = Ph

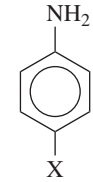

(**143**)

(**a**) X = MeO
(**b**) X = Me
(**c**) X = H
(**d**) X = Cl
(**e**) X = Br
(**f**) X = NO_2

TABLE 7. Bimolecular rate constants for the reaction of anilines **141**–**143** with *N*-acetoxy-*N*-butoxybenzamide (**137**, R = Bu) in methanol-d_4 at 308 K, 298 K and 278 K[89,90]

Aniline	$10^4\ k_2{}^{308}$ ($l\,mol^{-1}\,s^{-1}$)	$10^4\ k_2{}^{298}$ ($l\,mol^{-1}\,s^{-1}$)	$10^4\ k_2{}^{278}$ ($l\,mol^{-1}\,s^{-1}$)
141a	8.4		0.9
141b	15.4		1.0
141c	193.4		22.9
142a	581.5	290.9	62.8
142b	—	1.6	—
143f			36.7
143d			68.6
143c	—		89.6
143e			106.0
143b			273.3
143a			929.0

Rate constants at 278 K for the reaction of *N*-acetoxy-*N*-butoxybenzamide (**137**, R = Bu) with a series of substituted anilines (**141**–**143**) have also been measured (Table 7) and for **143a**–**f**, correlated with Hammett σ^+ with $\rho = -0.91$, which accords with the developing ammonium ion character in the transition state. Reactions of substituted anilines at alkyl and acyl carbon centres are more sensitive to electronic effects ($\rho = -2.0$ to -3.0)[202] and, together with the strong sensitivity to substituents on the leaving group, the lower ρ value of -0.91 reflects an early transition state in which positive charge is not transferred directly to the nucleophile. Rather, because of incipient stabilization by the alkoxyl group, there is significant nitrenium ion character.

As expected, bulky groups on the *N*-acyloxy-*N*-alkoxyamide as well as on the nucleophile have a significant impact on ease of S_N2 reaction at nitrogen.

Like alkyl halides, branching β to the nitrogen on both the acyl and the alkoxy side chains impedes S_N2 reactivity. Methyl and ethyl adjacent to the amide carbonyl (Table 6, **90**, R^3 = Me, Et) lowered rate constants by an order of magnitude relative to arylamides (Table 6, **137**, R = Bu, and **90**, R^1 = Bu, R^2 = Ph, R^3 = Ph) in keeping with the transition state depicted in Figure 19[13]. This is analogous to the reactions of α-chloroketones where α-chloroacetones are less reactive than the corresponding acetophenones[135]. Branching

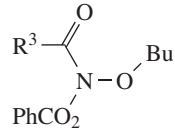

(**144**)

α to the amide carbonyl had a dramatic influence; **144** with $R^3 = i$-Bu, t-Bu, 1-Ad were unreactive while the neohexamide with the *tert*-butyl group-one carbon removed from the carbonyl also reacted very slowly at 313 K (Table 6, **90**, R^1 = Bu, R^2 = Ph, $R^3 = t$-$BuCH_2$)[99].

Azide reacted bimolecularly with analogous *N*-alkoxy-*N*-chloroamides. However, ionic nucleophiles such as azide and acetate are thought to react with α-haloketones through tighter classical S_N2 transition states, which are insensitive to steric effects[135, 148].

While substrates with unbranched propoxyl, butoxyl, pentoxyl and octyloxyl as well as isopentoxyl side chains all gave similar rate constants at 308 K (Table 6, **137**), isopropoxyl (**137**, R = i-Pr) and isobutoxyl (**137**, R = i-Bu) significantly lowered the rates relative to ethoxyl and propoxyl (**137**, R = Et, Pr) in accordance with their higher degree of steric hindrance brought about by branching. While *N*-acetoxy-*N*-benzyloxybenzamide and the 3,5-dimethylbenzyloxy analogue (**90**, R^1 = benzyl and 3,5-dimethylbenzyl, R^2 = Me, R^3 = Ph) reacted with similar rate constants at 308 K, a 2,6-dimethylbenzyloxy group (**90**, R^1 = 2,6-dimethylbenzyl, R^2 = Me, R^3 = Ph) strongly inhibited the reaction[187]. A *tert*-butoxyl group in **137** (R = t-Bu) completely inhibited S_N2 reaction with *N*-methylaniline at the same temperature[187].

Analysis of rate constants for the bimolecular attack of substituted anilines at 308 K clearly indicated that steric effects on the nucleophile play a role. 2,6-Dimethyl- and 2,6-diethylaniline react more than an order of magnitude slower than 3,5-dimethylaniline at the same temperature (Table 7)[89, 90]. A comparison of the rate constants for reaction of aniline and *N*-methylaniline at 278 K and *N*-methylaniline with *N*-phenylaniline at 298 K provides further evidence of steric effects although the very small rate constant for the diphenylamine could, in part, also be attributed to reduced nucleophilicity due to resonance into the additional phenyl ring.

Rate constants for the reaction of *N*-methylaniline with a range of *N*-butoxy-*N*-alkanoyloxybenzamides in methanol-d_4 at 303 K indicated that steric effects of branching on the acyloxyl side chain in **140** were insignificant (Table 6). The data, taken together with that for several *N*-butoxy-*N*-benzoyloxybenzamides (**140**, R = Ph, 4-$MeOC_6H_4$, 4-MeC_6H_4), correlated negatively with pK_A of the acid (slope = -4.8, $r^2 = 0.983$), supporting the theoretical transition state properties in which substantial charge transfer to the carboxyl group takes place.

Bimolecular reactions of aniline with *N*-acyloxy-*N*-alkoxyamides are model S_N2 processes in which the transition state for the reaction at nitrogen resembles that for classical S_N2 processes at carbon. Electronic influences of substituents support a non-synchronous process, which has strong charge separation at the transition state and which is subject to steric effects around the reactive centre, at the nucleophile but not on the leaving group. The sp^3 character of nitrogen and the disconnection between the amino group and the amide carbonyl renders these reactions analogous to the displacement of halides in α-haloketones.

The mutagenic activity of *N*-acyloxy-*N*-alkoxyamides is believed to involve S_N2 reactions of guanine N7 at the amide nitrogen with displacement of carboxylate and their biological activity is similarly affected by substituents at the amide nitrogen[13, 98, 113].

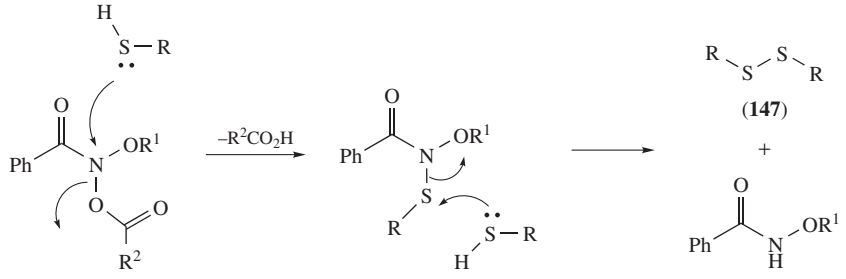

(**145**) (**146**) (**147**) + (**148**)

(**a**) RS = glutathiyl
(**b**) RS = (*L*)-cysteinyl methyl ester
(**c**) RS = (*L*)-cysteinyl ethyl ester

SCHEME 24

b. Reaction with thiols. *N*-Acyloxy-*N*-alkoxyamides (**145**) have been shown to react rapidly with thiols giving the oxidized form of the thiol (**147**), the parent hydroxamic ester (**148**) and carboxylic acid as products (Scheme 24)[13,203].

N-Acetoxy-*N*-butoxybenzamide (**145**, $R^1 = Bu$, $R^2 = Me$) reacted with glutathione in DMSO-d_6/D_2O and with (*L*)-cysteine methyl and ethyl esters in methanol-d_4. NMR studies indicated a bimolecular process, with thiol consumed at twice the rate of *N*-acyloxy-*N*-alkoxyamide. Like the *N*-aminohydroxamic esters described in the previous section, the intermediate *N*-thioalkylhydroxamic ester (**146**) is also unstable, being susceptible to a non-rate-determining, secondary nucleophilic reaction with the reactive thiol[13,203].

Rates of reaction were moderately fast. Glutathione reacted rapidly in DMSO-d_6/D_2O (k_2^{303} *ca* 2×10^{-2} l mol^{-1} s^{-1}) and a series of *N*-benzoyloxy-*N*-benzyloxybenzamides (**139**) and (*L*)-cysteine ethyl ester in methanol-d_4 reacted with low E_A values (8–16 kcal mol^{-1}) and negative $\Delta S^{\ddagger}$ (−19 to −43 cal K^{-1} mol^{-1}), similar to their reaction with anilines. Bimolecular rate constants at 298 K (Table 8) correlated positively with Hammett σ constants with slightly lower sensitivity ($\rho = 1.1$ as opposed to $\rho = 1.7$ for *N*-methylaniline)[13,203].

The S_N2 reaction has also been investigated theoretically at HF/6-31G* and BPDN*//6-31G* density functional levels using the model compounds methanethiol and *N*-formyloxy-*N*-methoxyformamide (**91**). As was reported for the ammonia reaction (Section

TABLE 8. Rate constants at 298 K for reaction of *N*-benzoyloxy-*N*-benzyloxybenzamides (**139**) with *L*-cysteine ethyl ester in methanol-d_4[13]

Z	$10^4\ k_2^{298}$ (l mol^{-1} s^{-1})
H	51.3
OMe	31.3
Me	57.0
Cl	200.0
NO_2	523.2

IV.C.3.a), nucleophilic displacement of formate is an asynchronous process with substantial alkoxynitrenium ion character at the transition state. The reaction is computed to be exothermic by 5.0 kcal mol^{-1} and to have an E_A of 4.2 kcal mol^{-1} [13, 157].

c. Reaction with hydroxide ion. *N*-Acyloxy-*N*-alkoxybenzamides (**149**) react rapidly with dilute aqueous sodium hydroxide at room temperature giving alkyl benzoates (**150**) (equation 17)[95]. A crossover experiment using **149a** and **149b** resulted in the exclusive formation of butyl 4-chlorobenzoate (**150a**, 46%) and benzyl benzoate (**150b**, 43%) along with their hydrolysis products, 4-chlorobenzoic acid and benzoic acid, indicating that esters were formed intramolecularly.

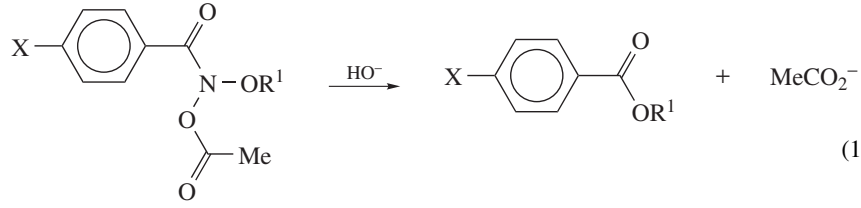

(17)

(**149**) (**150**)

(**a**) R^1 = Bu, X = Cl
(**b**) R^1 = Bn, X = H

Evidence pointed to an *N*-alkoxyhydroxamic acid intermediate (**151**), which is formed by base attack at the nitrogen of **90** rather than at the acyloxyl carbon ($B_{Al}2$ rather than normal $B_{Ac}2$ ester hydrolysis) according to Scheme 25. In the presence of excess base, conversion of the hydroxamic acid intermediate into its conjugate anion (**152**) resulted in a facile HERON reaction forming ester (**130**) and presumably nitrosyl hydride. **152** possesses a high-energy pair of electrons that enhances the $n_O-\sigma^*_{NOR}$ anomeric effect, driving the rearrangement. A theoretical study pointed to an early transition state, **153**, which leads to a tetrahedral intermediate **154** rather than directly to ester[87].

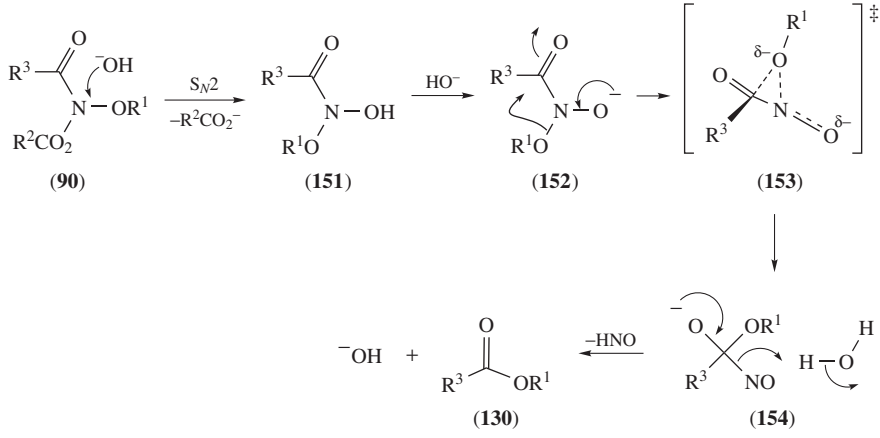

(**90**) (**151**) (**152**) (**153**)

(**130**) (**154**)

SCHEME 25

TABLE 9. Bimolecular rate constants for the reaction of dilute solutions of hydroxide ion with **139** at 275 K[95]

Z	k_2^{275} ($l\,mol^{-1}\,s^{-1}$) [a]
Me	2.27 (0.4)
H	3.16 (0.7)
Cl	3.82 (0.7)
CHO	4.91 (0.6)
CN	6.97 (0.1)
NO_2	8.14 (1.3)

[a] Errors in parentheses.

Bimolecular rate constants for reaction with the series of *N*-(4-substituted benzoyloxy) mutagens (**139**) are given in Table 9 and correlated with Hammett σ constants with positive slope ($\rho = +0.55$, $r = 0.992$). $B_{Ac}2$ base hydrolysis of benzoate esters correlated with Hammett ρ but with a much larger ρ-value in the range 2.0–2.4[198]. The observed sensitivity to substituent electronic effects is in keeping with stabilization by electron-withdrawing groups of partial carboxylate character in the transition state.

The HERON rearrangement of **152** to **154** is supported by B3LYP/6-31G*//HF/6-31G* calculations on **152** ($R^1 = Me$, $R^3 = H$), which gave an activation energy for formation of the HERON transition state (**153**, $R^1 = Me$, $R^3 = H$) of only 5.3 kcal mol^{-1} (10.0 kcal mol^{-1} including solvation effects). In contrast to the HERON reactions of *N*-amino-*N*-alkoxyamides described above (Section IV.C.3.a) and detailed in Section VI.C, the rearrangement, which is exothermic by 10.7 kcal mol^{-1}, leads to a stable tetrahedral intermediate (**154**, $R^1 = Me$, $R^3 = H$)[87]. An earlier AM1 study of methoxyl migration in the corresponding *N*-methoxyacetohydroxamate gave similar results ($\Delta H^{\ddagger} = 6.2$ kcal mol^{-1} and $\Delta H_{reaction} = 15.3$ kcal mol^{-1})[88].

d. Reaction with azide ion. *N*-Acyloxy-*N*-alkoxyamides (**90**) react rapidly with azide ion to give quantitative yields of esters (**130**) and two equivalents of nitrogen (equation 18). As with *N*-alkoxy-*N*-chloroamides (see Section III.C.4), crossover experiments showed that **130** are formed intramolecularly and presumably through the *N*-alkoxy-*N*-azidoamide intermediate (**155**), which decomposes with loss of nitrogen to 1-acyl-1-alkoxydiazene (**156**) followed by a HERON reaction (see Scheme 16)[97, 133, 151].

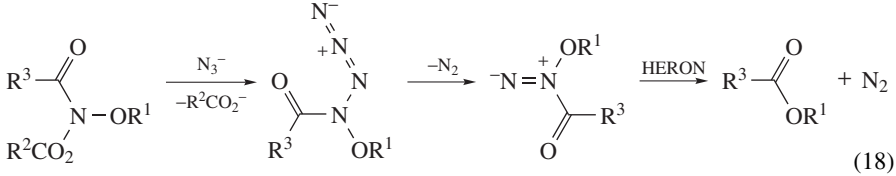

(**90**) (**155**) (**156**) (**130**) (18)

The rate of reaction with *N*-acetoxy-*N*-benzyloxybenzamide (**115**, Y = H), determined dilatometrically in aqueous acetonitrile at 294 K, showed first-order dependence upon concentrations of both mutagen and azide and yielded a bimolecular rate constant of *ca* 1.9 $l\,mol^{-1}\,s^{-1}$. Reaction of hydroxide ion with **139** proceeded with similar, large rate constants in aqueous organic media. Rate constants for the reaction of *N*-acyloxy-*N*-alkoxyamides with softer nucleophiles, aromatic amines or glutathione were slower by two to three orders of magnitude[13, 89, 90, 113, 203].

The nucleophilic attack of azide on an *N*-acyloxy-*N*-alkoxyamide has also been modelled at the pBP/DN*//HF/6-31G* level using *N*-formyloxy-*N*-methoxyformamide (**91**)[97]. In the gas phase with solvent correction, the reaction was computed to be exothermic by 13.3 kcal mol^{-1} and have an E_A of 6.7 kcal mol^{-1} in accord with a facile S_N2 reaction and in agreement with the experimental findings[13,97]. In the computed transition state the increase in negative charge of the formate group ($\Delta q_{formate} = -0.65$) was larger than the decrease in negative charge over the azide group ($\Delta q_{azide} = +0.24$), indicative of a non-synchronous process similar to that reported for the corresponding reactions of ammonia and methanethiol with **91**[157].

e. Reaction with carboxylate salts. Shtamburg and coworkers have reported that *N*-acyloxy-*N*-alkoxyureas (**157a**), -carbamates (**157b**) and -benzamides (**157c**) undergo acyloxyl group exchange with sodium or potassium carboxylates in MeCN. The reaction is reversible and the equilibria are driven further to product by the use of potassium salts. Benzamides were more reactive than the ureas or carbamates. Thus, for instance, *N*-acetoxy-*N*-alkoxyurea (**158a**), -carbamate (**158b**) and benzamide (**158c**) were generated from the corresponding *4*-chlorobenzoates **157a**, **157b** and **157c** in yields of 42, 70 and 87%, respectively (equation 19)[158].

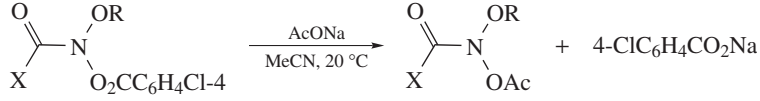

(**157**) (**158**) (19)

(**a**) X = NH_2, R = Bu, 42%
(**b**) X = EtO, R = Me, 70%
(**c**) X = Ph, R = Et, 87%

4. Reaction at the amide carbonyl

There is one report of competitive nucleophilic attack at the amide carbonyl in an *N*-acyloxy-*N*-alkoxyamide. Shtamburg and coworkers have reported that MeONa reacted with *N*-acetoxy-*N*-ethoxybenzamide (**159**) in DME giving methyl and ethyl benzoate (**160** and **161**) (Scheme 26)[68]. They attributed the formation of methyl benzoate to the direct attack of methoxide ion at the amide carbonyl rather than at nitrogen. The formation of **161** was attributed to a HERON reaction. Though not mentioned by the authors, it seems likely that under these aprotic conditions, **162** could also have been formed by methoxide attack at the acetate carbonyl leading to an anion-induced HERON reaction, by analogy with the reaction of *N*-acyloxy-*N*-alkoxyamides and aqueous hydroxide discussed above (Section IV.C.3.c)

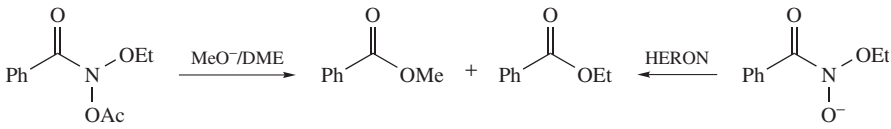

(**159**) (**160**) (**161**) (**162**)
23% 31%

SCHEME 26

5. Thermolysis reactions

Recent studies from the author's laboratory have focused upon the thermal reactions of *N*-acyloxy-*N*-alkoxyamides. For these, anomeric weakening of the $N-O$Acyl bonds is evident from their crystallographic structures and theoretical properties, and in polar solvents this results in the S_N1 and S_N2 reactions outlined above (Section III.C.1 and Section III.C.3). However, in non-polar solvents homolytic cleavage or rearrangements are a further manifestation of anomeric substitution. *N*-Acyloxy-*N*-alkoxyamides undergo both homolytic and rearrangement reactions in parallel at around 100 °C with E_A values in the range of 26–30 kcal mol^{-1} and small negative $\Delta S^{\ddagger}$ (1.6 to −9.0 cal K^{-1} mol^{-1}).

a. Free radical reactivity. A number of *N*-acyloxy-*N*-alkoxybenzamides (**163a–h**) have been shown to decompose in mesitylene or toluene at temperatures above 100 °C giving a complex mixture of products including the corresponding anhydride (**169**) and alkyl ester (**170**) and two significant additional radical reaction products, which were characterized as the 1,4,2-dioxazoline (**167**) and the *N*-alkyl adduct (**168**) (Scheme 27).

Yields of products are extremely variable and highly dependent upon reaction conditions (temperature, concentration, presence or absence of oxygen) and the nature of the side chains.

The radical-derived products, **167** and **168**, may be attributed to the persistence of alkoxyamidyl radicals. These are isoelectronic with nitroxyl radicals, having significant delocalization onto oxygen and hence thermodynamic stability. The ESR hyperfine coupling constant to nitrogen in amidyls (A_N) is typically 1.48 mT while that of *N*-alkoxyamidyls is 1.04 mT, indicating a significant delocalization away from the nitrogen atom[123–125, 127–129]. Unlike electrophilic amidyl radicals, which add to alkenes and arenes, alkoxyamidyls are more nucleophilic and persistent[127]. Sodiated alkoxyamidyls have been detected in the gas phase in ESI-tandem mass spectrometric studies on *N*-acyloxy-*N*-alkoxyamides[13, 87]. Their lifetimes in solution appear to enable very efficient capture of reactive free radicals formed in their presence in solvent cage reactions. Formation of both adduct (**168**) and heterocycle (**167**) can be ascribed to homolysis (Scheme 27, pathway (i)). Decarboxylation of acyloxyl radical gives radicals, $R^{2\bullet}$, which combine with the persistent free radical (**164**) giving **168**. Formation of the dioxazoline (**167**) requires hydrogen abstraction from the persistent radical (**164**) by either the acyloxyl (**165**) or alkyl radical $R^{2\bullet}$. Cyclization with **163a** and its analogue with deuterium replacing hydrogens α to the butoxyl oxygen gave a primary kinetic isotope effect of *ca* 3[204]. B3LYP/6-31G* calculations predict that the diradicals (**166**) reside in a strongly dipolar singlet state, which accounts for their cyclization to the dioxazoline[13].

Both radical reaction products are believed to be solvent cage reactions for the following reasons:

(1) Adduct and dioxazoline formation were not suppressed in the decomposition of the heptanoyloxyl derivative **163c** in the presence of tributyltin hydride.
(2) The sole adduct formed from thermolysis of **163e** was *N*-butoxy-*N*-(hex-5-en-1-yl)benzamide (**168e**) rather than the methylcyclopentyl isomer. The rate constant for trapping must at least exceed that for ring closure of hexenyl at these temperatures (*ca* 5×10^6 s^{-1})[205].
(3) While decarboxylation of alkyl acyloxyls is normally around the rate of diffusion from the solvent cage (typically $> 1 \times 10^9$ l mol^{-1} s^{-1} [206]), adduct **168b** was formed without a trace of propylbenzene in toluene.

The last point also favours acyloxyl radical as the abstracting radical $X^{\bullet}$ in pathway (i).

The persistence of alkoxamidyls (**164**) probably facilitates rebound capture of acyloxyl radicals in competition with their decarboxylation and hydrogen abstraction reactions.

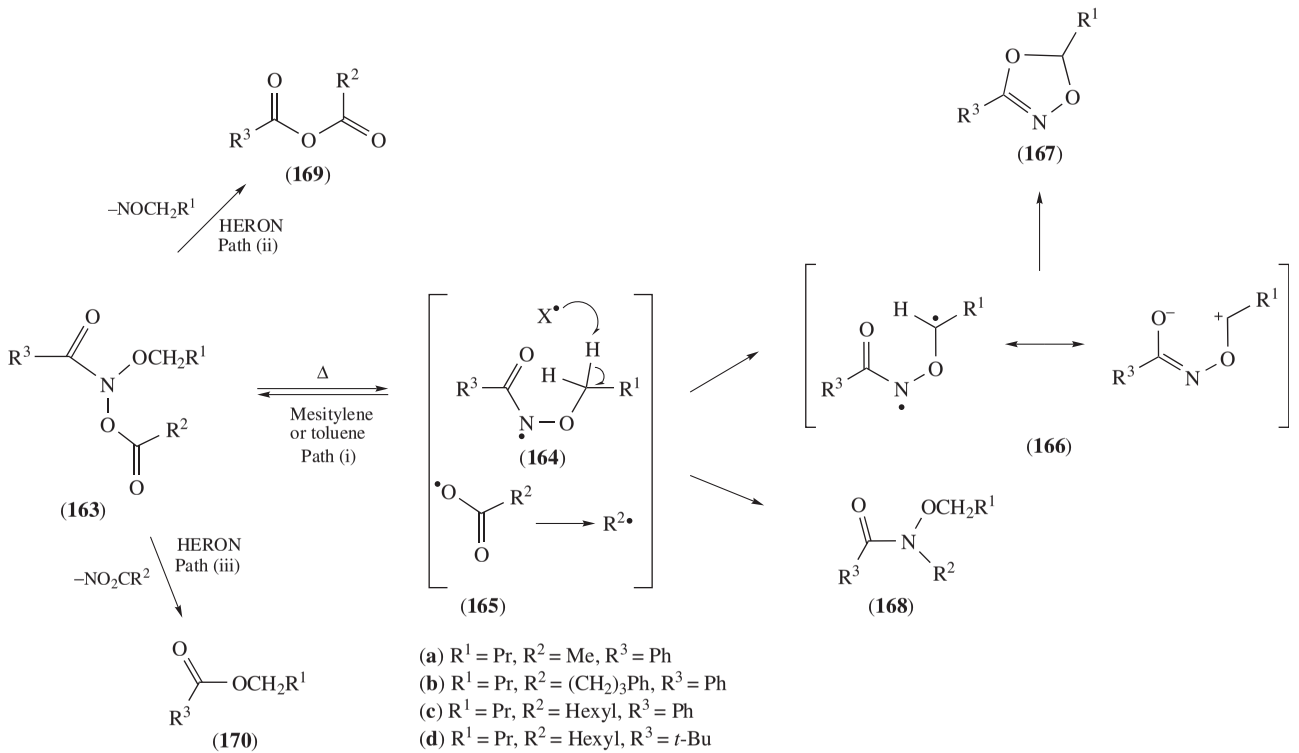

(**a**) R^1 = Pr, R^2 = Me, R^3 = Ph
(**b**) R^1 = Pr, R^2 = $(CH_2)_3$Ph, R^3 = Ph
(**c**) R^1 = Pr, R^2 = Hexyl, R^3 = Ph
(**d**) R^1 = Pr, R^2 = Hexyl, R^3 = *t*-Bu
(**e**) R^1 = Pr, R^2 = 5-Hexen-1-yl, R^3 = Ph
(**f**) R^1 = Pr, R^2 = R^3= Ph
(**g**) R^1 = 4-ClC_6H_4, R^2 = Me, R^3 = Ph
(**h**) R^1 = 4-ClC_6H_4, R^2 = Me, R^3 = *t*-Bu

SCHEME 27

b. Rearrangement reactions. Along with radical-derived products, the major products from thermolysis of *N*-acyloxy-*N*-alkoxyamides at around 100 °C are anhydrides (**169**) and esters (**170**). Anhydrides, which were formed preferentially, are almost certainly the consequence of HERON reactions (Scheme 27, pathway (ii)). Esters might also be formed by the alternative HERON process (Scheme 27, pathway (iii)).

HERON reactions of *N*-acyloxy-*N*-alkoxyamides in non-polar media would be expected to favour migration of acyloxyl groups since anomeric effects are strongest in this direction (Figure 15, Section IV.B.1).

B3LYP/6-31G* calculations on *N*-formyloxy-*N*-methoxyformamide (**91**), in the gas phase, predicted migration of formyloxyl group to give formic anhydride (**171**) and methoxynitrene (**172**) (equation 20) to be favoured over migration of the methoxyl group giving methyl formate (**173**) and formyloxynitrene (**174**) (equation 21) by about 4 kcal mol^{-1}. However, activation energies (39 and 43 kcal mol^{-1}, respectively) were large and these reactions are unlikely to compete with heterolysis of the *N*—*O*Acyl bond in polar solvents[13,87]. An earlier AM1 study on *N*-acetoxy-*N*-methoxyacetamide gave similar results[88].

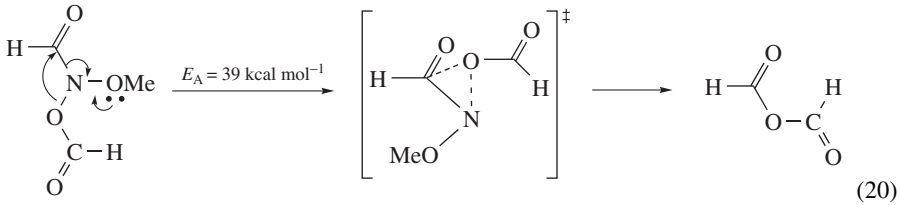

(**91**) (**171**) + (**172**) (20)

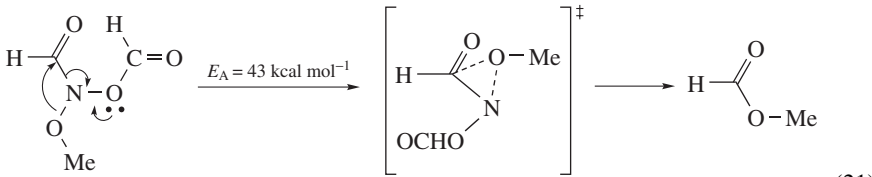

(**91**) (**173**) + (**174**) (21)

Other products of these rearrangements would be alkoxy- and acyloxynitrenes. In the decomposition of **163g**, which afforded acetic benzoic anhydride (**175**) as the major product, a significant component of the reaction mixture was 4-chlorobenzonitrile (**176**), the formation of which can be rationalized according to Scheme 28.

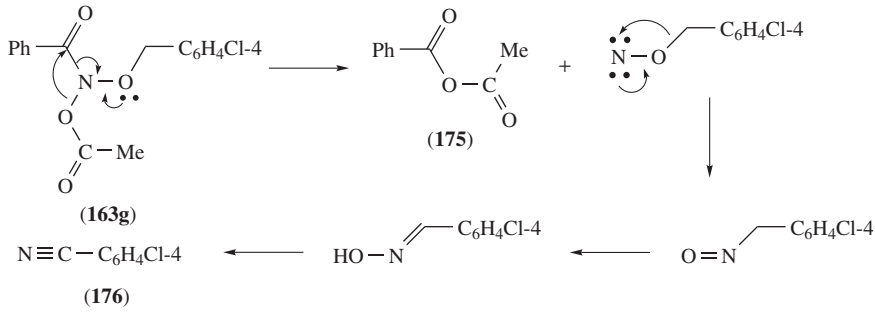

SCHEME 28

Evidence for HERON reactions of *N*-acyloxy-*N*-alkoxyamides in the gas phase was also obtained from ESI-tandem mass spectrometric studies on a number of *N*-acyloxy-*N*-alkoxyamides[87]. Under these conditions, free from solvent, the sodiated parent ion (**177**) can be detected, which fragments under collision-induced dissociative conditions into three sodiated product ions (Scheme 29). These products exhibited masses corresponding to the sodiated *N*-alkoxyamidyl radical (**178**), which in most cases was the major pathway (Scheme 29, pathway (i)). The second most intense product ion was the sodiated anhydride (**180**) formed through HERON rearrangement of the acyl group (Scheme 29, pathway (ii)). The ester (**182**) that would be formed through an alternative HERON migration of the alkoxyl group (Scheme 29, pathway (iii)) was a weak product ion in all cases where it was present, and absent in the fragmentations of all aliphatic amides. The fragments from these reaction processes are presumed to be acyloxyl radical (**179**), alkoxynitrene (**181**) and acyloxynitrene (**183**).

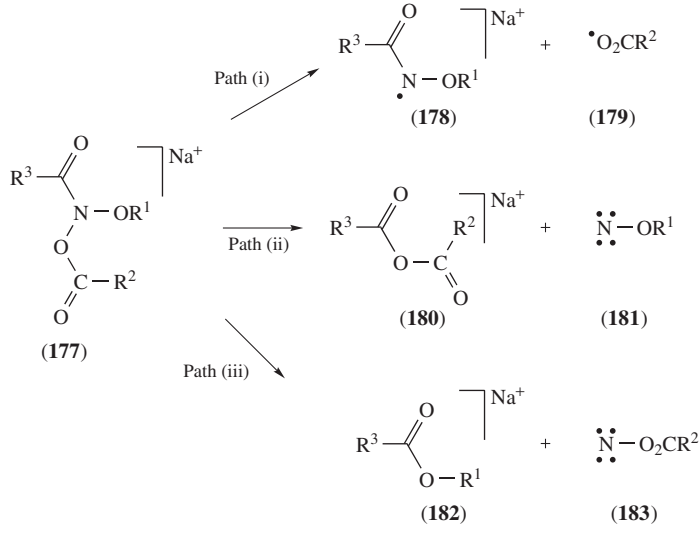

SCHEME 29

Clearly the ESI-MS-MS data reflect the expected migration tendencies of acyloxyl versus alkoxyl moieties in these substrates.

6. Reactions with DNA

N-Acyloxy-*N*-alkoxyamides are direct-acting mutagens as a consequence of their electrophilicity towards DNA. Mutagenic activity required the presence, at nitrogen, of both an acyloxyl and an alkoxyl substituent[98, 113].

Although they have been shown to generate highly reactive alkoxynitrenium ions under appropriate acid-catalytic conditions (see Section IV.C.1), these would not be expected to form at physiological pH and would be expected to react rapidly with water in a cellular environment.

In vitro studies with plasmid DNA showed that *N*-acyloxy-*N*-alkoxyamides react at G-N7 in what is most probably an S_N2 reaction within the major groove of DNA[98, 113]. However, mutagenic activity is negatively correlated with both S_N1 and S_N2 reactivity trends and their mutagenic capability appears to be dependent upon their survival in cellular environment. Hydrophobic binding to DNA is the major factor governing activity, and steric effects also play a role and can influence access to the major groove or reactivity once located there[13, 96, 99, 149].

A quantitative structure–activity relationship (QSAR) has been developed for a wide range of *N*-acyloxy-*N*-alkoxyamides that accurately predicts mutagenic activity in *S. typhimurium* TA100, and which incorporates hydrophobic, reactivity and steric dependencies[13, 149]. From equation 22 mutagenic activity (log of induced revertants at 1 μmol/plate) is correlated positively to hydrophobicity through the log P term, with stability through the positive dependence upon pK_A of the carboxylic acid of the leaving group, and negatively with the size of *para* substituents on a benzamide, benzyloxyl or benzoyloxyl side chain through respective Taft steric parameters, E_s^1, E_s^2 and E_s^3.

$$\begin{aligned}\text{Log TA100} = {} & 0.29(\pm 0.03)\log P + 0.21(\pm 0.09)pK_A + 0.15(\pm 0.04)E_s^1 \\ & + 0.16(\pm 0.04)E_s^2 + 0.11(\pm 0.05)E_s^3 + 0.86(\pm 0.46) \\ & (n = 43, r = 0.897, s = 0.16, F = 30.3) \end{aligned} \quad (22)$$

The QSAR has been used to demonstrate how S_N2 reactivity of *N*-acyloxy-*N*-alkoxyamides with DNA is critical in controlling their mutagenic activity. A range of mutagens with increasing branching α to the amide carbonyl (**144**, R^3 = Me, Et, *i*-Bu, *t*-Bu, 1-Ad and Neopentyl) and which, as a consequence of branching, resist S_N2 reactions with *N*-methylaniline at nitrogen, had mutagenic activities significantly below their activity predicted by equation 22[13, 99].

Thus, *N*-acyloxyl-*N*-alkoxyl substitution in these anomeric amides significantly impacts upon their biological activity in two ways: Inversely by affecting the ease of their nucleophilic reactivity towards intracellular bionucleophiles and hence their intracellular survival, and directly by controlling their ability to undergo S_N2 reactions once ultimately bound in the major groove of DNA.

V. *N,N*-DIALKOXYAMIDES

N,*N*-Dialkoxyamides (**1c**) are the least studied class of stable *N*-heteroatom-substituted hydroxamic esters. The combined electronegativity of two alkoxyl oxygen atoms is less than that of acyloxyl and alkoxyl oxygen in *N*-acyloxy compounds but properties are largely typical of anomeric amides. There is good spectroscopic evidence that the nitrogen

in *N*,*N*-dialkoxyamides is pyramidal and the X-ray structure of a related *N*,*N*-dimethoxyurea supports this. However, the reactivity patterns of *N*,*N*-dialkoxyamides are different from those of *N*-acyloxy-*N*-alkoxyamides in that the nitrogen does not bear an anomerically destabilized leaving group. This section deals with the synthesis, structure and reactivity of *N*,*N*-dialkoxyamides and their carbamate and urea analogues.

A. Synthesis of *N*,*N*-Dialkoxyamides

The limited number of compounds in this class have mostly been made by alcohol exchange of a better leaving group at anomeric hydroxamic esters.

A number of dialkoxyarylamides (**12**) have been formed by alcoholysis of the corresponding *N*-alkoxy-*N*-chloro precursors according to equation 3 (Section III.C.2). S_N1 solvolysis in aqueous alcohol mixtures afforded symmetrical as well as mixed *N*,*N*-dialkoxyamides in modest yields[62,64]. Rudchenko and coworkers made the analogous *N*,*N*-dialkoxy-*N*′,*N*′-dialkylureas (**124a**) by the S_N2 displacement of chlorine with alkoxides in alcohol[66] (equation 10, Section III.C.4).

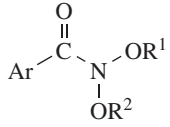

(**12**)

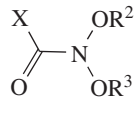

(**124**)

(**a**) X = NR_2
(**b**) X = OR

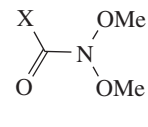

(**184**)

(**a**) X = H
(**b**) X = NH_2

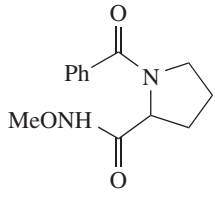

(**185**)

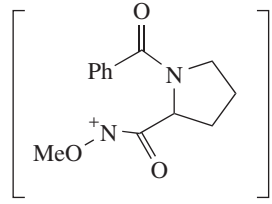

(**186**)

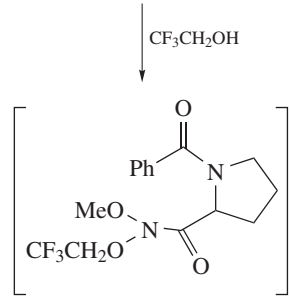

(**187**)

(23)

As described in Section IV.C.2, Shtamburg and coworkers found that *N*-acyloxy-*N*-alkoxyureas and -carbamates undergo alcoholysis in neat alcohol (methanol, ethanol, propanol) to give mixed and symmetrical *N*,*N*-dialkoxyureas (**124a**) and *N*,*N*-dialkoxycarbamates (**124b**)[68] (equation 14). The reactions are slow, ranging from several days to weeks, particularly where branched alcohols are used, but generally result in high yields. *tert*-Butanol was unreactive.

Oxidation of hydroxamic esters in an alcoholic solvent may prove to be useful in certain cases. Phenyliodine(III)bis(trifluoroacetate) (PIFA) oxidation of the proline derivative (**185**) in trifluoroethanol afforded a 26% yield of the *N*-methoxy-*N*-trifluoroethoxy derivative (**187**), presumably via an intermediate *N*-methoxy-*N*-acylnitrenium ion (**186**) (equation 23)[143].

Dialkoxyamines, though less nucleophilic than their dialkylamine counterparts, react with acyl chlorides to yield *N*,*N*-dialkoxyamides directly[74, 207]. For example, with 4-nitrobenzoyl chloride (**189**), dimethoxyamine (**188**) was converted to *N*,*N*-dimethoxy-4-nitrobenzamide (**190**) in 55% yield (equation 24).

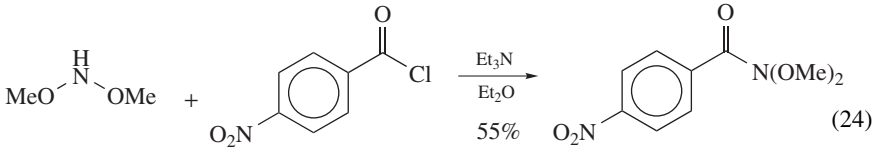

(**188**) (**189**) (**190**) (24)

B. Properties of *N,N*-Dialkoxyamides

In these systems, the nitrogen is expected to be strongly pyramidal with attendant $N-C(O)$ bond lengthening. Anomeric effects at nitrogen should operate; an oxygen p-type lone pair of one oxygen, n_O, can interact with a σ^*_{NO} orbital involving the second oxygen. Orbital overlap is optimal since both oxygen and nitrogen have similar sized p-orbitals, but the higher σ^*_{NO} energy and lower electron affinity of the alkoxyl group results in a weaker anomeric interaction than is the case for the *N*-alkoxy-*N*-chloroamides (Section III.B) or *N*-acyloxy-*N*-alkoxyamides (Section IV.B).

1. Structural properties

Evidence for pyramidality at nitrogen and anomeric effects in *N*,*N*-dialkoxyamides has been obtained from computational chemistry and is supported by X-ray data for a urea analogue.

B3LYP/6-31G* calculations on *N*,*N*-dimethoxyformamide (**184a**) have identified the lowest energy conformer as that in Figure 21a[10]. The geometry is characterized by a pyramidal nitrogen atom (average angle at nitrogen is 114.6°) and one anomeric interaction in which the $O_{(1)}-Me$ bond *anti* to the carbonyl is nearly orthogonal to the vicinal $N-O_{(2)}$ bond (Figure 21b). The methyl group *syn* to the carbonyl is *endo* to the nitrogen pyramid and steric effects preclude a mutual anomeric interaction. The $N-C(O)$ bond (1.396 Å) is significantly lengthened relative to formamide (1.362 Å) and *N*-methoxyformamide (1.380 Å) computed at the same level[10]. The best estimate for the amide isomerization barrier was around 7 kcal mol^{-1} while the nitrogen inversion barrier was once again predicted to be only around 2.5 kcal mol^{-1}. These characteristics are typical of other anomeric hydroxamic esters reviewed in this chapter.

Shtamburg and coworkers have recently reported X-ray data for *N*,*N*-dimethoxyurea (**184b**, Figure 22, Table 10)[159]. In this compound nitrogen is strongly pyramidal with

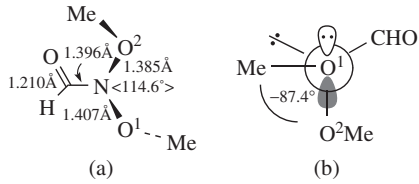

FIGURE 21. (a) B3LYP/6-31G* lowest energy conformation of *N*,*N*-dimethoxyformamide (**184a**); (b) Newman projection along the $O_{(1)}-N$ bond

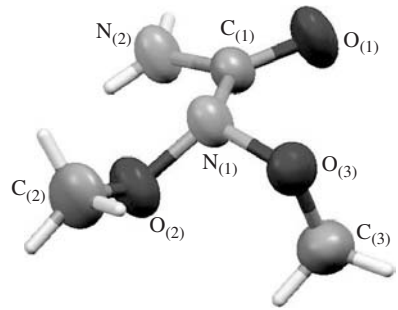

FIGURE 22. X-ray structure of *N*,*N*-dimethoxyurea (**184b**) with displacement ellipsoids shown at the 50% level. Bond lengths and angles are given in Table 10

TABLE 10. Selected structural properties of *N*,*N*-dimethoxyurea (**184b**)

Parameter	
$r_{C(1)O(1)}$ (Å)	1.220
$r_{C(1)N(1)}$ (Å)	1.438
$r_{N(1)O(2)}$ (Å)	1.401
$r_{N(1)O(3)}$ (Å)	1.397
$r_{N(2)C(1)}$ (Å)	1.320
$C_{(1)}-N_{(1)}-O_{(2)}$ (deg)	110.1
$O_{(3)}-N_{(1)}-O_{(2)}$ (deg)	110.3
$O_{(3)}-N_{(1)}-C_{(1)}$ (deg)	111.3
$\langle\beta\rangle$ (deg)[a]	110.6
τ (deg)[b]	0.8
χ_N (deg)[c]	57.4
$C_{(2)}-O_{(2)}-N_{(1)}-O_{(3)}$ (deg)	89.3
$C_{(3)}-O_{(3)}-N_{(1)}-O_{(2)}$ (deg)	55.2

[a] $\langle\beta\rangle = \Sigma(\beta)/3$.
[b] Angle subtended by the axes of the nitrogen lone pair and the carbonyl carbon $2p_z$ orbital.
[c] Amide distortion parameter defined in accordance with Winkler–Dunitz[107, 108].

average angles at nitrogen of 110.6° and Winkler–Dunitz nitrogen distortion of $\chi_N = 57.4°$. The conformation of the methoxyl groups is similar to that predicted for the lowest energy conformation of the corresponding formamide (Figure 21a) but the $C-N$ bond is significantly longer (1.438 Å). This can be accounted for by the competing urea nitrogen, which is sp^2 hybridized and strongly conjugated with the carbonyl ($C-N$ bond length of 1.32 Å). Respective $N-O$ bond lengths are similar (1.397 and 1.401 Å) and close to predicted values for the formamide (**184a**) (1.385 and 1.407 Å). The *N*,*N*-dimethoxyurea has a similar conformation to the corresponding *N*-acetoxy compound (Figure 17b). There is one strong anomeric interaction from the *anti*-oxygen, $O_{(2)}$, into the $N_{(1)}-O_{(3)}$ bond (the $C_{(2)}-O_{(2)}-N_{(1)}-O_{(3)}$ dihedral angle is almost 90° while the $C_{(3)}-O_{(3)}-N_{(1)}-O_{(2)}$ angle is only 55°).

Thus the experimental properties of the urea (**184b**) mirror remarkably well the theoretical properties of *N*,*N*-dimethoxyformamide.

2. Spectroscopic properties

The IR carbonyl stretch frequencies for a number of simple *N*,*N*-dialkoxyamides, -ureas and -carbamates are presented in Table 11 and reflect an increase of between 20 and 30 cm^{-1} relative to the hydroxamic esters from which they were derived. In confirmation of theoretical studies, $N-C(O)$ double-bond character is considerably less than in the hydroxamic esters, although the carbonyl stretch frequencies are not as

TABLE 11. IR carbonyl absorption frequencies for *N*,*N*-dialkoxyamides[a] [63,64], ureas[b] and carbamates[c] [68,100,116] ($R^1ON(OR^2)COR^3$) and their precursor hydroxamic esters ($R^1ONHCOR^3$)

R^1	R^2	R^3	Amide ν (cm^{-1})	Hydroxamic ester ν (cm^{-1})
Me	Me	Ph	1711	1683
Me	Me	4-MeC_6H_4	1710	1685
Me	Me	4-$MeOC_6H_4$	1705	1687
Me	Me	4-ClC_6H_4	1712	1687
n-Pr	Me	Ph	1713	1678
i-Bu	Me	Ph	1714	1684
Et	Me	Ph	1712	1679
Et	Et	Ph	1712	1679
n-Pr	Et	Ph	1711	1678
i-Bu	Et	Ph	1715	1684
Bu	Bu	Ph	1710	1654
Me	Me	NH_2	1720	1685
Et	Me	NH_2	1742	1680
n-Bu	Me	NH_2	1740	1680
i-Pent	Me	NH_2	1740	—
Benzyl	Me	NH_2	1725	1645
n-Octyl	Me	NH_2	1728	1680
n-Dodecyl	Me	NH_2	1728	1680
n-Pr	Me	NMe_2	1735	1695
Et	Me	NHBenzyl	1735	1685
Me	*n*-Bu	OMe	1780	1765
Et	Et	OMe	1780	1740
i-Bu	Me	OMe	1770	1745
n-Octyl	Me	OMe	1780	—

[a] Solution ($CHCl_3$).
[b] KBr disc or nujol.
[c] Nujol or neat.

high as in the corresponding *N*-alkoxy-*N*-chloroamides or *N*-acyloxy-*N*-alkoxyamides. Condensed-phase IR carbonyl stretch frequencies for *N*,*N*-dialkoxyureas and *N*,*N*-dialkoxycarbamates mirror the amide properties.

In the limited cases studied, no barrier to amide isomerization could be determined by ^{1}H NMR studies. In methanol-d_4, the methoxy methyl groups in *N*,*N*-dimethoxy-4-toluamide (**191**) resonated together as a sharp singlet down to −90 °C[50]. The benzylic protons of *N*-benzyloxy-*N*-methoxybenzamide (**192**) also remained isochronous down to the same temperature, putting an upper limit of about 8 kcal mol^{-1} on the free-energy barrier for any isomerization process. The barriers to inversion in some *N*,*N*-dialkoxy-*N*′,*N*′-dimethylureas (**193a–c**) have been measured in toluene-d_8 at between 10 and 13 kcal mol^{-1} [74]. These are much lower than those found for the configurationally stable acyclic dialkoxyamines ($\Delta G^{\ddagger}$ 20–23 kcal mol^{-1} [74]) and point to the significant role that an α-carbonyl group plays in stabilizing the inversion transition state. The fact that the ureas have a higher inversion barrier than that predicted for *N*,*N*-dialkoxyamides, which could not be observed, is in accord with the weaker electron demand of the α-aminocarbonyl substituent; in *N*,*N*-dialkoxy-*N*′,*N*′-dimethylureas, the amide isomerization barrier for rotation about the *CO*−*NMe*$_2$ bond has been measured at 13.3–14.5 kcal mol^{-1} [74], indicating a significant degree of delocalization of the adjacent nitrogen lone pair into the carbonyl. Conjugative stabilization of the planar transition state for inversion at the dialkoxyamine nitrogen should thus be reduced in ureas, leading to higher inversion barriers than those in the dialkoxyamides.

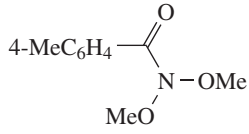

(**191**)

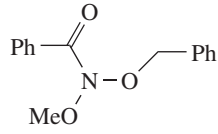

(**192**)

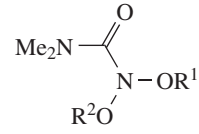

(**193**)

(**a**) R^1 = *i*-Bu, R^2 = CF_3CH_2
(**b**) R^1 = CH_2=$CHCH_2$, R^2 = CF_3CH_2
(**c**) R^1 = PhCH(Me)NHCOCMe$_2$, R^2 = Et

C. Reactions of *N*,*N*-Dialkoxyamides

1. Free radical decomposition reactions

The reactions of a limited number of *N*,*N*-dialkoxyamides have been investigated[50,63]. While they are relatively stable at RT, at temperatures above 100 °C in mesitylene, *N*,*N*-dimethoxy-4-substituted benzamides (**194**) have been found to undergo unimolecular decomposition giving parent hydroxamic ester (**195**), methyl esters (**196**) and *N*-methoxy-*N*-(3,5-dimethylbenzyl)benzamides (**197**) (equation 25).

In the presence of the hydrogen donor tri-*N*-butyltin hydride, only hydroxamic ester **195** is formed and the reaction is presumed to involve *N*−*O* bond homolysis to give the resonance-stabilized *N*-alkoxyamidyl radicals (**198**), which in the presence of Bu_3SnH are reduced to hydroxamic ester according to Scheme 30. In the absence of Bu_3SnH hydride, formation of esters probably involves alkoxyamidyl dimerization to hydrazines (**199**) as intermediates (see Section VI.C, Scheme 34), although HERON reactions of **194** with production of methoxynitrene cannot be discounted. Mesityl radicals, formed by the

abstraction of hydrogen from the solvent, are trapped by the persistent alkoxyamidyl radical giving **197**. Homolytic rather than heterolytic cleavage of $N-O$ bonds is presumably a direct consequence of the low electron affinity of the alkoxyl group which prevents anomerically assisted elimination of methoxide to give stabilized alkoxynitrenium ions.

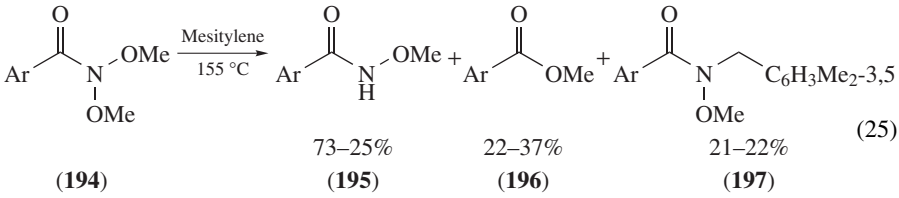

73–25% 22–37% 21–22% (25)

(**194**) (**195**) (**196**) (**197**)

(**a**) Ar = C_6H_5
(**b**) Ar = 4-ClC_6H_4
(**c**) Ar = 4-MeC_6H_4
(**d**) Ar = 4-$MeOC_6H_4$

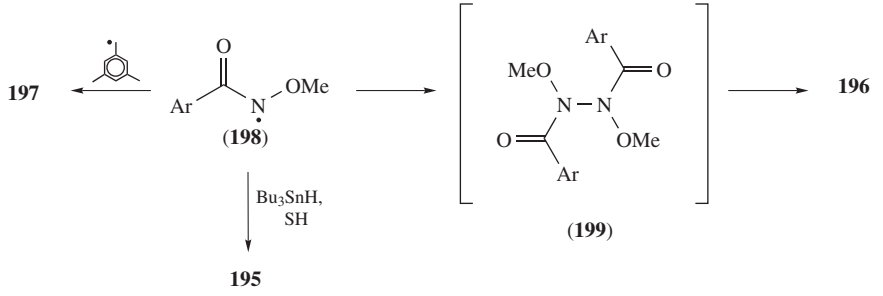

SCHEME 30

Table 12 gives Arrhenius activation parameters and rate constants for thermal decomposition of *N*,*N*-dimethoxybenzamides **194a–d**. $\Delta S^{\ddagger}$ values are low when compared to homolysis of diacyl peroxides and peroxides, for which values are typically around 8–11 cal K^{-1} mol^{-1} [208]. This has been attributed to significant π stabilization and restricted rotation in the alkoxyamidyl radical intermediates (**198**)[50]. Similar E_A and $\Delta S^{\ddagger}$ values were obtained for the thermal decomposition of *N*-acyloxy-*N*-alkoxyamides though those reactions involved both homolysis and rearrangements (Section IV.C.5)[13].

2. Alcohol exchange reactions

The reactions of *N*,*N*-dialkoxyamides with electrophiles or Lewis acids have not been investigated, although Rudchenko reported that the analogous ureas (**200**) undergo facile

TABLE 12. Arrhenius parameters and rate constants at 373 K for radical decomposition of *N*,*N*-dimethoxy-4-substituted benzamides (**194a–d**)[50]

X	E_A (kcal mol^{-1})	$\Delta S^{\ddagger}$ (cal K^{-1} mol^{-1})	$10^6 k^{373}$ (l mol^{-1} s^{-1})
H	29.9	−5.6	0.69
Cl	30.2	−4.1	4.24
Me	31.6	−1.6	2.12
MeO	32.1	−0.3	2.24

alcohol exchange in the presence of acids (R^2OH/TsOH or R^2OH/H^+) giving mixed and cyclic *N*,*N*-dialkoxyureas (**201**) (equation 26)[74].

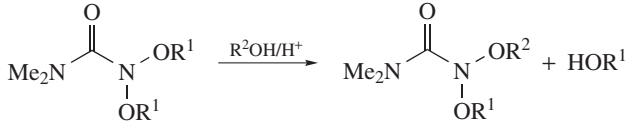

(**200**) (**201**) (26)

N,*N*-Dialkoxyureas (**200**) can also be cleaved by acetyl chloride to regenerate *N*-chloro-*N*-methoxy ureas (**202**) according to equation 27[74].

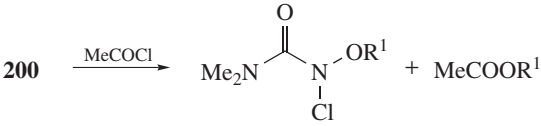

(**202**) (27)

3. Reaction at the amide carbonyl

Solvolysis of urea analogues (**200**) in aqueous KOH leads to hydrolysis of the amide rather than substitution at nitrogen, in keeping with the poor leaving capacity of alkoxide (equation 28). This reaction is an excellent source of *N*,*N*-dialkoxyamines (**203**), a relatively little known class of compounds[209].

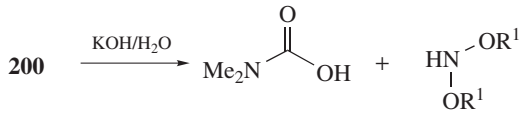

(**203**) (28)

Finally, the formation of methyl ketones (**205**) by displacement of *N*,*N*-dimethoxyamine from *N*,*N*-dimethoxyamides (**204**) using methyl lanthanum(III) triflate has been reported. However, under the reaction conditions employed, further alkylation occurs to give the alcohols (**206**) (equation 29)[210].

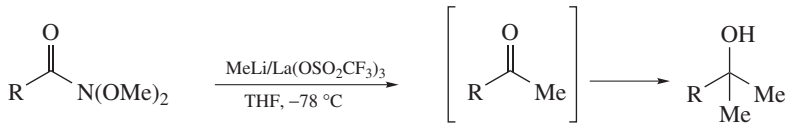

(**204**) R = Ph, (*E*)-MeCH=CH (**205**) (**206**) (29)

VI. *N*-ALKOXY-*N*-AMINOAMIDES

Amides bearing both an alkoxyl and an amino substituent at nitrogen (**207**) exhibit all the properties of anomeric amides. The electronegativities of nitrogen and oxygen combine to rehybridize the amide nitrogen from sp^2 to sp^3 with the attendant changes in amide properties. Although an alkoxyl oxygen possesses lower electron affinity than acyloxyl

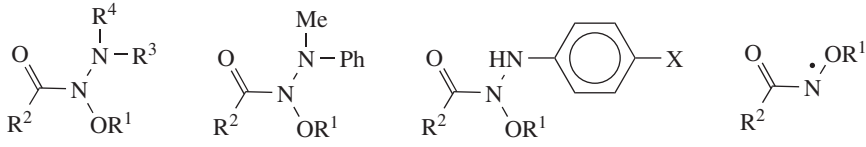

(**207**) (**208**) (**209**) (**210**)

(**a**) $R^1 = R^2 = Me$, $R^3 = R^4 = Ac$
(**b**) $R^1 = R^2 = Me$, $R^3R^4 =$ Succinyl
(**c**) $R^1 = R^2 = Me$, $R^3 = Ac$, $R^4 = OMe$

oxygen, the high-energy lone pair on the amino substituent results in pronounced anomeric effects in such amides. Properties have been investigated theoretically, by X-ray analysis and spectroscopically, and studies of their reactivity led to the discovery of the first HERON reaction of anomeric amides[114].

A. Synthesis of *N*-Alkoxy-*N*-aminoamides

A limited range of stable anomeric *N*-alkoxy-*N*-aminoamides is known. They have been implicated as reactive intermediates in the reaction of *N*-acyloxy-*N*-alkoxyamides and anilines (Section IV.C.3.a, Scheme 23). However, though *N*-alkoxy-*N*-(*N*′-methylanilino)amides (**208**) or *para*-substituted anilino analogues (**209**) are formed initially in those reactions, their susceptibility to HERON reactions makes them too short-lived to be detected at room temperature[13,89,90,99,114]. The HERON reaction has been studied both experimentally and theoretically (see Section VI.C) and the results of early modelling at the AM1 level of theory predicted that *N*-diacetylamino (**207a**), *N*-succinimido (**207b**) and *N*-(*N*′-acetyl-*N*′-methoxyamino) substitution (**207c**) would significantly raise the E_A for HERON reactions of *N*-alkoxy-*N*-aminoamides[88]. *N*,*N*′-Diacyl-*N*,*N*′-dialkoxyhydrazines (**212**) are, indeed, significantly more stable at room temperature and they have been isolated from oxidative dimerization of hydroxamic esters (**211**) using a range of metals[70,72,73,211], benzoyl peroxide[70] and persulfate[128] or from photolysis of *N*-alkoxy-*N*-halo- or *N*-nitroso amides (**213**)[51,70,123] (Scheme 31). Both methods probably involve formation and combination of alkoxyamidyls (**210**) although heterolytic displacement of metals or halogen by hydroxamic esters have been invoked in some cases[51,70,211].

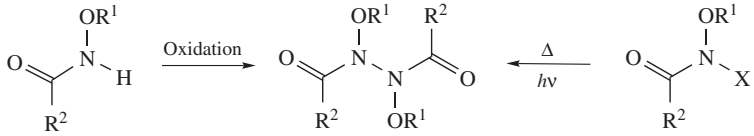

R^1 = Alkyl, R^2 = alkyl, aryl X = Cl, Br, I, NO

(**211**) (**212**) (**213**)

SCHEME 31

Oxidations of the hydroxamic esters have been carried out in good yields using lead tetraacetate[63,70,73,211,212], ammonium hexachloroplumbate(IV), peroxides and silver oxide[70]. Cooley and coworkers reported that only *N*,*N*′-diacyl-*N*,*N*′-dialkoxyhydrazines

with alkylamide groups could be isolated in benzene[70] although Norman's group successfully synthesized *N*,*N*′-dibenzoyl-*N*,*N*′-dibenzyloxyhydrazine in dichoromethane[211]. Barton and coworkers found that the hydrazines were formed in excellent yields at low temperatures using ceric ammonium nitrate (CAN) or nickel peroxide ($NiO_2 . H_2O$) in anhydrous THF. This method permitted formation of hydrazines bearing both aryl as well as bulky alkyl or acyl substituents, although the latter were measurably less stable[72].

Dimerization of alkoxyamidyls formed by thermolysis of *N*-alkoxy-*N*-nitrosoamides[129], *N*-alkoxy-*N*-bromo- or *N*-iodoamides[51] or photolysis of *N*-alkoxy-*N*-chloroamides[51, 123] has been reported, but yields of the hydrazines were lower and esters were secondary products (Scheme 31).

Crawford and Raap generated *N*,*N*′-dicarboalkoxy-*N*,*N*′-dialkoxyhydrazines (**212**, R^2 = alkoxyl) in good yields using Ag_2O in diethyl ether[213]. *N*,*N*′-Dicarbomethoxy-*N*,*N*′-dimethoxyhydrazine was also prepared by oxidation of the *N*-chloro-*N*-methoxyurethane (**213**, X = Cl, R^1 = Me, R^2 = MeO) with triethylamine in methanol[69].

N-Alkoxy-*N*-chloro-*N*′,*N*′-dialkylureas also react with dialkylamines, but the product *N*-dialkylamino-*N*-alkoxyureas (**207**, $R^2 = NR_2$, $R^3 = R^4$ = alkyl) are unstable under the acidic reaction conditions[65].

B. Properties of *N*-Alkoxy-*N*-aminoamides

1. Structural properties

In *N*-alkoxy-*N*-aminoamides, also termed HERON amides, since *NNO* systems were the first anomeric amides found to undergo the *N*-to-*CO* rearrangement of the alkoxyl group (although the HERON reaction has subsequently been found to be a general pathway for anomeric amides), anomeric overlap is facilitated by both the electronegativity of oxygen, the similarity in sizes of the interacting orbitals and, most importantly, the high-energy lone pair on nitrogen. With the exception of charged heteroatoms (see Section IV.C.3.c), in the context of anomeric interactions in bisheteroatom-substituted amides, the nitrogen lone pair is the highest in energy along the second row and should interact strongly with $N-O$ σ^* orbitals in these systems.

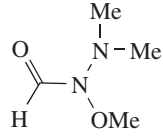

(**214**)

The stereoisomerism in the model HERON amide, *N*-methoxy-*N*-dimethylaminoformamide (**214**), has been studied in detail at the B3LYP/6-31G* level[214]. At the global minimum the oxygens are *syn* and the amide nitrogen deviates significantly from planarity with an average angle at nitrogen of 116° (Figure 23a), which results in a long $N-C(O)$ bond (1.387 Å) when compared to formamide (computed 1.362 Å[3, 10], experimental 1.352 Å, although slightly longer bond lengths of 1.360 Å and 1.376 Å have been reported[4, 14, 182, 215]). The computed E/Z amide rotational barrier of 12.6 kcal mol^{-1} was significantly smaller than that found in amides or hydroxamic esters (16.7–21.5 kcal mol^{-1} [1, 4–12, 105, 106]). Carbonyl stretch frequencies of *NNO* anomeric amides are therefore predicted to be higher than those of normal amides.

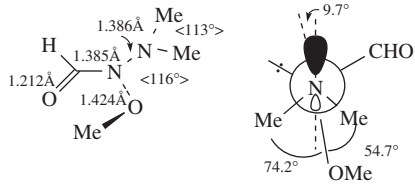

(**a**) (**b**)

FIGURE 23. (a) B3LYP/6-31G* optimized conformation for *N*-methoxy-*N*-dimethylaminoformamide (**214**); (b) Newman projection along the $N-N$ bond

The inversion at the amide nitrogen of **214** could not be computed but, like other anomeric amides reviewed in this chapter, was expected to be very low[10,214].

The lowest energy conformation illustrated in Figure 23b was favourable for an $n_N-\sigma^*_{NO}$ orbital overlap resulting in a long $N-O$ bond (1.424 Å) when compared to the $N-O$ bond in hydroxylamine (predicted to be only 1.399 Å at the HF/6-31G* level). The $N-N$ bond (1.386 Å) was correspondingly much shorter relative to hydrazine (experimental value 1.45 Å[216]) and the anomeric interaction resulted in a significant barrier of some 14.3 kcal mol^{-1} to rotation about the $N-N$ bond. An AM1 semiempirical study on a wide range of *N*-amino-*N*-methoxyacetamides predicted that the anomeric interaction was strongest with electron-donating substituents on the amino group and weakest with electron-withdrawing haloalkyl and acyl substituents[88].

The *N*,*N*′-diacyl-*N*,*N*′-dialkoxyhydrazines (**212**) are a special case of the HERON amide (**207**) and their theoretical properties have also been computed[133,212]. They should, to a large extent, exhibit characteristics similar to those predicted for the model *N*-methoxy-*N*-dimethylaminoformamide (**214**) although acyl substitution at both nitrogens must lower the energies of the nitrogen lone pairs.

Conformational analysis indicates that if both nitrogens are pyramidal, these hydrazines can exist in two arrangements about the $N-N$ bond that permit an anomeric overlap. A mutual anomeric interaction is possible in conformation **I** (Figure 24a), while in conformer **II** (Figure 24b), only one anomeric interaction is possible[212]. The second interaction in **II** is minimal on account of the *syn gauche* relationship between the $N_{(2)}$ lone pair and the vicinal $N_{(1)}-OR^1$ bond. In addition, in these systems, the amide groups can also have both *E* and *Z* configurations. Thus conformational analysis yields one anti-symmetrical (*ZE*) and two symmetrical starting conformations (*EE* and *ZZ*) for **I** (Figure 24a) and four anti-symmetrical (*EE*, *ZZ*, *ZE* and *EZ*) starting conformations for **II** (Figure 24b). The first stereochemical designator refers to the amide conformation at $N_{(1)}$ and the second refers to the conformation at $N_{(2)}$.

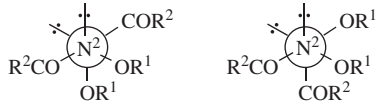

(a) (b)

FIGURE 24. Newman projections ($N_{(2)}$ to $N_{(1)}$) of staggered conformations of *N*,*N*′-diacyl-*N*,*N*′-dialkoxyhydrazines with lone pairs *syn* with (a) mutual $n_N-\sigma^*_{NO}$ anomeric effects and (b) a single $n_N-\sigma^*_{NO}$ anomeric effect

HF/6-31G* *ab initio* calculations on fully relaxed conformations of the model *N*,*N*′-diformyl-*N*,*N*′-dimethoxyhydrazine (**215a**) predicted **II** (*EE*) to be the most stable although **II**(*EZ*), **I**(*EE*) and **I**(*ZE*) were very similar in energy[212]. **I**(*EE*) and **I**(*ZZ*) resulted in symmetrical structures.

Nitrogens were predicted to be pyramidal in all cases and in asymmetrical structures, **I**(*ZE*) and **II**, pyramidality at respective nitrogen atoms differed significantly. $N-O$ bond lengths in those systems are affected by the degree of pyramidality of the nitrogen to which they are attached as well as anomeric effects. While all conformers of **II** must dictate an anomeric effect in one direction, the asymmetrical structure **I**(*ZE*) also showed clear evidence of this, with the $N_{(2)}-O\mathrm{R}^1$ bond (1.379 Å) much longer than $N_{(1)}-O\mathrm{R}^1$ (1.363 Å) and the donor nitrogen $N_{(1)}$ (average angle 116°) much less pyramidal than $N_{(2)}$ (average angle 113.7°). However, $N-N$ bond lengths (1.352–1.363 Å) in both forms **I** and **II** did not differ significantly, which suggests they have a similar degree of anomeric interaction. The dimethylamino nitrogen in **214** is strongly pyramidal (average angle 112.7°), resulting in a longer $N-N$ bond of 1.379 Å in spite of the stronger anomeric overlap that is possible in this system[212].

In the case of the **II**(*ZZ*) and **I**(*ZE*) stereo forms there was a marked difference in the degree of planarity at the nitrogens. In these cases at least, different carbonyl absorptions would be predicted in the IR as the carbonyls had significantly different equilibrium bond lengths. HF/6-31G* calculations on the unsymmetrical model **I**(*ZE*) gives scaled frequencies at 1765 and 1781 cm^{-1} corresponding to uncoupled stretch modes largely associated with different carbonyls. The lower stretch frequency corresponded to the carbonyl attached to the more planar donor nitrogen, which had a shorter $N-C(O)$ bond. However, a frequency calculation on one conformer with similar C=O bond lengths (**II**(*EZ*)) indicated that the carbonyls could be strongly coupled, leading to symmetrical and asymmetrical combination modes with scaled frequencies of 1786 and 1768 cm^{-1}.

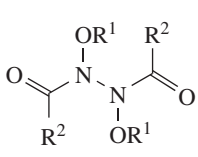

(**215**)

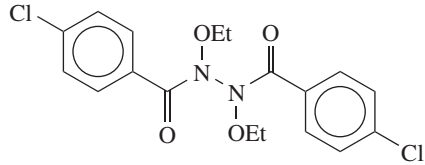

(**216**)

(**a**) R^1 = Me, R^2 = H
(**b**) R^1 = H, R^2 = Me
(**c**) $R^1 = R^2$ = H
(**d**) $R^1 = R^2$ = Me

Density functional calculations on **215b–d** at the B3P86 level have been carried out as part of a detailed study of the HERON reaction of hydrazines (see Section VI.C). These afforded symmetrical *gauche* structures **I**(*EE*) as lowest energy conformers[133]. $N-N$ (1.37 Å), $N-C(O)$ (1.38 Å) and $N-O$ (1.40 Å) bond lengths were similar to those from HF/6-31G* calculations[212].

X-ray data for *N*,*N*′-di(4-chlorobenzoyl)-*N*,*N*′-diethoxyhydrazine (**216**) have been published, which confirms the unsymmetrical nature of this structure (Figure 25, Table 13). The conformation in the solid state is *gauche* **II**(*ZE*) (Figure 24b) and, as predicted on both qualitative and theoretical grounds, both nitrogens are strongly pyramidal with average angles at nitrogen of 114.4 and 113.7°.

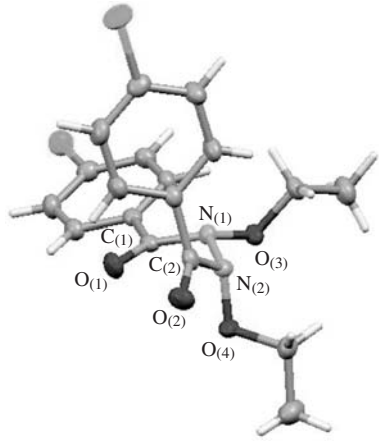

FIGURE 25. X-ray structure of *N*,*N*′-di-(4-chlorobenzoyl)-*N*,*N*′-diethoxyhydrazine (**216**) with thermal ellipsoids depicted at the 50% level. Bond lengths and angles are given in Table 13

TABLE 13. Selected structural properties of *N*,*N*′-di-(4-chlorobenzoyl)-*N*,*N*′-diethoxyhydrazine (**216**)

Parameter	
$r_{C(1)O(1)}$, $r_{C(2)O(2)}$ (Å)	1.213, 1.206
$r_{C(1)N(1)}r_{C(2)N(2)}$ (Å)	1.412. 1.410
$r_{N(1)N(2)}$ (Å)	1.389
$r_{N(1)O(3)}$, $r_{N(2)O(4)}$ (Å)	1.402, 1.412
$C_{(1)}-N_{(1)}-N_{(2)}$, $C_{(2)}-N_{(2)}-N_{(1)}$ (deg)	116.5, 116.7
$C_{(1)}-N_{(1)}-O_{(3)}$, $C_{(2)}-N_{(2)}-O_{(4)}$ (deg)	117.3, 113.2
$O_{(3)}-N_{(1)}-N_{(2)}$, $O_{(4)}-N_{(2)}-N_{(1)}$ (deg)	109.4, 111.2
$\langle\beta\rangle_{N(1)}$, $\langle\beta\rangle_{N(2)}$ (deg) [a]	114.4, 113.7
$\tau_{N(1)}$, $\tau_{N(2)}$ (deg) [b]	−8.5, −11.3
$\chi_{N(1)}$, $\chi_{N(2)}$ (deg) [c]	47.4, 48.9
$O_{(4)}-N_{(2)}-N_{(1)}-O_{(3)}$ (deg)	−66.7
$O_{(4)}-N_{(2)}-N_{(1)}-C_{(1)}$ (deg)	69.4

[a] $\langle\beta\rangle = \Sigma(\beta)/3$.
[b] Angle subtended by the axes of the nitrogen lone pair and the adjacent carbonyl carbon $2p_z$ orbital.
[c] Amide distortion parameters defined in accordance with Winkler–Dunitz[107,108].

There was a clear anomeric interaction in the direction of $N_{(2)}$. The $N_{(2)}-O_{(4)}$ bond nearly bisects the adjacent $C_{(1)}-N_{(1)}-O_{(3)}$ angle with torsion angles of 69.4° and −66.7° to $N_{(1)}-C_{(1)}$ and $N_{(1)}-O_{(3)}$ bonds, respectively, while the $N_{(2)}-O_{(4)}$ bond is 0.01 Å longer than the $N_{(1)}-O_{(3)}$ bond. The carbonyl bond lengths are similar; the $N_{(1)}C=O$ carbonyl [1.213(2) Å] is marginally longer than the $N_{(2)}C=O$ carbonyl [1.207(3) Å]) and the $N-C(O)$ bonds (1.412 and 1.410 Å) are extremely long relative to formamide (1.352 Å)[14,182,215], reflecting the reduced amide resonance. A comparison with the $N-C(O)$ bond lengths of the *N*-acyloxy-*N*-alkoxyamides **95a** and **95b** (Table 4, 1.44 Å) suggests that there is more resonance interaction in the hydrazines, although amide

nitrogens were more pyramidal in the *ONO* systems. The *N*−*N* bond length of hydrazine **216** is 1.389 Å, which, though longer than predicted for model systems **215a**–**d** (1.35–1.37 Å), is still well short of the hydrazine experimental value (1.45 Å)[216].

2. Spectroscopic properties

Analysis of the solution IR data for two series of hydrazines, **217** and **218**, indicates that the carbonyl stretch frequencies are all appreciably higher than for the monoheteroatom-substituted precursor hydroxamic esters, which confirms a significant degree of non-planarity at the nitrogen atoms (Table 14)[50,212]. Limited condensed-phase data from Barton's group demonstrated a similar increase[72]. In series **217** (Table 14, entries 1–5) and **218** (Table 14, entries 6–10) the carbonyl absorptions generally increased in wave number as the aryl substituent was varied from electron donor to electron acceptor, showing remarkable sensitivity to electron demand at amide nitrogen. In addition, IR spectroscopy also supported the unsymmetrical nature of hydrazines. In the solid state, with the exception of **217c**, all compounds **217** show two distinct carbonyl absorptions while in the benzyloxy series, **218**, two carbonyl absorptions are clearly evident in solution. Both absorptions are affected in predictable fashion by electronic effects of the substituents. The non-degeneracy of the carbonyls in hydrazines has been attributed to vibrational coupling; in the crystal structure of **216** as well as in the computed geometry of model **II**(*ZE*), the carbonyls are close together and the dipoles make rather small angles of around 40° with respect to one another[212].

The carbonyl stretch frequencies (in the condensed phase) for hydrazines bearing branched amide side chains (Table 14, entries 13, 14 and 17) exhibit the usual reduction

TABLE 14. IR carbonyl absorption frequencies ($CHCl_3$ and condensed phase) and selected carbonyl ^{13}C NMR chemical shifts ($CDCl_3$) for *N*,*N*′-diacyl-*N*,*N*′-dialkoxyhydrazines ($R^2CON(OR^1)N(OR^1)COR^2$) and precursor hydroxamic esters

Entry	R^1	R^2	Hydrazine [a] ν (cm^{-1}) ($\delta^{13}C$)	Hydrazine [b] ν (cm^{-1})	Hydroxamic ester [a] ν (cm^{-1}) ($\delta^{13}C$)
1[73]	Et	4-$MeOC_6H_4$	1700 (169.3)	1717/1708 (nujol)	1681 (162.4)
2[73]	Et	4-MeC_6H_4	1701 (169.9)	1712/1676 (nujol)	1682 (—)
3[73]	Et	Ph	1708 (170.0)	1696 (nujol)	1685 (166.5)
4[73]	Et	4-ClC_6H_4	1711 (168.7)	1718/1679 (nujol)	1680 (165.1)
5[73]	Et	4-$NO_2C_6H_4$	1722 (167.9)	1720/1695 (nujol)	1692 (169.8)
6[73]	4-MeO-benzyl	Me	1733/1707 (—)		1693 (—)
7[73]	4-Me-benzyl	Me	1734/1700 (171.3)		1693 (168.0)
8[73]	Benzyl	Me	1735/1711 (—)		1682 (168.1)
9[73]	4-Cl-benzyl	Me	1738/1715 (171.3)		1693 (—)
10[73]	4-NO_2-benzyl	Me	1744/1723 (—)	1731 (nujol)	1700 (—)
11[72]	Me	Ph		1718 (neat)	—
12[72]	*t*-Bu	Ph		1685 (KBr)	—
13[72]	*t*-Bu	1-Ad		1708 (neat)	1644 (neat)
14[72]	Me	*t*-Bu		1684 (neat)	—
15[72]	Me	$PhCH_2CH_2$		1725 (neat)	1685
16[72]	Benzyl	$PhCH_2CH_2$		1724 (neat)	—
17[72]	Me	Cyclohexyl		1711 (KBr)	—

[a] In solution.
[b] In the condensed phase.

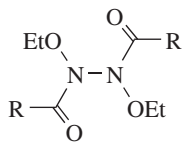

(**217**)

(**a**) R = 4-$MeOC_6H_4$
(**b**) R = 4-MeC_6H_4
(**c**) R = Ph
(**d**) R = 4-ClC_6H_4
(**e**) R = 4-$NO_2C_6H_4$

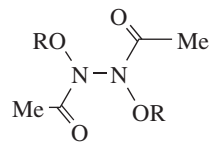

(**218**)

(**a**) R = 4-MeO-benzyl
(**b**) R = 4-Me-benzyl
(**c**) R = Benzyl
(**d**) R = 4-Cl-benzyl
(**e**) R = 4-NO_2-benzyl

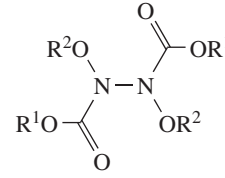

(**219**)

in wave number on account of inductive stabilization of the polar, single-bond amide resonance form.

Limited carbonyl ^{13}C NMR data are available for these anomeric amides. However, carbonyl shifts for hydrazines **217** and **218** were on average 3 ppm higher than their hydroxamic ester precursors. This reflects a higher degree of residual amide resonance in the hydrazines relative to *N*-acyloxy-*N*-alkoxyamides where the difference was closer to 8.0 ppm. As reported for *N*-acyloxy-*N*-alkoxyamides (see Section IV.B.2), analysis of variance in the hydrazine and hydroxamic ester shifts indicates that substituents affect the hydroxamic ester carbonyl shifts (±2.6) more than those of the hydrazines (±1.3 ppm).

Relative to *N*-chlorohydroxamic esters, *N*-acyloxy-*N*-alkoxyamides and *N*,*N*-dialkoxyamides, hydrazines exhibited quite different temperature-dependent behaviour in their ^1H NMR spectra. Whereas methylenic protons adjacent to oxygen on the alkoxyl group in the *ONO* anomeric systems are isochronous well below room temperature[15,50], the corresponding methylenes in **217** and **218** are diastereotopic well above room temperature[212]. Dynamic NMR studies gave free-energy barriers to topoisomerization of between 15 and 18 kcal mol^{-1} and a detailed conformational analysis has attributed these to restricted rotation about the *N*−*N* bond. They are significantly higher than the corresponding barriers of simple bipyramidal hydrazines (10–11 kcal mol^{-1} [217]) and are a direct measure of the strength of the anomeric interaction, which is stronger in these *NNO* systems than in an *ONCl* system (**2c** barrier 10 kcal mol^{-1}, Section III.B.2) and *ONO* systems, where the barrier to isomerization was too low to measure. In **218d**, for which the amide isomerization barrier was also measurable, the *N*−*N* rotational barrier (17.3 kcal mol^{-1}) was higher than the barrier to amide isomerization (12.9 kcal mol^{-1})[212]. Amide isomerization in *ONCl* and *ONO* systems could not be measured reinforcing the effect of electronegativity on pyramidality at nitrogen and amide resonance.

Shtamburg and coworkers have reported that *N*,*N*′-dialkoxy-*N*,*N*′-dicarboalkoxyhydrazines (**219**) have lower barriers to amide isomerization and weaker anomeric interactions[69]. They measured a barrier to amide isomerization of only 9.8 kcal mol^{-1}. Furthermore, benzylic methylenes in *N*-benzyloxy systems were isochronous down to at least −90 °C. These results are in line with observations for the *N*,*N*′-diacyl-*N*,*N*′-dialkoxyhydrazines since, in the carboalkoxy systems, the nitrogen lone pairs are lowered in energy by the additional electron demand, thereby reducing both amide conjugation and anomeric overlap.

C. Reactions of *N*-Alkoxy-*N*-aminoamides

A wide range of *N*-alkoxy-*N*-(*N*′-methylanilino)amides have been generated, but only as intermediates in the reactions of *N*-acyloxy-*N*-alkoxyamides with *N*-methylaniline and anilines from which esters, tetrazene and nitrogen were the products (See Section IV.C.3.a). The formation of non-crossover esters in these reactions led to the discovery of the HERON reaction pathway for *N*-alkoxy-*N*-aminoamides (Scheme 23, Section IV.C.3.a). The HERON process has been investigated extensively by several groups, from both a theoretical and physical organic as well as a synthetic utility point of view. It has been the subject of a recent review and has been introduced as named reaction in the literature[87, 91].

1. Theoretical treatment of the HERON reaction of N-alkoxy-N-aminoamides

The fate of *N*-alkoxy-*N*-aminoamides from *N*-methylaniline and *N*-acyloxy-*N*-alkoxyamides has been modelled at semiempirical, *ab initio* and density functional levels of theory[73, 88, 114]. B3LYP/6-31G* calculations predicted the HERON rearrangement of the model intermediate **214** to methyl formate (**173**) and 1,1-dimethyldiazene (**220**) to be exothermic by 5.5 kcal mol^{-1} and have an activation energy of 21.4 kcal mol^{-1} in the gas phase (Scheme 32).

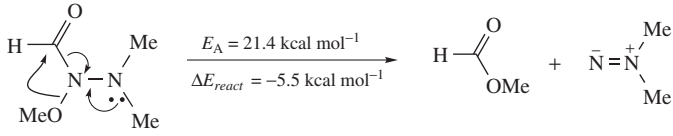

(**214**) (**173**) (**220**)

SCHEME 32

Like AM1 and HF/6-31G* methods, B3LYP/6-31G* calculations predicted an early transition state, shown in Figure 26, in which the migration of methoxyl from nitrogen to carbon takes place in a plane roughly perpendicular to that of the $N-C(O)$ group. The $N_{(1)}-C_{(1)}$ bond, though lengthened from 1.39 to 1.51 Å, is intact. A comparison with the ground-state structure (Figure 23) showed that the carbonyl bond length was virtually unchanged at 1.22 Å, and average angles around carbon were still 117.8°. The $N_{(1)}-N_{(2)}$ bond was shortened by 0.12 Å and the amino nitrogen was sp^2 hybridized (average angle 119.6°). Notably, an intrinsic reaction coordinate study indicated that the $N_{(1)}-C_{(1)}$ bond cleaves in concert with $O_{(2)}-C_{(1)}$ bond formation after the transition state and this reaction represents an intramolecular S_N2 reaction on the amide carbon. Further analysis of the computed transition state indicated significant charge redistribution. Predictably, $N_{(2)}(Me)_2$ becomes more positive (+0.51) at the transition state while $N_{(1)}$ (−0.19) and the migrating methoxyl group (−0.34) develop negative charge. Electron-releasing groups on the donor nitrogen, $N_{(2)}$, and electron-withdrawing groups on the migrating oxygen, $O_{(2)}$, should lower the energy of the transition state which, in accordance with experimental findings, should also proceed better in polar solvents that can stabilize this charge separation. Interestingly, there was no appreciable change in charge at the carbonyl and neither electron-donor groups nor electron-withdrawing groups at this position are predicted to exert a major influence upon the energetics of the reaction.

An extensive AM1 semiempirical study on a wide range of anomerically substituted acetamides was published in the first major paper describing this reaction[88]. For rearrangement of **221**, enthalpies of activation were clearly lowered in the sequence

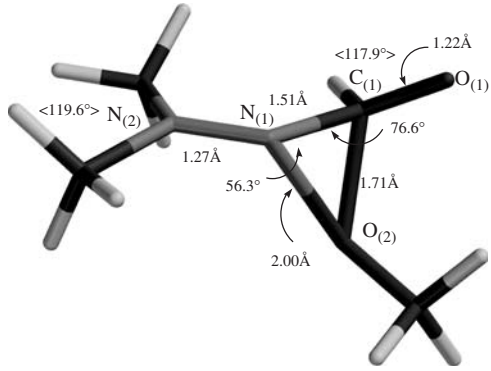

FIGURE 26. B3LYP/6-31G* transition state for the HERON reaction of *N*-formyloxy-*N*-(*N′*,*N′*-dimethylamino)formamide (**214**) to 1,1-dimethyldiazene (**220**) and methyl formate (**173**)

R = CF_3>CCl_3>$CHCl_2$>CH_2Cl>CH_3 and 4-$NO_2C_6H_4$>4-ClC_6H_4>C_6H_5>4-$NH_2C_6H_4$ and increased with R = acetyl, succinyl and acetyl/methoxyl. For migration of methoxyl in **222**, an alkoxide anion at *Y* resulted in a very low activation enthalpy but reactivity increased in the sequence Y = Cl<OH<OAc<OEt<NMe_2. With **223**, migration tendencies increased in the sequence X = Et<Me<H<Ac. Thus *NNO* systems are ideal for HERON reactivity.

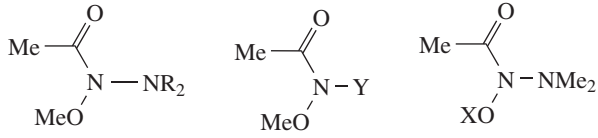

(**221**) (**222**) (**223**)

2. HERON reaction of N,N′-diacyl-N,N′-dialkoxyhydrazines

Both theoretically and structurally, *N*,*N′*-diacyl-*N*,*N′*-dialkoxyhydrazines (**212**) have been shown to possess all the anomeric amide properties of *N*-alkoxy-*N*-amino-amides[72,212], and they too have been shown to react by HERON rearrangements[63,72,73,87]. Cooley and coworkers first demonstrated the synthesis and the concerted thermal decomposition of symmetrical *N*,*N′*-diacyl-*N*,*N′*-dialkoxyhydrazines to esters[70]. Oxidation of hydroxamic esters with a variety of oxidants in benzene and ether also resulted in high yields of the corresponding esters. The hydrazines were less stable than the corresponding *N*,*N′*-dialkoxy-*N*,*N′*-dicarboalkoxyhydrazines (**219**) reported earlier by Crawford and Raap[213], who demonstrated that the carboalkoxy analogues were stable in refluxing methanol–water mixtures but were susceptible to acid and base catalysed decomposition. The effect of *para* benzoyl substituents in **224** and *para* benzyloxy substituents in **225** on the rates of decomposition in $CHCl_3$ was interpreted in favour of a rate-determining four-centre decomposition with incipient acylium and alkoxide character in the transition state **226** (Scheme 33)[71].

However, subsequent studies provided unequivocal evidence for consecutive three-centre rearrangements, the first step of which is a normal HERON reaction. Independent studies of decomposition of unsymmetrical hydrazines (**227a** and **227b**) produced esters

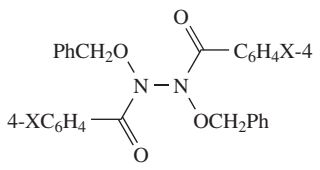

(**224**)

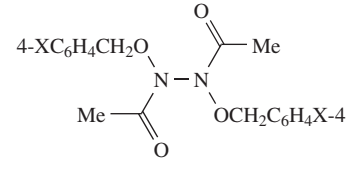

(**225**)

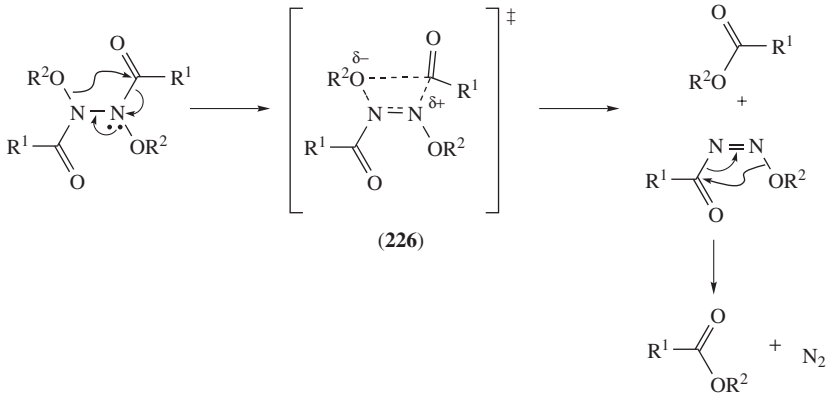

(**226**)

SCHEME 33

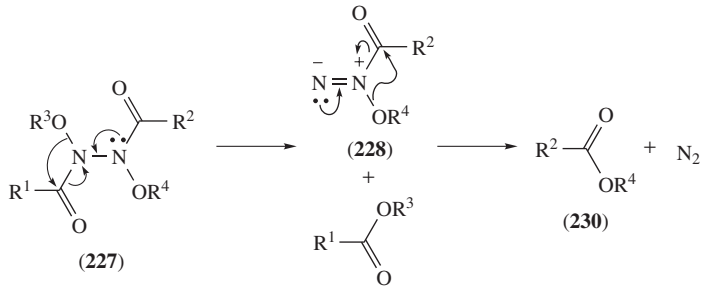

(**227**)

(**228**)

(**229**)

(**230**)

(**a**) R^1 = Ph, R^2 = 4-ClC_6H_4, R^3 = benzyl, R^4 = Bu
(**b**) R^1 = cyclohexyl, R^2 = benzyl, R^3 = Me, R^4 = $PhCH_2CH_2$

SCHEME 34

229a with **230a** and **229b** with **230b** rather than the alternate esters that would be formed through four-centre rearrangements (Scheme 34)[63,72].

227a decomposed in $CDCl_3$ with an E_A of 27 kcal mol^{-1}, an $\Delta S^{\ddagger}$ of 6.4 cal K^{-1} mol^{-1} and a rate constant, $k_2^{298} = 6.9 \times 10^{-6}$ s^{-1} [63]. Rate constants at 298 K and Arrhenius activation data for decomposition of **217** and **218** in mesitylene are presented in Table 15.

Activation barriers are similar to the gas-phase value of 21 kcal mol^{-1} for rearrangement of *N*-methoxy-*N*-dimethylaminoformamide (Scheme 32). Entropies of activation

TABLE 15. Arrhenius activation energies, entropies of activation and rate constants at 298 K for decomposition of *N*,*N*′-diacyl-*N*,*N*′-dialkoxyhydrazines **217** and **218** in mesitylene

Substrate	E_A(kcal mol^{-1})[a]	$\Delta S^{\ddagger}$ (cal K^{-1} mol^{-1})[a]	$10^8 k^{298}$ (s^{-1})
217a	23.7(1.0)	−5.1(3)	556
217b	24.0(2.0)	−4.7(6)	372
217c	24.0(1.2)	−5.7(4)	252
217c[b]	22.3(1.5)	−10.6(5)	353
217d	25.7(0.4)	0.2(1)	250
217e	24.8(0.4)	−3.7(1)	157
218a	26.6(0.2)	−5.0(1)	4.0
218b	30.1(0.2)	5.8(1)	2.8
218c	27.2(0.9)	−2.1(3)	6.2
218d	29.9(2.0)	6.5(6)	5.4
218e	23.6(0.1)	−11.1(0)	31.9

[a] Errors in parentheses.
[b] Reaction in cyclohexanone as solvent.

are modestly negative or positive in keeping with an intramolecular process with concerted bond formation and breaking, where the transition state has more constraints than the reactants and significant polar separation. Reaction rate constants at 298 K for the substituted benzoyl series **217a–e** correlated with Hammett σ^+ with $\rho = -0.4$, and those for the substituted benzyloxy series **218a–e** with Hammett σ constants and $\rho = +1.02$, entirely in accordance with the computed charge distribution in the model transition state for the HERON process[73]. The increased negative charge at the alkoxyl group in the model transition state is stabilized by *para* electron-withdrawing substituents on the benzyloxy groups (Figure 27a). In the case of the HERON reaction, the acceptor carbonyl moiety is computed to be nearly neutral in the transition state and thus relatively unaffected by donor or acceptor acyl groups. One nitrogen (the anomeric nitrogen) functions as an electron-pair donor and it is the increased positive charge at this nitrogen that is stabilized by *para* electron-donor substituents on the adjacent benzoyl group (Figure 27b). There was no evidence of the acylium character in the transition state as postulated by Cooley and coworkers[71].

The fact that members of the benzoyl series **217** reacted about two orders of magnitude faster at 298 K than the benzyloxy series **218** studied is also consistent with the theoretical properties of the transition state[73,150]. While an electron-withdrawing group on the alkoxy group will stabilize negative charge in the migrating group, it will destabilize a developing positive charge on the adjacent anomeric donor nitrogen (Figure 27a). In the benzoyl series, a donor group facilitates developing positive charge at the anomeric nitrogen but has little effect upon the acyl carbon, which neither gains nor loses charge (Figure 27b).

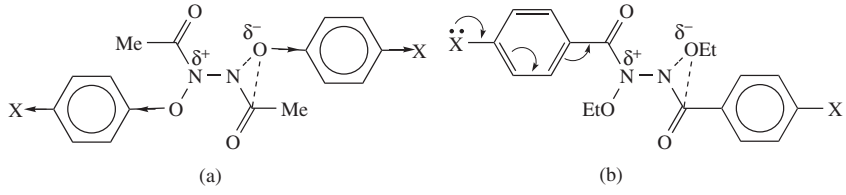

FIGURE 27. The influence on the HERON transition states of (a) electron-deficient benzyloxy groups in **218** and (b) electron-rich benzoyl groups in **217**

Arrhenius data for the decomposition of **218c** in cyclohexanone ($\varepsilon = 19$) are listed together with the data for mesitylene ($\varepsilon = 2.4$) in Table 15. Rates at 298K are similar, although in cyclohexanone both E_A and $\Delta S^{\ddagger}$ are smaller than the corresponding values in mesitylene; increased charge separation in the transition state is stabilized by more polar solvents but leads to ordering of polar solvent molecules, resulting in a more negative entropy of activation.

Using coupled cluster CCSD(T)//B3P86 methods, the E_A values for HERON rearrangement of model hydrazines **215b–d** have also been computed to be between 24 and 34 kcal mol^{-1} [133]. The authors ruled out alternative concerted rearrangements, which were computed to be energetically unfavourable.

The intermediate 1-acyl-1-alkoxydiazenes **228** in Scheme 34 have been computed independently by two groups to rearrange with very low E_A to ester and nitrogen[133, 151]. The same intermediate was postulated to form in the spontaneous decomposition of *N*-alkoxy-*N*-azidoamides (see Scheme 16, Section III.C.4 and equation 18, Section IV.C.3.d)[97, 150]. In model systems this step, which can also be envisaged as a HERON reaction, was computed to be extremely exothermic, by 95 kcal mol^{-1} at B3LYP/6-31G* for 1-formyl-1-methoxydiazene (**228**, $R^2 = H$, $R^4 = Me$)[151] or by 104, 103 and 95 kcal mol^{-1} at CCSD(T)//B3P86 for 1,1-diazenes from **215b–d**[133]. Activation energies were 2.8 kcal mol^{-1} and 2.2, 1.1 and 2.4 kcal mol^{-1} from the respective studies. Thus the facile ester formation through decomposition of 1-acyl-1-alkoxydiazenes is extremely exothermic, and on account of this the intermediates from thermal decomposition of *N*,*N*′-diacyl-*N*,*N*′-dialkoxyhydrazines or the reaction of azide with *N*-alkoxy-*N*-chloroamides or *N*-acyloxy-*N*-alkoxyamides have not been trapped[72, 73, 97, 133, 150, 151].

The characteristics of the HERON transition states for both steps in the thermal decomposition of *N*,*N*′-diacyl-*N*,*N*′-dialkoxyhydrazines facilitate the synthesis of esters. Notably, the alkoxyl group migrations in the internal S_N2 displacement of the 1,1-diazene in the first step, and nitrogen in the second step, do not involve a tetrahedral alkoxide intermediate and both Barton and coworkers[72] and Glover and Mo[97, 150] have utilized these properties in the synthesis of highly hindered esters.

Thermal decomposition of symmetrical hydrazines (**212a–d**) according to equation 30 resulted in excellent yields of hindered esters (**231a–d**)[72]. The hydrazines leading to the esters were generated as intermediates by the oxidation of *N*-alkoxyamides using ceric ammonium nitrate or $NiO_2.H_2O$ (Scheme 31).

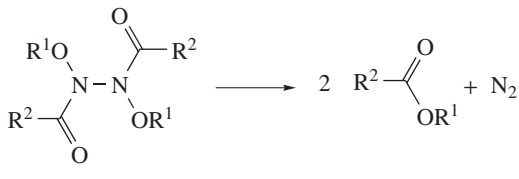

(**212**) (**231**) (30)

(**a**) R^1 = *t*-Bu, R^2 = Ph, 80–100 °C, 6 h, 92%
(**b**) R^1 = *t*-Bu, R^2 = 1-adamantyl, 40–65 °C, 6 h, 87%
(**c**) R^1 = Me, R^2 = *t*-Bu, 25 °C, 12 h, 100%
(**d**) R^1 = Me, R^2 = cyclohexyl, 50–80 °C, 4 h, 100%

Yields of hindered esters formed by HERON decomposition of the 1-acyl-1-alkoxydiazene intermediates from treatment of *N*-alkoxy-*N*-chloroamides with sodium azide in aqueous acetonitrile according to Scheme 16 are presented in Table 3[97] (Section III.C.4).

Both methods are successful since the formation of a tetrahedral intermediate about the ester carbonyl carbon, which is rate limiting in classical Fischer esterification[152–154], is avoided in the HERON reaction of hydrazines and 1-acyl-1-alkoxydiazenes.

3. HERON reactions in base-catalysed decomposition of azodicarboxylates

Treatment of dialkyl azodicarboxylates (**232**) with sodium methoxide or sodium acetate in methanol resulted in the generation of methyl alkyl carbonates (**235**) and alkyl formates (**236**) in a 1:1 ratio[87,150]. The reactions appear to involve methoxide addition at nitrogen giving **233** followed by amide anion-induced rearrangement. This is computed to be similar to HERON except that the tetrahedral intermediate **234** is formed, which decomposes in one step to acyl anion and nitrogen according to Scheme 35[87,150]. The rearrangement of the model intermediate (**233**, R = Me) is computed to be exothermic by 17.4 kcal mol^{-1} with an E_A of 14.8 kcal mol^{-1} at B3LYP/6-31G*//HF/6-31G* with solvation correction[87].

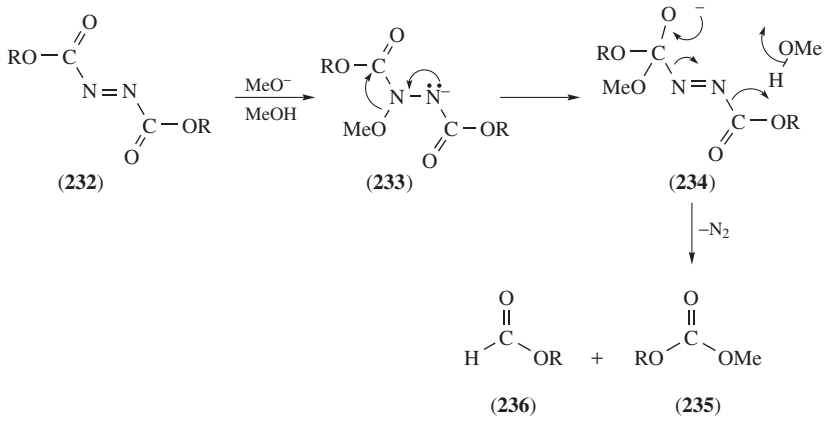

SCHEME 35

The reaction of *N*-acyloxy-*N*-alkoxyamides and aromatic amines, the thermal decomposition of *N*,*N*′-diacyl-*N*,*N*′-dialkoxyhydrazines as well as the base-induced decomposition of azodicarboxylates are examples of the HERON reaction, one of the newest-named reactions in the chemical literature[91], but one that seems to be common for these as well as a range of other bisheteroatom-substituted amides[87]. No doubt new examples will be discovered and it is entirely predicated upon the configurational and conformational properties of anomeric amides, attributes arising directly as a consequence of the dual electron demands of the heteroatoms at nitrogen.

VII. *N*-ALKOXY-*N*-THIOALKYLAMIDES

Amides substituted at nitrogen with both a sulfur and oxygen have only been generated as reactive intermediates. Sulfur is less electronegative than nitrogen and its role in anomeric substitution at nitrogen should be radically different.

A. Synthesis of *N*-Alkoxy-*N*-thioalkylamides

To date no stable examples of **1e** have been reported in the literature.

Structures of this type were generated in the reaction of *N*-acyloxy-*N*-alkoxyamides with thiols. Treatment of *N*-acetoxy-*N*-butoxybenzamide (**145**, $R^1 = Bu$, $R^2 = Me$) and a series of *N*-benzoyloxy-*N*-benzyloxybenzamides (**139**) with cysteine derivatives generated disulfides and hydroxamic esters (Section IV.C.3.b, Scheme 24). The intermediate *N*-alkoxy-*N*-thioalkylamides were unstable under the reaction conditions, reacting with a second thiol molecule at sulfur. The reaction of thiols at the anomeric nitrogen of *N*-acyloxy-*N*-alkoxyamides has been modelled theoretically and is predicted to be favourable energetically, leading to a stable substitution product[13,157].

B. Properties of *N*-Alkoxy-*N*-thioalkylamides

The structure of a model compound *N*-methoxy-*N*-thiomethylformamide (**237**) has been computed at the B3LYP/6-31G*//HF/6-31G* level as a means of comparing this configuration to other anomeric amides. Its properties are predicted to be radically different to those of hydroxamic esters **1a–d**. The conformer with sulfur and the carbonyl oxygen *syn* and *O*-methyl and *S*-methyl respectively *exo* and *endo* to the shallow nitrogen pyramid was lowest in energy by nearly 3 kcal mol^{-1} relative to the corresponding *anti* conformer (Figure 28).

The configuration at nitrogen suggests appreciably more amide character than found in **1a–d**. The nitrogen is only slightly pyramidal with an average angle of 117.5°. The $S-N-C$ angle is particularly large (123.3°). The Winkler–Dunnitz parameters of $\tau = 2.2°$ and $\chi_N = 31.1°$ point to a good deal of resonance in this structure. This is supported by bond lengths in **237**. The *C–N* bond (1.379 Å) is much shorter than the corresponding bond in *N*-formyloxy-*N*-methoxyformamide (**91**) calculated at the same level of theory (1.405 Å) and is only marginally longer than that of *N*-methoxyformamide (**92**) at the HF/6-31G* level (1.373 Å) (Section IV.B.1). In addition, the carbonyl bond length is the longest of all computed anomeric amide models at 1.185 Å and similar to that of methoxyformamide (1.188 Å). The small twist angle, as well as bond lengths and the low degree of pyramidality at nitrogen, suggest that *N*-alkoxy-*N*-thioalkylamides would exhibit properties that are much closer to those of normal amides than those of anomeric amides **1a–d**.

In confirmation of this, the barrier to rotation about the $C-N$ bond is computed to be 15.1 kcal mol^{-1}, which is significantly higher than other systems studied and similar to that computed for *N*-methoxyformamide (15.6 kcal mol^{-1})[10,13].

Of the two possible anomeric interactions the $n_O-\sigma^*_{NS}$ appears to dominate. The $Me-O-N-S(Me)$ dihedral angle is computed to be 92.4° whereas the reverse dihedral angle $(Me)O-N-S-Me$ is much smaller (76.4°). However, the $N-OMe$ bond

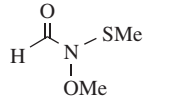

(**237**)

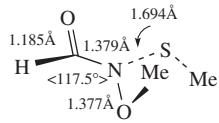

FIGURE 28. Lowest energy conformer of *N*-methoxy-*N*-thiomethylformamide calculated at the B3LYP/6-31G*//HF/6-31G* level

length (1.377 Å) is long when compared to that of *N*-formyloxy-*N*-methoxyformamide (**91**, 1.36 Å) despite the much lower degree of pyramidality at nitrogen, which would naturally shorten bonds. A low barrier to rotation about the $N-O$ bond of 7.6 kcal mol^{-1} was calculated at the B3LYP/6-31G*//HF/6-31G* level.

C. Reactions of *N*-Alkoxy-*N*-thioalkylamides

Theoretical properties of *N*-methoxy-*N*-thiomethylformamide (**237**) suggest that the reactivity patterns of *N*-alkoxy-*N*-thioalkylamides would be different to those of other anomeric hydroxamic esters described in this chapter. The reduced pyramidality at nitrogen together with the more conventional π overlap between the nitrogen lone pair and the carbonyl would disfavour reactions at the nitrogen atom, which dominates the reactivity patterns of other anomeric hydroxamic esters.

The only available evidence to support this is the fate of intermediates generated from the reaction of *N*-acyloxy-*N*-alkoxyamides with cysteine derivatives in methanol described in Section IV.C.3.b. The nucleophilic thiol reacts preferentially at the sulfur atom rather than at nitrogen, generating the hydroxamic ester and the disulfide (Scheme 24).

The theoretical properties of model **237** as well as the preferred mode of reaction with thiols can be rationalized in terms of the lower electronegativity of sulfur (2.5) as compared to nitrogen (3.0) and oxygen (3.5). In this case, the combined electronegativity of oxygen and sulfur appears to be insufficient to overcome the stabilization gained from amide resonance.

VIII. ACKNOWLEDGEMENT

The author is grateful to Dr Chris Fellows, Dr David Tucker and Ms Rhiannon Schumacher for their assistance in the production of this work.

IX. REFERENCES

1. A. Greenberg, C. M. Breneman and J. F. Liebman, *The Amide Linkage: Structural Significance in Chemistry, Biochemistry and Materials Science*, Wiley, New York, 2000.
2. K. B. Wiberg, in *The Amide Linkage. Structural Significance in Chemistry, Biochemistry and Materials Science* (Eds. A. Greenberg, C. M. Breneman and J. F. Liebman), Wiley, New York, 2000, p. 33.
3. K. B. Wiberg and C. M. Breneman, *J. Am. Chem. Soc.*, **114**, 831 (1992).
4. K. B. Wiberg, P. R. Rablen, D. J. Rush and T. A. Keith, *J. Am. Chem. Soc.*, **117**, 4261 (1995).
5. T. Drakenberg and S. Forsén, *J. Phys. Chem.*, **74**, 1 (1970).
6. T. Drakenberg, K. Dahlqvist and S. Forsén, *J. Phys. Chem.*, **76**, 2178 (1972).
7. M. Rabinowitz and A. Pines, *J. Am. Chem. Soc.*, **91**, 1585 (1969).
8. R. C. Neuman Jr., W. R. Woolfenden and V. Jonas, *J. Phys. Chem.*, **73**, 3177 (1969).
9. L. M. Jackman and F. A. Cotton, *Dynamic Nuclear Magnetic Resonance Spectroscopy*, Academic Press, New York, 1975, p. 203.
10. S. A. Glover and A. Rauk, *J. Org. Chem.*, **61**, 2337 (1996).
11. L. Bauer and O. Exner, *Angew. Chem., Int. Ed. Engl.*, **13**, 376 (1974).
12. D. A. Brown, W. K. Glass, R. Mageswaran and S. A. Mohammed, *Magn. Reson. Chem.*, **29**, 40 (1991).
13. S. A. Glover, *Adv. Phys. Org. Chem.*, **42**, 35 (2007).
14. B. Challis and J. Challis, in *Comprehensive Organic Chemistry Vol. 2, Nitrogen Compounds, Carboxylic Acids, Phosphorous Compounds* (Ed. I. O. Sutherland), Pergamon Press, Oxford, 1979, p. 957.
15. A.-M. E. Gillson, S. A. Glover, D. J. Tucker and P. Turner, *Org. Biomol. Chem.*, **1**, 3430 (2003).

16. J. H. Cooley, W. D. Bills and J. R. Throckmorton, *J. Org. Chem.*, **25**, 1734 (1960).
17. J. E. Johnson, E. A. Nalley, Y. K. Kunz and J. R. Springfield, *J. Org. Chem.*, **41**, 252 (1976).
18. S. Yamada, *Rev. Heteroatom Chem.*, **19**, 203 (1999).
19. S. Yamada, in *The Amide Linkage. Structural Significance in Chemistry, Biochemistry and Materials Science* (Eds. A. Greenberg, C. M. Breneman and J. F. Liebman), Wiley, New York, 2000, p. 215.
20. S. Yamada and A. Homma, *J. Chem. Soc., Chem. Commun.*, 2656 (2002).
21. S. Yamada and E. Noguchi, *Tetrahedron Lett.*, **42**, 3621 (2001).
22. C. N. Cow, J. F. Britten and P. H. M. Harrison, *J. Chem. Soc., Chem. Commun.*, 1147 (1998).
23. P. A. Duspara, C. F. Matta, S. I. Jenkins and P. H. M. Harrison, *Org. Lett.*, **3**, 495 (2001).
24. C. F. Matta, C. C. Cow, S. Sun, J. F. Britten and P. H. M. Harrison, *J. Mol. Struct.*, **523**, 241 (2000).
25. A. D. Bain, H. Chen and P. H. Harrison, *Can. J. Chem.*, **84**, 421 (2006).
26. C. F. Matta, C. C. Cow and P. H. M. Harrison, *J. Mol. Struct. (THEOCHEM)*, **660**, 81 (2003).
27. Y. Otani, O. Nagae, Y. Naruse, S. Inagaki, M. Ohno, K. Yamaguchi, G. Yamamoto, M. Uchiyama and T. Ohwada, *J. Am. Chem. Soc.*, **125**, 15191 (2003).
28. T. Ohwada, T. Achiwa, I. Okamoto, K. Shudo and K. Yamaguchi, *Tetrahedron Lett.*, **39**, 865 (1998).
29. I. Alkorta, C. C. Cativiela, J. Elguero, A. M. Gil and A. I. Jiménez, *New J. Chem.*, **29**, 1450 (2005).
30. G. V. Shustov, G. K. Kadorkina, S. V. Varlamov, A. V. Kachanov, R. G. Kostyanovskii and A. Rauk, *J. Am. Chem. Soc.*, **114**, 1616 (1992).
31. A. J. Kirby, I. V. Komarov, K. Kowski and P. Rademacher, *J. Chem. Soc., Perkin Trans. 2*, 1313 (1999).
32. A. J. Kirby, I. V. Komarov and N. Feeder, *J. Chem. Soc., Perkin Trans. 2*, 522 (2001).
33. A. J. Kirby, I. V. Komarov, P. D. Wothers and N. Feeder, *Angew. Chem., Int. Ed. Engl.*, **37**, 785 (1998).
34. A. Greenberg, in *The Amide Linkage. Structural Significance in Chemistry, Biochemistry and Materials Science* (Eds. A. Greenberg, C. M. Breneman and J. F. Liebman), Wiley, New York, 2000, p. 47.
35. A. Greenberg, D. T. Moore and T. D. DuBois, *J. Am. Chem. Soc.*, **118**, 8658 (1996).
36. K. Tani and B. M. Stoltz, *Nature*, **441**, 731 (2006).
37. T. P. Ribelin, A. S. Judd, I. Akritopoulou-Zanze, R. F. Henry, J. L. Cross, D. N. Whittern and S. W. Djuric, *Org. Lett.*, **9**, 5119 (2007).
38. W. B. Jennings, S. P. Watson and D. R. Boyd, *J. Chem. Soc., Chem. Commun.*, 1078 (1992).
39. P. C. B. Page, V. L. Murrell, C. Limousin, D. D. P. Laffan, D. Bethell, A. M. Z. Slawin and T. A. D. Smith, *J. Org. Chem.*, **65**, 4204 (2000).
40. E. Schmitz and S. Schramm, *Chem. Ber.*, **100**, 2593 (1967).
41. E. Schmitz, R. Ohme and S. Schramm, *Tetrahedron Lett.*, 1857 (1965).
42. A. J. Kirby, I. V. Komarov and N. Feeder, *J. Am. Chem. Soc.*, **120**, 7101 (1998).
43. C. G. Bashore, I. J. Samardjiev, J. Bordner and J. W. Coe, *J. Am. Chem. Soc.*, **125**, 3268 (2003).
44. R. S. Brown, in *The Amide Linkage. Structural Significance in Chemistry, Biochemistry and Materials Science* (Eds. A. Greenberg, C. M. Breneman and J. F. Liebman), Wiley, New York, 2000, p. 85.
45. X. Lopez, J. I. Mujika, G. M. Blackburn and M. Karplus, *J. Phys. Chem. A*, **107**, 2304 (2003).
46. K. L. Morgan, M. L. Rawlins and M. N. Montgomery, *J. Phys. Org. Chem.*, **18**, 310 (2005).
47. J. I. Mujika, J. M. Mercero and X. Lopez, *J. Am. Chem. Soc.*, **127**, 4445 (2005).
48. S. Yamada and H. Katsumata, *J. Org. Chem.*, **64**, 9365 (1999).
49. Z. Mucsi, A. Tsai, M. Szori, G. A. Chass, B. Viscolcz and I. G. Csizmadia, *J. Phys. Chem. A*, **111**, 13245 (2007).
50. S. A. Glover, *Tetrahedron*, **54**, 7229 (1998).
51. S. A. Glover, A. Goosen, C. W. McCleland and J. L. Schoonraad, *J. Chem. Soc., Perkin Trans. 1*, 2255 (1984).
52. S. A. Glover, A. Goosen, C. W. McCleland and J. L. Schoonraad, *Tetrahedron*, **43**, 2577 (1987).
53. S. A. Glover, C. A. Rowbottom, A. P. Scott and J. L. Schoonraad, *Tetrahedron*, **46**, 7247 (1990).

54. Y. Kikugawa and M. Kawase, *J. Am. Chem. Soc.*, **106**, 5728 (1984).
55. Y. Kikugawa and M. Shimada, *Chem. Lett.*, 1771 (1987).
56. M. Kawase, T. Kitamura and Y. Kikugawa, *J. Org. Chem.*, **54**, 3394 (1989).
57. Y. Kikugawa, M. Shimada and K. Matsumoto, *Heterocycles*, **37**, 293 (1994).
58. Y. Kikukawa, 'Nitrogen-containing heterocyclic compounds', Japanese Patent 60184063, 19 Sept. 1985; *Chem. Abstr.*, **104**, 68754 (1986).
59. Y. Kikukawa, 'Spirodienone derivatives', Japanese Patent 61227564, 09 Oct. 1986; *Chem. Abstr.*, **106**, 119699 (1987).
60. Y. Kikukawa, 'Preparation of spirocyclohexadienones by intramolecular cyclocondensation', Japanese Patent 62190176, 20 Aug. 1987; *Chem. Abstr.*, **109**, 190403 (1988).
61. Y. Kikukawa, 'Preparation of *N*-alkoxylactams from *N*-halo-*O*-alkylhydroxamic acids', Japanese Patent 63287765, 24 Nov. 1988; *Chem. Abstr.*, **111**, 7240 (1989).
62. R. G. Gerdes, S. A. Glover, J. F. Ten Have and C. A. Rowbottom, *Tetrahedron Lett.*, **30**, 2649 (1989).
63. J. M. Buccigross, S. A. Glover and G. P. Hammond, *Aust. J. Chem.*, **48**, 353 (1995).
64. S. A. Glover, J. P. Johns and R. M. Spence, Unpublished work.
65. V. F. Rudchenko, V. I. Shevchenko and R. G. Kostyanovskii, *Bull. Acad. Sci. USSR, Div. Chem. Sci.*, 551 (1986).
66. V. F. Rudchenko, V. I. Shevchenko and R. G. Kostyanovskii, *Bull. Acad. Sci. USSR, Div. Chem. Sci.*, 543 (1986).
67. O. V. Shishkin, R. I. Zubatyuk, V. G. Shtamburg, A. V. Tsygankov, E. A. Klots, A. V. Mazepa and R. G. Kostyanovsky, *Mendeleev Commun.*, 222 (2006).
68. V. G. Shtamburg, E. A. Klots, A. P. Pleshkova, V. I. Avramenko, S. P. Ivonin, A. V. Tsygankov and R. G. Kostyanovsky, *Russ. Chem. Bull.*, **52**, 2251 (2003).
69. V. G. Shtamburg, V. F. Rudchenko, S. S. Nasibov, I. I. Chervin and R. G. Kostyanovskii, *Izv. Akad. Nauk SSSR, Ser. Khim.*, 449 (1981); *Chem. Abstr.*, **95**, 61436 (1981).
70. J. H. Cooley, M. W. Mosher and M. A. Khan, *J. Am. Chem. Soc.*, **90**, 1867 (1968).
71. J. H. Cooley, D. H. Stone and H. Oguri, *J. Org. Chem.*, **42**, 3096 (1977).
72. M. V. De Almeida, D. H. R. Barton, I. Bytheway, J. A. Ferriera, M. B. Hall, W. Liu, D. K. Taylor and L. Thomson, *J. Am. Chem. Soc.*, **117**, 4870 (1995).
73. S. A. Glover, G. Mo and A. Rauk, *Tetrahedron*, **55**, 3413 (1999).
74. V. F. Rudchenko, *Chem. Rev.*, **93**, 725 (1993).
75. K. Müller and A. Eschenmoser, *Helv. Chim. Acta*, **52**, 1823 (1969).
76. G. V. Shustov, A. B. Zolotoi and R. G. Kostyanovsky, *Tetrahedron*, **38**, 2319 (1982).
77. N. D. Epiotis, W. R. Cherry, S. Shaik, Y. L. Yates and F. Bernardi, *Structural Theory of Organic Chemistry*, Springer-Verlag, Berlin, 1977, pp. 49, 131.
78. K. Müller, *Helv. Chim. Acta*, **53**, 1112 (1970).
79. P. Deslongchamps, *Stereoelectronic Effects in Organic Chemistry*, Vol. 1, Pergamon Press, Oxford, 1984, p. 4.
80. E. L. Eliel, S. H. Wilen and L. N. Mander, *Stereochemistry of Organic Compounds*, Wiley, New York, 1994, pp. 753, 1191.
81. A. Rauk, *Orbital Interaction Theory of Organic Chemistry*, Wiley, New York, 1994, p. 102.
82. A. Pross, *Theoretical and Physical Principles of Organic Chemistry*, Wiley, New York, 1995, p. 142.
83. S. A. Glover and A. P. Scott, *Tetrahedron*, **45**, 1763 (1989).
84. D. Schroder, F. Grandinetti, J. Hrusak and H. Schwarz, *J. Phys. Chem.*, **96**, 4841 (1992).
85. E. R. Thornton, *J. Am. Chem. Soc.*, **89**, 2915 (1967).
86. W. P. Jencks, *Chem. Rev.*, **72**, 705 (1972).
87. S. A. Glover, A. Rauk, J. M. Buccigross, J. J. Campbell, G. P. Hammond, G. Mo, L. E. Andrews and A.-M. E. Gillson, *Can. J. Chem.*, **83**, 1492 (2005).
88. J. M. Buccigross and S. A. Glover, *J. Chem. Soc., Perkin Trans. 2*, 595 (1995).
89. J. J. Campbell and S. A. Glover, *J. Chem. Res. (S)*, **8**, 474 (1999).
90. J. J. Campbell and S. A. Glover, *J. Chem. Res. (M)*, **8**, 2075 (1999).
91. S. A. Glover, in *Merck Index*, 14th ed., *Organic Name Reactions ONR-43* (Ed. M. J. O'Neil), Merck & Co., Inc., Whitehouse Station, N.J., 2006.
92. J. J. Campbell, S. A. Glover, G. P. Hammond and C. A. Rowbottom, *J. Chem. Soc., Perkin Trans. 2*, 2067 (1991).
93. A. M. Bonin, S. A. Glover and G. P. Hammond, *J. Chem. Soc., Perkin Trans. 2*, 1173 (1994).

94. S. A. Glover, K. M. Jones, I. R. McNee and C. A. Rowbottom, *J. Chem. Soc., Perkin Trans. 2*, 1367 (1996).
95. A. M. Bonin, S. A. Glover and G. P. Hammond, *J. Org. Chem.*, **63**, 9684 (1998).
96. A. M. Bonin, T. M. Banks, J. J. Campbell, S. A. Glover, G. P. Hammond, A. S. Prakash and C. A. Rowbottom, *Mutat. Res.*, **494**, 115 (2001).
97. S. A. Glover and G. Mo, *J. Chem. Soc., Perkin Trans. 2*, 1728 (2002).
98. T. M. Banks, A. M. Bonin, S. A. Glover and A. S. Prakash, *Org. Biomol. Chem.*, **1**, 2238 (2003).
99. L. E. Andrews, A. M. Bonin, L. Fransson, A.-M. E. Gillson and S. A. Glover, *Mutat. Res.*, **605**, 51 (2006).
100. V. G. Shtamburg, O. V. Shishkin, R. I. Zubatyuk, S. V. Kravchenko, A. V. Tsygankov, A. V. Mazepa, E. A. Klots and R. G. Kostyanovsky, *Mendeleev Commun.*, 323 (2006).
101. H. Teeninga and J. B. F. N. Engberts, *Recl. Trav. Chim. Pays-Bas*, **97**, 59 (1978).
102. A. Zwierzak and J. Brylikowska, *Synthesis*, 712 (1975).
103. M. J. Mintz and C. Walling, *Org. Synth.*, **49**, 9 (1963).
104. A. L. J. Beckwith and J. E. Goodrich, *Aust. J. Chem.*, **18**, 747 (1965).
105. H. Kamei, *Bull. Chem. Soc. Jpn.*, **41**, 2269 (1968).
106. B. Sunners, L. H. Piette and W. G. Schneider, *Can. J. Chem.*, **38**, 618 (1960).
107. F. K. Winkler and J. D. Dunitz, *J. Mol. Biol.*, **59**, 169 (1971).
108. J. D. Dunitz, *X-Ray Analysis and Structure of Organic Molecules*, Cornell University Press, London, 1979.
109. W. J. D. Klein, *Spectrochim. Acta*, **28A**, 687 (1972).
110. A. Goosen, C. W. McCleland and A. J. Merrifield, *J. Chem. Soc., Perkin Trans. 1*, 627 (1992).
111. W. J. D. Klein and A. R. Plesman, *Spectrochim. Acta*, **28A**, 673 (1972).
112. J. E. Devia and J. C. Carter, *Spectrochim. Acta*, **29A**, 613 (1973).
113. T. M. Banks, 'Reactivity, Mutagenicity and DNA Damage of *N*-Acyloxy-*N*-alkoxyamides', PhD thesis, University of New England, Armidale, Australia 2003.
114. J. J. Campbell and S. A. Glover, *J. Chem. Soc., Perkin Trans. 2*, 1661 (1992).
115. S. A. Glover and C. A. Rowbottom, Unpublished results.
116. V. G. Shtamburg, Private communication.
117. R. A. Nyquist, R. Streck and G. Jeschek, *J. Mol. Struct.*, **377**, 113 (1996).
118. S. A. Glover and D. Tucker, Unpublished results.
119. R. S. Neale, *Synthesis*, **1**, 1 (1971).
120. A. Goosen, *S. Afr. J. Chem.*, **32**, 37 (1979).
121. I. V. Koval, *Russ. J. Org. Chem.*, **37**, 297 (2001).
122. S. A. Glover, A. Goosen and H. A. H. Laue, *S. Afr. J. Chem.*, **26**, 127 (1973).
123. T. Koenig, J. A. Hoobler, C. E. Klopfenstein, G. Heddon, F. Sunderman and B. R. Russell, *J. Am. Chem. Soc.*, **96**, 4573 (1974).
124. A. R. Forrester and H. Irikawa, *J. Chem. Soc., Chem. Commun.*, 253 (1981).
125. K. U. Ingold and J. C. Walton, *Landolt Börnstein II 17c*, Springer-Verlag, Berlin, 1987.
126. R. Sutcliffe, D. Griller, J. Lessard and K. U. Ingold, *J. Am. Chem. Soc.*, **103**, 624 (1981).
127. S. A. Glover, A. Goosen, C. W. McCleland and J. L. Schoonraad, *J. Chem. Soc., Perkin Trans. 2*, 645 (1986).
128. A. R. Forrester, E. M. Johansson and R. H. Thomson, *J. Chem. Soc., Perkin Trans. 1*, 1112 (1979).
129. T. Koenig, J. A. Hoobler and W. R. Mabey, *J. Am. Chem. Soc.*, **94**, 2514 (1972).
130. S. A. Glover and A. Goosen, *J. Chem. Soc., Perkin Trans. 1*, 1348 (1977).
131. S. A. Glover and A. Goosen, *J. Chem. Soc., Perkin Trans. 1*, 653 (1978).
132. P. Mackiewicz and R. Furstoss, *Tetrahedron*, **34**, 3241 (1978).
133. L. M. Thomson and M. B. Hall, *J. Phys. Chem. A*, **104**, 6247 (2000).
134. Y. Kikugawa, M. Shimada, M. Kato and T. Sakamoto, *Chem. Pharm. Bull.*, **41**, 2192 (1993).
135. N. De Kimpe and R. Verhé, in *The Chemistry of α-Haloketones, α-Haloaldehydes and α-Haloimines* (Eds. S. Patai and Z. Rappoport), Wiley, Chichester, 1988, p. 38.
136. Y. Kikugawa, M. Kawase, Y. Miyake, T. Sakamoto and M. Shimada, *Tetrahedron Lett.*, **29**, 4297 (1988).
137. I. Fleming, R. C. Moses, M. Tercel and J. Ziv, *J. Chem. Soc., Perkin Trans. 1*, 617 (1991).
138. D. L. Savigni, D. Wege, G. S. Cliff, M. L. H. Meesters and E. H. Morgan, *Biochem. Pharm.*, **65**, 1215 (2003).

139. E. Miyazawa, T. Sakamoto and Y. Kikugawa, *J. Org. Chem.*, **68**, 5429 (2003).
140. D. J. Wardrop and A. Basak, *Org. Lett.*, **3**, 1053 (2001).
141. D. J. Wardrop, C. L. Landrie and J. A. Ortiz, *Synlett*, **9**, 1352 (2003).
142. A. G. Romero, W. H. Darlington and M. W. McMillan, *J. Org. Chem.*, **62**, 6582 (1997).
143. A. Correa, I. Tellitu, E. Dominguez, I. Moreno and R. SanMartin, *J. Org. Chem.*, **70**, 2256 (2005).
144. W. Forster and R. M. Laird, *J. Chem. Soc., Perkin Trans. 2*, 135 (1982).
145. F. A. Carrol, *Perspectives Structure and Mechanism in Organic Chemistry*, Brooks/Cole Publishing Company, New York, 1998, p. 489.
146. A. Halvorsen and J. Songstad, *J. Chem. Soc., Chem. Commun.*, 327 (1978).
147. D. J. McLennan and A. Pross, *J. Chem. Soc., Perkin Trans. 2*, 981 (1984).
148. J. W. Thorpe and J. Warkentin, *Can. J. Chem.*, **51**, 927 (1973).
149. L. E. Andrews, T. M. Banks, A. M. Bonin, S. F. Clay, A.-M. E. Gillson and S. A. Glover, *Aust. J. Chem.*, **57**, 377 (2004).
150. G. Mo, 'Properties and Reactions of Anomeric Amides', PhD thesis, University of New England, Armidale, Australia 1999.
151. S. A. Glover and A. Rauk, *J. Chem. Soc., Perkin Trans. 2*, 1740 (2002).
152. I. O. Sutherland, in *Comprehensive Organic Chemistry Vol. 2, Nitrogen Compounds, Carboxylic Acids, Phosphorous Compounds* (Ed. I. O. Sutherland), Pergamon Press, Oxford, 1979, pp. 871–909.
153. J. Mulzer, in *Comprehensive Organic Synthesis Vol 6, Heteroatom Manipulation* (Ed. E. Winterfeldt), Pergamon Press, Oxford, 1991, p. 323.
154. J. Mulzer, in *Comprehensive Organic Functional Group Transformations Vol. 5* (Ed. C. J. Moody), Pergamon, Oxford, 1995, p. 121.
155. J. Perronnet and J. P. Demoute, *Gazz. Chim. Ital.*, **112**, 507 (1982).
156. J. J. Campbell, S. A. Glover and C. A. Rowbottom, *Tetrahedron Lett.*, **31**, 5377 (1990).
157. S. A. Glover, *Arkivok*, Part xii, Issue in Honour of O. S. Tee, ms. OT-308C, 143 (2001).
158. V. G. Shtamburg, A. V. Tsygankov, E. A. Klots and R. G. Kostyanovsky, *Mendeleev Commun.*, 208 (2004).
159. V. G. Shtamburg, O. V. Shishkin, R. I. Zubatyuk, S. V. Kravchenko, A. V. Tsygankov, V. V. Shtamburg, V. B. Distanov and R. G. Kostyanovsky, *Mendeleev Commun.*, **17**, 178 (2007).
160. F. Kadlubar, P. P. Fu, H. Jung, A. U. Shaikh and F. A. Beland, *Environ. Health Perspect.*, **87**, 233 (1990).
161. F. A. Beland and F. F. Kadlubar, in *Chemical Carcinogenesis and Mutagenesis* (Eds. C. S. Cooper and P. L. Grover), Springer-Verlag, Secaucus, New Jersey, 1990, pp. 267–325.
162. D. X. Lin, M. S. Bryant, C. Maleveille, M. Friesen, H. Bartsch, N. P. Lang and F. F. Kadlubar, *Environ. Health Perspect.*, **102**, 11 (1994).
163. F. F. Kadlubar, *Environ. Health Perspect.*, **62**, 19 (1985).
164. F. F. Kadlubar, J. A. Miller and E. C. Miller, *Cancer Res.*, **38**, 3628 (1978).
165. W. G. Humphreys, F. F. Kadlubar and F. P. Guengerich, *Proc. Natl. Acad. Sci. U.S.A.*, **89**, 8278 (1992).
166. G. M. Blackburn and B. Kellard, *Chem. Ind.*, 607 (1986).
167. G. Boche, F. Bosold and S. Schroder, *Angew. Chem., Int. Ed. Engl.*, **27**, 973 (1988).
168. M. Famulok, F. Bosold and G. Boche, *Angew. Chem., Int. Ed. Engl.*, **28**, 337 (1989).
169. F. Bosold and G. Boche, *Angew. Chem., Int. Ed. Engl.*, **29**, 63 (1990).
170. M. Famulok and G. Boche, *Angew. Chem., Int. Ed. Engl.*, **28**, 468 (1989).
171. M. E. Colvin, F. T. Hatch and J. S. Felton, *Mutat. Res.*, **400**, 479 (1998).
172. M. Panda, M. Novak and J. Magonski, *J. Am. Chem. Soc.*, **111**, 4524 (1989).
173. J. S. Helmick and M. Novak, *J. Org. Chem.*, **56**, 2925 (1991).
174. J. C. Fishbein and R. A. McClelland, *J. Chem. Soc., Perkin Trans. 2*, 663 (1995).
175. M. Novak, M. J. Kahley, J. Lin, S. A. Kennedy and T. G. James, *J. Org. Chem.*, **60**, 8294 (1995).
176. M. Novak and S. A. Kennedy, *J. Am. Chem. Soc.*, **117**, 574 (1995).
177. R. A. McClelland, M. J. Kahley and P. A. Davidse, *J. Phys. Org. Chem.*, **9**, 355 (1996).
178. R. A. McClelland, M. J. Kahley, P. A. Davidse and G. Hadzialic, *J. Am. Chem. Soc.*, **118**, 4794 (1996).
179. M. Novak and S. Rajagopal, *Adv. Phys. Org. Chem.*, **36**, 167 (2001).
180. M. Novak and S. Rajagopal, *Chem. Res. Toxicol.*, **15**, 1495 (2002).

181. S. A. Glover and M. Novak, *Can. J. Chem.*, **83**, 1372 (2005).
182. W. J. Hehre, L. Radom, P. v. R. Schleyer and J. A. Pople, *Ab Initio Molecular Orbital Theory*, Wiley, New York, 1986.
183. A. P. Scott and L. Radom, *J. Phys. Chem.*, **100**, 16502 (1996).
184. F. H. Allen, *Acta Crystallogr.*, **B58**, 380 (2002).
185. S. A. Glover and R. R. Schumacher, Unpublished data.
186. S. A. Glover and C. Mary, Unpublished data.
187. S. A. Glover and H. Price, Unpublished data.
188. M. Collis and S. A. Glover, Unpublished data.
189. S. F. Clay and S. A. Glover, Unpublished data.
190. B. Clements and S. A. Glover, Unpublished data.
191. L. J. Bellamy, *The Infra-red Spectra of Complex Molecules*, Chapman and Hall, London, 1975.
192. R. M. Silverstein and F. X. Webster, *Spectrometric Identification of Organic Compounds*, Wiley, New York, 1998.
193. H. Neuvonen and K. Neuvonen, *J. Chem. Soc., Perkin Trans. 2*, 1497 (1999).
194. H. Neuvonen, K. Neuvonen, A. Koch, E. Kleinpeter and P. Pasanen, *J. Org. Chem.*, **67**, 6995 (2002).
195. G. C. Levy and R. L. Lichter, *Nitrogen-15 Nuclear Magnetic Resonance Spectroscopy*, Wiley, New York, 1979.
196. A. J. Bennet, V. Somayaji, R. S. Brown and B. D. Santarsiero, *J. Am. Chem. Soc.*, **113**, 7563 (1991).
197. V. F. Rudchenko, S. M. Ignatov, I. I. Chervin and R. G. Kostyanovsky, *Tetrahedron*, **44**, 2233 (1988).
198. N. S. Isaacs, *Physical Organic Chemistry*, 2nd ed., Longman Scientific and Technical, New York, 1995, pp. 511–529.
199. K. R. Adam, I. Lauder and V. R. Stimson, *Aust. J. Chem.*, **15**, 467 (1962).
200. J. E. Rowe and A. D. Ward, *Aust. J. Chem.*, **21**, 2761 (1968).
201. J. M. Harris, S. G. Shafer, J. R. Moffatt and A. R. Becker, *J. Am. Chem. Soc.*, **101**, 3295 (1979).
202. H. H. Jaffé, *Chem. Rev.*, **53**, 191 (1953).
203. M. Adams, S. A. Glover and D. J. Tucker, Unpublished results.
204. S. A. Glover and D. S. Pankhurst, Unpublished results.
205. A. L. J. Beckwith and S. A. Glover, *Aust. J. Chem.*, **40**, 157 (1987).
206. J. W. Hilborn and J. A. Pincock, *J. Am. Chem. Soc.*, **113**, 2683 (1991).
207. V. F. Rudchenko, S. M. Ignatov and R. G. Kostyanovskii, *Izv. Akad. Nauk SSSR, Ser. Khim.*, 2384 (1989); *Chem. Abstr.*, **112**, 197783t (1990).
208. T. Koenig, in *Free Radicals*, Vol. 1 (Ed. J. K. Kochi), Wiley, New York, 1973, p. 113.
209. V. F. Rudchenko, S. M. Ignatov, I. I. Chervin, V. S. Nosova and R. G. Kostyanovskii, *Bull. Acad. Sci. USSR, Div. Chem. Sci.*, 1045 (1986).
210. S. Collins, Y. Hong, G. J. Hoover and J. R. Veit, *J. Org. Chem.*, **55**, 3565 (1990).
211. R. O. C. Norman, R. Purchase and C. B. Thomas, *J. Chem. Soc., Perkin Trans. 1*, 1701 (1972).
212. S. A. Glover, G. Mo, A. Rauk, D. Tucker and P. Turner, *J. Chem. Soc., Perkin Trans. 2*, 2053 (1999).
213. R. J. Crawford and R. Raap, *J. Org. Chem.*, **28**, 2419 (1963).
214. S. A. Glover and A. Rauk, *J. Org. Chem.*, **64**, 2340 (1999).
215. E. Hirota, R. Sugisaki, C. J. Nielsen and G. O. Sorenson, *J. Mol. Struct.*, **49**, 251 (1974).
216. T. Kasuya and T. Kojima, *Sci. Pap. Inst. Phys. Chem. Tokyo*, **58**, 1 (1962).
217. J. R. Fletcher and I. O. Sutherland, *J. Chem. Soc., Chem. Commun.*, 706 (1969).

Author Index

This author index is designed to enable the reader to locate an author's name and work with the aid of the reference numbers appearing in the text. The page numbers are printed in normal type in ascending numerical order, followed by the reference numbers in parentheses. The numbers in *italics* refer to the pages on which the references are actually listed.

The chemistry of hydroxylamines, oximes and hydroxamic acids
Edited by Z. Rappoport and J. F. Liebman

Subject Index

Entries are in letter-by-letter alphabetical order ignoring spaces and punctuation marks. Page numbers in *italic* refer to Figures and Tables not included in the relevant page ranges.

The chemistry of hydroxylamines, oximes and hydroxamic acids
Edited by Z. Rappoport and J. F. Liebman

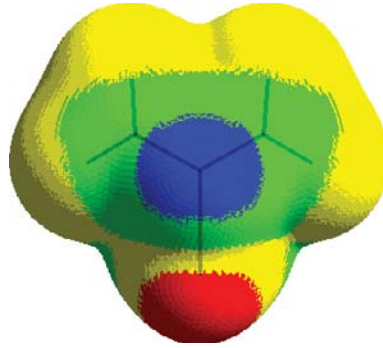

(a)

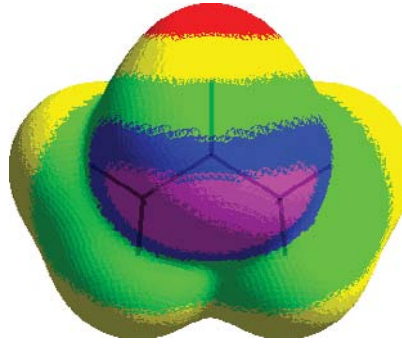

(b)

PLATE 1

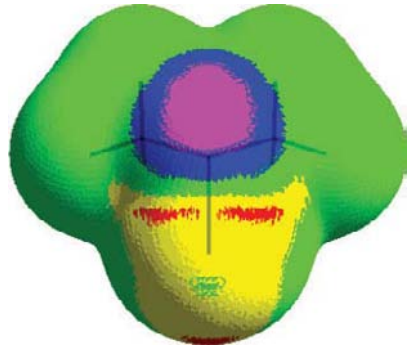

(a)

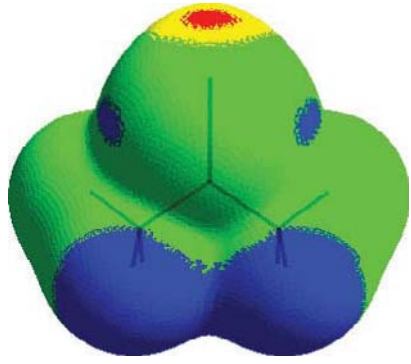

(b)

PLATE 2

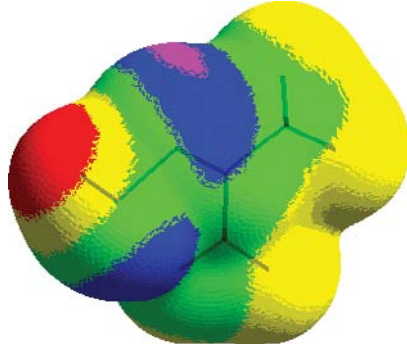

PLATE 3

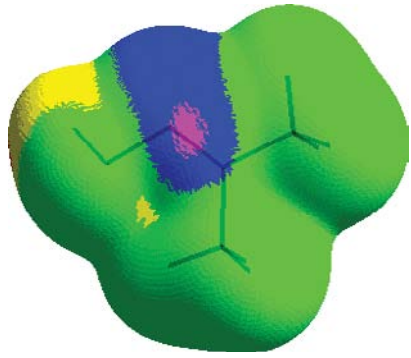

PLATE 4

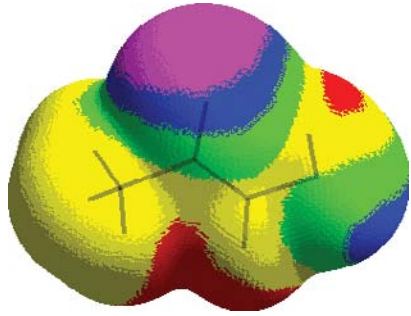

PLATE 5

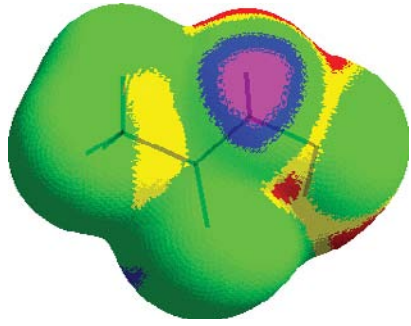

PLATE 6